RADIO RECEIVER DESIGN

By

K. R. STURLEY

Ph.D., B.Sc., A.M.I.E.E.
Marconi School of Wireless Communication

Part I

RADIO FREQUENCY AMPLIFICATION AND DETECTION

NEW YORK
JOHN WILEY & SONS, INC.
LONDON: CHAPMAN & HALL, LIMITED

First Published . . . 1943

IN THE REPRINTING OF THIS BOOK, THE RECOMMENDATIONS OF THE WAR PRODUCTION BOARD HAVE BEEN OBSERVED FOR THE CONSERVATION OF PAPER AND OTHER IMPORTANT WAR MATERIALS. THE CONTENT REMAINS COMPLETE AND UNABRIDGED.

3/45

PRINTED IN THE UNITED STATES OF AMERICA

AUTHOR'S PREFACE

AN attempt has been made in this book to bring together the fundamentals of radio receiver design. Difficulties were experienced in determining the order of treatment, and it was finally decided to follow introductory chapters on general considerations and valves by a detailed examination of the receiver, stage by stage, starting from the aerial. There are objections to this method from the teaching point of view ; for example, the chapter on aerials is better considered after that on R.F. amplifiers, whilst the chapter on I.F. amplifiers should be read before the latter half of that on R.F. amplifiers. To meet possible criticism a fairly detailed table of contents is given, so that the reader can develop his own plan of campaign.

Owing to war conditions the book has had to be divided into two parts, the first ending at the detector stage, leaving Part II to deal with audio frequency amplifiers, power supplies, receiver measurements, television and frequency modulated receiver design, etc.

The cosine expression, $\hat{E} \cos \omega t$, for a voltage of sinusoidal wave shape is used in preference to the sine expression because it is considered that it leads to a simpler mathematical analysis. For the same reason the grid bias voltage is written as $-E_b$, i.e., E_b represents a numerical and not algebraical value of bias. The advantage of so doing is most evident in Chapter 8.

Part I is practically self-contained, though there are one or two cross-references to sections in Part II. To facilitate cross-reference all sections, figures and expressions are prefixed by the chapter number.

No claim is made to an exhaustive bibliography, and reference is made, at an appropriate point in the text, only to those articles which have proved helpful in its preparation.

The author is indebted to his wife for help in reading the proofs, to Mr. R. M. Mitchell, B.Sc., for checking many of the calculations, to Mr. R. P. Shipway, B.A., for helpful discussion on parts of Chapter 8, and to Marconi's Wireless Telegraph Company for permission to publish material originally used by the author in lectures at the Marconi School of Wireless Communication.

August 1942.

ACKNOWLEDGMENTS

ACKOWLEDGMENTS are gratefully made to the following for permission to use figures and drawings taken from their publications.

Name of Journal	*Figure Numbers*
Electronics	3.22, 3.25 5.9 6.21
Journal of the Institution of Electrical Engineers	5.11*a*
Marconi Review	7.13*a* and *b*, 7.14, 7.15
Mullard Technical Bulletin	6.20
Proceedings of the Institute of Radio Engineers	2.17 5.23*a*, *b* and *c* 8.9
Wireless and Electrical Trader (*Pye Radio*)	5.24*a*
R.C.A. Review	5.8*b*
Wireless Engineer	3.8*a* to 3.19*b* 4.3, 4.11, 4.13, 4.14 5.8*a* 7.7, 7.9, 7.10, 7.11*a* 8.12, 8.13*a*, 8.17, 8.24
Wireless World	5.24*b* 6.13, 6.14 8.21*a* and *b*, 8.22

PART I

CONTENTS

PART I

CHAPTER 1

GENERAL CONSIDERATIONS

1.1. Introduction. The direct transmission and reception of speech or music over long distances, though not impossible, is impracticable and propagation of audio frequencies is usually accomplished by using them to modulate an R.F. wave acting as a carrier, i.e., the audio frequencies are used to control one of the three characteristics, amplitude, frequency, or phase, of the carrier. The most common method is by modulation of the carrier amplitude, the rate at which the amplitude is changed being directly proportional to the frequency of the original sound and the magnitude of the amplitude change being directly proportional to the intensity (a low intensity producing a small change of amplitude). This is illustrated in Figs. 1.1*a* and 1.1*b* for an unmodulated carrier amplitude of 1 volt peak. Fig. 1.1*a* corresponds to a low-intensity sound, the carrier amplitude varying between 0·9 and 1·1 volts, whilst Fig. 1.1*b* corresponds to a high-intensity sound, the carrier being 100% modulated, its amplitude varying from 0 to 2 volts. In frequency modulation, the carrier amplitude remains constant and its frequency is varied at a rate corresponding to the modulation frequency (50 times per second if f mod. = 50 c.p.s.), and the frequency deviation—rise and fall from the central unmodulated carrier frequency—is controlled by the intensity of the audio frequency. For example, suppose a 1,000 c.p.s. note is being transmitted on a carrier frequency of unmodulated value 1,000 kc/s, the variation of the carrier frequency takes place at the rate of 1,000 changes per second and the frequency limits may be

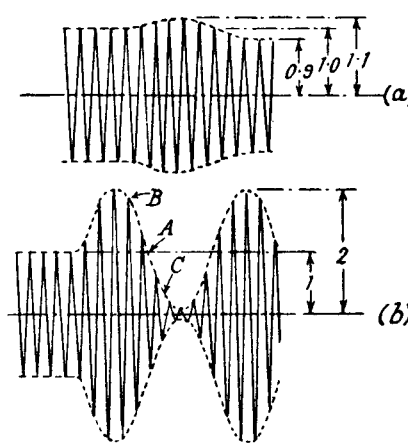

FIG. 1.1.—An Amplitude Modulated Wave.

± 100 c.p.s. (the carrier frequency changes between 1,000·1 and 999·9 kc/s) for a low intensity to $\pm 100{,}000$ c.p.s. for a high intensity note. These two conditions are illustrated in Figs. 1.2*a* and 1.2*b*. The frequency change of carrier is exaggerated in the figures for

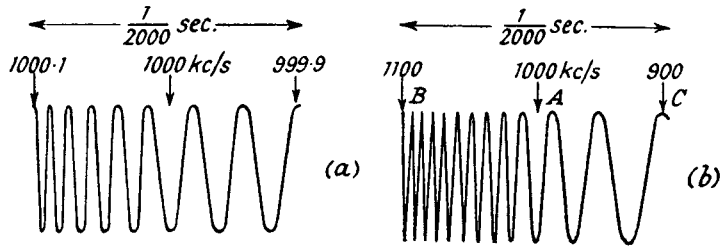

FIG. 1.2.—A Frequency Modulated Wave.

the purpose of illustration. With phase modulation the amplitude of the carrier remains constant and its phase angle with respect to its unmodulated condition is advanced and retarded at the frequency of the audio signal. The magnitude of the phase change is determined by the intensity of the audio frequency. Phase modulation has an effect on the carrier akin to frequency modulation, and whilst the phase of the carrier is varying, its frequency also is varying. There is a difference, but this is discussed later in Section 1.4.

Apart from the advantage of transmission over long distances the use of carriers enables many programmes to be transmitted simultaneously, any one of which may be selected by the listener with suitable receiving apparatus. This apparatus must abstract energy from the radiated electromagnetic carrier wave, separate desired from undesired signals, extract the audio frequency signal from the carrier, and amplify and reproduce the signal to any desired level. An aerial system is necessary to collect energy from the modulated carrier wave, the flux from which induces a voltage in the aerial as it passes. The function of the aerial is usually to act only as a collector, but it is sometimes employed as a discriminator against undesired signals, viz., in directional aerial systems. The separation of these signals is carried out by means of tuned circuits in the anode and grid circuits of the radio frequency valves, which amplify the desired modulated carrier. The audio frequency signal is extracted from the carrier by a suitable form of detector and is amplified to a level sufficient to operate the apparatus (telephones or loudspeaker) for converting electrical audio frequency energy into acoustical energy.

1.2. Amplitude Modulation. For understanding the function of any type of modulation a vector diagram is particularly useful, and amplitude modulation is quite simply illustrated if the envelope is sinusoidal as in Figs. 1.1*a* and 1.1*b*. The modulated signal is represented by

$$\hat{E} \cos \omega_c t(1+M \cos pt) \quad . \quad . \quad . \quad . \quad . \quad . \quad 1.1$$

where $\hat{E}$ = the unmodulated carrier peak voltage.
$\omega_c = 2\pi f_c$, the carrier pulsance.
$p = 2\pi f_m$, the modulating frequency pulsance.
M = modulation ratio, the maximum value of which is 1.

The factor 1 inside the bracket in expression 1.1 is necessarily included because the carrier still exists when there is no modulation, i.e., when $M = 0$. The vector representing expression 1.1 rotates at a speed of f_c c.p.s. and varies in amplitude f_m times per second between the limits $E(1+M)$ and $\hat{E}(1-M)$ as shown in Fig. 1.3*a*.

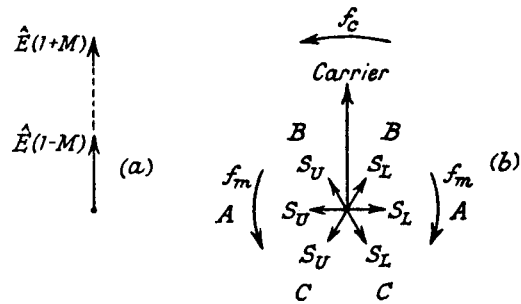

FIG. 1.3.—Alternative Vector Diagrams for an Amplitude Modulated Wave.

Expression 1.1 may be expanded as follows:

$$\hat{E} \cos 2\pi f_c t + \frac{\hat{E}M}{2} \cos 2\pi(f_c+f_m)t + \frac{\hat{E}M}{2} \cos 2\pi(f_c-f_m)t \quad . \quad 1.2$$

which consists of a carrier vector E rotating at f_c c.p.s. and two equal sideband vectors $\frac{\hat{E}M}{2}$ rotating at (f_c+f_m) and (f_c-f_m) c.p.s. about the same point as the carrier vector. Since these two sideband vectors only influence the carrier amplitude, it is clear that their resultant must always be in line with the carrier, and this is shown in Fig. 1.3*b*, for successive instants of time corresponding to points *A*, *B* and *C* on Fig. 1.1*b* The upper frequency sideband vector S_u is rotating round the carrier vector in an anti-clockwise direction (the accepted positive direction of frequency) at f_m c.p.s., whilst the lower frequency sideband vector S_L rotates in a clockwise direction round

the carrier vector at the same frequency. The carrier vector in Fig. 1.3*b* is, for convenience, shown as stationary, though actually it moves round in an anti-clockwise direction at f_c c.p.s.

Amplitude modulation of a carrier is achieved by controlling the gain of a carrier frequency amplifier in the transmitter by means of the A.F. signal. This can be realized by using the latter to vary the control grid or suppressor grid bias (of a pentode amplifier valve) or the anode voltage of a triode valve amplifier. Anode modulation requires a much larger A.F. signal than grid modulation, but the modulation envelope is much less distorted at high modulation percentages. To obtain the A.F. signal from the carrier, the amplitude variations must be detected at the receiver, i.e., a device is required to produce mean voltage variations in accordance with the carrier amplitude variations. This is achieved either by suppressing or reducing one-half of the amplitude modulated carrier, for this disturbs the symmetry of the wave shape (Fig. 1.4) with regard to the centre line and so produces a changing

FIG. 1.4.—A Detected Amplitude Modulated Wave.

mean voltage. A detector suppressing completely one-half of the modulated carrier and passing the other without changing its shape is known as a linear detector.

1.3. Frequency Modulation.[1, 4, 9] The problem of representing frequency modulation by a single vector is complicated by the fact that the frequency of the carrier is varying in accordance with the amplitude of the modulating frequency, and this means that the carrier vector rotates at varying speeds. Taking the example given above, for a frequency deviation of $\pm 100{,}000$ c.p.s. the carrier varies from 1,100 kc/s to 900 kc/s, and if we, acting as observers of the carrier vector, were to rotate at a frequency f_c c.p.s. (the carrier unmodulated value) in the same direction as the carrier vector, the latter would appear to oscillate backwards and forwards like a metronome, at the frequency of the modulating wave, i.e., 1,000 times per second. This condition is illustrated in Fig. 1.5*a*; like the metronome, the vector is stationary at the extremes, positions X' and X'', of its stroke so that the carrier frequency is instantaneously at its unmodulated value f_c (this is point A in Fig. 1.2*b*), whilst it is moving at its fastest, backwards

or forwards at the centre X of its swing. Movement of the vector in an anti-clockwise direction means that the frequency is greater than f_c and in a clockwise direction the reverse. Hence point X when the vector moves anti-clockwise corresponds to B in Fig. 1.2*b*, but when the vector is travelling clockwise X corresponds to C. In frequency modulation the carrier deviation is fixed for a given amplitude of modulating input, so that the speed of the vector as it passes through X is constant and independent of the frequency of oscillation backwards and forwards (that of the modulating input). Treating the problem as a mechanical one, the initial velocity at X' or X'' is zero, and the final velocity v at X is constant, so that the distance travelled from X' or X'' to X is proportional to velocity $\times$ time, but time is proportional inversely to the modulating frequency so that

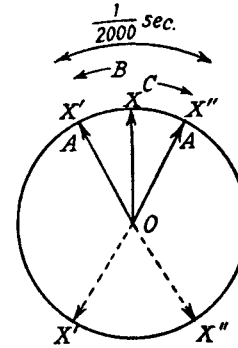

FIG. 1.5*a*.—Vector Diagram for a Frequency Modulated Wave.

$$X'X = X''X = Kvt = K_1 t = \frac{K_2}{f_m} \propto \frac{1}{f_m}$$

Hence the angle swept out by the carrier vector is large for low modulating frequencies and small for high modulating frequencies; dotted positions X' and X'' correspond to a lower modulating frequency than the full line positions. This again is analogous to the metronome, which increases its angle of sweep as the frequency decreases. The mathematical expression for a frequency modulated wave is

$$\hat{E} \cos\left[2\pi f_c t + \frac{Mf_c}{f_m} \cdot \sin 2\pi f_m t\right] \quad . \quad . \quad . \quad 1.3$$

where $$M = \frac{\text{deviation frequency}}{\text{carrier frequency}}$$

and the angle swept out by the vector is $\frac{Mf_c}{f_m}$ radians or $57{\cdot}3\ Mf_c/f_m$ degrees, which is seen to be inversely proportional to f_m. In the same way that expression 1.1 for amplitude modulation can be turned into a carrier and sidebands, so can expression 1.3 be treated, but instead of only two sidebands per fundamental modulating frequency it is found that there is a large number [1, 2] of sidebands spaced from the carrier by frequencies of $\pm f_m$, $\pm 2f_m$, $\pm 3f_m$, etc.

The expansion of expression 1.3 gives a carrier and infinite

series of sidebands having amplitudes corresponding to Bessel functions of ascending order, i.e.,

$$\hat{E}\cos\left[2\pi f_c t+\frac{Mf_c}{f_m}\sin 2\pi f_m t\right]$$
$$=\hat{E}\left\{J_0\left(\frac{Mf_c}{f_m}\right)\cos\omega_c t\right.$$
$$-J_1\left(\frac{Mf_c}{f_m}\right)[\cos(\omega_c-p)t-\cos(\omega_c+p)t]$$
$$+J_2\left(\frac{Mf_c}{f_m}\right)[\cos(\omega_c-2p)t-\cos(\omega_c+2p)t]$$
$$-J_3\left(\frac{Mf_c}{f_m}\right)[\cos(\omega_c-3p)t-\cos(\omega_c+3p)t]$$
$$\left.+\ \ldots\ \text{etc.}\right\}\quad .\quad .\quad .\quad .\quad .\quad .\quad 1.4$$

where $\omega_c = 2\pi f_c$ and $p = 2\pi f_m$.

$\frac{Mf_c}{f_m} = \frac{\text{deviation frequency}}{\text{modulating frequency}}$, sometimes designated as the modulation index,[2] may have any value from 1 upwards. For example, if the deviation frequency is ± 75 kc/s and the modulating frequency 10 kc/s, $\frac{Mf_c}{f_m} = 7{\cdot}5$. The amplitude of the carrier and sidebands can be obtained from tables of Bessel functions.[10, 11]

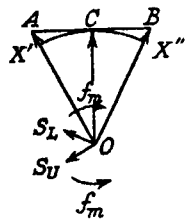

FIG. 1.5*b*.—Addition of Two Sidebands to Carrier to give Frequency Modulation.

The theoretically infinite number of sidebands is for all practical purposes fortunately limited, as the amplitudes of the sidebands more distant from the carrier normally decrease very rapidly. It is not only in the number of sidebands that frequency modulation differs from amplitude, but also in their position with respect to the carrier. All odd-numbered sideband vectors $\pm f_m$, $\pm 3f_m$, etc., from the carrier are so placed that their resultant falls on a line at right angles to the carrier [3] vector and all even-numbered sidebands have a resultant in line with the carrier vector. The addition of a carrier and two sideband vectors (spaced $\pm f_m$ from the carrier), having a resultant 90° displaced from the carrier vector, is shown in Fig. 1.5*b*. These two sideband vectors rotate round the carrier vector point 0 at f_m c.p.s., and their resultant adds to the carrier to cause the latter to oscillate backwards and forwards along the line AB. In fact, it is the same as Fig. 1.5*a*, apart from the ampli-

tude variation of the vector, and by adding suitable amplitudes of wider-spaced sidebands we can neutralize the amplitude variation, causing the point of the vector to describe an arc $X'X''$ giving only frequency modulation. Another important point to note with regard to frequency modulation sidebands is that the individual amplitudes are not directly proportional to the amplitude of the original modulating frequency as in amplitude modulation, but actually vary widely (sometimes becoming zero) as the angle swept out by the carrier vector changes. When this angle is small (f_m high) all sidebands except those nearest to the carrier are so small in amplitude that they can be neglected, but for a large angle of oscillation (f_m low) there are many sidebands of appreciable amplitude. For example, if $f_m = 50$ c.p.s. and its amplitude such as to give a carrier frequency change of $\pm 1{,}000$ c.p.s., the angle swept out by the vector moving from X' to X is $\frac{1000}{50} = 20$ radians (1,146°), and there are 23 sidebands of importance with amplitudes exceeding 1% of the fundamental sideband. If, however, $f_m = 1{,}000$ c.p.s., and the carrier frequency change is as before, the angle swept out by the vector is 1 radian (57·3°) and there are now only three sidebands of importance. It should be noted that the carrier vector may make a number of revolutions for low modulating frequencies.

Frequency modulation of a transmitter may be accomplished by varying the equivalent inductance or capacitance of the tuned circuit of the oscillator producing the carrier frequency (or a submultiple of this frequency). Since greater frequency stability is obtained at low frequencies it is quite common for the " master " oscillator driving the transmitter to generate a submultiple of the output carrier frequency, the submultiple being stepped up to the required output frequency by passing it through a series of multiplier stages, producing 2nd and 3rd harmonics of the input frequency. When the required frequency deviation of carrier is small compared with the carrier frequency—probable values are ± 75 kc/s at a carrier frequency of 45 Mc/s, representing a frequency deviation of $\pm 0{\cdot}001666 f_c$—the required change of tuning inductance or capacitance is linearly proportional to the frequency deviation. Hence a linear relationship between the amplitude of the A.F. signal and the change of inductance or capacitance results in frequency modulation having a deviation frequency linearly proportional to the amplitude of the A.F. signal. The variable reactance [8] valve (see Chapter 13 in Part II), as used in automatic frequency correction circuits, is particularly suitable for converting the A.F. amplitude into a change

of inductance or capacitance, since it acts as a reactance to any voltage source connected between its anode and cathode, the value of the reactance depending on the grid bias of the valve. If the relationship between the grid bias of the valve and its mutual conductance is linear, change of the former produces a linearly proportional change of reactance. Thus if the A.F. modulating voltage is applied to the grid circuit of the reactance valve it controls the mutual conductance in such a way as to produce a change of equivalent inductance or capacitance between the anode and cathode, which is linearly proportional to the A.F. voltage amplitude.

1.4. Phase Modulation. The vector representation of phase modulation is similar to that of frequency modulation with one important difference ; the angle swept out by the vector is constant for all modulating frequencies and is dependent only on the amplitude

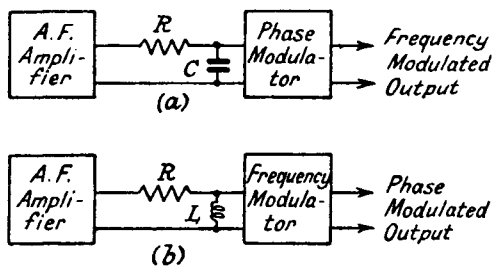

FIG. 1.6.
(*a*) Frequency Modulation from a Phase Modulator.
(*b*) Phase Modulation from a Frequency Modulator.

of the latter. This essentially means that the velocity of the vector at the centre X (Fig. 1.5*a*) increases as the speed of oscillation increases, i.e., the rise and fall in carrier frequency (frequency deviation) is directly proportional to the modulating frequency. It is possible to turn phase into frequency modulation by inserting in the modulation frequency amplifier a network having an amplification characteristic inversely proportional to frequency, giving a low frequency a large amplitude and a high frequency a small amplitude, i.e., the phase angle is no longer constant but increases as the modulation frequency falls. The reverse is also true ; frequency modulation can be converted to phase modulation by inserting in the modulation amplifier a network having an amplification characteristic directly proportional to frequency giving a low frequency a small and a high frequency a large amplitude. This is shown in Figs. 1.6*a* and 1.6*b* ; the first figure has a resistance–capacitance network in the modulation amplifier, thus producing

frequency modulation at the output of the phase modulator. In the second figure a resistance–inductance network produces phase modulation from a frequency modulator.

The modulated carrier expression is

$$\hat{E} \cos [2\pi f_c t + \phi M \cos 2\pi f_m t] \quad . \quad . \quad . \quad 1.5$$

and the phase angle swept out is equal to ϕM where ϕ is a constant and M is proportional to the amplitude of f_m but independent of its frequency. Phase modulation has an infinite number of sidebands spaced $\pm f_m$, $\pm 2f_m$, etc., from the carrier, but since the phase angle change is constant (unlike frequency modulation) the wider spaced sidebands for low as well as high modulating frequencies can usually be neglected. The resultants of all odd-numbered sidebands are 90° out of line with the carrier and those of the even-numbered ones are in line with the carrier vector. The amplitudes of the carrier and sidebands are Bessel Coefficients similar to those for frequency modulation, but the amplitude of the sidebands is dependent only on the amplitude of the modulating frequency. Thus

$$\begin{aligned} &\hat{E} \cos [2\pi f_c t + \phi M \cos 2\pi f_m t] \\ &= \hat{E} \{J_0(\phi M) \cos \omega_c t \\ &\quad - J_1(\phi M)[\cos (\omega_c - p)t - \cos (\omega_c + p)t] \\ &\quad + J_2(\phi M)[\cos (\omega_c - 2p)t - \cos (\omega_c + 2p)t] \\ &\quad - J_3(\phi M)[\cos (\omega_c - 3p)t - \cos (\omega_c + 3p)t] \\ &\quad + \ldots \text{ etc.}\} \quad . \quad . \quad . \quad . \quad . \quad . \quad 1.6 \end{aligned}$$

where ϕM is measured in radians.

The clearest distinction between frequency and phase modulation is indicated by considering a square-shaped modulating wave [7] as in Fig. 1.7. With frequency modulation the carrier frequency varies above and below its unmodulated value in accordance with the amplitude of the modulation. Phase modulation, however, shows that apart from the sudden instantaneous changes of phase when the carrier frequency becomes $+\infty$ or $-\infty$ the latter is constant at its unmodulated value.

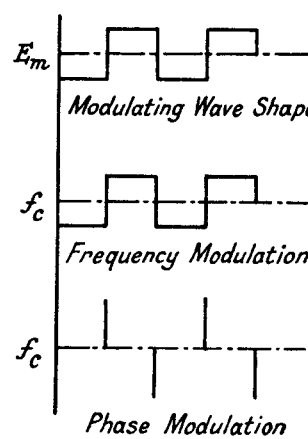

FIG. 1.7.—Illustration of the Difference between Frequency and Phase Modulation.

Phase modulation [5] can be achieved by separating the two sidebands of

an amplitude modulated carrier from the carrier and passing them through a phase adjusting network, which places their resultant at 90° to the carrier vector, as shown in Fig. 1.5*b*, and then recombines them with the carrier. Fig. 1.5*b* shows that amplitude modulation is also produced, but it can be suppressed by passing the phase modulated wave through a limiter (an amplitude distorting device giving almost constant carrier output for large changes of input). Phase change is not exactly proportional to the modulating voltage amplitude, but if its maximum value is limited to $\pm 25°$ deviation, distortion of the modulation does not exceed 3%.[6] Such a small phase change as $\pm 25°$ would represent a low modulation percentage, but if the original carrier is a submultiple of the required output frequency the phase angle is multiplied at the same time as the carrier in the frequency multiplier stages of the transmitter. For example, if the original carrier is one-tenth of the required, the phase angle is increased to $\pm 25° \times 10 = \pm 250°$ after passing through the multiplier stages. The extra sidebands essential to the larger phase angle are produced in the multiplier stages.

As far as the receiver is concerned, the main features of design are unaffected by the type of modulation. The frequency or phase modulation receiver requires two extra stages over its amplitude modulation counterpart; these are the amplitude limiter and frequency-amplitude converter. The latter is essential because the character of the original A.F. voltage modulating the carrier is that of amplitude variation, and it converts the frequency change of carrier into an amplitude change, which is then detected in the normal way by a diode or similar device. The converter does not remove the frequency variation, but this does not matter because the diode is sensitive only to amplitude change. The limiter stage is necessary to suppress amplitude change (due to transmission variations or noise) of the carrier before the converter, since the detector will respond to these undesired changes. Apart from these two modifications there is no vital difference between a frequency or phase modulation and an amplitude modulation receiver operating over the same range of carrier frequencies. In the chapters which follow, the amplitude modulation receiver is treated in detail, whilst the modifications necessary for reception of frequency or phase modulation are discussed in Chapter 15 of Part II.

1.5. Types of Amplitude Modulation Receivers. The simplest type of receiver is that consisting of a tuned circuit, connected to an aerial, and a detector, operating telephones. Selectivity

and output are low, though the latter may be increased to a value sufficient to operate a loud speaker by adding an audio frequency amplifier. Selectivity can be increased, but at the expense of output, by interposing more tuned circuits between the aerial and detector. With certain types of valve detectors selectivity and output may be increased by applying reaction, i.e., feeding radio frequency modulated carrier energy back from the anode to the grid circuit. The disadvantage of this method is that it produces a sharply peaked resonance curve, which discriminates against the higher audio frequencies modulating the carrier.

For adequate selectivity and low detector distortion, radio frequency amplification is essential. The selective property of a tuned circuit cannot be fully utilized if it is coupled to another tuned circuit, for each tends to damp the other. By separating tuned circuits with valves, maximum selectivity is achieved and the signal is also amplified. Most detectors are only linear over a limited range and above a given value of input signal, and R.F. amplification is necessary to raise the modulated carrier to this level.

A possible type of receiver is therefore one having R.F. and A.F. amplification. Owing to the difficulty of maintaining stability and the mechanical limitations imposed by the ganged variable capacitor, two stages of R.F. amplification are seldom exceeded for medium- and long-wave band operation. The amplification of an R.F. stage is proportional to $\frac{L}{CR}$, where L, C and R are the constants of the tuned circuit and, since L is constant and C decreases as frequency increases, amplification is not constant over the wave band but tends to increase with increasing frequency (in spite of the rise in R). Selectivity tends to fall as the frequency is increased. The tuning range of the capacitor is usually the same for each wave band, so that L is reduced as higher frequency wave ranges are selected. The value of L is so small on the short wave range that amplification is very low, and receivers for short wave operation are practically never dependent on the R.F. stages for amplification.

The difficulties of obtaining adequate carrier frequency amplification and constant selectivity over a given tuning range can largely be overcome by using the superheterodyne principle and converting all incoming R.F. carriers to a constant (generally) low R.F. frequency, at which high amplification and good selectivity can be obtained; the modulation sidebands are, of course, transferred to the new

fixed frequency carrier, which is called the intermediate frequency. The frequency conversion is carried out in a frequency changer valve by mixing the incoming modulated carrier with a local oscillation of frequency equal to the sum of the carrier and intermediate frequencies. The superheterodyne receiver is the most usual form of receiver for operation over all ranges from long to short waves. It tends to reduce the amplification and selectivity variations over the wave ranges by concentrating most of the amplification and selectivity in the intermediate frequency stage. There are disadvantages as well as advantages to the use of the superheterodyne principle, but they can be overcome by careful design. The local oscillator output may reach the aerial and be reradiated, causing interference in nearby receivers, and whistles may be produced by interaction between undesired carriers and the local oscillator and its harmonics. Reradiation can be reduced by

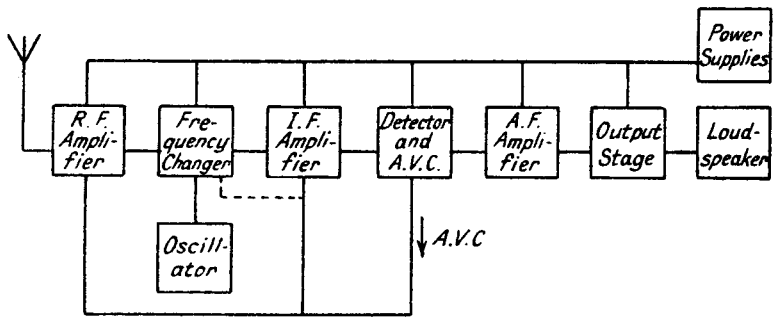

FIG. 1.8.—Schematic Diagram for a Typical Superheterodyne Receiver.

reducing the stray coupling in the frequency changer between the local oscillator and the aerial circuit. The inclusion of an R.F. amplifier valve between the aerial and signal circuit of the frequency changer almost entirely eliminates reradiation and has two other important advantages; it increases the signal-to-noise ratio when the noise is mostly produced in the first valve of the receiver, and it increases R.F. selectivity, so reducing undesired signals and whistle interference. The latter interference can be reduced by careful design of the frequency changer anode current-oscillator grid voltage characteristic.

A schematic diagram of a typical general purpose broadcast receiver is shown in Fig. 1.8. The aerial is coupled to the R.F. amplifier stage (usually a single valve, but in some communication type receivers two). This is followed by a frequency changer with

local oscillator, the output from which is fed to the intermediate frequency amplifier, consisting of one or two stages of amplification. A three-valve I.F. amplifier is usually necessary on receivers for television and frequency modulation. A diode detector is normally employed because of its linear detection characteristic with large signals ; carrier voltages exceeding 2 volts peak and modulated to 90% can be detected by the diode with very little distortion of the audio voltage output. An audio frequency amplifier usually precedes the power output stage. The amplification of the receiver should be such as to make it capable of reproducing with adequate output all signals above the noise level. Any increase in amplification beyond this is of little value except in so far as it improves automatic volume control action.

Most receivers incorporate accessory circuits aimed at making control less complicated, and two important ones are those providing automatic volume control, more correctly termed automatic gain control, and automatic frequency correction. Transmission of an electromagnetic wave through space is accomplished by direct and " sky reflected " waves, and beyond the service or local area much of the transmission is carried by the indirect ray reflected from the ionosphere surrounding the earth. The strength of the reflected ray is subject to slow or rapid fluctuations due to changes in the condition of the ionosphere, and the received input signal variations cause a corresponding change in audio output unless special measures are taken to vary the receiver gain in an inverse relationship to the signal strength. The gain of a receiver may be automatically controlled by using the D.C. component, produced by detection of the carrier, to vary the bias on the radio frequency, frequency changer (not always) and intermediate frequency stages, reducing the gain of these stages when the input signal increases, and vice versa. This is the principle involved in automatic gain control. A further advantage of A.G.C. is that it prevents " blasting " of the loudspeaker in tuning from a weak to a strong signal. Sometimes incorporated in an A.G.C. system is a device for silencing the receiver when the input signal is below a predetermined level—generally one governed by the noise level. Such a device, termed quiet automatic gain control or interstation noise suppression, removes one of the disadvantages of tuning with A.G.C., viz., that in the absence of a signal the gain of the receiver is maximum, thus amplifying receiver noise to an objectionable level.

Automatic frequency correction of the local oscillator in a superheterodyne receiver can be used to compensate for inaccuracy in

tuning, or drift of the oscillator, due to temperature changes, from its originally correct setting. It is particularly useful in remotely controlled and push-button operated receivers.

Push-button tuning is incorporated in order to facilitate rapid selection of, or changeover from, one station to another. The push-button switches may operate to switch in separate circuits tuned to the selected station or to control mechanically by cams, or electrically by a motor, the travel of the main tuning capacitor. Electrical motor control is readily adaptable to remote control.

In most receivers provision is made for the reproduction of gramophone records by switching the volume control of the receiver to the pick-up from the gramophone.

A third type is the superregenerative receiver, which may be used for ultra short wave communication purposes when quality of reproduction is unimportant and high sensitivity is required from simple apparatus. The receiver usually consists of a quenching valve, and an A.F. amplifier preceded by a detector, in which regeneration has been carried to the point of oscillation. The smallest signal is capable of initiating oscillation of the detector, and in the absence of control the oscillation will build up to a value determined by the valve characteristics. The rate of rise of oscillation amplitude, which is exponential, is proportional to the amplitude of the initiating signal and inversely to the inductance of the circuit tuning the signal. To make the valve useful as a detector it is necessary to stop periodically the oscillation and reset it to the sensitive condition. The interrupting frequency is supplied from a separate oscillator (in the simplest case the detector may be made self-setting by allowing it to develop a squegger oscillation) in series with the anode or grid circuit of the detector, so that with each negative half-cycle the latter is taken to cut-off and oscillation ceases. It is then ready for " triggering " by the signal once again. Since the rate of rise of oscillation is determined by the amplitude of the initiating signal, the average current taken by the valve follows approximately the modulation envelope of the signal. Owing to the very sensitive condition of the detector the smallest signal is capable of initiating oscillation and the noise level of the receiver is consequently high. In addition selectivity is low due to damping from the detector valve and it cannot be increased by including additional stages of R.F. amplification because positive feedback from the detector causes damped oscillations to occur in the added tuned circuits, thus masking the desired signal. For high sensitivity the ratio of initiating signal to quench frequency (about 40 kc/s) must be high ; this and

low selectivity confines the use of the superregenerative receiver to the ultra short wave band. Distortion of the modulation envelope of the received signal and high noise level make the receiver suitable only for communication for which reasonable intelligibility and not quality is the criterion.

1.6. Design Considerations Based on the Power Supply. The power supply has an important influence upon the receiver. For example, the H.T. battery in a battery receiver has a maximum voltage of 120 and a " life " capacity of approximately 0·2 kw. hrs., hence the power output of the receiver must be limited, the permissible distortion limit raised, and current consumption reduced to the lowest possible value. Since the output stage absorbs most of the current, economical working must be achieved by the use of special types of overbiased push-pull circuits, such as Class B and quiescent push-pull, which adjust their current consumption to the volume of the transmitted programme. Valves in the other stages of the receiver must be designed for maximum gain with minimum current and this can only be achieved in the R.F., frequency changer and I.F. stages at the expense of the variable-*mu* characteristic, the curvature of which must be greater, leading to higher distortion and cross-modulation effects than occur with their counterparts in the mains receiver.

In a mains-driven receiver for A.C./D.C. operation the H.T. voltage is limited by the mains connection, but large power can be obtained by high current consumption, and the output stage must be designed for low voltage and high current. The heaters of the valves are connected in series for economical operation.

A receiver for A.C. mains operation imposes practically no design limitations since with a suitable transformer the power source can be made to supply any desired current or voltage.

Cost also dictates the design of the receiver. High valve cost limits the number of stages and demands the highest amplification per stage. It also leads to the use of a pentode or beam tetrode valve in the output stage because of its high power sensitivity.

In the following chapters is described design procedure for each stage of the receiver, beginning at the aerial and progressing to the output. Part I ends with detectors and Part II, which begins with audio frequency amplifiers, includes chapters on television and frequency modulation receiver design.

BIBLIOGRAPHY

1. Notes on the Theory of Modulation. J. R. Carson, *Proc. I.R.E.*, Feb. 1922, p. 27.
2. Frequency Modulation. B. Van der Pol, *Proc. I.R.E.*, July 1930, p. 1194.
3. Note on the Relationship existing between Radio Waves Modulated in Frequency and Amplitude. C. H. Smith, *Wireless Engineer*, Nov. 1930, p. 609.
4. Amplitude, Phase and Frequency Modulation. H. Roder, *Proc. I.R.E.*, Dec. 1931, p. 2145.
5. A Method of Reducing Disturbances in Radio Signaling by a System of Frequency Modulation. E. H. Armstrong, *Proc. I.R.E.*, May 1936, p. 689.
6. Armstrong's Frequency Modulator. D. L. Jaffe, *Proc. I.R.E.*, April 1938, p. 475.
7. Frequency or Phase Modulation. Editorial Note, *Wireless Engineer*, Nov. 1939, p. 547.
8. Reactance Tube Frequency Modulators. M. G. Crosby, *R.C.A. Review*, July 1940, p. 89.
9. Amplitude, Frequency and Phase Modulation. Editorial, *Wireless Engineer*, Aug. 1940, p. 339.
10. *A Treatise on Bessel Functions.* Gray, Mathews and MacRobert. Text-book.
11. *Bessel Functions for Engineers.* N. W. McLachlan. Oxford University Press. Text-book.

CHAPTER 2

VALVES

2.1. Introduction.[9, 10] The all-important role played by the valve in receiver circuit design necessitates some knowledge of its constructional details and the principles, chief of which is thermionic emission, involved in its operation. An understanding of thermionic emission is helped by reference to the solar system hypothesis of the basic construction of matter. According to this theory, which, though superseded by later theories giving a more adequate explanation of certain phenomena, is very satisfactory in interpreting some of the simple actions, the atoms of all elements have a more-or-less compact central positively charged nucleus surrounded by electrons revolving in orbits rather like planets round the sun. The nucleus carries most of the mass of the atom and has a gross positive charge equal to the atomic weight of the element being considered ; part of this charge is neutralized by electrons in the nucleus itself and a net positive charge numerically equal to the atomic number is left. The atom is rendered electrically neutral by the orbital electrons, which equal in number the net positive charge on the nucleus. The maximum number of electrons, which can be maintained in each orbit, is limited, the first to 2 (2×1^2), the second and third to 8 (2×2^2), the third and fourth to 18 (2×3^2), and so on. The number of outer orbit electrons largely determines the activity of the element, inert elements like Helium, Argon, etc., having complete outer orbits and the most chemically active, the alkaline group (Lithium, Sodium, Potassium, etc.) headed by Hydrogen, having only one electron. The Potassium atom, fourth in the alkaline group, is illustrated in Fig. 2.1. Its atomic weight (total positive charge on the nucleus) is 39 and its atomic number (electrons in outer orbits) is 19, leaving 20 electrons in the nucleus. There is no evidence to fix the actual shapes of the orbits, which for convenience are shown as circular.

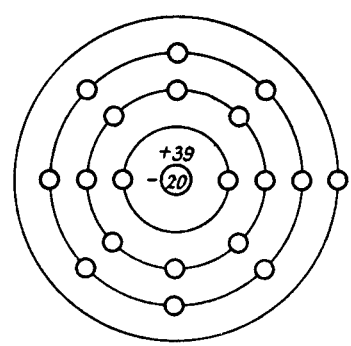

FIG. 2.1.—A Representation of the Potassium Atom.
(Atomic Weight 39, Atomic Number 19.)

In solid substances the atomic structure may allow the detachment of electrons from the atoms and the movement of these " free " electrons and the resultant positively charged atoms within the substance. Other solid media may, on the other hand, not allow the formation of these free electrons. Metals generally have many free electrons, and their motion is random except under the action of a driving potential, which causes them to move in one direction, so constituting a conduction current through the medium. The number of free electrons is indicative of the conductivity of the medium, a large number implying a good conductor. Insulating substances have practically no free electrons and an applied potential causes displacement of the orbits but no general drift of electrons. Electrical energy can be transferred across an insulator, if an alternating potential is applied, much in the same way that mechanical energy can be transferred through an elastic coupling.

In the metallic atom the velocity of the free electrons is largely determined by the temperature. At normal room temperatures the velocity is insufficient to carry the free electron beyond the boundary of the metallic surface, but as the temperature is raised its velocity increases and may reach a high enough value to allow it to break through and escape. This characteristic of liberating electrons under the action of heat is known as thermionic emission. A positive electrode placed near the metal will collect the electrons and show a small current. The number of electrons collected by this electrode depends on

(1) the metallic material forming the boundary of the emitting surface ;
(2) the temperature of the emitter ;
(3) the attractive power of the collector electrode, i.e., the positive voltage difference between it and the electron emitting surface ;
(4) the nature and density of the gaseous medium between the metal and electrode. When the density of the gas is high, the number of atoms per unit volume is large and the electrons collide with them, losing velocity so rapidly that many fail to reach the collector. If the gas density is very low, electron collisions are much less frequent and many more reach the collector anode.

This is the principle underlying the operation of the thermionic valve, which in its simplest form, a diode, consists of a metal filament or cathode heated to a high temperature, and a collector anode at a

suitable positive voltage. Earliest receiving valves used Tungsten for the heated filament since this could be raised to a high temperature without serious evaporation of the metal occurring. It was found, however, that the ease with which an electron escaped from its metallic barrier plane varied with different metals, and certain ones, notably the alkaline earth metals like Barium and Strontium, emitted electrons more readily and at a much lower temperature than Tungsten. Barium and Strontium oxides form the coating for the high efficiency low temperature valve, and during manufacture a thin film of the metals is distilled through to the surface of the cathode to act as an emitter, giving a copious flow of electrons.

We will now briefly touch upon the characteristics of the different types of valves, starting with the simplest, the diode.

2.2. The Diode. The diode consists of an electron-emitting hot cathode and a collector anode. For electrons to be collected, the anode generally must have a positive voltage applied between it and the cathode, though, owing to the initial velocity of the electrons, some may be collected at low negative anode voltages (between — 1 and 0 volt). The form of the anode current-anode voltage curves is shown in Fig. 2.2. Owing to the negative charge from the cloud of liberated electrons surrounding the cathode, maximum anode current does not flow immediately the anode becomes slightly positive. At low positive anode voltages this electronic negative space charge neutralizes the positive attractive field from the anode, and the anode current builds up to such a value that the number of electrons in transit produces a negative charge, just neutralizing the positive field from the anode. Increase of E_a requires a higher negative space charge for equilibrium, and so more electrons are drawn across to the anode to establish this equilibrium. The process continues as E_a is increased until all available electrons are being drawn off from the cathode; for higher values of E_a anode current remains constant. The maximum or saturation value of anode current is determined by the temperature of the cathode, i.e., the heater voltage, and increasing heater voltage raises the saturation current as shown in Fig. 2.2, though it has little effect on the current in the non-saturated region, since

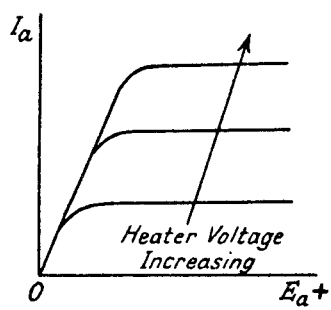

FIG. 2.2.—Diode I_aE_a Curves for Increasing Heater Voltage.

it is equivalent to increasing the reservoir of electrons without increasing the propulsive force from cathode to anode.

It can be shown that for concentric cathode and anode surfaces the anode current is

$$I_a = \frac{KE_a^{\frac{3}{2}}l}{r_a B^2} \quad . \quad . \quad . \quad . \quad . \quad . \quad . \quad . \quad 2.1$$

where K = constant depending on the emitting surface

l = length of cathode

r_a = radius of anode

B = a function of $\frac{r_a}{r_k}$

r_k' = radius of cathode.

Curve 1 in Fig. 2.3 shows an I_aE_a curve for expression 2.1.

This expression neglects the effect of the initial velocity of the electrons, which produces more initial curvature of the I_aE_a characteristic than that indicated by the $\frac{3}{2}$ power relationship and causes anode current to flow even for negative values of E_a (curve 2 in Fig. 2.3). Another factor controlling the I_aE_a curve is contact potential; this is due to the materials forming the cathode and anode, and it causes a shift of the curve in a positive anode voltage direction (curve 3 in Fig. 2.3). The use to which the valve is put determines the relative importance of these effects. A diode valve is employed either for rectification or for detection. As a rectifier it is required to convert A.C. to D.C. power, and for high efficiency it must allow large currents to flow for small positive voltage differences between anode and cathode. The current should be zero for negative anode voltages, and special precautions to prevent emission from the anode must be taken during manufacture. It is clear that a rectifier diode needs a high saturation current, i.e., the cathode should be long, for the temperature of an oxide-coated cathode, unlike that of the tungsten filament valve, must be maintained within fairly narrow limits if a long life is desired. Too high

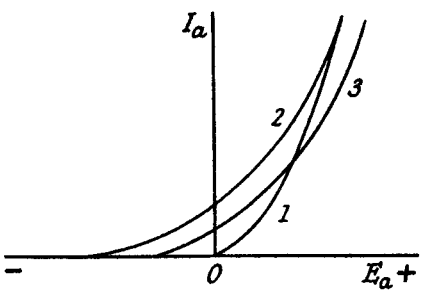

FIG. 2.3.—Effect of Initial Velocity and Contact Potential on the I_aE_a Curves of a Diode.

(Curve 1 : $I_a = kE_a^{\frac{3}{2}}$. Curve 2: Curve 1 with Initial Velocity Effect. Curve 3: Curve 2 with Contact Potential Effect.)

a temperature causes evaporation of the coating and loss of emission, and too low a value causes " poisoning " due to absorption of gas. The rate of rise of I_a with increasing E_a must be as steep as possible since this reduces the power loss in the valve and raises rectification efficiency. Hence from expression 2.1 we require a valve with a long cathode of large diameter, and minimum cathode-anode clearance. A small effective anode-cathode clearance is often obtained by including a grid (joined to the anode) close to the cathode. Since the A.C. peak voltages to be rectified are large, start of anode current at a small negative anode voltage and initial curvature of the I_aE_a characteristic at low anode voltages are not so important.

For detection purposes, linearity of I_aE_a characteristic is very necessary, and as the applied A.C. peak voltage will generally be small, the starting-point for anode current becomes important (Sections 8.2.6 and 7). On the other hand, detection current is small and a high saturation value is not essential.

2.3. The Triode. A triode valve has three electrodes, a grid being included between cathode and anode to control the flow of electrons. Its particular advantage is that small changes of grid voltage can produce large changes of anode current with negligible

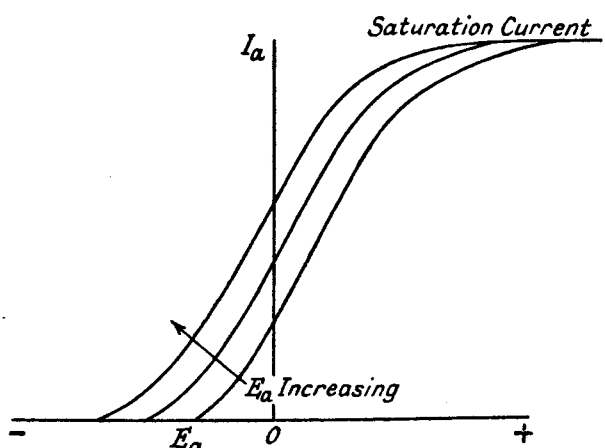

FIG. 2.4.—I_aE_a Curves for a Triode Valve.

expenditure of power in the grid circuit. The flow of electrons is now a result of the combination (at the cathode) of the electric fields from the grid and anode. Typical curves showing the effect of grid voltage variation on anode current are given in Fig. 2.4 for

different anode voltages. If the grid is made sufficiently negative it can completely neutralize the attractive power of the anode and stop the flow of electrons. As the negative grid voltage is reduced, I_a begins and increases until it finally reaches saturation at some positive value of grid voltage. When the grid voltage becomes positive (in mains valves with equipotential cathodes it may occur at a slightly negative value) electrons are collected by this electrode and grid current flows. The condition is rarely allowed to occur in practice because, as soon as grid current flows, power is taken from the driving source and this may cause distortion of the applied controlling voltage. Increase of E_a causes the I_aE_g curve to move to the left, but it does not appreciably affect the saturation current value.

The relationship between I_a, E_g and E_a can be more usefully expressed in the form of I_aE_a curves for different values of E_g, as shown in Fig. 2.11*a*. These curves are particularly helpful for indicating the performance of a valve in relation to its external anode circuit, and they also give three very important valve parameters, amplification factor (μ), mutual conductance (g_m), and internal resistance (R_a).

Amplification factor μ

$$= \frac{\text{change of anode voltage}}{\text{change of grid voltage to preserve constant anode current}}$$

$$= \frac{\Delta E_a}{\Delta E_g}(I_a = \text{constant}) \quad . \quad . \quad . \quad . \quad . \quad . \quad 2.2.$$

Thus if the grid voltage lines in Fig. 2.11*a* are separated by 1 volt intervals, amplification factor at a particular value of I_a is given by the horizontal distance between the intercepts of a horizontal line through this I_a value with the particular grid voltage lines. Hence the amplification factor for $I_a = 3\ mA$ and E_g from -3 to -4 volts is

$$\mu = \frac{XX'}{1} = 30.$$

Mutual conductance g_m

$$= \frac{\text{change of anode current}}{\text{change of grid voltage for constant anode voltage}}$$

$$= \frac{\Delta I_a}{\Delta E_g}(E_a = \text{constant}) \text{ expressed in mA/volt} \quad . \quad . \quad 2.3.$$

Mutual conductance is obtained in Fig. 2.11*a* by drawing a vertical line through a given E_a and measuring the vertical distance (in

milliamps) between any given E_g intercepts. Thus g_m at $E_a = 200$, E_g from -3 to -4 is

$$g_m = \frac{YY'}{1} = 3 \text{ mA/volt.}$$

Internal or Slope Resistance R_a

$$= \frac{\text{change of anode voltage}}{\text{change of anode current for a constant grid voltage}}$$

$$= \frac{\Delta E_a}{\Delta I_a}(E_g = \text{constant}) \quad . \quad . \quad . \quad . \quad . \quad . \quad 2.4.$$

This is measured by the inverse slope of the tangent to a given E_g curve at a particular value of E_a or I_a; R_a at $E_a = 200$, $E_g = -3$ is the cotangent of the angle that the tangent to the $E_g = -3$ volt curve at Y makes with the E_a axis,

$$\text{i.e., } R_a = 10{,}000\Omega.$$

By combining expressions 2.2, 3 and 4 we note that

$$\mu = \frac{\Delta E_a}{\Delta E_g} = \frac{\Delta E_a}{\Delta I_a} \times \frac{\Delta I_a}{\Delta E_g} = R_a.g_m$$

A point worth observing is that μ is a good guide to the grid base, i.e., the negative voltage required to stop anode current for

$$E_g(\text{cut-off}) \simeq \frac{E_a}{\mu}.$$

Actually E_g (cut-off) tends to be slightly greater than this because of the initial curvature of the I_aE_a characteristics.

The electrode construction of the valve determines the values of the three parameters. From Fig. 2.11*a* we see that decrease of the slope (increase of R_a) of the I_aE_a lines for the same perpendicular separation must increase XX' and hence increase μ. This can be achieved by reducing the effect of E_a on I_a, that is, by increasing the shielding power of the grid. Increase of the turns per inch, the thickness of the wire, or the distance between the grid and anode all increase μ.

Mutual conductance is raised by increasing the emitting surface and the control action of the grid. The former is realized by having a long cathode, and the latter by reducing the grid-cathode clearance. Increasing the turns per inch of the grid wire also tends to raise g_m.

The chief characteristics of a triode valve are that over the normal working ranges of I_a, E_a and E_g, μ, g_m and R_a are almost constant and only change as cut-off grid bias is approached, when μ and g_m fall and R_a rises.

2.4. The Tetrode. Between the control grid and anode, the tetrode valve has an additional grid positively biased with respect to the cathode. Two advantages are obtained; the anode-grid capacitance is very much reduced — 0·005 $\mu\mu$F in an R.F. tetrode as compared with about 3 $\mu\mu$F for a triode—so that coupling between anode and grid circuits is decreased, and the internal slope resistance becomes very high (not less than 0·5 MΩ). Both these effects are to be expected because the additional electrode screens the anode from the grid and the cathode, and very much reduces the influence of changes of anode voltage on the anode current.

The purpose for which the tetrode is to be used determines the details of its electrode construction. In an A.F. output stage, a low anode-grid capacitance and high resistance are not so essential and a coarse mesh screen allowing high g_m is desirable. For detection and amplification, particularly at radio frequencies, low anode-grid capacitance and high R_a are essential because the frequency response of an amplifier with tuned anode and grid circuits can be appreciably modified by regeneration and degeneration produced by the undesired anode-grid coupling. Furthermore, a low R_a reduces the selectivity of the anode tuned circuit. Metal skirts are often included at the top and bottom of the screen in order to reduce the stray capacitance between grid and anode.

R_a and g_m are the all-important parameters in a tetrode valve. The former is determined by the mesh of the screen wires (a close mesh screening the anode from the electron reservoir round the cathode), and the clearance between anode and screen (a large clearance producing a high R_a). Secondary emission from the screen to anode reduces R_a. A compromise is essential as screen current usually increases as the mesh becomes finer because a greater area of the electron stream is covered by the screen wires, and a large screen-anode clearance necessitates a large glass envelope. Mutual conductance is governed largely by the dimensions of the cathode, grid and screen and the anode has little effect.

The I_aE_g characteristics of a tetrode are similar to those of Fig. 2.4, except that E_s takes the place of E_a. The I_aE_a characteristics of the earliest form of tetrode, a screened grid, are illustrated in Fig. 2.5. Change of grid voltage alters the magnitude but not the general shape of the curves, and increase of screen voltage increases screen and anode current and also moves the point of minimum I_a to a higher E_a. Taking a particular curve, we see that for small increasing positive values of E_a, I_a rises quite steeply until at about +10 volts the velocity of the electrons striking the

anode is sufficient to detach electrons from the anode material. These low velocity secondary electrons are attracted to, and collected by, the screen because of its higher positive voltage. The secondary emission from the anode causes the anode current

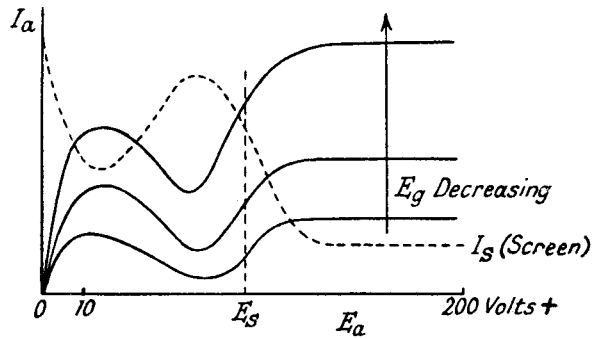

FIG. 2.5.—I_aE_a Curves for a Screened Grid Valve.

to fall and screen current to rise. Under suitable conditions the secondary electrons may exceed the primaries and I_a become negative. In the secondary emission region of falling I_a with increasing E_a, the anode presents a negative resistance to any external circuit and the valve can be made to act as an oscillator (known as a dynatron oscillator). When E_a approaches E_s, the attractive power of the screen lessens and the negative charge due to the electrons in the anode-screen space acts as a repulsive force driving the secondary electrons back to the anode. I_a therefore rises and I_s falls. As E_a is increased above E_s, secondary emission from the anode ceases and the anode collects all the primary electrons not intercepted by the screen wires. Thereafter I_a remains practically constant except for a small rise due to slight penetration of the anode field to the cathode, and to secondary emission from the screen to the anode. This secondary emission from the screen is much less effective than that from the anode since the secondaries are produced on the side away from the anode. The amount of secondary emission is dependent on the condition of the anode and screen surfaces, and if Barium and Strontium, volatilized from the cathode, are deposited on these the number of secondary electrons may be large. The emission from the anode can be greatly reduced by carbonising the surface.

Anode secondary emission is an undesirable characteristic in the tetrode because it limits the minimum working anode voltage to a little more than the screen voltage, i.e., it limits the maximum

output voltage from the valve. Its suppression can be achieved in a number of ways, all of which depend on the production of a voltage minimum in the anode and screen space, as shown in the curve of voltage distribution between the cathode and anode

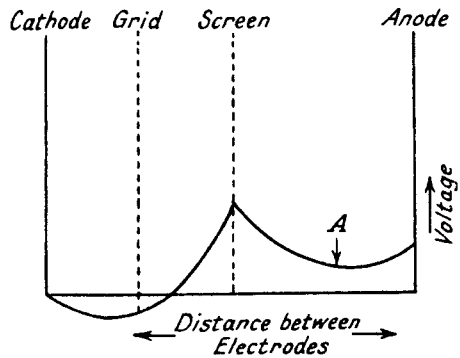

FIG. 2.6.—Voltage Distribution in a Tetrode Valve showing Suppression of Secondary Emission by a Voltage Minimum between Anode and Screen.

(Fig. 2.6). The secondary electrons are unable to pass this barrier (*A* in the figure) and so return to the anode. One of the simplest methods is to include an open-mesh grid (connected to the cathode) between the anode and screen. The pentode valve so formed has the I_aE_a characteristics of Fig. 2.7; the limitation of output voltage is now removed and an output voltage approaching 80% to 90% of the H.T. voltage can be obtained. The mesh of this grid

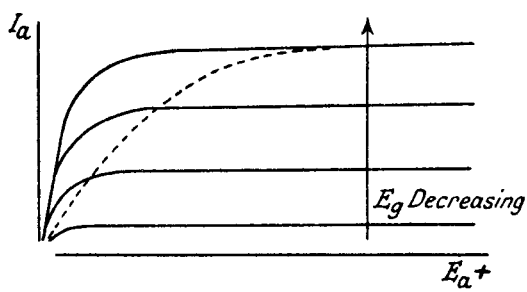

FIG. 2.7.—I_aE_a Curves for a Pentode Valve.

must be such as only just to suppress secondary emission, because if the mesh is made closer the flow of primary electrons to the anode at low E_a voltages is reduced, producing the dotted I_aE_a characteristic, which is demonstrably less efficient.

The potential minimum can be realized by fins [5] on the anode at right angles to the surface facing the screen, and also by increasing the anode-screen clearance.[4] In the latter instance the primary electrons in the anode-screen space provide the potential minimum by reason of their negative space charge. In a tetrode most of the anode secondary emission occurs in the region round the screen support wires where the primary electronic density is low. Plates, connected to the cathode and placed between the screen supports and the anode, return the secondary electrons to the anode and also tend to concentrate the primary electron stream into a beam, so producing the required potential minimum by the negative charge of the concentrated electrons, and preventing the return of secondaries in the main electron stream. This is the principle of secondary emission suppression employed in the beam tetrode, which often has the screen and control grids aligned so that the latter shades the former and reduces the pick-up of primary electrons by the screen.

In tetrodes required for R.F. amplification some form of gain control by variation of the D.C. electrode voltages is essential, and this is normally obtained by varying the grid bias of the control grid. This control would, without special grid construction, be much too rapid (curve 1 in Fig. 2.8) and would introduce serious distortion ; it is necessary to obtain a steady change of mutual conductance with grid bias as shown by curve 2 in Fig. 2.8. Curve 1 shows the variation of g_m against E_g for a normal grid construction of constant mesh. The curved characteristic 2 can be achieved by winding a grid of constantly variable pitch. The valve so produced is equivalent to a number of valves connected in parallel, each one having a different $g_m E_g$ characteristic, the close mesh part of the grid contributing mainly to the high g_m section (curve 3) and having a low negative cut-off voltage, and the open mesh giving a

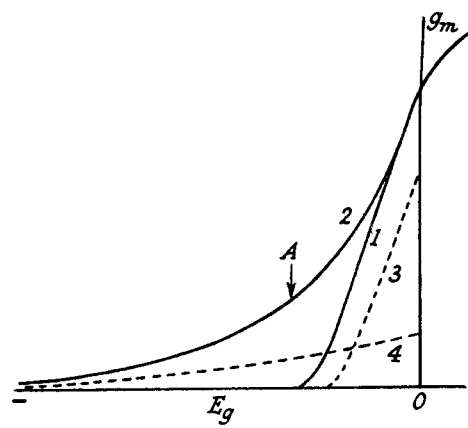

FIG. 2.8.—$g_m E_g$ Curves for a Tetrode or Pentode Valve.
(Curve 1 : Non-Variable *mu* Characteristic. Curve 2 : Variable *mu* Characteristic.)

low $g_m E_g$ curve (curve 4) with a high negative cut-off voltage. Generally, the mesh is fine at the ends of the grid electrode and coarse in the middle. Some distortion of the input voltage wave is inevitable with the variable *mu* (as it is called) valve, and it is a maximum at the point *A* (curve 2) of greatest curvature. A sudden change of mesh produces a sharp bend at this point, whilst a graded change of mesh produces a much smoother change.

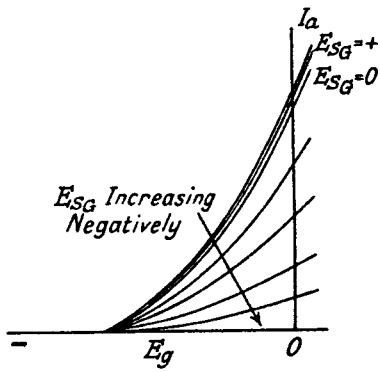

FIG. 2.9*a*.—$I_a E_g$ Curves of a Pentode Valve for Different Suppressor Grid Bias Voltages.

This variable *mu* or, more correctly, variable g_m effect can occur unintentionally in a non-variable *mu* valve if the grid electrode is out of line with the cathode or is conical in shape.

2.5. The Multi - electrode Valve. The multi-electrode valve, such as the pentagrid or heptode, octode, and hexode, is mainly used as a frequency changer. For an understanding of its action it is helpful to study the effect of negative bias on the suppressor grid of a pentode. Typical $I_a E_g$ curves showing the effect of negative bias on this grid are illustrated in Fig. 2.9*a*. As the bias increases, the electrons are repelled and the slope, g_m, of the characteristic decreases, and therefore the gain of the valve falls. Applying positive bias to the suppressor grid has little effect since the screen limits the flow of electrons from the cathode. As variation of suppressor grid negative bias controls gain, the valve may be used either as a modulator with the carrier applied to the control grid and modulation to the suppressor grid, or as a frequency changer with the signal applied to the control grid and the local oscillator output to the suppressor grid. There is, however, a disadvantage to the method and it can be seen from Fig. 2.9*b*. Increasing suppressor grid bias lowers R_a and eventually turns the $I_a E_a$ characteristic into that of a triode. This is due to the formation

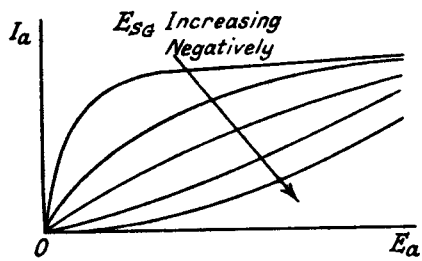

FIG. 2.9*b*.—$I_a E_a$ Curves for a Pentode Valve with Different Suppressor Grid Bias Voltages.

of a reservoir of electrons between the screen and suppressor grid ; the field from the anode can draw upon this virtual cathode and influence considerably the anode current. The reduction in R_a is a serious defect, particularly in a frequency changer, because it damps any highly selective anode circuit.

The difficulty can be overcome by converting the triode, formed by the virtual cathode, suppressor grid and anode, into a screened grid by interposing a positively biased grid between the suppressor grid and anode. Thus we have the hexode frequency changer of Fig. 2.10. The I_aE_{g1} characteristics for this valve are similar to those of Fig. 2.9*a* and the I_aE_{g3} characteristics for different values of E_{g1} are shown in Fig. 2.10. There is little increase in I_a for

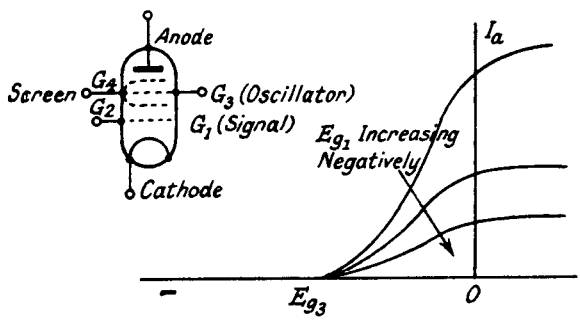

FIG. 2.10.—I_aE_{g3} Curves for a Hexode Valve with Different Signal Grid Bias Voltages.

positive values of E_{g3} since the first screen shields grid 3 from the cathode electron reservoir, and all available electrons between grids 2 and 4 have been collected by the anode. The I_aE_a characteristics are similar to those for a screened grid valve though the secondary emission " kink " is generally much less pronounced than that of Fig. 2.5.

The position of the signal and local oscillator grids may be interchanged, that is, the oscillator may be next to the cathode, and this occurs in pentagrid, heptode, and octode valve. In the heptode and octode valve another positively biased electrode is inserted between the oscillator grid and first screen to serve as an oscillator anode, and the valve acts as a combined oscillator and frequency changer. The octode has an extra suppressor grid between the anode and second screen to produce pentode I_aE_a characteristics. Details of these special valves are given in Section 5.3.

2.6. Representation of the External Anode Load Impedance on the I_aE_a Characteristic Curves. To illustrate the method of representing the external anode circuit on the I_aE_a curves we will consider a triode valve having the I_aE_a characteristic curves of Fig. 2.11*a*, with an external resistance R_0 of 10,000 ohms and an H.T. voltage $E_b = 200$ volts. This resistance is represented by a straight line AB passing through the points $I_a = 0$, $E_a = 200$

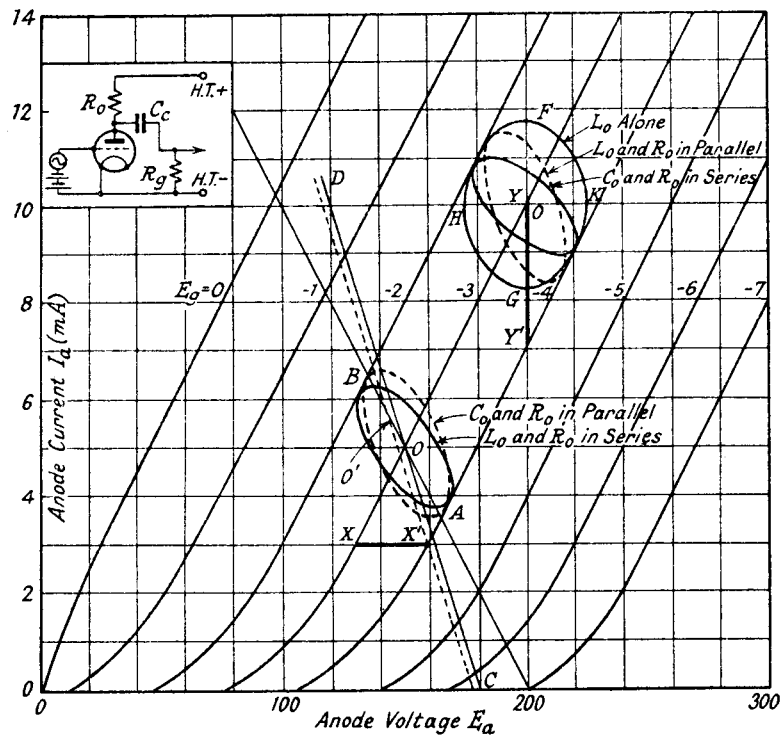

FIG. 2.11*a*.—Load Lines and Curves on the I_aE_a Characteristics.

(the anode voltage must equal E_b when $I_a = 0$ because no voltage drop occurs across R_0) and $I_a = 2$ *mA*, $E_a = 200 - I_aR_0 = 180$ volts. The resistance load line is straight because its equation is represented by

$$I_a = \frac{E_b - E_a}{R_0},$$

which shows that I_a is linearly proportional to E_a. We can use this line to determine the D.C. anode voltage and A.C. output voltage for any given D.C. grid bias and A.C. grid voltage. If the grid bias

is -3 volts and a sinusoidal A.C. voltage of peak value 1 volt is applied to the valve, the D.C. anode voltage is given by the intercept 0 of the R_0 line and the $E_g = -3$ volts curve measured on the E_a axis, i.e., it equals 150 volts. The A.C. anode peak voltage is 15, half the horizontal distance between the intercepts B and A of the R_0 line and the $E_g = -2$ and -4 volts curves. When a valve with a resistance load is used as a voltage amplifier the output from its anode circuit is coupled to the grid of the next valve through a capacitance C_c so as to isolate the D.C. voltage and allow only the A.C. component to be passed on. A grid leak R_g completes the D.C. path back to the cathode. The value of C_c is chosen so that at the lowest frequency its reactance is very much less than R_g. The effect of R_g is therefore to make the load resistance to A.C. of the first valve less than the D.C., i.e., the slope of the load line is $\frac{R_g R_0}{R_g + R_0}$, and it is shown on Fig. 2.11*a* as the line CD, which passes through the point O on the D.C. line. The A.C. voltage amplification is therefore reduced from

$$\frac{\mu R_0}{R_a + R_0} \text{ to } \frac{\mu \frac{R_g R_0}{R_g + R_0}}{R_a + \frac{R_g R_0}{R_g + R_0}},$$

but this is of much less importance than the fact that the bottom end of the A.C. line enters the cramped part of the $I_a E_a$ curves and distortion is produced with large outputs. R_g should therefore be chosen to have as high a value as possible so long as it does not produce softness in the succeeding valve. An interesting point to note is that the A.C. load line moves its position for large output voltages because rectification, and hence increased D.C. current, results from distortion. The line CD tends to move to a point O' corresponding to lower D.C. anode voltage in a manner similar to that described in Section 8.4.1. for anode bend detection.

To explain the construction of the locus load line for any form of load the simplest procedure is to start with the resistance case, dissociating the resistance locus load line from the $I_a E_a$ curves and drawing it as in Fig. 2.11*b* with reference to A.C. output voltage and current. To allow reference back to Fig. 2.11*a*, we will make the positive direction of output voltage to the left, because increasing positive load voltage means decreasing anode voltage E_a. The point O on the line AB in Fig. 2.11*a* becomes the origin for the line in Fig. 2.11*b*. Instantaneous values of E_0 and I_0 can be obtained

by projecting horizontally and vertically on to the two axes, for the voltage and current are in phase. Thus the A.C. cycle commences at O; 30° later E_0 and I_0 have values corresponding to OC and OD, which are half the maximum values of E_0 and I_0, OH and OP (at the 90° position of the cycle), for $\sin 30° = 0{\cdot}5$.

Now let us imagine that an inductive reactance of 15,000 ohms is connected in place of R_0 and that the peak voltage is arbitrarily

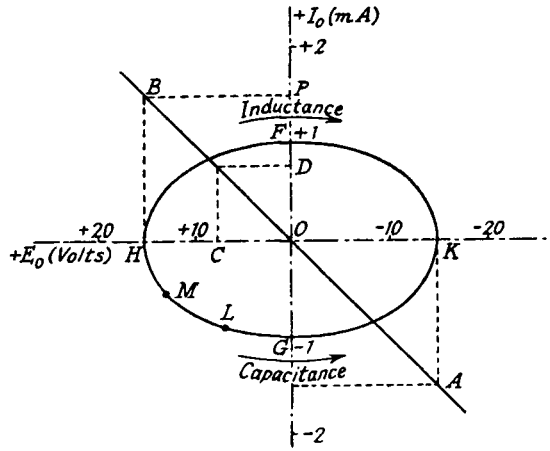

FIG. 2.11b.—Representation of the Locus Load Line for R_0, L_0, and C_0 Anode Loads.

chosen as 15, viz. OH, the same as that across R_0. Since the anode load is an inductive reactance, E_0 and I_0 are out of phase by 90°, I_0 lagging behind E_0. When E_0 is zero, I_0 has its maximum negative value of $\frac{-E_0}{X_0} = \frac{-15}{15{,}000} = -1$ mA; hence G is a point on the locus. 30° later E_0 has a value $15 \sin 30° = 7{\cdot}5$, and $I_0 = -1 \cos 30° = -0{\cdot}866$ mA. Therefore L is a point on the locus. Similarly after 60° of the cycle $E_0 = 13$ and $I_0 = -0{\cdot}5$, and point M is found. When $E_0 = 15$, its maximum value, $I_0 = 0$. If this procedure is repeated over the cycle the ellipse $GHFK$ is drawn out and this is the locus load line for an inductance L_0. The direction of progressive time instants is clockwise round the ellipse. A similar ellipse can be obtained for a capacitance C_0, but the point corresponding to progressive time instants now travels in an anti-clockwise direction because I_0 leads on E_0. The length of the I_0 axis of the ellipse is inversely proportional to the reactance X_0, being short for a large value of X_0.

In drawing out the reactive ellipse we assumed, for convenience,

that the output voltage was E_0, the same as that across R_0, but in actual fact the output voltage is dependent on the valve slope resistance R_a and on X_0. The shape of the locus curve is not affected, however, by the value of E_0 since I_0 is proportional to E_0, and a change of the former only means an increase or decrease in the size of the ellipse. In transferring the reactive ellipse to the I_aE_a curves we must adjust E_0 so that the ellipse is just tangential to the limit grid voltage curves, in this case $E_g = -2$ and -4 volts. Thus, if we have an H.T. voltage of 200 volts, a bias of -3 volts, an A.C. peak grid voltage of 1, and an inductance L_0 of reactance 15,000Ω and no D.C. resistance, the load curve is the ellipse $GHFK$ drawn on Fig. 2.11*a* with its centre O at the point $I_a = 10$ mA, $E_a = 200$ volts.

The size of the ellipse is adjusted to make it tangential to the $E_g = -2$ and -4 volt lines, and we find that E_0 has been increased to approximately 26 volts as compared with 15 volts arbitrarily chosen for constructing the ellipse in Fig. 2.11*b*. The major axis of the ellipse is vertical in Fig. 2.11*a* instead of horizontal as in Fig. 2.11*b*, because the scale relationship of I_a to E_a is changed.

Let us now consider the practical condition of a combined resistive and reactive load. Taking first a series circuit of resistance R_0 (10,000Ω) and reactance ωL_0 (15,000Ω), let us assume some arbitrary value of maximum current such as 1 mA, OF in Fig. 2.11*c*. We begin with current because a series circuit is being considered. The maximum voltage E_1 across R_0 is $IR_0 = 10$ volts (FB in Fig. 2.11*c*) and the maximum E_2 across L_0 is $IX_0 = 15$ volts (OH in the figure). By following the procedure outlined above we can draw the resistance line AB and the reactance ellipse $GHFK$. Since R_0 and L_0 are in series, their instantaneous voltages must be added for the combined locus load line. Thus for maximum $I_0 = OF$, the voltages E_1 and E_2 across R_0 and L_0 are FB and zero, and B is therefore a point on the combined locus. Similarly for $I_0 = 0$, the voltages across R_0 and L_0 are zero and OH respectively, and H is another point. For I_0 rising positively from zero, at a value $I_0 = OM$ we have $E_1 = MN$ and $E_2 = MP$ respectively, giving point Q. When I_0 is decreasing towards zero, for $I_0 = OM$ we have the total voltage $= MP - MN$ and point R is found. Continuing this process produces the locus curve $HQBKA$ similar in shape to a sheared ellipse, the direction of progressive time instants being clockwise. This curve must now be magnified or reduced for transferring to the I_aE_a curve in Fig. 2.11*a*. The resistance R_0, which will be assumed to have a D.C. resistance of

10,000Ω, and E_b (200 volts) determines the position of the centre point O of the "sheared" ellipse, and its overall size is adjusted until it is tangential to the grid voltage lines $E_g = -2$ and -4 volts as shown in Fig. 2.11.*a* A similar combined locus curve is obtained

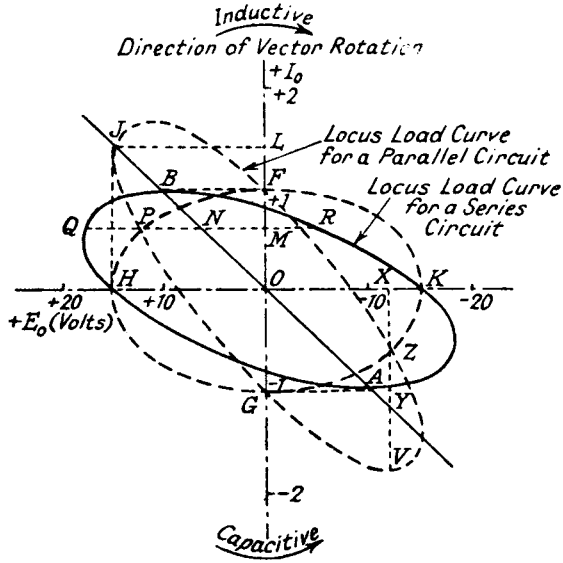

FIG. 2.11c.—Locus Load Curves for Series or Parallel Circuits of Resistance and Reactance.

for a series combination of R_0 and C_0, but the direction of vector rotation is anti-clockwise. We cannot transfer the series R_0C_0 circuit load curve directly to Fig. 2.11*a* because it has no D.C. path for the anode current. If, however, we assume the D.C. component to be carried by a choke of very high inductive reactance and zero D.C resistance, the combined locus is centred immediately above E_b (200 volts) at the intersection of $E_b = 200$ volts and $E_g = -3$ volts.

When the anode load is a parallel circuit of R_0 and L_0, we must take some arbitrary value of voltage E_0, OH in Fig. 2.11*c*, and draw the straight line for R_0 and ellipse for L_0. The maximum value of current I_1 through R_0 is $\frac{E_0}{R_0}$, OL in the figure, and the maximum value of current I_2 through L_0 is $\frac{E_0}{X_0}$, OF in the figure. Since the circuit is a parallel one we must add currents. When E_0 is zero, I_1 = zero and $I_2 = OG$, so that G is a point on the combined locus; for $E_0 = OH$ (its maximum positive value) $I_1 = OL$ but I_2 = zero,

hence J is a point on the combined locus. When E_0 is negative, equal to OX and decreasing to zero, $I_1 = XY$, $I_2 = XZ$ and V is a point on the combined locus where $XV = XY + XZ$. Continuing the process gives the " sheared " elliptical shape, $JFVG$, and this is increased or decreased in size, so that when transferred to Fig. 2.11a it becomes tangential to the $E_g = -2$ and -4 volt lines. The load curve for R_0 and C_0 in parallel is similar, with the direction of vector rotation in an anti-clockwise direction. The D.C. resistance component decides the position of the load curve above the E_a axis on Fig. 2.11a. The parallel R_0L_0 load curve is centred above the H.T. voltage E_b if L_0 has a negligible D.C. resistance, and the R_0C_0 curve about the intersection of the R_0 line with the $E_g = -3$ volt line if the D.C. resistance of R_0 is the same as its A.C. resistance.

2.7. Equivalent Circuits for a Valve. A valve may be represented by a constant voltage or a constant current generator [1]; the former representation is most suitable for a triode valve, which has a comparatively low resistance, whilst the latter is more useful in analysing the action of a tetrode or high resistance valve. The two circuits are shown in Figs. 2.12a and 12b; coupling between the anode and grid circuits has been assumed to be negligible.

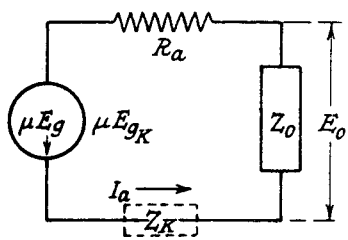

FIG. 2.12a.—The Valve as a Constant Voltage Generator.

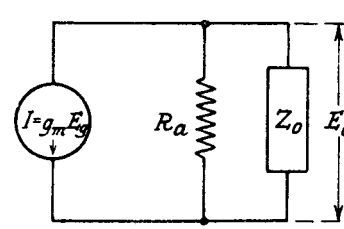

FIG. 2.12b.—The Valve as a Constant Current Generator.

The voltage developed across the external load Z_0 in Fig. 2.12a is

$$E_0 = \frac{\mu E_g Z_0}{R_a + Z_0} \quad . \quad . \quad . \quad . \quad 2.5a$$

whilst in Fig. 2.12b.

$$E_0 = \frac{IR_aZ_0}{R_a+Z_0} = \frac{g_mE_gR_aZ_0}{R_a+Z_0} = \frac{\mu E_gZ_0}{R_a+Z_0} \quad . \quad . \quad 2.5b.$$

The two circuits are therefore identical. Fig. 2.12b is very helpful when Z_0 is a tuned circuit, for it shows the desirability of having R_a as large as possible in order that the overall gain may be high and the maximum selectivity of Z_0 realized.

Sometimes an impedance is connected in the cathode-earth lead of a valve, notably for providing negative feedback ; the circuit of Fig. 2.12*a* is modified by the inclusion of the dotted impedance Z_k, and the effective grid input voltage becomes that between grid and cathode, E_{g_k}. The output voltage is

$$E_0 = \frac{\mu E_{g_k} Z_0}{R_a + Z_0 + Z_k}$$

where $$E_{g_k} = E_g - E_k$$

but $$E_k = \frac{\mu E_{g_k} Z_k}{R_a + Z_0 + Z_k}$$

$$\therefore E_{g_k} = E_g - \frac{\mu E_{g_k} Z_k}{R_a + Z_0 + Z_k}$$

$$= \frac{E_g(R_a + Z_0 + Z_k)}{R_a + Z_0 + (\mu + 1)Z_k}$$

$$\therefore E_0 = \frac{\mu E_g Z_0}{R_a + Z_0 + (\mu + 1)Z_k} \quad . \quad . \quad . \quad 2.5c.$$

Hence the inclusion of the cathode impedance has had the effect of increasing the equivalent valve impedance by $(\mu + 1)Z_k$. For high slope resistance valves, such as screened-grids or pentodes, g_m is the important parameter and expression 2.5*c* is modified as follows :

$$E_0 = \frac{g_m R_a E_g Z_0}{R_a + R_0 + (\mu + 1)Z_k} = \frac{g_m E_g Z_0}{1 + \frac{R_0}{R_a} + \left(g_m + \frac{1}{R_a}\right)Z_k} \simeq \frac{g_m E_g Z_0}{1 + g_m Z_k} \quad . \quad 2.5d$$

when $R_a \gg Z_0$. Thus the equivalent mutual conductance of the valve is reduced in the ratio $\frac{1}{1 + g_m Z_k}$. Expression 2.5*d* assumes that the screen is decoupled to cathode by a large capacitance and that there are no voltage changes across Z_k due to change of screen current. When the screen is decoupled to earth, a voltage is developed across Z_k due to screen current changes, and the following current voltage equations result.

$$E_k = (I_a + I_s)Z_k$$

$$I_a = \frac{\mu E_{g_k}}{R_a + Z_0 + Z_k} \simeq g_m E_{g_k}$$

$$I_s = \frac{\mu_s E_{g_k}}{R_s + Z_0 + Z_k}$$

where $$\mu_s = \frac{\Delta E_s}{\Delta E_g} (I_s \text{ constant}).$$

R_s = slope resistance of the $I_s E_s$ curves.

Generally $R_s \gg Z_k$ and

$$I_s = g_s E_{g_k}$$

where $$g_s = \frac{\Delta I_s}{\Delta E_g} (E_s \text{ constant}).$$

$$\therefore E_k = (g_m + g_s) Z_k E_{g_k}.$$

But $$E_g = E_{g_k} + E_k = [1 + (g_m + g_s) Z_k] E_{g_k}.$$

$$\therefore E_0 = g_m E_{g_k} = \frac{g_m E_g}{[1 + (g_m + g_s) Z_k]} \quad . \quad . \quad 2.5e.$$

$$= \frac{g_m E_g}{(1 + g_k Z_k)}.$$

Usually $g_m \propto I_a$ and $g_s \propto I_s$ so that

$$g_k = g_m \left(1 + \frac{I_s}{I_a}\right).$$

In non-aligned grid tetrode valves $\frac{I_s}{I_a}$ is about 0·25 and in aligned grid valves it is about 0·1.

2.8. The Grid Input Admittance of a Valve.[8]

2.8.1. Introduction. The grid input circuit of a valve can usually be represented by a resistance and capacitance in parallel. The magnitude of both components depends on the construction of the valve, the potentials applied to the electrodes, and the impedances in the external circuits connected to the electrodes.

The input resistance can be due to four causes:

(1) Leakage current between the grid and other electrodes. This can be measured when the valve heater or filament is cold, but it may change when it is hot.

(2) Electronic and positive ion current. The first may be produced by grid collection or emission of electrons. Collection of electrons by the grid may generally be prevented by applying sufficient negative bias. Emission from the grid is usually due to the volatilization of active material from the cathode and its condensation on the cooler grid. It can be reduced by preventing cathode temperatures in excess of that required for satisfactory operation, and by maintaining the temperature of grid and anode at as low a value as possible. A high temperature for the grid

electrode encourages emission from any material which has condensed upon it. Cooling fins are often connected to the top of the grid support wires of h gh current valves, and the anode is carbonized. Grid emission causes current in the opposite direction to that from electron collection, and produces across a grid leak resistance a positive bias on the grid. Positive ion current has this same effect and is due to the collection of positive ions—positively charged atoms of residual gas, which have been robbed of electrons by collisions with the primary electrons—by the negatively biased grid. Grid emission and positive ion current are more likely to occur in high current output valves, and the effect may be cumulative if a high grid leak resistance is employed. The positive bias caused by this grid current increases the anode current, thus raising the temperature of the anode, causing it to release absorbed gases; at the same time the grid temperature increases because of greater radiation from the anode, and grid emission current increases. A high grid leak may therefore quickly produce destruction of the vacuum and "softening" of the valve, and it is the probability of "softness" which limits the grid leak in output valves and most types of voltage amplifier valves to maxima of 0·5 and 2 MΩ respectively.

(3) Coupling between the grid and any other electrode containing an impedance to the input frequency. Anode-grid capacitance is the more usual source of this defect, but capacitance between the grid and cathode or screen can also contribute. The equivalent input resistance from this cause may be positive or negative, resulting in degeneration or regeneration of the input voltage, the sign depending on the sign of the particular electrode circuit reactance. The magnitude of this resistance is inversely proportional to the gain of the valve and directly proportional to the ratio of resistance to reactance in the given electrode circuit, zero reactance giving infinite resistance.

(4) Transit time of the electrons between the cathode and grid. When the time of flight of the electrons between grid and cathode becomes comparable with the reciprocal of the input frequency, electrons may be accelerated away from the grid in the direction of the cathode as well as in the direction of the screen of the R.F. amplifier valve. The negatively charged cloud of electrons moving away from both sides of the grid constitutes an A.C. current having a resistive and a capacitive component. The effect is dependent on the total electron flow and is greatest for high space currents, i.e., low grid biases.

The input capacitance is also dependent on four factors :

(1) The grid size and proximity to other earthed electrodes such as the cathode and screen. This capacitance can be measured when the valve is cold.

(2) Space charge. The negative charge due to the electrons clustered round the cathode is equivalent to a reduced distance between the cathode and grid, and the capacitance between the two electrodes is therefore increased upon that of the cold value. The increase is dependent on the grid bias and has a maximum of about 2 $\mu\mu$F at the minimum negative grid bias. It causes mistuning of the signal circuit when the gain of the valve is varied by changing the signal grid bias.

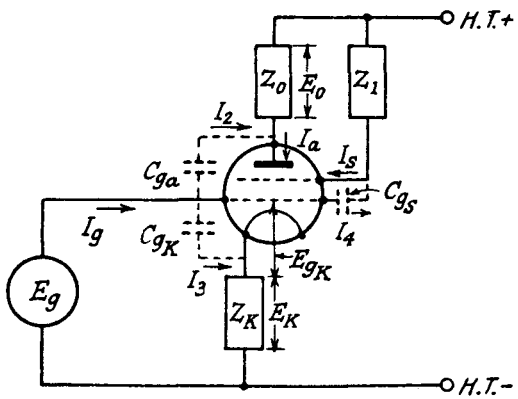

FIG. 2.13.—A Circuit showing Coupling to the Grid by Interelectrode Capacitance.

(3) Coupling between the grid and any other electrode, having an impedance to the operating frequency. This reflected reactance is always capacitive irrespective of the sign of the reactance in the other electrode, and the equivalent capacitance is a maximum for zero external circuit reactance and minimum grid bias, i.e., maximum valve gain.

(4) Transit time of the electrons as set out above.

We will now consider the resistance and capacitance reflected into the grid circuit due to coupling between it and other electrodes. A circuit showing coupling between the grid and other electrodes is given in Fig. 2.13.

2.8.2. Grid Input Admittance and Anode-Grid Capacitance Coupling. Assuming that $Z_k = Z_1 = C_{g_k} = C_{g_s} = 0$), the equivalent circuit for a valve having anode-grid capacitance coupling is shown in Fig. 2.14. Using the constant current generator

circuit and replacing the resistances and reactances by their equivalent conductances and susceptances, viz.

$$\frac{1}{R_a} \text{ by } G_a, \quad \frac{1}{Z_0} \text{ by } Y_0 = G_0 + jB_0 \text{ and } \frac{1}{X_{C_{g_a}}} \text{ by } B_{g_a},$$

the voltage and current relationships may be written as follows:

$$I_a = g_m E_g = E_0.[G_a + G_0 + jB_0] + [E_0 + E_g].jB_{g_a} \quad . \quad 2.6.$$

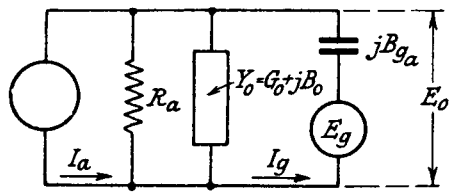

FIG. 2.14.—The Equivalent Constant Current ($I_a = g_m E_g$) Generator Circuit for Anode-Grid Capacitance Coupling.

Note.—E_0 and E_g are in the same direction as regards C_{g_a} and therefore additive.

$$I_g = (E_0 + E_g)jB_{g_a} \quad . \quad . \quad . \quad . \quad 2.7.$$

From 2.7 the admittance of the grid circuit is

$$Y_g = \frac{I_g}{E_g} = \left[1 + \frac{E_0}{E_g}\right].jB_{g_a}$$

and from 2.6

$$\frac{E_0}{E_g} = \frac{g_m - jB_{g_a}}{(G_a + G_0) + j(B_0 + B_{g_a})} \quad . \quad . \quad . \quad 2.8$$

$$\therefore \; Y_g = \frac{jB_{g_a}[G_a + G_0 + g_m + jB_0]}{(G_a + G_0) + j(B_0 + B_{g_a})}.$$

Rationalizing

$$Y_g = \frac{jB_{g_a}[G_a + G_0 + g_m + jB_0][G_a + G_0 - j(B_0 + B_{g_a})]}{(G_a + G_0)^2 + (B_0 + B_{g_a})^2}$$

$$= \frac{B_{g_a}.[[G_a + G_0 + g_m][B_0 + B_{g_a}] - B_0[G_a + G_0]] + jB_{g_a}[(G_a + G_0 + g_m)(G_a + G_0) + B_0(B_0 + B_{g_a})]}{(G_a + G_0)^2 + (B_0 + B_{g_a})^2}$$

$$= G_g + jB_g$$

$$\therefore \; R_g = \frac{1}{G_g} = \frac{(G_a + G_0)^2 + (B_0 + B_{g_a})^2}{B_{g_a}[g_m.B_0 + B_{g_a}(G_a + G_0 + g_m)]} \quad . \quad . \quad 2.9a$$

$$\text{and } C_g = \frac{B_g}{\omega} = \frac{C_{g_a}[(G_a + G_0 + g_m)(G_a + G_0) + B_0(B_0 + B_{g_a})]}{(G_a + G_0)^2 + (B_0 + B_{g_a})^2} \quad . \quad 2.9b.$$

These expressions show that when B_0 is positive or negative and infinite, R_g is infinite and $C_g = C_{g_a}$. This is to be expected since $B_0 = \infty$ means zero anode reactance and the anode is virtually connected to earth, leaving only the anode-grid capacitance across the grid input circuit. R_g is also infinite when $B_0 = -B_{g_a}\frac{(G_a+G_0+g_m)}{g_m}$. For values of $B_0 > -B_{g_a}\frac{(G_a+G_0+g_m)}{g_m}$, R_g is positive and for $B_0 < -B_{g_a}\frac{(G_a+G_0+g_m)}{g_m}$, R_g is negative. Thus anode-grid capacitive coupling with an inductive anode load can, and usually does, provide regeneration, whereas with a capacitive anode load, degeneration always occurs. There are two minima for R_g, one positive and the other negative, and they are found by differentiating 2.9*a*, with respect to B_0 and equating to 0. The resulting equation is

$$(B_0+B_{g_a})^2 g_m + 2B_{g_a}(B_0+B_{g_a})(G_a+G_0) - g_m(G_a+G_0)^2 = 0.$$

Hence $$B_0' = -B_{g_a} \pm (G_a+G_0)\left[\frac{B_{g_a}}{g_m} \pm \sqrt{1+\left(\frac{B_{g_a}}{g_m}\right)^2}\right] \quad . \quad 2.10a$$

The maximum value of C_g can be found in a similar manner from 2.9*b* and the resulting equation is

$$B_{g_a}(B_0+B_{g_a})^2 - 2(B_0+B_{g_a})(G_a+G_0)g_m - B_{g_a}(G_a+G_0)^2 = 0$$

$$B_0'' = -B_{g_a} \pm \left[\frac{g_m \pm \sqrt{{g_m}^2+{B_{g_a}}^2}}{B_{g_a}}\right](G_a+G_0)$$

the maximum condition is given from

$$B_0'' = -B_{g_a} + \left[\frac{g_m - \sqrt{{g_m}^2+{B_{g_a}}^2}}{B_{g_a}}\right](G_a+G_0) \quad . \quad 2.11a.$$

Generally, $B_{g_a} \ll g_m$ and (G_a+G_0) so that 2.10*a* and 2.11*a* reduce to

$$B_0' = \pm (G_a+G_0) \quad . \quad . \quad . \quad . \quad 2.10b$$

and $$B_0'' = -B_{g_a}. \quad . \quad . \quad . \quad . \quad 2.11b.$$

Combining 2.10*b* and 2.9*a* and neglecting B_{g_a} in comparison with the other factors

$$R_g(\text{min.}) = \pm\frac{2(G_a+G_0)}{g_m B_{g_a}} \quad . \quad . \quad . \quad 2.12.$$

Combining 2.11*b* and 2.9*b* and again neglecting B_{g_a}

$$C_g(\text{max.}) = C_{g_a}\left[\frac{G_a+G_0+g_m}{G_a+G_0}\right]$$

$$= C_{g_a}\left[1+\frac{g_m}{G_a+G_0}\right]$$

$$= C_{g_a}\left[1+\frac{g_m R_a R_0}{R_a+R_0}\right]. \quad . \quad . \quad 2.13a$$

$$= C_{g_a}\left[1+\frac{\mu R_0}{R_a+R_0}\right]. \quad . \quad . \quad 2.13b.$$

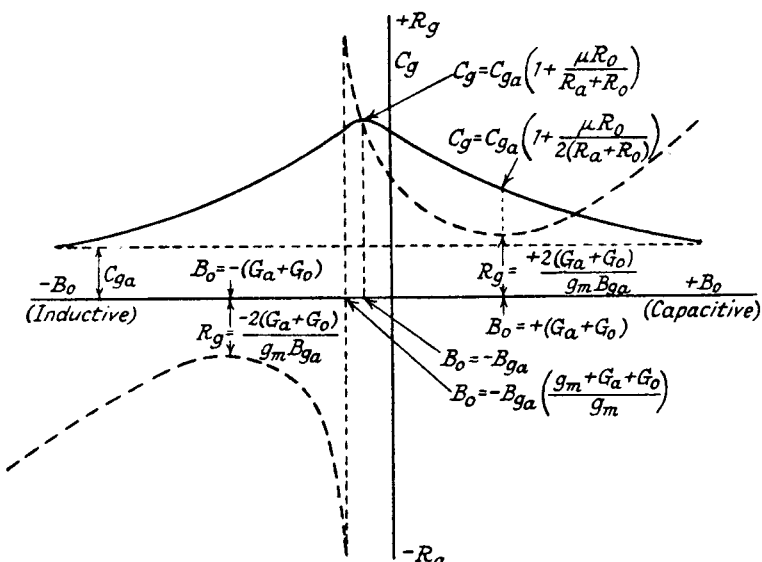

FIG. 2.15.—The Effect on Input Capacitance (C_g) and Input Resistance (R_g) of Varying Anode Circuit Susceptance (B_0).

Expression 2.13*b* is in the well-known form illustrating the Miller effect.

The changes of R_g and C_g for values of B_0 varying from $+\infty$ to $-\infty$ are shown in Fig. 2.15. These effects have a very important bearing on the frequency response of an R.F. amplifier and they are fully discussed in relation to this problem in Section 7.8.

In many practical examples $G_a \ll G_0$ and $B_{g_a} \ll B_0$ so that the expressions for R_g and C_g can be simplified to

$$R_g = \frac{G_0^2+B_0^2}{g_m B_{g_a} B_0} \quad . \quad . \quad . \quad . \quad . \quad . \quad . \quad . \quad 2.14a$$

$$= \frac{B_0}{g_m B_{g_a}} \text{ when } G_0 \ll B_0$$

$$= -\frac{1}{g_m \omega^2 L_0 C_{g_a}} \text{ when } B_0 \text{ is inductive.}$$

$$= \frac{C_0}{g_m C_{g_a}} \text{ when } B_0 \text{ is capacitive.}$$

$$C_g = C_{g_a}\left[\frac{(G_0+g_m)G_0+B_0^2}{G_0^2+B_0^2}\right] = C_{g_a}\left[1+\frac{g_m G_0}{G_0^2+B_0^2}\right] \quad . \quad 2.14b.$$

A valve may have an impedance in its cathode circuit (intentionally as in a negative feedback amplifier or unintentionally due to inductance of the lead from cathode to valve-pin) and the current-voltage equations are modified to (Fig. 2.13 with $C_{g_k} = 0$, $Z_1 = 0$, $I_2 = I_g$)

$$I_g = (E_g+E_0)jB_{g_a}$$

$$Y_g = \left[1+\frac{E_0}{E_g}\right]jB_{g_a} \quad . \quad . \quad . \quad . \quad . \quad . \quad 2.15.$$

$$I_a = \frac{\mu E_{g_k} - (E_0+E_k)}{R_a} = g_m(E_g - E_k) - (E_0+E_k)G_a$$

$$I_a = g_m E_g - E_k(g_m+G_a) - E_0 G_a$$
$$= E_k(G_k+jB_k)$$

$$\therefore\ E_k(G_a+G_k+g_m+jB_k)+E_0 G_a = g_m E_g \quad . \quad 2.16a$$

$$(I_a - I_g) = E_0(G_0+jB_0) = E_g(g_m - jB_{g_a}) - E_k(g_m+G_a) - E_0(G_a+jB_{g_a})$$

$$\therefore\ E_k(g_m+G_a)+E_0.[G_a+G_0+j(B_{g_a}+B_0)] = E_g(g_m - jB_{g_a}) \quad 2.16b.$$

Combining 2.16a and 2.16b to eliminate E_k

$$\frac{E_0}{E_g} = \frac{(g_m - jB_{g_a})(G_a+G_k+g_m+jB_k) - g_m(G_a+g_m)}{[G_a+G_0+j(B_{g_a}+B_0)][(G_a+G_k+g_m+jB_k)] - (G_a+g_m)G_a} \quad 2.17a.$$

It will be noted that when G_k and B_k are infinite, i.e., the cathode impedance is zero, 2.17a reduces to 2.8. Normally B_{g_a} and G_a can be neglected in comparison with the other components and so

$$\frac{E_0}{E_g} = \frac{g_m(G_k+jB_k)}{(G_0+jB_0)(G_k+g_m+jB_k)}. \quad . \quad . \quad 2.17b.$$

From 2.15 and 2.17*b*

$$Y_g = jB_{g_a}\left[\frac{(G_0+jB_0)(G_k+g_m+jB_k)+g_m(G_k+jB_k)}{(G_0+jB_0)(G_k+g_m+jB_k)}\right].$$

Rationalizing

$$Y_g = \frac{jB_{g_a}[(G_0+jB_0)(G_k+g_m+jB_k)+g_m(G_k+jB_k)]}{(G_0^2+B_0^2)((G_k+g_m)^2+B_k^2)}\cdot\frac{[(G_0-jB_0)(G_k+g_m-jB_k)]}{}$$

$$R_g = \frac{1}{G_g} = \frac{(G_0^2+B_0^2)((G_k+g_m)^2+B_k^2)}{g_m B_{g_a}[B_0(G_k^2+B_k^2)+g_m(B_0G_k-B_kG_0)]}$$

$$= \frac{G_0^2+B_0^2}{g_m B_{g_a} B_0}\left[1+\frac{g_m(g_m+2G_k)}{G_k^2+B_k^2}\right] \quad . \quad . \quad . \quad . \quad . \quad 2.18a$$

when $B_0G_k - B_kG_0$ is very small.

Comparing this with 2.14*a* we see that the reflected resistance is increased, i.e., the anode damping is reduced. The result was to be expected because the voltage across Z_k is a negative feedback voltage reducing the gain of the valve.

$$C_g = \frac{B_g}{\omega} = C_{g_a}\left[\frac{[(G_0+g_m)G_0+B_0^2][(G_k+g_m)^2+B_k^2] + g_m^2(B_kB_0 - G_kG_0) - g_m^3G^0}{(G_0^2+B_0^2)[(G_k+g_m)^2+B_k^2]}\right]$$

$$= C_{g_a}\left[\frac{(G_0+g_m)G_0+B_0^2}{G_0^2+B_0^2} - \frac{g_m[g_m^2G_0+g_m(G_kG_0-B_kB_0)}{(G_0^2+B_0^2)[(G_k+g_m)^2+B_k^2]}\right]. \quad 2.18b.$$

This is identical with 2.14*b* when G_k and B_k are infinite. The effect of Z_k is therefore to reduce C_g and this also agrees with the reduced valve amplification due to the negative feedback voltage across Z_k.

The above expressions assume that the screen voltage is decoupled by a capacitance to the cathode, and when it is decoupled to earth the following formulae are valid for R_g and C_g.

$$R_g = \frac{G_0^2+B_0^2}{g_m B_{g_a} B_0}\left[1+\frac{g_k(g_k+2G_k)}{G_k^2+B_k^2}\right] \quad . \quad . \quad . \quad . \quad . \quad 2.18c$$

$$C_g = C_{g_a}\left[\frac{(G_0+g_m)G_0+B_0^2}{G_0^2+B_0^2} - \frac{g_m[g_k^2G_0+g_k(G_kG_0-B_kB_0)}{(G_0^2+B_0^2)[(G_k+g_k)^2+B_k^2]}\right]. \quad 2.18d$$

where g_k = mutual conductance with reference to the cathode voltage

$$= g_m\left[\frac{I_a+I_s}{I_a}\right]$$

and I_a and I_s are the anode and screen currents respectively.

2.8.3. Grid Input Admittance and Grid-Cathode Capacitance Coupling. The grid-cathode capacitance of a valve is often comparatively large, about 3 $\mu\mu$F, but it acts only as a capacitance in parallel with the grid input circuit if there is no impedance in the cathode circuit of the valve. At high frequencies (from about 20 Mc/s) the inductance of the cathode lead can provide sufficient impedance to modify to a very great extent the grid input admittance. Fig. 2.13 shows the circuit (C_{g_a}, C_{g_s} and Z_1 are assumed to be zero, and $I_3 = I_g$) and the equations are given below

$$I_g = (E_g - E_k)jB_{g_k}$$

$$Y_g = \frac{I_g}{E_g} = \left[1 - \frac{E_k}{E_g}\right].jB_{g_k} \quad . \quad . \quad . \quad . \quad . \quad . \quad 2.19$$

$$I_a = \frac{\mu(E_g - E_k) - (E_0+E_k)}{R_a} = g_m(E_g - E_k) - (E_0+E_k)G_a$$

$$= E_0(G_0+jB_0)$$

$$I_a+I_g = E_k(G_k+jB_k)$$

from which $E_0(G_a+G_0+jB_0)+E_k(G_a+g_m) = g_mE_g$

and

$$E_0G_a+E_k[G_a+G_k+g_m+j(B_{g_k}+B_k)] = E_g(g_m+jB_{g_k}).$$

Combining the above equations to eliminate E_0

$$\frac{E_k}{E_g} = \frac{(g_m+jB_{g_k})(G_a+G_0+jB_0) - g_mG_a}{[G_a+G_k+g_m+j(B_{g_k}+B_k)][G_a+G_0+jB_0] - (G_a+g_m)G_a} \quad 2.20a.$$

If G_a can be neglected

$$\frac{E_k}{E_g} = \frac{g_m+jB_{g_k}}{G_k+g_m+j(B_{g_k}+B_k)} \quad . \quad . \quad . \quad 2.20b$$

and we see that the anode impedance (Z_0) has practically no effect on the result. Combining 2.19 and 2.20*b*

$$Y_g = jB_{g_k}\frac{(G_k+jB_k)(G_k+g_m - j(B_{g_k}+B_k))}{(G_k+g_m)^2+(B_{g_k}+B_k)^2}.$$

$$R_g = \frac{1}{G_g} = \frac{(G_k+g_m)^2+(B_{g_k}+B_k)^2}{B_{g_k}(G_kB_{g_k} - g_mB_k)} \quad . \quad . \quad 2.21a$$

$$C_g = \frac{B_g}{\omega} = \frac{C_{g_k}[G_k(G_k+g_m)+B_k(B_{g_k}+B_k)]}{(G_k+g_m)^2+(B_{g_k}+B_k)^2} \quad . \quad 2.21b.$$

These two expressions are similar in form to those for anode grid capacitance coupling.

Differentiating R_g with respect to B_k gives the following condition for minimum R_g.

$$B_k' = -B_{g_k} + (G_k + g_m)\left[\frac{B_{g_k}}{g_m} \pm \sqrt{1 + \left(\frac{B_{g_k}}{g_m}\right)^2}\right] \quad . \quad 2.22a.$$

C_g has a minimum value at

$$B_k'' = -B_{g_k} - \left[\frac{g_m - \sqrt{g_m^2 + B_{g_k}^2}}{B_{g_k}}\right](G_k + g_m) \quad . \quad 2.22b$$

and its maximum value is C_{g_k} for $B_k = \infty$.

This is the reverse of anode-grid coupling, but is to be expected since the voltage developed across a given impedance in the cathode circuit with regard to earth is 180° out-of-phase with that developed across the same impedance in the anode circuit. In the same way it is found that the sign of R_g is reversed, i.e., a positive or capacitive B_k gives a negative R_g. This is clearly shown below in the simplified expressions for R_g and C_g obtained by assuming $B_{g_k} \ll g_m$. Thus 2.22*a* and 22*b* become

$$B_k' = \pm (G_k + g_m)$$
$$B_k'' = -B_{g_k}$$

and

$$R_g(\text{min.}) = \mp \frac{2(G_k + g_m)}{g_m B_{g_k}} \quad . \quad . \quad . \quad 2.23$$

and

$$C_g(\text{min.}) = C_{g_k} \frac{G_k}{G_k + g_m}$$

$$= C_{g_k}\left[1 - \frac{g_m}{G_k + g_m}\right] \quad . \quad 2.24.$$

The general shape of the variations of R_g and C_g for changes of B_k from $-\infty$ to $+\infty$ is shown in Fig. 2.16. R_g is infinite when

$$B_k = +B_{g_k}\frac{G_k}{g_m}.$$

Many practical cases allow simplification of the general expressions 2.21*a* and 21*b* for R_g and C_g. Thus if $G_k \ll B_k$ and g_m.

$$R_g = -\frac{g_m^2 + (B_{g_k} + B_k)^2}{g_m B_{g_k} B_k} \quad . \quad . \quad . \quad 2.21c$$

and

$$C_g = C_{g_k}\frac{B_k(B_{g_k} + B_k)}{g_m^2 + (B_{g_k} + B_k)^2} \quad . \quad . \quad . \quad 2.21d.$$

Often B_{g_k} can be neglected in comparison with B_k and then

$$R_g = -\frac{g_m^2+B_k^2}{g_m B_{g_k} B_k} \quad . \quad . \quad . \quad 2.21e$$

and

$$C_g = C_{g_k}\frac{B_k^2}{g_m^2+B_k^2} \quad . \quad . \quad . \quad 2.21f.$$

In the simplest case when $g_m \ll B_k$

$$R_g = -\frac{B_k}{g_m B_{g_k}} = +\frac{1}{g_m \omega^2 L_k C_{g_k}} = -\frac{C_k}{g_m C_{g_k}}$$

when B_k is respectively inductive and capacitive.

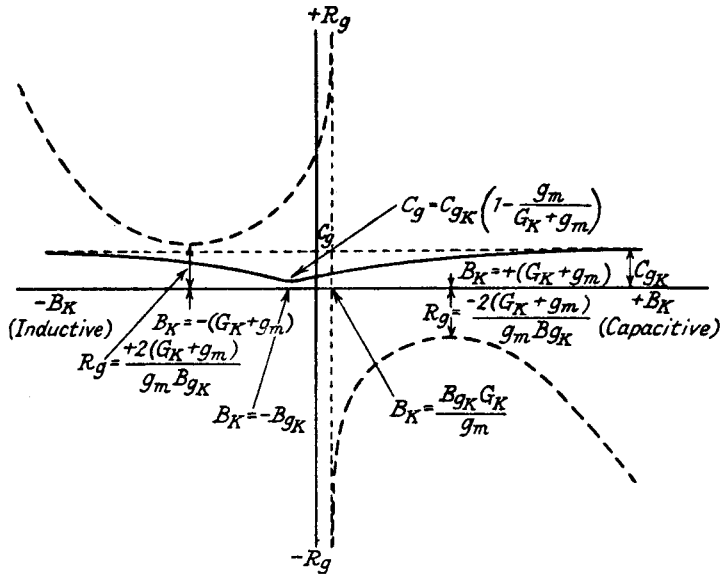

FIG. 2.16.—The Effect on Input Capacitance (C_g) and Input Resistance (R_g) of Varying Cathode Circuit Susceptance (B_k).

(Note that when the screen voltage is not decoupled to cathode, g_m in all the above expressions must be replaced by g_k, the mutual conductance referred to the cathode.)

In all the above expressions we have assumed that the screen is decoupled to cathode, and if it is decoupled to earth g_m must everywhere be replaced by g_k, where $g_k = g_m\left(1+\frac{I_s}{I_a}\right)$. When the effect of cathode lead inductance is considered, g_k must replace g_m. To illustrate the influence of the cathode lead inductance in an R.F. amplifier valve at high frequencies, let us consider a valve operating at 30 Mc/s. and having the following constants

$$g_k = 3 \text{ mA/volt}, \quad C_{g_k} = 3 \ \mu\mu\text{F}, \quad L_k = 0{\cdot}2 \ \mu\text{H}.$$

Using formula 2.21c

$$R_g = \frac{(3 \times 10^{-3})^2 + (0{\cdot}0565 \times 10^{-2} - 2{\cdot}65 \times 10^{-2})^2}{3 \times 10^{-3} \times 5{\cdot}65 \times 10^{-4} \times 2{\cdot}65 \times 10^{-2}}$$

$$= 15{,}200\Omega$$

$C_g \simeq C_{g_k}$ as $g_k \ll B_k$.

This result shows how serious an effect even a small cathode inductance can have when amplification at comparatively high frequencies is desired. Since R_g is inversely proportional to g_k, the amplifying properties of a high g_m valve may be completely nullified unless L_k is made very small. To reduce additions to L_k from external wiring, leads from the cathode decoupling capacitor to earth should be as short as possible and the capacitor itself must be non-inductive. The part contributed to L_k by the valve internal wiring may be reduced by bringing out by separate leads more than one connection from the cathode.

If the frequency is raised to 60 Mc/s, the resistance R_g falls to the very low value of 3,500Ω, i.e., almost in inverse proportion to the square of the frequency ratio change, 4 to 1.

It is possible to increase the input resistance of a valve by inserting a resistance R_k in the cathode lead, but this entails loss of amplification in the valve owing to the degenerative effect of R.F. voltages set up across R_k. Under certain circumstances the increase in input resistance may be greater than the decrease in valve amplification, and a net increase in overall amplification may result. An example in Section 4.10.3 illustrates this.

The formula for input grid resistance when R_k is included is that given in expression 2.21a.

$$R_g = \frac{(G_k + g_k)^2 + (B_k + B_{g_k})^2}{B_{g_k}(G_k B_{g_k} - g_k B_k)}.$$

To have any appreciable effect R_k must be comparable with the reciprocal of mutual conductance, so let us assume that $R_k = 300\Omega$, other components remaining as in the example quoted above. Converting the cathode impedance to an admittance

$$Y_k = \frac{1}{Z_k} = \frac{1}{300 + 37{\cdot}7j} = \frac{300}{300^2 + 37{\cdot}7^2} - \frac{37{\cdot}7j}{300^2 + 37{\cdot}7^2}$$

$$\therefore\ G_k = 3{\cdot}28 \times 10^{-3} \text{ mhos and } B_k = -0{\cdot}412 \times 10^{-3} \text{ mhos.}$$

$$R_g = \frac{(6{\cdot}28 \times 10^{-3})^2 + (1{\cdot}53 \times 10^{-4})^2}{5{\cdot}65 \times 10^{-4}(18{\cdot}5 \times 10^{-7} + 12{\cdot}36 \times 10^{-7})}$$

$$= 22{,}700\Omega.$$

The inclusion of R_k has, however, reduced the equivalent mutual conductance of the valve to (expression 2.5*e*).

$$g_m' = \frac{g_m}{1+g_k Z_k} \simeq \frac{g_m}{1+3 \times 10^{-3} \times 300} = 0{\cdot}526\ g_m.$$

This is a serious reduction and the increase in R_g could not be expected to offset it. However, in this example we have not taken into account the probable value of stray capacitance across R_k, and we shall see in the next example that even a small capacitance value can have a profound influence on the result. Let us consider R_k as paralleled by stray capacitance of 5 $\mu\mu$F. The cathode impedance Z_k now becomes

$$\begin{aligned} Z_k &= \frac{R_k}{1+j\omega C_k R_k} + j\omega L_k \\ &= \frac{R_k}{1+(\omega C_k R_k)^2} + j\left[\omega L_k - \frac{\omega C_k R_k^2}{1+(\omega C_k R_k)^2}\right] \\ &= 278 + j(37{\cdot}7 - 78{\cdot}5) \\ &= 278 - j40{\cdot}8 \end{aligned}$$

and $$\begin{aligned} Y_k &= 3{\cdot}52 \times 10^{-3} + j5{\cdot}17 \times 10^{-4} \\ &= G_k + jB_k. \end{aligned}$$

Hence $$\begin{aligned} R_g &= \frac{(6{\cdot}52 \times 10^{-3})^2 + (1{\cdot}082 \times 10^{-3})^2}{5{\cdot}65 \times 10^{-4}(19{\cdot}9 \times 10^{-7} - 15{\cdot}51 \times 10^{-7})} \\ &= 176{,}000\Omega \left(G_g = \frac{1}{R_g} = 5{\cdot}68\mu \text{ mhos}\right). \end{aligned}$$

This represents a very big improvement in input resistance, though the actual value of R_g is now much more dependent on frequency, and the application of this principle will clearly be more satisfactory in receivers operating at a fixed frequency (e.g., for television reception) or over a restricted tuning range.

One result of including R_k must not be overlooked; R_g is no longer infinite when $g_k = 0$. In the above example it has the comparatively low value of 12,050 ohms, steadily increasing as cathode mutual conductance is increased, to 176,000Ω at $g_k = 3$ mA/volt. This particular property may be used to reduce input resistance variations under A.G.C. conditions, for by a suitable choice of R_k it is possible to make R_g almost independent of changes of g_k. This can be illustrated by taking $R_k = 120\Omega$, all other components being as before:

$Z_k = 118{\cdot}3 + j24{\cdot}32.$

$G_k = 8{\cdot}11 \times 10^{-3}; \quad B_k = -1{\cdot}665 \times 10^{-3}$

$$R_g = \frac{(11{\cdot}11 \times 10^{-3})^2 + (1{\cdot}1 \times 10^{-3})^2}{5{\cdot}65 \times 10^{-4}[5{\cdot}65 \times 10^{-4} \times 8{\cdot}11 \times 10^{-3} + 3 \times 10^{-3} \times 1{\cdot}665 \times 10^{-3}]}$$

$= 23{,}050\Omega$ ($G_g = 43{\cdot}4$ micromhos)

for $g_k = 2$ mA/volt, $R_g = 23{,}100\Omega$, $G_g = 43{\cdot}2\mu$ mhos
" $= 1$ " " $= 23{,}800\Omega$, " $= 42{\cdot}0$ "
" $= 0$ " " $= 25{,}900\Omega$, " $= 38{\cdot}5$ "

The use of a cathode resistance may increase or decrease the variation of input capacitance when g_k is varied. From expression 2.21*b*.

$$C_g = AC_{g_k}$$

where

$$A = \frac{G_k(G_k + g_k) + B_k(B_{g_k} + B_k)}{(G_k + g_k)^2 + (B_{g_k} + B_k)^2}.$$

Least variation of A is obtained when $(B_{g_k} + B_k)$ is large compared with g_k, and under these conditions increase of G_k increases the variation of C_g. In the examples given above for $G_k = 0$, A varies from 1·01 ($g_k = 3$ mA/volt) to 1·02 ($g_k = 0$), whereas when $R_k = 120\Omega$, $C_k = 5$ $\mu\mu$F, it changes from 0·74 ($g_k = 3$ mA/volt) to 1·01 ($g_k = 0$). The inclusion of R_k therefore increases the variation of C_g as g_k is varied. If $(B_{g_k} + B_k)$ is comparable with g_k, increase of G_k generally reduces the capacitance variation, so that as the operating frequency increases (B_{g_k} and B_k decrease) we find that a cathode resistance can be used to advantage for reducing input capacitance variations.

2.8.4. Grid Input Admittance and Combined Anode-Grid and Grid-Cathode Capacitance Coupling. The circuit for this coupling is shown in Fig. 2.13. [$C_{g_a} = 0$ and $Z_1 = 0$] and the equations are

$$I_a = g_m(E_g - E_k) - G_a(E_k + E_0) \quad . \quad . \quad . \quad 2.25.$$
$$I_3 = (E_g - E_k)jB_{g_k} \quad . \quad . \quad . \quad . \quad . \quad 2.26.$$
$$I_2 = (E_g + E_0)jB_{g_a} \quad . \quad . \quad . \quad . \quad . \quad 2.27.$$
$$I_a + I_3 = E_k(G_k + jB_k) \quad . \quad . \quad . \quad . \quad . \quad 2.28.$$
$$I_a - I_2 = E_0(G_0 + jB_0) \quad . \quad . \quad . \quad . \quad . \quad 2.29.$$

$$Y_g = \frac{I_g}{E_g} = \frac{I_2 + I_3}{E_g} = \left(1 - \frac{E_k}{E_g}\right)jB_{g_k} + \left(1 + \frac{E_0}{E_g}\right)jB_{g_a} \quad 2.30.$$

Combining 2.25, 2.26 and 2.28

$$E_k[G_a+G_k+g_m+j(B_k+B_{g_k})]+E_0G_a = E_g[g_m+jB_{g_k}] \quad 2.31a.$$

From 2.25, 2.27 and 2.29

$$E_0[G_0+G_a+j(B_0+B_{g_a})]+E_k[g_m+G_a] = E_g(g_m - jB_{g_a}) \quad 2.31b.$$

Eliminating E_0 from 2.31a and b

$$\frac{E_k}{E_g} = \frac{[g_m+jB_{g_k}][G_a+G_0+j(B_0+B_{g_a})] - [g_m - jB_{g_a}]G_a}{[G_a+G_k+g_m+j(B_{g_k}+B_k)]\,[G_a+G_0+j(B_0+B_{g_a})] - [g_m+G_a]G_a} \quad 2.32.$$

If B_{g_a} can be neglected in comparison with its associated factors, 2.32 reduces to 2.20a, so that the part contributed to Y_g by the grid-cathode capacitance is the same as that given in Section 2.8.3.

Combining 2.31a and b to eliminate E_k

$$\frac{E_0}{E_g} = \frac{[g_m - jB_{g_a}][G_a+G_k+g_m+j(B_{g_k}+B_k)] - [g_m+jB_{g_k}][G_a+g_m]}{[G_a+G_0+j(B_0+B_{g_a})]\,[G_a+G_k+g_m+j(B_{g_k}+B_k)] - [g_m+G_a]G_a} \quad 2.33.$$

Again, if B_{g_k} can be neglected in comparison with the other factors, 2.33 reduces to 2.17a, and its contribution to Y_g is as calculated in the second part of 2.8.2. We may therefore take the values of G_g and C_g calculated in Sections 2.8.2. and 2.8.3, and obtain the combined effects of anode-grid and grid-cathode coupling by adding them.

Thus, from the modified expression 2.18a and from 2.21a (neglecting B_{g_k} in comparison with other factors)

$$G_g = \frac{g_m B_{g_a} B_0 (G_k^2+B_k^2)}{(G_0^2+B_0^2)[(G_k+g_m)^2+B_k^2]} - \frac{g_m B_{g_k} B_k}{(G_k+g_m)^2+B_k^2}$$

$$G_g = \frac{g_m}{[(G_k+g_m)^2+B_k^2]}\left[B_{g_a}B_0.\left[\frac{G_k^2+B_k^2}{G_0^2+B_0^2}\right] - B_{g_k}B_k\right]$$

$$R_g = \frac{[(G_k+g_m)^2+B_k^2][G_0^2+B_0^2]}{g_m[B_{g_a}B_0(G_k^2+B_k^2) - B_{g_k}B_k(G_0^2+B_0^2)]} \quad 2.34a.$$

Neglecting B_{g_a} and the second part in 2.18b, and also B_{g_k} in 2.21b.

$$C_g \simeq C_{g_a}.\left[\frac{(G_0+g_m)G_0+B_0^2}{G_0^2+B_0^2}\right]+C_{g_k}\left[\frac{(G_k+g_m)G_k+B_k^2}{(G_k+g_m)^2+B_k^2}\right] \quad 2.34b.$$

Examining 2.34a, we see that it is possible to make R_g infinite [7] and therefore independent of the mutual conductance of the valve if the denominator is zero, i.e.,

$$B_{g_a}B_0.(G_k^2+B_k^2) = B_{g_k}B_k(G_0^2+B_0^2)$$

or

$$\frac{B_{g_a}}{B_{g_k}} = \frac{\dfrac{B_k}{G_k^2+B_k^2}}{\dfrac{B_0}{G_0^2+B_0^2}} \quad . \quad . \quad . \quad 2.35a.$$

But $\dfrac{B_k}{G_k^2+B_k^2}$* is the reactance of the cathode circuit viewed as a series circuit consisting of R_k and L_k (or C_k, though this is less likely to be realized at ultra high frequencies), and similarly $\dfrac{B_0}{G_0^2+B_0^2}$ is the equivalent series reactance of the anode. Hence 2.35*a* becomes

$$\frac{B_{g_a}}{B_{g_k}} = \frac{C_{g_a}}{C_{g_k}} = \frac{L_k}{L_a} \quad . \quad . \quad . \quad 2.35b.$$

It will be noticed that B_0 and B_k must have the same sign (B_{g_a} and B_{g_k} are always capacitive and positive), i.e., they must both be inductive or capacitive. Thus in satisfying expression 2.35*b* by including an inductance $L_a = L_k\dfrac{C_{g_k}}{C_{g_a}}$ between the anode load impedance and the anode, it is possible to raise the input resistance to a very high value. Just as for the added cathode resistance method, there is loss of valve amplification due to the added anode inductance, which may need to be as much as fifty times that of the stray cathode inductance. Input resistance neutralization is also possible by means of an inductance in the screen electrode of the valve.

Expression 2.34*b* for input capacitance may be rewritten as

$$C_g = C_{g_a}.\left[1+\frac{g_mG_0}{G_0^2+B_0^2}\right]+C_{g_k}\left[1-\frac{(G_k+g_m)g_m}{(G_k+g_m)^2+B_k^2}\right]$$

$$= C_{g_a}+C_{g_k}+g_m\left[\frac{C_{g_a}G_0}{G_0^2+B_0^2}-\frac{C_{g_k}(G_k+g_m)}{(G_k+g_m)^2+B_k^2}\right] \quad . \quad 2.34c.$$

If $g_m \ll G_k$ it is also possible to prevent change of input capacitance when g_m is varied (under A.G.C. conditions); this is achieved by making

$$\frac{C_{g_a}}{C_{g_k}} = \frac{\dfrac{G_k}{G_k^2+B_k^2}}{\dfrac{G_0}{G_0^2+B_0^2}} = \frac{R_k}{R_0} \quad . \quad . \quad . \quad 2.36$$

* See Appendix 1A.

where R_k and R_0 are the equivalent series resistance components of the cathode and anode circuits.

It will similarly be found for capacitance coupling between the grid and other electrodes that each coupling can be treated independently of any other, and the resultant input conductances and capacitances can be added to obtain the combined effect.

2.8.5. Grid Input Admittance and Grid-Screen Capacitance Coupling. The equations for grid-screen capacitance coupling are identical with those for anode-grid coupling if G_a is replaced by G_s, the screen conductance $\frac{\Delta I_s}{\Delta E_s}$ (this is the slope of the I_sE_s curve), g_m by g_s, the screen mutual conductance, $\frac{\Delta I_s}{\Delta E_g}$, G_0, B_0 and B_{g_s} by G_1, B_1, the conductance and susceptance of the external impedance of the screen circuit, and B_{g_s}, the screen-to-grid capacitance.

Thus
$$R_g = \frac{(G_s+G_1)^2+(B_1+B_{g_s})^2}{B_{g_s}[g_sB_1+B_{g_s}(G_s+G_1+g_s)]} \quad . \quad . \quad . \quad 2.37a$$

$$C_g = C_{g_s}\left[\frac{(G_s+G_1+g_s)(G_s+G_1)+B_1(B_1+B_{g_s})}{(G_s+G_1)^2+(B_1+B_{g_s})^2}\right] \quad . \quad 2.37b.$$

In an R.F. amplifier, having undesired inductance in the screen lead, B_{g_s} and (G_s+G_1) can usually be neglected in comparison with B_1, so that

$$R_g \simeq \frac{B_1}{g_sB_{g_s}} \quad . \quad . \quad . \quad . \quad . \quad . \quad . \quad 2.38$$

$$\simeq -\frac{1}{g_s\omega^2L_1C_{g_s}} \text{ when } B_1 \text{ is inductive}$$

$$\simeq \frac{C_1}{g_sC_{g_s}} \text{ when } B_1 \text{ is capacitive.}$$

As for combined anode-grid and grid-cathode capacitance coupling, so for combined grid-screen and grid-cathode coupling it is possible to raise the input resistance to an infinite value; in this instance the condition is that

$$\frac{C_{g_s}}{C_{g_k}} = \frac{L_k}{L_s} \quad . \quad . \quad . \quad . \quad 2.39.$$

Since C_{g_s} and C_{g_k} are comparable in value it means that L_s is approximately equal to L_k.

2.8.6. Grid Input Admittance and Electron Transit Time.[3] Over the medium and long wave ranges the time taken for a given electron to travel from the cathode to the anode is a very small fraction of one period of the input voltage wave. Consequently the A.C. current flow in the grid circuit, due to the passage of electrons through the grid wires from cathode to anode, is almost entirely capacitive and leads the grid voltage producing it by 90°. Hence there is no absorption of power in the grid circuit and grid input resistance is very high. At the high-frequency end of the short wave range (from about 15 Mc/s upwards), the transit time of an electron between cathode and grid becomes an appreciable fraction of the grid voltage cycle. This causes the current action in the grid circuit to be delayed and grid current leads upon the

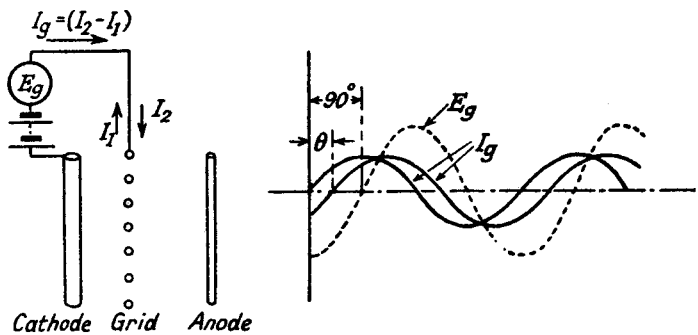

FIG. 2.17.—Grid Current due to Electrons Passing from the Cathode to Anode. (θ is the angle of lag due to the transit time of the electrons.)

grid voltage by an angle less than 90°; i.e., a conductance component is introduced into the grid input admittance. This conductance component increases as the frequency of the grid voltage input increases and in general-purpose valves is quite marked at 20 Mc/s.

Ferris [2] has explained the action as follows. In Fig. 2.17 is shown a cathode, grid and third electrode with electrons passing through the grid mesh. The approach of the negatively charged electrons, to the grid from the cathode, induces a charge on the grid which is equivalent to a current I_1 flowing into the grid circuit. Similarly as the electrons progress from the grid towards the third electrode they induce a charge on the grid mesh, which is equivalent to a current I_2 flowing out of the grid circuit. When there is no A.C. voltage on the grid and sufficient negative bias to prevent the collection of electrons, the grid current due to the approaching

electrons is completely neutralized by that due to the departing electrons. If an A.C. voltage is now applied to the grid, the distribution of the electrons is modulated by this voltage so that as E_g is increasing negatively the density of the electron stream is greatest on the cathode side, and there is a net current into the grid, i.e., I_g is negative. The reverse is true when E_g is decreasing and the density is greatest on the side opposite to the cathode, giving a net current out of the grid. The magnitude of the net current is dependent on the rate at which the electrons are being accelerated or decelerated, and is a maximum when this is maximum (provided there is no delay between the voltage E_g and its effect on the electrons), i.e., when E_g is changing at its greatest rate. This occurs when the A.C. component of E_g is passing through zero. The net current I_g (see Fig. 2.17) therefore leads E_g by 90°, being zero when E_g is maximum or minimum, increasing positively as E_g increases from its minimum value, and reaching a maximum when the A.C. component of E_g is zero. Thus the input admittance has no conductance component. If the time taken for electrons to travel from the cathode region to the grid is an appreciable fraction of the input voltage cycle, the effect of E_g on the electron stream distribution is delayed and the net current leads E_g by less than 90°. The new phase relationship is $(90° - \theta)$, where θ is the angular lag caused by the electron transit time from cathode to grid. The input grid admittance Y_g is

$$Y_g = \frac{I_g}{E_g} = |\, Y_g \,| \, \underline{/90 - \theta} \quad . \quad . \quad . \quad 2.40.$$

and it has a conductance component

$$G_g = |\, Y_g \,| \cos (90 - \theta) = |\, Y_g \,| \sin \theta \quad . \quad . \quad 2.41$$

Ferris suggests that the value of G_g is given by

$$G_g = K g_m f^2 \tau^2$$

where g_m = mutual conductance of the valve

K = a factor dependent on the ratio of the electron transit times in the cathode-grid and grid-third electrode spaces

f = frequency

τ = electron transit time to an arbitrary point in the system.

Electron transit time is reduced by using smaller electrode spacings as in the acorn type valve.

In the above description of electron transit time effects it is assumed that the valve is operating under space-charge current

limitations, i.e., the total current is far below its saturation value. If the current approaches its saturation value (due to reduced cathode temperature, or to a positively biased screen between the signal electrode and cathode as in the heptode frequency changer), current due to the flow of electrons past the grid wires may lag behind the voltage controlling the electrons, i.e., the input susceptance of the signal electrode is equivalent to a negative capacitance. Electron transit time causes the current to lag by more than 90°, so introducing a negative conductance component. This feature is discussed more fully in Section 5.8.3., where an alternative explanation of the positive conductance component under space-charge limited conditions is also given.

There are other forms of electron transit time effects in multi-electrode frequency changers, such as negative resistance [6] coupling between the oscillator and signal grids of a heptode (Section 5.8.3.), and the high negative bias start of grid current on the signal grid of a hexode valve (Section 5.8.2.).

BIBLIOGRAPHY

1. A Note on an Alternative Equivalent Circuit for the Thermionic Valve. N. R. Bligh, *Wireless Engineer*, Sept. 1930, p. 480.
2. The Input Resistance of Vacuum Tubes as Ultra High Frequency Amplifiers. W. R. Ferris, *Proc. I.R.E.*, Jan. 1936, p. 82.
3. The Analysis of the Effects of Space Charge on Grid Impedance. D. O. North, *Proc. I.R.E.*, Jan. 1936, p. 108.
4. The Anode to Accelerating Electrode Space in Thermionic Valves. J. H. O. Harries, *Wireless Engineer*, April 1936, p. 190.
5. Modern Receiving Valves. M. Benjamin, C. W. Cosgrove, and G. W. Warren, *Journal I.E.E.*, April 1937, p. 401.
6. Electron Transit Time Effects in Multigrid Valves. M. J. O. Strutt, *Wireless Engineer*, June 1938, p. 315.
7. Input Conductance Neutralization. R. L. Freeman, *Electronics*, Oct. 1939, p. 22.
8. Input Conductance. F. Preisach and I. Zakariás, *Wireless Engineer*, April 1940, p. 147.
9. *Theory of Thermionic Vacuum Tubes.* E. L. Chaffee. Text-book.
10. *Theory and Application of Electron Tubes.* H. J. Reich. Text-book.

CHAPTER 3

AERIALS AND AERIAL COUPLING CIRCUITS

3.1. Introduction. The difficulties presented by the design of the aerial circuit of a receiver are very largely due to the fact that the type of aerial with which the receiver will operate is unknown. For example, the aerial may be erected indoors, where it will have poor pick-up qualities and large capacitive and resistive components in its terminal impedance. (The terminal impedance is defined as the impedance between aerial and earth looking into the aerial from the receiver.) On the other hand, it may be erected outside, as a horizontal wire with perhaps a long lead-in, or as a short vertical wire at the highest point in the building and connected to the receiver by a screened cable. The characteristics of the two outside aerials are widely different, the former may have a terminal impedance with a low resistive and high reactive component varying appreciably over the tuning frequency range, whilst the latter, owing to the predominating effect of the screened cable, presents to the receiver a mainly resistive impedance less dependent on frequency. If the terminal impedance of the aerial is known over the tuning frequency range, the aerial may be replaced by a generator having an internal impedance equal to the terminal impedance of the aerial and an open circuit voltage equal to the effective pick-up voltage in the aerial. The problem then becomes one of matching aerial terminal and receiver input impedance, if maximum voltage transfer is desired. Before dealing with the aerial connection it is essential to set out briefly the chief features of electromagnetic wave propagation through space.

3.2. Propagation of Electromagnetic Waves. An A.C. current flowing through a wire produces a circularly disposed magnetic field about the wire in a plane perpendicular to the wire. The alternate collapse and reversal of the magnetic field due to the A.C. variation of current induces across the ends of the wire a voltage which is equal to the rate of change of the magnetic flux surrounding the wire and is in opposition to the applied voltage. The latter has, therefore, to overcome not only the resistance of the wire but also this induced component from the magnetic field and the voltage equation is represented by

$$E = RI + \frac{d\Phi}{dt} \quad . \quad . \quad . \quad . \quad 3.1a$$

but $$\frac{d\Phi}{dt} = \frac{d\Phi}{dI} \cdot \frac{dI}{dt} = L \cdot \frac{dI}{dt}$$

where L is the inductance of the wire. Expression 3.1*a* thus becomes

$$E = RI + L\frac{dI}{dt} \quad . \quad . \quad . \quad . \quad 3.1b.$$

If $I = \hat{I} \sin \omega t$ and we assume that there is no time lag between the appearance of the magnetic flux and the current producing it, the expression is again modified to

$$E = R\hat{I} \sin \omega t + L\frac{d\hat{I} \sin \omega t}{dt}$$

$$E = R\hat{I} \sin \omega t + \omega L\hat{I} \cos \omega t \quad . \quad . \quad . \quad 3.1c.$$

The power absorbed in the wire $= \frac{\omega}{2\pi}\int_0^{\frac{2\pi}{\omega}} E\hat{I} \sin \omega t \, dt$

$$= \frac{\omega}{2\pi}\int_0^{\frac{2\pi}{\omega}} [R\hat{I}^2 \sin^2 \omega t + \omega L\hat{I}^2 \cos \omega t \sin \omega t]dt.$$

$$= \frac{\omega}{2\pi}\int_0^{\frac{2\pi}{\omega}} \left[R\hat{I}^2\left[\frac{1 - \cos 2\omega t}{2}\right] + \frac{\omega L\hat{I}^2}{2} . \sin 2\omega t\right]dt$$

$$= \frac{\omega}{2\pi}\left[R\hat{I}^2\left(\frac{t}{2} - \frac{\sin 2\omega t}{4}\right) - \omega L\hat{I}^2 . \frac{\cos 2\omega t}{4}\right]_0^{\frac{2\pi}{\omega}}$$

$$= \frac{RI^2}{2}.$$

Hence there is no loss of energy when the magnetic flux is produced instantaneously, because the energy required to produce it is reabsorbed into the wire when the flux collapses again. This conception of instantaneous flux changes is largely true for low frequencies, such as 50 c.p.s. At much higher frequencies we would expect to find some time lag between the establishment of the magnetic field, especially at some distant point, and the current producing it. The expression for the flux is therefore modified to

$$\Phi = L\hat{I} \sin (\omega t - \theta)$$

and equation 3.1*b* to

$$E = R\hat{I} \sin \omega t + \frac{d}{dt}(L\hat{I} \sin (\omega t - \theta))$$

$$E = R\hat{I} \sin \omega t + \omega L\hat{I} \cos (\omega t - \theta)$$

$$= R\hat{I} \sin \omega t + \omega L\hat{I} (\cos \omega t \cos \theta + \sin \omega t \sin \theta)$$

$$= (R\hat{I} + \omega L\hat{I} \sin \theta) \sin \omega t + \omega L\hat{I} \cos \theta \cos \omega t \quad . \quad 3.1d.$$

The time lag in Φ has increased the resistance term by $\omega L\hat{I} \sin \theta$, and it is this energy component which is radiated into space and part of which is picked up by any suitably disposed conductor. It is known as the radiation resistance of the aerial, and it increases as the frequency increases (this explains the high radiating efficiency of the short wave aerial) and as the magnetic field is more spread out. The latter is achieved by the use of a straight open-ended wire. The magnetic field from a vertical open wire is best imagined in the form of concentric circles in a horizontal plane as shown in Fig. 3.1, and these circles grow in diameter, spreading outwards at the speed of light. The motion of the magnetic field automatically produces an electrostatic field at right angles to it in space but in phase as regards time. The electrostatic field is considered as a series of semicircles (if one end of the aerial is connected to earth)

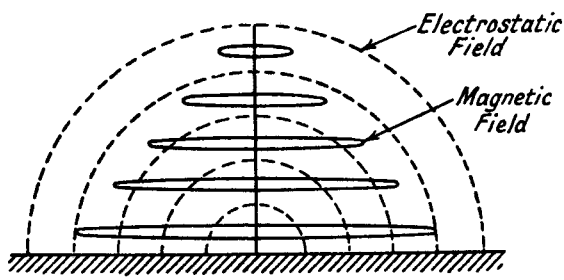

FIG. 3.1.—The Electrostatic and Electromagnetic Fields Developed by an Energised Vertical Aerial.

in a vertical plane (the dotted lines in Fig. 3.1), again moving outwards at the speed of light. The densities of the two fields vary together, i.e., when one is maximum so is the other, and sinusoidally if the current in the vertical wire is sinusoidal. At some distance from the wire (aerial) the magnetic and electrostatic fields are respectively horizontal and vertical, and they may be represented by two vectors at right angles to each other in a plane perpendicular to the direction of travel of the wave front. The horizontal magnetic vector is OM and the vertical electrostatic vector OE in Fig. 3.2*a*. Apart from the simultaneous sinusoidal variation of amplitude with time, the peak value of each vector decreases as the distance from the aerial increases (see $O'M'$ and $O'E'$ in the figure). When the electrostatic vector is vertical as in Fig. 3.2*a*, the wave is said to be vertically polarized, whereas if the electrostatic vector is horizontal (Fig. 3.2*b*), the wave is said to be horizontally polarized. The first condition is realized at some

distance from a vertical aerial if the earth over which the wave passes is a perfect conductor, whilst the second condition occurs by radiation from a horizontal aerial over a perfectly conducting earth. No voltage is induced in a horizontal wire by a vertically polarized wave because a voltage can only be induced in a con-

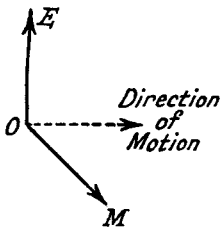

FIG. 3.2*a*.—The Representation of a Vertically Polarized Wave.

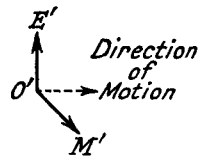

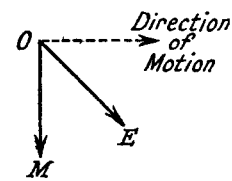

FIG. 3.2*b*.—A Horizontally Polarized Wave.

ductor which is at right angles both to the magnetic field and the direction of motion of the magnetic field.* Similarly a vertical aerial could not be employed for picking up horizontally polarized radiation. Radiation from a vertical aerial does not always result in vertical polarization, for the plane of polarization is tilted forward when the wave passes from a good to a poor conducting earth surface ; the electrostatic vector is tilted forwards and the wave is known as obliquely polarized. Radiation from an aerial at an angle (θ) to the vertical results in an obliquely polarized wave with the two E and M vectors at an angle between the vertical and horizontal polarization positions. Such radiation has vertical and horizontal components of electrostatic and magnetic field, and pick-up is possible with vertical or horizontal aerial. Close to a transmitting aerial, where radiation is mostly by direct ray, the wave is polarized in the plane of the aerial, i.e., is vertically polarized with a vertical aerial, but outside the area of direct ray transmission, where reception is mainly dependent on the indirect ray reflected from the ionosphere (a series of semiconducting layers round the earth), the wave may have any angle of polarization from vertical to horizontal and it may not even be plane polarized, i.e., the vertical and horizontal components of the electric or magnetic field may be out of phase with each other. For example, if the maximum amplitudes of the vertical and horizontal components are equal but have a 90° time phase difference—when the vertical

* This is the basis of Fleming's well-known Right Hand Rule as used in the theory of electrical machines.

is maximum the horizontal is minimum—the wave is said to be circularly polarized. Elliptical polarization is produced by unequal maximum amplitudes with a 90° time phase difference. From the point of view of reception, polarization of the wave front is important in deciding the best orientation of the aerial. For a plane polarized wave, pick-up is maximum when the aerial is parallel to the electrostatic field vector and it is zero at right angles to this. For a circularly or elliptically polarized wave pick-up is possible for any direction of the aerial ; this form of polarization is actually undesirable as it is often produced by conditions (liable to rapid variations) in the earth's upper atmosphere, and distortion of the modulation content of the wave is often severe.

The voltage generated in a receiving aerial may be due to direct or indirect rays from the transmitting aerial, which can be considered as projecting rays in all directions between the horizontal and vertical, though propagation is normally greatest in a horizontal direction or at some shallow angle to this direction. The direct ray travels parallel to the earth's surface, is vertically polarized and is attenuated as it travels away from the transmitting aerial due to the production of eddy currents in the earth. This attenuation increases rapidly as the frequency rises, and for short waves the radius of operation of the direct ray is very limited. An indirect ray is a ray projected at an angle to the earth's surface such that it would ordinarily be lost in space. Owing to the presence of semiconducting layers in the earth's upper atmosphere the ray may be reflected or refracted back to earth. Since the earth itself is a conductor the ray is reflected upwards and is again returned to earth at some distant point. Rays projected at a high angle to the horizontal may make several ricochets between the ionized layers and earth before they reach the receiving aerial.

The semiconducting layers, which return the indirect rays to earth, are caused by ionization of the upper atmosphere from solar radiation. Electrons have been detached from the neutral atoms of the gases in these layers so that besides neutral atoms there are free electrons and positively and negatively charged ions (atoms with a deficiency or excess respectively of electrons in their outer rings).

Subjecting a gas to ultra-violet light or bombardment by a stream of electrons are two methods of producing ionization, and these (due to radiation from the sun) are presumed to be the main causes of the ionized layers surrounding the earth. Pressure plays an important role in ionization and gases at low pressure can

generally be ionized fairly easily and recombine slowly when the cause of ionization is removed. On the other hand, high pressure makes ionization difficult, and recombination is rapid when the ionizing agency disappears. The exact number of ionized layers surrounding the earth is a matter of conjecture, but there are at least two important layers, called the *E* and *F* layers, located at heights of approximately 100 and 250 km. respectively. The lower *E* layer is in a region of comparatively high pressure, so that ionic density is not so high and recombination is rapid when the ionizing agent is removed, i.e., during the night the *E* layer is practically non-existent. The *F* layer, on the other hand, is in a region of lower pressure, ionic density is high and recombination is slow.

The effect produced by these ionized layers depends on their ionic density, the frequency of the transmitted wave, and the angle at which it strikes the layer. The latter may serve as an almost complete reflector, it may allow penetration followed by absorption and/or insufficient refraction for a ray to be returned to earth, or it may allow penetration with little absorption but sufficient refraction to cause the ray to return to earth.

For low frequencies (in the long wave range from approximately 20 to 600 kc/s) the ionosphere acts as an almost perfect reflector and the wave is propagated as if between two concentric reflecting shells formed by the earth and ionized layer. Practically no penetration occurs, and long distance transmission is obtained with steady reception. Direct ray attenuation is not very considerable and this, together with reflected indirect rays, causes the received signal strength to vary in a series of maxima and minima as the distance from transmitter increases. Since these frequencies do not penetrate the ionized layers to any great extent, the indirect ray is less susceptible to variations of ionization, and fading, which is seldom observed, is relatively slow. Owing to the concentric reflector characteristic of the ionosphere and earth, long wave band transmission is almost always vertically polarized at the receiver, though the wave front may be slightly oblique due to earth losses.

Transmission in the medium wave band from about 600 to 1,500 kc/s is characterised by a comparatively limited area of daylight reception; the useful service area, however, is considerably increased at night time. This is due to the fact that the direct ray is fairly rapidly absorbed, due to earth losses, whilst indirect rays penetrate and are absorbed by the lower *E* layer. Indirect rays striking the *E* layer at a shallow angle may be refracted back before penetrating to any depth, and the signal may therefore be

received at some considerable distance from the transmitter. At night when the *E* layer has disappeared, the *F* layer, of much greater ionic density, acts as a reflector for the indirect rays, which are thus returned to earth. High-angle radiation from the transmitting aerial is small, so that the signal from the indirect ray is negligible close to the transmitter ; as the distance from the transmitter increases, lower angle radiation contributes to the indirect ray, the field strength of which increases and remains comparatively high over a considerable distance. The increased power in the low-angle radiation more than compensates for the attenuation in the transmission path. At some point the direct and indirect rays will have comparable field strengths, and in this region night reception is generally unsatisfactory with rapid fading and distortion. This is due to variations in the ionized layer causing variations in the amplitude and phase of the indirect ray so that at one moment it may add and at another subtract from the direct ray. The refractive properties of the ionosphere vary according to frequency, and the phase and amplitude of the modulation sideband frequencies may be independently varied during refraction so that some sidebands may add to those of direct-ray sidebands whilst others subtract. The balance of the modulation frequencies may therefore be completely changed, resulting in severe distortion. The term selective fading is applied when the modulation sideband and carrier frequencies fade independently of each other. Beyond the area of equal direct and indirect ray reception, the signal may vary in strength, and distortion may be produced by the arrival of two indirect rays by different paths, but the resulting signal is generally very much more constant than that obtained in the intermediate area.

Over the short wave band, 2 Mc/s to 25 Mc/s, the direct ray is very rapidly attenuated as it travels over the earth's surface, and long-distance reception is entirely dependent on the indirect ray. The indirect rays penetrate the *E* layer but are refracted by the *F* layer of higher ionic density. If the angle of incidence of the ray is less than a certain critical angle, which falls as the frequency rises, the ray is completely refracted and returned to earth. Above a frequency of about 30 Mc/s, it is almost impossible to obtain a shallow enough critical angle for complete refraction but special freak conditions may produce occasional refraction to earth. Owing to this critical angle effect there are areas, beyond the range of the direct ray, over which no signal can be received except from scattered radiation very erratic in character. The

distance over which reception is almost impossible is known as the skip distance. This distance increases as the frequency increases and varies in length according to the time of day and year. For example, the skip distance at a given frequency is less over a daylight area in summer than over a night area in winter, i.e., refraction is greatest for greatest ionic density. The attenuation of the indirect ray by absorption in the ionized layers is inversely proportional to the square of the frequency (high frequencies in the short wave range are less attenuated than low) and is proportional to the ionic density (high ionic density causes high absorption). Attenuation is therefore greatest over a daylight path in the northern or southern hemisphere during summer.

Short wave reception may suffer from slow or rapid fading due to the arrival of several indirect rays by different paths, some after several ricochets between ionosphere and earth. Selective fading with distortion occurs, and occasionally reception may completely disappear for some hours, especially if the ray path runs close to the earth's magnetic poles. The latter effect normally only occurs during periods of intense solar activity. Another form of distortion sometimes met in short wave reception is that known as the echo effect which may result in either blurred or echoed reception. It is due to the time displacement between the arrival of indirect rays by different routes. The echo effect is often due to the combination of a ray by a more or less direct route and a ray which has made a complete circuit of the earth; a delay of about $\frac{1}{7}$ second occurs between the time of arrival of the same modulation cycle on each wave. It is more commonly noted close to a local short wave station rather than at normal distance operation.

3.3. Types of Aerials.

3.3.1. Introduction. Receiver aerials may conveniently be divided into open and closed (frame) aerials. A wire with an open circuited end is a good example of the former, whilst a frame aerial consisting of closed loops is an example of the latter. The open aerial is the more efficient collector and has maximum pick-up when it is perpendicular to the direction of travel of the wave and parallel to the electric field vector, e.g., with vertically polarized transmission (the electric field component is vertical) in a direction parallel to the earth's surface, an aerial perpendicular to the latter gives maximum pick-up. The voltage generated in the wire is proportional to the height of the wire, but is also considerably affected by the proximity of earthed objects, which tend to distort

the transmitted electric field. A frame aerial is a comparatively inefficient collector and maximum pick-up is obtained when the plane of the frame is that of the electric field and the direction of motion of the wave. The voltage generated is proportional to the area of the loop and the number of turns comprising it.

The open aerial can itself be further subdivided into the vertical, inverted L, the T, and the dipole aerial. The T and inverted L aerials are used principally for long and medium wave reception. They are less satisfactory (especially if they are long) for short wave reception, because the aerial becomes a resonant circuit when its length is approximately one-quarter of the wavelength of the desired transmission. This has a serious mistuning and damping effect on the first tuned circuit unless coupling is very loose. The dipole aerial, consisting of two symmetrical open aerials connected to the receiver by a feeder, is mainly employed for short wave operation, and its particular advantages are that it has directional pick-up and can be conveniently connected to the receiver by a balanced feeder, so reducing interference pick-up. For long and medium wave operation the inverted L aerial having a long horizontal top and vertical lead-in has been extensively used. Its horizontal top [13] enables the voltage picked up in the vertical limb to be used more efficiently, and the equivalent open circuit voltage generated in a given length of vertical is increased by the addition of a horizontal top. It has, however, the disadvantage of collecting vertically and horizontally polarized components of a transmitted wave. These components, having a random phase relationship, tend to cause fading and distortion. The vertical aerial is slowly superseding the inverted L aerial because it responds only to vertically polarized transmission, thus minimizing fading and distortion due to obliquely, circularly or elliptically polarized transmission. It is also simpler to construct and erect.

3.3.2. The Vertical Aerial. As far as reception is concerned there are two important aspects of the aerial connection, its voltage pick-up and its terminal impedance. The vertical aerial may be regarded as a network of series inductive and shunt capacitive arms distributed along its length, with a generator in series with each inductive arm as shown in Fig. 3.3*a*. Owing to the open circuited top the voltages generated in each section cannot be equally effective in driving a current through the receiver impedance. It is clear that the voltage generated at the top has no complete circuit and can therefore contribute nothing to the output, whilst the current sent to the base of the aerial by the second

generator is small because the return path provided by C_0 has a high reactance. The lowest generator is, however, working under most efficient conditions.

This means that standing waves of voltage and current are produced along the aerial as shown in Fig. 3.3*b*. Maximum voltage occurs at the top of the aerial and minimum at the base, whilst

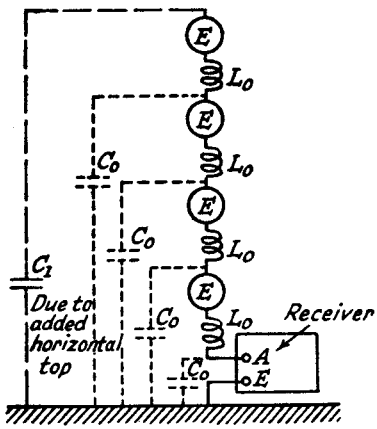

FIG. 3.3*a*.—The Equivalent Generator Circuit for a Vertical Aerial.

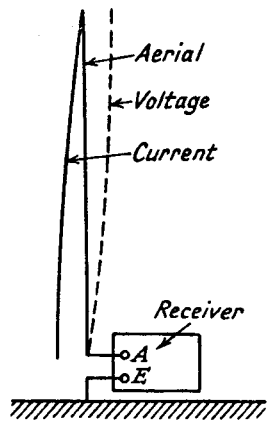

FIG. 3.3*b*.—The Distribution of Current and Voltage in a Vertical Aerial.

current is maximum at the base and minimum (in the special case of the vertical aerial it is zero) at the top. The shape of the standing waves is sinusoidal, but if the height of the aerial is much less than one-quarter of the wavelength the shape may be taken as triangular. Hence the equivalent generated voltage is the average voltage of the whole length of aerial, i.e., is $\frac{Eh}{2}$, where E is the voltage pick-up per unit length and h is the total length of the aerial. It is more usual to associate the $\frac{1}{2}$ with h than with E and $\frac{h}{2}$ is designated as the effective height of the aerial. Thus if we have a vertical aerial 3 metres (9·8 feet) high in a field of 20 μV per metre, the generated voltage is $20 \times \frac{3}{2} = 30$ μV. In this calculation we have assumed that the transmitted electromagnetic field is uniformly distributed from the earth upwards. Changes in earth conductivity and the presence of earthed conductors near the aerial distort and weaken the field. The effective height of low aerials is therefore usually less than $\frac{h}{2}$.

The analysis of aerial terminal impedance has been made by Howe,[1] who treats the aerial as an open-circuited transmission line. Neglecting end effects, he shows that the inductance and capacitance per unit length of a vertical wire close to earth are given by

$$\left.\begin{aligned} L_0 &= 2\left(\log_e \frac{h}{r} - 1\right) \times 10^{-3}\ \mu\text{H per cm.} \\ C_0 &= \frac{1}{1{\cdot}8\left(\log_e \frac{h}{r} - 1\right)}\ \mu\mu\text{F per cm.} \end{aligned}\right\} \quad . \quad 3.2$$

where h = length of aerial in cms.
and r = radius of wire in cms.
The characteristic or surge impedance of the aerial acting as a transmission line is

$$Z_{0} = \sqrt{\frac{R_0+j\omega L_0}{G_0+j\omega C_0}} \quad . \quad . \quad . \quad . \quad 3.3a$$

where R_0 and L_0 are the resistance and inductance per unit length, and G_0 and C_0 are the conductance and capacitance per unit length. Generally $\omega L_0 \gg R_0$ and $\omega C_0 \gg G_0$ so that

$$Z_0 = \sqrt{\frac{L_0}{C_0}} = 60\left(\log_e \frac{h}{r} - 1\right) = 138\left(\log_{10} \frac{h}{r} - 0{\cdot}435\right) . \quad 3.3b$$

(note that C_0 must be in μF per centimetre when L_0 is in μH per centimetre in the above formula).

Applying normal transmission line procedure, we have for the terminal impedance Z_{a0} of the aerial

$$\begin{aligned} Z_{a0} &= Z_0 \coth \sqrt{(R_0+j\omega L_0)(G_0+j\omega C_0)} \times h \\ &= Z_0 \coth (\alpha+j\beta)h \quad . \quad . \quad . \quad . \quad . \quad . \quad 3.4a \end{aligned}$$

where α = attenuation constant of the aerial

$$= \sqrt{\tfrac{1}{2}[\sqrt{(R_0^2+\omega^2L_0^2)\,(G_0^2+\omega^2C_0^2)}+(G_0R_0 - \omega^2L_0C_0)]}$$

and β = phase constant of the aerial

$$= \sqrt{\tfrac{1}{2}[\sqrt{(R_0^2+\omega^2L_0^2)\,(G_0^2+\omega^2C_0^2)} - (G_0R_0 - \omega^2L_0C_0)]}$$

when $\omega L_0 \gg R_0$ and $\omega C_0 \gg G_0$

$$\alpha = \sqrt{\tfrac{1}{2}(G_0R_0)} \quad . \quad . \quad . \quad . \quad 3.5a$$

and

$$\beta = \omega\sqrt{L_0C_0} \quad . \quad . \quad . \quad . \quad 3.5b.$$

Since the voltages and currents induced in the aerial by the transmitted wave themselves produce electrostatic and electromagnetic waves in space, the resistance term in the above formulae must

include the effect of the radiation resistance noted in expression 3.1*c*. In a well-constructed aerial R_0 and G_0 of the aerial and its insulators are negligible in comparison with the term due to radiation. The method of incorporating radiation resistance is illustrated in a later example. If we neglect the resistance and conductance components, the aerial terminal impedance has only a reactive component which is determined by combining 3.4*a* and 3.5*b*.

Thus
$$Z_{a0} = jX_{a0} = Z_0 \coth j\omega\sqrt{L_0C_0} \times h$$
$$= -jZ_0 \cot \omega\sqrt{(L_0C_0)} \times h$$
$$\therefore X_{a0} = -Z_0 \cot \omega h\sqrt{L_0C_0} \quad . \quad . \quad . \quad . \quad 3.6a.$$

If we assume that there is no retardation of the wave along the wire, the velocity of propagation (the speed of light) v cms. per second is related to $\sqrt{L_0C_0}$ as follows

$$v = \frac{1}{\sqrt{L_0C_0}} = \text{wavelength} \times \text{frequency} = \lambda f = \frac{\lambda\omega}{2\pi} \quad . \quad 3.7$$

$$\therefore X_{a0} = -Z_0 \cot \frac{2\pi h}{\lambda} \quad . \quad . \quad . \quad . \quad . \quad . \quad 3.6b.$$

From 3.6*b* we note that X_{a0} is 0, i.e., the aerial is resonant, when

$$\cot \frac{2\pi h}{\lambda} = 0 \text{ and } \frac{2\pi h}{\lambda} = \frac{\pi}{2}, \frac{3\pi}{2}, \text{ etc.},$$

or
$$h = \frac{\lambda}{4}, \frac{3}{4}\lambda, \text{ etc.} = \frac{n\lambda}{4}$$

where n is an odd positive integer.

Similarly X_{a0} is $-\infty$ when $h = 0, \lambda, 2\lambda$, etc., and is $+\infty$ at $h = \frac{\lambda}{2}, \frac{3\lambda}{2}$, etc. Generally we shall not be interested in the variation of X_{a0} for varying heights of aerial but for a fixed height h_0 and varying frequency. Expression 3.6*b* therefore becomes

$$X_{a0} = -Z_0 \cot \frac{2\pi h_0}{\lambda}$$

where h_0 = actual height of the aerial,

but
$$\frac{2\pi h_0}{\lambda} = \frac{2\pi}{\lambda}\cdot\frac{\lambda_0}{4} = \frac{\pi}{2}\,\frac{\lambda_0}{\lambda} = \frac{\pi}{2}\cdot\frac{f}{f_0}$$

where λ_0 = natural wavelength of the aerial
and f_0 = natural frequency of the aerial.

$$\therefore X_{a0} = -Z_0 \cot \frac{\pi}{2}\cdot\frac{f}{f_0} \quad . \quad . \quad . \quad . \quad . \quad 3.6c$$

which is negative, i.e., capacitive, when $\frac{f}{f_0} < 1$.

The equivalent terminal capacitance C_{a0} is

$$C_{a0} = \frac{1}{\omega Z_0 \cot(\pi/2.f/f_0)} = \frac{\tan(\pi/2.f/f_0)}{\omega Z_0} \quad . \quad 3.8a$$

but from 3.3*b* and 3.7

$$Z_0 = \sqrt{\frac{L_0}{C_0}} = \frac{1}{vC_0} = \frac{h_0}{vC_1} = \frac{\frac{1}{4}\lambda_0}{f_0\lambda_0 C_1} = \frac{1}{4f_0C_1} \quad . \quad 3.3c$$

where $C_1 = C_0h_0$ = total electrostatic capacitance of the aerial, measured when f is very much less than f_0.

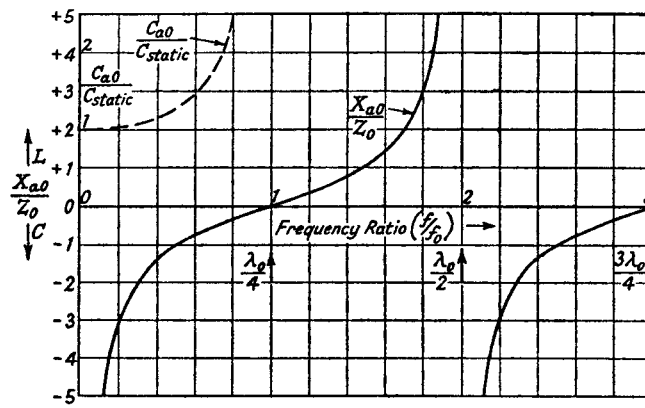

FIG. 3.4*a*.—The Variation of Aerial Terminal Reactance and Capacitance of a Vertical Aerial with Frequency.

Replacing Z_0 in 3.8*a* by 3.3*c*

$$C_{a0} = \frac{4f_0C_1 \tan(\pi/2.f/f_0)}{\omega} = \frac{4f_0C_1}{2\pi f}\tan\left(\frac{\pi}{2}.\frac{f}{f_0}\right)$$

$$= C_1\frac{2}{\pi}.\frac{f_0}{f}\tan\left(\frac{\pi}{2}.\frac{f}{f_0}\right) \quad . \quad . \quad . \quad . \quad . \quad 3.8b$$

when $\frac{f}{f_0}$ is small, $\tan\left(\frac{\pi}{2}.\frac{f}{f_0}\right) \simeq \sin\left(\frac{\pi}{2}.\frac{f}{f_0}\right) \simeq \left(\frac{\pi}{2}.\frac{f}{f_0}\right)$ and

$C_{a0} = C_1$, the electrostatic capacitance of the aerial.

The variation of the ratio of $\frac{C_{a0}}{C_1}$ against $\frac{f}{f_0}$ is shown by the dotted curve in Fig. 3.4*a* over the range $\frac{f}{f_0} = 0$ to 0·8, and the variation of $\frac{X_{a0}}{Z_0}$ (calculated from 3.6*c*) is the full line curve in the

same figure over the range $\frac{f}{f_0} = 0$ to 3. We note that for aerials short compared with the wavelength of the received signal $\left(\frac{f}{f_0} < 0{\cdot}5, \text{ i.e., } h_0 < \frac{\lambda_0}{8}\right)$ the terminal capacitance of the aerial is practically its electrostatic capacitance. Thus over the long and medium wave ranges most aerials can be replaced by a generator having an internal impedance consisting of a resistance (as yet unspecified) in series with the electrostatic capacitance of the aerial.

For $\frac{f}{f_0} > 1$ and < 2, $\cot \frac{\pi}{2} \cdot \frac{f}{f_0}$ is negative so that X_{a0} is positive and therefore inductive. It can be shown by a method similar to that used for calculating C_{a0} that.

$$L_{a0} = -L_1 \frac{\pi}{2} \cdot \frac{f}{f_0} \cot\left(\frac{\pi}{2} \cdot \frac{f}{f_0}\right)$$

$$= L_1 \text{ when } \frac{f}{f_0} \text{ approaches 2.}$$

where $L_1 = L_0 h$ = total inductance of the aerial.

From $\frac{f}{f_0} = 2$ to 3, the aerial is again capacitive and the curve of $\frac{C_{a0}}{C_1}$ is a repetition of that from $\frac{f}{f_0} = 0$ to 1. It is inductive from $\frac{f}{f_0} = 3$ to 4 and the process is repeated as f is increased. The variation of X_{a0} with frequency is that of a cotangent curve and it is plotted in Fig. 3.4*a* as a ratio of $\frac{X_{a0}}{Z_0}$ against $\frac{f}{f_0}$. Reactance is infinite at $\frac{f}{f_0} = 0$ and 2, corresponding to $h_0 = 0$ and $\frac{\lambda}{2}$, between $\frac{f}{f_0} = 0$ and 1 $\left(h_0 = 0 \text{ and } h_0 = \frac{\lambda}{4}\right)$ it is capacitive, being zero at $\frac{f}{f_0} = 1\left(h_0 = \frac{\lambda}{4}\right)$, whilst from $\frac{f}{f_0} = 1$ to 2 $\left(h_0 = \frac{\lambda}{4} \text{ to } \frac{\lambda}{2}\right)$ it is inductive. Above $\frac{f}{f_0} = 2$ it repeats itself periodically between $\frac{f}{f_0} = 2n$ and $2n+2$. If we neglect end effects the primary fundamental frequency, at which an aerial acts as a series resonant circuit

($X_{a0} = 0$), occurs when its height h_0 is equal to a quarter of the wavelength of the exciting frequency, and under these conditions standing quarter waves of E and I are produced on the aerial with maximum current at the base and maximum voltage at the top as shown in Fig. 3.3*b*. In the practical case the electric and magnetic fields do not cease abruptly at the end of the aerial but are projected for a short distance beyond, so that the equivalent electrical height as far as the resonant condition is concerned is rather greater than the actual. A more correct formula for the resonant wavelength and frequency is

$$\lambda_0 = 4{\cdot}2h_0\,;\quad f_0 = \frac{v}{4{\cdot}2h_0} \qquad . \qquad . \qquad . \qquad 3.9$$

and in determining the resonant frequency of any aerial the above formula should be used in preference to $f_0 = \frac{v}{4h_0}$.

So far in our discussion we have neglected the resistance component in the aerial terminal impedance. It is not easy to assess because of its dependence on a number of factors, the resistance and conductance characteristic of the aerial, the radiation resistance, and the earth loss due to circulating currents in an imperfectly conducting earth at the base of the aerial. The former, except in badly-erected and indoor aerials running close to earthed conductors, or semiconductors are not often very large and may be neglected, the earth losses are difficult to estimate and depend on site conditions, but the radiation resistance (assuming a perfect earth) has been calculated.

Thus a quarter-wave resonant aerial above a perfectly conducting earth has a terminal impedance which is non-reactive and equal to the radiation resistance, i.e., $36{\cdot}6\Omega$. The radiation resistance [21] for a given height of aerial varies approximately as the square of the signal frequency up to $h = 0{\cdot}4\lambda$, reaches a maximum of 108Ω at $h = 0{\cdot}45\lambda$ and then falls to about 46Ω at $h = 0{\cdot}675\lambda$, passing through 100Ω at $h = 0{\cdot}5\lambda$. To simplify the analysis let us assume that the radiation resistance is 40Ω at $h_0 = \frac{\lambda_0}{4{\cdot}2}$ (where h_0 is the physical height) and that radiation resistance is directly proportional to frequency up to $h_0 = \frac{\lambda}{2}$. The errors introduced by this simplification are not excessive. We can now illustrate the method of calculating terminal impedance in respect of an aerial of No. 12 S.W.G. copper wire 10 metres (30 ft. approx.) height.

From 3.9 the fundamental wavelength $= 4{\cdot}2 \times 10 = 42$ metres.
,, frequency $= 7{\cdot}14$ Mc/s.
Radius of No. 12 S.W.G. wire $= 0{\cdot}132$ cms.

From 3.2 the capacitance per unit length is

$$C_0 = \frac{1}{1{\cdot}8\left[\log_e \frac{1000}{0{\cdot}132} - 1\right]} \mu\mu\text{F/cm.}$$

$$= 0{\cdot}0705 \ \mu\mu\text{F/cm.}$$

The electrostatic capacitance is $C_0 l = 70{\cdot}5$ $\mu\mu$F.
From 3.3*b*

$$Z_0 = 138 \ (3{\cdot}445) = 475\Omega.$$

Combining expressions 3.4*a*, 3.5*b* and 3.9

$$Z_{a0} = Z_0 \coth \left(\alpha + j\frac{\pi}{2}\right)\frac{f}{f_0} \quad . \quad . \quad . \quad 3.4b.$$

For the quarter wave resonant condition $\frac{f}{f_0} = 1$ and Z_{a0} = radiation resistance $= 40\Omega$.

$$\therefore \ 40 = 475 \coth \left(\alpha + j\frac{\pi}{2}\right)$$

$$= 475 \tanh \alpha$$

or $$\alpha = 0{\cdot}0843.$$

$$\therefore \ Z_{a0} = 475 \coth \left(0{\cdot}0843 + j\frac{\pi}{2}\right)\frac{f}{7{\cdot}14}.$$

Note that

$$\coth(\alpha + j\beta) = \frac{\cosh(\alpha+j\beta)}{\sinh(\alpha+j\beta)} = \frac{\cosh(\alpha+j\beta)\sinh(\alpha-j\beta)}{\sinh(\alpha+j\beta)\sinh(\alpha-j\beta)}$$

$$= \frac{\sinh 2\alpha - \sinh j2\beta}{\cosh 2\alpha - \cosh j2\beta} = \frac{\sinh 2\alpha - j\sin 2\beta.}{\cosh 2\alpha - \cos 2\beta}$$

$$\therefore \ Z_{a0} = R_{a0} + jX_{a0} = Z_0\left[\frac{\sinh 2\alpha}{\cosh 2\alpha - \cos 2\beta} - \frac{j\sin 2\beta}{\cosh 2\alpha - \cos 2\beta}\right] \quad 3.10.$$

A graph showing the variation of R_{a0} and X_{a0} against frequency ratio from 0 to 3 is shown in Fig. 3.4*b*. The curve from 2 to 3 is calculated on the assumption that the radiation resistance falls back again to 40Ω at $\frac{3}{4}\lambda$, so that the value of R_{a0} is slightly lower than would occur in practice. X_{a0} is not appreciably altered by the radiation resistance except in the region of $\frac{f}{f_0} = 2$, at which value it is zero instead of infinite as for Fig. 3.4*a*, and it has a finite

maximum above and below $\frac{f}{f_0} = 2$. A vertical aerial greater than $\frac{\lambda}{4}$ long is seldom used for reception so that the curve from $\frac{f}{f_0} = 0$ to 1 is the important part.

We see that this particular aerial would function satisfactorily over the long and medium wave ranges because the highest received frequency is 1,500 kc/s giving $\frac{f}{f_0} = 0{\cdot}21$, and up to this frequency there is little difference between the terminal and static capacitance. It would not be satisfactory on the short wave range as

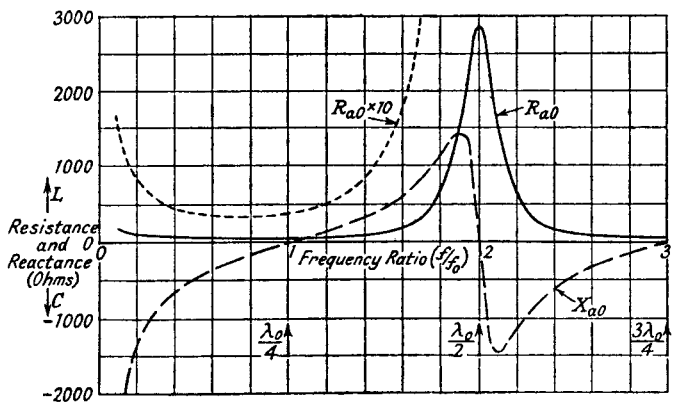

FIG. 3.4*b*.—The Resistance and Reactance Components of the Terminal Impedance of a Vertical Aerial having a Quarter Wavelength Radiation Resistance of 40 Ohms.

it passes through resonance, and would therefore affect considerably the performance of the first tuned circuit, causing large changes of the resistance and reactance components reflected from the aerial into this circuit. The need for keeping aerial resonance outside the desired frequency range is made clear in Section 3.4.

3.3.3. The Inverted L Aerial. The inverted L aerial is formed by adding a horizontal top to a vertical aerial. The addition of the horizontal top affects both generated voltage and terminal impedance : it is equivalent to adding a capacitance from the top of the aerial to earth, see C_1 in Fig. 3.3*a*. With vertically polarized transmission no voltage is induced in the horizontal top, but its capacitance to earth makes the voltage induced in each vertical section more effective, e.g., the top section generator is now operative because the horizontal top capacitance completes its return

path to earth. Similarly, succeeding generators operate more efficiently and the average effective voltage becomes greater than $\frac{Eh}{2}$, i.e., the effective height of the aerial is increased. An inverted L aerial having a ratio of horizontal to vertical length of unity has an effective height of the order of $0{\cdot}6h$.

The terminal impedance of an L aerial is calculated by considering vertical and horizontal sections separately. The horizontal section is treated as an open circuited transmission line parallel to earth, whilst the vertical part is treated as a line terminated by the terminal impedance of the horizontal part. The characteristic impedance Z_{0h} of this part is

$$Z_{0h} = 60\left(\log_e \frac{2h}{r} - 1\right) = 60\left(\log_e \frac{h}{r} + \log_e 2 - 1\right) \quad . \quad 3.11$$

and if $h \gg r$ we see that Z_{0h} is very nearly equal to Z_{0v} (expression 3.3*b*) when the radii of the horizontal and vertical sections are equal. The terminal or input impedance of the horizontal section is

$$Z_h = Z_{0h} \coth (\alpha_h + j\beta_h)l = Z_{0h} \coth \gamma_h l$$

where l = length of horizontal section

α_h and β_h = attenuation and phase constant of the section

and $\gamma_h = \alpha_h + j\beta_h$.

The vertical section is terminated by Z_h and applying the above nomenclature with the suffix "v" replacing "h" we have, by normal transmission line theory, for the terminal impedance of the vertical part

$$Z_{a0} = Z_{0v}\left[\frac{Z_h \cosh \gamma_v h + Z_{0v} \sinh \gamma_v h}{Z_h \sinh \gamma_v h + Z_{0v} \cosh \gamma_v h}\right] \quad . \quad 3.12a$$

where h = height of vertical section.

If $\alpha_v \ll \beta_v$ and $\alpha_h \ll \beta_h$.

$$Z_h = -jZ_{0h} \cot \beta_h l.$$

and $$jX_{a0} = Z_{0v}\left[\frac{-jZ_{0h} \cot \beta_h l. \cos \beta_v h + jZ_{0v} \sin \beta_v h}{Z_{0h} \cot \beta_h l. \sin \beta_v h + Z_{0v} \cos \beta_v h}\right] \quad 3.12b.$$

For aerial resonance $X_{a0} = 0$

i.e., $$\tan \beta_h l. \tan \beta_v h = \frac{Z_{0h}}{Z_{0v}} \quad . \quad . \quad 3.13.$$

If we assume $Z_{0h} = Z_{0v}$, we have that $L_{0h} = L_{0v}$, $C_{0h} = C_{0v}$ and $\beta_h = \beta_v$.

Hence expression 3.13 becomes

$$\tan \beta_v l. \tan \beta_v h = 1$$

$$\sin \beta_v l. \sin \beta_v h = \cos \beta_v l. \cos \beta_v h.$$

or $$\cos \beta_v (h+l) = 0$$

giving $$(h+l)\beta_v = \frac{\pi}{2}$$

so that from 3.5*b* and 3.7. $$(h+l) = \frac{\lambda_0}{4} \quad . \quad . \quad . \quad . \quad 3.14.$$

Similarly, expression 3.12*a* reduces to

$$X_{a0} = -Z_{0v}\left[\frac{\cot \beta_v l. \cos \beta_v h - \sin \beta_v h.}{\cot \beta_v l. \sin \beta_v h + \cos \beta_v h}\right].$$

$$= -Z_{0v}\left[\frac{\cos \beta_v l. \cos \beta_v h - \sin \beta_v h. \sin \beta_v l.}{\cos \beta_v l. \sin \beta_v h + \cos \beta_v h. \sin \beta_v l.}\right].$$

$$= -Z_{0v} \cot \beta_v (h+l) \quad . \quad . \quad . \quad . \quad . \quad 3.15.$$

We therefore see that an inverted L aerial erected well clear of earth has practically the same terminal impedance characteristics as a vertical aerial of height equal to the overall length of the L aerial.

3.3.4. The T Aerial. There is little essential difference in operation between the T and inverted L aerial. The split horizontal section acts as a capacitance to earth, increasing the effective height of the aerial. Terminal impedance is calculated in the same manner as for the inverted L aerial, but we must note that the impedance at the top of the vertical part consists of the impedances of the two horizontal sections in parallel, i.e., $Z_h = \frac{Z_{h1}.Z_{h2}}{Z_{h1}+Z_{h2}}$. Generally $Z_{h1} = Z_{h2}$, and if the T top has the same wire diameter as the vertical section and is not very close to earth

$$Z_h = \frac{Z_{h1}}{2} \simeq \frac{Z_{0v}}{2} \coth (\alpha_v + j\beta_v)\frac{l}{2}$$

where l is the total horizontal length of the T top.

3.3.5. The Dipole Aerial. The dipole (sometimes called the doublet) aerial consists of two equal lengths of open-ended wires connected at their near ends to a feeder balanced to earth. The two wires are in the same plane and at 180° to each other. Such an aerial is very suitable for short wave reception and it has the advantage that if the aerial itself is balanced to earth, i.e., erected horizontally, local interference effects tend to cancel out. Owing to the use of the reflected ray for short wave transmission, the wave

arriving at the aerial has an appreciable horizontally polarized component and this is picked up by the horizontally disposed dipole. The horizontal disposition gives the aerial a directive figure-of-eight diagram in the horizontal plane with maximum pick-up in the two directions perpendicular to the dipole. A vertically erected dipole has no directional effect in the horizontal plane and is unbalanced to earth so that local interference voltages are not cancelled to the same degree.

The terminal impedance of a dipole aerial can be calculated by the method employed for the vertical aerial. Let us assume that we have a horizontal dipole aerial, split at the centre to form two wires, each of 12 S.W.G. copper 7 metres long (Fig. 3.5 inset).

The fundamental wavelength is $4{\cdot}2 \times 7 = 29{\cdot}4$ metres

" " frequency is 10·2 Mc/s

which is in the centre of the short wave band (6 to 15 Mc/s).

The capacitance per unit length between each wire of the dipole when the latter is at least $\frac{\lambda}{2}$ (14 metres) from earth (the image effect can then be neglected) is [1]

$$C = \frac{1}{3{\cdot}6\left(\log_e \frac{l}{r} - 1\right)} \ \mu\mu\text{F/cm.}$$

where l = length of each wire

r = radius of wire = 0·132 cms.

$$C = \frac{1}{3{\cdot}6\left(\log_e \frac{700}{0{\cdot}132} - 1\right)} = 0{\cdot}0366 \ \mu\mu\text{F/cm.}$$

$$Z_0 = 120\left(\log_e \frac{700}{0{\cdot}132} - 1\right) = 910\Omega.$$

The radiation resistance of a $\frac{\lambda}{2}$ dipole split at the centre is twice that of the vertical $\frac{\lambda}{4}$ aerial, i.e., $72{\cdot}2\Omega$, and we will assume that the terminal impedance under these conditions is 80Ω.

Thus

$$80 = Z_0 \coth\left(\alpha + j\frac{\pi}{2}\right)$$

$$\tanh \alpha = \frac{80}{910} = 0{\cdot}0878$$

$$\alpha = 0{\cdot}0880$$

from 3.4*b*
$$Z_{a0} = Z_0 \coth\left(\alpha + j\frac{\pi}{2}\right)\frac{f}{10{\cdot}2}$$
$$= 910 \coth\left(0{\cdot}0880 + j\frac{\pi}{2}\right)\frac{f}{10{\cdot}2}.$$

The values of R_{a0} and X_{a0} are plotted against $\frac{f}{f_0} = 0$ to 3 in Fig. 3.5

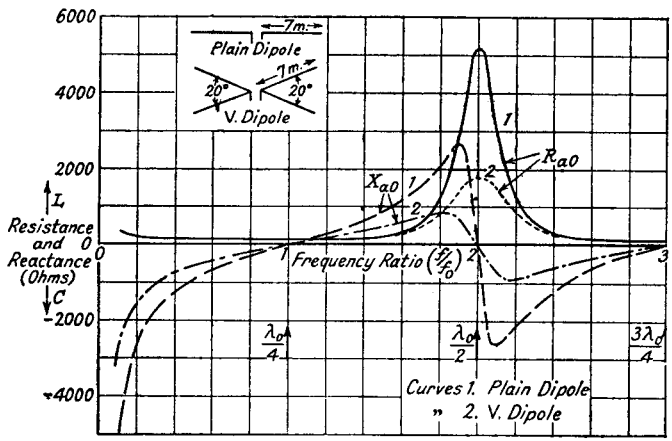

FIG. 3.5.—The Variation of Terminal Resistance and Reactance of a Plain and V Dipole having a Quarter Wavelength Radiation Resistance of 80 Ohms.
(The wavelength scale is referred to the length of one-half of the dipole.)

(curves 1). The variation of terminal impedance over the normal short wave range from 6 to 15 Mc/s (approximately from $\frac{f}{f_0} = 0{\cdot}6$ to 1·5) is considerable, though its effect on the receiver is generally reduced by the feeder connection, which is usually employed. Mismatching between feeder and aerial occurs and there is loss of efficiency in the power transfer at the junction. The loss of power, or transition loss as it is called, is discussed more fully in Section 3.5.3. The variation in terminal impedance can be reduced if the characteristic impedance [8] of the aerial is reduced. A decrease in Z_0 has no effect at $\frac{f}{f_0} = 1$, since the terminal impedance is determined by radiation resistance alone, but it has a large effect at $\frac{f}{f_0} = 2$. Then each half acts as a $\frac{\lambda}{2}$ aerial and

$$Z_{a0}\left(\frac{\lambda}{2}\right) = Z_0 \coth 2\alpha \simeq \frac{Z_0}{2\alpha} \text{ when } \alpha \text{ is small}$$

i.e.,
$$Z_{a0}\left(\frac{\lambda}{2}\right) = \frac{{Z_0}^2}{2R_r\left(\frac{\lambda}{4}\right)}.$$

Hence a small reduction of characteristic impedance reduces considerably Z_{a0}, e.g., halving Z_0 reduces Z_{a0} to 25% of its original value. This reduction of Z_0 can be achieved by making each half of the dipole into a V aerial [5] as shown by the inset in Fig. 3.5.

The capacitance $\mu\mu$F per cm. of this type of aerial is given by [2]

$$C = \frac{1}{1{\cdot}8\left[\log_e \frac{l}{r} - 1 + \log_e\left(1+\sqrt{1+(\operatorname{cosec}\theta+\cot\theta)^2}\right) - \log_e\left(1+\sqrt{1+[\operatorname{cosec}(180-\theta)+\cot(180-\theta)]^2}\right)\right]}$$

where θ = angle between the V.

If this angle is 20° and all other details the same as for the single dipole, the V dipole has a capacitance per centimetre of

$$C_0 = 0{\cdot}063 \ \mu\mu\text{F}.$$

and

$$Z_0 = 526\Omega.$$

Hence

$$\tanh\alpha = \frac{80}{526} = 0{\cdot}152$$

and

$$Z_{a0} = 526 \coth\left(0{\cdot}153 + j\frac{\pi}{2}\right)\frac{f}{10{\cdot}2}.$$

R_{a0} and X_{a0} are plotted as curves 2 in Fig. 3.5, and the reduction in terminal impedance variation is quite marked.

Since the curves in Fig. 3.5 are calculated on the assumption that R_r is directly proportional to frequency up to $\frac{f}{f_0} = 2$, the values of R_{a0} are not strictly correct, though they form a useful basis for the design of the aerial-to-receiver connection. The tendency is for the curves of R_{a0} to be high for values of $\frac{f}{f_0} < 1$ and low for values of $\frac{f}{f_0}$ from 1 to 1·8. A more accurate method of calculating aerial terminal impedance for many types of aerial is to be found in Bibliography 18.

The balanced horizontal dipole is an inefficient collector of signals in the long and medium wave ranges, for which transmission is mainly vertically polarized. If it is to be used for "all wave" reception, provision must be made to change its method of operation at lower frequencies. A method [5] of realizing this is shown in Fig. 3.6. The dipole is connected via a parallel wire feeder, crossed over at intervals, to a transformer at the receiver. The centre tap of the transformer primary is connected to earth by a series *LCR* circuit. One end of the secondary of the transformer is connected

to the aerial terminal of the receiver and the other to the capacitance C of the primary centre tap earth circuit. Over the short wave range the aerial acts as a dipole, the voltage being developed across the primary. The filtering action of the LCR circuit prevents voltages at short wave frequencies (desired or local interference) from appearing across C. An electrostatic screen is included between the primary and secondary to prevent interference currents passing to the unbalanced secondary. Local interference currents developed in each side of the aerial and feeder system cancel in the transformer primary and flow to earth through the LCR circuit. They tend to produce a voltage across C, but it is reduced to small proportions by the addition of the inductance L. As the desired frequency is decreased the reactance of C increases and the system begins to function as a T aerial, the two halves of aerial and feeder being considered as in parallel and the pick-up voltage appearing across C. With this method of operation there is practically no local interference protection at the lower frequencies, and some improvement may be achieved at the expense of signal strength by using a twin feeder enclosed in an earthed shield.

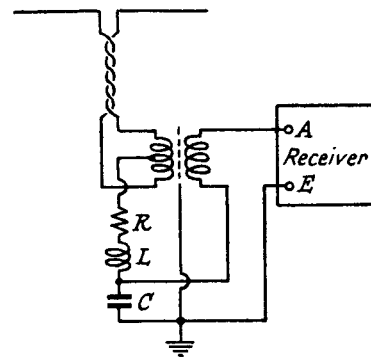

FIG. 3.6.—A Balanced Horizontal Dipole for All Wave Reception.

More complicated methods of making the dipole an all-wave collector have been employed, but the principle involved is the same, viz., the aerial acts as a dipole for short waves and then changes to a T or L aerial for long and medium waves. When a dipole aerial is intended for operation over a very limited range of frequencies, e.g., for television reception, one arm of the dipole may be connected through a parallel resonant wave trap circuit [19] (tuned to the centre of the short or ultra short wave band accepted by the dipole) to a long single wire, which acts as the aerial for the longer short wave ranges and the long and medium wave bands.

If increased signal is desired from a given direction, a reflector, often a similar dipole with the two halves either short circuited or connected together with an inductance or capacitance, is used. The inductance lowers and the capacitance raises the $\frac{\lambda}{2}$ resonant

frequency. The reflector is placed parallel to the first dipole at a distance of $\frac{\lambda}{8}$ to $\frac{\lambda}{4}$ behind it, looking from the direction of the desired transmission source. The effect of the reflector is also to suppress reception from sources behind the main aerial, the directional diagram being heart shaped with maximum pick up at right angles to, and in front of the first dipole. If the reflector is of different physical or electrical length (this is effected by inductance or capacitance at its centre) compared with the main aerial, a more constant response [20] can often be realized over a given frequency range.

3.3.6. The Frame Aerial. The frame or closed loop aerial is an inefficient collector as compared with the normal open aerial, and its chief advantage is its directional property. It operates for vertically polarized transmission only when there is a phase difference between the voltages induced in the two vertical sides. These voltages are equal and cancel each other when the plane of the loop is parallel to the electrostatic component of the transmitted field and perpendicular to its direction of travel. When the frame is not perpendicular to the motion of the field, there is a phase difference between the voltages induced in the two limbs, that induced in the limb nearest the source of the wave leading on the voltage in the other limb. This means that at any given instant the voltages are unequal and there is a net voltage to drive current round the loop. The phase angle between the two voltages is the distance in radians between the projections of the two vertical limbs on to a plane parallel to the motion of the wave. If λ is the wavelength of the desired signal, b the breadth of the frame and α the angle between the plane of the frame and the motion of the wave (Fig. 3.7*a*), the phase angle is $\frac{2\pi}{\lambda} b \cos \alpha$. The phase angle is clearly a maximum when α is 0, i.e., when the frame is parallel to the motion of the wave, and in this position the pick-up is maximum. The maximum effective voltage induced in the frame is $nEh \sin \frac{2\pi b}{\lambda}$ where n is the number of turns in the frame, E is the field strength of the signal at the frame and h is the length of a vertical side. When $\frac{2\pi b}{\lambda}$ is small the induced voltage is

$$\frac{nEh2\pi b}{\lambda} = \frac{2\pi nE}{\lambda} \times \text{area of frame} \quad . \quad . \quad 3.16.$$

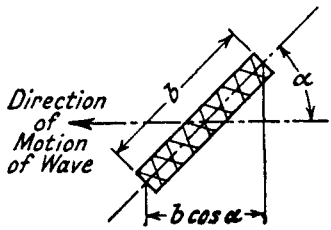

FIG. 3.7.*a*—Plan View of a Frame Aerial.

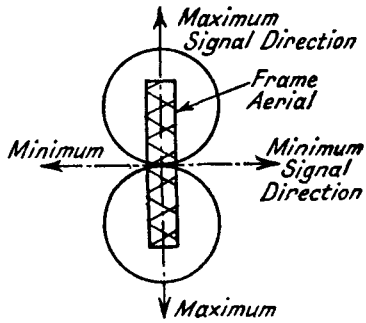

FIG. 3.7*b*.—The Directional Diagram of a Frame Aerial.

The directional diagram of the frame is a figure-of-eight with minimum from directions at right angles on either side of the frame and maximum from the two end-on positions (Fig. 3.7*b*).

3.4. The Coupling between the Aerial and Receiver.[3, 17]

3.4.1. Introduction. An aerial may be coupled to the first tuned circuit of a receiver by inductance and capacitance, separately or combined. Owing to this coupling, a resistance and reactance component is reflected from the aerial into the tuned circuit; this reduces its selectivity and also requires the tuning capacitor setting to be changed if resonance is to be maintained, a disadvantage when the circuit is ganged with succeeding tuned circuits. The object of the coupling is therefore to obtain maximum voltage transfer with minimum effect on the tuned circuit. For any given aerial and tuned circuit conditions, there is always an optimum coupling giving greatest voltage transfer, and if coupling is increased beyond this point voltage transfer falls and the reflected impedance effect from the aerial increases. Hence it is most undesirable to exceed optimum coupling, and indeed it is preferable to use couplings much less than critical since voltage transfer falls at a much slower rate than the reflected aerial impedance. For couplings less than optimum, maximum voltage transfer is realised by adjusting the tuning capacitance for resonance with the tuning coil and added reactance from the aerial.

In the analysis, which follows, the aerial circuit is assumed to consist of a generator of voltage E_1 with an internal impedance equal to the terminal impedance Z_{a0} of the aerial. This impedance is considered as a resistance R_{a0} in series with a reactance jX_{a0}; for most normal aerials the reactance is capacitive on the long and medium wave bands. The fundamental wavelength of an aerial is

given by 4·2 × height, and at this frequency it is resonant and its terminal impedance is resistive only. At frequencies greater than this the reactance becomes inductive. For resonance in the medium wave band (maximum frequency = 1,500 kc/s) the height or length of the aerial would have to exceed 47 metres, a condition hardly likely to be realized in practice. On the short wave range the resonant point may be reached and passed.

The first form of coupling to be considered is by mutual inductance, as it is possible to develop from this generalized formulae applicable to all types of coupling.

3.4.2. Mutual Inductance Coupling. Coupling between the aerial and first tuned circuit of a receiver is quite commonly effected by mutual inductance between a primary coil, to which the aerial is connected, and a secondary coil, which is the inductance element

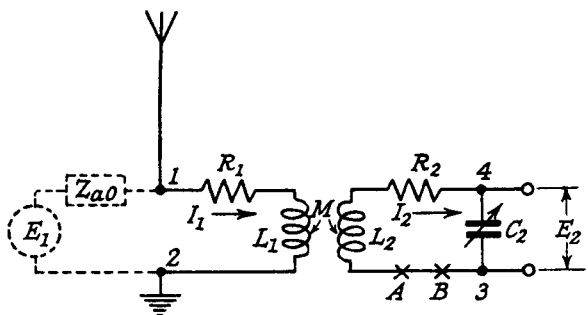

FIG. 3.8*a*.—An Aerial Circuit with Mutual Inductance Coupling.

L_2, of the first tuned circuit (Fig. 3.8*a*). Certain conventions and terms are used and these will first be stated.

The aerial is considered as a generator of voltage E_1 of internal impedance $Z_{a0} = R_{a0} + jX_{a0}$ equal to its terminal impedance.

The series impedance of the aerial terminal impedance and the coupling coil is designated as

$$Z_{a1} = R_{a1} + jX_{a1} = R_{a0} + R_1 + j(X_{a0} + \omega L_1)$$

where R_1 and L_1 are the resistance and inductance of the primary coil. Hence Z_{a1} is the impedance looking from the aerial input voltage E_1 with the tuning coil on open circuit.

The series impedance of the tuned secondary circuit with the aerial disconnected is designated as

$$Z_2 = R_2 + jX_2 = R_2 + j\left(\omega L_2 - \frac{1}{\omega C_2}\right)$$

Transfer Voltage Ratio T_R is the ratio of the voltage E_2 developed across the tuning capacitance C_2 to the aerial generated voltage E_1.

To express selectivity, we will use a term conveniently called the Selectivity Ratio defined as

$$S_R = \frac{R_2}{R_2+R_c+R_{ar}} = \frac{1}{1+\dfrac{R_c+R_{ar}}{R_2}}$$

where R_2 = resistance of the secondary coil
R_c = resistance (if any) of the coupling element
R_{ar} = resistance reflected into the secondary circuit from the aerial.

It is very nearly the ratio of the Q value of the secondary circuit, with the aerial connected, to that of the secondary coil alone. The coupling circuit resistance R_c (it is zero for mutual inductance but not necessarily for other forms of coupling) is excluded from the numerator since it can safely be assumed that the coupling element would not be included unless the aerial connection were required. The maximum value of selectivity ratio is 1, when the selectivity is that of the tuned circuit alone, and for all couplings it is less than 1.

Mistuning is definable in two forms, both of which are useful; the first states it as the capacitance correction, ΔC_2, required to maintain resonance of the secondary circuit. It is the difference in capacitance between C_2, the final tuning capacitance setting, and C_{20}, the initial tuning capacitance satisfying $C_{20} = \dfrac{1}{\omega^2 L_2}$. A knowledge of ΔC_2 indicates how far the ganging error can be corrected, e.g., if ΔC_2 is constant over a tuning range and within the range of the tuning trimmer capacitor, the ganging error can be reduced to zero. The second defines mistuning in the ratio form of $\dfrac{\Delta C_2}{C_{20}}$, and from this the frequency mistune ratio, the ratio of the frequency difference between the desired signal frequency and the actual resonant frequency of the secondary circuit (coupled to the aerial without correcting for reflected aerial and coupling reactance) to the desired signal frequency can be calculated. If $\Delta C_2 \ll C_{20}$, the frequency mistune ratio is half the capacitance mistune ratio, i.e.,

$$\frac{f_1 - f_2}{f_1} = \frac{\Delta C_2}{2C_{20}} = \frac{M_R}{2}$$

where f_1 = desired signal frequency, i.e., the resonant frequency of the uncoupled secondary circuit
f_2 = resonant frequency of the secondary coupled to the aerial
and M_R = mistune ratio.

The sign of mutual inductance is given with reference to the common limb of the equivalent T network in Fig. 3.8*b*. Thus positive M gives $(L_1 - M)$ and $(L_2 - M)$, whilst negative M gives (L_1+M) and (L_2+M) as the series arms. Referring to Fig. 3.8*a*, it means that M is positive if by joining 2 and 3 a measurement of

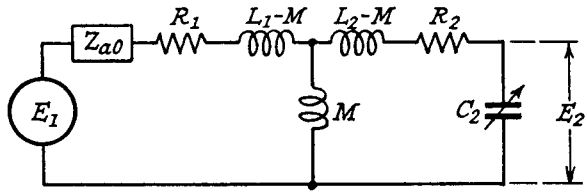

FIG. 3.8*b*.—The Equivalent Circuit for Mutual Inductance Aerial Coupling.

total inductance across 1 and 4 gives $L_T = L_1+L_2 - 2M$. Actually the sign of M is only important when additional coupling, e.g., by capacitance, is employed.

The current and voltage relationships from Fig. 3.8*a*, the actual circuit, are

$$E_1 = I_1[Z_{a0}+R_1+j\omega L_1]+I_2 j\omega M$$

$$0 = I_1 j\omega M+I_2\left(R_2+j\omega L_2+\frac{1}{j\omega C_2}\right)$$

$$E_2 = \frac{I_2}{j\omega C_2}.$$

Solving for the transfer voltage ratio

$$T_R = \frac{E_2}{E_1} = \frac{\dfrac{M}{C_2}}{Z_{a1}Z_2+\omega^2M^2}$$

$$= \frac{\dfrac{M}{C_2}}{(R_{a1}R_2 - X_{a1}X_2+\omega^2M^2)+j(X_2R_{a1}+X_{a1}R_2)} \quad . \quad 3.17.$$

Assuming L_1 to be fixed, there are two possible variables in 3.17, C_2 and M. In most practical circuits M is preset, but C_2 is variable over a wide range. In the absence of ganging requirements C_2 would be adjusted for maximum T_R, and this occurs when the total series reactance of the secondary circuit, including that reflected from the aerial, is zero, i.e., when the secondary circuit is resonant. If M also is variable, a maximum value of T_R, which we will call the optimum, is found.

To determine the resonant condition, the secondary circuit must be opened at points such as AB and E_1 must be short circuited.

The ratio of an applied voltage E (of any value) across these points to the current I it produces gives Z_{2T}, the secondary circuit equivalent series impedance.

Thus
$$Z_{2T} = \frac{E}{I} = R_2 + j\omega L_2 + \frac{1}{j\omega C_2} + \frac{\omega^2 M^2}{Z_{a1}}$$
$$= R_2 + \frac{\omega^2 M^2 R_{a1}}{|Z_{a1}|^2} + j\left[X_2 - \frac{\omega^2 M^2 X_{a1}}{|Z_{a1}|^2}\right] \quad . \quad 3.18.$$

The resistance and reactance reflected from the aerial are

$$\frac{\omega^2 M^2 R_{a1}}{|Z_{a1}|^2} \text{ and } -\frac{\omega^2 M^2 X_{a1}}{|Z_{a1}|^2} \text{ respectively.}$$

For secondary circuit resonance

$$X_2 = \frac{\omega^2 M^2 X_{a1}}{|Z_{a1}|^2} \quad . \quad . \quad . \quad . \quad 3.19.$$

Replacing X_2 in 3.17 by this value

$$\frac{E_2}{E_1}(\text{max.}) = \frac{\frac{M}{C_2}}{\left[R_{a1}R_2 - \frac{\omega^2 M^2 X_{a1}{}^2}{|Z_{a1}|^2} + \omega^2 M^2\right] + j\left[\frac{\omega^2 M^2 X_{a1} R_{a1}}{|Z_{a1}|^2} + X_{a1}R_2\right]}$$
$$= \frac{\frac{M}{C_2}}{Z_{a1}\left[R_2 + \frac{\omega^2 M^2 R_{a1}}{|Z_{a1}|^2}\right]} \quad . \quad . \quad . \quad . \quad . \quad . \quad 3.20a.$$

For optimum $\frac{E_2}{E_1}$ we must differentiate this expression with respect to M and equate to zero. This gives

$$M = \frac{Z_{a1}}{\omega}\sqrt{\frac{R_2}{R_{a1}}} \quad . \quad . \quad 3.21$$

and
$$\frac{E_2}{E_1}(\text{opt.}) = \frac{M}{2C_2 Z_{a1} R_2} \quad . \quad . \quad 3.20b$$
$$= \frac{1}{2\omega C_2 \sqrt{R_2 R_{a1}}} \quad . \quad . \quad 3.20c.$$

$$\text{Selectivity Ratio} = \frac{R_2}{R_2 + \frac{\omega^2 M^2 R_{a1}}{|Z_{a1}|^2}} \quad . \quad . \quad 3.22a$$
$$\left(\text{max. } \frac{E_2}{E_1}\right)$$

$$S_R\left(\text{opt. } \frac{E_2}{E_1}\right) = \frac{1}{2} \quad . \quad . \quad . \quad . \quad 3.22b.$$

Mistuning is calculated from 3.19 thus

$$X_2 = \omega L_2 - \frac{1}{\omega C_2} = \frac{\omega^2 M^2 X_{a1}}{|Z_{a1}|^2}$$

$$C_2 = \frac{1}{\omega^2 L_2 \left[1 - \frac{\omega^2 M^2 X_{a1}}{\omega L_2 |Z_{a1}|^2}\right]} \quad . \quad . \quad 3.23a$$

$$= \frac{C_{20}}{1 - \frac{\omega^2 M^2 X_{a1}}{\omega L_2 |Z_{a1}|^2}} \quad . \quad . \quad . \quad 3.23b.$$

Capacitance Correction $\Delta C_2 = C_2 - C_{20}$

$$= \frac{C_{20} \cdot \frac{\omega^2 M^2 X_{a1}}{\omega L_2 |Z_{a1}|^2}}{1 - \frac{\omega^2 M^2 X_{a1}}{\omega L_2 |Z_{a1}|^2}} \quad . \quad . \quad 3.24a$$

$$= \frac{C_{20}}{\frac{\omega L_2 |Z_{a1}|^2}{\omega^2 M^2 X_{a1}} - 1} \quad . \quad . \quad 3.24b.$$

Mistune Ratio $M_R = \frac{\Delta C_2}{C_{20}} = \frac{1}{\frac{\omega L_2 |Z_{a1}|^2}{\omega^2 M^2 X_{a1}} - 1} \quad . \quad . \quad 3.25.$

From expression 3.23*b* it is clear that when X_{a1} is positive, i.e., inductive, C_2 is greater than C_{20}. The reactance reflected into the secondary circuit from the aerial is equivalent to a negative inductance of $\frac{-\omega M^2 X_{a1}}{|Z_{a1}|^2}$ in series with the secondary coil. The reverse is true for capacitive X_{a1}, C_2 is less than C_{20}, and the reflected reactance is equivalent to positive inductance. Over the long and medium wave ranges, the aerial terminal reactance, X_{a0}, is almost certain to be capacitive, so that for X_{a1} to be inductive ωL_1 must be greater than X_{a0}, i.e., a large primary coil is required.

For optimum coupling

$$\Delta C_2 = \frac{C_{20}}{\frac{\omega L_2 R_{a1}}{X_{a1} R_2} - 1} \quad . \quad . \quad . \quad 3.24c.$$

Optimum coupling is rarely employed because M requires to be changed as the tuning frequency is varied $\left(M_{opt} = \frac{Z_{a1}}{\omega}\sqrt{\frac{R_2}{R_{a1}}}\right)$

unless Z_{a1} is proportional to ω (that is preponderatingly inductive) and the ratio $\frac{R_2}{R_{a1}}$ is constant. An added disadvantage is that selectivity ratio is halved and mistuning is large. The most important case is for a fixed value of M, and the expressions 3.20*a*, 22*a*, 24*b* and 25 are more useful.

By combining 3.20*a* and 23*a* we have

$$T_R = \frac{E_2}{E_1} = \frac{\omega M\left(\omega L_2 - \dfrac{\omega^2 M^2 X_{a1}}{|Z_{a1}|^2}\right)}{Z_{a1}\left[R_2 + \dfrac{\omega^2 M^2 R_{a1}}{|Z_{a1}|^2}\right]} \quad . \quad . \quad 3.26a$$

$$= \frac{\omega M}{Z_{a1}} Q_{21} \quad . \quad . \quad . \quad . \quad . \quad 3.26b$$

where Q_{21} = magnification of the secondary circuit when the aerial is coupled to it

$$= \frac{\text{coil reactance} + \text{reflected aerial reactance}}{\text{coil resistance} + \text{reflected aerial resistance}}.$$

A useful approximate formula is applicable when the coupling is loose, i.e., $M \ll \frac{Z_{a1}}{\omega}\sqrt{\frac{R_2}{R_{a1}}}$ for then $Q_{21} \simeq Q_2$, the magnification of the uncoupled secondary coil and

$$T_r = \frac{\omega M}{Z_{a1}} Q_2 = \frac{\text{coupling impedance}}{\text{aerial circuit impedance}} \times Q_2 \quad . \quad 3.26c.$$

In a similar way 3.24*a* may be written as

$$\Delta C_2 = \frac{C_{20}.\ \text{reflected aerial reactance}}{\text{coil reactance} + \text{reflected aerial reactance}} \quad . \quad 3.27.$$

Let us now consider combined mutual inductance and resistance coupling. Such a circuit (Fig. 3.9) is practically never used, but it is valuable in studying the effects of a more general form of coupling.

3.4.3. Combined Mutual Inductance and Resistance Coupling. The coupling impedance is $R + j\omega M$ and

$$T_R = \frac{\dfrac{R + j\omega M}{j\omega C_2}}{Z_{a1}Z_2 - (R + j\omega M)^2}$$

where $Z_{a1} = R_{a0} + R_1 + R + j(X_{a0} + \omega L_1)$

and $Z_2 = R_2 + R + j\left(\omega L_2 - \dfrac{1}{\omega C_2}\right)$.

The impedance reflected from the aerial into the tuned circuit is

$$\frac{-(R+j\omega M)^2}{Z_{a1}} = \frac{-(R+j\omega M)^2(R_{a1}-jX_{a1})}{|Z_{a1}|^2}$$

$$= \frac{(\omega^2M^2-R^2)R_{a1}-2R\omega MX_{a1}}{|Z_{a1}|^2} - \frac{j[X_{a1}(\omega^2M^2-R^2)+2\omega MRR_{a1}]}{|Z_{a1}|^2}.$$

Generally $\omega M \gg R$ and $X_{a1}\omega M \gg 2RR_{a1}$ so that the reflected aerial impedance is

$$Z_{a1} = \frac{\omega^2M^2R_{a1}-2R\omega MX_{a1}}{|Z_{a1}|^2} - \frac{j\omega^2M^2X_{a1}}{|Z_{a1}|^2}.$$

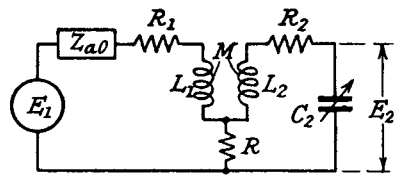

FIG. 3.9.—An Aerial Circuit with Combined Mutual Inductance and Resistance Coupling.

The resistance component is appreciably affected by the addition of R, but the reactance is almost unchanged. This means that T_R and S_R, but not ΔC_2 or M_R, are changed. The expression for T_R is

$$T_R = \frac{R+j\omega M}{j\omega C_2 Z_{a1}\left[R_2+R+\frac{\omega^2M^2R_{a1}}{|Z_{a1}|^2}-\frac{2R\omega MX_{a1}}{|Z_{a1}|^2}\right]} \quad . \quad 3.28$$

and

$$S_R = \frac{R_2}{R_2+R+\frac{\omega^2M^2R_{a1}}{|Z_{a1}|^2}-\frac{2R\omega MX_{a1}}{|Z_{a1}|^2}} \quad . \quad . \quad . \quad 3.29.$$

This analysis may be used as a basis for developing generalized formulæ applicable to any type of coupling which exists as, or is convertible into, a T section network.

3.4.4. Generalized Formulæ for T_R, S_R, ΔC_2 and M_R. The generalized form of T network for coupling common to aerial and secondary circuits is that of Fig. 3.10, and it is identical with Fig. 3.9, when

$$Z_\alpha+Z_\beta = Z_{a1} = R_{a0}+R_1+R+j(X_{a0}+\omega L_1)$$
$$Z_\beta = R+j\omega M$$
$$Z_\Delta = R_2+j\omega(L_2-M)$$
$$Z_\lambda = \frac{-j}{\omega C_2}.$$

By assuming that $Z_\alpha = R_\alpha + jX_\alpha$, etc., the generalized formula for transfer voltage ratio is from 3.28.

$$T_R = \frac{Z_\beta Z_\lambda}{(Z_\alpha+Z_\beta)\left[R_\beta+R_\Delta+R_\lambda+\dfrac{X_\beta^2(R_\alpha+R_\beta)}{|(Z_\alpha+Z_\beta)|^2}-\dfrac{2R_\beta X_\beta(X_\alpha+X_\beta)}{|(Z_\alpha+Z_\beta)|^2}\right]} \quad 3.30a$$

where $|(Z_\alpha+Z_\beta)|^2 = (R_\alpha+R_\beta)^2+(X_\alpha+X_\beta)^2$

and the formula for selectivity ratio is

$$S_R = \frac{R_2}{R_\beta+R_\Delta+R_\lambda+\dfrac{X_\beta^2(R_\alpha+R_\beta)}{|(Z_\alpha+Z_\beta)|^2}-\dfrac{2R_\beta X_\beta(X_\alpha+X_\beta)}{|(Z_\alpha+Z_\beta)|^2}} \quad . \quad 3.31a.$$

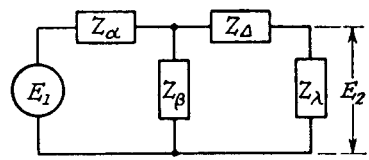

FIG. 3.10.—A Generalized T Network Coupling Circuit.

To obtain the generalized expressions for capacitance correction and mistune ratio we must return to 3.23*a*.

$$C_2 = \frac{1}{\omega\left(\omega L_2 - \dfrac{\omega^2 M^2 X_{a1}}{|Z_{a1}|^2}\right)} = \frac{1}{\omega\left(X_\beta+X_\Delta-\dfrac{X_\beta^2(X_\alpha+X_\beta)}{|(Z_\alpha+Z_\beta)|^2}\right)}$$

but $\dfrac{1}{\omega} = \omega L_2 C_{20}$.

$$\therefore C_2 = C_{20}\frac{\omega L_2}{X_\beta+X_\Delta-\dfrac{X_\beta^2(X_\alpha+X_\beta)}{|(Z_\alpha+Z_\beta)|^2}}$$

$$\Delta C_2 = C_2 - C_{20} = C_{20}\left[\frac{\omega L_2}{X_\beta+X_\Delta-\dfrac{X_\beta^2(X_\alpha+X_\beta)}{|(Z_\alpha+Z_\beta)|^2}}-1\right] \quad . \quad 3.32a$$

$$M_R = \frac{\Delta C_2}{C_{20}} = \left[\frac{\omega L_2}{X_\beta+X_\Delta-\dfrac{X_\beta^2(X_\alpha+X_\beta)}{|(Z_\alpha+Z_\beta)|^2}}-1\right] \quad . \quad . \quad 3.33a.$$

Simplification of the above expressions is possible by combining some of the terms into a single term as follows:

Let $R_{a1} = R_\alpha + R_\beta$ the series resistance of the aerial and coupling circuit with the secondary coil disconnected.

$X_{a1} = X_\alpha + X_\beta$ the series reactance of the same circuit.

$R_{21} = R_\beta + R_\Delta + R_\lambda$ the series resistance of the secondary and coupling circuit with the aerial disconnected.

$X_{21} + X_\lambda = X_\beta + X_\Delta + X_\lambda$ the series reactance of the same circuit.

and
$$x = \frac{X_\beta}{|(Z_\alpha + Z_\beta)|} = \frac{X_\beta}{|Z_{a1}|}.$$

Then
$$S_R = \frac{1}{\frac{R_{21}}{R_2} + \frac{x^2}{R_2}\left(R_{a1} - \frac{2R_\beta X_{a1}}{X_\beta}\right)} \quad . \quad 3.31b.$$

$$\Delta C_2 = C_{20}\left[\frac{\omega L_2}{X_{21} - x^2 X_{a1}} - 1\right] \quad . \quad . \quad 3.32b.$$

$$M_R = \frac{\omega L_2}{X_{21} - x^2 X_{a1}} - 1$$

$$= \frac{1}{\frac{\omega L_2}{\omega L_2 - X_{21} + x^2 X_{a1}} - 1} \quad . \quad . \quad 3.33b.$$

If $R_{a1} \ll X_{a1}$, a further simplification is possible for $x = \frac{X_\beta}{X_{a1}}$ and

$$S_R = \frac{1}{\frac{R_{21}}{R_2} + \frac{x^2 R_{a1}}{R_2} - \frac{2xR_\beta}{R_2}} \quad . \quad . \quad 3.31c.$$

$$M_R = \frac{1}{\frac{\omega L_2}{\omega L_2 - X_{21} + xX_\beta} - 1} \quad . \quad . \quad 3.33c.$$

If coupling is by mutual inductance $X_{21} = \omega L_2$ and

$$M_R = \frac{1}{\frac{\omega L_2}{xX_\beta} - 1} \quad . \quad . \quad 3.33d$$

and often for other forms of coupling $X_{21} = \omega L_2 + X_\beta$, hence

$$M_R = \frac{1}{-\frac{\omega L_2}{X_\beta(1-x)} - 1} \quad . \quad . \quad 3.33e.$$

Generally $R_\beta \ll X_\beta$ and transfer voltage ratio may be written as

$$T_R = \frac{xZ_\lambda S_R}{R_2}.$$

R_λ is usually very small so that

$$Z_\lambda = jX_\lambda = -\frac{j}{\omega C_2} = -\frac{j}{\omega C_{20}\left(1+\frac{\Delta C_2}{C_{20}}\right)}$$

$$= -\frac{j}{\omega C_{20}(1+M_R)}$$

$$\therefore\ T_R = \frac{xS_R}{j\omega C_{20}R_2(1+M_R)} = \frac{xQ_2S_R}{(1+M_R)} \quad . \quad . \quad . \quad 3.30b.$$

When x is much less than its optimum value $\sqrt{\frac{R_2}{R_{a1}}}$ (see expression 3.21) T_R is very nearly xQ_2; for $x = 0{\cdot}4$ and $0{\cdot}7.\sqrt{\frac{R_2}{R_{a1}}}$ the approximate value of T_R is about 10% and 25% high respectively.

Let us now consider the values of R_{a1}, X_{a1}, x, etc., for the probable forms of aerial coupling circuit The couplings will be designated as shunt, if the coupling impedance is common to aerial and tuned circuit (this is the procedure adopted in network analysis), and series when the impedance joins the aerial to the top or a tapping point on the secondary coil. The formulae for the resistance and reactance elements, together with selectivity and mistune ratio, are given. The formulae for capacitance correction and transfer voltage ratio are not listed since expressions 3.33a and 3.30b show their direct connection with M_R and S_R.

3.4.5. Combined Mutual Inductance and Shunt Capacitance Coupling. The circuit for this type is shown in Fig. 3.11.

$$R_{a1} = R_{a0}+R_1,\ R_{21} = R_2,$$

$$X_{a1} = X_{a0}+\omega L_1 - \frac{1}{\omega C_3},\ X_{21} = \omega L_2 - \frac{1}{\omega C_3}$$

$$x = (a)\ \frac{\omega M - \frac{1}{\omega C_3}}{Z_{a1}} \text{ and } (b)\ \frac{-\omega M - \frac{1}{\omega C_3}}{Z_{a1}}$$

where (*a*) refers to positive M

and (*b*) ,, ,, negative M.

$$S_R = \frac{1}{1+\frac{x^2 R_{a1}}{R_2}}$$

$$M_R = \frac{1}{\frac{\omega L_2}{x^2 X_{a1}+\frac{1}{\omega C_3}} - 1}.$$

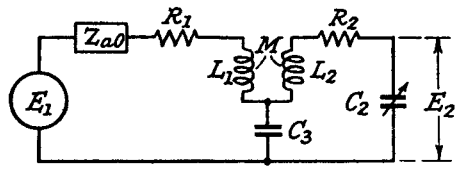

FIG. 3.11.—An Aerial Circuit with Combined Mutual Inductance and Shunt Capacitance Coupling.

Approximate expressions for M_R, obtained by assuming $x = \frac{X_\beta}{X_{a1}}$, are

$$M_R = (a) \quad \frac{1}{\frac{L_2}{Mx+\frac{1}{\omega^2 C_3}(1-x)} - 1}$$

and

$$M_R = (b) \quad \frac{1}{\frac{L_2}{-Mx+\frac{1}{\omega^2 C_3}(1-x)} - 1}.$$

3.4.6. Shunt Capacitance Coupling. Shunt Capacitance coupling is illustrated in Fig. 3.12.

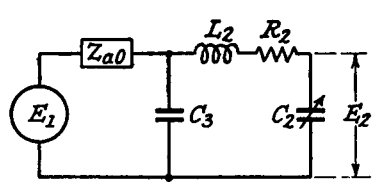

FIG. 3.12.—An Aerial Circuit with Shunt Capacitance Coupling.

$$R_{a1} = R_{a0}, \; R_{21} = R_2$$

$$X_{a1} = X_{a0} - \frac{1}{\omega C_3}, \; X_{21} = \omega L_2 - \frac{1}{\omega C_3}$$

$$x = \frac{-\dfrac{1}{\omega C_3}}{Z_{a1}}$$

$$S_R = \frac{1}{1+\dfrac{x^2 R_{a0}}{R_2}}$$

$$M_R = \frac{1}{\dfrac{\omega L_2}{x^2 X_{a1} + \dfrac{1}{\omega C_3}} - 1}$$

$$\simeq \frac{1}{\dfrac{\omega^2 L_2 C_3}{1-x} - 1} \qquad \left(x = \frac{X_\beta}{X_{a1}}\right).$$

3.4.7. The Tapped Tuned Circuit. Coupling to a tapping point on the tuned secondary coil is similar in form to mutual inductance coupling, and the equivalent T section can be deduced by analogy from Figs. 3.8*a* and 8*b*. The development is illustrated in Figs. 3.13*a* and *b*. The mutual inductance between the coils is such as to increase the total inductance between 1 and 4 and so by definition in Section 3.4.2 is given a negative sign

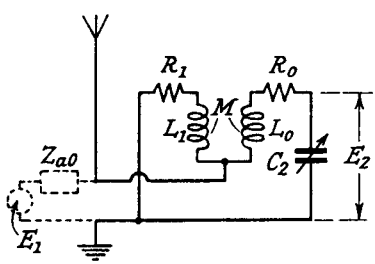

FIG. 3.13*a*.—Tapped Tuned Circuit Aerial Coupling.

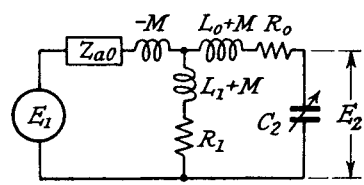

FIG. 3.13*b*.—The Equivalent Circuit of Tapped Tuned Circuit Aerial Coupling.

$$R_{a1} = R_{a0} + R_1, \quad R_{21} = R_1 + R_0,$$

$$X_{a1} = X_{a0} + \omega L_1, \quad X_{21} = \omega(L_1 + L_0 + 2M)$$

$$x = \frac{\omega(L_1+M)}{Z_{a1}}$$

$$S_R = \frac{1}{1+\dfrac{x^2 R_{a1}}{R_1+R_0} - \dfrac{R_1}{(R_1+R_0)}\dfrac{2x^2 X_{a1}}{X_\beta}}$$

$$\simeq \frac{1}{1+\dfrac{x^2R_{a1}}{R_1+R_0}-\dfrac{2xR_1}{R_1+R_0}} \left(x=\frac{X_\beta}{X_{a1}}\right)$$

$$M_R = \frac{1}{\dfrac{\omega(L_1+L_0+2M)}{x^2X_{a1}}-1}$$

$$\simeq \frac{1}{\dfrac{L_1+L_0+2M}{(L_1+M)x}-1}.$$

3.4.8. Series Capacitance Coupling. Fig. 3.14 gives the circuit diagram for series capacitance coupling.

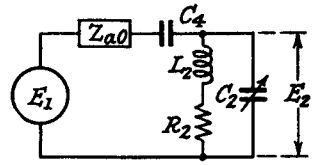

FIG. 3.14.—An Aerial Circuit with Series Capacitance Coupling.

$$R_{a1} = R_{a0}+R_2,\ R_{21} = R_2,$$

$$X_{a1} = X_{a0}+\omega L_2-\frac{1}{\omega C_4},\ X_{21} = \omega L_2$$

$$x = \frac{\omega L_2}{Z_{a1}}$$

$$S_R = \frac{1}{1+\dfrac{x^2R_{a1}}{R_2}-\dfrac{2x^2X_{a1}}{X_\beta}}$$

$$\simeq \frac{1}{1+\dfrac{x^2R_{a1}}{R_2}-2x}$$

$$M_R = \frac{1}{\dfrac{\omega L_2}{x^2X_{a1}}-1}$$

$$\simeq \frac{1}{\dfrac{1}{x}-1}.$$

3.4.9. Combined Series Capacitance and Shunt Inductance Coupling. In order to apply the generalized formulae the π section enclosed in the dotted lines (Fig. 3.15*a*) must be converted into the equivalent T section. The necessary transformation is

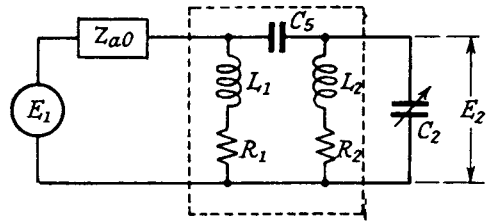

FIG. 3.15*a*.—An Aerial Circuit with Combined Series Capacitance and Shunt Inductance Coupling.

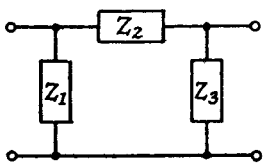

FIG. 3.15*b*.—An Unsymmetrical π Section.

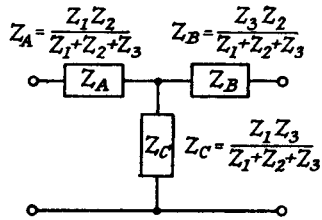

FIG. 3.15*c*.—The T Network Equivalent of Fig. 3.15*b*.

illustrated in Figs. 3.15*b* and 3.15*c*, and the impedances of the series and shunt arms of the T section are

$$Z_A = \frac{(R_1+j\omega L_1)\dfrac{1}{j\omega C_5}}{(R_1+R_2) - j\left(\dfrac{1}{\omega C_5} - \omega(L_1+L_2)\right)}$$

Rationalizing

$$Z_A = \frac{\left[(R_1+R_2)\omega L_1 + R_1\left(\dfrac{1}{\omega C_5} - \omega(L_1+L_2)\right)\right]\dfrac{1}{\omega C_5}}{(R_1+R_2)^2+\left[\dfrac{1}{\omega C_5} - \omega(L_1+L_2)\right]^2}$$

$$+\frac{j\left[\omega L_1\left(\dfrac{1}{\omega C_5} - \omega(L_1+L_2)\right) - R_1(R_1+R_2)\right]\dfrac{1}{\omega C_5}}{(R_1+R_2)^2+\left[\dfrac{1}{\omega C_5} - \omega(L_1+L_2)\right]^2}.$$

$$\text{Similarly } Z_B = \frac{\left[(R_1+R_2)\omega L_2+R_2\left(\frac{1}{\omega C_5}-\omega(L_1+L_2)\right)\right]\frac{1}{\omega C_5}}{(R_1+R_2)^2+\left[\frac{1}{\omega C_5}-\omega(L_1+L_2)\right]^2}$$

$$+\frac{j\left[\omega L_2\left(\frac{1}{\omega C_5}-\omega(L_1+L_2)\right)-R_1(R_1+R_2)\right]\frac{1}{\omega C_5}}{(R_1+R_2)^2+\left[\frac{1}{\omega C_5}-\omega(L_1+L_2)\right]^2}$$

$$-\left[(\omega^2L_1L_2-R_1R_2)(R_1+R_2)+(R_1\omega L_2+R_2\omega L_1)\left(\frac{1}{\omega C_5}-\omega(L_1+L_2)\right)\right]$$

$$\text{and } Z_C = \frac{}{(R_1+R_2)^2+\left[\frac{1}{\omega C_5}-\omega(L_1+L_2)\right]^2}$$

$$-\frac{j\left[(\omega^2L_1L_2-R_1R_2)\left(\frac{1}{\omega C_5}-\omega(L_1+L_2)\right)+(R_1+R_2)(R_1\omega L_2+R_2\omega L_1)\right]}{(R_1+R_2)^2+\left[\frac{1}{\omega C_5}-\omega(L_1+L_2)\right]^2}$$

In practice $\frac{1}{\omega C_5}-\omega(L_1+L_2) \gg R_1+R_2$, $\omega L_1 \gg R_1$ and $\omega L_2 \gg R_2$, so that Z_A, Z_B and Z_C can be simplified to

$$Z_A = A\left[R_1+\frac{(R_1+R_2)\omega L_1}{B}\right]+jA\omega L_1$$

$$Z_B = A\left[R_2+\frac{(R_1+R_2)\omega L_2}{B}\right]+jA\omega L_2$$

$$Z_C = -\left[\frac{R_2\omega L_1+R_1\omega L_2}{B}+\frac{\omega^2L_1L_2(R_1+R_2)}{B^2}\right]-j\frac{\omega^2L_1L_2}{B}$$

where $A = \frac{1}{B\omega C_5}$, and $B = \frac{1}{\omega C_5}-\omega(L_1+L_2)$.

Thus

$$R_{a1} = R_{a0}+A\left[R_1+\frac{(R_1+R_2)\omega L_1}{B}\right]-\frac{R_2\omega L_1}{B}-\frac{R_1\omega L_2}{B}$$

$$-\frac{\omega^2L_1L_2(R_1+R_2)}{B^2}$$

$$= R_{a0}+AR_1+\frac{A\omega L_1}{B}(R_1+R_2)\left(1-\frac{\omega L_2}{AB}\right)-\left[\frac{R_2\omega L_1+R_1\omega L_2}{B}\right]$$

$$R_{21} = AR_2+\frac{A\omega L_2}{B}(R_1+R_2)\left(1-\frac{\omega L_1}{AB}\right)-\left[\frac{R_2\omega L_1+R_1\omega L_2}{B}\right]$$

$$X_{a1} = X_{a0} + A\omega L_1 - \frac{\omega^2 L_1 L_2}{B}$$

$$X_{21} = A\omega L_2 - \frac{\omega^2 L_1 L_2}{B}$$

$$x = -\frac{\omega^2 L_1 L_2}{B Z_{a1}}$$

$$S_R = \frac{1}{\frac{R_{21}}{R_2} + \frac{x^2 R_{a1}}{R_2} + \left[\frac{R_2\omega L_1 + R_1\omega L_2}{B} + \frac{\omega^2 L_1 L_2 (R_1 + R_2)}{B^2}\right]\left(\frac{2x^2 X_{a1}}{X_\beta}\right)}$$

when $x \simeq \frac{X_{a1}}{X_\beta}$, the last factor in the denominator of S_R becomes $(2x)$

$$M_R = \frac{1}{\frac{\omega L_2}{(1-A)\omega L_2 + \frac{\omega^2 L_1 L_2}{B} + x^2 X_{a1}} - 1}$$

$$\simeq \frac{1}{\frac{1}{(1-A) + \frac{\omega L_1}{B}(1-x)} - 1} \left(x = \frac{X_\beta}{X_{a1}}\right).$$

3.4.10. Combined Mutual Inductance and Series Capacitance Coupling. The circuit is shown in Fig. 3.16*a*; the equivalent circuit is the same as that of Fig. 3.8*b* except that the capacitance C_5 joins the opposite ends of the resistances R_1 and R_2. The

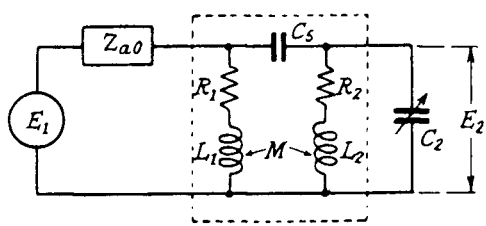

FIG. 3.16*a*.—An Aerial Circuit with Combined Mutual Inductance and Series Capacitance Coupling.

part enclosed between the dotted lines can therefore be transformed to the unsymmetrical bridged T network of Fig. 3.16*b*.

$$Z_1 = R_1 + j\omega(L_1 \mp M),\ Z_2 = R_2 + j\omega(L_2 \mp M);\ Z_3 = j\omega(\pm M),\ Z_4 = \frac{1}{j\omega C_5}$$

and this can in turn be changed to the T section of Fig. 3.16*c*. After making the same simplifications as in 3.4.9 we have

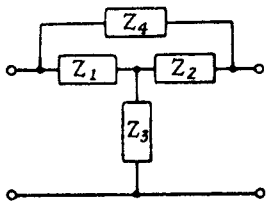

FIG. 3.16*b*.—An Unsymmetrical Bridged T Section.

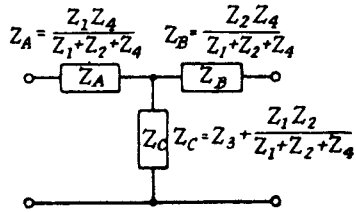

FIG. 3.16*c*.—The T Network Equivalent of Fig. 3.16*b*.

$$Z_A = A_1\left[R_1+\frac{(R_1+R_2)\omega(L_1\mp M)}{B_1}\right]+j\omega A(L_1\mp M)$$

$$Z_B = A_1\left[R_2+\frac{(R_1+R_2)\omega(L_2\mp M)}{B_1}\right]+j\omega A(L_2\mp M)$$

$$Z_C = -\left[\frac{[R_2\omega(L_1\mp M)+R_1\omega(L_2\mp M)]}{B_1}\right.$$
$$\left.+\frac{\omega^2(L_1\mp M)(L_2\mp M)(R_1+R_2)}{B_1^2}\right]+j\left[\omega M-\frac{\omega^2(L_1\mp M)(L_2\mp M)}{B_1}\right]$$

where $A_1 = \dfrac{1}{\omega C_5 B_1}$ and $B_1 = \dfrac{1}{\omega C_5} - \omega(L_1+L_2\mp 2M)$.

The sign taken by M when combined with L_1 or L_2 is negative for positive M and positive for negative M. It may be noted that when $M = 0$ the expressions for Z_A, Z_B and Z_C are identical with those in Section 3.4.9.

$$R_{a1} = R_{a0}+A_1\left[R_1+\frac{(R_1+R_2)\omega(L_1\mp M)}{B_1}\right]$$
$$-\left[\frac{R_2\omega(L_1\mp M)+R_1\omega(L_2\mp M)}{B_1}+\frac{\omega^2(L_1\mp M)(L_2\mp M)(R_1+R_2)}{B_1^2}\right]$$

$$R_{21} = A_1\left[R_2+\frac{(R_1+R_2)\omega(L_2\mp M)}{B_1}\right]-\left[\frac{R_2\omega(L_1\mp M)+R_1\omega(L_2\mp M)}{B_1}\right.$$
$$\left.+\frac{\omega^2(L_1\mp M)(L_2\mp M)(R_1+R_2)}{B_1^2}\right]$$

$$X_{a1} = X_{a0}+A_1\omega(L_1\mp M)\pm\omega M-\frac{\omega^2(L_1\mp M)(L_2\mp M)}{B_1}$$

$$X_{21} = A_1\omega(L_2\mp M)\pm\omega M-\frac{\omega^2(L_1\mp M)(L_2\mp M)}{B_1}$$

$$x = \frac{\pm\omega M - \dfrac{\omega^2(L_1 \mp M)(L_2 \mp M)}{B_1}}{Z_{a1}}$$

$$S_R = \frac{1}{\dfrac{R_{s1}}{R} + \dfrac{x^2 R_{a1}}{R_s} + \left[\dfrac{R_s\omega(L_1 \mp M) + R_1\omega(L_2 \mp M)}{B_1} + \dfrac{\omega^2(L_1 \mp M)(L_2 \mp M)(R_1 + R_2)}{B_1^2}\right]\left(\dfrac{2x^2 X_{a1}}{X_\beta}\right)}.$$

The last factor in the denominator becomes $2x$ when $x \simeq \dfrac{X_\beta}{X_{a1}}$.

$$M_R = \frac{1}{\dfrac{\omega L_2}{(1 - A_1)\omega(L_2 \mp M) + \dfrac{\omega^2(L_1 \mp M)(L_2 \mp M)}{B_1} + x^2 X_{a1}} - 1}$$

$$\simeq \frac{1}{\dfrac{1}{(1 - A_1)\dfrac{(L_2 \mp M)}{L_2} + \dfrac{\omega(L_1 \mp M)(L_2 \mp M)(1 - x)}{B_1 L_2} \pm \dfrac{Mx}{L_2}} - 1}$$

when $x = \dfrac{X_\beta}{X_{a1}}$

3.4.11. Selectivity Ratio Variation over a Tuning Range. From the approximate expression 3.31*c*, we can estimate the trend of selectivity ratio over a given tuning range. Neglecting the variation of the resistance ratios (these are less affected by frequency because numerator and denominator tend to vary together in the same direction), we see that S_R is dependent on x. When x is independent of frequency so is S_R, and hence if X_β and X_{a1} are the same type of reactance, both inductive or both capacitive, S_R is constant over the tuning range (see Curve 4 in Fig. 3.17*a*).

For X_β inductive and X_{a1} capacitive, x is proportional to $-f^2$, hence S_R decreases as the tuning frequency rises (curve 1*a* in Fig. 3.17*a*). The reverse is true when X_β is capacitive and X_{a1} inductive and S_R increases as the tuning frequency increases.

3.4.12. Mistune Ratio and Capacitance Correction Variation over a Tuning Range. An examination of Mistune ratio is possible, from expressions 3.33*d* and 3.33*e*. For mutual inductance coupling (3.33*d*) and X_{a1} capacitive, x is proportional to $-f^2$ and

$$M_R = \frac{1}{\dfrac{K}{-f^2} - 1}.$$

Hence M_R is negative and it increases as f is increased. Since $\Delta C_2 = C_{20}.M_R = \frac{K_1}{f^2}M_R$, ΔC_2 is negative and tends to fall as f is increased. In practice ΔC_2 tends to remain almost constant (curve 1*a* in Fig. 3.17*c*). When X_{a1} is inductive (large primary coil)

$$M_R = \frac{1}{\frac{L_2}{Mx} - 1} \text{ is positive and constant,}$$

because $\frac{L_2}{Mx} > 1$ and x is constant. ΔC_2 is also positive and it decreases as the frequency increases (curve 1*b* in Fig. 3.17*c*).

For couplings other than mutual inductance, expression 3.33*e* indicates that if X_β and X_{a1} are both inductive (x and $\frac{\omega L_2}{X_\beta}$ are positive constants) M_R is negative and independent of frequency. ΔC_2 is negative, decreasing for increasing frequency. For capacitive X_β and X_{a1}, x is a positive constant, but $\frac{\omega L_2}{X_\beta}$ is proportional to $-f^2$. Since X_β is generally much less than ωL_2 and x than 1, $\frac{\omega L_2}{-X_\beta(1-x)} > 1$ and M_R is positive, decreasing as the frequency increases. ΔC_2 is also positive and decreases (curve 4 in Fig. 3.17*c*).

If X_β is inductive and X_{a1} capacitive, x is proportional to $-f^2$ and $\frac{\omega L}{X_\beta}$ is constant. Hence

$$M_R = \frac{1}{-\left(\frac{K_1}{1+K_2f^2}\right) - 1},$$

i.e., is negative and increasing with increasing frequency. ΔC_2 is negative and increases slightly as the frequency rises.

When X_β is capacitive and X_{a1} inductive

$$\left(x = \frac{-K_1}{f^2},\ \frac{\omega L_2}{X_\beta} = -K_2f^2\right) M_R = \frac{1}{\frac{K_2f^2}{1+K_1f^2} - 1}$$

is positive and decreases as the frequency increases. ΔC_2 is positive and almost constant.

3.4.13. Transfer Voltage Ratio Variation over a Tuning Range. Expression 3.30*b* shows that T_R is almost proportional to x and its variation over a tuning range is largely that of x.

The above conclusions are best summarised in a table.

TABLE 3.1. TUNING FREQUENCY INCREASING

X_β	X_{a1}	x	S_R	M_R	ΔC_2	T_R	Δf
L	L	constant	constant	constant —	decreases —	constant	increases —
C	C	constant	constant	decreases +	decreases +	constant	decreases +
L	C	$-Kf^2$	decreases	increases —	decreases —	increases	increases —
C	L	$-\frac{K}{f^2}$	increases	decreases +	almost constant +	decreases	almost constant +
M	L	constant	constant	constant +	decreases +	constant	almost constant +
M	C	$-Kf^2$	decreases	increases —	slight decrease —	increases	increases —

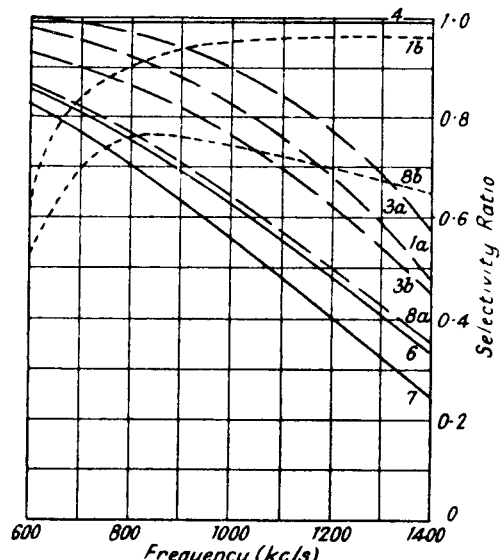

FIG. 3.17*a*.—Typical Selectivity Ratio Variations over the Medium Wave Range.

Typical examples of the variation of S_R, M_R, ΔC_2, T_R and Δf are shown in Figs. 3.17*a*, *b*, *c*, *d* and *e* for the following types of coupling.

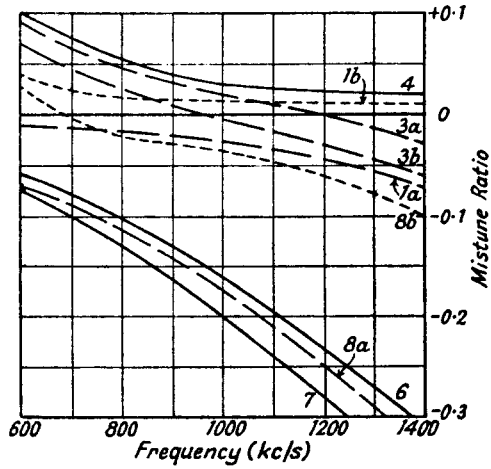

FIG. 3.17b.—Typical Mistune Ratio Variations over the Medium Wave Range.

1*a*. Mutual inductance, small primary coil, X_{a1} capacitive.
1*b*. ,, ,, , large ,, ,, , X_{a1} inductive.

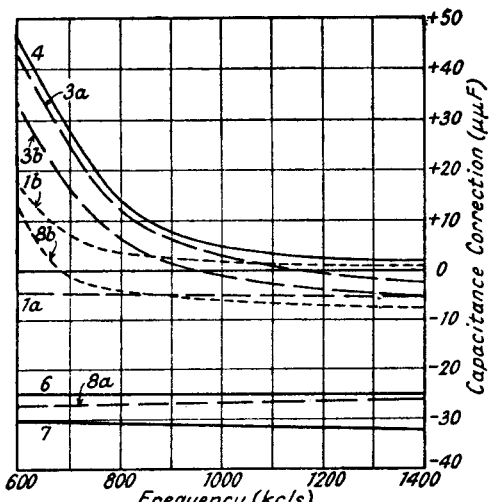

FIG. 3.17c.—Typical Capacitance Correction Variations over the Medium Wave Range.

3*a*. Positive mutual inductance, small primary coil, and shunt capacitance.
3*b*. Negative mutual inductance, small primary coil, and shunt capacitance.
4. Shunt capacitance.
6. Series capacitance.
7. Series capacitance and shunt inductance.
8*a*. Positive mutual inductance, small primary coil, and series capacitance.
8*b*. Negative mutual inductance, large primary coil, and series capacitance.

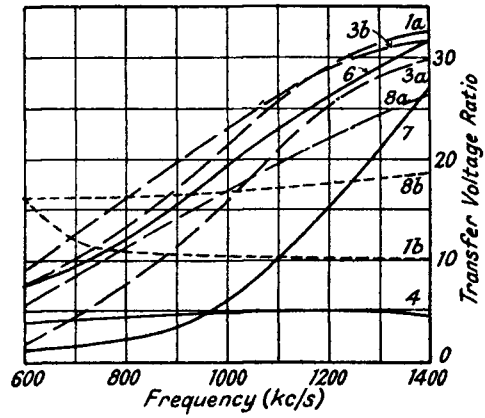

FIG. 3.17*d*.—Typical Transfer Voltage Ratio Variations over the Medium Wave Range.

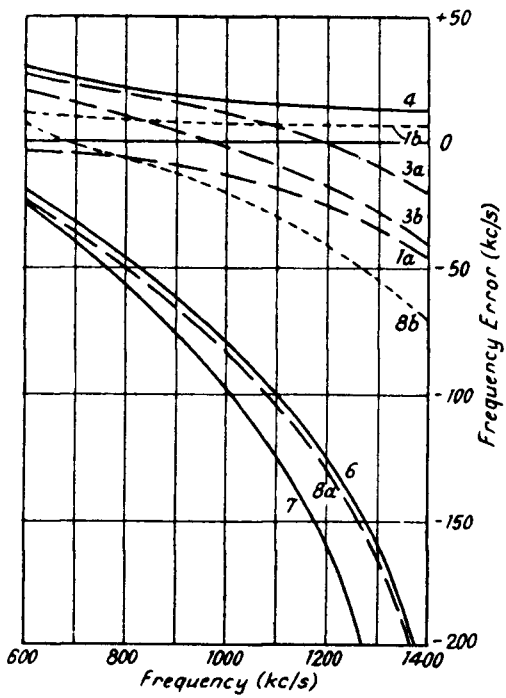

FIG. 3.17*e*.—Typical Frequency Error Variations over the Medium Wave Range.

The curves follow the predictions of Table 3.1, except for slight modifications due to an approach to aerial and coupling circuit resonance. Thus mutual inductance with a large primary coil (X_β and X_{a1} inductive) shows a decrease of S_R and an increase in M_R and T_R as the tuning frequency falls, because X_{a1} is approaching zero at the low frequency end of the range.

Combined couplings mainly affect x and those reducing the variation of x over the frequency range are advantageous in reducing the variation of T_R and S_R. For example, negative mutual inductance and shunt capacitance (curves 3*b*) giving $X_\beta = -\left(\omega M + \frac{1}{\omega C_5}\right)$ and positive mutual inductance with series capacitance (curves 8*a*) giving $X_\beta = +\omega M - \frac{\omega^2(L_1 - M)(L_2 - M)}{B}$ show reduced variation of T_R and S_R as compared with mutual inductance alone. There is a disadvantage; the average value of S_R is reduced and damping of the aerial circuit is therefore increased. Series capacitance coupling may be added to negative mutual inductance with a large primary coil so as to raise T_R at the high frequency end (curve 8*b*), but the average S_R is reduced.

The variation of ΔC_2 over the frequency range follows Table 3.1. For combined couplings it may change sign at some point in the frequency range (curves 3*a*, 3*b* and 8*b*), and this is due to the fact that the reflected aerial reactance $x^2.X_{a1}$ is opposite in sign to that of the coupling reactance. The most desirable curve of ΔC_2 against frequency is that giving a horizontal line, i.e., ΔC_2 is independent of frequency. Provided the constant value of ΔC_2 is within the range of the trimmer across the tuning capacitance, mistuning effects can be cancelled. From this point of view series capacitance (6), mutual inductance with small primary coil (1*a*), positive mutual inductance (small primary) and series capacitance (8*a*), and series capacitance with shunt inductance (7) are satisfactory.

We may note that if $R_{a0} \ll X_{a0}$ and X_{a0} is capacitive, ΔC_2 for three of the couplings may be written

Shunt capacitance (4) $\Delta C_2 = \dfrac{-C_{20}^2}{C_3 + C_{a0} - C_{20}}$

Series capacitance (6) $\Delta C_2 = \dfrac{-C_4 C_{a0}}{C_4 + C_{a0}}$ (independent of f)

Combined series capacitance and inductance (7) $\Delta C_2 = \dfrac{C_5}{1 - \dfrac{\omega^2 L_1 C_5}{1 - \omega^2 L_1 C_{a0}}}$.

Shunt capacitance coupling gives a large variation of ΔC_2 and it is not therefore desirable.

If no correction is made for coupling and reflected aerial reactance, mutual inductance with a large primary coil [9] gives least variation of frequency error (curve 1*b* in Fig. 3.17*e*). Shunt capacitance 4 is much better than series capacitance coupling 6. When frequency error varies over the range it is preferable to select a coupling giving least error at the low frequency end where the selective properties of the secondary circuit are greatest.

It is important next to consider the effect of aerial terminal impedance on S_R, M_R, ΔC_2 and T_R.

3.4.14. Aerial Terminal Impedance and S_R, ΔC_2 and T_R. —(*a*) *Increasing* R_{a0}. With a high value of X_{a1}, increase of R_{a0} increases R_{a1}, but hardly affects Z_{a1} and x. Hence M_R and ΔC_2 are almost unchanged; S_R is decreased because the second term in 3.31*c* is increased. If the aerial and coupling circuit approach resonance in the tuning range, i.e., $X_{a1} \rightarrow 0$, the reflected aerial reactance tends to disappear so that M_R and ΔC_2 fall. The second term in 3.31*c* approaches $\frac{X_\beta^2}{R_{a1}R_2}$ and so S_R tends to increase when R_{a0}, i.e., R_{a1}, increases. The general shape of S_R curve over a tuning range in which $X_{a1} = 0$ is shown in Fig. 3.18; it is a condition rarely occurring in practice, and increase of R_{a0} normally decreases S_R.

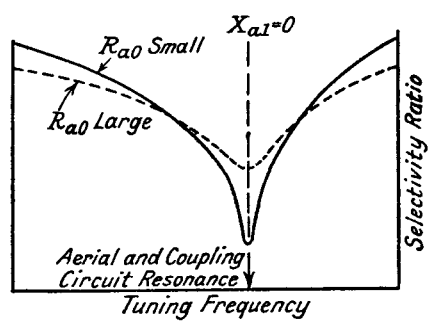

FIG. 3.18.—Selectivity Ratio Variation over a Tuning Range passing through Aerial and Coupling Circuit Resonance for a Large and Small Value of R_{a0}.

(*b*) *Increasing* X_{a0}. Increase of aerial terminal reactance X_{a0}, provided it has the same sign as X_{a1}, increases Z_{a1} and decreases x. Hence T_R is decreased and S_R increased. The statement with regard to T_R needs qualification if the coupling reactance X_β is initially greater than its optimum value, for increase of Z_{a1} then causes optimum coupling to be approached and T_R therefore increases. The normal decrease follows when optimum coupling is passed.

From 3.33*b* we see that M_R is decreased if X_{a1} and X_{a0} are negative, but is increased if X_{a1} is positive and X_{a0} is negative.

The following tables summarize the conclusions.

TABLE 3.2*a*. R_{a0} INCREASING

X_{a1}	x	S_R	M_R	ΔC_2	T_R
Very large	little affected	decreased	little affected	little affected	decreased
Small and comparable with R_{a0}	decreased	increased	tends to decrease	tends to decrease	decreased

TABLE 3.2*b*. X_{a0} INCREASING

X_{a1}	x	S_R	M_R	ΔC_2	T_R
Same sign as X_{a0}	decreased	increased	decreased	decreased	decreased if initial coupling < optimum increased if > optimum
Opposite sign to X_{a0}	increased	decreased	increased	increased	increased if initial coupling < optimum decreased if > optimum

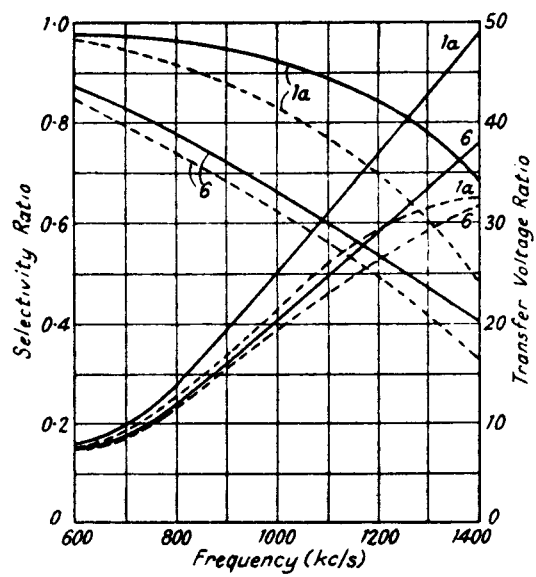

FIG. 3.19*a*.—The Effect on Selectivity and Transfer Voltage Ratios of a Change of R_{a0}.

Full line, R_{a0} = 15 ohms. C_{a0} = 177 $\mu\mu$ F.
Dotted line, R_{a0} = 42 ohms.

The result that a decrease of X_{a0} (X_{a1} of the same sign) tends to increase T_R when coupling is less than optimum shows that the addition of a horizontal top to a vertical aerial can not only increase the effective generated voltage (Section 3.3.3) but also give a greater transfer voltage ratio. The horizontal section reduces X_{a0} and X_{a1}, thus increasing x and T_R.

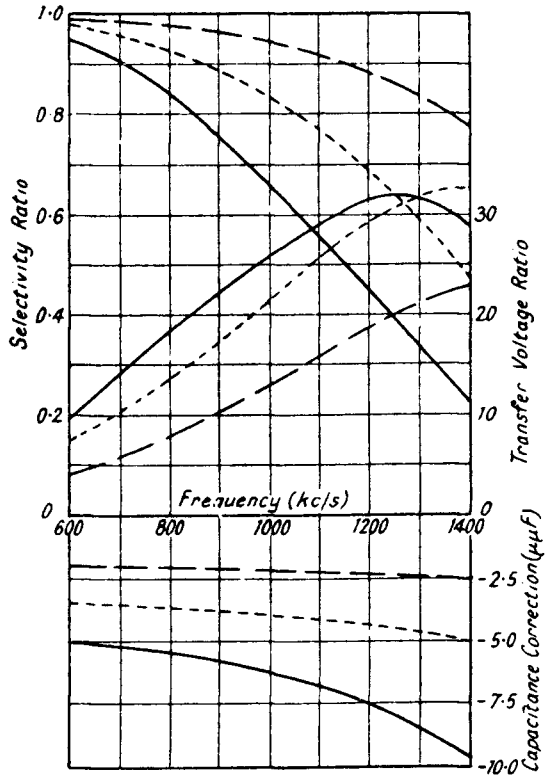

FIG. 3.19*b*.—The Effect on Selectivity and Transfer Voltage Ratios and Capacitance Correction of a Change of X_{a0} with Small Primary Coil.

Broken line, C_{a0} = 104 μμF. R = 42 ohms.
Dotted line, C_{a0} = 177 μμF. R = „ „
Full line, C_{a0} = 240 μμF. R = „ „

Typical examples of varying R_{a0} and X_{a0} are shown in Figs. 3.19*a* and 3.19*b* over the medium wave range for mutual inductance with a small primary coil (1*a*) and series capacitance coupling (6) (X_{a0} and X_{a1} capacitive). It is seen that increase of R_{a0} has greatest effect at the high frequency end of the range due to an approach to aerial circuit resonance (X_{a1} decreasing rapidly), and the variation

of T_R over the tuning range is reduced, though at the expense of a reduction of average S_R. This applies to all forms of inductive coupling with capacitive X_{a1} (e.g., 1*a*, 2, 3*a*, 3*b*, 6, 7 and 8). For inductive X_β and X_{a1} (large primary coil) variation of T_R is also reduced, but increase of R_{a0} has greatest effect at the low frequency end.

Increase of aerial terminal reactance X_{a0}, when X_{a0} and X_{a1} are both capacitive, increases Z_{a1} and decreases x. T_R is decreased and S_R increased. Most reduction of T_R and increase of S_R occurs at the end of the range approaching aerial circuit resonance, in this case the high frequency end. A modification occurs with $C_{a0} = 240$ $\mu\mu$F, T_R is reduced at the high frequency end as compared with $C_a = 177$ $\mu\mu$F, and this is due to optimum coupling having been exceeded. Capacitance correction (ΔC_2) and its variation over the tuning range is decreased because increase of X_{a0} increases X_{a1}.

3.5. Interference Reducing Aerial Systems.

3.5.1. Introduction. In the early days of broadcast reception the receiver was comparatively insensitive, and the aerial had therefore to be as good a collector as possible. As receiver design progressed and sensitivity was increased (mainly by the adoption of the superheterodyne principle), the necessity for a good aerial became less pressing and the tendency was to neglect this aspect of reception, employing inefficient indoor aerials or the mains wiring to supply the pick-up voltage. Attention is once again being focused on the aerial because of the increased use of electrical apparatus producing fortuitously or intentionally R.F. voltage components. For example, any form of sparking (in commutator machines, switching on apparatus, etc.), distortion of wave form by gas discharge illuminated signs, short wave therapy apparatus, etc., generate appreciable R.F. components, which can be transmitted for considerable distances over the supply lines, unless special precautions are taken to suppress or confine them to the apparatus. Since the supply lines are the transmission media the interference field is mainly localized in the building housing the receiver. The disadvantage of the indoor aerial is at once apparent; not only is it an inefficient collector (due to the screening effect of the building), but it is also located in the area of maximum interference field. It is possible to reduce the effect on the receiver by including R.F. filters in the incoming mains leads to the house, and by erecting an aerial well clear of the latter and coupling it to the

receiver by twisted, screened twin or concentric feeder, in which the interference voltage is either cancelled or eliminated. An example of a common type of interference reducing aerial [7] is shown in Fig. 3.20. The vertical aerial (often in the form of a spike attached to the highest point on the building outside the region of intense interference) is self-supporting and rarely longer than about 6 feet (1·83 metres), and is coupled at its base either direct to the screened twin feeder or by a matching transformer, T_1. At the other end of the feeder is a transformer T_2 (with earthed centre tapped primary), matching the low impedance feeder to the high impedance input of the receiver. It is almost impossible to obtain correct matching between the aerial and feeder over a large fre-

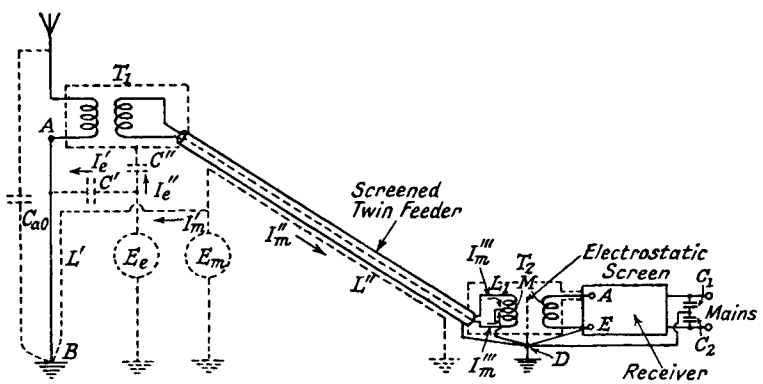

FIG. 3.20.—A Local-Interference Reducing Aerial System.

quency range, and the use of a transformer is only justified under certain conditions. The feeder-to-receiver transformer is generally designed on the basis of a receiver input impedance of 2,000 to 3,000 ohms. The dotted circuits in Fig. 3.20 indicate the possible ways by which interference is induced in the aerial circuit. The electrostatic component of the interference field is represented by the generator E_e and capacitances C' and C'', and the magnetic component by the generator E_m and loops L' and L''. The earthed lead AB from the aerial feeder matching transformer T_1, which is enclosed in a screening box earthed to the feeder shield but not to A, carries interference currents from E_e and E_m and an interference voltage is induced in the lead due to its inductive reactance. This voltage has a return path to earth via the aerial capacitance C_{a0}, but the current it produces in the primary of T_1 is usually negligible. If transformer T_1 is located in the interference field and connected by an unscreened lead to the aerial, considerable

interference is caused because the currents from E_e and E_m then pass through the primary of T_1. The earthed screen round T_1, the feeders and T_2 prevents electrostatic pick-up, but current in the loop L'' induces currents in the shield and feeders. The currents I_m''' in the feeders are equal and opposite, provided the feeders are balanced to earth; to ensure this the centre point of the primary of T_2 is earthed. An electrostatic screen between the primary and secondary also helps to preserve this balance and prevents interference voltage transfer (from the currents I_m''' in the half primaries) to the secondary by interwinding capacitance. The screening for feeders and transformers is earthed at one point only, preferably D, which is likely to be nearer to earth than A. If it is also earthed at A a loop ABD is formed in the interference field and pick-up due to the magnetic component is greatly increased. The earthed point of any filter system reducing interference entering by the mains (see capacitance C_1 and C_2 in Fig. 3.20) should be taken separately to earth rather than via the receiver earth. The improvement to be expected in signal-to-interference ratio by the use of this type of aerial circuit is from 30 to 40 dbs., but it is obtained at the cost of a reduction in desired signal (compared with the unshielded aerial and lead in) of from 3 to 6 dbs.

3.5.2. The Characteristic Impedance of Feeders. The characteristic impedance of any uniform feeder may be determined by measuring the capacitance of a comparatively short length of feeder at any suitable radio frequency, e.g., about 1,000 kc/s, and noting (expression 3.3c) that

$$Z_0 = \frac{l}{vC_1} = \frac{l \times 10^{12}}{3 \times 10^{10} C_1} = \frac{100l}{3C_1}\,\Omega$$

where l = length of feeder (cms.)
and C_1 = total capacitance of feeder in $\mu\mu$F.

The formula for calculating Z_0 of a concentric feeder from its dimensions is

$$Z_0 = \frac{138}{k} \log_{10} \frac{r_2}{r_1} \text{ ohms} \quad . \quad . \quad . \quad 3.34$$

where k = specific inductive capacitance of the dielectric separating the lines.
r_2 = inner radius of outer conductor.
and r_1 = outer radius of inner conductor.
For a pair of parallel unscreened wires

$$Z_0 = \frac{276}{k} \log_{10} \left(\frac{d}{r} + \sqrt{\frac{d^2}{r^2} + 1} \right) \quad . \quad . \quad . \quad 3.35$$

where d = distance between conductor centres.
and r = radius of conductor.

Curves are given in Fig. 3.21 of characteristic impedance against $\frac{r_2}{r_1}$ and $\frac{d}{r}$ for the concentric and parallel wire feeders with $k = 1$.

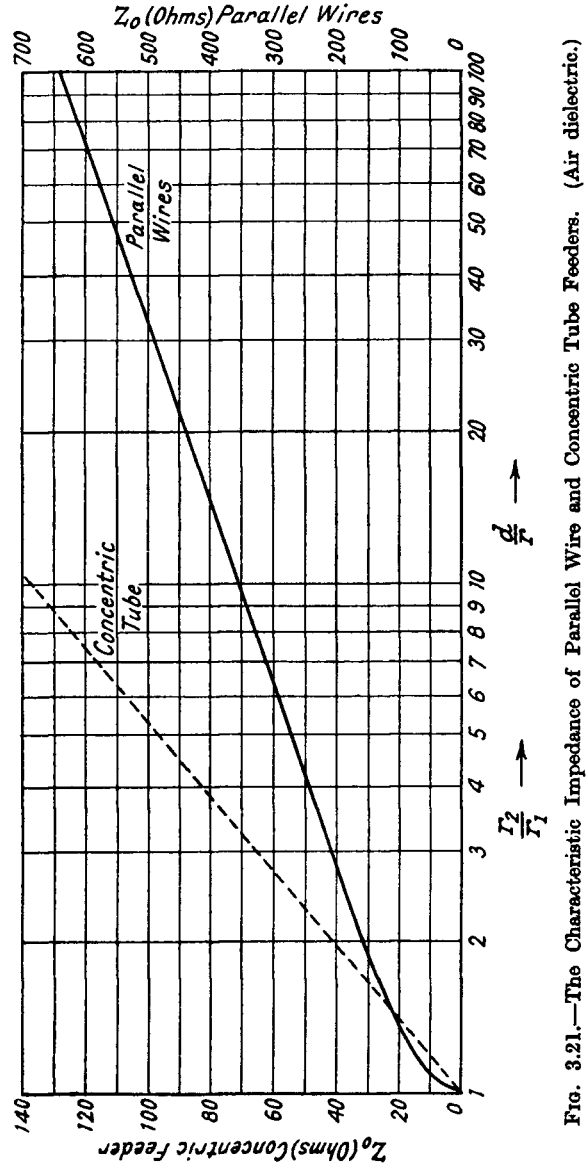

FIG. 3.21.—The Characteristic Impedance of Parallel Wire and Concentric Tube Feeders. (Air dielectric.)

3.5.3. The Aerial to Feeder Connection. We will consider first the case of a feeder correctly terminated at the receiver end in its characteristic impedance Z_0. Owing to the fact that the aerial input impedance varies over the frequency range and is reactive, except at its resonant frequencies, there must be a loss of power transfer at the junction of feeder and aerial. The maximum power transfer occurs when the load resistance (the characteristic impedance of the feeder) is equal to the generator (aerial) terminal resistance and the reactance of the latter is zero. The power transferred to the feeder under these conditions is

$$P_0 = \frac{E_1^2}{4R_{a0}} \quad . \quad . \quad . \quad . \quad 3.36$$

where E_1 = the generator (aerial) voltage.

Expression 3.36 is written as $\frac{E_1^2}{4R_{a0}}$ rather than $\frac{E_1^2}{4Z_0}$ since it is the generator resistive component which is variable and which determines the maximum power transfer.

When the generator (aerial) impedance is equal to $R_{a0} \pm jX_{a0}$, the power delivered to the feeder is

$$P_1 = I_1^2 Z_0 = \left[\frac{E_1}{\sqrt{(R_{a0}+Z_0)^2+X_{a0}^2}}\right]^2 Z_0 \quad . \quad . \quad 3.37.$$

The ratio of maximum to actual power is

$$\frac{P_0}{P_1} = \frac{(R_{a0}+Z_0)^2+X_{a0}^2}{4R_{a0}Z_0} \quad . \quad . \quad . \quad 3.38a$$

$$= \frac{\left(\frac{R_{a0}}{Z_0}+1\right)^2+\left(\frac{X_{a0}}{Z_0}\right)^2}{\frac{4R_{a0}}{Z_0}} \quad . \quad . \quad . \quad 3.38b.$$

Replacing $\frac{P_0}{P_1}$, $\frac{R_{a0}}{Z_0}$ and $\frac{X_{a0}}{Z_0}$ by a, x and y

we have $(x+1)^2+y^2 = 4ax$

or $x^2+2(1-2a)x+1+y^2 = 0.$

This is the equation to a circle with centre on the x axis, and solving for $y = 0$ gives the two values of x corresponding to the intersections of the circle with the x axis. Thus

$$x_2 = \frac{2(2a-1)+\sqrt{4(2a-1)^2-4}}{2}$$

$$= (2a-1)+\sqrt{(2a-1)^2-1}$$

and $$x_1 = (2a-1)-\sqrt{(2a-1)^2-1}.$$

The centre of the circle is at $x_3 = \frac{x_2+x_1}{2}$

or $$x_3 = 2a - 1$$

and the radius is $$r = \frac{x_2 - x_1}{2}$$

$$= \sqrt{(2a-1)^2 - 1}.$$

Taking a particular example, for a loss of 3 dbs., $a = 2$, $x_3 = 3$, $r = 2{\cdot}82$.

A series of curves, due to Wheeler,[4] are shown in Fig. 3.22. The semicircles connect values of $\frac{X_{a0}}{Z_0}$ and $\frac{R_{a0}}{Z_0}$ giving the particular

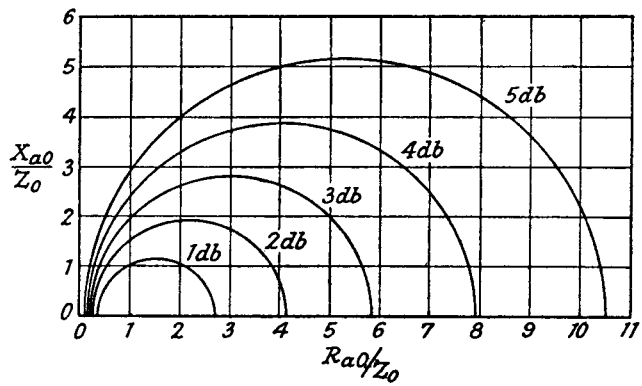

FIG. 3.22.—A Chart for Estimating Transition Loss due to Mismatching between an Aerial and Correctly Terminated Feeder.

transition loss marked. Thus the *V* dipole, whose impedance characteristic is given by curves 2 in Fig. 3.5, has at 13·2 Mc/s $\left(\frac{f}{f_0} = 1{\cdot}3\right)$ an impedance of $R_{a0}+jX_{a0} = 129+j255$, and coupling this to a correctly terminated 600Ω feeder gives $\frac{R_{a0}}{Z_0} = 0{\cdot}215$ and $\frac{X_{a0}}{Z_0} = 0{\cdot}425$, which from Fig. 3.22 corresponds to a loss of approximately 3 dbs. Calculation from $10 \log_{10} \frac{P_0}{P_1}$ (expression 3.38*b*) gives 2·8 dbs.

The loss (over the range 6 to 15 Mc/s) at the junction of the plain and *V* dipole aerials of Fig. 3.5 with a 600Ω feeder is shown in Fig. 3.23.

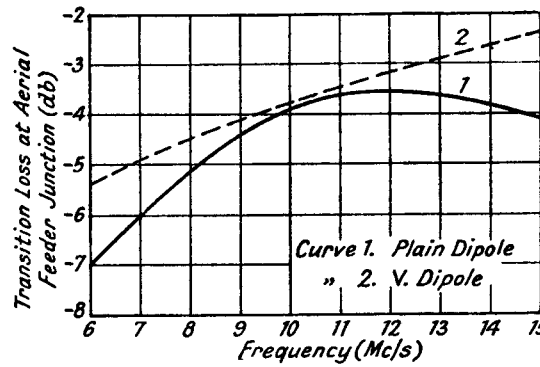

FIG. 3.23.—Curves of Transition Loss at the Junction of a Plain and *V* Dipole Aerial and a 600-ohm Feeder.

When the feeder is not correctly terminated the problem becomes more complicated. Let us suppose that a vertical aerial is connected to a receiver of input impedance Z_R via a feeder of characteristic impedance Z_0, having a propagation constant $Y = \alpha + j\beta$ (see Fig. 3.24). The aerial terminal impedance Z_{a0} (calculated as indicated in Section 3.3.2) is the terminating impedance of the

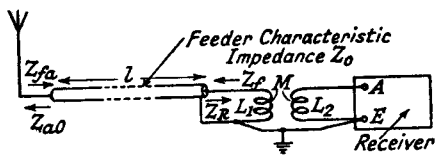

FIG. 3.24.—A Single Concentric Tube Feeder with no Aerial Matching Transformer.

feeder so that the impedance [6] at the receiver end of the feeder (Fig. 3.24) is given by

$$Z_f = Z_0 \frac{Z_{a0} \cosh \gamma l + Z_0 \sinh \gamma l}{Z_{a0} \sinh \gamma l + Z_0 \cosh \gamma l} \quad . \quad . \quad 3.39$$

$$= R_f + jX_f$$

where Z_0 = characteristic impedance of the feeder
and l = length of feeder.

The aerial and feeder may be replaced by a generator having an internal impedance Z_f and an open circuit voltage of $\frac{KE_1Z_R}{Z_{a0}+Z_R}$

where E_1 = aerial generated voltage

$$\text{and } K = \frac{2Z_0(Z_{a0}+Z_R)\varepsilon^{-\gamma l}}{(Z_{a0}+Z_0)(Z_R+Z_0)\left[1 - \frac{(Z_{a0}-Z_0)(Z_R-Z_0)}{(Z_{a0}+Z_0)(Z_R+Z_0)}\varepsilon^{-2\gamma l}\right]} \quad 3.40.$$

This formula is developed in Chapter 4, p. 116, of Bibliography 22, where curves of transition loss due to mismatching will also be found.

A simplification of the problem is possible in calculating over the long and medium wave ranges, because the feeder length is usually short compared with the lowest wavelength, and the attenuation constant α is negligible. In section 3.3.2 it is shown that the impedance of a vertical aerial of height less than $\frac{\lambda}{8}$ is practically equivalent to that of its electrostatic capacitance, and the same rule applies to a feeder line. Thus, if the lowest medium wavelength is 200 metres, feeder lines not exceeding 25 metres (82 feet) in length may be replaced by a shunt capacitance equal to the electrostatic capacitance. If the feeder attenuation constant cannot be neglected the feeder may be replaced by two shunt capacitances of half the feeder electrostatic capacitance and a series resistance. If a matching transformer [14] is employed between aerial and transformer, the equivalent circuit becomes that of Fig. 3.8*b* where C_2 is now the feeder capacitance C_f. Resonance effects between C_{a0}, L_1, L_2 and C_f can be used to produce a more level overall frequency response over a given range.

3.6. Aerials for Automobile Receivers.[11, 16] The design of aerials for automobile receivers is chiefly concerned with finding an aerial which is a reasonably efficient collector. Mechanical rigidity and location of the aerial, which should be as far from the ignition system as possible, are important. There is little difficulty in designing the coupling to the receiver first tuned circuit as it follows the lines set out in Section 3.4. Before the use of all-steel car construction the most efficient type of aerial consisted of gauze strip let into the roof of the car. The under-car aerial, mounted below the running-board, has been used, but it is a much less efficient collector, is liable to damage, and its pick-up properties are seriously impaired in wet weather due to mud adhering to the insulators and offering a low resistance path to earth. Owing to its position its capacitance to earth is comparatively high (about 200 $\mu\mu$F). The roof aerial mounted above and parallel to the roof of the car is a better collector and has a lower earth capacitance (about 50 $\mu\mu$F). A third type of aerial is the " telescopic whip "

vertical aerial located usually at the side of the car behind the bonnet. It may be capable of extension to a length of about 5 feet, and the sliding sections should have clamps making intimate contact between sections so as to prevent interference from intermittent contacts when travelling. Its capacitance to earth may be as low as 25 $\mu\mu$F. A concentric feeder with the outer conductor earthed to the car chassis is used to couple the aerial to receiver ; it should be as short as possible and should have the least possible capacitance value. The equivalent circuit is that of Fig. 3.24, and the feeder capacitance C_f acts with the aerial capacitance as a potential divider for the pick-up voltage ; a large value of C_f reduces the receiver input voltage and also necessitates looser coupling to the receiver for a given ganging error in the first tuned circuit.

3.7. The Connection of Several Receivers to one Aerial System. Difficulties are met if attempts are made to connect several receivers to the same aerial. Unless the coupling between each receiver and the aerial lead-in is loose, interaction may occur between the receivers, causing mistuning of the first tuned circuit of one receiver when the tuning of another is changed. There may also be sufficient oscillator voltage injected into the aerial circuit from the frequency changer to cause whistles in the other receivers as one is tuned over its range. It is possible, where loss of signal strength can be tolerated, to couple several receivers through suitable transformers to the feeder line of the interference reducing aerial described in Section 3.5.1. A more satisfactory arrangement, particularly for a large installation, such as that in a block of flats, is to distribute the signal frequencies via a low impedance feeder line, preceded by an aperiodic amplifier or with an aperiodic buffer amplifier between each receiver and the feeder. The second method has been employed but is obviously not so satisfactory economically as the first. A suitable circuit [15] for the first method is shown in Fig. 3.25. The aerial, a short vertical rod, erected at the highest point in the building, is connected by a short screened lead to two aperiodic amplifiers, covering a total frequency range from 150 kc/s to 15 Mc/s. It is not practicable to cover the whole range with one amplifier without appreciable loss of amplification. Between the aerial lead and each amplifier is a filter selecting the particular frequency range required ; to reduce further the possibilities of cross modulation the valves should have as near linear $I_a E_g$ characteristics as possible. Wave traps may also be necessary if the aerial is in the high field strength area of a local station. The outputs from the two amplifiers are connected in parallel, through step-

down transformers, to a low impedance feeder line of low loss terminated in its characteristic impedance. The advantage of the terminated feeder is that it has a wide frequency response and conveys power with low losses and small noise pick-up. Furthermore, its low impedance makes the reduction of interaction between receivers much simpler, and the comparatively high impedance inputs of the receivers can be connected to the feeder without impairing its transmission characteristics. The line is matched to the amplifier valves by transformers but no attempt is made to match the receiver input to the feeder. A resistance R is connected in series with

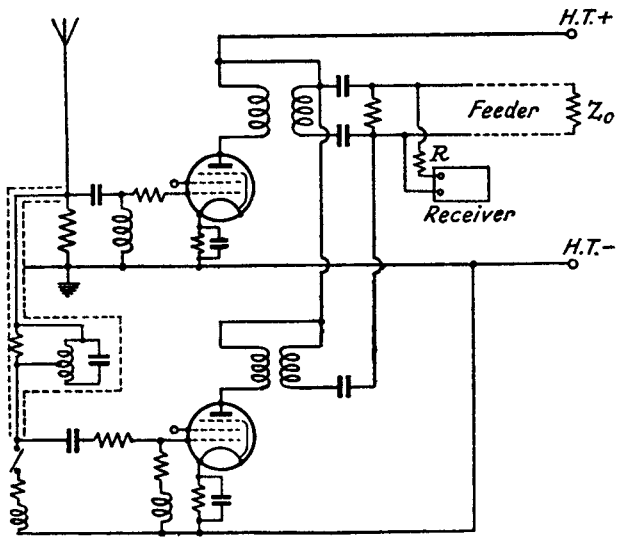

FIG. 3.25.—An Amplifier for a Feeder supplying Several Receivers.

each receiver input to reduce interaction still further. This resistance need only affect the input voltage at the receiver to a small extent, since it can be much lower than the receiver input impedance and yet much higher than the feeder impedance. For example, if the receiver input impedance is 3,000 Ω and the series resistance 1,000Ω, the greatest possible reduction of input voltage is to $\frac{3}{4}$ of the voltage at the feeder, whilst interaction is reduced to $\frac{70}{1070} \simeq 7\%$, if the characteristic impedance of the feeder is 70 ohms. The length of the feeder is determined by the highest received frequency because the feeder losses are greatest at this frequency; a length of 400 metres (about $\frac{1}{4}$ mile) is possible for the frequency range

quoted above, 150 kc/s to 15 Mc/s, but it may be increased to 2,000 metres (about $1\frac{1}{4}$ miles) if reception is restricted to the long and medium wave ranges.

3.8. Diversity Reception. Owing to its dependence on the reflected ray, short wave reception is liable to considerable variations in signal strength. The actual value of the signal at any given time instant depends on the position of the aerial, and there may be large differences in field strength between positions spaced only a few wavelengths apart. By suitably combining the outputs from two or more aerials with at least a wavelength separation, the average signal may be maintained at a more constant level. Diversity reception, as it is called, is quite often employed for commercial reception, and a large number of aerials are located at different positions and connected to the receiver by feeder lines. This is clearly not feasible for broadcast receiver purposes, but some improvement can be obtained by using two aerials, one vertical and the other horizontal, separated by at least a wavelength. One method [12] of combining the two aerial outputs is by means of a gas-filled valve with an interrupter relay in its anode circuit. The arm of the relay drives a sprocket wheel attached to a differential capacitor, the rotor of which is connected to the aerial terminal of the receiver. The stators are connected each to an aerial, and the gas-filled relay is biased by the D.C. component of the detected I.F. output voltage of the receiver. When the output is greater than a certain predetermined value, sufficient negative bias voltage is developed to render the gas-filled valve inoperative. If it falls below this value the bias is reduced, the valve conducts, and the interrupter relay drives the sprocket wheel until the output voltage is large enough to shut down the valve again. The sprocket wheel comes to rest with the capacitor giving more coupling to the aerial having greatest signal. If both aerials give outputs less than the value required to stop the relay the capacitor continues to rotate.

When the same programme is transmitted on two different carrier frequencies, improved reception may be gained by receiving each transmission on a separate receiver and combining the audio frequency outputs.[10]. A common A.G.C. system actuated from the strongest signal is employed for the two receivers, and A.F. combination may be achieved by dual loudspeakers, two output transformers, the secondaries of which are connected in series with the speech coil of a loudspeaker, or by a single centre-tapped-primary output transformer with the output valve of each receiver con-

nected to a half primary. A common aerial system may be used, but it is preferable to have (for example) a horizontal aerial for one receiver and a vertical for the other.

BIBLIOGRAPHY

1. On the Capacity of Radio Telegraphic Antennae. G. W. O. Howe, *Wireless Engineer*, Dec. 1914, p. 546; Jan. 1915, p. 612; Feb. 1915, p. 680.
2. The Capacity of Aerials of the Umbrella Type. G. W. O. Howe, *Wireless Engineer*, Oct. 1915, p. 426.
3. The Balance of Power in Aerial Tuning Circuits. F. M. Colebrook, *Wireless Engineer*, March, 1930, p. 129.
4. Transition Loss Chart. H. A. Wheeler, *Electronics*, Jan. 1936, p. 27.
5. The Design of Doublet Antenna Systems. H. A. Wheeler and V. E. Whitman, *Proc. I.R.E.*, Oct. 1936, p. 1257.
6. The Calculation of Input and Sending End Impedance of Feeders and Cables terminated with a Complex Load. H. Cafferata, *Marconi Review*, Jan.–Feb. and Sept.–Dec. 1937, pp. 12 and 21.
7. Screened Aerials. F. R. W. Strafford, *Wireless World*, Nov. 25th, 1937, p. 516.
8. The Impedance Characteristic of Short Wave Dipoles. T. Walmsley, *Phil. Mag.*, June 1938, p. 381.
9. The Aerial Connection. M. G. Scroggie, *Wireless World*, June 23rd, 1938, p. 548; June 30th, 1938, p. 579.
10. Diversity Reception at Home. R. H. Tanner, *Wireless World*, Sept. 1st, 1938, p. 194.
11. Car Aerials. F. R. W. Strafford, *Wireless World*. Oct. 20th, 1938, p. 344.
12. Dual Diversity Reception. *Wireless World*, March 2nd, 1939, p. 208.
13. Vertical or Inverted L Aerials. F. R. W. Strafford, *Wireless World*, June 15th, 1939, p. 554; June 22nd, 1939, p. 575.
14. Receiving Aerials. J. van Slooten, *Philips Technical Review*, Nov. 1939, p. 320.
15. A Central Antenna System. D. J. Fruin, *Electronics*, Nov. 1939, p. 37.
16. Design Problems in Automobile Radio Receivers. G. C. Hall, *A.W.A. Technical Review*, Vol. 4, No. 3, 1939, p. 105.
17. Receiver Aerial Coupling Circuits. K. R. Sturley, *Wireless Engineer*, April 1941, p. 137; May 1941, p. 190.
18. The Theory of Antennas of Arbitrary Size and Shape. S. A. Schelkunoff, *Proc. I.R.E.*, Sept. 1941, p. 493.
19. Antennas for Frequency Modulated Reception. J. G. Aceves, *Electronics*, Sept. 1941, p. 42.
20. The Design of Television Receiving Apparatus. B. J. Edwards, *Journal I.E.E.*, Wireless Section, Sept. 1941, p. 191.
21. Aerial Characteristics. N. Wells, *Journal I.E.E.*, June 1942, Part III, p. 76.
22. *Transmission Networks and Wave Filters*. T. E. Shea. Text-book.

CHAPTER 4

RADIO FREQUENCY AMPLIFICATION

4.1. Introduction. In this chapter radio frequency amplification is considered in relation to amplifiers which are tunable over a range of frequencies from a minimum of 150 kc/s to a maximum of 50 Mc/s. Special problems are involved due to the need for covering a range of frequencies ; for example, the gain and selectivity of an amplifier may vary widely over the frequency range, leading perhaps to instability at the high frequency end. Again owing to interelectrode capacitance coupling the grid input admittance of an R.F. amplifier valve (see section 2.8) may be comparable with the reciprocal of the dynamic resistance of the tuned circuit to which it is connected. An anode-grid capacitance of 0·005 $\mu\mu$F can produce a high input admittance at frequencies of the order of 1·5 Mc/s, if the anode external load impedance is high. At higher frequencies (50 Mc/s) in the short wave band other effects such as the inductance of the cathode-earth connection and electron transit time tend to give a very high input admittance, so that gain is limited.

The coupling impedances between the amplifier stages generally consist of parallel tuned circuits since high selectivity and gain are required (aperiodic circuits are rarely used). Band-pass filters are often employed, and the design of two coupled tuned circuits producing a band-pass effect is given in detail in Section 7.3 on I.F. amplifiers. We shall therefore only deal with those aspects of design which result from variable tuning. It is recommended that Sections 7.2 to 7.5 should be read before Sections 4.5 and 6, since the I.F. amplifier band-pass filter is a special case of the tuned R.F. filter operating at a fixed frequency.

The circuit analysis, which follows, begins with the simplest tuned filter, the parallel resonant circuit, and progresses to the more complicated band-pass filter. The R.F. valve, generally a multi-electrode valve, [19] is considered as a generator of constant current $I_a = g_m.E_g$ and its resistance R_a, except where stated otherwise, is assumed to be much larger than the resonant impedance of the tuned filter in its anode circuit.

4.2. The Parallel Resonant Circuit.

4.2.1. Magnification. The most important criterion for a coil forming part of a tuned circuit is its magnification. This term, designated by Q, is the ratio at resonance of the voltage across the inductance/or capacitance to the voltage injected in series with the circuit.

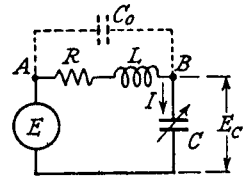

FIG. 4.1.—The Voltage Magnification of a Coil.

Referring to Fig. 4.1.

$$Q = \frac{E_L}{E} = \frac{I\omega_r L}{E}$$

Alternatively $$Q = \frac{Ec}{E} = \frac{I}{\omega_r CE}$$

But $$E = I\left[R + j\left(\omega_r L - \frac{1}{\omega_r C}\right)\right]$$

$$= IR \text{ at resonance, for } \omega_r L = \frac{1}{\omega_r C}$$

$$\therefore Q = \frac{\omega_r L}{R} = \frac{1}{\omega_r CR}. \quad . \quad . \quad . \quad . \quad . \quad . \quad 4.1.$$

4.2.2. The Impedance of a Parallel Resonant Circuit and its Equivalent Series and Parallel Circuits. The impedance of the parallel resonant circuit of Fig. 4.2 is

$$Z = \frac{R + j\omega L}{j\omega C} \Big/ R + j\left(\omega L - \frac{1}{\omega C}\right) \quad . \quad . \quad 4.2.$$

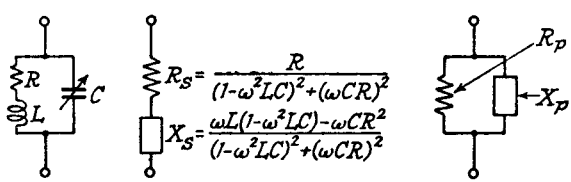

FIG. 4.2.—The Parallel Resonant Circuit and its Equivalent Series and Parallel Circuits.

$$Rp = \frac{R^2 + \omega^2L^2}{R}; \quad Xp = \frac{R^2 + \omega^2L^2}{\omega L(1 - \omega^2LC) - \omega CR^2}$$

At resonance if $R \ll \omega_r L$

$$Z_r = \frac{L}{CR} = \frac{\omega_r^2 L^2}{R} = Q\omega_r L = \frac{Q}{\omega_r C} \quad . \quad . \quad 4.3.$$

The resonant impedance Z_r is thus a resistance, and it is often called the dynamic resistance of the circuit and denoted by R_D.

To determine its frequency discriminating action, the impedance must be calculated for frequencies other than resonance.

Rewriting 4.2

$$Z = \frac{R+j\omega L}{1 - \omega^2 LC + j\omega CR}.$$

Rationalizing

$$Z = \frac{(R+j\omega L)(1 - \omega^2 LC - j\omega CR)}{(1 - \omega^2 LC)^2 + (\omega CR)^2}$$

$$= \frac{R}{(1 - \omega^2 LC)^2 + (\omega CR)^2} + j\frac{\omega L(1 - \omega^2 LC) - \omega CR^2}{(1 - \omega^2 LC)^2 + (\omega CR)^2} \quad . \quad 4.4$$

$$= R_S + jX_S$$

where R_S and X_S are the equivalent series resistance and reactance.

An interesting point to observe is that reactance resonance, i.e., $X_S = 0$, gives

$$\omega_r L(1 - \omega_r^2 LC) - \omega_r CR^2 = 0$$

or

$$\omega_r = \sqrt{\frac{1}{LC}\left(1 - \frac{CR^2}{L}\right)} \quad . \quad . \quad . \quad 4.5.$$

Replacing this in R_S (4.4) gives $Z_r = \frac{L}{CR}$, which is identical with expression 4.3, for which R was assumed to be much less than $\omega_r L$.

The equivalent series circuit is rarely so useful as the equivalent parallel circuit. The latter is determined by considering the admittance Y.

Thus

$$Y = j\omega C + \frac{1}{R+j\omega L}$$

$$= \frac{(1 - \omega^2 LC + j\omega CR)(R - j\omega L)}{R^2 + \omega^2 L^2}$$

$$= \frac{R}{R^2 + \omega^2 L^2} + j\frac{\omega CR^2 - \omega L(1 - \omega^2 LC)}{R^2 + \omega^2 L^2} \quad . \quad . \quad 4.6$$

$$= g + jb$$

$$= \frac{1}{R_p} + \frac{1}{jX_p}$$

where R_p and X_p are the equivalent parallel resistance and reactance. By making the assumption that $R \ll \omega L$ most useful approximate formulae for R_p and X_p are obtained as follows

$$\left.\begin{aligned} R_p &\simeq \frac{\omega^2 L^2}{R} \simeq R_D \\ X_p &\simeq \frac{\omega L}{1-\omega^2 LC} \end{aligned}\right\} \quad . \quad . \quad . \quad 4.7.$$

It is important to note that X_s and X_p are inductive for frequencies below and are capacitive for frequencies above the resonant frequency.

4.2.3. The Selectivity Characteristic.[6] The selectivity characteristic of a parallel tuned circuit may be defined as the ratio of the resonant impedance to the impedance at any given off-tune frequency. It is more conveniently expressed as loss in decibels, $20 \log_{10} \frac{|Z_r|}{|Z|}$, the reference level corresponding to 0 db. being the resonant impedance Z_r. Expression 4.2 simplifies to

$$\begin{aligned} Z &= \frac{\frac{L}{CR}}{1+j\frac{\omega_r L}{R}\left(\frac{\omega}{\omega_r} - \frac{\omega_r}{\omega}\right)} \\ &= \frac{R_D}{1+jQ\left(\frac{\omega}{\omega_r} - \frac{\omega_r}{\omega}\right)} \quad . \quad . \quad . \quad 4.8a \end{aligned}$$

when $R \ll \omega L$ and $\omega_r = \frac{1}{\sqrt{LC}}$.

But
$$\begin{aligned} \frac{\omega}{\omega_r} - \frac{\omega_r}{\omega} &= \frac{\omega^2 - \omega_r^2}{\omega_r \omega} = \frac{f^2 - f_r^2}{f_r f} \\ &= \frac{(f-f_r)(f+f_r)}{f_r f} \end{aligned}$$

If $f = f_r + \Delta f$, where Δf is the off-tune frequency

$$\begin{aligned} \frac{(f-f_r)(f+f_r)}{f_r f} &= \frac{\Delta f(2f_r+\Delta f)}{f_r(f_r+\Delta f)} \\ &\simeq \frac{2\Delta f}{f_r} \text{ when } \Delta f \ll f_r. \end{aligned}$$

For convenience we will designate $\frac{2\Delta f}{f_r}$ by F.

Expression 4.8*a* now becomes

$$Z = \frac{R_D}{1+jQF} \quad . \quad . \quad . \quad . \quad 4.8b$$

hence

$$20 \log_{10} \frac{|Z_r|}{|Z|} = 20 \log_{10} \sqrt{1+Q^2F^2}$$

$$= 10 \log_{10} (1+Q^2F^2) \quad . \quad . \quad 4.8c.$$

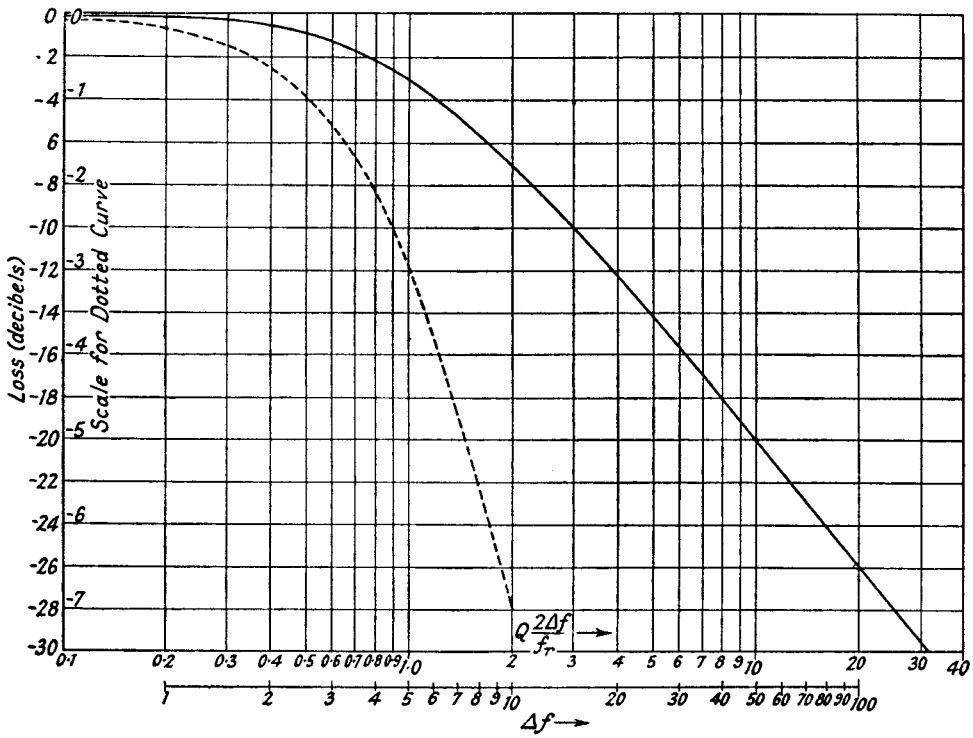

FIG. 4.3.—The Generalized Selectivity Curve for a Single Tuned Circuit.

Expression 4.8*c* is most important because it gives a generalized selectivity curve,[14] which enables the frequency response of any parallel tuned circuit to be obtained immediately. In Fig. 4.3 a curve is plotted of $10 \log_{10} (1+Q^2F^2)$ against QF. The scale of the latter is logarithmic. Only one-half of the curve is plotted since it is symmetrical about f_r, and the loss at equal numerical positive and negative values of Δf is the same.

Since $QF = \frac{2Q\Delta f}{f_r}$, $\Delta f = \frac{QF.f_r}{2Q}$

and $$\log_{10} \Delta f = \log_{10} QF + \log_{10} f_r - \log_{10} 2Q,$$

but for a given circuit f_r and Q are fixed, therefore

$$\log_{10} \Delta f = \log_{10} QF + \text{constant}.$$

Hence by sliding and locating correctly a logarithmic scale (identical with the QF scale) marked in Δf, the off-tune frequency, underneath the QF scale, the selectivity characteristic at different off-tune frequencies may be read directly. The correct position is obtained by locating $\Delta f' = \frac{f_r}{2Q}$ immediately beneath $QF = 1$. As an example, let $f_r = 1{,}000$ kc/s and $Q = 100$ be the constants of a particular tuned circuit, then

$$\Delta f' = \frac{f_r}{2Q} = \frac{1000}{200} = 5 \text{ kc/s}.$$

The Δf scale is therefore adjusted as shown in Fig. 4.3, with $\Delta f' = 5$ kc/s against $QF = 1$. The loss at any value of Δf may now be read directly, e.g., $\Delta f = 5$ and 10 kc/s gives a loss of 3 and 6·9 db. respectively.

The width of the pass band of any filter circuit is important, and in the case of a tuned circuit it is defined as the frequency range over which the loss is not greater than 3 db., i.e., between the frequency points at which the voltage has fallen to 0·707 of its maximum value. Referring to Fig. 4.3, the off-tune frequency corresponding to a loss of 3 db. is defined by

$$QF = \frac{Q2\Delta f}{f_r} = 1 \quad . \quad . \quad . \quad 4.9$$

so that the pass band $2\Delta f = \frac{f_r}{Q}$.

4.2.4. Constant Selectivity over a Range of Tuning Frequencies. In an ideal R.F. amplifier the overall selectivity should be independent of the tuning frequencies. From expression 4.8c we see that this requires a constant loss at a given off-tune frequency, i.e.,

$$1 + (QF)^2 = \text{constant at } \Delta f = \Delta f'$$

or $$QF' = \text{constant} = \frac{2Q\Delta f'}{f_r}$$

$$Q \propto f_r.$$

Hence for a constant selectivity characteristic over a range of resonant frequencies Q must vary linearly with f_r. For some types of coil, notably iron-cored coils, Q decreases as the frequency rises,

and the selectivity at low frequencies is much better than at high frequencies. This decrease of Q with increase of frequency has one advantage; the amplification of an R.F. stage is directly proportional to the dynamic resistance $R_D = Q\omega_r L$, which tends to remain more constant over the tuning range when Q decreases as the frequency increases. Permeability tuning,[16] i.e., tuning by variation of inductance with fixed capacitance, produces less change of selectivity and amplification over the tuning range because L decreases as the frequency increases. Its chief disadvantage is that variation of inductance is usually more difficult and costly to achieve than variation of capacitance over a wide tuning range.

In order to obtain constant selectivity from the normal type of coil it is necessary either to apply controlled reaction having greater effect at high than at low tuning frequencies, or to introduce resistance to reduce the Q of the coil as the tuning frequency is decreased. In the first method it is difficult to design a simple feedback circuit giving the desired Q compensation. The second method,[36] though not so satisfactory since it involves degrading the circuit, can be achieved by means of a simple resistance-reactance network.

It is essential in this method to obtain the highest Q possible at the highest frequency since the selectivity characteristic over the tuning range is to be entirely determined by the selectivity at the highest frequency. Let us assume that the highest possible Q is 150 for a medium wave band tuning inductance of 156 μH and that the Q varies as shown in Fig. 4.4. The variation of coil resistance is also plotted. Now $Q = \dfrac{\omega_r L}{R} = \dfrac{2\pi L}{R} f_r$, so that if Q is to be proportional to f_r the coil resistance R must remain constant over the range of f_r. It is therefore necessary to insert a resistance, in series with the coil, having a resistance variation with frequency shown by the curve $R_{required}$ (obtained from $R_{1,500\ kc/s} - R_{coil}$) in Fig. 4.4.

Let us consider the network shown in Fig. 4.4. It can be resolved into a series circuit of resistance and reactance of values, $R_2 = \dfrac{R_1 X_1^2}{R_1^2 + X_1^2}$ and $X_2 = X_1 \dfrac{R_1^2}{R_1^2 + X_1^2}$, where X_1 is the reactance of the L.C. arm. By a suitable choice of L_1 and C_1, X_1, and hence R_2, may be made zero at the highest tuning frequency. As the frequency is decreased X_1, and consequently R_2, increases, and this is the requirement for the compensating curve. By inserting this network in series with the coil it is possible to preserve an almost

constant resistance in the inductive arm over the tuning range. The variation of R_2 from the network cannot be made to give the exact R_2 curve required, but since there are three variables R_1, L_1 and C_1, three points of intersection are possible. The reactance term produced by the compensating network is usually very small

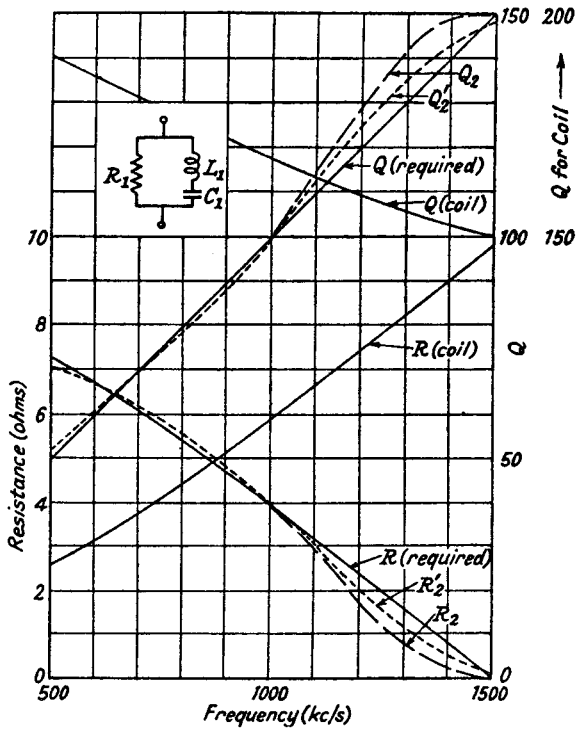

FIG. 4.4.—Correction Curves for a Tuned Circuit of Constant Q Value.

and can be neglected in comparison with the coil reactance. The reactance X_1 in the above expressions may be written

$$X_1 = j\omega L_1\left(1 - \frac{\omega_r^2}{\omega^2}\right)$$

$$= j\omega L_1\left(1 - \frac{f_r^2}{f^2}\right)$$

where

$$\omega_r = \frac{1}{\sqrt{L_1 C_1}}$$

To calculate the values of R_1, L_1 and C_1, we must fix the frequencies at which $R_2 = R_{required}$. Let us assume these are 600,

1,000 and 1,500 kc/s when $R_{required} = 6{\cdot}63$, $3{\cdot}94$ and 0 ohms respectively.

From $R_2 = 0$ at $f = 1{,}500$ kc/s, $f_r = 1{,}500$ kc/s.

At $f = 1{,}000$ kc/s.

$$3{\cdot}94 = R_1 \cdot \frac{[6{\cdot}28L_1(1 - (1{\cdot}5)^2)]^2}{R_1^2 + [6{\cdot}28L_1(1 - (1{\cdot}5)^2)]^2}$$

L_1 is in μH.

Hence
$$L_1^2 = \frac{3{\cdot}94R_1^2}{61{\cdot}8R_1 - 243} \quad . \quad . \quad . \quad . \quad . \quad 4.10.$$

For $f = 600$ kc/s

$$6{\cdot}63 = \frac{R_1\left[6{\cdot}28 \times 0{\cdot}6L_1\left(1 - \left(\frac{1{\cdot}5}{0{\cdot}6}\right)^2\right)\right]^2}{R_1^2 + \left[6{\cdot}28 \times 0{\cdot}6L_1\left(1 - \left(\frac{1{\cdot}5}{0{\cdot}6}\right)^2\right)\right]^2} \quad . \quad 4.11.$$

Replacing L_1 in 4.11 by 4.10 we find

$$R_1 = 7{\cdot}58\Omega$$

and from 4.10

$$L_1 = 1{\cdot}01\ \mu\text{H}$$

$$C_1 = \frac{1}{\omega_r^2 L} = 0{\cdot}01116\ \mu\text{F}.$$

The variation of R_2 with frequency is plotted in Fig. 4.4 (curve R_2). The variation of Q is also shown, and it can be seen to be almost identical with the required Q curve from 500 to 1,000 kc/s. Above 1,000 kc/s the departure is quite noticeable. If a calculation is made assuming f_r to be 1,600 kc/s, the curves R_2' and Q_2' result, and the discrepancy from 1,000 to 1,500 kc/s is much reduced, but from 600 to 1,000 kc/s it is less satisfactory. The values of the circuit constants are then

$$R_1 = 7{\cdot}8 \text{ ohms}, \quad L_1 = 0{\cdot}81\ \mu\text{H} \text{ and } C_1 = 0{\cdot}01225\ \mu\text{F}.$$

by making f_r still higher, the Q curve may be made to approximate even closer to the required up to 1,400 kc/s, but above this frequency the error is increased. The series reactance term (X_2) for the above R_1, L_1 and C_1 values has maximum effect at the lowest frequency (500 kc/s), and it reduces the inductance of the arm in which it is connected by approximately 0·5%, a negligible amount.

4.3. Coil Characteristics at Radio Frequencies.

4.3.1. Introduction. A coil possesses three characteristics of major importance when it is used for radio frequency amplifica-

tion purposes; they are its inductance, A.C. resistance and self-capacitance. To prevent undesirable pick-up and interaction between input and output circuits a metal screen is required round the coil, and its effect on the coil characteristics needs to be known.

4.3.2. The Inductance of a Coil. Calculation of the inductance of various types of air cored coils has formed the subject of many papers and it is possible to achieve very high accuracy of computation [1, 2] with some of the more common shapes of coil. For most practical purposes, however, a computation accuracy from 1 to 5% is sufficient, and the following simple formulae due to Wheeler [4] will be found most useful. Taking first the single-

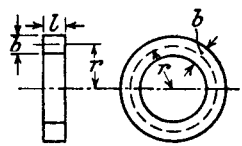

FIG. 4.5.—A Cylindrical Coil with Rectangular Section Winding Area.

layer helical solenoid—this is the coil of Fig. 4.5 with b = diameter of the wire forming the single layer—an approximate formula is

$$L = \frac{r^2N^2}{9r+10l}\ \mu\text{H} \quad . \quad . \quad . \quad . \quad 4.12$$

where l = length of the winding in inches
,, N = total number of turns on coil
and r = radius of the coil in inches to the centre of the wire layer. The error involved is less than 1% so long as $l > 0{\cdot}8r$. For values of l between $0{\cdot}8r$ to $0{\cdot}2r$ the following formula may be used with an error not exceeding 5%.

$$L = \frac{r^2N^2}{8r+11l} \quad . \quad . \quad . \quad . \quad 4.13.$$

An error not exceeding 2% over a range of r from 0 to $10l$ is obtained from

$$L = \frac{r^2N^2}{9r - \frac{r^2}{5l} + 10l} \quad . \quad . \quad . \quad 4.14.$$

Expression 4.13 is applicable to the thin spiral coil of one-wire thickness by replacing l by the breadth b, and taking r as the radius to the centre of the spiral face. The error is not greater than 5% so long as $b > 0{\cdot}2r$.

As an example of the single layer coil let us calculate the in-

ductance of a coil of 26 S.W.G. wire wound on a former of external radius 1 inch and 2 inches winding length.

Radius of wire = 0·009 inch.
Turns per inch of winding length with S.C.C. insulation = 50
Total number of turns = 100

using 4.12.

$$L = \frac{(1{\cdot}009)^2 100^2}{9(1{\cdot}009)+10(2)}$$
$$= 350\ \mu\text{H}.$$

A single-wire spiral of 1 inch breadth and inner radius of 1 inch using the same wire gives

$$b = 1,\ r = 1{\cdot}5,\ N = 50$$

and from 4.13.

$$L = \frac{(1{\cdot}5)^2 50^2}{12+11}$$
$$= 244\ \mu\text{H}.$$

Multilayer coils of approximately square section winding area may be calculated from

$$L = \frac{0{\cdot}8r^2N^2}{6r+9l+10b} \quad . \quad . \quad . \quad . \quad 4.15$$

with an error not exceeding 1% when l and b are approximately equal to $\frac{r}{2}$. A more accurate formula for small coil widths is

$$L = \frac{rN^2}{13\,5}\log_{10}\left(\frac{4{\cdot}9r}{l+b}\right)\mu\text{H} \quad . \quad . \quad . \quad 4.16$$

when the error is less than 3% if $(b+l) \leq r$.

Using 4.15, we will calculate the inductance of a coil of 26 S.W.G. S.C.C. wire of inner radius 1 inch, breadth 0·75 inch, and length 1 inch.

$$b = 0{\cdot}75 \text{ inch},\ l = 1 \text{ inch},\ r = 1+\frac{0{\cdot}75}{2} = 1{\cdot}375 \text{ inch}.$$

$$\text{Total turns} = \text{winding area} \times (\text{turns per inch})^2$$
$$= 0{\cdot}75 \times 1 \times 2{,}500$$
$$= 1{,}875.$$

$$L = \frac{0{\cdot}8(1{\cdot}375)^2(1875)^2}{6(1{\cdot}375)+9+7{\cdot}5}$$
$$= 215{,}000\ \mu\text{H}.$$

The accuracy of all the above formulae is reduced if the turn apacing is large and the equivalent inductance value at any par-

ticular frequency is influenced by skin effect and the coil distributed capacitance.

The inductance of single and multilayer coils has been also set out in the form of a series of abacs.[34]

For iron-cored coils the inductance depends on the permeability of the core material, and details are usually given by the makers of the latter.

4.3.3. The A.C. Resistance of a Coil. The effective resistance of a straight wire to A.C. currents is greater than to D.C. and it increases as frequency is increased. This is due to the fact that the magnetic flux, which produces a circular field around the conductor, also exists inside the conductor. The latter can be considered as made up of a series of concentric cylinders of elemental thickness, and the magnetic field surrounding each progressively decreases as the outside of the wire is approached. The surrounding field introduces an inductance component in each cylindrical element of the conductor and this component is greatest for that cylinder having the greatest surrounding magnetic field, i.e., the one nearest the centre of the wire. This inductance offers an impedance to the flow of current and there is therefore a tendency for the current to crowd to the outer edges or skin of the conductor. Increasing frequency means increasing effective inductive reactance and less current flow through the centre of the wire. At radio frequencies of about 1,000 kc/s, the current at the centre of the wire may be practically zero, and there is then little difference between a solid conductor and a thin hollow tube of the same external diameter. This concentration of current causes the resistance of a conductor at radio frequencies to be many times greater than its D.C. resistance.

If the wire is coiled, the current area is further restricted to the inside face nearest the coil former due to the magnetic field from adjacent turns, and there is usually a considerable increase in R.F. resistance. Coiling a wire initially increases the inductance at a much greater rate than resistance and there are optimum coil dimensions and wire diameters for minimum resistance with a given inductance. The classic paper on the subject is that [3, 18] by Butterworth. The ratio of A.C. to D.C. resistance is proportional to $\sqrt{\frac{\mu f}{\rho}}$, where μ is the average permeability of the material (conductor and core) in the magnetic field produced by the current in the conductor, f is the frequency, and ρ is the resistivity of the conductor. It is interesting to note that a magnetic material in the circuit (this

means increased μ) increases the A.C./D.C. coil resistance ratio as does decrease of ρ, i.e., a good conductor shows much greater change of resistance under A.C. operation than a poor conductor, and an iron-cored coil shows a much greater ratio change of resistance than does an air-cored coil.

General conclusions [28] on realizing minimum resistance depend on what parameters are fixed. There is an optimum wire diameter to winding pitch ratio, and it is given by $d_w \simeq \frac{0{\cdot}7l}{N}$, where l = length of coil and N = turns per layer. For a given diameter of wire, minimum resistance is obtained in single layer coils with a length to radius ratio $\left(\frac{l}{r}\right)$ of 0·6 to 0·9, single wire spirals require a breadth to mean radius ratio of approximately 1, and for multilayer coils the following relationship should be satisfied $5b+3l \simeq 2(b+r)$. Resistance is decreased for a given inductance by using larger gauge wire, and when there are no restrictions on wire size, resistance, for a given inductance value, coil radius and optimum wire diameter, is decreased by increasing the length of a single layer solenoid—this really means using a larger gauge wire as length is increased—but there is little advantage in making $l > 4r$. This gives a more economical shape than that cited above for a fixed wire diameter and is the one most used in practice. Multi-strand litz wire is effective for reducing resistance at frequencies up to about 5 Mc/s.

Additional sources of increased coil resistance are to be found in dielectric losses in the insulating material (these are greatly increased if the insulation is subject to moisture absorption, and it is essential to treat the coil with a non-hygroscopic varnish), coil self-capacitance, and eddy currents in the shield surrounding the coil. Coil self-capacitance is shown in Section 4.3.4 to increase the effective resistance of a coil. Losses in the coil shield are reduced by reducing the coupling to the screen, i.e., by increasing the ratio of shield-to-coil diameter (the ratio [28] should not be less than 2/1) and by using screen material of lowest resistivity.

4.3.4. Coil Self-Capacitance. Coil self-capacitance is caused by electrostatic coupling between turns, and between turns and earth. It is highest in multi-layer coils, in which there is a high potential between layers. To reduce self-capacitance it is essential to separate high potential points, thus a two-layer coil is preferably wound with interleaved turns—the third and fifth turns being wound on top of, and between the first and second and second and

fourth turns, etc. Winding in two separate layers, one on top of the other, causes a large self-capacitance. Large inductances, e.g., for R.F. chokes, are best separated into a number of independent sections, so reducing the potential between the ends of each section. The self-capacitance acts in parallel with the coil and tends to increase the equivalent inductance and series resistance. Referring to Fig. 4.1, let us suppose that the actual inductance L and series resistance R of the coil are paralleled by a self-capacitance C_0 (shown dotted). The impedance of the coil circuit is

$$\begin{aligned} Z &= \frac{\frac{R+j\omega L}{j\omega C_0}}{R+j\omega L+\frac{1}{j\omega C_0}} \\ &= \frac{R+j\omega L}{1-\omega^2 LC_0+j\omega C_0 R} \\ &= \frac{(R+j\omega L)(1-\omega^2 LC_0-j\omega C_0 R)}{(1-\omega^2 LC_0)^2+(\omega C_0 R)^2} \\ &= \frac{R}{(1-\omega^2 LC_0)^2+(\omega C_0 R)^2}+\frac{j\omega L(1-\omega^2 LC_0)-\omega C_0 R^2}{(1-\omega^2 LC_0)^2+(\omega C_0 R)^2} \qquad 4.17 \\ &= R_A+j\omega L_A \end{aligned}$$

where R_A and L_A are the apparent resistance and inductance of the coil.

If C_0 is small, the natural frequency of the coil is high and $(\omega C_0 R)^2$ and $\omega C_0 R^2$ can be neglected in comparison with the other factors.

$$\therefore\ R_A = \frac{R}{(1-\omega^2 LC_0)^2} \quad . \quad . \quad . \quad . \quad . \quad 4.18a$$

$$L_A = \frac{L}{(1-\omega^2 LC_0)} \quad . \quad . \quad . \quad . \quad . \quad 4.18b$$

and

$$\begin{aligned} Q_A &= \frac{\omega L_A}{R_A} = \frac{\omega L}{R}(1-\omega^2 LC_0) \quad . \quad . \quad . \quad 4.18c \\ &= Q(1-\omega^2 LC_0). \end{aligned}$$

Since the natural frequency due to resonance of L and C_0 can be assumed to be much higher than the highest tuning frequency in the range over which the coil is to be used, $\omega^2 LC_0 \ll 1$ and $(1-\omega^2 LC_0) < 1$. Hence the apparent series resistance and inductance of the coil are increased by the self capacitance; R_A is increased at a much greater rate than L_A, so that the apparent or effective Q of the circuit is reduced. The ratios of R_A/R, L_A/L and Q_A/Q vary with frequency, the first two increasing and the third

decreasing as the tuning frequency is increased. The tuning frequency condition is given by

$$\omega L_A = \frac{1}{\omega C}$$

where C = tuning capacitance setting required for resonance.

$$\omega L_A = \frac{\omega L}{1 - \omega^2 L C_0} = \frac{1}{\omega C}$$

$$\omega^2 L C = 1 - \omega^2 L C_0$$

or

$$\omega^2 = \frac{1}{L(C+C_0)}.$$

Replacing ω^2 in 4.18*a*, *b* and *c* by this value gives

$$R_A = R\left(1+\frac{C_0}{C}\right)^2. \quad . \quad . \quad . \quad 4.19a$$

$$L_A = L\left(1+\frac{C_0}{C}\right) . \quad . \quad . \quad . \quad 4.19b$$

$$Q_A = Q/\left(1+\frac{C_0}{C}\right) . \quad . \quad . \quad . \quad 4.19c.$$

The above expressions show quite clearly that the effect of self-capacitance is most pronounced at the highest tuning frequencies, for which C is small.

Average values of self-capacitance are 10 — 13 $\mu\mu$F, 7 to 10 $\mu\mu$F and 4 to 7 $\mu\mu$F for the long, medium and short wave ranges.

4.3.5. The Effect of Screening on the Inductance and Resistance of a Coil.[20] A shield surrounding a coil acts as a short-circuited turn coupled to the coil and reflects an impedance into the coil in the same manner as the aerial reflects an impedance into the first tuned circuit of a receiver (Section 3.4). The reflected impedance is equivalent to a resistance and negative inductance of values

$$\frac{\omega^2 M^2 R_s}{|Z_s|^2} \text{ and } -\frac{\omega^2 M^2 L_s}{|Z_s|^2} \text{ (expression 3.18)}$$

in series with the inductance of the coil, where $Z_s = R_s + j\omega L_s$ and R_s and L_s are the equivalent resistance and inductance of the short-circuited turn representing the shield. The effective resistance of the coil is therefore increased to

$$R\left[1+\frac{\omega^2 M^2 R_s}{|Z_s|^2 R}\right]$$

and its effective inductance reduced to

$$L\left[1 - \frac{\omega^2 M^2 L_s}{|Z_s|^2 L}\right]$$

As estimation of the effect of enclosing a coil in a screen has been made by Kaden [17] and more recently by Bogle,[33] who gives some very useful empirical formulae for the change in inductance and resistance. The following formula, applicable to single-layer coils, gives the ratio of the change in inductance (the difference between the unscreened and screened inductance values, L_1 and L_2 respectively) to the unscreened inductance value when the screen is of non-magnetic material of good electrical conductivity.

$$\frac{\Delta L}{L_1} = \frac{L_1 - L_2}{L_1} = \frac{\frac{l}{g}}{\left(\frac{l}{g} + 1{\cdot}55\right)} \left(\frac{r_c}{r_s}\right)^2 . \quad . \quad 4.20$$

where l = length of coil
$g = r_s - r_c$ = radial gap between the screen and coil
r_s = radius of screen.
r_c = radius of the coil.

Dimensions may be in inches or centimetres, as the result is in ratio form.

This formula has an error not exceeding 2% so long as the distance between the ends of the coil and the screen is not less than $2g$.

Thus if we place a single layer coil of winding length 1 inch and radius 1 inch inside a screen of radius 1·5 inches the ratio reduction of inductance is

$$\frac{\Delta L}{L_1} = \frac{\frac{1}{0{\cdot}5}}{\left(\frac{1}{0{\cdot}5} + 1{\cdot}55\right)} \left(\frac{1{\cdot}0}{1{\cdot}5}\right)^2$$

$$= \frac{2}{3{\cdot}55} \times 0{\cdot}445 = 0{\cdot}251.$$

Under most practical conditions the thickness of the shield is determined by mechanical rather than electrical considerations, as the eddy currents do not penetrate deeply. The minimum thickness for adequate shielding is a function of the resistivity ρ of the material and the frequency f, the actual relationship being that the thickness (inches)

$$t > \frac{2}{2{\cdot}54\pi}\sqrt{\frac{\rho}{f}}$$

$$> 0{\cdot}251\sqrt{\frac{\rho}{f}}$$

where ρ is in micro-ohms per cubic centimetre

f is in kilocycles per second.

For copper $\rho = 1{\cdot}68\ \mu\Omega$/c.c., so that for a minimum frequency of 100 kc/s, the thickness must be greater than $0{\cdot}251\sqrt{\frac{1{\cdot}68}{100}} = 0{\cdot}0325$ inch.

Most coil screens for mechanical rigidity require to be made of at least 20 S.W.G., which gives a thickness of 0·036 inch, a value greater than that required for electrical screening at this low frequency. At higher frequencies the required thickness decreases.

Bogle also gives the following formula for the ratio of the change in inductance to the screened inductance due to eccentricity of the axes of the coil and screen.

$$\frac{\delta L}{L_2} = 0{\cdot}535\,\frac{e^2}{g^2}\,\frac{g}{l+g}\cdot\frac{r_s}{r_c}\cdot\frac{\Delta L}{L_2} \qquad . \qquad . \qquad . \qquad 4.21$$

where e = the eccentricity of the axes.

Let us suppose the coil in the first example has an eccentricity of 0·02 inch.

$$\frac{\delta L}{L_2} = 0{\cdot}535\cdot\left(\frac{0{\cdot}02}{0{\cdot}5}\right)^2\cdot\frac{0{\cdot}5}{1{\cdot}5}\cdot\frac{1{\cdot}5}{1}\cdot\frac{\Delta L}{L_2}$$

$$= 4{\cdot}28 \times 10^{-4}\frac{\Delta L}{L_2}$$

$$\frac{\Delta L}{L_2} = \frac{L_1 - L_2}{L_2} = \frac{L_1}{L_2} - 1.$$

From the previous example

$$\frac{\Delta L}{L_1} = 1 - \frac{L_2}{L_1} = 0{\cdot}251$$

$$\therefore \frac{L_2}{L_1} = 0{\cdot}749$$

and

$$\frac{L_1}{L_2} = 1{\cdot}336$$

$$\therefore \frac{\delta L}{L_2} = 4{\cdot}28 \times 10^{-4} \times 0{\cdot}336$$

$$= 1{\cdot}43 \times 10^{-4}.$$

It is clear from this that eccentricity is a second-order effect and for most practical purposes may be neglected.

The increase in resistance to be expected due to placing the coil in a screen can be stated empirically as

$$\Delta R = \frac{\Delta L}{L_1}\left[\frac{N}{l}\,\frac{r_c}{r_s}\right]^2 . 4\pi^2 r_s l\sqrt{\rho f} . 10^{-6} \text{ ohms} \quad . \quad . \quad 4.22a$$

$$= 3{\cdot}95 \times 10^{-5}\frac{\Delta L}{L_1}\,\frac{N^2 r_c^{\,2}}{l r_s}\sqrt{\rho f} \text{ ohms} \quad . \quad . \quad 4.22b$$

where N = total turns of coil

ρ = resistivity of the screen material (μ ohms per cubic centimetre)

f = frequency in kc/s.

Expression 4.22*b* gives the increment in resistance due to losses in the screen, and this will not necessarily be the actual change in resistance that would be measured for a given coil. Referring to Expression 4.19*a* in the previous section, we note that owing to self-capacitance the apparent resistance of the coil is increased by $R\left[\frac{2C_0}{C}+\frac{C_0^2}{C^2}\right]$, where C is the value of the tuning capacitance. Now the inductance of the coil is reduced by placing it in a screen so that C must be increased for a given tuning frequency ; this reduces the value of apparent resistance, thus offsetting the increase in resistance due to screen losses. In a particular case we may therefore find that screening reduces the apparent coil resistance ; however, the apparent value of Q for the screened coil will be less than that of the unscreened coil owing to the reduction in inductance by the screening.

4.4. Types of R.F. Coupling Circuits.

4.4.1. The Tapped Parallel Tuned Circuit.[29] A generator supplying a parallel-tuned circuit may be connected across the complete coil or across only a part of it. Certain advantages may be gained by tapping down the coil. If the internal resistance of the generator is less than the dynamic resistance (R_D) of the tuned circuit, the output voltage across the latter is increased and the selectivity characteristic improved by tapping down. There is actually an optimum tapping point for maximum amplification, but maximum selectivity is obtained with the lowest tap.

When the generator resistance is greater than R_D, tapping down decreases the output voltage. This has advantages in the case of a valve generator having high g_m and comparatively high anode-grid capacitance. Feedback through this capacitance may cause instability if the voltage amplification of the anode circuit is high. Tapping down enables the latter to be reduced.

To estimate the performance of the tapped circuit the impedance between the tapping points, and the overall amplification must be calculated. The equivalent circuit is shown in Fig. 4.6, and the

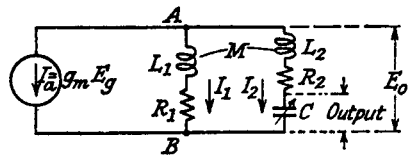

FIG. 4.6.—The Tapped Tuned Circuit.

current-voltage equations are given below. It is assumed that the valve has infinite resistance—a correction to the overall amplification is made later for a valve resistance R_a comparable with R_D—and that the resistances (R_1 and R_2) of the two sections of the coil are divided in proportion to the inductances L_1 and L_2.

$$I_a = I_1 + I_2 \quad . \quad . \quad . \quad . \quad 4.23a$$

$$I_1(R_1+j\omega L_1) - I_2 j\omega M = I_2\left[R_2+j\left(\omega L_2 - \frac{1}{\omega C}\right)\right] - I_1 j\omega M \quad 4.23b$$

$$\therefore\ I_1[R_1+j\omega(L_1+M)] = I_2\left[R_2+j\left[\omega(L_2+M) - \frac{1}{\omega C}\right]\right].$$

But the total coil inductance $L_T = L_1+L_2+2M$, so that

$$I_1[R_1+j\omega(L_1+M)] = I_2\left[R_2 - j\omega(L_1+M)+j\left(\omega L_T - \frac{1}{\omega C}\right)\right] \quad 4.23c.$$

Since $$\omega L_T - \frac{1}{\omega C} = \omega_r L_T\left(\frac{\omega}{\omega_r} - \frac{\omega_r}{\omega}\right) = \omega_r L_T F.$$

$$I_1 = \frac{I_2[R_2 - j\omega(L_1+M)+j\omega_r L_T F]}{R_1+j\omega(L_1+M)} \quad . \quad . \quad 4.23d.$$

Replacing 4.23*d* in 4.23*a*

$$I_a = \frac{I_2[R_T+j\omega_r L_T F)}{R_1+j\omega(L_1+M)} \quad . \quad . \quad . \quad . \quad . \quad . \quad 4.23e$$

where $R_T = R_1+R_2$, the total coil resistance.

$$E_0 = I_1(R_1+j\omega L_1) - I_2 j\omega M.$$

$$= \frac{I_2.[(R_1+j\omega L_1)(R_2 - j\omega(L_1+M)+j\omega_r L_T F) - j\omega M(R_1+j\omega(L_1+M)]}{R_1+j\omega(L_1+M)} \quad 4.24$$

$$= \frac{I_a[(R_1+j\omega L_1)(R_2 - j\omega(L_1+M)+j\omega_r L_T F) - j\omega M(R_1+j\omega(L_1+M))]}{R_T+j\omega_r L_T F}.$$

The impedance between the tapping points AB is

$$Z_{AB} = \frac{E_0}{I_a} = \frac{(R_1+j\omega L_1)(R_2 - j\omega(L_1+M)+j\omega_r L_T F) - j\omega M(R_1+j\omega(L_1+M))}{R_T+j\omega_r L_T F}$$

$$= \frac{(R_1+R_2+j\omega_r L_T F)(R_1+j\omega L_1) - [R_1+j\omega(L_1+M)]^2}{R_T+j\omega_r L_T F}$$

$$= R_1+j\omega L_1 - \frac{[R_1+j\omega(L_1+M)]^2}{R_T+j\omega_r L_T F} \quad . \quad . \quad . \quad . \quad 4.25a.$$

If $$R_1 \ll j\omega L_1 \ll \frac{[R_1+j\omega(L_1+M)]^2}{R_T+j\omega_r L_T F}$$

$$Z_{AB} \simeq \frac{\omega^2(L_1+M)^2}{R_T+j\omega_r L_T F} = \frac{\omega^2(L_1+M)^2}{R_T(1+jQF)} \quad . \quad . \quad 4.25b$$

where $$Q = \frac{\omega_r L}{R_T}.$$

At resonance $$F = 0 \text{ and}$$

$$Z_{AB} \simeq \frac{\omega_r{}^2(L_1+M)^2}{R_T} \quad . \quad . \quad . \quad 4.25c.$$

The overall amplification (A) of the stage is

$$A = \frac{I_2}{E_g j\omega C}.$$

Replacing I_2 with the value from 4.23*e*

$$A = \frac{I_a[R_1+j\omega(L_1+M)]}{jE_g\omega CR_T(1+jQF)}$$

$$\simeq g_m \frac{(L_1+M)}{CR_T(1+jQF)}$$

where $$I_a = g_m E_g \text{ and } R_1 \ll \omega(L_1+M)$$

$$|A| = g_m \frac{L_1+M}{CR_T\sqrt{1+(QF)^2}} \quad . \quad . \quad . \quad 4.26a.$$

At resonance

$$|A_r| = g_m \frac{(L_1+M)}{CR_T}$$

$$= g_m R_D \frac{(L_1+M)}{L_T} \quad . \quad . \quad . \quad 4.26b$$

where $$R_D = \frac{L_T}{CR_T}.$$

The selectivity, given by the ratio of $|A_r|$ to $|A|$ is $\sqrt{1+(QF)^2}$, and this is identical with that of the untapped circuit. This is

expected since R_a is assumed to be infinite. The overall gain is thus reduced in the ratio $\frac{L_1+M}{L_T}$ by tapping down but the selectivity is unaltered. When R_a is comparable with Z_{AB} the expression for (I_1+I_2) becomes

$$I_1+I_2 = g_m E_g \cdot \frac{R_a}{R_a+Z_{AB}}$$

$$A = \frac{g_m R_a}{R_a+\frac{\omega^2(L_1+M)^2}{R_T(1+jQF)}} \cdot \frac{R_D(L_1+M)}{(1+jQF)L_T} \quad . \quad 4.27a$$

and

$$A_r = \frac{g_m R_a}{R_a+R_D\left(\frac{L_1+M}{L_T}\right)^2} \cdot \frac{R_D(L_1+M)}{L_T} \quad . \quad 4.27b.$$

Differentiating 4.27*b* with respect to (L_1+M) and equating to 0 gives for a maximum A_r

$$R_a = \frac{R_D(L_1+M)^2}{L_T{}^2} = \frac{\omega^2(L_1+M)^2}{R_T}$$

so that the optimum tapping point is at $R_a = Z_{AB(resonance)}$ and

$$A_r = \frac{1}{2} \frac{g_m R_D(L_1+M)}{L_T}.$$

The Selectivity Ratio

$$\frac{|A_r|}{|A|} = \frac{\sqrt{(R_aQF)^2+\left[R_a+R_D\left(\frac{L_1+M}{L_T}\right)^2\right]^2}}{R_a+R_D\left(\frac{L_1+M}{L_T}\right)^2}$$

$$= \sqrt{1+(QF)^2\left[\frac{R_a}{R_a+R_D\left(\frac{L_1+M}{L_T}\right)^2}\right]^2}$$

is a maximum when R_a is infinite or (L_1+M) is zero, and is $\sqrt{1+\left(\frac{QF}{2}\right)^2}$ when $R_a = R_D \cdot \left(\frac{L_1+M}{L_T}\right)^2$. Hence selectivity is halved at the optimum amplification tapping point.

4.4.2. The Transformer Coupled Tuned Circuit.[9] The tapped tuned circuit is not an ideal practical arrangement and a better method is to use transformer coupling. This has two advantages ; a coupling coil is more easily adjusted than a tapping point,

and the tuned circuit is isolated from the positive H.T. voltage. The circuit is given in Fig. 4.7 and the equations are

$$E_0 = I(R_1+j\omega L_1)+I_2 j\omega M \quad . \quad . \quad . \quad 4.28a$$

$$0 = I_2[R_T+j\omega_r L_T F]+Ij\omega M \quad . \quad . \quad 4.28b$$

where $\omega_r L_T F = \left(\omega L_T - \frac{1}{\omega C}\right)$.

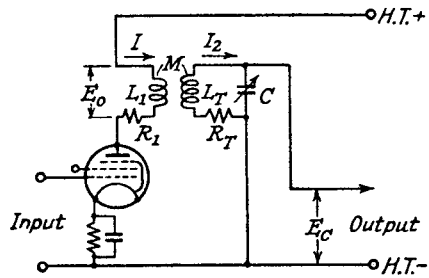

FIG. 4.7.—The Transformer Coupled Circuit.

From 4.28*b*

$$I_2 = -\frac{Ij\omega M}{R_T+j\omega_r L_T F} = -\frac{Ij\omega M}{R_T(1+jQF)}$$

$$\therefore\ E_0 = I\left[R_1+j\omega L_1+\frac{\omega^2 M^2}{R_T+j\omega_r L_T F}\right]$$

and

$$Z_0 = \frac{E_0}{I} = R_1+j\omega L_1+\frac{\omega^2 M^2}{R_T+j\omega_r L_T F}.$$

If

$$R_1+j\omega L_1 \ll \frac{\omega^2 M^2}{R_T+j\omega_r L_T F}$$

$$Z_0 = \frac{\omega^2 M^2}{R_T+j\omega_r L_T F} \quad . \quad . \quad . \quad . \quad 4.29a$$

and at resonance

$$Z_{0r} = \frac{\omega_r{}^2 M^2}{R_T} = R_D \frac{M^2}{L_T{}^2} \quad . \quad . \quad . \quad 4.29b.$$

The overall amplification A is

$$A = \frac{E_c}{E_g} = \frac{I_2}{E_g j\omega C} = \frac{-I}{j\omega C}\cdot\frac{j\omega M}{R_T(1+jQF)Eg}.$$

If R_a is very large $\mathrm{I} = \mathrm{I}_a = g_m E_g$

$$\therefore\ A = -g_m \frac{M}{CR_T(1+jQF)}$$

$$= -g_m \frac{R_D}{1+jQF}\cdot\frac{M}{L_T} \quad . \quad . \quad . \quad 4.30a.$$

The negative sign indicates that the sign of the mutual inductance coupling between primary and tuned secondary is negative, and it can be ignored when there is no other coupling between L_1 and L_T.

At resonance $$A_r = \frac{g_m M}{C R_T} = \frac{g_m R_D M}{L_T} \quad . \quad . \quad . \quad 4.30b.$$

When R_a is infinite (the assumption made above), amplification is reduced but selectivity is unchanged by reducing the coupling. For R_a comparable with Z_0, amplification is

$$A = \frac{g_m R_a}{R_a + \dfrac{\omega^2 M^2}{R_T(1+jQF)}} \cdot \frac{M}{C R_T(1+jQF)} \quad . \quad . \quad 4.31a$$

and the maximum value at resonance is obtained when $R_a = \dfrac{\omega^2 M^2}{R_T}$

Hence $$A_{r(max.)} = \frac{1}{2} g_m R_D \frac{M}{L_T} \quad . \quad . \quad . \quad 4.31b.$$

Selectivity is greatest when the coupling is least, and for maximum gain it is equivalent to that of a circuit of $\dfrac{Q}{2}$. Almost all the results are identical with those for a tapped circuit if M is replaced by (L_1+M).

It is clear from the above expressions that the primary coil inductance and resistance should be as small as possible and the coupling to the tuned circuit as large as possible. The position of the primary coil with respect to the tuned circuit is important as stray capacitive coupling between the two seriously modifies the selectivity characteristic. The primary must therefore be wound over the earthed end of the tuned coil.

4.4.3. The Choke-Capacitance Coupled Tuned Circuit. Another possible form of coupling to the tuned circuit is by R.F. choke and capacitance. Resistance-capacitance cannot be considered since a very high resistance is required for low damping of the tuned circuit, and this results in a very low D.C. anode voltage. The chief advantage of choke coupling is that the tuned circuit can be isolated from the positive H.T. voltage. The R.F. choke needs careful design; its inductance should be much higher (100 times at least) than the tuning coil and its self-capacitance should be low. The natural frequency of the choke must be well outside the frequency range of the tuned circuit if uneven frequency response and amplification characteristics are to be avoided. Generally the

natural frequency is much lower than the lowest tuned circuit frequency, and it therefore presents a high capacitive reactance over the tuning frequency range. This small equivalent capacitance can be compensated, for ganging purposes, by adjustment of the tuning capacitor trimmer. The coupling capacitance from the anode to the tuned circuit is not critical and a value of 0·0001 μF. is generally suitable. The minimum value of coupling capacitance is determined by R_D, and since R_D and this reactance are in phase quadrature a value of $X_c = \frac{R_D}{10}$ can give a voltage transfer of approximately 98%.

4.5. Band-Pass Tuned Circuits.[8, 10, 13, 15, 21, 22, 23, 24, 26]

4.5.1. Introduction. Band-pass tuned circuits are employed in R.F. amplifiers to obtain a wide and flat pass-band with sharp cut-offs. They consist usually of two tuned circuits coupled together by inductive or capacitive reactance, or a mixture of both. The theory of such band-pass filters is detailed in Chapter 7, and it is only necessary to indicate the special modifications which result from the need for variable tuning. The ideal tunable band-pass filter should maintain constant band width at all tuning frequencies, and we must examine the effect of different forms of coupling on the pass-band. The Howe method, detailed in Section 7.2, enables a preliminary examination of the pass-band to be made for a filter, having no resistance elements, as the tuned circuit resonant frequency is varied. Self-inductance coupling is not considered in the analysis, because it is but rarely employed in tunable filters.

4.5.2. Shunt Capacitance Coupling. The terms used to designate the position of the coupling are those normally employed in network theory as stated in Section 3.4.3. Taking first shunt (sometimes called common) capacitance coupling, the circuit is that

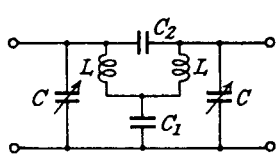

FIG. 4.8*a*.—Combined Series and Shunt Capacitance Coupling.

of Fig. 4.8*a* (showing combined shunt and series coupling) with the series capacitance C_2 open circuited. The peak frequencies are

$$f_2 = \frac{1}{2\pi\sqrt{\frac{LCC_1}{2C+C_1}}} \text{ and } f_1 = \frac{1}{2\pi\sqrt{LC}}$$

and for the trough or mid frequency

$$f_m = \frac{1}{2\pi\sqrt{\frac{LCC_1}{C+C_1}}}.$$

The pass-band is determined by $f_2 - f_1$ and

$$f_2 - f_1 = \frac{1}{2\pi}\left(\frac{1}{\sqrt{\frac{LCC_1}{2C+C_1}}} - \frac{1}{\sqrt{LC}}\right)$$

$$= \frac{1}{2\pi\sqrt{LC}}\left(\sqrt{\frac{2C}{C_1}+1} - 1\right) \quad . \quad . \quad 4.32a.$$

Expanding $\left(\frac{2C}{C_1}+1\right)^{\frac{1}{2}}$ by the Binomial Theorem

$$\left(\frac{2C}{C_1}+1\right)^{\frac{1}{2}} = 1+\frac{1}{2}\frac{2C}{C_1} - \frac{1}{8}\left(\frac{2C}{C_1}\right)^2 + \ldots$$

$$= 1+\frac{C}{C_1} - \frac{1}{2}\left(\frac{C}{C_1}\right)^2 + \ldots$$

$= 1+\frac{C}{C_1}$, when $C \ll C_1$, as is generally the case.

Thus $$f_2 - f_1 = \frac{1}{2\pi\sqrt{LC}} \cdot \frac{C}{C_1} = f_1\frac{C}{C_1} \quad . \quad . \quad 4.32b.$$

The semi-band width is

$$\Delta f = \frac{f_2 - f_1}{2} = \frac{f_1}{2}\frac{C}{C_1} \simeq \frac{f_m}{2}\frac{C}{C_1} \quad . \quad . \quad 4.33$$

for f_1 is very nearly equal to f_m, when Δf is small compared with f_m. Since $C \simeq \frac{1}{\omega_m^2 L}$, $\Delta f \simeq \frac{1}{8\pi^2 L C_1 f_m}$, so that Δf decreases as f_m is increased. It is plotted against f_m as curve 1, Fig. 4.9, for $L = 156$ μH and $C_1 = 0{\cdot}0162$ μF. The latter gives $\Delta f = 10$ kc/s at $f_m = 500$ kc/s falling to $\Delta f = 3{\cdot}33$ kc/s at $f_m = 1{,}500$ kc/s.

4.5.3. Series Capacitance Coupling. The circuit diagram for series capacitance coupling is that of Fig. 4.8*a*, with the shunt capacitance C_1 short circuited. The band-width is

$$f_2 - f_1 = \frac{1}{2\pi\sqrt{LC}}\left[1 - \frac{1}{\sqrt{1+\frac{2C_2}{C}}}\right] = f_1\frac{C_2}{C}$$

and the semi-band-width

$$\Delta f = \frac{f_1}{2}\frac{C_2}{C} \simeq \frac{f_m C_2}{2C} \quad . \quad . \quad . \quad 4.34.$$

Replacing C by $\frac{1}{\omega_m^2 L}$, $\Delta f \simeq 2\pi^2 L C_2 f_m^3$, and it increases as f_m increases.

It is plotted against f_m as curve 2, Fig. 4.9, for $L = 156$ μH and $C_2 = 0{\cdot}963$ $\mu\mu$F. The value of Δf is 10 kc/s at $f_m = 1{,}500$ kc/s, falling to 0·37 kc/s at $f_m = 500$ kc/s. Curve 2 is in the reverse direction to curve 1 and it would appear possible by combining the two curves to obtain a more constant band-width over the tuning range.

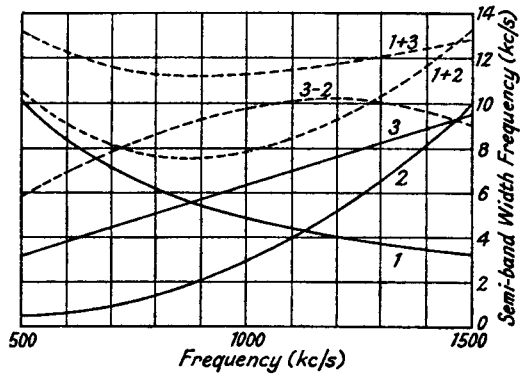

FIG. 4.9.—The Variation of Semi-Band-Width for Different Types of Coupling.
Curve 1.—Shunt Capacitance Coupling.
Curve 2.—Series Capacitance Coupling.
Curve 3.—Mutual Inductance Coupling.

4.5.4. Combined Shunt and Series Capacitance Coupling. The peak frequencies for combined capacitance coupling (Fig. 4.8*a*) are

$$f_2 = \frac{1}{2\pi\sqrt{L\left(\frac{CC_1}{2C+C_1}\right)}}; \text{ and } f_1 = \frac{1}{2\pi\sqrt{L(C+2C_2)}}$$

$$f_2 - f_1 = \frac{1}{2\pi\sqrt{LC}}\left[\sqrt{\frac{2C}{C_1}+1} - \frac{1}{\sqrt{\frac{2C_2}{C}+1}}\right]$$

$$\Delta f \simeq \frac{f_m}{2}\left[\frac{C}{C_1}+\frac{C_2}{C}\right] \quad . \quad . \quad . \quad . \quad . \quad . \quad 4.35.$$

Hence by adding curves 1 and 2, we obtain the semi-band-width variation for the combined couplings over the tuning frequency

range. The result is curve (1+2) Fig. 4.9, showing a much reduced semi-band-width variation.

4.5.5. Mutual Inductance Coupling. The semi-band-width for mutual inductance coupling is

$$\Delta f = \frac{1}{\pi\sqrt{LC}}\left[\frac{1}{\sqrt{1-\frac{M}{L}}} - \frac{1}{\sqrt{1+\frac{M}{L}}}\right]$$

$$\Delta f \simeq \frac{f_m}{2}\frac{M}{L} \quad . \quad . \quad . \quad . \quad . \quad . \quad . \quad 4.36.$$

Δf is plotted against f_m as curve 3, Fig. 4.9, and it rises linearly from 3·2 kc/s at 500 to 9·6 kc/s at 1,500 kc/s for $M = 2$ μH.

4.5.6. Combined Mutual Inductance and Shunt Capacitance Coupling.[5] Let us suppose that we have a combination

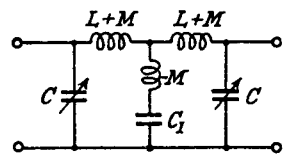

FIG. 4.8*b*.—Combined Mutual Inductance and Shunt Capacitance Coupling.

of negative mutual inductance and shunt capacitance coupling (Fig. 4.8*b*). The peak frequencies are

$$f_2 = \frac{1}{2\pi\sqrt{\frac{(L-M)CC_1}{2C+C_1}}} \text{ and } f_1 = \frac{1}{2\pi\sqrt{(L+M)C}}$$

$$f_2 - f_1 = \frac{1}{2\pi\sqrt{LC}}\left[\sqrt{\frac{\frac{2C}{C_1}+1}{1-\frac{M}{L}}} - \frac{1}{\sqrt{1+\frac{M}{L}}}\right] \quad . \quad . \quad 4.37a.$$

Expanding by the Binomial Theorem and assuming second-order terms to be negligible

$$f_2 - f_1 = \frac{1}{2\pi\sqrt{LC}}\left[\left(1+\frac{M}{2L}+\frac{C}{C_1}\right) - \left(1-\frac{M}{2L}\right)\right]$$

$$\simeq f_m\left[\frac{M}{L}+\frac{C}{C_1}\right] \quad . \quad . \quad . \quad . \quad . \quad 4.37b$$

or

$$\Delta f = \frac{f_m}{2}\left[\frac{M}{L}+\frac{C}{C_1}\right] \quad . \quad . \quad . \quad . \quad . \quad 4.37c.$$

For combined coupling we must add the curves 1 and 3 of Fig. 4.9,

and the result is curve (1+3). It is seen that this curve is an improvement on curves 1 and 3. As a general rule we shall find that combined shunt capacitance and negative mutual inductance gives a more constant band-width than combined shunt and series capacitance coupling.

If M is positive

$$\Delta f = \frac{f_m}{2}\left[\frac{C}{C_1} - \frac{M}{L}\right] \quad . \quad . \quad . \quad 4.37d$$

and curve 3 is subtracted from curve 1, thereby increasing the band-width variation.

4.5.7. Combined Positive Mutual Inductance and Series Capacitance Coupling. The circuit diagram for this coupling is shown in Fig. 4.8c.

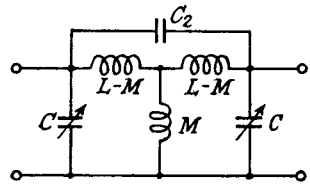

FIG. 4.8c.—Combined Mutual Inductance and Series Capacitance Coupling.

$$f_2 = \frac{1}{2\pi\sqrt{(L+M)C}} \text{ and } f_1 = \frac{1}{2\pi\sqrt{(L-M)(C+2C_2)}}$$

$$f_2 - f_1 = \frac{1}{2\pi\sqrt{LC}}\left[\frac{1}{\sqrt{1+\frac{M}{L}}} - \frac{1}{\sqrt{\left(1-\frac{M}{L}\right)\left(1+\frac{2C_2}{C}\right)}}\right]$$

$$\simeq f_m\left[1 - \frac{M}{2L} - \left(1+\frac{M}{2L}\right)\left(1-\frac{C_2}{C}\right)\right]$$

$$\simeq f_m\left[\frac{C_2}{C} - \frac{M}{L}\right]$$

$$\Delta f \simeq \frac{f_m}{2}\left[\frac{C_2}{C} - \frac{M}{L}\right] \quad . \quad . \quad . \quad . \quad . \quad . \quad 4.38.$$

The result of combining positive mutual inductance with series capacitance is shown in curve (3 − 2), Fig. 4.9, which is obtained by subtracting curve 2 from curve 3 multiplied by 2; i.e., M is assumed to be 4 μH instead of 2, so that the semi-band-width may have a maximum of the order of 10 kc/s. The result is not as satisfactory as curve (1+3).

Negative mutual inductance gives $\Delta f = \frac{f_m}{2}\left[\frac{C_2}{C} + \frac{M}{L}\right]$ and this

accentuates the band-width variation because curves 2 and 3, Fig. 4.9, are added.

4.6. The Design of a Tunable Band-Pass Filter. The analysis of 4.5 is most useful as a preliminary investigation and we have now to consider the practical filter, containing resistive as well as reactive components. The generalized curves for a two-circuit band-pass filter are given in Fig. 7.7, and in Section 7.5 it is shown that they are equally applicable to shunt or series reactance coupling. For the tunable filter, in which a mixture of shunt and series coupling is used, we have not discussed the application of the curves. If it is possible to replace either form of coupling by the other—the series reactance may, for example, be changed to a shunt reactance—then the curves are obviously applicable. Let us now take the series coupling reactance and try to convert it to the shunt coupling reactance. The first circuit is a symmetrical π section, whilst the second is a symmetrical T section network. The rules for conversion from one to the other are as follows: suppose the π section consists of two shunt arms of Z_1 and a series arm of Z_2, and the T section of two series arms of Z_a and a shunt arm of Z_b, then

$$Z_a = \frac{Z_1 Z_2}{2Z_1+Z_2} \text{ and } Z_b = \frac{Z_1^2}{2Z_1+Z_2}$$

If $Z_1 = \frac{1}{j\omega C}$, $Z_2 = \frac{1}{j\omega C_2}$ and $Z_2 \gg Z_1$ (this is usually true)

then $$Z_a = Z_1 \text{ and } Z_b = \frac{Z_1^2}{Z_2} = \frac{C_2}{j\omega C^2}.$$

We may therefore replace the series capacitance coupling by a shunt capacitance coupling of $\frac{C^2}{C_2}$, so that the combined coupling circuit of Fig. 4.8*a* may be replaced by a shunt coupling circuit having a shunt capacitance of C_1 and $\frac{C^2}{C_2}$ in series, i.e., $\frac{C_1 C^2}{C_1 C_2 + C^2}$.

In Section 7.4 the generalized selectivity response for the two circuit band-pass filter is shown to be

$$20 \log_{10} \frac{\sqrt{[1+Q^2(k^2-F^2)]^2+4Q^2F^2}}{2Qk}$$

and in Section 7.3 the meaning of Qk is indicated to be $\frac{\text{coupling reactance}}{\text{coil resistance}}$. Hence for combined series and shunt capacitance coupling we have $Qk = \frac{\omega C^2 C_1}{R}$, for mixed positive mutual

$$C_1 C_2 + C^2$$

inductance and series capacitance coupling $Qk = \dfrac{\left(\omega M - \dfrac{C_2}{\omega C^2}\right)}{R}$, and for mixed negative mutual inductance and shunt capacitance coupling $Qk = \dfrac{\left(\omega M + \dfrac{1}{\omega C_1}\right)}{R}$.

The particular value to be assigned to Qk at any frequency is determined by Q and the maximum band-width required, and it may be obtained from the curves of Fig. 7.7. Let us imagine that a band-pass filter is to be designed to operate over the medium wave range to give a semi-band-width Δf of approximately 8 kc/s. The inductance of the coils is 156 μH, and the Q values at three frequencies are as tabulated below. Since Q is fixed, the Δf scale is automatically fixed and it is adjusted for each frequency so that $\Delta f = \dfrac{f_m}{2Q}$ is immediately under $QF = 1$. By choosing the most suitable curves to give the required semi-band-width of 8 kc/s the values of Qk are as set out in Table 4.1. The curves are redrawn to the correct off-tune frequency scale in Fig. 4.10.

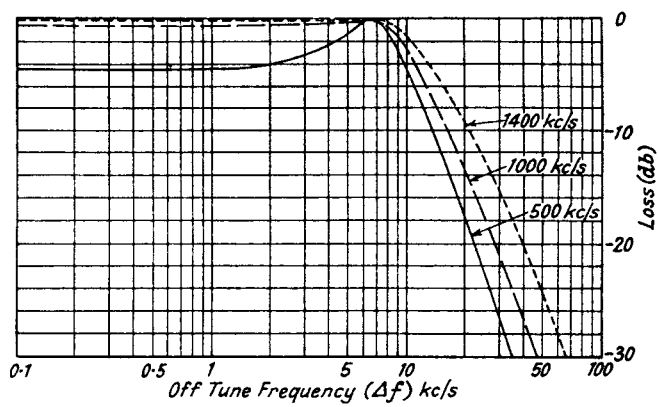

FIG. 4.10.—Selectivity Curves for a Tunable Band-Pass Filter.
[*Note.*—Read 600 kc/s for 500 kc/s in the above.]

TABLE 4.1

f_m(kc/s)	600	1,000	1,400
Q	120	100	80
$\Delta f(QF = 1)$(kc/s)	2·5	5	8·75
Qk	3	1·5	1·0
$R(\Omega)$	4·89	9·75	17·2
X coupling $= QkR(\Omega)$	14·67	14·63	17·2

Now we have the problem of finding the most suitable values of mixed coupling reactances. Let us first consider combined negative mutual inductance and shunt capacitance coupling. The coupling reactance is $\omega M + \frac{1}{\omega C_1}$, and as there are only two variables we cannot have the correct reactance at more than two frequencies. It is necessary to choose M and C_1, so as to give the nearest approach to the desired reactance over the tuning range.

Let us take some particular reference frequency f_0 at which the coupling $X = X_0 = \omega_0 M + \frac{1}{\omega_0 C_1}$ and assume $\omega_0 M$ to be some fraction A of X_0.

Thus $$\omega_0 M = AX_0$$

and $$\frac{1}{\omega_0 C_1} = (1 - A)X_0.$$

At any other frequency f

$$X = \omega M + \frac{1}{\omega C_1} = AX_0 \cdot \frac{\omega}{\omega_0} + (1 - A)X_0 \frac{\omega_0}{\omega}$$

or $$\frac{X}{X_0} = A\frac{f}{f_0} + (1 - A)\frac{f_0}{f} \quad . \quad . \quad . \quad . \quad . \quad 4.39.$$

The above expression, due to Beatty,[14] enables us to draw generalized curves, from which may be quickly estimated the values of M and C_1 to give a particular variation of coupling reactance over a given tuning range. Generalized curves of $\frac{X}{X_0}$ against $\frac{f}{f_0}$ for different values of A are plotted in Fig. 4.11. Both axes have logarithmic scales, as this allows the actual variation of X against f to be read directly by correctly registering similar logarithmic scales in X and f placed parallel to the two axes. For example, from the second column of Table 4.1. $X_0 = 14{\cdot}63\Omega$ and $f_0 = 1{,}000$ kc/s. The logarithmic reactance scale is set with $X = 14{\cdot}63\Omega$ registering with $\frac{X}{X_0} = 1$ and the frequency scale with $f = 1{,}000$ kc/s registering with $\frac{f}{f_0} = 1$ as shown in Fig. 4.11. If we choose any particular value of M such as $1{\cdot}165\ \mu$H, the value of $A = \frac{\omega_0 M}{X_0} = \frac{7{\cdot}325}{14{\cdot}63} = 0{\cdot}5$, and we can read from the curve

$A = 0{\cdot}5$ the values of coupling reactance for any desired frequency. Thus at $f = 600$ and 1,400 kc/s the coupling reactance is 16·7 and 15·4 ohms respectively. The shunt capacitance C_1 is 0·0217 μF obtained from $\dfrac{1}{\omega_0 C_1} = (1 - A)X_0$. Generally we shall wish to determine the values of M and C_1 to produce a coupling reactance variation over the tuning range as close as possible to values giving the desired band-pass characteristics. This is realized by plotting the required coupling reactance values, given in Table 4.1, against

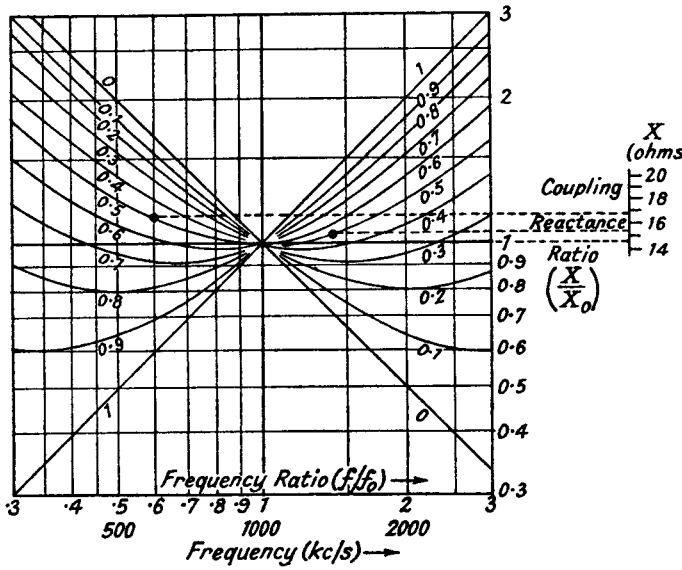

FIG. 4.11.—The Variation of Reactance Ratio Against Tuning Frequency Ratio for Combined Mutual Inductance and Shunt Capacitance Coupling.

frequency on tracing paper with X and f logarithmic scales identical with those of the generalized curves in Fig. 4.11. This curve is moved over the curves in Fig. 4.11, keeping the scale axes parallel, until the generalized curve most closely coinciding with the required coupling reactance curve is found. This occurs in our example for curve $A = 0{\cdot}6$, when $\dfrac{f}{f_0} = 1$ registers with $f = 920$ kc/s and $\dfrac{X}{X_0} = 1$ with $X = 14{\cdot}4\Omega$. The desired and generalized coupling reactance curves are curves 1 and 2 respectively in Fig. 4.12. Now we have all the data necessary to calculate M and C_1.

Thus

$$\omega_0 M = AX_0$$

$$M = \frac{AX_0}{\omega_0} = \frac{0{\cdot}6 \times 14{\cdot}4 \times 10^6}{6{\cdot}28 \times {\cdot}92 \times 10^6}\ \mu\text{H} = 1{\cdot}495\ \mu\text{H}$$

and $$\frac{1}{\omega_0 C_1} = (1 - A)X_0$$

or $$C_1 = 0{\cdot}03\ \mu\text{F}.$$

The same procedure can be applied to combined shunt and series capacitance coupling. The equivalent shunt coupling circuit gives a coupling reactance of $\left(\frac{C_2}{\omega C^2} + \frac{1}{\omega C_1}\right)$. C is a variable dependent

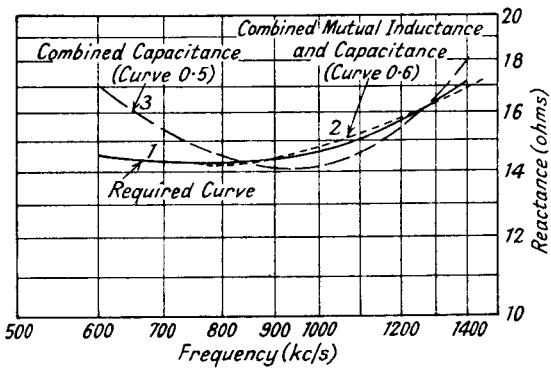

FIG. 4.12.—Required and Approximate Coupling Reactance-Frequency Curves.

on frequency and it may be eliminated by noting that $\omega = \frac{1}{\sqrt{LC}}$

$$\therefore\ X = \omega^3 L^2 C_2 + \frac{1}{\omega C_1}$$

$$= AX_0 \frac{f^3}{f_0{}^3} + (1 - A)X_0 \frac{f_0}{f} \quad . \quad . \quad 4.40$$

where $$\omega_0{}^3 L^2 C_2 = AX_0 \text{ and } \frac{1}{\omega_0 C_1} = (1 - A)X_0.$$

Generalized curves of $\frac{X}{X_0}$ against $\frac{f}{f_0}$ may be plotted as in Fig. 4.13.

The nearest curve is again found to the required $X - f$ curve from the tabulated figures. The $A = 0{\cdot}5$ curve gives the nearest approach, and this curve is curve 3 of Fig. 4.12. The agreement between the curves 1 and 3 is not so satisfactory as for MC_1 coupling

and this we should expect from the preliminary examination as illustrated in Fig. 4.9, which shows a much greater semi-band-width variation for C_1C_2 coupling. The reference point for curve 3 is $f_0 = 1{,}250$ kc/s and $X_0 = 16{\cdot}0\Omega$ and this gives

$$C_2 = \frac{AX_0}{\omega_0{}^3L^2} = \frac{0{\cdot}5 \times 16{\cdot}0 \times 10^{12} \times 10^{12}}{(6{\cdot}28 \times 1250 \times 10^3)^3.(156)^2}$$
$$= 0{\cdot}676\ \mu\mu\text{F}$$

and
$$C_1 = \frac{10^6}{(1-A)X_0.\omega_0} = \frac{10^6}{0{\cdot}5 \times 16{\cdot}0 \times 6{\cdot}28 \times 1250 \times 10^3}$$
$$= 0{\cdot}0159\ \mu\text{F}.$$

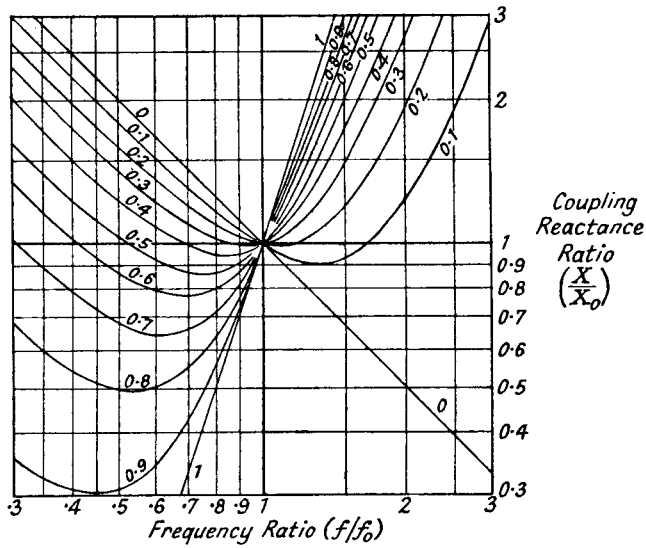

FIG. 4.13.—The Variation of Reactance Ratio Against Tuning Frequency Ratio for Combined Shunt and Series Capacitance Coupling.

Accurate adjustment of C_2 is not easily obtainable owing to its very low value. In addition, the coupling reactance variation cannot be made to follow closely the required law, so that mixed M and C_1 coupling is to be preferred.

In the above calculation we have chosen the values of Qk to give the required band-width by examination of the generalized curves. If we place a more explicit meaning to the term band-width, Qk can be calculated directly without reference to the curves. Using the definition of Section 7.7.4, the band-width becomes the difference between the frequencies at which the response is equal to

that at the minimum or trough. The transfer impedance from 7.2*c* is

$$|Z_T| = \frac{R_D Qk}{\sqrt{[1+Q^2(k^2-F^2)]^2+4Q^2F^2}}.$$

For the overcoupled case the minimum value $|Z_T|$ occurs for $F = 0$, i.e.,

$$|Z_T| = \frac{QkR_D}{1+Q^2k^2}$$

and the frequencies at the edge of the pass-band are obtained by equating the two expressions, thus

$$1+Q^2k^2 = \sqrt{[1+Q^2(k^2-F_p{}^2)]^2+4Q^2F_p{}^2}$$

where $$F_p = \frac{2\Delta f_p \text{ (to edge of pass-band)}}{f_m}.$$

squaring both sides

$$1+2Q^2k^2+Q^4k^4 = 1+2Q^2(k^2-F_p{}^2)+Q^4(k^2-F_p{}^2)^2+4Q^2F_p{}^2$$

$$Q^4F_p{}^4+Q^2F_p{}^2[2-2Q^2k^2] = 0$$

$$QF_p = \pm\sqrt{2(Q^2k^2-1)}.$$

$$F_p = \pm\sqrt{2\left(k^2-\frac{1}{Q^2}\right)}.$$

We may note that the frequency of maximum response is (Section 7.3).

$$F_{max.} = \pm\sqrt{k^2-\frac{1}{Q^2}}$$

$$\therefore\ F_p = \sqrt{2}\,.\,F_{max.}$$

or $$F_p{}^2 = \left(\frac{2\Delta f_p}{f_m}\right)^2 = 2\left(k^2-\frac{1}{Q^2}\right)$$

and $$k = \sqrt{2\left(\frac{\Delta f_p}{f_m}\right)^2+\frac{1}{Q^2}}.$$

Replacing Δf_p by 8 kc/s, and f_m and Q by the values tabulated above, the following values of k are found.

f_m(kc/s)	600	1,000	1,400
k	0·0206	0·0151	0·0149
Qk	2·48	1·51	1·19

These values do not differ greatly from those given in the first table except for $f_m = 600$ kc/s.

4.7. Distortion due to the R.F. Valve Characteristic.[11, 12]

4.7.1. Modulation Envelope Distortion and its Measurement. The characteristics required of a valve for R.F. ampli-

fication differ from those for A.F. amplification owing to the different nature of the anode load impedance. Tuned circuits discriminate in favour of a relatively narrow band of frequencies and require a high valve slope resistance for satisfactory operation. The constant-current generator circuit (Fig. 2.12*b*) indicates this very clearly, for the valve resistance is in parallel with and so damps the tuned circuit. The impedance of the latter is usually high so that a large stage gain is possible. Difficulties due to feedback are therefore greatly increased and the anode-grid capacitance must be as low as possible if instability is to be prevented. Another difference between R.F. and A.F. amplification is that, owing to the selective properties of R.F. tuned circuits, second harmonic R.F. distortion due to valve curvature is permissible and has no distorting effect on the modulation envelope. The most suitable valve for the purpose is the tetrode or pentode valve, since either can have a high R_a and low anode-grid capacitance. The tetrode having screened grid I_aE_a characteristics (Fig. 2.5) is less suitable when large output voltages are required because secondary emission limits the minimum anode voltage.

To see how the distortion effects occur in an R.F. amplifier we will take a simplified mathematical treatment, in which it is assumed that R_a is infinite and E_g is the only variable influencing I_a. The anode load is assumed to be zero to all frequencies outside the required pass-band and resistive to frequencies inside. We need therefore only consider components of anode current at frequencies within the pass-band. If the I_aE_g characteristic is represented by

$$I_a = a_0 + a_1E_g \quad . \quad . \quad . \quad . \quad 4.41$$

and $$E_g = \hat{E} \cos \omega t(1 + M \cos pt) - E_b$$

where $\hat{E}$ = carrier peak voltage

M = modulation ratio

$-E_b$ = grid-bias voltage,

no distortion can occur, and the output voltage is an amplified replica of the input and the valve functions as a linear amplifier. Let us next take an I_aE_g characteristic of the form.

$$I_a = a_0 + a_1E_g + a_2E_g^2 \quad . \quad . \quad . \quad . \quad . \quad . \quad . \quad 4.42$$

$$= a_0 + a_1[\hat{E} \cos \omega t(1 + M \cos pt) - E_b] + a_2[\hat{E} \cos \omega t(1 + M \cos pt) - E_b]^2$$

$$= a_0 + a_1[\hat{E} \cos \omega t(1 + M \cos pt) - E_b] + a_2[\hat{E}^2 \cos^2 \omega t(1 + 2M \cos pt + M^2 \cos^2 pt) - 2E_b\hat{E} \cos \omega t(1 + M \cos pt) + E_b^2] \quad . \quad 4.43$$

By noting that $\cos^2\theta = \frac{1+\cos 2\theta}{2}$, we may separate the anode current into the following components:

D.C. $$a_0 - a_1E_b + a_2\left[\frac{\hat{E}^2}{2}\left(1+\frac{M^2}{2}\right)+E_b^2\right]$$

Modulated R.F. fundamental $(a_1\hat{E} - 2a_2\hat{E}E_b)\cos\omega t(1+M\cos pt)$.

Distorted modulated R.F. 2nd Harmonic

$$\frac{a_2\hat{E}^2}{2}\cos 2\omega t\left(1+\frac{M^2}{2}+2M\cos pt+\frac{M^2}{2}\cos 2pt\right).$$

A.F. modulation fundamental $a_2\hat{E}^2M\cos pt$

A.F. ,, 2nd Harmonic $\frac{a_2\hat{E}^2M^2}{4}\cos 2pt$.

Since the anode-load impedance is assumed to be zero to all frequencies outside $\frac{\omega+p}{2\pi}$ to $\frac{\omega-p}{2\pi}$ the output voltage from the valve is

$$I_aZ_0 = (a_1\hat{E} - 2a_2\hat{E}E_b)\cos\omega t(1+M\cos pt)Z_0.$$

The voltage is dependent on E_b, decreasing as E_b is increased, and we see that a parabolic I_aE_g characteristic may be used to produce variable gain with variable bias without distortion of the modulation envelope. This effect is entirely due to the selective properties of the external anode impedance. With such a characteristic, aperiodic anode circuits would allow A.F. modulation distortion to appear at the detector output. The distortion products occur from the second power term in the I_aE_g characteristic, and consist of the distorted modulated R.F. second harmonic, the A.F. modulation and its second harmonic. A point to note is that the D.C. anode current increases as the input signal is increased, and it is also affected by the modulation ratio. Small variations of D.C. anode current are therefore to be expected in a variable mu valve when the signal is modulated.

Unfortunately it is difficult to achieve a parabolic I_aE_g curve, and a variable-mu characteristic is more nearly represented by a power series having a very large number of terms. If we add another term $a_3E_g^3$ to 4.42 we have, in addition to the component frequencies listed above, other frequencies obtained as follows:

$$a_3E_g^3 = a_3[\hat{E}^3\cos^3\omega t(1+M\cos pt)^3 - 3E_b\hat{E}^2\cos^2\omega t(1+M\cos pt)^2 + 3E_b^2\hat{E}\cos\omega t(1+M\cos pt) - E_b^3]. \quad . \quad 4.44.$$

Replacing $\cos^3\theta$ by $\frac{3\cos\theta+\cos 3\theta}{4}$ the following components can be separated

D.C.
$$-a_3E_b\left[\frac{3\hat{E}^2}{2}\left(1+\frac{M^2}{2}\right)+{E_b}^2\right]$$

Distorted modulated R.F. fundamental

$$a_3\hat{E}\cos\omega t\left[\frac{3\hat{E}^2}{4}\left(1+\frac{3M^2}{2}\right)+3{E_b}^2\right.$$
$$+\cos pt\left(\frac{9\hat{E}^2M}{4}+\frac{9\hat{E}^2M^3}{16}+3{E_b}^2M\right)+\cos 2pt\left(\frac{9M^2\hat{E}^2}{8}\right)$$
$$\left.+\cos 3pt\left(\frac{3\hat{E}^2M^3}{16}\right)\right].$$

Distorted modulated R.F. second and third harmonics, and A.F. modulation fundamental and second harmonic components are also present, but are not important because they do not contribute to the output voltage. The most important component is the distorted modulated R.F. fundamental, which is passed on through the amplifier to the detector and results in a distorted A.F. output. Power terms higher than the third all contribute to modulation envelope distortion.

It is therefore essential to reduce the factors, a_3, a_4, etc., in the I_aE_g power series to the smallest possible values, and rapid changes of curvature must be avoided. This is usually achieved by using a continuously variable pitch winding for the grid electrode as described in Section 2.4.

Distortion of the modulation envelope arising from these higher power terms limits the maximum modulated signal which can be accepted by an R.F. valve. The maximum signal generally increases as the negative bias voltage is increased, and the type of curve is shown in Fig. 7.19. A method of measuring directly the signal handling capacity of a R.F. valve is described in Section 7.11. The reason for the increase in maximum signal as the bias is increased is not very clearly shown by the power series, but it is actually due to a reduction in the rate of change of the g_m curve (see curve 2 in Fig. 2.8). Point A in Fig. 2.8 shows greatest rate of change of g_m and corresponds to the slight dip at $E_g = -12{\cdot}5$ volts in the input signal curve of Fig. 7.19.

A simpler method [32] of determining the signal handling capacity has been developed from the fact that the percentage second harmonic envelope distortion in a modulated R.F. output from the valve is directly related to the percentage third harmonic distortion produced by the same valve when an undistorted sinusoidal voltage is applied to its grid circuit. Expression 4.44 gives the amplitude of the second harmonic envelope distortion as

$$\frac{9a_3\hat{E}^3M^2}{8}$$

and by combining 4.43 and 4.44 the amplitude of the fundamental modulation envelope component is

$$[a_1 - 2a_2E_b + 3a_3E_b^2]\hat{E}M + \frac{9}{4}a_3\left(1+\frac{M^2}{4}\right)\hat{E}^3M.$$

Hence the second harmonic distortion percentage is

$$\frac{9a_3\hat{E}^2M \times 100}{8\left[[a_1 - 2a_2E_b + 3a_3E_b^2] + \frac{9}{4}a_3\left(1+\frac{M^2}{4}\right)\hat{E}^2\right]} \quad . \quad 4.45a.$$

By replacing $\frac{3a_3\hat{E}^2}{a_1 - 2a_2E_b + 3a_3E_b^2}$ by k, 4.45a becomes

$$\text{percentage second harmonic} = \frac{\frac{3}{8}kM100}{1+\frac{3}{4}k\left(1+\frac{M^2}{4}\right)} \quad . \quad 4.45b.$$

Applying a fundamental input voltage $\hat{E}\cos pt$ to

$$I_a = a_0 + a_1E_g + a_2E_g^2 + a_3E_g^3 \quad . \quad . \quad . \quad 4.46.$$

gives a fundamental amplitude of

$$(a_1 \quad 2a_2E_b + 3a_3E_b^2)\hat{E} \quad \tfrac{3}{4}a_3\hat{E}^3$$

and a third harmonic amplitude of $\frac{a_3\hat{E}^3}{4}$

$$\therefore \text{ percentage third harmonic} = \frac{\frac{a_3\hat{E}^2}{4}100}{a_1 - 2a_2E_b + 3a_3E_b^2 + \frac{3}{4}a_3\hat{E}^3}$$

$$= \frac{100k}{12\left(1+\frac{k}{4}\right)} \quad . \quad . \quad . \quad 4.47.$$

For any given percentage of second harmonic envelope distortion and percentage modulation, expression 4.45b gives a particular value of k, which inserted in 4.47, gives the corresponding value of third harmonic distortion. If therefore the valve is connected as an L.F. amplifier, and the input voltage adjusted to produce the calculated value of third harmonic percentage, the input voltage represents the signal handling capacity of the valve, i.e., it is equal to the carrier voltage which, modulated at the specified modulation percentage, gives the specified second harmonic distortion percentage of the modulation envelope. The values of k and percentage third harmonic distortion for different values of distortion and modulation percentage are tabulated below.

TABLE 4.2

Percentage 2nd Harmonic	30% M.		60% M.		80% M.	
	k.	Percentage 3rd.	k.	Percentage 3rd.	k.	Percentage 3rd.
2·5	0·2685	2·095	0·122	1·01	0·09	0·735
5	0·674	4·81	0·271	2·115	0·195	1·55
7·5	1·365	8·47	0·458	3·43	0·319	2·46
10	2·795	13·7	0·699	4·96	0·47	3·5

Since terms above the third power in the I_aE_g characteristic have been neglected the signal handling capacity determined by this method is not strictly accurate; as a general rule the error is quite small except at a grid-bias voltage where the characteristic has a rapid change of curvature or near cut-off of anode current.

The circuit recommended for this indirect measurement of signal handling capacity is shown in Fig. 4.14. The fundamental

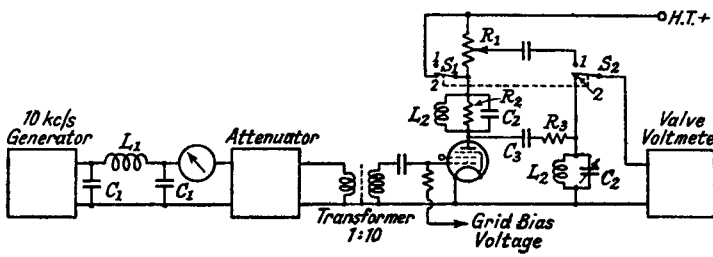

FIG. 4.14.—The Circuit Diagram for the Indirect Measurement of the Signal Handling Capacity of a R.F. Valve.

input voltage (frequency = 10 kc/s) is connected to the grid of the test valve through a low-pass filter ($L_1 = 3{\cdot}18$ mH, $C_1 = 0{\cdot}16$ μF), terminated by an attenuator of constant impedance 100 ohms and followed by a 1 : 10 step-up transformer. The anode circuit of the test valve contains a potentiometer R_1 (600Ω), across which the fundamental voltage is produced, and a frequency discriminating circuit L_2C_2 tuned to the third harmonic (30 kc/s). Ganged switches S_1 and S_2 enable the 30 kc/s output (position 2) to be compared with a proportion of the fundamental output (position 1), measured by a valve voltmeter. Potentiometer R_1 is adjusted so that the valve voltmeter indicates no change of reading between the two positions of the switches, and it is calibrated in terms of k by inserting a standard valve, the signal handling capacity of which

has either been calculated as described in Section 4.7.2 or measured as described in Section 7.11. The procedure for any valve is then to set R_1 to the required value of k, e.g., 0·271 for 60% modulation and 5% second harmonic envelope distortion, and to adjust the attenuator setting until the valve voltmeter indicates no change between the two switch positions. The signal handling capacity is then ten times the attenuator setting. An alternative method of calibrating R_1 in terms of k is to apply known amplitudes of 10 and 30 kc/s frequencies to the grid circuit of the valve in accordance with Table 4.2; thus for the condition set out above the amplitude ratio of 30 to 10 kc/s would be 2·115 to 100. Care must be taken to see that the amplitude of the 10 kc/s is small so that distortion of this frequency by the valve may be small.

The frequency discriminating network consists of two similar parallel tuned circuits of $L_2 = 10$ mH and $C_2 = 0{\cdot}01$ μF connected by a capacitor $C_3 = 0{\cdot}01$ μF in series with a high resistance R_3 (0·5 MΩ) to increase the selective properties of the second-tuned circuit. The first-tuned circuit is damped by a resistance R_2 (30,000Ω) to ensure that its dynamic resistance is much less than the anode impedance of any valve likely to be tested.

4.7.2. Calculation of Signal Handling Capacity from the g_mE_g Characteristic.[25] If 4.46 is differentiated with respect to E_g an expression for g_m in terms of E_g is obtained.

$$\frac{dI_a}{dE_g} = g_m = a_1 + 2a_2E_g + 3a_3E_g^2.$$

Now suppose $E_g = \hat{E}\cos\omega t - E_b$, then E_g varies between $\hat{E} - E_b$ and $-\hat{E} - E_b$. Denoting mutual conductance at these points by $g_m\,(max.)$ and $g_m\,(min.)$, and at $E_g = -E_b$ by g_{m0}, we have

$$\begin{aligned}
g_m\,(max.) &= a_1 + 2a_2(\hat{E} - E_b) + 3a_3(\hat{E} - E_b)^2 \\
g_m\,(min.) &= a_1 - 2a_2(\hat{E} + E_b) + 3a_3(\hat{E} + E_b)^2 \\
g_{m0} &= a_1 - 2a_2E_b + 3a_3E_b^2 \\
g_m\,(average) &= \frac{g_m\,(max.) + g_m\,(min.)}{2} \\
&= a_1 - 2a_2E_b + 3a_3E_b^2 + 3a_3\hat{E}^2 \\
&= g_{m0} + 3a_3\hat{E}^2 \\
&= g_{m0}\left[1 + \frac{3a_3\hat{E}^2}{a_1 - 2a_2E_b + 3a_3E_b^2}\right] \\
&= g_{m0}(1+k) \quad . \quad . \quad . \quad . \quad . \quad 4.48
\end{aligned}$$

where k has the same meaning as in Section 4.7.1.

Thus for 60% modulation and 5% second harmonic envelope distortion, $k = 0{\cdot}271$ and g_m (*aver.*) $= g_{m0}.1{\cdot}271$. Expression 4.48 may be used to calculate the signal handling capacity at any given bias $-E_b$, and the procedure is as follows. Using the g_mE_g curve draw a straight line through the point $g_m = g_{m0}(1+k)$, $E_g = -E_b$ to intersect the g_mE_g curve at two values, E_{g1} and E_{g2} such that $E_{g1} - E_b = E_b - E_{g2}$. The signal handling capacity is then $(E_{g1} - E_b)$ peak (unmodulated) carrier voltage or $0{\cdot}707$ $(E_{g1} - E_b)$ R.M.S. carrier voltage.

4.7.3. Cross-Modulation Distortion. One of the most undesirable forms of distortion in R.F. amplifiers is that known as cross-modulation. This effect can occur when a modulated undesired signal is applied to the grid of a valve at the same time as the desired signal. If the I_aE_g power series has terms above E_g^2, the undesired modulation is transferred to the desired carrier, and discrimination against the undesired carrier after this R.F. valve produces no reduction of undesired modulation. It can be shown by taking the $a_3E_g^3$ term and replacing E_g by

$$(\hat{E}_d \cos \omega_d t + \hat{E}_u \cos \omega_u t(1 + M \cos pt) - E_b),$$

where the suffix d denotes desired and u undesired signal. For simplicity the former is not modulated. Expanding

$$a_3(\hat{E}_d \cos \omega_d t + \hat{E}_u \cos \omega_u t(1 + M \cos pt) - E_b)^3$$

shows a term of the form

$$3a_3\hat{E}_d \cos \omega_d t \hat{E}_u^2 \cos^2 \omega_u t(1 + M \cos pt)^2,$$

which equals

$$3a_3\hat{E}_d \cos \omega_d t \hat{E}_u^2 \left(\frac{1 + \cos 2\omega_u t}{2}\right)(1 + M \cos pt)^2$$

and this contains a component

$$\frac{3a_3}{2}\hat{E}_d\hat{E}_u^2 \cos \omega_d t\left(1 + \frac{M^2}{2} + 2M \cos pt + \frac{M^2}{2} \cos 2pt\right).$$

The desired carrier is now modulated by the undesired modulation and its second harmonic. The remedy for this cross-modulation effect is to increase the selectivity of the circuits preceding the first R.F. amplifier so as to reduce $\hat{E}_u$, and also to decrease all the factors a_3, a_4, etc., in the power series for the I_aE_g curve. Thus the methods applied to reduce distortion of the desired modulation envelope also reduce cross-modulation. It will be noticed that the cross-modulating term is dependent on the square of $\hat{E}_u$ and independent of its frequency. In a well-designed receiver the

cross-modulating effect due to a strong local station signal should be confined to a band of tuning frequencies in its immediate neighbourhood, for the tuned circuits preceding the R.F. valve should quickly reduce E_u to a small value as the receiver is tuned away from the local station position. Special aerial rejector circuits may be fitted when a receiver operates in close proximity to a powerful transmitter.

4.8. Instability in R.F. Amplifiers.[7] Instability is always possible in an amplifier when coupling exists between input and output circuits. Energy feedback may occur via output to input leads, through the common supply voltages, or via the anode-grid capacitance. The first two causes are under the designer's control, and careful placing of the leads and adequate decoupling with short lead capacitors can prevent regeneration. The total anode-grid capacitance can be reduced by eliminating stray coupling external to the valve, but it cannot be made less than the inter-electrode capacitance. The only possible method of preventing instability from this source is to limit the gain of the stage. From Section 2.8 we note that feedback through the anode-grid capacitance produces, in conjunction with the anode load, a grid input admittance of resistance and capacitance in parallel. The sign of the resistive term depends on the reactance of the anode load, being positive for a capacitance and negative for an inductance. If the anode load is a tuned circuit we have for the input grid resistance R_g (see Section 7.8, expression 7.26*a*)

$$R_g = \frac{(QF)^2 + \left(1 + \frac{R_D}{R_a}\right)^2}{g_m B_{g_a} Q F R_D},$$

where $B_{g_a} = \omega C_{g_a}$ = anode-grid interelectrode susceptance, and the other terms have their usual meaning.

This is a minimum when $QF = \pm\left(1 + \frac{R_D}{R_a}\right)$ so that the minimum negative value of R_g is

$$R_g = \frac{-2\left(1 + \frac{R_D}{R_a}\right)}{g_m R_D B_{g_a}}$$

$$\simeq \frac{-2}{g_m R_D B_{g_a}}$$

when $$R_a \gg R_D.$$

Instability occurs when R_g is less than the parallel resistance component of the grid tuned circuit. If the anode and grid circuits are identical, the condition for stable operation is defined by

$$R_g > R_D$$

or

$$g_m R_D{}^2 B_{g_a} < 2$$

and for a given B_{g_a} either g_m or R_D must be limited. Generally it is better to reduce g_m by increasing grid bias, rather than to reduce R_D because selectivity is often reduced by decreasing R_D. However, the use of a tapped tuning coil allows the equivalent R_D to be reduced without loss of selectivity (see Section 4.4.1).

In estimating the condition for stability in a two-valve amplifier we will assume that all tuned circuits are identical. Owing to feedback, the dynamic impedance of the tuned circuit in the grid of the last valve is increased, and as this is the anode circuit of the next valve we have the following results:

Dynamic resistance of the last tuned circuit $= R_0' = R_D$

Grid input resistance of the last valve $= R_g' = \dfrac{-2}{g_m R_D B_{g_a}}$

Resultant dynamic resistance of the grid tuned circuit $= R_0''$

$$R_0'' = \frac{R_D R_g'}{R_D + R_g'} = \frac{2}{g_m B_{g_a}\left(\dfrac{2}{g_m R_D B_{g_a}} - R_D\right)}$$

Grid input resistance of the second valve $= R_g'' = \dfrac{-2}{g_m R_0'' B_{g_a}}$

$$= -\left[\frac{2}{g_m R_D B_{g_a}} - R_D\right].$$

The condition for stability is that

$$-R_g'' = \left[\frac{2}{g_m R_D B_{g_a}} - R_D\right] > R_D.$$

i.e.,

$$g_m R_D{}^2 B_{g_a} < 1.$$

For a three-valve amplifier the following results are obtained:
Resultant dynamic resistance of the third tuned circuit $= R_0'''$

$$R_0''' = \frac{R_g'' R_D}{R_D + R_g''} = \frac{R_D{}^2 - \dfrac{2}{g_m B_{g_a}}}{2R_D - \dfrac{2}{g_m R_D B_{g_a}}}.$$

$$\text{Grid input resistance of the valve} = R_g''' = -\frac{2}{g_m R_0'''.B_{g_a}}$$

$$= \frac{4\left[g_m R_D^2 - \frac{1}{B_{g_a}}\right]}{g_m R_D B_{g_a}\left(g_m R_D^2 - \frac{2}{B_{g_a}}\right)}.$$

For stability

$$R_D < -R_g'''$$

i.e., $$(g_m R_D^2 B_{g_a})^2 - 6 g_m R_D^2 B_{g_a} + 4 < 0$$

$$g_m R_D^2 B_{g_a} < \frac{+6 \pm \sqrt{20}}{2} < 0{\cdot}764.$$

Summarizing the results in the form of a table:

TABLE 4.3

No. of Amplifier Stages.	Maximum value of $g_m R_D^2 B_{g_a}$
1	2
2	1
3	0·764

In practice the maximum value of $g_m R_D^2 B_{g_a}$ will have to be much less than the value given in Table 4.3, otherwise feedback, though insufficient to cause oscillation, will have a serious effect on the overall frequency response of the amplifier. It causes greater amplification of frequencies below resonance and less amplification above resonance. The result is a lop-sided selectivity curve as discussed in Section 7.8.

4.9. Noise Limitation to Maximum Amplification.[35]

4.9.1. Introduction. By careful design a receiver may be constructed with very high amplification, and in the absence of a limiting factor it would be possible to obtain adequate output even from the weakest signal. The limiting factor is noise. Noise may be produced outside the receiver and be picked up in association with the desired signal or it may occur in the receiver itself. The desired signal must therefore be large enough to give with average modulation (about 30%) an A.F. output very much greater than that contributed by noise. Generally a signal-to-noise ratio of 15 db. is regarded as the minimum satisfactory level. External noise may be due to atmospheric disturbances (thunderstorm and magnetic storms), or to interference radiated from electrical

machinery. Over neither of these has the designer any control, though he can mitigate the effects of the latter, which is usually transmitted over the electric power lines, by including suitable R.F. filter chokes and by-pass capacitors between the supply and the receiver mains leads, and by locating the aerial as far as possible from the interference field of the supply lines (away from buildings) and connecting it to the receiver by screened leads (Section 3.5).

Noise produced in the receiver may be classed as accidental and inherent. The former is caused by faulty components—volume controls, variable capacitors, joints, can all contribute—and can be eliminated, but the latter cannot. Inherent noise is due to thermal effects in the conductors and shot noise in the valves. In both instances it is usually only the first stages of the receiver that have to be considered, since in later stages the signal is amplified and is much greater than any noise likely to be produced in these stages.

4.9.2. Thermal Noise. In Chapter 2 it was stated that all conductors contain free electrons, which are in a state of random motion. The average velocity of these free electrons is directly proportional to the absolute temperature and is only zero at 0° absolute. Each electron in motion constitutes a minute current and the sum total of these currents over a long period is zero. At any given instant, however, this will not necessarily be true, and there may be a net current in one direction or the other. These transient currents produce, across the ends of the conductor, voltages, the frequency components of which cover an infinite band. Nyquist assumes thermal noise to be equivalent to a voltage in series with the resistance of the conductor and computes its mean square value to be

$$E_{n_i}^2 = 4RkT(f_1 - f_2) \quad . \quad . \quad . \quad 4.49$$

where R = resistance of the conductor

k = Boltzmann's constant

T = Absolute temperature

$f_1 - f_2$ = Pass-band width of the receiver = $2\Delta f$.

The pass-band of the receiver must obviously affect the noise voltage since the wider this is the more noise frequency components are brought in. The pass-band is defined as the range of frequencies over which the response is greater than 70% of the maximum. Actually frequencies outside the normal pass-band of the stages preceding any non-linear device, such as a frequency changer or detector, have a noise-producing effect because the non-linear device can produce intermodulation frequencies in the overall pass-

band from noise frequencies normally outside it. Boltzmann's constant relates absolute temperature and electron energy, and the resistance R is the actual or equivalent shunt resistance of the first circuit. If the latter is a tuned circuit the resistance is the dynamic resistance (R_D) of the tuned circuit. The actual volume of noise produced at the output of the receiver—it appears generally as a hiss because of the greater sensitivity of the ear to the higher audio frequency components (500 to 5,000 c.p.s.)—is dependent on whether a carrier is being received. If there is no carrier the noise must provide its own, and as this is small in value the noise output is small. Section 8.2.8 states that detectors normally have a parabolic characteristic, and this makes the detection efficiency or sensitivity low for small signals. When a carrier is present detection sensitivity is increased and the noise voltages act as sidebands giving greater output. With no A.G.C. action in the receiver, increase of carrier up to a certain level increases the noise output, but beyond this level, at which the detector has reached the linear condition of maximum sensitivity, any further increase in carrier does not alter the noise output. If the receiver has A.G.C., as the carrier is increased beyond the point of operation of A.G.C., the receiver sensitivity is decreased and noise output reduced. The most important thermal noise voltage is that produced in the first tuned circuit, and if we assume normal operating temperature to be 63° F. (290° abs.) expression 4.49 becomes

$$E_{n_t} = 1{\cdot}25 \times 10^{-10}\sqrt{R_D(f_1 - f_2)} \quad . \quad . \quad 4.50.$$

Taking $R_D = 100{,}000\Omega$ and $(f_1 - f_2) = 10$ kc/s as typical of the medium wave band the noise R.M.S. voltage is

$$E = 1{\cdot}25 \times 10^{-10}\sqrt{10^5 \times 10^4} = 3{\cdot}95\ \mu\text{V}.$$

Hence a carrier (modulated 30%) of R.M.S. value 74 μV would be required to give the necessary 15 db. signal-to-noise ratio. The noise is assumed to have 1 sideband of the above value, whilst the carrier has two of 11·1 μV.

4.9.3. Shot Noise. A second important source of noise in a receiver is shot noise, produced by the flow of electrons from cathode to anode of the valve. The electrons making up the anode current have random motion, and the number arriving at the anode varies from one time-instant to another. This is equivalent to a small variable current of infinite number of frequency components superimposed upon the mean D.C. current. A mechanical analogy for shot noise is sand falling upon a gong; the resultant noise is dependent upon the resonant properties of the gong, the quantity

of sand falling per second and the size of the sand particles. In the same way shot noise is dependent on the external anode impedance (Z_0), the mean anode current I_a, and the electron charge e. For a saturated diode the mean square value of noise current has been shown to be

$$I_{n_s}^2 = 2I_a e(f_1 - f_2).$$

Replacing e by its actual value

$$I_{n_s} = 5{\cdot}54 \times 10^{-4}\sqrt{I_a(f_1 - f_2)}\ \mu\text{A}.$$

The noise voltage developed in the anode load Z_0 is

$$E_{n_s} = I_{n_s}Z_0 = 5{\cdot}54 \times 10^{-10} \times Z_0\sqrt{I_a(f_1 - f_2)} \quad . \quad 4.51.$$

This formula is not applicable to an amplifier valve operating under non-saturated space-charge conditions, for the space-charge reservoir of electrons acts as a cushion to smooth out the random variations, and the measured noise voltage is usually much less than this. Another theory assumes the valve to be replaced by its internal resistance at half the cathode temperature, and calculates the thermal noise voltage to be expected in the anode from this resistance. Calculations based on this assumption usually give too low a noise voltage. A convenient method of expressing shot noise is as the equivalent resistance, between grid and cathode of the valve, which would give at room temperature a thermal noise voltage in the anode circuit equal to that produced by the shot noise. This method has the advantage of allowing the relative magnitudes of shot and thermal noise to be compared by comparing the equivalent shot resistance with that of the input circuit. Since the thermal noise voltage across the anode circuit is proportional to $g_m Z_0\sqrt{R_D(f_1 - f_2)}$ and the shot noise voltage to $Z_0\sqrt{I_a(f_1 - f_2)}$, it follows that the equivalent shot noise resistance is proportional to $\frac{I_a}{g_m^2}$. Hence the best type of amplifier valve is one having a high value of g_m and low value of I_a. If the total space current exceeds the anode current, as in all multi-electrode valves except the triode, the equivalent shot noise is multiplied by a factor greater than 1 and is proportional to the ratio of total-to-anode current.

The following are average values of shot-noise resistance for different types of valves:

Valve Type.	Shot Noise Equivalent Resistance.
Triode	200 to 500Ω
Special beam tetrode	4,000 to 5,000Ω
Ordinary screened grid and pentode	20,000 to 50,000Ω
Frequency changer	50,000 to 100,000Ω

Frequency-changer valves are worst because g_c is never greater than $\frac{g_m}{4}$, i.e., signal gain is low for a given I_a. Ordinary screened grid or pentode valves are poor because of secondary emission and screen current. By concentrating the electrons into a beam and reducing screen current, shot noise can be much reduced, as shown by the beam tetrode value. The beam tetrode has the smallest shot noise of the multi-electrode valves because secondary emission is small and the space-charge reduces electron fluctuations.

If an R.F. amplifying stage is incorporated in a receiver, the impedance of the first-tuned circuit, except at ultra-high frequencies, is greater than the shot-noise resistance, so that thermal noise is the limitation. If, however, the first stage consists of a frequency changer the reverse is generally true and shot noise is greater than thermal. It should be noted that in a frequency changer stage shot noise is introduced by the oscillator valve as well ; shot and thermal noise components in the image or second channel region also add their quota. For a given overall gain a receiver without an R.F. valve before the frequency changer has normally at least twice the noise voltage of a receiver with an R.F. amplifier stage.

4.10. Problems in Short Wave and Ultra Short Wave Amplification.

4.10.1. Introduction. Amplification on the short wave range is chiefly complicated by the fact that selectivity is considerably reduced as the signal frequency is increased, and also that in many receivers the complete range from 6 to 15 Mc/s is covered by one coil using the same tuning capacitance, without modification, for short wave as for the medium and long wave ranges. As far as broadcast reception is concerned this method has two disadvantages : it makes tuning of the broadcast stations very sharp and difficult : it calls for a very small value of inductance which results in a low dynamic impedance and consequently low amplification. Much improved performance can be realized by band-spreading (selecting certain comparatively narrow bands in the short wave range). For communication receivers, required to cover completely the short wave band, the latter can be split up into a number of much smaller overlapping ranges. The tuning capacitance range is reduced by the use of a series or shunt capacitance (or combination of both), or in special cases much smaller tuning capacitances may be employed. The latter usually have the advantage of lower

losses, an important point at the higher frequencies, e.g., at 15 Mc/s.

The same problems also present themselves, though in a more acute form, at ultra high frequencies, and there are added complications due to low input valve conductance, stray inductance and capacitance.

4.10.2. Short Wave Amplification. In section 4.2.3 selectivity is shown to be a function of Q and the resonant frequency, and the pass-band is defined by

$$2\Delta f = \frac{f_r}{Q},$$

so that as f_r is increased the band-width is increased unless Q rises. The Q of short wave coils is often higher than corresponding coils for long and medium waves (values from 150 to 200 are common), but dielectric losses, valve input conductance, etc., lower considerably the effective Q of the tuned circuit, and a probable maximum value under favourable conditions is 50. This gives band-widths of 120 and 300 kc/s at 6 and 15 Mc/s respectively. The R.F. amplifier therefore only discriminates against undesired signal frequencies (reacting with harmonics of the oscillator—Section 5.4.3) well separated from the desired. Adjacent channel rejection is achieved in the I.F. amplifier. At an I.F. of 465 kc/s, the image signal (assuming $Q = 50$) is reduced by approximately 24 db. and 16·0 db. at 6 and 15 Mc/s respectively (see Fig. 4.3 for $QF = 15{\cdot}5$ and 6·2), and additional image rejection is really necessary. Circuits have been developed for application to band-spread receivers with preset signal tuning and these are described in Section 5.9.4. Little can be done to improve selectivity unless regeneration is employed, but this lack of selectivity may be used to advantage in band-spread broadcast receivers. Broadcast transmissions occur over certain quite narrow bands, rarely exceeding 200 kc/s width, and centred at 6·1, 9·6, 11·9, 15·2, 17·8 and 21·6 Mc/s. By reducing Q to 30 at 6·1 Mc/s, transmissions from 6 to 6·2 Mc/s can be accepted with a maximum loss of 3 db., i.e., the signal circuit can be preset tuned to 6·1 Mc/s and selection obtained by variation of oscillator frequency. At 15·2 Mc/s no decrease of Q is necessary. To obtain maximum amplification the signal-tuning capacitance should be as low as possible consistent with stray and valve capacitances, a minimum value being about 60 $\mu\mu$F. The required values of Q for a pass-band width of 200 kc/s, and the tuning inductance L for $C = 60$ $\mu\mu$F are tabulated below for the central frequencies listed.

Frequency.	Q	L
6·1 Mc/s	30·5	11·3 μH
9·6 ,,	48·0	4·57 ,,
11·9 ,,	59·5	2·97 ,,
15·2 ,,	76	1·82 ,,
17·8 ,,	89	1·32 ,,
21·6 ,,	108	0·9 ,,

The dynamic impedance is constant at 13,200Ω since $Q \propto f$. In actual fact it is unlikely that a Q value greater than 50 could be realized, and under these conditions the pass-band width increases as the frequency increases, whilst dynamic impedance and therefore amplification decrease as set out below.

Frequency.	R_D	Amplification Ratio. $\left(\frac{R_D \text{ at } f \text{ Mc/s}}{R_D \text{ at } 6{\cdot}1 \text{ Mc/s}}\right)$
11·9 Mc/s	11,100 Ω	0·841
15·2 ,,	8,700 ,,	0·66
17·8 ,,	7,380 ,,	0·588
21·6 ,,	6,120 ,,	0·464

Let us now consider the communication receiver required to cover with overlaps the short wave range from 6 to 25 Mc/s. Arbitrarily dividing into four ranges with overlaps gives

Range 1	6 to 9 Mc/s
,, 2	8·66 to 13 Mc/s
,, 3	12 to 18 Mc/s
,, 4	17 to 25·5 Mc/s

a frequency ratio change in each instance of 1 to 1·5, so that a capacitance change of 2·25 to 1 is required. We will assume that the frequency scale on the medium wave range is linear, and that we wish if possible to preserve this relationship while restricting the equivalent tuning capacitance change. If the signal-tuning inductance is 156 μH on the medium wave range and its self-capacitance is 10 $\mu\mu$F, the following tuning capacitance values are obtained at the equally spaced frequencies from 550 to 1,500 kc/s.

Frequency (kc/s) . .	550	788·5	1,025	1,263·5	1,500
Capacitance ($\mu\mu$F) .	526·8	252	145	92	62·17

and the problem is to obtain frequencies on the short wave ranges separated by a constant amount for these capacitance settings.

Restricting the capacitance range by a series padding capacitance gives the tuning frequency as

$$f = \frac{1}{2\pi\sqrt{L.\frac{C_p C}{C_p + C}}} \quad . \quad . \quad . \quad 4.52$$

where C_p = the series padding capacitance. By replacing f by 6 and 9 Mc/s and C by 526·8 and 62·17 $\mu\mu$F respectively in expression 4.52, the value of C_p is found to be 106 $\mu\mu$F. The frequencies corresponding to the chosen settings of C are

C ($\mu\mu$F)	526·8	252	145	92	62·17
Frequency (Mc/s)	6	6·52	7·2	8·02	9

whilst the frequencies for a linear frequency scale should be 6, 6·75, 7·5, 8·25 and 9 Mc/s. Hence the series padding capacitance has produced a reasonably satisfactory scale, which is slightly cramped at the high frequencies.

For a shunt trimmer capacitance the tuning frequency is

$$f = \frac{1}{2\pi\sqrt{L(C_t+C)}} \quad . \quad . \quad 4.53$$

and using the same tuning capacitance values C_t is calculated to be 310·5 $\mu\mu$F. The frequencies corresponding to the chosen settings of C are

C ($\mu\mu$F)	526·8	252	145	92	62·17
Frequency (Mc/s)	6	7·32	8·13	8·67	9

This means a very unsatisfactory scale with appreciable cramping at the low frequencies.

Since series and shunt capacitance restriction of tuning have opposite effects, it is possible to obtain a better approach to the linear frequency scale by a combination of both. Thus for C_p = 250 $\mu\mu$F and C_t = 46·5 $\mu\mu$F (C_p being between C and C_t), the frequencies are 6, 6·73, 7·51, 8·29 and 9 Mc/s, and the frequency scale is very nearly linear. From the point of view of maximum amplification over a tuning range, the series padding capacitance would be preferred to combined series and shunt capacitance because, although the frequency scale may be less satisfactory, the equivalent tuning capacitance is less and so the dynamic impedance is increased.

The values of C_p and C_t given above have the same effect on all ranges because the maximum-to-minimum frequency ratios are the same; thus for C_p = 250 and C_t = 46·5 $\mu\mu$F, the frequencies for range 4 are 17, 19·1, 21·3, 23·5 and 25·5 Mc/s.

4.10.3. Ultra Short Wave Amplification. In the previous section the difficulties of obtaining reasonable amplification in short wave amplifiers are outlined, and these are multiplied at ultra high frequencies. In spite of low stage amplification (about 5 times for general purpose receiving valves at the television frequency,

45 Mc/s and 12 for acorn valves [30]), there are definite advantages in including a R.F. stage between the aerial and frequency changer of a receiver. Overall amplification, signal-to-noise ratio, and selectivity against image and spurious I.F. responses due to interaction between undesired signals and the oscillator (Section 5.4) are all increased by the addition of a R.F. stage. The heavy damping from the R.F. valve (Section 2.8.3) prevents the realization of a high degree of selectivity against adjacent channels, but the I.F. amplifier discriminates satisfactorily against these. This fact, together with the probability of transmission being confined to comparatively narrow bands at certain selected positions in the ultra high frequency range, makes it possible to consider preset signal tuning to the centre of the band, tuning over it being accomplished by varying the oscillator frequency. Although the losses due to the valve input conductance, aerial connection and coil resistance predominate over all others, it is important to remember that components [27] such as the tuning capacitance, the trimmer, valve-holder, valve-base and any switches, which at lower frequencies generally have little effect, can contribute their quota. Expressing the losses as conductances, since they are circuits in parallel with the coil, typical values (at 45 Mc/s) for the components listed above are

Component	Bakelite Insulation.	Ceramic.
Tuning capacitance (minimum)	120 micromhos	30 micromhos
,, ,, (maximum)	20 ,,	5 ,,
Valve-holder	5 ,,	1 ,,
Valve-base	5 ,,	1 ,,
Range switch . . .	5 ,,	1 ,,

Let us consider the case of an amplifier stage operating at 45 Mc/s, and assume that the valve has characteristics identical with the one in Section 2.8.3, viz.,

$$g_k = 3 \text{ mA/volt}, \; C_{g_k} = 3 \; \mu\mu\text{F}, \; L_k = 0{\cdot}2 \; \mu\text{H}.$$

From expression 2.21*c*

$$R_g = -\frac{g_k{}^2+(B_k+B_{g_k})^2}{g_k B_{g_k} B_k}$$

$$B_{g_k} = 8{\cdot}48 \times 10^{-4} \text{ mhos}$$

$$B_k = -1{\cdot}768 \times 10^{-2} \text{ mhos}$$

$$R_g = \frac{(3 \times 10^{-3})^2+(-1{\cdot}683 \times 10^{-2})^2}{3 \times 10^{-3} \times 8{\cdot}48 \times 10^{-4} \times 1{\cdot}768 \times 10^{-2}}$$

$$= 6{,}480\Omega,$$

converting this to a conductance $G_g = 154$ μmhos. For maximum amplification the tuning capacitance should be as small as possible, and a probable minimum value is 30 $\mu\mu$F (valve and stray capacitance prevent it being less). For $C = 30$ $\mu\mu$F, $f = 45$ Mc/s, the tuning inductance is 0·416 μH, and taking Q as 150 for the coil, the dynamic resistance of the tuned circuit if C has no losses is

$$R_D = Q\omega L = 150 \times 6{\cdot}28 \times 45 \times 0{\cdot}416$$
$$= 17{,}700\Omega$$

or as a conductance

$$G_D = 56{\cdot}5 \ \mu\text{mhos}.$$

We will assume tuning capacitance loss to be 15 μmhos so that the overall total conductance including feedback loss due to the valve is made up as follows:

Part of the Circuit.	Conductance.
Coil	56·5 μmhos
Tuning capacitance	15·0 ,,
Valve-holder	2 ,,
Valve-base	2 ,,
Wiring	2·5 ,,
Range switch	2·0 ,,
Electron transit time in the valve	30·0 ,,
Total excluding feedback loss	110·0 ,,
Feedback loss due to L_k	154 ,,
Total conductance	264 ,,

To estimate the amplification from the aerial to the grid of the first R.F. valve we will assume that preset signal tuning is employed and that optimum coupling is therefore possible. Section 3.4.2 shows that the transfer voltage ratio is given by (expression 3.20c)

$$T_R = \frac{1}{2\omega C_2 \sqrt{R_2 R_{a1}}}$$

where C_2 is the tuning capacitance for the first-tuned circuit

R_{a1} is the total series resistance of the aerial circuit

R_2 is the total equivalent series resistance of the tuned circuit.

Taking R_{a1} as 80 ohms, the half-wave resonant impedance of a dipole aerial, the type most likely to be used at ultra high frequencies, and noting from expression 4.7 in section 4.2.2 that

$$R_2 = \frac{\omega^2 L^2}{R_D} = \omega^2 L^2 G_D$$
$$= (6{\cdot}28 \times 45 \times 0{\cdot}416)^2 \times 264 \times 10^{-6}$$
$$= 3{\cdot}65 \text{ ohms}$$

we find that

$$T_R = \frac{10^6}{2 \times 6{\cdot}28 \times 45 \times 30\sqrt{80 \times 3{\cdot}65}}$$
$$= 3{\cdot}45.$$

It will be seen from expression 3.20*c* quoted above, that $T_R \propto \frac{1}{\sqrt{R_2}}$ i.e., $\propto \frac{1}{\sqrt{G_D}}$, so that a decrease of G_D increases T_R. The overall Q of the tuned circuit in the absence of the aerial connection is $\frac{\omega L}{R_2} = \frac{117{\cdot}5}{3{\cdot}65} = 32{\cdot}2$, and for optimum coupling to the aerial, Q is halved, i.e., equals 16·1 (see expression 3.22*b* in Section 3.4.2). If we assume the band-width to be the frequency range over which the loss does not exceed 3 db., this condition is satisfied by

$$QF = \frac{Q2\Delta f}{f_r} = 1.$$

Hence the band-width $2\Delta f = \frac{45}{16{\cdot}1} = 2{\cdot}8$ Mc/s, and it is clear that preset signal tuning is a possibility when the band-width of the required transmissions is limited to the range 42·2 to 47·8 Mc/s. In Section 2.8.3 it is shown that a resistance R_k inserted in the cathode lead decreases the feedback conductance component of the valve. If $R_k = 150\Omega$ and $C_k = 5\ \mu\mu$F (this is stray capacitance, but it is essential in order to realize decreased input conductance).

$$Z_k = \frac{R_k}{1+\omega^2 C^2 R_k{}^2} + j\left(\omega L_k - \frac{\omega C_k R_k{}^2}{1+\omega^2 C_k{}^2 R_k{}^2}\right)$$
$$= 143{\cdot}3 + j(56{\cdot}5 - 30{\cdot}3)$$
$$= 143{\cdot}3 + j26{\cdot}2.$$

Thus $G_k = 6{\cdot}78 \times 10^{-3}$
$B_k = -1{\cdot}23 \times 10^{-3}$.

From expression 2.21*a*, Section 2.8.3

$$R_g = \frac{(G_k+g_k)^2+(B_k+B_{g_k})^2}{B_{g_k}(G_k B_{g_k} - g_k B_k)}$$
$$= \frac{(9{\cdot}78\times10^{-3})^2+(-0{\cdot}38\times10^{-3})^2}{8{\cdot}48\times10^{-4}(6{\cdot}78\times10^{-3}\times8{\cdot}48\times10^{-4}+3\times10^{-3}\times1{\cdot}23\times10^{-3})}$$
$$= 11{,}950\Omega$$
$G_g = 83{\cdot}6\ \mu$mhos.
Total $G_D = 193{\cdot}6\ \mu$mhos.

$$\frac{T_R(R_k = 150)}{T_R(R_k = 0)} = \sqrt{\frac{264}{193{\cdot}6}} = 1{\cdot}168.$$

This increase in transfer voltage ratio from the aerial to the grid of the first valve is, however, offset by the decrease in valve amplification due to negative feedback from the added cathode resistance. Section 2.7, expression 2.5*e*, indicates that the equivalent mutual conductance of the valve is reduced in the ratio $\frac{1}{1+g_kZ_k}$. Thus the valve equivalent g_m when $R_k = 0$ is

$$\frac{g_m}{1+g_k j\omega L_k} = \frac{g_m}{1+3 \times 10^{-3} \times 56{\cdot}5j} = \frac{g_m}{\sqrt{1+(0{\cdot}1695)^2}}$$
$$= 0{\cdot}972\ g_m$$

whereas for $R_k = 150\Omega$, $C_k = 5\ \mu\mu$F,

$$g_m' = \frac{g_m}{1+3 \times 10^{-3}(143{\cdot}3+j26{\cdot}2)}$$
$$= \frac{g_m}{\sqrt{(1+0{\cdot}4299)^2+(0{\cdot}0786)^2}}$$
$$= 0{\cdot}7\ g_m.$$

The actual reduction ratio of $g_m = \frac{0{\cdot}7}{0{\cdot}972} = 0{\cdot}72$ so that overall amplification, including the valve, has been reduced in the ratio 0·84 by inserting the resistance R_K. The advantages gained are:

(1) increase of selectivity in the ratio $\frac{264}{193{\cdot}6} = 1{\cdot}362$, and the band-width for a loss of 3 db. is reduced to 2·05 Mc/s; this is more important when variable tuned signal circuits are employed and may be a disadvantage with preset signal tuning.

(2) negative feedback tends to decrease distortion in the valve.

(3) there is less change of input conductance under A.G.C. operation, e.g., when $g_k = 0$, the valve input conductance = 106·2 μmhos ($R_g = 9{,}400\Omega$). It is practically independent of g_k in the particular example chosen.

Under certain conditions overall amplification can be increased by the use of a cathode resistance; for example, let us consider $R_k = 200$ ohms and $C_k = 15\ \mu\mu$F.

$$Z_k = \frac{200}{1{\cdot}715} + j\left(56{\cdot}5 - \frac{169{\cdot}0}{1{\cdot}715}\right)$$

$$= 116{\cdot}5 - j42.$$

$$G_k = 7{\cdot}58 \times 10^{-3},\ B_k = +2{\cdot}73 \times 10^{-3}$$

$$R_g = \frac{(10{\cdot}58 \times 10^{-3})^2 + (3{\cdot}58 \times 10^{-3})^2}{8{\cdot}48 \times 10^{-4}(7{\cdot}58 \times 10^{-3} \times 8{\cdot}48 \times 10^{-4} - 3 \times 10^{-3} \times 2{\cdot}73 \times 10^{-3})}$$

$$= -83{,}500\Omega$$

$$G_g = -11{\cdot}95\ \mu\text{mhos}.$$

Thus $G_D = 110 - 11{\cdot}95 = 98{\cdot}05\ \mu$mhos

and $$\frac{T_R(R_k = 200)}{T_R(R_k = 0)} = \sqrt{\frac{264}{98{\cdot}05}} = 1{\cdot}64.$$

The equivalent mutual conductance of the valve is

$$g_m' = \frac{g_m}{1 + 3 \times 10^{-3}(116{\cdot}5 - j42)} = \frac{g_m}{\sqrt{(1{\cdot}348)^2 + (0{\cdot}126)^2}}$$

$$= 0{\cdot}74\ g_m$$

and the ratio reduction of $g_m = \frac{0{\cdot}74}{0{\cdot}972} = 0{\cdot}76$.

The overall amplification ratio change is $1{\cdot}64 \times 0{\cdot}76 = 1{\cdot}245$. In this particular instance the overall amplification is increased by including R_k, but it will be noted that it is due to the cathode stray capacitance C_k overcompensating for the lead inductance L_k and so producing a negative input conductance. Selectivity is considerably increased, the ratio change being $\frac{264}{98{\cdot}05} = 2{\cdot}69$, and the bandwidth is reduced to 1·04 Mc/s from 2·8 Mc/s. Input conductance now varies considerably as g_k varies, from $-11{\cdot}95\ \mu$mhos at 3 mA/volt to 0 at 2·36 mA/volt and finally $+77{\cdot}5\ \mu$mhos at $g_k = 0$. This variation will help to improve the A.G.C. action and it has the merit of giving greatest selectivity for weak signals (lowest bias). An interesting feature of the particular component values chosen is the comparatively small change of conductance which occurs when the signal frequency is changed, e.g., at 40 Mc/s the conductance is $-15{\cdot}35\ \mu$mhos and it only decreases to $-5{\cdot}23\ \mu$mhos at 50 Mc/s. Care must be exercised to ensure that the negative input conductance is not increased sufficiently to cause an approach to oscillation.

Double-tuned transformers [31] may be employed for preset signal tuning between the R.F. valve and frequency changer, and they have the advantage of a flatter pass-band and sharper cut-off than a single circuit, though overall amplification is generally less. It is shown in Section 7.3 that maximum amplification with two tuned

circuits is only half that with a single-tuned circuit of identical L, C and Q values. However, a higher impedance may be possible with two tuned circuits since stray capacitance is approximately halved across each circuit, and the tuning inductance of either circuit may be increased upon that of a single circuit.

Adjustment of tuning at ultra high frequencies is preferably by variation of inductance, as fixed capacitors are less susceptible to ageing and temperature effects than variable ones, and variable inductances are more stable than variable capacitances. The tuning inductance usually consists of a few turns of copper wire with a metal plunger, which can be screwed into the axis of the coil. The plunger, which acts as a short-circuited turn to reduce inductance, must be of high conductivity material if it is not to alter appreciably the Q of the coil. The usual precautions appropriate to ultra high frequency operation must be taken in constructing the R.F. amplifier; leads must be as short as possible, all earth connections taken to the same point on the chassis, adequate decoupling, by small mica capacitors, of electrodes normally carrying only D.C. or A.C. supply voltages (screen, cathode and heaters).

BIBLIOGRAPHY

1. The Inductance Coefficients of Solenoids. Nagoka, *Journal of College of Science*, Tokyo, Aug. 15th, 1909, p. 1.
2. Bureau of Standards Circular No. 74 (1924).
3. The Effective Resistance of Inductance Coils at Radio Frequency. S. Butterworth, *Wireless Engineer*, April (p. 203), May (p. 309), July (p. 417), Aug. (p. 483), 1926.
4. Simple Inductance Formulas for Radio Coils. H. A. Wheeler, *Proc. I.R.E.*, Oct. 1928, p. 1398. Discussion on above (R. A. Batcher), *Proc. I.R.E.*, March 1929, p. 580.
5. An Improved Pre-Selector Circuit for Radio Receivers. E. A. Uehling, *Electronics*, Sept. 1930, p. 279.
6. The Design of Tuned Cicuits to fulfil Predetermined Conditions. A. L. M. Sowerby, *Wireless Engineer*, Jan. 1931, p. 23. Discussion (S. Butterworth), *Wireless Engineer*, April 1931, p. 199.
7. Oscillation in Tuned R.F. Amplifiers. B. J. Thompson, *Proc. I.R.E.*, March 1931, p. 421. Discussion, *Proc. I.R.E.*, July 1931, p. 1,281.
8. Theory and Operation of Tuned R.F. Coupling Systems. H. A. Wheeler and W. A. Macdonald, *Proc. I.R.E.*, May 1931, p. 738.
9. The Design of H.F. Transformers. M. Reed, *Wireless Engineer*, July 1931, p. 349.
10. The Design of the Band Pass Filter. N. R. Bligh, *Wireless Engineer*, Feb. 1932, p. 61.
11. Distortion in Screen-Grid Valves. R. O. Carter, *Wireless Engineer*, March 1932, p. 123.
12. The Theory of Distortion in Screen-Grid Valves. R. O. Carter, *Wireless Engineer*, Aug. 1932, p. 429.

13. Resistance in Band Pass Filters. G. H. Buffery, *Wireless Engineer*, Sept. 1932, p. 504.
14. Two Element Band Pass Filters. R. T. Beatty, *Wireless Engineer*, Oct. 1932, p. 546.
15. The Theory of Band Pass Filters for Radio Receivers. C. W. Oatley, *Wireless Engineer*, Nov. 1932, p. 608.
16. Ferro Inductors and Permeability Tuning. W. J. Polydoroff, *Proc. I.R.E.*, May 1933, p. 690.
17. Die Rückwirkung Metallischer Spulenkapseln auf Verluste Induktivität und Aussenfeld einer Spule. H. Kaden, *Elektrische Nachrichten Technik.*, July 1933, p. 277.
18. The Effective Resistance of Inductance Coils at Radio Frequency. B. B. Austin, *Wireless Engineer*, Jan. 1934, p. 12.
19. A Study of the Possibilities of R.F. Voltage Amplification with Screened Grid and with Triode Valves. F. M. Colebrook, *Journal I.E.E.*, Feb. 1934, p. 187.
20. The Effect of Screening Cans on the Inductance and Resistance of Coils. G. W. O. Howe, *Wireless Engineer*, March 1934, p. 115.
21. Band Pass Filter Characteristics. H. N. Jaderholm, *Electronics*, July 1936, p. 33.
22. Nomograms for the Design of Band Pass R.F. Circuits. C. P. Nachod, *Radio Engineering*, Dec. 1936, p. 13.
23. Two Mesh Tuned Coupled Circuit Filters. C. B. Aiken, *Proc. I.R.E.*, Feb. 1937, p. 230.
24. Universal Performance Curves for Tuned Transformers. J. E. Maynard, *Electronics*, Feb. 1937, p. 15.
25. A Graphical Estimation of the Signal Handling Capacity of Screened Grid Valves. R. W. Sloane, *Phil. Mag.*, April 1937, p. 529.
26. Using the R.F. Charts. C. P. Nachod, *Radio Engineering*, June 1937, p. 19.
27. The Resultant Q of Tuned Circuits. A. W. Barber, *Radio Engineering*, July 1937, p. 5.
28. The Design of Inductances for Frequencies Between 4 and 25 Mc/s. D. Pollack, *R.C.A. Review*, Oct. 1937, p. 184.
29. The Impedance of a Tapped Resonant Circuit. K. R. Sturley, *Marconi Review*, Oct.–Dec. 1938, p. 1.
30. A Receiver for Frequency Modulation. J. R. Day, *Electronics*, June 1939, p. 32.
31. Television Signal Frequency Circuits. G. Mountjoy, *R.C.A. Review*, Oct. 1939, p. 204.
32. The Signal Handling Capacity of H.F. Valves. R. W. Sloane, *Wireless Engineer*, Nov. 1939, p. 543.
33. The Effective Inductance and Resistance of Screened Coils. A. G. Bogle, *Journal I.E.E.*, Sept. 1940, p. 299.
34. *Radio Data Charts*. R. T. Beatty. Messrs. Iliffe.
35. *Spontaneous Fluctuations of Voltage*. E. B. Moullin, Oxford University Press. Text-book.
36. British Patent No. 518,969. J. D. Brailsford and Marconi's Wireless Telegraph Coy.

CHAPTER 5

FREQUENCY CHANGING

5.1. Problems in Frequency Changing.

5.1.1. Introduction.[1, 2, 3] The number of signal frequency amplifier stages in receivers covering a range of frequencies is generally limited, because ganging is difficult and, unless special precautions are taken, a considerable variation of sensitivity and selectivity occurs over the tuning range. For short wave reception it is almost impossible to obtain a high gain from an R.F. amplifier owing to the low value of tuning inductance (the dynamic resistance of a tuned circuit is $\frac{L}{CR}$) which must be employed, and at the high-frequency end of the range, cathode lead inductance and electron transit time combine to produce a high grid input admittance (Section 2.8). Many advantages are obtained if each signal frequency can be converted as desired to another fixed frequency and this is the principle involved in the superheterodyne method of reception. The frequency change is carried out by applying the signal and a local oscillator voltage (often known as the heterodyne * voltage) to a non-linear device, this term implying that frequencies, in addition to those applied at the input appear in the output voltage. Harmonics of, and the sum and difference frequencies of the signal and local oscillator, are produced in the output circuit, and any of these components may be selected by a suitable filter. The amplitudes of the sum $(f_h + f_s)$ and difference $(f_h - f_s)$ frequencies are equal, but the latter, called the intermediate frequency, is selected because possible amplification and selectivity are greater at the lower frequency. Any given signal can be converted to the intermediate frequency by a suitable choice of oscillator frequency.

In an ideal frequency changer the intermediate frequency amplitude varies directly as the signal frequency amplitude, and amplitude changes due to modulation of the signal frequency are reproduced without distortion with the intermediate frequency as carrier. It is, of course, assumed that no attenuation of the modula-

* All terms associated with the oscillator will be denoted by a suffix h, *e.g.*, $\hat{E}_h$ and f_h mean the local oscillator peak voltage and frequency respectively. The suffix h is used in preference to 0, as 0 is used to denote output circuit. The suffix s is used for the signal.

tion side-bands occurs in the intermediate frequency anode tuned circuit of the frequency changer.

5.1.2. The Advantages of Superheterodyne Reception. The chief advantages of superheterodyne reception are :

(1) The amplifier following the frequency changer can be designed for optimum performance because tuning controls are all preset.

(2) The overall sensitivity and selectivity of such a receiver is more constant over the tuning range because most is concentrated in the fixed frequency amplifier.

The intermediate frequency is generally, though not always, less than the signal frequency so that high sensitivity, selectivity and stability are obtainable. The gain of the frequency changer valve, itself, must be considered and it is therefore essential to define conversion conductance, g_c. This term, analogous to mutual conductance in an amplifier, is expressed as

$$g_c = \frac{\text{intermediate frequency component of } I_a \text{ for zero anode load}}{\text{signal voltage producing this component}}.$$

The output voltage from the frequency changer is

$$E_0 = g_c E_g Z_0$$

when Z_0, the external anode impedance, is much less than R_a, the frequency changer slope resistance.

Methods of measuring conversion conductance, and its relationship to mutual conductance, are discussed later. It should be noted, however, that g_c is generally less than 0·25 g_m. The lower value of g_c is offset to some extent by the higher anode impedance obtained at the intermediate frequency. This is made clear by Table 5.1, in which are listed typical values of coil constants used in radio receivers at intermediate frequencies of 110 and 465 kc/s, and at three signal frequencies of 200, 1,000, and 6,000 kc/s.

TABLE 5.1

Frequency (kc/s).	Inductance.	Q.	Impedance (Z_0).	Amplification.
110 (I.F.)*	9,000 μH	40	249,000	187
465 (I.F.)	1,000 μH	80	233,000	175
200 (S.F.)†	2,200 μH	45	124,000	372
1,000 (S.F.)	156 μH	100	98,000	293
6,000 (S.F.)	1·5 μH	200	11,300	34

* I.F.—intermediate frequency.
† S.F.—signal frequency.

For calculating amplification we have assumed that the mutual conductance of the amplifier is 3 mA/volt and that of the frequency changer 0·75 mA/volt. There is therefore a loss of amplification

by introducing frequency changing on the long and medium wave bands, but a considerable improvement on the short wave band—this is due to the low impedance of the short wave tuned circuit. The short wave inductance is low partly because it is assumed that the same tuning capacitor is used on all ranges. In receivers specially designed for short wave operation smaller capacitors (maximum value 150 $\mu\mu$F as compared with 500 $\mu\mu$F) are often employed. This allows an increase of inductance, which in turn increases the dynamic resistance of the signal tuned circuit and the amplification as an R.F. amplifier. The wave-range coverage is, of course, correspondingly reduced.

For medium and long wave operation the increased amplification obtained in the intermediate frequency amplifier tends to compensate for the lower amplification of the frequency changer.

5.1.3. The Principles of Frequency Changing.[16] Let us consider signal and oscillator voltages, represented by $\hat{E}_s \cos \omega_s t$ and $\hat{E}_h \cos \omega_h t$ respectively, applied to the grid circuit of a valve. If the valve has a linear $I_a E_g$ characteristic curve and the input voltages operate over the linear part, i.e., the valve is not biased near cut-off, we shall obtain the following result.

$$I_a = a_0 + a_1 E_g \quad . \quad . \quad . \quad . \quad . \quad 5.1a$$

but $$E_g = \hat{E}_s \cos \omega_s t + \hat{E}_h \cos \omega_h t - E_b$$

where $-E_b$ is the bias voltage

thus $$I_a = a_0 + a_1(\hat{E}_s \cos \omega_s t + \hat{E}_h \cos \omega_h t - E_b) \quad . \quad 5.1b.$$

The output circuit therefore contains only the two frequencies present in the input circuit.

If the valve has a characteristic curve represented by

$$I_a = a_0 + a_1 E_g + a_2 E_g^2 \quad . \quad . \quad . \quad 5.2a$$

we have

$$\begin{aligned} I_a &= a_0 + a_1[\hat{E}_s \cos \omega_s t + \hat{E}_h \cos \omega_h t - E_b] \\ &\quad + a_2[\hat{E}_s \cos \omega_s t + \hat{E}_h \cos \omega_h t - E_b]^2 \\ &= a_0 + a_1[\hat{E}_s \cos \omega_s t + \hat{E}_h \cos \omega_h t - E_b] \\ &\quad + a_2[\hat{E}_s^2 \cos^2 \omega_s t + \hat{E}_h^2 \cos^2 \omega_h t + E_b^2 + 2\hat{E}_s \hat{E}_h \cos \omega_s t \cos \omega_h t \\ &\quad - 2\hat{E}_s E_b \cos \omega_s t - 2\hat{E}_h E_b \cos \omega_h t] \end{aligned}$$

and by noting that

$$\cos^2 \theta = \frac{1 + \cos 2\theta}{2}$$

and $$\cos \theta \cos \phi = \frac{\cos(\theta + \phi) + \cos(\theta - \phi)}{2}$$

we can separate the anode current into its seven components as follows :

D.C. component	$a_0 - a_1E_b + a_2\left[\frac{\hat{E}_s^2 + E_h^2}{2} + E_b^2\right]$
Fundamental Frequencies f_s	$(a_1\hat{E}_s - 2a_2\hat{E}_sE_b)\cos\omega_s t$
Fundamental Frequencies f_h	$(a_1\hat{E}_h - 2a_2\hat{E}_hE_b)\cos\omega_h t$
Harmonic Frequencies $2f_s$	$\frac{a_2\hat{E}_s^2}{2}\cos 2\omega_s t$
Harmonic Frequencies $2f_h$	$\frac{a_2\hat{E}_h^2}{2}\cos 2\omega_h t$
Sum frequency $(f_h + f_s)$	$a_2\hat{E}_s\hat{E}_h\cos(\omega_h + \omega_s)t$
Difference frequency $(f_h - f_s)$	$a_2\hat{E}_s\hat{E}_h\cos(\omega_h - \omega_s)t.$

The valve has produced four frequencies in addition to the signal and oscillator, and the insertion of a suitable filter in its anode circuit allows any one of these frequencies to be selected. Thus we may reject all except the difference frequency voltage component, which is then passed on to the intermediate frequency amplifier. The difference frequency $(f_h - f_s)$ naturally assumes that the oscillator frequency is greater than the signal. From a mathematical point of view the difference frequency term may be written as $a_2\hat{E}_s\hat{E}_h\cos(\omega_h - \omega_s)t$ or $a_2\hat{E}_s\hat{E}_h\cos(\omega_s - \omega_h)t$ since $\cos\theta = \cos(-\theta)$ and in practice we have $(\omega_h - \omega_s)$ if $f_h > f_s$ and $(\omega_s - \omega_h)$ if $f_s > f_h$. The frequency changer is quite unable to discriminate against the two signal frequencies which can produce with a given oscillator frequency a difference frequency equal to the intermediate frequency. Usually the lower frequency signal giving $(f_h - f_s')$ as the difference frequency is regarded as the desired signal—the reasons for this are set out in Section 5.1.5—and the higher giving $f_s'' - f_h$ is regarded as an undesired frequency, generally called the second channel or image frequency.[5]

If the signal frequency is modulated, e.g., $\hat{E}_s\cos\omega_s t(1 + M\cos pt)$, all anode current components containing $\hat{E}_s$ are similarly modulated and the difference frequency component is

$$a_2\hat{E}_s\hat{E}_h(1 + M\cos pt)\cos(\omega_h - \omega_s)t;$$

so that according to the definition in 5.1.2 conversion conductance

$$g_c = \frac{I_a}{\hat{E}_s} = a_2\hat{E}_h \quad . \quad . \quad . \quad . \quad 5.3a.$$

It may be pointed out that the sum frequency is similarly modulated but is never selected because it is higher in frequency than either signal or oscillator. Many of the advantages of super-

heterodyne reception are lost when the intermediate frequency is higher than the signal, though in certain instances, over the long wave band of an all-wave receiver, the difference frequency often does exceed the signal frequency.

In the above analysis it has been shown that a valve having a linear I_aE_g characteristic curve does not normally produce frequency changing. It should, however, be noted that such a valve, biased either to cut-off or to a point where the total grid voltage swing of oscillator and signal passes over the cut-off discontinuity, produces frequency changing. It does so because the condition of non-linearity is fulfilled and the valve characteristic may be represented by an infinite power series containing a term such as $a_2E_g^2$.

A valve having two control electrodes giving the I_aE_g relationship

$$I_a = (a_0+a_1E_{g1})(b_0+b_1E_{g3}) \quad . \quad . \quad . \quad 5.2b$$

will also act as a frequency changer so long as the signal voltage is applied to grid 1 and the oscillator to grid 3, or vice versa. The term $a_1b_1E_{g1}E_{g3}$ corresponds to $a_2E_g^2$ in expression 5.2*a* and conversion conductance is

$$g_c = \frac{a_1b_1}{2}E_h \quad . \quad . \quad . \quad . \quad 5.3b$$

i.e., $\frac{1}{2}a_1b_1$ corresponds to a_2. Any frequency changer such as a pentagrid, heptode, octode or hexode, in which the oscillator voltage is applied to an electrode other than that of the signal, operates on this principle.

5.1.4. Considerations Governing the Choice of the Intermediate Frequency.[4, 14] The choice of the intermediate frequency is first of all limited to a position in the frequency range where there is little chance of direct interference from transmitting stations. As a rule, frequencies in the long or medium wave range are avoided because interference may be produced due to direct signal amplification in the intermediate frequency amplifier. The intermediate frequency is most commonly located in the frequency range 450 to 475 kc/s, though a lower frequency range 100 to 125 kc/s has been used for superheterodyne receivers covering only the medium and long wave-bands, and a higher [7, 22] frequency range 1,500 to 2,000 kc/s is employed for "single span" [18] and double superheterodyne receivers. The intermediate frequency range 450 to 475 kc/s is preferred to the 100 to 125 kc/s range because it gives greater frequency separation between the desired and the image signal. An amplifier operating at the lower intermediate frequency is generally more stable and has greater amplification and selectivity

than one operating at 450 kc/s, but these advantages are far outweighed by the fact that locking or control of the oscillator frequency by the signal circuit tuning becomes serious on the short wave band when a low intermediate frequency is used. Furthermore, the higher intermediate frequency produces less interference whistles (see Section 5.4) over a given range of signal frequencies.

5.1.5. The Oscillator Frequency. In Section 5.1.3 it is shown that there are two signal frequencies which can react with a given oscillator frequency to produce the intermediate frequency and, conversely, there are two oscillator frequencies which can give the intermediate frequency with a certain signal frequency. The two oscillator frequencies are higher and lower than the signal frequency by an amount equal to the intermediate frequency. The higher oscillator frequency is almost invariably chosen because the ratio of its maximum to minimum value over a given range is less than that of the signal. This means that the ratio of the maximum to minimum values of oscillator tuning capacitor is less than that of the signal tuning capacitor. For example, a receiver having a range from 550 to 1,500 kc/s calls for a signal capacitor ratio change of $7{\cdot}43 : 1\left(C \propto \frac{1}{f^2}\right)$, whilst the oscillator capacitor ratio is only $3{\cdot}75 : 1$ for an I.F. of 465 kc/s (frequency range from 1,015 to 1,965 kc/s) when $f_h > f_s$. Constructional and ganging difficulties are reduced, because the same tuning capacitor unit may be used for the oscillator as for the signal circuit, its range being adjusted by series and parallel padding capacitances. (See Section 6.12.)

5.1.6. Interference Whistles. Frequency changing possesses the disadvantage that it increases the possibility of obtaining interference from undesired signals. The interference may make itself evident by superimposing an undesired programme and a whistle on the desired, but generally it is shown by a whistling note only, the frequency of which varies when slight changes of oscillator capacitance tuning are made. The most serious is that due to image interference. Special measures to increase the filtering properties of the signal-tuned circuits at this particular frequency are often undertaken and are described in Section 5.9. There are many other forms of interference and a whistle is always possible if

$$\pm mf_h \mp nf_u \simeq f_1$$

where m and n are positive whole numbers

f_u = undesired signal frequency
f_1 = intermediate frequency.

Let us take as an example a receiver tuned to a signal of 750 kc/s with an I.F. of 465 kc/s. The oscillator frequency, 1,215 kc/s, may react with an undesired signal frequency of 982 kc/s at the input of the frequency changer to produce a 1 kc/s whistle in the I.F. amplifier for

$$2 \times 1{,}215 - 2 \times 982 = 466 \text{ kc/s}.$$

Similarly an undesired signal of 1,967 kc/s can produce a 2 kc/s whistle because

$$2 \times 1{,}215 - 1{,}967 = 463 \text{ kc/s}.$$

A more detailed discussion of these interference frequencies is given later in Section 5.4.

5.2. Frequency Changer Circuits.

5.2.1. Introduction. Frequency changer circuits may conveniently be divided into two classes; in the first the signal and oscillator frequencies are applied to a common electrode, usually the grid-cathode circuit of a valve, and in the second the two frequencies are applied at different electrodes. There is no fundamental difference between the two types of circuit, and frequency changing results in both cases because the oscillator voltage controls the mutual conductance and hence the amplification of the valve. Common electrode coupling entails a curved or discontinuous I_aE_g curve because frequency changing is determined by the E_g^2 term shown in equation 5.2*a*. For separate electrode coupling, the oscillator voltage causes a variation in the slope of the $I_aE_{sig.\,grid}$ characteristic curve, which may itself be a straight line, and frequency changing occurs in accordance with expression 5.2*b*.

5.2.2. Oscillator Application to the Grid-Cathode Circuit. Let us imagine that the signal and oscillator voltages are applied in series to the grid circuit of an R.F. amplifier valve having a curved I_aE_g characteristic, and that there is no interaction between the voltage sources.

If we wish to find the operating condition for maximum conversion conductance we have two dependent variables to consider, viz., the oscillator and bias voltages. The signal voltage is not a dependent variable since conversion conductance, in the same manner as mutual conductance, is independent of the signal voltage under normal operating conditions. The bias voltage must always be such that grid current does not flow, because damping of the signal-tuned circuit is not permissible. It is preferable therefore to vary the bias voltage with the oscillator voltage, keeping the bias

voltage always at least 1 volt more negative than the peak value of the oscillator voltage. Typical conversion conductance-oscillator voltage curves, obtained as described in Sections 5.6.3 and 5.6.4 are shown in Fig. 5.1*a*. The negative bias values for the three curves are adjusted to be 1, 2 and 3 volts, respectively, greater than the peak value of the oscillator voltage. The maximum value of conversion conductance and the oscillator voltage required to reach it tend to fall as the bias is increased. For small values of oscillator voltage the conversion conductance actually increases with increase

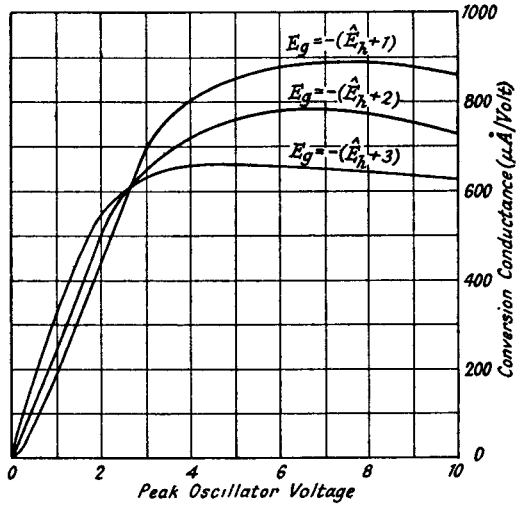

FIG. 5.1*a*.—Typical Conversion Conductance-Oscillator Voltage Curves for Signal and Oscillator Voltages in the Grid-Cathode Circuit.

of bias. If the latter is increased far enough the conversion conductance begins to fall and the effect is analogous to the optimum bias point for an anode bend detector as described in 8.4.1.

It is necessary now to consider the reason for maximum conversion conductance at a particular oscillator voltage, since the I.F. term $a_2\hat{E}_s\hat{E}_h \cos(\omega_h - \omega_s)t$ obtained from expression 5.2*a* would not suggest an optimum but an ever-increasing value as the oscillator is increased. This is due to the fact that a characteristic I_aE_g curve is never completely represented by the simple power series [16] in 5.2*a*, but more nearly by

$$I_a = a_0 + a_1E_g + a_2E_g^2 + a_3E_g^3 - a_4E_g^4 + \quad . \quad . \quad 5.4.$$

A negative sign for the a_4 term agrees with the known fact that

as E_g is increased positively I_a does not increase indefinitely but reaches some saturation value. Replacing E_g by

$$\hat{E}_s \cos \omega_s t + \hat{E}_h \cos \omega_h t - E_b$$

in $-a_4 E_g^4$ gives a term

$$\begin{aligned} &- 4a_4 \hat{E}_s \hat{E}_h^3 \cos \omega_s t \cos^3 \omega_h t \\ &= - 4a_4 \hat{E}_s \hat{E}_h^3 \cos \omega_s t (\tfrac{3}{4} \cos \omega_h t + \tfrac{1}{4} \cos 3\omega_h t) \\ &= - \tfrac{3}{2} a_4 \hat{E}_s \hat{E}_h^3 [\cos (\omega_h - \omega_s) t + \cos (\omega_h + \omega_s) t] \\ &\quad - \frac{a_4}{2} \hat{E}_s \hat{E}_h^3 [\cos (3\omega_h - \omega_s) t + \cos (3\omega_h + \omega_s) t]. \end{aligned}$$

The first term, $-\frac{3}{2} a_4 \hat{E}_s \hat{E}_h^3 \cos (\omega_h - \omega_s) t$, increases rapidly as the oscillator voltage is increased and subtracts from the I.F. component produced by $a_2 E_g^2$. There is also a term $-\frac{3}{2} a_4 \hat{E}_s^3 \hat{E}_h \cos (\omega_h - \omega_s) t$, but its effect is much less marked because $\hat{E}_s$ is usually much less than $\hat{E}_h$. Hence an optimum oscillator voltage value is obtained as shown by Fig. 5.1*a*, which gives curves typical of a valve of the variable mu type. For a non-variable mu valve the optimum oscillator voltage has a much more pronounced maximum. It will be noticed that the curves, after the initial rapid rise, reach a maximum rather slowly and it is preferable to operate at an oscillator voltage lower than maximum, e.g., 4 volts for $E_g = -(\hat{E}_h + 1)$ because the amplitude of the interference whistles generated by the frequency changer increases rapidly with increase of oscillator voltage (see Section 5.4.1).

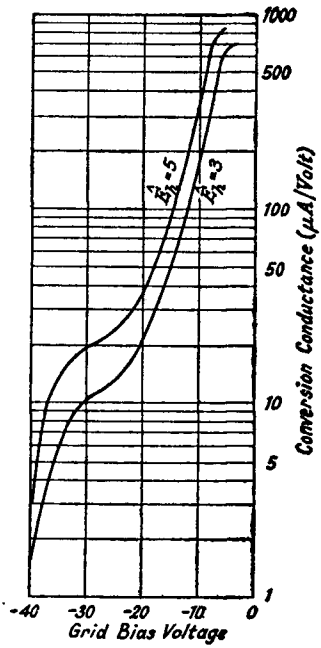

FIG. 5.1*b*.—Conversion Conductance-Grid Voltage Curves for Oscillator Voltage Application to the Cathode Circuit.

For good automatic gain control characteristics it is essential to control as many R.F. stages as possible so that the frequency changer valve may possess variable mu characteristics. Typical $g_c E_g$ curves are illustrated in Fig. 5.1*b* for two values of oscillator voltage. The larger gives greater conversion conductance and a longer cut-off (approximately longer by the difference between the two oscillator peak voltage values, i.e., 2 volts).

The oscillator voltage may be applied to the grid-cathode circuit

in a number of ways. One possible method is via a coil connected between the grid and the signal-tuned circuit. This has the disadvantage that the tuning range of the signal circuit is restricted by the coil capacitance to earth, and ganging with the preceding signal amplifier stages is rendered almost impossible. The alternative position for the coil, on the earthed side of the tuning circuit, necessitates insulation of rotor as well as stator plates of the tuning capacitance and is therefore impracticable. It can however be used when signal tuning is preset as for push-button operated receivers or band-spread receivers at high and ultra-high frequencies.

A second method is to apply the oscillator voltage via a coil coupled to the signal tuning coil. This suffers from the disadvantage that the actual value of the oscillator voltage applied to the grid circuit now depends on the selectivity of the signal circuit, and the frequency separation between oscillator and signal. The signal-tuned circuit is directly connected to the pick-up coil and interaction tends to cause a variation of oscillator frequency with variation of the signal-tuned circuit.

Coupling by capacitance to the grid of the frequency changer is a possibility, but it possesses the disadvantages of both the first two methods.

The best method of inserting the oscillator voltage in the grid-cathode circuit is by means of a coil in the cathode-earth lead. The coupling between the signal and oscillator circuits is limited to the grid-cathode capacitance and interaction is very much reduced. This circuit is very suitable for signal frequencies in the medium and long wave band, but is not satisfactory for short wave operation because the grid-cathode capacitance is sufficient to cause the signal circuit tuning to influence the amplitude and frequency of the oscillator voltage. The effect of this coupling at medium and long wave frequencies is chiefly to develop across the signal circuit an oscillator voltage in opposition to the cathode oscillator voltage, so that the net voltage applied between the grid and cathode of the frequency changer is decreased. A high I.F. reduces the feedback voltage developed in the signal circuit by increasing the frequency separation between signal and oscillator circuits. For an I.F. of 465 kc/s, the oscillator voltage developed in a signal circuit tuned to the centre of the medium wave-band is of the order of $\frac{1}{30}$ of that in the cathode circuit.

It is quite usual to combine the oscillator and frequency changer in one valve, and a typical circuit for grid-cathode coupling is shown in Fig. 5.2*a*. The valve is a triode-pentode with a cathode

common to both. The pick-up coil in the cathode is also the feedback coil for the oscillator, and this necessitates decoupling of the anode and screen circuits of the pentode to the cathode and not to earth. If these two circuits are decoupled to earth, current varia-

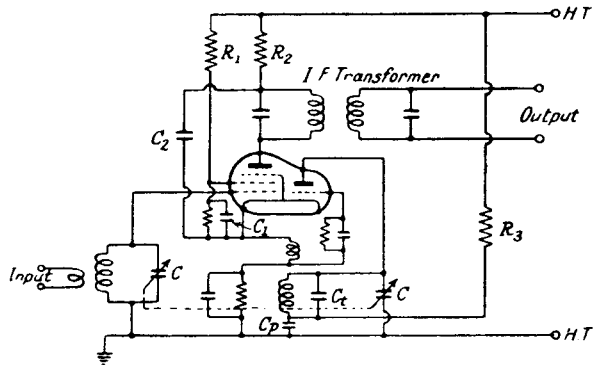

FIG. 5.2*a*.—The Circuit for Oscillator Voltage in the Cathode of a Triode-Pentode Valve.

tions in the pentode section at the oscillator frequency develop a voltage across the coil in opposition to that generated by the oscillator. This is more clearly demonstrated by considering the equivalent circuit in Fig. 5.2*b*. The I.F. circuit impedance is low to the oscillator frequency and is assumed to be zero. For convenience the cathode coil is replaced by a separate generator of

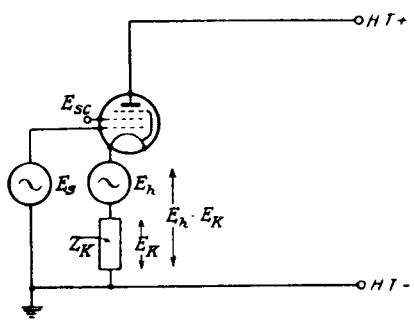

FIG. 5.2*b*.—The Equivalent Circuit for the Oscillator Voltage in the Cathode Circuit of a Pentode Valve.

open circuit voltage E_h (the oscillator voltage) with an internal impedance Z_k, the coil impedance at the oscillator frequency. The voltage applied to the grid-cathode electrodes of the pentode is $E_h - E_k$, where E_k is the voltage produced across the coil imped-

ance Z_k by the oscillator frequency variations of the pentode current. The value of E_k is

$$E_k = g_m(E_h - E_k)Z_k$$

where g_m = mutual conductance of the pentode.

Thus

$$E_k = E_h \frac{g_m Z_k}{1 + g_m Z_k}$$

and the net voltage between cathode and earth is

$$E_h - E_k = \frac{E_h}{1 + g_m Z_k} \quad . \quad . \quad . \quad 5.5.$$

The effective voltage is therefore reduced, and since this is also the driving voltage for the oscillator it means that there is a serious degenerative effect on the latter. This defect, which may even be sufficient to prevent oscillation altogether, can be eliminated by decoupling the screen and anode circuits to cathode. The resistances R_1 and R_2 and capacitances C_1 and C_2 in Fig. 5.2*a* perform this function, diverting pentode current variations at the oscillator frequency direct to cathode instead of via earth through Z_k to the cathode. I.F. current variations are diverted from Z_k at the same time. Capacitors C are ganged together and C_p acts as a padding capacitance for ganging purposes.

5.2.3. Oscillator Application to the Screen Circuit. Frequency changing may be accomplished by applying the oscillator voltage in the screen circuit of a multigrid valve. Owing to the low

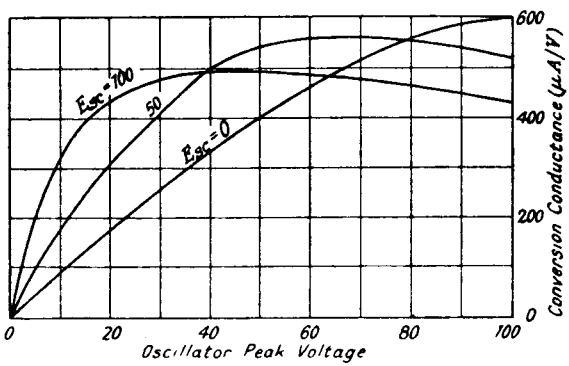

FIG. 5.3.—Typical Conversion Conductance-Oscillator Voltage Curves for Oscillator Voltage in the Screen Circuit of a Pentode Valve.

amplification factor between screen and anode a much larger voltage is required than for the cathode circuit. Typical conversion conductance-oscillator voltage curves are shown in Fig. 5.3 for a

pentode valve. Similar curves may be obtained for a screened-grid valve, but they are of little practical value since conversion gain under normal operating conditions is limited by the secondary emission characteristic, and falls off rapidly when the sum of the D.C. screen voltage and oscillator peak voltage approaches the minimum voltage developed in the anode under normal operating conditions. This voltage, which is equal to the H.T. voltage minus the peak value of the output voltage E_0, is dependent on the I F. external anode impedance and the signal voltage. In a pentode the effect does not occur since the minimum anode voltage is practically independent of screen voltage and can be very nearly zero.

An interesting point shown by the curves is that maximum g_c is obtainable with zero D.C. screen volts. The valve then operates as a half-wave frequency changer on the positive half of the oscillator voltage wave, the anode current being cut off for the negative half-cycle. Section 5.5 indicates that this is the most efficient method of frequency changing.

A serious disadvantage of screen application is the large oscillator voltages required. The screen-control grid capacitance is almost equal to that of the control grid-cathode so that the proportion of oscillator voltage transferred to the signal circuit is the same. Since the required value is so large (ten to twenty times greater than for cathode application) the voltage appearing across the signal circuit is much greater. Also the oscillator-tuned circuit has to be used to provide the screen voltage, and the signal-circuit tuning consequently influences the oscillator frequency to a great extent. For these reasons screen frequency changing is never used.

5.2.4. Oscillator Application to the Suppressor Grid. We have already shown in Section 2.5 that bias on the suppressor grid of a pentode may be used for controlling the amplification of the valve. Frequency changing can therefore be accomplished by applying the oscillator voltage to the suppressor grid circuit as in Fig. 5 4, and it takes place in accordance with expression 5.2*b*. The current taken by the suppressor grid on application of the oscillator provides the self-biasing voltage across R_s (about 1 MΩ). The optimum oscillator voltage depends on the suppressor grid cut-off bias voltage, and its peak value is usually 2 to 3 volts greater than half the latter. A typical curve of conversion conductance is shown in Fig. 5.4 for the self-bias condition. The maximum conversion gain $\left(g_c \cdot \frac{Z_0}{R_a + Z_0}\right)$ is generally little more than half that for cathode application because of the reduction in valve slope

resistance brought about by biasing the suppressor grid (Section 2.5). This resistance reduction causes loss of selectivity as well as of amplification when the valve is associated with an I.F. tuned transformer.

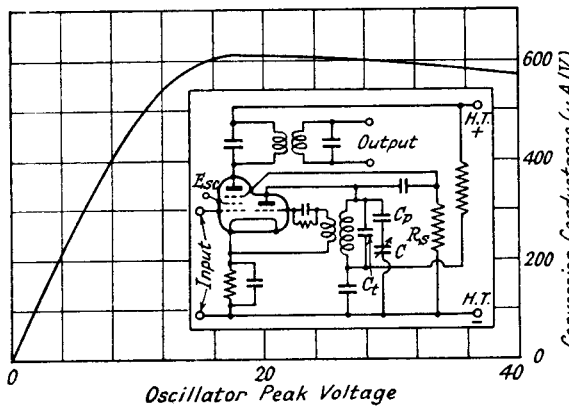

FIG. 5.4.—Typical Conversion Conductance-Oscillator Voltage Curves for Suppressor Grid Oscillator Voltage and Self-Bias on a Pentode Valve.

The chief advantage of suppressor grid application is the additional screening provided between signal and oscillator circuits by the screen-grid electrode and it therefore can be used for short wave operation.

5.2.5. Oscillator Application to the Anode Circuit.[9] Oscillator application to the anode circuit of a tetrode or pentode valve is not employed because the anode voltage has little effect on anode current unless the former is very low. For large conversion conductance the D.C. anode voltage must be low and the oscillator voltage must carry the anode voltage over the bend of the I_aE_a curve. Under these conditions the valve slope resistance is low and the I.F. transformer characteristics are adversely affected.

5.2.6. Frequency Changing and Oscillation from a Single Valve.[8] It is possible to combine the functions of frequency changer and local oscillator in one valve, though it is preferable to employ a separate oscillator as it is not easy to obtain high efficiency frequency changing with satisfactory oscillation and little interaction over a range of signal frequencies. Oscillation may be obtained by feedback coupling between cathode and anode or screen and anode, or by using the dynatron, or negative resistance characteristic (Section 2.4) of the screen or anode of a screened-grid valve. In one method a coil, inserted in the cathode lead of a tetrode or

pentode, is coupled to the oscillator-tuned circuit connected by capacitance to the anode, which contains an I.F. transformer with untuned primary, the latter acting as a choke to the local oscillator frequency. An alternative is to connect the feedback coil in the screen circuit, but this requires much tighter coupling as the amplification between screen and anode is generally low, and screen application requires a large oscillator voltage for satisfactory frequency changing. The position of the oscillator tuned circuit and feedback coil can be reversed, the latter being placed in series with the I.F. transformer primary, which can then be tuned. Oscillations may be generated by inserting the oscillator tuned circuit in either screen or anode of a screened grid valve and suitably biasing both electrodes to bring the dynatron characteristic into play, but this method is not very satisfactory and adjustments are critical. Combined single valve operation of this kind is only possible over medium and long wave ranges since there is considerable interaction between signal and oscillator circuits.

5.3. Special Types of Frequency Changers.[42]

5.3.1. The Triode Hexode.[10, 32] The triode-hexode frequency changer is a logical development from the triode pentode with suppressor grid application. It will therefore be treated before the heptode or octode, although it was preceded by them. The low slope resistance due to biasing the suppressor grid of the pentode is restored to a high value by the inclusion of a positively biased

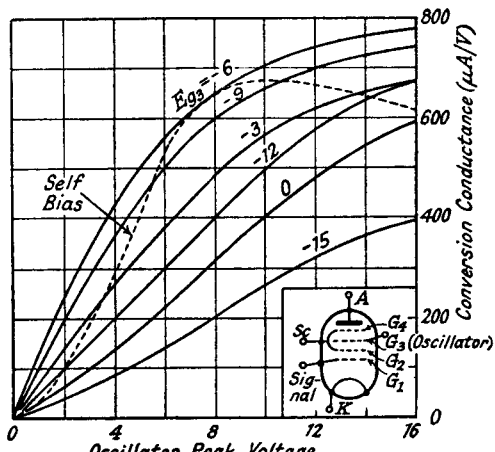

FIG. 5.5.—Typical Conversion Conductance Curves for a Hexode Valve.
(E_a = 250, E_{sc} = 70, E_{g1} = − 1·5.)

screen between the suppressor grid and anode. The effect of this screen, which converts the pentode to a hexode, is shown in Section 2.5 to be the conversion of the triode, formed by the virtual cathode round the first screen, the suppressor grid and anode, into a screen grid valve.

Typical conversion conductance-oscillator voltage curves are shown in Fig. 5.5. The dotted curve is the one obtained for self-bias of the oscillator grid. The rule for optimum oscillator peak voltage as given for self-biased suppressor grid application is again applicable, viz., that it is about half the cut-off bias voltage (— 16) plus 2 or 3. The additional screen (g_4) not only raises the valve slope resistance but also allows g_3 to have a closer mesh without seriously reducing anode current, and so the optimum oscillator voltage is much lower than for suppressor grid application. The signal grid g_1 is generally given variable mu characteristics, and variation of bias on this grid

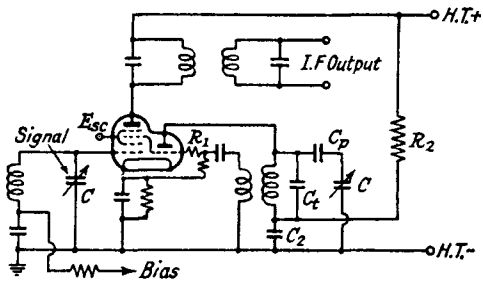

FIG. 5.6.—The Circuit for a Triode-Hexode Frequency Changer.

produces a curve similar in shape to those shown in Fig. 5.1*b*. A representative circuit for a triode-hexode frequency changer is shown in Fig. 5.6.

To avoid excessive interference whistle production it is advisable to operate the hexode at an oscillator voltage not exceeding the optimum and preferably less. Advantage should not be taken of the flat part of the self-biased conversion conductance curve to maintain constant g_c (in spite of large oscillator output variations over a tuning range), but rather attempts should be made to control oscillator output. The series grid resistance R_1 in Fig. 5.6 assists in preserving more constant voltage. (See Section 6.4.)

The hexode possesses the chief advantage of suppressor grid application, viz., low capacitance coupling between signal and oscillator circuits, and in addition gives high conversion conductance with high anode impedance. It is therefore particularly suitable for all-wave operation.

5.3.2. The Heptode.[13, 19, 29] The heptode (originally called pentagrid [5]) valve, which was an earlier development than the hexode, is a combined oscillator and frequency changer. It contains five grids, four are of normal construction and the fifth, so-called grid (G_2 in the circuit diagram of Fig. 5.7), consists of two rods,

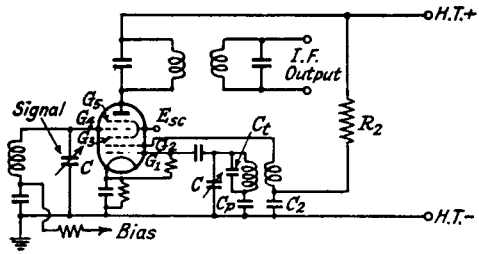

FIG. 5.7.—The Circuit Diagram for a Heptode Frequency Changer.

similar to grid support wires, placed between grids 1 and 3 These two rods constitute the anode of the oscillator, the grid of which is G_1 nearest the cathode. The grid G_1 is the active grid for frequency changing. Grids 3 and 5 are positively biased screening grids and grid 4 is the control grid. The valve, except for the oscillator anode, is similar to the hexode with the positions of the signal and oscillator voltages reversed. The rods forming the oscillator anode are only large enough just to maintain oscillation, and are set in line with the other grid support wires so that they are outside the main electron stream. Current for the oscillator anode, grid 2, is mainly derived by secondary emission from the screen, grid 3. It is essential that the oscillator anode should influence the main electron stream as little as possible, because changes of voltage on this electrode are in antiphase to those on grid 1 and tend to reduce the effective oscillator voltage applied for frequency changing.

The oscillator is of the tuned-grid type since the comparatively large voltage required on grid 1 can be obtained more easily from a tuned-grid than from a tuned-anode oscillator. A disadvantage of the valve is that variation of signal-grid bias (G_4), for amplification control purposes, affects the secondary emission from G_3 to the oscillator anode and causes amplitude and frequency variations of the oscillator. This can be overcome by the use of a separate oscillator section,[23] or greatly reduced by the constructions shown in Figs. 5.8*a* and 5.8*b*. In Fig. 5.8*a* [36] the first positively biased grid (G_3) is a pair of triangular plates, concentrating the main electron stream into a beam away from the oscillator anode (G_2). Variation of bias on G_4 has now very much less effect on the second-

ary emission from G_3 to G_2. Pentode I_aE_a characteristics are obtained by adding the suppressor grid (G_6). In Fig. 5.8*b* [35] the oscillator triode anode is separated from the frequency changing section by using half the cathode emission for the oscillator and half

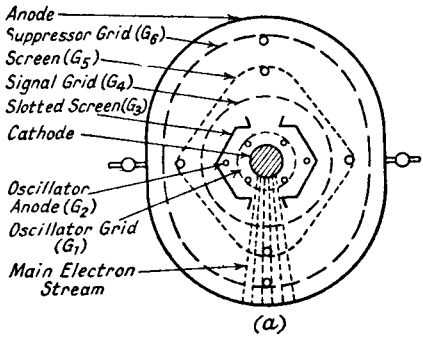

FIG. 5.8*a*.—The Electrode Structure of a Special Octode.

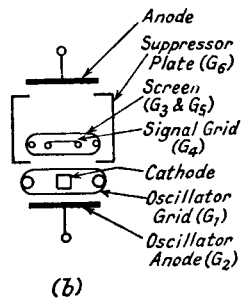

FIG. 5.8*b*.—An Improved Pentagrid Type of Frequency Changer.

for the frequency changer. The oscillator grid is, however, common to both circuits. The box-shaped suppressor plate helps to reduce capacitive coupling between oscillator and signal circuits and to suppress secondary emission from the frequency changer anode, thus raising the output impedance and giving pentode I_aE_a characteristics. Oscillator performance, especially on short waves, is greatly improved because of increased g_m, but conversion conductance suffers by using only one side of the cathode for frequency changing.

A disadvantage of a heptode operating over the short wave band is coupling between the oscillator and signal grids due to the common electron stream and this is discussed more fully in Section 5.8.3.

5.3.3. The Diode Frequency Changer. The detecting properties of the diode valve make its employment as a frequency changer possible, but it has not been used for this purpose to any extent because it has a low conversion gain (normally less than unity), a high oscillator harmonic response (Section 5.5 indicates that a high oscillator harmonic response is to be expected when a frequency changer valve operates into anode current cut-off), a comparatively poor signal-to-noise ratio,[41] grid current damping of the input signal circuit, and appreciable coupling between signal and oscillator circuits through the anode-cathode interelectrode capacitance. The property of high oscillator harmonic response (the oscillator second harmonic response ($2f_h - f_s'$) may be as much as

70% of the fundamental oscillator ($f_h - f_s$) conversion gain) may make it suitable as an ultra short wave frequency changer, since a lower oscillator frequency means increased oscillator frequency stability, a pressing problem on ultra short waves. Signal-to-noise ratio is low because of poor conversion gain and it is maximum for minimum diode conduction resistance (R_d of Section 8.2.5). Grid current damping can only be reduced by tapping down the signal-circuit coil and using a high conduction resistance diode with consequent loss of conversion efficiency. Interelectrode capacitance is decreased by increased electrode spacing (this, however, magnifies transit time effects at high frequencies) and decreased electrode area, both of which increase diode conduction resistance. A suitable circuit [30] for a diode frequency changer consists of an oscillator pick-up coil, tuned signal and intermediate frequency circuits, a diode valve, and a self-biasing resistance paralleled by a capacitance, all connected in series. The pick-up coil should be loosely coupled to the oscillator-tuned circuit so as to reduce interaction between it and the signal circuit, which is tapped down to reduce damping from the diode. The capacitance across the self-bias resistance must have a high enough value to bypass the I.F., but not too large to cause " non-tracking " distortion of the I.F. modulation envelope as described in Section 8.2.1. One point in favour of the diode is that when $\hat{E}_h$ is large, conversion gain is independent of the variation of $\hat{E}_h$, and I.F. output is linearly proportional to the input signal voltage.

5.4. Interference Whistle Production.[12, 17, 24, 27, 28]

5.4.1. Introduction. Interference whistles may be produced in a frequency changer whenever the signal circuit contains undesired frequencies which can combine amongst themselves or with the oscillator or its harmonics to produce a frequency near to the intermediate frequency. The former possibility is remote and need not be considered. Oscillator interference whistles, except that due to the image signal, against which even an ideal frequency changer cannot discriminate, are due mainly to distortion in the frequency changer. Harmonic distortion in the oscillator valve is rarely serious. To demonstrate the method by which interference may arise let us take the expression 5.4 for the $I_a E_g$ characteristic. Though this expression is concerned with common electrode application, similar results are obtained for separate electrode application by modifying the ideal expression of 5.2*b*. Using the same signal and oscillator designations but noting that the signal is an un-

desired frequency, i.e., $f_h - f_s \neq f_1$, and assuming for convenience that $E_b = 0$, expansion of the term $a_3 E_g^3$ in the series

$$I_a = a_0 + a_1 E_g + a_2 E_g^2 + a_3 E_g^3 - a_4 E_g^4$$

gives

$$\begin{aligned}
&a_3(\hat{E}_s \cos \omega_s t + \hat{E}_h \cos \omega_h t)^3 \\
&= a_3[\hat{E}_s \cos^3 \omega_s t + 3\hat{E}_s^2 \hat{E}_h \cos^2 \omega_s t \cos \omega_h t \\
&\qquad + 3\hat{E}_s \hat{E}_h^2 \cos \omega_s t \cos^2 \omega_h t + \hat{E}_h^3 \cos^3 \omega_h t] \\
&= a_3\left[\frac{\hat{E}_s^3}{4}(3 \cos \omega_s t + \cos 3\omega_s t) + \frac{3\hat{E}_s^2 \hat{E}_h}{2}(1 + \cos 2\omega_s t) \cos \omega_h t \right. \\
&\qquad \left. + \frac{3\hat{E}_s \hat{E}_h^2}{2}(1 + \cos 2\omega_h t) \cos \omega_s t + \frac{\hat{E}_h^3}{4}(3 \cos \omega_h t + \cos 3\omega_h t)\right] \\
&= a_3\left[\frac{\hat{E}_s^3}{4}(3 \cos \omega_s t + \cos 3\omega_s t)\right. \\
&\qquad + \frac{3\hat{E}_s^2 \hat{E}_h}{2}\left(\cos \omega_h t + \frac{\cos (2\omega_s + \omega_h)t + \cos (2\omega_s - \omega_h)t}{2}\right) \\
&\qquad + \frac{3\hat{E}_s \hat{E}_h^2}{2}\left(\cos \omega_s t + \frac{\cos (2\omega_h + \omega_s)t + \cos (2\omega_h - \omega_s)t}{2}\right) \\
&\qquad \left. + \frac{\hat{E}_h^3}{4}(3 \cos \omega_h t + \cos 3\omega_h t)\right] \qquad . \quad . \quad . \quad . \quad 5.6.
\end{aligned}$$

Eight frequencies are represented above by the pulsances ω_s, $3\omega_s$; ω_h, $3\omega_h$, $2\omega_s + \omega_h$, $2\omega_s - \omega_h$, $2\omega_h + \omega_s$, $2\omega_h - \omega_s$, and it is significant to note that they may be obtained by adding or subtracting the two fundamental pulsances ω_h and ω_s three at a time in all possible ways, but neglecting negative pulsances. For example

$$\begin{aligned}
&\omega_s + \omega_s - \omega_s = \omega_s, && \omega_h + \omega_h - \omega_h = \omega_h \\
&\omega_s + \omega_s + \omega_s = 3\omega_s, && \omega_h + \omega_h + \omega_h = 3\omega_h \\
&\omega_s + \omega_s + \omega_h = 2\omega_s + \omega_h && \omega_h + \omega_h + \omega_s = 2\omega_h + \omega_s. \\
&\omega_s + \omega_s - \omega_h = 2\omega_s - \omega_h && \omega_h + \omega_h - \omega_s = 2\omega_h - \omega_s
\end{aligned}$$

This rule may be extended to any term in the power series, and frequencies produced by the fourth power term can be obtained by taking the fundamental frequencies four at a time.

Most of the pulsances given by 5.6 do not contribute to the output voltage since the intermediate frequency circuit rejects them. However, if the signal frequency has certain values, the frequencies $\frac{2\omega_s - \omega_h}{2\pi}$ and $\frac{2\omega_h - \omega_s}{2\pi}$ may be very nearly equal to the intermediate frequency, and when this condition is fulfilled an interference whistle is produced. For example, for an I.F. of 465 kc/s and a signal frequency of 700 kc/s, the oscillator is

1,165 kc/s; undesired signal frequencies of 351, $(\omega_h - 2\omega_s)$, 816, $(2\omega_s - \omega_h)$, 1,867, $(2\omega_h - \omega_s)$ and 2,797 kc/s $(\omega_s - 2\omega_h)$, present at the grid of the frequency changer produce 2 kc/s interference tones if the I_aE_g characteristic of the latter has a third power term $(a_3E_g^3)$.

We can see from expression 5.6 that the amplitude of the terms bears a relationship to the frequency components; thus the frequency $\frac{2\omega_s - \omega_h}{2\pi}$ has an amplitude proportional to $\hat{E}_s^2\hat{E}_h$. The factor multiplying the fundamental frequency indicates that the fundamental amplitude is raised to a power equal to the multiplying factor. Interference involving signal frequency harmonics usually has a smaller amplitude than that involving the oscillator harmonic since $\hat{E}_s$ is less than $\hat{E}_h$.

Interference whistles are conveniently classified as follows, the suffixes u, h and 1 denote the undesired signal, oscillator and intermediate frequency respectively.

(1) Image frequency, $f_u - f_h \simeq f_1$

(2) Combination of the signal and oscillator harmonics of different integers

$$\pm mf_h \mp nf_u \simeq f_1$$

(3) Combinations of harmonics of equal integers

$$m(\pm f_h \mp f_u) \simeq f_1$$

(4) Intermediate frequency harmonics

$$f_s \simeq nf_1$$

where f_s = the desired signal frequency.

The " approximately equals " sign is used to denote that the resultant of undesired signal and oscillator is within audio range of the I.F., i.e., equals $f_1 \pm 15$ kc/s.

5.4.2. Image Signal Interference. Image interference is generally located at certain points in the tuning range corresponding to signal frequencies equal to those of any local powerful transmissions minus twice the intermediate frequency. Since the frequency changer cannot discriminate against the image signal special precautions are necessary to improve the selectivity of the signal frequency circuits at a frequency $2f_1$ kc/s above the desired frequency, and circuits for achieving this are considered in Section 5.9.

5.4.3. Interference due to Combination of Different Harmonics of the Signal and Oscillator. Oscillator and

signal harmonic interference whistles of this type are spread over the tuning range in an irregular manner. Harmonics produced by the oscillator and R.F. stage can cause this interference with an ideal frequency changer having an I_aE_g characteristic in accordance with expression 5.2*a* or 5.2*b*, but this rarely happens. Distortion in the frequency changer is the more usual source, and the interference effect can be reduced by reducing the curvature (the higher power terms in the power series) of the I_aE_g characteristics for the signal and oscillator electrodes. Generally oscillator harmonic interference is the more serious—the signal tuned circuits attenuate undesired signals so that $E_u \ll E_h$—and it is reduced by making the oscillator amplitude as small as possible consistent with good conversion conductance.

5.4.4. Interference due to Combination of Equal Harmonics of the Signal and Oscillator. The characteristic of this type of interference is that the whistles are grouped around the oscillator frequency. For example, with an I.F. of 465 kc/s, a desired signal of 700 kc/s, and an oscillator of 1,165, possible interfering frequencies are 932, 1,009, 1,049, 1,398, 1,321, 1281 kc/s, i.e., $2(f_h - f_s)$, $3(f_h - f_s)$, $4(f_h - f_s)$, $2(f_s - f_h)$, etc.

5.4.5. Intermediate Frequency Harmonics. Harmonics of the intermediate frequency may cause interference if there is feedback from the I.F. amplifier to the signal circuits when the latter are tuned to nf_1. Serious interference and even instability is possible for an I.F. of 465 kc/s at signal tuning settings of 930, 1,395, 1,860 kc/s, etc. The usual cause of feedback is inadequate filtering of the A.G.C. bias, but it may also occur due to insufficient decoupling of the R.F., frequency changer and I.F. stages of the receiver, and to insufficient R.F. filtering between the detector and first A.F. amplifier. Improved A.G.C. bias, R.F. decoupling and screening usually reduces the effect to small proportions.

5.4.6. Interference Charts.[6] Interference frequencies are most conveniently expressed in the form of charts. A chart for an I.F. of 465 kc/s is shown in Fig. 5.9, and it is constructed in the following manner. The horizontal axis gives the signal tuning frequency of the receiver, and the vertical axis, with one exception, the interfering frequency. The exception is a line at 45° through the origin. This line gives the desired frequency on the vertical axis and is designated $(h - s)$, where h is the oscillator frequency and s, for all lines except $(h - s)$, is the interfering frequency. Lines due to harmonics of the signal and oscillator higher than the third are not shown on the chart. The image signal line

$(s - h)$ is a line parallel to $(h - s)$ and vertically above it by twice the intermediate frequency.

Interference lines due to unequal harmonics of signal and oscillator are distributed over the chart at different angles. For

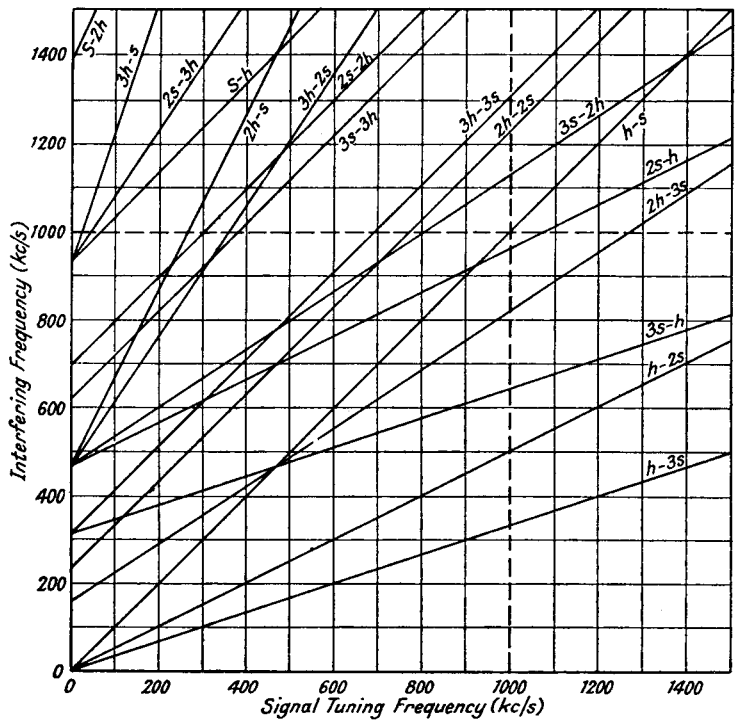

FIG. 5.9.—Interference Chart for an Intermediate Frequency of 465 kc/s.

example, the line corresponding to $(2h - s)$ passes through 100 kc/s (horizontal), 665 (vertical) and 500 (horizontal), 1,465 (vertical). The first point is calculated as follows :

$$\begin{aligned} \text{desired signal} &= 100 \text{ kc/s} ; \quad \text{oscillator} = 565 \text{ kc/s} \\ \text{undesired signal} &= 2 \times \text{oscillator} - f_1 \\ &= 1{,}130 - 465 = 665 \text{ kc/s}. \end{aligned}$$

Lines corresponding to equal harmonics of signal and oscillator are parallel to the desired frequency line $(h - s)$ and spaced vertically above it by $\left(\frac{n-1}{n}\right)f_1$ for $h > s$ and $\left(\frac{n+1}{n}\right)f_1$ for $s > h$, where n is the number of the harmonic. Hence $3(h - s)$ is 310 kc/s and $3(s - h)$ is 620 kc/s above $(h - s)$.

To interpret the charts, let us consider a desired frequency of 1,000 kc/s. By drawing a vertical line from 1,000 kc/s on the horizontal axis we find eight intersections with the interference lines from 333·3 ($h - 3s$) to 1,310 kc/s ($3h - 3s$). If any of these undesired frequencies is present in the input to the frequency changer a whistle may be produced. Conversely, if 1,000 kc/s is the frequency of a strong local station its interference possibilities may be estimated by drawing a horizontal line from 1,000 kc/s on the vertical axis. The points of intersection (read on the horizontal axis) with the interference lines give the tuning points at which interference due to the local station may be expected. In Fig. 5.9 there are 12 tuning points from 0 to 1,500 kc/s at which interference might be expected.

5.5. The Maximum Value of Conversion Conductance.[20, 21] In Section 5.1.2 it is stated that the ratio of conversion conductance g_c, to mutual conductance g_m, rarely exceeds 0·25 in practice. We will now determine the maximum value of this ratio under various oscillator operating conditions. Differentiating the I_aE_g expression for grid-cathode application

$$I_a = a_0 + a_1E_g + a_2E_g^2$$

we have

$$\frac{dI_a}{dE_g} = a_1 + 2a_2E_g \quad . \quad . \quad . \quad . \quad 5.7a.$$

But $\frac{dI_a}{dE_g}$ is the slope of the I_aE_g characteristic curve, i.e., it is the mutual conductance g_m.

At a fixed bias voltage $-E_b$, we have

$$\left[\frac{dI_a}{dE_g}\right]_{E_g=-E_b} = g_m' = a_1 - 2a_2E_b \quad . \quad . \quad 5.7b.$$

The anode current component for a signal grid voltage of $\hat{E}_s \cos \omega_s t$ at the above bias voltage is

$$\begin{aligned} I_a &= g_m'\hat{E}_s \cos \omega_s t \\ &= (a_1 - 2a_2E_b)\hat{E}_s \cos \omega_s t \quad . \quad . \quad 5.8a. \end{aligned}$$

If an oscillator voltage $\hat{E}_h \cos \omega_h t$ is also applied, $-E_b$ in 5.8a becomes $(\hat{E}_h \cos \omega_h t - E_b)$ and

$$I_a = [a_1 + 2a_2(\hat{E}_h \cos \omega_h t - E_b)]\hat{E}_s \cos \omega_s t.$$

The I.F. component (I_1) in I_a is contained in the term

$$2a_2\hat{E}_h\hat{E}_s \cos \omega_h t \cos \omega_s t,$$

thus

$$I_1 = a_2\hat{E}_h\hat{E}_s \cos (\omega_h - \omega_s)t \quad . \quad . \quad . \quad 5.8b$$

but from 5.3*a*

$$g_c = \frac{I_1}{\hat{E}_s} = a_2\hat{E}_h.$$

To interpret $a_2\hat{E}_h$, and hence g_c, in terms of g_m, let us imagine that the bias is decreased to $(-E_b+\hat{E}_h)$, at which the mutual conductance is $g_{m(max.)}$. Similarly at a bias of $-(E_b+E_h)$ let mutual conductance be $g_{m(min.)}$ Now

$$g_{m(max.)} = a_1+2a_2(\hat{E}_h - E_b)$$

and

$$g_{m(min.)} = a_1 - 2a_2(\hat{E}_h+E_b)$$

so that

$$g_{m(max.)} - g_{m(min.)} = 4a_2E_h.$$

Hence

$$g_c = \frac{g_{m(max.)} - g_{m(min.)}}{4} \quad . \quad . \quad . \quad 5.9a$$

or the conversion conductance is 0·25 of the change in mutual conductance produced by the application of the oscillator voltage. Maximum change of mutual conductance is obtained when g_m is varied from 0 to the value at which grid current begins. Since a valve operating as an R.F. amplifier would be biased initially almost to the start of grid current- -its mutual conductance is then $g_{m(max.)}$— we may say that the ratio of conversion conductance as a frequency changer to mutual conductance of the same valve acting as an R.F. amplifier is not greater than 0·25 as long as the oscillator takes the valve only to cut-off and not beyond.

The above method is not easily applicable when the oscillator voltage causes the anode current to be cut off for a part of the cycle, but if $\hat{E}_h \gg \hat{E}_s$ the following analysis may be employed. Suppose we take the expression for g_m in 5.7*b* and replace $-E_b$ by $-E_b+\hat{E}_h \cos \omega_h t$. At the left-hand side of Fig. 5.10, the curve of g_m against bias voltage (it is a straight line as shown by 5.7*b*) is drawn, whilst on the right-hand side the variation of g_m against time is plotted for two values of oscillator voltage; for curve 2 cut-off point is passed. Taking first curve 1, the coefficient of $\cos \omega_h t$ in this curve may be obtained by Fourier analysis, thus:

Coefficient of $\cos \omega_h t$ in curve 1

$$= \frac{\omega_h}{\pi}\int_0^{\frac{2\pi}{\omega_h}} [a_1+2a_2(\hat{E}_h \cos \omega_h t - E_b)] \cos \omega_h t \, dt$$

$$= \frac{\omega_h}{\pi}\left[\frac{a_1}{\omega_h} \sin \omega_h t+2a_2\hat{E}_h\left[\frac{t}{2}+\frac{\sin 2\omega_h t}{4\omega_h}\right] - \frac{2a_2}{\omega_h}E_b. \sin \omega_h t\right]_0^{\frac{2\pi}{\omega_h}}$$

$$= \frac{\omega_h}{\pi}2a_2\hat{E}_h\frac{2\pi}{2\omega_h} = 2a_2\hat{E}_h$$

$$= 2g_c \quad . \quad . \quad . \quad . \quad . \quad . \quad . \quad . \quad . \quad 5.9b.$$

Multiplying this fundamental oscillator component in the g_m curve by $\hat{E}_s \cos \omega_s t$ gives

$$2a_2\hat{E}_h\hat{E}_s \cos \omega_h t \cos \omega_s t$$

and the I.F. component in this is $a_2\hat{E}_h\hat{E}_s \cos (\omega_h - \omega_s)t$. We therefore see that half the coefficient of $\cos \omega_h t$ in the g_m curve plotted against time gives the conversion conductance. This method of attack is applicable to any shape of g_m curve provided $\hat{E}_h \gg \hat{E}_s$.

Let us apply it to the case where the oscillator voltage is large enough to cut off the anode current during a part of the cycle. For

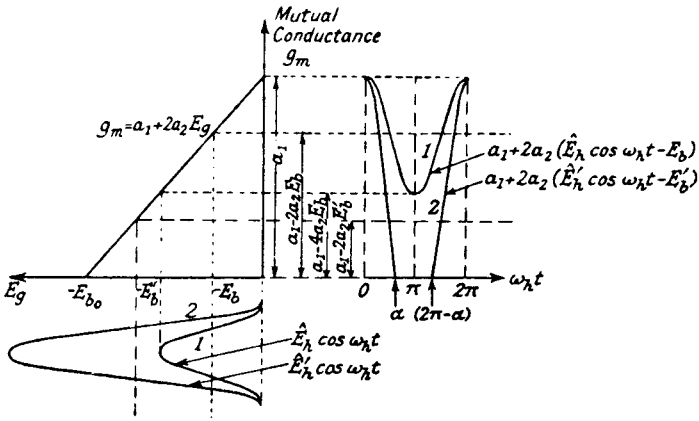

FIG. 5.10.—Linear Mutual Conductance Characteristic for the Normal Type of Frequency Changer.

simplification the maximum positive swing of the oscillator voltage will be assumed to be always 0 volts and the mutual conductance at this point to be $g_{m(max.)}$. The cut-off bias voltage, found by putting $g_m = 0$ in 5.7b, is $\dfrac{-a_1}{2a_2}$ and this we will designate by $-E_{b0}$. The equation to the g_mE_g curve in terms of $g_{m(max.)}$ and $-E_{b0}$ is

$$g_m = g_{m(max.)}\left[\frac{E_g}{E_{b0}} + 1\right] \quad . \quad . \quad . \quad 5.10a.$$

For oscillator and bias voltages of $\hat{E}_h' \cos \omega_h t$ and $-E_b'$ respectively we have

$$\begin{aligned} E_g &= \hat{E}_h' \cos \omega_h t - E_b' \\ &= \hat{E}_h'(\cos \omega_h t - 1) \end{aligned}$$

for $\hat{E}_h' \cos \omega_h t$ is assumed to take the bias to zero at the maximum

positive peak so that $E_b' = \hat{E}_h'$. To simplify let $\omega_h t = \theta$; equation 5.10*a* becomes

$$g_m = g_{m(max.)}\left[\frac{\hat{E}_h'}{E_{b0}}(\cos\theta - 1)+1\right] \quad . \quad . \quad 5.10b$$

and the angle α corresponding to cut-off bias $-E_{b0}$ is obtained from 5.10*b* by putting $g_m = 0$

$$\frac{\hat{E}_h'}{E_{b0}}(\cos\alpha - 1) = -1$$

or

$$\alpha = \cos^{-1}\left(1 - \frac{E_{b0}}{\hat{E}_h'}\right) \quad . \quad . \quad . \quad 5.11.$$

The coefficient of $\cos\theta$ in 5.10*b* is given by Fourier analysis over the intervals 0 to α and $(2\pi - \alpha)$ to 2π, or twice the value obtained from 0 to α. (See Appendix 2A.)

Coefficient of $\cos\theta$

$$= \frac{2}{\pi}\int_0^{\alpha} g_{m(max.)}\left[\frac{\hat{E}_h'}{E_{b0}}(\cos\theta - 1)+1\right]\cos\theta\, d\theta$$

$$= \frac{2g_{m(max.)}}{\pi}\left[\sin\alpha\left(1 - \frac{\hat{E}_h'}{E_{b0}}\right)+\frac{\hat{E}_h'}{E_{b0}}\left(\frac{\alpha}{2}+\frac{\sin 2\alpha}{4}\right)\right].$$

But from 5.11

$$\frac{\hat{E}_h'}{E_{b0}} = \frac{1}{1 - \cos\alpha}.$$

$\therefore$ Coefficient of $\cos\theta$

$$= \frac{2g_{m(max.)}}{\pi}\left[\frac{-\sin\alpha\cos\alpha}{1-\cos\alpha}+\frac{1}{1-\cos\alpha}\left(\frac{\alpha}{2}+\frac{\sin 2\alpha}{4}\right)\right]$$

$$= \frac{g_{m(max.)}}{\pi}\left[\frac{\alpha - \sin\alpha\cos\alpha}{1-\cos\alpha}\right] \quad . \quad . \quad . \quad . \quad 5.12a$$

$$= 2g_c$$

for as shown above in expression 5.9*b* $g_c = \frac{1}{2}$ the coefficient of $\cos\theta$ in the g_m expression.

The ratio of $\frac{g_c}{g_{m(max.)}}$ for different values of $\frac{\hat{E}_h}{E_{b0}}$ is plotted as curve 1 in Fig. 5.11*a*, and it is to be noted that a maximum g_c of 0·268 $g_{m(max.)}$ is obtained when $\hat{E}_h = 0{\cdot}65.E_{b0}$; i.e., when the valve is partially cut off by the oscillator voltage. There are disadvantages to operation into cut-off since oscillator harmonics, which can combine with undesired signals to cause interference whistles, are produced. If we limit $\hat{E}_h$ to $\frac{1}{2}E_{b0}$, no cut-off occurs, g_c is only reduced by about 8%, and for this particular (linear) g_m curve oscillator harmonic interference is absent, since the com-

ponent of cos $n\theta$, where n is greater than 1, in the Fourier analysis is zero over the intervals 0 to π and π to 2π. The practical form of $g_m E_g$ curve is seldom linear so that interference whistles are possible even when $\hat{E}_h < \frac{E_{b0}}{2}$ but they are considerably increased as soon as $\hat{E}_h$ exceeds $\frac{E_{b0}}{2}$.

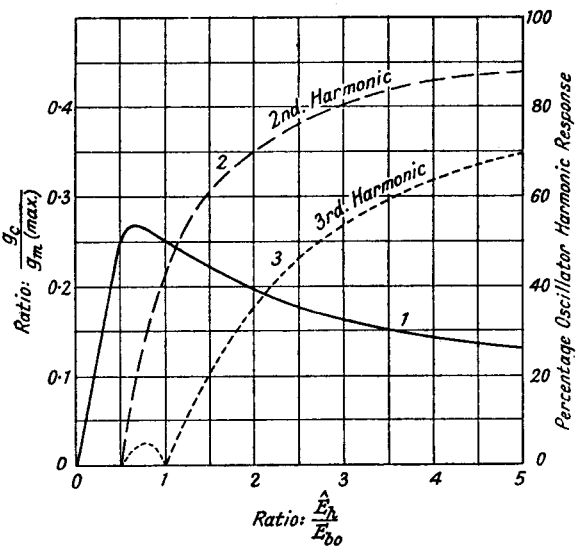

FIG. 5.11*a*.—Conversion Conductance and Oscillator Harmonic Response Curves for the Normal Type of Frequency Changer with Linear Mutual Conductance Characteristic.

We can calculate the ratio of oscillator harmonic to fundamental conversion conductance by finding the coefficient of cos $n\theta$ in 5.10*b* over the interval 0 to α in the same manner as for the fundamental. Thus for the second harmonic conversion conductance

$$g_c(2h) = \frac{g_{m(max.)}}{\pi}\int_0^{\alpha}\left[\frac{\hat{E}_h}{E_{b0}}(\cos\theta - 1)+1\right]\cos 2\theta\, d\theta.$$

$$= \frac{g_{m(max.)}}{\pi}\int_0^{\alpha}\left[\frac{\hat{E}_h}{E_{b0}}\left(\frac{\cos\theta+\cos 3\theta}{2} - \cos 2\theta\right)+\cos 2\theta\right]d\theta$$

$$= \frac{g_{m(max.)}}{\pi}\left[\frac{\hat{E}_h}{E_{b0}}\left(\frac{\sin\alpha}{2}+\frac{\sin 3\alpha}{6} - \frac{\sin 2\alpha}{2}\right)+\frac{\sin 2\alpha}{2}\right]$$

$$= \frac{g_{m(max.)}}{2\pi}\left[\frac{\hat{E}_h}{E_{b0}}\left(\sin\alpha+\frac{\sin 3\alpha}{3} - \sin 2\alpha\right)+\sin 2\alpha\right] \quad . \quad 5.12b$$

where α is as given in 5.11.

The ratio of $\frac{g_c(2h)}{g_c(h)} \times 100\%$, which we will call the percentage second harmonic response, is shown in curve 2 of Fig. 5.11*a*. It is zero until $\hat{E}_h$ exceeds $\frac{E_{b0}}{2}$ and steadily rises as $\hat{E}_h$ is increased.

Similarly it can be shown that the conversion conductance for the third harmonic of the oscillator is

$$g_c(3h) = \frac{g_{m(max.)}}{\pi}\left[\frac{\hat{E}_h}{E_{b0}}\left(\frac{\sin 4\alpha}{8}+\frac{\sin 2\alpha}{4}-\frac{\sin 3\alpha}{3}\right)+\frac{\sin 3\alpha}{3}\right]. \quad 5.12c.$$

The percentage third harmonic response $\frac{g_c(3h)}{g_c(h)} \times 100\%$ is the dotted curve 3 of Fig. 5.11*a*. It has zero value until $\hat{E}_h$ exceeds $\frac{E_{b0}}{2}$, rises to a maximum of 6·0% at $\hat{E}_h = 0{\cdot}8.E_{b0}$, falls to zero at $\hat{E}_h = E_{b0}$ and thereafter rises steadily. The need for preventing too high a value of oscillator voltage is made very clear from the curves.

The above analysis is applicable to all types of $g_m E_g$ curves, but when a separate electrode is used for the oscillator voltage the g_m curve for the oscillator grid must be considered.

Taking expression 5.2*b* as representative of the hexode valve we obtain after differentiating with respect to E_{g1}

$$\frac{dI_a}{dE_{g1}} = g_m = a_1(b_0+b_1E_{g3})$$

and plotting this against E_{g3}, the bias on the oscillator grid, we have a straight line similar to that in Fig. 5.10. Proceeding along the lines set out above, we obtain a result for conversion conductance which is identical with that for common electrode application of the oscillator. Thus the curves in Fig. 5.11*a* are also applicable to the hexode valve, where $g_{m(max.)}$ equals a_1b_0, the value of g_m when the oscillator grid bias is zero.

We can estimate the maximum conversion conductance obtainable from a linear I_aE_g characteristic, such as that for a non-variable mu valve or a diode frequency changer, by the same method. Since I_a is linearly proportional to E_g, the g_mE_g curve is a straight line parallel to the E_g axis, cutting the g_m axis at $g_{m(max.)}$. At the cut-off bias voltage, $-E_{b0}$, it falls sharply to zero. The curve of mutual conductance against time for a given oscillator peak voltage exceeding $-E_{b0}$ is therefore rectangular with zero g_m between α and $2\pi-\alpha$, where $\alpha = \cos^{-1}\left(1-\frac{E_{b0}}{\hat{E}_h}\right)$. Conversion

conductance is given by half the coefficient of cos θ in $g_m = g_{m(max.)}$ over twice the interval 0 to α

$$\therefore\ g_c = \frac{1}{2}\left[\frac{2}{\pi}\int_0^{\alpha} g_{m(max.)} \cos\theta\, d\theta\right]$$

$$= \frac{g_{m(max.)} \sin\alpha}{\pi} \quad . \quad . \quad . \quad . \quad 5.13a$$

$$= \frac{g_{m(max.)}}{\pi}\sqrt{\frac{2E_{b0}}{\hat{E}_h} - \frac{E_{b0}^2}{\hat{E}_h^2}} \quad . \quad . \quad 5.13b.$$

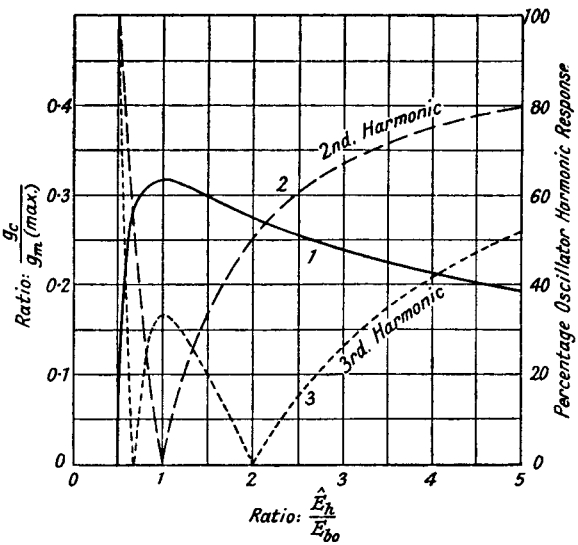

FIG. 5.11*b*.—Conversion Conductance and Oscillator Harmonic Response Curves for a Frequency Changer with Constant Mutual Conductance Characteristic.

This result is plotted in Fig. 5.11*b* as curve 1, and we see that when $\hat{E}_h < \frac{E_{b0}}{2}$ there is no cut-off and hence no frequency changing. This is to be expected since the output wave shape is an exact reproduction of the original input. Actually when $\hat{E}_h = \frac{E_{b0}}{2}$, the addition of the signal voltage causes the cut-off point to be passed and some small g_c value is obtained. When $\hat{E}_h = E_{b0}$, $g_c = \frac{g_{m(max.)}}{\pi}$ and this is its maximum value.

The percentage second and third harmonic responses are found from the coefficients of cos 2θ and cos 3θ in the g_m — time curve.

Thus $$g_c\left(\frac{2h}{h}\right) = 100 \cos \alpha\,\% = \left(1 - \frac{E_{b0}}{\hat{E}_h}\right) 100\,\%.$$

and $$g_c\left(\frac{3h}{h}\right) = \frac{100 \sin 3\alpha}{3 \sin \alpha}\,\%.$$

The curves 2 and 3 show the variation of harmonic response for different ratios of $\frac{\hat{E}_h}{E_{b0}}$. Second harmonic is zero at $\frac{\hat{E}_h}{E_{b0}} = 1$, whilst third harmonic response is zero at $\frac{\hat{E}_h}{E_{b0}} = 0{\cdot}66$ and 2. For large values of oscillator voltage the linear $I_a E_g$ characteristic has lower oscillator harmonic responses than the parabolic characteristic operated into cut-off, and this is largely due to a higher fundamental conversion conductance.

5.6. Measurements on Frequency Changers.

5.6.1. Introduction. The most important measurements which are required are those of conversion conductance, oscillator harmonic response, and signal handling capacity for a given modulation percentage and distortion of the modulation envelope.

5.6.2. Conversion Conductance. Conversion conductance may be measured by direct or indirect means. The first involves the use of low frequency input voltages for the signal and oscillator, whilst the second method uses frequencies in the range over which it is intended to operate. The former has the advantage of requiring only simple apparatus, but the results may not show close agreement with measurements made under short wave operating conditions, because of transit time of electrons and increased grid admittance. However, for the medium and long wave bands agreement between the two methods is generally good and variations rarely exceed 5%.

5.6.3. Indirect Measurements of Conversion Conductance. The voltages for one indirect method are obtained from the 50 c.p.s. mains supply, and Fig. 5.12 shows a diagram of connections for a hexode valve. The diagram is similar for a pentode except that oscillator and signal inputs may be applied to the same electrode. Suitable bias and screen voltages are applied, and the signal voltage is fixed at some convenient value such as 0·1 to 0·5 peak volts. A value of 0·5 volts should not be exceeded or it may be found that the measured g_c is not independent of the signal voltage. The change-over switch (S) in the signal circuit allows the phase relationship between signal and oscillator to be reversed. The oscillator

voltage is variable and is obtained from the same transformer as the signal voltage. Operation of the change-over switch produces a change of mean current in the D.C. milliammeter, and this change is proportional to the conversion conductance. The relationship is expressed by

$$g_c = \frac{I_{a1} - I_{a2}}{2\hat{E}_s} \quad . \quad . \quad . \quad . \quad 5.14$$

where I_{a1} = the mean current for the in-phase condition of $\hat{E}_s$ and $\hat{E}_h$
and I_{a2} = ,, ,, ,, ,, ,, out-of-phase ,, ,, ,, ,, ,,

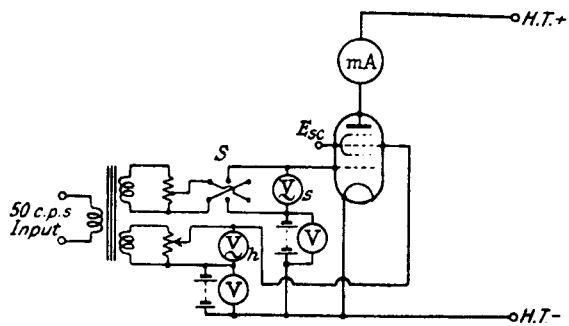

FIG. 5.12.—A Circuit for the Measurement of Conversion Conductance of a Hexode Valve by means of the 50 c.p.s. Mains Supply.

The proof of the above expression may be derived from 5.2*b*, thus:

$$I_a = (a_0 + a_1 E_{g1})(b_0 + b_1 E_{g3}).$$

Replacing E_{g1} by $(\hat{E}_s \cos\theta - E_{b1})$ and E_{g3} by $(\hat{E}_h \cos\theta - E_{b3})$ we have for the in-phase current

$$(a_0 + a_1(\hat{E}_s \cos\theta - E_{b1}))(b_0 + b_1(\hat{E}_h \cos\theta - E_{b3}))$$

the D.C. component of which is

$$I_{a1} = a_0 b_0 - a_1 b_0 E_{b1} - a_0 b_1 E_{b3} + \frac{a_1 b_1}{2}\hat{E}_s\hat{E}_h.$$

For the out-of-phase condition $E_{g1} = -\hat{E}_s \cos\theta - E_{b1}$, and the D.C. component is

$$I_{a2} = a_0 b_0 - a_1 b_0 E_{b1} - a_0 b_1 E_{b3} - \frac{a_1 b_1}{2}\hat{E}_s\hat{E}_h$$

$$I_{a1} - I_{a2} = a_1 b_1 \hat{E}_s \hat{E}_h.$$

But from expression 5.3*b* (Section 5.1.3)

$$g_c = \frac{a_1 b_1}{2}\hat{E}_h = \frac{I_{a1} - I_{a2}}{2\hat{E}_s}.$$

The above result assumes that there is no distortion of the hexode $I_a E_g$ characteristics, and since in practice it is rare to obtain

linear characteristics there are possibilities of error in the measurement. The error is, however, not usually very serious, particularly if the signal voltage is not made large.

A second indirect method [21] employs one A.C. voltage only—no signal voltage being used—and the circuit is shown in Fig. 5.13. A filter in the anode circuit attenuates all but the fundamental A.C. voltage. The input fundamental, which must be completely free

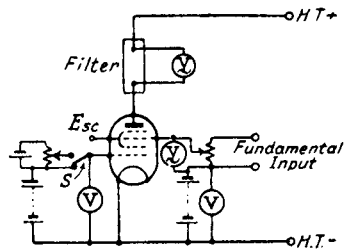

FIG. 5.13.—A Circuit for the Measurement of Conversion Conductance of a Hexode Valve by means of the Change of Fundamental Output.

from distortion, acts as the oscillator voltage, and the input signal is simulated by varying the signal grid bias a predetermined amount such as 0·5 volts. The change in fundamental output is noted and conversion conductance is given by,

$$g_c = \frac{\text{output fundamental voltage change}}{2 \times \text{signal grid bias change} \times Z_0 \text{ (anode circuit filter)}}.$$

This may be proved as follows:

$$I_a = (a_0+a_1E_{g1})(b_0+b_1E_{g3})$$

where $$E_{g3} = \hat{E}_h \cos\theta - E_{b3}$$

$$\therefore\ I_a = a_0b_0+a_1b_0E_{g1}+a_0b_1(\hat{E}_h \cos\theta - E_{b3})+a_1b_1E_{g1}(\hat{E}_h \cos\theta - E_{b3})$$

and the fundamental A.C. component in the above is

$$I_f = (a_0b_1+a_1b_1E_{g1})\hat{E}_h \cos\theta.$$

If E_{g1} is decreased by a value of $+E_s$ the change in fundamental current component is

$$\Delta I_f = a_1b_1E_s\hat{E}_h \cos\theta$$

but

$$g_c = \frac{a_1b_1}{2}\hat{E}_h$$

$$= \frac{\Delta I_f}{2E_s} = \frac{\Delta I_f Z_0}{2E_sZ_0} = \frac{\Delta E_f}{2E_sZ_0} = \frac{\Delta E_f}{Z_0} \quad . \quad . \quad 5.15$$

if $$E_s = 0{\cdot}5 \text{ volts.}$$

Both indirect methods can be made to give satisfactory results compared with direct measurements, but for frequency changers operating over short wave ranges it is often preferable to use a direct method which takes into account coupling between signal and oscillator circuits, and electron transit time effects.

5.6.4. Direct Measurement of Conversion Conductance. For direct measurement of conversion conductance a signal frequency is chosen at approximately the centre of the desired range of tuning frequencies. Suitable values are 700 kc/s for medium and long wave bands and 10 Mc/s for the short wave. A schematic diagram is given in Fig. 5.14. The signal voltage, supplied by a signal generator, must be limited to a value not exceeding 0·5 peak volts, though for high gain frequency changers, with a high anode impedance, it may be necessary to reduce to 0·1 peak volts if anode voltage distortion is to be prevented. The oscillator voltage is obtained from an oscillator followed by an amplifier, the gain of

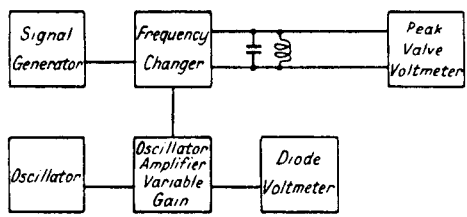

FIG. 5.14.—Schematic Diagram for the R.F. Measurement of Conversion Conductance.

which is changed by bias variation. In the anode circuit of the amplifier is a tuned circuit, which rejects oscillator harmonics. This is essential for harmonic response measurement. Large oscillator voltages are obtained by capacitance-resistance coupling from this tuned circuit to the appropriate oscillator electrode in the frequency changer. Voltages not exceeding about 15 peak volts are obtained from a pick-up coil wound on the earthed end of the tuned circuit. A diode voltmeter may conveniently be used for measuring the oscillator volts across the pick-up coil, and it may also be calibrated to give the voltage across the tuned circuit by noting the diode current for different voltages measured by a slide-back or peak voltmeter across the tuned circuit.

The anode circuit of the frequency changer consists of a parallel tuned circuit resonant at the I.F., and a slide-back or peak voltmeter is used to measure the output voltage. This type of voltmeter has two advantages; its range of measurement is large—the output

may reach a peak value of 100 volts—and its grid input conductance can be made very low so that there is little damping of the output circuit. To calculate conversion conductance we must measure the resonant or dynamic resistance of the tuned output circuit, and this can be accomplished as follows. The bias on the signal grid of the frequency changer is increased to a value (about — 8 volts) at which the anode slope resistance can be expected to be much higher than the tuned-circuit impedance. The input signal is adjusted to give a certain output voltage, such as 1 volt peak (a low value is chosen to prevent the possibility of non-linearity between input and output voltages). The tuned circuit is next paralleled by a known non-inductive resistance and the input signal increased to give the same output voltage, viz., 1 volt. If $\hat{E}_s'$ and $\hat{E}_s''$ are the input peak signal voltages with and without the non-inductive resistance R, we have

$$\hat{E}_0 = 1 = g_c\hat{E}_s'R_D = g_c\hat{E}_s''\frac{R_DR}{R_D + R}$$

where $\hat{E}_0$ = the output peak voltage
g_c = conversion conductance
R_D = the dynamic resistance of the tuned circuit

$$\therefore\ R_D = R\left[\frac{\hat{E}_s''}{\hat{E}_s'} - 1\right].$$

If we can assume that $R_a \gg R_D$ we can now calculate conversion conductance for

$$g_c = \frac{\hat{E}_0}{\hat{E}_sR_D} \quad . \quad . \quad . \quad . \quad 5.16.$$

5.6.5. Measurement of Oscillator Harmonic Response. Interference whistles from interaction between undesired signals and harmonics of the oscillator are normally more serious than undesired signal harmonic interference, and the ratio of conversion conductance for the second and third oscillator harmonics to that for the fundamental is a good indication of the interference capability of the frequency changer.

The apparatus is the same as that used in the previous section, but the signal frequency is adjusted to give the I.F. by interaction with the particular oscillator harmonic under consideration. For example, if desired signal and I.F. frequencies are 700 and 465 kc/s respectively, the signal frequencies for measuring second and third harmonic responses are 1,865 (2 × 1,165 — 465) and 3,030 kc/s (3 × 1,165 — 465). It is essential that the oscillator voltage source be free from harmonics, and this may be checked with

oscillator amplifier at full gain by placing a potentiometer across the output and reducing the oscillator voltage applied to the frequency changer to about one-fifth of its optimum value. The oscillator harmonic response under these conditions should be not greater than 1% of the fundamental. The percentage oscillator harmonic response $\left(\frac{g_c \text{ harmonic}}{g_c \text{ fundamental}} \times 100\%\right)$ is plotted in Fig. 5.15 against signal grid bias under normal conditions for the hexode type (full line), and the pentode with common electrode application. Increase of oscillator voltage increases both second and third harmonic response maxima and may change the position of third harmonic minima. The harmonic response for the hexode has generally lower maxima than the pentode and is less variable with

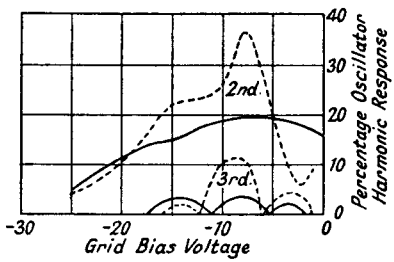

Fig. 5.15.—Typical Oscillator Harmonic Response Curves for a Pentode and Hexode Valve.
(Dotted Line—Pentode. Full Line—Hexode.)

bias change, because oscillator harmonics are caused by curvature of the $I_aE_{g_h}$ characteristic, which is less affected by signal grid-bias variation than the I_aE_g characteristic of the pentode.

5.6.6. Signal Handling Capacity. The maximum modulated input signal and output I.F. voltage, which can be handled by a frequency changer, is defined as the carrier peak voltage modulated K% which gives 5% total harmonic distortion of the audio frequency envelope of the carrier. The modulation percentage is usually fixed at 80% in order to keep distortion low in the apparatus other than the frequency changer. The apparatus is substantially similar to that described in Section 7.11, except for the inclusion of the oscillator voltage at the appropriate point.

Typical curves for a pentode with cathode application of the oscillator and for a hexode are illustrated in Fig. 5.16. The input and output carrier voltage curves for the hexode are lower than those for the pentode because of the semi-screened grid I_aE_a char-

acteristics of the former. Conversion conductance obtained by calculation from the input and output voltages is always higher at a large negative bias than conversion conductance measured with a small signal voltage. This is due to the fact that the input signal is large and the variable mu characteristic of the signal grid

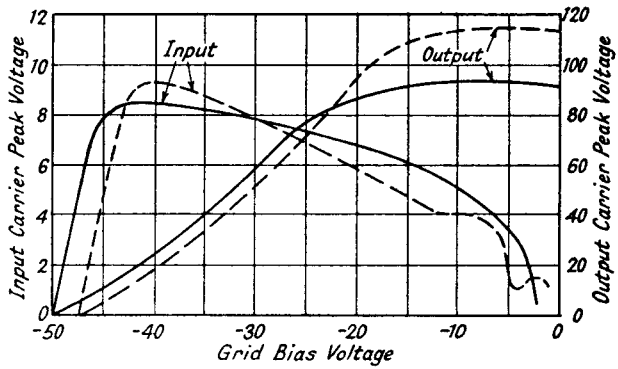

FIG. 5.16.—Typical Signal Handling Capacity Curves for Pentode and Hexode Frequency Changers.
(5% A.F. Envelope Distortion and 80% Modulation of Carrier.)
(Dotted Line—Pentode. Ful, Line—Hexode.)

causes the output voltage to increase at a greater rate than the input. The importance of these curves is discussed in Section 12.4.2 on automatic gain control.

5.7. The Properties Required of a Frequency Changer Valve.[31]

5.7.1. Introduction. Having discussed the salient features of frequency changing, we can now specify the essential requirements of a frequency changer valve. It should have

(1) A low value of anode and total current, and high slope resistance.
(2) A high value of conversion conductance, which is maintained in the short wave ranges.
(3) Low oscillator harmonic response.
(4) Minimum cross-modulation.
(5) Minimum coupling between oscillator and signal circuits.
(6) Minimum variation of signal grid-cathode capacitance for bias variations on the signal grid.
(7) Low signal grid input admittance.
(8) Small oscillator frequency drift.
(9) Minimum microphonic effects.

5.7.2. Anode and Total Current, Slope Resistance. Low values of anode and total currents aid economy of operation (this

is only an absolute essential in battery receivers), but their importance, in conjunction with g_c, is their influence on shot noise. The equivalent shot-noise voltage at the grid of the frequency changer is approximately $\frac{K\sqrt{I_a}}{g_c}.\sqrt{\frac{2.\Delta f}{10{,}000}}\mu$V; where K is a factor dependent on the type of valve and varying between 0·5 and 1·5, and $2\Delta f$ is the pass-band width of the I.F. amplifier. The total current does not appear directly in the formula, but is actually contained in K, which is increased as the total current is increased. The importance of minimum I_a and I_T is thus apparent.

Since for the triode valve, anode and total currents are equal, signal-to-noise ratio is comparatively high, but this type of valve is quite unsuitable for frequency changing because of its low slope resistance, R_a, which results in low amplification and heavy damping of the primary of the I.F. transformer with consequent loss of selectivity. The tetrode or pentode valve is superior to the hexode or heptode because it has a lower ratio of total cathode to anode current, about 1·3 to 1 as compared with from 2 to 3 to 1 for the heptode and hexode. In certain beam tetrodes with aligned grids, screen current is reduced from the usual value of 25% of the anode current to 10% or less, and signal-to-noise ratio for these valves approaches that of the triode. Taking the signal-to-noise ratio of the latter as a basis of comparison, the beam tetrode with aligned grids, the normal tetrode or pentode, and the heptode or hexode have signal-to-noise ratios of about 0·8, 0·5 and 0·25 (respectively) [38] of that for a triode. If the difficulties introduced by coupling between signal and oscillator circuits can be overcome, such as by using an untuned signal circuit, a tetrode with grid-cathode oscillator application is preferable to a hexode or heptode when there is no preceding R.F. stage, because of its greater signal-to-noise ratio. The effects of coupling on the short wave range can also be reduced by using a high I.F. and preset signal-tuned circuits, as occurs in some types of band-spread receivers. In the multi-electrode valve, any secondary emission currents to the anode add their quota of noise so that a high anode resistance R_a, which indicates small secondary emission from the screen or any other possible emitting surface (apart from the cathode) to the anode, is desirable; at the same time it increases the conversion stage gain, which leads to increased signal-to-noise ratio.

5.7.3. Conversion Conductance. In order to obtain the highest signal-to-noise ratio the conversion conductance should have the highest possible value. As this tends to produce high

harmonic response, a compromise value of conversion conductance must be chosen, and generally it is about 85% of the maximum value.

5.7.4. Oscillator Harmonic Response. For small oscillator harmonic response the curve connecting g_c and oscillator voltage should be straight, and oscillator voltage limited to the maximum value which can be obtained on the straight part of this curve.

5.7.5. Cross-Modulation. Cross-modulation is reduced by high R.F. selectivity before the frequency changer and by having minimum curvature of the $g_c E_g$ characteristic of the signal grid. Signal harmonic response is also reduced by this method.

5.7.6. Signal and Oscillator Circuit Interaction. In an ideal frequency changer, variation in signal circuit tuning should have no effect on oscillator frequency and amplitude. Coupling by interelectrode capacitance and the common electron stream occurs in practice, and the signal circuit tuning always has some influence. Its effect is most pronounced at the higher short wave frequencies where the frequency ratio between oscillator and signal is smallest.

5.7.7. Signal Grid-Cathode Capacitance Variation. A capacitance variation of about 2 $\mu\mu$F occurs when the signal grid bias is varied and is due to variation of the distance between the grid and the virtual cathode produced by space charge. It is a function of the total current passing through the control grid and the greatest mistuning effect occurs for small signal-tuning capacitances, i.e., at the high-frequency end of any given range. The effect is much less pronounced in the heptode than in the hexode valve.

5.7.8. Low Signal Grid Input Admittance. The conductance component of the signal grid input admittance of a hexode frequency changer generally increases as the signal frequency increases due to the inductance of the cathode lead and feedback through the grid-cathode capacitance, and also due to transit time of the electrons. A heptode valve may show a negative input conductance, which decreases as the signal grid bias is increased, becoming zero at a particular bias voltage and finally asymptotic to a positive value equal to the losses in the valve-holder, etc., as measured when the valve-heater is open-circuited (the valve is cold). Both these effects are discussed in Section 5.8. Anode-grid capacitance coupling has little influence on input conductance because the value of capacitance is small and the anode circuit is an I.F. transformer offering a very low impedance to the signal frequencies.

5.7.9. Oscillator Frequency Drift. Oscillator frequency variations due to the frequency changer valve itself are covered by

5.7.6 and are more fully discussed in Section 5.8.1. Those due to the oscillator and its component parts are dealt with in Sections 6.6 and 7.

5.7.10. Microphony. Microphony is largely affected by electrode structure and supports. The position of the valve with respect to the loud-speaker and the use of a shock-absorbing valve mounting can determine the extent of microphonic noises. Sound-wave coupling may also occur between the loudspeaker and rotor plates of the oscillator tuning capacitance, and to reduce this the complete tuning capacitance chassis is often mounted on rubber. Increasing the thickness and spacing of the rotor plates of the oscillator tuning capacitance also reduces the tendency to sound coupling.

5.8. Special Considerations in Short Wave Frequency Changing.[25]

5.8.1. Introduction. Short and ultra short wave frequency changing is chiefly complicated by the increased effect of capacitive and electronic coupling, the reduced frequency ratio between signal and oscillator and increased signal grid input admittance, which becomes comparable with the resonant conductance $\frac{1}{R_D}$ of the signal-tuned circuit.

Capacitance coupling has the same effect in hexode or heptode valves. It normally precludes the use of common electrode application of signal and oscillator frequencies, though for special reasons (such as increased signal-to-noise ratio) a tetrode [38] may be used as a frequency changer with common coupling for ultra high frequency conversion (40 Mc/s). The signal circuit is then either untuned or preset tuned, and the oscillator voltage made as low as possible consistent with satisfactory frequency changing; the oscillator frequency can be less than that of the signal. Inter-electrode capacitance coupling has a two-way effect which can be observed when the valve-heater is open-circuited (no emission). The signal circuit reflects through the signal grid-oscillator grid capacitance an impedance into the oscillator-tuned circuit, and both tuning and amplitude of the oscillator voltage are affected. In the reverse direction this coupling induces in the signal circuit an oscillator voltage component which is generally in phase with the initial oscillator voltage. Conversion conductance is consequently increased.

Frequency and amplitude variations of the oscillator due to

signal circuit tuning changes are illustrated in Fig. 5.17. Assuming that $f_s < f_h$, tuning the signal circuit towards the oscillator frequency, i.e., reducing the signal circuit capacitance, causes the oscillator frequency to fall because the signal circuit appears as a capacitance and resistance in parallel (Section 4.2.2). The capacitance component reaches a maximum at a signal tuning setting of C_3, and then falls to zero when signal and oscillator circuits are tuned to the same frequency. Below this value of C_2 the signal circuit is inductive and the oscillator frequency increases, reaches a maximum at C_1, where $C_2 - C_1 \simeq C_3 - C_2$, and then falls as the signal capacitance is further decreased. Amplitude is a minimum at the signal tuning capacitance setting of C_2.

The reverse direction effect of capacitance coupling causes an oscillator voltage component in the signal circuit, which adds to

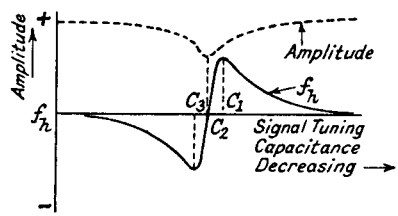

FIG. 5.17.—Curves showing the Effect of the Signal Tuning Circuit Capacitance on the Oscillator Frequency and Amplitude with Capacitance Coupling between the two Electrodes.

the true oscillator voltage when the signal circuit is capacitive, i.e., $f_s < f_h$, and opposes when the signal circuit is inductive, i.e., $f_s > f_h$. For grid-cathode application of the oscillator voltage the reverse is true, i.e., the oscillator voltage component in the signal circuit opposes the true oscillator voltage when the signal circuit is capacitive ($f_s < f_h$). A voltage in the grid circuit in phase with that in the cathode circuit means that the net voltage from grid to cathode is reduced. The magnitude of the oscillator component voltage depends on the value of intermediate and oscillator frequencies, the interelectrode capacitance, and to a less extent the Q of the signal circuit. As an example let us assume the following signal circuit constants $L_s = 2\ \mu\text{H}$, $C_s = 125\ \mu\mu\text{F}$, $f_s = 10$ Mc/s, $Q = 100$, $f_1 = 465$ kc/s, $C_{sig.\text{-}osc.\ elec.} = 0{\cdot}2\ \mu\mu\text{F}$. Using expression 4.8*a* (Section 4.2.2), the impedance of the signal circuit at the oscillator frequency 10·465 Mc/s is

$$Z = \frac{R_D}{1 + jQ\left(\frac{\omega_h}{\omega_s} - \frac{\omega_s}{\omega_h}\right)} = \frac{\omega_s L_s Q}{1 + 9{\cdot}1j} = \frac{12{,}560}{1 + 9{\cdot}1j}.$$

The reactance of the signal to oscillator interelectrode capacitance is

$$jX_{sig.\ osc.} = \frac{-j10^{12}}{6{\cdot}28 \times 10{\cdot}465 \times 10^6 \times 0{\cdot}2} = -76{,}000j$$

and the ratio of oscillator voltage across the signal-tuned circuit to oscillator electrode voltage is

$$\frac{12{,}560}{-76{,}000j(1+9{\cdot}1j)+12{,}560} = \frac{12{,}560}{712{,}000} = 0{\cdot}01762,$$

which is negligible. The undesirability of grid-cathode oscillator application under normal conditions can be demonstrated by assuming a grid-cathode capacitance of 3 $\mu\mu$F when the voltage ratio becomes 0·213.

Electron coupling and transit time give different results in the hexode valve from those in the heptode and they will be considered separately.

5.8.2. The Hexode as a Short Wave Frequency Changer. Since the signal grid of the hexode is next to the cathode, increase of operating frequency causes increased input admittance due to cathode lead inductance and electron transit time (Sections 2.8.3 and 2.8.6 show that input conductance is proportional to the square of the signal frequency.) The inclusion of a series resistance R_k in the cathode circuit decreases input capacitance and conductance and their variation with signal grid bias change. A resistance of from 20 to 50Ω may so reduce input conductance at high frequencies that the loss of amplification due to negative feedback (the equivalent conversion conductance is reduced to $\frac{g_c}{1+g_cZ_k}$) is more than offset, and overall amplification may actually be increased, as described in Section 4.10.3. Coupling from the signal to the oscillator circuit due to the common electron stream is not very important in the hexode, but in the reverse direction (from oscillator to signal) signal circuit performance is adversely affected by the repulsion of electrons from the neighbourhood of the oscillator grid back to the signal grid region. Some of these electrons (e.g., those repelled at the time when the oscillator voltage has its maximum negative value) may gain sufficient velocity to be collected by the signal grid. The effect occurs at all operating frequencies, but the occasions, when conditions favourable to the collection of electrons by the signal grid are realized, are multiplied as the oscillator frequency is increased. This electron collection causes grid current to flow in the signal circuit, and to prevent it the negative grid bias must be increased—about −2·5 volts may be required at 20 Mc/s as

compared with − 1·0 volt at 1 Mc/s. This increase in minimum negative bias means a lower conversion conductance in the short and ultra short wave ranges. The collection of electrons by the signal grid is proportional [34] to the square of the amplitude of the oscillator voltage, and to the square of the distance between the first screen G_2 and the oscillator grid G_3, and inversely to the D.C. voltage on G_2. Hence excessive oscillator voltage must be avoided, and the distance between G_2 and G_3 should be as small as possible. Raising the screen voltage on G_2 has disadvantages since G_2 and G_4 are connected together, and increasing E_{g4} reduces the anode slope resistance, thus causing damping of the I.F. transformer.

5.8.3. The Heptode as a Short Wave Frequency Changer. A frequency changer having an oscillator in the same electron stream suffers from a number of disadvantages. A high oscillator mutual conductance is difficult to obtain, so that oscillation at the low frequency end of a short wave range requires tight coupling, which tends to produce a large oscillation amplitude and possibly squeggering at the high-frequency end. Another defect is that mentioned in Section 5.3.2, viz., the oscillator anode current is affected by bias on the signal grid and therefore application of A.G.C. bias varies oscillator amplitude and frequency. The second defect is largely eliminated by the constructions shown in Fig. 5.8*a* and 5.8*b*, or by using " electron coupling " [15] for the oscillator with a cathode coupling coil as in Fig. 5.18. The current in the cathode

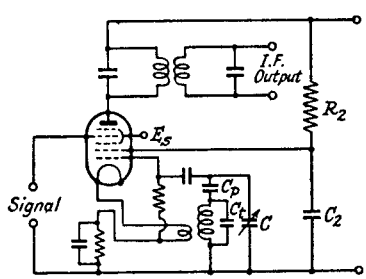

FIG. 5.18.—A Heptode Frequency Changer with Cathode Coupled Oscillator.

coil is independent of signal grid bias. Both defects are largely overcome by employing a separate oscillator valve.

The signal grid input admittance of the heptode valve may be positive or negative. It is often negative at low signal grid biases, i.e., it appears as a negative capacitance and negative resistance in parallel. This is due to the fact that there is no reservoir of electrons in the space between the two screens, G_3 and G_5 (Fig. 5.7), and the

space current tends to be constant and independent of signal grid bias variation (the shape of the I_aE_g characteristics of the signal grid are similar to those of the oscillator grid of the hexode as shown in Fig. 2.10). Let us consider an A.C. voltage applied to G_4; as this is increasing (the signal grid voltage is becoming less negative) electrons in the G_3G_4 space are accelerated and their velocity increased. Since the electron space current is the product of electron density and velocity, it follows that constant space current entails reduced electron density when velocity is increased. The reduced electron density means reduced negative charge in the neighbourhood of the signal grid, which is equivalent to reduced positive charge on the grid, i.e., the charge on the grid is 180° out of phase with the signal voltage producing it. If we assume that the signal voltage is

$$E_s = \hat{E} \sin \omega t,$$

the charge on the signal grid is

$$Q_g = -\hat{Q} \sin \omega t.$$

The current in the grid circuit due to this charge is the differential of Q_g with respect to time so that

$$I_g = \frac{dQ_g}{dt} = -\hat{I} \cos \omega t = \hat{I} \sin (\omega t - 90).$$

The phase relationships between E_s, Q_g and I_g are shown in Fig. 5.19*a*. I_g lags behind E_s by 90° and the input admittance

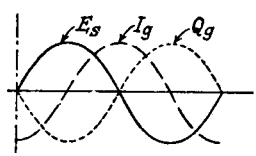

FIG. 5.19*a*.—The Phase Relationship of the Signal Voltage and the Grid Current due to Electron Motion.

appears as a negative capacitance, $-C_{g4}$ as shown by the vector diagram of Fig. 5.19*b*. Electron transit time causes a lag in the charge so that

$$Q_g = -\hat{Q} \sin (\omega t - \phi)$$

where ϕ = angle of lag due to the time of travel of electrons between G_3 and G_4 (the signal grid)

and $$I_g = \hat{I} \sin [\omega t - (90 + \phi)].$$

This modifies the vector diagram to that of Fig. 5.19*c*, which means an input admittance with a negative conductance ($-G_{g4}$) as well

as a negative capacitance component ($-C_{g4}$). The actual value of input admittance is determined by the voltage on the oscillator grid ; it is generally negative for low negative voltages on G_1, becoming smaller, and finally positive to a value equal to losses in the valve base and holder, as this bias is increased. Under normal conditions the signal grid input admittance varies considerably over a complete cycle of oscillator voltage and measurement gives an average value of input admittance. For television reception, the signal circuit

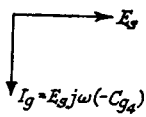

FIG. 5.19b.—The Vector Diagram for the Signal Voltage and Grid Current.

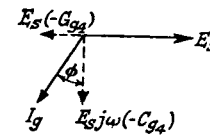

FIG. 5.19c —The Vector Diagram for the Signal Voltage and Grid Current showing the Lag due to Electron Transit Time.

connected to the frequency changer may require damping in order to prevent the negative input conductance from reducing to too great an extent the width of the pass-band. The average value of negative input conductance is generally decreased as the oscillator voltage amplitude is increased, because the latter increases the D.C. self-bias on the oscillator grid and also carries the frequency changer current into cut-off during some part of its negative half-cycle. Whilst the valve is cut off, the instantaneous input conductance is positive. The improvement to be obtained in this manner is limited and it has the disadvantage of increasing oscillator harmonic response.

It is interesting to note that the above description of the cause of negative input admittance can also be used as a basis for explaining positive input admittance when the signal grid is next to the cathode, as in the hexode. In this instance increasing signal voltage means increased density of electrons in the neighbourhood of the grid (the cathode forms a reservoir of electrons which can be drawn upon as required) and therefore increased positive charge on the grid, i.e., the signal voltage and induced charge due to the motion of the electrons are in phase and

$$E_s = \hat{E} \sin \omega t$$
$$Q_g = \hat{Q} \sin \omega t$$
$$\therefore\ I_g = \hat{I} \cos \omega t$$

so that I_g leads upon E_s by 90°, or the input admittance is equivalent to a positive capacitance. Similarly transit time introduces a lag

in I_g and a positive conductance component in the admittance. If the heater voltage is reduced so that current saturation is approached, the input admittance of the hexode signal grid can become negative, because the cathode electron reservoir disappears.

Electron coupling from the signal to oscillator grid has a tendency to start grid current at increasing negative biases on the oscillator grid as the operating frequency is increased, but electron repulsion from G_4 to G_1 is much less than in the hexode since the signal voltage is usually much less than the oscillator voltage, and in any case grid current is required on G_1 for self-bias purposes. Hence this form of electron coupling is unimportant. In the reverse direction, oscillator to signal electrode, a very undesirable form of coupling exists. It can be shown [33] by varying the signal circuit tuning; as this frequency, initially lower than that of the oscillator, approaches the latter, the anode current of the frequency changer decreases to a minimum, from which it rises to its normal value when $f_s = f_h$. From this point it increases to a maximum and then falls back, becoming asymptotic to its normal value as f_s is further increased. This can be explained if the oscillator voltage component induced in the signal circuit is out-of-phase with the true oscillator voltage for $f_s < f_h$ and in-phase for $f_s > f_h$. This is the reverse of what happens with capacitive coupling between the two circuits (Section 5.8.1, Fig. 5.17). Electron coupling must therefore be equivalent to a negative capacitance from G_1 to G_4, and it may be explained by considering the charge induced on the signal grid G_4 by electron movement due to the oscillator grid voltage. Increasing voltage (less negative) on the latter increases total current and the electron density in the G_3G_4 space. The increased negative space-charge induces an increased positive charge on G_4, i.e., the charge on G_4 is in-phase with the voltage on G_1. This is the reverse of positive capacitance coupling which, for increasing positive voltage on G_1, induces an increasing negative charge on G_4. The equivalent negative capacitance coupling, which has a value from -2 to $-0{\cdot}5$ $\mu\mu$F, can be neutralized by the addition of capacitance externally between G_1 and G_4. Neutralization is, however, only complete at one particular set of operating conditions, and change of the D.C. voltages on the electrodes, or oscillator voltage amplitude varies the electron coupling negative capacitance value.

The coupling current flowing from G_1 to G_4 lags behind the voltage applied to G_1 and the vector relationship is as shown in Fig. 5.19*b* when $E_s = E_{g1}$ and $I_g = I_{g1g4}$. Transit time of the electrons causes

a lag in the current vector and at high frequencies the vector diagram is similar to that of Fig. 5.19c ; the coupling admittance includes a negative conductance component and neutralization involves the use of a series RC circuit between G_1 and G_4. Another factor complicates the problem ; the negative conductance component increases as the operating frequency increases so that electron coupling is dependent on the oscillator frequency as well as on the electrode voltages. Only partial neutralization can therefore be achieved when operating over a range of frequencies.

Owing to the negative capacitance coupling the oscillator frequency is affected by signal tuning, but in the reverse direction to that due to positive capacitance coupling. A curve of oscillator frequency variation against signal-tuning capacitance shows the change in f_h to be positive when $f_s < f_h$ and negative when $f_s > f_h$; the curve is the reverse of Fig. 5.17.

5.9. Image Signal Suppression Circuits.[11, 26]

5.9.1. Introduction. Section 5.1.3. indicates the necessity for discrimination against the image signal (f_h+f_1) in the R.F. circuits preceding the frequency changer, and a special filter is sometimes

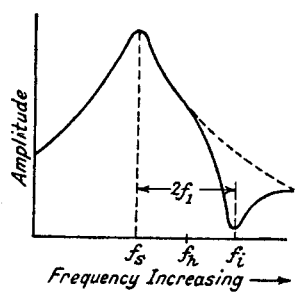

FIG. 5.20.—The Required Selectivity Curve for the R.F. Circuits preceding the Frequency Changer.

included to attenuate particularly this frequency. The effect of the filter is to give a selectivity curve with a pronounced dip at the image frequency (Fig. 5.20). There are two important methods of achieving image suppression, (1) by the use of series or parallel circuits tuned to the image signal and (2) by feedback of the image frequency component from a later stage into the input so as to neutralize the input component.

5.9.2. Series and Parallel Suppression Circuits. The simplest form of series circuit is obtained by tapping the output circuit down the coil of the parallel tuned signal circuit as shown

in Fig. 5.21. The top part of the coil and the tuning capacitor form the series resonant circuit rejecting the image frequency. The particular case shown is that of the aerial circuit and for the output voltage we have, neglecting resistance components

$$E_{AB} = I\left[j\omega L_2 + \frac{1}{j\omega C}\right] + Ij\omega M$$

and for E_{AB} to be zero

$$f = \frac{1}{2\pi\sqrt{(L_2+M)C}} \quad . \quad . \quad . \quad 5.17a.$$

If the input generator is a tetrode valve instead of an aerial, the constant current generator conception (Section 2.7) gives L_1 in

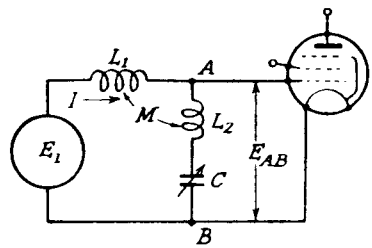

FIG. 5.21.—The Equivalent Circuit for the Tapped Coil Image Suppressor.

parallel with L_2C, and as L_2C are a short circuit at their resonant frequency there can be no current in L_1, so that

$$f = \frac{1}{2\pi\sqrt{L_2C}} \quad . \quad . \quad . \quad . \quad 5.17b.$$

is the condition for E_{AB} to equal 0.

Generally $M \ll L_2$ and 5.17*a* and 5.17*b* are almost identical.

This method suffers from two disadvantages; it reduces the amplitude of the desired signal, and it can only give maximum image suppression at one particular signal tuning frequency since variation of C over the tuning range makes it impossible to maintain the rejection frequency equal to the image frequency. We will illustrate this point for the aerial generator case. Let us assume that currents I_s and I_i flow in the circuit at the signal and image frequencies respectively. If tapping down is not employed, the image discrimination is given by the ratio of signal to image voltages across C and this is

$$\frac{E_{Cs}}{E_{Ci}} = \frac{I_s}{j\omega_s C} \cdot \frac{j\omega_i C}{I_i} = \frac{I_s}{I_i} \cdot \frac{f_i}{f_s} \quad . \quad . \quad . \quad 5.18$$

where $f_s = \dfrac{1}{2\pi\sqrt{(L_1+L_2+2M)C}}$, $f_i = f_s + 2f_1$, and f_1 = intermediate

frequency. Across the points AB the signal to image discrimination is $\frac{E_{ABs}}{E_{ABi}}$,

but $$E_{ABs} = I_s\left[R_{2s} + j\left(\omega_s(L_2+M) - \frac{1}{\omega_s C}\right)\right] \quad . \quad 5.19a$$

where R_{2s} = resistance of the L_2 part of the coil at f_s

$$E_{ABs} = I_s R_{2s}\left[1 + \frac{j\omega_s(L_2+M)}{R_{2s}}\left(1 - \frac{1}{\omega_s^2(L_2+M)C}\right)\right]$$

$$= I_s R_{2s}\left[1 + jQ_{2s}\left(1 - \frac{f_2^2}{f_s^2}\right)\right] \quad . \quad . \quad . \quad . \quad 5.19b$$

where $f_2 = \frac{1}{2\pi\sqrt{(L_2+M)C}} = \frac{1}{2\pi\sqrt{(L_1+L_2+2M)C}} \cdot \sqrt{\frac{L_1+L_2+2M}{L_2+M}}$

$= kf_s$

where $k = \sqrt{\frac{L_1+L_2+2M}{L_2+M}}$.

If we assume the total resistance R_1+R_2 to be proportionally divided between L_1 and L_2

$$Q_{2s} = \frac{\omega_s(L_2+M)}{R_{2s}} = \frac{\omega_s(L_2+L_1+2M)}{R_{1s}+R_{2s}} = Q_s.$$

$$\therefore\ E_{ABs} = I_s R_{2s}\left[1 + jQ_s\left(1 - \frac{f_2^2}{f_s^2}\right)\right]$$

and $$E_{ABi} = I_i R_{2i}\left[1 + jQ_i\left(1 - \frac{f_2^2}{f_i^2}\right)\right]$$

$$\therefore\ \frac{E_{ABs}}{E_{ABi}} = \frac{I_s R_{2s}\left[1 + jQ_s\left(1 - \frac{f_2^2}{f_s^2}\right)\right]}{I_i R_{2i}\left[1 + jQ_i\left(1 - \frac{f_2^2}{f_i^2}\right)\right]} \quad . \quad . \quad . \quad 5.20.$$

The improvement in rejection due to tapping down is

$$20\ \log_{10}\frac{|E_{ABs}|}{|E_{ABi}|} \cdot \frac{|E_{Ci}|}{|E_{Cs}|}\ \text{db.}$$

$$= 10\ \log_{10}\left[\frac{R_{2s} \cdot f_s}{R_{2i} f_i}\right]^2 \cdot \left[\frac{1 + Q_s^2\left(1 - \frac{f_2^2}{f_s^2}\right)^2}{1 + Q_i^2\left(1 - \frac{f_2^2}{f_i^2}\right)^2}\right] \quad . \quad 5.21.$$

If there is only a small variation in Q from f_s to f_i $\frac{R_{2s}}{R_{2i}} = \frac{f_s}{f_i}$ and 5.21 reduces to

$$10\ \log_{10}\frac{f_s^4 + Q^2(f_s^2 - f_2^2)^2}{f_i^4 + Q^2(f_i^2 - f_2^2)^2} \quad . \quad . \quad . \quad 5.22.$$

Curves in Fig. 5.22 show the increased image attenuation achieved by the tapped coil in comparison with the full coil over the medium wave-band of a receiver. The I.F. is 465 kc/s, the coil inductance 156 μH and $Q = 100$. Curve 1 gives $f_2 = f_i = 1{,}530$ kc/s at $f_s = 600$ kc/s, and curve 2 gives $f_2 = f_i = 1{,}930$ kc/s at $f_s = 1{,}000$ kc/s. Curve 1 is more satisfactory because attenuation is greatest for image frequencies either in the medium wave range or close to it. Curve 2 actually has less discrimination for these same image frequencies and gives greatest attenuation on frequencies well outside the medium wave range. If the optimum suppression

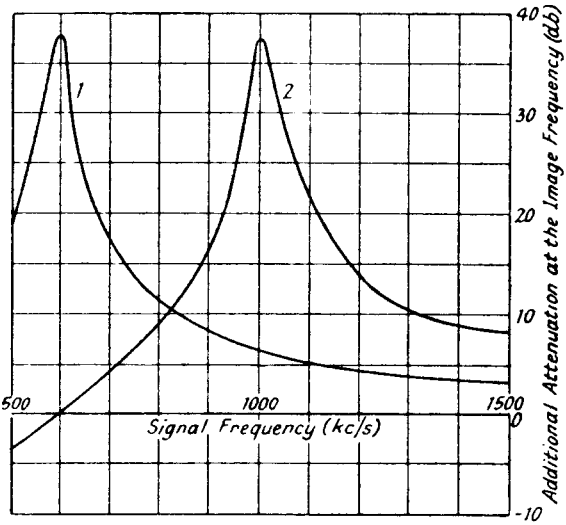

FIG. 5.22.—Image Frequency Rejection Curves for the Tapped Coil Suppressor.

point is chosen at too high a tuning frequency, the tapped coil may give less discrimination against the image than the full coil as the tuning frequency approaches the low-frequency end of the range. This occurs when

$$\frac{f_s^4+Q^2(f_s^2-f_2^2)^2}{f_i^4+Q^2(f_i^2-f_2^2)^2} < 1$$

or

$$(f_i^2+f_s^2)\frac{1+Q^2}{Q^2} > 2f_2^2 \quad . \quad . \quad . \quad 5.23a.$$

By noting that $f_i = f_s+2f_1$, $f_2 = kf_s$ and $\frac{1+Q^2}{Q^2} \simeq 1$, expression 5.23*a* reduces to

$$f_s < \frac{2f_1}{\sqrt{2k^2-1}-1} \quad . \quad . \quad . \quad 5.23b.$$

If an R.F. amplifier precedes the frequency changer, a better average image rejection curve is obtained by tapping down the aerial input and anode coils of this valve by differing amounts so as to stagger the frequencies of optimum rejection.

Tapping down the coil has the disadvantage of reducing the gain at the signal frequency and the loss is

$$20 \log_{10} \frac{|E_{Cs}|}{|E_{ABs}|}$$

Since $\omega_s(L_1+L_2+2M) = \dfrac{1}{\omega_s C}$, expression 5.19*a* may be rewritten

$$E_{ABs} = I_s[R_{2s}+j\omega_s(L_1+M)]$$

also

$$E_{Cs} = \frac{I_s\omega_s(L_1+L_2+2M)}{j}.$$

Thus

$$20 \log_{10} \frac{|E_{Cs}|}{|E_{ABs}|} = 20 \log_{10} \frac{\omega_s(L_1+L_2+2M)}{\sqrt{R_{2s}^2+\omega_s^2(L_1+M)^2}} \quad . \quad 5.24a$$

$$= 20 \log_{10} \frac{L_1+L_2+2M}{L_1+M}$$

if $R_{2s} \ll \omega_s(L_1+M)$,

$$= 20 \log_{10} \frac{1}{1-\dfrac{L_2+M}{L_1+L_2+2M}}$$

$$= 20 \log_{10} \frac{1}{1-\dfrac{1}{k^2}} \quad . \quad . \quad . \quad . \quad 5.24b.$$

The loss for curves 1 and 2 (Fig. 5.22) is 1·4 and 2·72 dbs. respectively.

5.9.3. Image Suppression by Neutralizing Feedback Voltage.[26] Image suppression by feeding back part of the output voltage into the input, or vice versa, necessitates some form of selective circuit (accepting the desired and rejecting the image) between input and output. Let us suppose that equal amplitudes of desired and image frequencies are applied to the input of the band-pass filter of Fig. 5.23*a*.

In the second tuned circuit of the filter the signal voltage is increased and the image voltage decreased owing to the selectivity characteristic of the first tuned circuit. By coupling to this circuit a coil connected to the input, signal and image voltages may be injected into the second tuned circuit direct from the input. By correct adjustment of the amplitude and phase of the image voltage complete cancellation may be obtained. Some reduction of the

signal voltage must also occur, but this may be made quite small with coils of normal Q value. Generally no attempt is made to secure accurate antiphase conditions, and maximum image suppression is obtained by adjustment of the number of turns of the coupling coil. A single turn, wound on the earthed end of the second tuned coil, is often adequate.

By assuming the resistance components to be zero, and the coupling reactance between the two tuned circuits to be small in

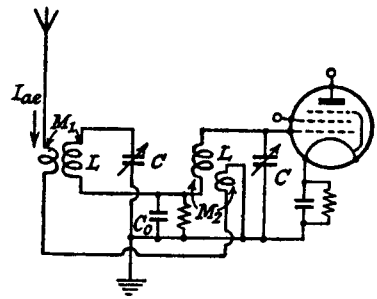

FIG. 5.23*a*.—Image Suppression by a Neutralizing Voltage applied from the Aerial to the Second Tuned Circuit.

comparison with the reactances in the tuned circuits at the image frequency, we have for the voltage transferred to the second circuit across the coupling capacitance C_0

$$E_{C_0} = \frac{I_{ae} j\omega_i M_1 \frac{1}{j\omega_i C_0}}{j\left[\omega_i L - \left(\frac{1}{\omega_i C} + \frac{1}{\omega_i C_0}\right)\right]} \quad . \quad . \quad . \quad 5.25$$

where I_{ae} = current in the aerial circuit
and M_1 = coupling from aerial to first tuned circuit.

The neutralizing voltage transferred to the second circuit by direct coupling from the second aerial coil is $I_{ae} j\omega_i M_2$ and for cancellation

$$I_{ae} j\omega_i M_2 = \frac{I_{ae} \frac{M_1}{C_0}}{j\left(\omega_i L - \frac{C+C_0}{\omega_i C C_0}\right)}$$

$$j\omega_i M_2 = \frac{\frac{M_1}{C_0}}{j\omega_i L\left(1 - \frac{C+C_0}{\omega_i^2 C C_0 L}\right)}$$

but
$$w_s^2 = \frac{C+C_0}{LCC_0} \quad . \quad . \quad . \quad . \quad 5.26$$

$$\therefore \omega_i^2 M_2 L\left(1 - \frac{\omega_s^2}{\omega_i^2}\right) = \frac{M_1}{C_0}$$

$$(\omega_i^2 - \omega_s^2) = \frac{M_1}{M_2 L C_0}.$$

Combining the above with 5.26

$$\frac{f_i^2}{f_s^2} - 1 = \frac{M_1 C}{M_2(C+C_0)} \quad . \quad . \quad . \quad 5.27.$$

Only one point of maximum suppression is obtained, but a second can be produced by tapping the output from a part of the second coil as described in Section 5.9.2.

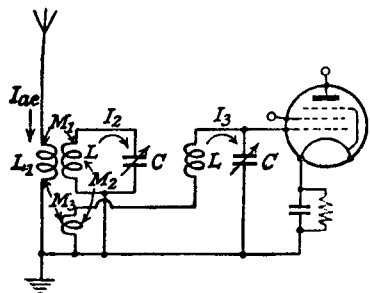

FIG. 5.23*b*.—An Alternative Circuit to Fig. 5.23*a* for Image Suppression by a Neutralizing Voltage.

An alternative circuit is that of Fig. 5.23*b*. The current and voltage equations are

$$E_{ae} = I_{ae}Z_1 + I_2 j\omega M_1 + I_3 j\omega M_3$$
$$0 = I_{ae} j\omega M_1 + I_2 Z_2 + I_3 j\omega M_2$$
$$0 = I_{ae} j\omega M_3 + I_2 j\omega M_2 + I_3 Z_3$$

where Z_1, Z_2 and Z_3 are the series impedances of each circuit, e.g., $Z_1 = R_{a0} + R_1 + j(X_{a0} + \omega L_1)$, where $R_{a0} + jX_{a0}$ is the aerial terminal impedance. If the resistance components are negligible $I_3 = 0$ at the optimum rejection frequency, thus

$$I_2 Z_2 = -I_{ae} j\omega_i M_1$$
$$I_2 j\omega_i M_2 = -I_{ae} j\omega_i M_3$$

from which
$$\frac{Z_2}{j\omega_i M_2} = \frac{M_1}{M_3} \quad . \quad . \quad . \quad . \quad 5.28.$$

But $$Z_2 = j\left(\omega_i L - \frac{1}{\omega_i C}\right) = j\omega_i L\left(1 - \frac{f_s^2}{f_i^2}\right)$$

where $$f_s = \frac{1}{2\pi\sqrt{LC}},$$ the desired frequency.

Replacing Z_2 in 5.28

$$\left[1 - \frac{f_s^2}{f_i^2}\right] = \frac{M_1 M_2}{M_3 L} \quad . \quad . \quad . \quad 5.29.$$

Again only one point of optimum suppression is obtained since the R.H.S. of the equation is a constant. The actual optimum suppression frequency may be set by sliding the coupling coil in the last circuit so as to vary M_3 and M_2 in opposite directions. Generally the aerial coil is wound on the earthed end of the first tuning coil,

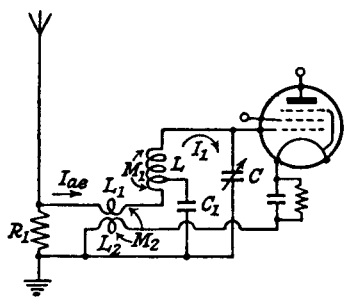

FIG. 5.23c.—Image Suppression by a Neutralizing Voltage Applied from the Aerial to the Cathode Circuit of the First R.F. Valve.

and the coupling coil in the last tuned circuit is arranged to slide over it.

A circuit permitting two points of optimum suppression in the wave range is shown in Fig. 5.23c. The neutralizing voltage is inserted in the cathode-earth lead of the first R.F. valve by a coil coupled to the aerial circuit, which is broadly tuned to the centre of the wave range to be accepted. By neglecting the resistance components, the rejection frequency may be calculated as follows: the equation for the tuned circuit is

$$(I_{ae} - I_1)\frac{1}{j\omega_i C_1} = I_1\left(j\omega_i L + \frac{1}{j\omega_i C}\right) + I_{ae} j\omega_i M_1$$

$$I_1 j\omega_i L\left(1 - \frac{f_s^2}{f_i^2}\right) = -I_{ae} j\left(\omega_i M_1 + \frac{1}{\omega_i C_1}\right)$$

where $$f_s = \frac{1}{2\pi\sqrt{\frac{LCC_1}{C + C_1}}}$$

C_1 is a comparatively large capacitance (about 0·005 μF) and its reactance is low enough to allow the impedance on the aerial side in parallel with it to be neglected, i.e., the tuned circuit frequency is determined by LC and C_1.

Voltage between grid and cathode $= E_C - E_{L_2}$

$$= \frac{I_1}{j\omega_i C} - I_{ae} j\omega_i M_2$$

$$= -I_{ae}\left[\frac{\left(\omega_i M_1 + \frac{1}{\omega_i C_1}\right)}{\omega_i L\left(1 - \frac{f_s^2}{f_i^2}\right) j\omega_i C} + j\omega_i M_2\right]$$

$$= 0$$

when $$\omega_i^2 LC\left(1 - \frac{f_s^2}{f_i^2}\right) = \frac{M_1}{M_2} + \frac{1}{\omega_i^2 M_2 C_1}.$$

But $$LC = \frac{C_1 + C}{\omega_s^2 C_1}$$

$$\therefore \left[\frac{f_i^2}{f_s^2} - 1\right]\frac{C_1 + C}{C_1} = \frac{M_1}{M_2} + \frac{f_3^2}{f_i^2} \quad . \quad . \quad 5.30$$

where $$f_3 = \frac{1}{2\pi\sqrt{M_2 C_1}}.$$

Two points of optimum suppression may be achieved over the wave range because the R.H.S. of equation 5.30 contains two independently variable terms. The first term is of importance at high frequencies. The circuit can give a fairly constant suppression over the wave range and has the advantage of introducing little damping from the aerial into the tuned circuit. The grid-cathode capacitance should be as low as possible as it modifies considerably the image suppression characteristics.

In all image suppression circuits the maximum reduction varies between 20 and 30 dbs.

5.9.4. Image Suppression on the Short Wave Range. The need for image signal suppression on the short wave range is even greater than on the long and medium wave ranges because the signal-tuned circuits are less selective, and the image-to-real signal-frequency ratio is less. For example, at a signal frequency of 1 Mc/s and an I.F. of 465 kc/s, the image signal is reduced by 43 dbs. (see expression 4.8*a*) for a single R.F. tuned circuit of $Q = 100$ (an average value), whereas for a signal frequency of 15 Mc/s and $Q = 50$ (an average value) the image signal is only reduced by 15.8 dbs. Methods of image signal rejection outlined in 5.9.2 and

5.9.3. are not successful for the short wave band because the frequency ratio between the image and real signal is so much smaller. The rejection of the image signal (10·930 Mc/s) for a signal frequency of 10 Mc/s is equivalent to the rejection of an image spaced 93 kc/s from a signal at 1 Mc/s. There have been no special developments for image suppression when a receiver is tuned over the whole of the short wave range, but two methods have been successfully applied with band-spread receivers having preset signal tuning.

One method [37] is illustrated in Fig. 5.24*a*. The preset signal circuit consists of a transformer, the primary and secondary of which are tuned to the centre of the band to be received. The aerial circuit is tuned by the series capacitance C_1 and the inductance L_1, and the latter is coupled to the secondary coil L_2 by combined

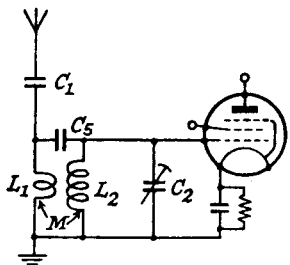

FIG. 5.24*a*.—Image Suppression on the Short Wave Band by Combined Mutual Inductance and Series Capacitance Coupling.

positive mutual inductance and series capacitance coupling (C_5 in Fig. 5 24*a*). The capacitance C_2 tunes the secondary circuit. Section 3.4.10 shows that the equivalent shunt coupling for this form of coupling is

$$Z_C = -\left[\frac{R_2\omega(L_1-M)+R_1\omega(L_2-M)}{B_1}+\frac{\omega^2(L_1-M)(L_2-M)(R_1+R_2)}{B_1^2}\right] + j\left[\omega M - \frac{\omega^2(L_1-M)(L_2-M)}{B_1}\right]$$

and the rejection frequency is obtained when the reactive component of Z_C is 0, i.e.,

when $$\omega M - \frac{\omega^2(L_1-M)(L_2-M)}{B_1} = 0.$$

Replacing B_1 by $\frac{1}{\omega C_5} - \omega(L_1+L_2-2M)$

$$\omega M\left[\frac{1}{\omega C_5} - \omega(L_1+L_2-2M)\right] = \omega^2(L_1-M)(L_2-M)$$

or
$$\omega = \frac{1}{\sqrt{\frac{C_5(L_1L_2 - M^2)}{M}}} \quad . \quad . \quad . \quad 5.31a$$
$$= \frac{1}{\sqrt{MC_5\left(\frac{1-k^2}{k^2}\right)}} . \quad . \quad . \quad . \quad 5.31b$$

where
$$k = \frac{M}{\sqrt{L_1L_2}}.$$

The method of adjusting the image rejection is as follows: With C_5 disconnected, C_1 and C_2 are tuned to give maximum signal frequency output at the centre of the band-spread range, the modulated input signal voltage being obtained from a signal generator through a standard dummy aerial. C_5 is next inserted between L_1 and L_2, so connected to give positive mutual inductance

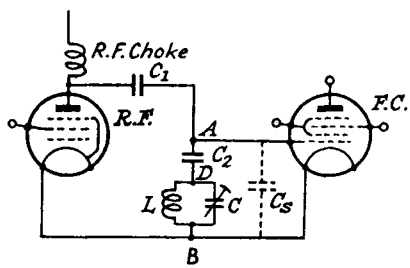

FIG. 5.24b.—Image Suppression on the Short Wave Band by a Series Parallel Suppression Circuit.

(see Section 3.4.2), and the signal generator is tuned to the image frequency (f_s+2f_1). C_5 is adjusted to give minimum audio output from the receiver. An average value for the extra image rejection is about 12 dbs.

Another circuit [40] for obtaining image suppression is shown in Fig. 5.24b. C_1 is the normal coupling capacitance (0·0001 μF) from the anode of the R.F. valve to the frequency changer. A capacitance C_2 is inserted between the top of the preset tuned-signal circuit and the grid of the frequency changer. It forms a series resonant circuit, at some frequency lower than the signal frequency, with the inductive reactance of the LC circuit, which itself is tuned to the signal frequency. In this instance it means that the image frequency must be less than the signal frequency, and the oscillator, contrary to normal practice, has a frequency of $f_s - f_1$. This causes no particular complication as the signal circuits are preset and no ganging problems therefore arise. The use of an inductance in place of C_2 would enable the more normal oscillator condition

of $f_h = f_s + f_1$ to be realized, but satisfactory rejection is difficult to obtain owing to resistance in the inductance, and stray capacitance from the grid of the frequency changer to earth. The series impedance of the LC circuit is (expression 4.4)

$$Z_{DB} = \frac{R}{(1-\omega^2LC)^2+(\omega CR)^2} + j\frac{\omega L(1-\omega^2LC)-\omega CR^2}{(1-\omega^2LC)^2+(\omega CR)^2}$$

$$Z_{DB} \simeq \frac{R}{(1-\omega^2LC)^2} + j\frac{\omega L}{(1-\omega^2LC)}$$

since R is usually much less than ωL. For series resonance at the image frequency

$$\frac{\omega_i L}{1-\omega_i^2 LC} = \frac{1}{\omega_i C_2}$$

$$\omega_i = \frac{1}{\sqrt{L(C+C_2)}} = \frac{\omega_s}{\sqrt{1+\dfrac{C_2}{C}}} \quad . \quad . \quad . \quad 5.32$$

and then $$Z_{AB} = \frac{R}{(1-\omega_i^2LC)^2}$$

$$= \frac{R}{\left[1-\dfrac{\omega_i^2}{\omega_s^2}\right]^2}$$

where $$\omega_s^2 = \frac{1}{LC}.$$

In the absence of the capacitance C_2

$$Z_{AB(C_2=0)} = Z_{DB} = \frac{\dfrac{L}{CR}}{1+jQ_s\left(\dfrac{\omega_i}{\omega_s}-\dfrac{\omega_s}{\omega_i}\right)} \qquad \text{[Expression 4.8}a\text{]}$$

so that the increase in image rejection is

$$20\log_{10}\frac{Z_{DB}}{Z_{AB}} = 20\log_{10}\frac{L}{CR^2}\,\frac{\left[1-\left(\dfrac{f_i}{f_s}\right)^2\right]^2}{\sqrt{1+Q_s^2\left(\dfrac{f_i}{f_s}-\dfrac{f_s}{f_i}\right)^2}} \text{ db.}$$

But $$\frac{L}{CR^2} = \frac{\omega_s L}{R}\cdot\frac{1}{\omega_s CR} = Q_s^2$$

and increased image rejection $= 20\log_{10}\dfrac{Q_s^2\left[1-\left(\dfrac{f_i}{f_s}\right)^2\right]^2}{\sqrt{1+Q_s^2\left[\dfrac{f_i}{f_s}-\dfrac{f_s}{f_i}\right]^2}}$. 5.33.

For $f_s = 15$ Mc/s, $Q = 50$ and $f_1 = 465$ kc/s

$$\text{increased image rejection} = 20 \log_{10} \frac{50^2\left[1 - \left(\frac{14{\cdot}07}{15}\right)^2\right]^2}{\sqrt{1+50^2\left[\frac{14{\cdot}07}{15} - \frac{15}{14{\cdot}07}\right]^2}}$$

$$= 15{\cdot}34 \text{ dbs.}$$

The ratio of $\frac{C_2}{C}$ for this signal frequency is given from expression 5.32.

$$\frac{C_2}{C} = \left(\frac{f_s}{f_1}\right)^2 - 1 = 0{\cdot}135$$

or $C_2 = 10{\cdot}8\ \mu\mu\text{F}$ if $C = 80\ \mu\mu\text{F}$. (An average value for band-spread signal tuning.)

The above represents the maximum image suppression for a signal tuned to the centre of the band-spread range and the average rejection over the whole range would be about 13 dbs. Higher values of image suppression are obtained at lower frequencies due to the increased ratio of $\frac{f_s}{f_i}$; thus at 6 Mc/s for the same Q the maximum extra image suppression is increased to 21·6 dbs. Expression 5.32 shows that the ratio $\frac{C_2}{C}$ must be changed when the range is varied, and it has to be increased as the central signal frequency is reduced. The required increase in C_2 is less when L is switched and C is fixed than when C is switched. Usually the first condition applies for reasons discussed in Section 4.10.2.

Stray capacitance C_s across the points AB should be reduced to the smallest possible value as it affects adversely the image rejection performance, chiefly by reducing the impedance to the signal frequency across the points AB. Thus, denoting the dynamic impedance of the LC circuit at the signal frequency by R_D,

$$Z_{AB}(C_s = 0) = R_D + \frac{1}{j\omega C_2}$$

$$Z_{AB}(C_s \neq 0) = \frac{\left[R_D + \frac{1}{j\omega C_2}\right]\frac{1}{j\omega C_s}}{R_D + \frac{1}{j\omega C_2} + \frac{1}{j\omega C_s}}$$

$$\simeq \left(R_D + \frac{1}{j\omega C_2}\right)\frac{C_2}{C_2 + C_s}$$

when $\frac{1}{\omega C_2} + \frac{1}{\omega C_s} \gg R_D$

$$\therefore\ Z_{AB} \simeq \frac{C_2}{C_2 + C_s} Z_{AB}.(C_s = 0). \quad . \quad . \quad 5.34.$$

5.10. Push-Pull Frequency Changing. Push-pull frequency changing possesses certain advantages over single valve frequency changing.

(1) The signal or oscillator frequency currents in the anode circuit can be cancelled. This is of most advantage when the signal or oscillator frequency approaches that of the I.F.

(2) The interaction between the signal and oscillator circuits due to electrode capacitance and electron coupling [39] may be considerably reduced.

(3) All even oscillator harmonic responses may be cancelled.

If the oscillator grids of the two valves are connected in parallel and the anode circuits are in push-pull, matched valves give no resultant oscillator current in the anode circuit. Even oscillator harmonic responses are therefore cancelled ; this may be proved by assuming the I_aE_g relationship of each valve to be represented by

$$I_a = (a_0+a_1E_{g1}+a_2E_{g1}^2+\ \ldots)(b_0+b_1E_{g3}+b_2E_{g3}^2+\ \ldots)$$

if

$$E_{g1} = \hat{E}_s \cos \omega_s t$$

$$E_{g3} = \hat{E}_h \cos w_h t$$

(the bias voltage for simplification is assumed to be zero)

the coefficient of I.F. current in the first valve $= \dfrac{\hat{E}_h\hat{E}_s a_1 b_1}{2}$

,, ,, ,, ,, ,, ,, ,, second ,, $= -\dfrac{\hat{E}_h\hat{E}_s a_1 b_1}{2}$.

Since the valves are in push-pull with regard to their anode circuits we must subtract the two currents, hence the total I.F. current $= \hat{E}_s\hat{E}_h a_1 b_1$.

The coefficient of the 2nd harmonic response current in the first valve

$$= \frac{\hat{E}_h^2\hat{E}_s a_1 b_2^2}{2}.$$

The coefficient of the 2nd harmonic response current in the second valve

$$= \frac{(-\hat{E}_h)^2\hat{E}_s a_1 b_2^2}{2}$$

$$= \frac{\hat{E}_h^2\hat{E}_s a_1 b_2^2}{2}.$$

Subtraction of these terms gives zero coefficient, and this will be found to occur for all even harmonic responses. If the valves are not matched, $a_1' \neq a_1''$ and $b_2' \neq b_2''$ and some oscillator harmonic response is found.

BIBLIOGRAPHY

1. A New System of Short Wave Amplification. E. H. Armstrong, *Proc. I.R.E.*, Feb. 1921, p. 3.
2. The Superheterodyne, Its Origin, Development and Some Recent Improvements. E. H. Armstrong, *Proc. I.R.E.*, Oct. 1924, p. 539.
3. On the Origin of the Superheterodyne Method. W. Schottky, *Proc. I.R.E.*, Oct. 1926, p. 695.
4. Recent Developments in Superheterodyne Reception. G. L. Beers and W. L. Carlson, *Proc. I.R.E.*, March 1929, p. 501.
5. Considerations in Superheterodyne Design. E. G. Watts, *Proc. I.R.E.*, April 1930, p. 690.
6. Undesired Responses in Superheterodynes. R. H. Langley, *Electronics*, May 1931, p. 618.
7. A Single Dial Control Short Wave Converter for Working a Broadcast Receiver as a Short Wave Superheterodyne. H. A. Chinn, *Q.S.T.*, June 1931, p. 9.
8. Single Valve Frequency Changers. W. T. Cocking, *Wireless World*, July 29th (p. 74), Aug. 5th (p. 110), 1932.
9. The Screen-Grid Valve as Frequency-Changer in the Superhet. E. L. C. White, *Wireless Engineer*, Nov. 1932, p. 618.
10. The Hexode Tube. H. A. Wheeler, *Radio Engineering*, March (p. 19) and April (p. 12), 1933.
11. Second Channel Suppression. R. I. Kinross, *Wireless World*, June 9th, 1933, p. 416.
12. A Note on Interference Tones in Superheterodyne Receivers. W. F. Floyd, *Proc. Phys. Soc.*, July 1st, 1933, p. 610.
13. The Pentagrid Converter. C. L. Lyons, *Wireless Engineer*, July 1933, p. 364.
14. Superheterodyne Receivers. The Advantage of a High Intermediate Frequency. *World Radio*, Jan. 19th, 1934, p. 87.
15. Suppression of Interlocking in First Detector Circuits. P. W. Klipsh, *Proc. I.R.E.*, June 1934, p. 699.
16. On Conversion Detectors. M. J. O. Strutt, *Proc. I.R.E.*, Aug. 1934, p. 981.
17. Second Channel and Harmonic Reception in Superheterodynes. G. W. O. Howe, *Wireless Engineer*, Sept. 1934, p. 461.
18. Developing Single Span Tuning. W. T. Cocking, *Wireless World*, March 23rd (p. 196), Nov. 16th (p. 391), Nov. 23rd (p. 418), 1934.
19. Heptode Frequency Changers. R. J. Wey, *Wireless Engineer*, Dec. 1934, p. 642.
20. Mixing Valves. M. J. O. Strutt, *Wireless Engineer*, Feb. 1935, p. 59.
21. The Operation of Superheterodyne First Detector Valves. J. Stewart, *Journal I.E.E.*, Feb. 1935, p. 227.
22. Frequency Transformation with Reference to Single Span. F. M. Colebrook, *Wireless World*, Feb. 15th, 1935, p. 174.
23. An Improved Short Wave Frequency Changer. E. J. Alway, *Wireless World*, March 1st, 1935, p. 213.
24. Whistling Notes in Superheterodyne Receivers. M. J. O. Strutt, *Wireless Engineer*, April 1935, p. 194.

25. The Application of Superheterodyne Frequency Conversion Systems to Multirange Receivers. W. A. Harris, *Proc. I.R.E.*, April 1935, p. 279.
26. Image Suppression in Superheterodyne Receivers. H. A. Wheeler, *Proc. I.R.E.*, June 1935, p. 569.
27. Superheterodyne Whistles. M. G. Scroggie, *Wireless World*, Sept. 13th, 1935, p. 302.
28. Interfering Responses in Superheterodynes. H. K. Morgan, *Proc. I.R.E.*, Oct. 1935, p. 1164.
29. A New Tube for use in Superheterodyne Frequency Conversion. C. F. Nesslage, E. W. Herold., W. A. Harris, *Proc. I.R.E.*, Feb. 1936, p. 207.
30. Diode Frequency Changers. M. J. O. Strutt, *Wireless Engineer*, Feb. 1936, p. 73.
31. Frequency Changers in All Wave Receivers. M. J. O. Strutt, *Wireless Engineer*, April 1937, p. 184.
32. Why the Triode Hexode ? J. A. Szabadi, *Wireless World*, May 7th (p. 446) and May 14th (p. 472), 1937.
33. Frequency Changing with the Octode. E. Lukacs, *Wireless World*, March 17th, 1938, p. 238.
34. Electron Transit Time Effects in Multigrid Valves. M. J. O. Strutt, *Wireless Engineer*, June 1938, p. 315.
35. A New Converter Tube for All Wave Reception. E. W. Herold, W. A. Harris, T. J. Henry, *R.C.A. Review*, July 1938, p. 67.
36. A New Converter Valve. J. L. H. Jonker and A. J. W. M. Van Overbeek, *Wireless Engineer*, Aug. 1938, p. 423.
37. Pye 906. International A.C. Superhet. *Supplement to Wireless and Electrical Trader*, Oct. 7th, 1939.
38. Superheterodyne Converter Systems. E. W. Herold, *R.C.A. Review*, Jan. 1940, p. 325.
39. A New Ultra Short Wave Frequency Changer. J. A. Sargrove, *Wireless World*, May 1941, p. 124.
40. Making the Most of Short Waves. L. A. Moxon. *Wireless World*, June 1941, p. 148.
41. The Diode as Rectifier and Frequency Changer. D. A. Bell, *Wireless Engineer*, Oct. 1941, p. 395.
42. *Moderne Mehrgitter-Electronenröhren.* M. J. O. Strutt. Text-book.

CHAPTER 6

OSCILLATORS FOR SUPERHETERODYNE RECEPTION

6.1. Introduction.[1] Any reversible system which is capable of storing and releasing energy, i.e., changing its form from potential to kinetic and back again, can be made to oscillate. If the release and storage can be achieved without loss of energy the system will continue to oscillate when once set in motion. This condition cannot be realized in practice because energy is always dissipated when any interchange takes place, and the oscillation amplitude decays according to an exponential law unless the loss is made good. The simplest form of oscillator is the pendulum, which stores energy when rising and releases it when falling. The potential energy is a maximum at the top of the stroke, when the pendulum is momentarily stationary, and storage is complete. Kinetic energy is maximum at the centre of the stroke, and the potential energy is then zero. The pendulum has as an electrical counterpart, the LC circuit, for energy storage is possible in the capacitance and energy release in the inductance. A fully charged capacitance corresponds to maximum potential energy in the pendulum at the top of its stroke, whilst maximum current in the inductance corresponds to maximum kinetic energy in the pendulum at the centre of its stroke. The energy stored in the capacitance is $\frac{1}{2}CE^2$, and is a maximum when the voltage is maximum and current through the system is zero. The energy released in the inductance is $\frac{1}{2}LI^2$ and is zero when I is 0, i.e., when $\frac{1}{2}CE^2$ is maximum. It is maximum one-quarter of a period later (90°) when E is zero. The analogy with the pendulum is therefore exact, for the potential energy and kinetic energy maxima are separated by one-quarter of the oscillation period.

In the pendulum, energy is lost mainly in friction at the bearings, and this loss is made up by energy transferred through a suitable impulsing mechanism to the pendulum from the unidirectional driving source, a tensioned spring, a suspended weight, or an electrical power supply. This impulsing must be made in the right direction and at the correct instant so as to restore the decaying amplitude to its original value. Correct timing or phasing of the impulse is essential if the natural oscillation of the pendulum is to remain

unaltered, and it should be applied when the pendulum is at the centre of its stroke. An impulse given at any other position increases or decreases the frequency of oscillation. If the impulse is given on the down stroke in the direction of pendulum motion, the frequency is increased, whereas it is decreased if given in the opposite direction.

Energy loss in the tuned circuit occurs due to the resistance component of the inductance and of the capacitance. The former is generally far more important than the latter, which can be reduced to a very low value by the use of suitable dielectrics. Make-up energy to compensate for these losses can be derived from a D.C. source, and the impulsing action may be supplied mechanically by a buzzer or electrically by a valve. In the case of a buzzer the impulse is of short duration and at intervals separated by perhaps many cycles of the *LC* circuit oscillation frequency. The result is a train of oscillations of decaying amplitude built up to the initial amplitude at regular time intervals, when the buzzer contacts close and connect it to the D.C. power source. Conditions are different in the case of a valve, which is able to sustain oscillations by virtue of its amplifying action. An essential condition is that energy is fed back from the valve output circuit to the input circuit. This input energy is amplified in the valve and helps to make up the losses in the output circuit, which is usually directly or indirectly the *LC* circuit. The decay of an oscillation once started in the *LC* circuit is prolonged by the energy feedback and amplification, and if sufficient feedback occurs oscillations can be prolonged indefinitely. The make-up energy may be supplied to the *LC* circuit during a part or the whole of the oscillation cycle. Short period impulsing (Class C operation) over about a third of the cycle is the most efficient method of operation, and is consequently widely used for transmitting oscillators. For a superheterodyne receiver oscillator, Class C impulsing is not normally employed and Class B operation is more usual. The impulse is applied over about three-quarters of the cycle and this has the advantage of causing less harmonic production. Low harmonic content is essential to prevent whistle interference in the frequency changer (Sections 5.4.3 and 5.4.4), and oscillator efficiency is of little consequence.

An essential component of the valve oscillator is the feedback impedance between the anode and grid circuits, which allows the valve to apply the make-up energy in the correct phase relationship. If the phase angle of the feedback voltage is not correct the oscillation frequency is different from the natural frequency of the

LC circuit and the frequency is decreased or increased in the same manner as that of the pendulum.

In a valve-driven circuit oscillation occurs as soon as the ratio of the energy feedback to the output energy exceeds the energy gain of the valve, and oscillation amplitude builds up to larger and larger values until balance is restored by a reduction in the energy gain of the valve. The efficiency of the valve as an energy amplifier is only independent of oscillation amplitude for small amplitudes, and usually the energy gain progressively falls when the amplitude is increased beyond a certain value. The limit of oscillation amplitude is determined by cut-off of anode current at one end, and either by grid current damping or saturation of anode current at the other. Grid current is usually the more important limiting factor. The non-linear action of the valve is essential to the stabilisation of amplitude and it is clear that harmonics of the oscillation frequency cannot be avoided. The amplitudes of the individual harmonics in comparison to the fundamental can, however, be made very small by careful design and operation.

6.2. Types of Valve Oscillators and the Conditions for Self-Oscillation.

6.2.1. Introduction. There are five chief types of valve-maintained oscillators. In the tuned anode oscillator (shown in Fig. 6.2*a*), the *LC* circuit is connected to the valve anode, and a coil coupled to the inductance branch is used to return energy to the grid circuit for amplification by the valve. The tuned grid oscillator is similar to the tuned-anode oscillator of Fig. 6.2*a* except that the positions of the *LC* circuit and feedback impedance are reversed, i.e., the former is connected between grid and earth.

The simplest form of back-coupled oscillator is the Hartley (Fig. 6.4). The tuned *LC* circuit, connected between anode and grid, is its own feedback impedance. The position of the tapping point of the cathode on the coil governs the amount of feedback, and is such that the latter is in the right direction to increase the energy supply from the anode of the valve to the *LC* circuit.

The Colpitts oscillator of Fig. 6.5 is a variant on the Hartley, the only difference being that the capacitance branch is split to provide a tapping for the cathode instead of the inductance branch. The *LC* circuit is again its own feedback impedance.

In the last form of oscillator (Meissner) shown in Fig. 6.1 the *LC* circuit is not inserted in either grid or anode circuit. Coils L_a and L_g, coupled to the tuned circuit, supply energy to the latter.

We will now proceed to an examination of the conditions necessary to start oscillations in all the above types of oscillator except the Meissner. One assumption is made, viz., that the valve is

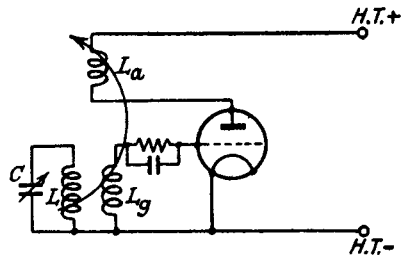

FIG. 6.1.—The Meissner Oscillator.

functioning as a linear amplifier. In actual fact, once oscillation has started, constant amplitude can only be maintained if the valve has non-linear characteristics.[10, 13] Nevertheless, the linear theory is most useful in giving an understanding of the principles underlying valve oscillators, and is helpful in indicating the effect of the valve on the frequency of oscillation.

6.2.2. The Tuned Anode Oscillator. The actual and equivalent circuits for the tuned anode oscillator are shown in Figs. 6.2*a* and 6.2*b*. Making the assumptions of linear [21] operation and high

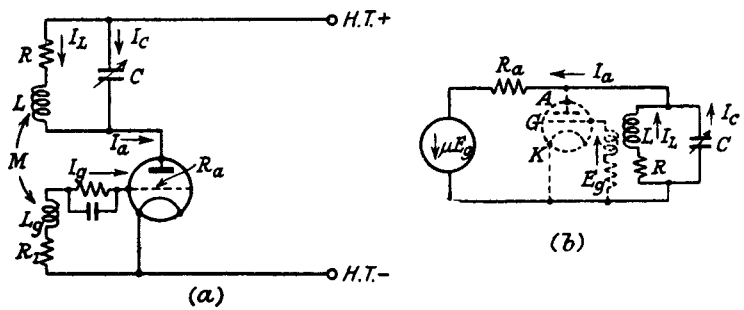

FIG. 6.2*a* and 2*b*.—The Tuned Anode Oscillator and its Equivalent Circuit.

grid input impedance, the current-voltage equation for the anode circuit is

$$\mu E_g = I_a R_a + I_L(R + j\omega L) \quad . \quad . \quad . \quad 6.1a$$

where $-E_g$ = voltage induced in the grid circuit, the negative sign must be included since the vector direction with reference to the cathode is opposite to that for the generated anode voltage, i.e.,

when μE_g is increasing in a positive direction, E_g is increasing in a negative direction. Hence the voltage equation for the grid circuit is

$$-E_g = j\omega M I_L \quad . \quad . \quad . \quad . \quad 6.2.$$

Combining 6.1*a* and 6.2.

$$-\mu j\omega M I_L = I_a R_a + I_L(R+j\omega L) \quad . \quad . \quad 6.1b$$

but

$$I_a = I_L + I_C \quad . \quad . \quad . \quad . \quad 6.3$$

and

$$I_L(R+j\omega L) = \frac{I_C}{j\omega C} \quad . \quad . \quad . \quad . \quad 6.4.$$

From 6.3 and 6.4

$$I_a = I_L[1+(R+j\omega L)j\omega C] \quad . \quad . \quad . \quad 6.5$$

replacing I_a in 6.1*b* by 6.5.

$$-\mu j\omega M I_L = I_L[R_a[(R+j\omega L).j\omega C+1)]+R+j\omega L]$$

$$I_L[R+R_a - \omega^2 LCR_a + j(\mu\omega M + \omega L + RR_a\omega C)] = 0 \quad 6.6.$$

Since $I_L = 0$ is obviously not a possible solution, the term in the bracket must be zero. Equating real and imaginary terms separately to zero we have

$$\omega = \frac{1}{\sqrt{LC}}\sqrt{1+\frac{R}{R_a}} = \omega_0\sqrt{1+\frac{R}{R_a}} \quad . \quad . \quad 6.7$$

where $\omega_0 = \dfrac{1}{\sqrt{LC}}$ the natural pulsance of the LC circuit

and

$$M = -\left[\frac{L+CRR_a}{\mu}\right] = -\left[\frac{L}{\mu}+\frac{CR}{g_m}\right] \quad . \quad . \quad 6.8.$$

The negative sign for M is to be expected since the grid voltage E_g with respect to the cathode must be in antiphase to μE_g also referred to the cathode. The physical significance of $-M$ is treated in Section 3.4.2, and the grid coil L_g is shown reversed in Fig. 6.2*a* to emphasise this feature. Two points of interest arise from expression 6.7 ; the valve slope resistance affects the oscillation frequency, making it higher than the natural frequency of the LC circuit, and the difference in frequency is least with smallest coil resistance and largest valve resistance. The increase of oscillation frequency means that the impedance of the LC tuned circuit is capacitive, and this is clearly shown from the vector diagram of Fig. 6.3, in which all voltage and current vectors are referred to the cathode. The generated voltage vector μE_g, shown as horizontal to the right, is taken as the datum. It has two components (see expression 6.1*a*), that represented by $I_a R_a$ across the valve resistance and that, $E_0 = I_L(R+j\omega L) = \dfrac{I_C}{j\omega C}$, across the tuned circuit. Since

the oscillation frequency exceeds the natural frequency of the tuned circuit, I_a is capacitive with respect to μE_g and leads it as shown. Of the two current components of I_a, I_C leads E_0 by 90° (assuming the capacitance C to have no resistance component) and I_L lags behind E_0 by less than 90° due to the coil resistance R. The grid voltage E_g lags behind I_L by 90° and is at 180° to μE_g; i.e., for continuous oscillation I_L must always lag behind μE_g by 90°. This is not possible if I_a is inductive, for E_0 then leads on μE_g, and as the angle between E_0 and I_L cannot exceed 90°, I_L can never be at 90° to μE_g. The effect of an increase of R_a is shown by the dashed vectors of Fig. 6.3, I_a is reduced to I_a', but the vector

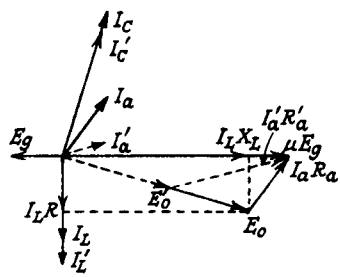

FIG. 6.3.—The Vector Diagram for the Tuned Anode Oscillator.

I_aR_a is increased to $I_a'R_a'$ because I_a' is reduced to a less extent than R_a' is increased. Since I_L', and therefore E_0', must remain at the same phase angle relative to μE_g it follows that $I_a'R_a'$ and therefore I_a' must have a smaller phase angle with respect to μE_g. I_a' must have a smaller angle of lead on E_0', which means that the LC circuit impedance is less capacitive and the oscillation frequency closer to the natural frequency of the tuned circuit thus confirming expression 6.7. The same process can also show that decrease of R reduces the difference between the oscillation and natural frequencies.

Let us now consider the effect of a finite grid input impedance due mainly to grid current. If I_g is the current in the grid circuit and R_g represents the grid input impedance (assumed to be resistive), the equations become

$$\mu E_g = -\mu I_g R_g = I_a R_a + I_L(R + j\omega L) + I_g j\omega M \quad . \quad 6.9$$

$$I_a = I_L + I_C \quad . \quad . \quad . \quad . \quad 6.10$$

$$I_L(R + j\omega L) + I_g j\omega M = \frac{I_C}{j\omega C} . \quad . \quad . \quad 6.11.$$

From 6.10 and 6.11

$$I_a = I_L[1+j\omega C(R+j\omega L)] - I_g\omega^2 MC \quad . \quad . \quad 6.12.$$

But $I_L j\omega M = I_g(R_g+j\omega L_g)$

$$I_g = \frac{I_L j\omega M}{R_g+j\omega L_g} \quad . \quad . \quad . \quad . \quad 6.13.$$

Replacing I_a and I_g in 6.9 by 6.12 and 6.13.

$$\frac{-\mu j I_L R_g \omega M}{R_g+j\omega L_g}$$

$$= I_L\left[R_a(1+j\omega C(R+j\omega L))+R+j\omega L+\frac{j\omega M}{R_g+j\omega L_g}(j\omega M-\omega^2 MCR_a)\right]$$

$$I_L[\mu j\omega M R_g+[R_a+j\omega C(R+j\omega L)R_a+R+j\omega L](R_g+j\omega L_g) + j\omega M(j\omega M - \omega^2 MCR_a)] = 0.$$

Equating the real term to zero gives the value of ω

$$R_g(R_a - \omega^2 LCR_a+R) - \omega^2 LL_g - \omega^2 L_g CRR_a - \omega^2 M^2 = 0 \quad . \quad 6.14.$$

Hence

$$\omega = \sqrt{\frac{R_g(R+R_a)}{LCR_aR_g+LL_g+L_gCRR_a+M^2}}$$

$$= \omega_0 \sqrt{\frac{1+\frac{R}{R_a}}{1+\frac{L_g}{CR_aR_g}+\frac{L_gR}{LR_g}+\frac{M^2}{LCR_aR_g}}} \quad 6.15.$$

It will be seen that expression 6.15 reduces to 6.7 when R_g is infinite. The frequency of oscillation is least affected when R_g is as large as possible, i.e., grid current should be small; L_g should also be as small as possible. The larger the value of C the less effect has R_g, so that we should expect the departure from the natural frequency to be less at the lower frequencies of a given tuning range.

6.2.3. The Tuned Grid Oscillator. If the effect of grid current is neglected the following equations are obtained for the tuned grid oscillator.

$$\mu E_g = I_a(R_a+j\omega L_a)+Ij\omega M \quad . \quad . \quad . \quad 6.16$$

where I = the circulating current in the tuned grid circuit

$$-E_g = \frac{I}{j\omega C} \quad . \quad . \quad . \quad . \quad 6.17$$

$$I_a j\omega M + I\left[R+j\left(\omega L - \frac{1}{\omega C}\right)\right] = 0 \quad . \quad . \quad 6.18.$$

Combining 6.16 and 6.17

$$I = \frac{I_a(R_a+j\omega L_a)}{-j\left(\omega M+\frac{\mu}{\omega C}\right)} \quad . \quad . \quad . \quad 6.19.$$

Replacing this value of I in 6.18

$$I_a\left[j\omega M+\frac{\left[R+j\left(\omega L-\frac{1}{\omega C}\right)\right](R_a+j\omega L_a)}{-j\left[\omega M+\frac{\mu}{\omega C}\right]}\right]=0$$

or

$$\omega^2M^2+\mu\frac{M}{C}+R_aR-\omega L_a\left(\omega L-\frac{1}{\omega C}\right)$$
$$+j\left[R_a\left(\omega L-\frac{1}{\omega C}\right)+R\omega L_a\right]=0 \quad . \quad 6.20.$$

Equating the imaginary term to zero gives the oscillation frequency as

$$\omega = \frac{1}{\sqrt{LC\left(1+\frac{L_aR}{LR_a}\right)}} \quad . \quad . \quad . \quad 6.21a$$

$$= \frac{\omega_0}{\sqrt{1+\frac{L_aR}{LR_a}}} \quad . \quad . \quad . \quad . \quad 6.21b.$$

This is less than ω_0 and the LC circuit is thus an inductive impedance at the oscillation frequency, exactly the reverse of the tuned anode oscillator. Least frequency variation is obtained when R_a is large, and R and L_a small.

Equating the real term to zero and replacing ω by expression 6.21a gives a quadratic in M

$$\frac{M^2}{LC(1+\alpha)}+\frac{\mu M}{C}+RR_a+\frac{L_a}{C}-\frac{L_a}{C(1+\alpha)}=0$$

where

$$\alpha=\frac{L_aR}{LR_a}$$

and

$$M=\frac{-\mu L(1+\alpha)\pm\sqrt{[\mu L(1+\alpha)]^2-4[L_aL\alpha+RR_aLC(1+\alpha)]}}{2} \quad . \quad 6.22a.$$

The minimum value of M required to start oscillation is that with the positive sign before the root.

Thus $$M = \frac{-\mu L(1+\alpha)+\mu L(1+\alpha)\left[1-\frac{4[L_aL\alpha+RR_aLC(1+\alpha)]}{[\mu L(1+\alpha)]^2}\right]^{\frac{1}{2}}}{2}$$

expanding the last term by the Binomial theorem.

$$M \simeq \frac{-[L_aL\alpha+RR_aLC(1+\alpha)]}{\mu L(1+\alpha)}$$

$$\simeq -\left[\frac{L_a\alpha}{\mu(1+\alpha)}+\frac{CR}{g_m}\right] \quad . \quad . \quad . \quad 6.22b.$$

Expression 6.22*b* is similar in form to 6.8 and M is again negative. The value of α is unlikely ever to be greater than 1 and L_a is usually much less than L, so that a smaller value of M is required to initiate oscillation for the tuned-grid oscillator than for the tuned-anode oscillator.

6.2.4. The Hartley Oscillator. The fundamental equations for the Hartley oscillator (Fig. 6.4), neglecting grid current, are as follows:

$$\mu E_g = I_aR_a+I_1(R_1+j\omega L_1) - I_2j\omega M.$$

In this equation and in all others that follow, M denotes the

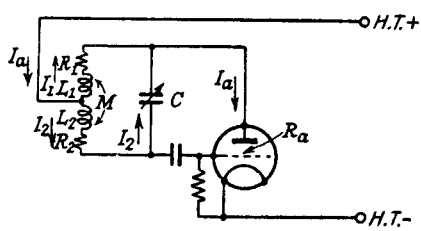

FIG. 6.4.—The Hartley Oscillator.

numerical value of mutual inductance and the negative sign, which the circuit clearly indicates is necessary, is placed outside M.

$$-E_g = I_2(R_2+j\omega L_2) - I_1j\omega M$$

$$I_a = I_1+I_2.$$

Hence

$$-\mu[I_2(R_2+j\omega L_2) - I_1j\omega M] = (I_1+I_2)R_a+I_1(R_1+j\omega L_1) - I_2j\omega M.$$

But $$I_1(R_1+j\omega L_1) - I_2j\omega M = I_2(R_2+j\omega L_2) - I_1j\omega M+\frac{I_2}{j\omega C}$$

$$\therefore\ I_2[R_a+R_1+j\omega(L_1-\mu M)]\left[R_2+j\omega(L_2+M)+\frac{1}{j\omega C}\right]$$

$$+[R_a+\mu R_2+j\omega(\mu L_2-M)][R_1+j\omega(L_1+M)] = 0 \quad 6.23.$$

Equating the imaginary term to zero we have

$$R_2\omega(L_1-\mu M)+(R_a+R_1)\left[\omega(L_2+M)-\frac{1}{\omega C}\right]$$
$$+R_1\omega(\mu L_2-M)+(R_a+\mu R_2)\omega(L_1+M)=0$$

$$\omega^2[R_a(L_1+L_2+2M)+R_2(\mu+1)L_1+R_1(\mu+1)L_2]=\frac{R_a+R_1}{C}.$$

Generally $R_a(L_1+L_2+2M)\gg R_2(\mu+1)L_1$ and $R_1(\mu+1)L_2$ so that

$$\omega\simeq\sqrt{\frac{1+\frac{R_1}{R_a}}{(L_1+L_2+2M)C}}=\omega_0\sqrt{1+\frac{R_1}{R_a}} \quad . \quad . \quad 6.24$$

where ω_0 = the natural frequency of the LC circuit. The oscillation frequency, as in the case of the tuned anode oscillator, is higher than ω_0, but the frequency difference is small when R_a is large and R_1 small.

The condition for oscillation is obtained by equating the real part of expression 6.23 to zero.

$$(R_a+R_1)R_2-\omega^2(L_1-\mu M)(L_2+M)+\frac{L_1-\mu M}{C}$$
$$+(R_a+\mu R_2)R_1-\omega^2(\mu L_2-M)(L_1+M)=0$$

$$R_a(R_1+R_2)+R_1R_2(1+\mu)+\frac{L_1-\mu M}{C}-\omega^2(L_1L_2-M^2)(\mu+1)=0.$$

Neglecting $R_1R_2(1+\mu)$ and replacing ω^2 by 6.24

$$\frac{(L_1L_2-M^2)(\mu+1)\left(1+\frac{R_1}{R_a}\right)}{(L_1+L_2+2M)C}=\frac{L_1-\mu M}{C}+R_a(R_1+R_2).$$

If $\frac{R_1}{R_a}\ll 1$.

$$(L_1L_2-M^2)(\mu+1)=(L_1-\mu M)(L_1+L_2+2M)$$
$$+CR_a(R_1+R_2)(L_1+L_2+2M)$$

which reduces to

$$\mu=\frac{L_1+M}{L_2+M}+\frac{CR_a(R_1+R_2)(L_1+L_2+2M)}{(L_1+M)(L_2+M)}. \quad . \quad 6.25a$$

for continuous oscillation.

By changing the ratio of $\frac{L_1+M}{L_2+M}$, i.e., the cathode tapping point on the coil, it is possible to adjust the oscillating conditions. A larger inductance between the grid and cathode makes for easier

oscillation. The frequency requirement of high R_a points to the need for a high g_m for expression 6.25*a* approaches

$$\frac{\mu}{R_a} = g_m = \frac{C(R_1+R_2)(L_1+L_2+2M)}{(L_1+M)(L_2+M)} \quad . \quad . \quad 6.25b.$$

6.2.5. The Colpitts Oscillator. The conditions for start of oscillation may be determined in the same manner as for the previous

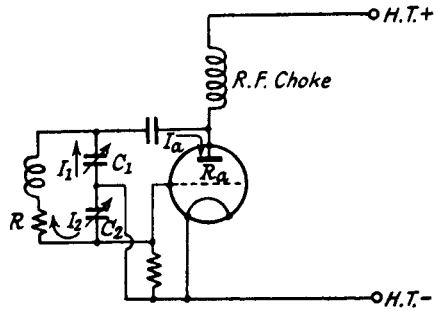

FIG. 6.5.—The Colpitts Oscillator.

circuits. Referring to Fig. 6.5, we find the following current and voltage relationships (neglecting grid current):

$$I_a = I_1+I_2$$

$$\mu E_g = I_aR_a+\frac{I_1}{j\omega C_1} = I_2R_a+I_1\left(R_a+\frac{1}{j\omega C_1}\right)$$

$$-E_g = \frac{I_2}{j\omega C_2}.$$

$$\frac{I_1}{j\omega C_1} = I_2\left(R+j\omega L+\frac{1}{j\omega C_2}\right)$$

$$-\frac{\mu I_2}{j\omega C_2} = I_2\left[\left(R+j\omega L+\frac{1}{j\omega C_2}\right)\left(R_a+\frac{1}{j\omega C_1}\right)j\omega C_1+R_a\right].$$

$$I_2[\mu+jR_a\omega C_2-\omega^2R_aRC_1C_2+j\omega C_2R-j\omega^3LR_aC_1C_2 - \omega^2LC_2+j\omega C_1R_a+1] = 0 \quad 6.26.$$

Equating the imaginary term to zero

$$R_a\omega C_2+\omega C_2R-\omega^3LR_aC_1C_2+\omega C_1R_a = 0.$$

$$\omega^2 = \frac{1}{LC_1}+\frac{1}{LC_2}+\frac{R}{R_aLC_1}$$

$$= \frac{1}{\frac{LC_1C_2}{C_1+C_2}}\left(1+\frac{RC_2}{R_a(C_1+C_2)}\right). \quad . \quad . \quad 6.27a$$

or

$$\omega = \omega_0\sqrt{1+\frac{R}{R_a}\left(\frac{C_2}{C_1+C_2}\right)}. \quad . \quad . \quad 6.27b$$

where ω_0 is the natural frequency of the LC circuit.

The condition for start of oscillation is obtained by equating the real term to zero.

I.e., $$\mu+1 = \omega^2(LC_2+RR_aC_1C_2)$$

Replacing ω by the value in 6.27*a*

$$\mu+1 = \left[\frac{C_1+C_2}{C_1}+\frac{R_aR(C_1+C_2)}{L}\right]\left[1+\frac{RC_2}{R_a(C_1+C_2)}\right]$$

If $$\frac{RC_2}{R_a(C_1+C_2)} \ll 1$$

$$\mu+1 = 1+\frac{C_2}{C_1}+\frac{R_aR(C_1+C_2)}{L}$$

or for oscillation to be sustained

$$\mu = \frac{C_2}{C_1}+\frac{R_aR(C_1+C_2)}{L} \quad . \quad . \quad . \quad 6.28a.$$

The ease with which a Colpitts circuit may be made to oscillate is very clearly indicated by expression 6.28*a*. In practice $C_2 \simeq C_1$, so that for normal values of circuit components even a very low μ valve can be made to sustain oscillation.

We also note that for small frequency variation due to the valve, R should be small and R_a large. When $\frac{R_aR}{L}(C_1+C_2) \gg \frac{C_2}{C_1}$ the valve parameter determining oscillation is g_m for expression 6.28*a* becomes

$$\frac{\mu}{R_a} = g_m = \frac{R(C_1+C_2)}{L} \quad . \quad . \quad . \quad 6.28b.$$

Summarizing the results of the examination assuming linear operation we find that for minimum frequency variation due to the valve, R_a and R_g (the grid circuit input resistance) should be as large as possible, whilst R, I_g, and the inductance of the feedback coil should be as small as possible. The valve makes the oscillation frequency greater than the resonant frequency of the LC circuit for the tuned anode, Hartley and Colpitts oscillators and less for the tuned-grid.

Ease of oscillation is secured in all cases by a low value of R and high value of g_m and oscillation conditions for the Hartley and Colpitts circuits are particularly easy to fulfil.

A lower value of M or μ is required as the tuning capacitance is decreased, i.e. frequency is increased.

6.3. The Conditions to be fulfilled by a Superheterodyne Receiver Oscillator. An oscillator supplying the oscillator voltage to a frequency changer must fulfil the following requirements if satisfactory operation is to be achieved:

1. The conditions for self-oscillation must be easily realizable. An oscillator requiring a feedback coil comparable in inductance to the *LC* circuit inductance is obviously unsatisfactory. Excessive anode current in the normal oscillating condition cannot be tolerated.

2. Oscillation must be maintained over the required frequency range without "blind spots", frequencies at which oscillation ceases.

3. The variation in amplitude over the frequency range should be as small as possible. The necessity for this is clearly indicated in Section 5.5.

4. The oscillator must not have a number of degrees of freedom, and must not be liable to parasitic or squegger oscillations.

5. Supply voltage variations should have minimum effect on the oscillation frequency.

6. The frequency should be independent of bias or supply voltage variations on the frequency changer.

7. Harmonic frequency voltages generated by the oscillator should be small.

8. Temperature and humidity variations should have minimum effect on the oscillation frequency.

Each of the four types of oscillator fulfils some of the requirements, and generally by careful design those not normally fulfilled can be approached.

The tuned anode oscillator, for example, has generally less harmonic content, a larger amplitude, and is more stable to supply voltage fluctuations than the tuned-grid, whilst the latter has a more constant amplitude as the oscillator frequency is varied over the tuning range.[2] The tuned anode oscillator has the added advantage of being less affected by bias variations on the frequency changer valve, when the oscillator grid of the frequency changer and grid of the oscillator valve are connected together.

The Hartley and Colpitts circuits, on the other hand, can be made to oscillate without difficulty even at high frequencies in the short wave range.

We will now consider requirement 3 in detail.

6.4. The Maintenance of Constant Output over the Frequency Range. In Section 5.5 it is shown that the oscillator voltage at the frequency changer must not be allowed to exceed a given value, otherwise harmonic interference whistles are produced by the frequency changer. Conversion conductance is rapidly reduced if the oscillator voltage falls much below the optimum

value. Hence it is essential to maintain the oscillator output voltage close to the required value over the frequency range.

The tendency in most oscillators is for the amplitude to increase as the frequency increases. The conditions for start of oscillation given in Section 6.2 indicate that this is to be expected, since decrease in the tuning capacitance C reduces the value of M or μ required to start oscillation. It is not practicable to reduce the value of M or μ as C is decreased. The decrease in C is offset to some extent by an increase of coil resistance R, but this is not sufficient to prevent increasing amplitude. The only alternative is to insert an impedance which increases the damping of the tuned circuit or reduces the feedback as the frequency rises. A normal method of achieving this is to include a resistance between the grid of the valve and the self-bias resistance and capacitance. This is

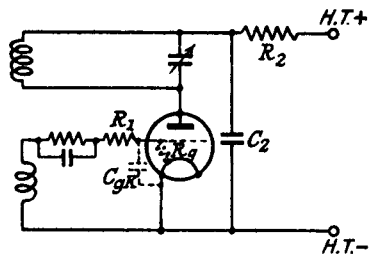

FIG. 6.6.—The Tuned Anode Oscillator with Series Grid Resistance as an Amplitude Stabilizer.

shown in Fig. 6.6 for the tuned-anode oscillator. The resistance R_1 forms with the grid input impedance a potentiometer which reduces the proportion of voltage transferred to the grid as the frequency increases. Its chief effect as an amplitude stabilizer is, however, in combination with the grid-earth capacitance for it produces across the grid coil a parallel damping resistance, which decreases as the frequency increases. For example, if $R_1 = 1{,}000\Omega$ and the grid earth capacitance $C_1 = 10\ \mu\mu$F, the admittance of these two in series is

$$Y = \frac{1}{R_1 + \dfrac{1}{j\omega C_1}} = \frac{j\omega C_1(1 - j\omega C_1 R_1)}{1 + \omega^2 C_1^2 R_1^2}$$

$$= \frac{R_1\omega^2 C_1^2}{1 + \omega^2 C_1^2 R_1^2} + \frac{j\omega C_1}{1 + \omega^2 C_1^2 R_1^2}$$

$$= +Gj B.$$

The damping resistance across the grid coil is therefore

$$R_g = \frac{1}{G} = \frac{1+\omega^2 C_1^2 R_1^2}{R_1 \omega^2 C_1^2}$$
$$= 0{\cdot}84 \text{ M}\Omega \text{ at } 550 \text{ kc/s}$$
$$= 0{\cdot}113 \text{ M}\Omega \text{ at } 1{,}500 \text{ kc/s}.$$

A typical curve showing the amplitude correction obtained by this method is given in Fig. 6.7. A value of 500 to 1,000Ω is suitable for long and medium waves and 50Ω for the short waves. R_2 and C_2 are R.F. decoupling components in the anode circuit and have values from 20,000 to 50,000Ω and 0·1 μF, respectively. Limitation of amplitude variation in the tuned-grid oscillator can also be

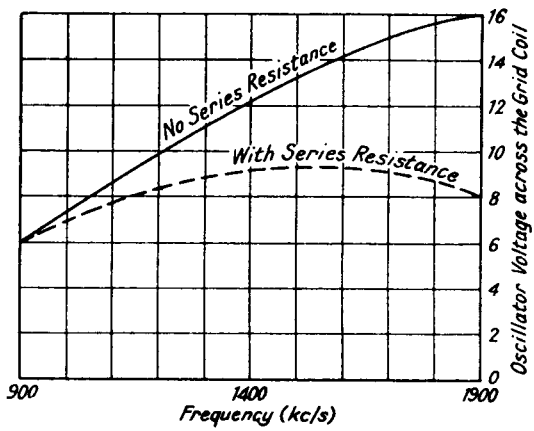

FIG. 6.7.—Curves showing the Stabilizing Effect of the Series Grid Resistance in the Tuned Anode Oscillator.

achieved by inserting a resistance between the anode and feedback coil, and the values given above are suitable.

Negative feedback, by inserting a small coil L_k in the cathode lead, can be applied to limit amplitude variation when the oscillator valve is separate from the frequency changer. The increasing impedance of L_k reduces the effective mutual conductance of the valve to $g_m' = \frac{g_m}{1+jg_m\omega L_k}$ as the frequency increases, and so reduces oscillator output.

Amplitude variation in a tuned anode oscillator may be reduced by using resistance-capacitance coupling to the LC circuit as in Fig. 6.8. The anode resistance R_a reduces the gain variation due to the increase in the tuned circuit impedance $\left(\frac{L}{CR}\right)$ as the oscillation

frequency increases. This resistance has the disadvantage of damping the LC circuit and increasing the possibility of harmonic production in the oscillator itself. It also reduces oscillator frequency stability with respect to changes of H.T. voltage, because R_0 is

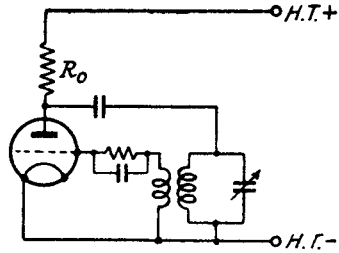

FIG. 6.8.—Amplitude Stabilization of the Tuned Anode Oscillator by a Shunt Resistance.

effectively in parallel with the tuned circuit; it increases R in expression 6.7 with the result that $\frac{R}{R_a}$ is increased and variations of R_a produced by changes of H.T. voltage have greater effect.

Amplitude stability may be increased for the tuned-anode oscillator by using a diode connected to the tuned circuit to supply the grid bias. A suitable circuit is shown in Fig. 6.9. This method considerably reduces the maximum amplitude, and a long grid-base

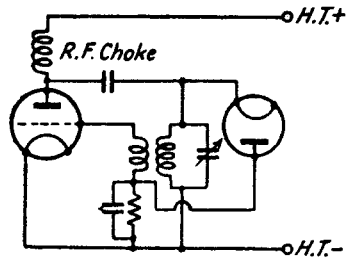

FIG. 6.9.—Amplitude Stabilization of the Tuned Anode Oscillator by Grid Bias derived from the Tuned Circuit with a Diode.

valve may be necessary to obtain sufficient voltage for the frequency changer.

6.5. Frequency Stability.[3, 8] One of the most important requirements in an oscillator is that its frequency should remain constant. Any variation of frequency from the correct setting causes the I.F. carrier to be displaced from the centre of the pass-band of the I.F. amplifier. For an amplitude modulated wave, frequency distortion, producing high-pitched shrill reproduction, is

the chief result, but if the off-centering is excessive the equivalent of single side-band transmission is obtained and amplitude distortion occurs. Rapid fluctuations of H.T. voltage, due to hum, interference, etc., are more serious in the frequency modulation receiver, since they cause frequency modulation of the oscillator rather than amplitude modulation. The detector system in the amplitude modulation receiver has no response to a frequency modulated I.F. carrier. In the case of frequency modulated reception, slow variation of oscillator frequency is serious because it limits the permissible frequency deviation of the carrier and causes amplitude distortion at high modulation levels.

Frequency variation may be separated into long- and short-period effects. Long-period changes, i.e., slow drift of oscillator frequency, are generally the most troublesome and produce greatest frequency variation ; heat and humidity are the chief causes by varying the inductance and capacitance of the tuning circuit. Increase of temperature normally increases inductance and capacitance and lowers the oscillation frequency. Heating of the valve also adds its quota by producing a change in the parameters, μ, g_m and R_a, and in the electrode spacings. Short-period changes are chiefly due to H.T. supply voltage fluctuation from hum, mains interference or feedback from the audio frequency stages, but an important source is also the frequency changer. Frequency variations from the latter are mainly a result of A.G.C. and coupling (electronic and capacitive—Sections 5.8.2 and 5.8.3) to the signal circuit. For this reason A.G.C. is often not applied to a frequency changer operating on the short and ultra short wave ranges.

Though long- and short-term fluctuations form a convenient classification it is preferable to analyse under the headings of the components, causing the frequency variations, e.g., the valve, the *LC* circuit and its associated components, such as the range switch, coupling capacitors, etc., and frequency changer.

6.6. Frequency Variations due to the Valve.[21]

6.6.1. Introduction. Frequency variations due to the valve may be ascribed to four causes :

1. The valve is not functioning as a pure negative resistance, but has a reactive component, the value of which is affected by power supply voltages. This reactance is in parallel with the *LC* circuit and directly affects the resonant frequency.

2. Harmonics are present. They are essential to stabilized

oscillation, but the smaller the harmonic content the less is the frequency variation.

3. Interelectrode capacitance change. This capacitance is made up of two components, one due to the electrode dimensions and spacing, and the other to the space-charge distribution of the electrons. Change of the former due to heating of the electrode structure is a long-period effect, whilst the latter may have a long-period effect due to heating of the valve changing the emission properties, and a short-period effect due to H.T. supply voltage variations. Greatest space-charge capacitance is usually in the neighbourhood of a negative electrode, and hence grid-cathode space-charge capacitance is greater than anode-cathode space-charge capacitance. A tuned grid oscillator therefore shows greater frequency variation than a tuned anode for given fluctuations of supply voltage.

4. Variation in valve slope resistance R_a resulting from power supply fluctuations. The frequency formulae developed in preceding sections indicate that changes of R_a affect the oscillation frequency.

6.6.2. Valve Reactance. The valve has the effect of reducing the resistance component of the LC circuit to zero so that the slightest random disturbance sets up oscillation. At the same time it introduces a reactive component which modifies the equation for start of self-oscillation to

$$R+j\left(\omega L-\frac{1}{\omega C}\right)-(R_1+jX_1)=0.$$

If $X_1=0$ we see that the oscillation frequency is $f=\dfrac{1}{2\pi\sqrt{LC}}$ and is independent of the valve. The frequency f is $\dfrac{1}{2\pi\sqrt{\left(L-\dfrac{X_1}{\omega}\right)C}}$ or $\dfrac{1}{2\pi\sqrt{L\left(C+\dfrac{1}{\omega X_1}\right)}}$ if X_1 is respectively inductive or capacitive.

From the above it would appear possible to neutralize the frequency variation due to X_1 by inserting a suitable correcting reactance in series with the grid or anode lead. An improvement in frequency stability can be brought about by the inclusion of a neutralizing reactance but, since the latter must be varied when the LC circuit frequency is varied, it is not feasible for correcting oscillators covering a large frequency range. Furthermore, owing to non-

linear operation of the valve, reactance neutralization cannot prevent, but can only reduce frequency variation due to the valve. The effect of valve reactance can be reduced by using very loose coupling between the valve and tuned circuit, and one way is to tap the valve connection into a part only of the tuning coil, rather than across the whole coil.

6.6.3. Harmonics. In oscillators there must be an energy as well as power balance. The latter entails neutralization of LC circuit resistance whilst the former requires equality of inductive and capacitive energy. Harmonic currents, generated by the valve, flow more easily through the capacitance than the inductance branch of the LC circuit so that the capacitive energy tends to exceed the inductive energy. To restore energy balance the current through the inductive branch must be increased. This may be realized by a reduction of fundamental oscillation frequency. Experiment has tended to show the opposite effect, viz., that increase of harmonics result in an increase of frequency, and it is assumed that another effect is occurring simultaneously in the opposite direction. Nevertheless, better frequency stability is registered when the harmonic content is low. A valve having a high R_a, a coil resistance as low as possible, a low L/C ratio, and minimum grid current all contribute to low harmonic content.

6.6.4. Interelectrode Capacitance Variation. Variation of interelectrode capacitance due to space-charge effects is greatest between grid and cathode. There is usually an increase in grid-cathode capacitance of about 2 $\mu\mu$F from the cold to hot condition (filament on and off), but the variation under operating conditions is much less than this, being of the order of 0·04 $\mu\mu$F. The magnitude of the variation is dependent on the anode current, grid voltage, heater voltage, and mutual conductance. A valve with a high anode current and mutual conductance generally produces large capacitance change. The space-charge capacitance change is not linearly proportional to grid voltage so that there is a mean as well as periodic change of capacitance. Any change in the oscillation amplitude therefore affects the interelectrode capacitance. This may be minimized by using a large value of tuning capacitance in the LC circuit, by employing a tuned anode in preference to a tuned grid oscillator, and by tapping the valve into a part of the tuning coil. Interelectrode changes between anode and cathode are usually less than 0·01 $\mu\mu$F, and their effect on the oscillator frequency may be reduced by the insertion of a resistance, R_3 in Fig. 6.10, between the anode and tuned circuit. This has the advantage of reducing

the effect of changes of R_a, but it is not very suitable for the short wave ranges because of stray capacitance across the resistance.

6.6.5. Valve Internal Resistance. The linear theory of oscillation shows that frequency is dependent on R_a, which should be as high as possible consistent with a high g_m value. One method of reducing the influence of changes of R_a is to use loose coupling between the valve and tuned circuit, i.e., tapping across a part instead of the whole tuning inductance. The series resistance mentioned in 6.6.4 helps in this direction, but the use of two valves, as in the Franklin oscillator of Fig. 6.12, is a better solution.

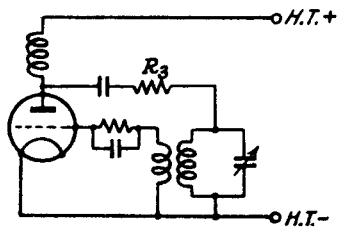

FIG. 6.10.—Reduction of Valve Effects on Frequency Stability by a Series Resistance.

6.6.6. Miscellaneous Effects causing Frequency Variation. Rapid fluctuations of the H.T. voltage may be prevented from influencing frequency by a resistance-capacitance decoupling circuit, R_2C_2 in Fig. 6.6. The decoupling resistance is also useful in reducing long-period variations in H.T. voltage, because it acts as one arm of a potentiometer with the oscillator valve D.C. resistance as the other, so making the D.C. anode voltage change less than the H.T. voltage change.

Frequency variation due to valve temperature change is a comparatively short-period effect occurring in the first 5 or 10 minutes after switching on, for the valve internal temperature settles down quite rapidly to a value not greatly affected by normal external temperature changes.

6.6.7. Special Methods of Reducing Frequency Variations due to the Valve. Various methods may be used to reduce the effect of the valve on frequency. One is by negative feedback ; an impedance, consisting of a resistance, or a resistance and inductance in series, is inserted in the cathode circuit of the valve. The series RL circuit is preferable since it is a better amplitude stabilizer than the resistance alone, across which there is stray capacitance tending to make negative feedback less effective at the higher oscillating frequencies. A triode oscillator with the tuned circuit connected

between grid and H.T. negative, the cathode tapped partway up the tuning inductance, and the anode connected to H.T. positive is an example of negative feedback control.

The electron coupled [4] oscillator is another alternative. A screened-grid or pentode valve is used with the grid and cathode as the active oscillating elements. Negative feedback compensation is

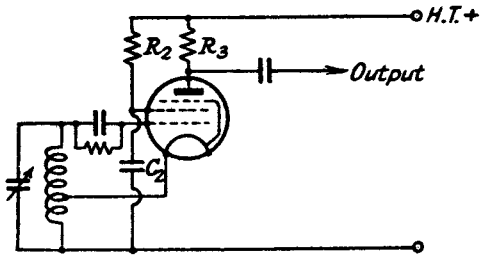

FIG. 6.11.—The Electron Coupled Oscillator.

realized because the cathode is connected to a tapping point on the *LC* circuit. The diagram of connections is shown in Fig. 6.11, and the normal anode merely serves as a means of developing the oscillator voltage for application to the frequency changer. The screen carries no R.F. voltages (capacitance C_2 has a high value—0·1 μF), and therefore reduces the capacitance coupling between the oscillator proper and the anode. Two advantages are gained from this type; the voltage applied to the frequency changer is not obtained directly from the oscillating circuit so that variations

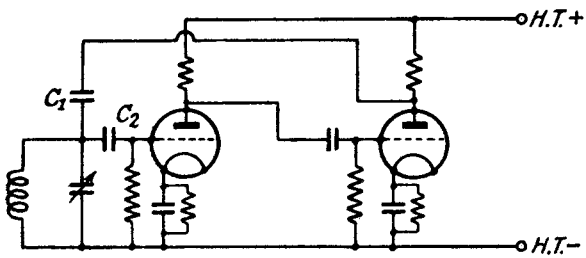

FIG. 6.12.—The Franklin Oscillator.

in frequency changer conditions have almost no effect on oscillator frequency. The second advantage is that the frequency variation due to increase or decrease of screen voltage is in the opposite direction to that for increase or decrease of anode voltage. Hence by suitably adjusting R_2 and R_3 the oscillation frequency can be made almost independent of H.T. supply voltage changes.

A very successful method of reducing valve effect is the Franklin

circuit [15] of Fig. 6.12. The capacitances C_1 and C_2 are very small (1 to 2 $\mu\mu$F) so that the LC circuit is only very loosely coupled to the valves. Since two valves are required the method is not very suitable for use in broadcast receivers.

6.7. Frequency Variations due to the LC circuit and its Associated Components.

6.7.1. Introduction. The chief cause of variation of the inductance, capacitance and resistance of the LC circuit and its associated components is temperature change, though humidity can have a more serious effect if care is not taken in moisture-proofing the coils or fixed capacitors. By the use of high-grade waxes or varnishes, humidity variations can generally be reduced to a second order effect. Increase of humidity has much the same effect as increase of temperature, viz., it increases the capacitance (in the case of a coil, its self-capacitance) and reduces the oscillator frequency. The increase in capacitance is due to the displacement of air in the insulating material by water vapour, which has a higher dielectric constant.

Variations in the values of inductance and capacitance of the LC circuit are largely responsible for the total frequency variation. Associated components, such as the padding and self-bias capacitances, the range switch and wiring, also add their quota to the frequency change but are much less important. The trimmer capacitance can cause very large changes of frequency when the tuning capacitance is small.

6.7.2. Inductance Variations. Changes of temperature produce a variation in the inductance, resistance and self-capacitance of a coil. The last two are not, however, important in comparison with the change in inductance. Taking the formula for a single-layer solenoid (the shape most likely to be used on the medium and short wave ranges) given by expression 4.12

$$L = \frac{r^2N^2}{9r+10l}$$

where l = length of winding
r = radius of winding
N = total turns in the coil

we see that increase of length decreases L, whereas increase of radius increases L. Change of radius has the greater effect and increasing temperature therefore increases L. If we assume that the coefficients

of radial and axial expansion, α_r and α_l respectively are equal, the inductance for an increase in temperature of $t°$ C. becomes

$$L+\Delta L = \frac{r^2(1+\alpha t)^2N^2}{9r(1+\alpha t)+10l(1+\alpha t)} \quad . \quad . \quad 6.29a.$$

$$L+\Delta L = \frac{r^2N^2}{9r+10l}(1+\alpha t)$$

i.e., the increase in inductance is directly proportional to the change in temperature multiplied by the coefficient of expansion of the conductor. Expressing the result in a more convenient form, the coefficient of inductance increase equals the coefficient of expansion of the conductor, or

$$\frac{\Delta L}{L.t} = \alpha ;$$

the value of α for copper is 16×10^{-6} parts per degree Centigrade. But

$$f = \frac{1}{2\pi\sqrt{LC}}$$

and

$$f - \Delta f = \frac{1}{2\pi\sqrt{(L+\Delta L)C}}$$

where Δf is the decrease in oscillator frequency due to the increase ΔL in L

$$\frac{f-\Delta f}{f} = \sqrt{\frac{L}{L+\Delta L}}$$

$$1 - \frac{\Delta f}{f} = \left(1+\frac{\Delta L}{L}\right)^{-\frac{1}{2}} \quad . \quad . \quad . \quad 6.30a.$$

Expanding by the Binomial Theorem and neglecting $\left(\frac{\Delta L}{L}\right)^2$ and all higher powers—this is justified because $\frac{\Delta L}{L}$ is so small—expression 6.30*a* may be rewritten

$$\frac{\Delta f}{f} = \frac{1}{2}\left(\frac{\Delta L}{L}\right) \quad . \quad . \quad . \quad . \quad 6.30b.$$

Thus the ratio change in frequency due to the unhindered expansion of a copper coil is 8×10^{-6} parts per degree centigrade, or for the normal temperature rise of 30° C. the ratio change of frequency is 240 in 10^6. Frequency variations, due to coil expansion, of 240 and 2,400 c.p.s. at oscillator frequencies of 1 and 10 Mc/s respectively, would be expected under these conditions.

Since increase of radius has the opposite effect to increase of length, it is possible by suitably choosing α_r and α_l to make inductance independent of temperature. Re-writing 6.29*a* with α_r and α_l

$$L+\Delta L = \frac{r^2(1+\alpha_r t)^2 N^2}{9r(1+\alpha_r t)+10l(1+\alpha_l t)} \quad . \quad . \quad . \quad 6.29b.$$

Differentiating the above with respect to temperature t and equating the result to 0 gives the condition for no change of inductance

$$\frac{d(L+\Delta L)}{dt} = \frac{r^2N^2[(9r(1+\alpha_r t)+10l(1+\alpha_l t))(1+\alpha_r t)2\alpha_r - (1+\alpha_r t)^2(9r\alpha_r+10l\alpha_l)]}{[9r(1+\alpha_r t)+10l(1+\alpha_l t)]^2}$$

when $t = 0$

$$\frac{d(L+\Delta L)}{dt} = 9r\alpha_r+10l(2\alpha_r - \alpha_l)$$

$$= 0$$

when $$\frac{\alpha_l}{\alpha_r} = 2+\frac{9r}{10l} \quad . \quad . \quad . \quad . \quad . \quad 6.31.$$

By satisfying the above expression for the ratio of axial to radial expansion, it is possible to make L independent of temperature. The practical application involves winding the coil turns loosely, and fixing the ends firmly to the coil former so that radial expansion is determined by the conductor, and axial by the coil former. Suitable coil-former materials, having coefficients of expansion greater than twice that for copper, are not easy to obtain, but experiments have shown the validity of the theoretical argument. An alternative is to reduce the radial and axial expansion, either by shrinking the coil on to a former having a lower coefficient of expansion, e.g., ceramic material having coefficient of 7×10^{-6} parts per degree centigrade, or by using copper-plated low-coefficient material, such as invar, for the coil. The latter is not an economic proposition for receivers, and the best alternative is the ceramic coil former. Synthetic resin or bakelite coil formers are not to be recommended because they tend to show a non-reversible ageing, which results in a permanent change in inductance after several cycles of temperature change. They are also more affected by humidity variation than ceramic material.

6.7.3. Capacitance Variations. Temperature variation has two effects in capacitors; it changes the permittivity of the dielectric and also changes the disposition of the plates. In fixed capacitors, mica is the most suitable dielectric and capacitance change is largely a result of pressure variation between the plates. This effect can be considerably reduced by replacing the metal

plates by metal (silver) sprayed on to the mica dielectric. Both sides of the mica are sprayed and each side forms an active plate; adjacent sides are connected together so that spacing variations due to changes of pressure become of little importance. This type of silvered mica fixed capacitor has a very small temperature coefficient and its effect on oscillator frequency variation is very small.

Fixed capacitors (maximum value about 3 $\mu\mu$F) with a bimetallic plate can be constructed to give a decrease of capacitance with increase of temperature, and they may be used to compensate for the increase in capacitance and inductance of the main elements of the tuning system.

Variable capacitors often have a high temperature coefficient and their effect on oscillator frequency is generally much greater than that of the coil. For this reason tuning by inductance variation with fixed capacitors, which can be constructed with low temperature coefficients, is to be preferred, and is employed in some short wave band-spread receivers. By observing the following points the temperature coefficient can be reduced. The dielectric should be air, as the use of a solid dielectric, such as mica, tends to distort the plates and increase the high-frequency resistance component. The insulating end supports have an important effect, particularly when the capacitance is minimum, and ceramic material is best as it has a low permittivity change with temperature. Synthetic plastic materials are not usually satisfactory and have non-cyclical variation. The rotor shaft and stator frame should be of the same material, so that expansion allows the rotor plates to remain centrally disposed with respect to the stator. Initial accurate alignment of a rotor plate midway between two stator plates reduces capacitance change due to differential expansion, because a given change of spacing has much greater effect when the rotor-to-stator plate spacings are unequal. Increase of stator-rotor plate spacing also reduces capacitance change for a given change of spacing. Good mechanical rigidity and construction are essentials for small capacitance variation with temperature.

Particular care is necessary in the choice of the trimmer capacitor, which can have a very large influence on the oscillator frequency as the temperature varies. Mica dielectric pressure-type capacitors are generally unsatisfactory and show an appreciable increase in capacitance with increase of temperature. Air dielectric capacitors with ceramic insulation should be employed.

6.7.4. Frequency Variations due to Associated Components. By the use of silvered mica construction, frequency

drift due to fixed capacitors associated with the tuned circuit can be reduced to very small proportions. That due to the wave-change switch and wiring [14] can also be made a second-order effect by observing certain precautions. The switch should be of rigid mechanical construction with ceramic insulation, and the wiring rubber-covered or enamelled. Especial care is necessary to ensure that leads are securely fixed and not in tension. Preliminary cyclical heating is an aid to frequency stability.

Stray capacitance between the tuning inductance and the feedback coil must be reduced to a minimum as this generally has a high temperature coefficient. It is preferable not to wind the feedback coil on top of the tuning inductance but to have an air space between them.

Examples of the capacitance-temperature coefficients of typical insulating materials given below show the desirability of using ceramic [20] rather than other forms of insulation.

Varnished cambric	+2,100	parts in	10^6	per	degree	Centigrade
Synthetic resin	+1,600	,,	,,	,,	,,	,,	,,
Enamel	+ 470	,,	,,	,,	,,	,,	,,
Ceramic	+ 100	,,	,,	,,	,,	,,	,,

6.7.5. Compensation for Temperature-Frequency Change. Certain types of capacitors can be constructed to give a negative temperature coefficient, i.e., capacitance decreases with increase of temperature, and they may be used to compensate for the positive temperature coefficient of the normal tuning inductance and capacitance. Compensation is only complete, however, at one particular frequency, and the temperature of the corrector must follow that of the component it is intended to compensate. Two corrector capacitors may be used, one, with a heater winding generally supplied from the A.C. mains transformer, to compensate for the rapid initial frequency change due to the valve warming-up, and the other placed so as to follow the temperature of the tuning system and to correct for change in L and C. The corrector capacitor may be connected in parallel with the tuning inductance or capacitance—the bimetallic construction described in Section 6.7.3 has a capacitance change of the order of 0·5 $\mu\mu$F for 30° C. variation—or in parallel with the padding capacitance. Compensation does not obviate the necessity for aiming at the smallest possible frequency variation of the uncompensated oscillator.

6.8. Frequency Variations due to the Frequency Changer. [9] The input admittance at the oscillator grid of the frequency changer

includes three possible variables, grid current, space-charge capaci tance, and space-charge and capacitance coupling to the signal grid. The effect of grid current variation due to bias changes on the frequency-changer valve is least important when the oscillator and frequency-changer grids are connected together, as in the triode-hexode. It is more important when an R.C. coupling is employed between the two grids, as for suppressor grid application in the pentode (Fig. 5.4), but the frequency variation can be reduced to small proportions by using a high resistance (1 MΩ) from suppressor grid to earth.

Frequency variation due to capacitive and space-charge effects is largely beyond the receiver designer's control, because it is most dependent on valve construction. All the effects can be reduced by making the coupling between the oscillator-tuned circuit and the frequency changer as loose as possible consistent with adequate oscillator voltage. The greatest load effect is produced when the oscillator grid is directly coupled to the tuned circuit as for the tuned grid oscillator connection. By the use of a tuned anode oscillator a reduction in frequency variation of about 5 to 1 may be obtained for a given change of frequency changer bias.

A reduction of load-frequency variation is achieved by using a low impedance LC circuit, i.e., a high capacitance and low inductance, for the addition of a resistance and reactance in parallel with any LC circuit has least effect when the L/C ratio is small.

Space-charge coupling between signal and oscillator grids is very much less in hexode than in heptode type frequency changers. The use of a neutralizing capacitance about 1 $\mu\mu$F may be used in the latter case as described in Section 5.8.3.

Stray capacitive coupling between the signal and oscillator grids must be avoided if the tuning of the signal circuit is not appreciably to affect the oscillator operation on the short wave ranges.

6.9. Precautions Necessary to Preserve Frequency Stability. The following summarizes the steps which may be taken to increase the frequency stability of the oscillator.

1. A valve having a high g_m and high R_a is required.

2. Grid current should be as low as possible, i.e., a high grid self-bias resistance, provided squeggering is not experienced, and feedback coupling only just sufficient to sustain oscillation at the required amplitude are necessary.

3. The coil resistance should be as low as possible.

4. The L/C ratio is required to be low so that variations of stray capacitance and load reflected from the frequency changer

have less effect. Too low a value, however, makes oscillation difficult. Except in band-spread receivers with fixed signal tuning, and push-button operated receivers, the values of L and C are fixed by ganging considerations, and little control is possible.

5. The use of a phase-correcting reactance is not feasible as it is only suitable for fixed-frequency operation.

6. The feedback coupling, if a coil, should have the smallest value of coil inductance with maximum value of mutual inductance coupling to the tuned LC circuit.

7. The tuned circuit should be loosely coupled to the valve, i.e., the valve should be connected across a part of the tuning inductance, and tuned anode is preferable to tuned grid because space-charge capacitance changes are greatest at the grid electrode.

8. The H.T. supply should be adequately decoupled and smoothed. The possibility of audio-frequency feedback from the power output stage may be reduced by a push-pull audio-output connection.

9. Temperature-frequency variations are reduced by mounting inductances and capacitances away from such sources of heat as the mains transformer, the power output and rectifier valves. Low-loss coil formers of ceramic material are to be recommended. Different rates of radial and axial expansion for the coil are a possible means of reducing the temperature effect. High-loss insulators must be avoided as these almost always have high positive temperature coefficients. Rigid mechanical construction of coils, variable capacitors, range switches and wiring is very necessary. Variable capacitance values should be minimum, and inductance tuning with fixed capacitance is desirable.

10. Compensation by a capacitance having a negative temperature coefficient may be provided.

11. Humidity effects demand the use of non-hygroscopic insulating material, waxes and varnish.

12. The optimum oscillator voltage required by the frequency changer should be as low as possible, as this allows loose coupling to and reduces the load reflected from the frequency changer into the oscillator tuned circuit.

13. A frequency correcting device may be connected to the oscillator in order to introduce additional reactance in parallel with the LC circuit as the frequency tends to vary from its correct setting. The magnitude of the reactance is determined by the amount of error, and high initial frequency errors may be reduced to quite small values. Thus an uncorrected oscillator frequency

error of 20 kc/s can be reduced to a final error of only about 200 c.p.s. Methods of automatically correcting frequency variations by means of a variable reactance valve are discussed in Chapter 13.

6.10. Squegger and Parasitic Oscillations. Two undesirable effects, known as squegger and parasitic oscillations, may be met in self-oscillating valve circuits. Squegger oscillation is a regular or irregular interruption of the normal oscillation, and is a result of excessive amplitude. The large positive pulses of grid voltage produce sufficient grid current to charge the capacitor across the self-biasing grid leak to a negative voltage much greater than anode current cut-off. The anode current ceases and oscillations cannot be maintained. The capacitor gradually discharges through the grid leak until the grid voltage is low enough to allow anode current to flow and oscillation to recommence. Grid current again biases the valve beyond cut-off and the cycle is repeated. The squegger effect is equivalent to a 100% modulation of the oscillator by an approximately square wave. The period of the interruption depends on the time constant of the capacitor and grid leak, and it may produce in the output of a receiver an audible note (if the interruption frequency is in the audible range), reduced desired output, excessive whistle interference and noise. It can normally be prevented by using a low value of self-biasing capacitance and grid leak, and feedback coupling only just sufficient to give the required oscillator amplitude at the frequency changer. Values of 100 $\mu\mu$F and 50,000 ohms are typical for the medium and long wave ranges, but for short wave operation the capacitance may be reduced to 50 $\mu\mu$F. A large H.T. decoupling resistance (R_2 in Fig. 6.6) also helps to prevent squegger oscillations, for the oscillator anode voltage is increased by decrease of mean anode current and this moves the cut-off voltage to a higher negative value.

Parasitic [16] oscillations are oscillations at a frequency other than that of the controlling *LC* circuit. Generally they are at very high frequencies and are due to the inductance of the leads from, and the stray capacitance across, the valve electrodes. These inductances and capacitances form tuned-anode and tuned-grid circuits (Fig. 6.13) and the necessary feedback coupling is provided by the anode-grid capacitance. High-frequency parasitic oscillation is more likely with high μ and g_m valves, but it may also be produced by a negative resistance characteristic in the I_aE_g curve of the oscillator grid of the frequency changer. This negative resistance

effect more often occurs at appreciable positive voltages on the oscillator grid, and it can be reduced by preventing excessive oscillator amplitude. A small resistance (about 20Ω) connected close to grid or anode pin of the valve is helpful in damping the parasitic control circuits. The series grid resistance R_1 of Fig. 6.6 performs this rôle as well as that of amplitude stabilizer.

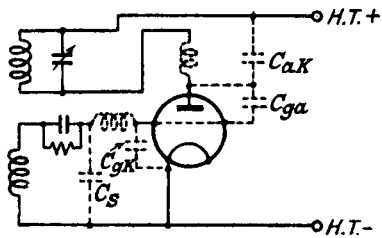

FIG. 6.13.—Parasitic Oscillation due to Lead Inductance and Stray Capacitance.

The modified Colpitts oscillator for short wave operation (Fig. 6.14) uses the anode-cathode, grid-cathode capacitances as the capacitance tap, and parasitic oscillation is possible when the tuning capacitance C is large, for the lead inductances can act as the control inductance, and C_{ak} and C_{gk} as the control capacitance. A remedy is to connect the tuning capacitor as close to the anode and grid pins as possible.

The Hartley oscillator may be troublesome at high frequencies by attempting to act as a modified Colpitts. The introduction of a small R.F. choke or resistance between the centre tap and

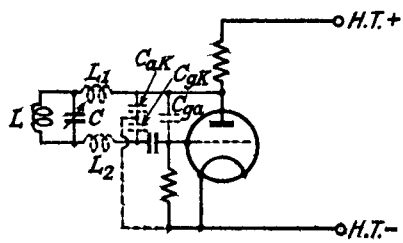

FIG. 6.14.—Parasitic Oscillation in the Modified Colpitts Oscillator.

the H.T. supply is a solution, for the oscillator functions as a Hartley for low frequencies and as a modified Colpitts for high frequencies.

Parasitic oscillation not far removed from the desired frequency is possible when the feedback coil has an inductance comparable

with that of the tuned *LC* circuit. Such a condition is unlikely to arise on the medium and long wave ranges, but it is quite possible on the short wave range. As the oscillator frequency is increased, i.e., the tuning capacitance decreased, a point is reached at which the oscillation frequency jumps to a value approximately given by the resonant frequency of the feedback coil and its stray capacitance. The original functions of the feedback and control *LC* circuit are now reversed, the former acting as the control. The remedy for this type of parasitic oscillation is to use the lowest possible value of feedback coil inductance and to obtain sufficient feedback by tight coupling to the coil of the *LC* circuit.

6.11. Problems in the Design of Short Wave and Ultra Short Wave Oscillators.[19] Oscillators for the short wave and ultra short wave ranges present in a more acute form all the problems encountered on the medium and long wave ranges. In addition they are more prone to squegger and parasitic oscillations and, in the case of the tuned grid and tuned anode circuits, are more difficult to maintain in oscillation over a range of frequencies.

A high g_m valve is an essential as it enables looser coupling to be employed, and this reduces the tendency to squegger and parasitic oscillation. With tuned grid and tuned anode circuits the feedback coil is often interleaved with the main tuning coil in order to obtain high coupling with a small feedback coil.

The ease with which the Hartley and Colpitts circuits can be made to oscillate is a great advantage at high frequencies, and the possibility of feedback coil frequency control is removed. The fact that the Hartley circuit tuning capacitor rotor is not earthed and that the Colpitts requires a split capacitor is no serious disadvantage on band-spread receivers with preset signal tuning. The negative feedback oscillator of Section 6.6.7, with the cathode tapped into the tuning coil, has the advantages of the Hartley circuit and also that one side of the tuning capacitor may be earthed. The modified Colpitts oscillator of Fig. 6.14 is satisfactory at high frequencies and obviates the necessity for a split capacitor, the anode-cathode and grid-cathode interelectrode capacitances performing this function. The tuning capacitor rotor cannot, however, be earthed. The disadvantages of having neither side of the tuning capacitance connected to earth can be overcome by using inductance tuning. On the short wave range this may be accomplished by varying the position of an iron dust core in the tuning coil, and on ultra short waves by inserting a metal plunger of high conductivity material into the coil axis.

Frequency drift of the oscillator due to changes of temperature is more serious as the frequency is increased, partly because the LC circuit components have to be reduced in value, but also because the frequency error Δf, even for a fixed ratio of frequency change $\left(\frac{\Delta f}{f}\right)$, increases as the oscillation frequency rises. Thus for a frequency ratio change of 1 part in 10^3 the frequency drift is 1 kc/s at a frequency of 1 Mc/s, whilst at 45 Mc/s it is 45 kc/s, sufficient to take the I.F. carrier outside the pass range of an I.F. amplifier for amplitude modulated sound signals. Since variable and stray capacitances are the chief offenders, it means that the frequency ratio tends to increase as the oscillation frequency is increased and the tuning capacitance decreased. A low L/C ratio helps to reduce the frequency ratio, but at the same time makes oscillation more difficult to sustain. When the I.F. has a high value, as for the vision signals of a television programme, and the sound signals of a frequency modulated transmission, the use of an oscillator frequency ($f_h = f_s - f_1$) lower than the signal frequency is an advantage in reducing frequency drift. An alternative is to employ a harmonic of the oscillator to combine with the signal ; Section 5.5 shows that a 2nd harmonic response approaching 80% of the fundamental oscillator response is obtainable when a large oscillator voltage is applied to the frequency changer. Provided the increase in possible interference whistle production is no disadvantage, oscillator frequency drift can be reduced to approximately one-half by using the second harmonic of the oscillator. For example, suppose temperature change produces an increase of capacitance by 0·05 $\mu\mu$F ; at 45 Mc/s, the maximum value of tuning capacitance is about 40 $\mu\mu$F if adequate oscillation amplitude is to be realized, and the frequency drift is

$$\Delta f = f \cdot \frac{1}{2} \frac{\Delta C}{C}$$

$$= \frac{45}{2} \times \frac{0{\cdot}05}{40} \times 1{,}000 \text{ kc/s}$$

$$= 28{\cdot}1 \text{ kc/s}.$$

(The proof of this is similar to that developed in Section 6.7.2 for inductance change.)

When the oscillator frequency is halved, the tuning capacitance may be increased to 80 $\mu\mu$F for the same $\frac{L}{CR}$ value (this is a measure

of the oscillation capability of the circuit, and doubling L and C doubles the frequency with little change of $\frac{L}{CR}$). Thus the frequency drift of the oscillator becomes

$$\Delta f = \frac{22{\cdot}5 \times 0{\cdot}05}{2 \times 80} \times 1{,}000$$
$$= 7{\cdot}025 \text{ kc/s},$$

which is one-quarter of that at 45 Mc/s. The frequency drift for the second harmonic is twice this value, i.e., 14·05 kc/s, so that the net frequency drift has been reduced to one-half of its original value for an oscillator of 45 Mc/s fundamental frequency.

The need for short, firmly secured, leads from the valve to the control LC circuit cannot be over-emphasized, and adequate decoupling with non-inductive mica capacitors (0·001 to 0·01 μF) of leads carrying D.C. or mains A.C. voltages is essential. Only a very small inductance can provide undesirable coupling at ultra high frequencies, and decoupling capacitors should therefore be returned to the same point on the chassis. In a shunt-fed circuit (see Fig. 6.10) with a choke between the anode and H.T. positive, particular care must be taken in the construction of the choke, which, if used to cover a number of ranges, should be wound in separate sections, becoming smaller at the anode side. This is to prevent resonance of the choke with its self-capacitance, thereby causing absorption and dead spots at particular frequencies corresponding to parallel resonance of the whole or a section of the choke with self and stray capacitance. When this does occur, it may be possible by adjustment of the turns in the sections nearest the anode to remove the absorption frequency outside the range. When the oscillator is intended for operation at ultra high frequencies only, adjustment of the anode choke, and also of any other decoupling choke in the cathode or heater circuits, may have considerable effect on oscillator amplitude, too large a value of choke reducing the amplitude as well as too small a value.

6.12. Ganging of the Oscillator and Signal Circuits.[5, 11, 12, 18] In order to reduce the number of receiver controls to a minimum, it is usual to couple mechanically the signal and oscillator capacitor rotor plates. Since the oscillator capacitance is required to tune its own circuit to a frequency greater than the signal frequency by a constant amount, a specially shaped rotor and stator are necessary to maintain the correct oscillator frequency. In certain types of receivers the oscillator capacitor is designed to

give the required capacitance law over the medium wave range, but then the same shaped capacitor is not correct for the long and short wave ranges. It is not economical to have a separate capacitor for each range and a compromise is obviously desirable. Such is possible by providing a number of preadjusted components in the oscillator tuned circuit, the term preadjusted or preset being applied to a component, the value of which is under the control of the designer. This component is constant for a given wave range, but is varied when the latter is changed. The oscillator frequency can be given its correct value at the same number of signal frequencies as there are preset components, and by using such a circuit an oscillator capacitor identical with that tuning the signal may be employed.

A circuit having two preset components, the tuning inductance L_h and the padding capacitance C_p, is shown in Fig. 6.15. The

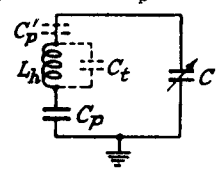

FIG. 6.15.—An Oscillator Ganging Circuit.

padding capacitance may be placed between the high potential ends of L_h and the tuning capacitance C, or it may be placed as shown between L_h and earth. The second position has the advantage of not adding to the capacitance in parallel with the coil, for in the first the capacitance to earth of C_p is in parallel with C_0, the coil self-capacitance (C_t in Fig. 6.15). The oscillator frequency is

$$f_h = \frac{1}{2\pi\sqrt{L_h\left[C_0+\frac{C_pC}{C_p+C}\right]}} \quad . \quad . \quad . \quad 6.32.$$

For any two values, f_{h1} and f_{h2}, this equation may be satisfied simultaneously by suitably selecting L_h and C_p. Suppose that these two oscillator frequencies correspond to two signal frequencies f_{s1} and f_{s2}, for which the tuning capacitance C has values of C_1 and C_2. The following simultaneous equations result

$$\frac{1}{[2\pi f_{h1}]^2} = \frac{1}{[2\pi(f_{s1}+f_1)]^2} = L_h\left[C_0+\frac{C_pC_1}{C_p+C_1}\right] \quad . \quad 6.33a$$

$$\frac{1}{[2\pi f_{h2}]^2} = \frac{1}{[2\pi(f_{s2}+f_1)]^2} = L_h\left[C_0+\frac{C_pC_2}{C_p+C_2}\right] \quad . \quad 6.33b$$

where f_1 = the intermediate frequency.

Solving for C_p gives a quadratic

$$C_p^2\left[\frac{C_1-C_2}{\alpha-1}-(C_0+C_2)\right]-C_p[C_0(C_1+C_2)+C_1C_2]-C_0C_1C_2=0. \quad 6.34$$

where $$\alpha=\left[\frac{f_{h2}}{f_{h1}}\right]^2=\left[\frac{f_{s2}+f_1}{f_{s1}+f_1}\right]^2$$

and

$$C_p=\frac{C_0(C_1+C_2)+C_1C_2+\sqrt{[C_0(C_1+C_2)+C_1C_2]^2+4C_0C_1C_2\left[\frac{C_1-C_2}{\alpha-1}-(C_0+C_2)\right]}}{2\left[\frac{C_1-C_2}{\alpha-1}-(C_0+C_2)\right]} \quad 6.35.$$

The second solution of C_p with a negative sign before the square root is not a practical possibility. The value of L_h is found by substituting expression 6.35 for C_p in either 6.33*a* or 6.33*b*.

Thus $$L_h=\frac{1}{[2\pi f_{h1}]^2\left(C_0+\frac{C_pC_1}{C_p+C_1}\right)} \quad . \quad . \quad 6.36$$

The most suitable values of f_{s1} and f_{s2} are those giving the minimum error variation over the wave range, and to determine them the error curve shape must be known. The best choice is

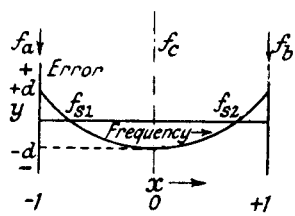

FIG. 6.16.—The Ideal Curve for Two-point Zero Error Ganging.

clearly either that which gives errors equal in magnitude at the ends and centre of the range, or least error at the low frequency end of the range where the signal circuits are normally more selective. Let us consider the first alternative and assume that the error curve is parabolic as in Fig. 6.16, with equal errors at the ends and centre of the range. By designating the error axis as y and the frequency axis as x, the general expression for the parabola is

$$y=ax^2+bx+c \quad . \quad . \quad . \quad . \quad 6.37.$$

Taking f_c, the frequency at the centre of the range, as the origin,

f_a and f_b the end frequencies, as $x = -1$ and $+1$ respectively, and the maximum error as d kc/s, the general expression reduces to

$$\begin{aligned} y &= ax^2 + c \\ &= d \text{ when } x = -1 \text{ and } +1, \\ &= -d \text{ when } x = 0 \end{aligned}$$

so that $a = -2c = 2d$ and

$$y = d(2x^2 - 1) \quad . \quad . \quad . \quad . \quad 6.38.$$

The frequencies of zero error are obtained by equating 6.38 to 0.

Thus $$x = \pm\sqrt{\tfrac{1}{2}} = \pm 0{\cdot}707.$$

The required signal frequency values are therefore

$$f_{s1} = f_c - 0{\cdot}707\,(f_c - f_a)$$

and $$f_{s2} = f_c + 0{\cdot}707\,(f_c - f_a)$$

for $$f_c - f_a = f_b - f_c.$$

Let us now consider the above procedure applied to the design of an oscillator circuit to gang with a signal circuit of 156 μH inductance for an I.F. of 465 kc/s, and covering the medium wave range from 550 to 1,500 kc/s. The capacitance required to tune the signal coil at selected frequencies is given below

f_s(kc/s)	550	600	700	800	900	1,000
C($\mu\mu$F)	536·8	451	331·1	253·7	200·5	162·38

f_s(kc/s)	1,100	1,200	1,300	1,400	1,500
C($\mu\mu$F)	134·48	112·76	96·1	82·84	72·17

Not all the tuning capacitance is found in the tuning capacitor and some is made up of stray capacitance due to the range switch, wiring, self-capacitance of the coil, and the trimmer capacitance (required for signal circuit ganging) across the coil. An average value for each of these capacitances is 10 $\mu\mu$F, making a total stray capacitance of 40 $\mu\mu$F. Hence the actual value of the tuning capacitance is obtained by subtracting 40 $\mu\mu$F from the values given in the above table. We will make the assumption that the oscillator tuning circuit has similar stray capacitance values, except that there is no trimmer capacitance, and that C_p is located close to L_h and permanently connected to it, i.e., the range switch and wiring is on the tuning capacitance side of C_p. The value of C at a signal frequency of 550 kc/s ($f_h = 1{,}015$) is therefore the value of the tuning capacitance (536·8 — 40) plus the stray capacitance (20 $\mu\mu$F) due to the wiring and range switch, i.e., equals 516·8 $\mu\mu$F. The centre signal frequency of the range is 1,025, so that the signal frequencies of zero error are 1,025 $\pm$ 0·707 (475),

589 and 1,361 kc/s. The oscillator frequencies f_{h1} and f_{h2} for zero error are 1,154 and 1,826 kc/s, the tuning capacitances C_1 and C_2 are 322 and 67·6 $\mu\mu$F; if the oscillator coil self-capacitance C_o is 10 $\mu\mu$F the quadratic for C_p (expression 6.34) is

$$9{\cdot}2\ C_p{}^2 - 2{,}564{\cdot}6\ C_p - 21{,}750 = 0$$

$$C_p = 288\ \mu\mu\text{F}.$$

Hence

$$L_h = 117{\cdot}3\ \mu\text{H}.$$

The actual oscillator frequencies at different signal frequencies may be calculated by replacing C_0, C, C_p and L_h in 6.32 by their appropriate numerical values. An error curve for the I.F. is plotted in Fig. 6.17 and it is seen that the parabolic shape is approached.

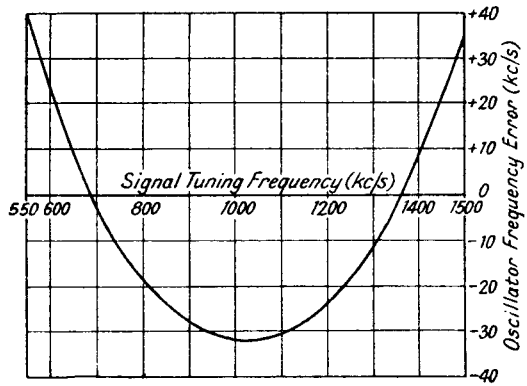

FIG. 6.17.—The Calculated Error Curve for Two-point Ganging.

A greatly improved error curve is obtained by adding another preset component, a trimmer capacitor C_t, in parallel with the coil L_h. It is more usual to place the trimmer C_t directly across L_h rather than across L_h and C_p, since in the first position it can compensate for variations in coil self-capacitance and stray capacitance. In the formulae given below, C_t is the total value of capacitance across L_h, including self and stray capacitance. Zero error can be realized at three signal frequencies f_{s1}, f_{s2} and f_{s3}, and from the following three equations the values of C_p, C_t and L_h can be calculated.

$$\left.\begin{aligned}
\frac{1}{[2\pi f_{h1}]^2} &= \frac{1}{[2\pi(f_{s1}+f_1)]^2} = L_h\left[C_t+\frac{C_pC_1}{C_p+C_1}\right]\\
\frac{1}{[2\pi f_{h2}]^2} &= \frac{1}{[2\pi(f_{s2}+f_1)]^2} = L_h\left[C_t+\frac{C_pC_2}{C_p+C_2}\right]\\
\frac{1}{[2\pi f_{h3}]^2} &= \frac{1}{[2\pi(f_{s3}+f_1)]^2} = L_h\left[C_t+\frac{C_pC_3}{C_p+C_3}\right]
\end{aligned}\right\} \qquad 6.39.$$

Eliminating L_h and C_t we have

$$C_p = \frac{AC_1(C_2 - C_3) + BC_2(C_3 - C_1) + C_3(C_1 - C_2)}{A(C_3 - C_2) + B(C_1 - C_3) + (C_2 - C_1)} \quad . \quad 6.40$$

where $$A = \left[\frac{f_{h3}}{f_{h1}}\right]^2 \text{ and } B = \left[\frac{f_{h3}}{f_{h2}}\right]^2.$$

Solving for C_t

$$C_t = \left[\frac{AC_3C_p}{C_3+C_p} - \frac{C_1C_p}{C_1+C_p}\right]\frac{1}{1-A} \quad . \quad . \quad 6.41$$

$$L_h = \frac{1-A}{[2\pi f_{h3}]^2\left[\frac{C_3C_p}{C_3+C_p} - \frac{C_1C_p}{C_1+C_p}\right]} \quad . \quad . \quad 6.42.$$

Now we must fix the optimum signal frequencies of zero error, and this we can do by assuming the error curve to be a cubic as shown in Fig. 6.18. The general expression for the curve is

$$y = ax^3 + bx^2 + cx + d \quad . \quad . \quad . \quad 6.43a$$

and it is clear that the optimum error curve should be symmetrical

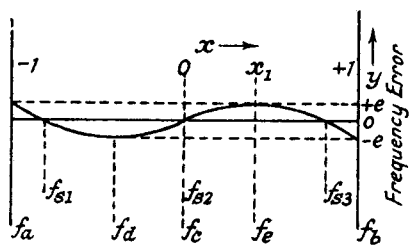

FIG. 6.18.—The Ideal Curve for Three-point Zero Error Ganging.

about the centre frequency f_c with zero error at this frequency. The maximum errors ($y = \pm e$) should all be equal at the four frequencies f_a, f_b, f_d and f_e. By letting $x = 0$, $+1$ and -1 correspond to the centre and end frequencies, f_c, f_b and f_a respectively, we find that $d = 0$ (for $y = 0$, when $x = 0$), $b = 0$ ($y = \pm e$, when $x = \mp 1$) and $(a+c) = -e$. Thus expression 6.43a reduces to

$$y = ax^3 + cx \quad . \quad . \quad . \quad . \quad 6.43b.$$

At f_e there is a point of inflection so

$$\frac{dy}{dx} = 0 = 3ax_1^2 + c$$

and $$x_1 = +\sqrt{\frac{-c}{3a}}.$$

Replacing this value in 6.43*b* and noting that $y = e = -(a+c)$

$$-(a+c) = a\left(\frac{-c}{3a}\right)^{\frac{3}{2}} + c\left(\frac{-c}{3a}\right)^{\frac{1}{2}} \quad . \quad . \quad . \quad 6.44.$$

A cubic equation is obtained by squaring 6.44

$$\frac{4c^3}{27} + ac^2 + 2a^2c + a^3 = 0$$

and one solution of this is $c = \frac{-3a}{4}$.

Inserting this value in 6.43*b* we have

$$y = ax(x^2 - \tfrac{3}{4}) \quad . \quad . \quad . \quad . \quad 6.43c.$$

Zero error is obtained when expression 6.43*c* equals 0, i.e., when $x = 0$ and $\pm\sqrt{\frac{3}{4}}$, and the signal frequencies of zero error are therefore

$$f_{s2} = f_c$$
$$f_{s1} = f_c - \sqrt{\tfrac{3}{4}}(f_c - f_a)$$
$$f_{s3} = f_c + \sqrt{\tfrac{3}{4}}(f_c - f_a).$$

Hence for the medium wave range (550 to 1,500 kc/s) the signal frequencies of zero error are

$$f_{s2} = 1{,}025 \text{ kc/s}, \; f_{s1} = 614 \text{ kc/s}, \; f_{s3} = 1{,}436 \text{ kc/s}.$$

Again assuming a stray and trimmer capacitance in the signal circuit of 40 $\mu\mu$F and a stray capacitance of 20 $\mu\mu$F across the

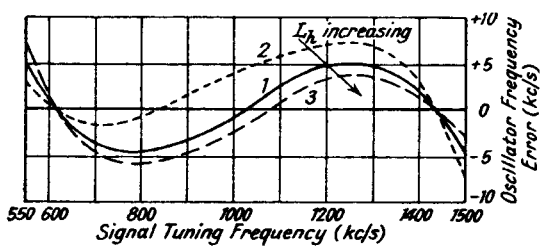

FIG. 6.19.—Calculated Error Curves for Three-point Ganging.

oscillator tuning capacitor, the values of C_1, C_2 and C_3 are 410·5, 134·58 and 58·74 $\mu\mu$F respectively. Replacing these in expressions 6.40, 6.41 and 6.42, and noting that f_{h1}, f_{h2} and f_{h3} are 1,079, 1,490 and 1,901 kc/s respectively, we find that

$$C_p = 601 \; \mu\mu\text{F}, \; C_t = 36{\cdot}5 \; \mu\mu\text{F} \text{ and } L_h = 77{\cdot}4 \; \mu\text{H}.$$

The calculated error curve is curve 1 of Fig. 6.19. A very considerable reduction of maximum ganging error (from 35 to 5 kc/s)

has been achieved by employing three instead of two preset components, and the form of the curve shows the use of the cubic expression for it to be justified.

Inspection of equations 6.39 indicates that variations of C_t affect the error curve at the high frequency end, whilst C_p controls the error curve mainly at the low-frequency end. This therefore suggests the procedure for ganging a receiver. The receiver should first be set to the highest required zero error signal frequency (f_{s3} = 1,436 kc/s), and C_t adjusted to give maximum audio output. The tuning is next changed to f_{s1} = 614 kc/s and C_p adjusted to give maximum output. Returning to 1,436 kc/s, C_t is readjusted if necessary and the procedure is repeated until the best results are obtained.

If we assume that this is the method employed for ganging we can calculate the error curve resulting from manufacturing errors in the value of L_h, and curves 2 and 3 (Fig. 6.19) show the result when L_h is 5% below and 5% above its correct value. High accuracy in calculating these errors is not easy to achieve as the difference between the actual and correct oscillator frequencies is very small (less than 1%) in comparison with the oscillator frequency itself. The values shown should therefore only be taken as indicative of the trend of the error curve against frequency. C_p and C_t have values of 665 and 41·5 $\mu\mu$F for L_h = 73·53 μH, and 546 and 32·9 $\mu\mu$F for L_h = 81·27 μH. In both cases maximum error is increased, and the central zero error frequency is changed to a lower value when L_h is 5% low and a higher value when L_h is 5% high. Curve 2 (L_h 5% low) has the advantage that the error is less at the low-frequency end of the range, where the signal circuits are usually more selective.

The effect of errors in the value of the tuning capacitance C cannot easily be assessed because it is unlikely that the error can be represented by a constant percentage over the wave range, as is possible for L_h.

6.13. Graphical Determination of the Oscillator Tracking Capacitances C_p and C_t.[6, 17] Graphical methods for determining C_p and C_t have been developed, and they are particularly helpful when a rapid calculation of C_p and C_t is required for a number of signal circuits having differing LC values. Their accuracy is, however, limited.

The method is well illustrated by taking the three numerical values C_1, C_2 and C_3 given above. The first step involves the construction of a diagram giving the total capacitance of C_1 and

C_p in series. Vertical lines, AB and DE in Fig. 6.20, are scaled in equal values of capacitance from A and D and are separated by any convenient distance. A and D are in the same horizontal straight line, AB is the C axis and DE the C_p axis. The C axis is

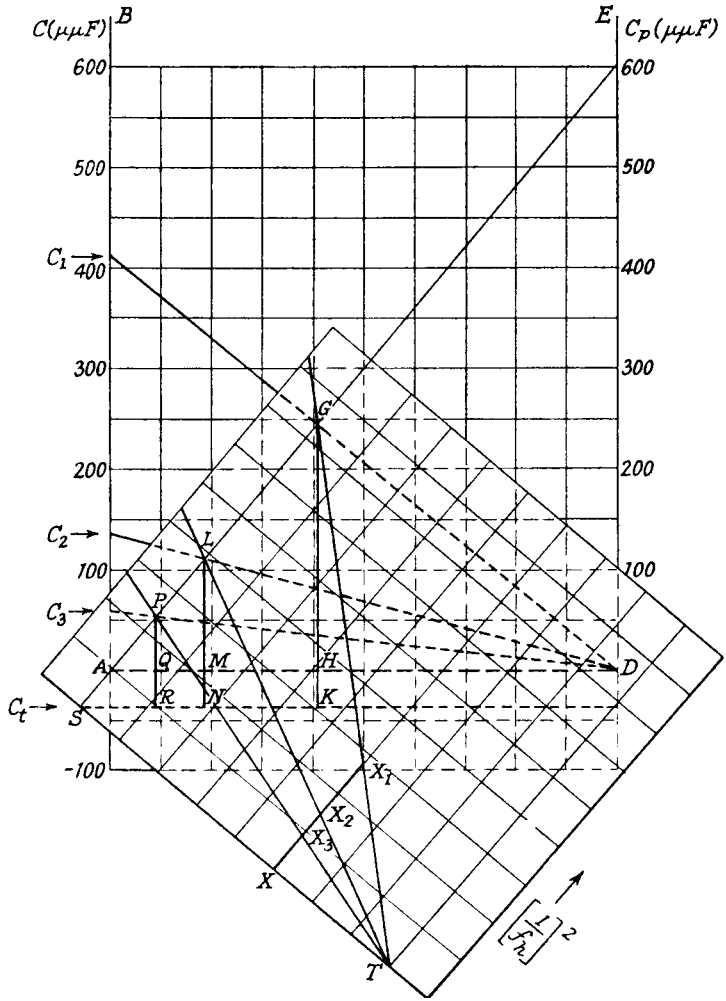

FIG. 6.20.—Graphical Construction for the Determination of the Padding and Trimming Capacitances.

projected below A and the reason for this is shown later. The length of a perpendicular on to the line AD from the intersection of lines drawn from A and D to particular points on the C_p and C scales respectively gives the capacitance for C_p and C connected

in series. Thus if $C = 410{\cdot}5\ \mu\mu F$ and $C_p = 601\ \mu\mu F$, we join D to $410{\cdot}5\ \mu\mu F$ on the C scale and A to $601\ \mu\mu F$ on the C_p scale and find that the capacitance of C and C_p in series is $GH = 244\ \mu\mu F$. The procedure for finding C_p and C_t is as follows. Join D with $C = C_1 = 410{\cdot}5\ \mu\mu F$, $C_2 = 134{\cdot}58$ and $C_3 = 58{\cdot}74\ \mu\mu F$; the line from A to the C_p scale cannot yet be drawn because C_p is unknown. We do, however, know that the total oscillator capacitances, $C_t + \frac{C_1 C_p}{C_1 + C_p}$, etc., must be proportional to $\left[\frac{1}{f_{h1}}\right]^2$, etc. The next step is therefore to draw three lines on transparent linear graph paper, the vertical intercepts XX_1, XX_2 and XX_3, of which from the base line ST are in the ratio of $\left[\frac{1}{f_{h1}}\right]^2 : \left[\frac{1}{f_{h2}}\right]^2 : \left[\frac{1}{f_{h3}}\right]^2$. The transparent sheet is placed over Fig. 6.20 and manœuvred until a " vertical " line on this sheet passes through A and the intersections P, L and G of the $\left[\frac{1}{f_{h3}}\right]^2$, etc., lines with DC_3, DC_2 and DC_1 lines. The point where this line SG cuts the C_p axis gives the required value of C_p, viz., 601 $\mu\mu F$. A line parallel to AD through S cuts the C axis below A, and this point gives the value of C_t, viz., $36{\cdot}5\ \mu\mu F$. The proof is as follows:

Triangles SPR, SLN and SGK are similar so

$$SP : SL : SG = \left[\frac{1}{f_{h3}}\right]^2 : \left[\frac{1}{f_{h2}}\right]^2 : \left[\frac{1}{f_{h1}}\right]^2$$
$$= PR : LN : GK$$
$$= (PQ + QR) : (LM + MN) : (GH + HK)$$

but $$QR = MN = HK = C_t.$$

and $$PQ = \frac{C_3 C_p}{C_3 + C_p}, \quad LM = \frac{C_2 C_p}{C_2 + C_p}, \quad GH = \frac{C_1 C_p}{C_1 + C_p}.$$

$$\therefore \left[\frac{1}{f_{h3}}\right]^2 : \left[\frac{1}{f_{h2}}\right]^2 : \left[\frac{1}{f_{h1}}\right]^2$$
$$= \left[C_t + \frac{C_3 C_p}{C_3 + C_p}\right] : \left[C_t + \frac{C_2 C_p}{C_2 + C_p}\right] : \left[C_t + \frac{C_1 C_p}{C_1 + C_p}\right].$$

The value of C_p can be found with reasonable accuracy, but C_t may be difficult to read exactly. The value of C_t may, however, be checked by substituting the graphical value of C_p in expression 6.41.

No particular difficulties are met in ganging band-spread receivers with signal tuning, and the design proceeds on the lines set out above, the formulae 6.40, 6.41 and 6.42 give the values of the

oscillator tuned circuit components. The values of the tuning capacitance for different signal frequencies are decided by the degree of band-spreading and may be calculated as indicated in Section 4.10.2.

6.14. Approximate Expressions for Ganged Oscillator Circuit Components for Different Intermediate Frequencies.[7] If the assumption is made that the oscillator tuning capacitance is equal to the total tuning signal capacitance, including strays and trimmer, expressions may be derived for the ratios $\frac{C_p}{C_{max.}}$, $\frac{C_t}{C_{max.}}$ and $\frac{L_h}{L_s}$, where $C_{max.}$ is the maximum value of total signal tuning capacitance at the minimum signal frequency, and L_h and L_s are the oscillator and signal inductances respectively. The above can then be given in terms of the ratios of the intermediate and the three zero error signal frequencies to the minimum signal frequency. The expressions defining the signal and oscillator frequencies for zero error are therefore

$$f_{s1} = \frac{1}{2\pi\sqrt{L_s C_1}} \qquad f_{h1} = \frac{1}{2\pi\sqrt{aL_s\left(C_t + \frac{C_p C_1}{C_p + C_1}\right)}}$$

$$f_{s2} = \frac{1}{2\pi\sqrt{L_s C_2}} \qquad f_{h2} = \frac{1}{2\pi\sqrt{aL_s\left(C_t + \frac{C_p C_2}{C_p + C_2}\right)}}$$

$$f_{s3} = \frac{1}{2\pi\sqrt{L_s C_3}} \qquad f_{h3} = \frac{1}{2\pi\sqrt{aL_s\left(C_t + \frac{C_p C_3}{C_p + C_3}\right)}}$$

where $L_h = aL_s$.
Combining the above expressions

$$\left[\frac{f_{s1}}{f_{h1}}\right]^2 = A_1 = \frac{a\left(C_t + \frac{C_p C_1}{C_p + C_1}\right)}{C_1}$$

$$\left[\frac{f_{s2}}{f_{h2}}\right]^2 = A_2 = \frac{a\left(C_t + \frac{C_p C_2}{C_p + C_2}\right)}{C_2}$$

$$\left[\frac{f_{s3}}{f_{h3}}\right]^2 = A_3 = \frac{a\left(C_t + \frac{C_p C_3}{C_p + C_3}\right)}{C_3}$$

Solving for C_p, a and C_t

$$C_p = \frac{A_1C_1^2(C_3 - C_2) + A_2C_2^2(C_1 - C_3) + A_3C_3^2(C_2 - C_1)}{A_1C_1(C_2 - C_3) + A_2C_2(C_3 - C_1) + A_3C_3(C_1 - C_2)} \quad . \quad 6.45a.$$

$$a = \frac{(A_1C_1 - A_2C_2)(C_p + C_1)(C_p + C_2)}{C_p^2(C_1 - C_2)} \quad . \quad . \quad . \quad . \quad 6.46a.$$

$$C_t = \frac{A_1C_1(C_p + C_1) - aC_pC_1}{a(C_p + C_1)} \quad . \quad . \quad . \quad . \quad . \quad . \quad 6.47a.$$

But $f_{min.} = \dfrac{1}{2\pi\sqrt{L_sC_{max.}}}$.

Writing

$$\left[\frac{f_{min.}}{f_{s1}}\right]^2 = B_1 = \frac{C_1}{C_{max.}}$$

$$\left[\frac{f_{min.}}{f_{s2}}\right]^2 = B_2 = \frac{C_2}{C_{max.}}$$

$$\left[\frac{f_{min.}}{f_{s3}}\right]^2 = B_3 = \frac{C_3}{C_{max.}}$$

and dividing the numerator of 6.45a by $(C_{max.})^3$ and the denominator by $(C_{max.})^2$, we have

$$\frac{C_p}{C_{max.}} = \frac{A_1B_1^2(B_3 - B_2) + A_2B_2^2(B_1 - B_3) + A_3B_3^2(B_2 - B_1)}{A_1B_1(B_2 - B_3) + A_2B_2(B_3 - B_1) + A_3B_3(B_1 - B_2)} \quad . \quad 6.45b.$$

But $$A_1 = \left[\frac{f_{s1}}{f_{h1}}\right]^2 = \frac{1}{\left[1 + \dfrac{f_1}{f_{s1}}\right]^2}$$

for $$f_{h1} = f_{s1} + f_1$$

where f_1 = the intermediate frequency.

$$\therefore\ A_1 = \frac{1}{\left[1 + \dfrac{f_{min.}}{f_{s1}} \cdot \dfrac{f_1}{f_{min.}}\right]^2}$$

$$= \frac{1}{(1 + \sqrt{B_1}.D)^2}$$

where $$D = \frac{f_1}{f_{min.}}.$$

Similarly $$A_2 = \frac{1}{[1 + \sqrt{B_2}.D]^2}$$

and $$A_3 = \frac{1}{[1 + \sqrt{B_3}.D]^2}.$$

Replacing A_1, A_2 and A_3 in 6.45*b*

$$\frac{C_p}{C_{max.}} = \frac{\dfrac{B_1^2(B_3-B_2)}{(1+D\sqrt{B_1})^2}+\dfrac{B_2^2(B_1-B_3)}{(1+D\sqrt{B_2})^2}+\dfrac{B_3^2(B_2-B_1)}{(1+D\sqrt{B_3})^2}}{\dfrac{B_1(B_2-B_3)}{(1+D\sqrt{B_1})^2}+\dfrac{B_2(B_3-B_1)}{(1+D\sqrt{B_2})^2}+\dfrac{B_3(B_1-B_2)}{(1+D\sqrt{B_3})^2}} \quad . \quad 6.45c.$$

Hence $\dfrac{C_p}{C_{max.}}$ is defined completely in terms of the ratios of the intermediate, and the three zero error frequencies to the minimum signal-tuning frequency.

Dividing the numerator and denominator in expression 6.46*a* by $(C_{max.})^3$.

$$a = \frac{\left[\dfrac{B_1}{(1+D\sqrt{B_1})^2}-\dfrac{B_2}{(1+D\sqrt{B_2})^2}\right](F+B_1)(F+B_2)}{F^2(B_1-B_2)} \quad . \quad 6.46b$$

where $F = \dfrac{C_p}{C_{max.}}$.

Dividing numerator by $(C_{max.})^2$ and denominator by $(C_{max.})$ in expression 6.47*a*.

$$\frac{C_t}{C_{max.}} = \frac{\dfrac{B_1}{(1+D\sqrt{B_1})^2}(F+B_1)-aFB_1}{a(F+B_1)} \quad . \quad 6.47b.$$

Thus a and $\dfrac{C_t}{C_{max.}}$ can also be defined in terms of the frequency ratios.

Expressions 6.45*c*, 46*b* and 47*b* are plotted in Fig. 6.21 against $\dfrac{f_1}{f_{min.}}$ for

$$\frac{f_{s1}}{f_{min.}} = 1{\cdot}091, \quad \frac{f_{s2}}{f_{min.}} = 1{\cdot}82, \quad \frac{f_{s3}}{f_{min.}} = 2{\cdot}545,$$

which means that for the medium wave range and $f_{min.} = 550$ kc/s, $f_{s1} = 600$ kc/s, $f_{s2} = 1{,}000$ kc/s, $f_{s3} = 1{,}400$ kc/s. These were the original zero error frequencies chosen by the authors of this method. From the curves in Fig. 6.21, the component ratios for an I.F. of 465 kc/s are $\left(\dfrac{f_1}{f_{min.}} = 0{\cdot}845\right)$

$$\frac{C_p}{C_{max.}} = 1{\cdot}067, \quad a = 0{\cdot}535, \quad \frac{C_t}{C_{max.}} = 0{\cdot}027$$

and if the maximum value of the total tuning capacitance is

536·8 $\mu\mu$F, and the signal inductance 156 μH as for the previous example in Section 6.12,

$$C_p = 572 \ \mu\mu\text{F}, \ L_h = 83{\cdot}5 \ \mu\text{H}, \ C_t = 14{\cdot}5 \ \mu\mu\text{F}.$$

These are not very different from the values calculated in Section 6.12. The difference is partly due to the assumption that the oscillator tuning capacitor has a value equal to the total signal-

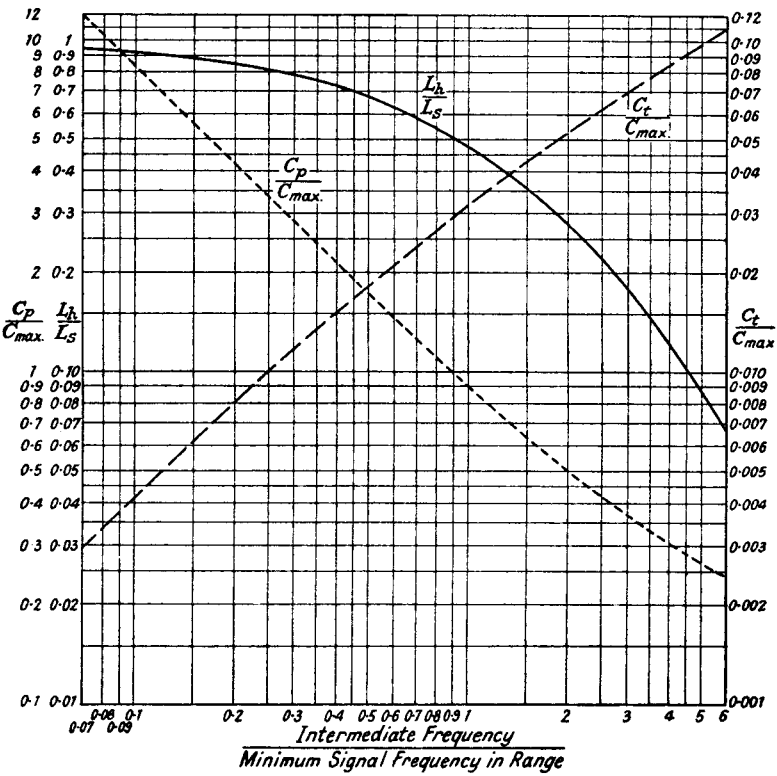

FIG. 6.21.—Curves for Ganging Component Ratios against Intermediate to Minimum Signal Frequency Ratios.

tuning capacitance, and partly to the fact that the zero error signal frequencies are different. If the latter are the same as in Section 6.12, viz., 614, 1,025 and 1,436 kc/s, the component values are

$$C_p = 578 \ \mu\mu\text{F}; \ L_h = 81{\cdot}2 \ \mu\text{H}, \ C_t = 13{\cdot}3 \ \mu\mu\text{F}.$$

In spite of these differences satisfactory ganging is obtained. The great advantage of the curves is that they may be used to give

oscillator component values for any intermediate frequency in the normal range, and for any maximum value of tuning capacitance having a capacitance range factor not less than 7·43. The ratio range of the extreme zero error signal frequencies is 2·33 : 1, and if a smaller range is desired, as for band-spread reception, a new set of curves is necessary. The curves of Fig. 6.21 are suitable for the long wave (165 to 450 kc/s), the medium wave (550 to 1,500 kc/s) and the short wave band (5·5 to 15 Mc/s).

BIBLIOGRAPHY

1. Frequency Variations in Thermionic Generators. K. E. Edgeworth *Journal I.E.E.*, Vol. 64, 1926, p. 349.
2. On the Variation of Generated Frequency of a Triode Oscillator. K. B. Eller, *Proc. I.R.E.*, Dec. 1928, p. 1,706.
3. Constant Frequency Oscillators. F. B. Llewellyn, *Proc. I.R.E.*, Dec. 1931, p. 2,063.
4. A Recent Development in Vacuum Tube Oscillator Circuits. J. B. Dow. *Proc. I.R.E.*, Dec. 1931, p. 2,095. Correction *ibid.*, Jan. 1932, p. 182,
5. Ganging the Tuning Controls of a Superheterodyne Receiver. A. L. M. Sowerby, *Wireless Engineer*, Feb. 1932, p. 70.
6. The Padding Condenser. B. F. McNamee, *Electronics*, May 1932, p. 160.
7. A Solution of the Superheterodyne Tracking Problem. V. D. Landon and E. A. Seen, *Electronics*, Aug. 1932, p. 250.
8. *Valve Oscillators of Stable Frequency.* F. M. Colebrook, H.M. Stationery Office, Special Report No. 13, 1933.
9. Suppression of Interlocking in First Detector Circuits. P. W. Klipsch, *Proc. I.R.E.*, June 1934, p. 699.
10. The Non-Linear Theory of Electric Oscillations. B. van der Pol, *Proc. I.R.E.*, Sept. 1934, p. 1,051.
11. Oscillator Padding. H. Roder, *Radio Engineering*, March 1935, p. 7.
12. Ganging a Superhet. C. P. Singer, *Wireless Engineer*, June 1936, p. 307.
13. The Non-Linear Theory of the Maintenance of Oscillations. P. Le Corbeiller, *Journal I.E.E.*, Sept. 1936, p. 361.
14. Thermal Drift in Superheterodyne Receivers. J. Miller, *Electronics*, Nov. 1937, p. 24.
15. Tuning Drift. E. L. Gardiner, *Wireless World*, Jan. 6th, 1938, p. 6.
16. Short Wave Oscillator Problems. W. T. Cocking, *Wireless World*, Feb. 9th, 1939, p. 127.
17. Design of the Oscillator Circuit of Superhet Receivers. *Mullard Technical Bulletin*, Feb. 1939, p. 149.
18. Ganging Superheterodyne Receivers. M. Wald, *Wireless Engineer*, March 1940, p. 105, and April 1941, p. 146.
19. Ultra High Frequency Oscillator Frequency Stability Considerations. S. W. Seeley and E. I. Anderson, *R.C.A. Review*, July 1940, p. 77.
20. Ceramic Insulations for High Frequency Work. W. G. Robinson, *Journal I.E.E.*, Nov. 1940, p. 570.
21. *Theory and Design of Valve Oscillators.* H. A. Thomas, Messrs. Chapman and Hall. Text-book.

CHAPTER 7

INTERMEDIATE FREQUENCY AMPLIFICATION

7.1. Introduction. The intermediate frequency amplifier is a special case of a radio frequency amplifier operating at a fixed frequency. The values of L and C forming the tuned circuits are not limited by the need for a variable capacitance range, but may be chosen to give the best performance as regards selectivity and amplification. High selectivity demands high Q values for the coils, and for a given selectivity the required Q value is linearly proportional to frequency. For example, a Q of 50 at 110 kc/s gives the same selectivity as a Q of 211 at 465 kc/s. Stranded wire generally becomes necessary in order to obtain the required selectivity at high intermediate frequencies.

The amplification of an I.F. amplifier stage is largely fixed by the impedance of the I.F. tuned circuits, i.e., $\frac{L}{CR}$, and it is greatest when L is large and C small. There is a limit to the possible reduction of C, for valve and stray capacitances must not form a large proportion of the tuning capacitance; variation of valve capacitance due to A.G.C. and replacement of valves may otherwise cause serious detuning. Furthermore, these stray capacitances have resistive components which reduce the Q value and the impedance of the circuit. A typical value for C is between 100 and 400 $\mu\mu$F. Too small a capacitance value not only means greater liability to variation during service but also greater variation with temperature change, for stray capacitance usually has a high positive temperature coefficient.

Inductance or capacitance tuning may be employed, but the former is preferable because a variable inductance is less affected by temperature change than a variable capacitance. Moreover, fixed capacitors, of the silvered mica type, may be made with very small temperature coefficients (Section 6.7.3). Inductance tuning is usually accomplished by a movable screwed iron-dust core at the centre of the coil. When capacitance tuning is employed, the dielectric should be air as this gives a much lower resistive component than mica and allows greater mechanical stability. Pressure-type mica capacitors are generally unsatisfactory owing to a high positive temperature coefficient and poor mechanical stability.

Single-tuned circuits are not normally used in an I.F. amplifier

since they give a selectivity curve with a comparatively narrow pass-band and poor attenuation outside the pass-range. Coupled circuits give a more satisfactory curve, approximating to the ideal of a flat pass-band with sharper attenuation outside the band. Often they have identical L, C and R values, an important advantage in manufacture.

7.2. Types of Coupled Circuits.[15] Capacitance or inductance coupling between two tuned circuits may be used to give a band-pass selectivity curve. The coupling impedance may be in shunt connection (sometimes called common coupling), e.g., Z_1 in Fig. 7.1, or it may be in series connection (sometimes called top-end coupling), e.g., Z_2 in the same figure. Alternatively, both forms of coupling may be used as illustrated in Fig. 7.1. Combined coupling may occur unintentionally, and an example of this is provided by stray capacitance between two circuits having mutual inductance coupling.

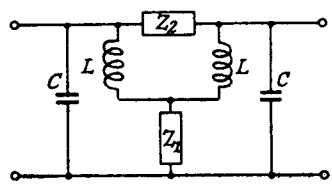

FIG. 7.1.—A Circuit with Combined Shunt and Series Coupling.

The I.F. valve is generally a pentode, so that the input source to the coupled circuits may conveniently be regarded as a generator of constant current $I_a = g_m E_g$. If E_2 is the voltage across the second tuned circuit, the selectivity curve is obtained by plotting the ratio $\frac{E_2}{I_a}$ against frequency. This ratio, $\frac{E_2}{I_a}$, often called the transfer impedance Z_T (note that $g_m E_g Z_T$ gives the secondary output voltage), may be calculated by normal procedure, but before doing so it is always advisable to estimate the frequency limits of the pass-band and any rejection frequencies. A rejection frequency can only occur for mixed inductive and capacitive coupling. If we assume the resistance components to be zero, the pass-band limit frequencies are obtained by making $\frac{E_2}{I_a} = \infty$, and the rejection frequencies by making $\frac{E_2}{I_a} = 0$. Calculation from the transfer impedance formula is laborious and a much simpler method (due to G. W. O. Howe [1, 2]) is possible.

Taking the shunt coupling impedance case, Howe shows that

one pass-band limit frequency is found by series resonance in the outer ring of impedances excluding Z_1 i.e., $\frac{1}{2\pi\sqrt{LC}}$. The second is obtained by separating the two circuits as in Fig. 7.2, the coupling impedance being doubled in the separation. This is logical because on joining up the two impedances $2Z_1$, we have Z_1. The second

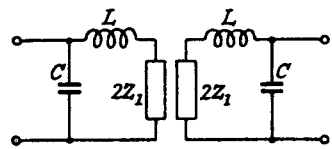

FIG. 7.2.—A Circuit with Separated Shunt Coupled Circuits.

pass-band frequency is given by series resonance of the LC circuit and $2Z_1$. Thus if $Z_1 = j\omega L_1$, the other limit frequency is

$$\frac{1}{2\pi\sqrt{(2L_1+L)C}}$$

or if $Z_1 = \frac{1}{j\omega C_1}$, it is

$$\frac{1}{2\pi\sqrt{\frac{LCC_1}{2C+C_1}}}$$

for the coupling capacitance C_1 must be halved to double Z_1.

It is important at this point to introduce the term,[4] coupling coefficient, k. This is defined, for shunt coupling, as the ratio of the coupling reactance to the sum of the coupling reactance and the reactance of the same form in either circuit. Thus for inductive coupling.

$$k = \frac{j\omega L_1}{j\omega(L+L_1)} = \frac{L_1}{L+L_1},$$

whilst for capacitance

$$k = \frac{\frac{1}{j\omega C_1}}{\frac{1}{j\omega C}+\frac{1}{j\omega C_1}} = \frac{C}{C+C_1}.$$

If the highest frequency is designated f_2, for inductive coupling

$$f_2 = \frac{1}{2\pi\sqrt{LC}} \text{ and } f_1 = \frac{1}{2\pi\sqrt{(2L_1+L)C}}$$

and

$$\frac{f_2^2 - f_1^2}{f_2^2+f_1^2} = \frac{L_1}{L+L_1} = k.$$

If

$$f_m = \frac{1}{2\pi\sqrt{(L_1+L)C}}$$

(note f_m is the primary resonant frequency with the secondary open-circuited or vice versa)

$$f_2 = \frac{f_m}{\sqrt{\frac{L}{L+L_1}}} = \frac{f_m}{\sqrt{1-k}} \text{ and } f_1 = \frac{f_m}{\sqrt{1+k}}.$$

For capacitive coupling

$$f_2 = \frac{1}{2\pi\sqrt{\frac{LCC_1}{2C+C_1}}}, \qquad f_1 = \frac{1}{2\pi\sqrt{LC}}$$

and $$\frac{f_2^2 - f_1^2}{f_2^2+f_1^2} = \frac{C}{C+C_1} = k. \quad \text{If } f_m = \frac{1}{2\pi\sqrt{\frac{LCC_1}{C+C_1}}}.$$

(Again, f_m is the resonant frequency of the primary with the secondary open circuited.)

$$f_2 = \frac{f_m}{\sqrt{\frac{C+C_1}{2C+C_1}}} = f_m\sqrt{1+\frac{C}{C+C_1}} = f_m\sqrt{1+k}$$

and $$f_1 = f_m\sqrt{1-k}.$$

The results for f_2 and f_1 in terms of f_m and k are different from those for inductive coupling. The difference is explained by the fact that capacitive reactance is the inverse of inductive reactance and that C_1 and C are in series, so that the total capacitance is reduced.

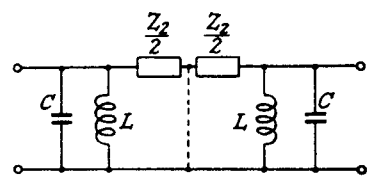

FIG. 7.3.—Separated Series Coupled Circuits.

For series coupling, the coupling impedance may be halved, as shown in Fig. 7.3, and the centre point joined to the junction of L and C. The two half-coupling impedances are in series, and when added make the total coupling impedance Z_2. The pass-band frequencies are given by resonance of the circuits, excluding $\frac{Z_2}{2}$, and then by including it. If $Z_2 = j\omega L_2$

$$f_2 = \frac{1}{2\pi\sqrt{\frac{LL_2C}{2L+L_2}}}; \quad f_1 = \frac{1}{2\pi\sqrt{LC}}$$

$$k = \frac{\text{Coupling susceptance } (L \text{ or } C)}{\text{circuit} + \text{coupling susceptance } (L \text{ or } C)}.$$

The coupling impedance is virtually in parallel with L and C, hence the use of susceptance to define it.

$$\therefore\ k = \frac{\frac{1}{j\omega L_2}}{\frac{1}{j\omega L}+\frac{1}{j\omega L_2}} = \frac{L}{L+L_2}$$

$$\frac{f_2^2 - f_1^2}{f_2^2+f_1^2} = \frac{L}{L+L_2} = k$$

$$f_m = \frac{1}{2\pi\sqrt{\frac{LL_2}{L+L_2}C}}$$

$$f_2 = f_m\sqrt{\frac{2L+L_2}{L+L_2}} = f_m\sqrt{1+k}$$

$$f_1 = f_m\sqrt{1-k}.$$

The coupling inductance is in parallel with the tuning inductance L so that the total inductance is decreased, and f_2 and f_1 in terms of f_m and k are identical with the expressions for shunt capacitance coupling. When $Z_2 = \frac{1}{j\omega C_2}$

$$f_2 = \frac{1}{2\pi\sqrt{LC}};\quad f_1 = \frac{1}{2\pi\sqrt{L(C+2C_2)}}$$

$$k = \frac{j\omega C_2}{j\omega C+j\omega C_2} = \frac{C_2}{C+C_2} = \frac{f_2^2 - f_1^2}{f_2^2+f_1^2}$$

$$f_m = \frac{1}{2\pi\sqrt{L(C+C_2)}}$$

$$f_2 = \frac{f_m}{\sqrt{1-k}};\quad f_1 = \frac{f_m}{\sqrt{1+k}}.$$

These last expressions are identical with those for shunt inductance coupling.

In all the above examples we see that only one of the limit frequencies is affected, and the results are best summarized in the form of a table.

Type of Coupling.	Frequency Peak Affected.	Effect of increase in Component on Frequency.	Peak Separation.
1. Shunt inductance	lower	decreases	increases
2. Shunt capacitance	higher	decreases	decreases
3. Series inductance	higher	decreases	decreases
4. Series capacitance	lower	decreases	increases

All possible forms of coupling have not been exhausted and there is yet mutual inductance coupling. The equivalent circuit is that of Fig. 7.4*a*, and the limit frequencies are

$$f_2 = \frac{1}{2\pi\sqrt{(L-M)C}}, \qquad f_1 = \frac{1}{2\pi\sqrt{(L+M)C}}$$

$$k = \frac{M}{L} = \frac{f_2^2 - f_1^2}{f_2^2 + f_1^2}$$

$$f_m = \frac{1}{2\pi\sqrt{LC}}, \quad f_2 = \frac{f_m}{\sqrt{1-k}}, \quad f_1 = \frac{f_m}{\sqrt{1+k}}.$$

Both limit frequencies are dependent on the coupling impedance and the pass-band range increases as M increases. If k is small ($< 0{\cdot}1$), $f_2 - f_m \simeq f_m - f_1$, so that symmetrical variable selectivity may be obtained by variation of M. With L and C coupling variation, f_m varies and the I.F. carrier must be varied if it is to be located in the centre of the pass-band, i.e., asymmetrical variable selectivity is obtained.

In Fig. 7.4*a* the mutual inductance is given a positive value,

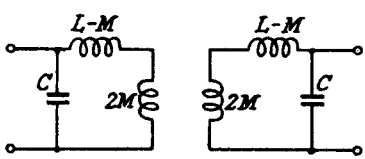

FIG. 7.4*a*.—Mutual Inductance Coupling with the Circuits Separated.

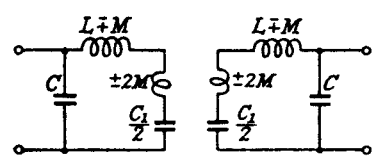

FIG. 7.4*b*.—Combined Mutual Inductance and Shunt Capacitance Coupling with the Circuits separated.

but it might equally be designated as $-M$. The horizontal inductances then become $(L+M)$ and the frequencies f_1 and f_2 merely reverse values. As long as no other coupling exists between the circuits the sign of M is unimportant. If, however, there is capacitance coupling, as in Fig. 7.4*b*, the sign of M is important. When M is positive the coupling impedance is $j\left(\omega M - \frac{1}{\omega C_1}\right)$ and the limit frequencies are

$$f_2 = \frac{1}{2\pi\sqrt{\frac{(L+M)CC_1}{2C+C_1}}} \text{ and } f_1 = \frac{1}{2\pi\sqrt{(L-M)C}}$$

with a rejection frequency

$$f_3 = \frac{1}{2\pi\sqrt{MC_1}}$$

produced by series resonance of the coupling arm. If M is negative $Z_1 = -j\left(\omega M + \frac{1}{\omega C_1}\right)$ and

$$f_2 = \frac{1}{2\pi\sqrt{\frac{(L-M)CC_1}{2C+C_1}}} \text{ and } f_1 = \frac{1}{2\pi\sqrt{(L+M)C}},$$

but there is no rejection frequency, for f_3 is imaginary. The sign of M is changed by reversing the primary or secondary coil connections as explained in Section 3.4.2.

A typical selectivity curve for positive M is shown in Fig. 7.4c, the rejection frequency f_3 can be varied by changing C_1 and can occur at any desired position. It may be used to increase attenua-

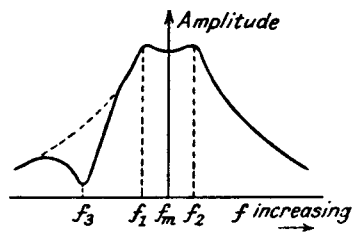

FIG. 7.4c.—A Typical Selectivity Curve for Combined Positive Mutual Inductance and Shunt Capacitance Coupling

tion at the edge of the pass-band, though the tendency is then to reduce the pass-band width and response nearest f_3 and to cause asymmetrical pass response.

If there is series capacitance as well as mutual inductance coupling, the equivalent circuit is that of Fig. 7.5. One limit frequency is obtained from resonance of the circuit excluding the mutual inductance (C_2 is doubled). Thus when M is positive

$$f_2 = \frac{1}{2\pi\sqrt{(L-M)(C+2C_2)}}.$$

The other limit frequency is given by resonance of the circuit excluding the series capacitance. The mutual inductance is doubled in separation and

$$f_1 = \frac{1}{2\pi\sqrt{(L+M)C}}.$$

Since there is mixed coupling, a rejection frequency is possible and its value may be found as follows.

For zero voltage across the second capacitance in Fig. 7.5

$$I_2 j\omega_3(L - M) + I_1 j\omega_3 M = 0$$

or
$$I_1 = -I_2\frac{(L - M)}{M}$$

also

$$\frac{I_2}{j\omega_3 C_2} + I_2 j\omega_3(L - M) + (I_2 - I_1)j\omega_3(L - M) = 0$$

$$jI_2\left[\omega_3\left(2(L - M) + \frac{(L - M)^2}{M}\right) - \frac{1}{\omega_3 C_2}\right] = 0$$

from which
$$f_3 = \frac{1}{2\pi\sqrt{\frac{(L+M)(L - M)}{M}C_2}}.$$

The selectivity curve is similar to that shown in Fig. 7.4*c*. The frequencies for negative M are found by replacing $+M$ by $-M$ in

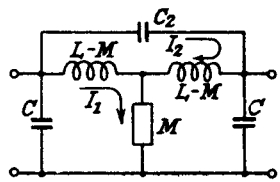

FIG. 7.5.—A Circuit with Combined Positive Mutual Inductance and Shunt Capacitance Coupling.

the above expressions and, as for shunt capacitance and mutual inductance coupling, there is no rejection frequency.

We see from this preliminary examination that variable pass-band width is most satisfactorily obtained by mutual inductance coupling, because increase of M moves both limit frequencies away from the mid-frequency. We will therefore proceed to a detailed analysis of the I.F. tuned transformer with mutual inductance coupling.

7.3. The Design of an I.F. Transformer with Mutual Inductance Coupling. The equivalent circuit diagram for the double-tuned transformer with mutual inductance coupling is shown in Fig. 7.6 ; the valve is represented as a constant current generator of $I_a = g_m E_g$, and its resistance is assumed to be much greater than the impedance of the primary of the transformer. The procedure for calculating the transfer impedance $Z_T\left(\frac{E_2}{I_a}\right)$ is considerably simplified by replacing the actual circuits by Z_1, Z_2, etc.

Then $$\frac{E_2}{E_1} = \frac{Z_5}{Z_4+Z_5}$$

$$\frac{E_1}{E} = \frac{Z_3(Z_4+Z_5)}{Z_3+Z_4+Z_5} \Big/ \frac{Z_3(Z_4+Z_5)}{Z_3+Z_4+Z_5}+Z_2$$

$$\frac{E_2}{E} = \frac{Z_3Z_5}{Z_3(Z_4+Z_5)+Z_2(Z_3+Z_4+Z_5)}.$$

But $$E = I_aZ_1\left[Z_2+\frac{Z_3(Z_4+Z_5)}{Z_3+Z_4+Z_5}\right] \Big/ Z_1+Z_2+\frac{Z_3(Z_4+Z_5)}{Z_3+Z_4+Z_5}.$$

Hence $$\frac{E_2}{I_a} = \frac{Z_1Z_3Z_5}{(Z_1+Z_2)(Z_3+Z_4+Z_5)+Z_3(Z_4+Z_5)}$$

or $$Z_T = \frac{Z_1Z_3Z_5}{(Z_1+Z_2+Z_3)(Z_3+Z_4+Z_5)-Z_3^2} \quad . \quad . \quad 7.1a$$

$$= \frac{Z_1Z_3Z_5}{Z_{s1}.Z_{s2}-Z_3^2} \quad . \quad . \quad . \quad . \quad . \quad . \quad 7.1b$$

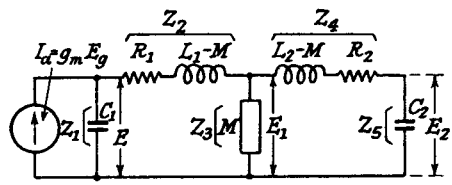

FIG. 7.6.—The Equivalent Circuit for a Double Tuned I.F. Transformer.

where Z_{s1} and Z_{s2} are the series impedances of first and second circuits taken separately, i.e.,

$$Z_{s1} = Z_1+Z_2+Z_3 \text{ and } Z_{s2} = Z_3+Z_4+Z_5.$$

But $$Z_1 = \frac{1}{j\omega C_1}, \quad Z_2 = R_1+j\omega(L_1-M), \quad Z_3 = j\omega M$$

$$Z_4 = R_2+j\omega(L_2-M) \text{ and } Z_5 = \frac{1}{j\omega C_2}.$$

It is assumed that the resistance components in the capacitive branches are negligible (this is usually true of air dielectric capacitors or of good quality mica fixed capacitors).

$$Z_{s1} = Z_1+Z_2+Z_3 = R_1+j\left(\omega L_1-\frac{1}{\omega C_1}\right)$$

$$= R_1(1+jQ_1F)$$

where $$Q_1 = \frac{\omega_m L_1}{R_1}$$

$$F = \frac{2\Delta f}{f_m} \text{ (see Section 4.2.3)}$$

and f_m = central or mid-band frequency

$$= \frac{1}{2\pi\sqrt{L_1C_1}} = \frac{1}{2\pi\sqrt{L_2C_2}}.$$

$$Z_{s2} = R_2 + j\left(\omega L_2 - \frac{1}{\omega C_2}\right)$$

$$= R_2(1 + jQ_2F).$$

Hence
$$Z_T = \frac{-\dfrac{j\omega M}{\omega^2 C_1C_2}}{R_1R_2(1+jQ_1F)(1+jQ_2F)+\omega^2M^2}$$

$$= \frac{-\dfrac{j\omega M}{\omega^2 C_1C_2R_1R_2}}{(1+jQ_1F)(1+jQ_2F)+\dfrac{\omega^2M^2}{R_1R_2}}.$$

But $k = \dfrac{M}{\sqrt{L_1L_2}}$ and $\dfrac{\omega^2M^2}{R_1R_2} = \dfrac{\omega_mL_1}{R_1}\cdot\dfrac{\omega_mL_2}{R_2}\cdot\dfrac{M^2}{L_1L_2}\cdot\left(\dfrac{\omega}{\omega_m}\right)^2 \simeq Q_1Q_2k^2$

$$\text{if } \frac{\omega}{\omega_m} \simeq 1$$

$$\frac{\omega M}{\omega^2 C_1C_2R_1R_2} = \frac{\omega_m}{\omega}\left[\frac{M}{\omega_m C_1C_2R_1R_2}\right] = \frac{\omega_m}{\omega}\left[\frac{\omega^3{}_mL_1L_2M}{R_1R_2}\right]$$

for $$\omega_mL_1 = \frac{1}{\omega_mC_1} \text{ and } \omega_mL_2 = \frac{1}{\omega_mC_2}.$$

$$\therefore \frac{\omega M}{\omega^2 C_1C_2R_1R_2} = \frac{\omega_m}{\omega}\left[\frac{\omega_m{}^2L_1{}^2}{R_1}\cdot\frac{\omega_mL_2}{R_2}\cdot\frac{M_1}{L_1}\right]$$

$$= \frac{\omega_m}{\omega}\left[R_{D1}\cdot Q_2\cdot\frac{M}{\sqrt{L_1L_2}}\cdot\sqrt{\frac{L_2}{L_1}}\right]$$

$$= \frac{\omega_m}{\omega}\left[R_{D1}Q_2k\sqrt{\frac{L_2}{L_1}}\right]$$

where R_{D1} = dynamic resistance of the primary when not coupled to the secondary circuit.

Generally we shall be concerned only with frequencies close to f_m (within $\pm$ 30 kc/s) so that $\dfrac{\omega_m}{\omega} \simeq 1$ and

$$\frac{\omega M}{\omega^2 C_1C_2R_1R_2} \simeq R_{D1}Q_2k\sqrt{\frac{L_2}{L_1}}$$

Thus
$$Z_T = \frac{-jR_{D1}Q_2k\sqrt{\frac{L_2}{L_1}}}{(1+jQ_1F)(1+jQ_2F)+Q_1Q_2k^2} \quad . \quad . \quad 7.2a$$

$$|Z_T| = \frac{R_{D1}Q_2k\sqrt{\frac{L_2}{L_1}}}{\sqrt{[1+Q_1Q_2(k^2-F^2)]^2+(Q_1+Q_2)^2F^2}} \quad . \quad 7.2b.$$

The conditions for maximum value of $|Z_T|$ are found by differentiating 7.2*b* with respect to F and equating to zero.

Thus $2[1+Q_1Q_2(k^2-F^2)](-2Q_1Q_2F)+2(Q_1+Q_2)^2F=0$

or
$$F_{(max.\,|Z_T|)} = \pm\sqrt{k^2-\frac{1}{2}\left(\frac{1}{Q_1^2}+\frac{1}{Q_2^2}\right)}.$$

We have now to estimate the importance of k, Q_1 and Q_2 in determining the behaviour of the coupled circuits. Three conditions arise, viz.,

$$k<\sqrt{\frac{1}{2}\left(\frac{1}{Q_1^2}+\frac{1}{Q_2^2}\right)};\ k=\sqrt{\frac{1}{2}\left(\frac{1}{Q_1^2}+\frac{1}{Q_2^2}\right)} \text{ and } k>\sqrt{\frac{1}{2}\left(\frac{1}{Q_1^2}+\frac{1}{Q_2^2}\right)}.$$

When $k<\sqrt{\frac{1}{2}\left(\frac{1}{Q_1^2}+\frac{1}{Q_2^2}\right)}$, $F_{(max.\,|Z_T|)}$ is imaginary and a maximum occurs at $F=0$, when

$$|Z_T| = \frac{R_{D1}Q_2k\sqrt{\frac{L_2}{L_1}}}{1+Q_1Q_2k^2} \quad . \quad . \quad . \quad 7.3a.$$

For $k=\sqrt{\frac{1}{2}\left(\frac{1}{Q_1^2}+\frac{1}{Q_2^2}\right)}$; $F_{(max.\,|Z_T|)}=0$ and

$$|Z_T| = \frac{R_{D1}\sqrt{\frac{1}{2}\left(\frac{Q_2^2}{Q_1^2}+1\right)}\sqrt{\frac{L_2}{L_1}}}{1+\frac{Q_1^2+Q_2^2}{2Q_1Q_2}} \quad . \quad . \quad 7.3b.$$

The above value of k represents critical coupling and greater values produce a double-peaked response.

When $Q_1=Q_2$

$$|Z_T| = \frac{R_{D1}\sqrt{\frac{L_2}{L_1}}}{2} \quad . \quad . \quad . \quad . \quad 7.3c.$$

Two maxima result when $k > \sqrt{\frac{1}{2}\left(\frac{1}{Q_1^2}+\frac{1}{Q_2^2}\right)}$

and $$F_{(max.)} = \pm\sqrt{k^2 - \frac{1}{2}\left(\frac{1}{Q_1^2}+\frac{1}{Q_2^2}\right)}.$$

This corresponds to off-tune frequencies

$$\Delta f_{(max.\ |Z_T|)} \text{ of } \pm\frac{f_m}{2}\sqrt{k^2 - \frac{1}{2}\left(\frac{1}{Q_1^2}+\frac{1}{Q_2^2}\right)}.$$

Replacing F by $\pm\sqrt{k^2 - \frac{1}{2}\left(\frac{1}{Q_1^2}+\frac{1}{Q_2^2}\right)}$ in expression 7.2*b* gives after simplification

$$|Z_T| = \frac{R_{D1}Q_2k\sqrt{\frac{L_2}{L_1}}}{\sqrt{1 - \frac{(Q_1^2+Q_2^2)^2}{4Q_1^2Q_2^2}+(Q_1+Q_2)^2k^2}} \quad . \quad 7.3d.$$

This reduces to

$$|Z_T| = \frac{R_{D1}\sqrt{\frac{L_2}{L_1}}}{2}$$

when $Q_1 = Q_2$, which is the same result as for $k = \sqrt{\frac{1}{2}\left(\frac{1}{Q_1^2}+\frac{1}{Q_2^2}\right)}$, i.e., after critical coupling is exceeded two-peaked response is obtained, but the two maxima have amplitudes equal to the amplitude at critical coupling. Increased coupling merely increases the frequency separation of the two peaks, but does not change their amplitude unless coupling is very large when the term $\frac{\omega_m}{\omega}$ in the expression $\frac{\omega M}{\omega^2 C_1 C_2 R_1 R_2}$ given above can no longer be neglected. The effect of this term is to increase the lower frequency maximum and decrease the higher frequency maximum. For couplings much less than critical, the transfer impedance at any frequency is

$$|Z_T| = \frac{R_{D1}Q_2k\sqrt{\frac{L_2}{L_1}}}{\sqrt{(1+Q_1Q_2(-F^2))^2+(Q_1+Q_2)^2F^2}}$$

$$= \frac{R_{D1}Q_2k\sqrt{\frac{L_2}{L_1}}}{\sqrt{(1+Q_1^2F^2)(1+Q_2^2F^2)}}.$$

The selectivity characteristic (Section 4.2.3), or the variation of $|Z_T|$ with respect to F, is equivalent to that of two circuits of Q_1 and Q_2 separated by a valve. The transfer impedance is however directly proportional to k, so that under these conditions amplification (in association with a valve) is low.

In most cases the primary and secondary circuits are identical and the expression for transfer impedance becomes

$$|Z_T| = \frac{R_D Qk}{\sqrt{[1+Q^2(k^2-F^2)]^2+4Q^2F^2}} \quad . \quad . \quad 7.2c$$

and its maximum value is obtained when

$$F = \pm\sqrt{k^2 - \frac{1}{Q^2}}$$

when $k < \frac{1}{Q}$, $F_{(max.\,|Z_T|)} = 0$ and

$$|Z_T| = \frac{R_D Qk}{1+Q^2k^2} \quad . \quad . \quad . \quad . \quad 7.3e.$$

For $k = \frac{1}{Q}$, $F_{(max.\,|Z_T|)} = 0$

$$|Z_T| = \frac{R_D}{2} \quad . \quad . \quad . \quad . \quad 7.3f$$

and $k > \frac{1}{Q}$ gives $F_{(max.\,|Z_T|)} = \pm\sqrt{k^2 - \frac{1}{Q^2}}$ and

$$|Z_T| = \frac{R_D}{2}.$$

It may be noted that $Qk = \frac{\omega L}{R} \cdot \frac{M}{L} = \frac{\omega M}{R} = \frac{\text{coupling reactance}}{\text{coil resistance}}$

This shows that the maximum amplification obtainable from a pair of coupled circuits is only one-half that obtained with one circuit. The loss of amplification is however offset by increased selectivity and pass-band response.

7.4. Generalized Selectivity Curves for Mutual Inductance Coupling. A series of generalized selectivity curves [5] may be obtained for a pair of identical coupled circuits by plotting $20 \log_{10} \frac{|Z_T|}{|Z_T|_{max.}}$ *db* against QF for selected values of Qk. The reference level, 0*db*, is conveniently taken as $|Z_T|_{(max.)}$, i.e., $\frac{R_D}{2}$ and the decibel loss at any particular frequency f is

$$20 \log_{10} \frac{R_D}{2|Z_T|_f} = 20 \log_{10} \frac{\sqrt{[1+Q^2(k^2-F^2)]^2+4Q^2F^2}}{2Qk} \quad 7.4.$$

This expression is independent of the sign of QF and it means that the selectivity curve is symmetrical about f_m. By plotting expression 7.4 against QF (to a logarithmic scale) we have the generalized curves of Fig. 7.7. The great advantage of these curves lies in the ease with which QF may be converted to the off-tune frequency Δf as soon as we have fixed Q and f_m. As indicated in

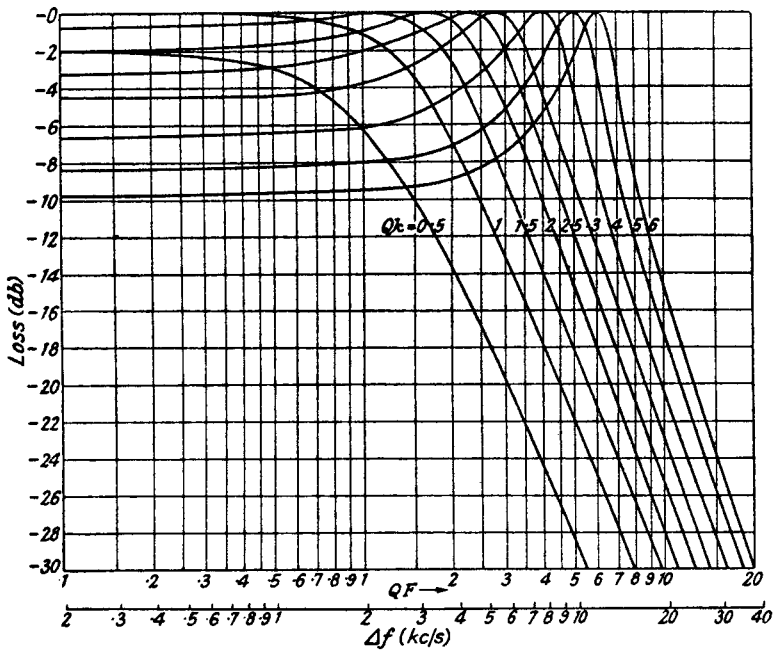

FIG. 7.7.—Generalized Selectivity Curves for an I.F. Transformer with two Identical Coupled Circuits.

Section 4.2.3, to obtain the selectivity curve against off-tune frequency it is only necessary to slide a logarithmic Δf scale underneath the QF scale until $\frac{f_m}{2Q}$ on the former corresponds to $QF = 1$. As an example of the use of these curves, let us consider coupled circuits having $Q = 120$ and $k = 0{\cdot}025$ at an I.F. of $f_m = 465$ kc/s.

$$Qk = 3 \text{ and } \frac{f_m}{2Q} = 1{\cdot}94.$$

The logarithmic Δf scale is adjusted so that $\Delta f = 1{\cdot}94$ lies immediately under $Qk = 1$ (Fig. 7.7). The decibel loss at any off-tune frequency is read directly from the curve $Qk = 3$. Thus

maximum $|Z_T|$ occurs at $\Delta f = 5{\cdot}5$ kc/s, whilst at $\Delta f = 15$ kc/s the frequency response is reduced by 18 dbs.

The assumptions made in order to obtain the generalized curves lead to only small errors with normal couplings at an I.F. of 465 kc/s or over and off-tune frequencies up to ± 50 kc/s. For lower intermediate frequencies (110 kc/s) and similar off-tune frequency limits, the generalized curves are useful but their accuracy is limited.

7.5. Generalized Selectivity Curves for Shunt and Series Coupling. Let us again assume that the primary and secondary circuits are identical, and that shunt capacitance (C_1) coupling is employed. The transfer impedance is found by inserting the following values for Z_1, Z_2, etc., in expression 7.1*b*.

$$Z_1 = Z_5 = \frac{1}{j\omega C}; \quad Z_3 = \frac{1}{j\omega C_1}$$

$$Z_{s1} = Z_{s2} = R + j\left(\omega L - \frac{1}{\omega C \frac{C_1}{C+C_1}}\right)$$

From Section 7.2

$$\omega_m = \frac{1}{\sqrt{LC\frac{C_1}{C+C_1}}} \text{ and } k = \frac{C}{C+C_1}$$

$$\therefore Z_{s1} = Z_{s2} = R(1+jQF)$$

and

$$Z_T = \frac{-\frac{1}{j\omega^3 C_1 C^2 R^2}}{(1+jQF)^2 + \frac{1}{\omega^2 C_1{}^2 R^2}} \qquad 7.5$$

$$\frac{1}{\omega^3 C_1 C^2 R^2} = \left(\frac{\omega_m}{\omega}\right)^3 \frac{C+C_1}{\omega_m C C_1 R} \cdot \frac{C}{C+C_1} \cdot \frac{(C+C_1)^2}{\omega_m{}^2 C^2 C_1{}^2 R} \cdot \frac{C_1{}^2}{(C+C_1)^2}$$

$$= \left(\frac{\omega_m}{\omega}\right)^3 . QkR_D \frac{C_1{}^2}{(C+C_1)^2}$$

$$\simeq QkR_D$$

since $\frac{\omega_m}{\omega}$ over the normal response range is nearly equal to unity and $C_1 \gg C$.

Similarly

$$\frac{1}{\omega^2 C_1{}^2 R^2} = \left(\frac{\omega_m}{\omega}\right)^2 \left[\frac{C+C_1}{\omega_m C C_1 R} \cdot \frac{C}{C+C_1}\right]^2$$

$$= \frac{\omega_m{}^2}{\omega^2} Q^2 k^2$$

$$\simeq Q^2 k^2.$$

Hence $$|Z_T| = \frac{R_D Q k}{\sqrt{[1+Q^2(k^2-F^2)]^2+4Q^2F^2}}$$

which is identical with expression 7.2c. The generalized selectivity curves are therefore applicable to this form of coupling so long as we note that

$$f_m = \frac{1}{2\pi\sqrt{\frac{LCC_1}{C+C_1}}},$$

i.e., it varies as the coupling $k = \frac{C}{C+C_1}$ is varied.

The curves may also be used to estimate the performance of shunt inductance coupling L_1 and in this instance

$$f_m = \frac{1}{2\pi\sqrt{(L+L_1)C}} \text{ and } k = \frac{L_1}{L+L_1}.$$

The generalized curves are also applicable to series coupling provided the coupling reactance is large compared with the reactance of the same kind in either of the tuned circuits. For series capacitance coupling

$$f_m = \frac{1}{2\pi\sqrt{L(C+C_2)}} \text{ and } k = \frac{C_2}{C+C_2}$$

and for series inductance

$$f_m = \frac{1}{2\pi\sqrt{\frac{LL_2}{L+L_2}C}} \text{ and } k = \frac{L}{L+L_2}.$$

7.6. The Impedance of the Primary of Two Coupled Circuits. In the solution of certain problems, e.g., the calculation of the voltage available for A.G.C., it is necessary to know the impedance (Z_p) of the primary of two coupled circuits. Referring to Fig. 7.6

$$Z_p = \frac{Z_1 Z}{Z_1+Z} \quad . \quad . \quad . \quad . \quad . \quad 7.6$$

where $$Z = Z_2 + \frac{Z_3(Z_4+Z_5)}{Z_3+Z_4+Z_5}$$

$$\therefore Z_p = \frac{Z_1[Z_2(Z_3+Z_4+Z_5)+Z_3(Z_4+Z_5)]}{(Z_1+Z_2)(Z_3+Z_4+Z_5)+Z_3(Z_4+Z_5)}$$

$$= \frac{Z_1[(Z_2+Z_3)(Z_3+Z_4+Z_5)-Z_3^2]}{(Z_1+Z_2+Z_3)(Z_3+Z_4+Z_5)-Z_3^2}.$$

Replacing Z_1, Z_2, etc., by their appropriate components

$$Z_p = \frac{\frac{1}{j\omega C_1}[R_1R_2(1+jQ_1)(1+jQ_2F)+R_1R_2Q_1Q_2k^2]}{R_1R_2[(1+jQ_1F)(1+jQ_2F)+Q_1Q_2k^2]}$$

where $Q_1 = \frac{\omega_m L_1}{R_1}$, $Q_2 = \frac{\omega_m L_2}{R_2}$ and $\frac{\omega}{\omega_m} \simeq 1$.

Since $Q_1 \gg 1$ and $\gg Q_1Q_2k^2$

$$Z_p \simeq \frac{Q_1(1+jQ_2F)}{\omega C_1[(1+jQ_1F)(1+jQ_2F)+Q_1Q_2k^2]}$$

$$\simeq \frac{\frac{\omega_m}{\omega}R_{D1}(1+jQ_2F)}{(1+jQ_1F)(1+jQ_2F)+Q_1Q_2k^2}$$

$$\simeq \frac{R_{D1}(1+jQ_2F)}{(1+jQ_1F)(1+jQ_2F)+Q_1Q_2k^2} \quad . \quad . \quad 7.7a$$

when $\omega_m \simeq \omega$

$$|Z_p| = \frac{R_{D1}\sqrt{1+Q_2{}^2F^2}}{\sqrt{[1+Q_1Q_2(k^2-F^2)]^2+(Q_1+Q_2)^2F^2}} \quad . \quad 7.7b$$

$$= \frac{|Z_T|\sqrt{1+Q_2{}^2F^2}}{Q_2k\sqrt{\frac{L_2}{L_1}}} \quad . \quad . \quad . \quad . \quad 7.7c.$$

When the primary and secondary circuits are identical

$$Z_p = \frac{R_D(1+jQF)}{(1+jQF)^2+Q^2k^2} \quad . \quad . \quad . \quad 7.7d.$$

At the mid-frequency f_m, $F = 0$ and

$$|Z_p|f_m = \frac{R_{D1}}{1+Q_1Q_2k^2},$$

from which we see that the primary impedance decreases progressively as k is increased. At critical coupling

$$k = \sqrt{\frac{1}{2}\left(\frac{1}{Q_1{}^2}+\frac{1}{Q_2{}^2}\right)}$$

$$|Z_p|f_m = \frac{R_{D1}}{1+\frac{1}{2}\left(\frac{Q_2}{Q_1}+\frac{Q_1}{Q_2}\right)}$$

$$\simeq \frac{R_{D1}}{2}$$

when $Q_1 \simeq Q_2$.

It is sometimes helpful to use the equivalent primary circuit developed from

$$Z_p = \frac{Z_1 Z}{Z_1 + Z}.$$

Now
$$Z = Z_2 + \frac{Z_3(Z_4+Z_5)}{Z_3+Z_4+Z_5}$$

$$= Z_2 + Z_3 - \frac{Z_3^2}{Z_3+Z_4+Z_5} = Z_2 + Z_3 - \frac{Z_3^2}{Z_{s2}}.$$

The term $-\dfrac{Z_3^2}{Z_3+Z_4+Z_5}$ can be separated into a resistive and reactive component connected in series.

$$-\frac{Z_3^2}{Z_3+Z_4+Z_5} = \frac{\omega^2 M^2}{R_2(1+jQ_2F)} = \frac{\omega^2 M^2}{R_2(1+Q_2^2F^2)} - \frac{j\omega^2 M^2 Q_2 F}{R_2(1+Q_2^2F^2)}.$$

This result may be compared with that indicated by expression 3.18 in Section 3.4.2. The equivalent primary circuit is shown in

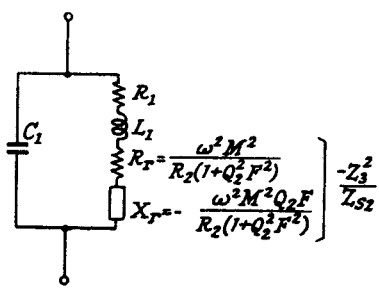

FIG. 7.8.—The Equivalent Circuit for the Primary of an I.F. Transformer.

Fig. 7.8, the total resistance and reactance in the inductive arm becoming

$$R = R_1 + R_r$$

$$= R_1\left[1 + \frac{\omega^2 M^2}{R_1 R_2(1+Q_2^2F^2)}\right]$$

$$\simeq R_1\left[1 + \frac{Q_1 Q_2 k^2}{1+Q_2^2F^2}\right] \quad . \quad . \quad . \quad 7.8a.$$

$$X = j(\omega L_1 + X_r)$$

$$\simeq j\omega L_1\left[1 - \frac{Q_2^2 k^2 F}{1+Q_2^2F^2}\right] \quad . \quad . \quad . \quad 7.8b$$

when $\dfrac{\omega_m}{\omega} \simeq 1$.

7.7. Variable Selectivity.

7.7.1. Introduction. The degree of selectivity required to suppress adjacent channel interference depends to a large extent on the strength of the received signal. For local station reception the selectivity can be reduced with consequent improvement in fidelity, but for distant station reception very high selectivity is often necessary. Hence some means of varying selectivity is an advantage, and in a superheterodyne receiver a very simple method is to control the selectivity of the I.F. amplifier.

Variable selectivity may conveniently be divided into asymmetrical (one side-band only is affected) and symmetrical variation (both side-bands are affected). Each has its merits and their advantages are listed below.

Asymmetrical.	*Symmetrical.*
1. One side-band only is reduced, that suffering from interference.	1. Both side-bands are reduced.
2. Tuning is critical and the carrier must be located correctly.	2. Tuning is not very critical.
3. Amplitude (harmonic) distortion can be high if not tuned correctly.	3. Amplitude distortion is small.
4. Frequency distortion is not so appreciable as only the high frequencies in one side-band are affected.	4. Frequency distortion may be considerable because the high frequencies in both side-bands are reduced.
5. Selectivity is better for given fidelity (audio frequency response) when interference is on one side of the carrier.	5. Selectivity is better when interference occurs on both sides of the carrier.
6. Signal to noise ratio is approximately − 3 dbs. down on that for symmetrical variable selectivity.	

Amplitude distortion due to asymmetrical variable selectivity can be reduced to a low value if there is symmetrical response for side-bands up to $\pm 1{,}500$ c.p.s.[6] on either side of the carrier. The audio frequency output with two side-bands is +6 dbs. above that with one, whilst noise is only +3 dbs. up due to the increased band width. Sections 4.9.2 and 4.9.3 show that circuit and valve noise is proportional to the square root of the band width, whereas the audio signal is directly proportional.

7.7.2. Asymmetrical Variation. Asymmetrical variation of selectivity is rarely used because of the need for skilled operation if satisfactory results are to be realized. It may be achieved by

detuning the oscillator so as to locate the carrier on the side of the selectivity curve, or by detuning one side of the I.F. coupled circuits. The second method varies the total pass-band, whereas the first varies only the relative widths of the pass region of each side-band.

7.7.3. Symmetrical Variation. Symmetrical variation of selectivity may be accomplished by varying the mutual inductance coupling between the I.F. circuits, or the damping of the circuits. The latter is not very satisfactory as it appreciably reduces the discrimination against frequencies outside the pass-band.

7.7.4. Variable Selectivity by Mutual Inductance Variation.[3, 9, 10] We have already seen from Section 7.2 that a double-peaked response may be obtained from two tuned circuits coupled by mutual inductance. Increase of coupling causes these two peaks

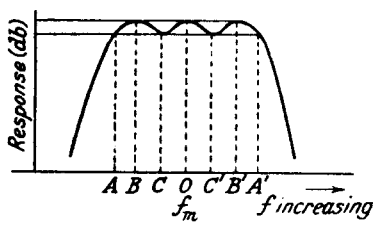

FIG. 7.9.—The Overall Selectivity Curve for an Overcoupled I.F. Transformer and a Single $\frac{1}{2}Q$ Circuit.

to travel by almost equal amounts from the mid-frequency f_m. It is important to note that the mutual inductance coupling between the circuits can only be satisfactorily varied by changing the relative positions of the two coils. The insertion of a shielding coil,[14] paralleled by a resistance between the two coils, is equivalent to a resistance shunting the mutual inductance arm. The effect is to reduce the lower frequency peak at $f_1 = \frac{1}{2\pi\sqrt{(L+M)C}}$, and if the resistance is made small enough this peak is completely suppressed. One disadvantage of mutual inductance coupling variation is that a trough is produced between the peaks and its depth increased as the peaks separate. This results in variable frequency response over the pass region between the peaks. It is, however, possible to overcome this difficulty if the overcoupled circuits are used in conjunction with a single tuned circuit of half the Q of the coupled circuits taken separately. The overall frequency response of the three circuits has three maxima of equal amplitude (see Fig. 7.9), and the frequency separation between the two outside maxima (contributed by the overcoupled circuits) is increased as the coupling

between the two circuits is increased. At the same time the two minima are reduced in amplitude so that an absolutely flat response over the pass-band is not obtained by this arrangement. Nevertheless, for normal pass-bands of ± 10 kc/s the variation can be reduced to very small proportions, less than 2 dbs. The proof that the maxima have equal amplitudes is as follows : the frequency response for the two coupled circuits is

$$20 \log_{10} \frac{R_D Q k}{\sqrt{[1+Q^2(k^2-F^2)]^2+4Q^2F^2}}$$

and that for the single tuned circuit

$$20 \log_{10} \frac{R_{D1}}{\sqrt{1+Q_1{}^2F^2}}.$$

The overall frequency response of the two circuits coupled by a valve is

$$20 \log_{10} \frac{R_D Q k R_{D1}}{\sqrt{([1+Q^2(k^2-F^2)]^2+4Q^2F^2)(1+Q_1{}^2F^2)}} \quad . \quad 7.9.$$

The variable factor is F, and since it occurs only in the denominator we can differentiate the latter and equate to zero in order to find the maxima and minima of the overall curve. We will replace Q_1 by $\frac{Q}{2}$ and check the final result by noting if three equal maxima are obtained.

$$(\text{Denominator})^2 = ([1+Q^2(k^2-F^2)]^2+4Q^2F^2)\left(1+\frac{Q^2F^2}{4}\right). \quad 7.10$$

$$\frac{d(D)^2}{dF} = \left(1+\frac{Q^2F^2}{4}\right)(-4Q^2F(1+Q^2(k^2-F^2))+8Q^2F) + ([1+Q^2(k^2-F^2)]^2+4Q^2F^2)\left(\frac{Q^2F}{2}\right)$$

$$= \frac{Q^2F}{2}[(9-6Q^2k^2+Q^4k^4)+Q^2F^2(12-4Q^2k^2)+3Q^4F^4] \quad . \quad 7.11$$

$$= 0$$

when $F = 0, \pm\sqrt{k^2-\frac{3}{Q^2}}$ and $\pm\sqrt{\frac{k^2}{3}-\frac{1}{Q^2}}$.

The three maxima in the overall frequency response curve, B, O and B' in Fig. 7.9, are given by the first three values of F $\left(0 \text{ and } \pm\sqrt{k^2-\frac{3}{Q^2}}\right)$ and the two minima, C and C', by the last

two values $\left(\pm\sqrt{\frac{k^2}{3}-\frac{1}{Q^2}}\right)$. Replacing F by 0 and $\pm\sqrt{k^2-\frac{3}{Q^2}}$ in expression 7.9 gives three equal maxima of

$$20\log_{10}\frac{R_D Q k R_{D1}}{1+Q^2k^2} \quad . \quad . \quad . \quad . \quad 7.12$$

thus proving the statement that one circuit of $\frac{Q}{2}$ in conjunction with two coupled circuits, each of magnification Q, gives three equal maxima in the response curve. The value at the minima, obtained by replacing F by $\pm\sqrt{\frac{k^2}{3}-\frac{1}{Q^2}}$ in expression 7.9, is

$$20\log_{10}\frac{3\sqrt{3}R_D.R_{D1}}{9+Q^2k^2} \quad . \quad . \quad . \quad 7.13.$$

Thus the ratio maximum-to-minimum response is

$$20\log_{10}\frac{(9+Q^2k^2)Qk}{3\sqrt{3}(1+Q^2k^2)} \quad . \quad . \quad . \quad 7.14$$

and from this expression the decibel ratio variation of frequency response over the pass range can be determined for any value of Qk.

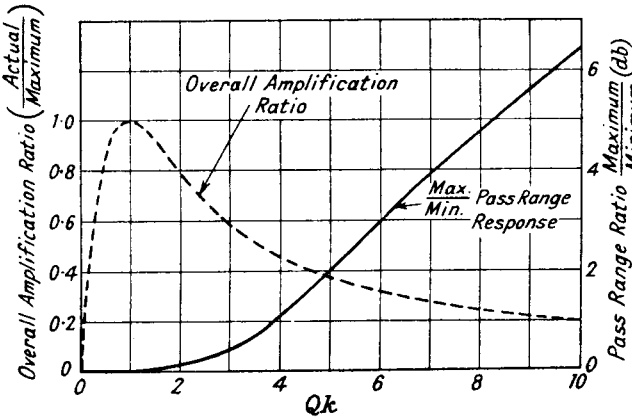

FIG. 7.10.—The Overall Amplification and Pass-band Ratios for an Overcoupled I.F. Transformer and a Single $\frac{1}{2}Q$ Circuit.

It is plotted in Fig. 7.10 against Qk. Expression 7.12 clearly shows that overall amplification is a function of Qk, and the condition for maximum is found by differentiating $\frac{R_D Q k R_{D1}}{1+Q^2k^2}$ with respect to Qk and equating to 0. This gives $Qk = 1$ and maximum amplification proportional to $\frac{R_D R_{D1}}{2}$. The ratio loss of amplification from the

maximum value is shown against Qk as the dotted curve in Fig. 7.10.

The pass-band is not strictly the frequency separation between the two maxima, B and B', but is more correctly that between the two points A and A' in Fig. 7.9, i.e., the extreme frequencies at which the response is equal to that at the minima, C and C'. The values of F corresponding to A and A' are found by equating expressions 7.9 and 7.13, which means that

$$[[1+Q^2(k^2-F^2)]^2+4Q^2F^2]\left(1+\frac{Q^2F^2}{4}\right)=\frac{Q^2k^2(+9Q^2k^2)^2}{27}$$

or

$$\left[Q^2F^2+1-\frac{Q^2k^2}{3}\right]^2\left(Q^2F^2+4-\frac{4Q^2k^2}{3}\right)=0$$

$$F=\pm 2\sqrt{\frac{k^2}{3}-\frac{1}{Q^2}} \quad . \quad . \quad . \quad 7.15a.$$

Since $F=\dfrac{2\Delta f}{f_m}$, we may write for the maximum off-tune frequency

$$\Delta f_{(max.)}=f_m\sqrt{\frac{k^2}{3}-\frac{1}{Q^2}}=\frac{R}{2\pi L}\sqrt{\frac{Q^2k^2}{3}-1} \quad . \quad 7.15b.$$

To illustrate the design of such a stage let us assume that the coupled circuits are preceded and succeeded by valves and that the $\dfrac{Q}{2}$ single circuit is in the anode of the second valve.

Let g_{m1} = 1 mA/volt = mutual conductance of the first valve.
g_{m2} = 3 mA/volt = ,, ,, ,, ,, second ,,
f_m = 465 kc/s
$\Delta f_{(max.)}$ = 10 kc/s.

The following requirements are to be met:

The variation of the pass-band is not to exceed 2 dbs., the amplification (A_1) of the stage supplying the coupled circuits is to be 50 at critical coupling and that (A_2) of the second stage 100.

Figure 7.10 gives $Qk = 5$ for a 2-db. difference between the maxima and minima of the response curve.

Hence from expression 7.15*b*.

$$\frac{L}{R}=\frac{1}{2\pi 10^4}\sqrt{\frac{25-3}{3}}=4{\cdot}31\times 10^{-5}$$

$$Q=\frac{\omega_m L}{R}=126.$$

The amplification of the coupled circuit stage at critical coupling is

$$A_1 = g_{m1}\frac{\omega_m LQ}{2}$$

or

$$L = \frac{2A_1}{g_{m1}\omega_m Q} = 272\ \mu\text{H}$$

$$R_D = \omega_m LQ = 100{,}000\Omega$$

$$C = 430\ \mu\mu\text{F}$$

$$R = \frac{\omega_m L}{Q} = 6{\cdot}28\Omega$$

$$Qk = 5 = \frac{\omega_m M}{R}$$

$$M = 10{\cdot}75\ \mu\text{H}.$$

The amplification of the single circuit stage is

$$A_2 = 100 = g_{m2}\omega_m L_1 \times \frac{Q}{2}\left[Q_1 = \frac{Q}{2}\right]$$

thus

$$L_1 = 181\ \mu\text{H}$$

$$R_{D1} = 33{,}000\Omega$$

$$C_1 = 645\ \mu\mu\text{F}$$

$$R_1 = \frac{2\omega_m L_1}{Q} = 8{\cdot}4\ \Omega$$

Referring to the curve for overall amplification given in Fig. 7.10, we note that the actual operating overall amplification at maximum desired coupling is only 0·38 of its maximum value ; i.e., the operating amplification of the first stage is $0{\cdot}38 \times 50 = 19$. If the pass-band is reduced by reducing Qk, overall amplification is increased as far as critical coupling, and the variation over the pass-band is reduced. When variable selectivity is obtained by this method there is often very little change in volume when Qk exceeds 1, because the increase in side-band width tends to offset the loss of amplification at the lower audio frequencies. Automatic gain control will also tend to compensate for the reduction in operating amplification.

In order to obtain sufficient maximum selectivity, more than two coupled and one single circuit are required in an I.F. amplifier, but to preserve the flat pass-band we must maintain the ratio of two coupled to one single circuit. Using two pairs of coupled circuits and two single circuits each separated by a valve is not very practical, and it is essential to consider a compromise. If we

couple two tuned circuits loosely together, we obtain a selectivity curve which approximates to that of two separate tuned circuits connected by a valve, having zero anode-grid capacitance. It is therefore possible to couple the tuned circuit of $\frac{1}{2}Q$ to the secondary of the overcoupled circuits, and to obtain an overall selectivity curve which very nearly approaches that of the circuits separated by a valve. The actual effect of coupling on the pass-band response is to depress the side maxima below the mid-frequency maximum. The chief problem in design is to obtain a sufficiently high transfer impedance with loose coupling.

By assuming that all three circuits have equal values of L and C but that the Q of the last loosely coupled circuit is only $\frac{1}{2}$ the Q of the overcoupled circuit, the current in the secondary of the overcoupled circuits is (from 7.1*a*)

$$I_2 = \frac{E_2}{Z_5} = \frac{I_a Z_1 Z_3}{(Z_1+Z_2+Z_3)(Z_3+Z_4+Z_5+Z') - Z_3^2} \quad . \quad 7.16a$$

$$= \frac{I_a \omega M_1}{\omega C[R(1+jQF)(R(1+jQF)+Z') + \omega^2 M_1^2)} \quad . \quad 7.16b$$

where M_1 = mutual inductance between the overcoupled circuits

,, R = effective series resistance of these two circuits

,, Z' = impedance reflected into the secondary of the two circuits from the loosely coupled $Q/2$ circuit

,, $= \frac{\omega^2 M_2^2}{Z''}$ (Section 7.6)

,, Z'' = series impedance of the $Q/2$ circuit

and M_2 = mutual inductance between the $Q/2$ circuit and the secondary of the overcoupled circuits

$$Z'' = 2R + j\omega_m L\left(\frac{\omega}{\omega_m} - \frac{\omega_m}{\omega}\right)$$

$$= R(2+jQF).$$

The current-voltage equation for the $Q/2$ circuit is

$$I_3 R(2+jQF) + I_2 j\omega M_2 = 0$$

where I_3 = the current in the $Q/2$ circuit.

The output voltage across the capacitance is

$$E_3 = \frac{I_3}{j\omega C} = \frac{-I_2 j\omega M_2}{j\omega C R(2+jQF)}$$

and the transfer impedance is

$$Z_T = \frac{E_3}{I_a}$$

$$= \frac{-\omega^2 M_1 M_2}{\omega^2 C^2 R(2+jQF)\left[R(1+jQF)\left[R\left(1+jQF+\frac{\omega^2 M_2{}^2}{R^2(2+jQF)}\right)\right]+\omega^2 M_1{}^2\right]}$$

$$= \frac{-\omega^2 M_1 M_2}{\omega^2 C^2 R^3\left[(2+jQF)(1+jQF)^2+\frac{\omega^2 M_2{}^2}{R^2}(1+jQF)+\frac{\omega^2 M_1{}^2}{R^2}(2+jQF)\right]}$$

But $$\frac{\omega^2 M_1 M_2}{\omega^2 C^2 R^3} = \frac{\omega_m{}^2 L^2}{R^2}\cdot\frac{1}{\omega_m{}^2 C^2 R}\cdot\frac{M_1 M_2}{L^2} = Q^2 R_D k_1 k_2$$

where $$k_1 = \frac{M_1}{L}, \text{ and } k_2 = \frac{M_2}{L}$$

$$\frac{\omega^2 M_2{}^2}{R^2} = \left(\frac{\omega}{\omega_m}\right)^2\cdot\frac{\omega_m{}^2 L^2}{R^2}\cdot\frac{M_2{}^2}{L^2} = \left(\frac{\omega}{\omega_m}\right)^2 Q^2 k_2{}^2$$

$$\simeq Q^2 k_2{}^2$$

if $$\frac{\omega}{\omega_m} \simeq 1.$$

Similarly $\frac{\omega^2 M_1{}^2}{R^2} \simeq Q^2 k_1{}^2$.

Thus

$$Z_T = \frac{-Q^2 k_1 k_2 R_D}{2\left[1+Q^2\left(k_1{}^2+\frac{k_2{}^2}{2}-2F^2\right)\right]+jQF[5+Q^2(k_1{}^2+k_2{}^2-F^2)]} \qquad 7.17a$$

or $|Z_T|$

$$= \frac{Q^2 k_1 k_2 R_D}{\sqrt{4\left[1+Q^2\left(k_1{}^2+\frac{k_2{}^2}{2}-2F^2\right)\right]^2+Q^2F^2[5+Q^2(k_1{}^2+k_2{}^2-F^2)]^2}} \qquad 7.17b$$

when Qk_2 is small

$$|Z_T| = \frac{Q^2 k_1 k_2 R_D}{\sqrt{4[1+Q^2(k_1{}^2-2F^2)]^2+Q^2F^2[5+Q^2(k_1{}^2-F^2)]^2}} \qquad 7.17c.$$

The square of the denominator of expression 7.17c can be expanded as follows

$$4\left[(1+Q^2(k_1{}^2-F^2)-Q^2F^2)^2+\frac{Q^2F^2}{4}(4+1+Q^2(k_1{}^2-F^2))^2\right]$$

$$= 4\left[(1+Q^2(k_1{}^2-F^2))^2-2Q^2F^2(1+Q^2(k_1{}^2-F^2))+Q^4F^4\right.$$

$$\left.+\frac{Q^2F^2}{4}(1+Q^2(k_1{}^2-F^2))^2+\frac{Q^2F^2}{4}[16+8(1+Q^2(k_1{}^2-F^2))]\right]$$

$$= 4\left[(1+Q^2(k_1^2-F^2))^2\left(1+\frac{Q^2F^2}{4}\right)+Q^2F^2(4+Q^2F^2)\right]$$

$$= 4[(1+Q^2(k_1^2-F^2))^2+4Q^2F^2]\left[1+\frac{Q^2F^2}{4}\right]$$

and this is 4 × expression 7.10; $|Z_T|$ therefore reduces to

$$|Z_T| = \frac{Q^2k_1k_2R_D}{2\sqrt{[(1+Q^2(k_1^2-F^2))^2+4Q^2F^2]\left[1+\frac{Q^2F^2}{4}\right]}} \quad . \quad 7.17d.$$

Hence the frequency response characteristic is the same as that when the overcoupled and single circuits are separated by a valve, and, provided Qk_2 is small, the curves for the loss over the pass range, and overall amplification ratio in Fig. 7.10 are applicable. The value of Qk_1 at which maximum amplification is realized, is moved to a slightly higher value by the coupling to the single tuned circuit and it can be found by differentiating the value of $|Z_T|$, for $F = 0$ ($f = f_m$), with respect to k_1. Thus from expression 7.17*b*

$$|Z_T|_{f_m} = \frac{Q^2k_1k_2R_D}{2\left[1+Q^2\left(k_1^2+\frac{k_2^2}{2}\right)\right]} \quad . \quad . \quad 7.18a$$

and $$\frac{d|Z_T|_{f_m}}{dk_1} = 0 \text{ when } Qk_1 = \sqrt{1+\frac{Q^2k_2^2}{2}}$$

so that if $Qk_2 = 0{\cdot}2$, $Qk_1 = 1{\cdot}01$, which is not very different from 1.

Replacing Qk_1 in expression 7.18*a* gives

$$|Z_T|_{f_m} = \frac{Qk_2R_D}{4\sqrt{1+\frac{Q^2k_2^2}{2}}} \quad . \quad . \quad . \quad 7.18b.$$

If the required maximum overall amplification, A, of the stage is known, the value of Qk_2 may be calculated from 7.18*b*, for

$$A = g_m|Z_T|_{f_m} = \frac{g_mQk_2R_D}{4\sqrt{1+\frac{Q^2k_2^2}{2}}}$$

from which

$$Qk_2 = \frac{4A}{\sqrt{g_m^2R_D^2-8A^2}} \quad . \quad . \quad . \quad 7.19.$$

To illustrate the design of the circuits, let us consider the problem given in the previous example, viz., the overall response in the pass range (±10 kc/s) is not to exceed 2 dbs., the amplification required at critical coupling is 50, $f_m = 465$ kc/s, and $g_m = 1$ mA/volt. If

it is assumed that the coupling k_2 is sufficiently loose to allow the curves in Fig. 7.10 to be used, the 2 dbs. variation gives

$$Qk_{1(max.)} = 5, \frac{L}{R} = 4{\cdot}31 \times 10^{-5} \text{ and } Q = 126.$$

The value of L must be as high as possible to obtain the highest transfer impedance. Let us assume that the maximum permissible value is 1,000 μH, which gives a tuning capacitance of 117 $\mu\mu$F.

Thus $L = 1{,}000\ \mu\text{H}. \quad C = 117\ \mu\mu\text{F}, \quad R = \frac{\omega L}{Q} = 23{\cdot}2\Omega.$

$$R_D = \omega L.Q = 368{,}000\Omega$$
$$g_m.R_D = 368.$$

From 7.19

$$Qk_2 = \frac{200}{\sqrt{368^2 - 8(50)^2}} = 0{\cdot}588.$$

This value of Qk_2 is too large, and the single circuit will affect the response of the overcoupled circuits to too great an extent. A more suitable value of Qk_2 is about 0·2. This entails increasing either R_D or g_m, or decreasing A. Increase of R_D involves an increase of L and decrease of C, and it is not very practicable since stray capacitance becomes an appreciable proportion of the total capacitance. A large ratio of stray-to-total capacitance increases the probability of mistuning during operation (due to valve or wiring lead changes, and to temperature effects). Furthermore, an increase in R_D may not result in a proportionate increase in amplification, due to R_D becoming comparable with the valve slope resistance R_a; when R_D approaches R_a the frequency response of the overcoupled circuits is affected and the variation over the pass-band increased. The only course is therefore to reduce A, if g_m cannot be increased; let us therefore take A as 17 as this gives $Qk_2 = 0{\cdot}2$. The critical value of Qk_1 corresponding to maximum amplification is

$$Qk_{1(crit.)} = \sqrt{1 + \frac{Q^2k_2^2}{2}} = 1{\cdot}01$$

$$M_{1(crit.)} = \frac{Qk_1R}{\omega_m} = \frac{1{\cdot}01 \times 23{\cdot}2 \times 10^6}{6{\cdot}28 \times 4{\cdot}65 \times 10^5}$$
$$= 8{\cdot}02\ \mu\text{H}$$

$$M_{1(max.)} = \frac{5}{1{\cdot}01} M_{1(crit.)} = 39{\cdot}7\ \mu\text{H}$$

$$M_2 = \frac{Qk_2R}{\omega_m} = \frac{0{\cdot}2 \times 23{\cdot}2 \times 10^6}{6{\cdot}28 \times 4{\cdot}65 \times 10^5}$$
$$= 1{\cdot}59\ \mu\text{H}.$$

The following component values satisfy all the requirements except that of amplification, the value of which cannot exceed 17 at critical coupling :

for the overcoupled circuits

$L = 1{,}000\ \mu H, \quad C = 117\ \mu\mu F, \quad R = 23{\cdot}2\Omega, \quad R_D = 368{,}000\Omega$
$Q = 126$
$M_1 = 8{\cdot}02\ \mu H$ (critical coupling)
$= 39{\cdot}7\ \mu H$ (for the required pass-band of $\pm$ 10 kc/s)

and for the single circuit

$L = 1{,}000\ \mu H, \quad C = 117\ \mu\mu F, \quad R = 46{\cdot}4\Omega, \quad R_D = 184{,}000\Omega$
$Q = 63$
$M_2 = 1{\cdot}59\ \mu H.$

Another possible arrangement for reducing the number of stages is to follow two pairs of overcoupled circuits by a pair of loosely coupled circuits of magnification $Q/2$, each pair being separated from the next by a valve. Since the $Q/2$ circuits form the last stage of the amplifier, the detector is connected across the secondary, and an A.G.C. detector will probably be connected across the primary. As a basis of design let us assume that each circuit has initially the same Q as the overcoupled circuits, and that the detector damping, and A.G.C. detector and amplifier anode damping reduce the magnification of secondary and primary to $Q/2$. We must now decide on the minimum coupling. If it is made too small in order that the selectivity curve of the coupled circuits may approach that of two valve-separated circuits, there is considerable loss of amplification to the detector. As a compromise let us take the coupling coefficient as one half critical. From section 7.3 critical coupling is realized when the coupling coefficient is equal to the reciprocal of the magnification of either circuit, therefore the required coupling coefficient is

$$k = \frac{0{\cdot}5}{Q/2} = \frac{1}{Q}$$

A lower value of coupling, for example $\frac{0{\cdot}2}{Q/2} = 0{\cdot}4Q$ is preferable for approaching the selectivity characteristics of two separated circuits, but this reduces appreciably the voltage to the detector.

The values of the circuit components are estimated as follows :

Let R_{DET} = parallel damping resistance due to the detector
R_p = parallel damping resistance due to the A.G.C. detector and the amplifier valve resistance R_a

and R_1 and R_2 = primary and secondary coil series resistances.

If the magnification of each circuit is reduced to one-half by damping, it follows that the initial resonant impedance of each circuit equals the parallel damping resistance, thus the circuit constants are (Section 4.2.2)

$$\omega L_1 Q = R_p\,; \quad \omega L_2 Q = R_{DET}$$

where Q = initial undamped magnification of either circuit.

$$L_1 = \frac{R_p}{\omega Q} \qquad L_2 = \frac{R_{DET}}{\omega Q}$$

$$C_1 = \frac{1}{\omega^2 L_1} \qquad C_2 = \frac{1}{\omega^2 L_2}$$

$$R_1 = \frac{\omega L_1}{Q} \qquad R_2 = \frac{\omega L_2}{Q}$$

$$Qk = \frac{\omega M}{\sqrt{R_1 R_2}} = 1 \text{ or } M = \frac{\sqrt{R_1 R_2}}{\omega}.$$

The damping resistance due to the detector (R_{DET}) and that in R_p due to the A.G.C. detector may be taken as one-half of the A.C. load resistance (see Section 8.2.10). If the A.G.C. detector is delayed, its damping resistance only becomes fully effective when the R.F. voltage is much greater than the delay voltage. However, the maximum band width is not likely to be used unless strong signals are being received. Taking the value of Q obtained in the previous example, i.e., 126, and assuming that the A.C. load resistance of A.G.C. and detector diodes is 0·5 MΩ and that the valve slope resistance R_a is 1 MΩ, we have

$$R_p = \frac{1 \times 0{\cdot}25}{1{\cdot}25} = 0{\cdot}2 \text{ M}\Omega. \qquad R_{DET} = 0{\cdot}25 \text{ M}\Omega$$

$$L_1 = \frac{0{\cdot}2 \times 10^{12}}{6{\cdot}28 \times 4{\cdot}65 \times 10^5 \times 126} \qquad L_2 = \frac{0{\cdot}25 \times 10^{12}}{6{\cdot}28 \times 4{\cdot}65 \times 10^5 \times 126}$$

$$= 544\ \mu\text{H} \qquad = 680\ \mu\text{H}$$

$$R_{D1} = \tfrac{1}{2}\omega L_1 Q = 100{,}000\Omega$$

$$C_1 = 215\ \mu\mu\text{F} \qquad C_2 = 172\ \mu\mu\text{F}$$

$$R_1 = 12{\cdot}6\Omega \qquad R_2 = 15{\cdot}75\Omega$$

$$M = \frac{\sqrt{R_1 R_2}}{\omega Q k} = 4{\cdot}82\ \mu\text{H}.$$

Owing to coupling between the two circuits there is a greater variation of overall frequency response over the pass-range, and the

maximum at f_m is less than the maxima at the side frequencies. The effect is not very serious if a coupling of one-half critical is not exceeded.

The number of stages may be still further reduced by coupling the two pairs of overcoupled circuits loosely together as shown in Fig. 7.11*a*. The equivalent circuit is shown in Fig. 7.11*b* and the

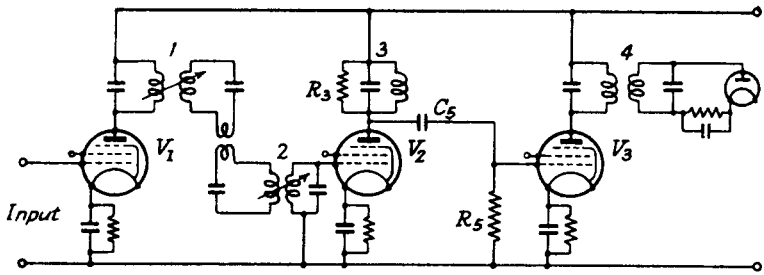

FIG. 7.11*a*.—A Variable Selectivity I.F. Amplifier with almost Constant Pass-band Response.

transfer impedance can be calculated by the method used in Section 7.3. By replacing the impedances by Z_1, Z_2, etc., the general expression for Z_T is

$$Z_T = \frac{E_2}{I_a}$$

$$= \frac{Z_1Z_3Z_5Z_7Z_9}{(Z_1+Z_2+Z_3)(Z_3+Z_4+Z_5)(Z_5+Z_6+Z_7)(Z_7+Z_8+Z_9) - Z_3^2(Z_5+Z_6+Z_7)(Z_7+Z_8+Z_9) - Z_5^2(Z_1+Z_2+Z_3)(Z_7+Z_8+Z_9) - Z_7^2(Z_1+Z_2+Z_3)(Z+Z_4+Z_5) + Z_3^2Z_7^2.}$$

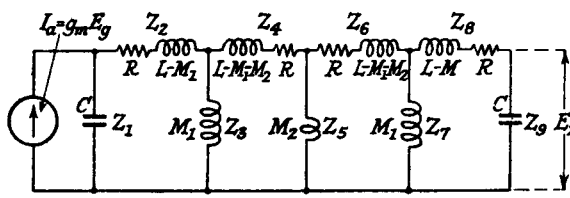

FIG. 7.11*b*.—The Equivalent Circuit for Two Loosely Coupled I.F. Transformers. [For Z_s read $L - M_1$ and R.]

If all the circuits have identical component values, as indicated in Fig. 7.11*b*

$$Z_1 = Z_9 = \frac{1}{j\omega C}; \quad Z_2 = Z_8 = R + j\omega(L - M_1)$$

$$Z_3 = Z_7 = j\omega M_1; \quad Z_4 = Z_6 = R + j\omega(L - M_1 - M_2), \quad Z_5 = j\omega M_2,$$

$$Z_1+Z_2+Z_3 = R+j\left(\omega l - \frac{1}{\omega C}\right) = Z_3+Z_4+Z_5 = Z_5+Z_6+Z_7$$
$$= Z_7+Z_8+Z_9 = R(1+jQF)$$

$$\therefore\ Z_T = \frac{j\dfrac{\omega^3 M_1^2 M_2}{\omega^2 C^2}}{R^4(1+jQF)^4+R^2\omega^2 M_1^2(1+jQF)^2+R^2\omega^2 M_2^2(1+jQF)^2 + R^2\omega^2 M_1^2(1+jQF)^2+\omega^4 M_1^4.}$$

$$\text{Numerator of } Z_T = \frac{\omega M_1^2 M_2}{C^2} = \frac{\omega}{\omega_m} R^4\left[\frac{\omega_m^3 L^3}{R^3}\cdot\frac{1}{\omega_m^2 C^2 R}\cdot\frac{M_1^2}{L^2}\cdot\frac{M_2}{L}\right]$$
$$= \frac{\omega}{\omega_m} R^4 Q^3 R_D k_1^2 k_2$$
$$\simeq R^4 Q^3 k_1^2 k_2 R_D.$$

Denominator of Z_T

$$= R^4\left[(1+jQF)^4+\frac{2\omega^2 M_1^2}{R^2}(1+jQF)^2+\frac{\omega^2 M_2^2}{R^2}(1+jQF)^2+\frac{\omega^4 M_1^4}{R^4}\right]$$
$$\simeq R^4[(1+jQF)^4+2Q^2k_1^2(1+jQF)^2+Q^2k_2^2(1+jQF)^2+Q^4k_1^4]$$
$$\simeq R^4[(1+Q^2(k_1^2-F^2))^2 - 4Q^2F^2+Q^2k_2^2(1-Q^2F^2) + j2QF(2+Q^2k_2^2+2Q^2(k_1^2-F^2))].$$

Hence

$$|Z_T| = \frac{Q^3 k_1^2 k_2 R_D}{\sqrt{[(1+Q^2(k_1^2-F^2))^2-4Q^2F^2+Q^2k_2^2(1-Q^2F^2)]^2 + 4Q^2F^2[2+Q^2k_2^2+2Q^2(k_1^2-F^2)]^2}} \quad . \quad 7.20a$$

when k_2 is small this approaches

$$|Z_T| = \frac{Q^3 k_1^2 k_2 R_D}{[1+Q^2(k_1^2-F^2)]^2+4Q^2F^2}$$

and the selectivity curve, which is determined by the denominator, is the same as that for two separated pairs.

At the mid-frequency f_m, $F = 0$ and

$$|Z_T| = \frac{Q^3 k_1^2 k_2 R_D}{(1+Q^2k_1^2)^2+Q^2k_2^2} \quad . \quad . \quad . \quad 7.20b$$

differentiating this with respect to k_1 and equating to zero gives for a maximum

$$Qk_{1(crit.)} = \sqrt[4]{1+Q^2k_2^2} \quad . \quad . \quad . \quad 7.21.$$

Replacing Qk_1 in 7.20*b* by this value

$$|Z_T| = \frac{Qk_2R_D\sqrt{1+Q^2k_2^2}}{(1+\sqrt{1+Q^2k_2^2})^2+Q^2k_2^2} = \frac{Qk_2R_D}{2(1+\sqrt{1+Q^2k_2^2})}. \quad 7.20c.$$

The overall amplification of the stage is

$$A = g_m \mid Z_T \mid = \frac{g_m Q k_2 R_D}{2(1+\sqrt{1+Q^2k_2^2})}$$

or $4\ A^2(1+Q^2k_2^2) = (g_m R_D Q k_2 - 2A)^2$

whence

$$Qk_2 = \frac{4Ag_mR_D}{g_m^2R_D^2 - 4A^2} \quad . \quad . \quad . \quad 7.22.$$

Taking the component values already used for the overcoupled circuits and loosely coupled single circuit, viz.,

$L = 1{,}000\ \mu H$, $C = 117\ \mu\mu F$, $Q = 126$, $Qk_2 = 0{\cdot}2$, $g_m = 1$ mA/volt
$R = 23{\cdot}2\Omega$, $R_D = 368{,}000\Omega$

$$A = g_m \mid Z_T \mid = \frac{1 \times 10^{-3} \times 368{,}000 \times 0{\cdot}2}{2(1+\sqrt{1{\cdot}04})}$$

$$= 18{\cdot}2.$$

This represents the maximum gain which can be obtained from the stage with loose enough coupling between the pairs of overcoupled circuits.

$$Qk_{1(crit.)} = \sqrt[4]{1+Q^2k_2^2} = \sqrt[4]{1{\cdot}04}$$

$$= 1{\cdot}01$$

$$M_{1(crit.)} = \frac{Qk_1R}{\omega_m} = \frac{1{\cdot}01 \times 23{\cdot}2 \times 10^6}{6{\cdot}28 \times 4{\cdot}65 \times 10^5}$$

$$= 8{\cdot}02\mu H.$$

For 2db. loss at ± 10 kc/s, Fig. 7.10 gives $Qk_{1(max.)} = 5$

$$\therefore\ M_{1(max.)} = 39{\cdot}7\ \mu H$$

$$M_2 = \frac{0{\cdot}2 \times 23{\cdot}2 \times 10^6}{6{\cdot}28 \times 4{\cdot}65 \times 10^5} = 1{\cdot}59\ \mu H.$$

The coupling reactance between the two circuits may, if desired, be a capacitance C_1, its value being determined from $Qk_2 = \frac{1}{\omega C_1 R}$,

thus

$$C_1 = \frac{10^6}{\omega R Q k_2} = \frac{10^6}{6{\cdot}28 \times 4{\cdot}65 \times 10^5 \times 23{\cdot}2 \times 0{\cdot}2}$$

$$= 0{\cdot}0738\ \mu F.$$

The three compromise circuits give a frequency response over the pass-band which is almost equal to that of the separated circuits if the loose coupling coefficient does not exceed appreciably the value given in the calculations. Stray capacitance coupling, in addition to the mutual inductance coupling, may occur and produce an asymmetrical overall frequency response. The effect can often

be reduced by reversing the sign of each mutual inductance element with respect to the preceding one.

7.8. Valve Input Admittance and Frequency Response. In the preceding theory we have assumed that the input admittance of each valve amplifier is zero over the pass-band. In practice the input admittance due to the valve anode-grid capacitance may be comparable with that of the circuits across which it is connected. This input admittance may be separated into two parallel components, resistive and reactive (see Section 2.8.2). The resistive component is from expression 2.9*a* (neglecting B_{g_a} in comparison with B_0)

$$R_g = \frac{(G_a+G_0)^2+B_0^2}{g_m B_{g_a} B_0} \quad . \quad . \quad . \quad 7.23a$$

where $G_a = \dfrac{1}{R_a}$ = anode slope conductance

G_0 = conductance of the external anode load admittance

B_0 = susceptance ,, ,, ,, ,, ,, ,,

g_m = mutual conductance of the valve

B_{g_a} = susceptance of the anode-grid capacitance.

The sign of R_g depends on B_0, being negative when B_0 is inductive and positive when B_0 is capacitive. With tuned anode circuits B_0 is inductive at frequencies lower than resonance, and capacitive for higher frequencies. The value of R_g is minimum when $B_0 = G_a+G_0$ and, for single or coupled circuits of normal Q, the minimum occurs in the pass-band of the amplifier. This tends to produce an overall lop-sided frequency response curve higher on the low-frequency side of resonance where R_g is negative. The grid parallel reactive component is always capacitive with a value (see expression 2.9*b*, again neglecting B_{g_a} in comparison with B_0).

$$C_g = C_{g_a}\left[1+\frac{g_m(G_a+G_0)}{(G_a+G_0)^2+B_0^2}\right] \quad . \quad . \quad 7.23b.$$

The variation of this component over the pass-band is generally negligible and compensation for its mistuning effect can be made on the grid-coil tuning capacitance. The resistive component cannot be ignored, and the only satisfactory solution is to isolate each stage from the next by a semi-aperiodic circuit. The dynamic resistance of this circuit must be much less than the minimum input resistance component of the succeeding valve, and it must also have a sufficiently low value to make the input resistance component of the valve, to which it is connected, very much greater than the dynamic resistance of the preceding circuit.. The ratio of minimum

grid input resistance to tuned circuit dynamic resistance R_D should not be less than 10 : 1. In order, therefore, to obtain satisfactory results it is necessary to insert an isolator semi-aperiodic stage between the variable coupling and the fixed coupling stages. The modified circuit appears as in Fig. 7.11*a*.

In order to determine the constants of the aperiodic circuit, we must calculate the input resistance component of valve V_3, connected to the two $Q/2$ loosely coupled circuits. Using the equivalent primary circuit developed in Section 7.6, the series resistive and reactive components reflected from the secondary into the primary inductance branch are

$$R_S = \frac{2\omega^2M^2}{R_2(4+Q^2F^2)} \text{ and } X_S = \frac{-\omega^2M^2QF}{R_2(4+Q^2F^2)}.$$

(Note that the equivalent secondary series resistance is $2R_2$ because the circuit is damped to $Q/2$, and that $Q = \frac{\omega L_1}{R_1} = \frac{\omega L_2}{R_2}$.)

The equivalent primary series resistance is $2R_1 + \frac{2\omega^2M^2}{R_2(4+Q^2F^2)}$ and the reactance of the inductive arm is

$$j\omega L_1 - \frac{j\omega^2M^2QF}{R_2(4+Q^2F^2)} \simeq j\omega L_1$$

when F is small, i.e., in the pass-band range.

Hence the total equivalent parallel resistance of the primary is very nearly (see Section 4.2.2.)

$$\frac{\omega^2L_1^2}{2R_1 + \frac{2\omega^2M^2}{R_2(4+Q^2F^2)}}$$

and, as this includes the amplifier valve anode resistance and A.G.C. damping because the primary series resistance is taken as $2R_1$, it is equal to $\frac{1}{G_a+G_0}$.

or

$$(G_a+G_0) = \frac{2R_1\left[1+\frac{\omega^2M^2}{R_1R_2(4+Q^2F^2)}\right]}{\omega^2L_1^2} = \frac{2\left[1+\frac{\omega^2M^2}{R_1R_2(4+Q^2F^2)}\right]}{\frac{\omega^2L_1^2}{R_1}} = \frac{2\left[1+\frac{Q^2k^2}{4+Q^2F^2}\right]}{R_{D1}} \quad . \quad . \quad . \quad 7.24a.$$

$$B_0 = \omega C_1 - \frac{1}{\omega L_1 - \dfrac{\omega^2 M^2 QF}{R_2(4+Q^2F^2)}}.$$

The reflected reactance term cannot now be neglected since ωC_1 is comparable with $\dfrac{1}{\omega L_1}$

$$B_0 = \frac{\omega^2 L_1 C_1 - 1 - \dfrac{\omega^2 M^2 QF \omega C_1}{R_2(4+Q^2F^2)}}{\omega L_1 - \dfrac{\omega^2 M^2 QF}{R_2(4+Q^2F^2)}}.$$

But $$\omega^2 L_1 C_1 - 1 = \left[\frac{\omega^2}{\omega_m{}^2} - 1\right] = F$$

and $$Q\omega C_1 = \frac{\omega^2 L_1 C_1}{R_1} = \frac{\dfrac{\omega^2}{\omega_m{}^2}}{R_1} \simeq \frac{1}{R_1}$$

$$\therefore\ B_0 \simeq \frac{F - \dfrac{\omega^2 M^2 F}{R_1 R_2(4+Q^2F^2)}}{\omega L_1}$$

$$= \frac{F}{\omega L_1}\left[1 - \frac{Q^2k^2}{4+Q^2F^2}\right]$$

$$= \frac{QF}{R_{D1}}\left[1 - \frac{Q^2k^2}{4+Q^2F^2}\right] \quad . \quad . \quad . \quad 7.24b.$$

Note that F is negative at frequencies below resonance, and hence B_0 is negative (inductive).

If we consider the case of the two loosely coupled $Q/2$ circuits, as shown in the anode circuit of V_3 in Fig. 7.11*a*, $Qk = 1$ and expressions 7.24*a* and 7.24*b* become

$$G_a + G_0 = \frac{2}{R_{D1}}\left[1 + \frac{1}{4+Q^2F^2}\right] \quad . \quad . \quad . \quad 7.25a$$

and $$B_0 = \frac{QF}{R_{D1}}\left[1 - \frac{1}{4+Q^2F^2}\right] \quad . \quad . \quad 7.25b$$

and replacing (G_a+G_0) and B_0 in expression 7.23*a* we have

$$R_g = \frac{4(5+Q^2F^2)^2 + Q^2F^2(3+Q^2F^2)^2}{g_m B_{g_a} R_{D1} QF (3+Q^2F^2)(4+Q^2F^2)}$$

$$= \frac{25+6Q^2F^2+Q^4F^4}{g_m B_{g_a} R_{D1} QF (3+Q^2F^2)} \quad . \quad . \quad . \quad . \quad 7.23c.$$

To find the condition for a minimum value of R_g, it is necessary to

differentiate 7.23c with respect to F and equate to 0. A cubic equation in Q^2F^2 results:

$$Q^6F^6+3Q^4F^4 - 57Q^2F^2 - 75 = 0.$$

One solution of which is

$$Q^2F^2 = 6{\cdot}86 \text{ or } QF = \pm 2{\cdot}62.$$

Replacing QF in 7.23c by 2·62 gives

$$R_{g(min.)} = \frac{4{\cdot}38}{g_m B_{g_a} R_{D1}}.$$

If we assume that the anode-grid capacitance of V_3 (Fig. 7.11a) = 0·005 $\mu\mu$F and g_m = 3 mA/volt and that the dynamic resistance of one $Q/2$ circuit is R_{D1} = 100,000Ω (as calculated for the previous example), the minimum grid input resistance of V_3 is

$$R_{g(min.)} = \frac{4{\cdot}38 \times 10^{12}}{3 \times 10^{-3} \times 6{\cdot}28 \times 4{\cdot}65 \times 10^5 \times 0{\cdot}005 \times 100{,}000} = 1\text{M}\Omega$$

so that the dynamic resistance R_{DA} of the isolator or semi-aperiodic tuned circuit must not exceed 100,000Ω if the ratio of $\frac{R_{g(min.)}}{R_{DA}}$ is not to exceed 10.

We have yet to consider the minimum grid input resistance of the isolator valve V_2, as this must not be less than 10 times the dynamic resistance of the circuit between grid and earth. The conductance and susceptance of the isolator anode circuit are from expressions 4.7 in Section 4.2.2.

$$G_0 = \frac{R}{\omega^2 L^2} = \frac{1}{R_{DA}}$$

$$B_0 = \frac{\omega^2 LC - 1}{\omega L} = \frac{F}{\omega L} \simeq \frac{QF}{R_{DA}}.$$

Note that X_p in expression 4.7 is positive and that a positive X_p is equal to $-B_0$. Hence the change of sign in the numerator of B_0.

$$\therefore R_g = \frac{\left(\frac{1}{R_a}+\frac{1}{R_{DA}}\right)^2+\left(\frac{QF}{R_{DA}}\right)^2}{g_m B_{g_a} \frac{QF}{R_{DA}}}$$

$$= \frac{Q^2F^2+\left(1+\frac{R_{DA}}{R_a}\right)^2}{g_m B_{g_a} QF R_{DA}} \quad . \quad . \quad . \quad 7.26a$$

where $R_a = \frac{1}{G_a}$ = the slope resistance of V_2.

At frequencies below resonance F is negative and R_g is negative. Regeneration of the input circuit therefore occurs. For frequencies above resonance R_g is positive and degeneration occurs.

The condition for minimum R_g is found by differentiating 7.26*a* with respect to F and equating to 0. Thus

$$QF = 1 + \frac{R_{DA}}{R_a} \quad . \quad . \quad . \quad . \quad 7.27.$$

If $R_a \gg R_{DA}$ — in practice this is generally true — $QF = 1$ and

$$R_{g(min.)} = \frac{2}{g_m B_{g_a} R_{DA}} \quad . \quad . \quad . \quad 7.26b.$$

Taking the maximum grid circuit resistance as the dynamic resistance of one of the tuned circuits forming the two pairs of overcoupled circuits in the anode of V_1, i.e., as 368,000Ω, the minimum grid input resistance of the isolator valve V_2 must not be less than 3·68 MΩ. If the grid-anode capacitance of V_2 is 0·005 $\mu\mu$F and g_m is 3 mA/volt, the maximum permissible dynamic resistance of the isolator-tuned circuit is from 7.26*b*.

$$R_{DA} = \frac{2}{g_m B_{g_a} R_{g(min.)}}$$

$$= \frac{2 \times 10^{12}}{3 \times 10^{-3} \times 6{\cdot}28 \times 4{\cdot}65 \times 10^5 \times 0{\cdot}005 \times 3{,}680{,}000}$$

$$= 12{,}400\Omega.$$

The amplification of this stage is $g_m R_{DA} = 37{\cdot}2$. It is clear in this particular example that the factor limiting R_{DA} is the input grid resistance of the valve V_2, in the anode circuit of which it is connected. Having fixed the value of R_{DA} it is necessary now to decide on the Q, L and C of the circuit. From 7.27, the grid input resistance is a minimum at $QF = 1$, i.e., at an off tune frequency $\Delta f = \frac{f_m}{2Q}$ and the only condition governing Δf is that it should be as far outside the pass range as possible. Let us assume that $\Delta f = 30$ kc/s, then

$$Q = \frac{465}{60} = 7{\cdot}75$$

and

$$L = \frac{R_{DA}}{\omega Q} = 547 \ \mu\text{H}$$

$$C = 214 \ \mu\mu\text{F}$$

$$R = 206\Omega.$$

The isolator circuit does not give an absolutely flat response over the pass-band and the loss in decibels is $20 \log \sqrt{1 + Q^2F^2} = 0{\cdot}44$ db. for $\Delta f = 10$ kc/s. The effect of the circuit on the overall response

may therefore be neglected. The variation of R_g (calculated from 7.26*b*) over a range of modulation frequencies from 1 to 100 kc/s is shown in Fig. 7.12. The variation of C_g over the same range of frequencies is also shown; its value from 7.23*b* is

$$C_g = C_{g_a}\left[1+\frac{g_m(G_a+G_0)}{(G_a+G_0)^2+B_0^2}\right]$$

$$\simeq C_{g_a}\left[1+\frac{g_m R_{DA}}{1+Q^2F^2}\right] . \quad . \quad . \quad . \quad 7.28$$

when $$R_a \gg R_{DA}.$$

Its variation over the pass-range is seen to be negligible; since it is dependent on g_m, C_g is reduced if the g_m of the valve is reduced,

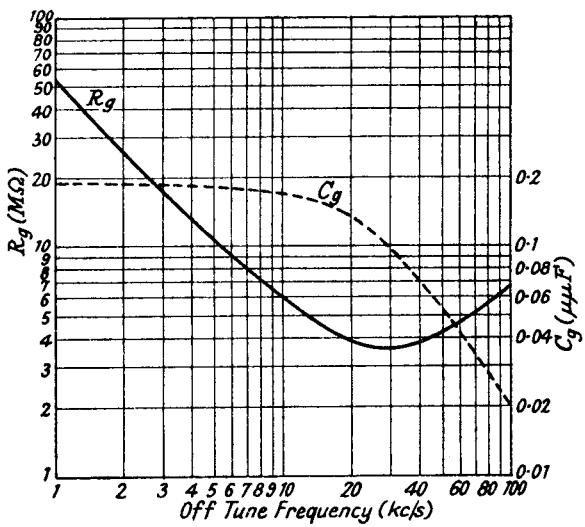

FIG. 7.12.—Curves showing the Variation of Grid Input Resistance and Capacitance for the Isolator Stage.

e.g., by A.G.C. action. A variation of g_m from 3 to 0·1 mA/volt causes a change of 0·1798 $\mu\mu$F in C_g, and this represents a mistuning of approximately 0·358 kc/s for the over-coupled circuit having a tuning capacitance of 117 $\mu\mu$F, a not very serious tuning error.

7.9. Cathode Feedback and Variable Selectivity.[16, 18] Cathode feedback may be used in an I.F. amplifier to give a level pass-band frequency response and to sharpen the attenuation outside this range, when variable selectivity is produced by changing mutual inductance between coupled tuned circuits. Two parallel-tuned circuits are included in series between the cathode and earth

as shown in Fig. 7.13*a*. One is tuned to (f_m+9) kc/s and the other to (f_m-9) kc/s. (Medium wave stations are normally separated by 9 kc/s.) These circuits provide negative feedback with considerable attenuation at the two resonant frequencies. The figure shows the tuned circuits as transformer coupled, and this is done

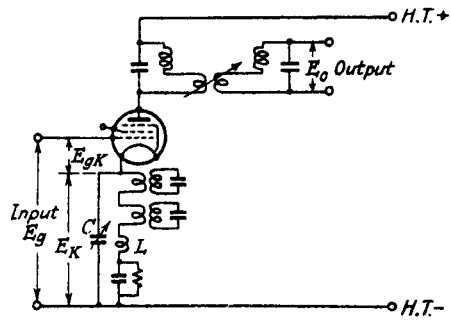

FIG. 7.13*a*.—An I.F. Amplifier with Cathode Feedback.

in order to reduce the impedance at f_m so that the loss over the pass-band range may be as small as possible. A fuller explanation is given at the end of this section. The coil L (of low inductance) and capacitance C (a small trimmer) are generally found necessary with the transformer coupling arrangement, in order to produce symmetry of the frequency response feedback characteristic. The frequency response due to feedback is shown in Fig. 7.13*b*, and by

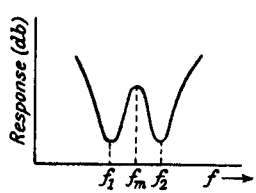

FIG. 7.13*b*.—The Frequency Response due to Cathode Feedback.

suitable design it is possible to neutralize the trough normally produced by overcoupled circuits in the anode and grid of the valve. The principle underlying the method has already been discussed in Section 2.7, where it is shown that the output voltage in the anode circuit is (expression 2.5*d*)

$$E_0 = \frac{g_m E_g Z_T}{1+g_m Z_k}$$

or overall amplification $= \dfrac{E_0}{E_g} = \dfrac{g_m Z_T}{1+g_m Z_k} = g_m' Z_T.$

By plotting $20 \log_{10} \frac{g_m}{g_{m'}}$ against frequency we obtain the frequency loss in decibels due to cathode feedback, and adding this curve to the Z_T curve gives the overall response of the stage. To do this we must obtain the generalized expression for the cathode impedance. The expression for a parallel resonant circuit impedance (obtained by rationalizing expression 4.8*b*) is

$$Z = \frac{R_D(1 - jQF)}{1+Q^2F^2}$$

where $R_D = \frac{\mathrm{L}}{CR}$; $F = \frac{2\Delta f'}{f_1}$ and $f_1 =$ the resonant frequency. However, we do not wish to refer to f_1 but to the intermediate frequency f_m. If $f_1 < f_m$

$$\frac{2\Delta f'}{f_1} = \frac{2(\Delta f_1+\Delta f)}{f_1} \quad . \quad . \quad . \quad 7.29$$

where $f_m - f_1 = \Delta f_1$ and Δf is now referred to f_m as zero, i.e., equals $-[f_m - (f_1+\Delta f')]$.

That this is correct is proved by noting that $\Delta f = -\Delta f_1$ referred to f_m gives $\Delta f'$ referred to f_1.

When Δf_1 is small, $f_1 \simeq f_m$, and 7.29 becomes

$$2\left[\frac{\Delta f_1}{f_m}+\frac{\Delta f}{f_m}\right]$$

and

$$Z_1 = \frac{R_D\left[1 - j2Q\left(\frac{\Delta f_1}{f_m}+\frac{\Delta f}{f_m}\right)\right]}{1+4Q^2\left(\frac{\Delta f_1}{f_m}+\frac{\Delta f}{f_m}\right)^2}$$

rewriting $\frac{2\Delta f_1}{f_m}$ as F_1 and $\frac{2\Delta f}{f_m}$ as F we have

$$Z_1 = \frac{R_D[1 - jQ(F_1+F)]}{1+Q^2(F_1+F)^2} \quad . \quad . \quad . \quad 7.30a.$$

Similarly for the other circuit ($f_2 > f_m$ and the j term is positive)

$$Z_2 = \frac{R_D[1+jQ(F_2 - F)]}{1+Q^2(F_2 - F)^2}$$

$$= \frac{R_D[1+jQ(F_1 - F)]}{1+Q^2(F_1 - F)^2} \quad . \quad . \quad 7.30b$$

for $f_2 - f_m = \Delta f_2 = f_m - f_1 = \Delta f_1$

$$\therefore \quad F_2 = \frac{\Delta f_2}{f_m} = F_1 = \frac{\Delta f_1}{f_m}$$

$$Z_k = Z_1 + Z_2 = \frac{2R_D[1+Q^2(F_1^2+F^2) - jQF(1 - Q^2(F_1^2 - F^2))]}{[1+Q^2(F_1+F)^2][1+Q^2(F_1 - F)^2]}$$

$$Z_k = \frac{2R_D\sqrt{[1+Q^2(F_1^2+F^2)]^2+Q^2F^2[1 - Q^2(F_1^2 - F^2)]^2}}{1+2Q^2(F_1^2+F^2)+Q^4(F_1^2 - F^2)^2} \quad . \quad 7.31a$$

$$= \frac{2R_D\sqrt{\begin{array}{r}([1+Q^2(F_1^2+F^2)]^2 - 4Q^4F_1^2F^2) \\ +Q^2F^2([1 - Q^2(F_1^2 - F^2)]^2+4Q^2F_1^2)\end{array}}}{[1+Q^2(F_1^2+F^2)]^2 - 4Q^4F_1^2F^2}$$

$$= \frac{2R_D\sqrt{\begin{array}{r}[(1+Q^2(F_1^2+F^2))^2 - 4Q^4F_1^2F^2] \\ +Q^2F^2[(1+Q^2(F_1^2+F^2))^2 - 4Q^4F_1^2F^2]\end{array}}}{[1+Q^2(F_1^2+F^2)]^2 - 4Q^4F_1^2F^2}$$

$$= \frac{2R_D\sqrt{1+Q^2F^2}}{\sqrt{[1+Q^2(F_1^2+F^2)]^2 - 4Q^4F_1^2F^2}} \quad . \quad . \quad . \quad . \quad 7.31b.$$

The above expression contains three possible variables R_D, QF_1 and QF, and it is desirable to reduce to two if generalized curves are to be obtained. It is possible to replace R_D, if the permissible loss due to feedback at f_m is fixed. Let us assume this to be 3 dbs.

At $f = f_m$, $F = 0$, expression 7.31*b* becomes $\frac{2R_D}{1+Q^2F_1^2}$; for 3db. loss $\frac{g_m}{g_m'} = 1{\cdot}414$

or $$1+g_mZ_k = 1{\cdot}414$$

$$g_mZ_k = 0{\cdot}414 = \frac{g_m2R_D}{1+Q^2F_1^2}$$

or $$2R_D = \frac{0{\cdot}414(1+Q^2F_1^2)}{g_m} \quad . \quad . \quad . \quad 7.32.$$

Replacing this in 7.31*b*.

$$|Z_k| = \frac{0{\cdot}414(1+Q^2F_1^2)}{g_m}\sqrt{\frac{1+Q^2F^2}{[1+Q^2(F_1^2+F^2)]^2 - 4Q^4F_1^2F^2}}$$

and the frequency response loss

$$20\log_{10}(1+g_mZ_k)$$

$$= 20\log_{10}\left[1+\frac{0{\cdot}414(1+Q^2F_1^2)\sqrt{1+Q^2F^2}}{\sqrt{[1+Q^2(F_1^2+F^2)]^2-4Q^4F_1^2F^2}}\right] . \quad 7.33.$$

This is plotted in Fig. 7.14 against QF for different values of $Q^2F_1^2$. The QF scale can be converted to an off-tune frequency scale as shown for the generalized coupled circuit curves in Fig. 7.7. To illustrate the use of the curves let us take the following example: $f_m = 465$ kc/s, the cathode circuits are to give maximum attenuation

at ± 9 kc/s, and a flat pass-band is required over a maximum range of ± 6 kc/s when the cathode circuits are used in conjunction with a pair of coupled circuits. The design procedure is as follows : the maximum permissible Q of the cathode circuits, which is the determining factor, should be as high as possible for maximum sharpness of cut-off outside the pass-band. At the same time the maximum Q curve may not give the flattest pass-band in conjunction with

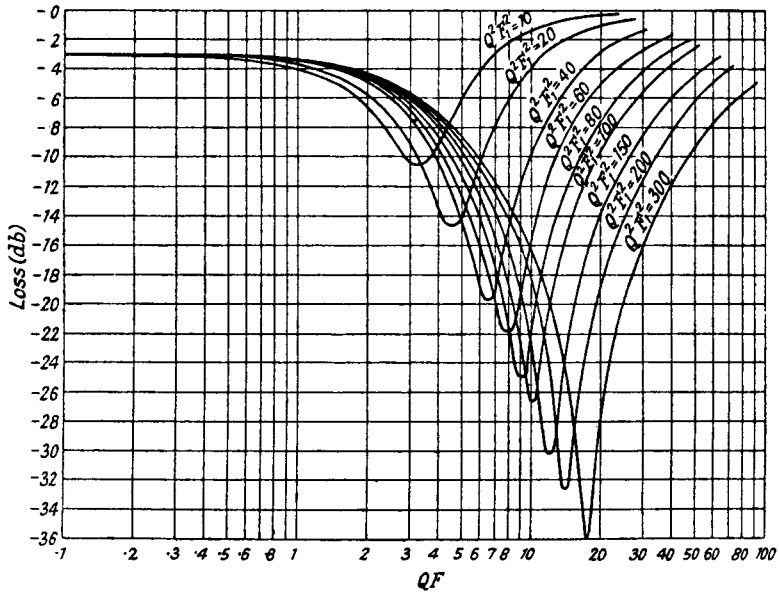

FIG. 7.14.—Generalized Selectivity Curves for Cathode Feedback.

the coupled circuits, and a compromise may be necessary. Let $Q = 225$; this automatically fixes $(QF_1)^2$ and the frequency scale

$$(QF_1)^2 = \left[\frac{225 \times 2 \times 9}{465}\right]^2 = 76 \simeq 80.$$

For a flat overall pass-band response the shape of the cathode feedback curve must be the reverse of the coupled circuit curve, and the former reversed should fit exactly over the latter in the pass-band range. The curve for $(QF_1)^2 = 80$ is therefore redrawn on tracing paper with the correct frequency scale but with the loss scale reversed. This curve is then placed on top of Fig. 7.7 and moved along until it fits as nearly as possible over a generalized coupled circuit curve up to 6 kc/s. The most suitable curve is that for $Qk = 6$ with $\Delta f = 1$ kc/s registering with $QF = 1$ on Fig. 7.7,

and the two curves are shown in Fig. 7.15. The overall response curve is obtained by plotting the difference between the two curves. The frequency scale for the coupled circuits is now fixed ($QF = 1$ when $\Delta f = 1$ kc/s), and Q and k are therefore 232·5 and 0·0258 respectively. The required value of Q for the coupled circuits is rather higher than would normally be obtainable, and a more practical value is found by assuming that two pairs of overcoupled

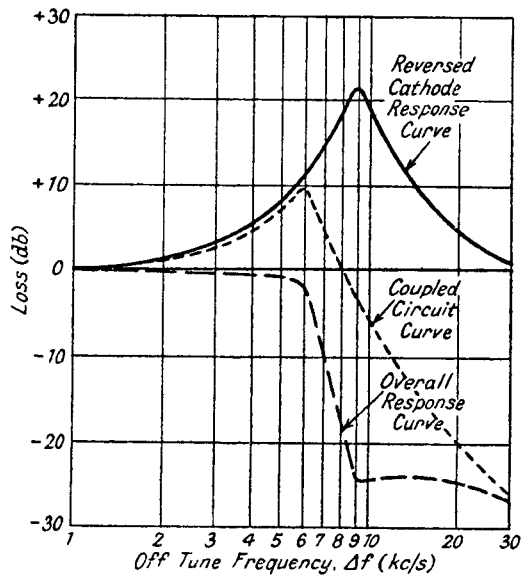

FIG. 7.15.—The Overall Frequency Response Curve for Cathode Feedback Compensation.

circuits (one in the grid and the other in the anode circuit of the valve) have to be compensated. The procedure then is to fit the curve from Fig. 7.14 over Fig. 7.7 with the loss scale of Fig. 7.7 multiplied by 2. The required Q of the overcoupled circuits is then approximately halved.

The constants for the cathode circuits can be determined by using 7.32.

$$R_D = \frac{0{\cdot}414(1+Q^2F_1^2)}{2g_m} = \frac{0{\cdot}414 \times 81}{2 \times 10^{-3}} = 16{,}800\Omega$$

if $g_m = 1$ mA/volt.

$$L = \frac{R_D}{\omega Q} = \frac{16{,}800 \times 10^6}{6{\cdot}28 \times 4{\cdot}65 \times 10^5 \times 225}\ \mu\text{H}$$
$$= 25{\cdot}5\ \mu\text{H}.$$

It is almost impossible to realize practically at 465 kc/s a Q of 225 for such a low inductance, and the most satisfactory method is to adopt transformer coupling to the tuned circuits. The resonant impedance of a transformer coupled tuned circuit is given in expression 4.29*b* (Section 4.4.2) as $\frac{\omega^2 M^2}{R_T}$ and it can be written as

$$\frac{\omega^2 M^2}{R_T} = \frac{\omega^2 M^2}{L_1 L_T} \cdot \frac{L_1 L_T}{R_T} = \frac{M^2}{L_1 L_T} \cdot \omega L_1 \cdot \frac{\omega L_T}{R_T} = k^2 \omega L_1 Q$$

where L_1 = inductance of the cathode coil
Q = the magnification of the tuned secondary coil.

By adjusting k any value of secondary coil inductance may be chosen to give the required resonant impedance.

Variable selectivity is produced in the normal manner by varying the mutual inductance between the coupled circuits, and an almost level pass-band response is maintained as selectivity is increased.

The cathode feedback curve is affected by varying the gain of the valve, and increasing bias decreases the loss. It is therefore possible to obtain variable selectivity by varying the grid bias of the valve. For example, suppose that the coupled circuits are adjusted to give a double-peaked frequency response, and the cathode circuits are designed to overcompensate at maximum gain so that a single-peaked overall response curve is obtained. Increase of bias reduces the cathode compensation and widens the pass-band. At high negative biases the cathode circuits have practically no effect, and the overall frequency response is the wide band double-peaked curve of the coupled circuits. The application of A.G.C. to such a stage automatically produces variable selectivity, with high selectivity for weak signals and low selectivity for strong signal voltages.

7.10. Automatic Variable Selectivity.[7, 11, 12] Many types of circuits have been developed for varying automatically the selectivity of a receiver. The control may be exercised by the desired signal or the interference. The ideal arrangement is by differential control from both, so that either decreasing desired signal or increasing interference causes an increase in selectivity. Methods of achieving automatic selectivity may be conveniently divided into three groups. In the first, selectivity is controlled by varying the damping of the tuned circuits,[8] in the second by varying the coupling reactance [13] between the circuits, and in the third by mistuning the circuits.

Variation of damping can be obtained by paralleling the tuned

circuits with triode valves, the anode-cathode resistance of which is controlled by varying their grid bias. The valves are initially biased so that anode current is almost cut off and the anode-cathode resistance is consequently very high. Positive bias, increasing as the desired signal increases, is derived from the detector load resistance, and the anode current of the damping valves thus increases, their resistance falls and selectivity decreases. This method is not very satisfactory because the ideal selectivity curve shape cannot be produced by damping, and widening of the pass-band is accompanied by appreciable loss of attenuation outside the band. In addition, owing to curvature of the valve characteristics, the anode-cathode resistance is not constant over the signal voltage cycle, and distortion of the latter occurs.

Automatic selectivity control by coupling reactance variation may be obtained by a relay, varying the disposition of the coupling coils between the primary and the secondary of the I.F. transformers. The relay may be controlled by the D.C. component of the input carrier at the detector, increasing the coupling as the carrier increases. Polarized variable capacitors [17] (as described in Chapter 13) may be employed as variable shunt and series couplings between the primary and secondary circuits of the I.F. transformer. Their capacitance values are controlled by varying the D.C. potential between their plates. The series capacitance coupling chiefly controls the low frequency side of the selectivity curve, whilst the shunt coupling controls the high frequency side. Increase of selectivity results from a decrease in the series capacitance and an increase in the shunt capacitance. For the most favourable conditions of reception the pass-range is a maximum, and the selectivity curve has a double-humped frequency response. Decrease of the series capacitance increases the frequency of the lower frequency peak, thus narrowing the pass-band on the low-frequency side of the carrier, whilst increase of the shunt capacitance decreases the frequency of the higher peak and narrows the pass-band on that side of the carrier. The selectivity curve can therefore be narrowed from either side, and the control voltages for the capacitors are derived from a discriminator circuit (similar to that for automatic frequency control and described in Chapter 13) responsive to the interference. Interference on the low-frequency side of the carrier produces a voltage reducing the series capacitance value, and that on the high-frequency side increases the shunt capacitance value.

Mistuning of the primary and secondary of the I.F. transformers in opposite directions, using these polarized capacitors, may also

be used to give the same result, but overall amplification is reduced.

A circuit [19] which combines mistuning with increased selectivity in the I.F. amplifier is shown in Fig. 7.16. The mistuning is brought about by moving the carrier away from the centre of the I.F. amplifier pass-band and in the direction of the interfering voltage. This asymmetric expansion is produced by the discriminator circuits T_1 and T_2 (generally tuned to $f_m \pm 9$ kc/s), the detected voltages from which are connected in series with the automatic frequency correction bias voltage to the variable reactance valve across the oscillator-tuned circuit. These discriminator circuits T_1 and T_2 are also used to produce a flat pass-band response and sharp cut-offs as described in Section 7.9. The A.F.C. discriminator circuits T_3 and

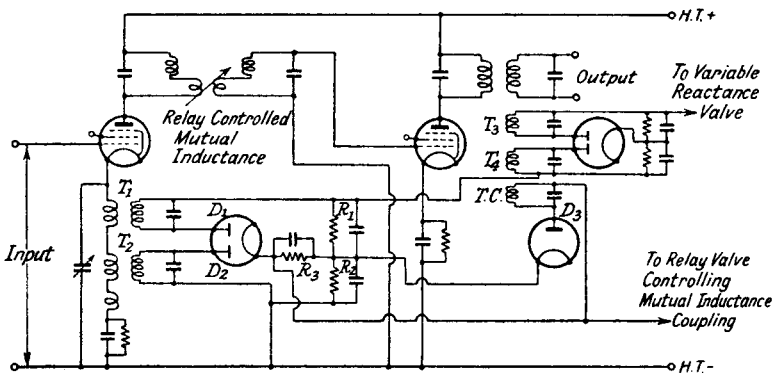

FIG. 7.16.—Automatic Variable Selectivity Control by Differential Action of the Signal and Interference Voltages.

T_4 correct for normal tuning errors and oscillator drift (see Section 13.4). The extra differential bias developed across the resistances R_1 and R_2 reacts on the oscillator frequency to move the interference more into the attenuating part of the I.F. amplifier frequency response. The overall width of the pass-band of the amplifier is controlled by a valve-operated relay connected across the resistance (R_3) in common with diodes D_1 and D_2. The relay controls the mutual inductance coupling between the I.F. tuned circuits. The circuit T.C. is tuned to the I.F. carrier frequency and its output is detected by the diode D_3, which is connected to R_3, so that the detected current opposes that due to the interference. Thus the I.F. selectivity is controlled by differential action of interference and desired signal, increase of the former and decrease of the latter increasing selectivity.

7.11. Signal Handling Capacity of the I.F. Amplifier Valve. For A.G.C. design purposes the signal-handling capacity of the I.F. amplifier valve requires to be known at different grid biases. The signal-handling capacity of a valve is defined as the maximum input (and output) carrier voltage, modulated at a given percentage, which can be accepted for a given percentage distortion of the modulation envelope. The percentage modulation should be as high as possible, and its maximum value is limited to some extent by distortion of the modulation envelope at the detector. A modulation percentage of 60 is a convenient practical value for measurement purposes, but 80% may be used if the detector circuit is designed to reduce envelope distortion (mainly due to an A.C. to D.C. load-resistance ratio less than unity) to a minimum. A usual value for audio frequency harmonic distortion is 5%, and

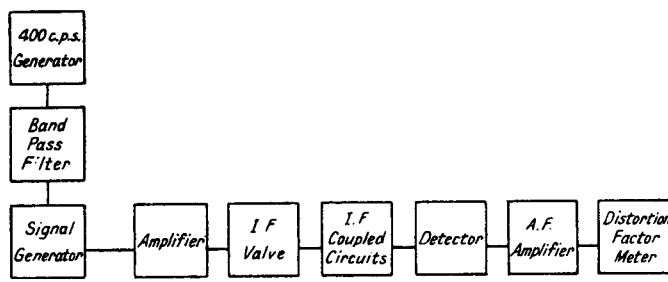

FIG. 7.17.—A Schematic Diagram for the Measurement of Signal Handling Capacity.

the results are expressed in the form of curves of input and output carrier peak voltage against grid bias for 5% total harmonic distortion of the audio output voltage from the detector.

A schematic diagram of the apparatus is shown in Fig. 7.17 and it is mainly self-explanatory. The modulating source has a frequency of 400 c.p.s., the normal test frequency for receiver measurements, and it is filtered so as to reduce distortion in the modulating voltage to very small values. The signal generator should be anode-modulated direct from the filtered 400 c.p.s., because modulation by anode voltage variation generally gives least modulation envelope distortion. An amplifier is required between the signal generator and I.F. valve because the maximum input signal carrier voltage is generally about 8 volts, and it may conveniently be a tetrode valve with an anode circuit tuned to the I.F. A diode detector, previously calibrated, is a suitable measuring device for the I.F. input carrier. The coupled circuits in the I.F. valve anode must be adjusted for single-peaked frequency response in order to

eliminate the possibility of asymmetrical side-band amplification due to mistuning. The diode detector has special features and the circuit is shown in Fig. 7.18. The D.C. load resistance consists of 0·5 MΩ fixed resistance, R_1, in series with a 20,000Ω potentiometer (R_2). A microammeter, which measures the mean current due to the output carrier voltage, is inserted in the detector cathode circuit. The A.F. output is taken from the potentiometer through a coupling capacitance C_2 and R.F. filter R_3C_3 to the grid of an A.F. amplifier. A 2 MΩ grid leak R_4 completes the D.C. path for the amplifier.

These precautions are taken in order to prevent the modulation

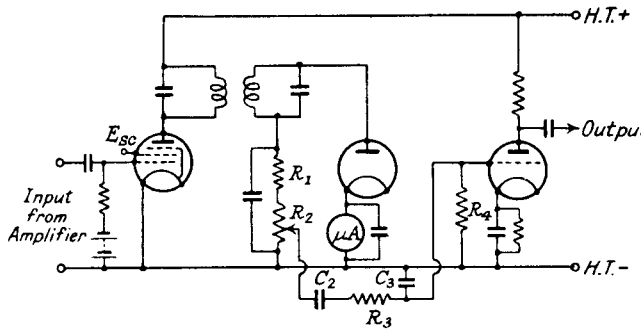

FIG. 7.18.—The A.F. Valve and Detector Circuit for the Measurement of Signal Handling Capacity

envelope distortion mentioned in Section 8.2.3. The maximum permissible modulation percentage is approximately

$$\frac{2 \times 10^6}{2{\cdot}03 \times 10^6} \times 100 = 98{\cdot}5\%,$$

so that distortion due to the detector A.C. load resistance is not likely to occur at a test modulation percentage of 80%. The first A.F. amplifier valve is followed by a second, preferably a power output triode, the output from which is connected to a distortion factor meter.

Care must be taken to ensure that distortion in the apparatus other than the test valve is as small as possible ; a minimum value of about 1% may be expected at 80% modulation. Distortion in the A.F. amplifier may be checked by connecting the output from the 400 c.p.s. filter to the 20,000-ohm potentiometer. The diode detector valve must be removed from its socket when the test is made. Distortion in the amplifier following the signal generator may be checked by connecting the diode detector to its output.

The procedure is to increase the input signal until 5% total harmonic distortion is registered on the distortion factor meter. Typical curves are shown in Fig. 7.19, and their usefulness is discussed in Section 12.4.2. A point which should be noted is that at high negative biases there may be two input voltages for 5% distortion, one a high value and the other a very low one. The first should be regarded as the correct, since the low value can only be found by starting from zero signal at the high negative bias. The high value is always obtained when the input is (as is normal in A.G.C.) increased as the bias is increased.

The mutual conductance of the valve under operating conditions

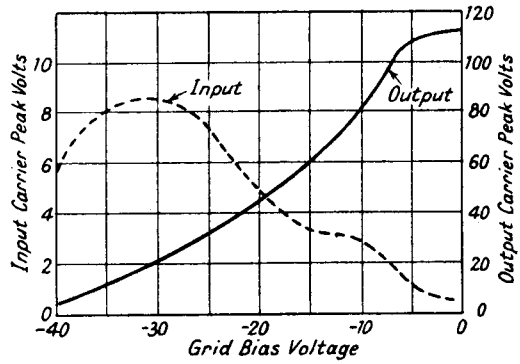

FIG. 7.19.—Typical Signal Handling Capacity Curves for an I.F. Amplifier for 5% Modulation Envelope Distortion and 80% Modulation of the Carrier.

may be calculated from the grid input carrier voltage, the output carrier voltage across the primary of the I.F. transformer, and the primary impedance. Thus

$$g_m = \frac{\hat{E}_p}{\hat{E}_s R_{Dp}}$$

where $\hat{E}_p$ = carrier peak voltage across the primary
$\hat{E}_s$ = ,, ,, ,, applied to the grid
R_{Dp} = resonant impedance of the primary.

R_{Dp} may be measured by using a peak voltmeter and a non-inductive resistance as described in Section 5.6.4. The current in the diode detector across the secondary may be used as a measure of primary volts by calibrating it against peak primary volts as measured by the peak voltmeter.

The signal handling capacity of an R.F. amplifier valve or a frequency changer may be measured in the same way. In th case

of a frequency changer a local oscillator is required and the signal generator carrier frequency is adjusted to any convenient signal frequency.

There are methods of measuring indirectly, and of calculating the signal-handling capacity of a valve, and a description of these is given in Sections 4.7.1 and 4.7.2.

BIBLIOGRAPHY

1. Analysis of Frequency in Oscillating Circuits. G. W. O. Howe, *Electrical World* (New York), August 19th, 1916.
2. Band-Pass Filters in Radio Receivers. G. W. O. Howe, *Wireless Engineer*, May 1931, p. 233.
3. The Analysis and Design of a Chain of Resonant Circuits. M. Reed, *Wireless Engineer*, May (p. 259) and June (p. 320), 1932.
4. Coupling and Coupling Coefficients. G. W. O. Howe, *Wireless Engineer*, Sept. 1932, p. 485.
5. Two Element Band Pass Filters. R. T. Beatty, *Wireless Engineer*, Oct. 1932, p. 546.
6. High Fidelity Receivers with Expanding Selectors. H. A. Wheeler and J. K. Johnson, *Proc. I.R.E.*, June 1935, p. 594.
7. Automatic Selectivity Control. B. D. Corbett, *Wireless World*. Nov. 29th, 1935, p. 554.
8. Automatic Selectivity Control. G. L. Beers, *Proc. I.R.E.*, Dec. 1935, p. 1,425.
9. Variable Selectivity and the I.F. Amplifier. W. T. Cocking, *Wireless Engineer*, March (p. 119), April (p. 179), May (p. 237), 1936.
10. Variable Selectivity. H. J. Benner, *Radio Engineering*, May 1936, p. 12.
11. Automatic Band Width Regulation. O. Köhler, *Funktechnische Monatshefte*, Sept. 1936, p. 337.
12. Variable Fidelity Control and Automatic Selectivity Control. A. W. Barber, and H. F. Mayer, *Radio Engineering*, Jan. 1937, p. 5.
13. American Automatic Selectivity Control. *Wireless World*, March 26th, 1937, p. 296.
14. Resistance Control of Mutual Inductance Coupling. K. R. Sturley, *Marconi Review*, March–April 1937, p. 1.
15. The Design of Coupling Filters in Broadcast Receivers. G. W. O. Howe, *Wireless Engineer*, June (p. 289) and July (p. 347), 1937.
16. Frequency Selective Feedback Applied to the Design of Band Pass Amplifiers. J. D. Brailsford, *Marconi Review*, January–March 1938, p. 10.
17. Broadcast Receivers. A Review. N. M. Rust, O. E. Keall, J. F. Ramsay and K. R. Sturley, *Jour. I.E.E.*, June 1941, Part III, p. 59.
18. British Patent No. 490,819. N. M. Rust, J. D. Brailsford and Marconi's Wireless Telegraph Coy.
19. British Patent No. 501,760. O. E. Keall, N. M. Rust and Marconi's Wireless Telegraph Coy.

CHAPTER 8

DETECTION

8.1. Introduction. To obtain the audio frequency intelligence conveyed in an amplitude modulated carrier it is necessary to employ a detector to suppress or reduce the amplitude of one-half of the modulation envelope. An example of a modulated wave before and after detection has already been given in Figs. 1.1 and 1.4. The suppression of the negative modulation envelope (shown in Fig. 1.4) produces a mean voltage which is an exact reproduction, to a smaller amplitude, of the modulation envelope. This mean voltage variation can be applied to an A.F. amplifier terminated by

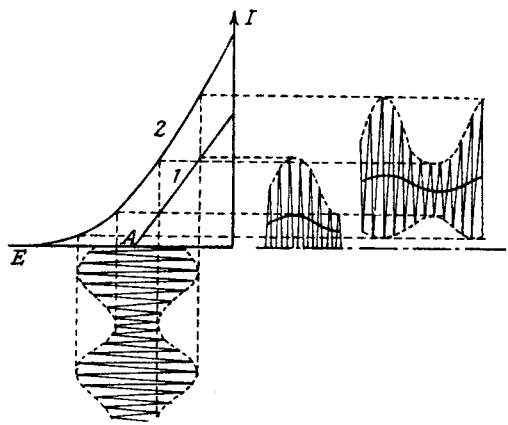

FIG. 8.1.—Detection with Linear (1) and Parabolic (2) Characteristics.

telephones or a loudspeaker, from which sound waves corresponding to the original audio frequencies modulating the carrier will be heard.

In the case of frequency and phase modulated transmission the modulation is first converted to amplitude modulation before application to the detector.

All detectors possess one feature in common, viz., their current-voltage characteristic curve is non-linear over the operating range, having either a point of discontinuity (Curve 1 in Fig. 8.1) or a curved shape (Curve 2 in the same figure). A detector having a discontinuous characteristic is generally called a linear [6] detector if it is biased to the point of discontinuity A ; the positive modulation envelope is reproduced without distortion and the shape of the mean current wave follows exactly that of the modulation envelope.

A detector having a characteristic similar to that of Curve 2 is generally (somewhat loosely) termed a "square law" or parabolic detector because detection depends on the squared term (a_2E^2) in the expression $I = f(E)$ connecting current and voltage. Such a detector distorts the modulation envelope, and the shape of the mean current wave is not an exact copy of the modulation envelope.

In this chapter we shall consider only valves as detectors, though it should be remembered that detection is not solely a property of valves but also of certain types of crystals and metallic surfaces (the copper oxide detector is an example of the latter). The fundamental principles are, however, the same whatever form the detector may take.

Valve detectors may be conveniently divided into four groups as follows:

(1) Diode
(2) Cumulative or leaky grid
(3) Power grid
(4) Anode bend.

We shall start with the diode as the simplest form of detector.

8.2. Diode Detection.

8.2.1. Introduction. A diode detector consists of a valve having two electrodes. Current flow is unidirectional from anode to cathode and a characteristic I_aE_a curve is shown in Fig. 2.3 (curve 3). The characteristic approximates to a parabolic shape for small values of E_a due to space charge and electron velocity effects, but for large values of E_a it becomes a straight line. In the preliminary theory which follows we shall neglect this initial curvature and assume a straight-line characteristic. Now suppose we apply an A.C. voltage to the detector. If the generator supplying this voltage has zero internal resistance, the current through the diode consists of a series of pulses of a shape approximating to a half-sine wave, and a D.C. milliammeter placed in series with the diode measures a mean current of approximately $\frac{\hat{I}}{\pi}$* where $\hat{I}$ is the maximum current through the diode.

When the generator has an internal resistance R_0, the pulses of

* The mean current in a half-sine wave of peak current $\hat{I}$

$$= \frac{1}{2\pi}\int_0^{\pi} \hat{I} \sin\theta \, d\theta$$

$$= \frac{\hat{I}}{2\pi}\Big[-\cos\theta \Big]_0^{\pi} = \frac{\hat{I}}{\pi}.$$

current are still half sinusoidal in shape but reduced in amplitude, giving a lower reading in the D.C. milliammeter.

Now let us assume that the voltage applied to the diode is a modulated R.F. carrier $\hat{E} \cos \omega t\ (1+M \cos pt)$. The amplitude variations of the carrier produce corresponding variations in the detected current pulses, but a D.C. milliammeter will give a reading which is dependent only on the " average " carrier voltage and not upon the modulation. This is so because a decrease of carrier

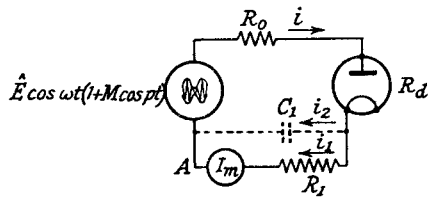

FIG. 8.2.—A Diode Detector.

amplitude (due to modulation) at one time instant is exactly counterbalanced by an increase at another time instant. Since, however, the pulses of current are varying in amplitude at an audio frequency there must be an A.C. current of that frequency in addition to the D.C. current measured by the milliammeter. The presence of this audio frequency current can be proved by noting that a thermal milliammeter, connected in series with the D.C. milliammeter, gives a higher reading than the latter.

An audio amplifier following the detector requires a voltage input so that a resistance (R_1) must be inserted in the diode circuit as in Fig. 8.2, in order that the mean current fluctuations may be converted into mean voltage variations. The voltage developed

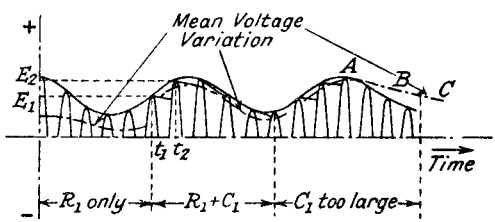

FIG. 8.3.—The Wave Shape of the Voltage across the Load Resistance in a Diode Detector.

across R_1 takes the form of half-sinusoidal pulses as shown to the left in Fig. 8.3. The reference point is A (Fig. 8.2), so that the pulses are in a positive direction. Their amplitude is dependent on R_1, the diode resistance R_d, the generator resistance R_0 and the

modulation envelope. If $R_1 \gg R_d + R_0$ the mean value of the voltage across R_1 is the mean value of half the input modulated carrier, i.e.,

$$\frac{\hat{E}(1+M\cos pt)}{2\pi}\int_{-\frac{\pi}{2\omega}}^{\frac{\pi}{2\omega}} \cos \omega t.dt = \frac{\hat{E}}{\pi} + \frac{\hat{E}M}{\pi}\cos pt,$$

the first term in the expression is the D.C. component and the second the A.C. component.

It is clear that such a method of detection is inefficient since the available output A.F. signal is reduced to approximately one-third $\left(\frac{1}{\pi}\right)$ of the input modulation envelope. The problem becomes one of increasing the mean voltage across R_1 by filling in the gaps between the pulses. This can be achieved by connecting a capacitance C_1 across R_1. Owing to its low reactance at radio frequencies it effectively short circuits R_1 and allows almost all the R.F. input voltage to be applied to the diode. Hence, during the diode conduction period, the detected current is only limited by the diode and generator resistance. This current is used to charge the capacitance C_1, the voltage across which rises nearly to the maximum value E_1 of the R.F. carrier, reached at some time instant t_1 (Fig. 8.3). After the time instant t_1 the voltage across R_1 tends to fall, but now the capacitance C_1 charged to E_1, begins to discharge through the resistance R_1, thus tending to maintain the voltage. The capacitance C_1 continues to discharge until a point on the next positive cycle when the input voltage equals that across C_1, and the diode conducts charging C_1 up to E_2. Then discharge begins again and the cycle is repeated. It will be seen that the discharge of C_1 has filled in the gaps between the voltage pulses and the mean voltage variation across R_1 is very little less than the peak voltage variation of the input wave. Thus the loss in the detector stage is almost entirely eliminated. The maximum permissible value of capacitance C_1 depends on the highest modulation frequency employed and the maximum modulation percentage, since if C_1 is too large the voltage across R_1 may be unable to fall to a value lower than the next positive peak. In this circumstance the mean voltage variation across R_1 is not a faithful reproduction of the modulation envelope but will be distorted when the modulation envelope decreases as shown by the line ABC in Fig. 8.3. This distortion is often called " non-tracking " distortion. If the value of C_1 is too small,[7] the detected voltage will be reduced because the gaps between the pulses are inadequately filled.

8.2.2. Diode Detection Characteristic Curves. If we assume that C_1 fills in completely the gaps between successive voltage pulses, the D.C. current through R_1 is determined solely by R_1 and the diode conduction resistance R_d. This means that we

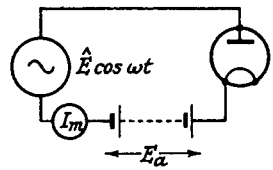

FIG. 8.4*a*.—The Circuit for Obtaining I_mE_a Curves for a Diode Detector.

may replace R_1C_1 by a fixed voltage, i.e., from a battery, and obtain a series of I_mE_a curves (I_m is the mean D.C. current through the diode), which have properties similar to those of the I_aE_a curves for a triode. It is possible on these curves (just as for triode I_aE_a curves) to draw load lines corresponding to the load resistance R_1 and to determine the output voltage for given input conditions. The circuit for obtaining a series of these curves (Fig. 8.4*b*) is shown in Fig. 8.4*a*; a low-frequency voltage [10] —the 50-c.p.s. mains supply—may be employed, but if it is desired to include such effects as anode cathode and stray capacitance, these capacitances must be artificially increased to make their reactances at 50 c.p.s. equal to their reactances at the particular radio frequency being considered, e.g., 0·0001 μF at 1,000 kc/s is equivalent to 2 μF at 50 c.p.s. Care must be taken to ensure that the D.C. resistance in the circuit is much less than the diode conduction resistance, R_d, or the curves will be incorrect. For this reason the microammeter measuring mean current should not be a multirange instrument with considerable variation of D.C. resistance between ranges. The battery voltage simulating the voltage produced across R_1 applies a negative voltage to the anode and each curve in Fig. 8.4*b* is obtained by maintaining the input signal voltage constant (at convenient peak values of, for example, 0·5, 1, 1·5, etc.) and varying the battery voltage E_a. The curves of Fig. 8.4*b* are typical of indirectly heated diodes with conduction current beginning at a negative voltage. The curve for $\hat{E}_1 = 0$ is not parallel to the other curves, which actually merge into this curve at certain positive voltages, and the reason for this is explained in Section 8.2.16.

We can now draw across these curves a line corresponding to R_1, making an angle to the horizontal axis of $\theta = \cot^{-1} R_1$, and in the absence of any fixed biasing voltage this starts from $E_a = 0$.

Subject to the condition stated at the beginning of the section, viz., $R_1 \gg R_d + R_0$, we can determine the D.C. voltage, developed across R_1 in the actual detector circuit in which C_1R_1 replace the battery, for any given peak input signal. If we consider the resistance R_1 to be represented by the line OB, an output peak voltage $\hat{E}_1$ gives a mean current in the resistance R_1 of I_1 and a mean voltage across it of E_1. If the input peak voltage rises to $\hat{E}_2$ or falls to $\hat{E}_3$, the mean voltage across R_1 rises to E_2 or falls to E_3. The line OB is therefore the locus for any variation of carrier amplitude. For example, if the input carrier peak voltage $\hat{E}_1$ is

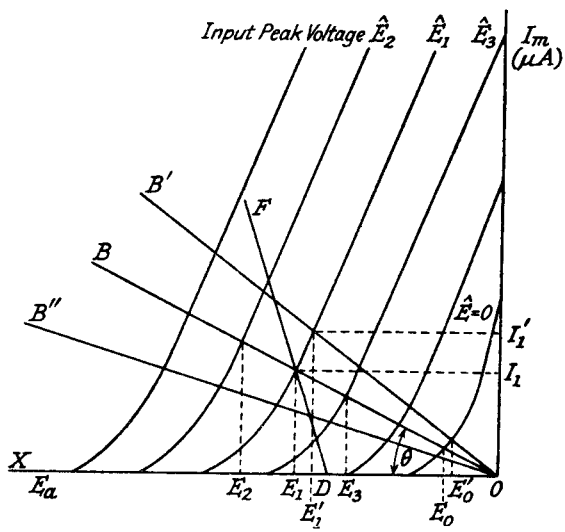

FIG. 8.4*b*.—Typical I_mE_a Curves for a Diode Detector.

modulated such that at the peak of the modulation envelope it reaches $\hat{E}_2$ and at the trough falls to $\hat{E}_3$, the mean voltage varies from E_2 to E_3. Since OB is a straight line, the mean voltage variations are an exact reproduction of the input modulation envelope reduced in amplitude in the ratio $\frac{E_1 - E_0}{\hat{E}_1}$ (E_0 = voltage across R_1 when $\hat{E}_1 = 0$), provided the carrier voltage lines are parallel and equally spaced. The peak value of the audio frequency voltage across R_1 is $\frac{E_2 - E_3}{2}$, since the modulation envelope varies by the voltage difference between positive and negative peaks of the audio frequency wave. The reduction ratio $\frac{E_1 - E_0}{\hat{E}_1}$ is generally called

the detection efficiency η_d and for normal values of R_1 (0·5 MΩ) it is about 0·9. The resistance R_1, in conjunction with R_d, determines η_d and the latter increases as R_1 increases. In most practical circuits C_1 has a low enough reactance and high enough time constant with R_1 to permit Fig. 8.4*b* to be used, but when C_1 is too small, mean detection voltage-carrier peak voltage curves can be used to estimate detector performance. The battery in Fig. 8.4*a* is replaced by the load resistance R_1, paralleled by a capacitance C_1, having a reactance value at 50 c.p.s. equal to the reactance of the actual value of C_1 at the desired radio frequency. Typical mean detection voltage-carrier peak voltage curves for decreasing values of C_1 are shown in Fig. 8.4*c* ; the loss of detection efficiency as C_1 is reduced is clearly indicated. The A.F. output voltage across the

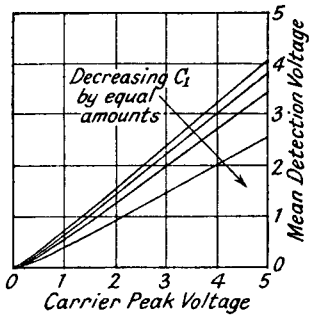

FIG. 8.4c.—Typical Detection Voltage-Carrier Peak Voltage Curves for a Diode Detector.

detector load resistance is estimated as follows : for a carrier peak voltage of 2 volts modulated 50%, carrier amplitude varies between 3 volts and 1 volt peak and the mean detection voltage change corresponding to this carrier change is for the top curve from 0·7 to 2·4 volts, a difference of 1·7 volts. Hence the A.F. peak output voltage for a sinusoidal modulation envelope is $\frac{1{\cdot}7}{2} = 0{\cdot}85$ volts, i.e., detection efficiency is 85%.

8.2.3. Effect of the Coupling Impedance from Diode to A.F. Amplifier.[23] The audio output from the detector is transferred to the A.F. amplifier through a capacitance-resistance coupling such as C_2R_2 shown in Fig. 8.5. Capacitive coupling prevents application of the D.C. component across R_1 to the grid of the amplifier valve, which is biased separately to the optimum point. In addition there is generally a resistance-capacitance filter (R_3C_3) to prevent the passage of R.F. voltages to the audio amplifier,

where they are likely to produce over-loading and perhaps instability. The capacitance of C_3 is about equal to C_1, so that its effect may be neglected at audio frequencies, and R_3 is usually much less than R_1.

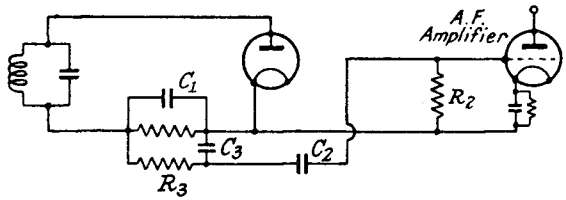

FIG. 8.5.—A Diagram of Connections for the Coupling from a Diode Detector to an A.F. Amplifier.

The actual value of R_3 is to a large extent controlled by R_2, since it forms with R_2 a potentiometer which reduces the A.F. voltage across R_2 to $\frac{R_2}{R_2+R_3}$ of that across R_1. Generally it has a value of about $\frac{R_2}{10}$. Adequate R.F. filtering is then obtained without appreciable reduction of A.F. voltage, or frequency discrimination against

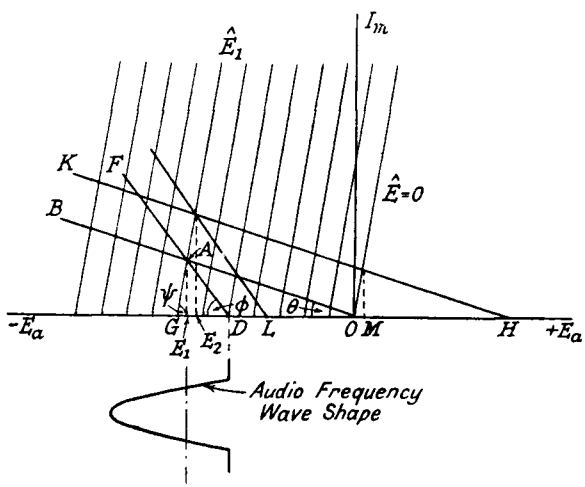

FIG. 8.6.—Ideal I_mE_a Curves for a Diode Detector showing the Effect of the Coupling Resistance R_2 and Positive Bias.
[OH = Positive Bias Voltage.]

the higher audio frequencies by C_3. The coupling reactance of C_2 must be small in comparison with R_2 at the lowest audio frequencies or frequency discrimination results. The resistances

R_2 and R_3 are thus in parallel with R_1 for all audio and radio frequencies. Referring to Fig. 8.6 (the I_mE_a curves are for convenience considered as straight lines) for a modulated input voltage to the detector of $\hat{E}_1[1+M\cos pt]\cos \omega t$, the D.C. operating point is at A, the point of intersection between OB and the voltage line $\hat{E}_1$, and the modulation envelope will travel up and down OB on either side of the point A as long as R_2 is infinite. As R_2 is decreased the locus of the modulation envelope changes to the line DF, where $\cot \widehat{FDG} = \dfrac{R_1R_2}{R_1+R_2}$. We are assuming for simplicity that R_3 is included in R_2. The first effect of R_2 is to reduce the audio voltage from the detector. The second effect, which is much more serious, occurs when the modulation trough falls below the carrier value corresponding to OD. The modulation envelope is cut off and the audio frequency wave shape is distorted as shown. The modulation ratio which can be accepted without distortion is thus limited by R_2. If we assume the I_mE_a characteristic curves for a diode to be straight lines as in Fig. 8.6, the critical modulation ratio is given by $\dfrac{DG}{OG}$.

But
$$DG = DE_1+E_1G$$
$$= AE_1\cot\phi + AE_1\cot\psi \quad . \quad . \quad 8.1$$

and
$$OG = OE_1+E_1G$$
$$= AE_1\cot\theta + AE_1\cot\psi . \quad . \quad . \quad 8.2.$$

From 8.1 and 8.2, the critical modulation ratio is

$$M = \frac{DG}{OG} = \frac{\cot\phi+\cot\psi}{\cot\theta+\cot\psi}$$
$$= \frac{\dfrac{R_1R_2}{R_1+R_2}+R_d'}{R_1+R_d'} \qquad 8.3.$$

It is important to note that R_d', the inverse of the slope of the diode I_mE_a characteristic curve, is the diode equivalent resistance to changes of voltage across R_1 and is not the diode conduction resistance R_d of Section 8.2.5. Its relationship to R_d is discussed in Sections 8.2.15 and 16.

Since detection efficiency $\eta_d = \dfrac{OE_1}{OG} = \dfrac{\cot\theta}{\cot\theta+\cot\psi}$

$$= \frac{R_1}{R_1+R_d'} \quad . \quad . \quad . \quad . \quad 8.4$$

rearranging expression 8.3

$$M = \frac{R_1+R_d'+\dfrac{R_1R_2}{R_1+R_2}-R_1}{R_1+R_d'} = 1-\frac{R_1^2}{(R_1+R_2)(R_1+R_d')}$$
$$= 1-\eta_d\cdot\left[\frac{R_1}{R_1+R_2}\right] \quad . \quad . \quad . \quad . \quad . \quad . \quad 8.5a.$$

It is clear from expression 8.5*a* that a high critical modulation ratio requires a high value of R_2. A reduction of detection efficiency also leads to a higher critical modulation ratio. This is to be expected since lower detection efficiency means either a reduced value for R_1 or increased value for R_d', i.e., a smaller angle ψ, which brings a lower carrier voltage line to the point D on Fig. 8.6. An equivalent increase in R_2 can be realized by tapping down the detector D.C. resistance R_1. Suppose R_2 is tapped across a part $KR_1(K<1)$ only, the A.C. load resistance is

$$(1-K)R_1+\frac{KR_1R_2}{KR_1+R_2} = R_1-\frac{(KR_1)^2}{KR_1+R_2}$$

and from 8.3 the critical modulation ratio is

$$M = \frac{R_1-\dfrac{(KR_1)^2}{KR_1+R_2}+R_d'}{R_1+R_d'}$$
$$= 1-\eta_d\frac{K^2R_1}{KR_1+R_2}$$
$$= 1-\eta_dK\cdot\left(\frac{R_1}{R_1+\dfrac{R_2}{K}}\right) \quad . \quad . \quad . \quad 8.5b.$$

Not only is R_2 equivalently increased to $\dfrac{R_2}{K}$, but the negative term is also reduced by the multiplying factor K.

The critical modulation ratio may also be increased by applying a positive bias [29] to the anode of the diode. The carrier locus line takes up a new position such as HK where OH is the positive bias voltage. The critical modulation ratio may be increased to 1 for any given value of R_2 and carrier peak voltage $\hat{E}_1$ by a suitable choice of OH. Expression 8.5*a* is modified by the addition of positive bias to

$$M' = \frac{LG}{HG} = 1-\eta_d\cdot\left(\frac{R_1}{R_1+R_2}\right)$$

where $\eta_d = \dfrac{ME_2}{OG} = \dfrac{OE_1}{OG} = \dfrac{R_1}{R_1+R_d'}$ since HK is parallel to OB.

The carrier modulation ratio, which is not M', is given by

$$M = \frac{LG}{OG} = \frac{LG}{HG} \cdot \frac{HG}{OG}$$

$$M = M'\left(\frac{\hat{E}_1 + E_b}{\hat{E}_1}\right) \text{ where } E_b = OH$$

thus

$$M = \left[\frac{\hat{E}_1 + E_b}{\hat{E}_1}\right]\left(1 - \eta_d\left(\frac{R_1}{R_1 + R_2}\right)\right) \quad . \quad . \quad 8.6.$$

The critical modulation ratio is now dependent on the carrier peak voltage and the positive bias applied to the diode. When this critical modulation ratio is exceeded the D.C. current in the resistance R_1 is increased owing to the fact that the bottom of the audio frequency voltage wave is cut off, i.e., is itself being detected. Thus any change of D.C. current in the diode circuit of a receiver, when a programme is being received from a steady carrier voltage source such as a local station, indicates distortion of the audio frequency output voltage by the detector stage.

There is a disadvantage to the use of positive bias due to the fact that the detector is generally supplied from a high impedance generator (a tuned circuit in the anode of a valve). A positively biased diode conducts in the absence of an input signal and so presents a low input resistance to the generator. This heavy damping is reduced as the input signal is increased, and the diode begins to function as a unidirectional device (see Section 8.2.6). Two effects are obtained; the detector is insensitive to signal inputs less than a certain value (about 0·3 of the positive bias) and it also distorts the modulation envelope of the applied signal. Hence for really satisfactory operation the positive bias needs to be variable and directly controlled by the input signal (decreasing as the signal decreases and vice versa).

In the above analysis we have assumed the diode $I_m E_a$ characteristic curves to be straight lines, but in Section 8.2.16 it is shown that a curved shape is obtained even for a diode with a linear $I_a E_a$ characteristic. This curvature tends to give a higher critical modulation ratio than that given in expressions 8.5*a*, 8.5*b* and 8.6.

8.2.4. Damping of the Input Circuit due to the Diode Conduction Current. The conduction current of the diode constitutes a load which may considerably modify the sensitivity and selectivity characteristics of the input, when the latter contains a tuned circuit. The load effect may be estimated by averaging over the complete R.F. cycle of the input voltage the resistance introduced

during the conduction period. In this way the equivalent damping resistance shunting the input can be calculated.

Two cases will be considered; in the first the diode will be assumed to have a linear I_aE_a characteristic given by $I_a = KE_a$, and in the second the diode characteristic will be assumed to be parabolic and given by $I_a = KE^2{}_a$.

8.2.5. Equivalent Damping Resistance due to a Diode with Linear I_aE_a Characteristic. We shall assume that the I_aE_a curve ($\hat{E}_1 = 0$) is a straight line given by the relationship

$$I_a = \frac{E_a}{R_d}.$$

Where R_d = diode conduction resistance, i.e., the inverse of the slope of this characteristic.

The diode conducts when the input voltage $\hat{E}_1 \cos \omega t$, which for convenience may be re-written $\hat{E}_1 \cos \theta$, exceeds the voltage across the resistance R_1 (Fig. 8.7).

The D.C. voltage (E_1) across the resistance-capacitance parallel

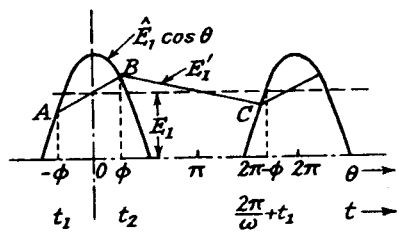

FIG. 8.7.—The Voltage Wave Shape Across the Load Resistance R_1 of a Diode Detector.

combination will not in actual practice remain constant but will fluctuate in the manner shown by the lines AB and BC in Fig. 8.7. This fluctuation, if taken into account, considerably complicates the analysis and its effect may be neglected except when the detection efficiency is much lower than is normally encountered in practice. It will therefore be assumed that E_1 is a constant voltage.

Mean Current I_m, and the Relationship between R_1, R_d, η_d.[20]

The expression for the mean current in the circuit is

$$I_m = \frac{1}{2\pi}\int_{-\phi}^{\phi} I_a \, d\theta$$

$$= \frac{1}{2\pi}\int_{-\phi}^{\phi} \frac{(\hat{E}_1 \cos\theta - E_1)d\theta}{R_d} \quad . \quad . \quad 8.7$$

where $\hat{E}_1 \cos \phi = E_1$, the voltage at which the diode conducts.

The limits of equation 8.7 may conveniently be changed to ϕ and 0 and the mean current then becomes

$$I_m = \frac{1}{\pi}\int_0^{\phi} \frac{(\hat{E}_1 \cos\theta - E_1)}{R_d} d\theta$$

$$= \frac{1}{\pi R_d}\{\hat{E}_1 \sin\phi - E_1\phi\}$$

$$= \frac{\hat{E}_1}{\pi R_d}\left\{\sin\phi - \frac{E_1}{\hat{E}_1}\phi\right\} \quad . \quad . \quad . \quad 8.8.$$

But $\cos\phi = \dfrac{E_1}{\hat{E}_1} = \eta_d$ = detection efficiency

thus $\sin\phi = \sqrt{1 - \eta_d{}^2}$

and $\phi = \cos^{-1}\eta_d$.

Replacing the expressions containing ϕ in 8.8 we get

$$I_m = \frac{\hat{E}_1}{\pi R_d}\{\sqrt{1 - \eta_d{}^2} - \eta_d . \cos^{-1}\eta_d\} \quad . \quad . \quad 8.9.$$

But $I_m = \dfrac{E_1}{R_1}$

$$\therefore \frac{R_1}{R_d} = \frac{\pi\eta_d}{(\sqrt{1 - \eta_d{}^2} - \eta_d \cos^{-1}\eta_d)} \quad . \quad . \quad 8.10.$$

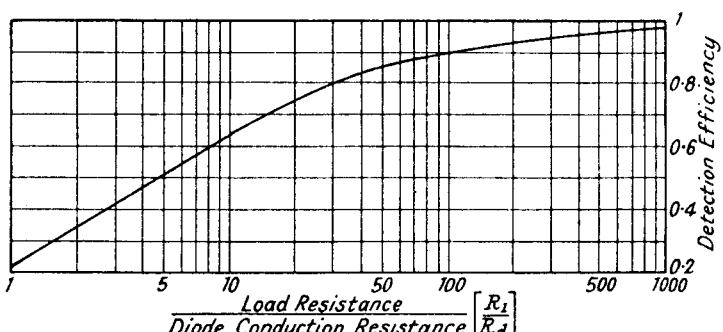

FIG. 8.8.—A Curve of Detection Efficiency against the Ratio of Load to Diode Conduction Resistance.

Expression 8.10 shows the relationship between the detection efficiency and the ratio $\dfrac{R_1}{R_d}$ and it is plotted in Fig. 8.8 for various values of $\dfrac{R_1}{R_d}$.

Effective Input Resistance R_E.

The effective input resistance may be determined by equating the power absorbed in the circuit to $\frac{\hat{E}_1^2}{2R_E}$, where R_E is the equivalent shunt resistance due to the diode conduction current.

Power absorbed in diode load resistance R_1

$$= \frac{1}{\pi}\int_0^{\phi} \hat{E}_1 \cos\theta \, I_a \, d\theta \quad . \quad . \quad . \quad . \quad 8.11$$

$$= \frac{1}{\pi R_d}\int_0^{\phi} \hat{E}_1 \cos\theta [\hat{E}_1 \cos\theta - E_1] \, d\theta$$

$$= \frac{\hat{E}_1^2}{\pi R_d}\int_0^{\phi}\left[\frac{1+\cos 2\theta}{2} - \frac{E_1}{\hat{E}_1}\cos\theta\right] d\theta$$

$$= \frac{\hat{E}_1^2}{2\pi R_d}\left\{\phi + \frac{\sin 2\phi}{2} - \frac{2E_1}{\hat{E}_1}\sin\phi\right\}$$

$$= \frac{\hat{E}_1^2}{2\pi R_d}\{\cos^{-1}\eta_d - \eta_d\sqrt{1-\eta_d^2}\}$$

$$= \frac{\hat{E}_1^2}{2R_E}$$

$$\therefore \; R_E = \frac{\pi R_d}{\cos^{-1}\eta_d - \eta_d\sqrt{1-\eta_d^2}} \quad . \quad . \quad . \quad 8.12.$$

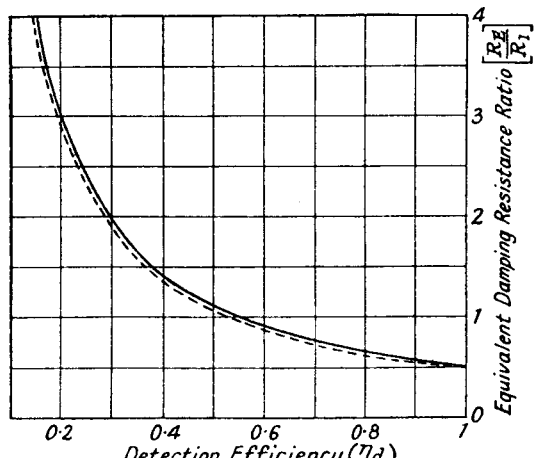

FIG. 8.9.—Curves of Damping Resistance Ratio against Detection Efficiency.
(Full Line—Linear Characteristic.
Dotted Line—Parabolic Characteristic.)

Inserting the value of R_d from 8.10 in 8.12

$$\frac{R_E}{R_1} = \frac{[\sqrt{1-\eta_d{}^2} - \eta_d \cos^{-1}\eta_d]}{\eta_d(\cos^{-1}\eta_d - \eta_d\sqrt{1-\eta_d{}^2})} \quad . \quad . \quad 8.13$$

The ratio $\frac{R_E}{R_1}$ is plotted in Fig. 8.9 for different values of η_d and it can be noted that the equivalent resistance R_E approaches $\frac{1}{2}R_1$ as η_d approaches unity. As η_d decreases R_E increases and at $\eta_d = 0{\cdot}55$, R_E is equal to R_1.

It is not usual for the diode to conduct exactly at $E_a = 0$, and in the more general case conduction starts when E_a is either positive or negative. In directly heated filament valves E_a is most often positive, whereas for indirectly heated mains valves with equipotential cathodes E_a is usually negative. The two conditions are more easily considered separately. Let us take first the case of the mains valve with current starting at $-E_0$.

8.2.6. Equivalent Damping Resistance for Conduction Current Beginning at a Negative Anode Voltage. The characteristic curve is given by line AB in Fig. 8.10, and the I_aE_a relationship by

$$I_a = \frac{(E_a+E_0)}{R_d}$$

where $-E_0$ is the voltage at which current starts. The expression E_0 thus represents a numerical and not an algebraic value.
The expression for mean current becomes:

$$I_m = \frac{1}{\pi R_d}\int_0^{\phi}(\hat{E}_1 \cos\theta - E_1+E_0)\,d\theta \quad . \quad . \quad 8.14a$$

$$= \frac{\hat{E}_1}{\pi R_d}\left[\sin\phi - \frac{E_1 - E_0}{\hat{E}_1}\phi\right] \quad . \quad . \quad 8.14b$$

where E_1 = D.C. mean voltage developed across R_1.

The signal voltage must exceed a certain value before detection can take place, since the diode conduction current must be cut off at some part of the cycle. Even though no detection takes place there is still a mean current flowing round the diode circuit due to the negative start of current. Its value, assuming the input circuit to have no resistance, will be $\frac{E_0}{R_1+R_d}$, and ϕ in expression 8.14*b* will be π

thus
$$I_m = \frac{E_0}{R_1+R_d} = \frac{\hat{E}_1}{\pi R_d}\left(-\frac{E_1' - E_0}{\hat{E}_1}\right)\pi$$
$$= \frac{E_0 - E_1'}{R_d}$$

where E_1' = voltage across the load resistance R_1 for no detection,

thus
$$E_1' = \frac{E_0 R_1}{R_1 + R_d} \quad . \quad . \quad . \quad . \quad 8.15.$$

The value of $\hat{E}_1$ which just fails to produce detection may be found by making the mean current (8.14a) due to detection equal to 0

or
$$\hat{E}_1' \cos\theta - E_1' + E_0 = 0$$

but
$$\cos\theta = \frac{E_1' - E_0}{\hat{E}_1'} = -1$$

when $\theta = \pi$ (the condition for no detection).

$$\therefore \hat{E}_1' = E_0 - E_1' = E_0 - \frac{E_0 R_1}{R_1 + R_d}$$
$$= \frac{E_0 R_d}{R_1 + R_d}.$$

That this is the voltage required to start detection may be seen from Fig. 8.10. AB is the $I_a E_a$ characteristic curve for the diode and AG the D.C. line for the diode resistance R_d and R_1. The

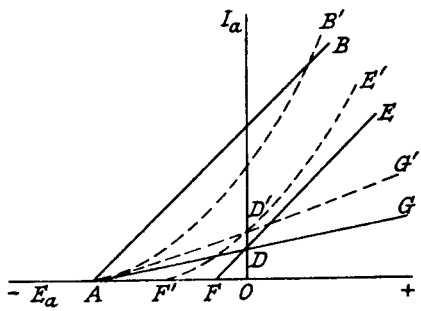

FIG. 8.10.—Operating Conditions for a Diode with Negative Start of Conduction Current.
(Full Line—Linear Conduction Characteristic.
Dotted Line—Parabolic Conduction Characteristic.)

reactance of the capacitance C_1 at radio frequencies is assumed to be negligible compared with R_d. Hence the only impedance to R.F. voltages in the circuit is the diode resistance R_d. The locus line for small variations of R.F. voltages is the line FE, which is parallel to AB and passes through D, the D.C. operating point. The current represented by OD is $OA \tan \widehat{DAO}$ which equals $\frac{E_0}{R_1 + R_d}$, so that the voltage OF is

$$OF = OD \cot \widehat{DFO}.$$
$$= \frac{E_0}{R_1 + R_d} . R_d$$

which confirms that no detection occurs until the input peak voltage $\hat{E}_1$ exceeds $\frac{E_0 R_d}{R_1+R_d}$, since only then can the input voltage take the diode into cut-off.

When the input voltage exceeds this critical value, detection takes place and the mean current is given by expression 8.14*b*. We may note that

$$\cos\phi = \frac{E_1 - E_0}{\hat{E}_1} \quad . \quad . \quad . \quad . \quad 8.16a$$

and

$$\eta_d = \frac{E_1 - E_1'}{\hat{E}_1} \quad . \quad . \quad . \quad . \quad 8.16b.$$

Replacing E_1' by $\frac{E_0 R_1}{R_1+R_d}$ and combining expressions 8.16*a* and 8.16*b*.

$$\cos\phi = \eta_d - \frac{E_0 R_d}{(R_1+R_d)\hat{E}_1} = \eta_d - A$$

where

$$A = \frac{E_0 R_d}{(R_1+R_d)\hat{E}_1}.$$

We may now re-write 8.14*b* as follows:

$$I_m = \frac{\hat{E}_1}{\pi R_d}\left[\sqrt{1-(\eta_d - A)^2} - (\eta_d - A)\cos^{-1}(\eta_d - A)\right]$$
$$= \frac{E_1}{R_1}.$$

From which

$$\frac{R_1}{R_d} = \frac{\pi\frac{E_1}{\hat{E}_1}}{\sqrt{1-(\eta_d - A)^2} - (\eta_d - A)\cos^{-1}(\eta_d - A)}$$
$$= \frac{\pi\left(\eta_d + \frac{AR_1}{R_d}\right)}{\left[\sqrt{1-(\eta_d - A)^2} - (\eta_d - A)\cos^{-1}(\eta_d - A)\right]} \quad . \quad 8.17a.$$

When $R_d \ll R_1$ and η_d approaches 1 this reduces to

$$\frac{R_1}{R_d} = \frac{\pi\left(\eta_d + \frac{E_0 R_1}{\hat{E}_1(R_1+R_d)}\right)}{\sqrt{1-\eta_d^2} - \eta_d\cos^{-1}\eta_d} \quad . \quad . \quad 8.17b.$$

Detection efficiency is plotted against $\frac{\hat{E}_1}{E_0}$ in Fig. 8.11*a* (curve 1) for $R_d = 5{,}000\Omega$ and $R_1 = 1$ MΩ; $-E_0 = -1$ volt.

The equivalent resistance R_E can be found by the same method as that used in Section 8.2.5, and is given by

$$R_E = \frac{\pi R_d}{\cos^{-1}(\eta_d - A) - (\eta_d - A)\sqrt{1-(\eta_d - A)^2}}$$

replacing R_d by the value derived from 8.17*a*.

$$\frac{R_E}{R_1} = \frac{[\sqrt{1-(\eta_d - A)^2} - (\eta_d - A)\cos^{-1}(\eta_d - A)]}{\left(\eta_d + \frac{AR_1}{R_d}\right)[\cos^{-1}(\eta_d - A) - (\eta_d - A)\sqrt{1-(\eta_d - A)^2}]} \quad . \quad 8.18$$

except where η_d is small, this reduces to

$$\frac{R_E}{R_1} = \frac{\sqrt{1-\eta_d{}^2} - \eta_d \cos^{-1}\eta_d}{\left[\eta_d + \frac{E_0 R_1}{\hat{E}_1(R_1+R_d)}\right][\cos^{-1}\eta_d - \eta_d\sqrt{1-\eta_d{}^2}]}.$$

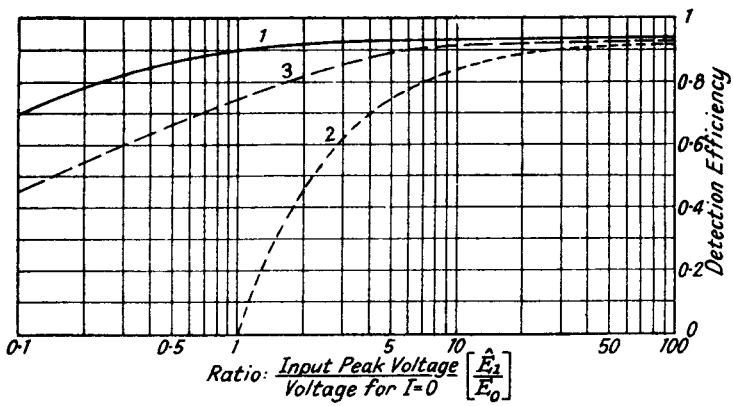

FIG. 8.11*a*.—Curves of Detection Efficiency against Voltage Ratio $\frac{\hat{E}_1}{E_0}$.

Curve 1. $-E_0 = -1$. Linear Characteristic.
Curve 2. $+E_0 = +1$. Linear Characteristic.
Curve 3. $-E_0 = -1$. Parabolic Characteristic.
($R_1 = 1M\Omega$. $R_d = 5{,}000\Omega$.)

It may be noted that when no detection takes place $\eta_d = 0$; $\hat{E}_1' \leq \frac{E_0 R_d}{R_1 + R_d}$, $A = 1$, and $R_E = R_d$.

The value of R_E for $R_d = 5{,}000\Omega$, $R_1 = 1\ M\Omega$, and $-E_0 = -1$ is plotted for various ratios of $\frac{\hat{E}_1}{E_0}$ as curve 1 in Fig. 8.11*b*. The variation of effective resistance with signal voltage is quite marked for $\hat{E}_1 < 10\ E_0$. When $\hat{E}_1 = 0{\cdot}005$ volt the effective resistance is very low indeed and almost equal to the diode resistance R_d. This

undesirable feature can be eliminated by neutralizing the negative start of current with negative bias to the diode anode of $-E_0$ volts. It should be noted that positive bias applied to a diode with conduction current starting at zero voltage has the same effect as current starting at a negative anode voltage.

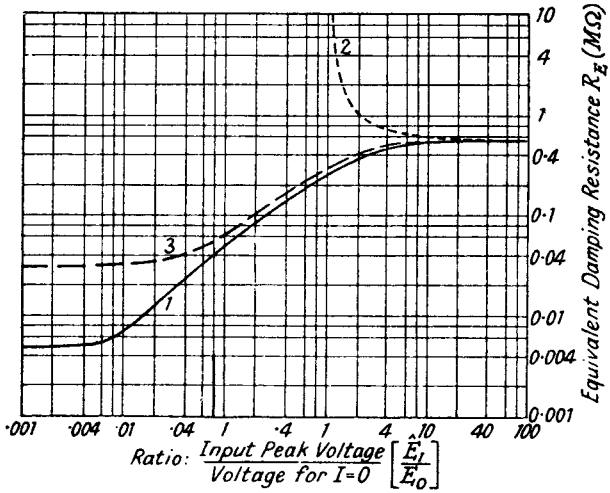

FIG. 8.11*b*.—Curves of Equivalent Damping Resistance against Voltage Ratio $\frac{\hat{E}_1}{E_0}$.

Curve 1. $-E_0 = -1$. Linear Characteristic.
Curve 2. $+E_0 = +1$. Linear Characteristic.
Curve 3. $-E_0 = -1$. Parabolic Characteristic.
($R_1 = 1$ MΩ. $R_d = 5{,}000\Omega$.)

8.2.7. Conduction Current Beginning at a Positive Anode Voltage. The equation to the characteristic curve is

$$I_a = \frac{(E_a - E_0)}{R_d}$$

where $+E_0$ is the positive voltage at which current starts.

By applying the procedure given above

$$I_m = \frac{\hat{E}_1}{\pi R_d}\left[\sin\phi - \frac{E_1+E_0}{\hat{E}_1}\phi\right]$$

$$\cos\phi = \frac{E_1+E_0}{\hat{E}_1}$$

$$\eta_d = \frac{E_1}{\hat{E}_1}$$

$$\cos\phi = \eta_d + \frac{E_0}{\hat{E}_1}.$$

Thus

$$I_m = \frac{\hat{E}_1}{\pi R_d}\left[\sqrt{1-\left(\eta_d+\frac{E_0}{\hat{E}_1}\right)^2}-\left(\eta_d+\frac{E_0}{\hat{E}_1}\right)\cos^{-1}\left(\eta_d+\frac{E_0}{\hat{E}_1}\right)\right]. \quad 8.19$$

$$= \frac{E_1}{R_1}.$$

$$\frac{R_1}{R_d} = \frac{\pi\eta_d}{\left[\sqrt{1-\left(\eta_d+\frac{E_0}{\hat{E}_1}\right)^2}-\left(\eta_d+\frac{E_0}{\hat{E}_1}\right)\cos^{-1}\left(\eta_d+\frac{E_0}{\hat{E}_1}\right)\right]}.$$

In a similar manner

$$R_E = \frac{\left[\sqrt{1-\left(\eta_d+\frac{E_0}{\hat{E}_1}\right)^2}-\left(\eta_d+\frac{E_0}{\hat{E}_1}\right)\cos^{-1}\left(\eta_d+\frac{E_0}{\hat{E}_1}\right)\right]R_1}{\eta_d\left[\cos^{-1}\left(\eta_d+\frac{E_0}{\hat{E}_1}\right)-\left(\eta_d+\frac{E_0}{\hat{E}_1}\right)\sqrt{1-\left(\eta_d+\frac{E_0}{\hat{E}_1}\right)^2}\right]} \quad 8.20.$$

The variation of η_d and R_E with $\frac{\hat{E}_1}{E_0}$ for $R_d = 5{,}000\Omega$, $R_1 = 1\ \mathrm{M}\Omega$, $E_0 = +1$ is shown in Curve 2, Figs. 8.11*a* and 8.11*b*, respectively. R_E rises rapidly to infinity when $\hat{E}_1$ approaches E_0 and detection efficiency falls to zero. The condition of positive start of current is thus much less desirable than negative start. A very much larger input voltage is required to begin detection, and the maximum modulation percentage which may be accepted is less, because the trough of the modulation envelope $\hat{E}_1(1 - M)$ must not fall below E_0, whereas for a negative value of E_0 the minimum value of $\hat{E}_1(1 - M)$ is $\frac{E_0 R_d}{R_1+R_d}$. This undesirable feature may be eliminated by the addition of a positive biasing voltage equal to E_0 in series with the diode, which then operates as if current starts at zero anode voltage.

It is interesting to note that this explains why with small signal voltages improved detection is generally obtained by returning the grid leak of a battery valve acting as a cumulative grid detector to the positive lead of the filament. This is equivalent to supplying the grid, which is acting as the anode of a diode, with positive bias, and removing the start of grid current from a positive to a negative value of E_0.

8.2.8. Equivalent Damping Resistance due to a Diode with a Parabolic I_aE_a Characteristic Curve. It is not usual to find that the I_aE_a characteristic curve of a diode is linear for all values of E_a and the relationship is more nearly represented by

$I_a = KE_a^2$ for small signal voltages, approaching $I_a = KE_a$ for large signals. We will therefore examine the effect of a parabolic characteristic on the equivalent damping resistance R_E.

Let us assume that the current-voltage relationship is given by :

$$I_a = \frac{E_a^2}{R_d}$$

where R_d is the inverse of the slope of the I_aE_a characteristic at $E_a = 1$ volt.

The mean current is

$$I_m = \frac{1}{\pi R_d}\int_0^{\phi}(\hat{E}_1 \cos\theta - E_1)^2\, d\theta$$

$$= \frac{E_1^2}{2\pi R_d}\left[\left(1+\frac{2E_1^2}{E_1^2}\right)\phi + \frac{\sin 2\phi}{2} - \frac{4E_1}{\hat{E}_1}\sin\phi\right]$$

but $$\cos\phi = \frac{E_1}{\hat{E}_1} = \eta_d.$$

$$\therefore\ I_m = \frac{\hat{E}_1^2}{2\pi R_d}[(1+2\eta_d^2)\cos^{-1}\eta_d - 3\eta_d\sqrt{1-n_d^2}]. \quad 8.21$$

$$= \frac{E_1}{R_1}.$$

$$\therefore\ \frac{R_1}{R_d} = \frac{2\pi\eta_d}{\hat{E}_1[(1+2\eta_d^2)\cos^{-1}\eta_d - 3\eta_d\sqrt{1-\eta_d^2}]} \quad . \quad 8.22.$$

$$\text{Power absorbed} = \frac{\hat{E}_1^2}{2R_E} = \frac{1}{\pi}\int_0^{\phi}\hat{E}_1\cos\theta I_a\, d\theta$$

$$= \frac{1}{\pi}\int_0^{\phi}\frac{\hat{E}_1\cos\theta\,(E_1\cos\theta - E_1)^2\, d\theta}{R_d}$$

$$= \frac{\hat{E}_1^3}{\pi R_d}\left[\sin\phi\left(\frac{3}{4}+\frac{E_1^2}{\hat{E}_1^2}\right) + \frac{\sin 3\phi}{12} - \frac{E_1}{\hat{E}_1}\phi - \frac{E_1}{\hat{E}_1}\frac{\sin 2\phi}{2}\right]$$

but $$\sin 2\phi = 2\cos\phi\sin\phi = 2\eta_d\sqrt{1-\eta_d^2}$$

$$\sin 3\phi = 3\sin\phi - 4\sin^3\phi = (\sqrt{1-\eta_d^2})(4\eta_d^2 - 1)$$

or $$\frac{\hat{E}_1^2}{2R_E} = \frac{\hat{E}_1^3}{\pi R_d}\left[\left(\frac{\eta_d^2}{3}+\frac{2}{3}\right)\sqrt{1-\eta_d^2} - \eta_d\cos^{-1}\eta_d\right]$$

$$R_E = \frac{\pi R_d}{2\hat{E}_1\left[\left(\frac{\eta_d^2}{3}+\frac{2}{3}\right)\sqrt{1-\eta_d^2} - \eta_d\cos^{-1}\eta_d\right]}. \quad . \quad 8.23.$$

Replacing R_d by the value obtained from 8.22.

$$\frac{R_E}{R_1} = \frac{[(1+2\eta_d^2)\cos^{-1}\eta_d - 3\eta_d\sqrt{1-\eta_d^2}]}{4\eta_d\left[\left(\frac{\eta_d^2}{3}+\frac{2}{3}\right)\sqrt{1-\eta_d^2} - \eta_d\cos^{-1}\eta_d\right]} \quad . \quad 8.24.$$

The ratio $\frac{R_E}{R_1}$ is plotted in Fig. 8.9 against detection efficiency and the curve is almost identical with the one obtained for the linear diode. Both approach $\frac{R_E}{R_1} = \frac{1}{2}$ as η_d is increased to 1, but for low values of η_d a lower value of $\frac{R_E}{R_1}$ is obtained for the parabolic diode.

8.2.9. Conduction Current Beginning at a Negative Anode Voltage. Negative start of current has a slightly different effect from that obtained for the linear diode on account of the detection properties of the square law I_aE_a relationship. Cut-off of current is not an essential as it is in the linear case. This is explained more fully in Section 8.4.1.

The equation for the characteristic curve is

$$I_a = \frac{(E_a+E_0)^2}{R_d}$$

where $-E_0$ is the voltage at which current flow begins. When $E_a = 0$, the voltage across the diode is the difference between E_0 and the voltage across R_1 so that the current flowing in the circuit is

$$I_0 = \frac{[E_0 - I_0R_1]^2}{R_d}$$

or

$$\frac{I_0^2R_1^2}{R_d} - I_0\left[\frac{2E_0R_1}{R_d}+1\right]+\frac{E_0^2}{R_d} = 0.$$

Solving for I_0 we get for the minimum root (the maximum root gives a value for I_0 greater than $\frac{E_0}{R_1}$ which is impossible)

$$I_0 = \frac{1+\frac{2E_0R_1}{R_d} - \sqrt{1+\frac{4E_0R_1}{R_d}}}{\frac{2R_1^2}{R_d}} = \frac{R_d}{2R_1^2}+\frac{E_0}{R_1} - \sqrt{\frac{R_d^2}{4R_1^4}+\frac{E_0}{R_1^3}R_d}.$$

Generally $R_d \ll R_1$, so that

$$I_0 = \frac{E_0}{R_1}\left[1 - \sqrt{\frac{R_d}{E_0R_1}}\right] \quad . \quad . \quad . \quad 8.25a.$$

The voltage across R_1 for zero input volts

$$E_1' = E_0\left[1 - \sqrt{\frac{R_d}{E_0R_1}}\right] \quad . \quad . \quad . \quad 8.25b.$$

The mean current $I_m = \frac{1}{\pi R_d}\int_0^{\phi}[\hat{E}_1 \cos\theta - (E_1 - E_0)]^2\, d\theta$

$$= \frac{\hat{E}_1^2}{\pi R_d}\left[\left(\frac{1}{2} + \frac{(E_1 - E_0)^2}{\hat{E}_1^2}\right)\phi + \frac{\sin 2\phi}{4} - \frac{2(E_1 - E_0)}{\hat{E}_1}\sin\phi\right]$$

$$\cos\phi = \frac{E_1 - E_0}{\hat{E}_1}$$

$$\eta_d = \frac{E_1 - E_1'}{\hat{E}_1}$$

where E_1' is the voltage across R_1 with $\hat{E}_1 = 0$.

thus $$\eta_d = \frac{E_1 - E_0\left(1 - \sqrt{\frac{R_d}{E_0 R_1}}\right)}{\hat{E}_1} = \frac{E_1 - E_0}{\hat{E}_1} + \frac{1}{\hat{E}_1}\sqrt{\frac{E_0 R_d}{R_1}}.$$

If we assume $-E_0 = -1$, $R_d = 5{,}000\Omega$ and $R_1 = 1\ M\Omega$

then $\eta_d \simeq \frac{E_1 - E_0}{\hat{E}_1}$ except when E_1 is comparable with E_0.

Thus $\cos\phi \simeq \eta_d$

and $$I_m \simeq \frac{\hat{E}_1^2}{\pi R_d}\left[\left(\tfrac{1}{2} + \eta_d^2\right)\cos^{-1}\eta_d - \frac{3}{2}\eta_d\sqrt{1 - \eta_d^2}\right] \quad . \quad 8.26$$

$$= \frac{E_1}{R_1}.$$

$$\frac{R_1}{R_d} \simeq \frac{2\pi\left(\eta_d + \frac{E_0}{\hat{E}_1}\right)}{\hat{E}_1\left[\left(1 + 2\eta_d^2\right)\cos^{-1}\eta_d - 3\eta_d\sqrt{1 - \eta_d^2}\right]} \quad . \quad 8.27.$$

It may also be shown that

$$R_E \simeq \frac{R_1\left[\left(1 + 2\eta_d^2\right)\cos^{-1}\eta_d - 3\eta_d\sqrt{1 - \eta_d^2}\right]}{4\left[\eta_d + \frac{E_0}{\hat{E}_1}\right]\left[\left(\frac{\eta_d^2}{3} + \frac{2}{3}\right)\sqrt{1 - \eta_d^2} - 2\eta_d\cos^{-1}\eta_d\right]}. \quad 8.28.$$

Detection efficiency and R_E are plotted as curve 3 in Fig. 8.11*a* and 8.11*b* for $-E_0 = -1$, $R_d = 5{,}000\Omega$, $R_1 = 1\ M\Omega$ for various values of $\frac{\hat{E}_1}{E_0}$. As $\hat{E}_1$ is reduced to zero R_E approaches a limiting value, which is the A.C. resistance of the diode at $E_a = 0$. This limiting value may be found by reference to Fig. 8.10. If AB' is the original $I_a E_a$ characteristic curve of the diode where $OA = E_0$, the D.C. characteristic, which includes the effect of R_1, is represented by a curve such as AG' intersecting the I_a axis at D'. The A.C. characteristic curve is represented by $F'E'$, which is parallel to

AB'. The effective resistance of the diode when $\hat{E}_1 = 0$ is the inverse of the slope of curve $F'E'$ at the point D'.

We have already found in 8.25*a* the value of the current represented by OD'; it is

$$I_0 \simeq \frac{E_0}{R_1}\left[1 - \sqrt{\frac{R_d}{E_0 R_1}}\right].$$

The equation to curve $F'E'$ is

$$I_a = \frac{(E_a + E_3)^2}{R_d}$$

where $-E_3 = OF' = \sqrt{I_0 R_d}$. (Note $I_a = I_0$ when $E_a = 0$.)

$$R_E = \frac{dE_a}{dI_a} = \frac{R_d}{2(E_a + E_3)},$$

at $E_a = 0$

$$R_E = \frac{R_d}{2E_3} = \frac{R_d}{2\sqrt{I_0 R_d}} = \frac{1}{2}\sqrt{\frac{R_d}{I_0}}$$

$$= \frac{1}{2}\sqrt{\frac{R_d R_1}{E_0\left(1 - \sqrt{\frac{R_d}{E_0 R_1}}\right)}}$$

$$\simeq \frac{1}{2}\sqrt{\frac{R_d R_1}{E_0}} \quad . \quad . \quad . \quad . \quad . \quad 8.29$$

when $R_d \ll R_1$.

In our particular example

$$R_E \simeq \frac{1}{2}\sqrt{\frac{5{,}000 \times 10^6}{1}} = 35{,}300\Omega.$$

From curve 3, Fig. 8.11*b*, it may be noted that R_E for the parabolic diode is higher for small values of $\hat{E}_1$, but for large values of $\hat{E}_1$ there is little difference between it and the linear diode. The detection efficiency is less in the parabolic case (curve 3 in Fig. 8 11*a*), except for very small signal voltages, when it is superior to the linear diode (curve 1) because, due to curvature of the characteristic, there is always some detection For the linear diode detection ceases when $E_1 < \frac{E_0 R_d}{R_1 + R_d}$. An added advantage of the square law diode is that there is much less damping of the input tuned circuit for small signal voltages. R_E, in the particular example given, is 35,300 Ω as compared with 5,000Ω for the linear diode.

The parabolic diode with positive start of current will not be detailed here as the results follow very similar lines to those obtained for the linear diode under such conditions. For example, no detection occurs until the signal voltage exceeds the voltage E_0 at which current starts.

8.2.10. Diode Detector Damping and the Preceding R.F. Amplifier Stage.[27, 28, 30] We have seen from preceding sections that a diode detector reflects a resistance load into the input tuned circuit, causing damping with loss of amplification and selectivity. The equivalent load due to the diode for normal detection efficiencies is $\frac{R_1}{2}$, but we must note that this applies only to the carrier frequency. In Section 8.2.3 it is shown that when the carrier is modulated the coupling resistance to the first A.F. amplifier must be taken into account, and the load reflected on to the tuned circuit for the modulated signal is approximately one-half the A.C. load resistance of the diode, i.e., $\frac{1}{2}\left(\frac{R_1R_2}{R_1+R_2}\right)$ if R_2 is tapped across the full resistance R_1. This means that the amplification for the modulation envelope is less than for the carrier, or, in other words, there is a reduction of the modulation ratio from input to output. If the modulation ratio at the grid of the R.F. tetrode valve supplying the detector is M, g_m and R_a, the mutual conductance and slope resistance of the valve, and R_D the dynamic resistance of the anode tuned circuit, the amplification at the carrier voltage is

$$g_m \Big/ \left(\frac{1}{R_a}+\frac{1}{R_D}+\frac{2}{R_1}\right)$$

and for the modulation envelope

$$g_m \Big/ \left[\frac{1}{R_a}+\frac{1}{R_D}+\frac{2(R_1+R_2)}{R_1R_2}\right]$$

so that the modulation ratio at the detector is reduced to

$$\frac{M.\left(\frac{1}{R_a}+\frac{1}{R_D}+\frac{2}{R_1}\right)}{\frac{1}{R_a}+\frac{1}{R_D}+\frac{2(R_1+R_2)}{R_1R_2}}.$$

8.2.11. Effect of the Capacitance in Shunt with the Load Resistance. In the above calculations we have assumed that the reactance of the shunt capacitance C_1 at the carrier frequency is small in comparison with the diode resistance R_d. When this is not true detection efficiency is reduced and the effective resistance

R_E increased. We will consider first the case with no shunt capacitance and then proceed to a development showing the effect of the capacitance.

8.2.12. Detection Efficiency and Effective Resistance for a Linear Diode with no Shunt Capacitance. If $I_a = \frac{E_a}{R_d}$ is the equation to the diode characteristic curve, the equation to the curve representing the circuit conditions including the load resistance R_1 is $I_a = \frac{E_a}{R_1+R_d}$.

The mean current is given by

$$I_m = \frac{1}{\pi}\int_0^{\frac{\pi}{2}} \frac{\hat{E}_1 \cos\theta}{R_1+R_d}\, d\theta,$$

the limits are from $\frac{\pi}{2}$ to 0, because there is no capacitance to maintain the voltage across R_1 and half-wave detection results.

$$I_m = \frac{\hat{E}_1}{\pi(R_d+R_1)} = \frac{E_1}{R_1}$$

thus
$$\frac{E_1}{\hat{E}_1} = \eta_d = \frac{R_1}{\pi(R_d+R_1)} \quad . \quad . \quad . \quad . \quad 8.30.$$

Power absorbed
$$= \frac{1}{\pi}\int_0^{\frac{\pi}{2}} \frac{\hat{E}_1^2 \cos^2\theta}{R_1+R_d}\, d\theta$$

$$= \frac{\hat{E}_1^2 \frac{\pi}{4}}{\pi(R_1+R_d)} = \frac{\hat{E}_1^2}{2R_E}$$

$$R_E = 2(R_1+R_d) \quad . \quad . \quad . \quad . \quad 8.31.$$

Thus when $C_1 = 0$ and $R_d \ll R_1$, detection efficiency approaches $\frac{1}{\pi}$ and R_E approaches $2R_1$. The latter result is to be expected since the diode conducts for exactly half a cycle, and during conduction the load resistance is very nearly R_1.

8.2.13. Effect of Shunt Capacitance on Detection Efficiency. When the reactance of C_1 cannot be neglected, as may be the case for a low radio frequency (110 kc/s) the curves in Fig. 8.4*b* will not give the true performance of the detector. An estimate of its behaviour may be made by obtaining a mean detection voltage-carrier peak voltage curve as described at the end of Section 8.2.2.

We will now turn to a theoretical examination of the effect of varying C_1.

In Fig. 8.7 is shown the shape of the voltage wave across the load resistance R_1. The interval during one cycle of the input wave, which will be assumed unmodulated, is divided into a charge and discharge period. The former starts at some time instant t_1 when the input voltage exceeds that across R_1, and ceases at t_2. If stable conditions prevail, charge will commence again at a time instant $t_3 = \frac{2\pi}{\omega} + t_1$ when the frequency of the input wave is $f = \frac{\omega}{2\pi}$.

Current and Voltage Relationships during Charge.

$$\hat{E}_1 \cos \omega t = E_1' + iR_d \quad . \quad . \quad . \quad 8.32$$

$$E_1' = i_1 R_1 = \frac{\int i_2 \, dt}{C_1} \quad . \quad . \quad . \quad 8.33$$

$$i = i_1 + i_2 \quad . \quad . \quad . \quad 8.34$$

where i, i_1 and i_2 are the instantaneous currents through diode, R_1 and C_1 respectively (Fig. 8.2) and E_1' is the instantaneous voltage across R_1 and C_1 (Fig. 8.7).

From 8.33 and 8.34

$$i = \frac{E_1'}{R_1} + C_1 \frac{dE_1'}{dt}.$$

Thus

$$\frac{\hat{E}_1 \cos \omega t}{C_1 R_d} = \frac{E_1'}{C_1 R_d}\left[1 + \frac{R_d}{R_1}\right] + \frac{dE_1'}{dt} \quad . \quad . \quad 8.35.$$

The particular solution is

$$E_{1p}' = K\hat{E}_1 \cos (\omega t - \phi)$$

where

$$\phi = \tan^{-1} \frac{\omega C_1}{\frac{1}{R_1} + \frac{1}{R_d}}$$

and

$$K = \frac{1}{R_d \sqrt{\omega^2 C_1^2 + \left(\frac{1}{R_1} + \frac{1}{R_d}\right)^2}} = \frac{\cos \phi}{\left(1 + \frac{R_d}{R_1}\right)}$$

$$\therefore \; E_{1p}' = \frac{E_1' \cos \phi}{\left[1 + \frac{R_d}{R_1}\right]} \cos (\omega t - \phi).$$

The complementary solution is

$$E_{1c}' = K_1 \varepsilon^{-\left(\frac{1}{R_d} + \frac{1}{R_1}\right)\frac{t}{C_1}} = K_1 \varepsilon^{-\frac{\omega t}{\tan \phi}}.$$

The complete solution is

$$E_1' = \frac{\hat{E}_1 \cos\phi}{\left[1+\frac{R_d}{R_1}\right]}\left[\cos(\omega t-\phi)+K_2\varepsilon^{-\frac{\omega t}{\tan\phi}}\right]. \quad . \quad 8.36a.$$

If diode conduction begins at some time instant t_1, the value of K_2 may be found by replacing E_1' by $\hat{E}_1 \cos \omega t_1$ in 8.36*a*

thus $$K_2 = \left\{\frac{\left(1+\frac{R_d}{R_1}\right)}{\cos\phi}\cos\omega t_1 - \cos(\omega t_1-\phi)\right\}\varepsilon^{\frac{\omega t_1}{\tan\phi}}.$$

Hence $$E_1' = \frac{\hat{E}_1\cos\phi}{\left(1+\frac{R_d}{R_1}\right)}\left\{\cos(\omega t-\phi)\right.$$
$$\left.+\left[\frac{\left(1+\frac{R_d}{R_1}\right)}{\cos\phi}\cos\omega t_1-\cos(\omega t_1-\phi)\right]\varepsilon^{\frac{-\omega(t-t_1)}{\tan\phi}}\right\}. \quad 8.36b.$$

Current and Voltage Relationships During Discharge.

$$E_1' = \frac{-\int i_2\,dt}{C_1} = R_1 i_1$$

$$i_1 = i_2$$

$$\frac{E_1'}{R_1} + C_1\frac{dE'_1}{dt} = 0$$

$$E_1'\left[D+\frac{1}{R_1C_1}\right] = 0$$

where $$D = \frac{d}{dt}.$$

The solution to this is

$$E_1' = K_3\varepsilon^{\frac{-t}{R_1C_1}}.$$

If diode conduction ceases at a time instant t_2, then replacing E_1' by $\hat{E}_1 \cos \omega t_2$ gives

$$K_3 = \hat{E}_1\cos\omega t_2\varepsilon^{\frac{t_2}{R_1C_1}}$$

$$E_1' = \hat{E}_1\cos\omega t_2\varepsilon^{-\left(\frac{t-t_2}{R_1C_1}\right)} \quad . \quad . \quad . \quad 8.37.$$

Steady State Conditions.

In the steady state condition the voltage at the end of discharge is equal to that at the beginning of charge, and vice versa.

By replacing t in equation 8.36*b* by t_2, in equation 8.37 by $\frac{2\pi}{\omega}+t_1$ and noting from Fig. 8.7 that E_1' is $\hat{E}_1 \cos \omega t_2$ and $\hat{E}_1 \cos(\omega t_1+2\pi)$ respectively, we obtain two simultaneous equations involving t_2 and t_1,

$$\text{thus } \cos \omega t_2 = \frac{\cos \phi}{\left(1+\frac{R_d}{R_1}\right)}\left\{\cos(\omega t_2 - \phi) + \left[\frac{\left(1+\frac{R_d}{R_1}\right)}{\cos \phi}\cos \omega t_1 - \cos(\omega t_1 - \phi)\right]\varepsilon^{\frac{-\omega(t_2-t_1)}{tan\,\phi}}\right\}$$

$$\text{and} \qquad \cos(\omega t_1+2\pi) = \cos \omega t_2 \varepsilon^{\frac{-\left(t_1+\frac{2\pi}{\omega}-t_2\right)}{R_1C_1}}$$

It is easier to deal with angles than time so we will replace ωt_2 by α_2 and ωt_1 by α_1, and rearrange these two equations into the following forms

$$\left\{\frac{\left(1+\frac{R_d}{R_1}\right)}{\cos \phi}\cos \alpha_1 - \cos(\alpha_1 - \phi)\right\}\varepsilon^{\frac{\alpha_1}{tan\,\phi}} = \left\{\frac{\left(1+\frac{R_d}{R_1}\right)}{\cos \phi}\cos \alpha_2 - \cos(\alpha_2 - \phi)\right\}\varepsilon^{\frac{\alpha_2}{tan\,\phi}} \quad . \quad 8.38a$$

$$\cos \alpha_1 \varepsilon^{\frac{2\pi+\alpha_1}{\omega C_1 R_1}} = \cos \alpha_2 \varepsilon^{\frac{\alpha_2}{\omega C_1 R_1}} \quad . \quad . \quad . \quad 8.38b.$$

The direct solution of 8.38*a* and 8.38*b* is not possible and the best method (suggested by Marique from whose paper [24] this analysis is taken) is by plotting the function

$$y = \left\{\left[\frac{1+\frac{R_d}{R_1}}{\cos \phi}\right]\cos \alpha - \cos(\alpha - \phi)\right\}\varepsilon^{\frac{\alpha}{tan\,\phi}}$$

for $$\alpha \text{ from } -\frac{\pi}{2} \text{ to } \frac{\pi}{2}$$

and the function

$$z = \cos \alpha \; \varepsilon^{\frac{2\pi+\alpha}{\omega R_1 C_1}} \text{ for } \alpha \text{ from } -\frac{\pi}{2} \text{ to } 0$$

and $$z = \cos \alpha \; \varepsilon^{\frac{\alpha}{\omega R_1 C_1}} \text{ for } \alpha \text{ from } 0 \text{ to } \frac{\pi}{2}.$$

Representative curves of y and z are shown in Fig. 8.12 between $-\frac{\pi}{2}$ and $\frac{\pi}{2}$; y has a positive value of $\sin\phi.\varepsilon^{-\frac{\pi}{2\tan\phi}}$ at $-\frac{\pi}{2}$ and a negative value of $-\sin\phi.\varepsilon^{\frac{\pi}{2\tan\phi}}$ at $+\frac{\pi}{2}$ whilst z is zero at both these angular values. The two values of α satisfying equations 8.38*a* and 8.38*b* for a particular value of y or z can be obtained by drawing lines parallel to the " α " axis and reading on that axis the intercepts with the y and z curves. The intercept between $-\frac{\pi}{2}$ and 0 gives α_1 and that between 0 and $\frac{\pi}{2}$, gives α_2. Two curves may be plotted of α_1 against α_2 (one for y, and one for z) obtained from the representative curves, and the point of intersection of these two curves

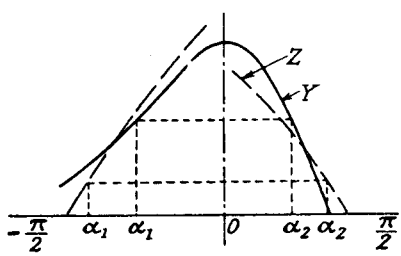

FIG. 8.12.—Typical Curves for the Charge and Discharge Functions.

for y and z gives the value of α_1 and α_2 satisfying the functions y and z simultaneously. Using these values of α_1 and α_2 and assuming the mean rectified voltage E_1 for the discharge period to be the same as for the charge period, we may calculate from 8.37 the value of this mean voltage. This assumption removes the necessity for calculating E_1 over the charge period by means of the more complicated expression 8.36*b*.

$$
\begin{aligned}
E_1 &= \frac{1}{2\pi+\alpha_1-\alpha_2}\int_{\alpha_2}^{\alpha_1+2\pi} E_1' d\alpha \\
&= \frac{\hat{E}_1\cos\alpha_2}{2\pi+\alpha_1-\alpha_2}\int_{\alpha_2}^{\alpha_1+2\pi} \varepsilon^{\frac{-(\alpha-\alpha_2)}{\omega C_1 R_1}}\, d\alpha \\
&= \frac{\omega C_1 R_1 \hat{E}_1\cos\alpha_2}{(2\pi+\alpha_1-\alpha_2)}\left[-\varepsilon^{\frac{-(\alpha-\alpha_2)}{\omega C_1 R_1}}\right]_{\alpha_2}^{\alpha_1+2\pi} \\
&= \frac{\omega C_1 R_1 \hat{E}_1\cos\alpha_2}{2\pi+\alpha_1-\alpha_2}\left(1-\varepsilon^{\frac{-(2\pi+\alpha_1-\alpha_2)}{\omega C_1 R_1}}\right)
\end{aligned}
$$

but detection efficiency $\eta_d = \dfrac{E_1}{\hat{E}_1}$

$$\therefore \eta_d = \frac{E_1}{\hat{E}_1} = \frac{\omega C_1 R_1 \cos \alpha_2}{2\pi + \alpha_1 - \alpha_2}\left[1 - \varepsilon^{\frac{-(2\pi+\alpha_1-\alpha_2)}{\omega C_1 R_1}}\right]$$

$$= \frac{R_1}{X_{C_1}} \cdot \frac{\cos \alpha_2}{2\pi + \alpha_1 - \alpha_2}\left[1 - \varepsilon^{\frac{-(2\pi+\alpha_1-\alpha_2)}{\omega C_1 R_1}}\right]. \quad . \quad 8.39$$

where X_{C_1} is the R.F. reactance of C_1.

The relationship between η_d and $\dfrac{R_1}{X_{C_1}}$ is shown in Fig. 8.13*a* for different values of $\dfrac{R_1}{R_d}$ and it will be noted that in each case there is a value of $\dfrac{R_1}{X_{C_1}}$ which, if exceeded, gives little improvement in

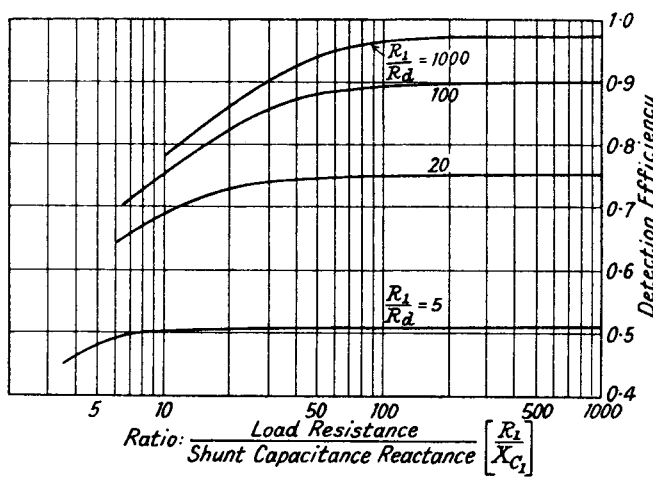

FIG. 8.13*a*.—Curves of Detection Efficiency against the Ratio of Load Resistance to Shunt Capacitance Reactance for Different Values of Load to Conduction Resistance.

detection efficiency. The curves are asymptotic to a value of η_d, which is that given in Fig. 8.8 for the particular value of $\dfrac{R_1}{R_d}$. The limiting value of $\dfrac{R_1}{X_{C_1}}$ is plotted in Fig. 8.13*b* against $\dfrac{R_1}{R_d}$, and if we take our previous case of $R_1 = 1$ MΩ and $R_d = 5{,}000\Omega$, a value

of $\frac{R_1}{X_{C_1}} = 80$ is obtained. The shunt capacitance has therefore little effect on η_d provided the following relationship is satisfied:

$$X_{C_1} \gtrsim \frac{R_1}{80}$$

or

$$C_1 \lesssim \frac{80 \times 10^6}{R_1 \times 2\pi f}\,\mu\text{F}$$

$$\lesssim \frac{12{\cdot}72 \times 10^6}{fR_1}\,\mu\text{F}$$

$$\lesssim \frac{12{\cdot}72}{f(\text{Mc/s}).R_1(\text{M}\Omega)}\,\mu\mu\text{F}.$$

If $f = 1{,}000$ kc/s, and $R_1 = 1$ MΩ, $C_1 \lesssim 12{\cdot}72$ $\mu\mu$F, whilst for $f = 100$ kc/s, $C_1 \lesssim 127{\cdot}2$ $\mu\mu$F.

In any practical case the value of C_1 is unlikely to be less than

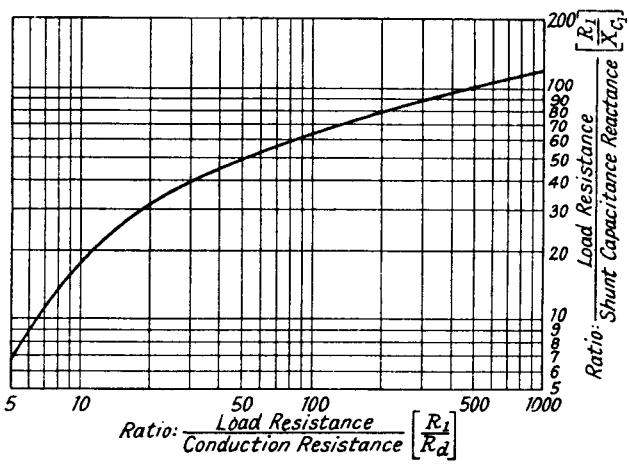

FIG. 8.13*b*.—A Curve of Load Resistance to Shunt Capacitance Reactance Ratio against Load Resistance to Conduction Resistance Ratio for Maximum Detection Efficiency.

0·0001 μF, so that we were justified in ignoring the effect of the shunt capacitance when calculating the equivalent damping resistance of the diode.

The above calculation suggests a minimum value for the capacitance C_1, and we must next consider its limiting value since too large a value can produce amplitude distortion (due to non-tracking) of the detected audio frequency wave shape.

8.2.14. Amplitude Distortion due to a Large Value of

Shunt Capacitance. Amplitude distortion [8, 17] has already been indicated in Fig. 8.3 and it is shown to be due to failure of the voltage across the capacitance to fall to a value below the succeeding carrier peak voltage. This effect only occurs as the modulation envelope is decreasing, and is worst at the point where the rate of change of the modulation envelope is greatest. Thus the rate of discharge of C_1R_1 must not be less than the maximum rate of change of the modulation envelope. If we assume a modulated input signal of $E_1(1+M\cos pt)\cos \omega t$, the rate of change of the modulation envelope is

$$\frac{dE}{dt} = -E_1 Mp \sin pt \quad . \quad . \quad . \quad 8.40$$

this is a maximum when $\frac{d^2E}{dt^2} = 0$

i.e., $$-\hat{E}_1 Mp^2 \cos pt = 0$$

this gives $\cos pt = 0$, and $t = \frac{\pi}{2p}$ or $\frac{\pi}{p}(n+\frac{1}{2})$.

The solutions $t = \frac{3\pi}{2p}, \frac{7\pi}{2p}$, etc., are inadmissible because the modulation envelope is rising, so that the required solutions are

$$t = \frac{\pi}{2p}, \frac{5\pi}{2p}, \text{ etc.}$$

The maximum rate of change of the modulation envelope is $-\hat{E}_1 Mp$.

The discharge equation for C_1R_1 is

$$E_{C_1} = E_0 \varepsilon^{-\frac{t}{R_1C_1}}$$

the rate of discharge $\frac{dE_0}{dt} = -\frac{E_0}{R_1C_1}\varepsilon^{-\frac{t}{R_1C_1}} = -\frac{E_{C_1}}{R_1C_1}$. 8.41.

At the time $t = \frac{\pi}{2p}$; $\cos pt = 0$, $E_{C_1} = E_1$.

Hence $$-\frac{E_1}{R_1C_1} \geqq -\hat{E}_1 Mp \quad . \quad . \quad . \quad 8.42a$$

and noting that $X_{C_1} = \frac{1}{pC_1}$, the reactance of C_1 at audio frequencies, expression 8.42*a* becomes [15]

$$\frac{X_{C_1}}{R_1} \geqq M \quad . \quad . \quad . \quad . \quad 8.42b.$$

Thus if amplitude distortion is to be avoided the ratio of the

reactance of C_1 at audio frequencies to the resistance R_1 must not be less than M, the modulation ratio.

Taking 5,000 c.p.s. as the maximum audio frequency that needs consideration (harmonics of frequencies higher than this are above 10,000 c.p.s. and are therefore unlikely to be troublesome), we have for $R_1 = 1$ MΩ and $M = 1$, a value of

$$C_1 = \frac{10^{12}}{2\pi \times 5{,}000 \times R_1} \mu\mu\text{F}$$
$$= 31{\cdot}9 \ \mu\mu\text{F}$$

which must not be exceeded if distortion is to be prevented at full modulation.

The usual practical value of C_1 is 0·0001 μF, so that the maximum acceptable modulation ratio is limited to 0·319 at 5,000 c.p.s. if distortion is to be avoided. The transmitted modulation ratio for the high audio frequency components is generally low and is normally much less than 0·319.

It is interesting to note that for a given ratio $\frac{X_{C_1}}{R_1}$ the maximum modulation ratio may be increased by applying positive bias [19] to the anode of the diode.

In the absence of a signal voltage there is a voltage across C_1 of very nearly $E_b (R_1 \gg R_d)$, and if we assume $\eta_d = 1$ the voltage rises to $\hat{E}_1 + E_b$ when a signal $\hat{E}_1 \cos \omega t$ is applied. The rate of discharge of C_1 thus becomes

$$\frac{dE_{C1}}{dt} = \frac{-(\hat{E}_1 + E_b)}{R_1 C_1}.$$

The conditions for no amplitude distortion are

$$\frac{\hat{E}_1 + E_b}{\hat{E}_1} \cdot \frac{X_{C_1}}{R_1} \geq M. \quad . \quad . \quad . \quad 8.42c.$$

8.2.15. Frequency Distortion due to the Shunt Capacitance. The capacitance C_1 can produce frequency distortion in addition to amplitude distortion if its value is increased unduly.

We have already noted in expression 8.8 that the mean current through the diode for an unmodulated carrier $\hat{E}_1 \cos \omega t$ is

$$I_m = \frac{\hat{E}_1}{\pi R_d}\left\{\sin \phi - \frac{E_1}{\hat{E}_1}\phi\right\}$$

but since $E_1 = I_m R_1$

$$I_m = \frac{1}{\pi R_d}[\hat{E}_1 \sin \phi - I_m R_1 \phi]$$

or

$$I_m = \frac{\hat{E}_1 \sin \phi}{\pi R_d + R_1 \phi} \quad . \quad . \quad . \quad . \quad 8.43.$$

If a modulated carrier $\hat{E}_1(1+M\cos pt)\cos\omega t$ is applied to the diode, substitution of $\hat{E}_1(1+M\cos pt)$ in 8.43 leads to

$$I_m = \frac{\hat{E}_1(1+M\cos pt)\sin\phi}{\pi R_d + R_1\phi}.$$

Since, however, the load resistance R_1 is shunted by the capacitance C_1, the expression for I_m is more correctly given by

$$I_m = \frac{\hat{E}_1\sin\phi}{\pi R_d + R_1\phi} + \frac{\hat{E}_1\sin\phi}{\pi R_d + Z_1\phi} M\cos pt.$$

The first part is the D.C. term produced by the carrier and the second is the A.C. term due to the modulation frequency. In this term R_1 is replaced by the impedance Z_1, which is the parallel impedance of C_1 and R_1 at the modulation frequency $\left(\frac{R_1}{jpC_1R_1+1}\right)$. The audio frequency voltage across the load resistance is

$$\begin{aligned} E_{AF} = I_m Z_1 &= \frac{E_1\sin\phi}{\pi R_d + Z_1\phi} M\cos pt . Z_1 \\ &= \frac{\hat{E}_1\sin\phi . M\cos pt}{\phi} \cdot \frac{Z_1}{\frac{\pi R_d}{\phi} + Z_1} \quad . \quad . \quad 8.44. \end{aligned}$$

The above expression 8.44 can be represented by a generator which has an open circuit voltage of $\frac{\hat{E}_1 M\sin\phi}{\phi}\cos pt$, an internal resistance $\frac{\pi R_d}{\phi}$ and an external load impedance Z_1. The internal resistance $\frac{\pi R_d}{\phi}$ is the equivalent resistance of the diode at audio frequencies. It is R_d' of Section 8.2.3 and the inverse slope of the $I_m E_a$ characteristic curves in Fig. 8.4*b*.

Two points of interest arise : (1) the resistance R_d' is dependent on detection efficiency for from Section 8.2.5. ϕ equals $\cos^{-1}\eta_d$. Expression 8.10 shows that η_d is controlled by R_d and R_1, so that R_d' itself must be dependent on R_d and R_1. The actual relationship is discussed in the next section ; (2) the reciprocal of the resistance R_d' may be obtained by partial differentiation of 8.8 with respect to E_1, thus

$$\frac{dI_m}{dE_1} = \frac{\phi}{\pi R_d} = \frac{1}{R_d'}.$$

Since the resistance R_d' is dependent on R_1, increasing as R_1 increases, the latter has a twofold effect on the frequency response

curve of the audio frequency output voltage from the detector. Increase of R_1 magnifies the influence of the capacitance C_1 and also increases R_d', and both effects tend to produce loss of high audio frequencies.

If $R_d = 5{,}000\Omega$, $R_1 = 1$ MΩ, $C_1 = 0{\cdot}0001$ μF, Fig. 8.8 gives $\eta_d = 0{\cdot}93$, and the audio output voltage is

$$E_{AF} = \frac{KZ_1}{R_d'+Z_1} = \frac{KR_1}{R_d'(1+jpC_1R_1)+R_1}$$
$$= \frac{KR_1}{\sqrt{(R_d'+R_1)^2+(pC_1R_1R_d')^2}}.$$

But
$$R_d' = \frac{R_d\pi}{\cos^{-1}\eta_d} = \frac{5{,}000\pi}{0{\cdot}3763}$$
$$= 41{,}700\Omega.$$

The reduction in voltage at 10,000 c.p.s. as compared with 50 c.p.s. is

$$\frac{E_{10,000}}{E_{50}} \simeq \frac{R_1}{\sqrt{(R_d'+R_1)^2+(pC_1R_1R_d')^2}} \cdot \frac{R_d'+R_1}{R_1}$$
$$\simeq \frac{1}{\sqrt{1+\left(\frac{pC_1R_1R_d'}{R_d'+R_1}\right)^2}} \simeq \frac{1}{\sqrt{1+(0{\cdot}2525)^2}}$$
$$= 0{\cdot}969 \text{ or } -0{\cdot}28 \text{ db.}$$

The loss of high-frequency response for the component values chosen is negligible. Should, however, the value of C_1 or the conduction resistance R_d of the diode be increased, the loss may become important. For example, suppose $C_1 = 0{\cdot}0005$ μF, then

$$\frac{E_{10,000}}{E_{50}} \simeq \frac{1}{\sqrt{1+(5 \times 0{\cdot}2525)^2}}$$
$$= \frac{1}{\sqrt{1+1{\cdot}59}} = 0{\cdot}621$$
$$\equiv -4.12 \text{ dbs.}$$

or if $R_d = 25{,}000\Omega$, $R_1 = 1$ MΩ and $C_1 = 0{\cdot}0001$ μF. Fig. 8.8 gives $\eta_d = 0{\cdot}84$

$$R_d' = \frac{25{,}000\pi}{0{\cdot}574} = 136{,}800\Omega$$

$$\frac{E_{10,000}}{E_{50}} = \frac{1}{\sqrt{1+(0{\cdot}756)^2}} = 0{\cdot}797 \equiv -1{\cdot}96 \text{ dbs.}$$

Increase of capacitance C_1 has therefore a greater effect than the same ratio increase in R_d. Decrease of R_1 reduces the high-frequency loss for given values of C_1 and R_d.

8.2.16. The I_mE_a Characteristic Curves[9] for a Linear Diode Conducting at $E_a = 0$. The mean current expression 8.8 may be written

$$I_m = \frac{\hat{E}_1}{\pi R_d}[\sin\phi - \phi\cos\phi] \quad . \quad . \quad . \quad 8.45$$

for $$\frac{E_1}{\hat{E}_1} = \cos\phi.$$

$$\therefore\ I_m = \frac{\hat{E}_1}{\pi R_d} f(\phi).$$

The function $f(\phi)$ is plotted in Fig. 8.14*a* between $\phi = 0$ and 4 radians. To obtain a particular I_mE_a characteristic curve it is

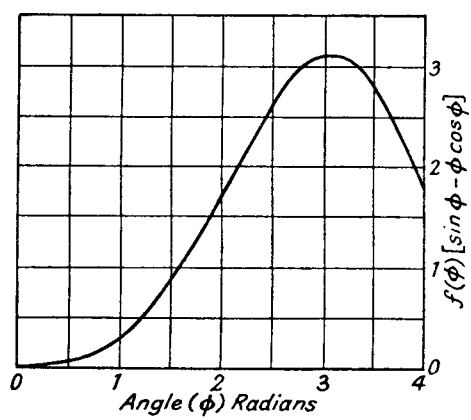

FIG. 8.14*a*.—The Curve of $f(\phi)$ against ϕ.

only necessary to replace E_1 in 8.45 by the required peak value and to note that $\frac{E_1}{\hat{E}_1} = \frac{-E_a}{\hat{E}_1} = \cos\phi$. For example, if $R_d = 5{,}000\Omega$, $E_1 = 1$ volt and $E_a = -0{\cdot}5$ volts, $\cos\phi = 0{\cdot}5$ or $\phi = \frac{\pi}{3}$, which gives a value of $f(\phi) = 0{\cdot}35$ and $I_m = 0{\cdot}022$ mA. If this is repeated for values of E_a from -1 to $+1$ the I_mE_a curve for $\hat{E}_1 = 1$ volt is obtained. When E_a exceeds $+\hat{E}_1$ each curve merges into the diode conduction curve because the diode current is not taken to cut-off and no detection occurs. In Fig. 8.14*b* I_mE_a curves are shown for $\hat{E}_1 = 1$ to 5 volts and $R_d = 5{,}000$ ohms. If a load line OB, corresponding to any particular value of R_1, is drawn across these

curves, it will be noted that I_m at the intersections is proportional to $\hat{E}_1$. Since $I_m = \frac{\hat{E}_1}{\pi R_d} f(\phi)$ it follows that $f(\phi)$ must be constant,

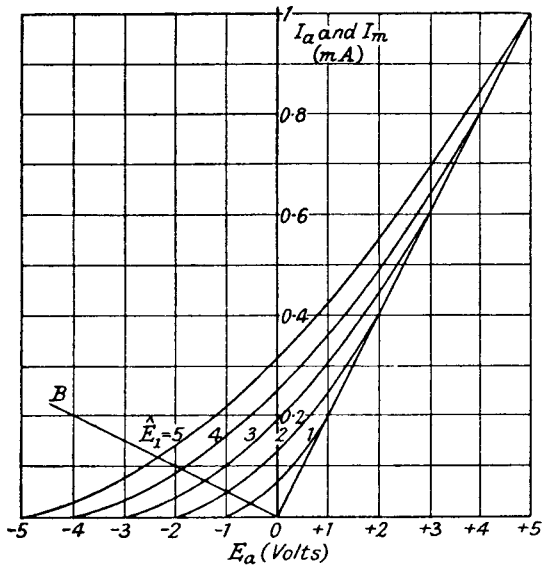

FIG. 8.14b.—Characteristic $I_m E_a$ Curves for a Diode with Linear Conduction Curve.
(R_d = 5,000Ω.)

i.e., ϕ is constant. But we have already shown in Section 8.2.15 that the slope of these curves is $\frac{1}{R_d'}$ or $\frac{\phi}{\pi R_d}$. Hence if ϕ is constant, R_d' is also constant for a given value of R_1. The relationship between R_d' and R_1 may be obtained for a fixed value of R_d by

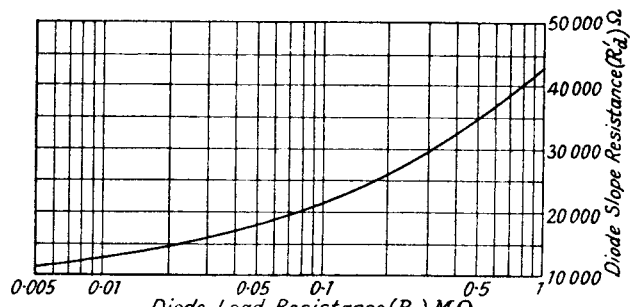

FIG. 8.14c.—A Curve of Diode Slope Resistance against Load Resistance.
(R_d = 5,000Ω.)

substituting the particular values of ϕ (obtained from the curves of $\eta_d(\phi = \cos^{-1}\eta_d)$ against $\frac{R_1}{R_d}$, Fig. 8.8), in the expression $R_d' = \frac{\pi R_d}{\phi}$, e.g., Fig. 8.8 gives $\eta_d = 0{\cdot}866$ at $\frac{R_1}{R_d} = 58$; $\phi = \cos^{-1} 0{\cdot}866 = \frac{\pi}{6}$, and replacing this in $R_d' = \frac{\pi R_d}{\phi}$ when $R_d = 5{,}000\Omega$, we find that $R_d' = 6R_d = 30{,}000\Omega$ for $R_1 = 58 \times 5{,}000 = 290{,}000\Omega$. A curve of R_d' against R_1 for $R_d = 5{,}000\Omega$ is plotted in Fig. 8.14c.

8.3. Cumulative Grid Detection.

8.3.1. Introduction. The cumulative grid detector operates in a manner similar to the diode by using the grid of a triode or multigrid valve as the diode anode. The I_gE_g characteristic curve is generally similar to curve AB' of Fig. 8.10 illustrating the parabolic detector. The audio frequency variations of small carrier amplitudes are detected due to curvature [5] of the characteristic, i.e.,

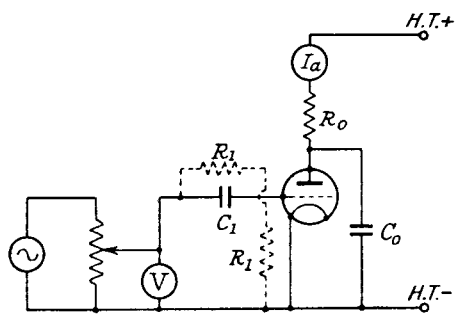

FIG. 8.15.—A Circuit for Measuring the Detection Characteristics of a Cumulative Grid Detector.

I_g [14] flows throughout the cycle and R_E is low, but for large carrier amplitudes the grid-cathode space acts as a unidirectional device and I_g flows over a small part of the cycle only.

The audio frequency variations across R_1 (Fig. 8.15) cause variations in the grid bias of the valve which in turn produce audio frequency variations of anode current. The cumulative grid detector may be viewed as a separate diode,[18] the anode of which is connected directly to the grid of an A.F. amplifier valve. Detection makes the grid voltage negative with respect to the cathode so that the D.C. anode current falls as the carrier input voltage is increased. This type of detector would therefore appear to offer the advantage of a combined detector and A.F. amplifier in one valve. It possesses,

however, two disadvantages, the D.C. grid-bias point is variable, and R.F. as well as A.F. voltages are applied to the grid. The bias point is fixed by the input carrier peak voltage, so that it is impossible to operate the valve under optimum audio frequency amplifying conditions except for a restricted range of carrier voltages. The presence of R.F. as well as A.F. voltages increases the possibility of overloading, and the A.F. output voltage is consequently restricted. Since R.F. voltages from the input tuned circuit are not filtered from the grid of the valve, the anode-grid capacitance will cause the anode circuit to reflect back a resistance and capacitance component into the grid circuit as described in Section 2.8.2. The resistance component is generally the more serious and its effect may be many times greater than that due to grid current damping.

There are two possible methods of connecting the detector load resistance R_1 as illustrated in Fig. 8.15. The only difference between the two positions so far as the operating conditions are concerned is that when R_1 is connected between grid and cathode it acts as an additional shunt resistance across the input circuit. This connection of R_1 is chiefly of advantage in battery valve detectors, having start of grid current at some positive voltage, for R_1 can be returned to the L.T. positive terminal without disturbing the valve or input circuit connections. The necessity for a positive bias voltage on the grid of the valve having a positive start of current has already been discussed in Section 8.2.7. If large signal voltages are applied, grid current is only taken on the peaks of the input signal, because the voltage across R_1 is maintained by the discharge of capacitance C_1 between the peaks in a manner exactly similar to that shown in Fig. 8.3 for the diode. This produces less damping on the grid circuit $\left(\text{see curve 1 in Fig. 8.11}b \text{ for } \frac{\hat{E}_1}{E_0} \text{ increasing}\right)$, a higher detection efficiency (curve 1 in Fig. 8.11a) and a mean grid voltage variation which is an almost exact reproduction of the modulation envelope.

Owing to the control of the bias by the input carrier voltage, though no distortion may occur in the grid circuit, distortion may be produced in the anode circuit. When the mean grid voltage variations are large the anode current variations may be carried into the bottom bend of the I_aE_g characteristic curve with resultant flattening [2] of the audio frequency wave shape. In extreme cases this may cause in a receiver a double-humped tuning effect with a distorted minimum output at the correct tuning point. This flattening of the audio frequency wave may be decreased by

increasing the detector anode voltage and reducing the mean grid voltage variations. A detector modified in this way is often called a power grid detector.

8.3.2. Power Grid Detection. The power grid detector—a modification of the cumulative grid detector—is intended for operation with large input carrier voltages, when the grid circuit acts as a unidirectional current device and current is taken only on extreme positive peaks of the signal. The grid leak resistance R_1 (Fig. 8.15) is reduced and the anode voltage increased so as to prevent distortion of the audio frequency output current in the anode circuit. The reduction of grid voltage variations by decreasing R_1 may be illustrated from Fig. 8.4*b* where it is shown that the line OB' (corresponding to a small R_1) reduces the grid voltage variations in the ratio $\frac{E_1' - E_0'}{\hat{E}_1}$.

8.3.3. Damping of the Input Circuit by a Cumulative Grid Detector. The cumulative grid detector introduces two forms of damping on the input signal circuit. The first, due to grid conduction current, has already been adequately discussed in Sections 8.2.5 to 8.2.9 on the diode. The second is due to the anode-grid capacitance of the valve. We have already developed in Section 2.8.2 expressions for the conductance and susceptance reflected into the grid circuit by feedback from the anode circuit through the anode-grid capacitance of the valve. Taking expressions 2.9*a* and 2.9*b*, substituting $\frac{1}{R_a}$ for G_a, $\frac{1}{R_0}$ for G_0 and ωC_0 for B_0, and neglecting B_{g_a} in association with other components we have

$$R_g = \frac{\left(\frac{1}{R_a}+\frac{1}{R_0}\right)^2+(\omega C_0)^2}{g_m \omega C_{g_a} \omega C_0} \quad . \quad . \quad . \quad . \quad . \quad 8.46a$$

and

$$C_g = \frac{C_{g_a}\left[\left(\frac{1}{R_a}+\frac{1}{R_0}+g_m\right)\left(\frac{1}{R_a}+\frac{1}{R_0}\right)+(\omega C_0)^2\right]}{\left(\frac{1}{R_a}+\frac{1}{R_0}\right)^2+(\omega C_0)^2} \quad . \quad 8.46b$$

where R_g and C_g are the equivalent parallel resistance and capacitance components of the grid input admittance. The load capacitance C_0 is an essential part of the circuit as it acts as a bypass for R.F. currents developed in the valve, and reduces the possibility of passing on R.F. voltages to the grid of the next valve. Its maximum value is limited by its discrimination against the high-frequency

components of the audio frequencies contained in the modulation; a suitable value is 100 $\mu\mu$F.

When $\omega C_0 \gg \frac{1}{R_a}+\frac{1}{R_0}$ and $g_m \gg \frac{1}{R_a}+\frac{1}{R_0}$.

$$R_g \simeq \frac{C_0}{g_m C_{g_a}} \quad . \quad . \quad . \quad . \quad . \quad . \quad 8.47a$$

and

$$C_g \simeq C_{g_a}\left(\frac{g_m\left(\frac{1}{R_a}+\frac{1}{R_0}\right)}{(\omega C_0)^2}+1\right) \quad . \quad . \quad 8.47b.$$

By using these expressions for R_g and C_g we can estimate the effect of g_m, C_{g_a}, R_0 and C_0 on the input admittance, and this is summarized in the table below.

Variable.	R_g	C_g
Increasing g_m	decrease	increase
Increasing C_{g_a}	decrease	increase
Increasing R_0		
(*a*) $R_0 \gg \frac{1}{\omega C_0}$	(*a*) little effect	decrease
(*b*) R_0 comparable to $\frac{1}{\omega C_0}$	(*b*) has minimum value when $\omega C_0 = \frac{1}{R_a}+\frac{1}{R_0}$	
(*c*) $R_0 \ll \frac{1}{\omega C_0}$	(*c*) decrease	
Increasing C_0	decrease to minimum when $\omega C_0 = \frac{1}{R_a}+\frac{1}{R_0}$	decrease

To show the order of R_g and C_g let us take the following example of a triode detector:

$$f = 1{,}000 \text{ kc/s}, \; R_0 = 30{,}000\Omega, \; C_0 = 100 \; \mu\mu\text{F}, \; C_{g_a} = 3 \; \mu\mu\text{F}$$

$$R_a = 10{,}000\Omega, \; g_m = 3 \text{ mA/volt}.$$

From 8.46*a* and 8.46*b*

$$R_g = 11{,}600\Omega$$
$$C_g = 5{\cdot}9 \; \mu\mu\text{F}.$$

The detuning effect of the parallel capacitance C_g is small and except for small values of tuning capacitance may be ignored. The parallel resistance R_g is so low that it shows anode circuit damping to be much more serious than grid current damping $\left(\frac{R_1}{2} \text{ approximately}\right)$. The resistance R_g can be conveniently increased only by reducing C_{g_a} or g_m. It is not possible to increase

C_0 unduly or loss of the high audio frequency modulation components results.

A reduction of g_m is not a satisfactory solution since this reduces the gain of the detector stage. (For large signal input voltages g_m is reduced because of increase of D.C. bias voltage, so that there is a tendency to decrease anode circuit damping as the input signal is increased.) The only real solution is a reduction of C_{g_a} and this can be accomplished by using a tetrode or pentode [21] valve as a detector. Care must be exercised to see that the external stray capacitance between grid and anode is very small if the full advantage of such a valve is to be gained, and it should be noted that the high internal resistance of a multigrid valve will tend to accentuate the loss of high audio frequencies due to the bypass capacitance C_0. The stage gain of a triode detector is proportional to $\frac{\mu Z_0}{R_a+Z_0}$, i.e., $\frac{g_m R_a Z_0}{R_a+Z_0}$, whilst for a tetrode it is more nearly proportional to $g_m Z_0$ or $\frac{\mu Z_0}{R_a}$; any variation of Z_0 will obviously affect the result to a much less extent in the triode case.

Anode circuit damping can be entirely eliminated when a separate diode and triode valve are used for detection and amplification. An R.F. filter (R_3C_3 in Fig. 8.5), included between the diode load resistance and the triode grid circuit, effectively isolates the latter from the tuned R.F. input circuit to the detector. The diode-triode combination usually produces a higher gain than that of the same triode operating as a cumulative grid detector because of the elimination of anode circuit damping. Furthermore, greater output voltage is possible for a given distortion since only A.F. voltages are applied to the triode grid circuit.

8.3.4. Estimation of the Performance of the Cumulative Grid Detector. The detection characteristic of the cumulative grid detector may be measured at a low frequency (50 c.p.s.) provided the capacitances C_1 and C_0 are increased to give the same reactances at 50 c.p.s. as at the normal carrier frequency. For example, 0·0001 μF at 1,000 kc/s is equivalent to 2 μF at 50 c.p.s. The circuit is given in Fig. 8.15 ; no special precautions are necessary except that since grid current flows the input potentiometer must not have a high resistance value. A series of curves of mean detection voltage plotted against peak input volts may be obtained as in Fig. 8.16. The mean detection voltage is given by $(I_{a0} - I_{a1})R_0$, where I_{a1} is the D.C. current at a particular peak input voltage,

I_{a0} is the D.C. current at zero input voltage, and R_0 is the resistance in the anode circuit. The initial curvature for small peak input voltages (less than 0·1 volt) due to square law detection is indicated in the curves.

The audio output voltage in the anode circuit is obtained by noting the change of mean detection voltage between the carrier peak voltage limits set by the modulation envelope maximum and minimum values. Taking a carrier peak voltage of 1 volt modulated by 50%, the maximum and minimum of the modulation envelope are 1·5 and 0·5 peak volts, respectively. The mean detected voltage change corresponding to these limits is from 10 to 28 volts. The relationship between carrier peak volts and mean detection volts is

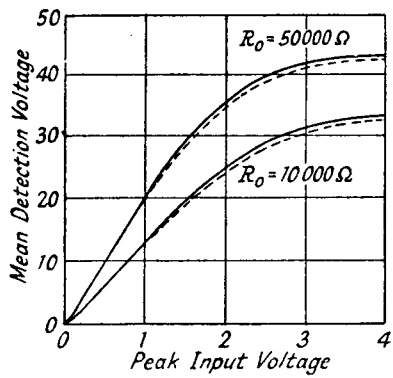

FIG. 8.16.—Typical Detection Curves for a Cumulative Grid Detector.
(Full Line—R_1 = 1 MΩ.
Dotted Line—R_1 = 0·1 MΩ.)

very nearly linear over this range, so that the peak value of the audio output voltage is one-half of the mean detection voltage change, i.e., 9·0 volts. The turn-over effect as I_a approaches the bottom bend of the I_aE_g curve is very clearly shown, and it will be observed that when the carrier voltage is increased beyond 2 volts the mean detection voltage change due to the modulation envelope decreases and becomes distorted. This is the effect producing an apparent double-humped response already discussed in Section 8.3.1.

Characteristic curves [16] rather similar to the I_mE_a characteristic curves of a diode may be obtained for a cumulative grid detector. The circuit is the same as that of Fig. 8.15, except that the anode resistance R_0 is replaced by a low-resistance milliammeter. I_mE_a curves are obtained for different values of input peak voltage for

fixed values of R_1 and C_1 (2 μF to correspond to 0·0001 μF at 1,000 kc/s), and these are indicated in Fig. 8.17. The audio output voltage for any particular H.T. voltage and anode external resistance R_0 can be obtained by drawing the appropriate load lines such as AB or AG. A separate set of curves must, of course, be drawn for each required value of R_1. These curves only represent detection conditions if the anode impedance to the carrier frequency is low. This assumption is generally valid owing to the presence of the R.F. bypass capacitor C_0. The great advantage of the curves lies in the fact that the effect of any values of R_0 with, or without, a decoupling resistance R' may be studied. When a decoupling resistance (R') is employed, a load line, such as AB, is drawn from a point

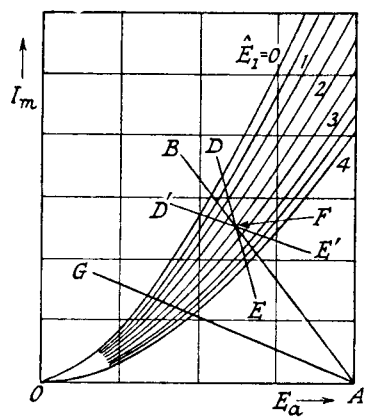

FIG. 8.17.—Typical I_mE_a Curves for a Cumulative Grid Detector.

on the E_a axis equal to the H.T. voltage at an angle $\cot^{-1}(R'+R_0)$, and then another load line DE is drawn at an angle $\cot^{-1} R_0$ through the intersection F of the line AB and the particular carrier peak voltage being considered. The A.F. output voltage is obtained from the intersections of DE with the appropriate carrier voltage lines. $D'E'$ represents the condition for a transformer load with a decoupling resistance R'; AB now has an angle given by $\cot^{-1} R'$.

8.4. Anode Bend Detection.

8.4.1. Introduction. A valve may be made to operate as an anode bend detector if the grid bias is so adjusted that the valve is working on the curved part of its I_aE_g characteristic. Such detection depends mainly on the second derivative [1] of the I_aE_g curve. If we assume that the I_aE_g relationship is given by $I_a = f(E_g)$, a

small change of grid voltage δE_g results in the following current-voltage relationship

$$(I_a+\delta I_a) = f(E_g+\delta E_g)$$

and using Taylor's expansion

$$(I_a+\delta I_a) = f(E_g)+\frac{df(E_g)}{dE_g}\delta E_g+\frac{d^2f(E_g)}{dE_g{}^2}\frac{\delta E_g{}^2}{2!}+\frac{d^3f(E_g)}{dE_g{}^3}\cdot\frac{\delta E_g{}^3}{3!}+\text{ etc.},$$

$$= f(E_g)+f'(E_g).\delta E_g+f''(E_g)\frac{\delta E_g{}^2}{2!}+f'''(E_g)\frac{\delta E_g{}^3}{3!}+\text{ etc.},$$

where $f'(E_g) = \frac{df(E_g)}{dE_g} = \frac{dI_a}{dE_g}$; $f''(E_g) = \frac{d^2I_a}{dE_g{}^2}$, etc.

If $\delta E_g = \hat{E}\cos\omega t(1+M\cos pt)$

$$\delta I_a = f'(E_g)[\hat{E}\cos\omega t(1+M\cos pt)]+f''(E_g)\frac{[\hat{E}\cos\omega t(1+M\cos pt)]^2}{2!}$$

$$+f'''(E_g)\frac{[\hat{E}\cos\omega t(1+M\cos pt)]^3}{3!} \quad . \quad . \quad 8.48.$$

The first and third terms contain only modulated radio frequency components and are therefore of no interest since we require audio frequency components. The second term is

$$\frac{f''(E_g)}{2!}\hat{E}^2\cos^2\omega t(1+M\cos pt)^2$$

$$=\frac{f''(E_g)}{2!}\left[\frac{\hat{E}^2(1+\cos 2\omega t)}{2}(1+2M\cos pt+M^2\cos^2 pt)\right].$$

The radio frequency term is not required and the D.C. and audio frequency components produced by this term are

$$\frac{f''(E_g)}{4}\hat{E}^2\left(1+2M\cos pt+\frac{M^2}{2}(1+\cos 2pt)\right). \quad . \quad 8.49a$$

of which the audio frequency component is

$$E_{AF} = \frac{f''(E_g)}{4}\hat{E}^2\left(2M\cos pt+\frac{M^2}{2}\cos 2pt\right) \quad . \quad . \quad 8.49b.$$

This contains a term of frequency $\frac{p}{2\pi}$ c.p.s., the original modulation component, and a second harmonic component of $\frac{2p}{2\pi}$ c.p.s.

The ratio of second harmonic to fundamental is

$$\frac{M^2}{2}\cdot\frac{1}{2M} = \frac{M}{4} \quad . \quad . \quad . \quad . \quad 8.50.$$

Hence, the modulation ratio of a carrier detected by a parabolic detector should not be high if distortion is to be kept low.

The coefficient $f''(E_g)$ otherwise $\frac{d^2I_a}{dE_g^2}$ is the slope of the mutual conductance-grid bias (g_mE_g) curve of the valve at the particular grid bias point. We may note that it is not only the second derivative term in the Taylor expansion which produces audio frequency components. All even derivatives can produce such components. A better understanding of the physical significance of these derivatives in the Taylor expansion may be gained by considering an I_aE_g curve represented by a power series such as

$$I_a = a_0+a_1E_g+a_2E_g^2+a_3E_g^3+a_4E_g^4+ \ . \ . \ .$$

The first derivative represents the mutual conductance

$$g_m = f'(E_g) = \frac{dI_a}{dE_g} = a_1+2a_2E_g+3a_3E_g^2+4a_4E_g^3 \ . \ . \ .$$

the second is

$$f''(E_g) = \frac{d^2I_a}{dE_g^2} = 2a_2+6a_3E_g+12a_4E_g^2+ \ . \ . \ .$$

In a true parabolic detector all terms above a_2 are zero, hence

$$f''(E_g) = 2a_2 = \text{constant}$$

and the detected audio frequency output voltage is then independent of the bias point on the I_aE_g characteristic. For an actual valve characteristic the terms a_3, a_4, etc., are rarely zero. The a_4 term is usually negative so that $f''(E_g)$ has a maximum value at a particular grid bias. This is clearly shown in the typical detection curves of Fig. 8.19*b*; a bias of -3 volts gives maximum detection. Two grid bias points can generally be found giving optimum detection conditions, for there is a position of maximum rate of change of curvature [$f''(E_g)$] near zero anode current (bottom bend) and near saturation current of the valve (top bend). The "top bend" of the I_aE_g characteristic is never used since it represents a waste of anode current and a considerable reduction in the life of the valve. Furthermore, saturation can usually be reached only by using positive grid bias, and grid current is an undesirable feature because it causes damping of the input circuit.

The operation of a valve as an anode bend detector using the "bottom bend" can be followed from the I_aE_g characteristic curve in Fig. 8.18*a*.

The curve AB is the characteristic curve for zero external anode resistance. This condition is of no use since an output voltage is

required from the detector. A resistance must therefore be inserted in the anode circuit. The operational I_aE_g curve then takes the shape shown by the line AG, and detection occurs because the negative envelope is amplified to a less extent than the positive envelope. This produces a mean current fluctuation which approximately follows the modulation envelope. Harmonics (mainly second) of the audio frequency are actually produced as shown by the mathematical analysis. As the resistance R_0 is increased, the rate of change of curvature decreases (i.e., the slope of AG is less),

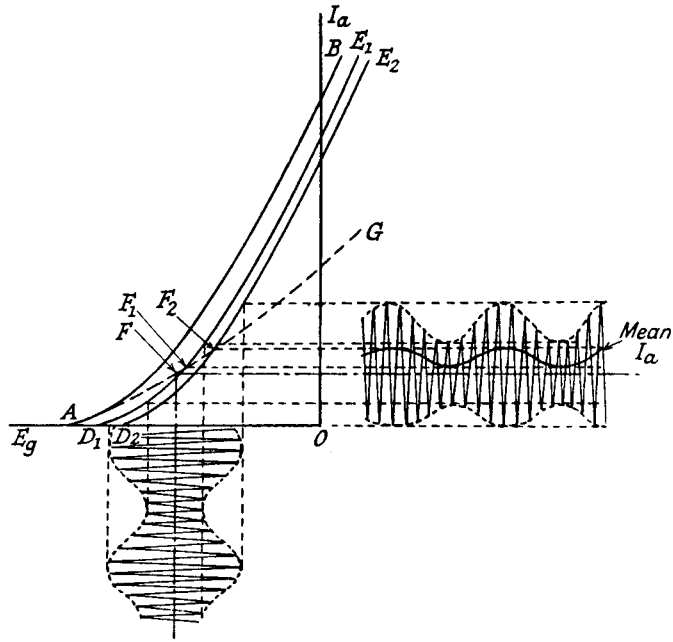

FIG. 8.18*a*.—Anode Bend Detection referred to the I_aE_g Characteristic.

thus decreasing the mean current, but the audio output voltage is actually increased. The case is analogous to that of a generator of fixed internal resistance connected to a variable resistance. As this resistance is increased the voltage across it rises, approaching in the limit the open circuit voltage of the generator.

The decrease in the rate of change of curvature as R_0 is increased is undesirable and we should prefer to maintain the original rate of change of I_a as R_0 is increased. This can be accomplished if the anode impedance is zero, or nearly so, for radio frequencies. The use of a capacitance (C_0 in Fig. 8.19*a*) in parallel with R_0 will produce this result. If the reactance of C_0 is small at radio fre-

quencies the characteristic curve along which detection takes place is one similar to D_1E_1 in Fig. 8.18*a*. It is substantially parallel to the original curve AB for $R_0 = 0$, but is moved towards zero grid volts by an amount governed by the mean current, which in turn is fixed by the carrier amplitude, R_0, and the original grid bias.

Since the mean current is proportional to the carrier amplitude, the position of the operating line varies with the modulation envelope. For minimum carrier amplitude, the mean current is minimum so that the correct line is D_1E_1, but for the maximum carrier amplitude it is D_2E_2. These two lines represent the limits of movement for the particular modulated wave shown, and the

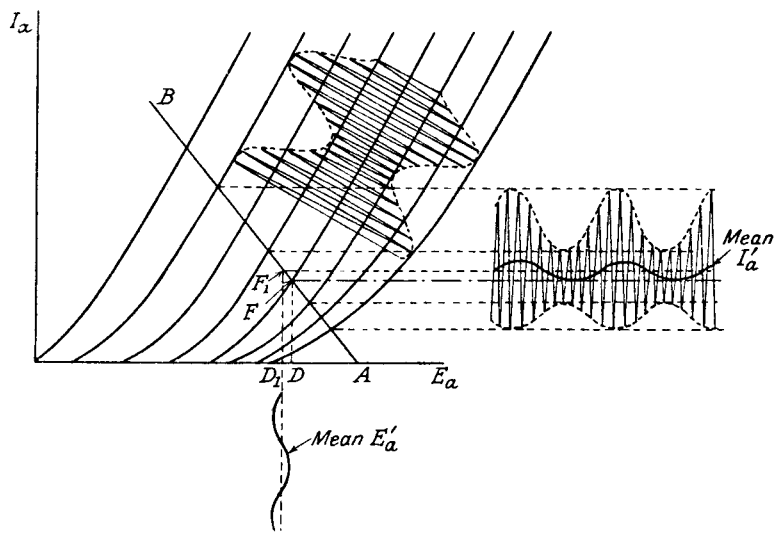

FIG. 8.18*b*.—Anode Bend Detection, with no Anode Capacitance, referred to the I_aE_a Characteristic.

R.F. detection line oscillates between the two positions at an audio frequency corresponding to that of the modulation envelope. Increase of modulation percentage causes F_1 to move nearer to F, the operating point in the absence of a signal, and F_2 to move further from F.

The effect of the capacitance C_0 may be more clearly shown by reference to the I_aE_a curves. Taking the case of the resistance R_0 only in the anode circuit, the conditions are represented in Fig. 8.18*b* where AB is the load line at an angle $\cot^{-1} R_0$. If F is the point corresponding to the grid bias, a modulated wave in the grid circuit produces a distorted modulated anode current wave

which has a mean current variation shown by the full line. The mean current variation is always above the point F unless the input signal is 100% modulated, because even the smallest signal causes some increase in anode current. The mean current variation produces a mean voltage variation given by the full line beneath the E_a axis. The D.C. anode voltage is decreased by detection from its zero signal value OD to OD_1. The mathematical analysis shows in equation 8.49*a* that detection increases the D.C. current by $\frac{f''(E_g)\hat{E}^2\left(1+\frac{M^2}{2}\right)}{4}$. Hence the true operating point moves from F to F_1; the exact position of F_1 depends on the signal voltage,

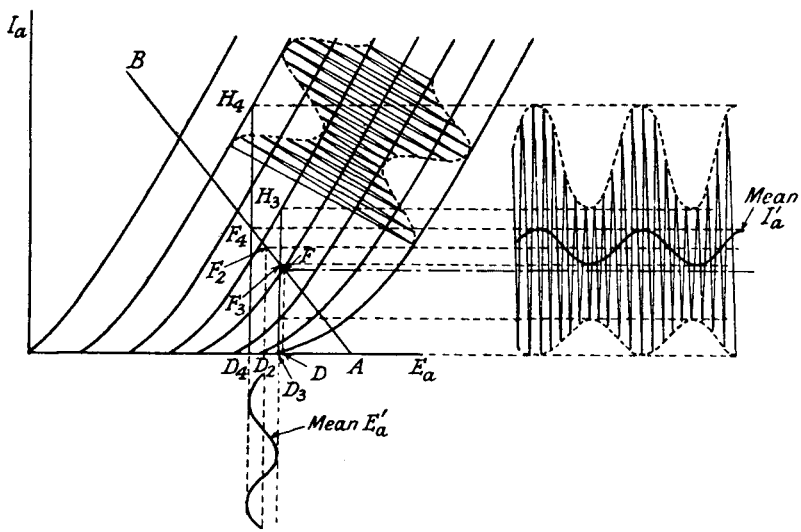

FIG. 8.18c.—Anode Bend Detection, with Anode Bypass Capacitance, referred to the I_aE_a Characteristic.

rising higher on the load line as the carrier amplitude and modulation percentage are increased.

When the resistance R_0 is paralleled by a capacitor C_0, the operating conditions become those of Fig. 8.18*c*. The audio frequency load line is as before, AB, because the reactance of C_0 is very much greater than R_0 at these frequencies, but the R.F. load line changes to an almost vertical line. This vertical line really approximates to a thin ellipse, the minor axis of which is small since the reactance of C_0 is much less than R_0. The position of this load line is not fixed but varies with the modulation envelope

amplitude between the two points F_3 and F_4. The load line position for maximum envelope amplitude is D_4H_4 and for minimum amplitude D_3H_3. The D.C. anode voltage, which is given by OD_2, is approximately the average of OD_4 and OD_3, and its value is determined by the carrier amplitude and modulation percentage. The anode current wave shape is shown to the right of Fig. 8.18*c*, where the thick curve indicates the fluctuations of mean current. This curve, projected on to the audio frequency load line AB, gives the mean voltage shown below the E_a axis. The addition of the capacitor C_0 has therefore two effects; it has for a given input signal: (1) decreased the D.C. anode voltage and (2) greatly increased the mean anode current and anode voltage variation. The resistance R_0 controls the mean output voltage variation, and maximum gain, which is limited by the amplification factor of the valve, is obtained when R_0 is large. Very high values of R_0 tend to reduce the amplification factor as in the analogous case of the A.F. amplifier (Section 9.3.1) and also cause discrimination against the high audio frequencies by reason of the parallel capacitance C_0. R_0 should not therefore exceed three to four times the internal resistance of the valve.

To obtain optimum detection, variation of anode or grid bias voltage is essential. With small signal voltages detection is generally a maximum for low anode voltages because the rate of change of curvature of the I_aE_g characteristic diminishes as the anode voltage increases. For the same reason a valve having high values of μ and R_a is generally better than one having low values.

If a large input signal is available an anode bend detector may be made to function in a manner approaching a linear[4] detector by biasing the valve almost to the point where $I_a = 0$. The negative modulation envelope is then suppressed and, provided the positive envelope passes over the straight part of the I_aE_g curve, the audio frequency components of the modulation envelope are reproduced without distortion. Under these conditions the output voltage approaches $\frac{\mu R_0}{R_a+R_0}$ times the input modulation envelope. The maximum signal voltage, however, must not be large enough to produce grid current.

8.4.2. Estimation of the Performance of an Anode Bend Detector. Measurements at 50 c.p.s. may be made on a valve to indicate its performance as an anode bend detector. The circuit is shown in Fig. 8.19*a*. The value of C_0 is chosen to give a reactance at 50 c.p.s. equal to the reactance of the capacitor normally used

at radio frequencies. Fig. 8.19*b* shows the presence of an optimum bias point and also the disadvantage of the anode bend detector,

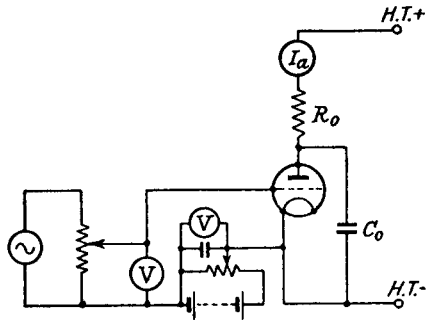

FIG. 8.19*a*.—A Circuit for determining Anode Bend Detection Characteristics.

viz., its inefficient detection of small signal voltages. This feature also limits the maximum modulation percentage of larger signals which can be accepted without serious distortion.

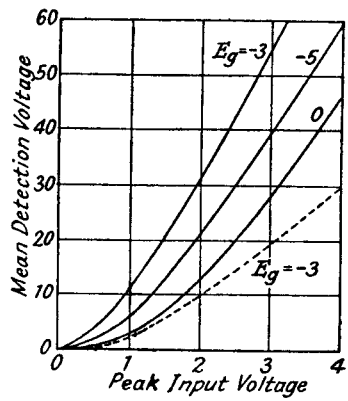

FIG. 8.19*b*.—Typical Detection Curves for an Anode Bend Detector.
(Full Line—R_0 = 50,000Ω.
Dotted Line—R_0 = 10,000Ω.)

8.4.3. Damping of the Input Circuit. The anode bend detector has the advantage that it produces no grid current damping. There is, however, damping due to the anode-grid capacitance,[3] the parallel components of resistance and capacitance being the same as for the cumulative grid detector, viz.,

$$R_g \simeq \frac{C_0}{g_m C_{g_a}}.$$

$$C_g \simeq C_{g_a} \cdot \left[\frac{g_m \left(\frac{1}{R_a} + \frac{1}{R_0} \right)}{(\omega C_0)^2} + 1 \right].$$

Since, however, the anode bend detector operates on the curved part of the characteristic, g_m will be lower than in the case of the cumulative grid detector. For small signals, therefore, the damping is small, but it increases as the signal increases because the valve begins to operate over the higher gain part of the characteristic. This is not a serious disadvantage since strong signals require generally less selectivity than weak signals. The low gain of the detector for small signals is, however, not offset by the lower damping.

8.4.4. Anode Bend Detection with Self-Bias. It is quite usual with indirectly heated anode bend detectors to provide self-bias by a resistance in the cathode circuit. A large capacitance (50 μF) must bypass the resistance if loss of the low audio frequency modulation components is to be prevented, since voltages across the self-bias resistance tend to cancel the anode current changes producing them (see Section 2.7). The resistance value should be chosen to give under no signal conditions the optimum bias. As the signal increases there is a tendency for self-bias to increase and detection efficiency to decrease.

8.5. The Advantages and Disadvantages of the Three Types of Detectors.[13] We may now summarize the advantages and disadvantages of the diode, cumulative grid, and anode bend detectors as follows :

1. *Diode Detector.*

Advantages.

(1) Distortion of the audio frequency components of the modulation envelope decreases as the carrier voltage is increased.
(2) The carrier modulation percentage may be high without distortion becoming appreciable provided certain coupling conditions are fulfilled.
(3) There is no damping of the input circuit other than conduction current damping.
(4) The maximum permissible carrier voltage is almost unlimited.

Disadvantages.

(1) The valve represents a loss of amplification ; this loss may be reduced to small proportions by a suitable choice of R_1 and C_1.
(2) Conduction current produces damping of the input circuit. The use of a high value of R_1 reduces this effect.

2. *Cumulative Grid Detector.*

Advantages.

(1) It is very sensitive for small carrier voltages.
(2) Amplification is obtained from input to output, approximating to that of the valve as an A.F. amplifier.
(3) Distortion is not very great provided the carrier voltage is not too large (the maximum permissible is generally about 1 volt).

Disadvantages.

(1) The input circuit is damped by conduction grid current and by a resistance component reflected from the anode circuit by the anode-grid capacitance.
The latter effect is generally much more serious than grid conduction current damping.
(2) The maximum carrier voltage is limited due to the bottom bend of the I_aE_g characteristic.

3. *Anode Bend Detector.*

Advantages.

(1) There is no damping of the input circuit due to grid current.
(2) Anode-grid capacitance damping is generally low owing to the fact that the valve operates on the low gain bottom bend of the I_aE_g characteristic.
(3) Amplification is obtained from input to output.

Disadvantages.

(1) Sensitivity is very low for small carrier voltages.
(2) Distortion of the audio frequency modulation components is high except for large carrier input voltages with low modulation percentages.
(3) The maximum carrier voltage is limited by grid current.

8.6. Reaction or Regeneration in Detectors. The term reaction, or more correctly regeneration, is used to describe the process by which the output voltage of a valve is coupled back to the input so as to increase the effective input voltage. Regeneration may be produced over any range of frequencies, but in a detector it is generally confined to the input carrier frequency and its modulation side-bands. The degree of regeneration depends on the input voltage, the grid and anode circuit characteristics and the phase relationship between the feedback and initial input voltages. It

leads to accentuation of any already existing frequency discrimination, i.e., it increases the selectivity of its input tuned circuit. In a detector quasi-correct phase relationship is generally established for the carrier frequency, but owing to phase changes of the side-band frequencies by the input circuit, regeneration progressively decreases at frequencies above and below the carrier. This causes a virtual increase in the selectivity of the input tuned circuit.

The improvement in selectivity due to regeneration is not as satisfactory as that produced by adding more tuned circuits. With a high degree of regeneration the virtual selectivity curve is sharply peaked with a narrow pass-band, which rapidly attenuates all the modulation side-bands except those due to the low audio frequencies. This leads to " woolly " A.F. reproduction. The virtual selectivity curve is considerably modified by the presence at the detector of a large undesired signal because the latter increases the bias on the valve (acting as a cumulative grid detector) and reduces its gain as an R.F. amplifier. Regeneration of the desired signal is decreased and the virtual selectivity reduced. To obtain maximum selectivity by regeneration a pre-detector volume control is essential so as to reduce any undesired signal. The desired is simultaneously reduced but the reduction is compensated by increasing regeneration. The need for reducing any undesired signal to the lowest possible value indicates the desirability of using an input tuned circuit having a high rather than a low Q value.

With added tuned circuits, instead of regeneration, the selectivity curve has a much wider and flatter pass-band and attenuation outside the pass region is independent of the magnitude of the undesired signal.

By regeneration the sensitivity of a cumulative grid detector may be increased and damping due to grid current and anode-grid capacitance coupling neutralized. The detector must operate as an R.F. amplifier and a suitable impedance (a R.F. choke) is inserted between the A.F. impedance and the anode. The R.F. anode voltage is returned to the input circuit via a variable capacitance (C_2) and a coil (L_1) as shown in Fig. 8.20. The feedback voltage due to the mutual inductance coupling increases as the frequency increases, and to prevent excessive regeneration at the highest frequency in the tuning range the feedback capacitor (C_2) is of the differential type. Decrease of the feedback capacitance coupling is thus accompanied by increasing shunt capacitance from anode to earth. The maximum value of the differential capacitance should not exceed 0·0003 μF as it is a shunt to the high audio frequency components

of the modulation envelope in the anode circuit. In an alternative circuit the feedback coil L_1 is inserted directly in the anode circuit and the variable capacitance, C_2, decrease of which increases the feedback voltage, is connected from anode to earth and acts as a shunt to R.F. voltages.

As the coupling between anode circuit and input is increased a point is reached where self-oscillation occurs. The transition from the stable to the oscillating condition should be smooth and free from backlash, i.e., a slight reduction of coupling from the oscillating point should stop oscillation. This is essential because the R.F. gain of a cumulative grid detector tends to fall owing to increasing bias as the input carrier signal is increased. With backlash, slight fading of the carrier voltage might cause oscillation which would persist when the carrier voltage returned to its original value.

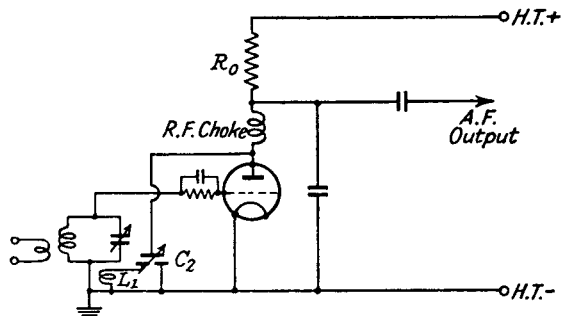

FIG. 8.20.—A Typical Circuit for a Regenerative Detector.

Unstable regeneration is generally due to incorrect phasing of the feedback and input voltages and to an R.F. amplification characteristic which increases as the input increases. Incorrect phasing may largely be avoided by making the resonant frequency of the feedback circuit much higher than the highest required input tuning frequency. The feedback coil, having a small number of turns, should therefore be tightly coupled to the earthed end (to avoid capacitance coupling) of the input coil. Combined capacitance and mutual inductance coupling may produce excessive regeneration or stop regeneration at some point in the tuning range of the input circuit.

Since increasing carrier voltage increases the bias on a cumulative grid detector, its gain as an R.F. amplifier tends to fall. This is quite different from the R.F. amplification characteristic of an anode bend detector, for owing to the curvature of the I_aE_g characteristic the R.F. anode voltage increases at a greater rate than the input

voltage, i.e., the gain increases as the signal increases. Hence unstable regeneration is usually a feature of such detectors.

Although the anode current characteristic of a cumulative grid detector tends to give stable regeneration, the grid detection characteristic can produce instability and backlash. In Fig. 8.11*b*, it is shown that the equivalent damping resistance due to detection is dependent on the input voltage when detection current begins at a voltage other than zero. If therefore grid current begins in the cumulative grid detector at some negative or equivalent negative voltage (as in an indirectly heated valve or a directly heated valve with the grid leak returned to the L.T. positive), damping of the input circuit decreases as the signal is increased. Reduced damping increases the R.F. voltage at the grid and the detector has therefore a tendency to unstable regeneration. Backlash is increased if the negative voltage start of grid current is increased. On the other hand, a detector having a positive voltage start of grid current tends to give stable regeneration since curve 2, Fig. 8.11*b*, shows increasing damping as the signal is increased. The positive voltage start is, however, undesirable because of distortion (see Section 8.2.7) and the ideal condition is obtained with zero start of grid current.

Increasing the detector grid leak resistance decreases the damping of the input tuned circuit and tends to more stable operation.

Regeneration may be applied to a diode detector followed by an A.F. amplifier valve by using the latter as the regenerator, but it is not usual because most of the advantages of diode detection are lost if R.F. voltages are passed to the succeeding A.F. amplifier. When regeneration is required the R.F. filter circuit (R_3C_3 in Fig. 8.5) between the detector and amplifier must be removed and an R.F. impedance, coupled back to the detector input tuned circuit, must be included in the A.F. amplifier anode circuit.

We may state the points for and against regeneration in detectors as follows. The advantages are : considerably increased sensitivity and selectivity (provided any undesired signal voltages are small). The disadvantages are that as regeneration is increased the tuning of the input circuit generally needs adjustment (the degree of correction depends on the phase angle between the feedback and input voltages and is small when this is small), adjustment of the regeneration control is necessary as the input tuning frequency is changed, radiation may occur if regeneration is carried as far as oscillation, and the presence of an undesired signal modifies the regeneration characteristic.

8.7. Detection with Push-Pull Output.[22] It may some-

times be advantageous to provide push-pull output from a detector and two possible circuits are shown in Figs. 8.21*a* and 8.21*b*. The first gives push-pull output from a diode, and is applicable when one side of the input circuit is earthed. When the circuit need not be earthed (the secondary of an I.F. transformer) the R.F. choke L

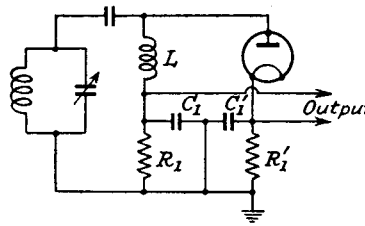

FIG. 8.21*a*.—Push-Pull Output from a Diode Detector.

may be removed and the tuned circuit inserted in its place. The two output voltages across R_1 and R_1' may be slightly unbalanced at high audio frequencies due to unequal stray capacitances, but this effect is not usually serious. Heater to cathode insulation must be high or interference from hum is likely to be experienced.

Fig. 8.21*b* shows how push-pull output may be obtained from a cumulative grid detector. Anode bend detection can equally well be employed, but both detectors require an input circuit isolated from earth. Capacitors C_0 (0·0001 μF) bypass R.F. to earth.

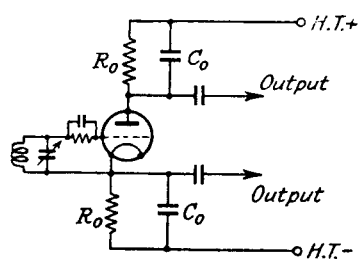

FIG. 8.21*b*.—Push-Pull Output from a Triode Detector.

8.8. Double-Wave Detection. The chief advantage of double-wave detection is the smaller R.F. ripple voltage across the load resistance R_1, which means that less R.F. filtering is required between R_1 and the A.F. amplifier. A centre tapped coil is necessary (see Fig. 8.22) and this reduces the available A.F. voltage from the load resistance to one-half that for half-wave detection. On the other hand, the equivalent damping resistance due to the diode conduction current is increased to twice that for half-wave detection. It

has been shown [25] that only under special circumstances can double-wave detection prove superior to half-wave detection, and the latter is almost universally employed in receivers.

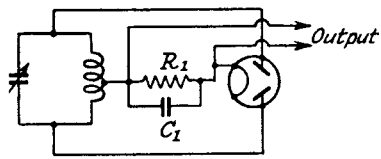

FIG. 8.22.—Double Wave Detection with a Diode.

8.9. The Anode Bend Detector with Negative Feedback.[26] The anode bend detector with negative feedback (see Fig. 8.23*a*) has an action similar to that of a diode with current starting at a high negative voltage. It has a linear detection characteristic for carrier voltages exceeding about 0·5 volts, a high critical modulation ratio (see Section 8.2.3), and the maximum permissible carrier voltage is almost unlimited. As in the case of the normal anode bend detector, detection is obtained by the parabolic or unidirectional property of the I_aE_g characteristic. No grid current is taken and there is therefore practically no damping of the input tuned circuit. In its action it is similar to the diode with a negative start of anode current, but it has no serious damping effect for small signal voltages as shown by the diode (Fig. 8.11*b*, curve 1). High input admittance, the resistance component of which may be negative, and high critical modulation ratio are the important ad-

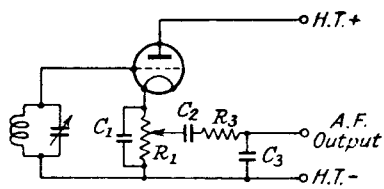

FIG. 8.23*a*.—The Anode Bend Detector with Negative Feedback.

vantages of this type of detector. Its chief disadvantage (shared by the diode) is that its amplification factor is less than 1 and its detection efficiency is of the same order as that of the diode, viz., about 90% for $R_1 = 1\ \text{M}\Omega$. Since the I_aE_g characteristic has usually a greater initial curvature than the I_aE_a characteristic of a diode the detection efficiency for small signals is lower than that of a diode with zero start of current, though not lower than that of the diode with negative start of current. We should note that the diode

with negative start of current (Section 8.2.6) is identical with the diode having zero start of current and positive bias (Section 8.2.3).

Detection $I_m E_g$ characteristic curves (Fig. 8.23*b*) similar to the diode curves of Fig. 8.4*b* may be obtained by using the 50 c.p.s. mains supply as an input and replacing $R_1 C_1$ in Fig. 8.23*a* by a microammeter and a battery as illustrated in Fig. 8.4*a* for the diode. The negative start ($-E_b$) of anode current gives a critical modulation ratio in accordance with expression 8.6, viz.,

$$M = \left[\frac{\hat{E}_1 + E_b}{\hat{E}_1}\right]\left[1 - \eta_d \frac{R_1}{R_1 + R_2}\right],$$

so that modulation distortion due to the grid leak (R_2) in the A.F. amplifier following the detector is appreciably reduced. The value

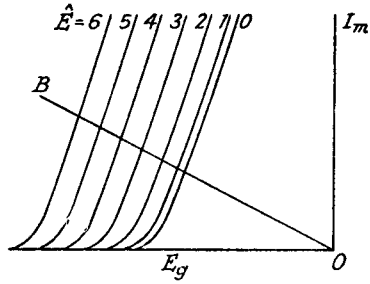

FIG. 8.23*b*.—Typical Curves for an Anode Bend Detector with Negative Feedback.

of $-E_b$, which is entirely controlled by the anode voltage, can be increased by increasing the latter. A characteristic of this type of detector is that it presents a negative input conductance, i.e., produces regeneration and improves the selectivity of the input tuned circuit across which it is connected. This negative conductance is due to feedback through the grid-cathode capacitance from the R.F. voltage developed across the capacitive cathode load impedance (see Section 2.8.3).

8.10. Interference Effects due to an Undesired R.F. Signal in the Detector Input Circuit. The desired A.F. output voltage from a detector is generally affected by the presence of an undesired R.F. voltage in the input circuit. The extent of the interference produced depends on the relative magnitudes and frequency separation of the desired and undesired carrier voltages.

If the frequency difference between the two carrier voltages is an inaudible frequency, the interference effect is entirely dependent on their relative magnitudes. An unmodulated R.F. signal compar-

able in value to the desired signal reduces and distorts the A.F. modulation components of the latter. If the former is modulated the undesired modulation (generally distorted) is also heard. The demodulation [11] effect (reduction of the A.F. output voltage from a modulated carrier due to the presence of another carrier at the detector input) occurs for either desired or undesired signals, and if the magnitude of the undesired signal is small it may be almost completely demodulated by the desired carrier. That is to say, the undesired modulation is audible in the absence of the desired carrier, but becomes inaudible when the latter is being transmitted.

If the frequency difference between the undesired and desired carrier voltages is an audible frequency, additional interference effects are observed. The difference frequency appears as a heterodyne whistle together with the modulation components of the undesired carrier, which are generally distorted. Another effect which may also occur is that of frequency inversion of the undesired modulation side-bands, the high-frequency components appearing in the A.F. output as low frequencies and vice versa. Both effects give rise to an A.F. output which is best characterized as a chatter. An example may often be found on the medium-wave range of a receiver tuned to a distant station adjacent in frequency to a strong local station. The frequency separation of 9 kc/s appears as a heterodyne whistle of 9 kc/s, and the modulation side-bands produce chatter due to distortion and frequency inversion, an undesired modulation frequency of 1 kc/s. being produced as a frequency of 8 kc/s, i.e., 9 − 1, a frequency of 3·5 kc/s as 5·5 kc/s, i.e., 9 − 3·5 ; and so on.

To examine the theory underlying these distortion effects we will consider separately the linear and parabolic detector. Let us imagine that the undesired carrier only is applied to a linear detector. It produces a detection current which causes a voltage, equivalent to a negative bias on the diode anode, to appear across the diode load resistance. As shown in Section 8.2.7, no detection occurs until the signal voltage exceeds any negative bias applied to the diode anode. The comparison of the effect produced by the undesired carrier to that produced by a fixed negative bias is not strictly correct since some detection of the desired signal takes place, even when the latter is much less than the undesired carrier. For a large desired signal, however, the undesired carrier has practically the same effect as a fixed negative bias equal in value to the D.C. voltage produced by the undesired carrier acting alone. The influence of the undesired on the mean detection voltage-desired

peak carrier curves is shown in Fig. 8.24. These are idealized curves calculated [12] on the assumption that the detector has an efficiency of $\eta_d = 100\%$. Similar curves may be obtained experimentally using the circuit in Fig. 8.2 with two signal voltages at differing frequencies connected in series in place of the generator

$$\hat{E}_1 \cos \omega t(1+M \cos pt).$$

Curves 1, 2 and 3 give the detection characteristic for undesired peak voltages of $\hat{E}_u = 0$, 0·25 and 1 volt. The A.F. output voltage wave shape for a desired carrier of $\hat{E}_d = 0{\cdot}2$ volts modulated 50% is shown to the right of the figure. Demodulation and distortion

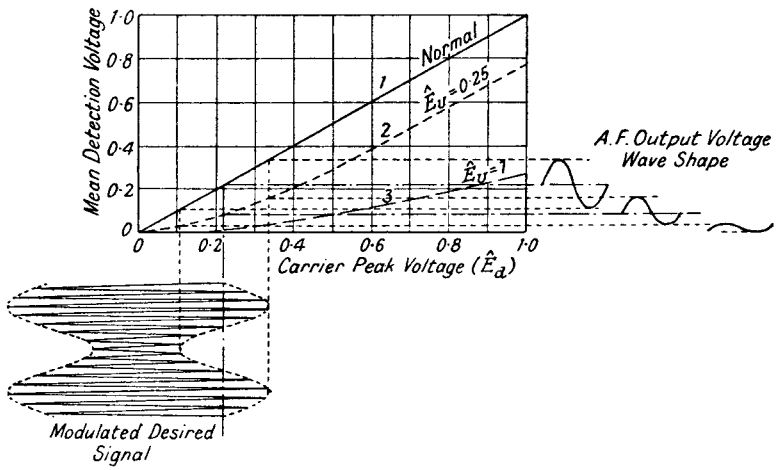

FIG. 8.24.—Demodulation of a Small by a Large Signal at the Detector.

of the modulation envelope are clearly marked as $\hat{E}_u$ is increased. Both effects are mutual and are greatest for the smaller signal, which in practice is generally $\hat{E}_u$. We see from curve 2 that when $\hat{E}_d$ exceeds $\hat{E}_u$, the detection curve becomes straight and parallel to curve 1, thus showing that $\hat{E}_u$ has an effect similar to that of negative bias. If $\hat{E}_u$ is unmodulated and differs from $\hat{E}_d$ by an inaudible frequency, the output A.F. voltage is unaffected when the modulation is restricted to operation over the straight part of curve 2, i.e., the modulation trough $\hat{E}_d(1 - M)$ must not fall below about 0·4 volts.

For the parabolic detector let us assume its $I_a E_g$ characteristic to be given by

$$I_a = a_0 + a_1 E_g + a_2 E_g^2 + a_3 E_g^3 - a_4 E_g^4 + \ldots \quad . \quad 8.51.$$

(The reason for the coefficient $-a_4$ is explained in section 8.4.1.)

But $E_g = \hat{E}_d \cos \omega_d t(1+M_d \cos p_d t)+\hat{E}_u \cos \omega_u t(1+M_u \cos p_u t) - E_b$ where $-E_b$ = the bias voltage.

Replacing E_g in equation 8.51 and analysing the anode current into its A.F. components as in Section 8.4.1, we find the following effects in the detector output.

1. Undesired modulation.

This results from the $a_2 E_g^2$ term and is

$$\frac{a_2 \hat{E}_u^2}{2}\left[2M_u \cos p_u t+\frac{M_u^2}{2} \cos 2p_u t\right].$$

The distortion term in the above expression is not for our purposes classed as such since it is due to the parabolic property and not to the interaction of the two signals.

2. Difference frequency and inversion of the undesired modulation components.

These are obtained from

$$a_2[2\hat{E}_d \cos \omega_d t(1+M_d \cos p_d t)\hat{E}_u \cos \omega_u t(1+M_u \cos p_u t)].$$

The difference frequency component

$$a_2 \hat{E}_d \hat{E}_u \cos (\omega_d - \omega_u)t$$

is contained in

$$2a_2 \hat{E}_d \cos \omega_d t \hat{E}_u \cos \omega_u t$$

for $\cos \theta \cos \phi = \frac{1}{2}[\cos (\theta - \phi)+\cos (\theta+\phi)]$

and the frequency inversion term

$$\frac{a_2 \hat{E}_d \hat{E}_u M_u}{2} \cos (\omega_d - \omega_u - p_u)t.$$

occurs in

$$a_2 2\hat{E}_d \hat{E}_u M_u \cos \omega_d t \cos \omega_u t \cos p_u t.$$

If $\frac{\omega_d - \omega_u}{2\pi} = 9$ kc/s, and $\frac{p_u}{2\pi} = 8$ kc/s

$$\frac{(\omega_d - \omega_u - p_u)}{2\pi} = 1 \text{ kc/s},$$

thus an 8 kc/s. undesired modulation frequency appears as a 1 kc/s. frequency in the output.

The desired modulation also has an inverted component for equation 8.51 gives

$$\frac{a_2 \hat{E}_d \hat{E}_u M_d}{2} . \cos (\omega_d - \omega_u - p_d)t.$$

3. Demodulation of the desired signal.

The demodulation term appears from $-a_4E_g^4$ for this contains $-a_4 6\hat{E}_d^2 \cos^2 \omega_d t(1+M_d \cos p_d t)^2 \hat{E}_u^2 \cos^2 \omega_u t(1+M_u \cos p_u t)^2$, which gives the component

$$-\frac{3a_4\hat{E}_d^2\hat{E}_u^2}{2}(1+M_d \cos p_d t)^2$$

$$= -\frac{3a_4\hat{E}_d^2\hat{E}_u^2}{2}\left(2M_d \cos p_d t+\frac{M_d^2}{2}\cos 2p_d t\right).$$

This subtracts from the A.F. term

$$\frac{a_2\hat{E}_d^2}{2}\left(2M_d \cos p_d t+\frac{M_d^2}{2}\cos 2p_d t\right)$$

in $a_2E_g^2$.

A similar demodulating term is also obtained for the undesired signal.

4. Distortion of the desired and undesired modulation components.

A distorted desired and undesired modulation component is contained in $-a_4E_g^4$

$$-\frac{6a_4\hat{E}_d^2\hat{E}_u^2}{4}(1+M_d \cos p_d t)^2(1+M_u \cos p_u t)^2$$

gives

$$-\frac{3}{4}a_4\hat{E}_d^2\hat{E}_u^2\left[M_d^2 \cos 2p_d t+M_u^2 \cos 2p_u t\right].$$

In addition there are sum and difference frequencies $\frac{(2p_d \pm p_u)}{2\pi}$, $\frac{2p_u \pm p_d}{2\pi}$, and $\frac{(2p_d \pm p_u)}{2\pi}$.

BIBLIOGRAPHY

1. A Theoretical and Experimental Investigation of Detection for Small Signals. E. L. Chaffee and G. H. Browning, *Proc. I.R.E.*, Feb. 1927, p. 113.
2. Detection by Grid Rectification with the High Vacuum Triode. S. Ballantine, *Proc. I.R.E.*, May 1928, p. 593.
3. Effect of Anode-Grid Capacity in Anode-Bend Rectifiers. E. A. Biedermann, *Wireless Engineer*, Feb., p. 71, March, 1929, p. 135.
4. Detection at High Signal Voltage—Plate Rectification with the High Vacuum Triode. S. Ballantine, *Proc. I.R.E.*, July 1929, p. 1,153.
5. The Numerical Estimation of Grid Rectification for Small Signal Amplitudes. W. A. Barclay, *Wireless Engineer*, Nov. 1929, p. 596.
6. The Theory of the Straight Line Rectifier. F. M. Colebrook, *Wireless Engineer*, Nov. 1930, p. 595.

7. The Estimation of the Sensitivity of the Grid Rectifier for Large Inputs. C. D. Hall, *Wireless Engineer*, Dec. 1930, p. 668.
8. Some Properties of Grid Leak Power Detection. F. E. Terman and N. R. Morgan, *Proc. I.R.E.*, Dec. 1930, p. 2,160.
9. Grid Circuit Power Rectification. J. R. Nelson, *Proc. I.R.E.*, March 1931, p. 489.
10. Test Procedure for Detectors with Resistance Coupled Output. G. D. Robinson, *Proc. I.R.E.*, May 1931, p. 806.
11. Mutual Demodulation and Allied Problems. G. W. O. Howe, *Wireless Engineer*, Aug. 1931, p. 405.
12. The Apparent Demodulation of a Weak Station by a Stronger One. F. M. Colebrook, *Wireless Engineer*, Aug. 1931, p. 409.
13. Quality Detectors. W. Greenwood and S. J. Preston, *Wireless Engineer*, Dec. 1931, p. 648.
14. The Graphical Solution of Detector Problems. G. S. C. Lucas, *Wireless Engineer*, April 1932, p. 202.
15. Some Notes on Grid Circuit and Diode Rectification. J. R. Nelson, *Proc. I.R.E.*, June 1932, p. 989.
16. A New Valve Characteristic. P. K. Turner, *Wireless Engineer*, July 1932, p. 384.
17. Discussion on Grid Circuit Detection and Diode Rectification. J. R. Nelson and F. E. Terman, *Proc. I.R.E.*, Dec. 1932, p. 1971.
18. Some Notes on the Use of a Diode as a Cumulative Grid Rectifier. E. A. Biedermann, *Wireless Engineer*, March 1933, p. 123.
19. Discussion on " Some Notes on Grid Circuit and Diode Rectification ". F. G. Kelly, *Proc. I.R.E.*, April 1933, p. 630.
20. Diode Detection Analysis. C. E. Kilgour and J. M. Glessner, *Proc. I.R.E.*, July 1933, p. 930.
21. Notes on Screened Grid Pentode Detectors. F. R. W. Strafford, *Wireless Engineer*, Sept. 1934, p. 484.
22. Push-Pull Input Systems. W. T. Cocking, *Wireless World*, Sept. 21st, 1934, p. 245.
23. Diode Detectors. J. B. L. Foot, *Wireless World*, Dec. 28th, 1934, p. 547.
24. Notes on the Theory of Diode Rectification. J. Marique, *Wireless Engineer*, Jan. 1935, p. 17.
25. The Detector Input Circuit. W. T. Cocking, *Wireless Engineer*, Nov. 1935, p. 595.
26. New Detector Circuit. W. N. Weeden, *Wireless World*, Jan. 1st, 1937, p. 6.
27. The Modulation Response and Selectivity Curves of a Resonant Circuit loaded by a Diode Rectifier. F. C. Williams, *Wireless Engineer*, April 1938, p. 189.
28. The Properties of a Resonant Circuit loaded by a Complex Diode Rectifier. F. C. Williams, *Wireless Engineer*, Nov. 1938, p. 600.
29. The Diode Detector with Positive Bias. K. R. Sturley, *Wireless World*, March 9th, 1939, p. 220.
30. Diode Operating Conditions. W. P. N. Court, *Wireless Engineer*, Nov. 1939, p. 548.

APPENDIX 1A

"j" NOTATION

THE use of "j" notation to represent complex quantities is a most useful aid in the solution of A.C. problems. In Fig. 1A.1 are shown two vectors of equal length "a" units, one OA is horizontal and the other OB is vertical.

Let us assume that the vectors are represented respectively by "a" and "ja," the factor "j" denoting that the original vector OA has been rotated through 90° in an anti-clockwise direction. By taking the process a step further we may multiply vector OB by j and obtain vector OC, which is a vector equal in length but opposite in direction to OA, thus

$$OC = j\,OB = j.(jOA) = j^2a = -a$$

or

$$j = \sqrt{-1} \quad . \quad . \quad . \quad . \quad 1A.1.$$

In the same manner dividing by "j" can denote rotation of a vector through 90° in a clockwise direction; hence $OD = \frac{OA}{j} = -j.OA$. The result is in agreement with normal co-ordinate axes for

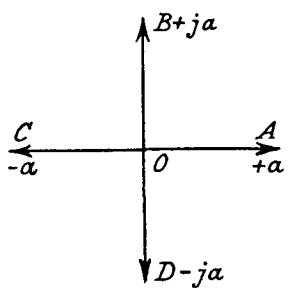

FIG. 1A.1.—Real and Imaginary Axes.

$OD = -j.OA = -OB$. The horizontal vectors OA and OC are known as real, and the vertical vectors as imaginary quantities. This method of vector representation is particularly useful in dealing with circuits containing inductance and capacitance as well as resistance. Taking as an example an inductance L and resistance R connected in series across a generator supplying a voltage E at a frequency f c.p.s., the voltages across L and R cannot simply be

added because that across L is advanced in time by 90° with respect to the current as shown in Fig. 1A.2. The voltage across the resistance R is in phase with the current I. By the theorem of Pythagoras the total voltage E is equal to $\sqrt{E_R^2+E_L^2}$. The voltage E_R across R is IR, and that E_L across L is IX_L.
The impedance Z of the whole circuit is

$$Z = \frac{E}{I} = \sqrt{R^2+(\omega L)^2} \quad . \quad . \quad . \quad \text{1A.2}$$

where $\omega = 2\pi f.$

Since the reactance ωL is 90° ahead of R we may write the impedance Z in terms of "j" notation as

$$Z = R+j\omega L \quad . \quad . \quad . \quad . \quad \text{1A.3.}$$

Similarly a series circuit of resistance R and capacitance C gives an impedance

$$Z = \sqrt{R^2+\left(\frac{1}{\omega C}\right)^2} = R+\frac{1}{j\omega C} = R-\frac{j}{\omega C} \quad . \quad \text{1A.4}$$

for the voltage across the capacitance lags 90° behind that across the resistance, and the capacitive reactance vector must therefore

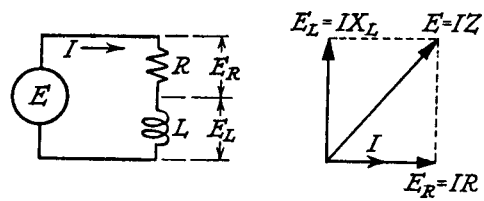

FIG. 1A.2.—The Vector Representation of the Voltages and Current in a Series Circuit.

be divided by "j." Before demonstrating the advantages of "j" notation (in the above elementary circuits it is difficult to see that simplification has resulted) certain points with regard to its use should be considered.

1. A vector impedance $Z = R+jX$ has an amplitude $|Z| = \sqrt{R^2+X^2}$, and a phase angle $\phi = \tan^{-1}\frac{X}{R}$; for a vector impedance $Z = R-jX$, the amplitude $|Z|$ is still unchanged and equal to $\sqrt{R^2+X^2}$, but its phase angle is $\phi = \tan^{-1}\frac{-X}{R}$; i.e., the reactance term is capacitive. Thus the amplitude is inde-

pendent of the sign of the real and imaginary terms in the "j" representation. Only the phase angle is affected.

2. A term containing a complex denominator must be rationalized before the phase angle is determined, for example, a circuit having an impedance $Z = R+jX$ has an admittance $Y=\frac{1}{Z} = \frac{1}{R+jX}$. The amplitude of the admittance $|Y| = \frac{1}{\sqrt{R^2+X^2}}$, but its phase angle is not $\phi = \tan^{-1}\frac{X}{R}$ but

$$\phi = \tan^{-1} -\frac{X}{R} \text{ for } Y = \frac{R-jX}{(R+jX)(R-jX)} = \frac{R-jX}{R^2+X^2}.$$

3. Complex vectors may be multiplied together; the product of the real and imaginary components gives an imaginary, whilst the product of two imaginaries gives a real term, for $j^2 = -1$.

4. For the impedance of parallel circuits or the admittance of series circuits, a complex denominator $a+jb$ must always be rationalized by multiplying numerator and denominator by $(a - jb)$. The real and imaginary parts, which result are the resistance and reactance term respectively in the case of impedance, and the conductance and susceptance term in the admittance case.

For example, $$Z = \frac{10-4j}{2+3j} = \frac{(10-4j)(2-3j)}{2^2+3^2}$$
$$= \frac{8-38j}{13} = 0{\cdot}615 - 2{\cdot}925j$$

thus Z is equivalent to a resistance of 0·615 ohms in series with a capacitive reactance of 2·925 ohms. Similarly $Y = \frac{10-4j}{2+3j}$ is equivalent to a conductance of 0·615 mhos in parallel with an inductive susceptance of 2·925 mhos.

5. An inductive impedance is always represented by $a+jb$ and a capacitive impedance by $a - jb$, whilst the reverse is true for admittance; the $+j$ term is in this case a capacitive susceptance. This may be seen by inverting an inductive reactance to obtain an inductive susceptance.

$$j\omega L \text{ reactance} = \frac{1}{j\omega L} \text{ susceptance}$$
$$= \frac{-j}{\omega L}.$$

The advantage of "j" notation can be demonstrated when it is

desired to convert a parallel circuit such as that of Fig. 1A.3 into its equivalent series circuit.

$$Z = \frac{\dfrac{Rj\omega L}{j\omega C}}{Rj\omega L + \dfrac{R}{j\omega C} + \dfrac{j\omega L}{j\omega C}} = \frac{j\omega LR}{R(1 - \omega^2 LC) + j\omega L}.$$

Rationalizing

$$Z = \frac{j\omega LR[R(1 - \omega^2 LC) - j\omega L]}{[R(1 - \omega^2 LC)]^2 + (\omega L)^2}.$$

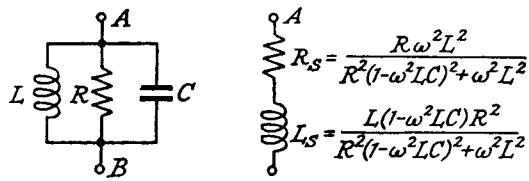

FIG. 1A.3.—A Parallel Circuit and its Series Equivalent.

The equivalent series circuit is obtained by separating the real or resistive term from the imaginary or reactive term, thus

$$Z = R_s + jX_s.$$

$$= \frac{R\omega^2L^2}{R^2(1 - \omega^2LC)^2 + (\omega L)^2} + \frac{j\omega L(1 - \omega^2LC)R^2}{R^2(1 - \omega^2LC)^2 + (\omega L)^2} \quad . \quad 1A.5.$$

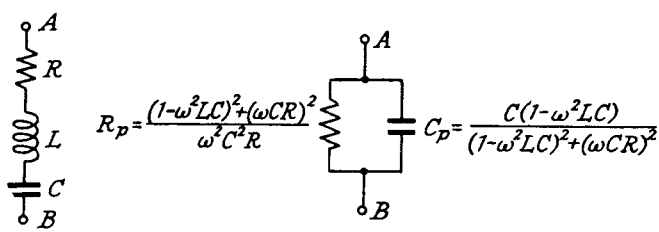

FIG. 1A.4.—A Series Circuit and its Parallel Equivalent.

In a similar manner the series circuit L, C and R (Fig. 1A.4) may be converted into an equivalent parallel circuit.

$$Y = \frac{1}{Z} = \frac{1}{R + j\omega L + \dfrac{1}{j\omega C}} = \frac{j\omega C}{(1 - \omega^2LC) + j\omega CR}$$

$$= \frac{j\omega C[(1 - \omega^2LC) - j\omega CR]}{(1 - \omega^2LC)^2 + (\omega CR)^2}$$

$$= \frac{R\omega^2C^2}{(1 - \omega^2LC)^2 + (\omega CR)^2} + \frac{j\omega C(1 - \omega^2LC)}{(1 - \omega^2LC)^2 + (\omega CR)^2} \quad . \quad 1A.6$$

$$= \frac{1}{R_p} + \frac{j}{X_p}$$

where R_p is the equivalent resistance in parallel with X_p the equivalent reactance.

The simplification resulting from the use of "j" notation is even more clearly demonstrated when the impedance or admittance of a complex circuit such as that of Fig. 7.6 is required and its importance cannot be over emphasised.

APPENDIX 2A

FOURIER SERIES

THE Fourier method of analysing a complex wave shape into a series of harmonically related sinusoidal waves has proved of paramount importance to the radio engineer. By the principle of superposition * it is possible to consider separately the action of each frequency component of a complex current or voltage wave applied to a circuit, and all effects may later be added together to give the final result at the output of the circuit. The complex wave is generally considered as periodic, but a transient wave can be treated by the Fourier Integral Method. We shall, however, limit ourselves to an examination of the periodic complex wave.

The Fourier theorem states that any periodic complex wave

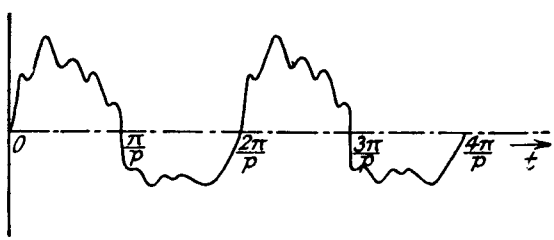

FIG. 2A.1.—An Example of a Periodic Wave which can be resolved into its Components by Fourier Analysis.

shape, such as that of Fig. 2A.1, may be represented by a series of sines and cosines of possibly infinite number, i.e.,

$$f(t) = a_1 \sin pt + a_2 \sin 2pt + \ldots a_n \sin npt$$
$$+\frac{b_0}{2} + b_1 \cos pt + b_2 \cos 2pt + \ldots b_n \cos npt \quad . \quad 2A.1.$$

The significance of writing $\frac{b_0}{2}$ as the first term of the cosine series is considered later. Certain conditions must be fulfilled if the above equation is to hold.

* The superposition theorem states that in any network consisting of generators and linear bilateral impedances the current flowing at any point is the sum of the currents which would flow if each generator were considered separately, all other generators being replaced at the time by impedances equal to their internal impedances.

1. The function $f(t)$ must have only one value for a given value of "t", except where there is a discontinuity, e.g., a circle cannot be treated, but the instantaneous fall from A to B in Fig. 2A.2 can be considered.

2. If the wave is not continuous the number of discontinuities must be finite. The value of $f(t)$ at the discontinuity must also be finite. At a point of discontinuity the Fourier series gives the average value of the wave.

Two terms, $a_1 \sin pt$ and $b_1 \cos pt$, make up the fundamental frequency which is the reciprocal of the periodic time of the complex wave. Two terms are necessary to define each frequency component since correct positioning on the time scale is as important as correct amplitude.

The double fundamental term may be rewritten

$$\sqrt{a_1^2+b_1^2}\left[\frac{a_1}{\sqrt{a_1^2+b_1^2}} \sin pt + \frac{b_1}{\sqrt{a_1^2+b_1^2}} \cos pt\right]$$

which can be simplified to

$$c_1 \sin (pt+\phi_1) \quad \text{where} \quad c_1 = \sqrt{a_1^2+b_1^2}$$
$$\text{and} \quad \phi_1 = \tan^{-1}\frac{b_1}{a_1}.$$

Similarly, every frequency component may be written as $c_n \sin (npt+\phi_n)$. The angle ϕ_n determines the position of each frequency component on the time scale since it fixes the value of any frequency term when $t = 0$.

The values of a_n and b_n may be obtained by multiplying $f(t)$ in equation 2A.1 by the appropriate sine and cosine function and integrating this product over the periodic interval from 0 to $\frac{2\pi}{p}$. Thus a_n may be found by integrating equation 2A.1 multiplied by $\sin npt$.

$$\int_0^{\frac{2\pi}{p}} f(t) \sin npt\, dt = \int_0^{\frac{2\pi}{p}} [a_1 \sin pt + \ldots a_m \sin mpt + \ldots + \frac{b_0}{2} + b_1 \cos pt + \ldots b_m \cos mpt + \ldots] \sin npt\, dt \quad \ldots \quad \text{2A.2.}$$

The right-hand side of equation 2A.2 simplifies considerably because for any value of m or n the expression $\int_0^{\frac{2\pi}{p}} \cos mpt \sin npt\, dt$

is zero and except when $m = n$ the expression $\int_0^{\frac{2\pi}{p}} \sin mpt \sin npt\, dt$ is also zero. Hence

$$\int_0^{\frac{2\pi}{p}} f(t) \sin npt\, dt = a_n \int_0^{\frac{2\pi}{p}} \sin^2 npt\, dt.$$

$$= a_n \int_0^{\frac{2\pi}{p}} \frac{(1 - \cos 2npt)}{2}\, dt$$

$$= a_n \left[\frac{t}{2} - \frac{\sin 2npt}{4np}\right]_0^{\frac{2\pi}{p}}$$

$$= a_n \frac{\pi}{p}$$

or

$$a_n = \frac{p}{\pi} \int_0^{\frac{2\pi}{p}} f(t) \sin npt\, dt \quad . \quad . \quad . \quad 2\text{A}.3$$

where n may have any value from 1 to ∞.
A similar expression is obtained for b_n

$$b_n = \frac{p}{\pi} \int_0^{\frac{2\pi}{p}} f(t) \cos npt\, dt \quad . \quad . \quad . \quad 2\text{A}.4$$

where n has any value from 0 to ∞.
The factor $\frac{1}{2}$ multiplying b_0 in 2A.1 is necessary to make expression 2A.4 true when $n = 0$. The Fourier expression for the curve represented by $f(t)$ becomes

$$f(t) = \frac{b_0}{2} + \sum_{n=1}^{\infty} a_n \sin npt + \sum_{n=1}^{\infty} b_n \cos npt. \quad . \quad 2\text{A}.5.$$

Let us now take certain examples which will make clear the process of Fourier analysis. Let us assume that we wish to know the frequency components of voltage produced across a resistance connected in series with a half-wave rectifier. The voltage wave shape is that of a sine wave with the negative half suppressed. If the pulsance of the applied voltage to the rectifier is p rads/sec.

$$a_n = \frac{p}{\pi} \int_0^{\frac{2\pi}{p}} f(t) \sin npt\, dt.$$

$f(t)$ is made up of two parts; from 0 to $\frac{\pi}{p}$ it is represented by $\hat{E} \sin pt$ and from $\frac{\pi}{p}$ to $\frac{2\pi}{p}$ by 0.

Therefore $$a_n = \frac{p}{\pi}\left[\int_0^{\frac{\pi}{p}} \hat{E} \sin pt \sin npt\, dt + \int_{\frac{\pi}{p}}^{\frac{2\pi}{p}} 0 \sin npt\, dt\right]$$

$$= \frac{p}{\pi}\int_0^{\frac{\pi}{p}} \hat{E} \sin pt \sin npt\, dt.$$

The particular coefficients a_1, a_2, etc., may be evaluated by replacing n in the above expression by 1, 2, etc. As a general rule, however, calculation is very much simplified by proceeding to the integrand before replacing n by its particular value. Thus by noting that $\sin\theta \sin n\theta = \dfrac{\cos(n-1)\theta - \cos(n+1)\theta}{2}$.

$$a_n = \frac{\hat{E}p}{2\pi}\int_0^{\frac{\pi}{p}} [\cos(n-1)pt - \cos(n+1)pt]\, dt$$

$$= \frac{Ep}{2\pi}\left[\frac{\sin(n-1)pt}{(n-1)p} - \frac{\sin(n+1)pt}{(n+1)p}\right]_0^{\frac{\pi}{p}}.$$

It is now only necessary to replace n by its particular value to obtain each coefficient.

Hence $$a_1 = \frac{\hat{E}p}{2\pi}\left[\frac{\sin 0pt}{0p} - \frac{\sin 2pt}{2p}\right]_0^{\frac{\pi}{p}}.$$

Since $\dfrac{\sin 0}{0}$ is indeterminate we must return to the original integral which then gives

$$a_1 = \frac{Ep}{\pi}\int_0^{\frac{\pi}{p}} \sin^2 pt\, dt = \frac{\hat{E}p}{2\pi}\int_0^{\frac{\pi}{p}} (1 - \cos 2pt)\, dt$$

$$= \frac{\hat{E}p}{2\pi}\left[t - \frac{\sin 2pt}{2p}\right]_0^{\frac{\pi}{p}}$$

$$= \frac{\hat{E}p}{2\pi}\cdot\frac{\pi}{p} = \frac{\hat{E}}{2}.$$

$$\left(\text{It is important to note that } \left[\frac{\sin 0pt}{0}\right]_0^{\frac{\alpha}{p}} = \alpha.\right)$$

All other sine function coefficients are zero because $\sin(n+1)pt$ and $\sin(n-1)pt$ are zero when $t = \dfrac{\pi}{p}$ or 0.

$$b_n = \frac{p}{\pi}\int_0^{\frac{\pi}{p}} \hat{E} \sin pt \cos npt\, dt$$

$$= \frac{\hat{E}p}{2\pi}\int_0^{\frac{\pi}{p}} (\sin(n+1)pt - \sin(n-1)pt)\, dt.$$

$$\left[\text{Note that } \sin\theta\cos n\theta = \frac{\sin(n+1)\theta - \sin(n-1)\theta}{2}\right]$$

or
$$b_n = \frac{\hat{E}p}{2\pi}\left[-\frac{\cos(n+1)pt}{(n+1)p} + \frac{\cos(n-1)pt}{(n-1)p}\right]_0^{\frac{\pi}{p}}$$
$$= \frac{\hat{E}}{2\pi}\left[\frac{1-\cos(n+1)\pi}{n+1} - \frac{1-\cos(n-1)\pi}{n-1}\right].$$

When n is odd, $\cos(n+1)\pi = \cos(n-1)\pi = 1$, hence b_1, b_3, b_5, etc., are zero.

When n is even $\cos(n+1)\pi = \cos(n-1)\pi = -1$, and

$$b_n = \frac{\hat{E}}{2\pi}\left[\frac{2}{n+1} - \frac{2}{n-1}\right] = \frac{\hat{E}}{\pi}\,\frac{-2}{(n-1)(n+1)}.$$

Thus
$$b_0 = \frac{\hat{E}}{\pi}.2,\quad b_2 = -\frac{\hat{E}}{\pi}.\frac{2}{3},\quad b_4 = -\frac{\hat{E}}{\pi}.\frac{2}{3.5}$$
$$b_6 = -\frac{\hat{E}}{\pi}.\frac{2}{5.7},\text{ etc.}$$

The expression for the half sine wave is

$$f(t) = \frac{2}{\pi}\left[\frac{1}{2} + \frac{\pi}{4}\sin pt - \frac{1}{3}\cos 2pt - \frac{1}{3.5}\cos 4pt - \frac{1}{5.7}\cos 6pt - \ldots\right]. \quad 2\text{A}.6a.$$

For a half cosine wave

$$f(t) = \frac{2}{\pi}\left[\frac{1}{2} + \frac{\pi}{4}\cos pt + \frac{1}{3}\cos 2pt - \frac{1}{3.5}\cos 4pt + \frac{1}{5.7}\cos 6pt \ldots\right] \quad . 2\text{A}.6b.$$

Any shape of wave may be so analysed and in computing the coefficients a_n and b_n for any discontinuous curve, the integrals may be split up into the appropriate functions and integrated between the limits of the discontinuities. For example, replacing the half-wave by a full-wave rectifier gives

$$a_n = \frac{p}{\pi}\left[\int_0^{\frac{\pi}{p}} \hat{E}\sin pt\sin npt\,dt + \int_{\frac{\pi}{p}}^{\frac{2\pi}{p}} -\hat{E}\sin pt\sin npt\,dt\right].$$

The second function contains $-\hat{E}\sin pt$ because the curve from $\frac{\pi}{p}$ to $\frac{2\pi}{p}$ is part of the sine curve $-\hat{E}\sin pt$. It is interesting to

note that the second integral is the negative of the first so that $a_n = 0$, for b_n we have the second integral equal to the first; hence

$$b_n = \frac{2p}{\pi}\int_0^{\frac{\pi}{p}} \hat{E} \sin pt \cos npt \, dt$$

and the expression for the full-wave rectifier-wave shape is

$$f(t) = \frac{4}{\pi}\left[\frac{1}{2} - \frac{1}{3}\cos 2pt - \frac{1}{3.5}\cos 4pt - \frac{1}{5.7}\cos 6pt - \ldots\right] \quad \text{2A.7}a$$

or for a full-wave rectifier with cosine input.

$$f(t) = \frac{4}{\pi}\left[\frac{1}{2} + \frac{1}{3}\cos 2pt - \frac{1}{3.5}\cos 4pt + \frac{1}{5.7}\cos 6pt - \ldots\right]. \quad \text{2A.7}b.$$

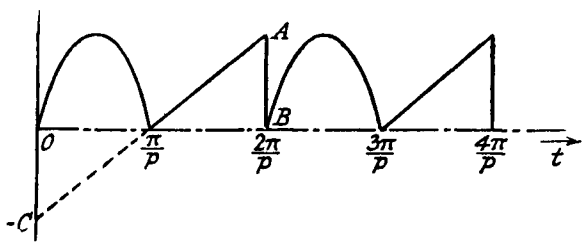

FIG. 2A.2.—A Combined Half Sine and Triangular Wave Shape.

If the wave has the shape shown in Fig. 2A.2, a half sine wave from 0 to $\frac{\pi}{p}$ and a triangular wave from $\frac{\pi}{p}$ to $\frac{2\pi}{p}$ the value of a_n is

$$a_n = \frac{p}{\pi}\left[\int_0^{\frac{\pi}{p}} \hat{E} \sin pt \sin npt \, dt + \int_{\frac{\pi}{p}}^{\frac{2\pi}{p}} (Kt - C) \sin npt \, dt\right]. \quad \text{2A.8}$$

where $(Kt - C)$ is the expression for the wave shape (a straight line) from $\frac{\pi}{p}$ to $\frac{2\pi}{p}$. K is the slope of the line and $-C$ the intercept at $t = 0$.

There is often no objection to changing the initial position of the curve as this only alters the relative initial time positions of the frequency components. In so doing the amount of analysis involved may be greatly reduced. In our first example (the half-wave rectifier) we could have moved the origin forward by $\frac{\pi}{2p}$ seconds, thus turning the function from a half sine wave to a half cosine wave. We would then have found the fundamental frequency component changed to a cosine function and all sine

components zero. Expression 2A.6*b* is the Fourier analysis for the changed position. In this connection it is useful to note the following six important cases of symmetry and their significance.

(1) $f(t) = -f(-t)$.

This condition is represented by the curve in Fig. 2A.3.

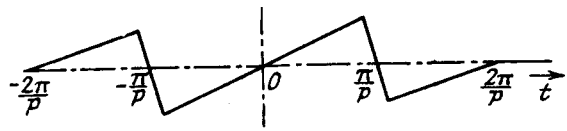

FIG. 2A.3.—A Wave Shape having Sine Functions only.

$$\text{Now } f(t) = \frac{b_0}{2} + \sum_{n=1}^{\infty} a_n \sin npt + \sum_{n=1}^{\infty} b_n \cos npt$$

$$\text{and } f(-t) = \frac{b_0}{2} + \sum_{n=1}^{\infty} a_n \sin np(-t) + \sum_{n=1}^{\infty} b_n \cos np(-t)$$

$$\text{thus } f(t)+f(-t) = 0 = b_0 + \sum_{n=1}^{\infty} a_n[(\sin npt + \sin(-npt)] + \sum_{n=1}^{\infty} b_n[\cos npt + \cos(-npt)]$$

$$\text{but} \qquad \sin(-npt) = -\sin npt.$$

$$\text{and} \qquad \cos(-npt) = \cos npt.$$

$$\therefore\ b_0 + 2\sum_{n=1}^{\infty} b_n \cos npt = 0$$

$$\text{or} \qquad f(t) = \sum_{n=1}^{\infty} a_n \sin npt \qquad . \quad . \quad . \quad \text{2A.9.}$$

Hence the curve contains only sine functions of the fundamental and harmonic frequencies.

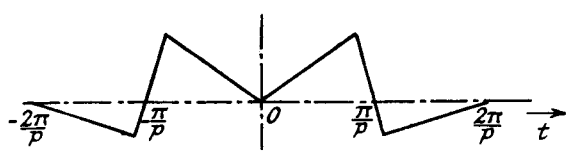

FIG. 2A.4.—A Wave Shape having Cosine Functions only.

(2) $f(t) = f(-t)$.

A curve such as that of Fig. 2A.4 fulfils this equation, which yields the following result.

$$\sum_{n=1}^{\infty} a_n[\sin npt - \sin np(-t)] + \sum_{n=1}^{\infty} b_n[\cos npt - \cos np(-t)] = 0.$$

Hence $$2\sum_{n=1}^{\infty} a_n \sin npt = 0$$

and $$f(t) = \frac{b_0}{2} + \sum_{n=1}^{\infty} b_n \cos npt \quad . \quad . \quad . \quad 2A.10.$$

Moving the origin of the half wave in the first example produces a wave fulfilling this condition and reduces considerably the extent of the analytical investigation.

(3) $f(t) = -f\left(\frac{\pi}{p} + t\right)$ gives

$$f(t) = \sum_{n=1}^{\infty} a_{2n-1} \sin (2n-1)pt + \sum_{n=1}^{\infty} b_{2n-1} \cos (2n-1)pt \quad . \quad 2A.11$$

i.e., b_0 and all even integer sine and cosine coefficients such as a_2, b_2, etc., are zero. A typical curve is shown in Fig. 2A.5.

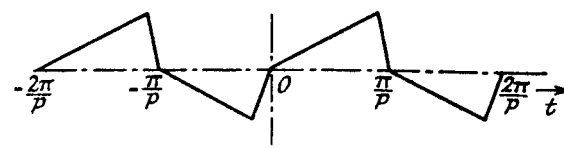

FIG. 2A.5.—A Wave Shape with Odd Sine and Cosine Functions.

(4) $f(t) = f\left(\frac{\pi}{p} + t\right)$.

The expression for the wave shape, which is illustrated in Fig. 2A.6, is

$$f(t) = \frac{b_0}{2} + \sum_{n=1}^{\infty} a_{2n} \sin 2npt + \sum_{n=1}^{\infty} b_{2n} \cos 2npt \quad . \quad 2A.12.$$

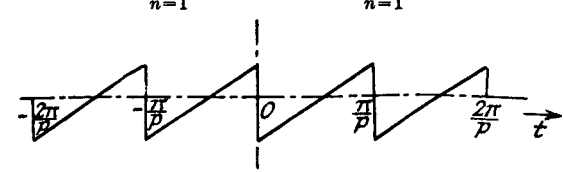

FIG. 2A.6.—A Wave Shape with Even Sine and Cosine Functions.

This is to be expected since the wave repeats itself after every $\frac{\pi}{p}$ interval shown and this interval should really be considered as the complete instead of half interval, viz., $\frac{2\pi}{p}$ instead of $\frac{\pi}{p}$.

(5) $f(t) = -f\left(\frac{\pi}{p} - t\right)$.

A wave shape conforming to this condition (see Fig. 2A.7) gives

$$f(t) = \sum_{n=1}^{\infty} a_{2n} \sin 2npt + \sum_{n=1}^{\infty} b_{2n-1} \cos (2n - 1)pt \quad . \quad 2A.13,$$

i.e., a_1, a_3, etc., b_0, b_2, b_4, etc., are zero.

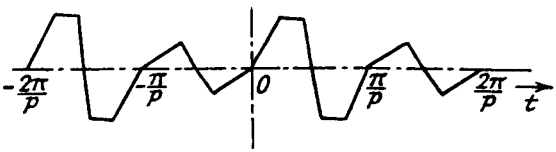

FIG. 2A.7.—A Wave Shape with Even Sine and Odd Cosine Functions.

(6) $f(t) = +f\left(\frac{\pi}{p} - t\right)$.

The curve of Fig. 2A.8 illustrates this and its expression is

$$f(t) = \frac{b_0}{2} + \sum_{n=1}^{\infty} a_{2n-1} \sin (2n - 1)pt + \sum_{n=1}^{\infty} b_{2n} \cos 2npt \quad . \quad 2a.14.$$

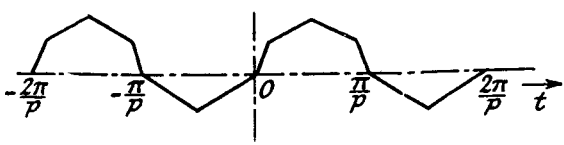

FIG. 2A.8.—A Wave Shape with Odd Sine and Even Cosine Functions.

The special conditions of symmetry are for convenience tabulated below.

Condition.	b_0	Sine coefficients.	Cosine coefficients.
1. $f(t) = -f(-t)$	Zero	All present	All zero
2. $f(t) = f(-t)$	Present	All zero	All present
3. $f(t) = -f\left(\frac{\pi}{p} + t\right)$	Zero	Even integers zero	Even integers zero
4. $f(t) = f\left(\frac{\pi}{p} + t\right)$	Present	Odd integers zero	Odd integers zero
5. $f(t) = -f\left(\frac{\pi}{p} - t\right)$	Zero	Odd integers zero	Even integers zero
6. $f(t) = f\left(\frac{\pi}{p} - t\right)$	Present	Even integers zero	Odd integers zero.

If a wave shape satisfies more than one of the conditions listed above, then $f(t)$ does not comprise any of the terms eliminated.

Taking as an example the curve in Fig. 2A.6, we find that it satisfies

$$f(t) = -f(-t)$$

and

$$f(t) = f\left(\frac{\pi}{p}+t\right).$$

$$\therefore\ f(t) = \sum_{n=1}^{\infty} a_{2n} \sin 2npt \quad . \quad . \quad . \quad \text{2A.15}$$

i.e., the curve contains only sine term coefficients of even suffix.

As a final example of Fourier analysis let us find the distortion present in the output current of a valve having a curved I_aE_g characteristic and an undistorted sinusoidal input voltage. Fig. 2A.9 illustrates a possible set of conditions.

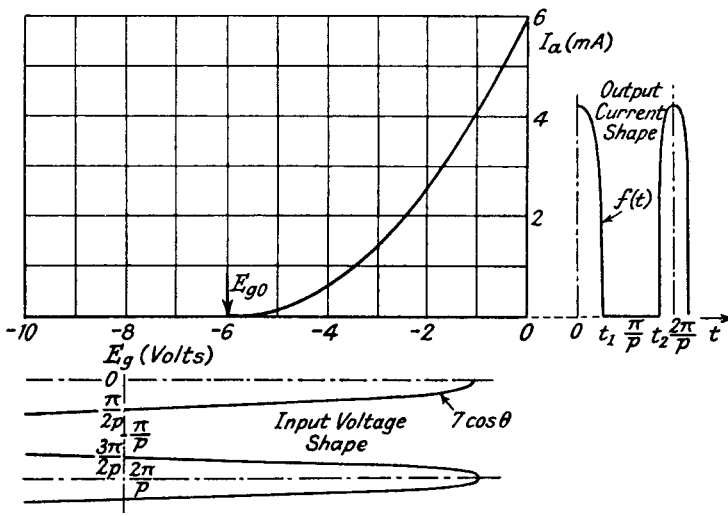

FIG. 2A.9.—An Example of the Application of Fourier Analysis to the Calculation of Distortion produced by the I_aE_g Characteristic of a Valve.

The first step must be to find the equation to the I_aE_g characteristic and this may be achieved by assuming that

$$I_a = c_0+c_1E_g+c_2E_g{}^2+ \ . \ . \ . \ +c_nE_g{}^n \quad . \quad . \quad \text{2A.16.}$$

The curve represented by expression 2A.16 may be made to coincide with the original curve at $(n+1)$ points; $(n+1)$ simultaneous equations are obtained by replacing the particular values of I_a and E_g at these points so that the coefficients c_0, c_1, etc., may be found. Generally it is unnecessary to proceed beyond $n = 4$, and in our particular example we need not consider above $n = 2$. Thus the expression for the I_aE_g curve of Fig. 2A.9 is

$$I_a = 6+2E_g+0{\cdot}166\ E_g{}^2 \quad . \quad . \quad . \quad \text{2A.17}$$

anode current cut-off occurring at $E_{g_0} = -6$. Let us suppose that the input voltage is represented by $7 \cos \theta$ and that the initial bias, $-E_b$, is -8 volts. The output current wave may be drawn out on its time axis to the right of the I_aE_g curve as shown.

The next step is to find the equations to the curve between the discontinuities and the time instants corresponding to the discontinuities. The time instant t_1 is easily determined because $\hat{E} \cos pt_1 = E_b + E_{g_0} = 8 - 6 = 2$.

$$\therefore\ t_1 = \frac{\cos^{-1}\dfrac{2}{\hat{E}}}{p} = \frac{\cos^{-1}\dfrac{2}{7}}{p} = \frac{1{\cdot}28}{p} \text{ radians}$$

and $$t_2 = \frac{2\pi}{p} - t_1 = \frac{5}{p} \text{ radians.}$$

Between t_1 and t_2 the equation to the curve is $f(t) = 0$ so that the Fourier coefficients are

$$b_n = \frac{p}{\pi}\int_0^{\frac{1{\cdot}28}{p}} f(t) \cos npt\, dt + \frac{p}{\pi}\int_{\frac{5}{p}}^{\frac{2\pi}{p}} f(t) \cos npt\, dt$$

$$= \frac{2p}{\pi}\int_0^{\frac{1{\cdot}28}{p}} f(t) \cos npt\, dt$$

where $f(t)$ is the equation to the curve between $t = 0$ and $t = t_1$. a_n is zero because $f(t) = f(-t)$ (see condition 2 above).

The expression for $f(t)$ is obtained by replacing E_g in 2A.17 by $\hat{E} \cos pt - E_b$, i.e., $7 \cos pt - 8$.

Thus $$f(t) = 4{\cdot}75 - 4{\cdot}66 \cos pt + 4{\cdot}083 \cos 2pt.$$

The next step involves finding a general expression for b_n. An attempt to obtain a formula containing only the variable n should always be made as it greatly simplifies the analysis. It can be achieved in this case by separating b_n into its three components, thus :

$$b_n = \frac{2p}{\pi}\Bigg[4{\cdot}75\int_0^{\frac{1{\cdot}28}{p}} \cos npt\, dt - 4{\cdot}66\int_0^{\frac{1{\cdot}28}{p}} \cos pt \cos npt\, dt + 4{\cdot}083\int_0^{\frac{1{\cdot}28}{p}} \cos 2pt \cos npt\, dt\Bigg]$$

$$= \frac{2}{\pi}\Bigg[\frac{4{\cdot}75 \sin 1{\cdot}28n}{n} - \frac{4{\cdot}66}{2}\left(\frac{\sin 1{\cdot}28(n+1)}{n+1} + \frac{\sin 1{\cdot}28(n-1)}{n-1}\right) + \frac{4{\cdot}083}{2}\left(\frac{\sin 1{\cdot}28(n+2)}{n+2} + \frac{\sin 1{\cdot}28(n-2)}{n-2}\right)\Bigg]$$

Where replacing n by a particular value gives $\frac{\sin 1{\cdot}28 \times 0}{0}$, this function becomes 1·28, thus

$$b_0 = 1{\cdot}74,\ b_1 = 1{\cdot}56,\ b_2 = 1{\cdot}09,\ b_3 = 0{\cdot}56,\ b_4 = 0{\cdot}16.$$

The output current therefore consists of the following components :

$$I_a = 0{\cdot}87 + 1{\cdot}56 \cos pt + 1{\cdot}09 \cos 2pt + 0{\cdot}56 \cos 3pt + 0{\cdot}16 \cos 4pt.$$

INDEX

END OF PART ONE.

RADIO RECEIVER DESIGN

By

K. R. STURLEY

Ph.D., B.Sc., M.I.E.E., Sen. M.I.R.E.

Head of Engineering Training Department,
British Broadcasting Corporation

Late of Marconi School of Wireless Communication

Part II

AUDIO FREQUENCY AMPLIFIERS TELEVISION AND FREQUENCY MODULATED RECEIVER DESIGN

Second Impression

NEW YORK

JOHN WILEY & SONS INC.

440 FOURTH AVENUE

1948

First Published . . . *1945*
Second Impression . . *1948*

THIS BOOK IS PRODUCED IN COMPLETE
CONFORMITY WITH THE AUTHORIZED
ECONOMY STANDARDS

Printed in Great Britain by Butler & Tanner Ltd., Frome and London

AUTHOR'S PREFACE

STARTING with A.F. amplification, the procedure of analysing the remaining stages of a radio receiver is similar to that adopted in Part I. The principle of progressing from aerial to output is followed in the two chapters devoted to the special requirements of frequency modulated and television reception. To preserve continuity with Part I, the first chapter is numbered 9, and all sections, figures and expressions are prefixed by their chapter number. A glossary of the more important symbols and units, as well as a detailed table of contents, is included.

The author is again indebted to his wife for help in reading the proofs and to Marconi's Wireless Telegraph Company for permission to incorporate material originally used in lectures given at the Marconi School of Wireless Communication. In addition, he wishes to record his gratitude to Mr. M. Esterson, B.Sc., for useful criticism of the script and checking of the calculations.

May 1944.

ACKNOWLEDGMENTS

REFERENCES to sources of information will be found in the Bibliographies and footnotes, but the author particularly wishes to acknowledge his indebtedness to the following for permission to use diagrams from their publications.

Name of Journal or Manufacturer	*Figure Numbers*
Electronic Engineering	15.3 to 15.10
Journal of the Institution of Electrical Engineers	16.1
Marconi Review	13.19
Proceedings of the Institute of Radio Engineers	9.15 10.15, 10.25 13.4, 13.11 14.1*a*, 14.1*b*
Radio Manufacturers Association (England)	14.6*a*, 14.6*b*
R.C.A. Journal	15.1 16.9*a*, 16.11, 16.13, 16.14, 16.16
Wireless Engineer	10.4, 10.6, 10.20, 10.21 11.16, 11.17 12.9*a*, *b* and *c* 15.18*a* to 15.21
Wireless World	9.18 to 9.21 11.15*a*, 11.19, 11.20 12.20 13.3 16.22, 16.27 Table 11.1
Messrs. Cosmos Manufacturing Company	16.26
Messrs. Electrical Musical Industries	13.14
Messrs. Pye Radio	16.20, 16.24, 16.31
Messrs. Radio Corporation of America	12.19 13.9*a*, 13.9*b* 15.11, 15.22 to 15.24, 15.26, 15.27

PART II

CONTENTS

GLOSSARY

OF THE MORE IMPORTANT SYMBOLS USED IN THE TEXT

Symbols

R . . . . resistance.

L . . . . inductance.

M . . . . mutual inductance, also modulation ratio.

C . . . . capacitance.

I . . . . current (R.M.S. or D.C. value), $\hat{I}$ peak value of A.C. current.

E . . . . voltage (R.M.S. or D.C. value), $\hat{E}$ peak value of A.C. voltage.

P . . . . power.

X . . . . reactance of an inductance ($2\pi fL$), or of a capacitance $\left(\frac{1}{2\pi fC}\right)$.

Z . . . . impedance of a resistance and reactance.

G . . . . conductance, the reciprocal of resistance.

B . . . . susceptance (when with suffix), the reciprocal of reactance.

Y . . . . admittance, the reciprocal of impedance.

g_m . . . . mutual conductance of a valve, $\frac{\partial I_a}{\partial E_g}$.

R_a . . . . internal or slope resistance of a valve, $\frac{\partial E_a}{\partial I_a}$.

μ . . . . amplification factor of a valve, $\frac{\partial E_a}{\partial E_g}$.

μ . . . . permeability (chapters 10 and 11).

$\Delta\mu$ . . . . incremental permeability.

R_D . . . . resonant impedance of a tuned circuit.

Z_T . . . . transfer impedance of a pair of coupled circuits, $\frac{\text{output voltage}}{\text{input current}}$.

Q . . . . magnification of a coil or tuned circuit, $\frac{2\pi fL}{R}$ or $\frac{1}{2\pi fCR}$.

F . . . . frequency ratio, twice the off-tune frequency Δf to the resonant or mid-frequency (f_r or f_m).

ω . . . . radio frequency pulsance, $2\pi f_c$.

p . . . . low or audio frequency pulsance, $2\pi f_m$.

k . . . . coupling coefficient, normally, $\frac{M}{\sqrt{L_p L_s}}$.

n . . . . ratio of secondary to primary turns in a transformer.

N_p . . . . number of turns on primary of a transformer.

N_s . . . . number of turns on secondary of a transformer.

A . . . . amplification when with suffix (chapter 9).

A . . . . area when without suffix (chapters 10 and 11).

V . . . . volume (chapters 10 and 11).

Φ . . . . total flux.

Symbols

B	flux density when without suffix (chapters 10 and 11).
H	magnetic field strength.
H_p	polarizing D.C. magnetic field strength.
A.C.	alternating current.
D.C.	direct current.
C.R.	cathode ray.
A.F.	audio frequency.
I.F.	intermediate frequency.
R.F.	radio frequency.
V.F.	vision frequency.
H.T.	high tension.
L.T.	low tension.
A.F.C.	automatic frequency correction.
A.G.C.	automatic gain control (sometimes A.V.C.).
R.M.S.	root mean square.

Signs

$\sqrt{\ }$	square root.
$<$	less than.
$\ll$	much less than.
$>$	greater than.
$\gg$	much greater than.
$=$	equals.
$\simeq$	approximately equals.
$\times$	multiplied by.
$\lvert A \rvert$	modulus of A.
$\angle$	angle between 0° and 180°.
$\supset$	angle between 180° and 360°.
%	percentage.
+db.	gain.
− db.	loss.
λ	wavelength.
η	efficiency.
$\tan^{-1} A$	angle whose tangent is A.
j	$\sqrt{-1}$, vector operator.
Δ	small change of.
∂	partial differential.

Suffixes

a	anode circuit.
$a1$	aerial and coupling circuit.
b	bias or battery.
c	carrier signal (exception C_c, coupling capacitance, chapter 9).
co	cut-off.
d	desired signal.
f	fundamental (exception feedback circuit in Section 10.10).
g	grid circuit.
h	high (chapter 9), harmonic (chapter 10), local oscillator (chapter 13), hum (chapter 14).

Suffixes

k	cathode circuit.
l	low.
m	middle
mod	modulation
n	noise.
1	input.
0	output.
p	primary.
r	resonance.
s	secondary (chapters 9, 10 and 11), screen (chapters 9 and 16), stray (chapter 9).
sc	speech coil.
u	undesired.

Units

H	henrys.
*m*H	millihenrys.
μH	microhenrys.
μF	microfarads.
$\mu\mu$F	micro-microfarads.
mA	milliamperes.
μA	microamperes.
mV	millivolts.
μV	microvolts.
mW	milliwatts.
Ω	ohms.
MΩ	megohms.
db.	decibel.
c.p.s.	cycles per second.
kc/s	kilocycles per second.
Mc/s	megacycles per second.
μ (as prefix)	micro.

PART II

CHAPTER 9

AUDIO FREQUENCY AMPLIFIERS

9.1. Introduction. An audio-frequency voltage amplifier stage is generally required between the detector and output valve, especially when the latter has a low power-sensitivity,* or when an amplified A.G.C. system is employed (in this instance the maximum carrier voltage applied to the detector valve is about 3 volts R.M.S.). An A.F. stage is also necessary if the receiver is used in conjunction with a gramophone pick-up. In certain types of receivers an A.F. amplifier is not included, the detector being fed directly to a high power-sensitivity pentode or tetrode valve requiring about 4 volts R.M.S. input for maximum power output. It is not usual to find more than one stage of A.F. amplification—except in receivers with push-pull output—partly because it adds almost nothing to the selectivity of a receiver and partly because high A.F. amplification tends to instability (motor boating) and increased hum output. The design of the A.F. voltage amplifier is somewhat different from that of the output amplifier stage since maximum voltage, and not power, is required at the output. Resistance-capacitance or transformer coupling is generally employed ; choke-capacitance coupling is rarely used because it is more expensive, has a less satisfactory frequency response and only a slightly higher amplification than resistance-capacitance coupling. The particular features of the first two types of coupling are discussed in Sections 9.3 and 9.4.

9.2. The Characteristics Required of an A.F. Amplifier. The most important characteristic required of an amplifier is that it shall reproduce faithfully at its output the shape of the input wave without adding noise or hum voltages. This statement may be qualified in the case of an audio frequency amplifier to " shall reproduce at its output the component input frequencies (and no others) in the same amplitude proportions as exist for the input signal ". Undesirable hum voltages are generally associated with the valve heater and H.T. supply, and they can be reduced to negligible proportions by adopting special forms of heater (e.g., the

* Power sensitivity is defined as the output power (milliwatts) per volt (R.M.S.) input.

spiral type) and electrode construction, and by careful smoothing of the H.T. supply. In special cases when the input signal is small and considerable amplification is needed, for example, in a condenser microphone amplifier, the H.T. supply may be stabilized by using a gas discharge valve across it, and the heater of the first valve may be supplied with smoothed rectified D.C. Thermal and shot noise voltages are generally of no consequence in the A.F. stages of a receiver because A.F. amplification is not sufficient to bring them into prominence.

Distortion of the output wave shape from an A.F. amplifier may be of four kinds: attenuation (variation of amplification for the individual frequency components of the input signal), harmonic or non linear (involving the production of frequencies harmonically related to the input frequency components), phase (a variation in the time delay of the individual frequency components of the signal from input to output terminals), and transient distortion. The latter is caused by damped oscillations following upon shock excitation of the amplifier by a steep-fronted pulse.

Attenuation distortion results from the unequal amplification of the frequency components of the input signal, i.e., for zero attenuation distortion the frequency response of the amplifier must be flat over the range it is desired to accept. A reasonably sharp cut-off with considerable attenuation is desirable outside the required range as this assists in removing interference, hum or noise voltages from the output. A range from 30 to 18,000 c.p.s. is generally considered necessary for the faithful reproduction of musical sounds—a much smaller range is needed for speech—and an amplifier should normally be designed to have a flat frequency response over this range. Attenuation distortion resulting in loss of low-frequency response causes reproduction to be unnaturally brilliant, whilst high-frequency attenuation produces a muffled tone with reduced intelligibility for speech. If high and low frequencies are attenuated, reproduction is intelligible but lacks naturalness. An exception to the rule calling for a flat-frequency response is provided by tone control, which allows adjustment of the high and low frequency components relative to the middle frequencies (1,000 to 3,000 c.p.s.). Tone control may be used to compensate for deficiencies in the frequency response of other parts of the receiver. For example, attenuation of the high frequency modulation sidebands in the R.F. and I.F. stages can be counteracted to a large extent by an increase in the high-frequency response of the A.F. amplifier. Alternatively, greater attenuation of the high frequencies in the A.F. amplifier may be used

as an aid to selectivity. Control of low-frequency response may be included to give a better frequency balance when interference requires severe attenuation of the high audio frequencies. Furthermore, the characteristics of the ear are such that a change in average sound level causes an apparent change in the balance of the frequency components, a reduction in volume leading to an apparently greater reduction in the low and high frequency components compared with the middle frequencies. Discrimination in favour of the high and

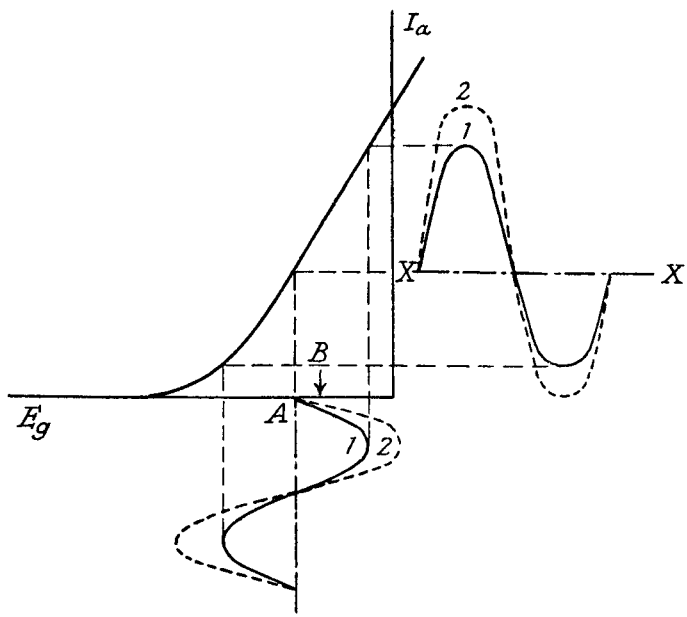

FIG. 9.1.—Distortion due to Curvature of the I_aE_g Characteristic and Grid Current.

low frequencies enables the balance to be retained as volume is reduced.

Amplitude or harmonic distortion is caused by variation of the instantaneous amplification over the input voltage cycle. It may be introduced by the valve, its associated circuits, or a combination of both. The valve produces amplitude distortion because of a non-linear I_aE_g relationship, or because grid current flattens the positive tip of the input voltage wave. The first causes flattening of the negative peak of anode current (see curve 1, Fig. 9.1), whilst the second causes the positive peak of the wave to be flattened (see curve 2, Fig. 9.1). Owing to curvature of the I_aE_g character-

istic as I_a approaches zero, the optimum working grid bias is always less than half the bias voltage needed to cut-off anode current; it is generally about 0·4 of this voltage. The positive peak of anode current may be flattened, as shown by curve 2, Fig. 9.1, even though the input voltage is insufficient to draw grid current, and this is due to the anode load resistance causing a turn-over, or top bending, of the I_aE_g characteristic. Triode valves seldom have this type of characteristic, but with tetrodes it is quite apt to occur, particularly if the load resistance is high. It is due to the load line entering the "knee" of the I_aE_a characteristic (see line AB' in Fig. 9.8). Amplitude distortion from a valve having a resistance anode load is caused usually by incorrect biasing and/or too large an input signal. Curve 1 (Fig. 9.1) shows the result of overbiasing, and distortion could be appreciably reduced by changing the bias point from A to B. Overloading by too large an input signal is illustrated by curve 2 (Fig. 9.1). It may be noted that both curves are symmetrical about a vertical line drawn through maximum or minimum amplitude. This is to be expected because the operating I_aE_g characteristic with a resistance anode load cannot exhibit a "hysteresis" loop, i.e., it must be the same for increasing input voltage (grid voltage becoming less negative) as for decreasing input voltage amplitude.

Amplitude distortion always produces frequencies additional to those present in the input, and Fourier analysis of the wave shape of curve 1 in Fig. 9.1 shows that it contains mainly even harmonics, the wave shape being asymmetrical about the datum line XX'; curve 2, on the other hand, contains mainly odd harmonics, the wave shape being almost symmetrical about XX'. Figs. 9.2*a* and 9.2*b* show that the addition of a second and third harmonic frequency respectively to the fundamental results in wave shapes similar to those of curves 1 and 2. As a general rule the input voltage wave to an A.F. amplifier does not consist of a single sinusoidal frequency but of a number of such components, and amplitude distortion may cause intermodulation frequencies to appear in the output as well as harmonics of the original frequency components. These intermodulation products are sum and difference frequencies (the upper and lower sidebands) formed by combining the original frequency components or their harmonics. Thus for an input of two frequencies, f_1 and f_2, the output may contain fundamental and harmonic frequencies of f_1, mf_1, f_2 and nf_2, and also intermodulation frequencies of $mf_1 \pm nf_2$, and $nf_2 \pm mf_1$, where m and n are integers. Intermodulation tones generally have an inharmonic relationship to

the original frequencies, and in consequence tend to harsh and discordant reproduction.

A valve, which may not produce amplitude distortion of a given input signal with a resistance anode load, may, however, distort with a reactive anode load. A linear * impedance of reactance and resistance is represented on the I_aE_a characteristics by a locus curve similar to a sheared ellipse, which may pass through the low I_a non-linear part of the characteristics (see Section 2.6, Part I, and Section 10.5) as shown by the section *CD* in Fig. 10.7*a*. The wave shape is distorted in the manner shown in Figs. 10.7*a* and 10.7*b* for an inductive and capacitive load respectively, the leading edge

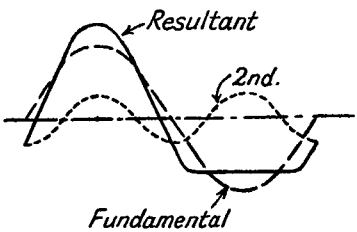

FIG. 9.2*a*.—Addition of Fundamental and Second Harmonic to produce a Wave Shape similar to Curve 1 in Fig. 9.1.

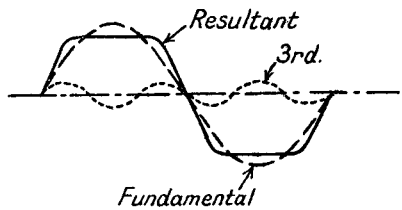

FIG. 9.2*b*.—Addition of Fundamental and Third Harmonic to produce a Wave Shape similar to Curve 2 in Fig. 9.1.

(increasing I_a) rising more slowly than the trailing edge with an inductive load (Fig. 10.7*a*), and vice versa for a capacitive load (Fig. 10.7*b*). It should be noted that the wave shapes are asymmetric about a vertical line through maximum or minimum amplitude, i.e., the operating I_aE_g characteristic is no longer the same for increasing as for decreasing signal amplitude, but is rather similar to an iron *B-H* hysteresis loop as shown in Fig. 10.7*b*. The direction of progress round the loop is anticlockwise for an inductive anode load, maximum I_a (point F_1, Fig. 10.7*b*) occurring after maximum positive input voltage has been passed, whilst it is clockwise for a capacitive load, maximum I_a (point F_2, Fig. 10.7*b*) occurring before maximum positive input voltage.

Amplitude distortion may also be produced by circuits associated with the valve ; for example, an iron-cored coil may act as a non-linear impedance, its inductance varying with the current through it because of a non-linear relationship between the magnetic flux

* A linear impedance consists of an inductance, capacitance and/or resistance, the value of which is constant and independent of the amplitude or frequency of the voltage applied to it, or of the current passing through it.

and current. Distortion of a symmetrical input wave by non-linear action of an iron-cored inductance usually results in an asymmetrical output wave owing to the hysteresis loop of the *B-H* curve.

Phase distortion occurs in an amplifier when the frequency components of the input wave suffer differing time delays in passing through the amplifier. An example of the change in output wave shape caused by delaying the fundamental frequency component of Fig. 9.2*b* by 60° of its cycle, i.e., $\frac{60}{360f} = \frac{1}{6f}$ seconds with respect to the third harmonic frequency, where f = frequency of the fundamental, is illustrated in Fig. 9.2*c*. Despite the difference in wave shape between the two figures, the ear is unable to detect any noticeable difference in sound characteristic. This applies also to frequencies not harmonically related, so that we can ignore phase distortion in A.F. amplification unless the time delay becomes much larger than is usually encountered in practice. Phase distortion is very important in television reception because there is a marked difference between the equivalent light contents of the output waves of Figs. 9.2*b* and 9.2*c*.

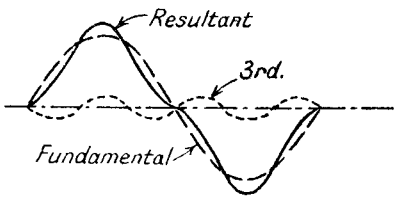

FIG. 9.2*c*. — The Effect of Phase Change on Wave Shape shown in Fig. 9.2*b*.

Transient distortion can occur in an amplifier if the latter contains a tuned circuit, or its equivalent, comparatively lightly damped, i.e., has a frequency response peaked over a narrow band. A steep-sided pulse shock-excites the tuned circuit, and a train of damped oscillations follows the leading edge of the pulse. The decay of these oscillations is determined by the degree of damping on the tuned circuit, which is measured by the height of the peak above the average frequency response level in the vicinity of the peak. Transient distortion can usually be ignored if the peak-to-average response is less than 1 db., provided a peak in one stage of an amplifier is not being cancelled by a dip in another. Large transient distortion produces blurring of the sound output.

9.3. Resistance-Capacitance Coupling Circuits.[10]

9.3.1. Frequency Response and Amplification. A typical resistance-capacitance coupled A.F. amplifier is shown in Fig. 9.3; triode valves are illustrated in the figure, but they may be replaced

by tetrodes, and the modifications needed to make the formulae applicable to tetrodes will be indicated as the analysis proceeds. The input voltage variations, developed in amplified form across R_0, are transferred to the next stage through the coupling capacitance C_c, which prevents the application of the D.C. component of

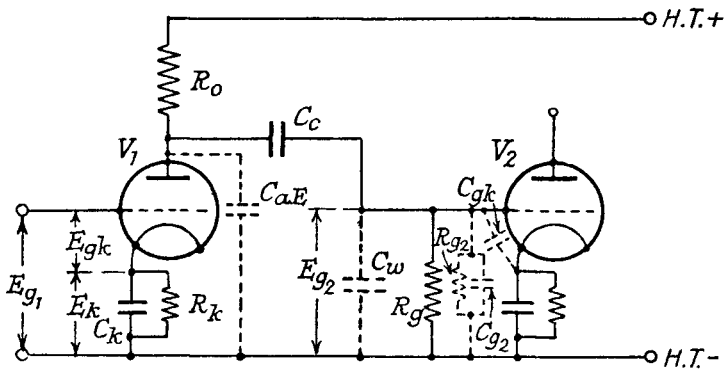

FIG. 9.3.—The Circuit for a Typical Resistance-Capacitance Coupled A.F. Amplifier.

anode voltage to the grid of the second valve V_2. The D.C. path from the grid of valve V_2 to H.T. negative or a suitable bias voltage is completed by the grid leak resistance R_g. Grid bias for the

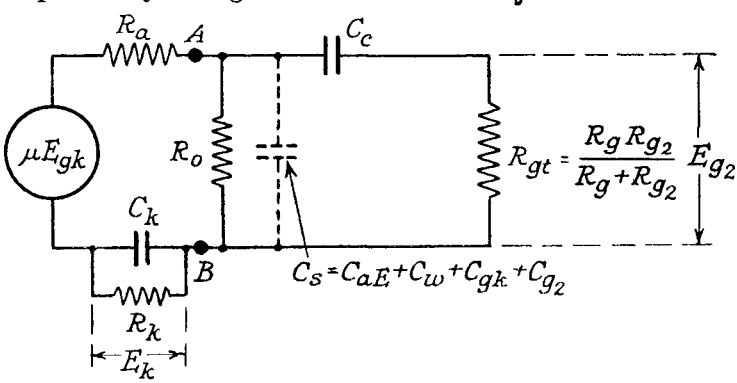

FIG. 9.4*a*.—A Simplified Diagram of a Resistance-Capacitance Coupled A.F. Amplifier.

stages may be derived from the anode current passing through a self-bias resistance (R_k between the cathode of V_1 and H.T. negative) if the valves are indirectly heated. Directly heated valves (battery) generally require the bias to be inserted between the end of the grid leak, R_g, and H.T. negative or earth. A potential divider carrying the total anode current of all stages or a separate bias

battery may be provided. The self-bias resistance R_k must be paralleled by a capacitance C_k if reduced amplification by degenerative A.F. voltages across R_k is to be prevented.

A simplified diagram of the stage is shown in Fig. 9.4*a*; the valve is considered as a constant voltage generator of μE_{gk}—μ is the amplification factor of the valve V_1—and the output capacitance of $V_1(C_{aE})$, the input capacitance of $V_2(C_{g2}+C_{gk})$, and the wiring capacitance C_w are represented by C_s across R_0. This is permissible because C_c is, as a rule, much larger than C_s. C_{gk} is the grid-cathode interelectrode capacitance of V_2; C_{g2} and R_{g2} are the parallel capacitance and resistance components reflected from the anode of V_2 through its anode-grid capacitance (see Section 2.8.2, Part I). Overall amplification, given by the ratio of the output to input voltage, $\frac{E_{g2}}{E_{g1}}$, varies over the frequency range due to the reactance variations of C_c and C_s.

Taking first the separately biased amplifier ($R_k = 0$), amplification is

$$A = \frac{E_{g2}}{E_{g1}} = \frac{\mu Z_{AB}}{R_a+Z_{AB}} \cdot \frac{R_{gt}}{R_{gt}+\frac{1}{jpC_c}}$$

where R_a = the slope resistance of the valve, V_1,
Z_{AB} = impedance across the points AB looking from the generator
R_{gt} = the effective resistance of R_g and R_{g2} in parallel.

Generally for an A.F. amplifier stage R_{g2} is large compared with R_g and can be neglected; in the analysis which follows we shall assume that only R_g need be considered.

$$Z_{AB} = \frac{\frac{R_0}{jpC_s}\left(R_g+\frac{1}{jpC_c}\right)}{\frac{R_0}{jpC_s}+R_0\left(R_g+\frac{1}{jpC_c}\right)+\frac{1}{jpC_s}\left(R_g+\frac{1}{jpC_c}\right)}$$

$$A = \frac{\mu R_0 R_g}{R_0\left(R_g+\frac{1}{jpC_c}\right)+R_a\left(R_0+jpC_sR_0\left(R_g+\frac{1}{jpC_c}\right)+R_g+\frac{1}{jpC_c}\right)} \quad 9.1.$$

The effect of the variables, the reactances of C_c and C_s, on the frequency response of the amplifier is best examined by dividing the audio frequency range into three separate bands, of low, medium and high frequencies. In the medium frequency band, the series reactance of C_c is negligible compared with R_g, and the parallel

reactance of C_s is large compared with R_0; the equivalent circuit is that of Fig. 9.4*b* and the amplification at the medium frequencies is therefore :

$$A_m = \frac{\mu R_0 R_g}{R_0 R_g + R_a(R_0 + R_g)} \quad . \quad . \quad . \quad 9.2a$$

$$= \frac{\mu R_0'}{R_a + R_0'} \quad . \quad . \quad . \quad . \quad . \quad 9.2b$$

where $R_0' = \frac{R_0 R_g}{R_0 + R_g}$ = effective anode load resistance at the medium frequencies.

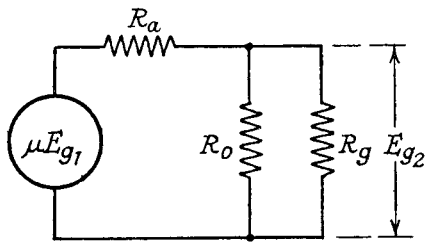

FIG. 9.4*b*.—The Equivalent Circuit of a Resistance-Capacitance Coupled A.F. Amplifier over the Medium Frequency Band.

In the low frequency band, the reactance of C_c increases and becomes comparable with R_g, whilst the reactance of C_s can still be

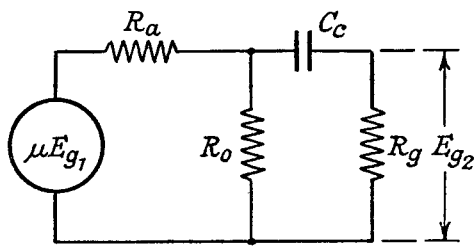

FIG. 9.4*c*.—The Equivalent Circuit of a Resistance-Capacitance Coupled A.F. Amplifier over the Low Frequency Band.

neglected. Fig. 9.4*c* is the equivalent diagram and expression 9.1 is amended to

$$A_l = \frac{\mu R_0 R_g}{R_0\left(R_g + \frac{1}{jpC_c}\right) + R_a\left(R_0 + R_g + \frac{1}{jpC_c}\right)} \quad . \quad . \quad 9.3a$$

$$= \frac{\mu R_0 R_g}{(R_a + R_0)\left(R_g + \frac{1}{jpC_c}\right) + R_a R_0} \quad . \quad . \quad . \quad 9.3b$$

Combining 9.2*a* and 3*b*

$$\frac{A_l}{A_m} = \frac{\dfrac{R_0R_a}{R_0+R_a}+R_g}{\dfrac{R_0R_a}{R_0+R_a}+R_g+\dfrac{1}{jpC_c}}$$

$$= \frac{1}{1-j\dfrac{X'}{R'}} \quad . \quad . \quad . \quad . \quad 9.4a$$

where $X' = \dfrac{1}{pC_c}$ and $R' = \dfrac{R_0R_a}{R_0+R_a}+R_g$.

Hence $$\left|\frac{A_l}{A_m}\right| = \frac{1}{\sqrt{1+\left(\dfrac{X'}{R'}\right)^2}} \quad . \quad . \quad . \quad 9.4b.$$

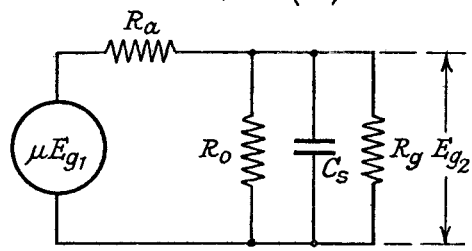

FIG. 9.4*d*.—The Equivalent Circuit for a Resistance-Capacitance Coupled A.F. Amplifier over the High Frequency Band.

For the high frequency band, the shunting effect of C_s is important, but the reactance of C_c is very small. The equivalent circuit is shown in Fig. 9.4*d* and expression 9.1 is modified to

$$A_h = \frac{\mu R_0R_g}{R_0R_g+R_a(R_0+jpC_sR_0R_g+R_g)}$$

$$= \frac{\mu\dfrac{R_0R_g}{R_0+R_g}}{\dfrac{R_0R_g}{R_0+R_g}+R_a+\dfrac{jpC_sR_0R_gR_a}{R_0+R_g}} \quad . \quad . \quad . \quad 9.5.$$

Combining 9.2*a* and 5

$$\frac{A_h}{A_m} = \frac{\dfrac{R_0R_g}{R_0+R_g}+R_a}{\dfrac{R_0R_g}{R_0+R_g}+R_a+\dfrac{jpC_sR_0R_gR_a}{R_0+R_g}}$$

$$= \frac{1}{1+j\dfrac{R''}{X''}} \quad . \quad . \quad . \quad . \quad . \quad . \quad 9.6a$$

where $R'' = \dfrac{R_0R_gR_a}{R_0R_g+R_a(R_0+R_g)}$ = resistance of R_0, R_g and R_a in parallel.

$$X'' = \frac{1}{pC_s}.$$

Thus
$$\left|\frac{A_h}{A_m}\right| = \frac{1}{\sqrt{1+\left(\dfrac{R''}{X''}\right)^2}} \quad . \quad . \quad . \quad 9.6b.$$

By denoting zero level (0 db.) as $20 \log_{10} A_m$ we can express the reduction in amplification over the low and high frequency ranges as

$$-20 \log_{10}\left|\frac{A_m}{A_l}\right| = -10 \log_{10}\left(1+\left(\frac{X'}{R'}\right)^2\right) \text{ db.}$$

$$= -10 \log_{10}\left(1+\frac{1}{x^2}\right) \text{ db.} \quad . \quad . \quad 9.4c$$

and
$$-20 \log_{10}\left|\frac{A_m}{A_h}\right| = -10 \log_{10}\left(1+\left(\frac{R''}{X''}\right)^2\right) \text{ db.}$$

$$= -10 \log_{10}(1+x^2) \text{ db.} \quad . \quad . \quad . \quad 9.6c.$$

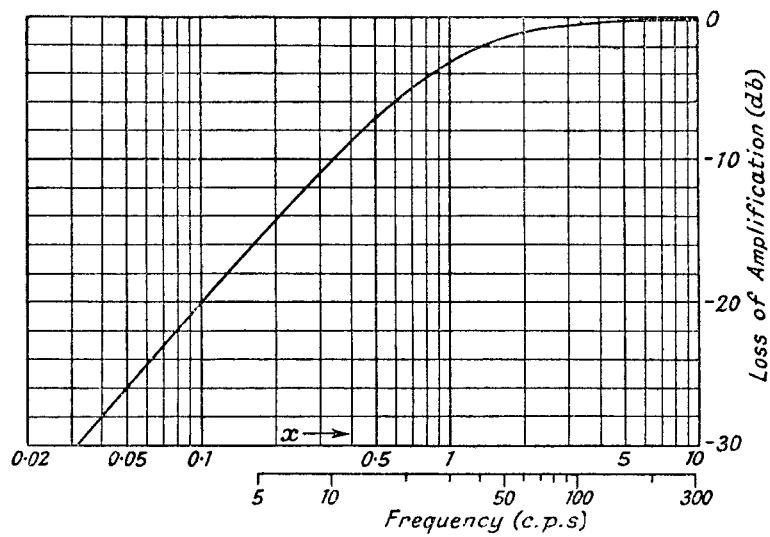

FIG. 9.5a.—Generalised Low Frequency Response of a Resistance-Capacitance Coupled A.F. Amplifier.

The negative sign in expressions 9.4c and 9.6c denote that it is a loss of amplification. From these two expressions we may plot two generalised amplification curves of frequency response (db.) against

$x\left(\frac{R'}{X'} \text{ and } \frac{R''}{X''}\right)$ to a logarithmic scale as in Figs. 9.5*a* and 9.5*b*. Since these two ratios, $\frac{R'}{X'}$ and $\frac{R''}{X''}$, are both directly proportional to frequency, we can find the frequency response of any amplifier by suitably positioning a logarithmic scale, marked in frequency, beneath the x scale in a similar manner to the method described in Sections 4.2.3 and 7.4 (Part I).

Taking as an example the following values for the constants of an amplifier

$$R_0 = 200{,}000\ \Omega$$
$$R_a = 50{,}000\ \Omega$$
$$R_g = 1\ \text{M}\Omega$$
$$C_c = 0{\cdot}005\ \mu\text{F}$$
$$C_s = 0{\cdot}0005\ \mu\text{F}$$

$$R' = R_g + \frac{R_a R_0}{R_a + R_0} = 1{\cdot}04 \times 10^6\ \Omega$$

$$R'' = \frac{R_a R_0 R_g}{R_0 R_g + R_a(R_0 + R_g)}$$
$$= 3{\cdot}84 \times 10^4\ \Omega.$$

For the low frequency response $\frac{R'}{X'} = 1$ when $R' 2\pi f C_c = 1$

or $$f = 30{\cdot}6 \text{ c.p.s.}$$

The logarithmic frequency scale is therefore moved until 30·6 c.p.s. is located immediately beneath $x = 1$ as shown in Fig. 9.5*a*, and the response at any frequency is read directly. Thus at 50 c.p.s. the response is − 1·4 db., whilst at 100 and 25 c.p.s. it is − 0·4 and − 3·95 db. respectively.

For the high frequency response $\frac{R''}{X''} = 1$,

$$\text{when } f = \frac{1}{2\pi C_s R''}$$
$$= 8{,}280 \text{ c.p.s.}$$

The frequency scale is moved until 8,280 c.p.s. is located immediately beneath $x = 1$ (see Fig. 9.5*b*) and the response at any particular frequencies such as 5,000 and 10,000 c.p.s. is noted to be − 1·35 and − 3·9 db. respectively. The complete frequency response of this amplifier over the frequency range 30 to 18,000 c.p.s. is obtained by joining the two curves for the low and high frequency sections.

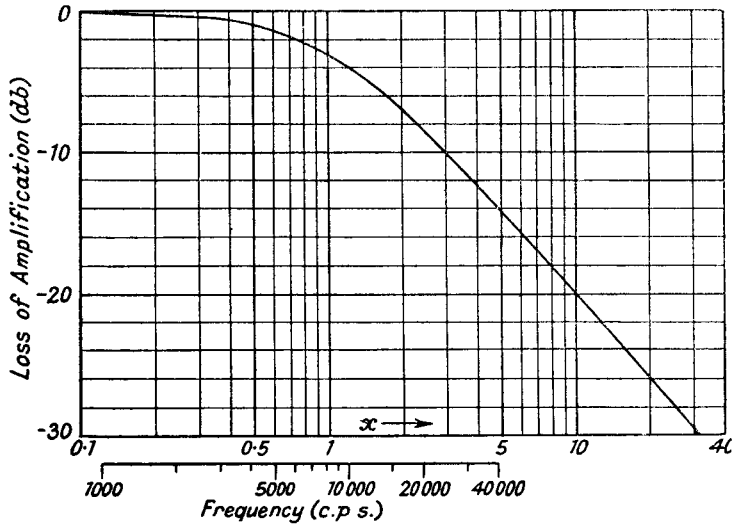

FIG. 9.5*b*.—Generalised High Frequency Response of a Resistance-Capacitance Coupled A.F. Amplifier.

The maximum overall amplification of the amplifier (in the middle range of frequencies) may be calculated from expression 9.2*b*, and it is conveniently expressed in terms of the amplification factor of the valve as

$$\frac{A_m}{\mu} = \frac{1}{1+\frac{R_a}{R_0'}} \quad . \quad . \quad . \quad . \quad 9.2c.$$

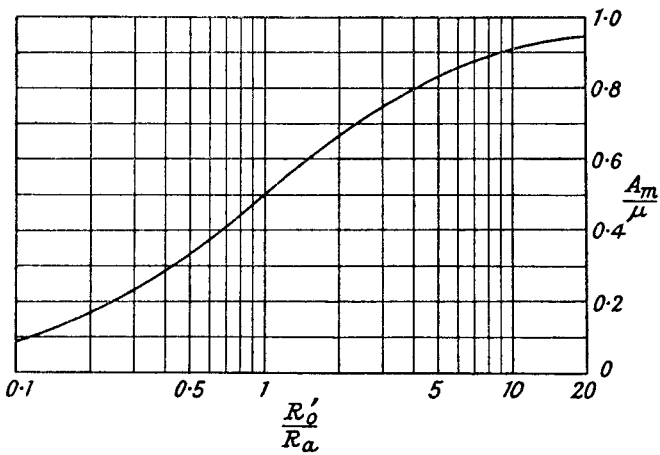

FIG. 9.6.—The Variation of Medium Frequency Amplification with Change of Anode Load Resistance.

Plotting 9.2c against $\frac{R_0'}{R_a}$ (Fig. 9.6) shows that the overall gain increases to μ as R_0' is made much greater than R_a. A point to be noted in connection with Fig. 9.6 is that μ is not necessarily a constant, but is often dependent upon the R_0 component in R_0'. This is made clear by reference to the triode I_aE_a characteristics of Fig. 9.7; as R_0 is increased the load line AB is carried into the curved lower part of the characteristics (see line AB') where μ falls and R_a increases. On this account it is inadvisable to make R_0 much greater than $3R_a$. The importance of ensuring that R_0' is not much less than R_0, i.e., that R_g is as large as possible, is stressed in Section 9.3.3.

An alternative expression to 9.2*b* may be derived by replacing μ by g_mR_a.

$$A_m = g_m\frac{R_aR_0'}{R_a+R_0'} \quad . \quad . \quad . \quad . \quad 9.2d$$

$= g_m \times$ the parallel combination of R_a, R_0 and R_g.

This result is also obtained by considering the valve as a constant current generator (Section 2.7, Part I). Expression 9.2*d* is very useful in the case of a tetrode valve, for which g_m and R_a, and not μ, are known. In this instance R_a is usually high ($> 0{\cdot}5$ MΩ), and it would be almost impossible to fulfil the condition $R_0 > R_a$. The maximum value of R_0 is limited by the shape of the tetrode I_aE_a characteristics, by the stray capacitance, and by the permissible loss at high audio frequencies. It is often much less than R_a, so that expression 9.2*d* may be modified to

$$A_m = g_mR_0' \quad . \quad . \quad . \quad . \quad 9.2e.$$

9.3.2. A Comparison between the Triode and Tetrode Valve as an A.F. Amplifier. The chief advantages of the triode valve as an A.F. amplifier are its low slope resistance and its capability of delivering a large output voltage with smaller harmonic distortion (of lower order harmonics) than the tetrode, but it does require generally a much larger input voltage to produce a given output voltage. A low slope resistance means that high frequency response is less dependent on the characteristics of the anode load impedance, because R'' in expression 9.6*b* is decreased by decrease of R_a. Low frequency response is, however, less satisfactory since decrease of R' in 9.4*b* increases the loss at low frequencies. The important features of the tetrode are higher amplification (it is generally about twice that of a triode of the same g_m value) and very much reduced feedback through the anode-grid capacitance.

The latter has an important bearing on high frequency response, because it increases the grid input capacitance by an amount equal to the grid-anode capacitance multiplied by $(1+A)$, where A is the amplification from the grid to the anode of the valve. For example, average values of C_{ga} and A for a triode valve are 3 $\mu\mu$F and 50, respectively, giving a grid input capacitance, additional to the "cold" input capacitance of $3 \times 51 = 153$ $\mu\mu$F; average values for a tetrode are 0·01 $\mu\mu$F and 100, respectively, giving an additional input capacitance of $0{\cdot}01 \times 101 = 1{\cdot}01$ $\mu\mu$F. Hence the use of a tetrode contributes to an improved high frequency response from the stage preceding it, because it reduces the stray capacitance C_s. The chief disadvantages of a tetrode are greater

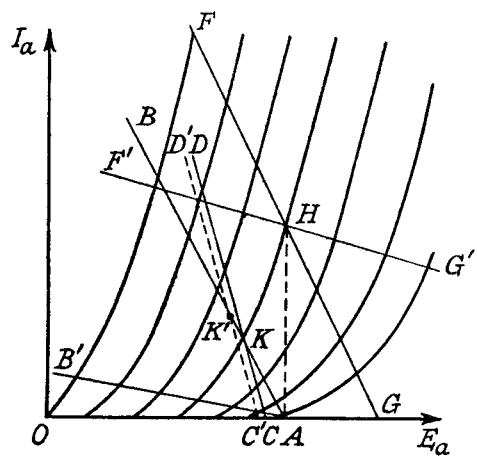

FIG. 9.7.—The Representation of Load Resistance on the I_aE_a Characteristics of a Triode Valve.

circuit complication (a screen resistance and capacitance are required) and the more objectionable type of distortion, consisting of higher order harmonics and intermodulation products (see Section 10.7).

The reason for the smaller distortion (of lower order harmonics) produced by the triode can be seen by referring to the I_aE_a characteristic curves in Fig. 9.7. The anode load resistance R_0 is represented by the straight line AB starting from an anode voltage equal to the total H.T. voltage to the stage (if there is no decoupling resistance). The angle of AB to the E_a axis is determined by the value of R_0, a large value being represented by a line of lower slope such as AB'. Maximum harmonic distortion for a fixed large input voltage is obtained when R_0 is small; the output voltage

wave shape is flattened at the high E_a end where the load line enters the cramped part of the I_aE_a characteristics and is peaked at the low E_a end. This type of wave is shown in Fig. 9.2*a* to contain mainly even harmonic (chiefly second) distortion. As R_0 is increased, the top end (low E_a) of AB leaves the region where the I_aE_a characteristics have opened out, and enters the lower current cramped region, where the intercepts with the constant grid voltage lines are smaller but more equal. Hence distortion progressively falls as R_0 is increased, and at the same time output voltage amplitude tends to increase. The maximum value of R_0 is fixed by the grid leak resistance of the succeeding valve (Section 9.3.3)

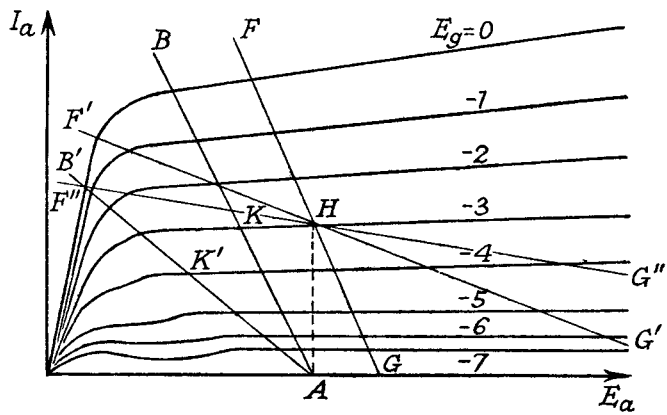

FIG. 9.8.—The Representation of Load Resistance on the I_aE_a Characteristics of a Tetrode Valve.

and also by high frequency considerations, because the larger R_0 is made the greater is attenuation and phase distortion due to stray capacitance. As pointed out in the previous section the rate of increase of amplification for a constant value of μ and R_a falls as R_0 is increased above R_a, and there is seldom any advantage in making the ratio of $\frac{R_0}{R_a}$ greater than 3 to 4.

The effect on harmonic distortion of varying R_0 is different in the case of the tetrode valve. Referring to the tetrode I_aE_a characteristic curves of Fig. 9.8, we see that a low load resistance (line AB) produces an output voltage wave which is flat at high E_a and peaked at low E_a values in a manner similar to that for low R_0 with a triode valve. Hence distortion consists mainly of even harmonics. As R_0 is increased the high E_a end of the output wave tends to become less flat and the low E_a end less peaked;

a value of R_0 is eventually reached when the output wave has both ends flattened to almost the same degree. The resulting symmetrically shaped wave, as shown in Fig. 9.2*b*, contains chiefly odd higher harmonics, and intermodulation products are produced if more than one frequency is present at the input. A further increase in R_0 flattens the low E_a part of the output wave, which now enters the very cramped " knee " of the characteristic, and opens out the opposite end. This results in the reappearance of even harmonics ; odd harmonics are also increased in amplitude. Reduced harmonic distortion and increased amplification are realized for high values of R_0 by increasing grid bias so as to bring the low E_a part of the output voltage away from the knee. For example, in Fig. 9.8, greater amplification with less distortion is obtained for R_0 corre-

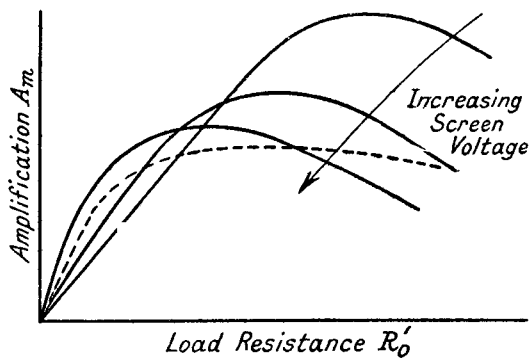

FIG. 9.9.—The Effect of Screen Voltage on the Amplification at Medium Frequencies of a Tetrode A.F. Amplifier with Resistance-Capacitance Coupling.

sponding to line AB' by increasing the bias from -3 to -4 volts (point K'). Thus we see that, unlike the triode, the tetrode has for maximum amplification an optimum bias, which increases with increase of R_0. If the bias voltage is fixed, an optimum value of R_0 is found for maximum amplification ; this optimum value depends on screen voltage and it increases as the latter is decreased. Usually there is an optimum screen voltage for maximum possible amplification, and Fig. 9.9 gives curves of amplification against R_0 for three values of screen voltage. For low values of R_0, expression 9.2*e* is applicable and maximum amplification is determined solely by g_m, the greater this is the greater is amplification, i.e., a high screen voltage is required. For high values of R_0 maximum amplification is determined by g_m and R_a, increase of both increasing amplification (expression 9.2*d*). Increase of screen voltage generally causes R_a to

fall and it falls at a greater rate than g_m increases. Hence greatest amplification is obtained with low screen voltages.

The optimum value of grid bias is often greater than that of a triode of similar g_m, and maximum permissible output voltage is obtained without the positive peak of the input voltage approaching close to the bias voltage at which grid current starts, i.e., it is the knee of the I_aE_a characteristics which limits input voltage rather than grid current. With triodes of high μ, optimum bias is the lowest consistent with zero grid current on peak signals, and the bias must be adjusted to be able to deal with the valve having the most negative start of grid current. This type of triode tends to show considerable variation of anode current cut-off from valve to valve, so that fairly large changes of amplification are likely to be experienced between valves.

Summarising, we may say that the triode is the better type of valve for audio frequency amplification because the harmonic distortion it produces can be made small and is, in any case, less objectionable than that from a tetrode. Attenuation distortion due to its greater input capacitance need not present a serious problem because the highest required frequency is 20,000 c.p.s.

9.3.3. The Grid Leak and its Effect on the Anode Load. The grid leak resistance R_g in Fig. 9.3 is only in parallel with R_0 as far as the A.C. load is concerned, so that if R_0' is very much less than R_0 we must represent this condition by two lines on the I_aE_a characteristics as described in Section 2.6, Part I. This is shown in Fig. 9.7 by the two lines AB and CD, the former is the D.C. load line corresponding to R_0, whilst the latter is the A.C. load line corresponding to $R_0' = \frac{R_0R_g}{R_0+R_g}$. The point K, the intersection between AB and CD for small A.C. grid voltages, is the intersection of the D.C. load line AB and the normal operating bias line. If, however, the A.C. grid voltage is large enough to take the anode current down to the curved part of the characteristics, the output wave is flattened, i.e., partially rectified, and the D.C. anode current is increased so that the A.C. operating line is centred at K' instead of at K. The chief effect of the difference between the A.C./D.C. load lines is that distortion is increased for large input signal voltages, and output voltage is decreased; it is important therefore to make the ratio A.C./D.C. load resistance as near unity as possible.

The maximum permissible value of R_g is determined by the succeeding valve. If it is a voltage amplifier, the safe limit is usually from 1 to 2 MΩ, whereas the limit may be as low as 0·1 MΩ for

a large power-output valve, if softness (Section 2.8.1, Part I) is to be avoided. A *RC* coupled amplifier stage connected to a large power-output valve cannot therefore be designed with a very high effective load resistance, for it is inadvisable to make the ratio of A.C./D.C. load (R_0'/R_0) less than about 0·8.

9.3.4. Self Bias for a *RC* Coupled Amplifier. A valve with an indirectly heated cathode can be made to provide its own grid bias voltage by inserting a resistance (R_k) between the cathode and H.T. negative line as in Fig. 9.3. The D.C. anode current component flowing through R_k produces a positive voltage between the cathode and H.T. negative, and since the grid leak is returned to H.T. negative it means that the grid is biased negatively with respect to the cathode. The cathode resistance R_k must be by-passed by a large capacitor C_k in order to prevent A.F. voltages being developed across R_k by the A.C. components of the anode current. A.C. voltages developed across this resistance are in opposition to the grid voltages producing them, and overall amplification may be seriously reduced. This can be seen by considering the applied grid voltage as increasing positively; this increases the anode current and the voltage across R_k, so that the net positive increase in grid-to-cathode voltage, the difference between the positive increase of the input voltage and the positive increase of cathode voltage, may therefore be quite small. The insertion of R_k without a by-pass capacitor is a form of current negative feedback (see Section 10.10.4).

The capacitor C_k clearly cannot be equally effective at all frequencies, and negative feedback occurs at the lower end of the frequency range due to an increase in its reactance. Its influence on the overall frequency response can be calculated as follows:

Neglecting the effect * of C_c and C_s, the output voltage (see Fig. 9.4*a*)

$$E_{g2} = \frac{\mu E_{gk} R_0'}{R_a + R_0' + Z_k} \quad . \quad . \quad . \quad . \quad 9.7a$$

where E_{gk} = net A.F. voltage input from grid to cathode.

$$R_0' = \frac{R_0 R_g}{R_0 + R_g}$$

Z_k = impedance of the self-bias circuit

but $E_{gk} = E_{g1} - E_k$

* C_s normally has little influence as its reactance is important only at frequencies where C_k has no effect. If C_c is small enough for its reactance to be greater than R_g over the frequency range affected by C_k, R_0' in expression 9.7*a* should be replaced by R_0.

where E_{g1} = input voltage from grid to earth (Fig. 9.3)
and E_k = voltage developed across Z_k.

but $$E_k = \frac{\mu E_{gk} Z_k}{R_a + R_0' + Z_k}$$

$$\therefore E_{gk} = \frac{E_{g1}(R_a + R_0' + Z_k)}{R_a + R_0' + Z_k(1+\mu)}$$

Replacing this in 9.7*a*

$$E_{g2} = \frac{\mu E_{g1} R_0'}{R_a + R_0' + Z_k(1+\mu)} \quad . \quad . \quad . \quad 9.7b.$$

Amplification with feedback $$= A_f = \frac{E_{g2}}{E_{g1}}$$

$$= \frac{\mu R_0'}{R_a + R_0' + Z_k(1+\mu)}.$$

Normal amplification without feedback $= A_m = \frac{\mu R_0'}{R_a + R_0'}$.

The ratio loss of amplification due to feedback is therefore

$$\frac{A_m}{A_f} = \left(1 + \frac{Z_k(1+\mu)}{R_a + R_0'}\right) \quad . \quad . \quad . \quad 9.8a.$$

Replacing Z_k in 9.8*a* by $\frac{R_k}{1 + jpC_kR_k}$, we have

$$\frac{A_m}{A_f} = 1 + \frac{R_k(1+\mu)}{(R_a + R_0')(1 + jpC_kR_k)}$$

$$= \frac{1 + \frac{R_k(1+\mu)}{R_a + R_0'} + jpC_kR_k}{1 + jpC_kR_k}$$

$$\left|\frac{A_m}{A_f}\right| = \sqrt{\frac{\left(1 + \frac{R_k(1+\mu)}{R_a + R_0'}\right)^2 + (pC_kR_k)^2}{1 + (pC_kR_k)^2}} \quad . \quad . \quad 9.8b$$

The loss in amplification (db.) is $-20 \log_{10} \left|\frac{A_m}{A_f}\right|$

$$= -10 \log_{10} \left[\frac{B^2 + x^2}{1 + x^2}\right] \quad . \quad . \quad . \quad 9.8c$$

where $$x = pC_kR_k = \frac{R_k}{X_k}$$

and $$B = 1 + \frac{R_k(1+\mu)}{R_a + R_0'}.$$

Expression 9.8*c* is plotted in Fig. 9.10 against x, i.e., $\frac{R_k}{X_k}$, to a

logarithmic scale for different values of B. As x increases, i.e., C_k becomes more effective as a by-pass, the loss of amplification decreases to zero, but when it decreases, the loss tends to the value which would be realized with $C_k = 0$.

This value depends on B and is given from 9.8*c* as

$$\text{loss} = -20 \log_{10} B = -20 \log_{10} \left[1 + \frac{1+\mu}{R_a + R_0'} . R_k\right] . \quad 9.8d.$$

For a particular value of R_k, the loss is increased when μ is increased, or R_a or R_0' decreased. Expression 9.8*d* for a pentode amplifier becomes $20 \log_{10} (1+g_m R_k)$, since $\mu \gg 1$ and $R_a \gg R_0'$.

The curves in Fig. 9.10 are generalized curves, and the frequency response may be determined by suitably locating (as for Figs. 9.5*a* and 9.5*b*) a logarithmic frequency scale beneath the x scale. We shall illustrate this by the following example.

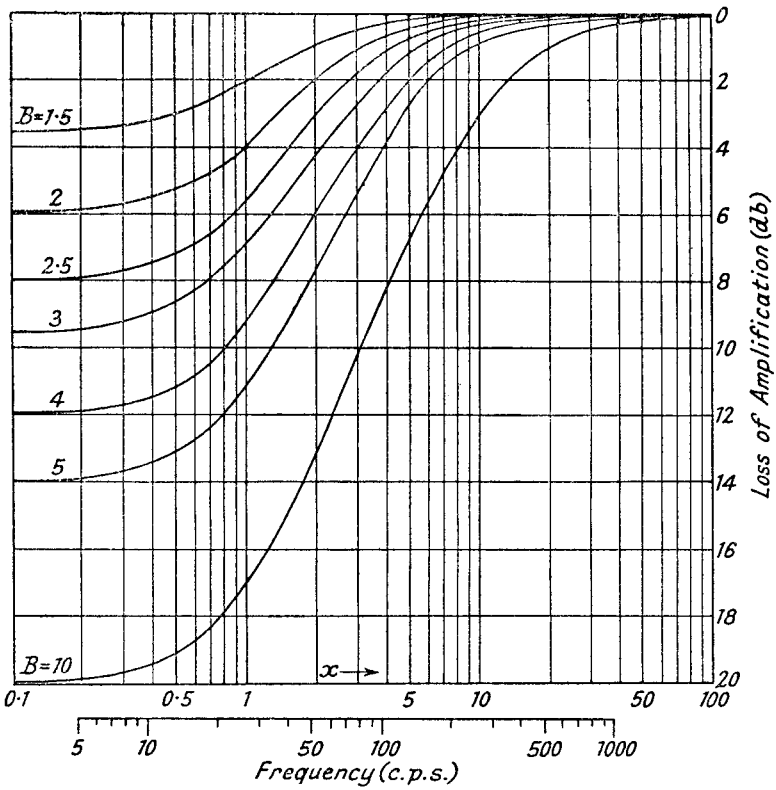

FIG. 9.10.—Generalised Curves for the Frequency Response of an A.F. Amplifier with Cathode Self Bias and Resistance-Capacitance Coupling.

$R_0 = 200{,}000\ \Omega$, $R_a = 50{,}000\ \Omega$, $R_g = 1\ \text{M}\Omega$, $\mu = 100$, $R_k = 3{,}000\ \Omega$, $C_k = 2\mu\text{F}$, $R_0' = 166{,}666\ \Omega$.

$$\frac{\mu+1}{R_a+R_0'} = \frac{101}{216{,}666} = 4{\cdot}65 \times 10^{-4}$$

$$B = 2{\cdot}395.$$

When $\frac{R_k}{X_k} = 1$, $f = \frac{10^6}{2\pi \times 2 \times 3{,}000} = 26{\cdot}5$ c.p.s.

The logarithmic frequency scale is adjusted beneath the x scale as in Fig. 9.10, so that 26.5 c.p.s. locates with $x = 1$, and the frequency response due to self bias is then read by interpolating between the $B = 2$ and $B = 2{\cdot}5$ curves. Thus at frequencies of 20 and 50 c.p.s. the loss is approximately $-6{\cdot}1$ and $-3{\cdot}0$ db. respectively.

The value of R_k required for any set of operating conditions is obtained by drawing the D.C. load line on the I_aE_a characteristic curves and estimating by inspection the bias voltage which gives maximum voltage output with minimum distortion. The locus of operation should be over that part of the load line which makes equal intercepts with lines of constant grid voltage difference; at the same time it must not be allowed to pass beyond the start of grid current. The ratio of the bias voltage, finally selected, to the anode current at the intersection of the load line with this bias voltage curve gives the required value of R_k. In many cases R_k will be a non-standard value and it is usual to select the nearest standard value. For a triode amplifier it is preferable to take the nearest lower standard value of R_k, since this reduces bias and takes the locus of operation further from the cramped low anode current region producing distortion. This does not necessarily apply to a pentode because cramping may occur at high as well as low anode current. The D.C. load line should be drawn for R_0+R_k, but R_k is so much less than R_0 that its effect may usually be neglected.

The total overall frequency response, including the effect of C_s and C_c, is obtained by adding the loss due to these two capacitances, as found from Figs. 9.5*a* and 9.5*b*, at the appropriate frequencies. Some error is introduced at the low frequencies due to the assumption in the above analysis that the reactance of C_c is small compared with R_g, but the effect will not usually be very serious and can be overcome by replacing R_0' by R_0 in the above expressions.

9.3.5. The Effect of the Screen Decoupling Circuit on the Frequency Response of a Tetrode Amplifier. The screen

decoupling circuit of a tetrode amplifier has a capacitance to earth acting as a by-pass for audio frequencies. A voltage in this circuit (see Fig. 9.11), due to variations in screen current produced by the input grid voltage, tends to reduce the gain of the amplifier. Since the reactance of this capacitance increases with decrease of frequency, the effect is greatest at lowest frequencies, and is similar to that due to the rising reactance of the self-bias capacitor. For calculating the reduction in frequency response we shall take the fundamental equations for screen and anode currents, which are as follows :

$$\Delta I_a = g_m \Delta E_g + g_s \Delta E_s + g_a \Delta E_a \quad . \quad . \quad . \quad 9.9$$

$$\Delta I_s = G_m \Delta E_g + G_s \Delta E_s + G_a \Delta E_a \quad . \quad . \quad 9.10$$

where $g_m = \frac{\partial I_a}{\partial E_g}$, $g_s = \frac{\partial I_a}{\partial E_s}$, $g_a = \frac{\partial I_a}{\partial E_a} = \frac{1}{R_a}$,

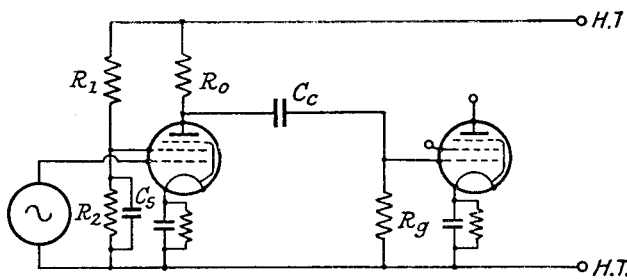

FIG. 9.11.—A Tetrode A.F. Amplifier with Resistance-Capacitance Coupling.

[*Note*: for C_s read C_s''.]

and G_m, G_s, G_a, are similar derivatives of I_s with respect to the voltages. The voltage changes ΔE_a and ΔE_s are those produced across the anode-cathode and screen-cathode circuit and, when they are caused by changes of I_a and I_s, are in such a direction as to oppose the current changes, i.e., increasing I_a and I_s causes a reduction in anode and screen voltage. Hence

$$\Delta E_a = -\Delta I_a Z_0 \quad . \quad . \quad . \quad . \quad 9.11.$$

$$\Delta E_s = -\Delta I_s Z_s' \quad . \quad . \quad . \quad . \quad 9.12$$

Z_s' is the total impedance of the external screen circuit, $\frac{R_s'}{1+jpC_s''R_s'}$.

where R_s' = the equivalent A.C. resistance component in the screen circuit, which may be made up of a potential divider for D.C. voltages consisting of two resistances R_1 and

R_2. These two resistances, in series for D.C., are in parallel as far as A.C. is concerned.

$$= \frac{R_1 R_2}{R_1 + R_2}.$$

C_s'' = the decoupling capacitance to earth in the screen circuit.

Combining 9.9, 9.10, 9.11 and 9.12.

$$\Delta I_a(1+g_a Z_0) = g_m \Delta E_g - g_s \Delta I_s Z_s'$$

$$\Delta I_s(1+G_s Z_s') = G_m \Delta E_g - G_a \Delta I_a Z_0$$

$$\Delta I_a(1+g_a Z_0) = g_m \Delta E_g - \frac{g_s Z_s'(G_m \Delta E_g - G_a \Delta I_a Z_0)}{1+G_s Z_s'}$$

$$\therefore \frac{\Delta I_a}{\Delta E_g} = \frac{g_m(1+G_s Z_s') - g_s G_m Z_s'}{(1+g_a Z_0)(1+G_s Z_s') - g_s G_a Z_0 Z_s'}$$

$$\text{Amplification } A = \frac{\Delta I_a Z_0}{\Delta E_g} = \frac{Z_0[g_m(1+G_s Z_s') - g_s G_m Z_s']}{(1+g_a Z_0)(1+G_s Z_s') - g_s G_a Z_0 Z_s'}. \quad 9.13.$$

When $Z_s' = 0$

$$A_0 = \frac{g_m Z_0}{1+g_a Z_0} = \frac{\mu Z_0}{R_a + Z_0}$$

$$\frac{A_0}{A} = \frac{1+Z_s'\left(G_s - \frac{g_s G_a Z_0}{1+g_a Z_0}\right)}{1+Z_s'\left(G_s - \frac{g_s G_m}{g_m}\right)} = \frac{1+jpC_s''R_s'+R_s'\left(G_s - \frac{g_s G_a Z_0}{1+g_a Z_0}\right)}{1+jpC_s''R_s'+R_s'\left(G_s - \frac{g_s G_m}{g_m}\right)}. \quad 9.14a.$$

If $Z_0 = R_0' = \frac{R_0 R_g}{R_0 + R_g}$.

$$\frac{A_0}{A} = \sqrt{\frac{B^2 + p^2 R_s'^2 C_s''^2}{D^2 + p^2 R_s'^2 C_s''^2}} \quad . \quad . \quad . \quad 9.14b$$

where $$B = 1+R_s'\left(G_s - \frac{g_s G_a R_0'}{1+g_a R_0'}\right)$$

and $$D = 1+R_s'\left(G_s - \frac{g_s G_m}{g_m}\right).$$

But $$\frac{G_m}{g_m} = \frac{\partial I_s}{\partial I_a} = \frac{G_s}{g_s} = \frac{G_a}{g_a}$$

so that $$B = 1+R_s' G_s\left(1 - \frac{g_a R_0'}{1+g_a R_0'}\right)$$

$$= 1+\frac{R_s' G_s}{1+g_a R_0'}$$

$$= 1+\frac{\frac{R_s'}{R_{sg}}}{1+\frac{R_0'}{R_a}} = 1+\frac{R_s'R_a}{R_{sg}(R_a+R_0')}$$

and $D = 1$

where $R_{sg} = \frac{1}{G_s} = \frac{\Delta E_s}{\Delta I_s}$ = slope of the E_sI_s characteristic.

If $R_0' \ll R_a$ then $B = 1+\frac{R_s'}{R_{sg}}$.

The loss of amplification is given by $-20\log_{10}\left|\frac{A_0}{A}\right|$

$$= -10\log_{10}\left[\frac{B^2+p^2C_s''^2R_s'^2}{1+p^2C_s''^2R_s'^2}\right] \quad . \quad 9.15a$$

$$= -10\log_{10}\left[\frac{B^2+x^2}{1+x^2}\right] \quad . \quad . \quad . \quad 9.15b$$

where $x = pC_s''R_s' = \frac{R_s'}{X_s'}$.

This expression is identical in form to that of expression 9.8*c* and the generalized curves of Fig. 9.10 may be used as long as we note that x is $\frac{R_s'}{X_s'}$ and $B = 1+\frac{R_s'R_a}{R_{sg}(R_a+R_0')}$. The loss tends to become asymptotic to a value $-10\log_{10}B^2$ as the frequency is decreased and X_s' increased.

Hence max. loss (db.) $= -20\log_{10}\left[1+\frac{R_s'R_a}{R_{sg}(R_a+R_0')}\right]$. 9.15*c*.

9.3.6. The Effect of the Anode Decoupling Circuit on the Frequency Response of an A.F. Amplifier. The reactance of the smoothing capacitance for the H.T. supply of a mains-operated receiver increases with decrease of frequency, and forms a common coupling impedance for the A.F. stages. (An 8-μF capacitor has a reactance of 398 Ω at 50 c.p.s.) Voltages may be produced in this reactance by low-frequency current components from the output stage ; other stages can likewise produce voltages, but their effect is much less important because current values are much smaller. These voltage components, if fed back to the grid of the output valve, or of a previous stage, via the preceding anode load connection to the H.T. supply, can either decrease or increase the overall A.F. response to the low frequencies. With *RC* coupling, the phase of the voltage is such as to cause low frequency degenera-

tion, if fed to the grid of the output valve, or regeneration if fed to the grid of the previous stage. For diode detection and one stage of A.F. amplification before the output valve (the A.F. amplifier grid circuit is not connected to the H.T. supply), the feedback is to the grid of the output valve only, and is degenerative. For two stages of A.F. amplification it is to the grid of the stage preceding the output valve as well, and the effect is predominantly regenerative. In extreme cases it may lead to low frequency oscillation (about 5 to 10 c.p.s.) known as " motorboating ".* Regenerative feedback can occur with one stage of *RC* coupled A.F. amplification if a cumulative-grid or anode-bend detector is employed, since the grid of the A.F. stage is then directly connected to the H.T. supply via the detector anode load resistance. For transformer-coupled A.F. stages

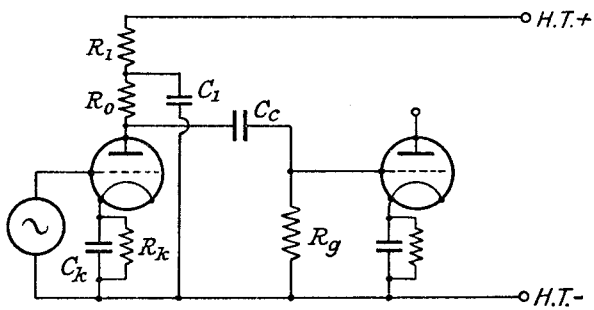

FIG. 9.12.—A Resistance-Capacitance Coupled A.F. Amplifier with an Anode Decoupling Circuit.

the phase of the feedback also depends on the sign of the mutual anductance coupling between the primary and secondary.

To reduce this form of feedback, a resistance-capacitance decoupling filter circuit is almost always included in the anode circuit of each A.F. amplifier as shown by R_1C_1 in the diagram of Fig. 9.12. A similar circuit is also included in all R.F. stages, but resistance and capacitance values are then much smaller, about 1,000 Ω and 0.1 μF as compared with 5,000 Ω and 2 μF for A.F. decoupling.

The inclusion of the decoupling circuit R_1C_1 affects the frequency response because it forms with R_0 the anode load impedance of the valve. It tends to raise the amplification at low frequencies. For example, the amplification at medium frequencies, where the reactances of C_c, C_k and C_1, can be neglected, is

* The circuit acts as a multivibrator or relaxation oscillator.

$$A_m = \frac{\mu R_g}{R_a+R_g} \cdot \frac{R_0}{\frac{R_a R_g}{R_a+R_g}+R_0}.$$

[Note that the alternative Thévenin development (see Appendix 3A) is more convenient and is used here.]

At low frequencies, assuming that the reactance of C_c is small and can be neglected,

$$A_l = \frac{\mu R_g}{R_a+R_g} \cdot \frac{R_0+\frac{R_1}{1+jpC_1R_1}}{\frac{R_a R_g}{R_a+R_g}+R_0+\frac{R_1}{1+jpC_1R_1}}.$$

Replacing $\frac{R_a R_g}{R_a+R_g}+R_0$ by R' we have

$$\frac{A_l}{A_m} = \frac{\frac{R_1}{R_0}+1+jpC_1R_1}{\frac{R_1}{R'}+1+jpC_1R_1} = \frac{\left(\frac{R'}{R_1+R'}\right)\left(\frac{R_1}{R_0}+1+jpC_1R_1\right)}{1+\frac{jpC_1R_1R'}{R_1+R'}}$$

or

$$\left|\frac{A_l}{A_m}\right| = \sqrt{\frac{\left(\frac{(R_1+R_0)R'}{(R_1+R')R_0}\right)^2+\left(\frac{pC_1R_1R'}{R_1+R'}\right)^2}{1+\left(\frac{pC_1R_1R'}{R_1+R'}\right)^2}} \quad . \quad . \quad 9.16a$$

$$= \sqrt{\frac{B^2+x^2}{1+x^2}} \quad . \quad . \quad . \quad . \quad . \quad . \quad 9.16b$$

where $B = \frac{(R_1+R_0)R'}{(R_1+R')R_0}$

and $x = \frac{R_1}{X_1} \cdot \frac{R'}{R_1+R'} = \frac{pC_1R_1R'}{R_1+R'}$,

i.e., low frequency increase in amplification is

$$+20 \log \left|\frac{A_l}{A_m}\right| = +10 \log \left(\frac{B^2+x^2}{1+x^2}\right) \text{ db.} \quad . \quad .9.16c.$$

Expression 9.16c is identical with 9.8c except for the sign, and the curves plotted in Fig. 9.10 can be used, but the vertical scale now represents a gain instead of a loss of amplification.

Since the decoupling circuit produces the opposite effect from that due to the self-bias capacitor, it is possible to choose values to cancel the loss of amplification due to the self-bias circuit. The conditions for exact compensation are that the values of x and the values of B for the two circuits should be equal. The former gives

$$C_kR_k = C_1R_1\frac{\dfrac{R_aR_g}{R_a+R_g}+R_0}{\dfrac{R_aR_g}{R_a+R_g}+R_0+R_1} \quad . \quad . \quad . \quad 9.17a$$

and this fixes the position of the horizontal frequency scale.

The second condition is fulfilled by making

$$1+\frac{R_k(1+\mu)}{R_a+\dfrac{R_0R_g}{R_0+R_g}} = \frac{(R_1+R_0)\left(\dfrac{R_aR_g}{R_a+R_g}+R_0\right)}{\left(R_1+R_0+\dfrac{R_aR_g}{R_a+R_g}\right)R_0} \quad . \quad . \quad 9.17b$$

and this ensures that the maximum loss for the cathode circuit is exactly equal to the maximum gain of the anode circuit. Generally it will not be possible to satisfy expression 9.17*b* unless R_0 is small compared with R_a and R_1. This method of compensation has been employed in the video-frequency amplifiers of television receivers (Section 16.8.3). It may also be used in tone-control circuits when increased amplification is required at low audio frequencies.

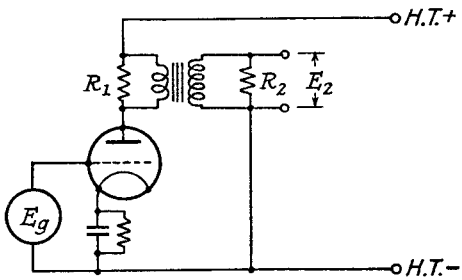

FIG. 9.13*a*.—A Transformer Coupled A.F. Amplifier.

9.4. The Transformer Coupled Amplifier.

Transformer coupling is shown in Fig. 9.13*a*. The resistances R_1 and R_2 may be included across the primary and secondary in order to improve the frequency response. R_1 reduces the increase of amplification at the medium frequencies caused by the increasing reactance of the primary inductance, whilst R_2 tends to flatten any peak in the high-frequency response due to resonance between the leakage inductance and stray capacitance across the secondary. The equivalent circuit of Fig. 9.13*b* indicates the separate impedances making up the transformer circuit, thus

C_{aE} = anode-earth capacitance of the valve
C_p = self-capacitance of primary of the transformer
R_{he} = resistance simulating the hysteresis and eddy current losses in the core
R_p = A.C. resistance of the primary winding, for all practical purposes this is the D.C. resistance of the primary winding

L_p = inductance of primary
C_w = interwinding capacitance
n = ratio of secondary to primary turns
M = mutual inductance between primary and secondary $= k\sqrt{L_p L_s}$
k = coupling coefficient
R_s = A.C. resistance of the secondary winding, approximately the D.C. resistance of the secondary winding
L_s = inductance of secondary
C_s = self-capacitance of secondary
C_g = input capacitance of the next stage
R_g = input resistance of the next stage.

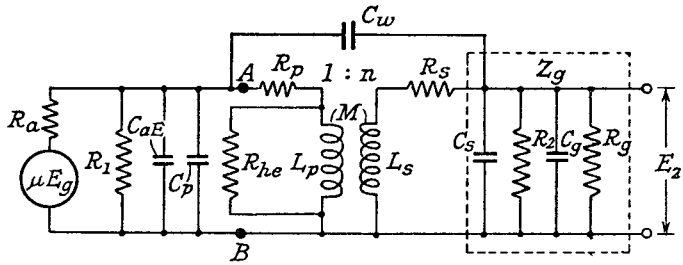

FIG. 9.13b.—The Equivalent Circuit for a Transformer Coupled A.F. Amplifier.

Generally C_{aE}, C_p, C_w and R_{he} have very small effects and will be neglected. For analysis it is convenient to transfer the secondary impedances to the primary side and include at the output a perfect

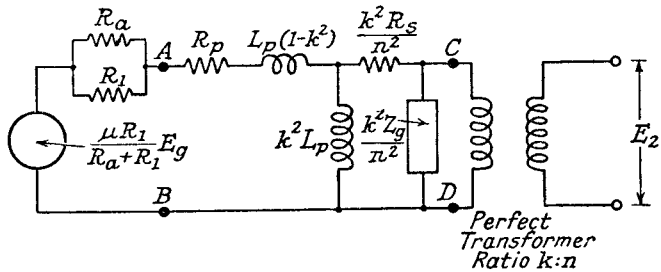

FIG. 9.13c.—A Simplified Diagram for a Transformer Coupled A.F. Amplifier.

transformer having a primary to secondary turns ratio of k to n. This is shown in Fig. 9.13c. That this circuit is equivalent to Fig. 9.13*b* can be proved by noting from Section 7.6 (Part I) that the impedance reflected from the secondary into the primary in

series with R_p and L_p is $\frac{p^2M^2}{R_s+jpL_s+Z_g}$; where Z_g is the impedance of C_s, R_2, R_g and C_g in parallel. Hence the total impedance across points AB in Fig. 9.13*b* is (neglecting C_{aE}, C_p, C_w, and R_{he})

$$Z_{AB} = R_p+jpL_p+\frac{p^2M^2}{R_s+jpL_s+Z_g} \quad . \quad . \quad . \quad 9.18.$$

The impedance across the same points AB in Fig. 9.13*c* is

$$Z_{AB} = R_p+jpL_p(1-k^2)+\frac{jpL_pk^2.\frac{(R_s+Z_g)k^2}{n^2}}{jpL_pk^2+\frac{(R_s+Z_g)k^2}{n^2}}$$

$$= R_p+jpL_p+\frac{p^2L_p{}^2k^2n^2}{n^2jpL_p+(R_s+Z_g)}$$

but $k = \frac{M}{\sqrt{L_pL_s}}$, and $n = \sqrt{\frac{L_s}{L_p}}$

$$\therefore Z_{AB} = R_p+jpL_p+\frac{p^2M^2}{R_s+jpL_s+Z_g}$$

which is identical with 9.18.

From Section 7.3 (Part I) the secondary voltage developed across Z_g in Fig. 9.13*b* is (neglecting C_{aE}, C_p, C_w and R_{he}),

$$E_2 = \frac{Z_3Z_5E}{Z_3(Z_4+Z_5)+Z_2(Z_3+Z_4+Z_5)} = \frac{Z_3Z_5E}{(Z_2+Z_3)(Z_3+Z_4+Z_5)-Z_3{}^2}$$

where $E = E_{AB}$, $Z_2 = R_p+jp(L_p-M)$, $Z_3 = jpM$,

$$Z_4 = R_s+jp(L_s-M), \text{ and } Z_5 = Z_g.$$

$$\therefore E_2 = \frac{jpM.Z_g.E_{AB}}{(R_p+jpL_p)(R_s+jpL_s+Z_g)+p^2M^2} \quad . \quad . \quad 9.19a.$$

The secondary voltage, from Fig. 9.13*c*, is

$$E_2 = \frac{n}{k}E_{CD} = \frac{n}{k}.\frac{Z_g}{R_s+Z_g}.\frac{jk^2pL_p(R_s+Z_g)\frac{k^2}{n^2}E_{AB}}{\left[jk^2pL_p+(R_s+Z_g)\frac{k^2}{n^2}\right]Z_{AB}}$$

$$= \frac{jknpL_pZ_gE_{AB}}{(jpL_s+R_s+Z_g)Z_{AB}} \quad . \quad . \quad . \quad . \quad 9.19b.$$

Replacing Z_{AB} in the above by 9.18 and noting that $knpL_p = pM$

$$E_2 = \frac{jpMZ_gE_{AB}}{(R_p+jpL_p)(R_s+Z_g+jpL_s)+p^2M^2}.$$

Expression 9.19*b* is therefore identical to 9.19*a*, so that Fig. 9.13*c* is the correct equivalent of Fig. 9.13*b*.

A further simplification is possible since k in a well-designed transformer is very nearly unity, and it may be assumed such in all cases except in the term for the leakage inductance $L_p(1 - k^2)$. In any practical case all the transformer circuit constants can be measured by suitable D.C. and A.C. bridge methods. Thus the primary and secondary winding resistances R_p and R_s can be measured with D.C., and the primary inductance L_p can be measured on a suitable A.C. bridge by noting the inductance across the primary terminals. If the transformer is directly coupled to the anode of a valve, L_p should be measured with the rated D.C. current flowing in the primary, or a commensurate D.C. current in the secondary when this is more convenient. The leakage inductance $L_p(1 - k^2)$ is the inductance across the primary terminals when the secondary is short-circuited.

The frequency response and amplification of a transformer stage is best calculated by dividing the pass range into three frequency bands, as was done for the *RC* coupled stage.

For the medium frequencies, leakage and primary inductance in Fig. 9.13*c* can be neglected, and Z_g may be replaced by R_{2t}, which has a value of $\frac{R_g R_2}{R_g + R_2}$, because the reactance of C_s and C_g is negligible.

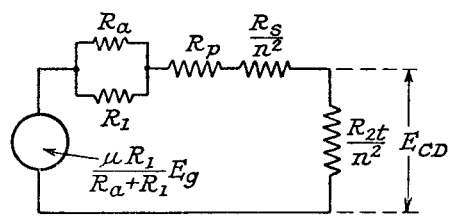

FIG. 9.14*a*.—The Transformer Coupled A.F. Amplifier at Medium Frequencies.

The equivalent circuit is shown in Fig. 9.14*a*, the valve-generated voltage, slope resistance and primary shunt resistance R_1 being converted according to Thévenin's Theorem (Appendix 3A). The amplification is

$$A_m = \frac{E_2}{E_g} = \frac{nE_{CD}}{E_g}$$

$$= \frac{n\mu R_1}{R_a + R_1} \cdot \frac{\frac{R_{2t}}{n^2}}{\frac{R_a R_1}{R_a + R_1} + R_p + \frac{R_s + R_{2t}}{n^2}} \quad . \quad . \quad 9.20a.$$

Rewriting the above in terms of maximum possible amplification, $\frac{n\mu R_1}{R_a+R_1}$,

$$\frac{A_m}{n\mu'} = \frac{1}{1+\frac{R_a'+\frac{R_s}{n^2}}{\frac{R_{2t}}{n^2}}} \quad . \quad . \quad . \quad 9.20b$$

where $\mu' = \frac{\mu R_1}{R_a+R_1}$, and $R_a' = \frac{R_a R_1}{R_a+R_1}+R_p$.

The similarity between expressions 9.20*b* and 9.2*c* can be noted and Fig. 9.6 is applicable when $n\mu'$ replaces μ. An important point is that maximum A_m is realized when R_1 and $\frac{R_{2t}}{n^2}$ are infinite. From the point of view of maximum amplification it is preferable to dispense with them. They also reduce the anode load impedance and therefore tend to increase distortion; their inclusion is only

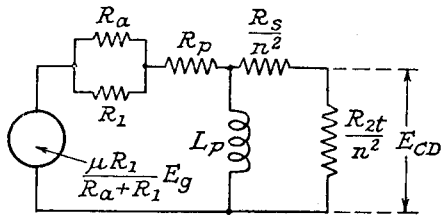

FIG. 9.14*b*.—The Transformer Coupled A.F. Amplifier at Low Frequencies.

justified for the purpose of improving low- and high-frequency response.

At low frequencies the reactance of the leakage inductance and secondary capacitance can be neglected, but L_p must be taken into account as its reactance is comparable with $\frac{R_s+R_{2t}}{n^2}$, with which it is in parallel. The equivalent circuit is that of Fig. 9.14*b*. Low-frequency amplification is

$$A_l = \frac{E_2}{E_g} = \frac{nE_{CD}}{E_g}$$

$$= \frac{n\mu' \frac{R_{2t}}{n^2} jpL_p}{R_a'\left(jpL_p+\frac{R_s+R_{2t}}{n^2}\right)+jpL_p\left(\frac{R_s+R_{2t}}{n^2}\right)} \quad . \quad . \quad . \quad 9.21a$$

$$= \frac{n\mu' \frac{R_{2t}}{n^2} jpL_p}{\left(R_a' + \frac{R_s + R_{2t}}{n^2}\right) jpL_p + R_a' \left(\frac{R_s + R_{2t}}{n^2}\right)}$$

$$= \frac{n\mu' \frac{R_{2t}}{n^2}}{\left(R_a' + \frac{R_s + R_{2t}}{n^2}\right)\left(1 + \frac{\frac{R_a'(R_s + R_{2t})}{n^2}}{\left(R_a' + \frac{R_s + R_{2t}}{n^2}\right) jpL_p}\right)} \quad . \quad 9.21b$$

$$= \frac{A_m}{1 + \frac{R_l}{jX_l}} \quad . \quad . \quad . \quad . \quad . \quad . \quad . \quad . \quad 9.21c$$

where R_l = resistance of R_a' and $\frac{R_s + R_{2t}}{n^2}$ in parallel and $X_l = pL_p$.

Hence $$\left|\frac{A_m}{A_l}\right| = \sqrt{1 + \left(\frac{R_l}{X_l}\right)^2} = \sqrt{1 + \frac{1}{x^2}} \quad . \quad . \quad 9.22a$$

where $x = \frac{X_l}{R_l}$.

The loss of amplification at low frequencies in decibels is

$$-20 \log_{10} \left|\frac{A_m}{A_l}\right| = -10 \log_{10} \left(1 + \left(\frac{R_l}{X_l}\right)^2\right)$$

$$= -10 \log_{10} \left(1 + \frac{1}{x^2}\right) \quad . \quad . \quad . \quad 9.22b,$$

and a universal curve of loss against x, i.e. $\frac{X_l}{R_l}$, to a logarithmic scale is identical with that of Fig. 9.5*a*. The same method is employed for finding the frequency response for particular values of X_l and R_l as was adopted for the *RC* coupling, viz., a logarithmic frequency scale is located so that $f = \frac{R_l}{2\pi L_p}$ is immediately below $x = 1$ in Fig. 9.5*a*. From this curve we note that the low-frequency response is best when R_l is small, i.e., when R_a' or $\frac{R_s + R_{2t}}{n^2}$, or both are small. Since for maximum A_m and minimum distortion R_l should be greater than R_a, this leads directly to the conclusion that a low R_a valve should be used. A disadvantage possessed by this type of valve is that it usually requires a high I_a, and this increases transformer core saturation and reduces L_p. The use of

a *RC* coupling to the transformer, as described in Section 9.5, offers a solution to this difficulty.

The equivalent circuit for the high-frequency range is shown

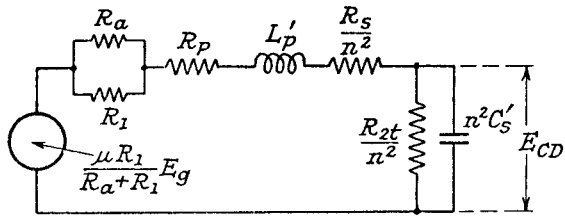

FIG. 9.14c.—The Transformer Coupled Amplifier at High Frequencies.

in Fig. 9.14c. The primary inductive reactance has little effect, but the leakage inductance and total stray capacitance C_s' across the secondary now have considerable influence. The amplification is

$$A_h = \frac{\dfrac{n\mu'\dfrac{R_{2t}}{n^2}}{1+jpC_s'R_{2t}}}{R_a'+\dfrac{R_s}{n^2}+jpL_p'+\dfrac{\dfrac{R_{2t}}{n^2}}{1+jpC_s'R_{2t}}}$$

where $L_p' = L_p(1-k^2)$

$$= \frac{n\mu'\dfrac{R_{2t}}{n^2}}{\left(R_a'+\dfrac{R_s}{n^2}+jpL_p'\right)(1+jpC_s'R_{2t})+\dfrac{R_{2t}}{n^2}}$$

$$A_h = \frac{n\mu'}{1+\dfrac{R_a'+\dfrac{R_s}{n^2}}{\dfrac{R_{2t}}{n^2}}-p^2L_p'C_s'n^2+jp\left(C_s'n^2\left(R_a'+\dfrac{R_s}{n^2}\right)+\dfrac{L_p'}{\dfrac{R_{2t}}{n^2}}\right)} \quad . \quad 9.23a.$$

Let $p_0 = \dfrac{1}{\sqrt{L_p'C_s'n^2}}$, the resonant pulsance of L_p' and n^2C_s' and

$$X_0 = p_0L_p' = \frac{1}{p_0C_s'n^2}$$

then $$A_h = \frac{n\mu'}{1+\dfrac{R_a'+\dfrac{R_s}{n^2}}{\dfrac{R_{2t}}{n^2}}-\left(\dfrac{p}{p_0}\right)^2+j\dfrac{p}{p_0}\left[\dfrac{R_a'+\dfrac{R_s}{n^2}}{X_0}+\dfrac{X_0}{\dfrac{R_{2t}}{n^2}}\right]}$$

$$= \frac{A_m\left(1+\dfrac{R_a'+\dfrac{R_s}{n^2}}{\dfrac{R_{2t}}{n^2}}\right)}{1+\dfrac{R_a'+\dfrac{R_s}{n^2}}{\dfrac{R_{2t}}{n^2}} - \left(\frac{p}{p_0}\right)^2 + j\frac{p}{p_0}\left[\dfrac{R_a'+\dfrac{R_s}{n^2}}{X_0}+\dfrac{\dfrac{X_0}{R_{2t}}}{n^2}\right]} \quad . \quad 9.23b.$$

Owing to the series resonance of L_p' and C_s' there may be a gain or a loss at f_0, and it is preferable to express the response as

$$\text{Amplification} = 20 \log_{10}\left|\frac{A_h}{A_m}\right|$$

$$= 10 \log_{10} \frac{\left(1+\dfrac{R_a'+\dfrac{R_s}{n^2}}{\dfrac{R_{2t}}{n^2}}\right)^2}{\left[1+\dfrac{R'_a+\dfrac{R_s}{n^2}}{\dfrac{R_{2t}}{n^2}} - \left(\frac{f}{f_0}\right)^2\right]^2 + \left[\frac{f}{f_0}\left(\dfrac{R_a'+\dfrac{R_s}{n^2}}{X_0}+\dfrac{\dfrac{X_0}{R_{2t}}}{n^2}\right)\right]^2} \quad 9.24.$$

When expression 9.24 has a positive sign an increase in amplification is obtained at high frequencies, whereas if it has a negative sign there is loss of amplification relative to the medium frequency amplification.

It is difficult to produce a series of generalized curves from expression 9.24 because there are three independent variables $\frac{f}{f_0}$; $\dfrac{R_a'+\dfrac{R_s}{n^2}}{X_0}$ and $\dfrac{\dfrac{X_0}{R_{2t}}}{n^2}$. The amplification (or loss) when $f = f_0$ is, however, a valuable guide to the high frequency response, and Klipsch [4] has suggested a convenient method of graphing 9.24 when $f = f_0$. He joins points of $\dfrac{R_a'+\dfrac{R_s}{n^2}}{X_0}$ and $\dfrac{\dfrac{X_0}{R_{2t}}}{n^2}$, giving constant loss (−) and amplification (+), as illustrated by the full line curves in Fig. 9.15. For convenience, both parameters are plotted to a tangent scale, e.g., $\dfrac{R_a'+\dfrac{R_s}{n^2}}{X_0} = 1 = \tan y$ gives $y = 45°$, and $\dfrac{R_a'+\dfrac{R_s}{n^2}}{X_0} = \infty$ gives

$y = 90°$. Hence the first point is half-way between 0 and ∞. It is important to note that f_0 is not the frequency of maximum amplification, which is determined by the ratio of the two parameters, $\dfrac{\dfrac{R_{2t}}{n^2}}{R_a' + \dfrac{R_s}{n_2}}$ and always occurs at a frequency lower than f_0. The dotted-line curves in Fig. 9.15 join points of constant ratio $\dfrac{\dfrac{R_{2t}}{n^2}}{R_a' + \dfrac{R_s}{n^2}}$.

The latter also governs the general shape of the high-frequency response; a low ratio means that the frequency for maximum

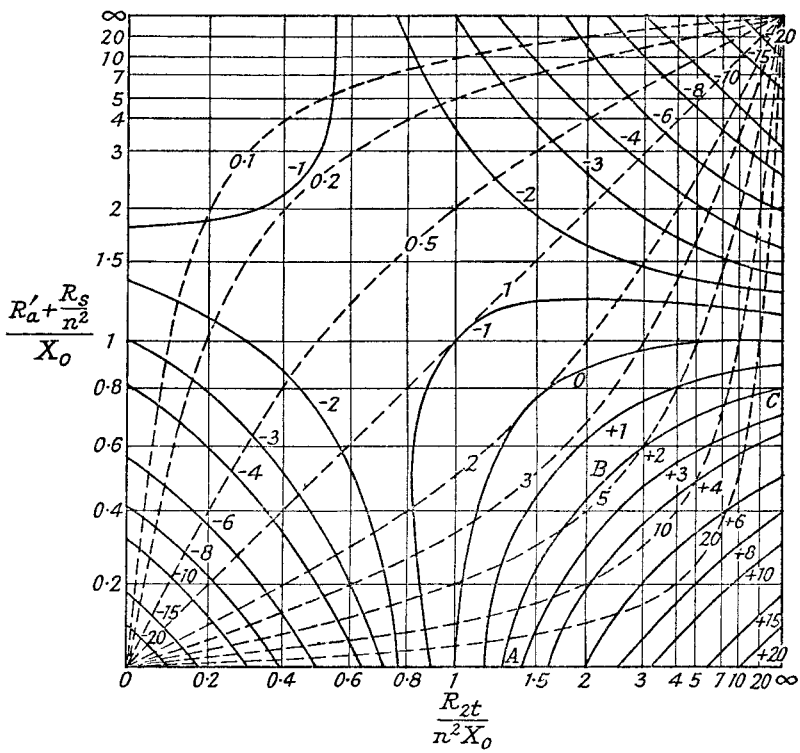

FIG. 9.15.—Loss or Gain in Frequency Response of a Transformer Coupled A.F. Amplifier at the Resonant Frequency of Leakage Inductance and Secondary Stray Capacitance.

Full Lines: Loss (−) or Gain (+) of Amplification (db.).

Dashed Lines: Constant Ratios of $\dfrac{\dfrac{R_{2t}}{n^2}}{R_a' + \dfrac{R_s}{n^2}}$.

amplification is close to f_0, maximum amplification is very little greater than amplification at f_0, and cut-off above f_0 is not rapid; i.e., the response is generally flat. The converse is also true; a high ratio of $\dfrac{\dfrac{R_{2t}}{n^2}}{R_a'+\dfrac{R_s}{n^2}}$ means a more peaked high frequency response with sharper cut-off. This is to be expected since $R_a'+\dfrac{R_s}{n^2}$ is the series resistance element in the series resonant circuit, while $\dfrac{R_{2t}}{n^2}$ is a parallel resistance element.

To illustrate the use of the curves we shall find values of R_1 and R_{2t} to give an amplification of +2 db. at f_0 and a loss not exceeding − 2 db. at 50 c.p.s., when the transformer and valve characteristics are as follows:

$L_p = 100$ H, $R_p = 500\ \Omega$, $R_s = 5000\ \Omega$, $n = 3$, $L_p' = 0{\cdot}3$ H, $f_0 = 8$ kc/s, $\mu = 30$, $R_a = 10{,}000\ \Omega$.

Low frequency response; since $R_a' = R_p + \dfrac{R_a R_1}{R_a + R_1}$, R_a' cannot exceed the value for $R_1 = \infty$, i.e., 10,500 Ω. Hence R_l in expression 9.22*b*, which consists of R_a', and $\dfrac{R_s + R_{2t}}{n^2}$ in parallel, must be less than 10,500 Ω. Now $X_l = 2\pi \times 50 \times 100 = 31{,}400\ \Omega$, and if we take the maximum possible value of R_l, we have $\dfrac{X_l}{R_l} = \dfrac{31{,}400}{10{,}500} = 3$. From Fig. 9.5*a* we find the loss for $x = 3$ as − 0·5 db., and this is the maximum possible. Hence, whatever value of R_l is fixed by high-frequency response, the loss at 50 c.p.s. will always be less than − 0·5 db. High-frequency response; the curve for +2 db. gain is *ABC* in Fig. 9.15 and any values of $\dfrac{R_a' + \dfrac{R_s}{n^2}}{X_0}$ and $\dfrac{R_{2t}}{n^2 X_0}$ lying on this curve satisfy the amplification requirement at f_0. Since the most level high-frequency response may be considered as desirable, we need to choose the lowest ratio value of $\dfrac{\dfrac{R_{2t}}{n^2}}{R_a' + \dfrac{R_s}{n^2}}$. This, from Fig. 9.15, is seen to be about 4.6 and we will

select 5. The latter intersects ABC at two points, $\frac{R_{2t}}{n^2X_0} = 3$ and 1·7 and $\frac{R_a'+\frac{R_s}{n^2}}{X_0} = 0{\cdot}6$ and 0·34. Both the ratios for $\frac{R_a'+\frac{R_s}{n^2}}{X_0}$ are possible since the maximum value of $R_a'+\frac{R_s}{n^2}$ is $10{,}500+555 = 11{,}055\ \Omega$, $X_0 = 2\pi \times 8{,}000 \times 0{\cdot}3 = 15{,}080\ \Omega$ and $\frac{R_a'+\frac{R_s}{n^2}}{X_0}$ must not therefore exceed 0·738. For maximum medium frequency amplification R_a' and $\frac{R_{2t}}{n^2}$ require to be as high as possible. We will therefore choose $\frac{R_{2t}}{n^2X_0} = 3$ and $\frac{R_a'+\frac{R_s}{n^2}}{X_0} = 0{\cdot}6$. This gives

$$R_{2t} = 3n^2X_0 = 27 \times 15{,}080 = 407{,}000\ \Omega$$

$$R_a'+\frac{R_s}{n^2} = 0{\cdot}6X_0 = 9050\ \Omega$$

$$R_a' = 8{,}495\ \Omega = R_p+\frac{R_aR_1}{R_a+R_1}$$

$$\therefore\ R_1 = 39{,}800\ \Omega.$$

Amplification at the medium frequencies is

$$A_m = \frac{n\mu R_1}{(R_a+R_1)\left(1+\frac{R_a'+\frac{R_s}{n^2}}{\frac{R_{2t}}{n^2}}\right)}$$

$$= 59{\cdot}9.$$

Thus values for R_1 and R_{2t} of 39,800 Ω and 0·407 MΩ satisfy the frequency response requirements with the particular valve and transformer constants given, and amplification at medium frequencies is 59·9.

9.5. The *RC* Coupled Transformer Amplifier. Considerable advantages are gained if the D.C. anode current component is by-passed from the transformer primary. Core material of high permeability may be used and the size of transformer for a given primary inductance reduced. This leads to a lower leakage inductance and secondary capacitance, with consequent improvement in

high-frequency response. A resistance or L.F. choke may be employed to carry the D.C. current component, the former is preferable on account of cost, saving of space and absence of iron, which may cause distortion or pick-up hum. Slightly less amplification is generally obtained from the resistance because of the lower D.C. anode voltage and consequently lower μ and higher R_a.

In the typical circuit of Fig. 9.16, the transformer is shown with separated primary and secondary, but auto-transformer action with increased amplification can be obtained by connecting the earthed end of the secondary, point B, to the anode end of the primary, point A. The formulæ developed in Section 9.4 for high and medium frequency response are unaffected by the coupling capacitance C_c, since at these frequencies its reactance is negligible in comparison

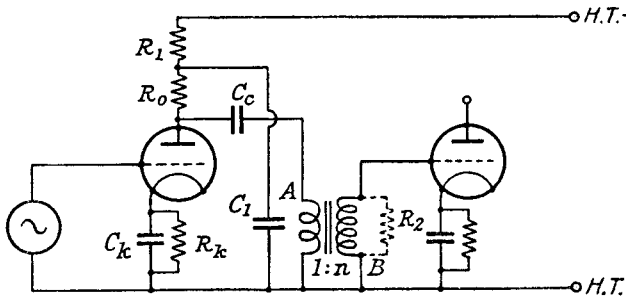

FIG. 9.16.—The *RC* Transformer Coupled A.F. Amplifier.

with other components. At low frequencies the reactance of C_c may become comparable with X_{L_p} and the amplification in expression 9.21*b* is modified by replacing R_a' by $R_a'+\frac{1}{jpC_c}$ to

$$A_l=\frac{n\mu'\frac{R_{2t}}{n^2}}{\left[R_a'+\frac{1}{jpC_c}+\frac{R_s+R_{2t}}{n^2}\right]\left[1+\frac{\left(R_a'+\frac{1}{jpC_c}\right)\left(\frac{R_s+R_{2t}}{n^2}\right)}{\left(R_a'+\frac{1}{jpC_c}+\frac{R_s+R_{2t}}{n^2}\right)jpL_p}\right]}$$

$$=\frac{n\mu'\frac{R_{2t}}{n^2}}{R_a'+\frac{R_s+R_{2t}}{n^2}-\frac{R_s+R_{2t}}{n^2}\left(\frac{p_0'}{p}\right)^2-j\left[\frac{X_0'p_0'}{p}+\frac{R_a'(R_s+R_{2t})}{n^2X_0'}\frac{p_0'}{p}\right]}$$

where $p_0' = \dfrac{1}{\sqrt{L_p C_c}}$ and $X_0' = p_0' L_p = \dfrac{1}{p_0' C_c}$

$$\frac{A_l}{A_m} = \frac{R_a' + \dfrac{R_s + R_{2t}}{n^2}}{R_a' + \dfrac{R_s + R_{2t}}{n^2} - \dfrac{R_s + R_{2t}}{n^2}\left(\dfrac{p_0'}{p}\right)^2 - j\dfrac{p_0'}{p}\left[X_0' + \dfrac{R_a'(R_s + R_{2t})}{n^2 X_0'}\right]}.$$

The gain (+) or loss (−) in decibels relative to A_m is

$$20 \log_{10} \left| \frac{A_l}{A_m} \right|$$

$$= 10 \log_{10} \frac{\left[1 + \dfrac{n^2 R_a'}{R_s + R_{2t}}\right]^2}{\left[1 + \dfrac{n^2 R_a'}{R_s + R_{2t}} - \left(\dfrac{f_0'}{f}\right)^2\right]^2 + \left[\dfrac{f_0'}{f}\left(\dfrac{X_0' n^2}{R_s + R_{2t}} + \dfrac{R_a'}{X_0'}\right)\right]^2}. \qquad 9.25.$$

The above expression is seen to be similar in form to that of expression 9.24, and Fig. 9.15 may be used for calculating the loss or gain at the low frequency f_0' by considering the vertical axis as scaled in terms of $\dfrac{R_a'}{X_0'}$, and the horizontal in terms of $\dfrac{R_s + R_{2t}}{n^2 X_0'}$.

The values of R_0 and R_2 for a particular low- and high-frequency response at f_0' and f_0 can be obtained as follows: Suppose both high- and low-frequency responses at f_0 and f_0' are required to be +2 db. above the amplification at medium frequencies; curve ABC in Fig. 9.15 gives pairs of values of $\dfrac{R_a' + \dfrac{R_s}{n^2}}{X_0}$ and $\dfrac{R_{2t}}{n^2 X_0}$, satisfying the high-frequency response requirement. Pairs of values of $\dfrac{R_a'}{X_0'}$ and $\dfrac{R_s + R_{2t}}{n^2 X_0'}$ corresponding to the high-frequency response pairs are calculated and plotted on a separate transparent sheet scaled according to a tangent law in the same manner as Fig. 9.15. This curve now represents values of $\dfrac{R_a'}{X_0'}$ and $\dfrac{R_s + R_{2t}}{n^2 X_0'}$, which satisfy the high-frequency response condition of +2 db., and it is placed on top of Fig. 9.15. The point of intersection of the first curve on the transparent sheet with the + 2 db. curve ABC gives values of R_a' and $\dfrac{R_s + R_2}{n^2}$, which satisfy both high- and low-frequency response simultaneously. If the curve does not intersect ABC the chosen

values of response cannot be realized. A compromise is, however, usually possible giving responses within 1 db. of those required.

It should be noted that there is an upper limit to the value of R_0 because it carries the D.C. anode current component, and it is generally inadvisable to exceed about $3R_a$. $R_a' = \frac{R_a R_0}{R_a + R_0} + R_p$ must be made up bearing this limitation in mind.

9.6. Tone Control Circuits.

9.6.1. Introduction.[1, 8] Usually an A.F. amplifier is designed to have as little attenuation distortion as possible, but there are occasions when control of frequency response is desirable, and tone control circuits are then included to allow variation of amplification at the high and at the low frequencies as compared with the medium frequencies.

High-frequency attenuation is useful when interference, due either to an adjacent frequency transmission or to noise, is experienced. It is also advantageous for suppressing needle scratch from gramophone records. Noise interference may be caused by atmospherics or by electrical apparatus connected to the mains supply wiring. Reproduction is characterized by a mellow tone, which becomes muffled if attenuation is severe. High-frequency intensification is of service, when receiving a powerful local station, in compensating for loss of the high-frequency sidebands due to the selectivity of the R.F. and I.F. tuned circuits. An average broadcast receiver often attenuates severely modulation sideband frequencies exceeding 3 kc/s, and reproduction from the higher pitch instruments in an orchestral programme may lose its character or be absent from the output unless there is discrimination by the A.F. amplifier in favour of the high frequencies. Reproduction with marked high-frequency intensification is usually described as brilliant.

Low-frequency attenuation is often helpful in combating the tendency to muffled reproduction when severe high-frequency attenuation is necessary to eliminate interference. Low-frequency intensification relative to other frequencies leads to more balanced reproduction as volume is reduced. The characteristics of the average ear are such that a general reduction in the levels of all frequencies appears to reduce the output of lower frequencies (50 to 200 c.p.s.) to a much greater extent than the medium frequencies (1,000 to 3,000 c.p.s.). Thus for an output volume of about 6 dynes/sq. cm.[6] (intensity level of 90 db.) at each frequency (this corresponds to a very loud radio receiver output) balanced

reproduction is obtained and all frequencies appear of very nearly equal loudness, whereas for an output volume of 0·02 dynes/sq. cm. (intensity level 40 db.), frequencies below 100 c.p.s. are not heard, i.e., the output is below the threshold of audibility ; at 1,000 c.p.s. the output appears to be 40 db. louder than at 100 c.p.s. For this same intensity level, viz., 40 db., there is a progressive decrease in loudness level as the frequency is increased above 2,000 c.p.s. Owing to limitations on needle movement, the low-frequency components in gramophone recordings are attenuated (about 15 db.) and low-frequency intensification in the A.F. amplifier can be used to compensate for this. It is also an aid in mitigating the effect of inadequate output transformer primary inductance and loudspeaker baffle area, but care must then be exercised to prevent overloading of the output stage.

For certain purposes it may be necessary to amplify or suppress a comparatively narrow band of audio frequencies ; e.g., telegraphic communication generally calls for a very narrow pass range (about ± 50 c.p.s.) in the neighbourhood of 1,000 c.p.s. This band-pass characteristic is secured by the use of tuned circuits in the A.F. amplifier. Similar circuits arranged to perform the opposite function are occasionally employed to suppress heterodyne interference from an adjacent transmission, and needle scratch in gramophone reproduction.

9.6.2. Types of Tone Control Circuits.[10] Tone control circuits require the use of reactances in order to obtain variable frequency response, and almost always involve a reduction in the general level of amplification. A valve associated with these circuits should not, therefore, be primarily intended as an amplifier but should be considered as a tone controller, the desired A.F. amplification being obtained in other stages. Parallel or series resonant circuits, except for special purposes, are undesirable unless they are heavily damped. If in a parallel circuit of R, L and C, the parallel resistance R is $> \frac{1}{2}\sqrt{\frac{L}{C}}$, damped oscillations may be set up by shock excitation from transients in the A.F. signal. In practice, owing to the series resistance of L, it is found that as long as $R < \sqrt{\frac{L}{C}}$,[7] reproduction is not seriously impaired by " hangover " or " ringing ". When tuned circuits are employed, the parallel resonant type is to be preferred to the series ; the latter has a reduced impedance at resonance, thus tending to cause amplitude distortion in its associated triode valve anode circuit. A tetrode

valve has an optimum anode load impedance, and amplitude distortion increases for impedances greater or less than this value, so that series or parallel circuits produce much the same effect.

Tone control circuits depending on variation of anode load impedance, as distinct from the potential divider type, are less effective in the anode circuit of a triode than of a tetrode, because the former has a much lower slope resistance. In all types it is preferable to use capacitance rather than inductance elements. The inductance element is, as a rule, more costly, has a much higher resistance component, is liable to pick up hum and interference voltages, and has stray capacitance.

Control of tone may be in steps, by variation of the reactance element, or it may be continuously variable, the resistance element being adjustable. In some cases [9] the A.F. signal voltage may be passed to three separate amplifiers. One amplifies all frequencies equally, the second contains a low-pass filter which accepts only the low frequencies (below about 250 c.p.s.), and the third uses a high-pass filter to accept the high frequencies (above 2,000 c.p.s.). The outputs of the three amplifiers may be combined in a single loudspeaker, or may be fed to separate loudspeakers specially designed to cover the desired frequency range. Separate adjustment of a potentiometer in each amplifier enables almost any required tonal balance to be obtained.

Negative feedback, with frequency selective feedback circuits, can also be used to provide tone control. Thus, if there is maximum feedback in the range of medium frequencies, the result is equivalent to an intensification of the low and high frequencies.

9.6.3. High-Frequency Attenuation. Control of the higher audio frequencies is possible prior to the A.F. amplifier, and variable selectivity in the I.F. amplifier (see Section 7.7, Part I) can be used for high-frequency tone control as well as for discriminating against undesired signals. Reduced coupling between the I.F. tuned circuits causes high-frequency attenuation, and overcoupling, producing double-humped frequency response, causes high-frequency intensification.

In an A.F. amplifier high-frequency attenuation can be obtained by adding a capacitance in parallel with the anode load resistance. Its effect is identical with that of stray capacitance C_s in Fig. 9.4*a*. The loss of amplification for given values of R_a, R_0, R_g and C_1+C_s, where C_1 is the additional control capacitance, can be read from Fig. 9.5*b* as explained in Section 9.3.1. Variation of the high-frequency loss (in actual fact it is a variation in the maximum

amplification at the medium frequencies) is achieved by varying the load resistance R_0. Increase of R_0 increases the high-frequency attenuation by increasing the amplification at the medium frequencies. A similar effect could be achieved by including a suitable inductance L_1 between the anode of V_1 and the junction of R_0 and C_c in Fig. 9.3, or in series with C_c between the anode of V_1 and the junction of R_g and the grid of V_2. Series resonance of C_c and L_1 would be damped by the grid leak resistance, R_g. With the first connection, increase of R_0 decreases the high-frequency attenuation, and with the second, tone control is achieved by variation of R_g, increase of R_g reducing the high-frequency loss. Stray capacitance across R_g may produce a series resonance peak in the frequency response at a high audio frequency; its effect is similar to that of leakage inductance and stray capacitance in the transformer coupled amplifier (Section 9.4). Other disadvantages of using inductance control are listed in 9.6.2.

9.6.4. High-Frequency Intensification. Increase of frequency response at the high audio frequencies can be obtained with either of the two circuits shown in Figs. 9.17*a* and 17*b*. Analysing Fig. 9.17*a* by means of Thévenin's Theorem, we have for the amplification at medium frequencies:

$$A_m = \frac{\mu R_g R_0}{(R_a+R_0)\left(R_g+\frac{R_a R_0}{R_a+R_0}\right)}$$

if the reactances of C_c and L_1 are negligible. At the high frequencies

$$A_h = \frac{\mu(R_g+jpL_1)R_0}{(R_a+R_0)\left(R_g+jpL_1+\frac{R_a R_0}{R_a+R_0}\right)} \quad . \quad . \quad 9.26.$$

Thus

$$\left|\frac{A_h}{A_m}\right| = \sqrt{\frac{1+\left(\frac{X_1}{R_g}\right)^2}{1+\left(\frac{X_1}{R}\right)^2}} \quad . \quad . \quad . \quad 9.27a$$

where $R = R_g+\frac{R_a R_0}{R_a+R_0}$ and $X_1 = pL_1$.

The increase in amplification at the high frequencies expressed in decibels is therefore

$$+10\log_{10}\frac{1+\left(\frac{X_1}{R_g}\right)^2}{1+\left(\frac{X_1}{R}\right)^2} = +10\log\frac{1+x^2}{1+(Bx)^2} \quad . \quad . \quad 9.27b$$

where $x = \frac{X_1}{R_g}$ and $B = \frac{R_g}{R} = \frac{1}{1+\frac{R_a R_0}{R_g(R_a+R_0)}}$.

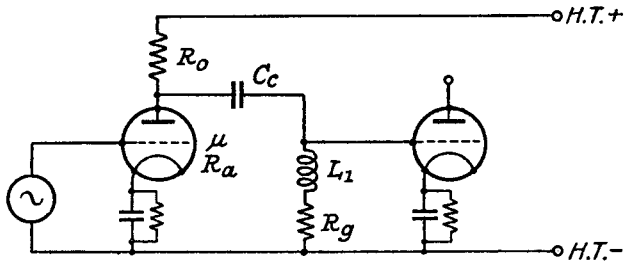

FIG. 9.17*a*.—A Circuit for Increasing High Frequency Response.

We may note that tone control, by varying R_g, is again obtained actually by reducing the amplification at the medium frequencies. Maximum amplification, $A_{max.} = \frac{\mu R_0}{R_a+R_0}$, is realized at the highest audio frequencies and is independent of B. Increased high-fre-

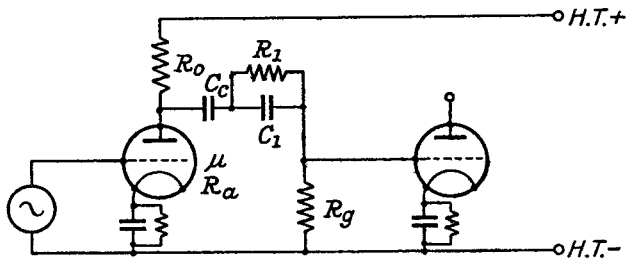

FIG. 9.17*b*.—A Circuit for Increasing High Frequency Response.

quency intensification is obtained by decreasing R_g. A series of curves of gain at high frequencies relative to the medium frequencies is plotted in Fig. 9.18 against x, i.e., $\frac{X_1}{R_g}$, to a logarithmic scale for selected values of B. The horizontal x scale is converted to frequency by locating $f_1 = \frac{R_g}{2\pi L_1}$ with $x = 1$, thus if $R_a = 50{,}000\ \Omega$, $R_0 = 200{,}000\ \Omega$, $R_g = 40{,}000\ \Omega$, $L_1 = 3$ H, frequency response is read from the curve for $B = 0{\cdot}5$, and $f_1 = \frac{40{,}000}{6{\cdot}28 \times 3} = 2{,}120$ c.p.s. is located with $x = 1$. Amplification at 5,000 and 10,000 c.p.s. is $+4{\cdot}5$ and $+5{\cdot}5$ db. respectively.

It may be observed in the above example that the A.C./D.C. load resistance ratio $\frac{R_g}{R_g+R_0}$ is only $\frac{1}{6}$; hence a large output voltage cannot be obtained from the tone control valve if distortion (see Section 9.3.3) is to be small.

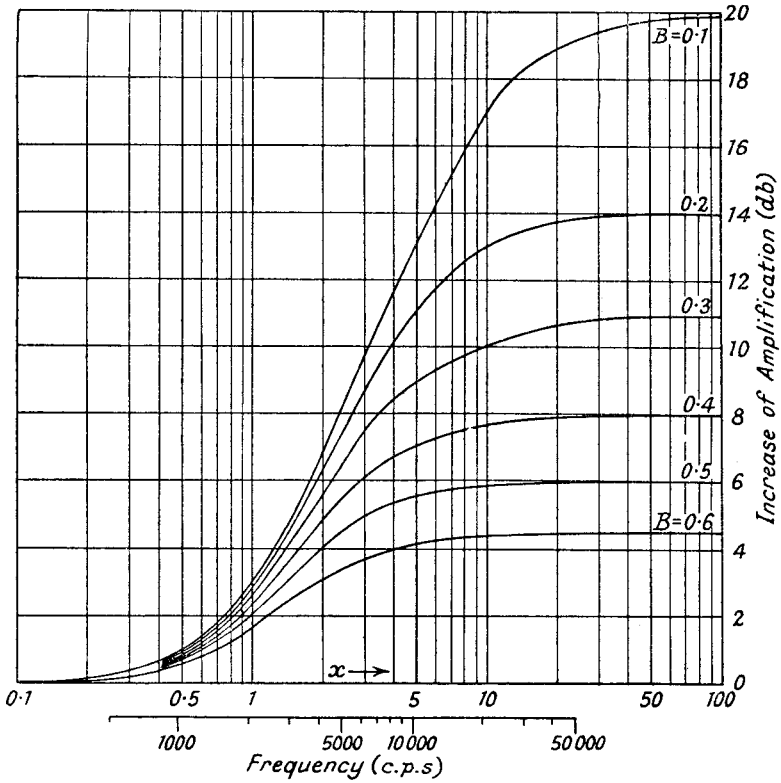

FIG. 9.18.—Generalised Curves of High Frequency Intensification Circuits.

For the circuit of Fig. 9.17*b*

$$A_m = \frac{\mu R_0 R_g}{(R_a+R_0)\left(\frac{R_a R_0}{R_a+R_0}+R_1+R_g\right)}$$

and

$$A_h = \frac{\mu R_0 R_g}{(R_a+R_0)\left(\frac{R_a R_0}{R_a+R_0}+\frac{R_1}{1+jpC_1R_1}+R_g\right)}$$

$$\frac{A_h}{A_m} = \frac{1+jpC_1R_1}{1+j\frac{R}{R+R_1}pC_1R_1}$$

where again $R = R_g + \dfrac{R_a R_0}{R_a + R_0}$

or
$$20 \log_{10} \left| \frac{A_h}{A_m} \right| = +10 \log_{10} \frac{1 + \left(\dfrac{R_1}{X_1}\right)^2}{1 + \left(\dfrac{R}{R+R_1} \cdot \dfrac{R_1}{X_1}\right)^2}$$
$$= +10 \log_{10} \frac{1+x^2}{1+(Bx)^2} \quad . \quad . \quad . \quad 9.28$$

where $x = \dfrac{R_1}{X_1}$ and $B = \dfrac{R}{R+R_1}$.

Expression 9.28 is identical with 9.27*b* and the curves in Fig. 9.18 are therefore again applicable, the horizontal x, i.e., $\dfrac{R_1}{X_1}$, scale being converted to frequency by locating $f_1 = \dfrac{1}{2\pi R_1 C_1}$ with $x = 1$. Thus for the same values of R_a, etc., as in the previous example, $R_1 = 80{,}000\ \Omega$ and $C_1 = 0{\cdot}00094\ \mu\text{F}$, $B = 0{\cdot}5$, $f_1 = 2{,}120$ c.p.s., and the frequency response is identical with that of the first circuit having an inductance element. A disadvantage of this circuit compared with that of Fig. 9.17*a* is that overall amplification is reduced in the ratio of B to 1, maximum amplification at the high frequencies being equal to amplification at the medium frequencies for the inductance element. For the component values listed above there is a loss of 6 db. in overall amplification with the capacitance element; on the other hand, the A.C./D.C. load resistance ratio is higher at the medium frequencies.

9.6.5. Low-Frequency Attenuation. Reduced amplification of the low audio frequencies can be obtained either by reducing the coupling capacitance C_c, or the self-bias capacitance C_k in Fig. 9.3. Figs. 9.5*a* and 9.10 enable the frequency response for selected com-

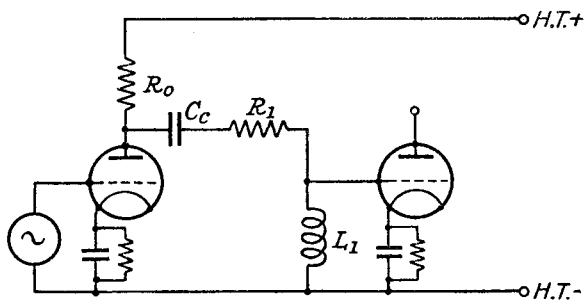

FIG. 9.19.—A Circuit for Producing Low Frequency Attenuation.

ponent values, or vice versa, to be estimated rapidly. A circuit also producing low-frequency attenuation is shown in Fig. 9.19 ; variation of the resistance R_1 controlling the frequency at which attenuation sets in. At medium frequencies, amplification is

$$A_m = \frac{\mu R_0}{R_a + R_0}$$

and at low frequencies, assuming that the reactance of C_c is so small that it can be neglected (the analysis becomes unduly complicated if this is not done)

$$A_l = \frac{\mu R_0}{R_a + R_0} \cdot \frac{jpL_1}{R_1 + \frac{R_a R_0}{R_a + R_0} + jpL_1} \quad . \quad . \quad 9.29$$

$$\left| \frac{A_m}{A_l} \right| = \sqrt{1 + \left(\frac{R}{X_1} \right)^2}$$

where $R = R_1 + \frac{R_a R_0}{R_a + R_0}$

and low-frequency loss is

$$-20 \log_{10} \left| \frac{A_m}{A_l} \right| = -10 \log_{10} \left(1 + \left(\frac{R}{X_1} \right)^2 \right) = -10 \log_{10} \left(1 + \frac{1}{x^2} \right). \quad 9.30.$$

The above expression is identical with 9.4*c*, so that the curve in Fig. 9.5*a* gives the frequency response by locating $f_1 = \frac{R}{2\pi L_1}$ c.p.s. with $x = 1$. There is a possibility of parallel resonance at a high audio frequency due to stray capacitance across L_1.

9.6.6. Low-Frequency Intensification. Increased amplification of the low frequencies relative to medium and high frequencies

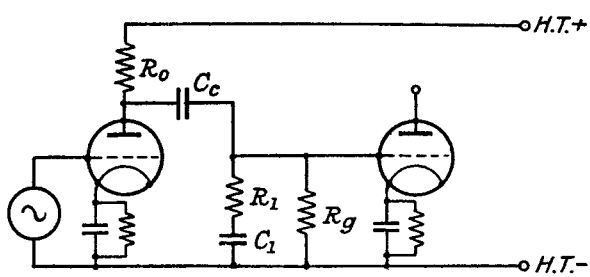

FIG. 9.20.—A Circuit for Increasing Low Frequency Response.

can be accomplished by the circuit shown in Fig. 9.20. At the medium frequencies

$$A_m = \frac{\mu R_0' R_1}{(R_a + R_0')\left(\frac{R_a R_0'}{R_a + R_0'} + R_1\right)}$$

where $$R_0' = \frac{R_0 R_g}{R_0 + R_g}$$

$$A_l = \frac{\mu R_0'}{R_a + R_0'} \cdot \frac{R_1 + \frac{1}{jpC_1}}{\frac{R_a R_0'}{R_a + R_0'} + R_1 + \frac{1}{jpC_1}} \quad . \quad . \quad 9.31.$$

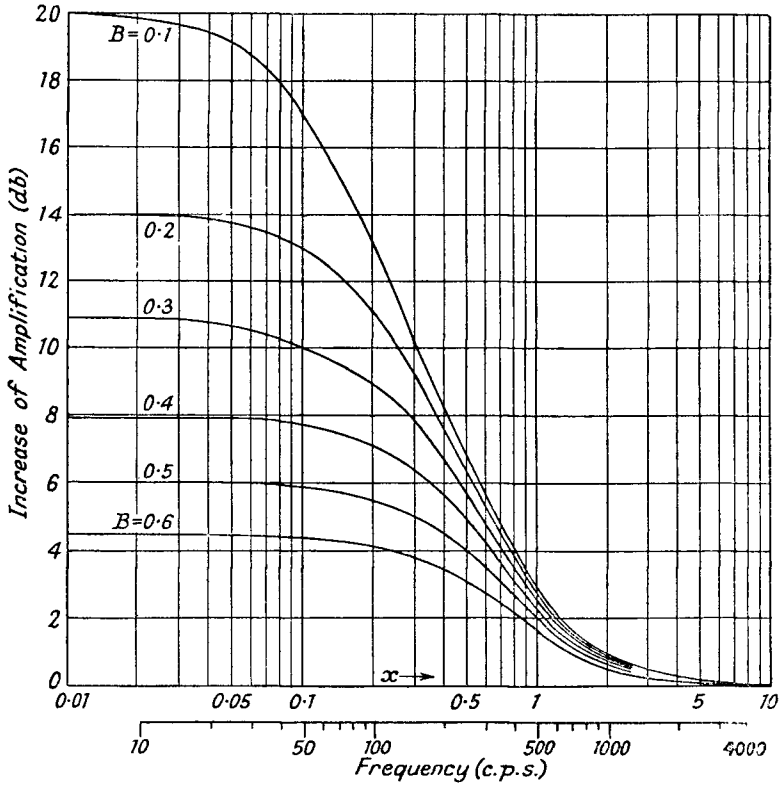

FIG. 9.21.—Generalized Curves for Low Frequency Intensification Circuits.

Increase in amplification at low frequencies is

$$+20 \log_{10} \left| \frac{A_l}{A_m} \right| = +10 \log_{10} \frac{1 + \frac{1}{x^2}}{1 + \left(\frac{B}{x}\right)^2} \quad . \quad . \quad 9.32$$

where $x = pC_1R_1$, $B = \frac{R_1}{R}$ and $R = \frac{R_aR_0'}{R_a+R_0'}+R_1$.

Curves are plotted in Fig. 9.21 of amplification in decibels against x for selected values of B, and the frequency response is read by locating $f_1 = \frac{1}{2\pi C_1R_1}$ with $x = 1$. Thus if $R_a = 50{,}000\ \Omega$, $R_0 = 200{,}000\ \Omega$, $R_g = 1\ \text{M}\Omega$, $R_1 = 40{,}000\ \Omega$, and $C_1 = 0{\cdot}008\ \mu\text{F}$, $f_1 = \frac{10^6}{6{\cdot}28 \times 40{,}000 \times 0.008} = 497$ c.p.s. is registered with $x = 1$ and frequency response is obtained from the curve for $B = 0{\cdot}5$ (the nearest curve to the actual value of $B = 0{\cdot}51$). Thus the increase in amplification at 50 and 100 c.p.s. is $+5{\cdot}8$ and $+5{\cdot}5$ db. respectively.

Yet another method of obtaining increased amplification at low frequencies is by a suitable choice of anode decoupling RC values as described in Section 9.3.6.

9.6.7. Response confined to a Band of Audio Frequencies. When a receiver is intended for telephonic communication, its audio frequency range can with advantage be confined to a band from 250 to 2,750 c.p.s. This comparatively narrow band contains almost all the frequency components necessary for good intelligibility, and at the same time tends to eliminate undesired frequencies due to hum, atmospherics, etc. As a rule a correctly terminated filter ($R_0 = 600\ \Omega$) is inserted in the A.F. amplifier; design procedure for this is beyond the scope of the book and reference should be made to Bibliography Nos. 13 and 14.

Frequency response limited to a very narrow band (about ± 50 c.p.s.) in the neighbourhood of 1,000 c.p.s. is quite often employed in communication receivers for telegraph operation. The narrow pass-band may be achieved by the use of a double-tuned iron-cored transformer with critical coupling between primary and secondary. The frequency response is similar to that for I.F. double-tuned coupled circuits, and the curves of Fig. 7.7 (Part I) can be used either to estimate the performance for given values of primary and secondary inductance, capacitance and Q, and the mutual inductance between the circuits, or to calculate component values for a given performance. An average value Q for iron-cored inductances is 5, but by special design, such as thinner iron laminations, it may be raised to 20. The factors influencing the Q of iron-cored coils have been examined in considerable detail by Arguimbau [5, 11], who found that Q reaches a maximum value of

$$Q_{(max)} = \frac{1}{\delta}\sqrt{\frac{3\rho_i SA\alpha}{\rho_c tl}} \quad . \quad . \quad . \quad 9.33$$

at a particular frequency of

$$f_1 = \frac{10^9}{4\pi^2 \Delta\mu\delta}\sqrt{\frac{3\rho_c\rho_i tl}{SA\alpha}} \quad . \quad . \quad . \quad 9.34a$$

$$= \frac{3.10^9\rho_i}{4\pi^2\Delta\mu\delta^2 Q_{(max)}} \quad . \quad . \quad . \quad . \quad 9.34b$$

where δ = thickness of laminations in cms.
ρ_i = resistivity of lamination material in ohms per c.c.
ρ_c = resistivity of copper winding in ohms per c.c.
$S = \frac{N\pi d^2}{4}$ = effective coil window area (total cross-sectional area of winding window in sq. cm.)
d = diameter of wire.
N = number of turns of copper.
A = cross-sectional area of magnetic path in sq. cm.
α = stacking factor of iron (the ratio of effective area of core iron to inside area of coil tube, allowance is to be made for lamination insulation).
t = average length of one turn of winding.
l = mean length of magnetic flux path.
$\Delta\mu$ = incremental permeability of magnetic material.

In determining the above expressions it is assumed that the A.C. flux density is very small, i.e., hysteresis loss is small, that skin effect of the copper in the winding, leakage flux and eddy currents between laminations are negligible, and that resonance is remote. The following conclusions are reached by an examination of expressions 9.33, 9.34*a* and 9.34*b*:

(1) Multiplication of overall dimensions by a factor "r" increases $Q_{(max)}$ to $rQ_{(max)}$ and decrease f_1 to $\frac{f_1}{r}$.

(2) Decrease of lamination thickness, δ, increases $Q_{(max)}$ (not quite in the same proportion as δ is decreased, because the stacking factor, α, is altered) and increases f_1.

(3) When the winding area is not fully occupied (S is reduced), $Q_{(max)}$ is decreased and f_1 increased.

(4) When the core is loosely stacked (α reduced) $Q_{(max)}$ is decreased and f_1 increased.

(5) Increase of core cross-sectional area increases $Q_{(max)}$ and decreases f_1, but the change in A is offset by a similar

change in t. Doubling A only increases $Q_{(max)}$ about 1·25 times.

(6) Decrease of core material resistivity, ρ_i, decreases $Q_{(max)}$ and f_1.

(7) Increase of winding material resistivity, ρ_c, decreases $Q_{(max)}$ and increases f_1.

(8) Increase of air gap in a given design has no effect on $Q_{(max)}$, but decreases f_1 if $\Delta\mu$ is increased. If the core carries D.C. current, $\Delta\mu$ may be increased by increase of air gap.

The value of Q obtained at a frequency, f, can be expressed in terms of $Q_{(max)}$, f and f_1 as follows:

$$Q = \frac{2\,Q_{(max)}}{\frac{f}{f_1}+\frac{f_1}{f}} \quad . \quad . \quad . \quad . \quad 9.35$$

For a Q of 5, and $f_r = 1{,}000$ c.p.s., frequency response for critical coupling is (see Fig. 7.7.) about 1 db. and 7 db. down at 100 and 200 c.p.s. respectively off-tune from 1,000 c.p.s., whilst for $Q = 20$, $f_r = 1{,}000$ c.p.s., the losses at the same frequencies are 18 and 30 db. respectively. When reduced overall amplification can be considered, greater selectivity is possible by using couplings less than critical. For example, at one-half critical coupling, the losses in the first case are increased to 4 and 11·5 db. respectively, but overall amplification is reduced by 2 db.

9.6.8. Elimination of a Narrow Band of Frequencies. The elimination of a narrow band of frequencies in the A.F. range is sometimes used for reducing needle scratch in the reproduction of gramophone records (the predominant frequency is about 11 kc/s), and also for reducing heterodyne whistle interference (about 9 kc/s) from an adjacent channel transmission. A possible circuit is shown in Fig. 9.22.

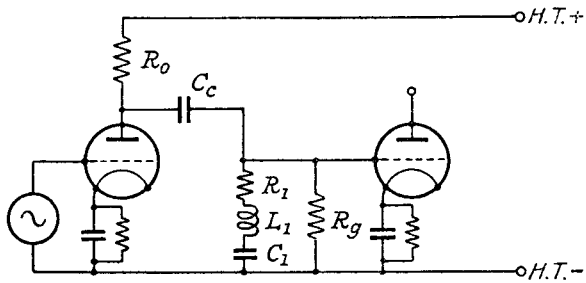

FIG. 9.22.—A Circuit for Eliminating a Narrow Band of Audio Frequencies.

The amplification at frequencies far removed from resonance is

$$A_n = \frac{\mu R_0'}{R_a + R_0'}$$

where $$R_0' = \frac{R_0 R_g}{R_0 + R_g}$$

and at other frequencies

$$A = \frac{\mu R_0'}{R_a + R_0'} \cdot \frac{R_1 + j\left(pL_1 - \frac{1}{pC_1}\right)}{\frac{R_a R_0'}{R_a + R_0'} + R_1 + j\left(pL_1 - \frac{1}{pC_1}\right)}.$$

At resonance, amplification is minimum and given by

$$A_r = \frac{\mu R_0'}{R_a + R_0'} \cdot \frac{R_1}{\frac{R_a R_0'}{R_a + R_0'} + R_1}.$$

The ratio of A_n to amplification at any particular frequency is

$$\frac{A_n}{A} = \frac{\frac{R_a R_0'}{R_a + R_0'} + R_1 + j\left(pL_1 - \frac{1}{pC_1}\right)}{R_1 + j\left(pL_1 - \frac{1}{pC_1}\right)} = \frac{\frac{R''}{R_1} + \frac{jp_r L_1}{R_1}\left(\frac{p}{p_r} - \frac{p_r}{p}\right)}{1 + \frac{jp_r L_1}{R_1}\left(\frac{p}{p_r} - \frac{p_r}{p}\right)}$$

$$= \frac{B + jQ\left(x - \frac{1}{x}\right)}{1 + jQ\left(x - \frac{1}{x}\right)} \quad . \quad . \quad . \quad . \quad . \quad . \quad . \quad 9.33$$

where $R'' = \frac{R_a R_0'}{R_a + R_0'} + R_1$, $p_r = \frac{1}{\sqrt{L_1 C_1}}$; $B = \frac{R''}{R_1}$, $Q = \frac{p_r L_1}{R_1}$

and $x = \frac{p}{p_r} = \frac{f}{f_r}$.

The loss relative to A_n is

$$-20 \log \left| \frac{A_n}{A} \right| = -10 \log_{10} \frac{B^2 + Q^2\left(x - \frac{1}{x}\right)^2}{1 + Q^2\left(x - \frac{1}{x}\right)^2} \quad . \quad 9.34.$$

There are three possible variables, B, Q and x, in 9.34, and a single series of generalized frequency response curves cannot be produced. Representative curves showing the effect of varying B for constant Q, and vice versa, are plotted in Fig. 9.23 against x. A similar

logarithmic frequency scale with $f_r = \frac{1}{2\pi\sqrt{L_1C_1}}$ registered against $x = 1$ enables frequency response for particular component values to be read. Thus if $R_a = 50{,}000\ \Omega$, $R_0 = 200{,}000\ \Omega$, $R_g = 1\ \text{M}\Omega$, $R_1 = 10{,}000\ \Omega$, $Q = 10$ and $f_r = 9$ kc/s the frequency scale is registered at 9 kc/s as shown and frequency response read from the curve $Q = 10$, $B = 5$ (this is nearest to the actual value of $B = 4{\cdot}85$), i.e., maximum loss at 9 kc/s is very nearly 14 db., whilst at 8 (or 10·1) kc/s and 7 (or 11·6) kc/s the loss is 7·2 and 3 db. respectively. The curves show quite clearly that Q controls the

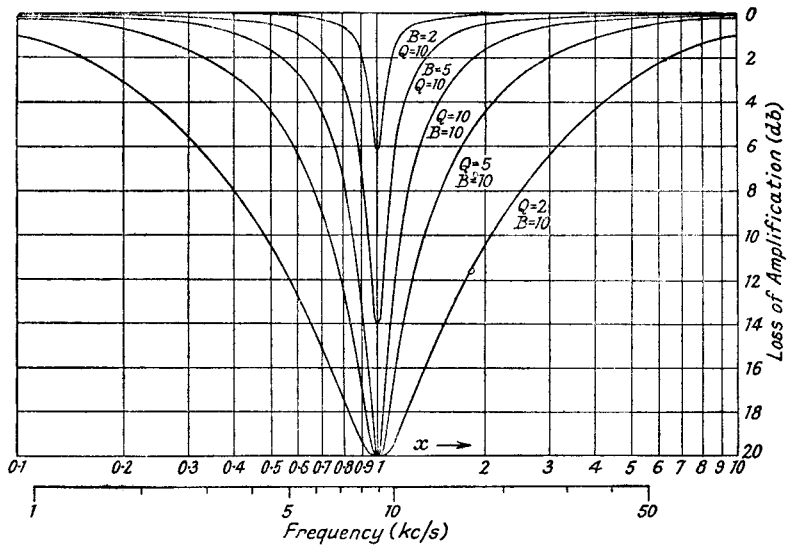

FIG. 9.23.—Generalized Curves for Narrow Band Elimination Circuit.

shape of the frequency response and B the maximum loss at the resonant frequency.

9.6.9. Combined Volume and Tone Control. Attempts have been made to overcome the lack of tonal balance as the loudspeaker average sound intensity is reduced (due to a greater apparent reduction in the low and high A.F. components) by linking the volume and tone control action. One of the simplest and earliest methods was by means of a parallel resonant circuit [3] (tuned to about 50 c.p.s.) or a series resonant circuit [2] (tuned to about 1,000 c.p.s.) connected to a fixed tapping point on the volume control potentiometer. As this point is approached by the slider of the potentiometer, low-frequency response is intensified (by the

parallel resonant circuit) or medium-frequency response is reduced (by the series resonant circuit). This method has the disadvantage that frequency response is not exactly related to the sound output as should be the case for correct tone-volume compensation. Combined volume and tone control can be realized by ganging the volume potentiometer and the resistance tone-control element. A separate tone control is, however, generally preferable since best tonal balance depends on site conditions (size and furnishing of room, signal-to-noise ratio, etc.), and is, to a large extent, a matter of personal taste.

BIBLIOGRAPHY

1. The Design of Tone Control Circuits. K. W. Jarvis, *Electronics*, Aug. 1930, p. 230.
2. Acoustically Compensated Volume Control. I. Wolff and J. I. Cornell, *Electronics*, Jan. 1933, p. 50.
3. Tone Compensation. M. G. Scroggie, *Wireless World*, Aug. 30th, 1935, p. 252.
4. Design of Audio Frequency Amplifier Circuits Using Transformers. P. W. Klipsch, *Proc. I.R.E.*, Feb. 1936, p. 219.
5. Losses in Audio Frequency Coils. L. B. Arguimbau, *General Radio Experimenter*, Nov. 1936, p. 1.
6. The Evolution of the Phon. D. B. Foster, *Wireless World*, July 9th, 1937, p. 32.
7. Flexible Tone Control. M. G. Scroggie, *Wireless World*, Sept. 10th, 1937, p. 263.
8. Tone Control. "Cathode Ray." *Wireless World*. Sept. 15th and 22nd, 1938, pp. 247 and 269.
9. New American Quality Receiver. L. G. Pacent and H. C. Likel, *Wireless World*, March 23rd, 1939, p. 271.
10. Tone Control Systems. W. T. Cocking, *Wireless World*, June 8th, 1939, p. 532.
11. How Good is an Iron-Cored Coil? P. K. McElroy and R. F. Fields, *General Radio Experimenter*, March 1942, p. 1.
12. *Radio Engineering*. F. E. Terman. McGraw Hill. Text-book.
13. *Transmission Circuits for Telephonic Communication*. K. S. Johnson. Van Nostrand. Text-book.
14. *Transmission Networks and Wave Filters*. T. E. Shea. Van Nostrand. Text-book.

CHAPTER 10

THE POWER OUTPUT STAGE

10.1. Introduction. The audio frequency output stage of a receiver differs from the other stages in that maximum power, as distinct from maximum voltage, is required from its anode circuit. This usually entails a definite relationship between the output load and the valve internal resistance, though the optimum load resistance is not determined only by maximum power but also by distortion considerations. Normally the optimum load is taken as that value of resistance which gives maximum output power for a total harmonic distortion of 5%.

Two types of valves are used, the triode and the beam tetrode or pentode, and each has its particular advantages. The output load may be supplied from a single valve, or a pair operating in push-pull, the particular features of the latter being (if matched valves, having identical I_aE_a characteristics are employed) cancellation of even harmonics, and zero D.C. polarization in the output transformer. Neither of these features is possessed by a pair of valves in parallel, and the only advantage of the parallel connection is that the equivalent generator internal resistance is halved. When a single valve supplies the output stage, it is usually biased to the centre of the straight part of its I_aE_g characteristic; this is not essential in push-pull stages, and in order to economize in current consumption both valves may be biased to the bend of their I_aE_g characteristic. Even harmonic distortion is produced in each valve but is cancelled by the push-pull connection. The first method is known as Class A operation and the second as Class B operation. There is also a third method, known as Class AB, which, together with the second method, is discussed in Section 10.8. Inverse or negative feedback from the output stage is employed to reduce amplitude and frequency distortion and to damp loudspeaker resonances, and details of the various forms of feedback circuits are given in Section 10.10.

10.2. Conditions for Maximum Power Output.[48] In order to calculate the load for maximum output power, some assumption of the form of the I_aE_a characteristics must be made. For convenience we shall consider a triode having a series of straight equally-spaced parallel lines, of slope $\frac{\Delta I_a}{\Delta E_a}$ equal to the reciprocal of the valve

internal resistance R_a. The line OA in Fig. 10.1 is the boundary curve for $E_g = 0$, beyond which the valve may not operate unless the previous stage has been designed to supply the necessary power absorbed by grid current.

The analysis can also be applied to a tetrode, but the valve resistance R_a must then be taken as the value obtained from the boundary curve OA, and is not the normal valve slope resistance obtained with high anode voltage.

Five possible cases have to be considered, for all of which neither grid current nor distortion are permitted. The first has fixed A.C. input voltage to the grid, the second has fixed D.C. anode voltage and no limitations on D.C. anode current or A.C. input grid voltage. The third case is the same as the second except that the maximum D.C. power dissipation at the anode is fixed, i.e., maximum D.C. anode current, is fixed. The fourth has fixed D.C. power dissipation, but D.C. anode current and voltage can be varied so long as their product is constant. The fifth applies all the results to the practical form of triode I_aE_a characteristic, curved at low anode currents. This means that there is a minimum value of anode current, below which the valve must not be operated if distortion is to be small, and also that the straight part produced (MA in Fig. 10.2*b*) of the boundary line does not pass through the origin but a point corresponding to an anode voltage of ε.

CASE 1. *Grid current and distortion zero, fixed A.C. input voltage to the grid.*

The valve functions as a generator of constant voltage μE_g, having an internal resistance of R_a.

$$\text{A.C. power output } P_0 = \frac{(\mu E_g)^2 R_0}{(R_a + R_0)^2} \qquad . \quad 10.1a$$

and is a maximum when $\dfrac{dP_0}{dR_0} = 0$,

i.e., when $R_0 = R_a$.

This condition is illustrated on the I_aE_a characteristics of Fig. 10.1 by the load line $B'D'$, which can be located anywhere between OA and MN (the limiting grid voltage lines) so long as $F'H' = H'B'$. The best position is that shown, B' and M coinciding, since raising $B'D'$ merely increases the D.C. power taken by the valve without increasing A.C. power output, which is the area of triangle $H'F'Q$.

Therefore $P_0 = \frac{1}{2}(E_1' - E_2')I_1'$

But $E_1' = \frac{3}{2}E_2'$ because $R_0 = R_a$

Therefore $P_0' = \frac{1}{6}E_1'I_1' = \frac{1}{18}\frac{E_1'^2}{R_a}$ 10.1*b*

D.C. power to the valve $= E_1'I_1' = \frac{E_1'^2}{3R_a}$

so that A.C./D.C. power conversion efficiency = 16·6%

If it is possible for grid current to flow and E_2' can be taken to zero, power output is increased to $\frac{1}{2}E_1'I_1'$ and A.C./D.C. power conversion efficiency to 50%.

CASE 2. *Grid current and distortion zero, fixed D.C. anode voltage, no limitations on D.C. anode current or A.C. input voltage to the grid.*

The load line is *BD* on Fig. 10.1, and the equation to this line is

$$I_a = -\frac{E_a}{R_0} + C$$

where C = anode current at the intersection of *BD* with the I_a axis. For zero distortion $E_1 - E_2 = E_3 - E_1$, or $E_3 = 2E_1 - E_2$.

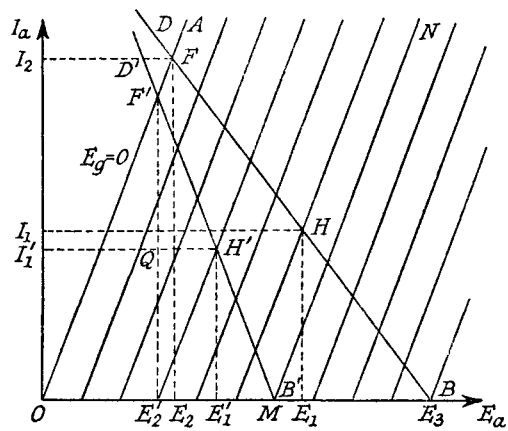

FIG. 10.1.—Load Lines on the Idealized I_aE_a Characteristics of a Triode.

The point *B* on line *BD* corresponds to

$$I_a = 0 = \frac{-(2E_1 - E_2)}{R_0} + C.$$

Therefore $$C = \frac{2E_1 - E_2}{R_0}.$$

Current and voltage at the intersection *F* of *OA* and *BD* are

$$I_2 = \frac{E_2}{R_a} = -\frac{E_2}{R_0} + \frac{2E_1 - E_2}{R_0} = \frac{2}{R_0}(E_1 - E_2).$$

Therefore $E_2 = \dfrac{2E_1R_a}{2R_a+R_0}$

and $I_2 = \dfrac{2E_1}{2R_a+R_0}$.

Power output $P_0 = \frac{1}{2}(E_1 - E_2)\dfrac{I_2}{2}$

$$= \tfrac{1}{2}\frac{E_1^2R_0}{(2R_a+R_0)^2} \quad . \quad . \quad . \quad . \quad 10.2a.$$

For maximum power output $\dfrac{dP_0}{dR_0} = 0$;

or $R_0 = 2R_a$.

Therefore $P_0(max.) = \dfrac{E_1^2}{16R_a}$ . . 10.2*b*.

Input D.C. power $= \dfrac{E_1I_2}{2} = \dfrac{E_1^2}{4R_a}$.

A.C. to D.C. power conversion efficiency = 25%.

Hence for a given D.C. anode voltage E_1, case 2 gives more power output and a higher A.C. to D.C. conversion efficiency than case 1. On the other hand, a larger input A.C. voltage is required at the grid. Conversion efficiency is increased to 50% if E_2 can be taken to zero. This condition can be approached with a tetrode without grid current, but the grid current region must be entered if a triode is used. Class AB (Section 10.8.7) and Class B positive-drive (Section 10.8.5) are examples of this, the previous stage being specially designed to supply the power needed when grid current is taken.

The optimum load for curved I_aE_a characteristics having the relationship $I_a = KE_a^{\frac{3}{2}}$ has been calculated[2] and found to be $R_0 = 1{\cdot}6R_a$. However, the rule giving optimum load as $R_0 = 2R_a$ proves in practice to be nearer the measured optimum value for single triode Class A amplifiers giving 5% total harmonic distortion.

CASE 3. *Grid current and distortion zero, fixed D.C. anode voltage and anode current.*

For every valve there is a maximum value, $P_D(max.)$, for the power which can be dissipated at the anode, and care must be taken to see that the D.C. power (E_1I_1) taken by the valve does not exceed this value. If I_1 for $R_0 = 2R_a$, is less than $\dfrac{P_D(max.)}{E_1}$, this represents optimum load conditions and there will be actually less power output by increasing I_1 to $\dfrac{P_D(max.)}{E_1}$. When $I_1(R_0 = 2R_a)$

exceeds $\frac{P_D(max.)}{E_1}$, the D.C. grid-bias voltage must be increased to reduce I_1 to its maximum permissible value, and maximum power output is then obtained for $R_0 > 2R_a$. This condition is illustrated in Fig. 10.2*a*; the hyperbolic relationship between D.C. anode current and voltage for a fixed value of $P_D(max.)$ is represented by the curve *GHK*. *OA* is the boundary line for zero grid current and *BD* is the load line drawn through the reference point *H* on the curve *GHK*. For zero distortion the change in anode current and voltage above *H* must equal the change below *H*. It is not an essential condition, however, that the full extent of the load line from *B* to *F* should be used, and the problem is one of determining whether maximum power output is obtained by an excursion over less than the length *BF*. If we ignore the limitations imposed by the negative anode voltage swing (below *H*), maximum power output is obviously obtained by using the full extent of *HB* and by making *PB* as large as possible. Power output, equal to $\frac{1}{2}(E_3 - E_1)I_1$ is the area of the triangle *HBP*, and this is clearly a maximum when E_3 is maximum. It must therefore be the negative anode voltage swing, which always determines the maximum power output. Power output, equal to the area of triangle *HFL*, is zero when R_0 is infinite (*BD* is horizontal) and when $R_0 = 0$ (*BD* vertical); it is maximum when the slope of *BD* equals that of *OA*. It is equivalent to working with a fixed grid input A.C. voltage and is therefore case 1 over again. Two possible conditions, depending on the position of *H* relative to *OA* and the E_a axis, have to be considered. Suppose *H* is much closer to the E_a axis than to *OA*; we find that as the point *B* on the load line, pivoted at *H*, is brought closer to E_1, the area of the triangle *HBP* is decreasing and that of triangle *HFL* increasing. Since *H* is assumed to be close to the E_a axis, the condition for maximum power output is that the areas of the triangles *HBP* and *HFL* are equal. When $R_0 = R_a$ (giving maximum area of triangle *HFL*) the area of triangle *HFL* is greater

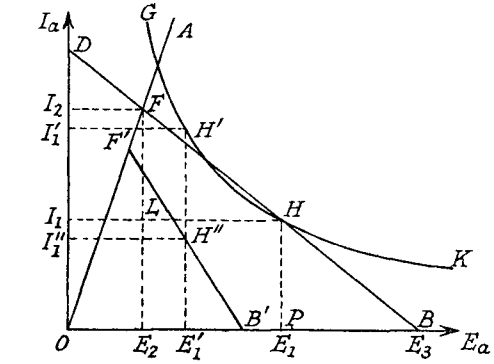

FIG. 10.2*a*.—Optimum Load Conditions for a Triode Valve of Fixed D.C. Power Dissipation.

than that of triangle HBP, and if distortion is to be avoided it entails reducing the negative anode voltage excursion from HF to a length equal to HB. This is clearly inefficient. For equal areas of the triangles, the maximum current I_2 must be twice I_1 and

$$E_2 = I_2R_a = 2I_1R_a.$$

$$\text{Power output } P_0 = \tfrac{1}{2}(E_1 - E_2)I_1$$
$$= \tfrac{1}{2}(E_1 - 2I_1R_a)I_1 \quad . \quad 10.3a.$$

$$\text{Optimum load resistance } R_0 = \frac{HL}{FL} = \frac{E_1 - E_2}{I_1}.$$
$$= \frac{E_1}{I_1} - 2R_a$$
$$= R_{\text{D.C.}} - 2R_a$$

where $R_{\text{D.C.}}$ = D.C. resistance of the valve

$$\text{A.C. to D.C. conversion efficiency} = \frac{\tfrac{1}{2}(E_1 - 2I_1R_a)I_1}{E_1I_1}$$
$$= \tfrac{1}{2}\left(1 - \frac{2R_a}{R_{\text{D.C.}}}\right) \quad . \quad 10.4.$$

Maximum A.C./D.C. conversion efficiency approaches the same maximum value as for case 2, viz., 50% when $R_{\text{D.C.}}$ is large compared with R_a. This is to be expected since a large value of $R_{\text{D.C.}}$ implies a high value of E_1 and low value of I_1; both these effectively reduce E_2, as does a decrease in R_a.

The second condition, for which H is much closer to OA than to the E_a axis (see position H' in Fig. 10.2a), requires R_0 to equal R_a for maximum power output, but the valve is then operating very inefficiently, only a small part of the load line between H' and B being used. The most efficient method of operation would be to reduce I_1' to I_1'', which gives $H''F' = H''B'$ with a load line of $R_0 = 2R_a$.

The conclusion to be drawn from the analysis is that I_1 should never exceed $\dfrac{E_1}{4R_a}$ (this corresponds to an optimum load resistance of $R_0 = 2R_a$), for increase of current above this value decreases power output and A.C./D.C. conversion efficiency. Optimum load resistance when $I_1 > \dfrac{E_1}{3R_a}$ is $R_0 = R_a$ but for $I_1 < \dfrac{E_1}{3R_a}$ it is $R_0 = \dfrac{E_1}{I_1} - 2R_a$. Maximum power output is always realized for $I_1 = \dfrac{E_1}{4R_a}$, when optimum load resistance is $R_0 = 2R_a$.

CASE 4. *Zero grid current and distortion, fixed D.C. anode dissipation loss, no limitations on D.C. anode voltage.*

Expression 10.3*a* for power output may be written

$$P_0 = \tfrac{1}{2}(E_1 I_1 - 2I_1^2 R_a) = \tfrac{1}{2}(P_D(max.) - 2I_1^2 R_a) \quad . \quad 10.3b.$$

Since $P_D(max.)$ is a constant, it follows that maximum power output is obtained when I_1 is as small as possible, i.e., E_1 is as large as possible. A.C. to D.C. conversion efficiency is a maximum at the same time. It must, however, be noted that increased efficiency in the anode circuit, brought about by increased D.C. anode voltage, entails a lower grid input voltage efficiency by requiring a steadily increasing input voltage. In most practical cases of Class A triode

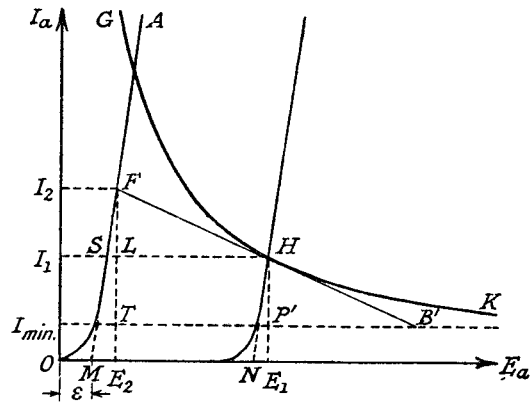

FIG. 10.2*b*.—Optimum Load Conditions for a Triode of Fixed D.C. Power Dissipation and Minimum Anode Current.

operation optimum overall input and output conditions are realized by making $R_0 = 2R_a$.

As pointed out at the beginning of this section the analysis may be applied to a Class A tetrode valve provided it is remembered that R_a is the slope resistance of the boundary curve for small values of anode voltage. In almost all cases $I_1 < \dfrac{E_1}{4R_a}$ and optimum load is

$$R_0 = R_{\text{D.C.}} - 2R_a.$$

Often R_a, the slope resistance of the OA boundary line for small anode voltages (not exceeding 30 volts), is negligible in comparison with $R_{\text{D.C.}}$ and

$$R_0 = R_{\text{D.C.}}$$

gives a good approximation to the optimum load.

CASE 5. *Grid current and distortion zero, fixed D.C. anode dissipation loss, fixed minimum D.C. anode current, boundary line produced from its straight part passes through some positive value of* E_a.[46]

The practical form of I_aE_a characteristic is generally non-linear for low values of I_a, and this sets a limit on the minimum operative value of I_a if distortion is not to be excessive. For a triode valve the foot of the boundary characteristic ($E_g = 0$) is often curved and the straight part (produced) cuts the E_a axis at some positive voltage. Fig. 10.2*b* illustrates the condition, the intersection of the boundary line OA (produced) cutting the E_a axis at $+\varepsilon$ volts. The hyperbolic curve GHK is the fixed anode dissipation loss and it is cut eventually by the minimum anode current line drawn at $I_a = I_{min.}$. Cases 1 and 2 are not affected by the new conditions, i.e., optimum load for fixed grid A.C. input voltage is R_a, and for fixed D.C. anode voltage and unlimited grid input voltage is $2R_a$, where R_a is the slope resistance of the line MA. Case 3 is, however, slightly modified; the triangles HFL and $HP'B'$ must be equal, which means that

$$I_2 - I_1 = I_1 - I_{min.}$$

or

$$I_2 = 2I_1 - I_{min.}$$

A.C. power output $P_0 = \frac{1}{2}(E_1 - E_2)(I_1 - I_{min.})$

$$= \tfrac{1}{2}[E_1 - (2I_1 - I_{min.})R_a - \varepsilon][I_1 - I_{min.}] \quad 10.5.$$

Optimum load resistance $R_0 = \dfrac{E_1 - E_2}{I_1 - I_{min.}}$ 10.6*a*

$$= \frac{E_1 - (2I_1 - I_{min.})R_a - \varepsilon}{I_1 - I_{min.}}$$

$$= \frac{E_1}{I_1}\left(\frac{I_1}{I_1 - I_{min.}}\right) - R_a\left(2 + \frac{I_{min.}}{I_1 - I_{min.}}\right) - \frac{\varepsilon I_{min.}}{I_{min.}(I_1 - I_{min.})}$$

$$= R_{\text{D.C.}} - 2R_a + (R_{\text{D.C.}} - R_a - R_{min.})\frac{I_{min.}}{I_1 - I_{min.}} \quad . \quad . \quad 10.6b$$

where $R_{\text{D.C.}}$ and $R_{min.}$ are $\dfrac{E_1}{I_1}$ and $\dfrac{\varepsilon}{I_{min.}}$ respectively.

The above expression is the same as for case 3 when $I_{min.}$ and ε are zero.

A.C. to D.C. power conversion efficiency

$$= \frac{[E_1 - (2I_1 - I_{min.})R_a - \varepsilon][I_1 - I_{min.}]}{2E_1I_1}$$

$$= \tfrac{1}{2}\left(1 - \frac{2R_a}{R_{\text{D.C.}}} + \frac{R_aI_{min.}}{R_{\text{D.C.}}I_1} - \frac{\varepsilon}{E_1}\right)\left(1 - \frac{I_{min.}}{I_1}\right). \quad . \quad 10.7$$

since $R_a I_{min.} < \varepsilon$, and $\left(1 - \frac{I_{min.}}{I_1}\right) < 1$, expressions 10.5 and 10.7 for P_0 and conversion efficiency are clearly less than 10.3*a* and 10.4, and this is to be expected since minimum anode current is no longer zero.

Case 4 (unlimited D.C. anode voltage) is also modified, for maximum P_0 is now obtained at some finite value of E_a. This must be so since the D.C. anode voltage cannot possibly exceed half the anode voltage corresponding to the intersection of $I_{min.}$ with the hyperbola *GHK*. The condition for maximum power output is obtained by differentiating P_0 (expression 10.5) with respect to I_1 and equating to 0.

Thus $$\frac{dP_0}{dI_1} = 0 = (3I_{min.} - 4I_1)R_a - \varepsilon - \frac{dE_1}{dI_1}.I_{min.}$$

for $$E_1 I_1 = P_D(max.) = \text{constant}$$

$$E_1 = \frac{P_D(max.)}{I_1}.$$

Therefore $$\frac{dE_1}{dI_1} = -\frac{P_D(max.)}{I_1^2}.$$

The condition for maximum P_0 is

$$\frac{P_D(max.)}{I_1^2} = \left[\frac{4I_1}{I_{min.}} - 3\right]R_a + R_{min.}.$$

This is a cubic equation in I_1, which is generally fairly easily solved by trial and error.

By noting that $\frac{P_D(max.)}{I_1^2} = R_{\text{D.C.}}$ and replacing $R_{\text{D.C.}}$ in 10.6*b* by its value in terms of I_1, $I_{min.}$ and $R_{min.}$, we have

$$R_0 = \left[\frac{4I_1}{I_{min.}} - 1\right]R_a + R_{min.} \quad . \quad . \quad . \quad 10.6c$$

as the optimum value for R_0. It is a function of $I_{min.}$ and ε ($I_{min.}R_{min.}$). The smaller the value of $I_{min.}$ the larger is R_0, and when $I_{min.}$ is zero, optimum R_0 is infinite as for case 4.

It is useful to note that the A.C. input voltage required at the grid in all cases where I_a is taken down to $I_{min.}$ is

$$E_g = \frac{MN}{\mu} = \frac{SH}{\mu} = \frac{SL + LH}{\mu} = \frac{(I_2 - I_1)(R_a + R_0)}{\mu}$$

$$= \frac{(I_1 - I_{min.})(R_a + R_0)}{\mu} \quad . \quad . \quad . \quad . \quad . \quad 10.8$$

and it increases as R_0 is increased.

10.3. The Characteristics Required of an Output Valve. Certain characteristics are required of an output valve and the most important are :

(1) *High power sensitivity.* Power sensitivity is expressed as the R.M.S. output power (milliwatts) per input R.M.S. grid volt. The higher this value the lower is the grid voltage required for maximum power, so that less amplification is needed in preceding stages, and the possibility of distortion before the output valve is consequently reduced.

(2) *Low distortion.* Distortion should be low and confined mainly to the second harmonic. Higher harmonics indicate the probability of intermodulation products, which tend to produce rough and rasping reproduction.

(3) *High D.C. to A.C. conversion efficiency.* High efficiency, though desirable, is less necessary in A.C. mains than in battery operated receivers. It may be achieved by making the minimum anode voltage as low as possible, by using a high H.T. voltage and a Class B push-pull output stage.

(4) *High power output.* Power outputs of about 3,000 mW maximum are generally adequate for most living rooms, but much larger values are required for public address systems.

(5) *Low slope resistance.* This helps to damp out loudspeaker cone resonances. Most loudspeakers have several resonances, a major one occurring between 50 and 100 c.p.s., and they can be objectionable if not adequately damped.

A comparison can now be made between the two types of output valve, the triode, and the tetrode or pentode. The triode has a low power sensitivity ; an average value for a D.C. power dissipation of 12 watts is about 150 mW per 1 volt R.M.S. grid input. The beam tetrode has a sensitivity of about 1,000 mW per volt for the same D.C. power. In a triode, distortion is largely confined to the second harmonic, and it falls as the load resistance increases. The beam tetrode has characteristics similar to the pentode and it therefore produces distortion containing a proportion of the higher harmonics. There is a load resistance value at which second harmonic is a minimum, but third harmonic steadily rises with increase of load resistance (see Fig. 10.10*b*). This is a disadvantage because the impedance of the loudspeaker speech-coil increases at the higher frequencies. This increase in load impedance [8] is often limited by a series combination of capacitance and resistance connected across the primary of the output transformer. The reactance of the capacitance falls as the frequency increases, and

the effect of the series resistance becomes more and more pronounced, thus tending to stabilize the output load. This also has the advantage of reducing the accentuation of the high frequencies. The accentuation is due to the rising impedance of the speech-coil in association with the high internal resistance of the tetrode, which tends to maintain a constant current through the speech-coil if no correcting circuit is applied.

Owing to the shape of its I_aE_a characteristics, the beam tetrode has a lower minimum anode voltage than the triode, and its maximum D.C. to A.C. conversion efficiency, in spite of the loss of power due to screen current, is therefore higher, about 35% as compared with 23% for the triode. For the same reason the tetrode produces a larger power output than a triode operating under similar H.T. conditions. The lower internal resistance of the triode is of considerable advantage in damping loudspeaker resonances.

Summarizing, the triode is preferable when high quality is essential, whilst the tetrode is better when high power sensitivity and efficiency are desirable.

10.4. The Calculation of Power Output and Harmonic Distortion.[6, 9, 15, 17] The power output and distortion produced by an output valve supplying a resistance load may be calculated from I_aE_a characteristic curves, taken at specified grid-bias voltages, generally equally spaced; the number of curves required is at least one more than the number of the harmonic, the amplitude of which is to be calculated. Thus, if distortion up to the fourth harmonic is to be calculated, curves are needed for five grid bias voltages. We shall take first the case of a triode having mainly second harmonic distortion. The normal grid bias for any given anode voltage is estimated from the I_aE_g characteristic curves; it should correspond approximately to the centre of the straight part of the characteristic, and generally is less than half (about 35 to 45% of) the cut-off grid bias voltage. Having determined the normal operating bias voltage ($-E_{g1}$), the minimum negative grid voltage ($-E_{g2}$) is fixed by start of grid current (in battery valves E_{g2} is slightly positive, but in mains valves it is negative, being about $-0{\cdot}5$ to -1 volt). For a sinusoidal input voltage the maximum negative grid voltage $-E_{g3}$ is equal to $-(2E_{g1}-E_{g2})$. The three I_aE_a characteristic curves for these grid bias voltages, $-E_{g2}$, $-E_{g1}$ and $-E_{g3}$, are the ones selected for calculating second harmonic distortion and power output, and they correspond to angular positions for a cosine *

* The cosine expression for input voltage is used in preference to the sine as was the case for Part I.

wave input voltage of 0°, 90°, 180°, 270° and 360°. Fig. 10.3*a* shows the curves with a load line *ZZ'* drawn across them. Although

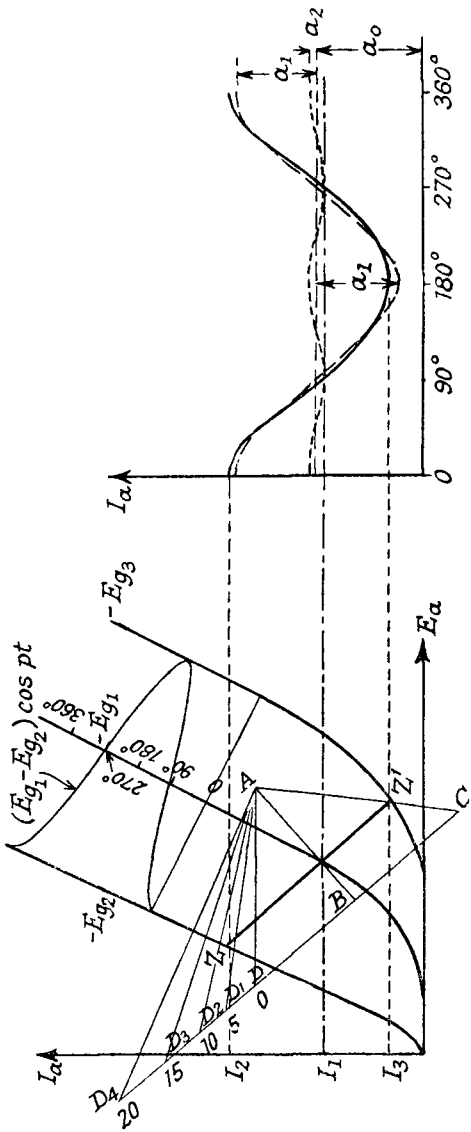

FIG. 10.3.—(*a*) Load Characteristic and Distortion with a Triode Valve.
(*b*) Time Relationships of the Fundamental and Harmonic Components of the Output Wave from (*a*).

the grid voltages are equally spaced, the separations between the curves are unequal, showing that the I_aE_g characteristic is non-linear and harmonic distortion is present. The shape of the output current

wave is shown to the right in Fig. 10.3*b*, and we will assume that it can be completely analysed into D.C., fundamental and second harmonic components; the expression for the output current is therefore

$$I_a = a_0 + a_1 \cos pt + a_2 \cos 2pt \quad . \quad . \quad . \quad 10.9$$

where a_0 = D.C. component of current
a_1 = fundamental A.C. peak current
a_2 = second harmonic A.C. peak current
and $p = 2\pi f$ = pulsance of the input frequency.

The three characteristic curves give three values of current I_2, I_1 and I_3, which satisfy expression 10.9, so that the values of a_0, a_1 and a_2 in terms of these currents can be found as follows:

At $-E_{g2}$, $pt = 0$; $I_a = I_2 = a_0 + a_1 + a_2$. . 10.10.
At $-E_{g1}$, $pt = 90°$; $I_a = I_1 = a_0 - a_2$ . . 10.11
and at $-E_{g3}$, $pt = 180°$; $I_a = I_3 = a_0 - a_1 + a_2$. 10.12.

Subtracting 10.12 from 10.10 gives

$$a_1 = \frac{I_2 - I_3}{2} \quad . \quad . \quad . \quad . \quad 10.13.$$

Therefore Power output,

$$P_0 = \frac{a_1^2 R_0}{2} = \frac{(I_2 - I_3)^2 R_0}{8} \quad . \quad . \quad . \quad 10.14.$$

Adding 10.10 and 10.12

$$I_2 + I_3 = 2(a_0 + a_2)$$
$$= 2(I_1 + 2a_2).$$

Therefore $$a_2 = \frac{I_2 + I_3 - 2I_1}{4} \quad . \quad . \quad . \quad 10.15.$$

$$\text{Second Harmonic ratio} = \frac{a_2}{a_1} = \frac{I_2 + I_3 - 2I_1}{2(I_2 - I_3)} \quad . \quad 10.16.$$

A direct reading harmonic scale may be constructed [20] for placing over the $I_a E_a$ curves so as to read percentage second harmonic directly. It is developed as follows:

If the Second Harmonic percentage $= x$

$$\frac{x}{100} = \tfrac{1}{2} \times \frac{(I_2 - I_1) - (I_1 - I_3)}{(I_2 - I_1) + (I_1 - I_3)}$$

$$= \tfrac{1}{2} \cdot \frac{y-1}{y+1} \quad . \quad . \quad . \quad . \quad 10.17$$

where $$y = \frac{I_2 - I_1}{I_1 - I_3}.$$

Rearranging 10.17 to express y in terms of x,

$$y = \frac{50+x}{50-x} \quad . \quad . \quad . \quad . \quad 10.18.$$

The values of y for different percentages of second harmonic are tabulated below.

$x\%$	1	2	3	4	5	10	15	20
y	1·04	1·082	1·127	1·173	1·221	1·5	1·86	2·33

To form the direct reading harmonic scale a right angled-triangle ABC is constructed as in Fig. 10.4, where AB and BC have any convenient lengths. A series of lines AD_1, AD_2, etc., is drawn to meet BC produced (on the opposite side of B to C) such that $BD/BC = y$.

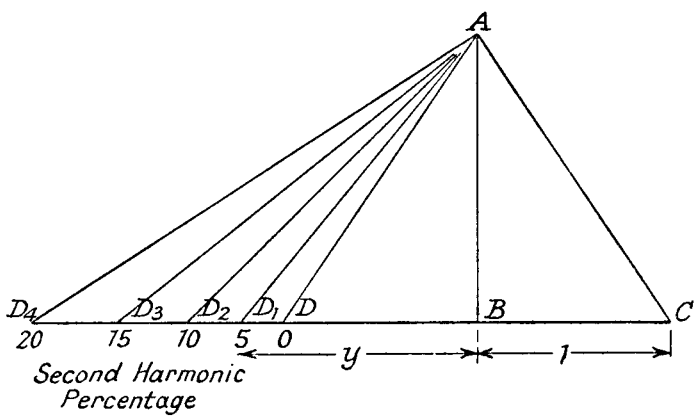

FIG. 10.4.—A Direct Reading Second Harmonic Scale.

Thus for 10% second harmonic $BD_2/BC = 1{\cdot}5$; corresponding lines are drawn for other values and each is marked with its appropriate harmonic percentage. The triangle ABC (on transparent paper) is placed on top of the I_aE_a curves so that DBC is parallel to the selected load line, and it is moved about until AB and AC pass through I_1 and I_3 respectively as shown in Fig. 10.3*a*. The AD line passing through Z gives the percentage second harmonic directly. If it should happen that $I_2 - I_1 < I_1 - I_3$, the triangle is reversed and adjusted so that AB and AC pass through I_1 and I_2 respectively and the AD line passing through Z' gives the percentage second harmonic distortion.

For an output valve (such as a beam tetrode) having the I_aE_a characteristics shown in Fig. 10.5, five grid bias voltages are needed for calculating up to the fourth harmonic. The bias voltages are

chosen to be equally spaced so that they correspond to angular positions of the cosine wave input voltage of 0°, 60°, 90°, 120°, 180°, etc. Three of the voltages are the same as for the second harmonic measurement, viz., $-E_{g2}$, $-E_{g1}$, and $-E_{g3}$, and the other two

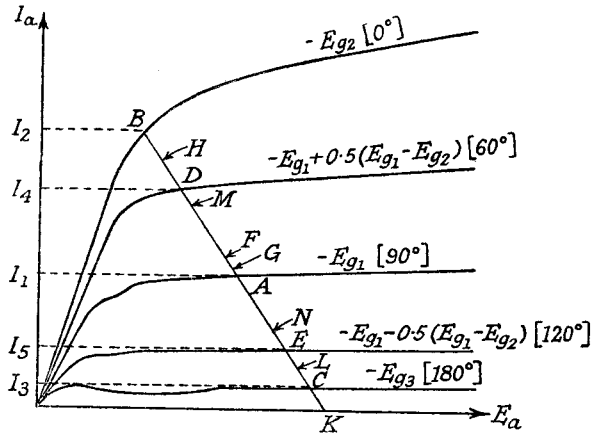

FIG. 10.5.—The Load Characteristic on the I_aE_a Curves of a Tetrode Valve.

voltages are $-E_{g1}\pm 0{\cdot}5(E_{g1}-E_{g2})$. We will assume that the anode current expression is

$$I_a = a_0+a_1\cos pt+a_2\cos 2pt+a_3\cos 3pt+a_4\cos 4pt \quad . \quad 10.19.$$

At $-E_{g2}$, $pt=0$. $I_2 = a_0+a_1+a_2+a_3+a_4$ . . . 10.20

$-E_{g1}+0{\cdot}5\,(E_{g1}-E_{g2})$, $pt=60°$.

$$I_4 = a_0+0{\cdot}5a_1-0{\cdot}5a_2-a_3-0{\cdot}5a_4 \quad . \quad 10.21.$$

$-E_{g1}$, $pt=90°$. $I_1 = a_0-a_2+a_4$ 10.22

$-E_{g1}-0{\cdot}5\,(E_{g1}-E_{g2})$, $pt=120°$.

$$I_5 = a_0-0{\cdot}5a_1-0{\cdot}5a_2+a_3-0{\cdot}5a_4 \quad . \quad 10.23$$

$-E_{g3}$, $pt=180°$. $I_3 = a_0-a_1+a_2-a_3+a_4$ . . 10.24.

Subtracting 10.24 from 10.20

$$I_2-I_3 = 2(a_1+a_3)$$

and 10.23 from 10.21

$$I_4-I_5 = a_1-2a_3.$$

Solving the above for a_1

$$a_1 = \frac{(I_2-I_3)+(I_4-I_5)}{3} \quad . \quad . \quad . \quad 10.25.$$

Therefore Power output,

$$P_0 = \tfrac{1}{2}a_1^2R_0 = \frac{[(I_2-I_3)+(I_4-I_5)]^2R_0}{18} \quad . \quad 10.26a.$$

Solving for a_3

$$a_3 = \frac{(I_2 - I_3) - 2(I_4 - I_5)}{6} \quad . \quad . \quad 10.27.$$

$$\text{Third harmonic ratio} = \frac{a_3}{a_1} = \frac{(I_2 - I_3) - 2(I_4 - I_5)}{2[(I_2 - I_3)+(I_4 - I_5)]} \quad 10.28a.$$

Adding 10.24 to 10.20

$$I_2+I_3 = 2(a_0+a_2+a_4)$$
$$= 2(I_1+2a_2).$$

Therefore

$$a_2 = \frac{I_2+I_3 - 2I_1}{4} \quad . \quad . \quad . \quad 10.29.$$

$$\text{Second harmonic ratio} = \frac{a_2}{a_1} = \tfrac{3}{4}\,\frac{I_2+I_3 - 2I_1}{(I_2 - I_3)+(I_4 - I_5)} \quad . \quad 10.30.$$

Adding 10.21 and 10.23

$$I_4+I_5 = 2a_0 - a_2 - a_4$$
$$I_2+I_3 = 2a_0+2a_2+2a_4.$$

Therefore

$$I_2+I_3 - I_4 - I_5 = 3a_2+3a_4.$$

Substituting 10.29 for a_2 in the above

$$a_4 = \frac{1}{12}(I_2+I_3 - 4I_4 - 4I_5+6I_1) \quad . \quad 10.31.$$

$$\text{Fourth harmonic ratio} = \frac{a_4}{a_1} = \tfrac{1}{4}\frac{(I_2+I_3) - 4(I_4+I_5)+6I_1}{(I_2 - I_3)+(I_4 - I_5)} \quad .10.32.$$

Solving for a_0 gives

$$a_0 = \tfrac{1}{6}(I_2+I_3+2I_4+2I_5) \quad . \quad . \quad . \quad 10.33.$$

A direct reading third harmonic scale may be constructed in a similar way to the scale for second harmonic in the first example. Expression 10.27 may be written in terms of the percentage harmonic, x, and y, the ratio $\dfrac{I_2 - I_3}{I_4 - I_5}$,

$$\frac{x}{100} = \frac{a_3}{a_1} = \frac{y - 2}{2(y+1)}. \quad . \quad . \quad .10.34a.$$

Rewriting 10.34a so as to give y in terms of x

$$y = \frac{100+x}{50 - x} \quad . \quad . \quad . \quad 10.34b.$$

The above expression is true when $(I_2 - I_3) > 2(I_4 - I_5)$, but for $(I_2 - I_3) < 2\,(I_4 - I_5)$, a_3 is negative and

$$y = \frac{100 - x}{50+x} \quad . \quad . \quad . \quad .10.34c.$$

The values of y for different distortion percentages and the two conditions, (*a*) $(I_2 - I_3) > 2(I_4 - I_5)$ and (*b*) $(I_2 - I_3) < 2(I_4 - I_5)$ are as follows:

$x\%$		0	1	2	3	4	5	10	15	20
y	(*a*)	2	2·065	2·125	2·19	2·26	2·335	2·75	3·29	4
	(*b*)	2	1·942	1·885	1·83	1·777	1·728	1·5	1·308	1·142

For the direct reading scale, an isosceles triangle ABC is constructed as in Fig. 10.6. (The isosceles shape is merely for convenience and is not essential.) The base BC is bisected at E, which is joined to A. Lines AD, etc., are drawn from A to cut BC (condition *b*) or BC produced (condition *a*) such that $BD/BC = y/2$. The triangle ABC (on transparent paper) is placed over the I_aE_a curves with BC parallel to the load line, AB passing through

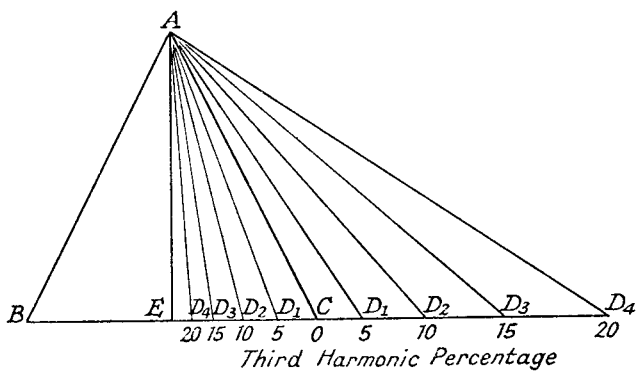

FIG. 10.6.—A Direct Reading Scale for Third Harmonic Percentage Distortion.

I_4 and AE through I_5. The triangle is now moved, maintaining BC parallel to, and at the same perpendicular distance from, the load line until AB passes through I_2. The distortion line AD passing through the intersection of I_3 and the load line, i.e., point C in Fig. 10.5, gives the percentage distortion directly.

Second harmonic distortion may be measured using the direct reading scale with I_1, I_2 and I_3 as indicated in the first example. This assumes that $I_2 - I_3 \simeq 2(I_4 - I_5)$, i.e., the third harmonic percentage is almost zero. The error introduced in the second harmonic percentage reading by this assumption is of the same percentage order as the third harmonic percentage. Thus the error introduced by 2% third harmonic is approximately 2% of the second harmonic percentage, i.e., a measurement of 5% second harmonic by the direct reading scale might be either 4·9% or 5·1%.

When the output wave shape is symmetrical about I_1

$$\frac{I_2+I_3}{2} = I_1 = \frac{I_4+I_5}{2}$$

and there is no second and fourth harmonic.

The amplitudes of the individual current components in expression 10.19 can be determined by comparatively simple geometrical constructions.[44] The increase in D.C. component due to the application of the signal is, from 10.33,

$$\begin{aligned} a_0 - I_1 &= \tfrac{1}{3}\left[\left(\frac{I_2+I_3}{2} - I_1\right)+2\left(\frac{I_4+I_5}{2} - I_1\right)\right] \\ &= \tfrac{1}{3}(FA+2GA) \end{aligned}$$

where F bisects the line BC in Fig. 10.5 and G bisects DE. From 10.25

$$\begin{aligned} a_1 &= \tfrac{2}{3}\left[\frac{I_2+I_4}{2} - \frac{I_3+I_5}{2}\right] \\ &= \tfrac{2}{3}(HK - LK) = \tfrac{2}{3}HL \end{aligned}$$

where H bisects BD and L bisects EC.
Expression 10.29 can be written

$$\begin{aligned} a_2 &= \tfrac{1}{2}\left[\frac{I_2+I_3}{2} - I_1\right] \\ &= \tfrac{1}{2}(FK - AK) = \tfrac{1}{2}FA. \end{aligned}$$

The value of a_3 can be expressed from 10.27 as

$$\begin{aligned} a_3 &= \tfrac{1}{3}\left[\left(\frac{I_1+I_2}{2} - I_4\right) - \left(\frac{I_1+I_3}{2} - I_5\right]\right) \\ &= \tfrac{1}{3}(MD - NE), \end{aligned}$$

where M bisects BA and N bisects AC.

If M is a lower current point than D, as in Fig. 10.5, MD becomes $-DM$ where DM is the distance from D to M.

From 10.31

$$\begin{aligned} a_4 &= \tfrac{1}{6}\left[\left(\frac{I_2+I_3}{2} - I_1\right) - 4\left(\frac{I_4+I_5}{2} - I_1\right)\right] \\ &= \tfrac{1}{6}(FA - 4GA). \end{aligned}$$

10.5. Audio Frequency Distortion with a Complex Anode Load Impedance. The analysis of Section 10.4 is developed on the assumption that the load impedance in the anode circuit of the output valve is resistive only, and this is generally true for the medium frequencies with transformer coupling. At low audio frequencies (50 to 150 c.p.s.) the inductance of the transformer primary may be comparable with the resistance load, whilst at high

frequencies (over 3,000 c.p.s.) stray capacitance and leakage inductance combine to produce a complex load. Furthermore, when the load on the output valve is the loudspeaker speech-coil, this forms a complex load, the resistive and reactive components of which vary with frequency. At low frequencies it is almost entirely resistive, but at high frequencies it is a mainly inductive impedance; there are rapid changes of impedance at frequencies in the neighbourhood of diaphragm resonances.[1] In spite of this, calculations and measurements assuming resistance loads are of value in determining the best practical operating conditions. Matching of the loudspeaker speech-coil to the output valve is performed by choosing an output transformer turns-ratio, which converts the modulus of the impedance of the speech coil at 400 c.p.s. to an impedance equal to the optimum load for the output valve. For example, suppose the optimum load is R_0 and the speech-coil impedance at 400 c.p.s. is $R_{sc}+jX_{sc}$, then the primary/secondary turns-ratio is chosen as

$$\frac{N_p}{N_s} = \sqrt{\frac{R_0}{\sqrt{R_{sc}^2+X_{sc}^2}}}$$

The representation of a complex load on the I_aE_a characteristics is (see Section 2.6, Part I) to be a closed curve similar in shape to a sheared ellipse, the inclination of the curve to the horizontal normally being fixed by the resistance component, and the width by the reactance component. When the reactance and resistance are in parallel, a large reactance leads to a narrow ellipse, but the reverse is true for a series circuit. The chief effect of a complex output load in the anode circuit of a valve having linear I_aE_a characteristics is to produce attenuation (frequency) distortion, causing a reduction in power output at low or high frequencies. The extent of the reduction depends on the relative value of the resistance and reactance and whether they are in parallel or series. Harmonic distortion is produced if the load curve enters the cramped low I_a region or if it cuts the E_a axis, i.e., if the valve is taken into the cut-off point of anode current.

With the practically realizable I_aE_a characteristics illustrated in Fig. 10.7*a*, it is important to note that harmonic distortion tends to be greater with a complex load than with a resistance load, for the locus curve passes through the more cramped low anode current region of the I_aE_a characteristics (see *CD* in Fig. 10.7*a*). A typical locus load line for an impedance consisting of resistance and reactance is shown in Fig. 10.7*a*. The direction of rotation round the locus curve depends on the type of reactance. If it is inductive

the direction is clockwise for input signal increasing in a positive direction, i.e., decreasing negative grid voltage, causes the anode current to rise according to the lower curve. The current wave shape tends to be asymmetric with respect to a vertical line through

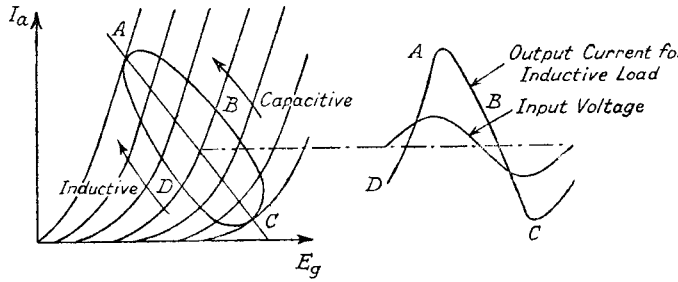

FIG. 10.7*a*.—A Reactive Locus Load Curve on the I_aE_a Characteristics with the Output Current for an Inductive Anode Load.

maximum amplitude, its leading edge being concave and trailing edge convex as shown in Fig. 10.7*a*. This is typcial of the conditions obtaining with an output transformer at low audio frequencies. The direction round the locus curve is reversed for a capacitive load, increasing input signal causing anode current to rise according to the top curve. The operating I_aE_g characteristic has a shape similar to that of the locus curve on the I_aE_a characteristics as

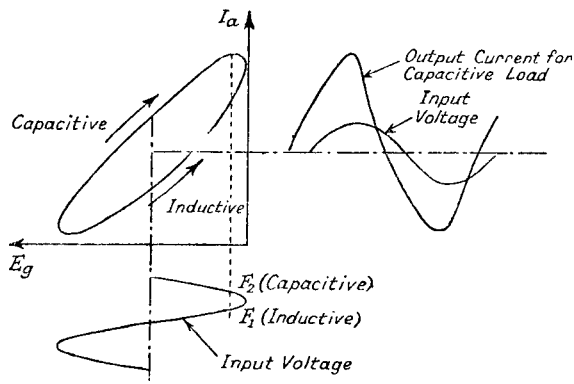

FIG. 10.7*b*.—A Reactive Locus Load Curve on the I_aE_g Characteristics with the Output Current for a Capacitive Anode Load.

illustrated in Fig. 10.7*b*. The lower curve represents the condition for increasing (positively) input voltage and the upper decreasing input voltage when the anode load is inductive ; the reverse is true of a capacitive load. The current wave shape for the latter

is shown in Fig. 10.7*b*, and it is the reverse of that in Fig. 10.7*a*, its leading edge being convex and trailing edge concave. Maximum anode current does not occur at maximum instantaneous input voltage but later in the cycle (point F_1) for an inductive load and earlier (point F_2) for a capacitive load.

10.6. Measurement of Power Output and Distortion. Measurement of power output and distortion is usually carried out at a fixed frequency, generally either the mains frequency or 400 c.p.s.

10.6.1. Measurement with a Mains Frequency Voltage Source. A schematic diagram of the apparatus is shown in

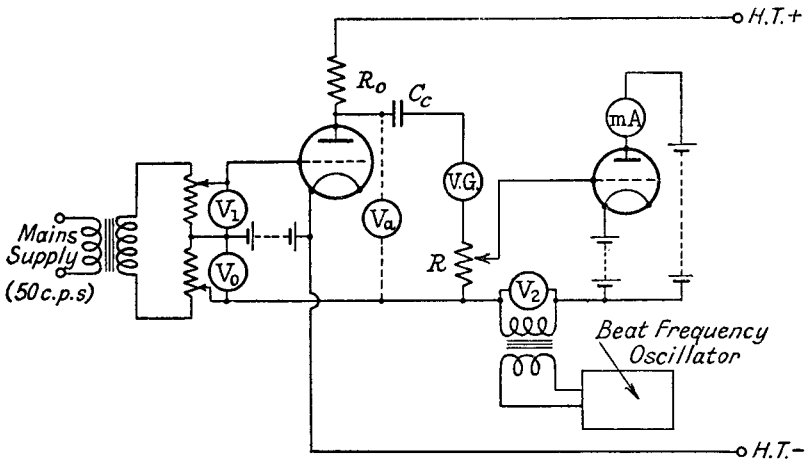

FIG. 10.8.—Measurement of Power Output at the Mains Frequency.

Fig. 10.8. Owing to the low frequency of the input signal the anode load is not by-passed by a choke, since it is difficult to make a choke with a high enough inductance. (100 H at 50 c.p.s. is only 31,416 ohms.) The resistance load is connected directly in the anode of the output valve, and constant D.C. anode voltage (the condition occurring when using a transformer) is maintained by increasing the H.T. voltage as the load resistance is increased. This is a serious disadvantage since very high H.T. voltages may be required; furthermore, push-pull measurements cannot be made. The fundamental 50 c.p.s. output anode voltage is measured by means of voltmeter V_0, connected across a back-balancing voltage obtained from the transformer supplying the input voltage V_1; this back-balancing voltage is connected to the anode through a vibrating galvanometer (V.G.) and coupling capacitance C_c.

Between the galvanometer and the back balancing voltage is a high resistance (R), across which are developed the harmonic distortion voltages. These voltages may be measured by a detector valve [4] or a dynamometer type milliammeter [10] acting as an harmonic analyser. In series with the grid circuit of this detector valve is a beat frequency oscillator, the frequency of which is adjusted close (within 1 c.p.s.) to that of the harmonic to be measured. The detector produces a beat, between the beat frequency oscillator output and the harmonic voltage, which causes the needle of a milliammeter (mA) in its anode circuit to oscillate at the difference frequency of approximately 1 c.p.s. The amplitude of this oscillation is a measure of the amplitude of the particular harmonic voltage. Each harmonic amplitude may be measured independently by suitably adjusting the frequency of the beat frequency oscillator, e.g., the fourth harmonic is measured by adjusting to approximately 201 or 199 c.p.s. The voltage output of the beat frequency oscillator, measured by V_2, must be maintained constant while the frequency is changed, and the detector may be calibrated initially against the fundamental mains frequency voltage with the oscillator frequency set at 49 or 51 c.p.s. For correct operation the input signal to the detector must not be excessive if the calibration is to hold, and for this reason it is essential that the fundamental component should be balanced out. A disadvantage of this type of harmonic analyser is the difficulty of reading an oscillating pointer, and the strain imposed on the operator.

10.6.2. Measurement with a 400 c.p.s. Voltage Source. The great advantage of using 400 c.p.s. as the fundamental frequency is that a choke may be used to by-pass the D.C. current and, if a centre-tapped connection is employed, push-pull measurements may be made (see Fig. 10.9). A distortion factor meter or a harmonic analyser can be connected to the output to measure total harmonic distortion or to read the ratios (or percentages) of individual harmonics. It is important that the input impedance of the harmonic measuring equipment should be high and much greater than the highest load resistance (about 20,000 ohms) likely to be required. A high input impedance buffer amplifier may be necessary to ensure this. Alternatively a transformer connection may be used between the output valve and distortion measuring equipment, and this is the type of circuit shown in Fig. 10.9. An output voltmeter may be used to determine power output—its resistance must be taken into account as it forms part of the load resistance—or a variable (in steps) resistance output power meter

can be employed, combining the function of adjustable load resistance and power output meter.

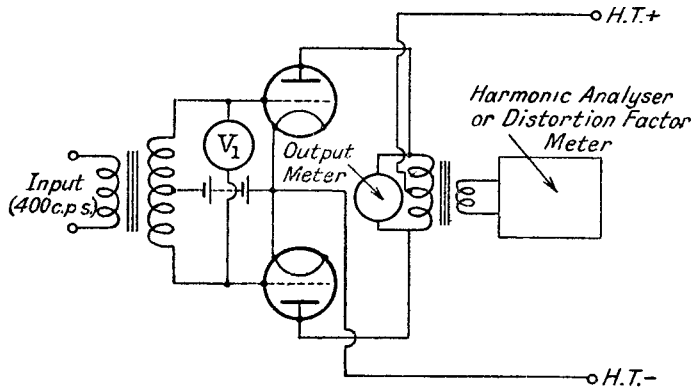

FIG. 10.9.—Measurement of Power Output at 400 c.p.s.

Representative curves of power output and distortion against load resistance are shown in Figs. 10.10*a* and 10.10*b* for a triode and tetrode valve. Referring to Figs. 9.7 and 9.8 showing characteristic I_aE_a curves for a triode and tetrode, respectively, we can see the reason for the particular shapes of the distortion curves. Since the output transformer primary carries the D.C. anode current,

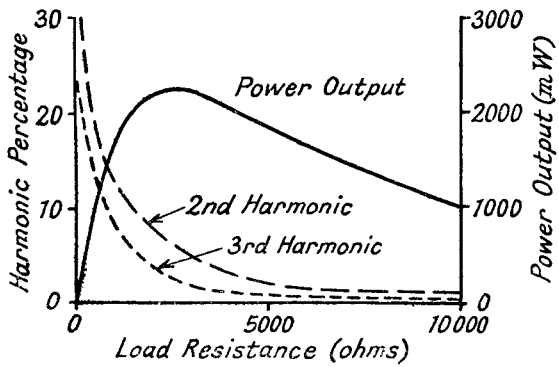

FIG. 10.10*a*.—Typical Power Output and Distortion Curves Against Load Resistance for a Triode Valve.

the D.C. anode voltage is practically the H.T. voltage. The load line FG is therefore pivoted at a point, such as H in Figs. 9.7 and 9.8, on the appropriate bias voltage line, immediately above an anode voltage equal to the H.T. voltage point A.

For the triode valve when the load resistance, R_0, is small, the

line FG in Fig. 9.7 approaches the vertical position, and its lower end projects into the cramped grid voltage—low anode current region. The output anode current wave shape tends to be flattened at its lower end, indicating chiefly second harmonic distortion. As R_0 is increased the line FG becomes less vertical and its lower end is taken out of the cramped low I_a region (see $F'G'$). Hence harmonic distortion decreases with increase of load resistance as shown in Fig. 10.10a.

The tetrode I_aE_a characteristics in Fig. 9.8 indicate that for low values of R_0, load line FG, the output current wave shape is cramped at the low current end, and second harmonic distortion is large. For an intermediate load resistance, line $F'G'$, high and low current

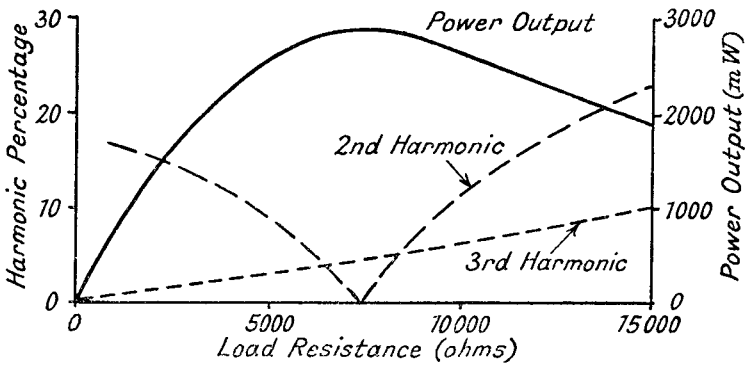

FIG. 10.10b.—Typical Power Output and Distortion Curves Against Load Resistance for a Tetrode or Pentode Valve.

ends of the line are cramped and distortion consists mainly of third harmonic, with second harmonic almost zero. This corresponds to a load resistance of 7,500 ohms on Fig. 10.10b, and usually to maximum power output. At high values of R_0, line $F''G''$, the high current end of the line is more, and the low current end is less, cramped. Second, as well as third, harmonic is now present.

10.7. Non-Linear Harmonic and Intermodulation Distortion in Power Output Valves. An absolute standard for permissible non-linear distortion is difficult to fix because of the number of different factors involved. The critical faculty of the listener and the overall frequency range of the receiver both play an important part; the tolerable distortion is reduced if direct comparison is possible between the undistorted and distorted sound. If the frequency range is reduced greater distortion can be permitted. Massa [14] gives the following as average values for distortion produc-

ing a detectable change of quality on speech. The effect of restricting the high-frequency range is indicated for three cut-off frequency limits. The lowest cut-off frequency (5,000 c.p.s.) gives a frequency range comparable to that of an average broadcast receiver.

	DIRECT COMPARISON		NO COMPARISON.	
Cut-Off Frequency.	Single Stage.	Push-Pull.	Single Stage.	Push-Pull.
14,000 c.p.s. .	5%	3%	10%	5%
8,000 ,, .	5%	3%	10%	7%
5,000 ,, .	12%	> 10%	17%	> 10%

More distortion is tolerable with the single stage having chiefly second harmonic than with the push-pull stage in which third harmonic distortion predominates, and greater distortion can be considered if the high-frequency range is reduced. The value of 5% total harmonic distortion, commonly used to specify the maximum power output condition, is open to criticism since the order of the predominant harmonic is so important in determining quality. The table shows that 3% of third harmonic is as objectionable as 5% of second. If, however, instead of total harmonic distortion the percentages of the individual harmonics are measured, a better estimate of distortion can be obtained. For comparison purposes the percentage of each harmonic is multiplied by the number of the harmonic, i.e., the distortion property of 5% second harmonic is represented by $5 \times 2 = 10$, and that of 3% third harmonic by $3 \times 3 = 9$. This is in accord with the results set out in the table above. Another method [49] is to insert in the distortion factor meter a network having an output voltage frequency response linearly proportional to frequency for a fixed amplitude of input signal. This is equivalent to multiplying the amplitude of each harmonic by its number.

Let us now consider why a given percentage of a higher order harmonic represents greater apparent distortion than the same percentage of a lower order harmonic. Relating harmonics to the musical scale we find that of the first ten all but the seventh and ninth are concordant with the fundamental. For most operational conditions the percentages of the discordant harmonics are very small—an exception is sometimes found in Class B operation—and it is not often possible to read the amplitudes of harmonics greater than the fifth. Hence it would appear that harmonic frequencies are not themselves generally responsible for harsh and discordant reproduction, and, for a single frequency input, whilst distortion causes a change in quality, reproduction is not necessarily rendered unpleasant. With the more usual input signal consisting of a series of frequencies, the property producing harmonic distortion can also

cause intermodulation between the frequency components; a low frequency, f_l may modulate a high-frequency component, f_h, to produce sidebands of $f_h \pm f_l$, $f_h \pm 2f_l$, etc., which can be, and often are, discords with the input frequency components. The relationship between harmonic and intermodulation distortion can be shown by considering the following expression for anode current in terms of grid voltage:

$$I_a = a_0 + a_1 E_g + a_2 E_g^2 + a_3 E_g^3 \quad . \quad . \quad . \quad 10.35.$$

If $E_g = \hat{E}_l \cos p_l t + \hat{E}_h \cos p_h t - E_b$

where $\hat{E}_l \cos p_l t$ represents the low audio frequency

$\hat{E}_h \cos p_h t$,, ,, high ,, ,,

and $-E_b$,, ,, grid bias voltage.

Replacing E_g in 10.35

$$\begin{aligned}
* I_a &= a_0 + a_1(\hat{E}_l \cos p_l t + \hat{E}_h \cos p_h t - E_b) \\
&\quad + a_2(\hat{E}_l \cos p_l t + \hat{E}_h \cos p_h t - E_b)^2 \\
&\quad + a_3(\hat{E}_l \cos p_l t + \hat{E}_h \cos p_h t - E_b)^3 \\
&= a_0 + a_1(\hat{E}_l \cos p_l t + \hat{E}_h \cos p_h t - E_b) \\
&\quad + a_2\left[\frac{\hat{E}_l^2}{2}(1 + \cos 2p_l t) + \frac{\hat{E}_h^2}{2}(1 + \cos 2p_h t) + E_b^2\right. \\
&\qquad \left. + \hat{E}_l\hat{E}_h[\cos(p_h + p_l)t + \cos(p_h - p_l)t] \right. \\
&\qquad \left. - 2\hat{E}_h E_b \cos p_h t - 2\hat{E}_l E_b \cos p_l t\right] \\
&\quad + a_3\left[\frac{\hat{E}_l^3}{4}(\cos 3p_l t + 3\cos p_l t) + \frac{\hat{E}_h^3}{4}(\cos 3p_h t + 3\cos p_h t) - E_b^3\right. \\
&\qquad \left. - \tfrac{3}{2}\hat{E}_l^2 E_b(1 + \cos 2p_l t) - \tfrac{3}{2}\hat{E}_h^2 E_b(1 + \cos 2p_h t)\right. \\
&\qquad \left. + 3\hat{E}_l E_b^2 \cos p_l t + 3\hat{E}_h E_b^2 \cos p_h t\right. \\
&\qquad \left. + \tfrac{3}{4}.\hat{E}_l^2\hat{E}_h(2\cos p_h t + \cos(p_h + 2p_l)t + \cos(p_h - 2p_l)t)\right. \\
&\qquad \left. + \tfrac{3}{4}\hat{E}_l\hat{E}_h^2(2\cos p_l t + \cos(2p_h + p_l)t + \cos(2p_h - p_l)t)\right. \\
&\qquad \left. - \tfrac{3}{2}\hat{E}_l\hat{E}_h E_b(\cos(p_h + p_l)t + \cos(p_h - p_l)t)\right] \quad . \quad . \quad 10.36.
\end{aligned}$$

The modulation ratio of the first intermodulation sideband $\frac{(p_h \pm p_l)}{2\pi}$ of the high audio frequency $\frac{(p_h)}{2\pi}$ is

$$\begin{aligned}
M_1 &= \frac{a_2\hat{E}_l\hat{E}_h - \frac{3}{2}a_3\hat{E}_l\hat{E}_h E_b}{a_1\hat{E}_h - 2a_2\hat{E}_h E_b + a_3\left[\frac{3\hat{E}_h^3}{4} + 3\hat{E}_h E_b^2 + \frac{3}{2}\hat{E}_h E_l^2\right]} \\
&= \frac{\hat{E}_l(a_2 - \frac{3}{2}a_3 E_b)}{a_1 - 2a_2 E_b + a_3[\frac{3}{4}\hat{E}_h^2 + 3E_b^2 + \frac{3}{2}\hat{E}_l^2]} \quad . \quad . \quad 10.37.
\end{aligned}$$

---

* $\cos^2\theta = \dfrac{1 + \cos 2\theta}{2}$; $\cos\theta + \cos\phi = \dfrac{\cos(\theta+\phi) + \cos(\theta-\phi)}{2}$.

$\cos^3\theta = \dfrac{3\cos\theta + \cos 3\theta}{4}$.

The modulation ratio for the second sideband $\frac{p_h \pm 2p_l}{2\pi}$ is

$$M_2 = \frac{\frac{3}{4}a_3\hat{E}_l^2}{a_1 - 2a_2E_b + a_3[\frac{3}{4}\hat{E}_h^2 + 3E_b^2 + \frac{3}{2}\hat{E}_l^2]} \quad . \quad . \quad 10.38.$$

If $\hat{E}_h = 0$, we have as the second harmonic $\left(\frac{2p_l}{2\pi}\right)$ ratio of $\frac{p_l}{2\pi}$

$$H_2 = \frac{\hat{E}_l\left[\frac{a_2}{2} - \frac{3}{2}a_3E_b\right]}{a_1 - 2a_2E_b + a_3[\frac{3}{4}\hat{E}_l^2 + 3E_b^2]} \quad . \quad . \quad 10.39$$

and for the third harmonic $\left(\frac{3p_l}{2\pi}\right)$ ratio

$$H_3 = \frac{\frac{1}{4}a_3\hat{E}_l^2}{a_1 - 2a_2E_b + a_3[\frac{3}{4}\hat{E}_l^2 + 3E_b^2]} \quad . \quad . \quad 10.40.$$

If we neglect the second term $-\frac{3}{2}a_3E_b$ in the numerators of 10.37, and 10.39, and terms containing $\hat{E}_h$ and $\hat{E}_l$ in the denominators of 10.37, 10.38, 10.39, and 10.40, we find that

$$M_1 = 2H_2$$

and

$$M_2 = 3H_3.$$

It is clear from the above expressions that the intermodulation terms responsible for unpleasant reproduction are proportional to the product of the individual harmonic of a single frequency input multiplied by the harmonic number. Hence " weighting " (as it is called) of the harmonics from a single frequency input is justified as a method of estimating apparent distortion. Higher power terms in the I_aE_g expression 10.35 introduce additional harmonic sidebands, and sidebands to harmonics of the high frequency. For example, $a_4E_g^4$ added to 10.35, produces in the output the following additional intermodulation sidebands,

$$\frac{p_h \pm 3p_l}{2\pi}, \quad \frac{2p_h \pm 2p_l}{2\pi} \text{ and } \frac{3p_h \pm p_l}{2\pi}.$$

An illustration of the way in which intermodulation [24] occurs is given in Fig. 10.11. The input signal consists of a large amplitude low audio frequency and a smaller amplitude high frequency. Typical operating I_aE_g characteristics for a triode (dotted extension) and tetrode (full line) are shown in the figure ; the flattening of the tetrode I_a curve at low bias voltages is due to the load line projecting into the knee of the I_aE_a characteristics (see $F'G'$ in Fig. 9.8). The wave shape of the high-frequency output current—the low frequency is omitted for the sake of clarity—shows that it is modu-

lated by the low frequency. For the tetrode the modulation envelope changes at the rate of $2f_l$, because amplification is reduced when the low-frequency input carries the grid voltage into the region BC and into the region of high negative voltage beyond A. With the triode, modulation in the region BC is absent; the modulation envelope has a fundamental frequency of f_l, i.e., there is no

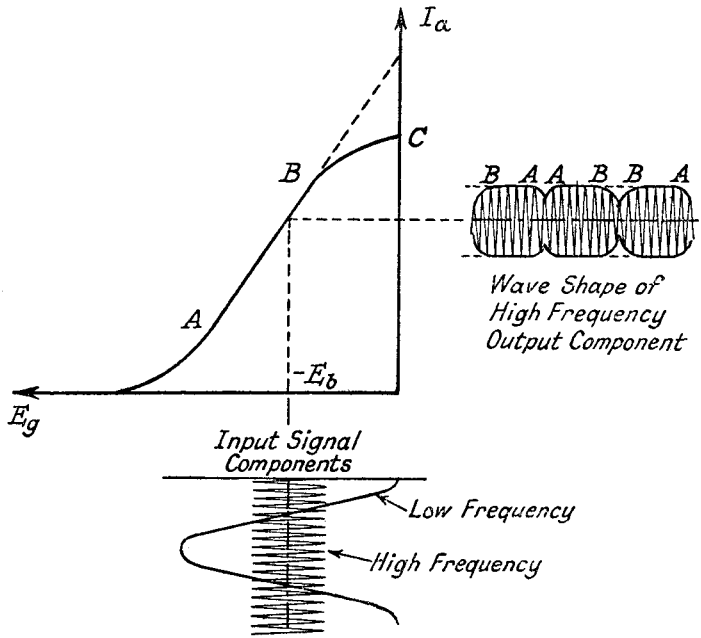

FIG. 10.11.—Intermodulation of a High Audio Frequency by a Low Audio Frequency.

dip in the envelope from B to B, and intermodulation distortion is much less.

Methods of estimating distortion by measuring intermodulation tones have been developed,[35, 45] though it is doubtful if the added complication of apparatus justifies their use in comparison with the single frequency method and harmonic ratios multiplied by their harmonic number. Harries, who appears to have been the first to suggest intermodulation distortion measurements, used two input frequencies of 70 c.p.s. and 1,000 c.p.s., having an amplitude ratio of 9 to 1. The amplitudes of the 1,000 c.p.s. frequency and its sidebands were measured with a harmonic analyser, the sidebands being expressed as a percentage of the 1,000 c.p.s. output. A triode was found to produce mainly first sideband voltages (1,000 $\pm$ 70 c.p.s.),

and all sideband amplitudes were generally small. A pentode valve showed a greater range of sidebands with the second (1,000±140 c.p.s.) as the largest. The second harmonic frequency (2,000 c.p.s.) was overmodulated and had sidebands larger than itself. Under these conditions distortion was marked, and reproduction harsh. Harries finally suggests the following quality grades:

(1) high quality: no sideband should represent more than 5% modulation where modulation percentage

$$= \frac{2 \times \text{sideband amplitude} \times 100}{\text{fundamental}};$$

(2) good commercial quality: first and second sideband modulation percentages to be less than 30% and 5% respectively;

(3) objectionable: this to be denoted by second sideband modulation percentage exceeding 5%.

"Undistorted" power output is to be defined as the power output given by a single frequency sine wave input of amplitude equal to the sum of the amplitudes of the two frequencies satisfying condition 2.

10.8. Push-Pull Operation.

10.8.1. Introduction.[7] Push-pull operation is obtained from a pair of valves by applying to the grid of one valve a voltage in phase opposition to that applied to the other (see Fig. 10.12). The anodes of these valves are joined to opposite ends of the primary of a transformer, the centre tap of which is connected to H.T. positive. The D.C. anode currents produce opposing voltages in the transformer primary, but the A.C. output currents, owing to the 180° phase shift between the grid voltages, are additive. Thus the total A.C. current in the primary is

$$\begin{aligned} I_{at} &= I_{a1} - (-I_{a2}) \\ &= I_{a1} + I_{a2}. \end{aligned}$$

Push-pull operation has four important advantages.

(1) Even harmonic distortion produced in each output valve is partially (completely, if matched valves are employed) cancelled.

(2) The D.C. current component in the output transformer is reduced considerably or cancelled. This means less attenuation (frequency) and non-linear (harmonic) distortion from, and more efficient operation of, the output transformer. A much smaller air gap is required so that

primary inductance, for a given number of turns, is greater than for the single-valve output transformer.

(3) Hum voltages in the H.T. supply and cathode or grid bias circuits, if common to both valves, are cancelled.

(4) Instability due to a high impedance H.T. supply circuit is made less likely because A.F. voltages produced in this circuit by the output valves cancel each other.

Cancellation of hum in a common cathode bias circuit and of second harmonic distortion can be demonstrated by assuming the following power series to represent the I_aE_g characteristic of each valve

$$I_a = a_0+a_1E_g+a_2E_g{}^2+a_3E_g{}^3 \quad . \quad . \quad . \quad 10.41.$$

Let $$E_g = \pm\hat{E}_1 \cos p_1t+\hat{E}_u \cos p_ut - E_b$$

where $\pm\hat{E}_1 \cos p_1t$ = signal voltage applied in push-pull connection to each valve,

$\hat{E}_u \cos p_ut$ = undesired hum or interference voltage applied in parallel connection to each valve

and $-E_b$ = grid bias voltage.

$$\begin{aligned} I_{a1} = a_0&+a_1[\hat{E}_1 \cos p_1t+\hat{E}_u \cos p_ut - E_b] \\ &+a_2[\hat{E}_1 \cos p_1t+\hat{E}_u \cos p_ut - E_b]^2 \\ &+a_3[\hat{E}_1 \cos p_1t+\hat{E}_u \cos p_ut - E_b]^3. \end{aligned}$$

$$\begin{aligned} I_{a2} = a_0&+a_1[- \hat{E}_1 \cos p_1t+\hat{E}_u \cos p_ut - E_b] \\ &+a_2[- \hat{E}_1 \cos p_1t+\hat{E}_u \cos p_ut - E_b]^2 \\ &+a_3[- \hat{E}_1 \cos p_1t+\hat{E}_u \cos p_ut - E_b]^3 \end{aligned}$$

Subtracting I_{a2} from I_{a1}, makes all terms except those containing $\hat{E}_1$ and $\hat{E}_1{}^3$ disappear, hence

$$\begin{aligned} \Delta I_{at} &= 2a_1\hat{E}_1 \cos p_1t - 4a_2E_b\hat{E}_1 \cos p_1t+4a_2\hat{E}_1\hat{E}_u \cos p_1t.\cos p_ut \\ &\quad +2a_3[\hat{E}_1{}^3 \cos^3 p_1t+3\hat{E}_1\hat{E}_u{}^2 \cos p_1t \cos^2 p_ut+3E_b{}^2\hat{E}_1 \cos p_1t \\ &\qquad - 3\hat{E}_1\hat{E}_uE_b \cos p_1t.\cos p_ut] \\ &= 2[a_1 - 2a_2E_b+2a_3(\tfrac{3}{4}\hat{E}_1{}^2+\tfrac{3}{2}\hat{E}_u{}^2+3E_b{}^2)]\hat{E}_1 \cos p_1t \\ &\quad +\frac{a_3}{2}\hat{E}_1{}^3 \cos 3p_1t \\ &\quad +2[a_2\hat{E}_1\hat{E}_u - \tfrac{3}{2}\hat{E}_1\hat{E}_uE_b] \cos (p_1\pm p_u)t \\ &\quad +\tfrac{3}{4}a_3\hat{E}_1\hat{E}_u{}^2 \cos (p_1\pm 2p_u)t \quad . \quad . \quad . \quad . \quad . \quad 10.42. \end{aligned}$$

The fundamental, third harmonic, and intermodulation sidebands of the fundamental with the undesired voltage are the only components in the output, the D.C., second harmonic and undesired components being cancelled. If the power series of 10.41 is carried further all parallel connected interference voltages, even harmonics and intermodulation sidebands of the even harmonics are found to

cancel in the output, leaving only the fundamental and odd harmonics with their intermodulation sidebands. If the two valves have slightly different I_aE_g characteristics, i.e., are not exactly matched, the proportion of even harmonic remaining depends on the amount of mismatching. If, for example, each valve normally produces 5% second harmonic and the mismatch in the values of a_2 is 10%, the output contains 0·5% second harmonic.

Before considering the various types of push-pull operation we will consider the methods of obtaining the push-pull antiphase voltages for the grid circuits of the output valves.

10.8.2. Methods of Producing the Push-Pull Grid Voltage.[21, 32] A method of obtaining the push-pull grid voltage from

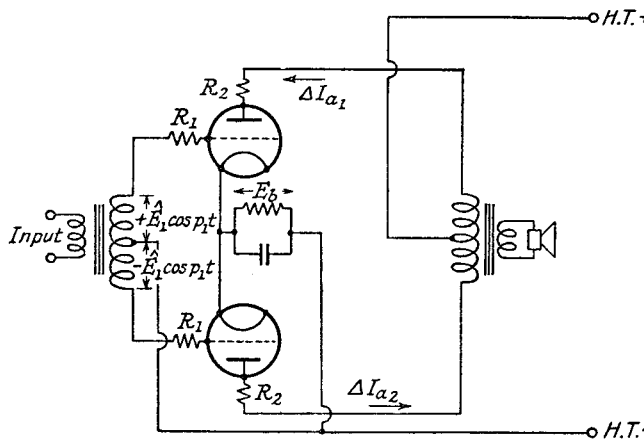

FIG. 10.12.—A Transformer Coupled Push-pull Output Stage.

a diode detector is described in Section 8.7, Part I. The disadvantage from which this suffers is that two ganged potentiometers are required for volume control, so that it is preferable to obtain the antiphase voltages from an A.F. stage after the detector volume control. One of the simplest methods is to use a transformer with centre-tapped secondary as in Fig. 10.12. Provided the transformer is designed to have a high primary inductance, low leakage inductance, and small and equal half secondary self-capacitances, and that the primary and half secondaries are electrically balanced with regard to the centre tap (this implies equal leakage inductances and interwinding capacitances from the primary to half secondaries), satisfactory performance over the A.F. range and the 180° phase shift between the two secondary voltages can be maintained.

A second method (Fig. 10.13), known as paraphase,[3] uses the

phase reversing property of a *RC* coupled A.F. amplifier. Part of the input voltage to one of the push-pull output valves V_3 is taken to the valve V_2, the output of which is connected to the other push-pull valve, V_4. The proportion of voltage taken from the grid of V_3 is equal to the inverse of the amplification from V_2 to V_4, so that the input voltages to V_3 and V_4 are equal but 180° out-of-phase. Correct push-pull operation is achieved by adjustment of the potentiometer R_1 to give minimum sound, with a suitable input frequency (400 or 1,000 c.p.s.), in telephones connected between the H.T. supply and the centre point of the primary of the output transformer. The disadvantages of the paraphase connection are :

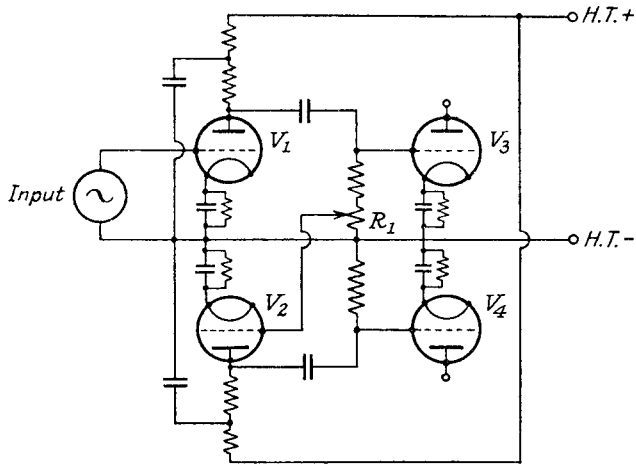

FIG. 10.13.—A Paraphase Push-pull Circuit.

(1) phase changes may occur between the input and output of V_2 at high audio frequencies due to stray capacitance, so that the 180° phase relationship is not maintained, and (2) hum and noise voltages may be introduced and amplified by the extra valve V_2.

A third system employs a cathode as well as an anode load resistance in an amplifier, the voltage for one valve being derived from the cathode and that for the other from the anode circuit as in Fig. 10.14. The objection to this method is the high D.C. voltage between heater and cathode, the possibility of producing hum voltage from the heater circuit across the cathode load resistance R_k, and the comparatively large stray capacitance across the latter, which causes a reduction in gain at high frequencies. An alternative method of connection using negative feedback reduces the stray capacitance and also allows the input to the valve to be earthed.

The dotted lines in Fig. 10.14 show the change in the circuit. The grid leak connection does not affect the A.F. operation of the valve but merely ensures that the correct D.C. bias is applied. Connecting directly from grid to earth applies a large bias to the valve, causing it to operate over the curved portion of its I_aE_g characteristic. When negative feedback is employed, the output voltage to each push-pull stage is less than the input voltage to the phase-changing stage, but distortion is also very low. The preceding amplifier must therefore deliver a larger voltage than is required to operate the push-pull valves, and it is important to guard against distortion in this stage. Chokes [40] wound on the same core, so that D.C. currents neutralize each other, may replace the resistances R_0 and

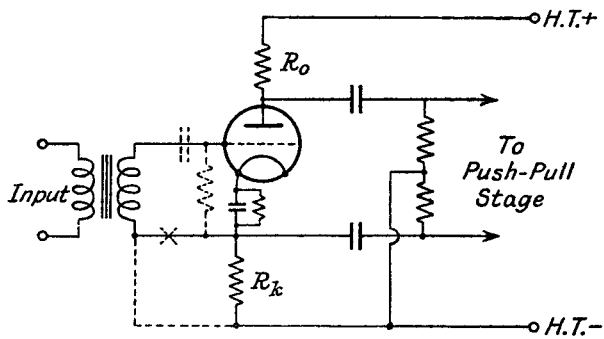

FIG. 10.14.—Push-pull Voltage Output by Means of Equal Anode and Cathode Load Resistances.

R_k if the H.T. voltage is low. Tone control may be achieved by a capacitance shunting R_k; this increases the output across R_0 at high frequencies relative to that across R_k, so that the push-pull outputs at these frequencies are unequal. This is less important since the amplitude of high frequencies is usually small and their harmonics are approaching the inaudible range.

A small secondary winding on the output transformer has been employed to provide the input to the second valve of a push-pull stage. This cannot be entirely satisfactory since it tends to defeat the object of push-pull by applying distortion in the output of one of the push-pull valves to the grid of the second, and cancellation of even harmonics cannot be complete.

The possibility of using the antiphase relationship between screen and anode currents in a heptode [37] valve has been suggested, but great care has to be exercised if equal amplitudes of undistorted push-pull voltages are to be produced.

10.8.3. Types of Push-Pull Stages. Push-pull output stages may be divided into three groups, depending on the biasing point relative to the I_aE_g characteristic. In Class A operation both valves are biased to the centre of the straight part of their I_aE_g characteristics though, owing to the cancellation of even harmonics, the valves may be operated in push-pull beyond the straight part of their characteristics. This method is very satisfactory since distortion is low and anode current to both valves substantially constant; efficiency is, however, low (25% to 35%).

In Class B operation both valves are biased to the curved lower part of their I_aE_g characteristics, i.e., almost into cut-off, and each valve supplies approximately half the output wave shape. Its chief advantages are low current consumption with zero input voltage, and high efficiency (about 60%) for maximum input voltage. The D.C. anode current is initially small but increases with increase of input voltage, and there is considerable economy in H.T. consumption, a very desirable characteristic for the output stage of a battery receiver. For mains receivers H.T. economy is not so important and Class B operation is hardly ever employed. The varying current of a Class B stage would require a H.T. source having very good D.C. voltage regulation. If triodes are used in Class B push-pull, they are usually operated into the positive grid region in order to obtain high efficiency. A special amplifier stage, known as the driver, is needed to supply the power absorbed by the grid current taken on the peaks of input voltage, and the method of operation is generally known as Class B positive drive. With tetrodes the shape of the I_aE_g characteristic makes positive drive of no value, and the term quiescent push-pull is often applied to this mode of operation without grid current.

Class AB operation is sometimes employed in mains receivers with triode output valves to obtain high efficiency and power output. The valves are biased approximately half-way between Class A and Class B conditions and a driver stage is used to allow grid current to be taken. Anode current varies with signal voltage but to a much less extent than with Class B.

Push-pull stages are particularly liable to parasitic oscillation at ultra high frequencies since capacitance coupling between the grid of one valve and the anode of the other is in the correct phase to initiate oscillation. Short leads and resistances of 1,000 and 100 ohms in the grid and anode leads (see R_1 and R_2 in Fig. 10.12), as close to the valve pins as possible, help to prevent this.

10.8.4. Class A Push-Pull. The performance of a push-pull

output stage can be determined by constructing IE_a curves [13] from the I_aE_a characteristics of the individual valves. If the instantaneous anode currents in each valve are I_{a1} and I_{a2} and the coupling coefficient between the two half primaries is very nearly unity (a justifiable assumption for most iron-cored transformers), the effective composite current, $I = I_{a1} - I_{a2}$, can be considered as flowing through one of the half primaries. The composite IE_a curves are therefore obtained by subtracting appropriate pairs of I_aE_a curves of the two valves, so arranged that the grid voltage and anode voltage scales of one valve are in the reverse direction to

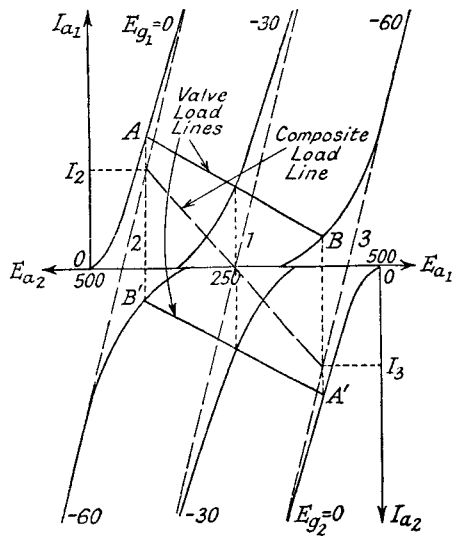

FIG. 10.15.—Composite Current-Anode Voltage Curves for a Class A Push-pull Amplifier.

those of the other. This essential condition of the push-pull connection is fulfilled by Fig. 10.15 ; the I_aE_a curves of the second valve, inverted and reversed with the E_{a2} scale running from right to left, are moved until the E_a points, corresponding to H.T. voltages of 250 on the normal and reversed scales register with each other. If the D.C. grid bias voltage on each valve is — 30 volts, the two I_aE_a curves for $E_g = -30$ volts are added to form the dotted composite IE_a curve 1. The process is repeated for each appropriate pair of I_aE_a curves, thus the composite curve 2 is obtained by adding the curve for $E_g = 0$ of the first valve to that for $E_g = -60$ of the second. Composite curve 3 is plotted by a similar process. It is most important to remember that these composite curves refer to

one-half of the primary, and a load line drawn across them represents a load resistance across a half primary. Hence the equivalent load resistance across the whole primary, i.e., the anode-to-anode load on the valves, is four times this value. For example, an optimum load resistance for the composite curves of 2,000 ohms, requires an anode-to-anode load resistance of 8,000 ohms, and the secondary to total primary turns ratio is adjusted to give the equivalent of 8,000 ohms across the total primary winding. The composite load line passes through the H.T. voltage and a composite current point equal to the difference between the D.C. anode currents of the valves ; if the latter are perfectly matched the composite current is zero as shown in Fig. 10.15. Power output and distortion may be calculated from the composite characteristics in the same manner as for a single stage. Thus, assuming even harmonics to be small in amplitude and third harmonics to be greatest, the power output is, from expression 10.26*a*,

$$P_0 = \frac{[(I_2+I_3)+(I_4+I_5)]^2 R_0}{18} \quad . \quad . \quad 10.26b$$

where I_2 is the intercept of the load line with the composite IE_a curve corresponding to $E_g = 0$ on the first valve and measured on the I_{a1} scale and I_3 is the counterpart of I_2 measured on the I_{a2} scale. The negative sign before I_3 and I_5 in expression 10.26*a* becomes positive because I_3 and I_5 are numerical values of current. The currents I_4 and I_5, measured on the I_{a1} and I_{a2} scales, respectively, are the load line intercepts with composite IE_a curves corresponding to $E_g = -15$ and -45 volts on the first valve. Third harmonic ratio is from 10.28*a*,

$$H_3 = \frac{(I_2+I_3) - 2(I_4+I_5)}{2((I_2+I_3)+(I_4+I_5))} \quad . \quad . \quad .10.28b.$$

Although the composite load line gives the equivalent half-primary load resistance, it is important to note that this is not the load resistance across each valve. The load line for each valve is obtained by projecting vertically (up or down) from the intersections of the composite load line and composite curves on to the corresponding I_aE_a curves for the single valve. Thus the valve load lines are represented by lines AB and $A'B'$ in Fig. 10.15 and, since the valves are operating in Class A push-pull, each has a slope of nearly half that of the composite load line ; i.e., it corresponds to twice the composite load resistance. If both valves have linear I_aE_a characteristics the composite curves are straight lines of twice the slope of the I_aE_a lines, and it may then be proved geometrically

that each equivalent valve load line has a slope of one-half that of the composite line. If the optimum load for a single valve stage is $2R_a$ (the valve resistance), the optimum composite load is half this value, i.e., R_a, so that the optimum anode-to-anode load becomes $4R_a$. The same conclusion is reached if we consider the push-pull stage as consisting of two valve generators connected in series. Their total internal resistance is $2R_a$, and by analogy with the single stage, the optimum load (from anode-to-anode) will be $2 \times 2R_a = 4R_a$. An important advantage of push-pull illustrated by the curves is that owing to the linearity of the composite characteristics, a complex load impedance giving an " elliptical " locus line as in Fig. 10.7*a* produces practically no harmonic distortion.

Owing to the predominance of odd harmonics when distortion occurs in push-pull stages, maximum " undistorted " power output should be assessed for a lower total harmonic percentage than a single valve, approximately in the ratio of 2 to 3 for triodes.

10.8.5. Class B Push-Pull.[18, 25, 29, 31] The performance of push-pull valves under Class B conditions may be shown by constructing composite IE_a curves in exactly the same way as for Class *A*, and these are shown in Fig. 10.16 for three grid bias voltages. Triode characteristics are used in the above illustration to preserve continuity with Fig. 10.15, but tetrode composite curves can be developed in like manner. The load line for each valve is obtained

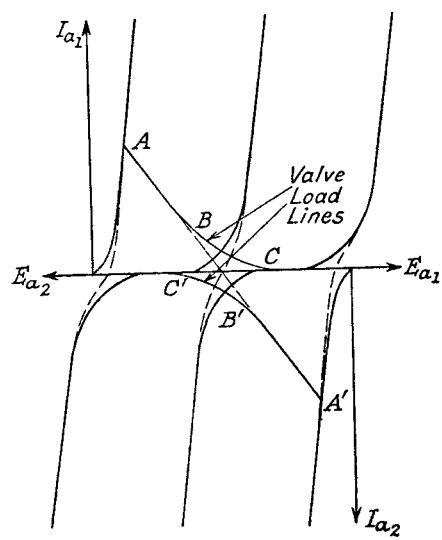

FIG. 10.16.—Composite Current-Anode Voltage Curves for a Class B Amplifier with High Grid Bias and Low Load Resistance.

by projection from the composite to the valve curves as described in the previous section. If the valves have linear I_aE_a characteristics and are biased to cut-off, each valve operates over half a cycle only, and the composite characteristics and load line are identical with the valve characteristics and load line. The anode-to-anode load resistance, which is four times the composite load resistance, is also four times the valve load resistance compared with twice for Class A. Since practical I_aE_a characteristics are always curved, the valves cannot be biased to cut-off and the valve load line only approaches the composite at the extremities of the grid voltage swing. Towards the centre, where both valves are operating, the valve load

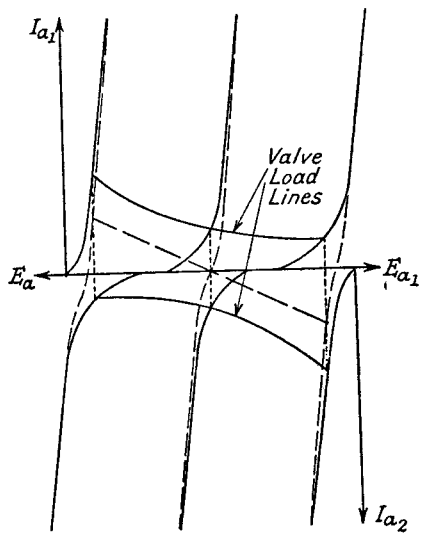

FIG. 10.17.—Composite Current-Anode Voltage Curves for a Class B Amplifier with Low Grid Bias and High Load Resistance.

resistance increases, eventually becoming infinite when the valve reaches cut-off. Hence the valve load line *ABC* is sharply curved as in Fig. 10.16. The degree of curvature is dependent on the grid bias voltage relative to the cut-off bias voltage and also upon the load resistance, a grid bias approaching cut-off bias and a low load resistance producing a more sharply curved load line (similar to *ABC* in Fig. 10.16), which rapidly approaches the composite load line. Conversely for a high load resistance and a bias voltage much less than cut-off bias, the valve load line is less sharply curved and has a slope of nearly twice that of the composite line; this is illustrated in Fig. 10.17.

It is much more difficult to obtain linear composite curves for Class B than for Class A operation, and generally there is a " kink " near zero current, the " kink " becoming more pronounced as the initial bias is increased. This " join-up " distortion,[28] as it is called, is greatest for small output voltages, and it places a limit on the maximum negative initial grid bias which can be employed.

The great advantage of Class B operation, apart from its low quiescent current consumption, is its high anode circuit efficiency. The theoretical maximum, assuming that each valve is biased to cut-off and that the anode voltage of each valve is taken to zero at the extremities of grid swing, is 78·5%. Each valve supplies half the wave shape so that the D.C. current is $\hat{I}/\pi$ where $\hat{I}\cos pt$ is the A.C. output current wave.

$$\text{Therefore D.C. power for two valves} = \frac{2E_1\hat{I}}{\pi}$$

where E_1 = H.T. voltage.
The A.C. output voltage wave is represented by $E_1 \cos pt$.

$$\text{Therefore A.C. power from two valves} = \frac{E_1\hat{I}}{2}$$

$$\text{A.C./D.C. efficiency} = \frac{\frac{E_1\hat{I}}{2}}{\frac{2E_1\hat{I}}{\pi}} = \frac{\pi}{4} = 78{\cdot}5\%.$$

There is little essential difference between the two types of Class B operation, quiescent push-pull (Q.P.P.) and positive drive. With quiescent push-pull, tetrode valves are employed and the input voltage is restricted to the region where there is no grid current. Positive-drive Class B operation is applied to triodes to obtain a high anode circuit efficiency by reducing the minimum anode voltage (see Section 10.2), below that permitted by the bias line $E_g = 0$. Grid current is taken during the period while the input voltage swing makes the grid voltage positive. The amplifier (driver stage) before the Class B valves must supply power when grid current flows, and the points to be observed in its design are discussed in Section 10.8.6.

The chief features of a Q.P.P. stage are the centre-tapped high ratio step-up input transformer, and the output transformer. The former is necessary since each half of the secondary must supply a peak voltage very nearly equal to the cut-off bias (at the operating H.T. voltage) of the Q.P.P. valves. The self-capacitance of the secondary should be low to prevent peaked high-frequency response due to resonance with the leakage inductance. The output trans-

former also needs to have low leakage inductance and self-capacitance, because the resonant circuit so formed is capable of producing damped oscillations [33] under shock excitation from the half wave current impulses of each valve. Since each valve supplies half the output wave it is essential that the half-primary inductance and the leakage inductance between each half primary and secondary should be very nearly equal. Inequality causes the amplitudes of the two halves of the wave delivered to the output load to be unequal at low and high frequencies, thus producing distortion. Parasitic oscillation due to the push-pull connection is usually prevented by capacitors (0·002 to 0·005 μF) connected across each half primary. High peak currents are taken during loud signals and the primary D.C. resistance must therefore be low. If high-frequency tone control is used, it should be included before the Q.P.P. output stage rather than across the output transformer. When the tone-control circuit is in parallel with the latter it tends to increase the peak output current during loud signals, and this may cause damage to the valves.

Triode valves in Class B positive drive may be designed to have high internal resistances and operate with zero grid bias, or to have low internal resistances and to operate with negative grid bias. Quiescent anode currents are approximately the same for both types of valves. The zero grid bias stage has the advantage of requiring no bias battery, but there is generally more " join up " distortion and heavier grid current damping of the driver stage. In addition, the optimum load resistance is high, and the output transformer primary inductance must consequently be large to prevent excessive attenuation (frequency) distortion at low frequencies. The second type has several advantages over the first, the grid bias of each valve can be adjusted to give reduced " join-up " distortion, a resistance can be included in parallel with the grid bias battery to reduce its voltage and keep it in step with the H.T. voltage as the H.T. battery becomes exhausted, driver stage damping is reduced, and the lower internal resistances of the valves assist in damping loudspeaker resonances. Class B positive drive is not now used to any large extent in receivers because quiescent push-pull gives results as satisfactory, without the complications of a driver stage. The design of the output transformer is similar to that for quiescent push-pull.

10.8.6. The Driver Stage for Class B Positive Drive. If the anode load resistance, R_0', of a triode A.F. amplifier is steadily increased, overall amplification, at first proportional to R_0', becomes

asymptotic to the amplification factor of the valve and is almost independent of changes of R_0. This occurs for values of R_0 exceeding about $4R_a$ (see Fig. 9.6). Owing to the fact that grid current is taken by each Class B valve, the equivalent load resistance in the driver valve anode circuit varies over its output voltage cycle from a very high to a low value, and unless this is controlled the output voltage wave shape is flattened at both ends of the cycle. If, however, the equivalent grid current load resistance is not allowed to fall below $4R_a$, the distortion produced in the output wave will not be serious. This result may be achieved by a suitable step-down intervalve transformer,[26] the step-down ratio being calculated from

$$\frac{\frac{1}{2}N_s}{N_p} = \sqrt{\frac{R_{g\ (min.)}}{4R_{a\ (driver\ valve)}}}$$

where N_p = total primary turns,
N_s = total secondary turns,
$R_{g(min.)}$ = minimum grid input resistance of the Class B stages

A higher step-down ratio would have the advantage of reducing the effect of variations of R_g, but this reduces the driver output voltage to the Class B valves, and the driver valve may then be overloaded before maximum output is obtained from the Class B stage. $R_{g(min.)}$ is the slope resistance of the I_gE_g characteristic curve of the Class B valve at the maximum required positive value of grid voltage; a satisfactory approximation is given by the ratio of the positive bias voltage equal to the maximum positive voltage reached on the grid of the Class B valve to the D.C. grid current flowing at this bias voltage, i.e., it is the resistance corresponding to the chord to the I_gE_g characteristic curve instead of the tangent. A normal step-down ratio from primary to half secondary is 1 to $\frac{3}{4}$, or the ratio from primary to total secondary is 1 to 1·5. The transformer must have a high primary inductance, small leakage inductances between primary and both half secondaries—this is particularly important since the minimum grid input resistance may be as low as 20,000 ohms for battery-operated Class B positive drive—and the D.C. resistance of each half secondary must be low so as to reduce the D.C. voltage developed when grid current occurs.

An improved driver stage may be obtained by using a "cathode follower" [12] connection, i.e., the transformer is placed in the cathode circuit of the driver valve. This reduces the effective impedance of the valve to $\frac{R_a}{1+\mu}$ (see Section 10.10.6), so that a step-up ratio may even be used. At the same time the effective amplification

of the valve is less than unity so that it acts simply as an impedance matching device.

10.8.7. Class AB Positive Drive. Class AB positive drive is sometimes used in A.C. mains-operated amplifiers to obtain the advantages of triode operation with high D.C. to A.C. conversion efficiency and high A.C. output. The triode valves are biased to a voltage approximately midway between the Class A and Class B positions. The zero-to-maximum signal D.C. current ratio is much less than that for Class B, about 2 to 1 as compared with 4 to 1, and "join-up" distortion is low. The changing anode current makes fixed grid bias (instead of cathode self-bias) and an inductance loaded H.T. supply (Section 11.2.6) essential.

10.9. The Output Transformer.

10.9.1. The Design of an Output Transformer. The basic principles, involved in output transformer design, are practically the same as for smoothing choke and mains transformer design, and we shall illustrate the method of procedure by the following example. Suppose the optimum load resistance referred to the primary side of the transformer is 6,000 ohms, the speech-coil impedance 5 ohms, and the primary D.C. current 40 mA. The required value of primary inductance is determined by the maximum permissible loss of response at a given low audio frequency, and we will assume this to be 2 db. at 50 c.p.s. From expression 9.22*b*, Section 9.4, 2 db. loss corresponds to a ratio of primary reactance to the total resistance of valve and load in parallel of very nearly 2 to 1. If the output valve is a tetrode the total parallel resistance can, for all practical purposes, be taken as the load resistance 6,000 ohms. Should the valve slope resistance be comparable with 6,000 ohms it merely improves the low-frequency response, making the loss less than 2 db. Hence the required value of primary inductance is

$$L_p = \frac{2 \times 6{,}000}{2\pi \times 50} = 38{\cdot}2 \text{ H.}$$

For convenience let us take the same stampings as are used for the mains transformer design in Section 11.2.2, viz., Stalloy 32A. For one secondary and two primary sections, interleaved as shown in Fig. 10.18, insulation thicknesses of 0·075 ins. between winding and core, and winding and outside limb, and of 0·05 ins. between windings, and windings and sides, the total available winding area is $(2{\cdot}25 - 0{\cdot}1)(1 - 0{\cdot}25) = 1{\cdot}612$ sq. ins. The most efficient use of the winding area is to divide it equally between secondary and

primary windings, so that the total area occupied by primary or secondary is 0·806 sq. ins. A suitable gauge of wire is 34 S.W.G.,

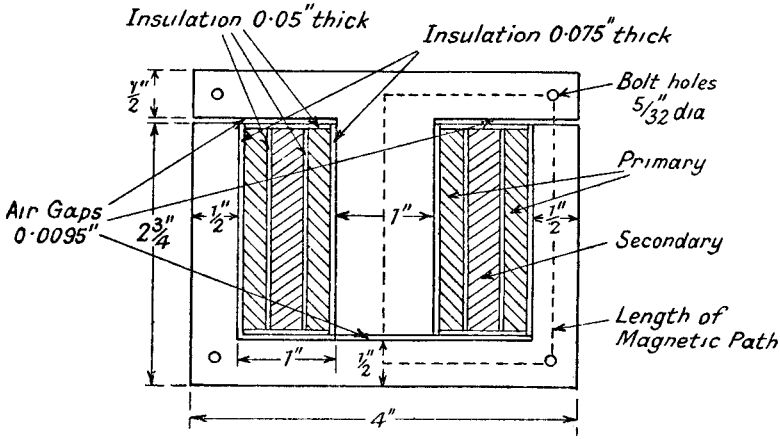

FIG. 10.18.—A Section Through a Typical Output Transformer.

which is rated to carry 66·5 mA, and if SSC is used, 8,730 turns can be accommodated per square inch (see Table 11.1).

The total primary turns in the available space $= 8{,}730 \times 0{\cdot}806$
$= 7{,}040$

Length of the magnetic path (Fig. 10.18), $l = 9$ ins.

Therefore turns per inch of magnetic path $= \dfrac{7{,}040}{9} = 782.$

D.C. ampere turns per inch of magnetic path $= \dfrac{782 \times 40}{1{,}000} = 31{\cdot}28.$

In Fig. 11.17 we have two curves for the ratio of inductance, with and without D.C. polarizing, against D.C. polarizing ampere-turns per inch, curve 1 for a very small A.C. flux density and curve 2 for a R.M.S. flux density of 60 lines per square centimetre, and either can be chosen for design purposes. If the former is used a larger transformer is obtained and low-frequency response for all A.C. input voltages is better than required. Curve 2 is more often used, the flux density of 60 lines per square centimetre corresponding to an input voltage of 7% of the maximum in our particular example (the peak flux density for maximum input voltage is calculated at the end of the section to be 1,200 lines per square centimetre). Incremental permeability, $\Delta\mu$,[23, 27] is shown in Fig. 10.20 to be proportional to peak A.C. flux density so that primary inductance for

voltages less than 7% of the maximum will tend to be less than that required, and conversely will be greater for larger voltages. The reduction in primary inductance is not generally sufficient to justify calculation on the basis of curve 1. From curve 2 the ratio of inductance with and without the D.C. polarizing current giving 31·28 D.C. ampere turns per inch is

$$\frac{L_{2(opt.)}}{L_1} = 0{\cdot}273$$

and the optimum air gap ratio is

$$\frac{a_0}{l} = 0{\cdot}0021.$$

Hence

$$L_1 = \frac{38{\cdot}2}{0{\cdot}273} = 140 \text{ H.}$$

Volume of iron required

$$= \frac{L_1 \times 10^8}{1{\cdot}255 \times 2{\cdot}54 \times \Delta\mu \times (\text{turns per inch of magnetic path})^2}$$

$$= \frac{140 \times 10^8}{1{\cdot}255 \times 2{\cdot}54 \times 900 \times (782)^2}.$$

Volume of iron = 8·0 cu. ins.

Incremental permeability is 900 for a R.M.S. flux density of 60 lines per square centimetre.

The area of Stalloy 32A stamping allowing for $\frac{5}{32}$-in. diameter bolt holes is 8·4236 sq. ins. (Section 11.2.2).

Therefore thickness of core = 0.95 ins.

Let us take a thickness of 1 in., i.e., an overall thickness of 1·1 ins. (allowing for 10% insulation between laminations)

Number of laminations of 0·014 ins. thickness $\simeq$ 79.

Total length of air gap = 0·0189 ins.

= 2 of 0·0095 ins. (the gap is divided between central and outside limbs).

It is of interest to compare with the above, the transformer design resulting from the use of curve 1.

$$\frac{L_{2(opt.)}}{L_1} = 0{\cdot}465$$

and optimum air gap ratio

$$\frac{a_0}{l} = 0{\cdot}00246.$$

Hence

$$L_1 = \frac{38{\cdot}2}{0{\cdot}465} = 82{\cdot}1 \text{ H.}$$

Volume of iron required ($\Delta\mu = 333$ for B very small)

$$= \frac{82{\cdot}1 \times 10^8}{1{\cdot}255 \times 2{\cdot}54 \times 333 \times (782)^2}$$

$$= 12{\cdot}65 \text{ cu. ins.}$$

Thickness of core $= 1{\cdot}5$ ins.

$= 1{\cdot}65$ ins., allowing 10% insulation.

Total length of air gap $= 0{\cdot}02215$ ins.

$= 2$ of $0{\cdot}01107$ ins. (the gap is divided between central and outside limbs).

Greatly increased core thickness is needed if the required value of primary inductance is to be maintained at extremely low flux densities.

Details of windings.

(1) *Primary.*

Mean length of one turn $= 8{\cdot}2$ ins.

$$\text{Total length of wire} = \frac{7{,}040 \times 8{\cdot}2}{36} = 1{,}605 \text{ yards}$$

$$\text{Total primary resistance} = 1{\cdot}605 \times 361{\cdot}2 = 580 \text{ ohms}$$

$$\text{D.C. voltage drop} = \frac{580 \times 40}{1{,}000} = 23{\cdot}2 \text{ volts.}$$

(2) *Secondary.*

$$\text{Step-down turns ratio} = \sqrt{\frac{6{,}000}{5}} = 34{\cdot}6$$

$$\text{Total turns in secondary} = \frac{7{,}040}{34{\cdot}6} \simeq 204$$

$$\text{Available winding area} = 0{\cdot}806 \text{ sq. in.}$$

$$\text{Therefore turns per square inch} = \frac{204}{0{\cdot}806} = 253.$$

No. 18 S.W.G. SSC wire giving 400 turns per square inch is the nearest size.

$$\text{Total length of secondary wire} = \frac{204 \times 8{\cdot}2}{36} = 46{\cdot}5 \text{ yards.}$$

Total resistance of secondary $= 0{\cdot}0465 \times 13{\cdot}267 = 0{\cdot}617$ ohms.

Neglecting iron losses, which are usually small compared with the copper resistance loss, the A.C. power efficiency for a 5-ohm secondary load resistance is

$$\eta = \frac{5}{5 + 0{\cdot}617 + \frac{580}{(34{\cdot}6)^2}} = \frac{5}{6{\cdot}102} = 82\%.$$

This is a normal value for efficiency, though it could be made higher at the cost of a slight increase in step-down turns ratio by using No. 16 S.W.G. enamelled wire for the secondary winding. The area required by the 18 S.W.G. secondary is only 0·51 sq. in. (less than that available, 0·806 sq. in.), and from a practical viewpoint this has advantages since it allows insulation between windings to be increased, and ensures that the windings can be fitted into the winding window.

It will be noted that a section through the central core limb is almost square ; this is considered to be the most economical shape of cross-section.

Losses in the Iron Core. Losses in the iron core of the transformer are a function of peak flux density $\hat{B}$, and, as $\hat{B}$ is directly proportional to the applied voltage and inversely to the frequency, they are greatest at the lowest audio frequency. Taking the latter as 50 c.p.s., and the maximum applied R.M.S. voltage as 120 (this is a reasonable figure for a tetrode valve operating at a H.T. voltage of 250), we have for the flux

$$\Phi = \frac{E \times 10^8}{4{\cdot}44 f N_p}$$

where N_p = total primary turns

$$\therefore \hat{\Phi} = \frac{120 \times 10^8}{4{\cdot}44 \times 50 \times 7{,}040}$$

$$= 7{,}680 \text{ lines.}$$

$$\hat{B} = \frac{\hat{\Phi}}{A} = 7{,}680 \text{ lines per square inch.}$$

$$\simeq 1{,}200 \text{ lines per square centimetre.}$$

Actual volume of iron in core of 1 in. thickness = 8·4236 cu. ins.

Total weight of core = 8·4236 × 0·28 lbs.

= 2·36 lbs.

Milliwatts lost per lb. for $\hat{B}$ of 1,200 lines per square centimetre = 12.
Therefore total milliwatts iron loss = 28·32

total output power milliwatts = 2,400.

The iron loss is therefore equivalent to a resistance of

$$6{,}000 \times \frac{2{,}400}{28{\cdot}32} = 508{,}000\ \Omega$$

in parallel with the primary inductance. Its effect on frequency response and general performance can justifiably be neglected.

The interleaved or sandwich type [38] of winding shown in

Fig. 10.18 has the merit of reduced leakage inductance compared with the non-interleaved type with a single primary winding. Interwinding capacitance is, however, usually slightly higher, though it can be reduced by bakelite separators. The self-capacitance of the windings can be reduced by sectionalizing instead of using a single continuous layer across the whole of the winding length. Reduced leakage inductance, winding and self-capacitance can be achieved by " pancake " coil construction with bakelite or bakelized paper spacers between the pancakes. For example, the above design could have employed three primary and two secondary interleaved pancake windings. The chief disadvantage of this type of winding is that it calls for a greater area of winding window and is not so robust ; on the other hand, a defective winding is more easily replaced. The windings should be vacuum impregnated with a suitable varnish to prevent the ingress of moisture, and an iron case is required to give magnetic screening and some measure of electrical screening and mechanical protection. It is not usual to seal the transformer in a bituminous compound.

Push-pull transformer design follows the same lines except that the D.C. polarizing current can be assumed to be small. Since only matched valves give a total effective D.C. current of zero it is usual to design on the basis of 10 mA D.C. current.

10.9.2. Output Transformer Attenuation (Frequency) Distortion. The frequency response of an output transformer is calculated in the same manner as that of the intervalve transformer in Section 9.4. The A.F. band is divided into three ranges, and the response at low and high audio frequencies is determined relative to that at the medium frequencies. Thus the loss of response at the low frequencies is from expression 9.22*b*.

$$-10 \log_{10}\left[1+\left(\frac{R_l}{X_l}\right)^2\right]$$

where $X_l = pL_p$, the reactance of the primary inductance,

R_l = the resistance of R_a+R_p in parallel with $\frac{R_s+R_{sc}}{n^2}$

R_p = resistance of primary winding
R_s = ,, ,, secondary winding
R_{sc} = resistance equivalent of the speaker speech-coil
n = secondary to primary turns ratio, which is generally much less than 1.

The resistance equivalent of the speech-coil is usually taken from the amplitude of the impedance ($\sqrt{R_{sc}^2 + X_{sc}^2}$) at 400 c.p.s., so

that the calculated frequency response is simply a measure of transformer performance, and not that of the output stage in association with the loudspeaker. Most loudspeakers have a mechanical resonance at a low frequency near 100 c.p.s., and several resonances in the high-frequency range. At and around these resonant frequencies the speech-coil impedance varies appreciably.

At high audio frequencies leakage inductance plays an important part but, owing to the low impedance of the speech coil, secondary self-capacitance can often be neglected. Expression 9.24 is therefore modified to a loss at high frequencies relative to medium of

$$-10\log_{10}\left(1+\left(\frac{R_h}{X_h}\right)^2\right)$$

where $R_h = R_a+R_p+\dfrac{R_s+R_{sc}}{n^2}$

$X_h = pL_p'$

L_p' = leakage inductance.

If the pass range of the output transformer is specified by those frequencies between which the maximum to minimum response is not greater than 3 db. (1·414 to 1), the lowest frequency is given by

$$X_l' = R_l'$$

or

$$f_l' = \frac{(R_a+R_p)\left(\dfrac{R_s+R_{sc}}{n^2}\right)}{\left(R_a+R_p+\dfrac{R_s+R_{sc}}{n^2}\right)2\pi L_p}$$

and the highest frequency by

$$X_h' = R_h'$$

or

$$f_h' = \frac{R_a+R_p+\dfrac{R_s+R_{sc}}{n^2}}{2\pi L_p'}$$

$$\text{Ratio } \frac{\text{highest frequency}}{\text{lowest frequency}} = \frac{L_p(1+G^2)}{L_p'G} \quad . \quad . \quad 10.43$$

where

$$G = \frac{R_s+R_{sc}}{n^2(R_a+R_p)}.$$

Thus, for a given value of G, the pass-band of the output transformer is proportional to the ratio of primary to leakage inductance,[30] and it will therefore be clear that there is no advantage in increasing primary inductance (by, for example, increasing primary turns) if leakage inductance is proportionally increased. Push-pull, by

balancing out the D.C. polarizing current, does increase primary inductance without increasing leakage inductance. The use of a high inductance choke to carry the output valve D.C. current with capacitance coupling to the output transformer has the same effect. Primary inductance is dependent on the applied voltage, and it generally increases as the latter increases, because incremental permeability increases (see Fig. 10.20). Frequency response tends, therefore, to be best with high output voltages and it is usual to design for the required response at low output voltages. In the preceding section primary inductance is calculated on the assumption of an output voltage of 7% of the maximum.

10.9.3. Output Transformer Amplitude (Harmonic) Distortion.[47] A non-linear relationship between the flux density B and magnetizing force H is responsible for amplitude distortion in iron-cored transformers. When a generator of sinusoidal voltage is applied to an unloaded transformer, it may produce almost equal distortion of flux and magnetizing force, greater distortion of flux than magnetizing force, or vice versa. The final result actually depends on the relative magnitudes of the generator internal impedance and the non-linear impedance of the transformer. If the former is very large (e.g., for the tetrode valve) the current, and hence magnetizing force, in the transformer core is practically sinusoidal; flux and the unloaded secondary voltage are distorted n shape. On the other hand, a low generator impedance (e.g., for a triode valve) implies a voltage applied to, and flux in, the transformer of nearly sinusoidal shape, with a distorted magnetizing force (input current to the transformer primary). The unloaded secondary voltage is therefore almost sinusoidal. A point worth noting is that the transformer induced voltage, which opposes the applied voltage, is proportional to $\frac{d\Phi}{dt}$, where Φ is the total flux in the iron core, so that each harmonic component in the flux wave is multiplied by its harmonic number in arriving at the harmonic voltage component. Hence the secondary output voltage wave shape has greater distortion than the flux wave shape.

The relative amplitudes of the harmonic currents produced in the transformer depend on the shape of the B–H loop curve. This is symmetrical in the absence of a D.C. polarizing current, and distortion is confined mainly to odd harmonics with third predominating. An asymmetrical loop is obtained with a D.C. polarizing current, and both even and odd harmonics are present with second and third as the most important.

The application of a load impedance to the secondary terminals affects the distortion, which now depends on the load impedance as well as upon the valve and the non-linear transformer impedance. This can be shown by referring to Fig. 10.19. The non-linear transformer impedance is designated by Z_p—it is the impedance of the parallel combination of primary inductance and the resistance due to hysteresis and eddy currents, L_p and R_{he} respectively, in Fig. 9.13*b*, but it excludes R_p, the primary winding resistance, since this is not a function of the conditions in the iron core. The primary winding resistance is added to the generator internal impedance in Z_a, and the secondary impedance, transferred to the primary by dividing by the square of the secondary to primary turns ratio, is indicated by Z_0. The sinusoidal generator voltage has an R.M.S. value of E volts, the current from the generator has fundamental

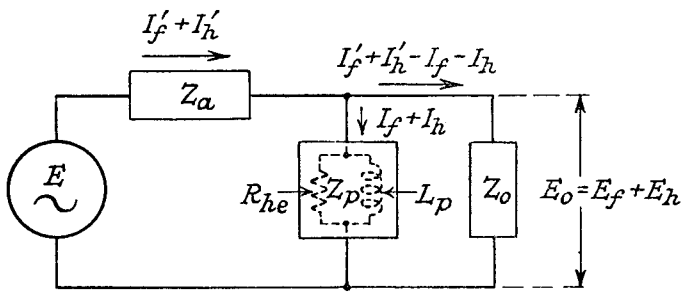

FIG. 10.19.—Current and Voltage Relationships in an Output Transformer.

and particular harmonic R.M.S. components of I_f' and I_h', corresponding currents in the non-linear transformer impedance (excluding the load) are I_f and I_h, and the output voltage E_0 has fundamental and particular harmonic components of E_f and E_h. The plus sign used in the figure indicates the vector sum of the component voltages and currents. Since the generator voltage contains no harmonics, it follows that the harmonic voltages produced across Z_a must equal those across Z_0,

i.e.,
$$E_h = (I_h' - I_h)Z_0 = -I_h'Z_a$$
$$I_h' = \frac{I_h Z_0}{Z_a + Z_0}$$
$$E_h = \frac{I_h Z_a Z_0}{Z_a + Z_0} \quad . \quad . \quad . \quad . \quad . \quad 10.44.$$

Thus we see that the harmonic output voltages are dependent on the generator and load impedances as well as the harmonic currents

produced in the non-linear transformer impedance. The ratio of any one harmonic voltage to the fundamental output voltage is

$$\frac{E_h}{E_f} = \frac{I_h \cdot \dfrac{Z_a Z_0}{Z_a + Z_0}}{I_f Z_f} \quad . \quad . \quad . \quad 10.45a$$

where I_f = fundamental current component in the transformer non-linear impedance

and Z_f = fundamental component of the non-linear impedance Z_p.

Z_0 and Z_a can generally be taken as resistances, and replacing them in 10.45*a* by R_0 and $R_a + R_p$, where R_a is the slope resistance of the output valve and R_p the primary winding resistance, we have

$$\frac{E_h}{E_f} = \frac{I_h R_0'}{I_f Z_f} \quad . \quad . \quad . \quad . \quad 10.45b$$

where

$$R_0' = \frac{R_0(R_a + R_p)}{R_0 + R_a + R_p}.$$

The above expression is limited in application because I_h varies when the load and generator impedances are varied. Partridge [47] has found empirically that all harmonic current components can be expressed quite simply in terms of the corresponding no-load harmonic current, R_0 and Z_f. The third harmonic current (I_3) in the unpolarized condition or the R.M.S. current of the second and third harmonics ($\sqrt{I_2^2 + I_3^2}$) in the polarized condition can be written

$$I_h = I_H\left(1 - \frac{R_0'}{4Z_f}\right) \quad . \quad . \quad . \quad 10.46$$

where I_H = no load harmonic current for $R_a + R_p = 0$.

The difference between measured and calculated (from 10.46) I_h is, in most cases, quite small when $R_0' \ll Z_f$ rising to about 5% when $R_0' = Z_f$.

Hence the harmonic voltage ratio is

$$\frac{E_h}{E_f} = \frac{I_H R_0'}{I_f Z_f}\left(1 - \frac{R_0'}{4Z_f}\right) \quad . \quad . \quad 10.45c.$$

The no-load current distortion ratio $\dfrac{I_H}{I_f}$ is a function of the peak flux density $\hat{B}$—the peak value is used in preference to R.M.S. because the shape of the flux density wave is often far from sinusoidal, and experimentally it has been found that the peak value and not the general shape is the determining factor. The no-load current distortion ratio can be estimated for different values of peak flux density (i.e., fundamental peak voltage across Z_p) by measuring with a harmonic analyser the fundamental and harmonic voltages across

a known low resistance in series with the unloaded transformer, which should have the lowest possible primary winding resistance. Alternatively the known series resistance may be varied, and the ratio of the harmonic to fundamental voltages, measured across it, plotted against the sum of the known and primary winding D.C. resistance. The line so obtained can be produced to give the no-load current distortion ratio for zero known and primary winding resistance. The peak flux density can be calculated from the R.M.S. value of the fundamental voltage (E_f) across the unloaded primary, by using the formula given in Section 11.2.2 (expression 11.2).

$$\hat{B} = \frac{E_f 10^8}{4{\cdot}44\, N_p A f} \text{ lines per square centimetre.}$$

where N_p = total primary turns
A = area of iron core section in square centimetres.
f = fundamental frequency.

Since $\hat{B}$ is inversely proportional to f, it is clear that a given applied voltage produces maximum flux density, and hence maximum amplitude distortion, at the lowest audio frequency.

Expression 10.45*c*, as it stands, is applicable only to one particular design, and it would be preferable to convert it to a product of two factors, one dependent on the core material and peak flux density, and the other dependent on the shape and winding details of the transformer. This is possible because, in most practical cases, Z_f can be taken as the reactance of the primary inductance at the fundamental frequency. Taking the expression 11.19*a*, Section 11.2.9, for the primary inductance we have

$$Z_f = pL_p = \frac{2\pi f\, 1{\cdot}255\, N_p{}^2 A \Delta\mu}{10^8 l}$$

where $\Delta\mu$ = incremental or A.C. permeability
l = length of the magnetic path in centimetres (see Fig. 10.18) and N_p and A are as expressed above for $\hat{B}$.

Therefore
$$Z_f = 7{\cdot}88 \times 10^{-8} \Delta\mu \frac{N_p{}^2 A f}{l} \quad . \quad . \quad . \quad 10.47.$$

Replacing Z_f in the $\frac{I_H}{I_f Z_f}$ part of 10.45*c* by 10.47 gives

$$\frac{I_H}{I_f Z_f} = \frac{I_H}{I_f} \frac{10^8}{7{\cdot}88 \Delta\mu} \times \frac{l}{N_p{}^2 A f} \quad . \quad . \quad . \quad 10.48$$

and both the variables $\frac{I_H}{I_f}$ and $\Delta\mu$ in the first factor relate to the core material and peak flux density, whilst the second factor relates

to the particular design details of the transformer. $\frac{I_H}{I_f}$ and $\Delta\mu$ can be measured for different peak flux densities and D.C. polarizing field. The current distortion ratio generally increases with increase of peak flux density and D.C. polarizing field. If incremental permeability $\Delta\mu$ is plotted against $\hat{B}$ it is found to have a maximum at some value of peak flux density dependent on the core material and D.C. polarizing voltage. Generally $\Delta\mu$ decreases for all flux densities as the D.C. polarizing voltage increases, but flux density for maximum $\Delta\mu$ increases. Typical curves of current distortion and incremental permeability abstracted from the article [47] by Partridge (note

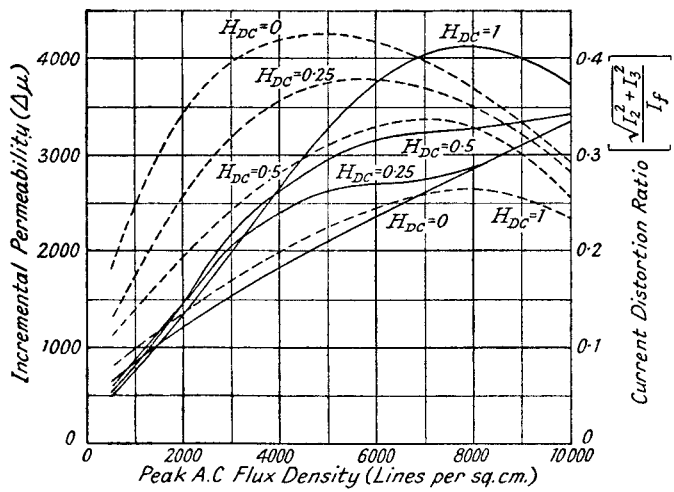

FIG. 10.20.—Incremental Permeability and Current Distortion Curves Against Peak A.C. Flux Density for Normal Stalloy Core.

Dotted Line: Incremental Permeability.
Full Line: Current Distortion.

that his relative specific choke impedance $Z_{sp} = 7{\cdot}88\Delta\mu 10^{-8}$) are plotted in Fig. 10.20 against peak flux density for different values of D.C. polarizing field; the core material is Silcor 2 ($3\frac{1}{2}\%$ silicon content) as used for the stalloy stamping of Section 10.9.1. The D.C. polarizing field is given in oersteds (gilberts per centimetre) and it is necessary to multiply by 2·02 to convert to D.C. ampere-turns per inch (see Section 11.2.9). The product $\frac{I_H}{I_f}\frac{10^8}{7{\cdot}88\Delta\mu}$ can be termed the distortion factor, D, of the core material, and it is plotted in Fig. 10.21 against peak flux density. The values are obtained from the curves in Fig. 10.20.

To illustrate the use of Fig. 10.21, let us consider the transformer designed in Section 10.9.1 and determine the transformer distortion occurring when operating under the full load conditions.

The peak flux density for a maximum applied R.M.S. voltage of 120 is 1,200 lines per square centimetre and the D.C. polarizing field is 31·28 ampere-turns per inch.

The curves in Fig. 10.21 are given for a maximum D.C. polarizing field of 2·02 ampere turns per inch, so we shall have to estimate a likely value for distortion coefficient. The correctness, or otherwise, of the estimate will not affect the general principles. For

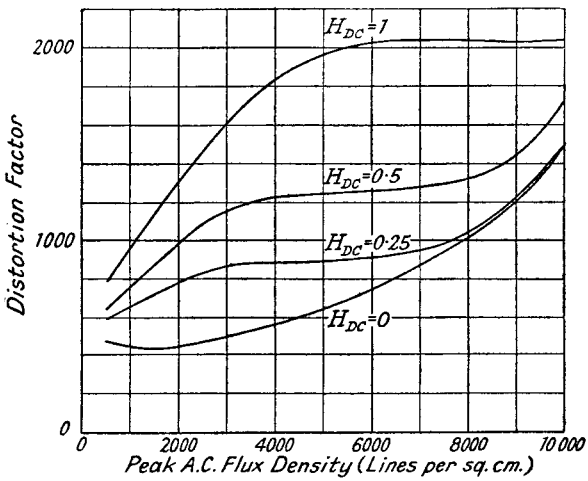

FIG. 10.21.—Distortion Factor-Peak A.C. Flux Density Curves for Normal Stalloy Core.

$H = 2{\cdot}02$ ampere turns per inch the distortion coefficient at $\hat{B} = 1{,}200$ lines per square centimetre is 1,050. The form of the current distortion curves suggests that an increase in D.C. field is unlikely to affect greatly the current distortion at $\hat{B} = 1{,}200$ lines per square centimetre. The chief effect of an increase in H is to reduce incremental permeability, and a probable decrease of $\Delta\mu$ of about 3 to 1 by changing H from 2 to 31·28 ampere turns per inch is suggested by the change in ratio of $\frac{L_{2(opt.)}}{L_1}$ in Fig. 11.17. Let us therefore assume a distortion coefficient of 3,150. A probable value for valve (a tetrode) slope resistance is 30,000 ohms, thus for $f = 50$ c.p.s.

$$R_0' = \frac{R_0(R_a+R_p)}{R_0+R_a+R_p} = \frac{6{,}000(30{,}580)}{36{,}580}$$
$$\simeq 5{,}000\ \Omega$$
$$Z_f = pL_p = 12{,}000\ \Omega.$$

By combining 10.45*c* and 10.48, voltage distortion

$$\frac{E_h}{E_f} = \frac{Dl}{N_p{}^2Af}.R_0'\left(1-\frac{R_0'}{4Z_f}\right)$$
$$= \frac{3{,}150 \times 9 \times 2{\cdot}54}{(7{,}040)^2 \times (1 \times 2{\cdot}54)^2 \times 50}.5{,}000\left(1-\frac{5{,}000}{48{,}000}\right)$$
$$= 0{\cdot}0201 = 2{\cdot}01\%.$$

Note that l and A are in centimetres and square centimetres respectively.

Certain general conclusions can be drawn from the analysis.

(1) Harmonic distortion is a function of Z_f, and it can be decreased to very small proportions at any given frequency by increasing Z_f, i.e., by increasing $\frac{N^2A}{l}$. However, for any given shape of transformer, leakage inductance and Z_f are directly proportional so that an increase in Z_f results in increased loss of high-frequency response. There is thus a limit to the improvement in harmonic distortion which can be achieved with any given transformer shape, and this limit is set by the tolerable loss at high frequencies.

(2) If attenuation (frequency), harmonic distortion and D.C. polarizing field are specified, the power-handling capacities of transformers of the same core material and geometrical proportions with given generator and load impedances are proportional to their volumes.

Specified attenuation (frequency) distortion implies that primary and leakage inductances are constant; the former decides the low-frequency response. Leakage inductance, which determines high-frequency response, is directly proportional to primary inductance for a given core material and geometrical proportions. Specified harmonic distortion for a constant D.C. polarizing field means that the peak A.C. flux density is constant, hence from expression 11.19*a*, Section 11.2.9.

$$L_p \propto \frac{N_p{}^2A}{l}$$

and from expression 11.2, Section 11.2.2.

$$E_f \propto N_pA.$$

If the linear dimensions of the transformer are multiplied by k, and attenuation distortion is to be unchanged

$$L_p = L_{p1} \propto N_{p1}{}^2 \frac{k^2 A}{kl} \propto \frac{N_p{}^2 A}{l}$$

$$\therefore N_{p1} \propto \frac{N_p}{\sqrt{k}}.$$

Using this in the expression for E_f

$$E_{f1} \propto \frac{N_p}{\sqrt{k}} k^2 A \propto k^{\frac{3}{2}} E_f,$$

but power $P_{f1} \propto E_{f1}{}^2 \propto k^3 P_f \propto$ volume of the transformer. When the D.C. current remains constant, increase in overall dimensions reduces the value of $H_{\text{D.C.}}$ in the polarizing D.C. field, because

$$H_{\text{D.C.}} \propto \frac{N_p}{l} \propto \frac{1}{k^{\frac{1}{2}}},$$

and this allows a greater increase in power handling capacity to be obtained over that due to the increase in volume.

10.10. Negative Feedback.[11, 16, 19]

10.10.1. Introduction. Negative or inverse feedback is applied to A.F. amplifiers in order to change the frequency response and/or to reduce harmonic distortion, hum and noise produced in the amplifier itself. It is achieved by feeding back a proportion of the output to the input in such a way as to oppose the input voltage. The opposition voltage may be fed back through a resistive network or a circuit arranged to give phase and amplitude discrimination.

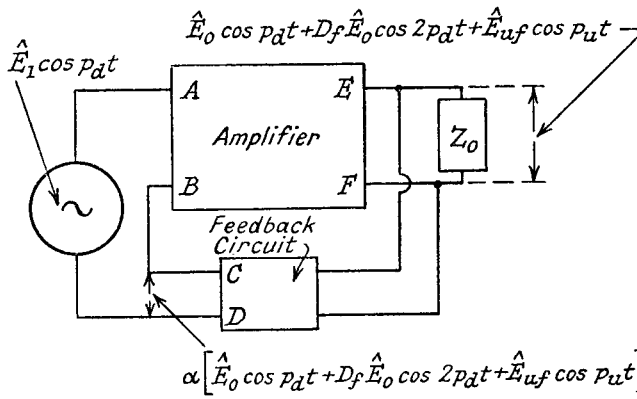

FIG. 10.22.—Schematic Diagram of Negative Feedback.

In both instances there is a possibility that at some frequency (usually outside the desired pass range of the amplifier) the phase shift may be such as to produce positive feedback, and special precautions are sometimes necessary, particularly when feedback occurs over a number of stages, to prevent self-oscillation. The usual method is to design the feedback circuit to attenuate severely frequencies outside the normal pass range of the amplifier.

Some of the properties of negative feedback can be demonstrated by considering the diagram in Fig. 10.22.

Let $\hat{E}_1 \cos p_d t$ = input voltage

μ_0 = overall amplification of the amplifier without feedback

μ_f = overall amplification of the amplifier with feedback.

$\hat{E}_0 \cos p_d t$ = fundamental component of the output voltage from the amplifier with feedback

D_0 = distortion ratio of the amplifier without feedback, the ratio of the amplitude of second harmonic (if this is the largest harmonic) to that of the fundamental in the output voltage

D_f = distortion ratio of the amplifier with feedback

$\hat{E}_u \cos p_u t$ = undesired hum or noise voltage produced by the amplifier itself without feedback

$\hat{E}_{uf} \cos p_u t$ = undesired hum or noise voltage produced by the amplifier with feedback

α = feedback factor, i.e., the proportion of the output voltage applied to the input.

Voltage across CD due to feedback

$$= \alpha[\hat{E}_0 \cos p_d t + D_f \hat{E}_0 \cos 2p_d t + \hat{E}_{uf} \cos p_u t].$$

Voltage applied to the amplifier across terminals AB

$$= \hat{E}_1 \cos p_d t - E_{CD}.$$
$$= (\hat{E}_1 - \alpha\hat{E}_0) \cos p_d t - \alpha D_f \hat{E}_0 \cos 2p_d t - \alpha \hat{E}_{uf} \cos p_u t.$$

Output voltage across EF

$$= \mu_0[(\hat{E}_1 - \alpha\hat{E}_0) \cos p_d t - \alpha D_f \hat{E}_0 \cos 2p_d t - \alpha \hat{E}_{uf} \cos p_u t] + \mu_0 D_0 (\hat{E}_1 - \alpha\hat{E}_0) \cos 2p_d t + \hat{E}_u \cos p_u t$$
$$= \hat{E}_0 \cos p_d t + D_f \hat{E}_0 \cos 2p_d t + \hat{E}_{uf} \cos p_u t.$$

Equating fundamental components

$$\hat{E}_0 = \mu_0(\hat{E}_1 - \alpha\hat{E}_0)$$

or
$$\frac{\hat{E}_0}{\hat{E}_1} = \mu_f = \frac{\mu_0}{1+\mu_0\alpha}. \quad . \quad . \quad . \quad 10.49$$

and equating second harmonic components

$$\mu_0 D_0(\hat{E}_1 - \alpha\hat{E}_0) - \mu_0\alpha D_f\hat{E}_0 = D_f\hat{E}_0.$$

Replacing $\hat{E}_1$ by the value obtained from 10.49

$$\mu_0 D_0\left(\frac{\hat{E}_0(1+\mu_0\alpha)}{\mu_0} - \alpha\hat{E}_0\right) = D_f\hat{E}_0(1+\mu_0\alpha).$$

Therefore
$$D_f = \frac{D_0}{1+\mu_0\alpha} \quad . \quad . \quad . \quad . \quad 10.50.$$

Equating undesired voltages

$$\hat{E}_{uf} = \hat{E}_u - \mu_0\alpha\hat{E}_{uf}$$

or
$$\frac{\hat{E}_{uf}}{\hat{E}_u} = \frac{1}{1+\mu_0\alpha} \quad . \quad . \quad . \quad . \quad 10.51.$$

We therefore see that negative feedback decreases overall amplification, distortion ratio and undesired hum and noise voltages due to the amplifier. The distortion ratio D_0 (without feedback) is generally a function of the fundamental input voltage and is less when the latter is less. Since with feedback the effective fundamental input is reduced from $\hat{E}_1 \cos p_d t$ to $(\hat{E}_1 - \alpha\hat{E}_0) \cos p_d t$, there is actually a greater reduction in distortion than is represented by the factor $\frac{1}{1+\mu_0\alpha}$. As a rule, however, the same output voltage will be required with feedback as without, and the fundamental input voltage is increased until this condition is achieved. The factor $\frac{1}{1+\mu_0\alpha}$ does then represent the reduction in distortion ratio. With any negative feedback amplifier it is essential to ensure that the preceding amplifier is capable of delivering the increased input voltage without increased harmonic distortion, for negative feedback can only cancel harmonics produced in its own amplifier stage. Another important point to note is that, although the general level of harmonic distortion is decreased, certain harmonics may be introduced or increased by the application of negative feedback. In the above example fourth harmonic of amplitude $D_f D_0 \mu_0 \alpha \hat{E}_0$ is introduced into the output by feedback of the second harmonic. The effect is not usually very serious.

The change in frequency response, which can be obtained by negative feedback, may be illustrated by rearranging 10.49.

thus
$$\frac{\hat{E}_0}{\hat{E}_1} = \frac{1}{\alpha}\left[\frac{1}{1+\frac{1}{\mu_0\alpha}}\right]$$
$$\simeq \frac{1}{\alpha}$$
if
$$\mu_0\alpha \gg 1$$
i.e., $\frac{\hat{E}_0}{\hat{E}_1}$ is independent of the amplification and frequency response of the amplifier and only dependent on that of the feedback circuit. Even when α has the normal practical values of 0·1 to 0·2, the feedback circuit frequency response has an appreciable effect on overall response. Negative feedback may therefore be used to compensate for deficiencies in amplifier response or to produce tone control. Thus a resistive feedback circuit (α is a pure number) tends to give a flat overall frequency response, whereas a reactive circuit (α is a complex number) tends to cause a variable frequency response. It should be noted that the frequency response of the amplifier without feedback is implicit in the overall amplification μ_0, which is generally a complex number of the form $\frac{\mu_{om}}{1\pm jx}$, where μ_{0m} = amplification at the medium audio frequencies, x is a function of frequency and is due to the reactance components in the amplifier.

10.10.2. Types of Negative Feedback.[41] The generally accepted classification of negative feedback circuits is according to the method of tapping the feedback voltage from the output. There are three important types, voltage, current and bridge feedback. In the first case the feedback voltage is taken from a potential divider across the output and is directly proportional to the output voltage. In the second case the feedback voltage is taken from an impedance in series with the output load, and is directly proportional to the output current. Bridge feedback is a combination of voltage and current feedback.

10.10.3. Voltage Feedback. Voltage feedback is illustrated in Fig. 10.23*a*. The potential divider R_1 is assumed to be much greater than the output load impedance Z_0, so that the current through it can be neglected. For the sake of simplicity we will refer to the R.M.S. values of voltage and current in the following analysis, and so dispense with $\cos p_d t$

$$E_0 = \frac{\mu E_{AB} Z_0}{R_a + Z_0} \quad . \quad . \quad . \quad . \quad 10.52$$

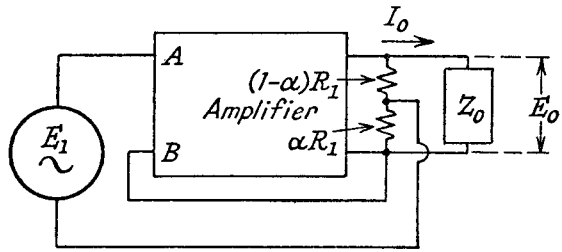

FIG. 10.23*a*.—Voltage Negative Feedback.

where μ = amplification of the amplifier when $Z_0 = \infty$
and R_a = the slope resistance of the output valve
$E_{AB} = E_1 - \alpha E_0$.
Replacing the above for E_{AB} in 10.52.

$$\frac{E_0}{E_1} = \frac{\mu Z_0}{R_a + Z_0(1+\mu\alpha)} = \frac{\frac{\mu}{1+\mu\alpha} Z_0}{\frac{R_a}{1+\mu\alpha} + Z_0} \quad . \quad . \quad . \quad . \quad 10.53.$$

By noting that $\mu_0 = \frac{\mu Z_0}{R_a + Z_0}$, expression 10.53 shows the expected reduction of overall amplification to $\mu_f = \frac{\mu_0}{1+\mu_0\alpha}$, and at the same time the equivalent slope resistance of the output valve is decreased to $\frac{R_a}{1+\mu\alpha}$. This reduction of generator resistance is particularly valuable when the load impedance is a loudspeaker speech coil, since it assists in damping cone resonances. One of the disadvantages of using a tetrode output valve, the accentuation of cone resonances, can be overcome by the application of voltage feedback, without losing the advantages of high A.C./D.C. power efficiency and (if feedback is not excessive) of high power sensitivity.

Some interesting effects result from the application of voltage feedback in special cases. For example, if $R_a \ll Z_0$, expression 10.53 becomes

$$\frac{E_0}{E_1} \simeq \frac{\mu}{1+\mu\alpha} \quad . \quad . \quad . \quad . \quad 10.54$$

i.e., output voltage is independent of Z_0. On the other hand if $R_a \ll Z_0$, $\mu\alpha \gg 1$ and $\alpha = \frac{K}{Z_0}$, output current instead of voltage is independent of Z_0.

$$I_0 = \frac{E_0}{Z_0} = \frac{\mu E_1}{\mu \alpha Z_0} = \frac{E_1}{K} \quad . \quad . \quad . \quad 10.55$$

10.10.4. Current Feedback. Current feedback is illustrated by the circuit in Fig. 10.23*b*, the feedback voltage being developed across the resistance R_f in series with the load impedance Z_0.

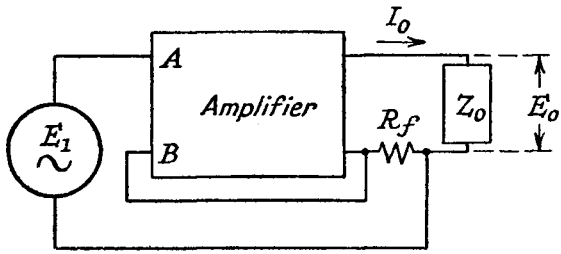

FIG. 10.23*b*.—Current Negative Feedback.

$$E_0 = \frac{\mu E_{AB} Z_0}{R_a + R_f + Z_0}$$

where R_a = slope resistance of the output valve

$$E_{AB} = E_1 - I_0 R_f$$

$$= E_1 - \frac{\mu E_{AB} R_f}{R_a + R_f + Z_0}.$$

Therefore

$$E_0 = \frac{\mu E_1 Z_0}{R_f(1+\mu) + R_a + Z_0} \quad . \quad . \quad . \quad 10.56.$$

We see from the above expression that current feedback increases the equivalent slope resistance of the output valve by $R_f(1+\mu)$, and the amplification factor with feedback is reduced only by reason of increased generator resistance.

Two special cases again arise; if μ is very large

$$E_0 = \frac{E_1 Z_0}{R_f}$$

and

$$I_0 = \frac{E_0}{Z_0} = \frac{E_1}{R_f} \quad . \quad . \quad . \quad . \quad 10.57.$$

When, in addition, $R_f = KZ_0$

$$E_0 = I_0 Z_0 = \frac{E_1}{K} \quad . \quad . \quad . \quad . \quad 10.58.$$

In the first instance output current is independent of Z_0, and in the second output voltage is unaffected by Z_0.

Current feedback is not often employed in output stages, partly because of the increased equivalent generator resistance, which tends

to exaggerate cone resonances when the output load is a loudspeaker speech coil, but mainly because it is difficult to develop sufficient feedback voltage without considerable loss of output power.

10.10.5. Bridge Feedback. Bridge feedback is indicated in the diagram of Fig. 10.23c.

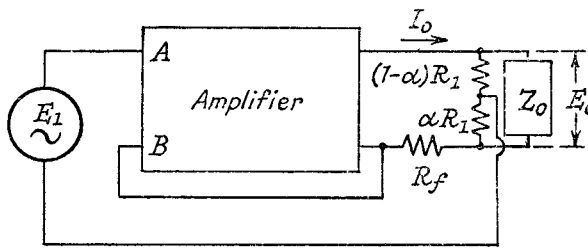

FIG. 10.23c.—Bridge Negative Feedback.

$$E_0 = \frac{\mu E_{AB} Z_0}{R_a + R_f + Z_0}$$

$$E_{AB} = E_1 - I_0 R_f - \alpha E_0$$
$$= E_1 - I_0(R_f + \alpha Z_0).$$

The current taken by R_1 is assumed to be negligible

$$E_{AB} = E_1 - \frac{\mu E_{AB}(R_f + \alpha Z_0)}{R_a + R_f + Z_0}$$
$$= \frac{E_1(R_a + R_f + Z_0)}{R_a + R_f(1+\mu) + Z_0(1+\mu\alpha)}$$

$$\therefore E_0 = \frac{\mu Z_0 E_1}{R_a + R_f(1+\mu) + Z_0(1+\mu\alpha)} \quad . \quad . \quad 10.59.$$

Rewriting 10.59 in the form $\frac{KZ_0}{K_1 + Z_0}$

$$\frac{E_0}{E_1} = \frac{\mu}{1+\mu\alpha} \cdot \frac{Z_0}{\frac{R_a + R_f(1+\mu)}{1+\mu\alpha} + Z_0}.$$

The effect of bridge feedback is a combination of the effects produced by voltage and current feedback; overall amplification and the equivalent slope resistance (increased by current feedback to $R_a + R_f(1+\mu)$) of the output valve are both reduced, by the factors $\frac{1}{1 + \mu_0\left(\frac{R_f}{Z_0} + \alpha\right)}$ and $\frac{1}{1+\mu\alpha}$ respectively. The equivalent slope resistance is constant if μ is very large and R_f and α are constant.

There are a number of possibilities with bridge feedback. It can provide:

(1) Constant output current and an equivalent generator impedance of Z_0 by making $\alpha = \frac{R_f}{Z_0}$ where R_f is constant. Neglecting R_a and Z_0 in comparison with μR_f and $\mu\alpha Z_0$ we have from equation 10.59.

$$E_0 = \frac{\mu Z_0 E_1}{\mu R_f + \mu\alpha Z_0} = \frac{E_1 Z_0}{R_f + \alpha Z_0} = \frac{E_1 Z_0}{2R_f}$$

$$\therefore I_0 = \frac{E_0}{Z_0} = \frac{E_1}{2R_f} = \text{constant}$$

and the equivalent generator impedance $= \frac{R_f}{\alpha} = Z_0$.

(2) Constant voltage and an equivalent generator impedance of Z_0 by making $R_f = \alpha Z_0$ where α is constant.

$$E_0 = \frac{Z_0 E_1}{R_f + \alpha Z_0} = \frac{E_1}{2\alpha} = \text{constant}$$

and the equivalent generator impedance $= \frac{R_f}{\alpha} = Z_0$.

Other variations in the feedback circuit can be made to give constant equivalent generator impedance with constant voltage or current.

10.10.6. Negative Feedback with a Cathode Follower Valve.[43] A valve with its load resistance placed between the cathode and H.T. negative is a special case of negative feedback for which the feedback factor α is 1. By analysis of the circuit in Fig. 10.24 we have

$$E_k = \frac{\mu E_{g_k} Z_k}{R_a + Z_k}$$

$$E_{g_k} = E_g - E_k$$

Therefore

$$E_k = \frac{\mu E_g Z_k}{R_a + (1+\mu) Z_k}$$

$$= \frac{\frac{\mu}{1+\mu} E_g Z_k}{\frac{R_a}{1+\mu} + Z_k}.$$

The output voltage E_k is therefore less than the input, and the valve equivalent slope resistance is reduced to a very small value by the factor $\frac{1}{1+\mu}$, and, if $\mu \gg 1$, it equals $\frac{1}{g_m}$. This type of negative feedback generator has two important advantages, low equivalent

generator internal resistance and low grid input admittance. The first means that it is particularly useful when constant output voltage is required across a variable load impedance. This property makes it a very satisfactory driver stage preceding Class B or Class AB

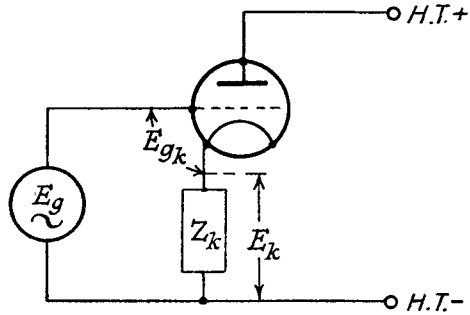

FIG. 10.24.—The Cathode Follower Circuit.

positive-drive output valves, the variable input impedance due to grid current causing practically no harmonic distortion of the output voltage. The valve may also be used as a D.C. voltage stabilizer; the D.C. voltage being taken between cathode and H.T. negative. Positive voltage between the grid and H.T. negative determines the D.C. output voltage, which is given by

$$E_{0\text{D.C.}} = E_b + E_{c0}$$

where E_b = positive voltage applied to the grid

$-E_{c0}$ = grid bias voltage required to cut off anode current for the given H.T. supply voltage.

Variations of the H.T. supply voltage are reduced by $\frac{1}{1+\mu}$ at the cathode circuit. Good regulation is also obtained by reason of low generator internal resistance.

Low grid input admittance is of greatest value for radio frequency operation, and at ultra high frequencies this property has the effect of improving signal-to-noise ratio. Low input admittance is realized because the voltage between grid and cathode is so very much less than the input voltage; this necessarily implies a comparatively small current flowing in the interelectrode grid-cathode capacitance. Formulæ for the parallel resistance and capacitance of the input admittance components are developed in Section 2.8.3, Part I. Thus, from expression 2.21*a*, the equivalent parallel resistance is

$$R_g = \frac{(G_k+g_m)^2+(B_{g_k}+B_k)^2}{B_{g_k}(G_k B_{g_k} - g_m B_k)}$$

and, from expression 2.21*b*, the equivalent parallel capacitance is

$$C_g = \frac{C_{g_k}[G_k(G_k+g_m)+B_k(B_{g_k}+B_k)]}{(G_k+g_m)^2+(B_k+B_{g_k})^2}$$

where $B_{g_k} = \omega C_{g_k}$

C_{g_k} = grid-cathode interelectrode capacitance

g_m = mutual conductance of the valve

and G_k and B_k = conductance and susceptance of the cathode load admittance.

At audio frequencies B_k is often zero and B_{g_k} can be neglected in the numerator, so that

$$R_g \simeq \frac{(G_k+g_m)^2}{G_k B_{g_k}^2}$$

which is very large because B_{g_k} is small, and

$$C_g \simeq C_{g_k}\left(1 - \frac{g_m}{G_k+g_m}\right) = C_{g_k}\left(1 - \frac{\mu R_k}{R_a+\mu R_k}\right).$$

Generally G_k is much less than g_m so that C_g approaches zero, i.e., the effective input capacitance is much reduced. It is clear, therefore, that grid input admittance will be low. The result of the cathode load resistance is actually a reversed Miller effect, the interelectrode capacitance being multiplied by 1 minus the approximate amplification of the stage. The negative sign is to be expected since a voltage across the cathode load resistance is 180° out-of-phase with a voltage across the same resistance placed in the anode circuit.

10.10.7. Balanced Feedback.[42] The chief disadvantage of negative feedback is that it reduces the overall amplification of any amplifier to which it is applied, and for the same output requires a larger input signal. This can be overcome if a combination of equal positive and negative feedback is employed, and this system is known as balanced feedback. It includes most of the advantages of negative feedback, viz., reduced interference voltages and distortion, and improved frequency response, without reducing the overall amplification (if the positive feedback is made equal to the negative).

Two controlling voltages are required; the negative feedback voltage is obtained from the output of the amplifier in the usual manner, but the positive feedback voltage is obtained either directly from the input voltage source or from the anode circuit of the first valve in the amplifier to which negative feedback is being applied.

The positive feedback voltage cannot be obtained from the amplifier output otherwise the negative feedback reduction of interference and distortion is cancelled as well as the input signal reduction.

The principle of balanced feedback is best shown by the following analysis.

Let E_{0f} = fundamental output voltage with feedback
$D_f(E_{0f})$ = distortion output voltage with feedback
E_{uf} = undesired interference output voltage with feedback
α = negative feedback factor
β = positive feedback factor
μ_0 = overall amplification without feedback
E_1 = fundamental input voltage
D_0 = distortion coefficient without feedback
E_u = undesired interference voltage without feedback.

The total input voltage to the amplifier is

$$E_1+\beta E_1 - \alpha[E_{0f}+D_f(E_{0f})+E_{uf}]$$

$$\therefore E_{0f}+D_f(E_{0f})+E_{uf} = \mu[E_1(1+\beta) - \alpha(E_{0f}+D_f(E_{0f})+E_{uf})]+E_u + D_0(\mu E_1(1+\beta) - \mu\alpha E_{0f})$$

$$= \frac{\mu(1+\beta)}{1+\mu\alpha}E_1+\frac{D_0(\mu E_1(1+\beta) - \mu\alpha(E_{0f})]}{1+\mu\alpha} + \frac{E_u}{1+\mu\alpha} \quad . \quad . \quad . \quad . \quad 10.60.$$

If $\mu\alpha = \beta$, i.e., the negative feedback voltage is equal to the positive

$$E_{0f}+D_f(E_{0f})+E_{uf} = \mu E_1+\frac{D_0(E_{0f})}{1+\mu\alpha}+\frac{E_u}{1+\mu\alpha}.$$

The function of balanced feedback is seen to be that only distortion and interference voltages are fed back in the negative direction, the negative fundamental voltage being cancelled by the positive fundamental voltage. If an attempt were made to derive the positive fundamental voltage from the output it would be necessary to filter the distortion and interference voltages before application to the input circuit. Such a method would not be possible except for a single frequency input or a very narrow band of frequencies.

With balanced feedback the frequency response can be made independent of the amplifier response and dependent only on that of the input voltage source. Suppose the amplification of the amplifier is represented by $\mu\phi(f)$ where $\phi(f)$ indicates a function of frequency, and the positive feedback factor is $\beta\phi'(f)$, where $\phi'(f)$ is

the frequency function for the input source. If the negative feedback circuit is independent of frequency,

$$\frac{E_{0f}}{E_1} = \frac{\mu\phi(f)(1+\beta\phi'(f))}{1+\mu\alpha\phi(f)} \quad . \quad . \quad . \quad 10.61$$

if $\mu\alpha.\phi(f) \gg 1$, $\beta\phi'(f) \gg 1$ and $\mu\alpha = \beta$.

$$\frac{E_{0f}}{E_1} = \mu\phi'(f)$$

i.e., is dependent only on the frequency characteristic of the input voltage.

A possible circuit for obtaining balanced feedback is shown in Fig. 10.25. Positive voltage feedback is obtained via the resistances R_1 and R_2 from the anode of V_2 to the grid of V_1. C_1 acts as a coupling capacitance and has a high value. Negative voltage

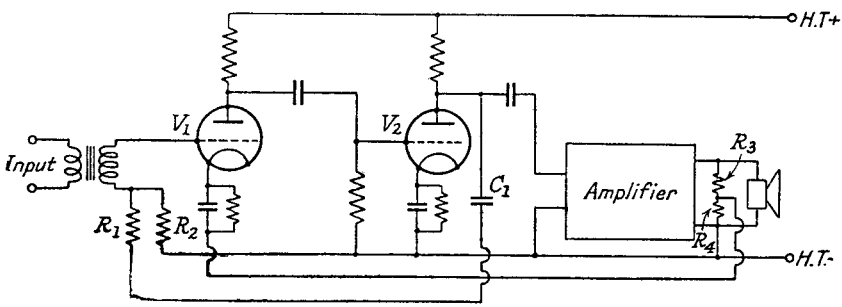

FIG. 10.25.—A Circuit for Obtaining Balanced Feedback.

feedback is obtained by connecting the cathode of V_1 to earth through R_4, which forms with R_3 a potential divider for the output voltage.

10.10.8. Instability in Feedback Amplifiers. From Section 9.3 we see that the gain of an amplifier over a frequency range must normally be represented by a complex number $\frac{\mu_m}{1 \pm jx}$, so that unless the feedback factor is a conjugate $\left(\frac{\alpha}{1 \pm jx}\right)$ of this, the feedback voltage phase relationship cannot be maintained at 180° to the input voltage for all frequencies. If it should happen at any frequency that the feedback phase-shift has been moved through 360°, positive feedback and, if $\mu\alpha > 1$, oscillation result, for expression 10.49 becomes

$$\frac{E_0}{E_1} = \frac{\mu}{1-\mu\alpha} = \frac{\mu}{0} = \infty.$$

Let us examine the case of a *RC* coupled amplifier with a resistive feedback circuit. A single stage gives a gain $\frac{\mu}{1 \pm jx}$ and the maximum possible phase shift through the amplifier is $\pm 90°$. Such a stage cannot be unstable with negative feedback because the feedback voltage vector must lie between 90° and 270° with respect to the input voltage. A two-stage *RC* coupled amplifier gives an overall amplification of

$$\mu_t = \frac{\mu_1}{1+jx_1} \cdot \frac{\mu_2}{1+jx_2}.$$

The alternative negative sign is not included because it leads to the same conclusion as the positive.

$$\mu_t = \frac{\mu_1 \mu_2}{1 - x_1 x_2 + j(x_1 + x_2)}.$$

Owing to the term $-x_1x_2$, the feedback voltage vector associated with μ_t can be rotated beyond 270°, and tends, as x_1 and x_2 increase, to approach the in-phase position with the input voltage. It does not reach the 360° position until $x_1 = x_2 = \infty$ when μ_t is zero. Thus a two-stage *RC* amplifier with resistive feedback is theoretically stable. In practice phase changes in decoupling and feedback circuits occur, and oscillation is possible.

The gain for a three-stage amplifier is

$$\mu_t = \frac{\mu_1 \mu_2 \mu_3}{(1+jx_1)(1+jx_2)(1+jx_3)}$$

$$= \frac{\mu_1 \mu_2 \mu_3}{1 - (x_1x_2 + x_1x_3 + x_2x_3) + j(x_1 + x_2 + x_3 - x_1x_2x_3)}.$$

The imaginary term disappears when

$$x_1 + x_2 + x_3 = x_1x_2x_3$$

and oscillation then occurs if

$$x_1x_2 + x_1x_3 + x_2x_3 > 1.$$

By suitable proportioning of the stages, such as making $x_1 = x_2$ and x_3 as different as possible from x_1 and x_2, the limiting feedback factor may be raised.

In transformer-coupled amplifiers leakage inductance and stray secondary capacitance produce resonance at some high frequency, and above this resonance the output voltage phase shift exceeds 270°. A single stage transformer coupling with resistive feedback is stable because the phase shift only reaches 360° when the amplification is too small to produce oscillation. Two stages of

transformer coupling, or one stage of *RC* and one stage of transformer coupling can, however, produce instability.

In a broadcast receiver we are mostly concerned only with one stage of amplification before the output stage, and the transformer of the latter is sufficiently damped by the load to reduce the phase-shift and amplification due to leakage inductance and stray capacitance resonance. If an intervalve transformer is used before the output stage, the tendency to instability may be checked by damping the secondary by a resistance. As the frequency of instability is often outside the pass range of the amplifier, self-oscillation can be prevented by inserting, in the amplifier or feedback circuit, a filter sharply attenuating undesired frequencies with little attenuation or phase shift in the desired frequency range.

10.10.9. The Application of Negative Feedback to the Output Stage. There is usually little advantage in applying negative feedback to a triode output stage, since a comparatively large input signal is needed without feedback and the slope resistance of the valve is in any case low. Furthermore, with feedback the increased input for a given power output tends to increase distortion in the preceding stage. The performance of a tetrode output stage can, however, be improved by voltage negative feedback, because distortion and generator impedance are reduced while still retaining the tetrode features of high efficiency and power output. Its power sensitivity is reduced, but since this is usually initially high, the extra input signal can often be obtained with little increase in distortion from the previous stage. Current feedback is practically never used in an output stage as it increases generator impedance and exaggerates loudspeaker resonances. Two methods of applying voltage feedback are shown in Figs. 10.26*a* and 10.26*b*. The first uses feedback into the grid circuit from the anode, the feedback ratio being $\frac{R_2}{R_1+R_2}$. This method may not be used in a positive-drive output stage taking grid current because of the resistance R_2. The capacitance C_1, which serves to isolate the D.C. anode voltage, may also be employed to reduce feedback at low frequencies, thus partially compensating for loss of low-frequency output due to the falling reactance of the output transformer primary. The earth capacitance of the input transformer secondary is in parallel with R_2, so that feedback at high frequencies is decreased. The feedback circuit cannot be connected directly to the grid of the output valve because coupling between anode and grid reduces its grid input resistance (Section 2.8.2, Part I), and so tends to increase distortion

in the preceding amplifier stage (Section 9.3.3). Fig. 10.26*a* cannot be used when the stage before the output valve has *RC* coupling because the grid leak from the grid to the junction of R_1 and R_2

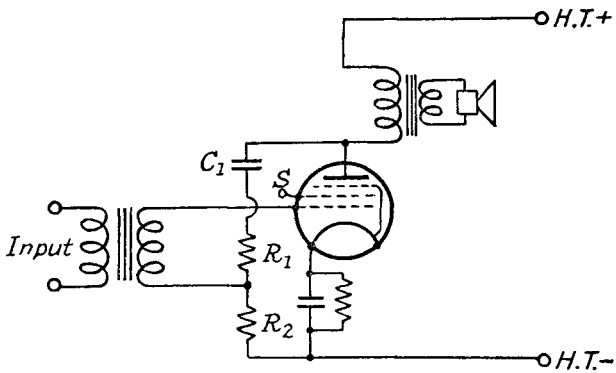

FIG. 10.26*a*.—Voltage Negative Feedback from the Output Transformer Primary to the Grid Circuit.

forms a potential divider, with the load and slope resistance of the previous valve, which reduces the proportion of feedback voltage across R_2 effectively applied to the output valve grid.

The second circuit feeds back from the output transformer secondary to the cathode, and this helps to compensate for output

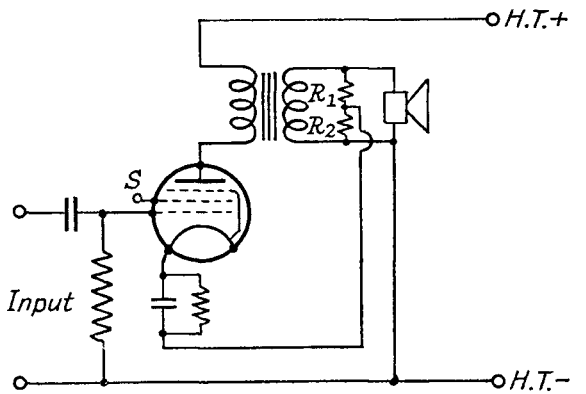

FIG. 10.26*b*.—Voltage Negative Feedback from the Output Transformer Secondary to the Cathode Circuit.

transformer harmonic distortion and the loss of low- and high-frequency response due to primary and leakage inductance. The resistance R_2 produces some degree of undesired current feedback because it is included in the cathode circuit; this and the

secondary load impedance limit the maximum value of voltage feedback and make the circuit more satisfactory for feedback applied over two stages.

The circuit of Fig. 10.26*a* is suitable for application to a push-pull stage, but each half of the push-pull input transformer must have its own feedback circuit; the transformer must therefore have two separate secondary windings.

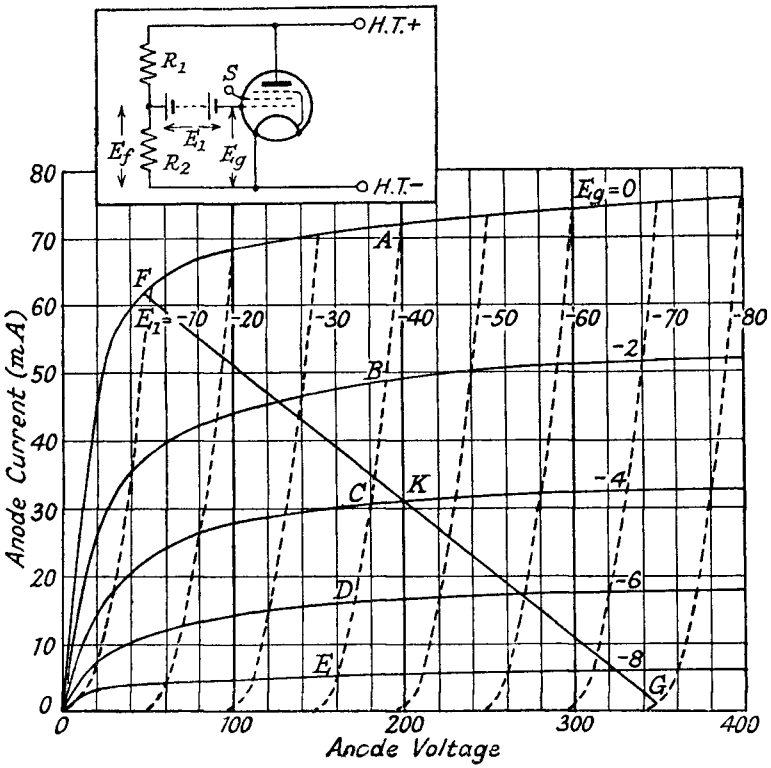

FIG. 10.27.—The Construction of Voltage Negative Feedback Curves for a Tetrode Valve.

Dotted Curves: Equivalent Negative Feedback Characteristics.

The performance of a tetrode output valve having voltage negative feedback may be examined by constructing special feedback curves on the I_aE_a characteristics. The circuit diagram for these curves is shown in Fig. 10.27, and in this same figure the feedback curves, shown dotted, are superimposed on the I_aE_a curves. The method of calculating the feedback curves from the I_aE_a curves is as follows. Suppose the total anode voltage is 200 and the feedback

ratio $\alpha\left(\frac{R_2}{R_1+R_2}\right)$ is 20% ; the voltage (E_f) across R_2 is +40. Now the actual bias voltage (E_g) applied between the grid and cathode is the sum of the grid to feedback point voltage (E_1) and the feedback voltage (E_f),

i.e., $E_g = E_1 + E_f = E_1 + \alpha E_a$ . . . 10.62*a*

where α = feedback ratio.

If $E_1 = -40$, $E_g = -40+40 = 0$ volts.

Hence point A the intersection of the I_aE_a curve for $E_g = 0$ with $E_a = 200$ must give a point on the input feedback curve corresponding to $E_1 = -40$. When $E_a = 190$ volts, $E_f = +38$ and if $E_1 = -40$, $E_g = -2$; thus point B, the intersection of $E_a = 190$ and the I_aE_a curve for $E_g = -2$, must be another point on the feedback curve for $E_1 = -40$. Points C, D and E for $E_f = +36$, $+34$ and $+32$ respectively are found by a similar process, which can be extended to produce feedback curves for other values of E_1 as shown in the figure. For a different feedback ratio another set of curves must be constructed.

To illustrate the use of these curves we will assume that the optimum load (it is unaltered by feedback) is 5,000 ohms, the H.T. voltage = 200 volts, and normal operating bias is -4 volts. The load line is FKG. The feedback curve passing through K is $E_1 = -44$, and this is the datum curve. Maximum input voltage is determined by the peak input signal which just takes the load line excursion to F, the intersection of the load line and $E_g = 0$. The input voltage line through F is $E_1 = -9$ so that the peak input voltage required is $44 - 9 = 35$ volts.

It is important to note that the datum and boundary conditions (points K and F) are fixed by the I_aE_a curves and not by the feedback curves. Power output and distortion may be calculated from the intersection of the load line with the appropriate input voltage lines, and, if the procedure set out in Section 10.4 is followed, the current intercepts must be measured for $E_1 = -9$; $-26{\cdot}5(-44+35 \times 0{\cdot}5)$, -44, $-61{\cdot}5$ and -79 volts. The feedback curves make quite clear that distortion and equivalent generator impedance are considerably reduced. The generator impedance is decreased from an average of about 40,000 ohms to 700 ohms by this degree of feedback.

In designing an output stage for optimum performance, the highest feedback ratio is required, and the limit is set by the maximum output possible with low distortion from the previous

stage. If, for example, this must not exceed 20 volts peak, we can calculate the maximum permissible feedback ratio by using the modified form of expression 10.62*a*.

$$\Delta E_g = \Delta E_1 - \Delta E_f \quad . \quad . \quad . \quad 10.62b.$$

The negative sign before the change of feedback voltage, ΔE_f, is necessary because feedback is negative and opposes the change of input voltage, ΔE_1. Now $\Delta E_f = \alpha \Delta E_a$, so that $\Delta E_g = \Delta E_1 - \alpha E_a$ and

$$\alpha = \frac{\Delta E_1 - \Delta E_g}{\Delta E_a} \quad . \quad . \quad . \quad . \quad 10.63.$$

Assuming the output valve to be operating for maximum power, the maximum change of anode voltage is

$\Delta E_a \simeq 150$ volts (the horizontal distance between K and F)
$\Delta E_1 = 20$.

From inspection of Fig. 10.27,

$$\Delta E_g = 4 \text{ volts.}$$

Therefore

$$\alpha = \frac{20 - 4}{150}$$

$$= \frac{16}{150} = 10{\cdot}66\%.$$

Curves may be constructed for this value of α as set out above and the performance of the output stage estimated.

10.10.10. Two-Stage Feedback Circuits.[34, 36] The application of negative feedback to a two-stage amplifier confers two advantages: (1) it raises the value of μ_0 in expression 10.49, so that for a fixed feedback ratio the output voltage approaches more closely to $\frac{E_1}{\alpha}$ and overall frequency response is controlled to a large extent by the feedback circuit; (2) it reduces distortion and compensates for frequency response deficiencies in the stage preceding the output, and (3) it requires less feedback voltage than a single stage so that this voltage may be derived from the secondary of the output transformer.

In a two-stage amplifier it is only possible to indicate the general lines of a design since the particular form of feedback circuit has to be suited to amplifier and load characteristic. A representative circuit [39] is shown in Fig. 10.28. The chief points to note are that R_1 and R_3 are sufficiently large to prevent serious loss of power and that R_2 is small enough to cause negligible current feedback

in the first valve. The inductance L_2 is placed in parallel with R_2 to reduce feedback at low frequencies (less than 100 c.p.s.), and compensate for the limited size of loudspeaker baffle, but sufficient feedback is allowed to reduce to some extent the resonance usually found between 50 and 100 c.p.s. Owing to the rise in speech-coil impedance as the frequency increases, it is advantageous to try to

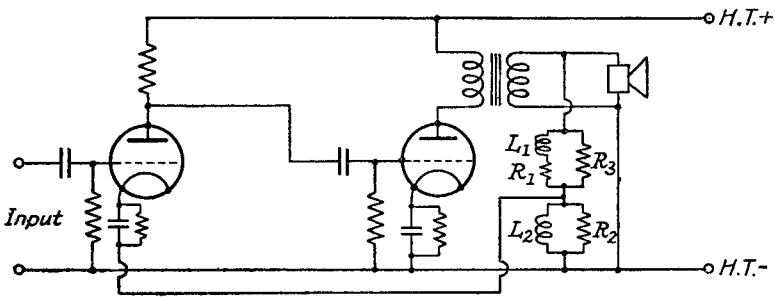

FIG. 10.28.—Negative Feedback in a Two-stage Amplifier.

maintain constant output current, and this is achieved by adjusting L_1R_1 and R_3 to satisfy expression 10.55 which requires α to be $\frac{K}{Z_0}$. As an example, let us assume that the first valve has $\mu = 30$ and $R_a = 10{,}000$ ohms with a total anode load resistance $\frac{(R_0R_g)}{R_0+R_g}$ of 50,000 ohms; the second valve is a tetrode of $g_m = 10$ mA/volt and an optimum output load resistance of 5,000 ohms, the speech-coil impedance is 5·5 ohms, and feedback reduces the overall amplification to $\frac{1}{5}$ of its initial value.

Amplification of the first stage neglecting current feedback in R_2

$$= \frac{\mu R_0'}{R_a+R_0'} = \frac{30 \times 50{,}000}{60{,}000} = 25.$$

Amplification of the second stage $= g_mR_0' = \frac{10}{1{,}000} \times 5{,}000 = 50.$

Step-down ratio of output transformer

$$= \sqrt{\frac{5{,}000}{5{\cdot}5}} \simeq 30.$$

Overall voltage amplification to the secondary of the output transformer

$$= \frac{25 \times 50}{30} = 41{\cdot}6.$$

$$\frac{1}{1+\mu_0\alpha} = \frac{1}{5}.$$

Therefore $\mu_0\alpha = 4$ and $\alpha = \frac{4}{\mu_0} = \frac{4}{41{\cdot}6} = \frac{1}{10{\cdot}4} = 9{\cdot}6\%$.

Assuming that L_1 has not much effect at the medium frequencies,

$$\frac{R_2}{R_2+\frac{R_1R_3}{R_1+R_3}} = \frac{1}{10{\cdot}4}.$$

A suitable value for $\frac{R_1R_3}{R_1+R_3}$ is 200 ohms, for the loss of power is then negligible, and

$$R_2 = \frac{200}{9.4} = 21{\cdot}3 \text{ ohms}.$$

Examining the effect of R_2 in the cathode circuit of the first valve, we find that the voltage amplification of the first valve is

$$\text{Amplification} = \frac{\mu R_0}{R_a+R_2(1+\mu)+R_0} = \frac{30 \times 50{,}000}{10{,}000+660+50{,}000}$$
$$= \frac{30 \times 5}{6{\cdot}066} = 24{\cdot}7,$$

which shows that current feedback due to R_2 can be neglected. The inductance of L_2 must depend on the low-frequency compensation required and a probable value is that making the reactance at 100 c.p.s. equal to R_2, i.e.,

$$L_2 = \frac{21{\cdot}3 \times 1{,}000}{6{\cdot}28 \times 100} = 33{\cdot}9 \text{ mH}.$$

The values of L_1, R_1 and R_3 depend on the speech coil and should be adjusted to give an impedance at high frequencies proportional to the speech-coil impedance.

A similar circuit may be adopted with a push-pull stage. The feedback voltage must not be taken from either half primary of the output transformer, but from the secondary or a suitable third winding. The voltage across each half primary of the output transformer contains some of the distortion components produced by the valve, which are not cancelled because of the leakage inductance and resistance of the windings. These components do, however, cancel each other when the voltage is taken across the total primary and are therefore not present in the secondary. If these distortion components are fed back they tend to increase the overall distortion, and one advantage of feedback is lost.

If the first stage is transformer-coupled, a resistance may be required across the secondary to damp the resonance due to leakage inductance and stray capacitance, and to prevent excessive phase

shifts, which might lead to positive feedback and self-oscillation at some high frequency outside the normal audio frequency range.

BIBLIOGRAPHY

1. An Apparatus for the Projection of Frequency Output Characteristics. C. G. Garton, and G. S. Lucas, *Wireless Engineer*, Feb. 1929, p. 62.
2. Output Characteristics of Thermionic Amplifiers. B. C. Brain, *Wireless Engineer*, March 1929, p. 119.
3. Push-Pull Amplification. F. Aughtie, *Wireless Engineer*, June 1929, p. 307.
4. A Thermionic Voltmeter Method for the Harmonic Analysis of Electrical Waves. C. G. Suits, *Proc. I.R.E.*, Jan. 1930, p. 178.
5. Effect of Output Load upon Frequency Distortion in Resistance Amplifiers. H. A. Thomas, *Wireless Engineer*, Jan. 1931, p. 11.
6. Percentage Harmonic Distortion. G. W. O. Howe, *Wireless Engineer*, July 1931, p. 347.
7. Push-Pull Problems. W. T. Cocking, *Wireless World*, 5th Aug. 1931, p. 128.
8. The Problem of Pentode Output Fidelity. L. Tulauskas, *Electronics*, Oct. 1931, p. 142.
9. Distortion in Valve Characteristics. G. S. C. Lucas, *Wireless Engineer*, Nov. 1931, p. 595. *Correspondence*, Dec. 1931, p.660, Feb. 1932, p. 76.
10. A Simple Harmonic Analyzer. M. G. Nicholson and W. M. Perkins, *Proc. I.R.E.*, April 1932, p. 734.
11. Regeneration Theory. H. Nyquist, *Bell Technical Journal*, July 1932, p. 126.
12. Grid Current Compensation in Power Amplifiers. W. Baggally, *Wireless Engineer*, Feb. 1933, p. 65.
13. Graphical Determination of Performance of Push-Pull Audio Amplifiers. B. J. Thompson, *Proc. I.R.E.*, April 1933, p. 591.
14. Permissible Amplitude Distortion of Speech in an Audio Reproducing System. F. Massa, *Proc. I.R.E.*, May 1933, p. 682.
15. A Theory of Available Output and Optimum Operating Conditions for Triode Valves. M. V. Callendar, *Proc. I.R.E.*, July 1933, p. 909.
16. Distortion Cancellation in Audio Amplifiers. W. Baggally, *Wireless Engineer*, Aug. 1933, p. 413.
17. The Calculation of Harmonic Production in Thermionic Valves with Resistive Loads. D. C. Espley, *Proc. I.R.E.*, Oct. 1933, p. 1439.
18. High Quality Class B Amplification. K. A. Macfadyen, *Wireless World*, Dec. 15th, 1933, p. 454.
19. Stabilised Feedback Amplifiers. H. S. Black, *Electrical Engineering*, Jan. 1934, p. 114.
20. Direct Reading Harmonic Scales. D. C. Espley and L. I. Farren, *Wireless Engineer*, April 1934, p. 183.
21. Push-Pull Input Systems. W. T. Cocking, *Wireless World*, Sept. 21st, 1934, p. 245.
22. Measurement of Non-Linear Distortions. H. Faulhaber, *Elecktrische Nachrichten Technik*, Oct. 1934, p. 351.
23. Incremental Permeability and Inductance. L. G. A. Sims, *Wireless Engineer*, Jan. (p. 8), Feb. (p. 65) 1935.

24. Intermodulation in Audio Frequency Amplifiers. A. C. Bartlett, *Wireless Engineer*, Feb. 1935, p. 70.
25. High Efficiency Push-Pull Output Stages. K. S. Macfadyen, *Wireless World*, 15th March 1935, p. 256.
26. Class B Transformers. N. Partridge, *Wireless World*, 22nd March 1935, p. 280.
27. Incremental Magnetization. L. G. A. Sims and D. L. Clay, *Wireless Engineer*, May (p. 238), June (p. 312) 1935.
28. Join-Up Distortion in Class B Amplifiers. F. R. W. Strafford, *Wireless Engineer*, Oct. 1935, p. 539.
29. Modifications of the Push-Pull Output Stage. K. S. Macfadyen, *Wireless Engineer*, Oct. and Dec. 1935, pp. 528 and 639.
30. Output Transformer Response. F. E. Terman and R. E. Ingebretsen, *Electronics*, Jan. 1936, p. 30.
31. Class B and Class AB Audio Amplifiers. G. Koehler, *Electronics*, Feb. 1936, p. 14.
32. Feeding Push-Pull Amplifiers. W. T. Cocking, *Wireless World*, Feb. 7th, 1936, p. 126.
33. Quasi Transients in Class B Audio Frequency Push-Pull Amplifiers. A. Pen-Tung Sah, *Proc. I.R.E.*, Nov. 1936, p. 1522.
34. Feedback Amplifier Design. F. E. Terman, *Electronics*, Jan. 1937, p. 12.
35. Amplitude Distortion. J. H. O. Harries, *Wireless Engineer*, Feb. 1937, p. 63.
36. Practical Feedback Amplifiers. J. R. Day and J. B. Russell, *Electronics*, April 1937, p. 16.
37. Phase Reversal in Push-Pull Amplifiers. C. C. Inglis, *Wireless World*, April 30th, 1937, p. 416.
38. Audio-Frequency Transformers. E. T. Wrathall, *Wireless Engineer*, June (p. 293), July (p. 363), Aug. (p. 414) 1937.
39. Inverse Feedback. B. D. H. Tellegen and V. C. Henriquez, *Wireless Engineer*, Aug. 1937, p. 409.
40. A New Push-Pull Feed Circuit. L. H. Cooper, *Wireless World*, Oct. 22nd, 1937, p. 411.
41. Some Properties of Negative Feedback Amplifiers. L. I. Farren, *Wireless Engineer*, Jan. 1938, p. 23.
42. Balanced Feedback Amplifiers. E. L. Ginzton, *Proc. I.R.E.*, Nov. 1938, p. 1367.
43. The Marconi-E.M.I. Television System. C. O. Browne, Part II, *Journal I.E.E.*, Dec. 1938, p. 767.
44. Distortion in Valves with Resistive Loads. A. Bloch, *Wireless Engineer*, Dec. 1939, p. 592.
45. Distortion Tests by the Intermodulation Method. J. K. Hilliard, *Proc. I.R.E.*, Dec. 1941, p. 614.
46. Optimum Conditions for Maximum Power in Class A Amplifiers. W. B. Nottingham, *Proc. I.R.E.*, Dec. 1941, p. 620.
47. Harmonic Distortion in Audio Frequency Transformers. N. Partridge, *Wireless Engineer*, Sept. (p. 394), Oct. (p. 451), Nov. (p. 503) 1942.
48. Optimum Conditions in Class A Amplifiers. G. W. O. Howe, *Wireless Engineer*, Feb. 1943, p. 53.
49. *Specification for Testing and Expressing Overall Performance of Radio Receivers.* Part II, Acoustic Tests, p. 15. Radio Manufacturers Association (England).

CHAPTER 11

POWER SUPPLIES

11.1. Introduction. The power supply circuits for the A.C., the A.C./D.C., the transportable (car) and the battery receiver have some common features, but also certain important differences. The power supply for the A.C. receiver consists of a mains transformer for the required heater and H.T. voltages, a rectifier and a smoothing filter for attenuating the rectified ripple voltage. In the A.C./D.C. receiver the mains transformer is omitted and the valve heaters are series-connected. The car receiver often uses the car battery for heater and H.T. supply, a vibrator (very occasionally a motor generator) acting as the converter for the H.T. supply. The battery receiver normally has an accumulator for L.T. and a dry battery for H.T. supply. The latter raises few problems ; adequate decoupling is essential in each stage of the receiver, to prevent feedback coupling as the internal resistance of the battery rises during life. Only supply circuits for the first three types of receivers are reviewed in this chapter.

11.2. A.C. Receiver Power Supply.

11.2.1. Introduction. A typical power supply circuit for an A.C. receiver is shown in Fig. 11.1. To suppress R.F. interference entering the receiver via the mains supply leads, an electrostatic

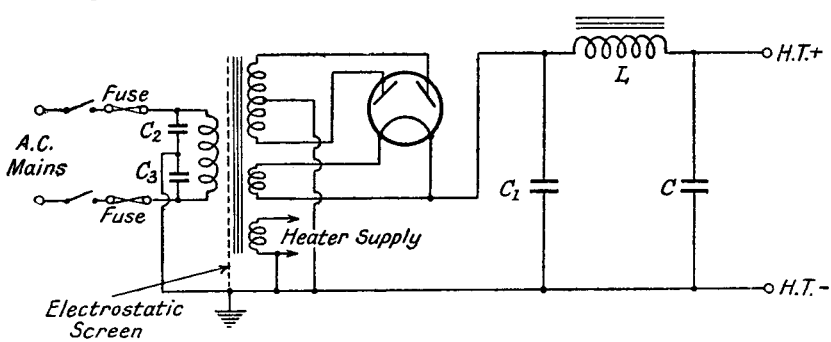

FIG. 11.1.—A Typical A.C. Receiver Power Supply Circuit.

screen is inserted between the primary and secondaries of the mains transformer, and two capacitances, C_2 and C_3 (about 0·001 μF) may be included from each mains lead to earth. The heater winding

may have a centre-tapped earth connection, but it is more common to earth one side of the winding. With indirectly-heated valves, hum and noise pick-up from the heaters can be almost entirely eliminated by connecting some point on the winding to earth. Directly-heated valves (normally only the output valves) must, however, be earthed at the centre tap in order to obtain electrostatic hum balance. An LC filter follows the reservoir capacitance C_1, and the full-wave rectifier. The filter choke has an air gap to prevent saturation of the iron core by the rectified current, and to maintain a high inductance value to the ripple voltage. The loud-speaker field coil is often employed as the filter choke. A small coil wound over the field winding is inserted in series with the speech coil to neutralize the effect on the latter of the A.C. ripple field.

11.2.2. The Mains Transformer.[11] The equivalent circuit for a mains transformer, having two secondary windings, shown in Fig. 11.2, gives a good indication of the features contributing to the production of a satisfactory component. The secondary winding resistances R_{s1} and R_{s2}, and the load resistances R_1 and R_2 are transferred to the primary side by dividing by the square of the ratios, n_1 and n_2, of the secondary to primary turns. The primary winding resistance and inductance are R_p and L_p respectively, and the leakage inductance is $L_p(1 - k^2)$ (Section 9.4), where k is the

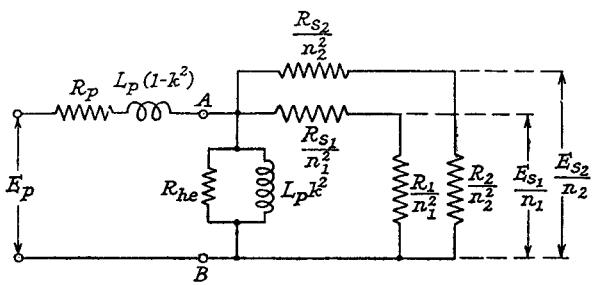

FIG. 11.2.—The Equivalent Circuit of a Mains Transformer.

coupling coefficient between primary and secondary. The leakage inductance is, in this case, considered to be the same for both secondary windings; the error involved in this assumption is not very large. R_{he} represents the hysteresis and eddy current loss in the iron core. The efficiency is governed by R_p, R_{s1}, R_{s2}, R_{he} and k, and decrease of the first three and increase of the last two lead to a higher efficiency. For good regulation, low values of R_p, R_{s1} and R_{s2}, and a high value of k are essential; R_{he} has little effect.

There are two alternatives for the winding positions; primary

and secondaries may be wound on top of each other, or they may be placed in separate sections side by side. In the first position the primary is usually nearest the centre limb of the core, and between it and the secondaries is the electrostatic screen, an open-circuited turn of copper foil or thin sheet. The H.T. and rectifier windings occupy the first two secondary positions respectively, and the L.T. heater winding is located in the outside position. For the second arrangement the primary winding is usually divided into two sections, each section being placed at the ends of the winding space. This reduces the leakage field (increases k) between the primary and secondaries, which are separate windings placed between the half primaries. Adequate insulation must be provided between the layers. Joints in the wire should have no projections and should occur at the centre of the layer, because electrical stress between layers is least at this position. Electrical stress is increased at projections, and insulation breakdown at joints due to mechanical puncture or corona effects may occur. Sharp corners to winding bobbins are avoided since electrical and mechanical (heating and cooling) stresses are greatest at these points. The ingress of moisture is prevented, preferably by sealing the windings (by pitch compound impregnation).

The design of a mains transformer is best illustrated by an example. Suppose a transformer fulfilling the following requirements is to be designed:

Primary . . .	230-volt 50-c.p.s. mains supply.
Secondaries . .	H.T. 300–0–300 volts 120 mA for full wave rectification, i.e., there is no D.C. polarizing current. The D.C. output for the above A.C. output would be about 280 volts, 90 mA. (See Section 11.2.5 for the method of calculating it.)
	L.T. 6·3 volts 2 amps.
	L.T. 6·3 volts 6 amps.

The fundamental equation for the induced voltage in any coil placed in a sinusoidal A.C. magnetic field is

$$E = 4{\cdot}44\ \hat{\Phi} f \times 10^{-8} \times N \text{ R.M.S. volts.} \qquad 11.1$$

where $\hat{\Phi}$ = peak value of the flux of the magnetic field.
= peak flux density ($\hat{B}$) × area (A) of a cross-section through which the field is threading.
f = frequency in c.p.s.
N = number of turns in the coil.

Rearranging 11.1.

$$\text{Turns per volt } \frac{N}{E} = \frac{10^8}{4{\cdot}44\,\hat{B}Af} \quad . \quad . \quad 11.2$$

where E has its R.M.S. value.

For Stalloy stampings a suitable value of $\hat{B}$ is 10,000 lines per square centimetre (64,500 lines per square inch) and taking A as 1·5 sq. ins.

$$\text{turns per volt} = 4{\cdot}65.$$

This permits the total primary turns to be calculated, but for estimating the secondary turns allowance must be made for the voltage drop in the primary and secondary winding resistance; i.e., the turns per volt for the secondary windings must be increased.

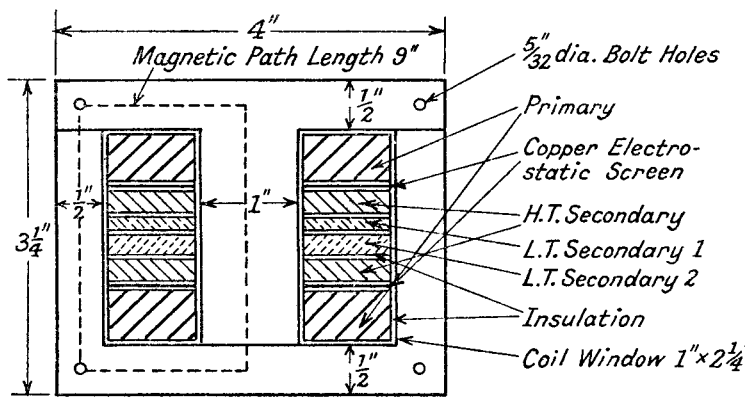

FIG. 11.3*a*.—A Section through a Typical Mains Transformer.

If we assume a power efficiency on full load of 85%, the voltage efficiency is approximately the square root of this, viz., 92%. For convenience the secondary turns per volt in subsequent calculations are taken as 5; this corresponds to a voltage efficiency of 92·5%.

The arrangement of the windings is shown in Fig. 11.3*a*, the primary winding being divided into two sections to reduce leakage inductance. The total number of turns for each winding and the number of sections are listed below.

Winding.	Total Turns.	Number of Sections.
Primary	1,070	2
H.T. Secondary	3,000	2
L.T. Secondary 1	31·5	1
L.T. Secondary 2	31·5	1

$$\text{Total output power from the transformer} = 300 \times 0{\cdot}12 + 6{\cdot}3 \times 8$$
$$= 86{\cdot}4 \text{ watts.}$$
$$\text{Total input power for 85\% efficiency} = 101{\cdot}6 \text{ watts.}$$
$$\text{Primary current} = \frac{101{\cdot}6}{230} = 0{\cdot}442 \text{ amps.}$$

Taking the permissible current density in all windings as 1,200 amps. per square inch, the required wire diameter can be calculated. The most suitable gauge of wire is then selected from Table 11.1 below, and the area taken by each winding estimated on the basis of double silk covering insulation for the primary and H.T. secondary, and enamel for the L.T. secondaries. The turns per square inch listed below [21] are calculated on the assumption that wires in consecutive layers are wound immediately above each other and not in the grooves between the wires of the layer below.

TABLE 11.1

S.W.G.	Wire Diameter (inches).	Resistance. Ohms per 1,000 yards.	Turns per Square Inch.				Enamel.
			SCC.	DCC.	SSC.	DSC.	
10	0·128	1·8657	54·1	49·6	58·3	57	—
12	0·104	2·8626	79·7	71·8	87·3	85	—
14	0·08	4·776	129	113	145	140	145
16	0·064	7·463	198	173	223	213	226
18	0·048	13·267	343	297	400	377	400
20	0·036	23·59	567	472	692	641	692
22	0·028	38·99	865	692	1,110	1,010	1,110
24	0·022	63·16	1,280	977	1,770	1,600	1,770
26	0·018	94·35	1,740	1,280	2,560	2,270	2,560
28	0·0148	139·55	2,310	1,630	3,650	3,160	3,760
30	0·0124	198·8	2,950	1,990	5,180	4,500	5,370
32	0·0108	262·1	4,010	2,550	6,610	5,650	6,890
34	0·0092	361·2	4,960	3,020	8,730	7,310	9,610
36	0·0076	529·2	7,430	4,110	12,100	10,300	13,500
38	0·006	849·1	10,000	5,100	17,800	14,700	20,400
40	0·0048	1,326·7	12,900	6,100	25,200	20,100	32,500

SCC = Single Cotton Covered. SSC = Single Silk Covered.

The details of each winding are therefore as follows :

Winding.	Required Wire Diameter (ins,) I = 1,200 Amps. per sq. in.	Suitable S.W.G.	Winding Area (Sq. ins.).
Primary . .	0·02165	24	0·669
H.T. Secondary .	0·00797	34	0·41
L.T. Secondary 1 .	0·0460	18	0·0788
L.T. Secondary 2 .	0·0797	14	0·217
		Total =	1·3748

Note that the average current from each half-secondary is only 60 mA because it delivers 120 mA each half-cycle. The wire diameter is therefore calculated as for 60 mA.

The next step is to decide on the stamping for the core. The cross-section of the central limb must be 1·5 sq. ins. in order to satisfy expression 11.2, and a suitable width for the limb is 1 in. The area of the winding window must be able to accommodate the coils (1·3748 sq. ins.) and the insulation between them. Let us try Stalloy No. 32A, the dimensions of which are given in Fig. 11.3*a*, and assume that the insulation between the windings themselves, and the windings and core is 0·075 ins. thick, and that the insulation from the primary to electrostatic screen is 0·05 ins. The available winding area dimensions are

$$\begin{aligned}\text{Effective width} &= \text{total width} - \text{insulation}\\ &= 1 - (2 \times 0{\cdot}075) = 0{\cdot}85 \text{ ins.}\\ \text{Effective height} &= \text{total height} - (\text{interwinding insulation}\\ &\qquad + \text{winding to screen insulation}\\ &\qquad + \text{electrostatic screens})\\ &= 2{\cdot}25 - (5 \times 0{\cdot}075 + 2 \times 0{\cdot}1 + 2 \times 0{\cdot}01)\\ &= 1{\cdot}655 \text{ ins.}\\ \text{Therefore total winding area} &= 1{\cdot}408 \text{ sq. ins.}\end{aligned}$$

There is a reasonable factor of safety upon that actually required, 1·3748 sq. ins.

The iron loss, copper loss and efficiency must now be checked.

(1) *Iron Losses.*

$$\begin{aligned}\text{Area of face of stamping} &= \text{total area} - \text{winding window area}\\ &\qquad - \text{area for } \tfrac{5}{32} \text{ in. diameter bolts.}\\ &= 4 \times 3{\cdot}25 - 2{\cdot}25 \times 2 - \pi\left(\frac{5}{32}\right)^2\\ &= 8{\cdot}4236 \text{ sq. ins.}\\ \text{Thickness of iron core} &= 1{\cdot}5 \text{ ins.}\\ \text{Total volume of iron} &= 8{\cdot}4236 \times 1{\cdot}5 = 12{\cdot}63 \text{ cu. ins.}\\ \text{Weight of iron (density 0·28 lbs. per cubic inch)} &= 12{\cdot}63 \times 0{\cdot}28 = 3{\cdot}54 \text{ lbs.}\\ \text{Loss in standard Stalloy at } \hat{B} &= 10{,}000 \text{ lines per square centimetre}\\ &= 0{\cdot}65 \text{ watts per lb.}\\ \text{Therefore loss in iron core} &= 2{\cdot}3 \text{ watts.}\end{aligned}$$

Allowing 10% insulation between stampings, the total thickness of core = 1·65 ins.

Number of laminations 0·014 in. thick = 118.

(2) *Winding Copper Loss.*

From Figs. 11.3*a* and 11.3*b*, the mean length of a winding turn is 9·3 ins. The total length of each winding, its resistance (obtained from Table 11.1) and power loss are tabulated below.

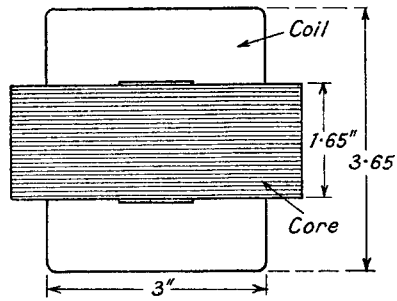

FIG. 11.3*b*.—A Plan View of the Mains Transformer of Fig. 11.3*a*.

Winding.	Total Turns.	Yards.	Ohms.	Current.	Power Loss.
Primary	1,070	276·5	17·7	0·442	3·42
H.T. Secondary	3,000	775	280	0·06	1·01
L.T. Secondary 1	31·5	8·14	0·1079	2	0·432
L.T. Secondary 2	31·5	8·14	0·0389	6	1·40

$$\text{Total loss (iron+copper)} = 6{\cdot}262+2{\cdot}3 = 8{\cdot}562 \text{ watts.}$$

$$\text{Efficiency} = \frac{86{\cdot}4}{94{\cdot}962} = 91\%.$$

This is slightly higher than the value assumed initially, but there is some increase in primary loss due to magnetizing current, which has not been considered in the above.

(3) *No-load and Full-load Operating Conditions.*

The no-load current of the transformer is determined mainly by the primary inductance, the formula for which is given in expression 11.19*b*, Section 11.2.9.

$$L = 1{\cdot}255\ \Delta\mu n^2 V 10^{-8}$$

where n = turns per centimetre of the magnetic path in the core.

$\Delta\mu$ = incremental A.C. permeability.

V = volume of iron core in cubic centimetres.

From Fig. 10.20, $\Delta\mu$ is 2,400 at $\hat{B} = 10{,}000$ lines per square centimetre, $H_{\text{D.C.}} = 0$, but let us assume $\Delta\mu$ is 2,000. The primary inductance is therefore

$$L_p = \frac{1{\cdot}255 \times 2{,}000 \times 2{\cdot}54 \times (1{,}070)^2 \times 12{\cdot}63}{9^2 \times 10^8}.$$

The factor 2·54 is included to convert turns per inch of magnetic

path and volume in cubic inches to turns per centimetre and cubic centimetres. The length of the magnetic path is 9 ins. (See Fig. 11.3*a*.)

Therefore $L_p = 11{\cdot}38$ H

$$X_p = 2\pi f L_p = 3{,}570\ \Omega.$$

The primary winding resistance has practically no effect on the no-load current which is

$$I_0 = \frac{230}{3{,}570} = 64{\cdot}4 \text{ mA}.$$

By assuming a leakage inductance of 0·5% of L_p (a probable value), we can estimate the no-load and full-load voltages at the secondary terminals. On no load the primary winding resistance has practically no effect, so that all no-load secondary voltages are 0·5% lower than the values given from the turns ratio.

H.T. half secondary open-circuit voltage $= \dfrac{230 \times 1{,}500 \times 0{\cdot}995}{1{,}070} = 320$

L.T. secondary (1) and (2) open-circuit voltage

$$= \frac{230 \times 31{\cdot}5 \times 0{\cdot}995}{1{,}070} = 6{\cdot}72.$$

To determine the full-load voltages it is necessary to estimate the secondary load resistances referred to the primary side. Thus, for the H.T. secondary, the total load resistance (including the winding resistance) for each half secondary is

$$\left[140 \text{ (winding)} + \frac{300}{0{\cdot}06}\text{(load)}\right] = 5{,}140 \text{ ohms},$$

and the load resistance for both half secondaries referred to the primary side becomes $2{,}570 \times \left(\dfrac{1{,}070}{1{,}500}\right)^2 = 1{,}310$ ohms. Similarly, the primary load resistances due to L.T. secondaries 1 and 2 are 3,770, $\left[\left(0{\cdot}1079 + \dfrac{6{\cdot}3}{2}\right)\left(\dfrac{1{,}070}{31{\cdot}5}\right)^2\right]$ and 1,260 ohms. The total resistance load across the points AB in Fig. 11.2 is the resultant of 1,310, 3,770 and 1,260 in parallel, i.e., 549 ohms.

The equivalent impedance across the points AB, including the reactance of $L_p k^2$, (j 3,552 ohms) is

$$R_{AB} + jX_{AB} = \frac{549 \times (3{,}552)^2}{(549)^2 + (3{,}552)^2} + j\frac{3{,}552 \times (549)^2}{(549)^2 + (3{,}552)^2}$$

$$= 537 + j\ 83.$$

The induced voltage in the transformer primary, i.e., the voltage across AB

$$= E_p \sqrt{\frac{(R_{AB})^2+(X_{AB})^2}{(R_{AB}+R_1)^2+(X_{AB}+\omega L_p(1-k^2))^2}}$$

$$= 230 \sqrt{\frac{(537)^2+(83)^2}{(554{\cdot}5)^2+(100{\cdot}85)^2}}$$

$$= 222 \text{ volts.}$$

The voltage across each pair of secondary terminals is

$$E_{AB} \frac{N_s}{N_p} \cdot \frac{R_L}{R_W+R_L}$$

where N_s and N_p are the secondary and primary turns, R_L and R_W are the load and winding resistances of the secondary.

$$\text{H.T. half secondary voltage} = 222 \frac{1{,}500}{1{,}070} \frac{5{,}000}{5{,}140} = 302 \text{ volts.}$$

$$\text{L.T. secondary 1 voltage} = 222 \frac{31{\cdot}5}{1{,}070} \frac{3{\cdot}15}{3{\cdot}2579} = 6{\cdot}3 \text{ volts.}$$

$$\text{L.T. secondary 2 voltage} = 222 \frac{31{\cdot}5}{1{,}070} \frac{1{\cdot}05}{1{\cdot}089} = 6{\cdot}3 \text{ volts.}$$

It is interesting to note the effect of an increase in leakage inductance to 1% of L_p; E_{AB} becomes 220 volts and the secondary voltages are reduced to 299 and 6·25 respectively. The need for keeping leakage inductance to the lowest possible value cannot be overstressed.

(4) *Transformer Temperature Rise on Full-load.*

For an air-cooled transformer an approximate value for the area required to dissipate 1 watt for a temperature rise of 1° C. in the iron is 30 sq. ins. and for the coils is 50 sq. ins.

The cooling area for the iron includes the top, sides, front and back faces, except that just underneath the coil, but does not include the bottom or central limb. The effective iron thickness of the core is 1·5 ins. Hence, from Figs. 11.3*a* and 11.3*b*.

$$\text{Total cooling area} = (4 \times 1{\cdot}5)+(3{\cdot}25 \times 1{\cdot}5)2+(4 \times 0{\cdot}5)2 + (2{\cdot}75 \times 0{\cdot}5)4 = 25{\cdot}25 \text{ sq. ins.}$$

$$\text{Watts lost in the iron core} = 2{\cdot}3$$

$$\text{Temperature rise of iron core} = \frac{30 \times 2{\cdot}3}{25{\cdot}25} = 2{\cdot}73° \text{ C.}$$

The cooling area for the coil includes all the area outside the iron core but excludes that at the bottom of the transformer.

$$\text{Cooling area of coil} = (3 \times 1)2+(2{\cdot}25 \times 1)4+(3 \times 2{\cdot}25)2$$
$$= 29{\cdot}5 \text{ sq. ins.}$$
$$\text{Watts lost in the coil} = 6{\cdot}262$$
$$\text{Temperature rise of coil} = \frac{50}{29{\cdot}5} \times 6{\cdot}262 = 10{\cdot}6^\circ \text{ C.}$$

In actual practice some heat is transferred from the coil to the core so that the average temperature of the coil is likely to be slightly lower than that given, and that of the core slightly higher. The calculated temperature rises are, however, well within the permissible values.

In the above example we have assumed that there is no polarizing D.C. field since a full-wave rectifier is being used. If half-wave rectification is employed, there is a D.C. polarizing field in the core due to the rectified current flowing in the secondary winding. The chief effect of the D.C. polarizing field is to reduce the primary inductance, thereby increasing the magnetizing current and reducing efficiency. An air gap is desirable, and the design principles involved are as set out in Section 11.2.9, but modified by the fact that the A.C. flux density is large and in most cases greater than the D.C. polarizing flux density.

11.2.3. The H.T. Rectifier. There are four important types of rectifier circuits, the full-wave, half-wave, bridge and voltage-doubler. Examples of the last three are given in Figs. 11.4*a*, 11.4*b* and 11.4*c*. The full-wave rectifier, illustrated in Fig. 11.1, is the most common type of receiver rectifier, and among its outstanding features are cancellation of the fundamental mains frequency com-

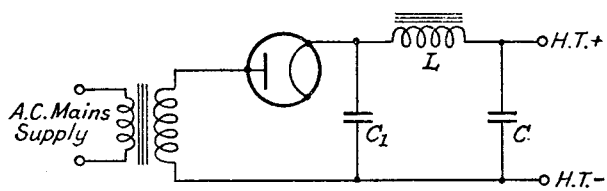

FIG. 11.4*a*.—A Half-wave Rectifier.

ponent in the rectified output, and cancellation of the D.C. current components through the mains transformer. This allows a smaller transformer core to be used and better voltage regulation to be obtained. On the other hand, a centre-tapped secondary winding is required, having a total A.C. peak voltage of approximately twice the D.C. output voltage. The half-wave rectifier has the merit of simplicity, reduced rectifier cost and only one secondary winding.

The secondary is half that of the full-wave rectifier secondary for the same D.C. output voltage. The D.C. output current is, however, only half that of the full-wave rectifier with similar secondary windings, and voltage regulation is worse. The simplified analysis of Section 11.2.5 shows that there should be little difference [2] between the R.M.S. to D.C. current ratios, but in practice it is generally found to be about 1·6 compared with 1·35 for full-wave operation. This, combined with the D.C. polarizing current in the secondary winding, tends to reduced transformer efficiency, whilst hum level of the D.C. output voltage is increased by the presence of a large mains fundamental frequency voltage component. The half-wave rectifier is most suitable for providing a high-voltage low-current D.C. output, such as that required for cathode-ray tube power supply circuits, but it is also used for A.C./D.C. operated receivers, which have no transformer connection to the mains supply.

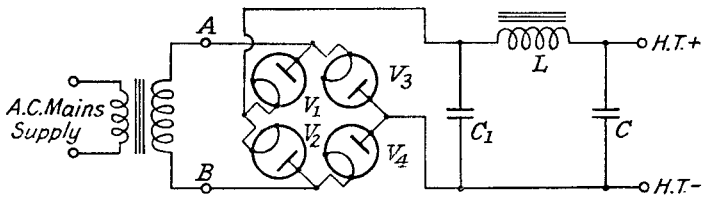

FIG. 11.4*b*.—A Bridge Rectifier.

Valves are practically never used in the bridge rectifier since four independent valve structures would be required, but the circuit is quite often employed with metal rectifiers. The bridge circuit, shown in Fig. 11.4*b*, is equivalent to a full-wave rectifier, but requires only a single secondary winding of half the A.C. voltage for the same D.C. output voltage as the full-wave circuit. The principle of operation is as follows. During the half-cycle when A is positive with respect to B, valves V_1 and V_4 are conducting, the current passing from the cathode of V_1, through the reservoir capacitor C_1, to the anode of V_4 and thence to B. For the opposite half wave, B is positive with respect to A, and valves V_2 and V_3 are conducting (V_1 and V_4 are inoperative), the current passing through C_1 in the same direction as when V_1 and V_4 conduct. Voltage regulation is practically the same as for the full-wave rectifier.

The voltage doubler rectifier of Fig. 11.4*c* requires two separate half-wave rectifiers, each charges its own reservoir capacitor (C_1 is that for V_1) on alternate half-cycles. The two reservoir capacitors, C_1 and C_2, are connected in series to give a D.C. output voltage of

approximately twice the secondary peak A.C. voltage. D.C. voltage regulation is usually not so good as that of the half-wave rectifier.

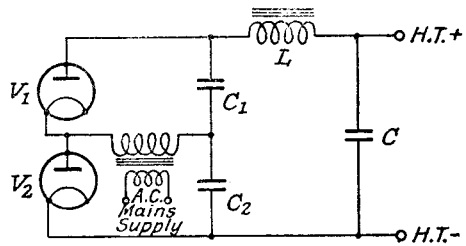

FIG. 11.4c.—A Voltage Doubler Rectifier.

The D.C. charging currents for capacitors, C_1 and C_2, oppose in the secondary winding of the transformer, and the permeability of the core is unaffected by the rectifier action.

The most popular type of rectifier for receiver H.T. supply is the high vacuum diode valve. It is robust and can be made to have a high inverse negative voltage. The inverse voltage is the negative voltage which can be withstood without taking appreciable current in the reverse direction, from cathode to anode. For high rectification efficiency the conduction slope resistance should be low, and this is achieved by having a large emitting surface and minimum anode-to-cathode spacing. The former can be realized with little difficulty in a directly-heated valve by having a long filament, but there are limits to the size of the cathode in an indirectly-heated valve, and increased rectification efficiency is largely obtained by reducing the equivalent spacing between anode and cathode. A comparatively coarse mesh grid, connected to the anode, is inserted between anode and cathode to neutralize the electron space-charge at the cathode, and this effectively reduces the anode-cathode spacing without decreasing to any large extent the inverse voltage. With a very narrow anode-cathode spacing there is a possibility of some of the active cathode coating being deposited on the anode, the temperature of which may become sufficiently high, due to heat radiation from the cathode as well as electron bombardment, to cause " back " emission in the reverse direction, and so reduce rectification efficiency. The chief value of the indirectly-heated rectifier is that the H.T. supply is not applied until the valves in the receiver are conductive, and high initial D.C. voltages, imposing undue strain on capacitors or resistors, are avoided.

A possible alternative to the high vacuum diode is the mercury

vapour rectifier, which generally has a higher rectification efficiency. The voltage drop across the valve during conduction is constant at about 15 volts and independent of load current. Its disadvantages are that it tends to produce R.F. interference, is less robust, and, unless special precautions are taken, has a shorter life than the high vacuum diode. Inverse voltage is also limited, though this effect is of little importance in receiver H.T. supplies. The nature of the conduction characteristic is such that a very peaked current wave, rich in the higher harmonics, is produced in the reservoir capacitance, and these harmonics enter the R.F. range and may cause interference in the receiver. Bombardment of the cathode coating by positive ions of mercury vapour tends to reduce valve life ; the velocity of these ions can become dangerously high if the A.C. anode voltage is switched on before the cathode is hot enough to emit a copious flow of electrons and so reduce the positive voltage between anode and cathode during conduction. Since practically all the mass of the gas atom is contained in the ion, its kinetic energy is considerable when its velocity is high, and the active material is stripped from the cathode.

The rectifier valve normally has a reservoir capacitance, which forms a capacitive load impedance. This increases rectification efficiency and attenuates A.C. fundamental and harmonic voltage components in the rectified output. An inductive load impedance may be used when high D.C. voltage regulation is desired, but rectification efficiency is then reduced. The mercury-filled diode valve is particularly suitable for use with an inductive load. A " pure " resistance load is never employed because it causes a low rectification efficiency—the D.C. output voltage is approximately $\frac{1}{3}$ (half wave) or $\frac{2}{3}$ (full wave) of that obtained with a capacitance load—and there is no attenuation of the A.C. voltage components in the rectified output. An examination of rectifier performance when supplying a resistance load is, however, helpful in understanding its operation with capacitive or inductive load.

11.2.4. The H.T. Rectifier with Resistance Load. When a H.T. rectifier has a resistance load, the unidirectional current pulses have half cosine wave shapes. For a half-wave rectifier these current pulses may be analysed into the Fourier Series * given below

$$I_0=\frac{2\hat{I}}{\pi}\left[\frac{1}{2}+\frac{\pi}{4}\cos pt+\frac{1}{3}\cos 2pt-\frac{1}{3.5}\cos 4pt+\frac{1}{5.7}\cos 6pt\ \ldots\right]. \quad 11.3a$$

where I_0 = current through the resistance load R.

* See Appendix 2A, Part I.

and $\hat{I}\cos pt$ = instantaneous current through the diode during the conduction period.

In a full-wave rectifier, the fundamental component is cancelled and the Fourier Series * becomes

$$I_0 = \frac{4\hat{I}}{\pi}\left[\frac{1}{2}+\frac{1}{3}\cos 2pt - \frac{1}{3.5}\cos 4pt+\frac{1}{5.7}\cos 6pt \ldots\right] \quad . \quad 11.3b.$$

The D.C. components for half- and full-wave operation are $\frac{\hat{I}}{\pi}$ and $\frac{2\hat{I}}{\pi}$ respectively. The voltage across the load resistance R is obtained by substituting E_0 and $\frac{\hat{E}_1 R}{R+R_d+R_t}$ for I_0 and $\hat{I}$ in the above expressions. R_d is the conduction resistance of the rectifier, R_t the sum of the winding resistance of the secondary and that reflected from the primary of the transformer supplying the rectifier, and $\hat{E}_1\cos pt$ is the secondary voltage. Generally, $R \gg R_d+R_t$, so that the D.C. output voltage, $\frac{\hat{E}_1}{\pi}$ or $\frac{2\hat{E}_1}{\pi}$, is almost independent of load resistance. The resistance loaded rectifier, therefore, has the advantage of good D.C. voltage regulation, but rectification efficiency is low (31·8% for the half-wave and 63·6% for the full-wave rectifier). To reduce A.C. voltages across the load resistance it is usual to insert an *LC* filter between the load resistance and rectifier. A single *LC* filter between rectifier and load resistance, as shown in Fig. 11.10, can, with suitable choice of L, give almost as good D.C. regulation as the resistance alone, and it is particularly useful for supplying a circuit requiring a variable current with little voltage variation, i.e., an output stage operating under Class B or Class AB conditions. The more common type of rectifier circuit includes a reservoir capacitance immediately following the rectifier. This raises rectification efficiency and D.C. output voltage, but decreases voltage regulation. We shall examine the capacitively loaded rectifier first.

11.2.5. The H.T. Rectifier with Capacitive Load. The action of the rectifier with a reservoir capacitance (Fig. 11.5) is similar to that of a diode detector having a capacitance shunted load resistance (Sections 8.2.5, 6, 7, and 13, Part I). The capacitance acts as a reservoir, storing energy when the A.C. voltage applied to the rectifier exceeds the voltage across the capacitance C_1. The stored energy is released through the load resistance R when the A.C. voltage falls below that across C_1, and the rectifier ceases to conduct. The gaps between successive half waves of A.C. voltage

* See Appendix 2A, Part I.

are therefore filled as shown by the dotted curve E_c in Fig. 11.6. The diode starts to conduct at some angle such as $-\alpha_1$, and ceases at an angle corresponding to α_2, α_1 being numerically greater than

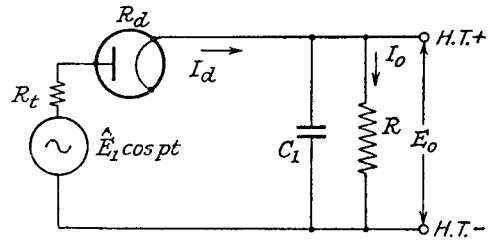

FIG. 11.5.—A Half-wave Rectifier with Capacitive Load.

α_2. The current pulse, I_d, through the diode, is shown under the second half wave.

The performance of the rectifier may be calculated by using the analyses developed in Sections 8.2.5 to 8.2.7, which assume that the voltage across the load resistance R is constant, and that diode conduction starts at $-\phi$ and ends at $+\phi$. The error involved is not very large provided rectification efficiency is greater than 50%, i.e., the D.C. voltage exceeds half the peak A.C. voltage. The shape of the conduction current-anode voltage characteristic of the high vacuum diode rectifier is generally of the form shown in Fig. 11.7, the

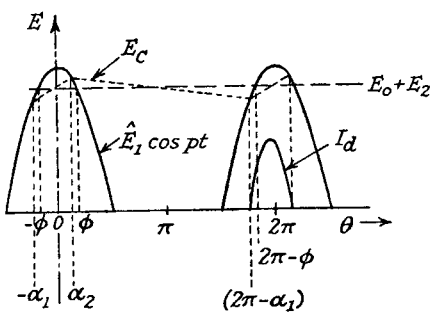

FIG. 11.6.—Voltage and Current Characteristics of a Half-wave Rectifier.

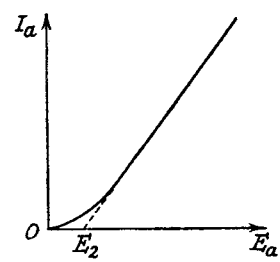

FIG. 11.7.—Conduction Current-Anode Voltage Characteristic of a Diode Rectifier.

straight part, produced, cutting the E_a axis at some positive voltage, E_2. If we neglect the initial curvature, and assume that the conduction characteristic is a straight line of slope resistance R_d passing through an anode voltage of $+E_2$, the expression for the rectified D.C. current through the load resistance R is, from Section 8.2.7,

$$I_o = \frac{\hat{E}_1 K}{\pi(R_d + R_t)} \quad . \quad . \quad . \quad . \quad . \quad 11.4$$

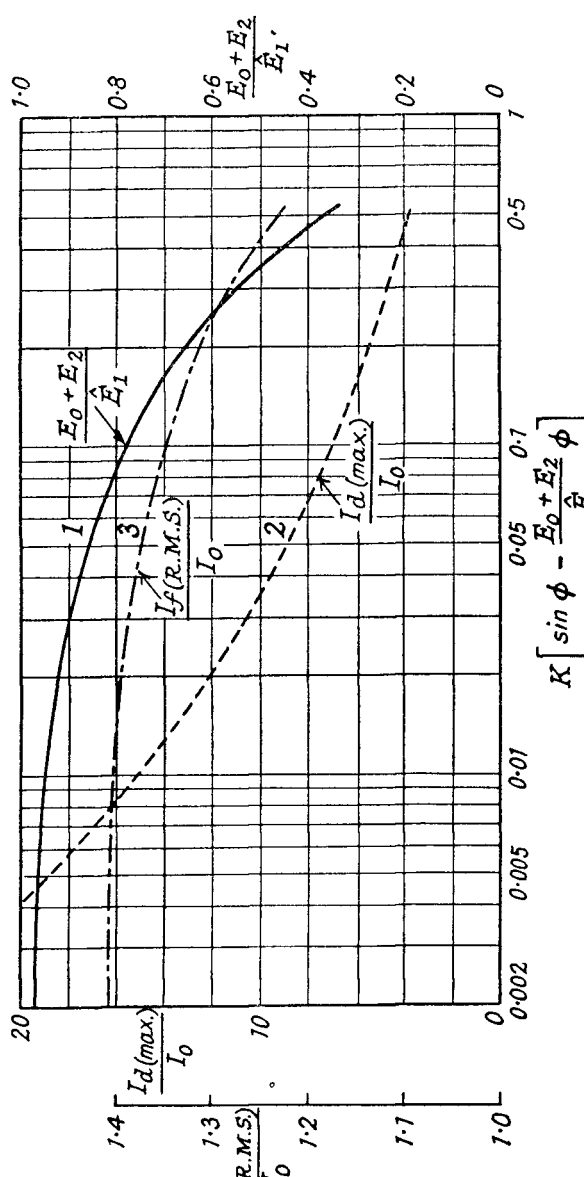

FIG. 11.8a.—Voltage and Current Relationships in a Diode Rectifier for Different Angles of Conduction.

where $\hat{E}_1 \cos pt$ = A.C. voltage of the secondary on open circuit

$$K = \left[\sin\phi - \left(\frac{E_0+E_2}{\hat{E}_1}\right)\phi\right]$$

E_0 = D.C. voltage across the load resistance R.

$$\phi = \cos^{-1}\left[\frac{E_0+E_2}{\hat{E}_1}\right]$$

and R_t = total winding resistance of secondary plus that reflected from primary.

The relationship between $\frac{E_0+E_2}{\hat{E}_1}$ and K is shown by the full line curve 1 in Fig. 11.8*a*. To illustrate its application, the D.C. output voltage-current relationship will be calculated for a half-wave rectifier circuit having the following component values. The transformer secondary and reflected primary resistances are 300 and 100 ohms respectively (the R.M.S. voltage of the secondary is 300 volts). The half-wave rectifier has a conduction resistance of 200 ohms and begins conducting at the equivalent of +5 volts. The total resistance of the rectifier circuit (excluding the load) is 600 ohms, so that the D.C. load current is

$$I_0 = \frac{300 \times 1{\cdot}414}{3{\cdot}14 \times 600} K = 225K \text{ mA.}$$

Inserting selected values for I_0 in the above gives the corresponding value of K, and reference to Fig. 11.8*a* enables the D.C. output voltage at the selected D.C. current to be calculated. The result is tabulated below.

I_0(mA) .	0	10	20	30	40	50	60
K . .	0	0·0444	0·0889	0·1333	0·1778	0·2223	0·2667
$\frac{E_0+E_2}{\hat{E}_1}$.	1	0·875	0·8	0·732	0·68	0·62	0·575
E_0 (volts)	419	366	334	306	283	258	239

In order to obtain these output voltages the reservoir capacitance is assumed to be large enough adequately to sustain the voltage across the load resistance during the non-conducting period of the rectifier. In Section 8.2.13, Part I, a curve (Fig. 8.13*b*) is developed for the minimum value of capacitance necessary to ensure this for different values of load and rectifier resistance. It is reproduced in

Fig. 11.9 as a curve of RC_1 against $\frac{R}{R_d+R_t}$, where $R = \frac{E_0}{I_0}$. The vertical scale on the right is for half-wave rectification (ripple frequency 50 c.p.s.), and that on the left is for full-wave rectification (ripple frequency 100 c.p.s.). Thus for given values of R, R_d and R_t, the minimum required value of C_1 for full-wave rectification is half that for half-wave rectification. The values of C_1 for the

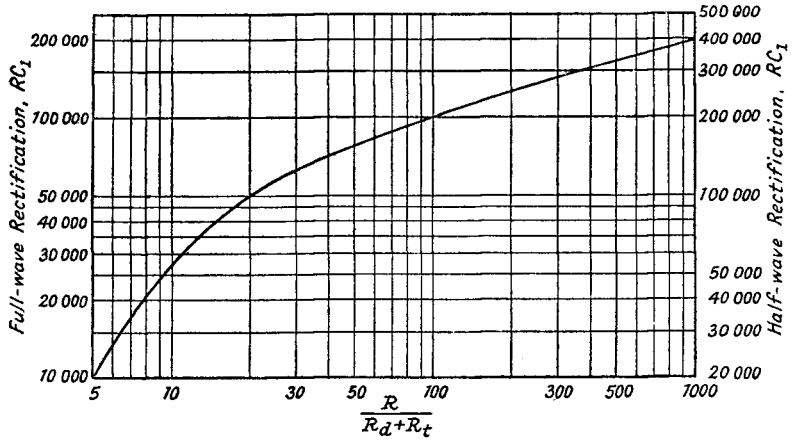

FIG. 11.9.—Optimum Capacitance Curves for a Full-wave and Half-wave Rectifier.

R in ohms, C in μF.

selected values of I_0 in the above example are tabulated below: a maximum is found at $\frac{E_0+E_2}{\hat{E}_1} = 0{\cdot}7$, which corresponds to conduction starting at $\phi = 45°$.

I_0 (mA) .	10	20	30	40	50	60
R (ohms) .	36,600	16,700	10,200	7,075	5,160	3,983
$\frac{R}{R_d+R_t}$.	61	27·8	17	11·8	8·6	6·64
C_1 (μF) .	4·64	7·2	8·65	9·2	8·8	8·05

An average practical value for a half-wave rectifier capacitance is 8 μF. For full-wave operation the minimum values of reservoir capacitance given above are halved for the same D.C. current; the D.C. voltage across the load resistance is greater because the value of K for the same D.C. current is halved.

As a second illustration let us assume that the turns ratio, and

secondary voltage of a transformer, together with the reservoir capacitance, are to be found in order that a full-wave rectifier may deliver 50 mA at 400 volts. The supply is 230 volts, 50 c.p.s. and the rectifier conduction resistance is 200 ohms starting at +5 volts. Probable values of primary and secondary resistance are 20 and 300 ohms, respectively. As a first attempt let us try a primary to secondary turns ratio of 1 to 2. The total A.C. resistance in the rectifier circuit is

$$R_d+R_t = 200+300+2^2 \times 20 = 580 \text{ ohms.}$$

The D.C. current expression is twice that for half-wave working, i.e.,

$$I_0 = \frac{2\hat{E}_1 K}{\pi(R_d+R_t)}.$$

Therefore $$K = \frac{50 \times \pi \times 580}{1{,}000 \times 460 \times 1{\cdot}414 \times 2} = 0{\cdot}07$$

From Fig. 11.8*a*

$$\frac{E_0+E_2}{\hat{E}_1} = 0{\cdot}83$$

$$E_0 = 535 \text{ volts.}$$

This is too high ; a primary to secondary turns ratio of 1 to 1·6 gives

$$R_d+R_t = 551$$

$$K = 0{\cdot}083$$

$$\frac{E_0+E_2}{\hat{E}_1} = 0{\cdot}81$$

and $$E_0 = 416 \text{ volts.}$$

This is slightly higher than required, but a lower ratio would be inadvisable because no account has been taken of the voltage drop due to leakage inductance. This tends to reduce the voltage induced in the secondary, and would bring the D.C. voltage close to the required 400 volts. The load resistance $R = \frac{E_0}{I_0} = 8{,}320\ \Omega$, and $\frac{R}{R_d+R_t} = \frac{8{,}320}{551} = 15{\cdot}1$; reference to Fig. 11.9 gives RC_1 as 40,000, and the minimum required value of reservoir capacitance is therefore 4·8 μF.

A characteristic of the rectifier with capacitive load is that the conduction current takes the form of pulses of large amplitude and short duration as shown in Fig. 11.6, and maximum current may be many times greater than the D.C. current. The reservoir capacitance, the rectifier conduction resistance and the transformer winding

resistance all influence the maximum rectification current. A large capacitance and low resistances lead to large maximum amplitudes of short duration. In some cases, when the mains supply to the rectifier has a very low resistance, it may be necessary to insert a resistance in series with the rectifier to limit the maximum conduction current and prevent damage to the valve. An example of this is afforded by the A.C./D.C. receiver, the half-wave rectifier for which often has a series resistance of about 50 ohms included to make up for the absence of the transformer winding resistances.

The maximum current, assuming conduction from $-\phi$ to $+\phi$ (Fig. 11.6) is given by

$$I_{d\,(max)} = \frac{\hat{E}_1(1 - \cos\phi)}{R_d + R} \quad . \quad . \quad . \quad 11.5a$$

and the ratio of maximum to D.C. current is

$$\frac{I_{d\,(max.)}}{I_0} = \frac{\pi(1 - \cos\phi)}{K} = \frac{\pi(1 - \cos\phi)}{\sin\phi - \phi\cos\phi} \quad . \quad . \quad 11.5b.$$

This ratio is plotted against K as curve 2 in Fig. 11.8*a*, and it can be seen that even under normal operating conditions (K between 0·1 to 0·5), the maximum conduction current is about six times that of the D.C. output current. For convenience the ratio of $I_{d\,(max.)}$ to I_0 is plotted against the ratio of $(E_0 + E_2)$ to $\hat{E}_1$ as curve 1 in Fig. 11.8*b*.

An estimate of the fundamental R.M.S. current supplied by the secondary winding of the transformer is required in order that the load from the rectifier can be determined for transformer design purposes. This can be obtained by calculating the fundamental peak current in the pulses shown in Fig. 11.6 and dividing by $\sqrt{2}$. Thus

$$\hat{I}_f = \frac{2}{\pi}\int_0^{\phi} \frac{(\hat{E}_1\cos pt - \hat{E}_1\cos\phi)}{R_d + R_t}\cos pt.d(pt)$$

$$\hat{I}_f = \frac{2\hat{E}_1}{\pi(R_d + R_t)}\int_0^{\phi}\left[\frac{1+\cos 2pt}{2} - \cos\phi.\cos pt\right]d(pt)$$

$$= \frac{2\hat{E}_1}{\pi(R_d + R_t)}\left[\frac{\phi}{2} + \frac{\sin 2\phi}{4} - \cos\phi.\sin\phi\right]$$

$$= \frac{\hat{E}_1}{\pi(R_d + R_t)}[\phi - \tfrac{1}{2}\sin 2\phi] \quad . \quad . \quad . \quad . \quad 11.6a.$$

The R.M.S. value of fundamental current

$$= I_f = \frac{\hat{E}_1}{\pi\sqrt{2}}\left(\frac{\phi - \frac{1}{2}\sin 2\phi}{(R_d + R_t)}\right).$$

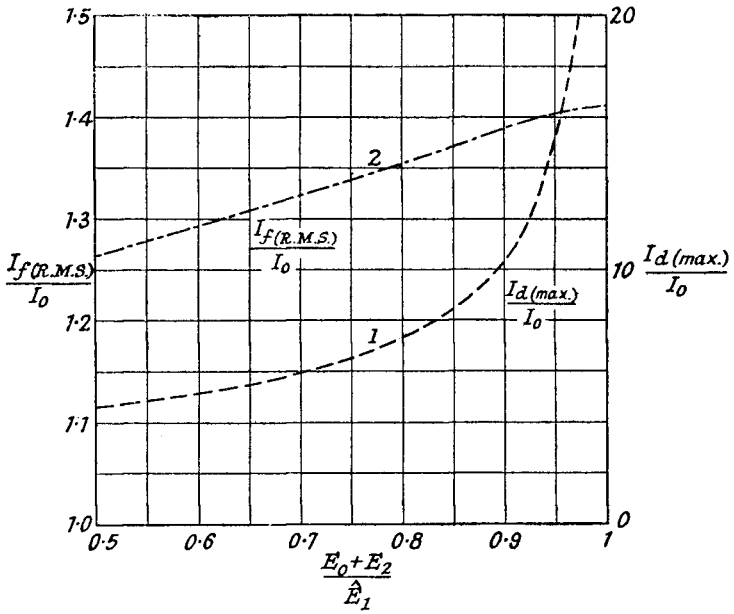

FIG. 11.8*b*.—R.M.S. and Conduction Current Ratios of a Diode Half-wave Rectifier in Terms of the D.C. Output Current.

The most useful method of expression for the above is in terms of the D.C. current I_0, hence using 11.4.

$$\frac{I_f}{I_0} = \frac{\phi - \frac{1}{2}\sin 2\phi}{\sqrt{2}K}$$

$$= \frac{0{\cdot}707(\phi - \frac{1}{2}\sin 2\phi)}{(\sin\phi - \phi\cos\phi)} \quad . \quad . \quad . \quad 11.6b.$$

This is plotted against K as curve 3 in Fig. 11.8*a* and against $\frac{E_0+E_2}{\hat{E}_1}$ as curve 2 in Fig. 11.8*b*. The interesting point is that as K is decreased, or $\frac{E_0+E_2}{\hat{E}_1}$ increased, the ratio of R.M.S. to D.C. current increases and approaches 1·414. On light loads the ratio is greatest, and as the load increases the ratio decreases.

The above calculation is based on half-wave operation, but the result is the same for full-wave working. For the same voltage ratio, i.e., a given value of $\cos\phi$, the D.C. and R.M.S. currents are doubled when full-wave rectification is employed, and their ratio is unaltered. An average value for the ratio of R.M.S. to mean current is about 1·35, and this is the figure used in estimating the

D.C. full load output from a rectifier connected to the transformer designed in Section 11.2.2.

11.2.6. The H.T. Rectifier with Inductive Load.[7] If a large inductance is inserted between the load resistance R and the rectifier, the D.C. performance is practically the same as that for a resistance load alone, viz., the D.C. voltage is much less than the peak A.C. applied voltage, but is practically independent of variations of R. The fall in D.C. voltage with increase of current is determined almost entirely by the resistance elements associated with the transformer, rectifier and added inductance. The chief advantage of the latter is that the A.C. current components in the load resistance are appreciably reduced, and all A.C. voltages across R are reduced by the factor $\frac{R}{\sqrt{R^2+(pL)^2}}$ in comparison with their values before the inductance L. The reduction factor has more and more effect at the higher harmonic frequencies. The filter action of L can be

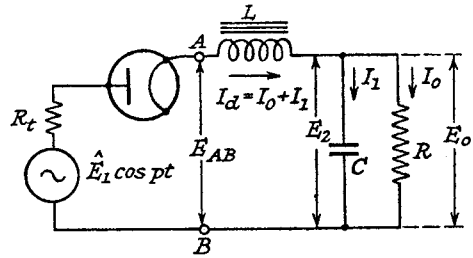

FIG. 11.10.—A Half-wave Rectifier with Inductive Load.

greatly increased by providing a by-pass capacitance C across the load resistance R as in Fig. 11.10, and D.C. performance is practically unaffected by the added capacitance unless the D.C. current falls below a certain value. For lower current values than the minimum, the D.C. current component is less than the A.C. current component; pulse charging of C results like that for the capacitively loaded rectifier, and, as the current is reduced, the D.C. voltage rises steeply to a value almost equal to the peak value of the A.C. voltage. Typical D.C. voltage-current curves (3 and 5) for the rectifier, with different values of inductance and a given value of by-pass capacitance C are shown in Fig. 11.11. Curve 3 is for a smaller inductance than curve 5. For comparison a curve (1) for the capacitively loaded rectifier is included to show the improved regulation obtained by the inductive load for currents above the critical minimum.

The action of this type of rectifier circuit can be quite simply analysed for D.C. currents exceeding the minimum value, if it is

assumed that the diode conduction resistance and transformer resistances are much less than the impedance of L and R. The wave shape of the voltage across the points AB in Fig. 11.10 is almost that of a half-cosine curve, so that the voltage applied to L and R is represented by

$$E_{AB} = \frac{2\hat{E}_1}{\pi}\left[\frac{1}{2}+\frac{\pi}{4}\cos pt + \frac{1}{3}\cos 2pt \ldots \text{etc.}\right] \quad . \quad 11.7$$

where $\hat{E}_1 \cos pt$ = A.C. voltage applied to the rectifier.

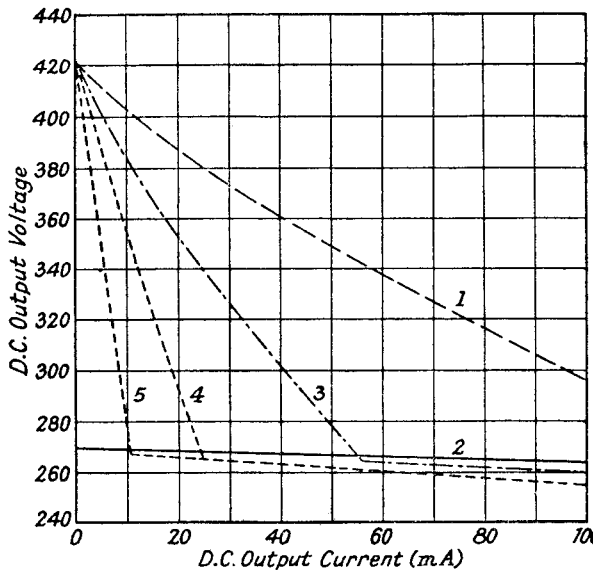

FIG. 11.11.—D.C. Output Voltage-Current Curves for a Half-wave Rectifier with Inductive Load.

Owing to the frequency discrimination of L the current I_d flowing from the rectifier has only two important components, a D.C. and fundamental A.C. The harmonic current amplitudes are inversely proportional to their harmonic number and directly proportional to the harmonic voltages, which themselves are much less than the fundamental voltage. The current I_d through the rectifier is therefore continuous, so long as its D.C. component exceeds the peak value of the A.C. current, i.e., the rectifier conducts during the whole of the cycle. This is an interesting case of the duality theorem [22] in networks, for it may be noted that the series combination of L and R is the dual of the parallel combination of C and R (the capacitively loaded rectifier). The voltage in the latter instance

is continuous, with a ripple voltage consisting almost entirely of fundamental frequency, and by the duality theorem the current should have that characteristic for the dual circuit, the series combination of L and R. Similarly duality is found between the current through the rectifier for the capacitive load and the voltage across the rectifier for the inductive load. The voltage wave shape in the latter case is actually 180° out of phase with the current wave shape in the CR case, i.e., the voltage has constant positive value for the majority of the cycle and has a downward peak in the opposite direction to the upward peak of current (see Fig. 11.6).

Having established that for good D.C. regulation the D.C. current must be not less than the fundamental A.C. peak current, we can use this to determine the minimum value of L for a given D.C. current, or vice versa. The value of the smoothing capacitance C has an effect, though not a large one, on the equivalent value of L required, its chief duty being that of reducing the fundamental voltage component across R. Denoting the D.C. and R.M.S. fundamental A.C. currents by I_0 and I_1 respectively, and the ratio of R.M.S. fundamental A.C. to D.C. voltage, $\frac{E_2}{E_0}$, across the load resistance R by r (conveniently called the ripple voltage ratio), we have

$$I_0 = \frac{E_0}{R} \quad . \quad . \quad . \quad . \quad 11.8a.$$

But E_0 is the D.C. component of E_{AB} (if the resistance of L is much less than R), which equals $\frac{\hat{E}_1}{\pi}$ (see 11.7).

Therefore

$$I_0 = \frac{\hat{E}_1}{\pi R} \quad . \quad . \quad . \quad . \quad 11.8b$$

$$I_1 = \frac{E_1}{X_C} = \frac{E_{AB\sim}}{X_L - X_C}.$$

The R.M.S. fundamental alternating current component of E_{AB} is $\frac{\hat{E}_1}{2\sqrt{2}}$ (expression 11.7)

and

$$I_1 = \frac{\hat{E}_1}{2\sqrt{2}(X_L - X_C)} \quad . \quad . \quad . \quad 11.9a$$

$$= \left[\frac{\hat{E}_1}{2\sqrt{2}} - E_2\right]\frac{1}{X_L}$$

where E_2 = R.M.S. fundamental voltage component across C

$$= \frac{E_0}{X_L}\left[\frac{\pi}{2\sqrt{2}} - r\right] \quad . \quad . \quad . \quad . \quad 11.9b.$$

$$\text{The ripple ratio } r = \frac{E_2}{E_0} = \frac{\hat{E}_1 X_c}{2\sqrt{2}(X_L - X_C)} \cdot \frac{\pi}{\hat{E}_1}$$

$$= \frac{\pi X_c}{2\sqrt{2}(X_L - X_c)}.$$

Solving the above for LC,

$$LC = \frac{\frac{\pi}{2r\sqrt{2}} + 1}{(2\pi f)^2} = \frac{\frac{1{\cdot}11}{r} + 1}{39{\cdot}5f^2} \quad . \quad . \quad 11.10a$$

where f = mains fundamental frequency.

The limiting condition for good D.C. voltage regulation is that the minimum D.C. current equals the A.C. peak current. Thus from 11.8*a* and 11.9*b*

$$I_{0(min.)} = \frac{E_0}{R_{(max.)}} = \frac{\sqrt{2}E_0}{X_L}\left(\frac{\pi}{2\sqrt{2}} - r\right)$$

and solving for L gives

$$L = \frac{\left(\frac{\pi}{2\sqrt{2}} - r\right)1{\cdot}414\ R_{(max.)}}{2\pi f}$$

$$= \frac{0{\cdot}225\ R_{(max.)}(1{\cdot}11 - r)}{f}. \quad . \quad . \quad 11.11a.$$

If full-wave rectification is employed the A.C. fundamental voltage across AB is zero; the second harmonic becomes the important voltage component, $E_{AB\sim} = \frac{4\hat{E}_1}{3\pi\sqrt{2}}$ and expression 11.10*a* is modified to

$$LC = \frac{\left[\frac{2}{3r\sqrt{2}} + 1\right]}{(2\pi 2f)^2} = \frac{\frac{0{\cdot}471}{r} + 1}{158f^2}. \quad . \quad . \quad 11.10b$$

where f is still the mains fundamental frequency.

Similarly, expression 11.11*a* becomes

$$L = \frac{0{\cdot}1125\ R_{(max.)}(0{\cdot}471 - r)}{f}. \quad . \quad . \quad 11.11b.$$

Comparing 11.11*a* with 11.11*b*, it is clear that half-wave rectification requires a larger value of inductance (approximately 4·7 times greater) than full-wave for the same value of $R_{(max.)}$ or $I_{0(min.)}$.

As an example we shall calculate the values of L and C for a D.C. output voltage of 400 volts, a minimum D.C. current of 20 mA, and

a ripple voltage ratio of 1% from (1) half-wave and (2) full-wave rectification of a 50-c.p.s. supply.

$$R_{(max.)} = \frac{E_0}{I_{0(min.)}} = \frac{400 \times 1{,}000}{20} = 20{,}000 \text{ ohms.}$$

From 11.11*a* and 11.11*b*

$$L \text{ (half-wave)} = \frac{0{\cdot}225 \times 20{,}000\,(1{\cdot}11 - 0{\cdot}01)}{50} = 99 \text{ H}$$

$$L \text{ (full-wave)} = \frac{0{\cdot}1125 \times 20{,}000\,(0{\cdot}471 - 0{\cdot}01)}{50} = 20{\cdot}8 \text{ H.}$$

Substituting in 11.10*a* and 11.10*b*

$$C \text{ (half-wave)} = \frac{112 \times 10^6}{39{\cdot}5 \times 50^2 \times 99} = 11{\cdot}5\ \mu\text{F}$$

$$C \text{ (full-wave)} = \frac{48{\cdot}1 \times 10^6}{158 \times 50^2 \times 20{\cdot}8} = 5{\cdot}82\ \mu\text{F.}$$

Since the value of L determines the D.C. current minimum, above which good regulation is obtained, it cannot be reduced without increasing $I_{0(min.)}$. The effective impedance of L to the fundamental frequency may be increased (I_1 and hence $I_{0(min.)}$ are thus reduced) by tuning [13] with a suitable capacitance. The disadvantage of the method is that L is less effective as a filter for the harmonic currents of the ripple voltage. Yet another method of decreasing $I_{0(min.)}$ is by means of a swinging choke. This is an iron-cored choke with an air-gap smaller than that required for maximum L at maximum D.C. current; its inductance is high for small D.C. currents and, though it falls for normal and maximum currents, it is high enough to provide satisfactory filtering. The dotted curves 4 and 5, Fig. 11.11, illustrate the effect of reducing air gap in a given iron-cored inductance, a smaller air gap being used for curve 5.

When the minimum D.C. load current taken by apparatus connected to the rectifier output is likely to fall below $I_{0(min.)}$, a resistance may be connected in parallel with the output to ensure that the output current is never less than $I_{0(min.)}$.

The inductive load is particularly suitable for use with gas-filled (mercury vapour) rectifier valves because of its low maximum conduction current to D.C. current ratio of about 2. Owing to the very low conduction resistance of these valves, very high peak currents are passed when the load is capacitive, and the emission property of the filament (or cathode) may be seriously damaged. The conduction angle (ϕ in Fig. 11.6) may be as low as 10°, giving $K = 0{\cdot}00195$ and a maximum to D.C. current ratio of 24·5 : 1.

Besides providing good regulation, the inductive load also gives a better utilization factor (ratio of D.C. to A.C. power) to the transformer. The utilization factor is reduced by taking current pulses of large amplitude and short duration from the transformer.

It is possible that leakage inductance in the transformer supplying a capacitively loaded rectifier may act in a similar manner to L, but it is generally too small for the good regulation characteristic to be reached with normal load currents. The usual result of leakage inductance is to decrease the A.C. voltage applied to the rectifier and to make D.C. voltage regulation worse.

11.2.7. Voltage Multiplier Rectifier Circuits.[19, 20] It is possible to obtain a high D.C. voltage from a low voltage A.C. source by using voltage multiplier rectifier circuits. The voltage-doubler

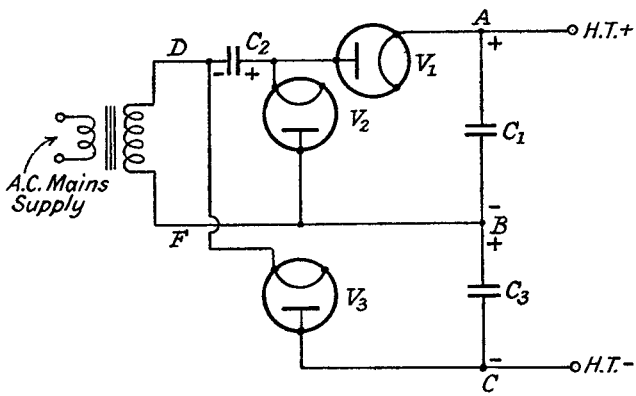

FIG. 11.12.—A Voltage Tripler Rectifier.

of Fig. 11.4c is an example of the multiplier circuit; two separate half-wave rectifiers, the D.C. output voltages of which are combined, are used with a mains supply voltage common to both. An alternative method of producing voltage doubling is shown by the two rectifiers V_1 and V_2 in the tripler circuit of Fig. 11.12. The double voltage is developed across the points AB. The circuit is like that of Fig. 11.4c, except that the positions of the mains input and C_1 of Fig. 11.4c, are interchanged, and the C_1 end of C_2 in the same figure is connected to the junction of L and C_1. This changes the mode of operation since the two rectifiers no longer act independently of each other. When the point F is positive with respect to D, rectifier V_2 conducts and charges C_2 almost to the peak value of the A.C. voltage input, the polarity of C_2 being as shown in Fig. 11.12. When F becomes negative with respect to D, V_2 ceases to conduct

and a positive voltage, equal to the sum of the D.C. voltage across C_2 and the A.C. input, is applied to the anode of V_1. The latter conducts and charges C_1 almost to twice the peak A.C. input voltage at DF. This circuit is less efficient than that of Fig. 11.4c and requires capacitance C_1 to be rated for twice the voltage developed across it in Fig. 11.4c. D.C. voltage regulation is also lower.

The voltage-tripler rectifier consists of the doubler already described with an additional rectifier V_3, which acts independently of the other two. The voltage across its reservoir capacitance C_3 is added to that across C_1 to produce a total voltage equal to approximately three times the peak A.C. input voltage.

A voltage quadrupler rectifier is shown in Fig. 11.13, and it

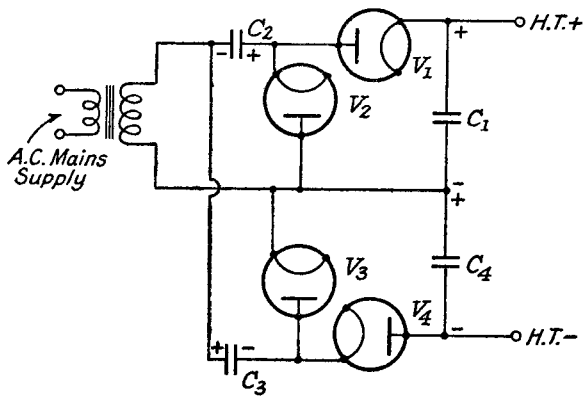

FIG. 11.13.— A Voltage Quadrupler Rectifier.

consists of two doubler circuits connected in series so that their D.C. output voltages add.

D.C. voltage regulation becomes worse as more multiplication is included; larger reservoir capacitances can help to counteract this, but are liable to cause damage to the valves because of high maximum conduction currents. Such circuits are, therefore, only suitable for supplying limited and constant D.C. currents.

11.2.8. The Rectifier Ripple Filter.[8, 9, 14] To reduce ripple voltages to the low level required for a receiver H.T. supply, an additional filter is needed between the D.C. load resistance R and reservoir capacitance. The most common type of filter consists of an iron-cored inductance L (often the loudspeaker field coil), in the H.T. positive lead from the rectifier, followed by a smoothing capacitance C. For some purposes (Section 12.5.4) the filter may be inserted in the negative lead[6]; care must then be taken to

reduce the mains transformer H.T. secondary-earth capacitance to a minimum, because it acts as a by-pass across the filter inductance. The reduction of the ripple voltage due to the filter is

$$\frac{R}{1+jpCR}\Big/\left[R_L+jpL+\frac{R}{1+jpCR}\right] \quad . \quad .11.12a.$$

Usually the resistance R_L of the filter inductance is small enough to be neglected so that 11.12a becomes

$$\frac{R}{jpL-p^2LCR+R} \quad . \quad . \quad .11.12b.$$

The loss in decibels is $-20\log_{10}\sqrt{[1-p^2LC]^2+\left(\frac{pL}{R}\right)^2}$. 11.13$a$.

As a general rule $p^2LC \gg 1$ and $\frac{pL}{R}$; hence expression 11.13a can be simplified to

$$\text{loss} = -20\log_{10} p^2LC \quad . \quad . \quad .11.13b.$$

The negative sign before p^2LC is ignored because it is really an indication of the phase relationship between the ripple voltage at the input and at the output of the filter.

The loss expression for a two-stage filter and the same assumptions is

$$\text{loss} = -20\log_{10} p^4LCL'C'. \quad . \quad . \quad 11.14.$$

Expression 11.13b is plotted in Fig. 11.14 against the product of LC for a frequency of 50 c.p.s. The minimum selected value of

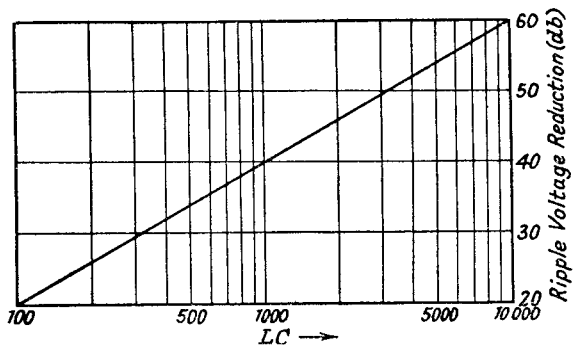

FIG. 11.14.—Ripple Filter Loss—LC Product Curve for 50 c.p.s. Mains Frequency.

LC (L is in Henrys and C in μF) is 100, because the assumption $p^2LC \gg 1$ is hardly valid for lower values of this product. Fig. 11.14 is applicable to harmonic frequencies of 50 c.p.s. by adding 12·04, 19·08, 24·08, and 27·96 db. to the loss scale for frequencies of 100,

150, 200 and 250 c.p.s. respectively. The loss for two similar filters is obtained by multiplying the loss scale by two.

As long as the product LC is constant and the conditions given above are fulfilled, viz., $p^2LC \gg 1$ and $\gg \frac{pL}{R}$, the actual values of L and C have little effect on filter characteristics, but for practical reasons it is better to use a large value of capacitance rather than a very large value of inductance. The latter is more difficult to make and has a higher D.C. resistance. Average values for L and C are 30 H and 8 μF giving $LC = 240$ and a loss of 27·5 db. at 50 c.p.s.

The iron-cored inductance must have an air gap to prevent saturation of the core by the D.C. current, and its design is detailed in the next section 11.2.9.

Special parallel and series circuits [13] tuned to the fundamental ripple frequency were at one time employed, but the use of electrolytic capacitances of comparatively high value has rendered these methods unnecessary. Furthermore, a tuned filter gives less discrimination against frequency components other than that to which it is tuned.

Resistance-capacitance smoothing filters may be used for low D.C. current outputs. The loss for this type is

$$-20 \log_{10} \sqrt{1+(pCR_1)^2} \quad . \quad . \quad . \quad 11.15a$$

where R_1 = filter resistance

C = by-pass capacitance in parallel with the load resistance R, which is assumed to be much greater than $\frac{1}{pC}$.

Generally $pCR_1 \gg 1$ and 11.15a becomes

$$\text{loss} = -20 \log_{10} pCR_1 \quad . \quad . \quad . \quad 11.15b.$$

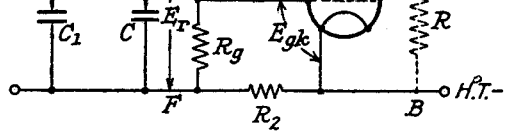

FIG. 11.15a.—Ripple Voltage Suppression by Means of a Valve.

An interesting method of neutralizing ripple voltage by means of a valve [17] is shown in Fig. 11.15a. The initial ripple voltage E_r across DF is applied to the valve grid through the large capacitance C_2, so that E_r effectively appears across the grid leak resistance

R_g. The ripple voltage developed by the valve across AB is 180° out of phase with the grid voltage, i.e., with E_r. Some of the ripple voltage appearing across AB due to the potential divider action of R_3 and R_a is cancelled by that in the valve, and E_{AB} has therefore a reduced ripple content. If the amplification of the valve is suitably adjusted and the initial ripple voltage is not large enough to cause distortion in the valve, complete cancellation is possible. The condition for ripple-free D.C. voltage across AB can be found from the equivalent circuit of Fig. 11.15*b*.

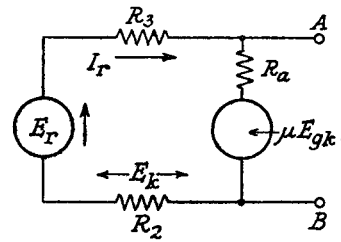

FIG. 11.15*b*. The Equivalent Circuit of Fig. 11.15*a*.

$$E_{AB} = \mu E_{gk} - I_r R_a = 0 \quad . \quad . \quad . \quad 11.16$$

where I_r is the ripple current in the circuit.

$$I_r = \frac{E_r + \mu E_{gk}}{R_2 + R_3 + R_a} \quad . \quad . \quad . \quad 11.17$$

because E_r and μE_{gk} are in phase with reference to the driving voltage for I_r.

Combining 11.16 and 11.17

$$\mu E_{gk}(R_2 + R_3) = E_r R_a$$

or

$$R_2 + R_3 = \frac{1}{g_m}\frac{E_r}{E_{gk}} \quad . \quad . \quad . \quad 11.18a$$

is the condition for zero ripple volts across AB.

But

$$E_{gk} = E_r - E_k$$

$$= E_r - \frac{(E_r + \mu E_{gk})R_2}{R_2 + R_3 + R_a}$$

$$E_{gk} = \frac{E_r(R_3 + R_a)}{R_3 + (1+\mu)R_2 + R_a} = \frac{E_r}{1 + \dfrac{(1+\mu)R_2}{R_3 + R_a}}.$$

Replacing E_{gk} in 11.18*a*

$$R_2 + R_3 = \frac{1 + \dfrac{(1+\mu)R_2}{R_3 + R_a}}{g_m} \quad . \quad . \quad . \quad 11.18b.$$

To illustrate the action of the circuit, let the total D.C. load and valve current be 50 mA, and the valve constants be $\mu = 30$, $g_m = 3$ mA/volt, $R_a = 10{,}000$ ohms at $E_g = -2$ volts. $E_a = 250$.

$$R_2 = \frac{E_g}{I_a} = \frac{2 \times 1{,}000}{50} = 40 \text{ ohms.}$$

From 11.18*b*

$$R_3+40 = \frac{1+\dfrac{31 \times 40}{R_3+10{,}000}}{3 \times 10^{-3}}.$$

Solving the above for R_3 gives

$$R_3 = 333 \text{ ohms.}$$

The total D.C. voltage drop between DF and AB is

$$I_0(R_2+R_3) = 18{\cdot}65 \text{ volts.}$$

One disadvantage of the method is that the A.C. impedance of the H.T. supply looking from the points AB is large, and adequate decoupling is necessary in all amplifier stages to prevent common impedance coupling and possible motorboating.

11.2.9. The Filter Inductance with an Air Gap.[1] The inductance of an iron-cored coil is given by

$$L = \frac{\Phi}{I}N10^{-8} \text{ Henrys.}$$

where Φ = total flux lines in the iron core
I = current (in amps.) producing the flux
N = total number of turns in coil
Now $\Phi = B \times A$
where B = flux density, lines per square centimetre
A = area of core cross-section in square centimetres
$B = \mu H$
where H = A.C. magnetizing force in oersteds
μ = permeability of the core when there is no air gap and no D.C. polarizing current.

$$H = \frac{4\pi NI}{10\ l} = 1{\cdot}255\frac{NI}{l}$$

where l = the mean length (centimetres) of the magnetic path in the core.

The inductance to A.C. for no air gap and zero D.C. polarizing current is

$$L_1 = \frac{1{\cdot}255\mu\ N^2A10^{-8}}{l} \text{ Henrys.} \quad . \quad . \quad 11.19a$$

or expressed in a more convenient form

$$L_1 = 1{\cdot}255\mu\frac{N^2}{l^2}Al10^{-8}$$

$$= 1{\cdot}255\ \mu n^2V10^{-8} \text{ Henrys} \quad . \quad . \quad 11.19b$$

where n = coil turns per centimetre of the magnetic path in core
V = volume of iron (cubic centimetres) in the core.

The term μ in the above expression needs qualification, and it is generally defined as the incremental permeability,[23] being dependent in this particular case upon the core material and magnitude of the A.C. flux density in the core. In the more normal filter inductance having an air gap and carrying D.C. current it is also dependent on the length of air gap and on the D.C. current. As far as the A.C. flux density is concerned, incremental permeability, which is designated as $\Delta\mu$ in succeeding expressions, is usually least for smallest A.C. flux densities (Fig. 10.20 shows curves of $\Delta\mu$ against peak A.C. flux density), and in designing an inductance it is preferable to calculate for this value of $\Delta\mu$, which gives the minimum value of inductance. A polarizing D.C. current through the coil reduces appreciably the incremental permeability, and the effect is clearly shown in Table 11.2, which gives $\Delta\mu$ for Stalloy [3] at different values of D.C. polarizing flux density and magnetizing force.

TABLE 11.2

D.C. Flux Density (B) (lines per square centimetre)	0	1,860	5,120	7,300	9,210	10,800	11,580
D.C. Magnetizing Force in iron (H_i) (oersteds) . .	0	0·3	0·5	0·7	1	1·5	2
Incremental Permeability $\Delta\mu$ . .	333	328	278	233	180	125	100
B . . .		12,300	12,960	13,280	13,580	13,900	14,180
H_i . .		3	5	7	10	15	20
$\Delta\mu$ . .		75	57	48	42	40	38

The table shows that any method of reducing the D.C. magnetizing force for the iron increases incremental permeability and, if the A.C. magnetizing force for the iron remains unchanged, A.C. flux density and inductance. This can be partially achieved by including an air gap in the magnetic circuit; the total D.C. magnetizing force, H_t, is then divided between the iron and air gap such that $H_t = \frac{H_i l + H_a a}{l + a}$, where H_i and H_a (H_a is numerically equal to B because $\mu = 1$ for air) are the magnetizing forces for the iron and air gap respectively, and l and a are the lengths of the magnetic path in the iron and air. As H_t is constant for a given D.C. current

and coil turns, increase of the air gap, a, must reduce H_i and, hence, increase $\Delta\mu$. However, the A.C. magnetizing force, ΔH, for the iron is also reduced in accordance with the D.C. reduction, but it is decreased, at first, at a slower rate than $\Delta\mu$ is increased. Thus A.C. flux density, ΔB, and inductance, L_2, are increased. Eventually an air-gap width is reached at which the rate of decrease of ΔH equals that of increase of $\Delta\mu$, and increase beyond this width reduces ΔB and inductance. The air gap giving maximum ΔB and inductance is known as the optimum air gap, a_0. The A.C. inductance $L_{2(opt.)}$ for optimum air gap is always less than the A.C. inductance L_1 for zero D.C. current and no gap. The ratio $\frac{L_{2(opt.)}}{L_1}$ decreases as the D.C. polarizing force is increased, and the air-gap ratio $\frac{a_0}{l}$ increases. Beatty [4] has developed a graphical method of determining the inductance L_2 for any air-gap ratio, $\frac{a}{l}$, and also the maximum value of L_2 ($L_{2(opt.)}$) and optimum air-gap ratio $\frac{a_0}{l}$; it is illustrated in Fig. 11.16. At the right-hand side is drawn the B–H curve for Stalloy, the figures being taken from Table 11.2, whilst on the left-hand side from the same origin is drawn a curve of B against $\frac{B}{\Delta\mu} - H_i$ derived from the B-H curve and the values of $\Delta\mu$ given in the table above. For a given air-gap ratio $\frac{a}{l}$ and D.C. polarizing force H_i oersteds (corresponding to OP in Fig. 11.16), a line is drawn from P to meet the BH curve at S', such that the ratio $\frac{S'U'}{PU'}$ of the sides of the right-angled triangle $PS'U'$ (U' is vertically above P) is equal to the air-gap ratio $\frac{a}{l}$, where $S'U'$ is the numerical value of the D.C. polarizing force in oersteds and PU' is the numerical value of the flux density in lines per square centimetre. The horizontal line $S'U'$ is produced to cut the left-hand curve 2 of Fig. 11.16 at the point R', which is then joined to P by the straight line PL'. The area of the triangle OPQ' enclosed by the line PL' and the BH axes is equal to $\frac{1}{2}\frac{L_2 I^2 10^7 4\pi}{V}$, where L_2 is in henrys, I is the D.C. current (amps.) and V is the volume of the iron core in cubic centimetres. Maximum area for triangle OPQ' (triangle OPQ, cross hatched in Fig. 11.16), which means maximum value

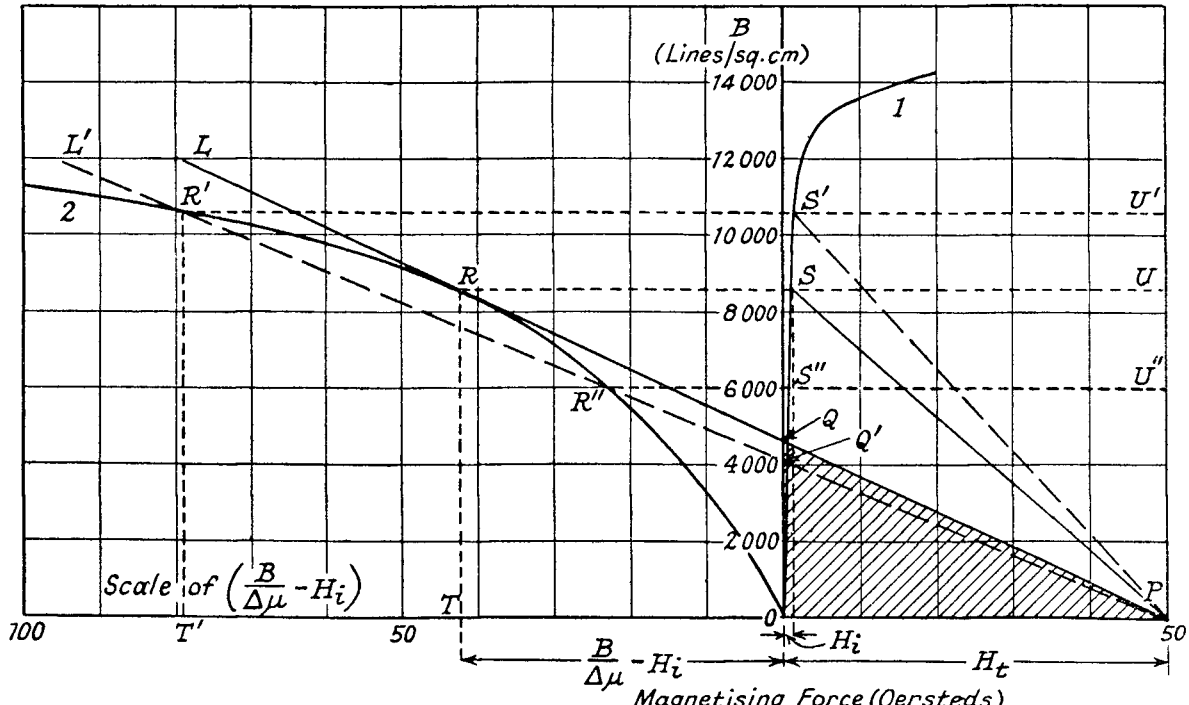

FIG. 11.16.—The Construction of *B-H* Curves to give Optimum Inductance and Air Gap.

for L_2, is obtained when PL' is tangential to curve 2 as at point R in Fig. 11.16. A horizontal line from R intersecting curve 1 at S and the perpendicular from P at U gives the optimum air-gap ratio $\frac{a_0}{l}$ as $\frac{SU}{PU}$. The proof that triangle OPQ' is equal to $\frac{1}{2}\frac{L_2 I^2 10^7 4\pi}{V}$ is as follows:

The total magnetizing force = that for the iron + that for the air-gap

$$= H_i l + H_a a = H_i l + Ba.$$

In the succeeding analysis, the term H_a is dropped and B is substituted, but it must not be forgotten that the numerical value of B only is used, the actual units being in oersteds and not lines per square centimetre.

The total magnetizing force per centimetre of magnetic path

$$= \frac{H_i l + Ba}{l + a} = H_t.$$

Generally $l \gg a$ and

$$H_t = H_i + \frac{Ba}{l} \quad . \quad . \quad . \quad . \quad 11.20.$$

Differentiating 11.20 with respect to B:

$$\frac{dH_t}{dB} = \frac{dH_i}{dB} + \frac{a}{l} = \frac{1}{\Delta\mu} + \frac{a}{l} \quad . \quad . \quad . \quad 11.21.$$

Combining 11.20 and 11.21 and eliminating $\frac{a}{l}$

$$B\frac{dH_t}{dB} = \frac{B}{\Delta\mu} + H_t - H_i \quad . \quad . \quad . \quad 11.22.$$

area of triangle $OPQ' = \frac{1}{2}OP.OQ' = \frac{1}{2}OP^2.\frac{OQ'}{OP}$

$$= \tfrac{1}{2}H_t^2\frac{OQ'}{OP}$$

but $$\frac{OQ'}{OP} = \frac{R'T'}{PT'} = \frac{B}{\frac{B}{\Delta\mu} - H_i + H_t}$$

$$= \frac{dB}{dH_t} \text{ (see expression 11.22)}$$

and the area of triangle OPQ'

$$= \tfrac{1}{2}H_t^2\frac{dB}{dH_t} \quad . \quad . \quad . \quad . \quad 11.23.$$

Now the inductance L_2 to small A.C. currents is

$$L_2 = \frac{d\Phi}{dI} N 10^{-8}$$

$$= \frac{dB}{dI} NA 10^{-8}$$

$$= \frac{dB}{dH_t} \frac{dH_t}{dI} NA 10^{-8} \quad . \quad . \quad . \quad 11.24.$$

But $$H_t = \frac{4\pi NI}{10l}$$

where I = D.C. current in the coil.

Therefore $$\frac{dH_t}{dI} = \frac{H_t}{I}$$

and $$N = \frac{H_t l 10}{4\pi I}$$

Replacing $\frac{dH_t}{dI}$ and N in 11.24 by the above expressions

$$L_2 = \frac{dB}{dH_t} \frac{H_t}{I} \frac{H_t l 10 A}{4\pi I} 10^{-8}$$

$$= \frac{dB}{dH_t} \frac{H_t^2}{I^2} V \frac{10^{-7}}{4\pi} \quad . \quad . \quad . \quad 11.25.$$

Rearranging 11.25

$$\frac{1}{2} \frac{L_2 I^2 4\pi \times 10^7}{V} = \frac{1}{2} \frac{dB}{dH_t} H_t^2$$

= area of triangle OPQ' (expression 11.23) . 11.26.

From 11.20

$$\frac{a}{l} = \frac{H_t - H_i}{B} = \frac{S'U'}{PU'} \quad . \quad . \quad . \quad 11.27.$$

For most practical purposes the gap ratio may be taken as $\frac{H_t}{B}$.

The ratio $\frac{L_{2(opt.)}}{L_1}$ and optimum gap ratio as determined from Fig. 11.16 is plotted against D.C. ampere turns per inch of the mean length of magnetic path as curves 1*a* and 1*b* in Fig. 11.17. The D.C. magnetizing force H_t is converted to D.C. ampere turns per inch (a more useful design parameter) by multiplying H_t oersteds by $\frac{2{\cdot}54}{1{\cdot}255}$, i.e., 2·02. Curves 1*a* and 1*b* are for a very small A.C. flux density, and for comparison similar curves 2*a* and 2*b* for a larger

flux density of R.M.S. value 60 lines per square centimetre are included on Fig. 11.17. These curves are often used for the design of an output transformer,[21] which normally has a higher average A.C. flux density than that produced by the ripple voltage in a filter inductance. The maximum inductance and optimum air-gap ratios are both decreased by having a larger A.C. flux density, though the actual value of $L_{2(opt.)}$ at any given D.C. ampere turns is higher because L_1 is so much higher. For example, $\Delta\mu$ for zero D.C. current is 900 at $\Delta B = 60$ lines per square centimetre (R.M.S. value), as compared with 333 at very small values of ΔB, and

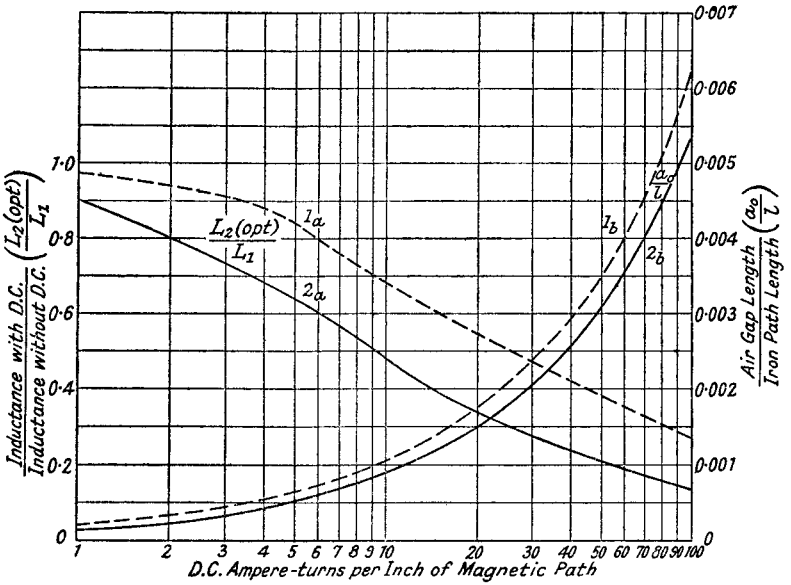

FIG. 11.17.—Optimum Inductance and Air Gap for Different D.C. Polarizations.
Curve 1: Low Flux Density.
Curve 2: R.M.S. Flux Density, 60 lines per sq. cm.

although the inductance ratio is (under worst conditions with large D.C. ampere-turns) halved for $\Delta B = 60$ lines per square centimetre, the actual value of $L_{2(opt.)}$ is approximately 1·35 times larger than when ΔB is very small. This result is to be expected, for in Fig. 11.16 increase in $\Delta\mu$ causes the rise of the left-hand curve 2 to become steeper; the line PL is therefore steeper and the area of the triangle OPQ is increased. At the same time the tangent point R is raised and PU increased, thus reducing the air-gap ratio $\frac{a_0}{l}\left[\frac{SU}{PU}\right]$.

This is a characteristic of iron-cored inductances up to an A.C. flux density of about 4,000 lines per square centimetre (R.M.S.) as shown by the incremental permeability curves in Fig. 10.20. Hence, as curves 1*a* and 1*b* are used in the design, the result represents the lowest possible value of A.C. inductance which will be obtained. If the A.C. flux density becomes very large (10,000 lines per square centimetre), lower values of inductance may then be obtained, but this is hardly likely to occur. A point worth noting is that there are always two air-gap ratios which will give a particular value of L_2 less than the optimum value, for the line PL' cuts curve 2 at two points R' and R''. The second possible air-gap ratio is given by $\frac{S''U''}{PU''}$ and is larger than the first $\frac{S'U'}{PU'}$.

Let us now use Fig. 11.17 to design a filter inductance having the following characteristics: $L_{2(opt.)} = 20$ H for a D.C. current of 120 mA, the D.C. voltage drop is not to exceed 40 volts and Stalloy No. 32A stampings are to be used.

The dimensions of No. 32A Stalloy stampings are shown in Fig. 11.3*a*.

Total winding area $= 2{\cdot}25 \times 1$ sq ins.

and allowing for insulation thickness of 0·075 ins. all round the coil

Available winding space $= (2{\cdot}25 - 0{\cdot}15) \times (1 - 0{\cdot}15)$

$= 2{\cdot}1 \times 0{\cdot}85$

$= 1{\cdot}785$ sq. ins.

Let us try SCC. 30 S.W.G. wire for the coil. Table 11.1 gives 2,950 turns per square inch for this wire, so that

Total turns in available space $= 1{\cdot}785 \times 2{,}950$

$= 5{,}260.$

Mean length of magnetic path in core $= 9$ ins.

Therefore turns per inch of magnetic path $= 585$.

D.C. ampere turns per inch $= 585 \times 0{\cdot}12 = 70{\cdot}2$.

From curves 1*a* and 1*b*, Fig. 11.17.

$$\frac{L_{2(opt.)}}{L_1} = 0{\cdot}33 \text{ and } \frac{a_0}{l} = 0{\cdot}0046$$

$$L_1 = \frac{20}{0{\cdot}33} = 60{\cdot}6 \text{ H}$$

and $a_0 = 9 \times 0{\cdot}0046 = 0{\cdot}0414$ ins.

The total air gap is divided between the core and side limbs, each of which has a gap of 0·0207 ins.

From 11.19*b*, after converting from centimetres to inches

$$L_1 = 1{\cdot}255\,\Delta\mu n^2 V \times 10^{-8} \times 2{\cdot}54$$

where n = turns per inch of magnetic path
V = volume of iron in cubic inches
$\Delta\mu$ = 333 from Table 11.2 (D.C. current zero).

Therefore
$$V = \frac{60{\cdot}6 \times 10^8}{1{\cdot}255 \times 333 \times (585)^2 \times 2{\cdot}54}$$
$$= 16{\cdot}63 \text{ cu ins.}$$

From Section 11.2.1

Area of No. 32A Stalloy = 8·4236 sq. ins.
Therefore required core thickness = 1·975
= 2·17 (allowing 10% for insulation).
Number of laminations 0·14 ins. thickness = 155.
Mean length of 1 turn of wire in coil = 10·34 ins.
Total length of wire = 1,514 yards.
Total resistance at 198·8 ohms per 1,000 yards = 301 ohms.
D.C. voltage drop = 301 × 0·12 = 36·1 volts.

Summarizing the design, which fulfils the stated requirements; the inductance consists of 160 Stalloy 32A stampings, 5,260 turns of SCC. 30 S.W.G. wire and 3 air gaps, each of length 0·0207 ins.

11.2.10. Grid Bias Supplies. The grid bias voltage for an indirectly-heated valve is generally derived from a resistance, paralleled by a capacitance, connected between its cathode and the H.T. negative lead. The cathode current flowing through this resistance produces the required grid bias voltage. The reactance of the capacitance must be low enough to by-pass A.C. anode current components, because these components develop A.C. voltages in the cathode circuit, which oppose the input voltage causing degenerative effects with attenuation (frequency) distortion (Section 9.3.4). A suitable value for the by-pass capacitance is 0·1 μF for R.F., and from 25 to 100 μF for A.F. amplifiers. Occasionally when an output valve, such as a triode, requiring a high grid bias voltage is employed, the bias voltage is obtained from a potential divider across the H.T. filter inductance, connected in the negative H.T. lead. The potential divider should have a resistance much greater than the inductive reactance of the filter inductance at 50 c.p.s., and an *RC* filter is necessary between the potential divider and output valve grid to filter the H.T. ripple voltage.

11.3. The Power Supply for the A.C./D.C. Receiver.

A typical power supply circuit for an A.C./D.C. receiver is shown in Fig. 11.18. It differs from that of the A.C. receiver in the direct connection to the A.C. mains supply, the series connection of the valve heaters, and the use of half-wave rectification. The direct mains connection necessitates an R.F. filter (L_2C_2), for diverting from the receiver any R.F. interference conveyed by the mains leads, and also a capacitance earth connection (C_3). The series heater connection calls for a certain valve order if hum voltages in the receiver output are to be minimum. The two valves which function by reason of non-linear I_aE_g characteristics (or their equivalent), the frequency changer and detector, must have the lowest A.C. voltage between heater and cathode. The frequency changer precedes the detector because it has the greater amplification following it. After

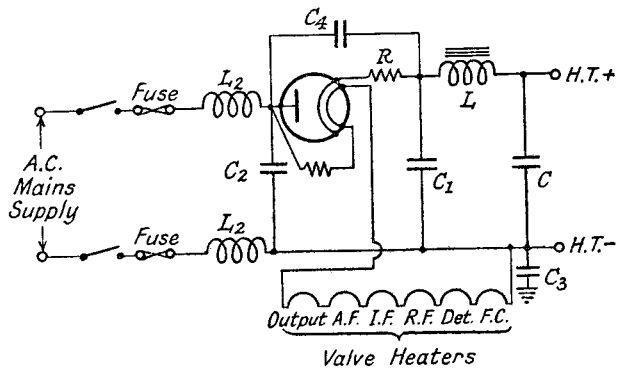

FIG. 11.18.—A Typical A.C./D.C. Power Supply Circuit.

the detector is placed the R.F. valve, and then the I.F. valve ; owing to the tuned anode circuits of these valves, hum voltages can be amplified only after modulating the signal voltage. Modulation hum is possible from the R.F. and I.F. amplifier because the variable mu. characteristic, needed for gain control purposes, necessarily involves a non-linear I_aE_g characteristic. It is greatest at a grid bias voltage (often about -10 volts) corresponding to greatest change of curvature of the I_aE_g characteristic. Hum in the A.F. valve, following the I.F., is directly amplified, but it is less serious because there is less amplification after this stage. If a high power-sensitivity output valve is used, the A.F. amplifier may be omitted, the detector being directly coupled to the former. The rectifier valve, the last of the heaters to be connected, has to deliver as much (or more) D.C. current as the full-wave rectifier in the A.C. receiver, so that its conduction resistance must be low. This entails

a long cathode of large radius and small anode-to-cathode spacing. The anode-to-cathode gap is usually equivalently reduced by inserting a grid, connected to the anode, between these two electrodes, as described in Section 11.2.3. To prevent excessive peak conduction currents a limiting resistance R of about 50 ohms is normally included in series with the rectifier anode or cathode. If R.F. signal voltages are present in the rectifier circuit, due to insufficient decoupling or screening of the receiver R.F., I.F. or oscillator stages, or to pick-up from the mains leads, rectification may cause them to be modulated by hum voltages, which are then reproduced in the output of the receiver. This type of modulation hum can be eliminated by paralleling the rectifier with a small capacitance (C_4) of about 0·001 μF, which by-passes the R.F. voltages and prevents modulation occurring.

11.4. Vibrator H.T. Supply.[5, 10, 15, 16] L.T. supplies for a car receiver can satisfactorily be obtained from the car accumulator, and it is advantageous if the H.T. supply is derived from the same source. This can be achieved by means of a vibrator, which, by periodical interruption, can produce a comparatively high A.C. voltage pulse from a low voltage D.C. source. The A.C. voltage pulses are applied to a suitable transformer, which steps up the voltage prior to rectification. Alternatively, the primary of the transformer may be connected to the low voltage source via a pair of contacts on the vibrator reed, and its action is then independent of the current actuating the reed. The rectifying action is often performed by an extra contact on the reed. The frequency of vibration of the reed is comparatively low (between 50 and 100 c.p.s.), in order to prevent high transient voltages across the transformer and sparking at the contact points A high frequency requires more energy for driving the reed, and makes it difficult to transfer sufficient energy to the transformer primary. The secondary, and often the primary, of the transformer is tuned to the reed frequency for single contact operation, or to twice that frequency for double contact excitation. This greatly improves transformer performance and efficiency, besides reducing sparking at the contacts.

A typical vibrator circuit is shown in Fig. 11.19. Double-wave excitation and rectification are achieved with contacts on both sides of the reed and a centre-tapped transformer primary and secondary. Double-wave excitation has the advantages of reduced ripple voltage, neutralization of the rectified D.C. current in the transformer secondary, and higher efficiency. The coil actuating the reed is independent of the transformer ; this is a better arrangement than

a coil connected in series with the primary, for the performance of the latter is adversely affected by the exciting coil impedance. The resonant frequency of the primary and secondary is adjusted to twice the reed frequency by the capacitances C_p and C_s. Owing to the pulse form of excitation, the vibrator current and voltage waves have sharp changes of shape, and contain appreciable amplitudes of the higher (chiefly odd) harmonics of the reed frequency. These harmonics may extend into the R.F. range, and the vibrator can radiate considerable R.F. interference. Careful electrostatic and magnetic screening is required and, in addition, R.F. filters must be included in the H.T. output leads, the vibrator input, the L.T. supply and loudspeaker field coil (if any), to prevent the interference entering the receiver via these leads. The filters consist of air-cored inductances (about 100 μH) and mica capacitances (about 500 $\mu\mu$F) marked L_2 and C_2 respectively, in the diagram. The D.C. resistance of the inductances in the vibrator input leads, the L.T. supply and loudspeaker field coil must be small since appreciable D.C. currents are taken in these circuits. Average current values with a 6-volt accumulator are 3 amps. for the vibrator

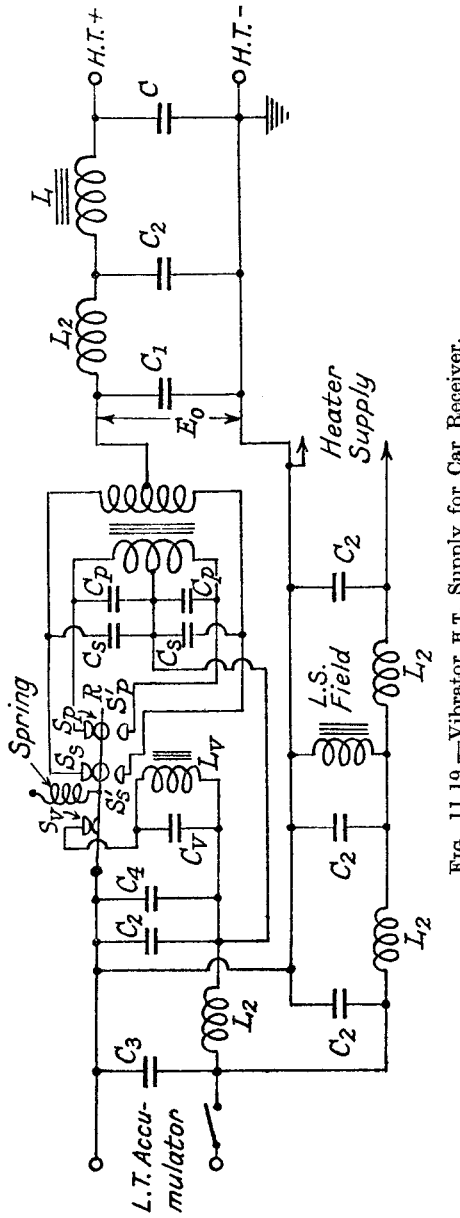

FIG. 11.19.—Vibrator H.T. Supply for Car Receiver.

input, 2 amps. for the L.T. supply, and 1·5 amps. for the loud-speaker field. Capacitances C_3 and C_4 are used to absorb low-frequency interference from the reed and have values of about 1 μF; C_v acts as an absorber across the vibrator coil when the contacts S_v open. Direct mechanical coupling between vibrator and receiver must be avoided, otherwise low-frequency interference may be experienced due to vibration of the valve electrodes or of the vanes of the oscillator tuning capacitance. Spring mounting of the vibrator element,[12] a double-walled container with a rubber seal and an air-tight inner container for the vibrator, have been used to reduce this type of interference. The R.F. interference filters for the vibrator input and output are usually contained in shielded com-

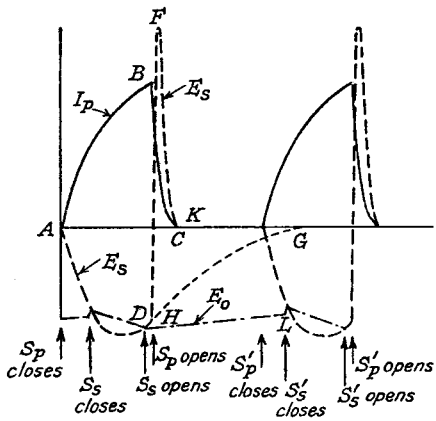

FIG. 11.20.—Primary Current and Secondary Voltage Wave Shapes for a Vibrator H.T. Supply.

partments, separate from the vibrator compartment but an integral part of the whole unit.

The operation of the vibrator is as follows. In the quiescent condition the reed R is held over by a spring, and contacts S_p, S_s and S_v are all closed. A current I_p begins to flow in the half primary of the transformer as soon as the switch is closed, and it increases steadily in an exponential manner (see Fig. 11.20), becoming asymptotic to $\frac{E}{R_p}$ amps., where E is the D.C. applied voltage and R_p is the half-primary resistance. A normal maximum value is about 4 amps. The shape of the secondary voltage E_s depends on the damping of the secondary circuit and, to a certain extent, on the characteristics of the transformer iron core. The shape generally obtained is of the form shown by the part AD of the

curve E_s in Fig. 11.20. The current in the vibrator coil (L_v) rises in a similar manner to I_p and, eventually, the reed is attracted, opening contacts S_p and S_s. The primary current I_p collapses very rapidly by discharging through C_p as shown by the section BC in Fig. 11.20 (point B corresponds to the opening of S_p). The sudden collapse of primary current induces a voltage in the secondary, and there is a very rapid reversal of secondary voltage from H to F. The shape of the curve from H through F to K, and the maximum value at F are determined by the rate of collapse of I_p, the secondary load, i.e., the D.C. output power supplied, and the value of the secondary capacitance C_s. A low D.C. output load resistance means heavier secondary damping, reduced rate of reversal of E_s and a lower maximum at F. Without collapse of I_p, the voltage E_s would decay exponentially as shown by the dotted curve HG. The D.C. reservoir capacitance C_1 is connected to the half secondary when the contacts S_s are closed, and it is charged to a voltage, E_0, corresponding to D when S_s opens. It then discharges through the D.C. load until at L the second pair of contacts S_s' are closed and connect it to the other half secondary. The contacts S_s and S_s' are always arranged to close after, and to open before S_p and S_p'. The advantage of this is that the secondary voltage has had time to rise to a value approximately equal to that across the reservoir capacitance C_1; the net voltage across S_s is therefore low and the reverse current (due to the discharge of C_1) through the secondary is small. The importance of opening S_s before S_p is obvious from Fig. 11.20; the reverse secondary voltage from H to F would discharge C_1 and produce severe sparking at the contacts.

The effect of incorrect choice of component values and contact operation can readily be understood from Fig. 11.20. If the primary capacitance C_p is too large, energy is diverted from the transformer primary, and the primary current rises slowly. This reacts on the secondary voltage reducing its rate of rise and maximum value. When C_p is too small the decay of primary current is rapid, producing high inverse secondary voltages. Too large a secondary capacitance C_s produces a slow rise of secondary voltage, reduced maximum value, and low D.C. efficiency, whilst too small a value causes a high inverse secondary voltage (point F in Fig. 11.20). A low resistance (not exceeding 50 ohms) is sometimes included in series with C_s to prevent damped oscillations occurring when S_s is opened. The D.C. load on the secondary plays an important rôle by affecting the rate of rise, and the maximum of the secondary voltage; any appreciable variation from the rated value causes sparking at the

contacts and a serious loss of efficiency. For example, an efficiency of 80% to 90% at a rated output of 200 volts 50 mA may fall to about 20% at 100 volts 10 mA. If reduced output is required from a vibrator it is preferable to reduce the applied battery voltage rather than to insert a resistance in series with the primary. A series resistance affects the rate of rise of primary current as well as the maximum value, and gives a lower efficiency than reduced battery voltage. Incorrect contact operation also reduces efficiency and increases sparking. If contacts S_p and S_s open too early the ripple voltage increases and D.C. regulation is worse, though there may be a slight increase in D.C. voltage. If S_s opens too soon the primary current is flowing without doing useful work, whilst if it opens after S_p, the inverse secondary voltage discharges C_1 and causes sparking at the contacts. There is a tendency for the contact gap widths to increase during the life of the vibrator so that S_p and S_s close late and open early, and an initial efficiency of about 85% may fall to 70% after 1,000 hours' service because of contact wear. Increased reed amplitude, by increased current through the vibrator magnet coil, helps to offset this by keeping S_p and S_s closed for a longer time, and a variable resistance [18] may be included between the magnet coil and L.T. battery. The value of this resistance is decreased as the contact points wear. A possible alternative is a tapped magnet coil, though this is likely to be less satisfactory because the increase in current is partially cancelled by a decrease in the inductance of the magnet coil.

BIBLIOGRAPHY

1. The Design of Reactances and Transformers which carry Direct Current. C. R. Hanna, *Transactions Amer. I.E.E.*, p. 155, 1927.
2. The Design of Power Rectifier Circuits. D. McDonald, *Wireless Engineer*, Oct. 1931, p. 522. Correspondence, *ibid.*, M. V. Callendar, Jan. 1932, p. 24.
3. The Air Gap Transformer and Choke. F. W. Lanchester, *Journal I.E.E.*, Oct. 1933, p. 413.
4. The Alternating-Current Inductance of an Iron Cored Coil carrying Direct Current. R. T. Beatty, *Wireless Engineer*, Feb. 1934, p. 61.
5. Vibrator Power Supply from Dry Cells. W. Van B. Roberts, *Electronics*, July 1934, p. 214.
6. Note on a Cause of Residual Hum in Rectifier-Filter Systems. F. E. Terman and S. B. Pickles, *Proc. I.R.E.*, Aug. 1934, p. 1040.
7. Some Considerations in the Design of Hot Cathode Mercury Vapour Rectifier Circuits. C. R. Dunham, *Journal I.E.E.*, Sept. 1934, p. 278.
8. Analysis of Rectifier-Filter Circuits. M. B. Stout, *Electrical Engineering*, Sept. 1935, p. 977.

9. Power Supply Filter Curves. W. W. Waltz, *Electronics*, Dec. 1935, p. 29.
10. Vibrators. *Electronics*, Feb. 1936, p. 25.
11. Mains Transformer Design. H. B. Dent, *Wireless World*, June 18th, 1937, p. 593.
12. A Vibrator for the Connection of A.C. Receiving Sets to D.C. Mains. J. W. Alexander, *Philips Technical Review*, Nov. 1937, p. 346.
13. Solving a Rectifier Problem. R. Lee, *Electronics*, April 1938, p. 39.
14. Rectifier Filter Design. H. J. Scott, *Electronics*, June 1938, p. 28.
15. Vibrator Power Supplies. G. Hall, *Wireless World*, Dec. 22nd, 1938, p. 553.
16. Vibrators. W. H. Cazaly, *Wireless World*, June 29th, 1939, p. 594.
17. Valve Operated Smoothing Circuit. *Wireless World*, Nov. 1939, p. 28.
18. Vibratory H.T. Generators. *Wireless World*, March 1941, p. 90. Correspondence, *ibid.*, April 1941, p. 106.
19. Voltage Multiplying Rectifiers. W. T. Cocking, *Wireless World*, March 1942, p. 60.
20. The Half-Wave Voltage-Doubling Rectifier Circuit. D. L. Waidelich and C. H. Gleason, *Proc. I.R.E.*, December 1942, p. 535.
21. *Radio Data Charts*. R. T. Beatty, *Wireless World*, Messrs. Iliffe.
22. *Communication Networks*. E. A. Guillemin, Volume II, p. 246. Messrs. J. Wiley. Text-book.
23. British Standard Specification for Magnetic Materials for Use under Combined D.C. and A.C. Magnetisation. No. 933.

CHAPTER 12

AUTOMATIC GAIN CONTROL

12.1. Introduction.[1, 7] Automatic gain control, sometimes wrongly termed automatic volume control, denotes the process by which the amplification of a receiver is controlled by the output carrier voltage, so that only small changes of the latter result from large variations of input carrier voltage.

Its chief advantages are:

(1) The increase in output voltage, which normally occurs when tuning from a weak to a strong station can be reduced to small proportions. For example, an 80-db. input change can be reduced to 10 db. output change.

(2) The effects of fading can be minimized.

A satisfactory A.G.C. system must possess certain features. The control must be dependent on the output carrier voltage of the received signal, but be independent of the modulation envelope. Modulation envelope variation of A.G.C. bias leads to a reduction [4] in the output carrier modulation percentage. The A.G.C. should be inoperative until the aural volume is adequate. Variation in the gain of the receiver must not produce distortion, and the speed of control should be sufficient to follow normal fading. In superheterodyne receivers the control should not cause appreciable variation of oscillator frequency.

12.2. Principle of Operation. As early as 1923 [6] a form of A.G.C. was obtained by using triodes, biased from the detector valve, to shunt the aerial circuit. In this instance it was intended for limiting the noise produced by strong atmospherics. A later method [2] employed a mechanical control to reduce the capacitance between the aerial and receiver; the moving coil of a milliammeter connected in the detector anode circuit actuated the moving vanes of the aerial capacitance.

The introduction of variable mu R.F. valves marked a most important step in the history of A.G.C., for control of R.F. gain by grid bias, derived from the D.C. component of the detected carrier output voltage, became possible. Automatic control of A.F. stage gain has been used to improve A.G.C. action, but it is not very satisfactory because the variable mu characteristic produces second

harmonic distortion (see Section 4.7.1, Part I). This distortion can be reduced by controlling two valves operating in push-pull, or a single multielectrode valve such as a hexode (Section 12.10.2). In the R.F. amplifier, the effect is not serious because the anode circuit rejects the second harmonic distortion of the carrier voltage and, if no higher harmonics are present, no distortion of the modulation envelope occurs. In Section 4.7, Part I, we see that modulation distortion can only be produced by terms higher than the second in the $I_a E_g$ power series expression.

Absolutely level output voltage is not possible from an A.G.C. system controlling only stages before the detector, because the output carrier produces the bias variations for the controlled valves. The actual variation is dependent on the number, and the $g_m E_g$ characteristics, of the controlled valves. It is least when there are several valves, each giving large changes of g_m for small changes of E_g. The maximum amplification of the receiver fixes a lower limit to the input signal voltage amenable to control, the upper limit being fixed by overloading of the detector or controlled valves. If the detector is a diode, the maximum input signal is limited only by distortion in the controlled valves, generally the last. Level or even falling output voltage for increasing input voltage is possible if the A.G.C. bias is used to control the gain of the A.F. amplifier stages. This method [9, 13] is, however, practically never used for the reasons stated above.

12.3. Methods of Obtaining the A.G.C. Bias Voltage.[8, 17] The A.G.C. bias voltage is always produced by detection of the output carrier voltage, the D.C. component of which is arranged to increase the negative bias on the R.F. stages. Filters must be inserted to prevent application of the A.F. modulation components to the grids of the R.F. valves, and to decouple each R.F. stage from the others so that instability due to R.F. feedback may be prevented. The characteristics of this filter are discussed in Section 12.6. Methods of deriving the A.G.C. voltage are conveniently treated under two headings, non-amplified and amplified. With non-amplified A.G.C., the bias voltage, which is never greater than the output carrier voltage, may be obtained from the receiver detector or from a separate diode. A diode, additional to the receiver detector, is always required when the A.G.C. is only intended to come into operation above a given input signal voltage. With amplified A.G.C., the control bias voltage is considerably greater than the carrier voltage applied to the receiver detector.

12.4. Non-Amplified A.G.C.[18, 32]

12.4.1. Unbiased Diode A.G.C. The simplest form of A.G.C. bias circuit is shown in Fig. 12.1. The diode cathode is earthed, and the negative voltage, developed between A and earth when a carrier signal is received, is supplied through filters to the grid circuits of the R.F. valves. In this arrangement the last tuned circuit cannot be earthed, and it is therefore only applicable to a superheterodyne or preset-tuned R.F. receiver which has no tuning capacitor with an earthed rotor. When the tuned circuit must be earthed, the detector D.C. load resistance R_1 may be connected in

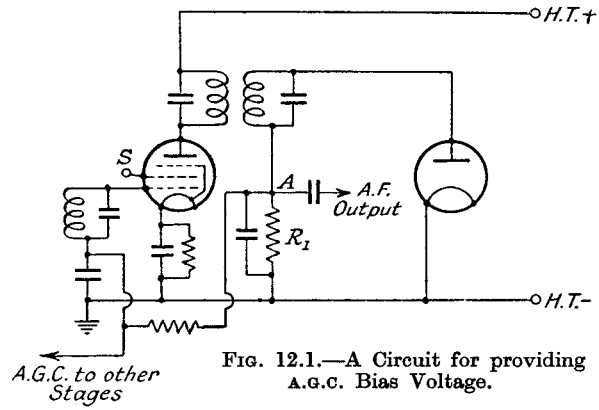

FIG. 12.1.—A Circuit for providing A.G.C. Bias Voltage.

parallel with the diode, at the cost of increased damping of the output circuit.

Calculation of the control[17] exercised by the unbiased diode is greatly facilitated by making the assumption that the cathode self-bias and screen voltages of the controlled valves are unaffected by A.G.C. action. There is generally a decrease of the first and increase of the second, but the effect causes only slight modifications to the A.G.C. curve. Let us first consider the case of a single controlled stage, the valve for which has the g_mE_g characteristic shown in Fig. 12.2; the detection characteristic of the diode is curve 1 in Fig. 12.3. The maximum A.G.C. bias must next be fixed; for calculation purposes the actual value is not important provided it is less than the bias voltage corresponding to zero anode current in the controlled stages. Let us assume a maximum A.G.C. bias of -40 volts, making a total of $-41{\cdot}5$ volts with the cathode bias of $-1{\cdot}5$ volts. The next step involves conversion of the g_mE_g curve to a decibel ratio g_mE_g curve by plotting $20 \log_{10} \frac{g_m}{g_m(E_g = -41{\cdot}5)}$

for various values of E_g (see Fig. 12.4). Fig. 12.3 is similarly transformed to a decibel ratio curve of applied carrier voltage—total

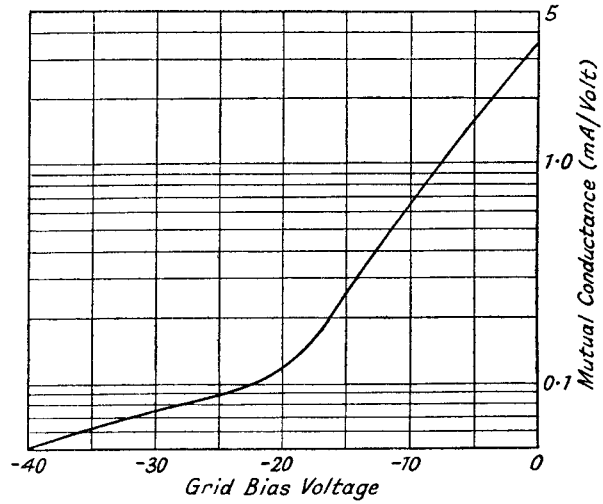

FIG. 12.2.—A Typical $g_m E_g$ Curve of a Variable-Mu Valve.

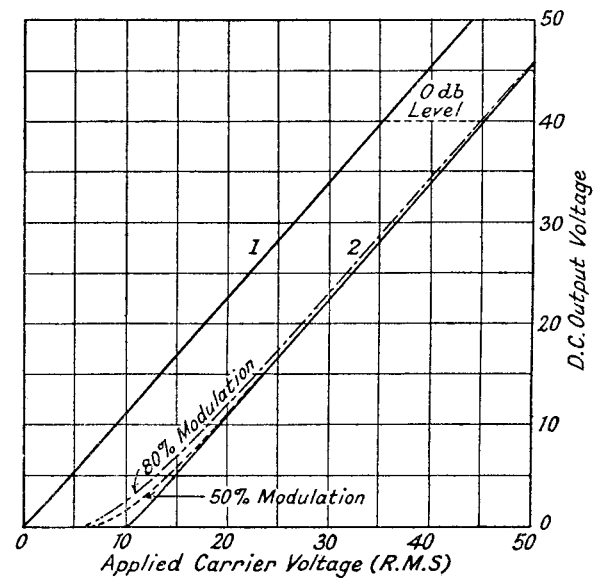

FIG. 12.3.—D.C. Output Voltage—R.M.S. Carrier Input Voltage Curves for Biased and Unbiased Diode Detector.

D.C. bias voltage as in Fig. 12.5 (curve 1). Any desired output carrier may be regarded as zero level (0 db.), but it is best to choose

the value giving the maximum required total bias, in our example — 41·5 volts, i.e., 40 volts A.G.C. bias. Thus 0 db. is equivalent to a R.M.S. carrier voltage of 35·6; this corresponds to 40 volts D.C.

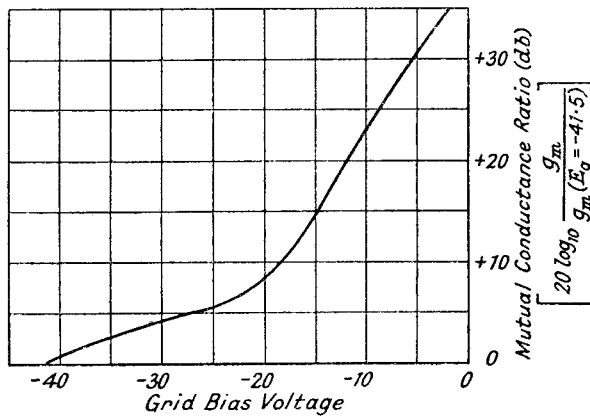

FIG. 12.4.—Decibel Ratio $g_m E_g$ Curve of a Variable-Mu Valve.
[Reference level 0 db. $\equiv g_m$ at $E_g = -41{\cdot}5$ volts.]

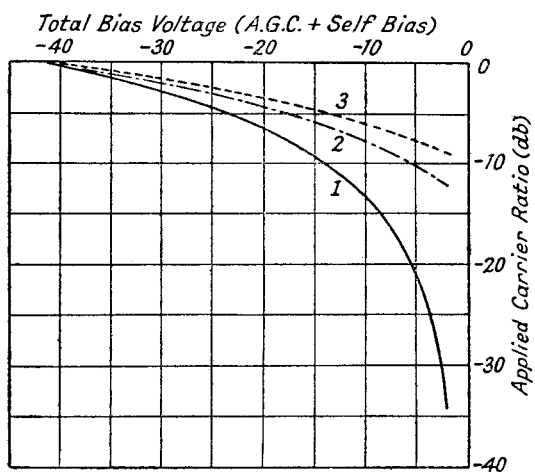

FIG. 12.5.—Decibel Ratio Applied Carrier Voltage—Total Bias Voltage Curves.
[Reference level 0 db. $\equiv$ carrier voltage at $E_g = -41{\cdot}5$.]
Curve 1: Unbiased Diode.
Curve 2: Biased Diode, $E_d = -10$ volts.
Curve 3: Amplified D.C. Control.

output in Fig. 12.3. We can now combine Figs. 12.4 and 12.5 in the input-output decibel ratio curve 1 of Fig. 12.6. To illustrate the method let us find the input carrier level corresponding to — 10 db. output carrier. Fig. 12.5 shows that this corresponds to

a total bias of — 14 volts, or an A.G.C. bias of — 12·5 volts, and referring to Fig. 12.3, the R.M.S. output carrier for this A.G.C. bias is 11·25 volts. A total bias of — 14 volts results in an increase of mutual conductance ratio of 16·5 db. (Fig. 12.4) over that at — 41·5 volts total bias. Overall amplification has therefore been increased by 16·5 db. in reducing the output signal by 10 db. In the absence of A.G.C. action it would have been necessary to reduce the input carrier by 10 db. in order to achieve the same reduction of output carrier, but since overall amplification has been increased at the same time, it follows that the input carrier must be still further reduced by an amount equal to the increase in amplification. Thus for an output carrier of — 10 db. the input carrier must be

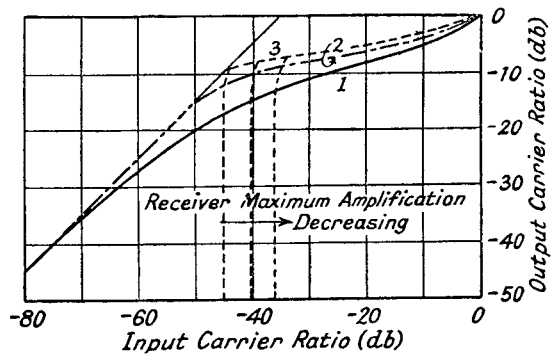

FIG. 12.6.—A.G.C. Characteristic of a Single Controlled Stage.

Curve 1: Unbiased Diode.
Curve 2: Biased Diode, E_d = — 10 volts.
Curve 3: Amplified D.C. Control.

— (16·5+10) = — 26·5 db. below the level required to give an output carrier of 0 db. (35·6 volts R.M.S.). One point on the input-output curve must therefore be — 10 db. output, — 26·5 db. input, and other points can be found by a similar method.

Curve 1, Fig. 12.6, shows that A.G.C. has a decreasing effect as the output falls to small values (less than 1 volt) and it becomes asymptotic to the 45° line corresponding to the non-A.G.C. condition. This is due partly to curvature of the diode characteristic, but it is mainly a result of g_m approaching a finite value as the A.G.C. bias falls to zero. To preserve constant control, the ratio change of g_m from — 1 to — 0·1 volt A.G.C. bias must be the same as from — 0·1 to — 0·01 volt, i.e., g_m must rise to infinity as the A.G.C. bias is decreased. Over the useful range of curve 1 (Fig. 12.6) an input variation of 50 db. is reduced to an output variation of 20 db. At high output

voltages the control decreases owing to the reduced slope of the $g_m E_g$ characteristic.

By controlling two similar R.F. stages the decibel input variation for a given output variation is doubled, and for n stages it is increased n times. If the R.F. stages have different $g_m E_g$ characteristics, curves similar to Fig. 12.4 must be obtained for each stage. The separate curves are added together giving a composite curve, which then replaces Fig. 12.4 in the original calculations.

12.4.2. Biased or Delayed Diode A.G.C.[10] Unbiased A.G.C. is not ideal because it tends to reduce amplification for the smallest signal. It is preferable to delay the action until the output carrier voltage with average modulation (about 50%) gives a satisfactory aural output. This may be done by negatively biasing the anode of

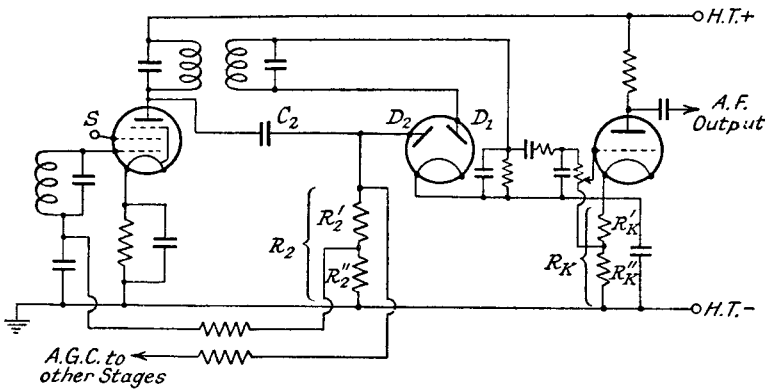

FIG. 12.7.—Biased or Delayed Diode A.G.C.

the diode producing the A.G.C. voltage, so that there is no detection until the applied signal exceeds a certain value. The receiver detector cannot be biased negatively without serious distortion accompanied by muting (no aural output below a certain carrier voltage), but a separately biased A.G.C. detector may be connected as in Fig. 12.7. In this diagram the cathode of the double diode is taken to the positive end of a split resistance R_k, inserted in the cathode circuit of the first A.F. amplifier valve. The voltage across this resistance is applied as negative bias to the anode of the A.G.C. diode D_2 by returning its load resistance R_2 to the earth line. The load resistance of the detector diode D_1 is connected to the cathode of the double diode, and hence no bias is applied to it. Part of the voltage across R_k is also applied as bias to the first A.F. valve by returning its grid leak to the junction of R_k' and R_k''. A combined

double-diode triode valve may be used in place of the two separate double-diode and triode valves The A.G.C. diode load resistance R_2 may be tapped so that a portion only of the A.G.C. bias is applied to the last controlled stage, and the reason for this is explained later in this section.

In Fig. 12.7 the output voltage supplying the A.G.C. diode is obtained from the primary of the R.F. transformer. The primary is less selective than the secondary, and, as the receiver is detuned, the amplification rises less rapidly than is the case when the A.G.C. bias is obtained from the more selective secondary. This markedly reduces the tendency to screechy reproduction in tuning out of a station. The distorted reproduction is due to the unequal amplification of the modulation sidebands and an effective increase in modulation percentage of carrier voltage produced by the mistuned selectivity characteristic. It only becomes unpleasant when detuning causes a rapid increase in receiver amplification.

The performance of biased A.G.C. may be calculated in the manner indicated in 12.4.1. The delay voltage modifies the detector characteristic as shown by curve 2 in Fig. 12.3. The diode detects when the R.M.S. carrier voltage exceeds 0·707 × the bias or delay voltage. Taking a bias voltage on the A.G.C. diode of — 15 (this corresponds to a R.M.S. carrier of 10·6 volts for start of detection) we may redraw curve 2 of Fig. 12.3 as an output carrier voltage ratio-grid bias curve. This gives curve 2, Fig. 12.5, zero level (0 db.) being the R.M.S. carrier output (45·5 volts) giving an A.G.C. bias of — 40 or a total bias of — 41·5 volts. The input-output curve 2 of Fig. 12.6 is obtained by combining Fig. 12.4 and curve 2, Fig. 12.5. Thus for an A.G.C. bias of — 18·5, i.e., a total bias of — 20, curve 2, Fig. 12.5, gives a carrier voltage ratio of — 4·5 db. and Fig. 12.4, a mutual conductance ratio of 8·5 db. The input carrier ratio is therefore — (8·5+4·5) = — 13 db. and a point on curve 2, Fig. 12.6, is output carrier ratio — 4·5, input carrier ratio — 13 db.; other points can be found by a similar process. The A.G.C. characteristic is noticeably flatter, and an even greater improvement can be obtained with a larger delaying bias. This must, however, be limited because the maximum required peak output carrier is approximately equal to the sum of the delay bias and maximum required bias voltage. Distortion in the R.F. amplifier supplying the carrier voltage to the A.G.C. diode results if the carrier output voltage is increased beyond a certain value. The critical value of output carrier and bias is obtained by superimposing the detection characteristic curves from Fig. 12.3 on the

signal handling capacity curves for the valve supplying the A.G.C. detector. Section 7.11, Part I, gives the method of determining this and a typical curve is shown in Fig. 12.8. The D.C. output voltage scale of Fig. 12.3 is taken to be the horizontal grid-bias voltage scale of Fig. 12.8 plus 1·5 volts (the assumed cathode self-bias on the valve); the same vertical scale is used for the R.M.S. carrier output voltage. The intersections of the detection curves for 0 and — 15 volts delay bias with the output carrier curve give limiting total bias voltages of — 25 and — 22, respectively. If

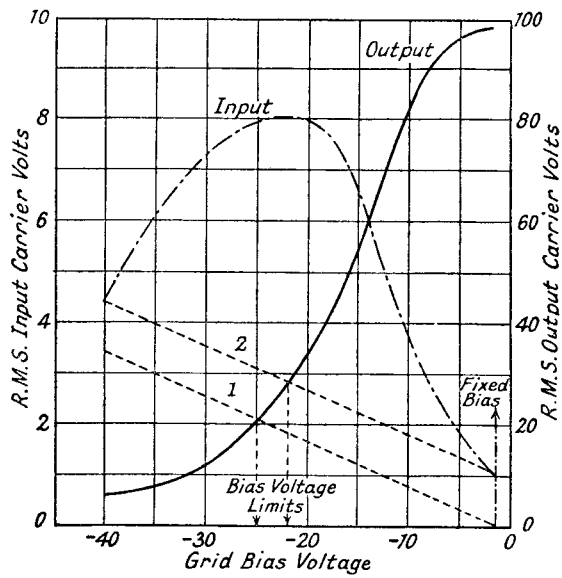

FIG. 12.8.—Output Voltage-Grid Bias Voltage Curve of the Last Controlled Valve illustrating A.G.C. Bias Voltage Limits.

only one stage is controlled, it means that the variation of input carrier, over which control is exercised, must be limited, and greater variations can only be accommodated by the inclusion of some form of manual control, such as a local-distant switch, to reduce the amplification before the controlled stage. When more than one stage is supplied with A.G.C. bias, all except that preceding the A.G.C. detector can be fully controlled. To the last stage a proportion only (generally $\frac{1}{2}$ to $\frac{1}{3}$) of the total A.G.C. bias is applied. The actual proportion depends on the maximum bias required by the other stages. For example, suppose for a delay bias of — 15 we need a maximum A.G.C. bias of — 40 volts; from Fig. 12.3 we note that with this delay bias 40 volts D.C. output requires a carrier

of 45·5 volts R.M.S., which can be obtained for a total bias voltage of — 17 (Fig. 12.8). The A.G.C. bias voltage is 1·5 volts less than the total, i.e., is — 15·5, so that only $\frac{15{\cdot}5}{40}$ or 0·388 of the A.G.C. voltage can be applied to this stage.

An exception to the rule that all stages but the last should be fully controlled may occur with a frequency changer operating on the short-wave bands. Current variations in this valve tend to produce frequency drift (Section 5.8, Part I) of the receiver oscillator, and the effect is magnified as the operating signal frequency increases. A.G.C. may therefore be omitted to this valve.

Improved signal-to-noise ratio may also be obtained by only partial control of the R.F. amplifier stage, because generally maximum value of $\frac{g_m}{\sqrt{I_a}}$, which is an important factor in determining signal-to-noise ratio (Section 4.9.3, Part I), is obtained at normal biases, and it decreases as the bias is increased. The best course would be to prevent A.G.C. being applied to this valve until a given input signal is reached, and afterwards to allow full A.G.C., but this is not so easily achieved as partial control.

12.4.3. Distortion due to Biased Diode A.G.C.[27] A negatively biased diode produces variable damping of the tuned circuit to which it is connected because, during the conduction period of the diode, an additional load is placed on the R.F. amplifier reducing its amplification. This effect may cause distortion of the modulation envelope. Figs. 12.9*a*, 12.9*b* and 12.9*c*, show what may happen for three different values of output carrier voltage. In Fig. 12.9*a*, the maximum modulation envelope amplitude is less than the delay bias voltage E_d. The A.G.C. diode is inoperative and there is no distortion. In Fig. 12.9*b*, the output carrier voltage is equal to the delay bias, and the top half of the positive modulation envelope is reduced in amplitude because of A.G.C. diode conduction current damping. Envelope as well as R.F. harmonic distortion is produced. The tuned transformer between A.G.C. diode and the A.F. detector rejects the R.F. harmonic distortion, leaving the original carrier with equal but distorted positive and negative envelopes. Detection of the modulated carrier results in an A.F. output containing harmonics of the original modulating frequency. In Fig. 12.9*c* the positive modulation envelope is completely damped, and it is identical in shape though reduced in size in comparison with the negative envelope. This represents R.F. harmonic distortion, which is rejected by the tuned transformer before the A.F. detector, leaving a modu-

lated carrier with equal undistorted positive and negative envelopes. The A.F. output from the detector is therefore undistorted. The A.G.C. diode only causes distortion of the detector output if the delay bias line cuts the positive modulation envelope; hence distortion is restricted to a range of carrier peak voltages from

$$\hat{E}_1 = \frac{E_d}{1+M} \text{ to } \hat{E}_3 = \frac{E_d}{1-M} \quad . \quad . \quad . \quad 12.1$$

with maximum distortion at $\hat{E}_2 = E_d$. The limits of the range are dependent on the modulation ratio M, being larger when the latter

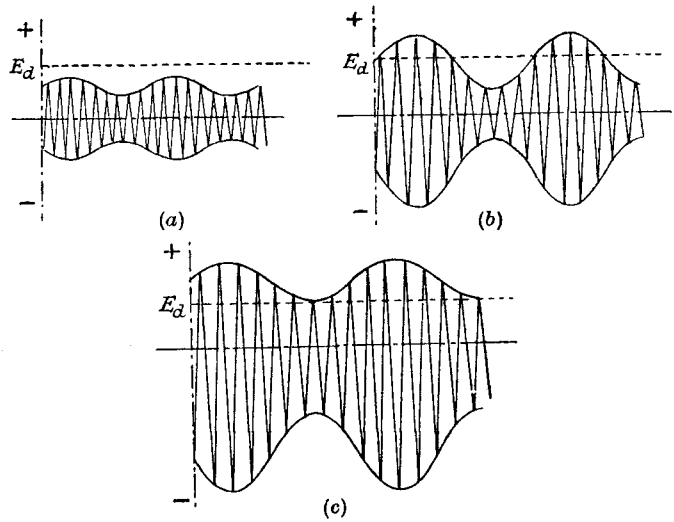

FIG. 12.9.—Various Stages of Input Voltage Damping due to Biased Diode A.G.C.
(a) Modulation envelope less than bias voltage.
(b) Carrier peak voltage equal to bias voltage.
(c) Modulation envelope greater than bias voltage.

is larger. The carrier peak voltage $\hat{E}_1$ gives the condition for the onset of distortion—the positive modulation envelope is just entering the A.G.C. diode conduction current region, and $\hat{E}_3$ defines the end of distortion when the positive envelope is completely damped. These distortion limits are true only as long as the A.C. and D.C. load resistances of the diode are equal, and this is never so in practice because of the filter required between the A.G.C. diode and the grid circuits of the controlled valves. An A.C./D.C. load resistance ratio less than unity has no effect on $\hat{E}_1$, but $\hat{E}_2$ and $\hat{E}_3$ are increased to

$$\hat{E}_2 = \frac{E_d}{1 - \frac{M}{\pi}\frac{R_1}{R_2}} \text{ and } \hat{E}_3 = \frac{E_d}{1 - \frac{M(R_1+R_2)}{R_2}} \quad . \quad 12.2$$

where R_1 = the diode D.C. load resistance
and R_2 = the input A.C. resistance of the filter looking from R_1.
The maximum value of distortion at $\hat{E}_2$ is proportional to the ratio of the dynamic or resonant impedance of the tuned circuit, across which the A.G.C. diode is connected, to the equivalent damping resistance of this same diode. The damping resistance is itself proportional to the A.C. load resistance $\frac{R_1R_2}{R_1+R_2}$. Thus, for small distortion, a low value of tuned circuit impedance and a large value of A.C. load resistance are required. A reduction in the former reduces the maximum output voltage which can be obtained from the R.F. valve supplying the A.G.C. diode, so that it is desirable to aim at the highest possible value of A.C. load resistance. This entails a high value of R_1 and R_2. The upper carrier limit $\hat{E}_3$ is a minimum when R_2 is as large as possible.

Another effect, which should be noted, is that with biased A.G.C. performance is no longer independent of the modulation envelope. When the positive modulation envelope is cut by the delay bias line, the envelope as well as the carrier is detected, and the D.C. component is greater than it would be in the absence of modulation. The effect of modulation on the detection characteristic is shown by the dotted curves in Fig. 12.3, which merge into curve 2 when the positive modulation envelope is completely damped. The initial curvature of the detection characteristic due to envelope detection affects the start of the A.G.C. output-input characteristic. Curve 2 in Fig. 12.6 begins at a smaller input voltage (less than — 50 db.), is initially more curved, and finally merges into the curve for no modulation envelope detection towards an input voltage corresponding to 0 db. The range of carrier output voltage over which modulation influences A.G.C. performance is the same as that over which A.G.C. diode conduction current produces distortion.

12.4.4. Biased A.G.C. using the Audio Frequency Detector. A biased A.G.C. circuit, which uses the A.F. detector as the source of control voltage and largely avoids the variable damping distortion of the negatively biased diode, is shown in Fig. 12.10. The A.F. detector cathode is connected to earth through a resistance R_3 producing a positive voltage between cathode and earth. The A.F. detector load resistance R_1 is returned to cathode in the usual manner. A.G.C. bias is taken from the negative end A of R_1 through the filter formed by R_2 and C_2. The positive delay voltage across R_3 means that there can be no negative A.G.C. voltage across C_2 until the voltage across R_1 exceeds that across R_3. To prevent the

application of positive bias (before A.G.C. comes into action) to the controlled valves, a second diode D_2 is connected across C_2, and it acts as a short-circuit when the voltage across C_2 is positive. It ceases to conduct when the voltage becomes negative, i.e., as soon as A.G.C. is functioning. It should be noted that distortion may be introduced into the A.F. output from D_1 when D_2 is conducting, for

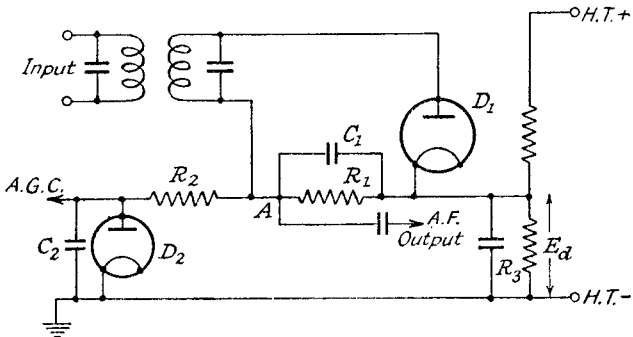

FIG. 12.10.—A Circuit for Reducing Distortion due to Biased Diode A.G.C.
[*Westinghouse Brake and Signal Company, Patent No.* 413,731.]

its conduction current passing through R_1 applies a negative bias to the anode of D_1. The actual biasing voltage can be made small by using a large value for R_2 and a small value for R_1. This form of distortion disappears when D_2 ceases to conduct and A.G.C. bias is applied.

12.5. Amplified A.G.C. Systems.

12.5.1. Introduction. Distortion due to a delay bias and to overloading of the valve preceding the A.G.C. diode may largely be eliminated by amplifying the A.G.C. bias. The control action of the latter, measured by the slope of the input-output curve, is actually dependent only on the equivalent delay bias and the $g_m E_g$ characteristics of the controlled valves. The improvement normally obtained from amplified A.G.C. is essentially due to an effective increase in the delay bias. For example, if in Section 12.4.1 an amplifier multiplying the A.G.C. bias by 10, is inserted between the D.C. output voltage from the A.G.C. detector and the controlled valves, the result is to change the reference level 0 db., for Fig. 12.5, e.g., the output carrier R.M.S. voltage for an A.G.C. bias of — 40 volts becomes approximately 3·56 instead of 35·6 volts. This has no influence on the shape of the input-output curve 1 of Fig. 12.6, and the only advantage gained is the reduced possibility of overloading the last controlled stage, which can be fully, instead of partially, controlled.

There are two important methods of obtaining amplified A.G.C. : (1) by R.F. amplification between the last controlled valve and the A.G.C. diode (it is assumed that the A.F. detector is connected to the output of the controlled valve and not to the output of the A.G.C. amplifier), and (2) by D.C. amplification between the A.G.C. bias voltage source and the controlled valves.

12.5.2. R.F. Amplified A.G.C. R.F. amplified A.G.C. in its simplest form consists of a fixed gain R.F. amplifier inserted between the A.G.C. diode and the R.F. valve supplying the A.F. detector. The amplifier should have an almost flat pass-band for frequencies within about ± 20 kc/s of the carrier frequency, as this reduces the tendency to sideband screech in the off-tune position as described in Section 12.4.2. The required pass-band may be obtained either by using an aperiodic anode circuit, or a double-tuned transformer with coupling greater than critical. When an aperiodic or low impedance circuit is employed, voltage doubling detectors can be used to increase the A.G.C. bias. Voltage doubling is not of much value with tuned circuits because it produces heavy damping, the damping resistance being reduced to half that for half-wave detection. The method of calculating the input-output curves is as described in Section 12.4 and, for the same delay bias voltages at the A.G.C. detector, the input-output curves are the same. The only difference is that the R.M.S. output carrier voltage corresponding to 0 db. is reduced in proportion to the increased amplification between A.G.C. detector and controlled R.F. stage. Owing to the A.G.C. amplification a larger delay bias may be applied to the A.G.C. detector without overloading the last controlled stage, and A.G.C. action can consequently be improved. The maximum delay bias depends on the maximum output carrier voltage which can be obtained from the A.G.C. amplifier. Referring to Fig. 12.8 we see that this may be as high as 100 volts, so that a delay bias of 50 volts is a possibility. Fig. 12.8 shows that there are limitations to the magnitude of input voltage which can be applied to the A.G.C. amplifier, but these can usually be overcome by supplying a proportion only of the output voltage from the last controlled stage to the A.G.C. amplifier. Anode circuit distortion can be tolerated in this amplifier as long as there is no feedback into the A.F. detector circuit, but grid circuit distortion, due to grid current, should not be permitted because it can produce variable damping distortion in a similar manner to the delay biased diode.

12.5.3. A.G.C. Using a Combined R.F. and A.F. Amplifier. A circuit producing R.F. amplified A.G.C. and requiring

no extra valves is shown in Fig. 12.11. The valve following the A.F. detector is used as a combined R.F. and A.F. amplifier.

The R.F. ripple voltage, produced across the detector load resistance R_1, is passed to the grid of the triode amplifier by means of the capacitance C_2. This capacitance (100 $\mu\mu$F) allows wide variation of A.F. volume control without appreciably affecting the R.F. voltage applied to the amplifier. An R.F. choke L is inserted in the A.F. amplifier anode circuit, and the capacitance C_3 transfers the R.F. output voltage to the diode. Detection of the A.F. anode voltages is avoided by making C_3 small (about 0·0001 μF). A disadvantage of the method is the danger of overloading the amplifier and distorting the A.F. output voltage, the maximum value of which

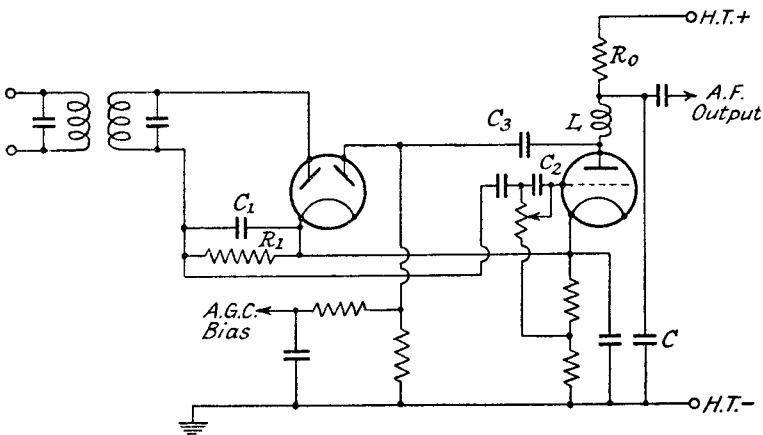

FIG. 12.11.—Amplified Biased or Delayed Diode A.G.C.

is reduced by the presence of the R.F. voltage. The A.F. amplification must be limited, and the load resistance, R_0, should not exceed the valve slope resistance.

It is possible to use the triode valve as a combined cumulative-grid detector and R.F. amplifier, but A.G.C. action may not then be so satisfactory since increasing carrier voltage biases the valve negatively and reduces its R.F. gain. This is to some extent offset if the delay bias voltage is obtained from a resistance through which the anode current from the cumulative grid detector is passing, because increasing carrier voltage decreases the anode current and delay bias voltage, and so tends to increase A.G.C. bias. The valve may also be used as an anode-bend detector and A.G.C. amplifier. This method of amplified A.G.C. has the usual disadvantages encountered when one valve is used for dual purposes, and much

more satisfactory operation is obtained by separating the functions of R.F. and A.F. amplification.

12.5.4. D.C. Amplified A.G.C.[11] D.C. amplification of the A.G.C. voltage may be achieved by the circuit shown in Fig. 12.12. A source of negative voltage is required, and it may be provided by the voltage drop across a resistance R_5 (or the loudspeaker field coil) between the earth line and H.T. negative, or by a separate H.T. supply. The second method is generally more stable and free from hum. The A.G.C. voltage is derived from the cathode of the double-diode-triode valve through the diode D_2, and delay bias is obtained by adjusting the resistance R_4 to give, in the absence of a carrier voltage, a positive bias on the cathode with respect to earth. A comparatively large capacitance C_4 (about 4 μF, paper, an electrolytic capacitor cannot be used because the cathode voltage changes from

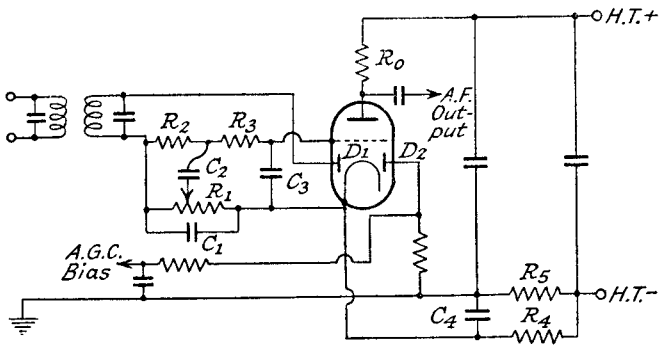

FIG. 12.12.—D.C. Amplified A.G.C.

positive to negative with respect to earth) is connected from the cathode end of R_4 to earth in order to prevent A.F. voltages being developed in the cathode circuit. Any such voltages may be rectified by D_2 to interfere with normal A.G.C. bias. The diode D_2 prevents positive bias being applied to the controlled valves since it cannot conduct with a positive cathode. The triode portion is biased from the A.F. detector load resistance R_1, the voltage across which becomes increasingly negative as the applied carrier voltage increases. Consequently the triode-anode current decreases, and the voltage between its cathode and earth falls to zero from its initial positive value and finally becomes negative. Diode D_2 then conducts, and a negative bias is applied to the controlled valves. The triode valve may be used as an A.F. as well as D.C. amplifier, the A.F. volume control being arranged as in Fig. 12.12 to leave the D.C. bias to the valve unchanged. The resistance R_2 (about $4R_1$) and capacitance

C_2 (about 0·01 μF) make this possible. It is undesirable that the R.F. ripple voltage should be passed to the triode grid, and R_3 and C_3 form an R.F. filter to prevent this. The A.F. output voltage from the triode is developed across R_0. It should be noted that the variable D.C. bias on the triode section may cause distortion of the A.F. output, because a large carrier voltage may take the operating bias voltage into the curved lower part of the triode I_aE_g characteristic.

The design procedure for this type of A.G.C. circuit is as follows. The negative voltage required across R_5 must first be determined; this should be about twice the maximum desired A.G.C. bias, i.e.,

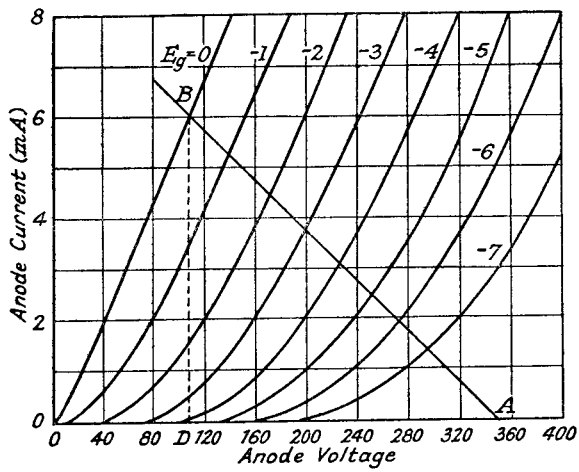

FIG. 12.13.—I_aE_a Characteristics for D.C. Amplified A.G.C. using a Triode Valve.

about 100 volts. If the D.C. voltage applied to the other circuits in the receiver is 250, the total H.T. voltage required is 350 volts; the I_aE_a characteristics of the triode section are assumed to be those in Fig. 12.13, and the detection curve of D_1 to be curve 1, Fig. 12.3. The triode slope resistance is approximately 20,000 ohms, so that a suitable value for R_0 is 20,000 ohms (it must not be too high because it reduces the A.G.C. delay bias voltage and also the A.G.C. bias voltage to the controlled valves). R_4 may be chosen to have the same value as R_0. The D.C. load line, AB in Fig. 12.13, having an inverse slope of 40,000 ohms, is drawn from E_a = 350 volts (the total H.T. voltage). The D.C. voltage available across R_4 is given by half the voltage difference between 350 and the intersection of AB with the particular grid bias voltage line being considered. Hence the relationship between the voltage across R_4 and grid bias

can be obtained, and curve 1, Fig. 12.3, allows the conversion of grid bias (this is the D.C. output voltage of Fig. 12.3) to R.M.S. output carrier voltage. In Fig. 12.14 the cathode-to-earth voltage, i.e., the A.G.C. bias voltage when it is negative, is plotted against R.M.S. carrier voltage applied to D_1, and this is next converted to a decibel ratio output carrier voltage—total bias voltage curve, reference level 0 db. again corresponding to the R.M.S. carrier voltage giving an A.G.C. bias of — 40 volts, i.e., 3·95 volts. This curve is shown in Fig. 12.5 as curve 3. Using the decibel g_mE_g characteristic of Fig. 12.4, we can now calculate the decibel ratio input-output curve 3 of Fig. 12.6, which gives the A.G.C. characteristic for a single

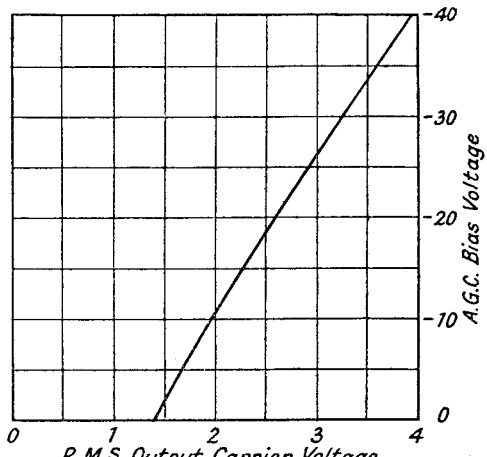

FIG. 12.14.—A.G.C. Voltage—R.M.S. Carrier Voltage for D.C. Amplified A.G.C.

controlled stage. Thus for an A.G.C. bias voltage of — 8·5 (output carrier = 1·9 from Fig. 12.14), the total bias voltage is — 10 volts and the output carrier is — 6·4 db. (Fig. 12.5, curve 3). A total bias of — 10 volts gives an increased amplification ratio of 23 db. (Fig. 12.4) so that the input voltage ratio is — (6·4 + 23) = — 29·4 db. One point on curve 3 of Fig. 12.6 is output carrier ratio — 6·4 db., input carrier ratio — 29·4 db. If more stages are biased, a composite g_mE_g curve must be obtained as discussed in Section 12.4.1. Curve 3 shows better control of output voltage than is obtained by the non-amplified systems, because of the increase in delay bias voltage, which is equal to the positive voltage between cathode and earth when the carrier voltage to D_1 is zero. The delay voltage is therefore half the voltage difference AD (Fig. 12.13) minus 100 volts (the voltage across R_5), which is 21 volts. The same curve can be

obtained from the non-amplified A.G.C. system with a delay bias of — 21 volts, but the output carrier voltage required to produce maximum A.G.C. bias cannot be realized without reduced control of the last R.F. stage.

12.5.5. Anode-Bend Amplified A.G.C.[3, 25] Another method of obtaining amplified A.G.C. is to use an anode-bend detector as shown in Fig. 12.15. The source of negative bias voltage may be a resistance between the earth and H.T. negative lead as for the D.C. amplified system, or a separate H.T. supply may be employed. In Fig. 12.15, two resistances, R_3 and R_2, are connected between earth and H.T. negative to supply the negative bias. The voltage

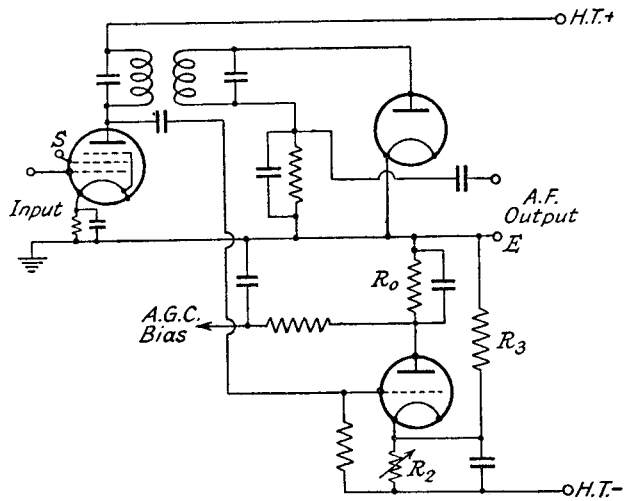

FIG. 12.15.—Anode Bend A.G.C.

drop across R_2, which can be varied, is used to bias the anode-bend A.G.C. detector. Variation of R_2 changes the delay bias for A.G.C. operation, and the detector anode current is generally zero in the absence of a carrier voltage. The anode resistance R_0 has a value of about 100,000 ohms. The parabolic detection characteristic of the anode-bend detector (see Fig. 8.19*b*, Part I) tends to give an improved A.G.C. characteristic, because A.G.C. bias increases at a greater rate than the carrier voltage.

12.6. The Filter between the A.G.C. Detector and the Controlled Stages. A filter must be inserted between the source of A.G.C. bias and the grid of the controlled valves in order—

(1) to complete the circuit for R.F. voltages from the grid of the controlled valve to earth, and

(2) to by-pass R.F. and A.F. voltages developed across the A.G.C. detector load resistance, and to permit only the D.C. component to reach the controlled stages.

Inadequate filtering may result in R.F. voltage feedback, causing instability and, in the superheterodyne receiver, interference whistles. If the A.F. voltages are not removed, the effective modulation ratio of the carrier applied to the A.F. detector is reduced, because the A.F. voltage feedback provides a variable A.G.C. bias. This bias operates on the input carrier envelope to reduce the output carrier envelope variation,[5] in the same way as the normal A.G.C. bias operates to reduce the much slower carrier variation due to fading.

The two objects mentioned above may be realized by employing a filter consisting of resistances and capacitances. The first condition merely requires a low R.F. impedance from the " earthed " end of the tuning impedance in the controlled valve grid circuit to the earth line. The second condition calls for the largest possible value of C and R. There is, however, one important condition which must be fulfilled by the filter, viz., its time constant must be low enough to allow the quick release or application of the A.G.C. bias when the input carrier varies. A time constant of $CR = 0{\cdot}1$ seconds is generally regarded as sufficiently fast to control normal fading variations. In any single stage RC filter the filtering action is dependent on the product of R and C, and a large value of R may be used with a small value of C, or vice versa. In Section 12.4.3 stress is laid upon the need for making the ratio of A.C. to D.C. load as near unity as possible, so that the highest value of R is required. The maximum value must, however, be limited if " softening " (Section 2.8.1, Part I) of the controlled valves is to be avoided, and generally the total D.C. resistance in the grid circuit must not be allowed to exceed $2M\Omega$. This limits R to 1 or $1{\cdot}5\ M\Omega$ if the A.G.C. detector D.C. load resistance is $0{\cdot}5\ M\Omega$, and hence C may have a value of about $0{\cdot}1\ \mu F$.

There is always a difference between the charge and discharge time constants of the A.G.C. filter, the former being more rapid than the latter. During discharge the A.G.C. diode is non-conducting, and the resistance in the circuit is the sum of the filter and diode D.C. load resistances, whilst for charge the latter is effectively short-circuited by the conduction resistance of the diode. When more than one valve is controlled, separate filters may be necessary for each stage in order to prevent R.F. feedback between stages. Interaction between the filters modifies the time constant of each individual filter; this effect has been calculated,[31] and the time

constant of various types of coupled filters is estimated by the following procedure.

In Fig. 12.16*a* is given an example of the series type of filter applying the A.G.C. bias to three controlled stages. The resistance R is the A.G.C. detector load resistance ; the R.F. coupling capacitance (C_2 in Fig. 12.7) is virtually in parallel with R, but it is so small that it has practically no effect on the time constant and is therefore omitted. During the charging period, i.e., increasing carrier voltage,

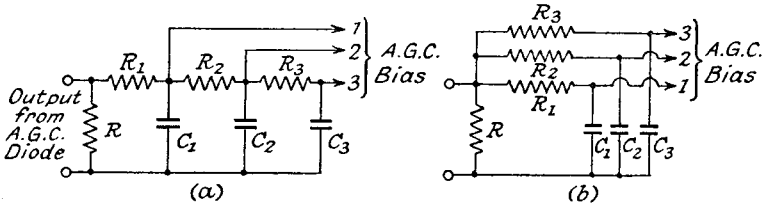

FIG. 12.16.—A.G.C. Filter Circuits.
(*a*) Series type. (*b*) Parallel type.

the diode is conducting, R has no effect, and the maximum time constant, which occurs in A.G.C., line 3, is

$$T_c = R_1(C_1+C_2+C_3)+R_2(C_2+C_3)+R_3C_3 \quad . \quad . \quad 12.3a.$$

During discharge the diode is non-conducting, and the total discharge current passes through R ; the time constant (line 3) for this condition is

$$T_d = C_3(R+R_1+R_2+R_3)+C_2(R+R_1+R_2)+C_1(R+R_1) \quad . \quad 12.3b$$

which is greater than T_c by $R(C_1+C_2+C_3)$.

The alternative parallel type of filter shown in Fig. 12.16*b* is more common. The time constant for charge is that of the largest separate filter (e.g., C_1R_1 or C_2R_2, etc.), whilst for discharge it is

$$T_d = C_1(R_1+R)+(C_2+C_3)R \quad . \quad . \quad . \quad 12.4.$$

The discharge time constant is modified when the capacitances and resistances are very different in value, and this is fully discussed in the article [31] to which reference has already been made.

To determine the relative advantages of the two types of filters, let us assume that $R = 0{\cdot}5$ MΩ, all the capacitances are $0{\cdot}1$ μF, the A.C./D.C. load resistance ratio is to be not less than 2 : 3, and all filter resistances are equal.

For the three stage series filter

$$\frac{R_{\text{A.C.}}}{R_{\text{D.C.}}} = \frac{2}{3} = \frac{R_1}{R_1+0{\cdot}5}$$

or

$$R_1 = 1{\cdot}0 \text{ M}\Omega.$$

The reactance of capacitance C_1 at audio frequencies is considered to be negligible in comparison with R_1, so that the resistances R_2 and R_3 contribute nothing to the A.C. load resistance. Substituting numerical values in expressions 12.3*a* and 12.3*b* gives the charge time constant T_c as 0·6 seconds and the discharge T_d as 0·75 seconds.

Assuming that the same conditions hold for the parallel filter, i.e., $R_1 = R_2 = R_3$,
$C_1 = C_2 = C_3 = 0{\cdot}1\ \mu F$, $R = 0{\cdot}5\ M\Omega$ and A.C./D.C. load ratio $= \frac{2}{3}$,

we have
$$\frac{R_{A.C.}}{R_{D.C.}} = \frac{2}{3} = \frac{\frac{R_1}{3}}{0{\cdot}5+\frac{R_1}{3}}$$

or
$$R_1 = 3\ M\Omega.$$

Hence $T_c = 0{\cdot}3$ seconds.
and $T_d = 0{\cdot}45$ seconds.
Thus we see that the parallel filter gives a lower time constant for charge and discharge than the series filter.

In both cases discussed above, the resistance in the grid return path of the controlled valves is 3·5 $M\Omega$, which is a higher figure than can be allowed ; it would be necessary to reduce either the A.C./D.C. load resistance ratio or R, in order to reduce the grid D.C. resistance, and so prevent softness developing in the controlled valves.

For the D.C. amplified A.G.C. system (Fig. 12.12) two circuits separated by a valve contribute to the overall time constant, the value of which is very nearly given by the sum of the grid and cathode circuit time constants. Theoretically it is found [35] that the overall time constant is not exactly determined by the sum of the individual time constants, the error, which is not greater than 7%, being maximum when the individual time constants are equal. In the practical case an added complication is found due to the fact that μ and R_a of the valve do not remain constant as the D.C. bias is varied, and a more correct expression for overall time constant is

$$T = KR_gC_g + \frac{R_kR_a'}{R_k+R_a'}C_k \quad . \quad . \quad . \quad 12.5$$

where K is a correction factor, a function of the grid bias, and is < 1 for discharge and > 1 for charge.

R_gC_g is the time constant of the grid circuit.

R_k is the cathode resistance across which the A.G.C. bias is developed (R_4 in Fig. 12.12).

R_a' is the sum of the valve slope resistance R_a and the anode circuit resistance R_0.

C_k is the cathode-earth capacitance, C_4 in Fig. 12.12.

12.7. Dual A.G.C.[33] When A.G.C. is applied to receivers having an R.F. stage before the frequency changer, certain conditions may arise to cause overloading of the latter. This is possible when a receiver is tuned to a weak station in the high field strength area of a local station, particularly if the two frequencies are not widely separated. The impedance of the signal tuning circuit in the anode of the R.F. valve at the undesired local station frequency may be sufficiently high to give amplification of this undesired signal, which can then produce interfering whistles (see Section 5.4) in the frequency changer. The undesired response is often large enough to cause serious interference with the A.F. output, but is not sufficient (owing to the selectivity of the I.F. circuits) to increase the A.G.C. bias to any great extent. By employing for the R.F. valve a separate A.G.C. bias obtained from an early, less selective, stage in the receiver, where the undesired signal is comparable with the desired, the A.G.C. bias is then controlled by both signals, and R.F. amplification is reduced as the undesired signal is increased. A diode detector produces the D.C. voltage component, and the A.G.C. source is usually a wide pass-band I.F. transformer (440 to 490 kc/s) in the anode of the frequency changer in series with the normal narrow band transformer to the first I.F. valve. The frequency response of the A.G.C. voltage source is therefore practically the same as that of the signal circuits, with the added advantage that the signal is amplified in the frequency changer. The wide pass-band transformer should have adequate cut-off at the oscillator frequency (615 kc/s) corresponding to the lowest required signal frequency (150 kc/s) otherwise the A.G.C. may be actuated by the oscillator voltage. A.G.C. bias, derived in the normal way from the last I.F. stage, is used to control I.F. and frequency changer stages, though the latter may be controlled from the R.F. amplifier bias. Such a scheme is known as dual A.G.C.

12.8. Inter-Channel Noise Suppression or Quiet A.G.C.[4, 15, 22]

12.8.1. Introduction. A noticeable feature of receivers having A.G.C. is the increase in noise which occurs when tuning out a signal. This is due to the increase of amplification resulting from the decrease of input carrier voltage. It can be overcome to some extent by increasing the bias on the R.F. controlled valves to reduce their maximum amplification, but this is not a very satisfactory method as it limits the A.G.C. action at the same time. The ideal system is to silence the receiver for small input signals without affecting receiver performance for signals exceeding a given value, and this

may be realized by overbiasing the A.F. amplifier or negatively biasing the detector [14] by a voltage controlled by the input signal. Release of this biasing voltage is usually achieved by a valve controlled circuit. The use of a mechanical shorting device [12] is rare because the relay needed to operate it must be very sensitive and free from chatter.

12.8.2. Biased Detector Quiet A.G.C. Serious distortion occurs over a range of input signal voltages in a detector having negative bias, and it is therefore essential to obtain rapid and complete removal of the negative silencing voltage when the desired input voltage is reached. To operate successfully, the negatively

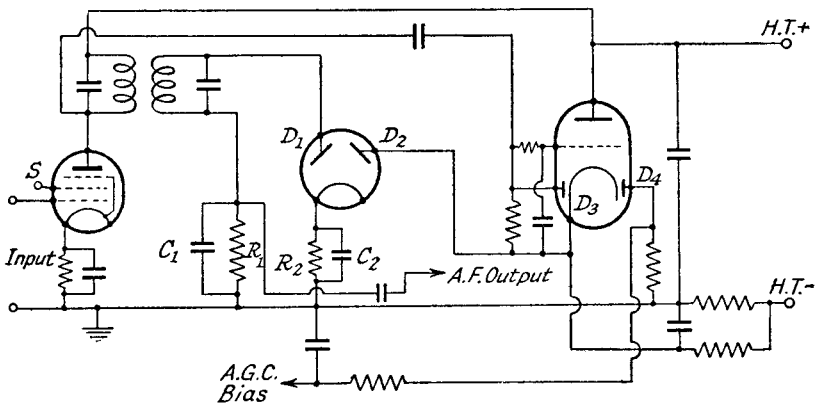

FIG. 12.17.—Quiet Delayed A.G.C. by Means of a Biased A.F. Detector Diode.

biased detector requires to be used with amplified A.G.C., and a suitable circuit is shown in Fig. 12.17.* One diode (D_3) of the double-diode triode acts as the A.G.C. detector, and the D.C. component from this is amplified by the triode section. The second diode (D_4) prevents the application of positive bias to the controlled valves as described in Section 12.5.4. The A.F. detector is the diode (D_1) of the double-diode valve; the other diode (D_2) is connected to the cathode of the A.G.C. amplifier valve, and in the common cathode circuit of these two diodes is a resistance R_2 paralleled by a capacitance C_2. As long as the cathode of the A.G.C. amplifier is positive with respect to earth, the diode D_2 conducts and applies a negative bias to D_1. This bias disappears when the cathode becomes negative, i.e., when A.G.C. bias begins to function, and D_1 detects normally. Part of the detected voltage

* British Patent 498,842, Marconi's Wireless Telegraph Co. and K. R. Sturley.

is developed across R_2, but this loss need not be great, because R_2 can be about $\frac{1}{10}$ R_1. The value of C_2 should be such as to make $C_2R_2 = C_1R_1$. Typical input-output curves are indicated as the dotted vertical lines in Fig. 12.6. The input voltage at which suppression is released may be controlled to a limited degree by varying the H.T. voltage of the triode D.C. amplifier, but it is preferably varied by reducing the maximum gain of the controlled valves. A similar method to the above, using a triple-diode triode, has also been developed.[14]

12.8.3. Interchannel Noise Suppression by a Variable Capacitance across the A.F. Detector Load Resistance. The A.F. output from a detector can be decreased by adding a large capacitance in parallel with the detector load resistance, and if it

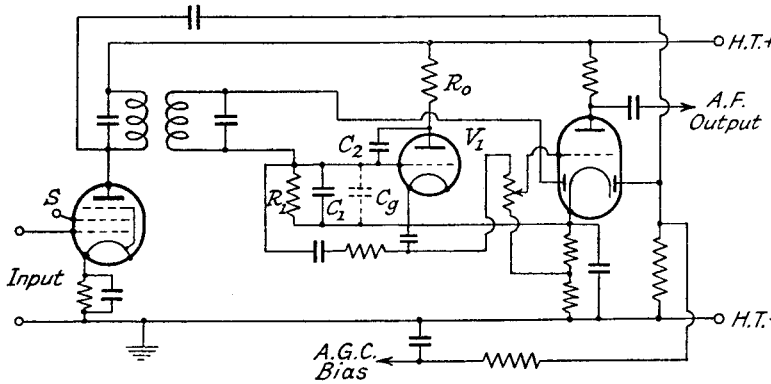

FIG. 12.18.—Quiet A.G.C. Using Miller Effect from a Triode across the A.F. Detector Load Resistance.

can be made to vary inversely as the carrier voltage, noise suppression can be achieved. This is possible by using the Miller effect, viz., the variation of grid input capacitance of a valve when its overall amplification is changed. A suitable circuit is illustrated in Fig. 12.18. The variable capacitance is provided by valve V_1, the anode-grid capacitance of which is increased by C_2 in order to increase the variation of grid input capacitance C_g. The value of the latter is, from expression 2.13*b*, Part I,

$$C_g = C_{ga}\left(1+\frac{\mu R_0}{R_a+R_0}\right)$$

where C_{ga} = total anode-grid capacitance including C_2.
R_0 = anode external circuit resistance.

It should be noted that maximum C_g is obtained by making the

anode external impedance a resistance, any reactance element due to stray capacitance reduces C_g. As an example of the possible maximum value of C_g, let us consider the following component and valve parameter values, $R_0 = 1\,\text{M}\Omega$, $R_a = 10{,}000\,\Omega$, $C_{ga} = 0{\cdot}001\,\mu\text{F}$, $\mu = 30$; a maximum value for C_g of $0{\cdot}0307\,\mu\text{F}$ is obtained. By connecting the grid circuit of V_1 across the D.C. load resistance R_1 (Fig. 12.18) the valve is automatically biased by the detected carrier voltage D.C. component, which becomes increasingly negative as the carrier voltage is increased. For small carrier voltages, the negative bias is small, μ is large, R_a small, and C_g is large. A.F. voltages across the load resistance R_1 are therefore very much reduced and A.F. output is almost negligible. Increasing carrier voltage decreases C_g, until a bias voltage is reached which takes V_1 to zero anode current and allows the detector circuit to function normally, giving full A.F. output. Since the shunt capacitance due to V_1 has greater by-passing effect on the higher audio frequencies, a form of automatic tone control occurs. This has advantages for noise suppression, because the amplification of the receiver increases with decrease of carrier voltage, and interference voltages, having appreciable high audio frequency sideband components, normally become more noticeable. A disadvantage of the method is that distortion tends to occur if the A.F. voltage across R_1 carries V_1 over the anode current cut-off point or curved part of the I_aE_g characteristic of the valve; the grid input admittance then varies appreciably over the cycle of A.F. voltage.

12.8.4. Noise Suppression by means of a Biased A.F. Amplifier. Noise suppression may also be achieved by applying additional negative bias, controlled from the carrier voltage, to cut off the anode current of the first A.F. amplifier valve. This bias is either gradually reduced as the carrier voltage increases or is short-circuited at a particular value of the latter. In one method the negative voltage is developed across a resistance in the anode circuit of a valve biased from the A.F. detector or the A.G.C. diode. Increase of carrier voltage decreases the anode current of this valve to zero, so that the initial negative voltage between the H.T. positive for the biasing valve and its anode disappears. A disadvantage of the system is that the total H.T. voltage must be increased because the H.T. positive of the biasing valve is the H.T. negative of the A.F. amplifier.

An alternative method is to short the suppressing bias by a mechanical relay or a glow discharge tuning indicator,[16] fitted with an auxiliary anode. In the latter case the cathode and auxiliary

anode of the indicator are connected across the additional bias. When the glow column reaches the auxiliary anode, conduction occurs and the bias is shorted.

12.9. Noise Limiters.[34] A noise limiter differs from a noise-suppressing device in that it allows the normal A.F. signal to be accepted and seeks only to limit the unpleasant effects produced by atmospheric and similar disturbances. The simplest method is to use a biased diode in the A.F. or R.F. circuits. For normal signal amplitudes the diode is non-conducting, but a peaked signal of excessive amplitude (a typical noise pulse shape) applies a voltage exceeding the bias, and conduction current damps the circuit, so flattening the resultant A.F. output peak voltage. Two diodes, connected to conduct in opposite directions, are often used, one limiting excessive positive and the other excessive negative peaks. A circuit * which avoids the necessity for fixed bias on the limiting

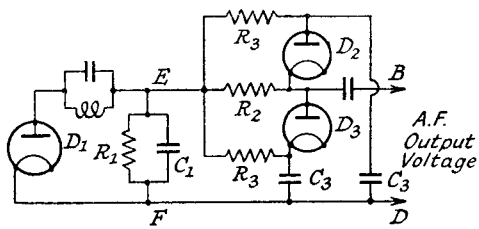

FIG. 12.19.—A Circuit for Limiting Interference on Noise Voltage Peaks.

diodes is shown in Fig. 12.19. The A.F. detector is D_1, and the noise limiting diodes, D_2 and D_3, function to damp negative and positive peaks of noise respectively. Their biasing voltage is derived from detection of the A.F. output voltage across the detector load resistance, R_1. The damping of positive and negative half-cycles due to the load imposed by D_2 and D_3 is equal, so that the A.F. voltage across BD is undistorted. A short duration positive noise pulse of large amplitude, appreciably exceeding the bias due to detection of the desired A.F. voltage, causes diode D_3 to take a large momentary current, which damps and flattens the output voltage noise peak across BD compared with the input voltage peak at EF. Diode D_2 functions in the same manner for negative noise pulses. The resistances R_3 (2 MΩ) and the common resistance R_2 form the load resistances for D_2 and D_3, and capacitances C_3 (0·001 μF) act as the coupling to D_2 and D_3. The resistance R_2 (0·2 MΩ) is included

* U.S. Patent Application, No. 391, 162. (1941) R. C. V. and V. A. Landon.

to form one arm of a potential divider, the other arm being the diodes D_2 and D_3, and it aids in suppressing the noise peaks.

In another method of noise limiting [19, 21] the noise voltage peaks are amplified and detected separately from the desired signals ; the D.C. component of the detected noise voltages is used to bias the I.F. amplifier before the A.F. detector and reduce considerably its amplification during interference peaks. The input voltage for the noise amplifier is derived from the input to the I.F. amplifier before the A.F. detector. The valve for the noise amplifier is of the non-variable-mu type and it is overbiased. The input-output voltage characteristic is parabolic, and normal modulated signals are not amplified to any great extent ; the large amplitude noise peaks, however, produce appreciable output voltages, which are detected by a biased detector across the output circuit. Biasing is applied to this detector in order to ensure that there is no detection of normal modulated signals. The I.F. amplifier preceding the A.F. detector is of the heptode or hexode type, the negative bias from the noise detector being connected to the " oscillator " grid, and the desired modulated carrier to the control grid. The filter between the noise detector and hexode grid must have a low time-constant (not greater than about 0·01 seconds) in order to obtain a rapid increase and decrease of bias voltage. If the action is slow the noise suppression is ineffective at the beginning of the pulses, and also the normal signal may be rendered inaudible for some time after the noise pulse has passed. This low time-constant makes filtering difficult, and a push-pull noise detector is an advantage because of the lower I.F. ripple voltage.

12.10. Audio Frequency A.G.C.

12.10.1. Introduction. Automatic gain control may be applied to A.F. amplifiers to give decreasing or increasing gain as the A.F. signal is increased. Decreasing gain control is generally only applied in public address systems to prevent blasting, or to preserve a reasonably level output when amplifying speech. Increasing gain control, known as contrast expansion, may be used to counteract the compression in intensity level range that must be made at a transmitter to obtain efficient modulation operation without overloading. It can only be satisfactory if compression at the transmitter is performed automatically by apparatus, the characteristics of which can be reproduced in inverse form as expansion at the receiver. At present compression is performed manually by skilled operators, so that an expansion circuit giving

correct compensation is not possible. Expansion can, however, be used with advantage to compensate for volume contraction (which is usually performed electrically) in gramophone records.

Whilst contrast expansion often adds to the realism of an orchestral transmission, it is not suitable for all types of programme. For speech or song it is less satisfactory owing to the discontinuous nature of the signal.

12.10.2. A.G.C. with Decreasing Amplification for Increasing A.F. Input.[29] The basic principle is the same as that involved in the application of A.G.C. to R.F. amplifiers. The A.F. voltage is amplified, then detected, and the D.C. component from detection is used to control the amplification of one or more of the A.F. stages. Control of a single A.F. tetrode valve is not usually

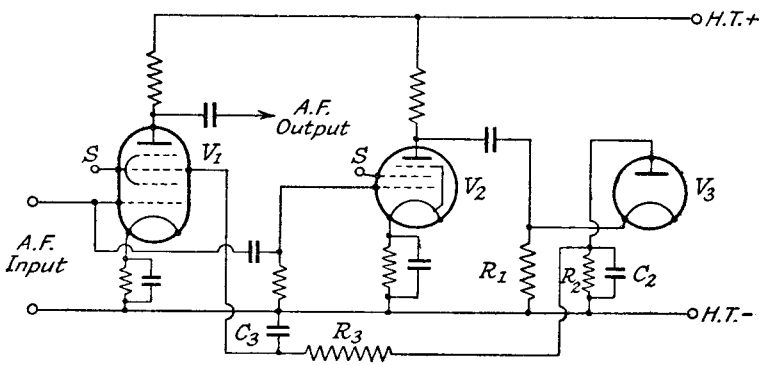

FIG. 12.20.—A.G.C. of an A.F. Signal Voltage.

satisfactory, because the curvature of its $I_a E_g$ characteristic (this is essential in order to make g_m variable with grid-bias voltage) produces distortion of the A.F. voltage. This distortion results chiefly in even harmonic frequencies, and it may be almost entirely eliminated by using two valves in push-pull with the A.G.C. bias applied to the grid-earth return lead common to both valves. An alternative is to employ a pentode, heptode or hexode valve, and to apply the A.G.C. bias to the suppressor grid or the oscillator grid. If suppressor grid control [30] is used with a pentode valve, the latter usually has to be designed with a finer mesh suppressor grid than is normal, otherwise very large biases are required before any appreciable reduction in amplification can be achieved. A possible circuit using a hexode valve is shown in Fig. 12.20. The A.F. input voltage is applied to the signal grid of the hexode valve V_1, and also

to the grid of the buffer valve V_2, before the A.G.C. detector, V_3. The buffer valve is necessary to prevent distortion of the input A.F. wave shape by conduction current damping from V_3, but it also increases the effectiveness of the A.G.C. control. It should be noted that this circuit is not the same as that for amplified A.G.C. of R.F. stages, because the bias voltage is being used to control the gain of an amplifier after the point from which the operative voltage for A.G.C. is taken. In this case the effectiveness of control is dependent on the amplification of the buffer valve as well as upon the delay bias (if any). The A.G.C. detector D.C. load resistance is divided between two resistances, R_1 and R_2, and the bias voltage is taken from R_2. Although the available bias voltage is reduced in the ratio $\frac{R_2}{R_1+R_2}$, this method of divided load resistance has the advantage of making filtering of the A.F. voltages from the D.C. component easier. Only the ripple A.F. voltages appear across R_2, whilst across R_1 is the full A.F. voltage as well as the ripple A.F. voltage. The time-constant of the A.G.C. filter circuit R_3C_3 must not be so high as to cause overloading on the first syllables of words, nor low enough to cause serious mutilation of the A.F. output wave shape. A value of about 0·5 seconds is generally satisfactory. The degree of input-output control may be calculated by plotting input voltage change, expressed as a decibel ratio, against input voltage ratio increase plus the ratio reduction of g_m (due to the A.G.C. bias change) of V_1.

12.10.3. A.G.C. providing Contrast Expansion.[26] To make efficient use of a transmitter when broadcasting music, the normal intensity level variation (70 db.) of an orchestral programme must be compressed. The maximum possible modulation percentage is 100%, and the minimum, which is determined by the noise level, is about 1%, so that a maximum possible intensity variation of 40 db. only is permissible. Conditions at the receiver are usually such (owing to noise) as to limit the variation further to about 25 db. Although expansion to, the original 70-db. range would not be desirable, and indeed would sound unnatural in a normal listening room, some degree of expansion is advantageous.

The circuit in Fig. 12.20 may be used for contrast expansion by reversing the anode-cathode connections to the A.G.C. diode V_3. This reverses the polarity of the A.G.C. bias to the hexode, so that increasing input voltage applies positive bias. An initial negative bias must be included in this circuit in order that the A.G.C. grid of the hexode may have a small negative bias even when the positive

A.G.C. bias is maximum. A filter circuit time-constant of 0·5 seconds is generally found to be satisfactory.

Another method of obtaining volume expansion is to include, in the speech-coil circuit of the loudspeaker, a variable resistance, the value of which is dependent on the current passing through it. The variable resistance may be produced by a lamp in parallel with the speech-coil, or two lamps in the opposite arms of a bridge circuit as shown in Fig. 12.21. In the first method the lamp resistance, of low value when cold, rises to a high value when the A.F. current passing through it causes it to glow. The result is that for small applied A.F. voltages a large proportion of the output current is diverted through the lamp. Increase of A.F. voltage increases the

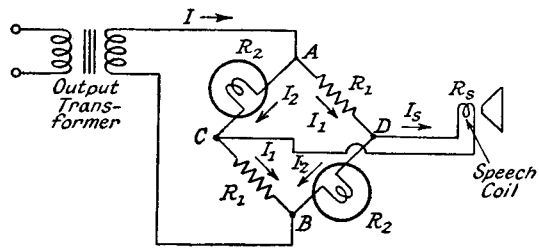

FIG. 12.21.—A.F. Contrast Expansion by means of Indicator Lamps.
[*Note.*—Read R_{sc} for R_s.]

lamp resistance and decreases the proportion of current diverted from the speech-coil. In the second method [20, 23, 24] the bridge is arranged to be almost in balance for small A.F. applied voltages. Increasing the latter causes the lamps to take more current and increase their resistance; the bridge is thrown more and more out of balance and a greater voltage is produced across the speech-coil. Both methods suffer from the disadvantage that much of the available power is dissipated in parts of the circuit other than the speech-coil even at maximum output. In either case a D.C. polarizing voltage [28] may be required across the lamps in order to raise their minimum resistances, and prevent too much attenuation of weak passages. The currents in the bridge circuit, which is symmetrical, are as marked in Fig. 12.21; R_2 is the lamp resistance, R_1 the resistance in the other two opposite arms, and R_{sc} the equivalent resistance of the speech-coil. The current and power relationships in the circuit are as follows:

$$I_1 - I_2 = I_s \quad . \quad . \quad . \quad . \quad . \quad 12.6$$

$$I_2R_2 = I_1R_1 + I_sR_{sc} \quad . \quad . \quad . \quad . \quad 12.7.$$

Solving 12.6 and 12.7 for I_1

$$I_1 = \frac{I_s(R_2+R_{sc})}{R_2 - R_1} \quad . \quad . \quad . \quad . \quad 12.8$$

and for I_2

$$I_2 = \frac{I_s(R_1+R_{sc})}{R_2 - R_1} \quad . \quad . \quad . \quad . \quad 12.9.$$

Power Output, $P_0 = I_s{}^2R_{sc}$

Power Input, $P_1 = 2(I_1{}^2R_1+I_2{}^2R_2)+I_s{}^2R_{sc}$.

Replacing I_1 and I_2 in the above by expressions 12.8 and 12.9.

$$P_1 = \frac{I_s{}^2[2(R_2+R_{sc})^2R_1+2(R_1+R_{sc})^2R_2+(R_2 - R_1)^2R_{sc}]}{(R_2 - R_1)^2}$$

$$= \frac{I_s{}^2[R_1+R_2+2R_{sc}][2R_1R_2+R_{sc}(R_1+R_2)]}{(R_2 - R_1)^2} \quad . \quad . \quad . \quad 12.10.$$

The power loss due to the insertion of the bridge is

$$\text{loss (db.)} = -10 \log_{10} \frac{P_1}{P_0}$$

$$= -10 \log_{10} \frac{[R_1+R_2+2R_{sc}][2R_1R_2+R_{sc}(R_1+R_2)]}{(R_2 - R_1)^2R_{sc}} \quad . \quad 12.11a.$$

It is convenient to express the input power in terms of the lamp current I_2 and the resistances, and combining 12.9 and 12.10, we have

$$P_1 = I_2{}^2\frac{(R_1+R_2+2R_{sc})[2R_1R_2+R_{sc}(R_1+R_2)]}{(R_1+R_{sc})^2} \quad . \quad 12.12$$

and the degree of contrast expansion is obtained by plotting the loss expression 12.11a against the input power P_1 (expression 12.12). A straight line parallel to the P_1 axis indicates no volume expansion.

The characteristics of the lamp $\left(I_2 \text{ against } R_2 = \frac{E_2}{I_2}\right)$ may be determined experimentally by measuring the current for different applied A.F. voltages (E_2), but, before the performance can be estimated, the relationship between R_1, $R_2(max.)$, the maximum hot resistance of the lamp, and R_{sc} must be established. This is obtained from the condition of maximum power transfer. Thus the bridge input resistance across AB must be matched to the valve, or, if the transformer is unchanged, the bridge input resistance across AB should equal the speech-coil resistance R_{sc}. The power loss ratio then becomes

$$\text{loss (db.)} = -10 \log_{10} \frac{(I_1+I_2)^2}{I_s{}^2}.$$

Substituting 12.8 and 12.9 for I_1 and I_2 in the above, and noting that R_2 is now $R_2(max.)$

$$\text{loss (db.)} = -20 \log_{10} \frac{(R_1+R_2(max.)+2R_{sc})}{(R_2(max.) - R_1)} \quad .12.11b.$$

Equating 12.11*a* and 12.11*b* gives

$$R_1R_2(max.) = R_{sc}^2.$$

Thus for $R_{sc} = 2{\cdot}5$ ohms, and loss at maximum power output from the valve of 3 db., we have,

$$\frac{R_1+R_2(max.)+2R_{sc}}{R_2(max.) - R_1} = \text{antilog}_{10}\, 0{\cdot}15 = 1{\cdot}413$$

and replacing $R_2(max.)$ by $\frac{R_{sc}^2}{R_1}$ gives after simplification

$$2{\cdot}413R_1^2+5R_1 - 2{\cdot}58 = 0$$

$$R_1 = 0{\cdot}425\ \Omega.$$

$$R_2(max.) = 14{\cdot}7\ \Omega.$$

BIBLIOGRAPHY

1. Automatic Gain Control. A. Dinsdale, *Wireless World*, Sept. 23rd (p. 290), and Sept. 30th (p. 327), 1932.
2. Automatic Volume Control. C. H. Smith, *World Radio*, Dec. 30th, 1932 (p. 1378), and Jan. 13th, 1933 (p. 53).
3. Practical Automatic Volume Control. W. T. Cocking, *Wireless World*, Jan. 6th (p. 2), and Jan. 13th (p. 29), 1933.
4. Automatic Volume Control. C. N. Smyth, *Wireless World*, Feb. 17th, 1933, p. 134.
5. The Influence of Fading Compensation on Contrast in Music. T. Sturm, *Funktechnische Monatshefte*, Feb. 1933, p. 139.
6. The History of A.V.C. *Wireless World*, March 31st, 1933, p. 236.
7. Automatic Gain Control of Radio Receivers. I. J. Cohen, *Post Office Electrical Engineers' Journal*, April 1933, p. 58.
8. Automatic Volume Control for Radio Receivers. C. B. Fisher, *Wireless Engineer*, May 1933, p. 248.
9. Corrected A.V.C. *Wireless World*, June 2nd, 1933, p. 386.
10. Delayed Diode A.V.C. W. T. Cocking, *Wireless World*, Sept. 8th, 1933, p. 208.
11. Delayed Amplified A.V.C. W. T. Cocking, *Wireless World*, Sept. 22nd, 1933, p. 244.
12. Q.A.V.C. F. L. Hossell, *Wireless World*, Jan. 19th, 1934, p. 43.
13. A.V.C. applied to A.F. Amplifier Tubes. J. R. Nelson, *Electronics*, Feb. 1934, p. 50.
14. Quiet, Amplified and Delayed A.V.C. with a Single Valve. *Wireless World*, April 27th, 1934, p. 296.
15. A.V.C. without Loss of Maximum Sensitivity. H. Pitsch, *Funktechnische Monatshefte*, May 1934, p. 182.

16. Methods of "Crack Killing". T. Sturm, *Funktechnische Monatshefte*, July 1934, p. 259.
17. The Design of A.V.C. Systems. W. T. Cocking, *Wireless Engineer*, Aug. (p. 406), Sept. (p. 476) and Oct. (p. 542), 1934.
18. The Determination of the Effectiveness of Antifading Devices. P. Mandel, *L'Onde Électrique*, Aug. 1935, p. 531.
19. A Noise Silencing I.F. Circuit for Superhet Receivers. J. J. Lamb, *Q.S.T.*, Feb. 1936, p. 11.
20. Light Bulb Volume Expander. *Electronics*, March 1936, p. 9.
21. Noise Elimination. *Wireless World*, March 27th, 1936, p. 314.
22. Delayed Detector Operation. J. H. Reyner, *Wireless World*, April 10th, 1936, p. 364.
23. Simplified Volume Expansion. W. N. Weeden, *Wireless World*, April 24th, 1936, p. 407.
24. Inexpensive Volume Expansion. R. H. Tanner and V. T. Dickins, *Wireless World*, May 22nd, 1936, p. 507.
25. Distortionless A.V.C. Systems. W. T. Cocking, *Wireless World*, June 12th, 1936, p. 574.
26. Contrast Amplification. W. N. Weeden, *Wireless World*, Dec. 18th, 1936, p. 636.
27. Distortion produced by Delayed Diode A.V.C. K. R. Sturley, *Wireless Engineer*, Jan. 1937, p. 15.
28. Contrast Expansion. G. Sayers, *Wireless World*, April 16th, 1937, p. 378.
29. A.V.C. in P.A. Equipment. *Wireless World*, Aug. 6th, 1937, p. 119.
30. Volume Expansion Problems. M. C. Pickard, *Wireless World*, Aug. 27th, 1937, p. 186.
31. Time Constants for A.V.C. Filter Circuits. K. R. Sturley, *Wireless Engineer*, Sept. 1938, p. 480.
32. A.V.C. Characteristics and Distortion. E. G. James and A. J. Biggs. *Wireless Engineer*, Sept. 1939, p. 435.
33. A.V.C. Developments. W. T. Cocking, *Wireless World*, Dec.1939, p. 51.
34. Noise Suppression by Means of Amplitude Limiters. M. Wald, *Wireless Engineer*, Oct. 1940, p. 432.
35. D.C. Amplified A.V.C. Circuit Time Constants. K. R. Sturley and F. Duerden, *Wireless Engineer*, Sept. 1941, p. 353.

CHAPTER 13

PUSH-BUTTON, REMOTE AND AUTOMATIC TUNING CONTROL[17]

13.1. Introduction. Push-button tuning is incorporated in receivers so that predetermined stations may be tuned in immediately by pressing a switch.

By the extension, when practicable, of the push-button switching to a position at some distance from the receiver, remote control of tuning is possible. Special circuits have also been designed to give continuous tuning over a range of frequencies at a remote point. The A.G.C. action of a remotely-tuned receiver must be such as to reduce output volume changes due to input signal variations to small proportions, unless a remote volume control is used. The ideal remotely-tuned receiver should, of course, include remote control of all the functions normally operated by hand. Methods of achieving this are, however, discussed in their appropriate chapters, i.e., automatic variable selectivity in Section 7.10, Part I, and automatic gain control in Chapter 12.

The use of highly selective I.F. circuits in a superheterodyne receiver makes accurate tuning a necessity if correct reproduction, free from distortion, is to be obtained. An early method of ensuring correct manual tuning was to use a highly selective circuit, tuned to the I.F. carrier, to operate a muting device. The receiver was silenced until the I.F. carrier entered the narrow pass range of this circuit. This offered no solution to the problem of accurate tuning of push-button receivers. The method now adopted (known as automatic frequency correction) is to adjust automatically the oscillator frequency so as to set the I.F. carrier in the centre of the I.F. amplifier pass-band irrespective of the signal tuning. This means that the signal circuits may be mistuned, but the effect is much less serious than off-centring the I.F. carrier. A variable reactance, connected in parallel with the oscillator tuned circuit, is controlled by the degree of I.F. carrier tuning error and is varied in such a direction as to reduce the error.

13.2. Push-Button Tuning.

13.2.1. Introduction.[7] A broadcast receiver is usually operated on a few selected (often local) stations, and there are advantages

in being able to switch over almost instantaneously from one programme to another. This is possible with push-button tuning, which may be accomplished in either of two ways. In the first the tuning capacitor may be rotated mechanically by means of cams operated from push buttons, or electrically by a motor. The second switches in pretuned circuits. In both systems it is usual to silence the receiver whilst the change is being made from one station to another. Automatic frequency correction of the oscillator is almost an essential requirement if accurate tuning is to be achieved and maintained.

13.2.2. Mechanical Rotation of the Tuning Capacitor.[13] There are a number of methods of mechanical tuning by push-button. One uses selecting levers connected to specially shaped cams equal in number to the stations required. Each cam is fixed to the rotor shaft of the capacitor. Pressure on the lever rotates the cam to the position corresponding to the desired station setting. The disadvantage of this system is that considerable pressure is required to operate the push-button, very careful mechanical design is necessary for reasonably accurate tuning, and wear of moving parts leads eventually to incorrect tuning.

Another mechanism employs spiral-shaped stator and rotor capacitor plates. Change of capacitance is obtained by moving the " rotor " in or out of mesh with the stator. The amount of mesh is determined by the travel of the push-button, the position of which is adjustable by means of a set screw. Each push-button can easily be set to any desired station in the wave range covered by the tuning capacitor variation, after the receiver has been installed.

A third method of rapid mechanical station selection is by an automatic telephone type dial fixed to the tuning capacitor shaft. A finger is inserted in the hole marked with the appropriate station and the dial is rotated until a stop is encountered. At this point the capacitor setting is correct for the desired station. Unlike the automatic telephone dial there is no return to the original position. The width of the finger-hole prevents the selection of stations close together in frequency though this difficulty may be overcome by staggering the holes. Another disadvantage is that the user cannot change to stations other than those already selected by the manufacturer.

13.2.3. Electrical Rotation of the Tuning Capacitor.[10] Electrical rotation of the tuning capacitor is accomplished by a small reversible induction motor (24-volt) geared to the capacitor shaft. The motor is generally of the shaded pole type, with two field

windings, connected in series, and a metal disc (copper or brass) as a rotor. One of the two field windings is centre-tapped, only one half of the coil being in circuit at a time, and the centre tap is connected to one end of the other field winding. By changing the supply from one-half of the coil to the other, the direction of the motor is reversed. The motor may be arranged to reverse direction only at the ends of the capacitor shaft travel (the reversing switch is operated by a cam on the shaft), or the selector mechanism may be so connected that the capacitor is always turned towards the tuning point of the desired station, i.e., direct " homing " is used. The first method is less satisfactory because the capacitor is taken to the end of the scale and then reversed, when it is desired to accept a transmission " behind " the initial tuning setting. This entails loss of time in tuning and greater wear on moving parts.

In the first type each station has its own disc mounted on the capacitor shaft, and let into the disc is an insulating segment at a position corresponding to the correct station setting. One side of the push-button switch is connected to a brush rubbing on the disc circumference ; the other side is joined to the motor, which itself is connected to a secondary of the mains supply transformer. The circuit is completed by the lead from transformer to disc. Closing of the push-button switch energizes the motor, which rotates until the insulating segment on the disc open-circuits the motor supply. The reversing switch is operated by a cam on the capacitor shaft when the latter reaches either end of its travel. A clutch disengages the motor drive immediately the supply is switched off. This is achieved by a spring-loaded armature, which in the rest position is out of line with the stator. Current induced in the armature pulls it into line with the stator, thus actuating the clutch. Contacts short-circuiting the loudspeaker speech-coil are also closed by the lateral movement of the armature.

Slight modification of the selector disc can give automatic reversal of the motor when the desired station setting is behind the starting position of the capacitor. The disc is divided into two equal sectors, one insulated from, and the other connected to, the tuning capacitor shaft as shown in Fig. 13.1. The insulated sector is connected via an insulated slip ring and sliding contact S_1 to one end of the " forward " coil A of the driving motor. The other sector is connected through the sliding contact S_2 on the capacitor shaft to the " reversing " coil B of the motor. The station selector contacts, two of which, $SS1$ and $SS2$, are shown in Fig. 13.1, are joined to their appropriate push-button switches, B_1, B_2, etc. They ($SS1$,

etc.) are often mounted on a semicircular rail, coaxial with the disc, and their positions are adjustable in order that any desired transmissions can be selected. The selective operation is best illustrated by reference to Fig. 13.1. With push-button B_1 closed, the supply is connected through $SS1$, the uninsulated sector, the tuning capacitor shaft and sliding contact S_2 to the reversing field coil B. The motor rotates the capacitor shaft in an anti-clockwise direction until the insulation between the sectors breaks the supply circuit. The clutch from motor to the gear drive immediately dis-

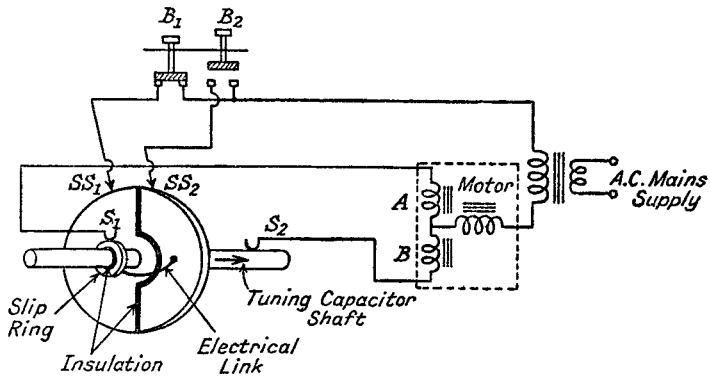

FIG. 13.1.—Reversible Motor Driven Tuning.

engages as described above, at the same time open-circuiting the loudspeaker speech-coil and allowing station 1 to be heard. Pressing $B2$ releases $B1$ and connects the supply through $SS2$, the insulated sector, slip-ring and sliding contact S_1 to the forward coil A of the motor, which rotates the capacitor shaft in a clockwise direction until the insulation comes under $SS2$. The motor supply and speech-coil are open-circuited and station 2 is heard.

13.2.4. Preset Tuned Circuits. Push-button selection of desired transmissions may be achieved by switching capacitors in parallel with a given coil, or vice versa. The switched capacitor or inductor must be capable of being trimmed in order that receiver circuits can be either correctly tuned to the desired transmission or changed from their initial setting to any other within reasonable frequency range of the original. The trimming range (the variation from maximum to minimum capacitance or inductance) should not be too large otherwise tuning frequency adjustment becomes critical and susceptible to mechanical jarring and the effects of temperature. From this point of view a switched trimmed inductance is preferable

to a capacitance, its actual value varying less with temperature and humidity change than that of a trimmed capacitance.

With inductance switching a fixed capacitor of the silvered mica type is often used, because it can be made with a low negative capacitance-temperature coefficient, which helps to balance the positive inductance-temperature coefficient of the coil. Inductance trimming is generally realized by having a screwed central iron-dust core, with a slotted head to take a screwdriver. Alternatively the dust core may be attached to a metal screw, having a lock-nut; this has advantages because the threading on the iron-dust core is liable to wear, must be of coarser pitch and is less easy to lock than a metal threaded screw. A separate trimmed inductance is required for each push-button switch, but the same fixed tuning capacitance may be employed, e.g., in changing from the long- to medium-wave range, it is only necessary to switch the inductance. With switched capacitors it is generally necessary to change the fixed inductance when transferring from one range to another.

Of the two types of circuit involved in tuning the superheterodyne receiver, the oscillator is more critical than the signal-tuned circuit, and the highest possible stability is required of the tuning components of the former, unless automatic frequency correction is employed. Stability of component values, though desirable, is not so essential in the signal circuits, particularly in the case of short-wave operation.

There are three types of push-button switches meriting description. The simplest is the shorting bar, shown shaded in Fig. 13.2*a*;

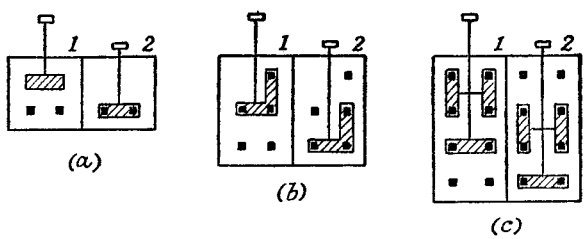

FIG. 13.2.—Examples of Push Button Switching.
(*a*) Simple short-circuit strip. (*b*) L-shaped short-circuit strip.
(*c*) A more complicated three-section short-circuit strip.

in position 2 the switch is operative. It is suitable for selecting an inductance or capacitance and connecting it to its other tuning element, which must be permanently connected to the grid of the amplifying valve. The L-shaped shorting strip with three rows of contacts, as shown in Fig. 13.2*b*, has the following advantages:

(1) the extra contact in the top row can be used to short-circuit unwanted coils, the coil being connected between this contact and the right-hand one of the middle row immediately below it ; (2) the grid of the valve and the appropriate tuning capacitance need not be permanently connected, the former being connected to the bottom left-hand contact and the latter to the bottom right-hand contact. This is a particularly useful feature when one of the push-button switches is used to convert to manual tuning with the normal variable capacitor.

A more complicated four-row switch is illustrated in Fig. 13.2*c*. In the operating position 2, rows 1 and 2 are disconnected from each other, 2 and 3 are joined and row 4 is short-circuited. Such a switch could be used to open circuit a selected coil, connect it to its tuning capacitor and also select a reaction winding in an oscillator circuit.

13.3. Remote Control.

13.3.1. Introduction. Many methods of station selection at a point remote from the receiving apparatus have been developed. Rotation of the variable tuning capacitor by a magnetic relay or motor, a ratchet relay selecting preset components and operated by pulses sent via the mains supply wiring or direct from a portable oscillator, transfer of the R.F. and frequency changer stages to the remote point, magnetic tuning, and the use of tuned lines are some of the methods which have been successfully employed.

13.3.2. Rotation of the Tuning Capacitor. A very early method [1] of remote control used an iron-armature motor driving the tuning capacitor. The position of the armature was controlled by two field coils at right angles. Resistances across the end of the lines at the remote point controlled the current in each field coil, and the armature was rotated to the position of maximum magnetic field. The disadvantage was that only a small torque was available and friction had to be reduced to a low value. However, selection of any station in the wave band was possible.

The motor drive described in 13.2.3 is very suitable for remote control, since the push-button switches can easily be located at a distance from the receiver. Continuous tuning over the wave range is not, however, practicable.

13.3.3. Pulse Control using Mains Supply Wiring. Two methods of remote control by sending pulses to the receiver via the internal mains wiring have been developed. One uses D.C. pulses and the other R.F. pulses.

A simplified diagram of the circuit for D.C. control pulses [16] is shown in Fig. 13.3. The source of D.C. is a transformer T_1, developing a secondary voltage of about 8 volts, and a full wave rectifier producing about 1·5 amps. at 10 volts. The primary of T_1 is connected in series with the D.C circuit to act as a choke allowing the D.C. pulses to be passed without short-circuiting the mains supply. Closing switch S sends to the mains leads, a D.C. pulse which energizes a low voltage relay R (0·35 volts, 5 mA) at the receiver. The D.C. voltage across the relay is small because of the low resistance of the incoming mains supply network, which forms with the primary of T_1 a potential divider for the D.C. voltage. A.C. must not be allowed to energize the relay, or chattering results. Cancellation of the A.C. voltage is obtained by connecting the relay between one terminal A of the primary and one terminal B of the secondary of a 1 : 1 transformer T_2. The A.C. voltages across

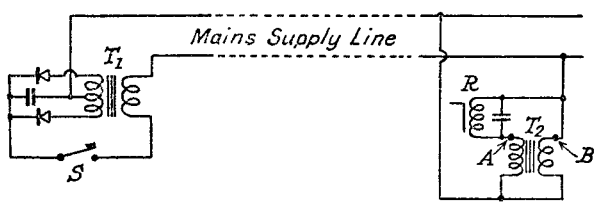

FIG. 13.3.—Remote Control by D.C. Pulses sent via the Mains Wiring.

primary and secondary are equal, so that the net A.C. voltage from A to B is zero and no A.C. load is applied to the transformer. The D.C. resistances of the primary and secondary are unequal so that a D.C. voltage is developed across the terminals AB during pulse excitation. The primary side A, which is in series with the relay, has a low resistance (about 3·5 Ω), and the secondary side B has a high resistance (200 Ω). A large capacitance is connected across the relay as a precaution to by-pass any out-of-balance A.C. voltage. The relay itself has insufficient torque to drive a ratchet selector mechanism, and it is used to operate an intermediate relay from an auxiliary rectifier at the receiver. The number of pulses sent determines the station selected.

An interesting development [11] of remote control by transmission of modulated pulses of R.F. voltage along the mains leads is illustrated in Fig. 13.4. The R.F. oscillator heater and H.T. supplies are obtained by transformer from the mains supply, and no rectifier is used in the H.T. source. The result is that the oscillator output is modulated by half-sine waves of the mains frequency, oscillation

ceasing when the A.C. anode-to-cathode voltage begins its negative half-cycle. Apart from the elimination of a rectifier there are other important advantages conferred by using a half-sine modulated pulse, and these are discussed below. The modulated output is transmitted via the coupling coil L_1 and capacitance C_1 to the mains lead. The capacitance C_1 (about 0·001 μF) has a low reactance to the radio frequency and a high reactance to the mains frequency, thus preventing a short-circuit of the mains supply by L_1. The R.F. voltage is accepted at the receiver via the capacitance C_2, of the same value as C_1, and coil L_2, and it operates one of two anode-bend detector valves, V_2 and V_3, having in their anode circuits relays driving ratchet selector mechanisms. The H.T. supply to the detectors is derived from the mains without using a rectifier. This

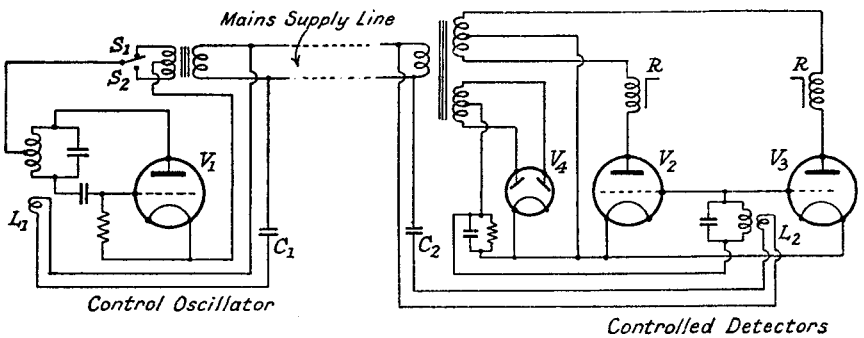

FIG. 13.4.—Remote Control by Pulses from a R.F. Oscillator.

method of detector and oscillator H.T. supply allows one oscillator to perform two functions, such as station selection and volume control, at the receiver. The relay in V_2 anode circuit performs, for example, the first, and that in V_3 anode circuit the second. Thus, with the oscillator switch in the S_1 position, the positive H.T. cycle on the oscillator coincides with the positive H.T. cycle on the anode of V_2, and V_2 is operative. Conversely with the switch in the S_2 position, detector V_2 is non-conducting when the oscillator functions and its relay is not energized. Detector V_3, with reversed H.T. supply, conducts during the same half-cycle as the oscillator, and its relay is, therefore, energized. The ratchet mechanism is operated each time switch S_1 or S_2 is closed. The pulse oscillator frequency is about 400 kc/s, and radiation beyond the house wiring is not usually serious. A R.F. filter may be inserted in the incoming mains leads as an additional protection. Loading of the mains

supply by other electrical apparatus, such as soldering irons and lamps, has little effect on the R.F. transmission characteristics of the leads. The oscillator has an output of about 100 watts and the resonant circuit at the detectors steps up the control voltage at the receiver from about 0·8 to 30 volts R.M.S. The rectifier valve V_4 supplies D.C. grid bias for the anode-bend detectors.

A special cold cathode gas-filled valve is used for switching on the supply to the receiver, and no energy is consumed by the receiver until a suitable R.F. pulse is received from the control oscillator. The cold cathode valve is very suitable for use on a mains voltage of 110, but cannot be operated from 230 volts. It is similar in principle to the gas-filled discharge valve used for time-base operation with cathode ray tubes. The R.F. pulse from the oscillator starts conduction between auxiliary electrodes, and this initiates the main discharge which energizes the on-off relay. The H.T. for the discharge path is obtained from the mains, and ceases on negative half-cycles, so that the valve only functions as long as the R.F. pulse maintains the auxiliary discharge, i.e., switching off the oscillator also shuts down the receiver.

13.3.4. R.F. Pulses from a Portable Oscillator.[14] A small battery-operated oscillator is situated at the remote point, and R.F. pulses, produced by interruption of the filament supply to the oscillator, are transmitted direct to the receiver. A tuned circuit coupled to a detector at the receiver accepts the pulses, which operate a ratchet relay selecting the required coil or capacitor. An automatic telephone type dial is used to interrupt the portable oscillator, and the required station is selected in accordance with the number of pulses transmitted.

13.3.5. Transfer of R.F. and Frequency Changer Stages to the Remote Point.[15] The signal and frequency changer stages are connected to the rest of the receiver by a multi-core cable carrying the aerial, earth, I.F., A.G.C., manual volume control, H.T. and L.T. supplies, and on-off switch leads. Matching transformers are required at each end of the aerial and I.F. lines. The method has the advantage of allowing continuous tuning over the wave range, but the unit is comparatively bulky.

13.3.6. Magnetic Remote Tuning.[6, 12] The inductance of an iron-dust-cored coil may be varied by placing it in a strong D.C. magnetic field. An inductance variation of about 9 : 1 is achieved for a change of 1·5 to 5 watts in the D.C. power to the electromagnet. Inductance tuning is possible by controlling the D.C. polarizing field. The control resistances for each electromagnet coil are ganged and

placed at the remote control point. Continuous tuning over a wave band is possible.

13.3.7. Tuned Lines.[5] The reactance and standing wave properties of R.F. cables have been employed to give push-button and continuous tuning control. First circuit noise is usually of secondary importance in remote control since only stations of reasonable daylight strength are normally selected, and a low impedance cable is not therefore a serious disadvantage. Station selection on long and medium waves can be achieved at distances up to 100 feet from the receiver.

Signal and oscillator frequency preselection is shown in Fig. 13.5. The aerial is coupled through a R.F. cable to coil L_1, which is loosely

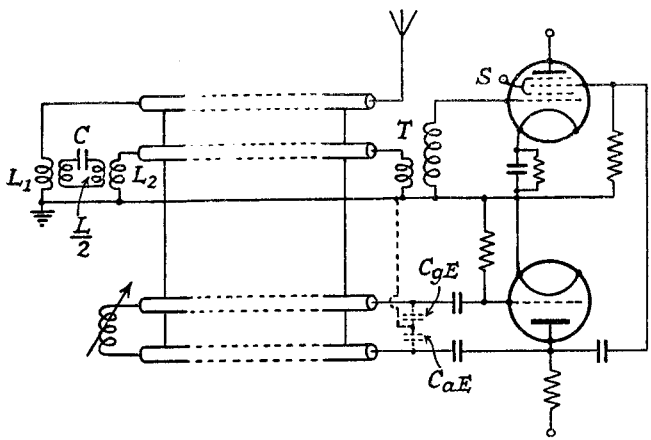

FIG. 13.5.—Remote Signal and Oscillator Tuning by means of Feeder Lines.

coupled to half the coil, $\frac{1}{2}L$, of the remote tuned circuit. The other half of L is loosely coupled to L_2, which connects to the screened cable. The receiver end of the screened cable is terminated in a wide frequency-acceptance-band transformer T, which steps up the voltage to the frequency changer grid. The tuning capacitance C has a series of preset values, which are switched in by push-buttons, and the tuning coil has a high Q value. The aerial-to-grid amplification is less than that of a single tuned circuit, but the selectivity is comparable. A Colpitts oscillator is shown, the cable acting as the splitting capacitance, but a back-coupled oscillator may also be used. For continuous tuning a high I.F. (about 2 Mc/s) is necessary, and the oscillator lead is used as a quarter-wave line. A small variable capacitor in series with an inductance at the remote end

controls the oscillator frequency, and it may be ganged with the capacitor tuning the signal circuits.

13.4. Automatic Frequency Correction.[3]

13.4.1. Introduction. Two effects, sideband "screech" and harmonic distortion, become very pronounced if the I.F. carrier frequency at the output of the frequency changer stage of a superheterodyne receiver is not correctly centred in the comparatively narrow pass-band of the I.F. amplifier. Sideband "screech" is characterized by high-pitched distorted reproduction, and it occurs when the I.F. signal carrier is detuned to the side of the I.F. selectivity curve. In this condition the equivalent of single sideband reception with over-accentuated high-frequency sideband components is obtained, because one set of sidebands is almost entirely eliminated, and the carrier and low-frequency sidebands are reduced by being outside the pass range. Harmonic distortion of the audio output is caused by the diode detector when one set of sidebands is removed. With normal pass-band widths (± 5 kc/s) the maximum tolerable mistune is about ± 1 kc/s. Automatic correction of the oscillator frequency overcomes this difficulty by reducing the error produced by inaccurate tuning, or frequency drift of the oscillator due to temperature and other effects. For example, a signal-tuning error of 5 kc/s may be reduced to an I.F. carrier error of 50 c.p.s. by this method.

The two units of the automatic frequency corrector are a discriminator or error detector, and a control device. The former translates the error in the I.F. carrier into a voltage, the magnitude and sign of which is a function of the error. The latter, operated from the discriminator voltage, provides frequency correction of the oscillator tending to reset the I.F. carrier in the centre of the I.F. amplifier pass-band. The operation of the system can be represented by an overall characteristic giving the final intermediate frequency error with different signal frequency tuning settings, and this is described in Section 13.4.4. The shape of the overall control characteristic is mainly dependent upon the discriminator, but the action of the control device, especially if it has a non-linear characteristic, modifies the result.

13.4.2. The Discriminator. A typical discriminator voltage-frequency curve is shown as dashed curve *ABODE* in Fig. 13.6*a*. The accuracy of control is determined by the slope *BOD*, and the final frequency error after correction is least when *BOD* has the greatest slope. It should be noted that automatic frequency

correction is similar to A.G.C., i.e., control is only exercised when there is a change in frequency, and correction can very much reduce, but not eliminate (except in special cases), the error. Two important frequencies in A.F.C. are the " pull-in " and " throw-out " points. The former is the signal-tuning setting at which A.F.C. comes into operation when approaching the required station setting; it is governed by the outer portions *AB* and *DE* of the characteristic. The latter is the signal-tuning setting at which A.F.C. loses control when tuning away from a station; it is mainly determined by the

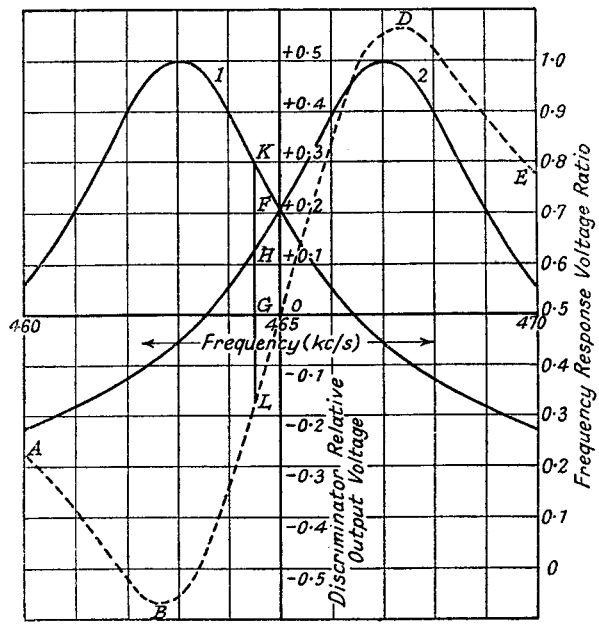

FIG. 13.6*a*.—Characteristic Curves for the Amplitude Discriminator.

distance of *B* and *D* from the horizontal axis. The " throw-out " signal-tuning setting is always greater than the " pull-in ", and it may be several channels away from the correct setting, thus causing a number of stations to be skipped when tuning away from the station. For this reason during manual tuning it is usual to disconnect A.F.C. with a friction switch operated by rotation of the tuning capacitor. The actual values of the throw-out and pull-in frequencies can be calculated from the discriminator and control device curves as described in Section 13.4.4.

There are two types of discriminator, one known as the amplitude [2] and the other as the phase discriminator.[4] An example of

the first is shown in Fig. 13.7. Two circuits, one (No. 1) tuned to a frequency about 2 kc/s below, and the other (No. 2) to 2 kc/s above the correct I.F. carrier frequency, are transformer-coupled to the anode circuit of a valve, deriving its input voltage from a proportion of the output voltage of the last I.F. stage in the receiver. Provided stray coupling between 1 and 2 is small and the slope resistance of V_1 is large compared with the maximum impedance across the primaries of 1 and 2, the frequency response of either circuit is unaffected by the other. The frequency response of each circuit relative to the response at the resonant frequency is shown by the curves 1 and 2 in Fig. 13.6*a*; these curves are obtained from the generalized selectivity curve of Fig. 4.3, Part I, as described below. They are identical in shape and displaced from each other by 4 kc/s. Diode detectors (D_1 and D_2 in Fig. 13.7) across these

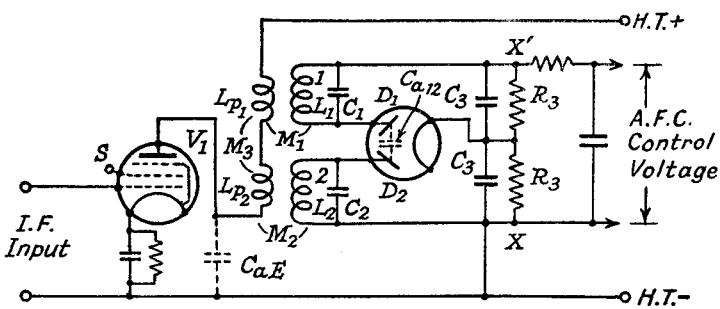

FIG. 13.7.—A Typical Amplitude Discriminator Circuit.

circuits, have their D.C. output voltages connected in series opposition. When there is no tuning error, the I.F. carrier voltages across 1 and 2 are equal (proportional to OF in Fig. 13.6*a*) and there is zero D.C. voltage across points XX' in Fig. 13.7. Mistuning to a lower I.F. carrier frequency (point G in Fig. 13.6*a*) increases to GK the proportional voltage applied to D_1 and decreases to GH that applied to D_2. Hence the D.C. output voltage at XX' is negative and proportional to HK, i.e., to GL; its actual value can be found by multiplying GL by the product of a constant K and the voltage detection efficiency of the diodes. The constant K is a function of the input unmodulated carrier peak voltage to, and g_m of, the valve V_1 in Fig. 13.7, the ratio of mutual inductance to secondary tuning inductance, and the resonant or dynamic impedance of the secondary. Voltage detection efficiency, η_d in Chapter 8, Part I, is the ratio of the D.C. voltage across one of the load resistances, R_3, in Fig. 13.7 to the unmodulated carrier peak voltage output from 1 or 2. The

steepness of the slope *BOD* (Fig. 13.6*a*) is fixed by the Q of the circuits 1 and 2, the intermediate frequency mid-carrier value, and the frequency separation of points B and D, so long as the stray coupling between the circuits is small. For any particular frequency separation of the points B and D, there is a value of Q which gives maximum slope to *BOD* at O. Lower or higher values of Q give a smaller slope at O and also greater curvature to the line *BOD*.

Assuming that the Q values of circuits 1 and 2 are equal, the optimum Q can be calculated as follows : from Section 4.2.3, Part I, the selectivity of a single tuned circuit, i.e., its frequency response in terms of that at the resonant frequency, is shown to be equal to $\frac{1}{\sqrt{1+Q^2F^2}}$, where $F = \frac{2\Delta f}{f_r}$, and Δf is the frequency difference (or off-tune) between the particular frequency considered and the resonant frequency f_r. Thus

$$\text{Selectivity} = \frac{1}{\sqrt{1+Q^2F^2}} \quad . \quad . \quad . \quad 13.1$$

and the slope S of the selectivity curve at any off-tune frequency Δf is

$$\begin{aligned} S &= \frac{d(\text{Sel}^y)}{d\Delta f} = \frac{d(\text{Sel}^y)}{dF} \cdot \frac{2}{f_r} \\ &= \frac{-Q^2F}{(1+Q^2F^2)^{\frac{3}{2}}} \cdot \frac{2}{f_r} \\ &= \frac{-4Q^2\Delta f}{f_r^2(1+Q^2F^2)^{\frac{3}{2}}} \quad . \quad . \quad . \quad . \quad 13.2. \end{aligned}$$

The value of Q which gives maximum slope for a fixed value of Δf is found by differentiating 13.2 with respect to Q and equating to zero. This gives

$$2Q\left[1+\left(\frac{Q2\Delta f}{f_r}\right)^2\right]^{\frac{3}{2}} - 3Q^3F^2\left[1+\left(\frac{Q2\Delta f}{f_r}\right)^2\right]^{\frac{1}{2}} = 0$$

or

$$Q = \frac{f_r}{\sqrt{2}\Delta f} = \frac{0{\cdot}707f_r}{\Delta f} \quad . \quad . \quad . \quad 13.3a.$$

It is important to note that expression 13.3*a* does not give maximum possible slope with a given Q ; this is found by differentiating 13.2 with respect to Δf and equating to zero, when

$$\Delta f = \frac{f_r}{2\sqrt{2}Q} = \frac{0{\cdot}3535f_r}{Q} \quad . \quad . \quad . \quad 13.3b.$$

Expression 13.3*b* gives a larger value of Δf than that used for

calculating Q in expression 13.3*a*, but, though it produces a more sensitive discriminator characteristic, it is less satisfactory because it tends to increase the "pull-in" and "throw-out" frequency separations from f_m.

Although the condition for maximum slope at O for a fixed value of Δf is provided by expression 13.3*a*, a larger value of Q, such as $Q = \frac{f_r}{\Delta f}$ actually gives a better discriminator characteristic. The slope at O is only slightly reduced compared with that for $Q = \frac{0{\cdot}707 f_r}{Q\Delta f}$, but the frequencies corresponding to the peaks B and D (Fig. 13.6*a*) are closer to $\pm\Delta f$, and the characteristic falls much more rapidly outside the peaks, which means less difference between the "throw-out" and "pull-in" frequencies. However, the value of Q calculated from expression 13.3*a* is often higher than can conveniently be achieved in practice, and a suitable compromise is

$$Q = \frac{f_r}{2\Delta f} = \frac{0{\cdot}5 f_r}{Q} \quad . \quad . \quad . \quad . \quad 13.3c.$$

Examples of the discriminator characteristic for $Q = \frac{f_r}{\Delta f}, \frac{f_r}{2\Delta f}$ and $\frac{f_r}{4\Delta f}$ are shown by curves 1, 2 and 3 in Fig. 13.6*b* (only half the character-

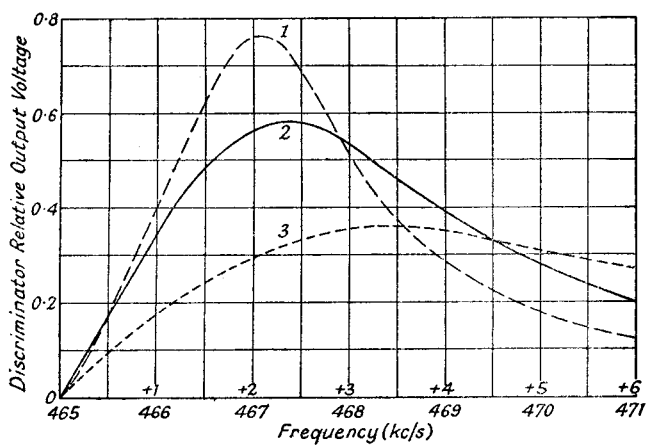

FIG. 13.6*b*.—Output Voltage Curves for an Amplitude Discriminator.

Curve 1.—$Q = \frac{f_r}{\Delta f}$. Curve 2.—$Q = \frac{f_r}{2\Delta f}$. Curve 3.—$Q = \frac{f_r}{4\Delta f}$.

istic is illustrated, the other half on the negative side being identical in shape). The curves are derived from the single tuned circuit generalized selectivity curve of Fig. 4.3 (Part I) for $f_r = 465$ kc/s,

$\Delta f = 2$ kc/s, as described later in this section. As Q is increased the frequency separation of peaks B and D is reduced and approaches $2\Delta f$, the peaks themselves increase in amplitude and the sections AB and DE fall away much more rapidly. Curve 1 $\left(Q = \frac{f_r}{\Delta f}\right)$ is similar to two S shapes joined at O; the tail of the S at O is exaggerated in Fig. 13.6*b* in order to demonstrate the effect more clearly. Curve 2 $\left(Q = \frac{f_r}{2\Delta f}\right)$ is linear over most of the range BOD whilst curve 3 $\left(Q = \frac{f_r}{4\Delta f}\right)$ is appreciably curved from B to D, being similar to a single S shape. Frequencies of maximum response for curves 1, 2 and 3 are $\pm 2{\cdot}02$, $\pm 2{\cdot}4$ and $\pm 3{\cdot}5$ kc/s respectively. The " throw-out " and " pull-in " frequencies both tend to decrease as Q is increased, though the actual difference between the " throw-out " frequencies for curves 1 and 2 is dependent on the shape of the variable reactance characteristic (see Section 13.4.4) and may be quite small.

Substituting values of 465 and 2 kc/s for f_r and Δf gives Q values of 232·5, 116·25 and 58·125 kc/s for curves 1, 2 and 3. The first value is difficult to realize in practice, and in subsequent calculations we shall use expression 13.3*c* in determining Q. The discriminator characteristic is therefore that represented by curve 2, the resonant frequencies of circuits 1 and 2 (Fig. 13.7) are 463 and 467 kc/s and

$$Q_1 = \frac{463}{4} = 115{\cdot}75.$$

$$Q_2 = \frac{467}{4} = 116{\cdot}75.$$

For practical purposes we may take $Q_1 = Q_2 = 116$.

The two curves in Fig. 13.6*a* are obtained from Fig. 4.3, Part I, by taking Q as 116 and f_r as 465 kc/s, i.e., the off-tune frequency scale is positioned such that $\Delta f = \frac{f_r}{2Q} = \frac{465}{232} \simeq 2{\cdot}0$ kc/s registers with $QF = 1$. The decibel scale of Fig. 4.3 is converted to a voltage ratio scale for plotting in Fig. 13.6*a*, curve 1 being plotted from a resonant frequency of 463 kc/s and curve 2 from a frequency of 467 kc/s. The error involved in fixing the position of the off-tune frequency scale for Fig. 4.3 by taking f_r as 465 instead of 463 and 467 kc/s is negligible.

Expression 13.2 gives the slope of the frequency response of one

of the tuned circuits, and it must be multiplied by 2 in order to obtain the slope at O. Hence maximum slope at O when $\Delta f = 2$ kc/s is

$$S_{(max.)} = 2.\frac{4.(116)^2.2}{(465)^2(2)^{\frac{3}{2}}} = 0{\cdot}352$$

$$= 0{\cdot}352\ \eta_d K \text{ volts per kc/s off-tune per 1 volt peak input carrier.}$$

If Δf is not fixed and a value larger than 2 kc/s can be tolerated, maximum slope for $Q = 116$ is obtained when $\Delta f = 2{\cdot}828$ kc/s (expression 13.3*b*) and is

$$max.\ S_{max.} = 2.\frac{4.(116)^2 2{\cdot}828}{(465)^2(1{\cdot}5)^{\frac{3}{2}}} = 0{\cdot}765.$$

In subsequent calculations we shall consider the condition that Δf is fixed and equal to 2 kc/s. On the assumption that R_a is much greater than the maximum primary impedance of circuit 1 or 2, the constant K is, from expression 4.30*b*, Section 4.4.2, Part I,

$$K = g_m \hat{E}_C R_D \frac{M}{L}$$

where g_m = mutual conductance of V_1 in mA/volt
$\hat{E}_C$ = peak (unmodulated) carrier voltage applied to the grid of V_1
R_D = resonant or dynamic impedance of the secondary of **1 or 2.**
M = mutual inductance between primary and secondary
L = inductance of the secondary.

Clearly greatest discriminator characteristic slope for a fixed g_m and $\hat{E}_C$ requires R_D and $\frac{M}{L}$ to be as large as possible. On the other hand, too large a value of $\frac{M}{L}$ and R_D produces a large primary impedance and causes the frequency response of one circuit to be affected by the other. Furthermore, stray capacitance coupling between the secondaries has a greater effect when R_D is increased. Suitable values for R_D and $\frac{M}{L}$ are 75,000 ohms and 0·3 respectively. From Section 4.4.2, Part I, the maximum impedance across either primary (when the secondary is resonant) is $R_D\frac{M^2}{L^2}$ (expression 4.29*b*), i.e., $R_p = 75{,}000 \times 0{\cdot}09 = 6{,}750$ ohms. This value is small compared with the probable minimum slope resistance of a tetrode

valve and the stray capacitance, C_{aE}, from anode to earth, so that we can safely assume that the series connection of the two primaries has little effect on the individual secondary frequency responses.

For the above selected values

$$K = g_m \hat{E}_G \; 75{,}000 \times 0{\cdot}3$$
$$= 67{\cdot}5 \; \hat{E}_G$$

if $g_m = 3$ mA/volt.

Taking $\hat{E}_G$ as 1 volt and η_d as 0·8, the maximum slope at O is

$$0{\cdot}352 \times 0{\cdot}8 \times 67{\cdot}5 = 19{\cdot}0 \text{ volts per kc/s off-tune per 1 volt peak input.}$$

The circuit constants for 1 and 2 may be calculated as follows :

Circuit 1.

$$Q_1 = 116, \; f_1 = 463 \text{ kc/s}, \; R_{D1} = 75{,}000 \text{ ohms}$$
$$L_1 = \frac{R_{D1}}{\omega_1 Q_1} = \frac{75{,}000 \times 10^6}{6{\cdot}28 \times 463 \times 10^3 \times 116}$$
$$= 222 \; \mu\text{H}$$
$$C_1 = 532 \; \mu\mu\text{F}$$
$$M_1 = 0{\cdot}3 L_1 = 66{\cdot}6 \; \mu\text{H}.$$

A probable value for coupling coefficient, $k_1 = \dfrac{M_1}{\sqrt{L_{p1} L_1}}$ between primary and secondary is 0·5, so that

$$L_{p1} = 80{\cdot}5 \; \mu\text{H}.$$

If the detector load resistances R_3 in Fig. 13.7 are 0·5 MΩ, the damping resistance due to diode conduction current is very nearly 0·25 MΩ. Hence the resonant impedance of the tuned secondary, in the absence of diode conduction current, must be

$$R_{D1}' = \frac{250{,}000 \times 75{,}000}{250{,}000 - 75{,}000} = 107{,}000 \text{ ohms}$$

and the Q of the coil is

$$Q_1' = \frac{R_{D1}'}{\omega_1 L_1} = \frac{107{,}000}{6{\cdot}28 \times 463 \times 10^3 \times 222} = 165,$$

which is a practically realizable value.

Circuit 2.

Since the resonant frequency of circuit 2 is so close to that of 1, the circuit constants are almost equal, and the most practical

method is to use nominally identical circuits, and to off-tune the required 2 kc/s from 465 kc/s by trimming either the inductance or capacitance element.

The performance of the discriminator is adversely affected by stray coupling between the primaries or the secondaries of 1 and 2. These stray couplings cause the two peaks B and D to be unequal in distance from the frequency base line, and the line BOD tends to be curved in concave shape looking from A. Coupling is produced by the anode-earth capacitance C_{aE} of valve V_1, which allows a current to circulate in the two primaries, and also by the anode-to-anode capacitance C_{a12} of diodes D_1 and D_2. The first effect is not very serious if the primary impedance is small and the primary to secondary coupling is loose. For example, the circuit constants selected above give a maximum primary impedance R_p of 6,750 ohms, so that the average stray anode-to-earth capacitance for V_1 of 15 $\mu\mu$F $\left(X_{aE} = \dfrac{10^{12}}{6{\cdot}28 \times 465 \times 10^3 \times 15} = 22{,}800 \text{ ohms}\right)$ would have little influence on performance. The anode-to-anode capacitance C_{a12} of the diodes is much less (about 1 $\mu\mu$F), but the secondary impedances are much higher than the primary. Both effects may be reduced or even cancelled by including positive mutual inductance coupling M_3 (see Section 3.4.2, Part I) between the circuits, a small coil in series with L_1 being coupled to L_2, or vice versa. The direction of M_3 is important, for if it is negative it adds to the stray capacitance coupling.

To economize in space the two circuits 1 and 2 may be wound at opposite ends of the same coil former, the stray mutual inductance being used to cancel the stray capacitance.

It is important to ensure that the resonant frequency of the two primaries with the stray capacitance C_{aE} is far removed from the I.F. or a low harmonic of the I.F., otherwise an asymmetrical discriminator characteristic with unequal positive and negative peak results. In the example quoted above the resonant frequency is 3·24 Mc/s with 15 $\mu\mu$F stray capacitance.

The two primaries may be connected in parallel instead of in series, or the tuned circuits 1 and 2 may each be loosely coupled through small capacitances (5 $\mu\mu$F) to the anode of the last I.F. amplifier valve in the receiver, but in both instances performance is less satisfactory and a symmetrical discriminator curve is difficult to obtain. The capacitively coupled circuits, even with small capacitance coupling, tend to modify the frequency response of the last I.F. transformer before the detector and to react one on the

other. The slope of the discriminator characteristic at O is also reduced.

An alternative method of connection using circuits 1 and 2 without transformer coupling is shown in Fig. 13.8. Its disadvantage is that the anode-earth capacitance of V_1 has greater effect because R_{D1} and R_{D2} are much greater than R_{p1} and R_{p2}, but this stray

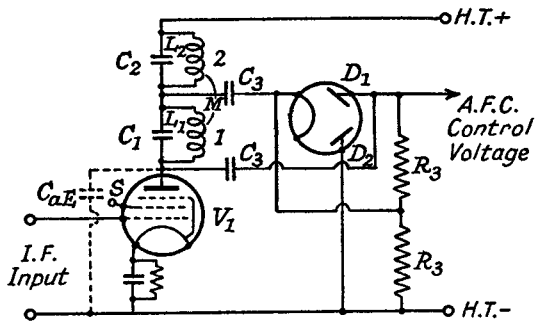

FIG. 13.8.—A Modified Form of the Amplitude Discriminator.

coupling may be cancelled by positive mutual inductance between the circuits satisfying

$$\frac{M}{\sqrt{L_1L_2}} = \frac{C_{aE}}{\sqrt{C_1C_2}}.$$

The voltage applied to the discriminator circuits must not be allowed to vary over wide limits because this affects A.F.C. performance, increase of applied voltage improving control but also increasing the " throw-out " and " pull-in " signal frequency separations from the correct signal setting. This means that A.G.C. must be combined with A.F.C. if the latter is to be satisfactory.

Increased control accuracy (greater slope to *BOD*) may be obtained by inserting between Nos. 1 and 2 and their respective diodes a circuit having a rejection frequency approximately equal to the correct I.F. carrier frequency f_m. The fall-away of the frequency response curves from each peak towards f_m is consequently made much steeper and the slope *BOD* increased. A suitable circuit [17] consists of two series inductance arms having positive mutual inductance between them, and a shunt capacitance arm connected to their junction point. The positive mutual inductance and shunt capacitance form a series rejection circuit at the frequency f_m.

A modification of the amplitude discriminator using only one tuned circuit is shown in Fig. 13.9*a*. Circuit L_1C_1 is tuned to a frequency about 2 kc/s above the correct I.F. value, so that for

frequencies below this value it presents an inductive reactance. Capacitance C_2 across the diode D_2 forms with the inductive reactance of L_1C_1 a series circuit tuned to a frequency about 2 kc/s below the correct I.F. value. The R.F. choke L_2 provides a D.C. return path for the conduction currents in diodes D_1 and D_2.

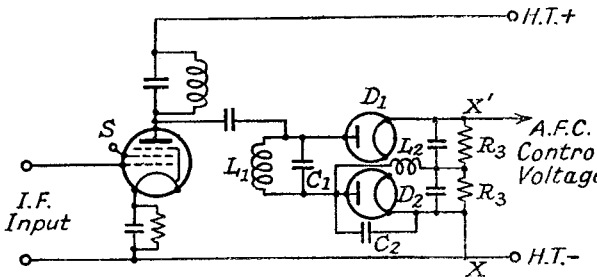

FIG. 13.9*a*.—An Amplitude Discriminator using a Single Tuned Circuit in Conjunction with a Capacitance.

The amplitude variation of the voltage applied to diode D_1 (curve 1 in Fig. 13.9*b*) is a maximum at (f_m+2) kc/s and a minimum at (f_m-2) kc/s when the series circuit of L_1C_1 and C_2 is resonant. The amplitude variation of the voltage applied to D_2 (curve 2 in Fig. 13.9*b*) is an image of that across D_1, being maximum at

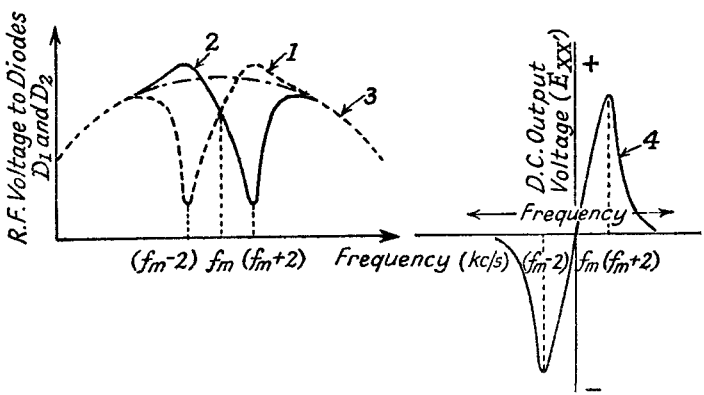

FIG. 13.9*b*.—Response Curves for the Single Tuned Circuit Amplitude Discriminator.

(f_m-2) kc/s and a minimum at (f_m+2) kc/s when the circuit L_1C_1 is resonant. The dashed curve 3 in Fig. 13.9*b*, symmetrical about f_m, is the frequency response of the source of I.F. The D.C. voltages across the load resistances R_3 are in series opposition so that the total D.C. output voltage across points XX' varies with frequency as shown by curve 4 in Fig. 13.9*b*. Curve 4 can be moved above

or below f_m kc/s by varying L_1 without changing the general shape of the curve, i.e., the frequencies of maximum positive and negative voltage maintain the same frequency spacing from the new value of mid-frequency, and the amplitudes are practically unchanged apart from the effect of curve 3. The frequency of the highest frequency peak is controlled by variation of C_1 (rising to a higher frequency when C_1 is decreased), and that of the lower by variation of C_2. The larger the ratio $\frac{C_1}{C_2}$ the smaller is the frequency spacing between the peaks. If $\frac{C_1}{C_2}$ and the Q of the circuit L_1C_1 are constant, a decrease of C_1 and C_2 and increase of L_1 increases the slope of the curve between the two peaks, i.e., increases A.F.C. sensitivity.

The amplitude discriminator, largely because of the necessity in its original form for two extra tuned circuits, has been almost entirely superseded by the phase discriminator. The term phase is applied because the principle of operation depends on the 90° phase shift that occurs at the mid-frequency (f_m) between the primary and secondary output voltages from a double-tuned transformer. The great advantage of the phase discriminator is its simplicity and economy of components. It is possible, at some sacrifice of quality, selectivity and overall amplification, to use the last I.F. transformer for A.F.C. as well as A.G.C. and normal A.F. detection.

The theory [9] of the phase discriminator can be developed from Sections 7.3 and 7.6, Part I, which give the secondary and primary output carrier peak voltages from a tuned transformer for 1 volt peak input (unmodulated) as

$\hat{E}_2 = g_m Z_T$, where Z_T has the value given in 7.2*a* (Section 7.3, Part I)

and $\hat{E}_1 = g_m Z_p$, where Z_p has the value given in 7.7*a* (Section 7.6, Part I)

$$\hat{E}_2 = g_m \frac{-jR_{D1}Q_2k\sqrt{\frac{L_2}{L_1}}}{(1+jQ_1F)(1+jQ_2F)+Q_1Q_2k^2} \quad . \quad . \quad . \quad . \quad 13.4$$

and $$\hat{E}_1 = g_m \frac{R_{D1}(1+jQ_2F)}{(1+jQ_1F)(1+jQ_2F)+Q_1Q_2k^2} \quad . \quad . \quad . \quad . \quad 13.5.$$

In the phase discriminator the secondary is centre tapped as shown in Fig. 13.10 and the diode detectors derive their R.F. applied voltages from the primary in series with one-half secondary. The R.F. choke L_3 and capacitance C_4 couple the primary to the secondary

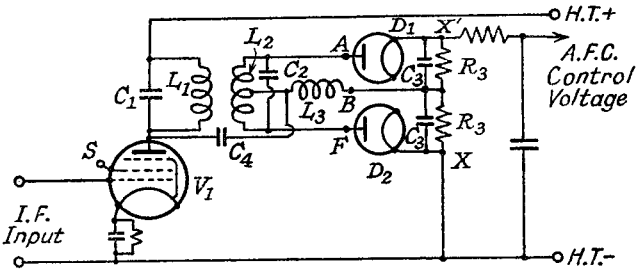

FIG. 13.10.—The Phase Discriminator.

centre tap and the centre point of the two diode load resistances R_3. Hence the carrier peak voltages applied to the diodes are

$$\hat{E}_{AB} = g_m \hat{E}_c R_{D1} \frac{1 + jQ_2\left(F + \frac{k}{2}\sqrt{\frac{L_2}{L_1}}\right)}{(1 + jQ_1F)(1 + jQ_2F) + Q_1Q_2k^2} \quad . \quad 13.6a$$

and

$$\hat{E}_{FB} = g_m \hat{E}_c R_{D1} \frac{1 + jQ_2\left(F - \frac{k}{2}\sqrt{\frac{L_2}{L_1}}\right)}{(1 + jQ_1F)(1 + jQ_2F) + Q_1Q_2k^2} \quad . \quad 13.6b$$

where $\hat{E}_c$ = peak value (unmodulated) of the carrier voltage applied to the grid of V_1.

Converting 13.6*a* and 13.6*b* to voltage amplitudes $|\hat{E}_{AB}|$ and $|\hat{E}_{FB}|$ and plotting them against frequency produces curves somewhat similar to those for the amplitude discriminator shown in Fig. 13.6*a*, provided the coupling between primary and secondary is loose. The peaks are displaced from the correct I.F. carrier value f_m by almost equal off-tune frequencies. If the coupling coefficient is increased to the critical value $\left[k = \sqrt{\frac{1}{2}\left[\frac{1}{Q_1^2} + \frac{1}{Q_2^2}\right]}\right]$ (Section 7.3, Part I) and greater, the off-tune frequency peaks are displaced further from f_m and a second, much smaller peak appears on the opposite side of f_m to the main peak.

By subtracting $|\hat{E}_{FB}|$ from $|\hat{E}_{AB}|$ and multiplying by the voltage detection efficiency, η_d, of the diode detectors, the expression for the discriminator voltage-frequency characteristic is found to be

$$\eta_d[|\hat{E}_{AB}| - |\hat{E}_{FB}|] = g_m R_{D1} \hat{E}_c \eta_d \frac{\left[1 + Q_2^2\left(F + \frac{k}{2}\sqrt{\frac{L_2}{L_1}}\right)^2\right]^{\frac{1}{2}} - \left[1 + Q_2^2\left(F - \frac{k}{2}\sqrt{\frac{L_2}{L_1}}\right)^2\right]^{\frac{1}{2}}}{[[1 + Q_1Q_2(k^2 - F^2)]^2 + (Q_1 + Q_2)^2F^2]^{\frac{1}{2}}} \quad 13.7.$$

The slope of the discriminator characteristic at the mid-frequency

f_m is obtained by differentiating 13.7 with respect to Δf and equating F in the resulting expression to 0. Hence

$$S_{(F=0)} = \frac{d(\eta_d[|\hat{E}_{AB}| - |\hat{E}_{FB}|])}{dF} \cdot \frac{dF}{d(\Delta f)}$$

$$= \frac{2g_m R_{D1}\eta_d Q_2{}^2\sqrt{\frac{L_2}{L}}}{f_m}\left[\frac{k}{(1+Q_1Q_2k^2)\left[1+\frac{Q_2{}^2k^2L_2}{4L_1}\right]^{\frac{1}{2}}}\right]. \quad 13.8$$

S in 13.8 is in D.C. volts per kc/s off-tune per 1 volt grid peak input. The slope at $F = 0$ can be varied by changing k and a maximum is found by differentiating the part of 13.8 inside the bracket with respect to k and equating the result to zero. Replacing Q_1Q_2 by a and $\frac{Q_2{}^2L_2}{4L_1}$ by b

$$\frac{k}{(1+Q_1Q_2k^2)\left[\frac{1+Q_2{}^2k^2L_2}{4L_1}\right]^{\frac{1}{2}}} = \frac{k}{(1+ak^2)(1+bk^2)^{\frac{1}{2}}}.$$

Differentiating with respect to k and equating to zero gives

$$1 - ak^2 - 2ab\,k^4 = 0$$

$$k^2 = +\frac{\sqrt{a^2+8ab} - a}{4ab}$$

$$\sqrt{Q_1Q_2}\,k = \sqrt{\frac{+\sqrt{Q_1{}^2Q_2{}^2+2Q_1Q_2{}^3\frac{L_2}{L_1}} - Q_1Q_2}{Q_2{}^2\frac{L}{L_1}}}. \quad 13.9.$$

The optimum values of $\sqrt{Q_1Q_2}\,k$ for different values of $\frac{L_2}{L_1}$ and $\frac{Q_2}{Q_1}$ are tabulated below.

TABLE 13.1

$\frac{L_2}{L_1}$	1	2	4	6	8	10	
$Q_1 = 0{\cdot}5Q_2$	0·786	0·707	0·625	0·578	0·544	0·52	$\sqrt{Q_1Q_2}\,k.$
$Q_1 = Q_2$	0·856	0·785	0·707	0·657	0·625	0·598	
$Q_1 = 2Q_2$	0·909	0·855	0·786	0·740	0·707	0·68	

The optimum value of $\sqrt{Q_1Q_2}\,k$ is always less than 1 and, for a given value of $\frac{L_2}{L_1}$, decreases as $\frac{Q_2}{Q_1}$ decreases.

For discriminator design purposes it is necessary to determine the off-tune frequencies, which give maximum positive or negative

D.C. output voltage, corresponding to points B and D in Fig. 13.6*a*. These frequencies are found by differentiating expression 13.7 with respect to Δf and equating to zero. A complicated equation in Δf raised to the 5th power results, and a simpler solution of the problem is possible if it is assumed that the variation * of the primary voltage $\hat{E}_1$ over the frequency range between the two peaks B and D is negligible. The voltage vector diagram for the discriminator then becomes that of Fig. 13.11. The primary voltage is repre-

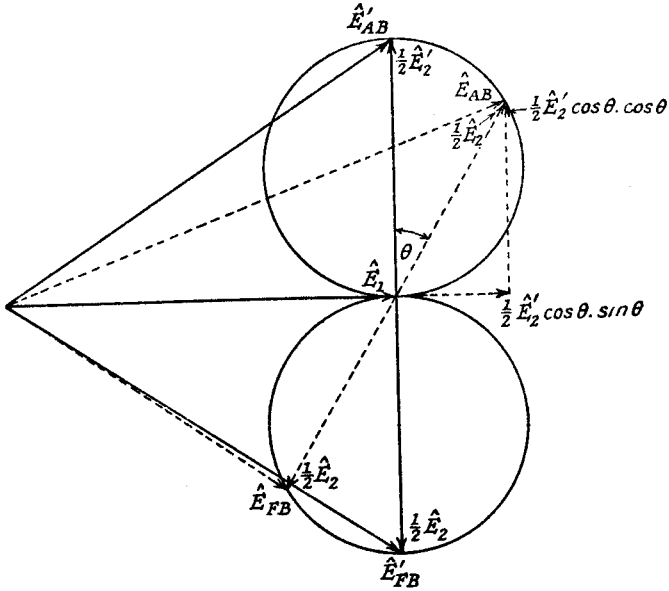

FIG. 13.11.—Vector Relationships of the Primary and Half Secondary Voltages in the Phase Discriminator.

sented by the horizontal vector $\hat{E}_1$ of constant length, and the half-secondary voltages by vectors $\pm\frac{1}{2}\hat{E}_2$. The locii of the two half-secondary voltages are the two circles shown (the impedance of a parallel tuned circuit has a circle locus). The diameter of either circle is equal to the half-secondary voltage, $\frac{1}{2}\hat{E}_2'$, at $f_m(F = 0)$, which in turn depends on the coupling coefficient k and Q_2. From expressions 13.4 and 13.5

$$\hat{E}_2'(F = 0) = -jQ_2k\sqrt{\frac{L_2}{L_1}}.\hat{E}_1(F = 0) = -j\alpha\hat{E}_1(F = 0)$$

where $$\alpha = Q_2k\sqrt{\frac{L_2}{L_1}}.$$

* The effect of the variation of E_1 upon the discriminator characteristic is considered in Section 15.9.3.

Referring to Fig. 13.11

$$\hat{E}_{AB}' = \hat{E}_1 + \frac{\hat{E}_2'}{2}\sin\theta\cos\theta + j\frac{\hat{E}_2'}{2}\cos\theta\cos\theta$$

where θ is the angle between the half-secondary voltage vector when $F \neq 0$ and the vector $\frac{\hat{E}_2'}{2}$ when $F = 0$, and

$$\tan\theta = \frac{\text{secondary series reactance component}}{\text{secondary series resistance component}}$$

$$= \frac{\omega L_2 - \dfrac{1}{\omega C_2}}{R_2} = Q_2 F$$

$$\therefore\ |\hat{E}_{AB}| = \hat{E}_1\sqrt{\left(1+\frac{\alpha\sin\theta\cos\theta}{2}\right)^2 + \left(\frac{\alpha\cos^2\theta}{2}\right)^2}$$

$$= \hat{E}_1\sqrt{\left(1+\frac{\alpha\sin 2\theta}{4}\right)^2 + \alpha^2\left(\frac{1+\cos 2\theta}{4}\right)^2}$$

$$= \hat{E}_1\sqrt{1+\frac{\alpha^2}{8}+\frac{\alpha\sin 2\theta}{2}+\frac{\alpha^2\cos 2\theta}{8}} \quad . \qquad .13.10a.$$

Similarly $|\hat{E}_{FB}| = \hat{E}_1\sqrt{1+\frac{\alpha^2}{8}-\frac{\alpha\sin 2\theta}{2}+\frac{\alpha^2\cos 2\theta}{8}}$ . .13.10b.

The maximum value of ($|\hat{E}_{AB}| - |\hat{E}_{FB}|$) is obtained by differentiating the difference between 13.10*a* and 13.10*b* with respect to θ and equating to zero. Hence

$$\left[1+\frac{\alpha^2}{8}+\frac{\alpha\sin 2\theta}{2}+\frac{\alpha^2\cos 2\theta}{8}\right]^{-\frac{1}{2}}\left(\alpha\cos 2\theta - \frac{\alpha^2\sin 2\theta}{4}\right)$$

$$-\left[1+\frac{\alpha^2}{8}-\frac{\alpha\sin 2\theta}{2}+\frac{\alpha^2\cos 2\theta}{8}\right]^{-\frac{1}{2}}\left(-\alpha\cos 2\theta-\frac{\alpha^2\sin 2\theta}{4}\right)=0.$$

This finally reduces to

$$\cos^2 2\theta\left(1+\frac{\alpha^2}{16}\right)+\cos 2\theta\left(1+\frac{\alpha^2}{8}\right)+\frac{\alpha^2}{16} = 0$$

or

$$\cos 2\theta = \frac{-\alpha^2}{16+\alpha^2} \quad \text{or} \quad -1.$$

The first root is the one required as it is a function of the coupling coefficient.

When the coupling coefficient is very small, α is very small, $\cos 2\theta$ is zero, and θ is 45°, but as α is increased θ is increased above 45°. Thus the minimum value of $\tan\theta$ is unity and this gives the

minimum value of off-tune frequency, at which the peaks B or D of the discriminator characteristic occur, as

$$\Delta f_{(min.)} = \frac{f_m}{2Q_2}.$$

Increase of coupling increases α, $\tan\theta$ and $\Delta f_{B \text{ or } D}$ to

$$\Delta f_{B \text{ or } D} = \frac{f_m}{2Q_2} \tan\theta = \Delta f_{(min.)} \tan\theta.$$

The factor, $\tan\theta$, by which $\Delta f_{(min.)}$ must be multiplied in order to find the actual value of $\Delta f_{B \text{ or } D}$, is tabulated below for different values of α, i.e., $Q_2 k\sqrt{\frac{L_2}{L_1}}$.

TABLE 13.2

$Q_2k\sqrt{\frac{L_2}{L_1}}$	0·01	0·1	0·25	0·5	0·75	1	1·5	2	3	4
$\tan\theta$	1	1	1·004	1·015	1·034	1·0605	1·1322	1·224	1·457	1·73

In determining the effective Q of the primary and secondary circuits of the transformer, consideration must be given to the influence of conduction current damping from the diode detectors, D_1 and D_2 in Fig. 13.10. The equivalent damping resistance from each diode may be taken as one-half the D.C. load resistance, $\frac{1}{2}R_3$ (Section 8.2.5, Part I); the resistance reflected across each half-secondary by each diode is therefore $\frac{1}{2}R_3$, and this is stepped up due to the centre tap to $2R_3$ across the complete secondary, thus giving $2R_3$ in parallel with $2R_3$, or a total of R_3 for both diodes. The equivalent Q of the secondary circuit is therefore

$$Q_2 = \frac{\omega L_2}{R_2 + \frac{(\omega L_2)^2}{R_3}} \quad . \quad . \quad . \quad . \quad 13.11$$

where R_2 = series resistance due to the secondary coil and capacitor. The conduction current of both diodes passes through the primary, hence the effective damping resistance is due to $\frac{1}{2}R_3$ in parallel with $\frac{1}{2}R_3$, i.e., $\frac{1}{4}R_3$, and

$$Q_1 = \frac{\omega L_1}{R_1 + \frac{4(\omega L_1)^2}{R_3} + \frac{(\omega L_1)^2}{R_a}} \quad . \quad . \quad . \quad 13.12$$

where R_1 = series resistance due to the primary coil and capacitor
R_a = slope resistance of the valve amplifier before the primary.

It is clear from expressions 13.11 and 13.12 that the diodes contribute very heavy damping to primary and secondary, particularly to the former. To obtain maximum slope of discriminator characteristic (expression 13.8 shows that R_{D1} and Q_2 need to be large) and the required peak at 2 kc/s off-tune frequency, the detector load resistances must be made as high as possible. A maximum practical value for R_3 is usually about 0·5 MΩ.

To illustrate the design features of the phase discriminator, let us take the following example :

$f_m = 465$ kc/s, $R_3 = 0{\cdot}5$ MΩ, $L_1 = 300$ μH, $Q_1' = Q_2' = 100$

where Q_1' and Q_2' are the normal undamped Q values for the primary and secondary circuits. For the amplifier valve preceding the discriminator primary $R_a = 1$ MΩ and $g_m = 2{\cdot}5$ mA/volt. The damping resistances in parallel with the discriminator primary are 1 MΩ from the amplifier valve and 0·125 MΩ ($\frac{1}{4}R_3$) from the discriminator detectors.

Thus
$$Q_1 = \frac{\omega L_1}{\dfrac{\omega L_1}{Q_1'} + \dfrac{(\omega L_1)^2}{R_a} + \dfrac{4(\omega L_1)^2}{R_3}}$$

$$\omega L_1 = \frac{6{\cdot}28 \times 465 \times 10^3 \times 300}{10^6} = 875 \text{ ohms.}$$

Therefore
$$Q_1 = \frac{875}{8{\cdot}75 + \dfrac{875^2}{10^6} + \dfrac{875^2}{0{\cdot}125 \times 10^6}} = \frac{875}{15{\cdot}638}$$

$$= 56.$$

We have seen from the previous analysis that Q_2 determines the minimum value of the off-tune frequencies at which the peaks B and D (Fig. 13.6*a*) of the discriminator curve occur, and, if no conduction current damping of the secondary circuit is assumed, the off-tune frequency cannot be less than $\Delta f_{(min.)} = \dfrac{f_m}{2Q_2'} = \pm 2{\cdot}325$ kc/s. Since $\Delta f_{(min.)}$ should not be large (the " throw-out " and " pull-in " frequencies are both increased with increase of $\Delta f_{(min.)}$), it follows that Q_2 should be as nearly equal to Q_2' as possible, i.e., L_2 must not be high in value. On the other hand, L_2 must not have too low a value, because the factor $\dfrac{L_2}{L_1}$ then reduces the slope of the discriminator characteristic (expression 13.8).

Let us take $L_2 = L_1$.

The diode conduction current damping across the secondary is 0·5 MΩ (R_3), so that the final Q of the secondary circuit is

$$Q_2 = \frac{\omega L_2}{\frac{\omega L_2}{Q_2'} + \frac{(\omega L_2)^2}{R_3}} = \frac{875}{8{\cdot}75 + 1{\cdot}535}$$
$$= 85.$$

Substituting 0·658 Q_2 for Q_1, and 1 for $\frac{L_2}{L_1}$ in expression 13.9 gives $\sqrt{Q_1 Q_2}\, k = 0{\cdot}813$ for maximum slope at f_m, i.e., $k = 0{\cdot}0118$. The mutual inductance coupling between primary and secondary is $M = k\sqrt{L_1 L_2} = 0{\cdot}0118 \times 300 = 3{\cdot}54\ \mu$H. The off-tune frequency corresponding to B and D in Fig. 13.6*a* is from Table 13.2

$$\left(Q_2 k \sqrt{\frac{L_2}{L_1}} \text{ very nearly equals } 1\right) 1{\cdot}0605 \times \Delta f_{(min.)}$$

or
$$\Delta f_{(B \text{ or } D)} = \pm 2{\cdot}91 \text{ kc/s}.$$

The slope of the discriminator characteristic at f_m is from expression 13.8.

$$S_{(F=O)} = \frac{2 \times 2{\cdot}5 \times 10^{-3} \times R_{D1} \times 0{\cdot}8 \times (85)^2 \times 1}{465} \cdot \left[\frac{0{\cdot}0118}{[1 + (0{\cdot}813)^2]\left[1 + \frac{1}{4}\right]^{\frac{1}{2}}}\right]$$

where $R_{D1} = \omega_m L_1 Q_1 = 875 \times 56 = 49{,}000\ \Omega$

and $\eta_d = 0{\cdot}8$.

Therefore $S_{F=O} = 19{\cdot}35$ volts per kc/s off-tune per 1 volt peak input carrier. Since the slope of the discriminator characteristic is dependent on the input carrier voltage at its amplifier valve, it is important, if A.F.C. is to hold its performance over wide variations of aerial input carrier voltage, that the receiver should have A.G.C. and that the discriminator voltage should be taken from the source supplying the A.G.C. detector.

The phase discriminator can itself be used as the A.F. detector at some sacrifice of quality by taking the A.F. output from one diode load resistance, R_3, and the A.G.C. diode may be supplied from the primary. Such a circuit is shown in Fig. 13.12. The R.F. choke L_3 in Fig. 13.10 has been omitted, the centre tap on the secondary being connected to the centre point of the D.C. load resistances R_3, and the capacitances C_3 being replaced by a single

capacitance C_3 across both load resistances. There are disadvantages to this method of saving components; by using one of the discriminator diodes as A.F. detector, there is practically no gain in selectivity from the secondary circuit because the voltage applied to the detector is the sum of primary and secondary voltages. The overall amplification is, however, greater than if the A.F. detector were connected across the secondary only (the normal procedure). A further objection is that the frequency response for the applied voltage to diode D_2, providing the AF frequency output, has a maximum about 3 kc/s off-tune from f_m, and A.F. distortion tends to occur due to asymmetric sideband amplitudes. A better method giving much improved selectivity is to use a separate pick-up coil (coupled to the discriminator transformer) and tuned circuit for the

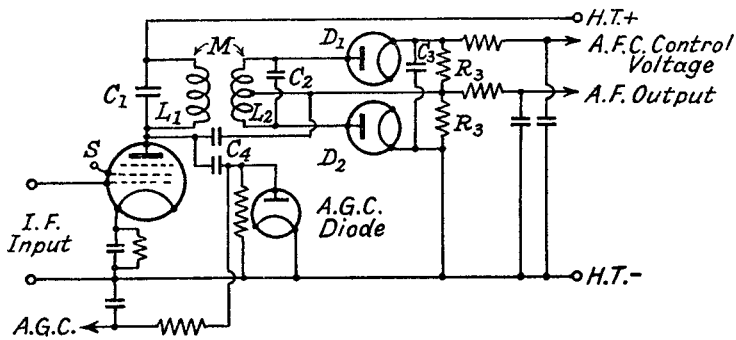

FIG. 13.12.—A Combined Phase Discriminator and A.F. Detector Circuit.

A.F. detector. The pick-up coil must be capacitively balanced to the discriminator secondary in order to prevent an asymmetric discriminator characteristic. This is achieved by disposing the pick-up coil symmetrically with respect to each half-secondary and by separating its output leads from the secondary leads. The third tuned circuit has an absorption effect, which decreases the slope of the discriminator characteristic and increases the frequency separation of the peaks B and D (Fig. 13.6*a*). Reduction of pick-up coil coupling reduces the effect, but at the same time decreases the A.F. output from the detector. The omission of the R.F. choke L_3 and the substitution of R_3 as the coupling impedance increases the damping on the primary, an additional damping resistance of $\frac{1}{2}R_3$ being applied.

The capacitances to earth of each half-secondary should be equal, otherwise an asymmetric discriminator characteristic results;

a small trimmer capacitance may be included from the anode to cathode of one of the diodes in order to ensure this.

In adjusting the phase discriminator to give the required characteristic, the following points should be borne in mind:

(1) The mutual inductance coupling, when it is small, affects chiefly the amplitude and not the frequency separation of the peaks B and D. As it is increased, a point is reached after which the amplitudes of the peaks increase at a slower rate, but their frequency separation begins to be increased. Table 13.2 shows that variation of coupling coefficient has little effect on the off-tune frequency separation until $Q_2 k \sqrt{\frac{L_2}{L_1}}$ exceeds 1.

(2) The primary tuning controls the symmetry of the discriminator characteristic about f_m; a decrease in primary resonant frequency increases the off-tune frequency of the lower frequency peak B (moving it further from f_m) and increases its amplitude. Conversely, increase of primary resonant frequency moves the upper frequency peak D further from f_m and increases its amplitude. The slope of BOD tends to become S-shaped.

(3) The secondary tuning has greatest effect on the central frequency (O in Fig. 13.6a), where the discriminator D.C. voltage passes through zero. If the secondary resonant frequency is decreased, the central frequency is reduced below f_m.

The procedure for obtaining the required discriminator characteristic is to disconnect C_4 from the secondary centre tap and, with loose coupling between the primary and secondary, to tune both circuits for maximum voltage across one of the diode load resistances R_3 when the frequency equals f_m. C_4 is next joined to the centre tap of the secondary, and the primary retuned to give approximately equal positive and negative maximum voltages from the cathode of diode D_1 in Fig. 13.10 to earth, i.e., across points XX', when the input frequency is varied over the range $f_m + 5$ kc/s to $f_m - 5$ kc/s. The stray capacitance to earth from the secondary centre tap is often appreciable and retuning of the primary is essential. The secondary circuit is now trimmed to bring zero D.C. volts across the points XX' in Fig. 13.10 at $f = f_m$, and afterwards the primary tuning is again checked for equal positive and negative maxima. Finally, the mutual inductance coupling is increased until the off-tune frequencies at which the positive and negative maxima occur begin to move outwards from f_m. Finer adjustment necessitates taking the discriminator D.C. output voltage-frequency curve and is seldom necessary.

The discriminator D.C. output voltage is connected to the control device by a R.F. filter, consisting of a resistance and capacitance having a time-constant of about 0·1 seconds.

13.4.3. The Variable Reactance Control Unit. The discriminator D.C. output voltage, which is proportional to the I.F. carrier frequency error, must be translated into a correcting reactance across the oscillator-tuned circuit. This reactance, which can be capacitive or inductive, may actually be a variable capacitor or inductor, or it may be simulated by a valve.

One of the simplest forms of control is the motor-operated variable capacitor. The motor, similar to that already described in Section 13.2.3, is reversible; the A.C. currents in the forward and reverse coils are obtained from valves, the amplifications of which are controlled in opposite directions from the discriminator D.C. output voltage. When there is no error of the I.F. carrier, the currents exercise opposing effects on the rotor disc and the motor is stationary, but if the I.F. carrier is off-tune, the current in one coil increases and that in the other decreases, causing the motor to rotate and, through gears, drive the correcting capacitor. The motor continues to rotate until the currents in the coil are again equal. This method is unsuitable for broadcast reception on account of cost, but it has been used for large commercial receivers operating mostly on telegraph signals. Its outstanding advantages are: (1) the control is very sensitive and high tuning accuracy is easily secured, (2) the inertia in the control unit renders it less liable to lose control when the carrier signal is discontinuous as with keyed C.W. transmission, and (3) the device has a floating datum line, i.e., disappearance of the discriminator D.C. voltage output causes practically no change in oscillator frequency. Many variable reactance devices fail under similar conditions and sometimes transfer reception from the desired to an undesired transmission.

Another method of using a variable capacitor to control the oscillator frequency is by means of a milliammeter with a vane, interleaved between two fixed plates, in place of the pointer. The milliammeter coil is actuated by the anode current of a valve, biased from the discriminator voltage. Such a device is too fragile for most purposes and it suffers from the disadvantage that if the discriminator voltage fails the capacitor returns to its "zero" setting and changes the oscillator frequency. The latter may be within range of an adjacent transmission, which then tends to actuate the control and prevent tuning back to the desired transmission when it reappears.

A direct control device, which has the merit of extreme simplicity and reasonable sensitivity, is a capacitor, the value of which is varied by changing a D.C. polarizing voltage applied between the plates. One electrode of this polarized capacitor* is a flat aluminium plate (about $\frac{1}{32}$ in. thick) having a thin polished anodized surface. The other is a thin leaf of polished duralumin foil (0·001 in. thick) lying flat on the first electrode. Application of a D.C. polarizing voltage (its direction is unimportant, either surface can be positive) brings the foil into closer contact with the anodized surface and capacitance is increased. The polarizing voltage can be applied

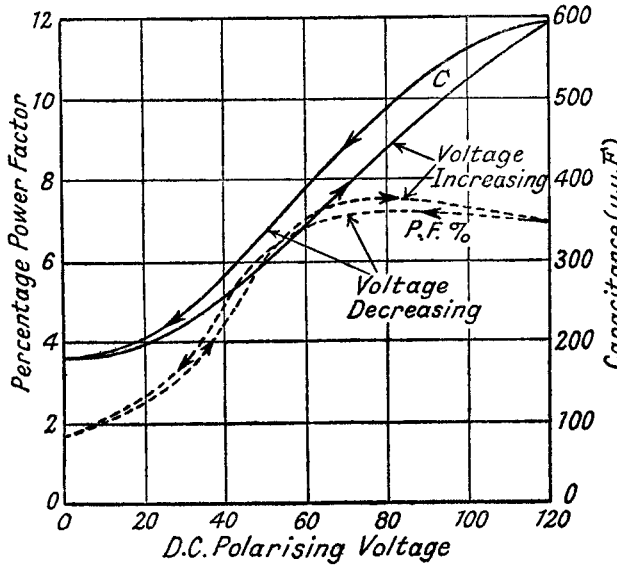

FIG. 13.13.—Curves of Capacitance—D.C. Voltage for the Polarized Capacitor with Increasing and Decreasing D.C. Voltage.

through a high resistance, 10 MΩ, so that circuit loss is negligible. A 3 to 1 change in capacitance is easily achieved by a polarizing voltage change of ±50 volts about a mean of 70 volts. Typical curves of capacitance and percentage power factor $\left[\frac{R}{\sqrt{R^2+\left(\frac{1}{\omega C}\right)^2}}\right]$ variation against polarizing voltage are shown in Fig. 13.13. The dimensions of the surfaces in contact for the capacitor whose

* British Patent Nos. 522,476 and 522,564. Marconi's Wireless Telegraph Company. N. M. Rust, J. D. Brailsford, A. L. Oliver and J. F. Ramsay.

performance is illustrated in the figure are approximately $\frac{3}{4}$ in. by 1 in. A hysteresis effect is obtained, the capacitance for increasing voltage being less than that for decreasing voltage, and the change of capacitance is only established some time after the change of polarizing voltage. Minimum capacitance is rather high, but this can be counteracted by inserting the device in series with a smaller capacitance across the oscillator-tuned circuit; this does, however, reduce the control exercised on the oscillator frequency. These disadvantages are not of very serious consequence in a simple A.F.C. circuit correcting oscillator frequency drift on push-button selected transmissions.

Another type of direct control is illustrated in Fig. 13.14. An iron-cored coil L_1, of mu-metal laminations, is inserted in series with

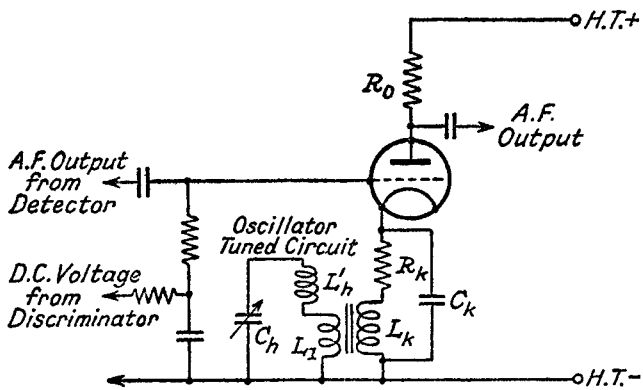

FIG. 13.14.—A Variable Reactance by Changing the D.C. Polarization of an Iron-cored Coil.

the oscillator main tuning coil L_h', and the permeability of its iron core is controlled from the discriminator D.C. output voltage. This is achieved by varying the D.C. current through a secondary winding, L_k, connected in the cathode-circuit of a triode valve biased from the discriminator D.C. voltage. The variation in cathode current varies the D.C. polarizing field and changes the inductance of L_1, 1 mA change of cathode current producing approximately 8% variation of L_1. The resistance R_k applies the normal bias voltage to the valve in the absence of the discriminator bias, and allows a positive increase in the latter without causing grid current. To save components the triode valve is also used as the A.F. amplifier following the detector, C_k being a large electrolytic capacitor (about 25 μF).

The most common method of obtaining the correcting reactance

is by means of a valve. Many circuits have been devised, but the majority depend on the application of R.F. voltages between the anode and cathode, and between grid and cathode, having a phase difference of 90°. If the valve has a high slope resistance, R_a, e.g., it is a tetrode, pentode, hexode, etc., the R.F. anode current component is in phase with the applied grid voltage. Hence there is a 90° phase difference between the R.F. anode current component and the applied R.F. anode voltage, so that the valve functions as a reactance. The latter is inductive if the R.F. grid voltage lags behind the anode voltage, and is capacitive if the grid voltage leads upon the anode voltage. The magnitude of the reactance, which is inversely proportional to the R.F. anode current, decreases as the amplification of the valve is increased by decreasing the D.C. bias on the control grid or another electrode. Thus by connecting the anode and cathode of the valve across the oscillator-tuned circuit, and biasing it from the discriminator D.C. output voltage, the valve functions as a variable correcting reactance. Care must be taken to see that the bias is connected to give a change of reactance in the right direction. Let us suppose that the valve anode-cathode circuit appears as a capacitive reactance and the I.F. carrier frequency is higher than its correct value. Since the oscillator frequency is almost always greater than that of the signal, it follows that the former must be greater than its correct value, and it must be reduced by decreasing the valve capacitive reactance, i.e., by increasing the capacitance of the anode-cathode space. This is achieved by decreasing the negative bias on the valve; in other words, the discriminator D.C. output voltage must be connected to give a positive voltage when the I.F. carrier exceeds its correct frequency and a negative voltage when it falls below the correct frequency. This condition is fulfilled by the circuit shown in Fig. 13.7. If the anode-cathode circuit of the valve is equivalent to an inductive reactance, the discriminator voltage connections must be reversed in order to give a negative voltage when the I.F. carrier exceeds its correct frequency.

The properties required of a variable reactance valve are that it should affect oscillator frequency and not amplitude, that it should produce large changes of reactance over a restricted range of bias voltages, and, outside this desired range of bias voltages, the reactance should not vary appreciably. The advantage of this limited reactance characteristic is discussed in Section 13.4.4.

The basic reactance valve circuit is shown in Fig. 13.15. The valve is a hexode, the control grid being connected to the centre

point of the phase-shifting network Z_1 and Z_2, and the oscillator grid to the discriminator D.C. output voltage. Considerable advantages are gained by using a hexode rather than a tetrode with the discriminator D.C. voltage applied to the control grid. The bias on the control grid can be set to its optimum value (often about — 5 volts), and variation of discriminator D.C. output voltage has little effect on the self-bias voltage derived from the cathode current of the valve. With the tetrode valve, change of control grid bias affects the self-bias voltage so as to reduce the reactance change for a given discriminator voltage change, and the initial bias must be much greater than optimum in order to allow the discriminator D.C. voltage to become positive without causing the control grid to take current. A pentode valve can be made to function in a manner similar to the hexode by applying the dis-

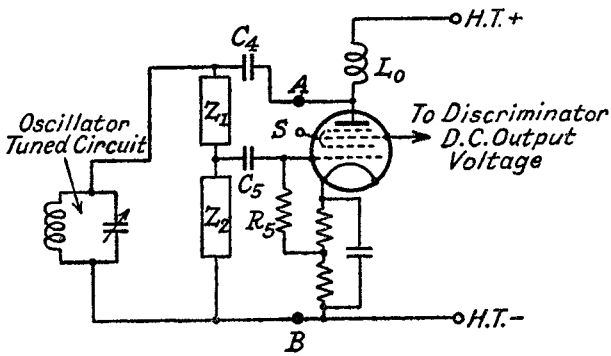

FIG. 13.15.—The Variable Reactance Valve Circuit.

criminator voltage to the suppressor grid, but a fine mesh suppressor grid is required if the control is to be sufficiently sensitive. The slope resistance of the valve is reduced (Section 2.5) by applying negative bias to the suppressor grid and its performance is not so satisfactory as that of a hexode. Impedances Z_1 and Z_2 act not only as a phase-shifting network but also as a potential divider for stepping-down the voltage applied to the grid from the oscillator-tuned circuit. A suitable peak value for the R.F. voltage at the grid of the reactance valve is about 4 volts. Capacitance-resistance coupling (C_5 and R_5) is shown from Z_2 to the reactance valve grid in Fig. 13.15, but in certain cases this may be unnecessary. For example, C_5 and R_5 can be omitted if Z_1 is a capacitance and Z_2 a resistance. H.T. voltage for the reactance valve anode is obtained via the R.F. choke L_0 and the R.F. voltage from the oscillator-tuned circuit is applied through the coupling capacitance C_4. If

the oscillator-tuned circuit is connected to a H.T. voltage source (e.g., a tuned anode oscillator), the anode of the reactance valve can be joined direct to the high R.F. potential end of the tuned circuit; C_4 and L_0 are then no longer required. If Z_1 is a resistance R, and Z_2 a capacitance C, and the valve has a high slope resistance, the admittance from anode to cathode (points AB) is given by

$$Y_{AB} = \frac{I_a}{E_a} = \frac{g_m E_g}{E_a} \quad . \quad . \quad . \quad . \quad 13.13a$$

where g_m = mutual conductance of the variable reactance valve.

But
$$E_g = \frac{E_a Z_2}{Z_1 + Z_2}$$

$$\therefore \; Y_{AB} = \frac{g_m Z_2}{Z_1 + Z_2} = g_m \frac{1}{1 + jR\omega C}$$

$$= \frac{g_m}{1 + (R\omega C)^2} - j\frac{g_m R\omega C}{1 + (R\omega C)^2} \quad . \quad . \quad 13.13b$$

which is equivalent to a resistance

$$R_{AB} = \frac{1 + (R\omega C)^2}{g_m}$$

in parallel with an inductance

$$L_{AB} = \frac{1 + (R\omega C)^2}{g_m R\omega^2 C}.$$

Three other combinations of R and L or C are possible, and the resultant parallel resistance and reactance components of Y_{AB} are tabulated below. Approximate expressions for R_{AB} and X_{AB}, obtained by assuming that Z_2 is small in comparison with Z_1 (this is often true in practice because the R.F. voltage required at the grid of the reactance valve is generally much less than that across the oscillator-tuned circuit), are also given.

TABLE 13.3

Z_1	R	C	R	L
Z_2	C	R	L	R
R_{AB}	$\frac{1 + (R\omega C)^2}{g_m}$	$\frac{1 + (R\omega C)^2}{g_m (R\omega C)^2}$	$\frac{R^2 + \omega^2 L^2}{g_m \omega^2 L^2}$	$\frac{R^2 + \omega^2 L^2}{g_m R^2}$
X_{AB}	$L_{AB} = \frac{1 + (R\omega C)^2}{g_m R\omega^2 C}$	$C_{AB} = \frac{g_m RC}{1 + (R\omega C)^2}$	$C_{AB} = \frac{g_m RL}{R^2 + \omega^2 L^2}$	$L_{AB} = \frac{R^2 + \omega^2 L^2}{g_m R\omega^2 L}$
	Approximate expressions $Z_2 \ll Z_1$			
R_{AB}	$\frac{(R\omega C)^2}{g_m}$	$\frac{1}{g_m (R\omega C)^2}$	$\frac{R^2}{g_m \omega^2 L^2}$	$\frac{\omega^2 L^2}{g_m R^2}$
X_{AB}	$L_{AB} = \frac{RC}{g_m}$	$C_{AB} = g_m RC$	$C_{AB} = \frac{g_m L}{R}$	$L_{AB} = \frac{L}{g_m R}$

From the above table it will be noted that the values of the resistance and reactance components of Y_{AB} are independent of R and L, or R and C, as long as $\frac{L}{R}$ and RC remain constant. It is generally undesirable that the resistance and reactance of the phase-shifting network should be small because the latter is in parallel with the oscillator-tuned circuit. A low reactance makes ganging of the oscillator and signal circuits difficult, whilst a low resistance damps the tuned circuit and reduces oscillator amplitude. Hence C should be small and R large, or L and R both large. The components of Y_{AB}, when Z_1 and Z_2 are equal to R and C respectively, are similar in form to those when Z_1 and Z_2 are equal to L and R respectively. In like manner the components for a CR phase-shifting network are similar to those for a RL network. As a rule a resistance-capacitance phase shifting circuit is to be preferred to a resistance-inductance combination because a capacitance has negligible resistance component. The internal resistance component of the inductance prevents an exact 90° phase shift being realized, and stray capacitance across the inductance also introduces complications.

Some interesting conclusions may be drawn from the approximate expressions for R_{AB} and X_{AB} : the value of the resistance component is in every case inversely proportional to g_m so that an increase of discriminator D.C. output voltage in a positive direction tends to reduce oscillator amplitude. The change in amplitude can be made very small by a suitable choice of R and C, or R and L, and generally the effect may be ignored. In the RC and LR network, R_{AB} is directly proportional to the square of the frequency, and if A.F.C. is applied to a variable-tuned circuit, as distinct from a preset circuit, R_{AB} has greatest damping at the low-frequency end of the range. This is undesirable because the oscillator amplitude is usually a minimum at this end. With the CR and RL network the reverse is true, and the decrease in R_{AB} as frequency increases helps to stabilize oscillator amplitude (Section 6.4, Part I). Examination of the approximate equivalent inductance or capacitance due to the reactance valve shows that it is independent of frequency, and dependent only on g_m and the resistance and reactance components of the phase splitter. For preset oscillator tuning all of the reactance valve circuits are equally suitable, but for variable oscillator tuning the inductive variable reactance valve (the RC or LR network) is preferable, because it provides a more constant corrective effect over the frequency range than does the capacitive reactance valve.

This can be shown as follows: the oscillator frequency for the inductive reactance valve is given by

$$f_h = \frac{1}{2\pi\sqrt{\frac{L_h' L_{AB}}{L_h' + L_{AB}} . C_h}} \quad . \quad . \quad . \quad 13.14$$

where L_h' and C_h are the oscillator main tuning components when the variable reactance valve is in circuit. Change of bias on the reactance valve alters L_{AB} to KL_{AB}, and the oscillator frequency to

$$f_h + \Delta f = \frac{1}{2\pi\sqrt{\frac{L_h' K L_{AB}}{L_h' + K L_{AB}} C_h}} \quad . \quad . \quad 13.15a$$

where $K = \frac{g_{m0}}{g_m}$, and g_{m0} is the mutual conductance for zero discriminator D.C. voltage.

Combining 13.14 and 13.15*a*

$$\frac{f_h + \Delta f}{f_h} = 1 + \frac{\Delta f}{f_h} = \sqrt{\frac{L_h' L_{AB}}{L_h' + L_{AB}} . \frac{L_h' + K L_{AB}}{L_h' K L_{AB}}}$$

$$= \sqrt{1 + \frac{(1-K)}{K} . \frac{L_h'}{L_h' + L_{AB}}}$$

If L_h is the oscillator-tuning inductance in the absence of the reactance valve

$$L_h = \frac{L_h' L_{AB}}{L_h' + L_{AB}}$$

or

$$\frac{L_h}{L_{AB}} = \frac{L_h'}{L_h' + L_{AB}}.$$

Therefore

$$1 + \frac{\Delta f}{f_h} = \sqrt{1 + \frac{1-K}{K} . \frac{L_h}{L_{AB}}} . \quad . \quad 13.15b.$$

Now $\frac{1-K}{K} . \frac{L_h}{L_{AB}}$ is generally very much less than 1, so that expression 13.15*b* may be written

$$1 + \frac{\Delta f}{f_h} \simeq 1 + \frac{1-K}{2K} . \frac{L_h}{L_{AB}}$$

or

$$\Delta f \simeq f_h \frac{1-K}{2K} . \frac{L_h}{L_{AB}} \quad . \quad . \quad 13.16a$$

$$\propto f_h \quad . \quad . \quad . \quad . \quad 13.16b$$

when $\frac{1-K}{2K} \frac{L_h}{L_{AB}}$ is a constant. Hence the degree of frequency

correction, exercised by the reactance valve is directly proportional to the oscillator mean frequency, i.e., A.F.C. gives least error for a given off-tune signal frequency setting at the high-frequency end of a range.

With the capacitive reactance valve the oscillator frequency is

$$f_h = \frac{1}{2\pi\sqrt{L_h(C_h'+C_{AB})}} \quad . \quad . \quad . \quad 13.17$$

where C_h' is the oscillator-tuning capacitance when the reactance valve is in circuit, and C_h is the tuning capacitance in the absence of the reactance valve, i.e., it equals $C_h'+C_{AB}$.

$$f_h+\Delta f = \frac{1}{2\pi\sqrt{L_h(C_h'+KC_{AB})}} \quad . \quad . \quad . \quad 13.18$$

where $K = \frac{g_m}{g_{m0}}$.

Combining 13.17, and 13.18.

$$1+\frac{\Delta f}{f_h} = \sqrt{\frac{C_h'+C_{AB}}{C_h'+KC_{AB}}} = \frac{1}{\sqrt{1+\frac{(K-1)C_{AB}}{C_h'+C_{AB}}}}$$

or

$$\frac{\Delta f}{f_h} \simeq \frac{(1-K)C_{AB}}{2(C_h'+C_{AB})} \quad . \quad . \quad . \quad 13.19$$

because $(1-K)\frac{C_{AB}}{C_h'+C_{AB}}$ is generally $\ll 1$.

Expression 13.19 may be rewritten.

$$\Delta f = f_h\frac{(1-K)C_{AB}}{2C_h} \quad . \quad . \quad . \quad 13.20$$

but

$$f_h = \frac{1}{2\pi\sqrt{L_hC_h}}$$

or

$$\frac{1}{C_h} = (2\pi)^2 f_h^2 L_h.$$

Therefore

$$\Delta f \propto f_h^3.$$

This means that the degree of frequency correction is very much greater at the high-frequency end of a given range than at the low-frequency end. It is desirable to have smallest error at the low-frequency end because the signal circuits are more selective than at the high-frequency end, so that the capacitive reactance valve is much less satisfactory than the inductive reactance valve when oscillator tuning is by variable capacitance. When permeability

oscillator tuning is employed (the inductance is varied), the reverse is true, and the capacitive reactance valve is more suitable.

Let us take an example to illustrate these points, dealing first with a capacitive reactance valve applying A.F.C. to the medium wave band of a receiver. The signal frequency limits are 550 to 1,500 kc/s, the I.F. 465 kc/s and the oscillator limits 1,015 to 1,965 kc/s. The $g_m E_{g3}$ characteristic of a typical hexode valve is shown in Fig. 13.16, for a bias of — 5 volts on the control grid, G_1. A bias voltage of — 5 means that the R.F. grid voltage should not exceed about 4 volts peak value if grid current is to be avoided. Taking $Z_1 = R = 20{,}000$ ohms, a possible value for C is 50 $\mu\mu$F, giving $Z_2 = -j\,3{,}140$ ohms at 1,015 kc/s and $-j\,1{,}624$ ohms at

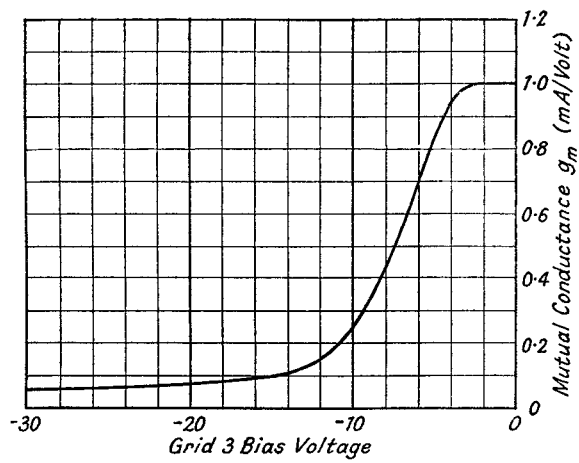

FIG. 13.16.—The Assumed $g_m E_g$ Characteristic of the Variable Reactance Valve.

1,965 kc/s. The step-down voltage ratios from anode to grid are 0·155 and 0·0812 respectively, so that the oscillator-tuned circuit peak voltages should not exceed 25·8 and 49·3 respectively if the oscillator voltage at the grid of the reactance valve is not to exceed 4 volts. The voltages are greater than are likely to be met in a tuned-grid oscillator, but are less than might be obtained with a tuned-anode oscillator unless it is heavily damped. In the latter instance C should be increased to 75 $\mu\mu$F, thus raising the anode maximum peak voltages to about 38·5 and 74 respectively.

The centre of the straight part of the $g_m E_{g3}$ characteristic of Fig. 13.16, is at about — 7 volts, where $g_{m0} = 0{\cdot}56$ mA/volt, so let us take this as the initial setting of the reactance valve corresponding to zero discriminator D.C. output voltage. At the low-frequency

end of the medium wave range, $f_h = 1{,}015$ kc/s, the parallel resistance component of the reactance valve is

$$R_{AB}(g_{m0} = 0{\cdot}56) = \frac{1+(R\omega C)^2}{g_{m0}} = \frac{41{\cdot}7}{0{\cdot}56 \times 10^{-3}}$$
$$= 74{,}500\ \Omega$$

and its minimum value at $g_m = 1$ mA/volt is $41{,}700\ \Omega$

$$L_{AB}(g_{m0} = 0{\cdot}56) = \frac{1+(R\omega C)^2}{g_{m0}R\omega^2 C} = \frac{41{\cdot}7 \times 10^6}{0{\cdot}56 \times 10^{-3} \times 4{\cdot}07 \times 10^7}\mu\text{H}.$$
$$= 1{,}832\ \mu\text{H}.$$

The frequency correction-discriminator D.C. voltage curve can be calculated by using expression 13.16a. Thus when $g_m = 1$ mA/volt, $E_{g3} = -2$ volts (from Fig. 13.16), $K = \frac{0{\cdot}56}{1} = 0{\cdot}56$. The oscillator-tuning inductance for the medium wave range is $77{\cdot}4\ \mu$H (see Section 6.12, Part I) so that

$$\Delta f = f_h\left(\frac{1-K}{2K}\right)\left(\frac{L_h}{L_{AB}}\right) = f_h\frac{0{\cdot}44}{1{\cdot}12}\frac{77{\cdot}4}{1{,}832}$$
$$= +0{\cdot}0166\, f_h$$
$$= +16{\cdot}8 \text{ kc/s for } f_h = 1{,}015 \text{ kc/s}.$$

The frequency correction for other values of E_{g3} may be calculated in a similar manner, and the result is shown as the full line curve 1 of Fig. 13.17. The horizontal axis is scaled in E_{g3} bias volts as well as discriminator D.C. output voltage.

The effect of the phase-shifting network on the oscillator-tuned circuit must also be considered, and converting the series combination of 20,000 ohms and 50 $\mu\mu$F into its equivalent parallel circuit we have for the parallel damping resistance

$$R_p = \frac{1+(R\omega C)^2}{R(\omega C)^2} = \frac{41{\cdot}7}{2{\cdot}035 \times 10^{-3}} = 20{,}450\ \Omega$$

$$C_p = \frac{C}{1+(R\omega C)^2} = \frac{50}{41{\cdot}7} = 1{\cdot}2\ \mu\mu\text{F}.$$

The resistance damping effect is fairly considerable but, although it makes oscillation more difficult to sustain, it has the advantage of rendering variations of R_{AB} with change of discriminator bias of less importance. The added capacitance is seen to be negligible.

At the highest frequency in the oscillator tuning range, $f_h = 1{,}965$ kc/s,

$$R_{AB}(g_{m0} = 0{\cdot}56) = \frac{153{\cdot}5}{0{\cdot}56 \times 10^{-3}} = 274{,}000\ \Omega$$

and its maximum value at $g_m = 1$ mA/volt is 153,500 Ω. The value of R_{AB} given above is very nearly $\left[\frac{1,965}{1,015}\right]^2$ times that at $f_h = 1,015$ kc/s, thus confirming the discussion on Table 13.3.

$$L_{AB}(g_{m0} = 0{\cdot}56) = \frac{153{\cdot}5 \times 10^6}{0{\cdot}56 \times 10^{-3} \times 15{\cdot}25 \times 10^7}$$
$$= 1{,}795\ \mu\text{H}.$$

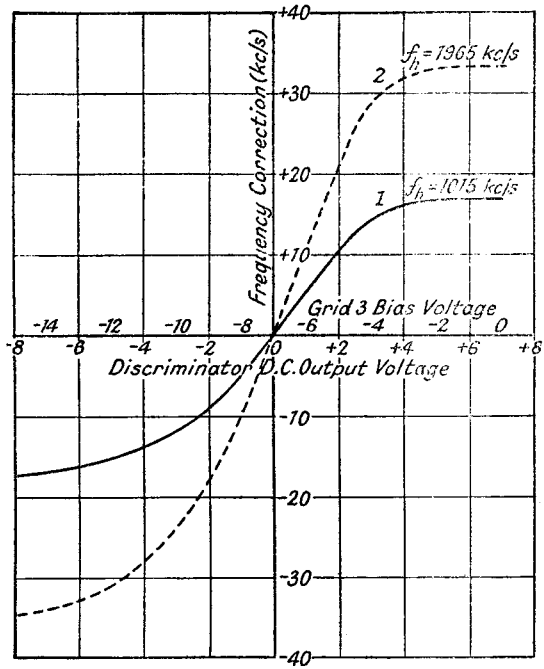

FIG. 13.17.—Frequency Correction—Discriminator Voltage Curves for the Inductive Reactance Valve.

Calculating the frequency correction from expression 13.16*a* we find that for $g_m = 1$ mA/volt, $E_{g3} = -2$ volts,

$$\Delta f = +f_h \cdot \frac{0{\cdot}44}{1{\cdot}12} \cdot \frac{77{\cdot}4}{1{,}785}$$
$$= +0{\cdot}0169\ f_h$$
$$= +33{\cdot}2 \text{ kc/s, for } f_h = 1{,}965 \text{ kc/s}.$$

The frequency correction is plotted as the dotted curve 2 in Fig. 13.17, against discriminator D.C. output voltage and E_{g3} bias.

The A.F.C. sensitivity measured by the slope of the curve at zero discriminator voltage is 10·3 kc/s per volt as compared with 5·2 kc/s per volt at f_h = 1,015 kc/s, i.e., it is very nearly $\frac{1,965}{1,015}$ times as sensitive, a result confirming expression 13.16*b*.

The equivalent parallel resistive and capacitive components of the phase-shifting network are

$$R_p = \frac{153{\cdot}5}{7{\cdot}625 \times 10^{-3}} = 20{,}100\ \Omega$$

$$C_p = \frac{50}{153{\cdot}5} = 0{\cdot}326\ \mu\mu\text{F}.$$

The damping resistance is very nearly the same as for f_h = 1,015 kc/s, so that there is a tendency to stabilize oscillator amplitude. The capacitive component is again negligible.

Suitable values for the phase-shifting network over the long-wave range (signal frequencies from 150 to 400 kc/s) are R = 20,000 Ω, C = 100 $\mu\mu$F. The oscillator frequency range is from 615 to 865 kc/s and the oscillator inductance is about 370 μH. Using these values, the results for the long-wave band are as follows :

Oscillator frequency	615 kc/s	865 kc/s
Step-down ratio anode to grid	0·1283	0·0915
$R_{AB}(g_{m0} = 0{\cdot}56)$	108,600 Ω	214,000 Ω
$R_{AB}(g_m = 1)$	60,800 Ω	119,500 Ω
$L_{AB}(g_{m0} = 0{\cdot}56)$	3,630 μH	3,600 μH
$\Delta f(g_m = 1)$	+24·6 kc/s	+35 kc/s
A.F.C. sensitivity (kc/s per volt)	7·6	10·8
R_p	20,380 Ω	20,200 Ω
C_p	1·64 $\mu\mu$F	0·835 $\mu\mu$F

Over the short-wave range (signal frequencies from 6 to 15 Mc/s), suitable values for the phase-shifting network and L_h are 20,000 Ω, 5 $\mu\mu$F and 1·5 μH and the results are as tabulated below :

Oscillator frequency	6,465 kc/s	15,465 kc/s
Step-down ratio anode to grid	0·2395	0·1022
$R_{AB}(g_{m0} = 0{\cdot}56)$	31,400 Ω	170,500 Ω
$R_{AB}(g_m = 1)$	17,550 Ω	95,500 Ω
$L_{AB}(g_{m0} = 0{\cdot}56)$	190 μH	180·5 μH
$\Delta f(g_m = 1)$	+20 kc/s	+50·4 kc/s
A.F.C. Sensitivity (kc/s per volt)	6·2	15·6
R_p	21,200 Ω	20,250 Ω
C_p	0·285 $\mu\mu$F	0·0523 $\mu\mu$F

It is clear from the above that satisfactory A.F.C. operation is less easy to achieve as the oscillator frequency increases. Stray capacitance across R becomes important and tends to prevent the 90° phase shift being obtained. It is therefore most necessary to

see that the leads from R and C to the reactance valve grid and anode are as short as possible. Interelectrode anode-grid capacitance is usually so small that it can be neglected, but allowance must be made for the grid-cathode interelectrode capacitance, which is a part of and may be comparable to the required value of C.

The less satisfactory performance of the capacitive reactance valve in correcting a capacitively tuned oscillator can be demonstrated by considering the medium-wave range. Suitable values for C and R are 5 $\mu\mu$F and 5,000 ohms ; a large value of R cannot be used because the grid-cathode capacitance of the valve is comparatively large (about 3·5 $\mu\mu$F), and if R is comparable with this

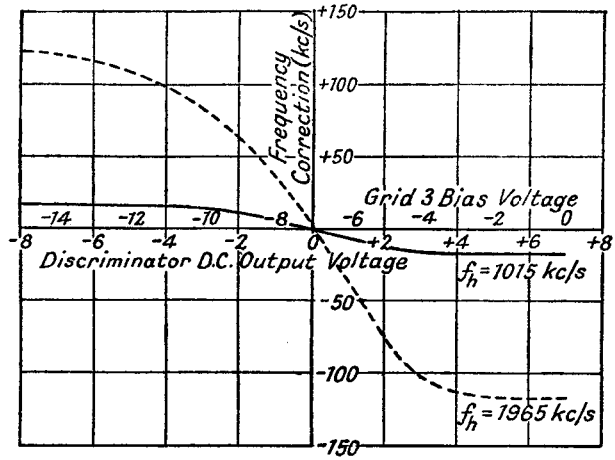

FIG. 13.18.—Frequency Correction—Discriminator Voltage Curves for the Capacitive Reactance Valve.

reactance the required 90° phase shift cannot be realized. The results at the extremes of the oscillator frequency range are tabulated below, and the frequency correction-discriminator voltage curve is shown in Fig. 13.18. The oscillator tuning capacitance at 1,015 and 1,965 kc/s is assumed to be 317 and 84·8 $\mu\mu$F respectively, i.e., $L_h = 77{\cdot}4$ μH.

Oscillator frequency	1,015 kc/s	1,965 kc/s
Step-down ratio anode to grid	0·158	0·295
$R_{AB}(g_{m0} = 0{\cdot}56)$	71,800 Ω	20,550 Ω
$R_{AB}(g_m = 1)$	40,200 Ω	11,500 Ω
$C_{AB}(g_{m0} = 0{\cdot}56)$	13·63 $\mu\mu$F	12·75 $\mu\mu$F
$\Delta f(g_m = 1)$	− 17·15 kc/s	− 116·1 kc/s
A.F.C. sensitivity (kc/s per volt)	5·3	36·0
R_p	202,000 Ω	57,900 Ω
C_p	4·87 $\mu\mu$F	4·56 $\mu\mu$F

This type of circuit is clearly less satisfactory because of the greater variation of damping resistance and A.F.C. sensitivity over the range.

A modified form [2] of the inductance-resistance phase-shifting network has been successfully employed; the actual oscillator tuning coil being used in series with an added resistance R. The input admittance of the reactance valve across the points AB is

$$Y_{AB} = \frac{g_m R}{R+R_h+j\omega L_h}$$

where L_h = inductance of the oscillator tuning coil
and R_h = the R.F. resistance of the tuning coil.

The total admittance of the inductive arm of the oscillator-tuned circuit and the reactance valve is

$$Y_T = \frac{1}{R+R_h+j\omega L_h} + \frac{g_m R}{R+R_h+j\omega L_h}$$

$$Y_T = \frac{1+g_m R}{R+R_h+j\omega L_h} \quad . \quad . \quad . \quad . \quad . \quad 13.21.$$

The oscillator tuning inductance is therefore multiplied by $\frac{1}{1+g_m R}$.

If the oscillator frequency is correct when $g_m = g_{m0}$, then

$$f_h = K\sqrt{1+g_{m0}R}$$

and

$$f_h+\Delta f = K\sqrt{1+g_m R}$$

or

$$1+\frac{\Delta f}{f_h} = \sqrt{\frac{1+g_m R}{1+g_{m0}R}}$$

$$= \sqrt{1+\frac{(g_m-g_{m0})R}{1+g_{m0}R}}$$

but $\frac{(g_m-g_{m0})R}{1+g_{m0}R}$ is usually $\ll 1$ so that

$$\frac{\Delta f}{f_h} \simeq \frac{1}{2}\frac{(g_m-g_{m0})R}{1+g_{m0}R}$$

$$\Delta f \simeq \frac{f_h}{2}\frac{(g_m-g_{m0})R}{1+g_{m0}R}.$$

Thus if $g_{m0} = 0{\cdot}56$ mA/volt and $R = 100$ ohms

$$\Delta f(g_m = 1) = \frac{f_h}{2}\frac{(1-0{\cdot}56)100\times 10^{-3}}{1{\cdot}056}$$

$$= 0{\cdot}0208\, f_h$$

$$= 21{\cdot}1 \text{ kc/s for } f_h = 1{,}015 \text{ kc/s}$$

$$= 40{\cdot}9 \text{ kc/s for } f_h = 1{,}965 \text{ kc/s}.$$

This result is very similar to that obtained for the inductive reactance valve with a *RC* phase-splitting network. The chief disadvantage of the method is that the addition of R in the oscillator-tuned circuit makes oscillation more difficult to sustain, and an oscillator valve having a high g_m is required.

The admittance of the capacitive arm of the oscillator-tuned circuit may be multiplied in the same manner by connecting the tuning capacitance in place of the inductance, but this is only possible with preset-tuned circuits which do not require the capacitance to be earthed.

Many other valve circuits are possible, and the variable reactance valve may, if desired, be applied via a separate coil coupled to the oscillator-tuned circuit. For satisfactory operation and high A.F.C. sensitivity, the control valve should have a high R_a, and a rapid and linear change of g_m with change of discriminator bias voltage.

13.4.4. Estimation of A.F.C. Overall Performance.[8] The operation of an A.F.C. circuit may be represented by an overall performance curve connecting signal tuning frequency setting with I.F. error. Such a curve is not satisfactory for design purposes since any change in the discriminator or variable reactance unit requires a different performance curve to be plotted. The overall characteristic is the result of two separate actions, and it is desirable to combine the characteristics of the discriminator and variable reactance unit in a way which preserves their separate identities. The method employed is illustrated in Fig. 13.19. The discriminator D.C. output voltage plotted against frequency error is represented by curve *ABODE*. The variable reactance characteristic *FGH* (frequency correction against control bias voltage), drawn on transparent paper, is rotated anti-clockwise through 90° so that its frequency correction axis is coincident with the frequency error axis of the discriminator and the two voltage axes are parallel. The reactance characteristic is moved over the discriminator curve for different tuning errors, always keeping the two frequency axes coincident. Thus the intersection of the voltage axis of the reactance unit with the frequency error axis, e.g., point M_1, gives the frequency error of the signal-tuned circuits, whilst a perpendicular from its intersection, N_1, with the discriminator characteristic on to the frequency axis gives the final I.F. tuning error OP_1. The proof of this is that the following equation is satisfied:

signal tuning error − frequency correction = final oscillator tuning error

$$OM_1 - M_1P_1 = OP_1.$$

By sliding the reactance unit characteristic over the discriminator curve (always maintaining the frequency axes coincident), the final oscillator (or I.F.) tuning error can be read directly for any value of signal tuning error. The " throw-out " and " pull-in " frequencies can also be found.

Five positions of signal frequency setting are illustrated on Fig. 13.19. In the first position the two curves intersect at the origin; the tuning setting is correct and no error exists. In position 1 the signal frequency setting error, OM_1, is corrected to an I.F. tuning error of OP_1. If the signal frequency error is progressively increased through M_2, M_3 to M_4, the final I.F. errors are OP_2, OP_3 to OP_4. At position 3 the reactance corrector curve just touches the discriminator characteristic, and a slight increase in

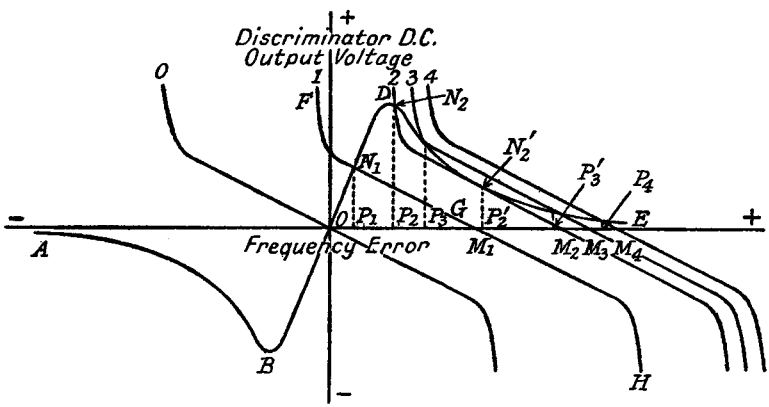

FIG. 13.19.—A Combined Form of Discriminator and Control Characteristic.

signal frequency error causes the I.F. error to jump from OP_3 to OP_3', i.e., A.F.C. has practically lost control. OM_3 therefore gives the " throw-out " signal frequency. In position 4 the error is slightly less than the signal frequency error, but for all practical purposes the A.F.C. can be regarded as inoperative. Progressive decrease of signal frequency tuning error from OM_4 towards O produces final I.F. errors of OP_3', OP_2' and OP_1. It should be noted that in position 3, the final I.F. error OP_3' is much greater when tuning towards O than away from O. At position 2, the reactance corrector curve is tangential to the discriminator curve at N_2', and the slightest movement towards O causes the working point to jump from N_2' to N_2. A.F.C. now takes full control, the I.F. error falling from OP_2' to OP_2. The signal frequency error corresponding to OM_2 gives the " pull-in " frequency setting. Between positions

2 and 3, there are three intersections of the reactance corrector and discriminator curves. The two extreme points give the operating points when tuning away from a signal (the I.F. error is less) and when tuning towards a signal (the I.F. error is greater), whilst the centre point represents an unstable position.

The reactance unit curve is shown in Fig. 13.19 as having a limited control characteristic, i.e., correction is confined to a range of discriminator voltages, and outside this range the reactance remains almost constant. Its chief advantage compared with the unlimited control characteristic is that it reduces the " throw-out " frequency and so reduces the transmission channel blotted out by A.F.C. action on either side of a strong signal. This is illustrated

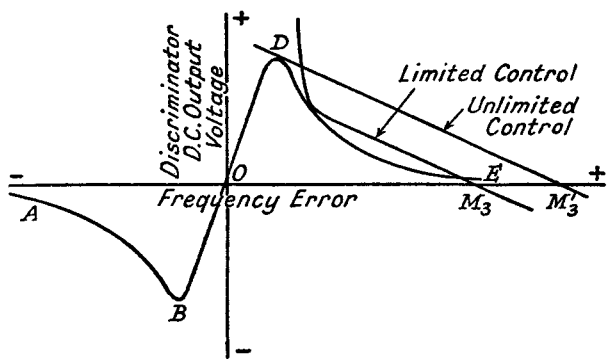

FIG. 13.20.—The Effect of Limited and Unlimited Control Characteristic on A.F.C.

in Fig. 13.20; the " throw-out " frequency, corresponding to OM_3', for the unlimited control characteristic is greater than that, OM_3, for the limited characteristic. In other respects there is little difference between the two, and the " pull-in " frequency is the same for both.

BIBLIOGRAPHY

1. A New System for the Remote Control of Radio Broadcast Receivers. J. B. Sherman, *Proc. I.R.E.*, Jan. 1935, p. 47.
2. Automatic Frequency Control. C. Travis, *Proc. I.R.E.*, Oct. 1935, p. 1125.
3. A.F.C. Design Considerations. S. Y. White, *Electronics*, Sept. 1936, p. 28.
4. Automatic Tuning. D. E. Foster and S. W. Seeley. *Proc. I.R.E.*, March 1937, p. 289.
5. Remote Tuning Control. J. F. Ramsay, *Wireless World*, Sept. 3rd, 1937, p. 231.
6. Magnetic Tuning Devices. L. de Kramolin, *Wireless World*, Feb. 24th (p. 160) and March 3rd, 1938 (p. 186).
7. Push-Button Tuning Systems. *Wireless World*, March 10th, 1938, p. 206.

8. Automatic Frequency Correction. O. E. Keall and G. Millington, *Marconi Review*, April–June 1938, p. 1.
9. Theory of the Discriminator Circuit for Automatic Frequency Control. H. Roder, *Proc. I.R.E.*, May 1938, p. 590.
10. Automatic Tuning Systems. W. E. Felix, *Wireless World*, June 16th, 1938, p. 526.
11. Teledynamic Control by Selective Ionization with Application to Radio Receivers. S. W. Seeley, H. B. Deal, and C. N. Kimball, *Proc. I.R.E.*, July 1938, p. 813.
12. More about Magnetic Tuning. L. de Kramolin, *Wireless World*, July 7th, 1938, p. 5.
13. Olympia Show Review. *Wireless World*, Sept. 1st, 1938, p. 207.
14. Mystery Control. *Radio and Television*, Jan. 1939.
15. Remote Frequency Changer. E. Martin, *Wireless World*, March 16th, 1939, p. 249.
16. Remote Control. Cathode Ray, *Wireless World*, March 23rd, 1939, p. 266.
17. Broadcast Receivers. A. Review. N. M. Rust, O. E. Keall, J. F. Ramsay and K. R. Sturley, *Journal I.E.E.*, Part III, June 1941, p. 59.

CHAPTER 14

MEASUREMENT OF RECEIVER OVERALL PERFORMANCE

14.1. Introduction. The overall performance of a radio receiver requires to be measured not only to assess the relative merits of a particular design, but also to indicate its usefulness under any special operating conditions. In broadcast reception the exact location of a particular receiver is unlikely to be known so that the first viewpoint is the more important. The approximate site conditions may, however, be known to a designer of a communication receiver, and these may have considerable influence on the measurement tests required.

A series of tests has been standardized in America by the Institute of Radio Engineers [1, 5] and in England by the Radio Manufacturers Association [2, 4] as a guide for the designer of broadcast receivers. Their recommendations form the basis of the methods discussed in this chapter, and grateful acknowledgement is made for permission to use the specifications. The two series differ in certain respects, and where this occurs an attempt is made to assess the relative advantages of each method. Modifications or elaborations of any test are included—in their appropriate sections—after the standard specification. Electrical and acoustical tests are covered by the recommendations, which include measurements of sensitivity, selectivity, frequency response, automatic gain control, noise and hum. The electrical tests are treated first. The meanings of certain terms and a short description of the measuring apparatus are given before dealing with procedure.

14.2. Definitions.

14.2.1. Standard Input Voltage. This is the R.M.S. value * of the input carrier in microvolts, or the ratio (in decibels) of the carrier referred to 1 microvolt as zero level (R.M.A.). A reference level of 1 volt is suggested by the I.R.E., but in most cases 0 db. $\equiv$ 1 μV is to be preferred. The standard modulation frequency and percentage is 400 c.p.s. and 30% respectively. Terms

* Wherever the term R.M.S. value of input carrier is employed it refers to the carrier voltage only, and excludes the sideband voltages ; i.e., it is the R.M.S. value of the carrier voltage before it is modulated.

distant, mean, local and strong are applied (by the I.R.E.) to R.M.S. carrier voltages of 50, 5,000, 100,000 μV and 2 volts respectively.

14.2.2. Standard Output Power. The I.R.E. suggest 50 mW and 500 mW as the standard outputs for receivers having maximum outputs less than and greater than 1,000 mW respectively. The R.M.A. recommend 50 mW for all receivers. There are advantages in the use of 500 mW for larger output receivers, because hum and noise may produce outputs comparable with 50 mW, particularly if the receiver is a superheterodyne with considerable I.F. amplification. The power is measured in a non-inductive resistance connected in place of the speaker speech-coil and having the same value as the modulus $(\sqrt{R_{sc}^2+X_{sc}^2})$ of the coil impedance at 400 c.p.s.

For communication receivers intended for phone operation or connection to a land line a suitable standard output power is 1 mW in a resistance equal to the impedance of the phones at 400 c.p.s., or equal to the characteristic impedance of the line (often 600 ohms).

14.2.3. Sensitivity. The sensitivity of an open aerial receiver is defined as the R.M.S. value of input carrier modulated 30% at 400 c.p.s. which, applied through an appropriate dummy aerial, gives the standard output power. Alternatively, sensitivity may be expressed in ratio form as decibels with reference to 1 μV as zero level (R.M.A.). If other than standard output is used the actual power should be stated or the input carrier value corrected by multiplying it by $\sqrt{\frac{P_s}{P_a}}$ where P_a is the actual and P_s the standard power. This correction is only applicable when the characteristic of the A.F. detector is linear.

For a frame aerial receiver sensitivity is defined in microvolts per metre.

14.2.4. Selectivity. The selectivity of a receiver is defined as its capability of discriminating against undesired signals. It may be expressed in terms of the ratio of the sensitivity of the receiver when a standard modulated carrier is off-tuned a specified amount, to its sensitivity when the carrier is correctly tuned to the receiver signal tuning frequency. It may also be expressed in terms of the undesired modulated carrier level required to produce a given interference output.

14.2.5. Fidelity or Frequency Response. The fidelity (better termed frequency response) of a receiver is the degree to which it responds to different modulation frequencies. It is measured by

noting the variation in A.F. power output as the modulation frequency is varied from 30 to 15,000 c.p.s.

14.2.6. Harmonic Distortion. Audio frequency harmonic distortion is expressed as the percentage ratio of the R.M.S. value of the total harmonic voltages in the output to the R.M.S. value of the fundamental and harmonic voltages together. Usually the harmonic voltages are small enough not to affect the second reading to any great extent.

14.2.7. Noise. The noise produced in a receiver is the A.F. output power registered with an unmodulated input carrier voltage. Hum voltages must be excluded from mains receivers by suitable filters attenuating all frequencies below 300 c.p.s. When a receiver is used for C.W. reception, the definition may be modified to read the A.F. output power registered in the absence of an input carrier voltage.

14.2.8. Hum. Hum is measured in the same way as noise except that a low-pass filter is used for attenuating noise output. Both hum and noise outputs are best expressed as decibel ratios referred to the normal output power as zero level.

14.2.9. Automatic Gain Control. The performance of an A.G.C. device is measured by the change of output power produced by a given change of modulated input carrier.

14.2.10. Standard Aerial. An open single-wire aerial of 4 metres effective height is considered as the standard aerial for medium and long waves, and a non-inductive resistance of 400 ohms for short waves.

14.3. The Apparatus required for the Overall Electrical Measurements. The apparatus required for the overall electrical tests includes a standard signal generator, a dummy aerial for an open aerial receiver, a special shielded pick-up coil for frame aerial receivers, an output meter, a beat frequency oscillator and a distortion factor meter, or harmonic analyser.

14.3.1. Standard Signal Generator. This is a frequency calibrated R.F. oscillator capable of modulation to 90%. The output is taken from an attenuator calibrated in microvolts. The attenuator input, supplied from a pick-up coil connected direct to the oscillator or to a buffer valve, is monitored by a thermal instrument or a valve voltmeter. The thermal instrument may also be used as a percentage modulation indicator, for the R.M.S. value of modulated carrier current is

$$I_{c+m} = I_c\sqrt{\left(1+\frac{M^2}{2}\right)}$$

where I_c is the R.M.S. value of unmodulated carrier. The initial modulation setting is made at 80% and lower modulation percentages are obtained from a calibrated potentiometer. When monitoring by valve voltmeter the latter is used to make direct comparison between the carrier and A.F. modulating voltage.

An internal 400 c.p.s. oscillator is incorporated, but external modulation can also be applied.

A slow-motion drive is required on the frequency control to allow selectivity measurements to be made.

The range of the attenuator is normally continuously variable from 1 μV to 0·1 or 1 volt R.M.S., and it is an advantage if the attenuator scale is calibrated in decibel ratios (referred to 1 μV as zero level) as well as microvolts. The output impedance of the attenuator should be low, and the oscillator frequency should not be affected by change of attenuator setting.

14.3.2. Standard Dummy Aerial. A standard dummy aerial is required between the signal generator and receiver to simulate an open aerial. The components are given in Fig. 14.1*a* and the

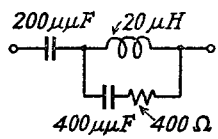

FIG. 14.1*a*.—Circuit Constants of a Standard Dummy Aerial for Long, Medium and Short Wave Bands.

impedance variation in Fig. 14.1*b*. The impedance approaches that of an open aerial of 4 metres effective height over the medium- and long-wave bands, whilst over the short-wave range it is equivalent to a resistance of 400 ohms. The impedance characteristic is affected by the signal generator attenuator output resistance, which should be much less than the series resistance or reactance component of the dummy aerial.

14.3.3. The Shielded Pick-Up Coil for Frame Aerial Receivers. A cylindrical shielded pick-up coil is necessary to provide magnetic coupling to frame aerial receivers. The following are the dimensions recommended by the R.M.A.: radius 5 cms., length 6 cms., turns 20 and approximate inductance 40 μH. Electrostatic coupling is prevented by enclosing the coil in a wire cage. The shunt capacitive reactance of the coil and the leads to the signal generator attenuator must be large compared with the inductive reactance of the coil, and the latter should be much larger (at least 20 times) than the attenuator output resistance so that the output

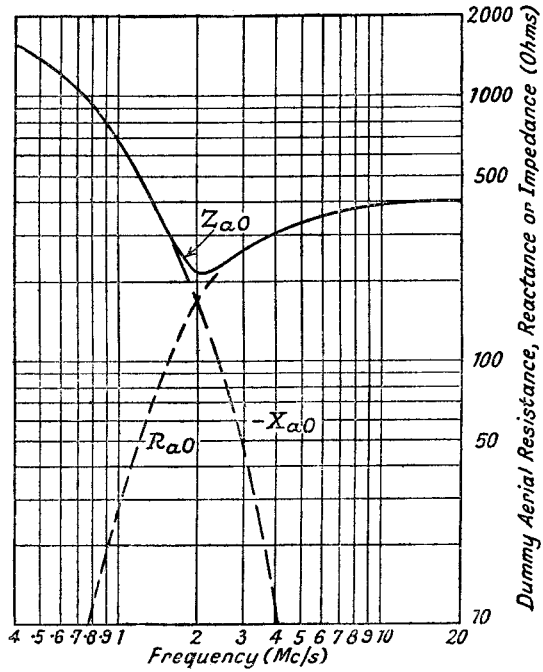

FIG. 14.1*b*.—Impedance Characteristics of a Standard Dummy Aerial.

voltage is unaffected by the coil connection. The coil and frame aerial are placed coaxially and the input to the receiver is

$$\frac{18{,}800\,Nr^2E}{(r^2+l^2)^{\frac{3}{2}}\omega L} \text{ microvolts/metre} \quad . \quad . \quad . \quad 14.1a.$$

where E = attenuator R.M.S. carrier output in microvolts.
N = number of coil turns.
r = coil radius in centimetres.
l = axial distance between the geometric centres of the coil and frame in centimetres.
L = coil inductance in Henries.

This reduces to

$$\frac{4{,}670E}{f} \text{ microvolts/metre} \quad . \quad . \quad 14.1b$$

for the above coil and the recommended distance l of 2 metres, where f is in c.p.s.

14.3.4. Output Meter. The output meter should be non-reactive and should present a constant resistance to frequencies from 30 to 10,000 c.p.s. If the resistance is variable in steps the meter

is usually scaled in milliwatts, but if it is fixed the reading is generally given in volts.

14.3.5. Beat Frequency Oscillator. A beat frequency oscillator is required to provide sufficient output to modulate the signal generator to 100%. Its total harmonic distortion at this output should not exceed 1%.

14.3.6. Distortion Factor Meter. The distortion factor meter consists of a filter for eliminating the fundamental, and a R.M.S. meter for measuring the harmonic voltages. A comparison method is employed, and a calibrated potentiometer across the input to the meter enables a proportion of the distorted input to be compared against the harmonic input. This potentiometer is scaled in percentage distortion. The distortion factor meter input impedance must be high enough not to affect the loading of the circuit to which it is connected. If this is not so, a buffer amplifier producing negligible harmonic distortion must be inserted before the meter.

14.3.7. Harmonic Analyser. A harmonic analyser is required for measuring the ratio of individual harmonics to the fundamental. Such apparatus generally uses the highly selective properties of a quartz crystal filter to separate each harmonic. The A.F. fundamental and harmonics are used to modulate a carrier frequency which is adjusted so as to bring the desired harmonic sideband into the very narrow pass-band of the crystal filter.

14.4. Receiver Adjustments. No special adjustments should be made to the receiver and the following recommendations are made by the R.M.A.

The receiver, in its own cabinet, is to be tested after it has been switched on for a half-hour. Mains receivers should be operated at the mean voltage of the particular transformer tapping point. Battery receivers are to have a resistance of ohmic value equal to the number of cells in the H.T. battery, inserted in the H.T. negative lead. This exaggerates any tendency to instability and is equivalent to a partially used battery. Tone, volume and selectivity controls are normally to be set for maximum 400 c.p.s. response. A " local-distant " switch, when fitted, is to be set to " distant " for sensitivity and selectivity tests.

14.5. Test Specifications.

14.5.1. Sensitivity. All sensitivity measurements on an open aerial receiver are to be made with the standard dummy aerial between the signal generator and receiver (see Fig. 14.2*a*). When the latter is intended to operate with a special aerial, the standard

is replaced by components giving an impedance characteristic similar to the special aerial. The R.F. input carrier modulated 30% at 400 c.p.s., is adjusted to give the standard output (1, 50 or 500 mW). If readings are not taken over each frequency range the suggested test frequencies are, long-wave range, 160, 200 and

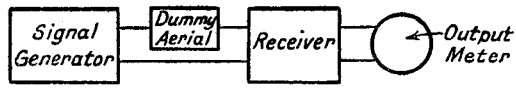

FIG. 14.2a.—Schematic Diagram of Apparatus for Measurement of Sensitivity.

300 kc/s, medium-wave range, 600, 1,000 and 1,400 kc/s, and short-wave ranges at the centre and ends of each range. The sensitivity may be plotted as a series of curves with a uniformly divided vertical decibel scale or logarithmically divided R.M.S. input carrier voltage scale against a linear or logarithmic frequency scale. The logarithmic frequency scale has the advantage that all the ranges can be accommodated on one graph as shown by the specimen full line curves in Fig. 14.2b.

For frame aerial receivers the shielded coil of 14.3.3, connected directly to the output of the signal generator, is placed coaxially with the frame at a distance of 2 metres (between geometric centres). Sensitivity is defined in microvolts per metre in accordance with the formula, 14.1b.

An additional test (I.R.E.) to show the sensitivity at maximum "undistorted" output (10% R.M.S. of A.F. total harmonic distortion) is

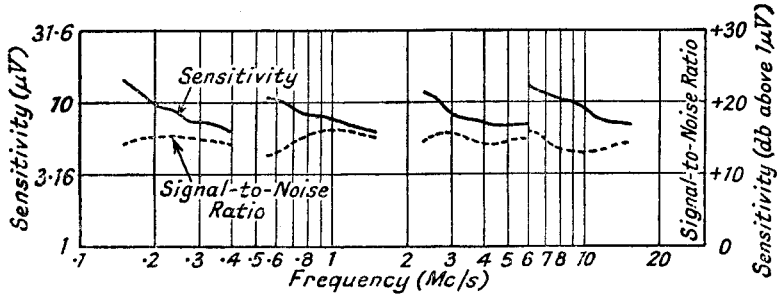

FIG. 14.2b.—Typical Sensitivity and Signal-to-Noise Ratio Curves for a Receiver.

useful, and it is carried out in the same manner as the normal test except that the input carrier is modulated 80%.

In the above tests no account is taken of noise level in determining the sensitivity, and it is clear that high sensitivity is quite valueless if the noise output is comparable with the standard 400 c.p.s. output.

Complete information on sensitivity therefore calls for a statement of signal-to-noise ratio, and the power output of noise at the sensitivity level of unmodulated carrier should be measured. The ratio, expressed in decibels, of standard modulated output to noise output, is included with the sensitivity curve for each range as shown by the dotted specimen curves in Fig. 14.2*b*.

A better estimate of sensitivity is obtained by associating it with a definite minimum signal-to-noise ratio. For example, sensitivity may be defined as the R.M.S. value of input carrier, which, modulated 30% at 400 c.p.s., gives standard output with a signal-to-noise ratio of not less than 15 db. This ratio is reasonably satisfactory for communication purposes, but a higher value is preferable for pleasurable reception. The procedure is to increase the modulated input carrier until standard power output is obtained, e.g., 50 mW ; the modulation is then turned off and the noise power output measured. If this is less than 1·585 mW (this represents — 15 db. on 50 mW), the sensitivity is taken as the R.M.S. input carrier registered by the signal generator. On the other hand, if the noise power exceeds this, the volume control on the receiver is adjusted until the noise power is reduced to 1·585 mW. This reduces the modulated output from 50 mW, and it is returned to its original value by increasing the modulated carrier input. The modulation is again switched off and the noise power checked to see that it is still 1·585 mW ; generally it is not changed to an appreciable extent by the increase in carrier voltage. The new carrier voltage giving the required signal-to-noise ratio with standard output is taken as the sensitivity of the receiver.

For receivers fitted with regeneration (reaction) control it is usual to take sensitivity with minimum and maximum reaction. The normal procedure is to increase the regeneration until oscillation begins. The control is then reduced until slight detuning of the receiver on either side of correct signal setting gives no sign of oscillation. The input carrier is then adjusted to give standard output. The values so obtained are liable to considerable variation, and to a large extent depend on the skill of the operator. A method giving more reliable results is to set the reaction control just to the oscillating point, and to detune the signal generator so that a difference frequency of approximately 400 c.p.s. is obtained. The unmodulated input carrier is then adjusted for standard output of the difference frequency, and this value is considered as the sensitivity. It generally gives a higher sensitivity value than that obtained by the first method.

14.5.2. Selectivity.[7] The large number of independent factors which affect selectivity make it extremely difficult to find an infallible measurement of the receiver discrimination against undesired signals. The chief interference effects are conveniently classified as follows:

(1) A heterodyne whistle, when the frequency difference between the desired and undesired carriers is equal to an audio frequency.

(2) Cross-modulation, the modulation frequencies of the undesired carrier are transferred to the desired carrier (see Section 4.7.3, Part I).

(3) A reduction in the desired audio output due to A.G.C. action and to demodulation at the detector (see Section 8.10, Part I) by the undesired carrier.

(4) "Monkey chatter" due to sidebands (or harmonic * sidebands) of the undesired carrier, which fall in the pass range of the receiver and become sidebands to the desired carrier. The resultant A.F. output has an "inverted" frequency relationship to the undesired modulating frequency. For example, suppose a receiver having a pass range of ± 15 kc/s is tuned to a desired carrier of 1,000 kc/s in the presence of an undesired carrier of 1,020 kc/s modulated by 5, 8, and 13 kc/s. The lower sideband frequencies of the undesired signal are 1,015, 1,012 and 1,007 kc/s respectively, and these enter the pass range of the receiver to form sidebands for the desired carrier. Subsequent detection produces A.F. outputs of 15, 12, and 7 kc/s, i.e., the original low modulating frequency appears as a high audio frequency and the original high frequency as a low audio frequency, a process which is termed frequency inversion.

Distorted undesired output due to frequency inversion is the most serious form of interference, since the receiver cannot be made to discriminate against it without restricting the pass range to an undesirable extent. The effect is worse when the receiver is operating at a site close to a strong local station, and several frequency channels on either side of the local station tuning point may show serious interference. For example, suppose a local transmission of 1,000 kc/s frequency induces a voltage of 1 volt in the aerial of a receiver tuned to 1,023 kc/s. If it is modulated 50% (the voltage of each of the two sidebands if 0·25) at 5 kc/s and there is a fourth

* The term harmonic sideband signifies a sideband produced from modulation of the carrier by a harmonic of the modulating frequencies, i.e., it is represented by $f_c \pm nf_{mod}$, where f_c and f_{mod} are the carrier and modulating frequencies, and n is a positive integer greater than 1.

harmonic sideband percentage of 0·1%, the amplitude of the upper frequency harmonic sideband (1,020 kc/s) is 500 μV. A desired carrier of 1,023 kc/s and 100 μV is overmodulated by the undesired harmonic sideband and the result is an A.F. output, which is a distorted reproduction of the frequency difference (3 kc/s) between the undesired harmonic sideband and the desired carrier. The only method of reducing this form of interference when the harmonic sidebands are produced by the transmitter is to reduce harmonic generation in the A.F. modulation amplifier stages and harmonic sideband production in the R.F. stages of the transmitter, and to include suitable filters attenuating severely modulating frequencies exceeding about 15 kc/s and radio frequencies outside the range $f_c \pm 15$ kc/s, where f_c is carrier frequency.

The receiver itself can produce these harmonic sidebands due to distortion in the first R.F. stage (see Section 4.7.1, Part I), and high selectivity in the aerial-tuned circuits can appreciably reduce the interference effect by decreasing the undesired carrier and its sidebands. As a general rule, however, harmonic sideband production in the receiver is a second order effect, and is negligible in comparison with that produced by the transmitter. Under present conditions of transmission and reception little is to be gained in trying to develop a test to determine the interference due to the receiver itself from frequencies inside the pass-band. Measurements of heterodyne whistle, cross-modulation and demodulation, as far as interference outside the pass-band is concerned, are, however, useful.

There are two recognized methods of estimating selectivity, the first, using a single modulated R.F. carrier, indicates the discrimination of the receiver-tuned circuits against modulated off-tune carrier frequencies, and the graph obtained is really a tuning frequency response curve. The second method uses two signals, one (unmodulated) representing the desired and the other (modulated) the undesired. Adjustment of the modulated undesired is made until a certain A.F. output power level is reached.

We shall first consider the tuning frequency response method of selectivity measurement. The particular signal tuning frequencies at which these measurements are to be made are the same as those recommended for the sensitivity tests. In certain receivers, having high I.F. selectivity, measurements on the short-wave ranges may be unnecessary because the R.F. tuned circuits contribute very little to adjacent channel selectivity. The procedure is as follows: the receiver is tuned to one of the three selected frequencies in a given wave range, e.g., 1,000 kc/s, and readings are taken of the input

carrier voltage (modulated 30% at 400 c.p.s.) required to maintain a constant output power (usually the standard, 50 mW) as the frequency of the carrier is detuned on either side of 1,000 kc/s. The input carrier, preferably expressed in decibels as the ratio of the voltage at the off-tune to that at the correctly tuned position (1,000 kc/s), is plotted against a linear horizontal off-tune frequency scale. The off-tune frequency is carried to a point where the input carrier ratio is 80 db. or its actual value is 1 volt, and a specimen curve is shown in Fig. 14.3*a*. If the magnitude of the carrier voltage is plotted it should be to a logarithmic scale.

Selectivity may also be expressed in tabular form as the band

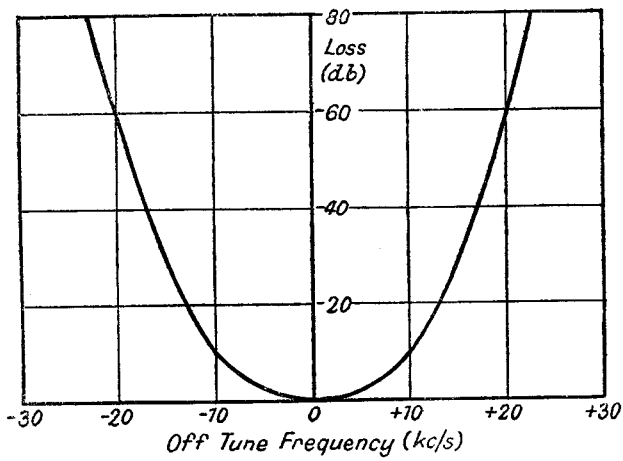

FIG. 14.3*a*.—An Example of a Tuning Response Curve.

width at certain specified input carrier ratios such as — 6, — 20 and — 40 db.

When the I.F. circuits are fitted with a variable selectivity control, its effect need only be tested at one signal frequency. Overall tests are normally carried out for minimum selectivity. Automatic (valve controlled) selectivity devices should be tested at different bias settings of the control valve or valves corresponding to maximum, half and minimum selectivity.

For receivers fitted with manual R.F. volume control, it is often desirable to check the selectivity curves at minimum and half-control settings, because bias changes affect the internal resistances of the amplifier valves and also feedback from the anode to grid due to the anode-grid capacitance. Both change the damping of the tuned circuit, and feedback also alters the tuning frequency (generally to

a lower frequency value). Receivers fitted with A.G.C., which cannot easily be disconnected, should be tested at a power output below that at which A.G.C. is operative. For broadcast receivers, 50 mW is likely to be satisfactory, but for communication receivers it should be limited to 1 mW. The effect of A.G.C. is to give a response wider than the true tuning frequency response.

This test yields results of value for assessing the performance of the tuned circuits, and it is a guide to the discrimination of the receiver against the first type of interference, viz., heterodyne whistle, but it provides incomplete information with regard to interference from undesired signals present at the grid of the first R.F. valve at the same time as the desired, i.e., cross-modulation and distortion in the first amplifier valve is ignored.

The second test (R.M.A.) is designed to include cross-modulation. The outputs from two signal generators, connected in series, are applied through a dummy aerial to the receiver. The two generators should be checked to ensure that the series connection has not affected their voltage calibration. Each in turn, with the other switched off, is set to the receiver tuning frequency, and the receiver output is noted for the same modulated signal generator voltage. The receiver output will be the same in both cases, if the series connection is satisfactory.

The selected test tuning frequencies are as for the first method. A low-pass filter is inserted in the receiver output to cut off all frequencies above 400 c.p.s. This is to prevent the beat frequency due to the desired and undesired carrier frequency separations from masking the cross-modulation effect. Correct tuning is first carried out with the undesired carrier off and the desired carrier modulated 30% at 400 c.p.s. and set for 1 millivolt R.M.S. The receiver volume control is adjusted to give one-quarter of the maximum rated output. The modulation of the desired carrier is switched off, and the undesired carrier modulated 30% at 400 c.p.s. is applied at different off-tune frequencies. Its voltage is adjusted to give an output power 40 db. below the original one-quarter maximum power. Thus an interference power of 0·1 mW is required from a receiver having maximum output of 4,000 mW. The undesired signal frequency is not normally adjusted closer than ± 5 kc/s to the desired frequency.

A specimen curve is shown as full line curve 1 of Fig. 14.3*b*. The interfering carrier is plotted to a vertical scale (logarithmic in μV or linear in decibels relative to 1 μV) against off-tune frequency to a linear horizontal scale. Except for receivers having very poor

selectivity before the first R.F. amplifier valve, little difference is found to exist between the curves obtained by this and the first method. Since the second method is so much more complicated there is little value in using it in preference to the first. It is, however, useful in determining the selectivity of a receiver fitted with automatic selectivity or automatic frequency control. A similar test, known as the two-signal cross-talk interference test, is suggested by the I.R.E., but the interference power output is adjusted to 30 db. below standard output and three different levels of desired carrier, 50, 5,000 and 100,000 μV, are used.

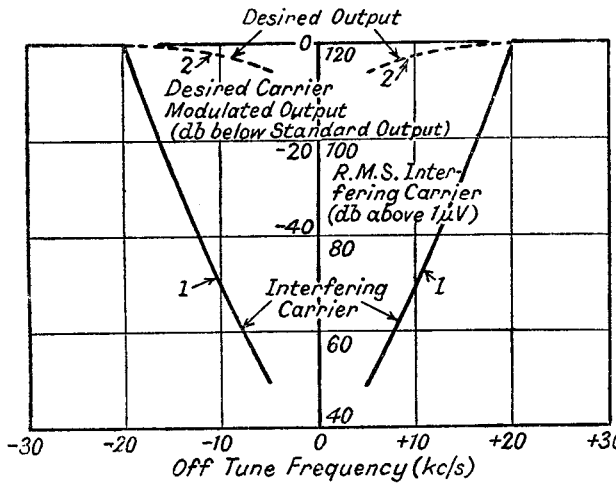

FIG. 14.3*b*.—A Selectivity Curve Obtained by the Two-signal Method.

This method of measuring selectivity gives no indication of the demodulating effect of the undesired carrier on the modulation of the desired at the detector, nor does it show the contribution of the undesired carrier to the A.G.C. voltage. The I.R.E. two-signal blocking interference test allows this effect to be measured, and is a further modification of the two-signal selectivity test. The modulation of the undesired signal is switched off after the correct interference power output has been obtained; the desired carrier is modulated at 30%, and the A.F. power output with the undesired carrier on is compared with its value when the undesired carrier is switched off. The reduction in desired output is plotted against off-tune frequency on the same graph as the two-signal selectivity curve (see dotted curve 2 in Fig. 14.3*b*).

Heterodyne whistle and " monkey-chatter " frequency-inverted

interference are not included in the above two-signal interference tests, but the latter can be modified to show this effect. The procedure is as follows: The two-signal generators are connected in series to the receiver through the dummy aerial and only the desired carrier is switched on. It is modulated 30% at 400 c.p.s. and its output set at a specified level (values are given later). If the A.F. output volume at this carrier level is greater than half the rated maximum output, the A.F. volume control is reduced to give this value. The desired modulation is now switched off and the undesired modulated carrier switched on and adjusted to a specified level. A 400 c.p.s. filter is not used, so that the interference power output includes heterodyne whistle and frequency-inverted components as well as cross-modulation. The interference power output is noted at different off-tune frequency settings of the undesired carrier and it is plotted in decibel ratio with reference to 1 mW as zero level. The minimum undesired-desired carrier spacing at which measurements are taken is that giving an interference power output equal to half the rated maximum. The test is carried out for the following carrier inputs—the suffix D denotes desired and U undesired carrier—50 μV (D) and 50 μV (U); 50 μV (D) and 100,000 μV or 1 volt (U); 5,000 μV (D) and 5,000 μV (U); 5,000 μV (D) and 100,000 μV or 1 volt (U). This simulates conditions for interference between two weak, a weak and powerful, two average, and an average and powerful signal. A typical result is shown by curve 1 in Fig. 14.3*c*; the curve is asymptotic to the inherent noise level of the receiver as the undesired carrier off-tune frequency separation from the desired is increased.

A 400 c.p.s. band-pass filter is next inserted between the output and output meter, and a test is carried out with the desired carrier modulated and the undesired unmodulated at the same input levels as those listed above. This measures the demodulating effect of the undesired and also the volume reduction of the desired modulation due to operation of the A.G.C. by the undesired carrier. Desired output is plotted against off-tune frequency as a decibel ratio with reference to 1 mW as zero level; curve 2 in Fig. 14.3*c* is a typical example.

The overall selectivity characteristic is expressed as the ratio of the desired to undesired output, and is obtained by plotting the difference between curves 1 and 2 in Fig. 14.3*c*. The result is indicated by curve 3 in Fig. 14.3*c*. This final curve gives a truer indication of interference discrimination than either single or normal two-carrier tests. For example, neither of the latter can indicate

the effect of a whistle filter in the A.F. stages, whereas the improvement in signal-to-interference ratio due to inclusion of the whistle filter is shown by the modified two-signal test as a dip in the interference output curve 1 at an off-tune frequency corresponding to the rejection frequency of the whistle filter and a rise in the signal-to-interference ratio curve 3. The whistle filter has no effect on the desired power output at 400 c.p.s., since it occurs after the detector where the demodulation is occurring.

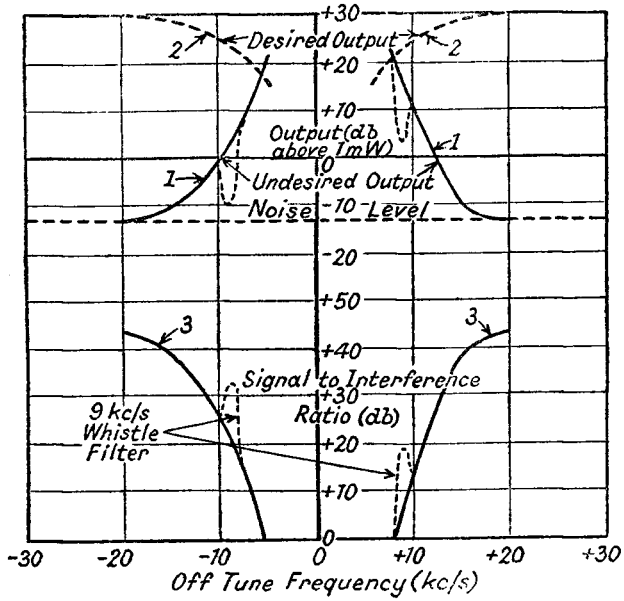

FIG. 14.3c.—A Modified Selectivity Test Curve.

14.5.3. Electrical Frequency Response. The electrical (as distinct from the acoustical) frequency response of a receiver is useful for assessing the attenuation of the higher-frequency modulation sidebands by the selectivity of the R.F. and I.F. tuned circuits, and the reduction of high or low audio frequencies due to tone control. The curve has only a general resemblance to the acoustical frequency response, which is chiefly determined by the audio radiation characteristics of the loudspeaker.

The test is performed at a carrier frequency of 1,000 kc/s, modulated 30%. The modulation frequency is varied from 30 to 10,000 c.p.s., and the power output variation noted. The carrier input is set at 5,000 μV, and the volume control adjusted to give one-quarter of the rated maximum or 500 mW, whichever is the

greater, at a modulation frequency of 400 c.p.s. If the power output approaches the maximum at any modulation frequency (this might occur with tone control circuits), the output level at 400 c.p.s. must be reduced below the rated one-quarter maximum. The results are plotted in the form of a vertical logarithmic power output scale, or a linear power output decibel ratio scale (zero level being the output at 400 c.p.s.), against a logarithmic scale of modulation frequency. Curves (see the dotted extensions in Fig. 14.4) are taken for tone control and variable selectivity (if included) settings giving maximum and minimum low and high audio frequency response. If the setting of the volume control affects fidelity,

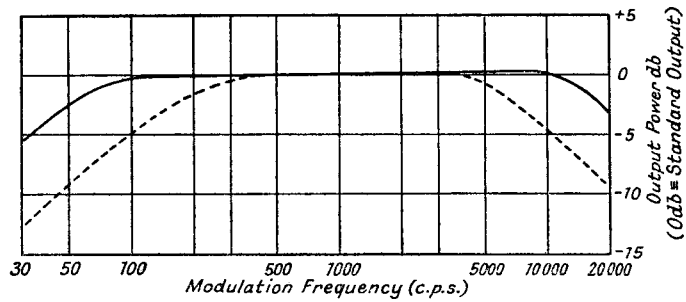

FIG. 14.4.—The Electrical Frequency Response of a Receiver.

curves should be taken at 400 c.p.s. power output levels differing by 10 db.

Electrical frequency response may be taken at carrier frequencies other than 1,000 kc/s, e.g., at the centre of the long-wave band, 200 kc/s; there is usually little to be gained by taking fidelity curves in the short-wave range because the selectivity of the signal-tuned circuits is relatively poor. Different input carrier levels should be tried if the receiver has automatic selectivity or tone control.

14.5.4. Harmonic Distortion. For this measurement care must be taken to ensure that the signal generator and audio frequency modulating source produce minimum sideband and audio frequency distortion. The tests can be conveniently subdivided to show the distortion introduced by the different stages in the receiver.

The A.F. stages may be checked by applying the audio frequency modulating source to the pick-up terminals or to the grid of the first A.F. amplifier valve. Readings of power output against distortion are obtained at, usually, three frequencies, 400, 1,500 and 3,000 c.p.s.

For measurement of R.F. modulation envelope distortion, the R.F. input carrier, modulated 30% and 60%, is varied, the A.F. volume control being adjusted each time to maintain constant power output at a value low enough to produce low distortion in the A.F. amplifier. Readings should also be taken of distortion against modulation percentage for an input carrier of 5,000 μV and the same low audio power output. The three frequencies listed above are used to modulate the carrier.

The effect of tone control on distortion should be examined by repeating the first test with tone control settings for minimum high- and low-frequency response.

14.5.5. Noise. The noise level of a receiver is specified by the R.M.A. as the R.F. input unmodulated carrier for which the R.M.S. audio output from the receiver is equal to the output given by 10% modulation at 1,500 c.p.s. of the same carrier.

For measuring the noise level the carrier is adjusted until the power output is doubled by applying the specified modulation, and this carrier is then regarded as the equivalent noise voltage level. A filter attenuating hum voltages below 300 c.p.s. is included. Noise from external sources is to be excluded, and it may be necessary to operate the signal generator from batteries.

This definition of noise is somewhat arbitrary and a more satisfactory method is to quote signal-to-noise power ratio as suggested for the sensitivity tests.

The I.R.E. specification differs slightly from the above. The input unmodulated carrier is set to some suitable value, such as the sensitivity value, and the noise power output, P_n, is measured by a thermal instrument (this gives R.M.S. value). A 400-c.p.s. band-pass filter is inserted between output and milliwattmeter, the 400-c.p.s. modulation of the carrier is switched on at 30%, and the power output P_0 noted. The equivalent noise voltage is defined as

$$E_n = 0{\cdot}3E^c\sqrt{\frac{P_n}{P_0}} \quad . \quad . \quad . \quad . \quad 14.2$$

where 0·3 is the modulation factor and E_c is the carrier voltage.

In order that the noise output may be proportional to the noise side-band voltages, the carrier voltage (E_c) should be at least $3E_n$ and preferably $10E_n$. If the original E_c gives E_n greater than $\frac{E_c}{3}$, it should be increased until expression 14.2 gives $E_n \leqslant \frac{E_c}{3}$. Noise from hum and external causes should be reduced to the lowest value as suggested for the first test.

14.5.6. Hum. In measuring interference due to hum from the mains power supply, noise frequencies must be severely attenuated, and a low-pass filter, having a cut-off frequency of 300 c.p.s., is inserted between the output and the output meter. Hum may appear in the loudspeaker from the speaker field coil, the A.F. or the R.F. amplifier stages. Hum from the former is a result of using it as the smoothing coil. A " hum-bucking " coil (a few turns of thick wire wound on top of the field coil) in series with the speech-coil is employed for neutralizing purposes. In measuring hum injected into the speech-coil from the field coil, the voltage across, or current in the speech-coil is noted when the output valve anode is disconnected from the output transformer primary and connected direct to H.T. positive, and the primary shunted by a resistance equal to the output valve slope resistance. For A.F. and R.F. amplifier hum measurement the speech-coil is replaced by an output meter having a resistance equal to the modulus of the speech-coil at 400 c.p.s. Hum from the A.F. amplifier is due to direct amplification of hum voltages produced in the grid-cathode circuits by the heaters or is due to insufficient smoothing of the H.T. power supply. The R.F. circuits can only produce hum by modulation of the input carrier or of the oscillator in the frequency changer circuit. Since modulation is dependent on non-linear valve characteristics, the hum from the R.F. circuits usually reaches a maximum at some particular bias corresponding to maximum rate of change of the I_aE_g characteristic.

Hum due to the A.F. stages may be measured on the output meter with the A.F. volume control set to zero, but it is preferable to remove the last I.F. valve from its socket and to take the reading with the A.F. volume control at maximum. If the latter is at zero, hum in the grid-earth circuit of the first A.F. amplifier is not measured, and this may form an appreciable proportion of the interference.

Measurement of modulation hum is only necessary when it is comparable with hum from the post-detector stages, and it is made with an unmodulated 1,000 kc/s carrier. The receiver volume control is set at maximum and the output meter reading is observed as the carrier voltage is increased. If the output reaches a maximum at a particular carrier voltage (this is generally so if the receiver has A.G.C.), the power is noted and compared with the output registered when the 400 c.p.s. (30%) modulation is switched on. The hum filter is removed for the 400-c.p.s. reading and volume control adjustments are made if overloading of the A.F. amplifier is experienced, the hum power output being measured at the new volume

control setting. The hum modulation is expressed as a percentage modulation

$$M_h = 30\sqrt{\frac{P_h}{P_0}}\,\% \quad . \quad . \quad . \quad 14.3$$

where P_h = hum power output

P_0 = 400-c.p.s. power output obtained for the same volume control setting as P_h.

14.5.7. Automatic Gain Control. The A.G.C. performance is normally measured at the mid-frequency of each waveband. The R.M.A. recommend that the input carrier modulated 30% at 400 c.p.s. should be set to 1 volt and the volume control adjusted to give one-quarter of the maximum rated output. The carrier input is reduced in suitable steps and the output noted. A curve is plotted of

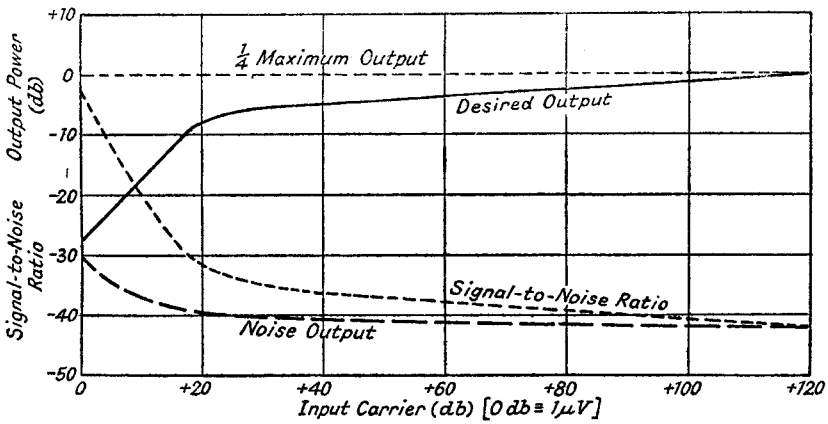

FIG. 14.5.—A.G.C. Characteristic Curves of a Receiver.

output power against input voltage to logarithmic scales, or of power and input carrier in decibel ratios to linear scales (Fig. 14.5), zero level being one-quarter of the rated maximum and 1 μV respectively.

The I.R.E. test is very similar; the output power is adjusted to one-half the rated maximum when the carrier voltage is 1 volt. The output power ratio (0 db. = $\frac{1}{2}$ maximum rated power) is plotted against a horizontal decibel scale of input carrier referred to a zero level of 1 volt. The suggested figure of merit is the input decibel reduction below 100,000 μV necessary to produce a 10-db. change of output. For receivers operating on small signals the input decibel reduction may be taken from 5,000 μV.

If an interchannel noise suppression circuit (Quiet A.G.C.) is

incorporated, the A.G.C. curve about the noise-suppression point should be taken for increasing as well as decreasing input carrier in order to show any backlash effect.

An alternative[6] method of measurement is to begin from minimum input carrier with the volume control set at maximum. The input is increased until the output reaches one-quarter of the maximum output. At this point the volume control is changed to reduce the output to one-tenth of its value. The input is again increased and the procedure repeated until 1 volt carrier is reached. The A.G.C. curve is made continuous by multiplying the second set of output readings by 10, the third by 100, and so on. The great advantage of this method is that it gives sensitivity directly and also indicates any need for changing the A.G.C. delay voltage. For example, suppose the maximum rated output is 3 watts, the A.G.C. delay — 15 volts, and the curve shows A.G.C. operation to commence at 10 watts output. This suggests that the delay voltage should be reduced to bring A.G.C. into operation at about 2,500 watts output, i.e., the delay voltage should be reduced to $-15 \times \sqrt{\frac{2{\cdot}5}{10}} = -7{\cdot}5$.

It is of considerable advantage to include with the A.G.C. characteristic a curve of noise power output against input carrier, the noise being measured for the unmodulated carrier. A suitable filter removing hum voltages is included between the A.F. output and the meter. Noise power output is plotted in decibel ratios (Fig. 14.5) with zero level the same as that for the A.G.C. curve. The signal-to-noise ratio for a given input carrier is found immediately by the difference between the A.G.C. and noise power levels.

14.5.8. Frequency Changer Interference Effects. The image signal, and harmonics of the oscillator, intermediate and undesired signal frequencies can interact in the frequency changer to produce interference with the desired signal. The first two are the most important and a measure of oscillator harmonic interference is usually an adequate guide to the smaller interference from intermediate and undesired signal harmonics.

The image signal sensitivity is found by varying the signal generator carrier frequency over a range covering a frequency of f_s+2f_1, where f_s is the receiver tuning frequency and f_1 is the intermediate frequency. The carrier is modulated 30% and its voltage is adjusted, when the frequency point of maximum audio output has been found, until standard power output is obtained. The result is plotted as $20 \log_{10} \frac{\text{image signal sensitivity}}{\text{real signal sensitivity}}$ against real

signal frequency. Variation of the carrier frequency over a small range on either side of f_s+2f_1 is necessary because the receiver tuning-dial frequency setting cannot usually be read with sufficient accuracy.

For oscillator harmonic response the same procedure is followed. The signal generator frequency is varied over a small range, which includes an undesired signal frequency spaced from second and third harmonics of the oscillator by an amount equal to the intermediate frequency. Thus for an I.F. of 465 kc/s and a receiver tuning frequency of 1,000 kc/s, the oscillator frequency is 1,465, giving second and third harmonics of 2,930 and 4,395 kc/s. The signal generator is therefore set in turn to 2,465 and 3,930 kc/s, and the sensitivity measured. Curves are plotted of decibel ratio oscillator harmonic sensitivity to real-signal sensitivity against real-signal frequency.

14.5.9. Oscillator Frequency Drift. The oscillator for the frequency changer should be checked to determine the variation of frequency due to power supply changes, normal operating temperature variations and A.G.C. A detector having a grid circuit tuned to the oscillator frequency is loosely coupled to the oscillator (a wire connected to the detector grid lead placed near the oscillator valve or tuning capacitor is usually sufficient). In series with the detector grid circuit is the output from a frequency stabilized oscillator operating at a frequency separated from the receiver oscillator frequency by about 500 c.p.s. The audio note of 500 c.p.s. produced in the detector output is measured by a calibrated beat frequency oscillator. The receiver oscillator drift causes the detector output A.F. frequency to vary and the variation is noted on the beat frequency oscillator.

Frequency variation is measured for $\pm 5\%$ mains supply variations, and readings are taken rapidly so as not to include temperature effects. The latter are noted by observing the variation of frequency over a given time period (about $\frac{1}{2}$ hour) from switching on. A curve is plotted of frequency drift (vertical linear scale) against time (horizontal).

Automatic gain control causes frequency drift by varying the H.T. voltage and the frequency changer load on the oscillator (Section 6.6 and 6.8, Part I). A curve is suggested of frequency drift against microvolts input to a logarithmic scale or decibel ratio to a linear scale (zero level 1 μV). This and the first test should only be performed after the receiver has settled down to normal operating temperatures (about $\frac{1}{2}$ hour after switching on). It is

not usual to take readings at other than the centre frequency of each wave range.

14.5.10. Automatic Frequency Correction. The performance of the automatic frequency corrector is checked by noting the off-tune frequencies at which the desired signal disappears and reappears. The signal generator input carrier is tuned away from the receiver tuning frequency, and the frequency at which the 400-c.p.s. output disappears is noted.

The carrier is then retuned towards the receiver frequency and the pull-in position noted. The A.F.C. is dependent on the amplitude of the input carrier, and it should be checked at the sensitivity input and also inputs of 5,000 and 100,000 μV. The test should preferably be carried out at each end of a wave range.

14.6. Acoustical Tests. Acoustic measurements on a radio receiver are more difficult to perform than electrical tests. Recommendations have been made by the R.M.A. for the measurement and calculation of frequency response, acoustic sensitivity, output and hum. Two tests only are suggested by the I.R.E., one on frequency response similar to the R.M.A. specification and the other a qualitative examination of noise audibility. Some further definitions must be given and additional apparatus described before the tests are stated.

14.7. Definitions.

14.7.1. Frequency Response. The acoustic frequency response of a receiver is the relationship between the output intensity level, measured at a given position relative to the loudspeaker, and the output audio frequency.

14.7.2. Intensity Level. The intensity level of an audio frequency is the ratio in decibels of the measured output with reference to a sound pressure of $2{\cdot}04 \times 10^{-4}$ dynes/sq. cm. (i.e., a power of 10^{-16} watts per square centimetre).

14.7.3. Loudness Level. The loudness level of an audio frequency note is the intensity level (expressed in phons) of a 1,000-c.p.s. note judged by the listener to be equal in loudness to the test frequency output. A direct measurement of loudness entails switching from the test to the 1,000-c.p.s. frequency. An examination by a number of observers [3] has produced an agreed average figure for loudness level for different frequencies and the relationship between loudness and intensity level for a 400-c.p.s. note is tabulated below.

Intensity Level (db.)	10	20	30	40	50	53	60	70	80	90	100
Loudness Level (phons)	0	11	22·5	35	47	50	58	69·5	80	91	99

14.7.4. Overall Acoustic Sensitivity. The overall acoustic sensitivity for an open aerial receiver is the input in microvolts needed to give a loudness level, at the measuring position, of 50 phons. The input carrier is modulated 30% at 400 c.p.s.

14.7.5. Distortion Factor. The distortion factor is defined as

$$\frac{1}{2}\sqrt{\frac{\sum_{n=2}^{\infty} n^2 E_n^2}{\sum_{n=1}^{\infty} E_n^2}} \quad . \quad . \quad . \quad 14.4$$

where E_n is the voltage across the speech-coil due to the nth harmonic. The arbitrary multiplication of E_n by n in the numerator is included since higher harmonics generally have greater interference capability (see Section 10.7). For example, 5% of third harmonic gives relatively greater interference than 5% of second harmonic.

14.7.6. Total Harmonic Content. The total harmonic content is

$$100\sqrt{\frac{\sum_{n=2}^{\infty} E_n^2}{\sum_{n=1}^{\infty} E_n^2}}\% \quad . \quad . \quad . \quad . \quad 14.5.$$

14.7.7. Free Space Conditions and their Approximation. Free space conditions of still air, absence of reflected waves and no distortion of the sound field by the microphone can be approached in the open air on a windless day at a considerable distance from the ground or any reflecting surface. They may also be simulated in a heavily damped room, the minimum internal volume of which should be 1,000 cubic feet.

14.7.8. Hum. Hum applies only to low-frequency mains interference due to inadequate filtering of D.C. voltage sources, vibration of mains transformers, and A.C. voltages induced from the heater supply. The result is expressed in phons.

14.8. Additional Apparatus. The apparatus required in addition to that listed in 14.3 is a pressure-operated microphone, calibrated in volts per dyne per square centimetre, an amplifier having a straight-line frequency response ($\pm 0{\cdot}5$ db.) from 30 to 10,000 c.p.s. for amplifying the microphone output, and distortion factor apparatus. The latter consists of an amplifier, having a flat frequency response from 30 to 10,000 c.p.s., a filter for attenuating

the fundamental, a circuit having a frequency response directly proportional to frequency, and a valve voltmeter. For measuring distortion factor, the filter and special frequency discriminating circuit are inserted and the R.M.S. output voltage noted. The filter and special circuit are next removed and a potentiometer calibrated in distortion factor is adjusted to give the same R.M.S. output voltage reading.

A diagram of the apparatus is shown in Fig. 14.6*a*, and details of the high-pass filter attenuating the fundamental are given in Fig. 14.6*b*. The frequency discriminating circuit consists of L_1 and R_4 connected to the anode of the first valve V_1. In the up position (1) of switch S_1 a flat frequency response is obtained (R_4 only is in circuit), whilst in the down position (2) L_1 is inserted and the required rising fre-

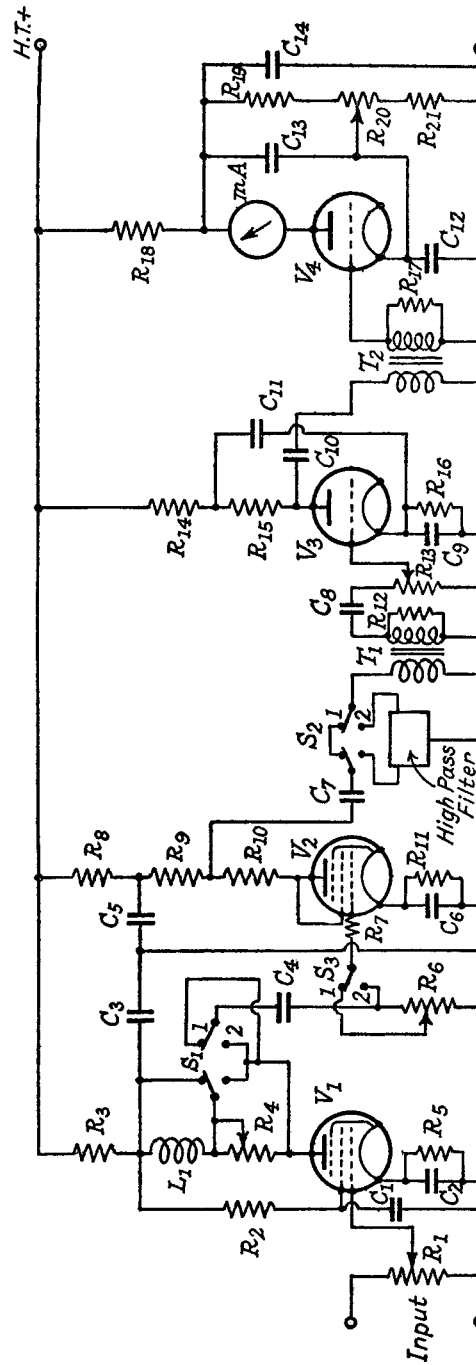

FIG. 14.6*a*.—Circuit Diagram of the Distortion Factor Test Apparatus for Acoustical Measurements.

quency characteristic is obtained, i.e., the amplitude of the output voltage from V_1 for a fixed input voltage is directly proportional to frequency. Switch S_2 in the up position (1) connects the output of the amplifier valve V_2 direct to the transformer T_1 in the grid circuit of another amplifier valve V_3. The latter is followed by the anode bend valve voltmeter V_4. With switch S_2 in the down position (2), the high-pass filter is inserted between V_2 and T_1 and the fundamental 400-c.p.s. frequency is eliminated. Potentiometer R_1 is an input control, selecting any desired proportion of the audio output voltage from the receiver. Potentiometer R_6 measures and is directly calibrated in distortion factor. R_{13} is a preset gain control initially adjusted to give a satisfactory valve voltmeter reading. Switch S_3 enables the total voltage across R_6 or the voltage from the slider to earth to be measured.

The component values for Fig. 14.6*a* are :

Inductance $L_1 = 0{\cdot}1$ *H*. Transformer T_1. 1 : 5 step-up ratio. Transformer T_2. 1 : 3·5 step-up ratio. Milliammeter 0 to 0·5 mA.

	Resistances.	Capacitances.
1.	0·1 MΩ (variable)	8 μF
2.	10,000 Ω	25 μF
3.	2,500 Ω	8 μF
4.	1,000 Ω (preset variable)	0·1 μF
5.	250 Ω	8 μF
6.	0·1 MΩ (variable)	50 μF
7.	100 Ω	4 μF
8.	1,000 Ω	0·1 μF
9.	750 Ω	25 μF
10.	2,500 Ω	1 μF
11.	60 Ω	1 μF
12.	25,000 Ω	25 μF
13.	0·1 MΩ (preset variable)	1 μF
14.	5,000 Ω	8 μF
15.	25,000 Ω	
16.	320 Ω	Valves.
17.	0·1 MΩ	1. MKT4
18.	15,000 Ω	2. KT41
19.	20,000 Ω	3. MH41
20.	1,000 Ω (variable)	4. MH41
21.	100 Ω	

The procedure for the initial calibration of R_6 in terms of distortion factor is as follows. The filtered output voltage from a 400-c.p.s. oscillator is applied across R_1, and with switch S_2 on position 1, the resistance R_4 is adjusted until there is no change in the valve voltmeter reading when switch S_1 is changed from position 2 to 1. This means that the amplification of V_1 to the fundamental frequency is the same in position 2 as in position 1.

The filtered output from the 400 c.p.s. oscillator is used to modulate the signal generator and the output voltage from the receiver is applied across R_1. With switches S_1, S_2 and S_3 in position 2, R_1 is adjusted to give a convenient reading on the valve voltmeter; this measures the total distortion quality of the harmonics, i.e., the voltage represented by the numerator of expression 14.4.

Switches S_1, S_2 and S_3 are now moved to position 1 and the slider of R_6 is adjusted to give the same selected reading on the valve voltmeter; this is a measure of the voltage represented by the denominator of expression 14.4. The distortion factor is $\frac{a}{2}$, where a is the fraction of R_6 needed to give the same voltmeter reading in position 1 as in position 2.

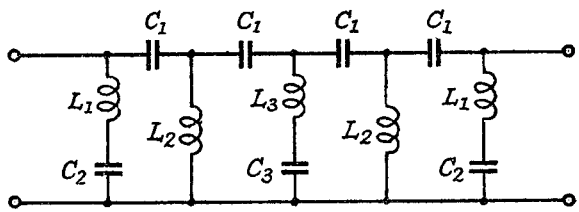

FIG. 14.6*b*.—The High Pass Filter for the Distortion Factor Apparatus.

Component values of the high-pass filter of Fig. 14.6*b* (used for removing the fundamental 400 c.p.s.) are as follows:

Inductance.	Capacitance.
1. 0·424 H	1. 0·249 μF
2. 0·127 H	2. 0·373 μF
3. 0·212 H	3. 0·746 μF

Cut-off frequency, 500 c.p.s.
Maximum attenuation frequency, 400 c.p.s.
$R_0 = 800\ \Omega$.
Attenuation at and above 800 c.p.s. less than 1 db.
Attenuation at 400 c.p.s. 80 db. (minimum) for Q of coils = 50.

14.9. Acoustical Measurements.

14.9.1. Frequency Response. Measurements of frequency response are to be made in the free space approximate conditions. Calibrated records are used in the gramophone pick-up, and for the complete receiver a 1,000 kc/s carrier modulated at 30% and of R.M.S. value 20,000 μV is applied through the dummy aerial. The tone and variable selectivity controls are set for maximum frequency

response. The input to a frame aerial receiver through the shielded coil is to be 20,000 μV per metre. The receiver volume control is adjusted to give one-quarter of the maximum electrical power output to a load resistance corresponding to the speech-coil modulus at a frequency of 400 c.p.s.

The modulation frequency of the signal generator is varied from 30 to 10,000 c.p.s. and measurements of intensity level are made for two positions of the microphone :

(1) On the axis of the speaker, with a distance of 3 feet between the planes of the microphone diaphragm and the loudspeaker grille or cabinet opening.

(2) At a point in the horizontal plane at 45° to the axis of the loudspeaker ; the microphone and speaker separation is to be 3 feet and the microphone diaphragm is to be set perpendicular to the line joining microphone and speaker.

For all tests the centre of the loudspeaker is 3 feet from any boundary surface.

If recording apparatus is used to note the intensity level-frequency curve, all maxima and minima must be registered, and stopping the apparatus at one frequency must not change the intensity level reading by more than 2 db.

The axial and 45° responses are plotted on the same graph to a vertical linear decibel ratio scale and a logarithmic horizontal frequency scale. The reference level of 0 db. for the curves is the intensity level corresponding to the geometric mean of the pressures at 200 and 600 c.p.s., i.e., the intensity level is referred to $\sqrt{P_{200}.P_{600}}$ instead of 0·000204 dynes/sq. cms. For radio gramophone receiver tests the type of needle used must be stated.

14.9.2. Acoustic Sensitivity. The acoustic sensitivity is the modulated carrier required to give a loudness of 50 phons, or at 400 c.p.s. modulation an intensity level of 53 db. Its value may be calculated from the measurement made for the previous test (14.9.1). The intensity level at 400 c.p.s. is taken as the geometric mean of the pressures at 200 and 600 c.p.s. referred to a pressure of 0·000204 dynes per square centimetre.

Let In_W denote this geometric mean intensity level, S_E the electrical sensitivity giving 50 mW electrical output, S_A the acoustical sensitivity giving a 400 c.p.s. output intensity level corresponding to 53 db., W the electrical power output at 400 c.p.s. for the frequency response test (of value about one-quarter of the maximum output).

If the electrical power output is directly proportional to the square of the input carrier

$$\frac{S_A}{S_E} = \sqrt{\frac{W_{53}}{50}}$$

where W_{53} is the electrical power output (mW) giving a 400-c.p.s. intensity level at the microphone of 53 db.

But $$In_W = 10 \log_{10} \frac{W}{W_0},$$

where W_0 is the electrical power output (mW) giving zero intensity level at the microphone (a pressure of 0·000204 dynes/sq. cm.).

and $$53 = 10 \log_{10} \frac{W_{53}}{W_0}.$$

$$\frac{In_W - 53}{10} = \log_{10} \frac{W}{W_{53}}$$

$$\frac{W}{W_{53}} = 10^{\left(\frac{In_W - 53}{10}\right)}$$

or $$W_{53} = \frac{W}{10^{\left(\frac{In_W - 53}{10}\right)}}.$$

Replacing this in the first expression, the acoustical sensitivity is

$$S_A = S_E \sqrt{\frac{W}{50 \times 10^{(0{\cdot}1\, In_W - 5{\cdot}3)}}} \quad . \quad . \quad . \quad 14.6.$$

14.9.3. Hum. For hum measurements, test-room disturbances and noise in the microphone amplifier are to be at least 5 phons below the lowest hum level. The microphone diaphragm is to be located on the speaker axis at a distance of 12 inches from the speaker grille. The mains supply voltage should contain approximately 3% of fifth harmonic. The fifth harmonic of the mains fundamental is chosen because it is found that this is the harmonic most frequently picked up by an unshielded grid lead. This requirement may be fulfilled by using a low-pass filter in the mains leads to suppress harmonics, the 3% of fifth harmonic being inserted from a valve generator, the output from which is connected across a series resistance in the filtered mains lead.

The overall frequency response characteristic of the microphone and amplifier is to be as follows to within ±2 db.

Frequency.	Gain relative to 25 c.p.s.
25 c.p.s.	0
50 ,,	+12·5
100 ,,	+25
150 ,,	+31·5
200 ,,	+36
250 ,,	+40
300 ,,	+43·5
400 ,,	+48
500 ,,	+51·5
600 ,,	+52·5
700 ,,	+54
800 ,,	+55
Above 1,000 c.p.s.	Less than −10

The above frequency characteristic may be realized by inserting a T-section equalizer at a suitable point in the straight-line frequency response amplifier mentioned in 14.8. The two series arms of the equalizer are capacitors of $\frac{398}{R_0}$ μF, and the shunt arm consists of a resistance of $0{\cdot}117R_0$ ohms and inductance $7{\cdot}17R_0$ μH, where R_0 is the characteristic impedance of the equalizer. Frequencies above 800 c.p.s. must be attenuated by additional apparatus. The voltmeter at the output of the microphone amplifier is to measure R.M.S. values.

The hum loudness level is expressed as

$$L = 65+20 \log_{10} \frac{E}{pq} \text{ phons} \quad . \quad . \quad 14.7$$

where E = the R.M.S. output voltage from the microphone amplifier
p = the ratio of the voltage across the output meter in the receiver to the voltage at the microphone at 400 c.p.s.
q = the sensitivity of the microphone in volts per dyne per square centimetre at 400 c.p.s.

The hum level is quoted for (1) maximum output hum obtainable without the carrier but with any control setting, and (2) the maximum output for any carrier voltage up to 1 volt and any control setting.

14.9.4. Acoustic Output and Distortion Factor. For the acoustic output-distortion factor measurements, the input carrier (1,000 kc/s) modulated 60% at 400 c.p.s. is adjusted to 20,000 μV.

Readings are taken of distortion factor for different settings of the A.F. volume control, and the result is plotted to a scale as

shown in Fig. 14.7. The intensity level In is calculated from the 400 c.p.s. electrical power output as follows:

$$In_{W_1} = In_W + 10 \log \frac{W_1}{W} \quad . \quad . \quad . \quad 14.8$$

where In_W is the intensity level defined in 14.9.2,
W is the electrical power output defined in 14.9.2,
W_1 is the actual 400 c.p.s. electrical power output measured,
and In_{W_1} is the intensity level corresponding to an electrical power output of W_1.

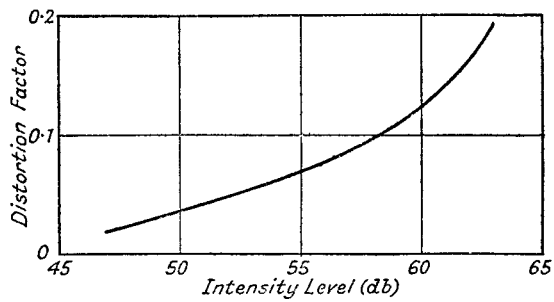

FIG. 14.7.—An Example of a Distortion Factor-Intensity Level Curve.

BIBLIOGRAPHY

1. *Year Book of the Institute of Radio Engineers*, 1931, p. 121.
2. Specification for Testing and Expressing Overall Performance of Radio Receivers. Part 1. Electrical Tests. Part 2. Acoustic Tests. Published by the Radio Manufacturers' Association (England). Dec. 1936.
3. The Evolution of the Phon. D. B. Foster, *Wireless World*, July 9th, 1937, p. 32.
4. Discussion on R.M.A. Specification. *Journal I.E.E.*, July 1937, p. 111.
5. *Standards on Radio Receivers*. The Institute of Radio Engineers. 1938.
6. The A.V.C. Characteristic. M. G. Scroggie, *Wireless World*, May 4th, 1939, p. 427.
7. Broadcast Receivers, A Review. N. M. Rust, O. E. Keall, J. F. Ramsay, K. R. Sturley, *J.I.E.E.*, Part III, June 1941, p. 59.

CHAPTER 15

FREQUENCY MODULATED RECEPTION[19]

15.1. Introduction. The difference between amplitude and frequency modulated transmissions has already been discussed in Chapter 1, Part I, where the corresponding vector and sideband representations are given. In frequency modulated transmission the amplitude of the carrier remains constant, variation of carrier frequency playing the same rôle as amplitude change in the amplitude modulated carrier. The magnitude of the frequency variation, or deviation, of the carrier is directly proportional to the intensity of the modulating signal. Thus, if the modulating signal voltage is doubled, the frequency deviation of the carrier is doubled. The rate at which the latter is varied is that of the modulating frequency. For example, if the intensity of the A.F. signal is such as to vary the carrier frequency by ± 50 kc/s, this variation occurs 1,000 times per second when the modulation frequency is 1,000 c.p.s. In the same manner as with amplitude modulation, the frequency modulated carrier can be resolved into a carrier, of fixed frequency equal to its unmodulated value, and sidebands spaced on either side of the carrier by frequency differences equal to the modulation frequency ; unlike the amplitude modulated carrier, frequency modulation produces more than two sidebands for each modulation frequency. For a given modulating A.F. voltage, the frequency spectrum covered by the essential sidebands is practically independent of the modulating frequency, i.e., a low modulating frequency of given amplitude has a large number of sidebands closely spaced, and a high modulating frequency of the same amplitude has few sidebands widely spaced, covering approximately the same frequency range as the low modulating frequency sidebands. The amplitudes of the carrier and sideband components are a function of the modulating frequency and voltage, and each component passes through a series of zero amplitudes as the amplitude of the modulating voltage is increased from zero. The actual relationship between component amplitudes and modulating frequency and voltage is shown in expression 1.4, Part I, to be of Bessel function form in terms of the modulation index. The latter, which is the ratio of the frequency deviation of the carrier to the modulation frequency, is a function of the modulating voltage because frequency deviation is a result of, and is directly proportional to, the modulation ampli-

tude. The variation of the carrier (f_c) and first ($f_c \pm f_{mod.}$), second ($f_c \pm 2f_{mod.}$) and third ($f_c \pm 3f_{mod.}$) sideband component amplitudes are plotted against modulation index in Fig. 15.1. Taking the carrier component and a modulating frequency of 1,000 c.p.s., we see that the carrier component is zero at modulating voltages corresponding to the following carrier frequency deviations, 2,405, 5,520, 8,654, 11,792, 14,931, 18,071 c.p.s., etc. This feature [8] has been used to measure frequency deviation in a frequency modulated transmitter and to determine the range of modulating voltage over which there is a linear relationship between modulating voltage and carrier frequency deviation. The unmodulated carrier is tuned in on an

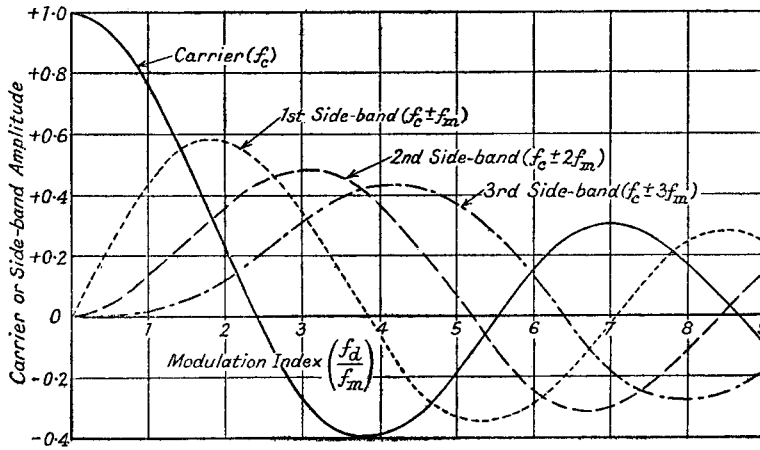

FIG. 15.1.—The Variation of Carrier and Sideband Amplitudes of a F.M. Transmission against Modulation Index $\left[\frac{f_d}{f_{mod.}}\right]$.

[*Note*: For f_m read $f_{mod.}$; f_d = carrier deviation frequency.]

amplitude modulation receiver having a heterodyne oscillator and a highly selective A.F. band-pass filter. The latter is tuned to some convenient audio frequency, such as 1,000 c.p.s., and has a sufficiently narrow pass range to prevent appreciable response from frequencies separated from the tuning frequency by an amount equal to, or greater than, the modulating frequency. Thus if $f_{mod.} = 1{,}000$ c.p.s. the filter should attenuate severely frequencies above about 1,800 c.p.s. and below 200 c.p.s. The filter is terminated by an amplifier and any suitable indicator such as telephones or valve voltmeter. The carrier is now modulated and the modulating amplitude increased until the heterodyne whistle or voltage at the indicator falls to a minimum. This corresponds to a frequency

deviation of 2,405 c.p.s. when $f_{mod.} = 1{,}000$ c.p.s. Other minima are found as the modulating voltage is increased and these correspond to 5,520, 8,654 c.p.s., etc., frequency deviations.

In a frequency modulated receiving system the semi-pass-band width of the receiver must never be less than the highest modulating frequency it is desired to accept, even though the frequency deviation of the carrier is less than the modulating frequency. For example, if the modulating frequency is 10,000 c.p.s. and its amplitude such as to give a carrier frequency deviation of 4,000 c.p.s., there are three pairs of sidebands up to $(f_c \pm 3f_{mod.})$ kc/s, which have amplitudes exceeding 1% of the carrier component, and all these must be accepted by the receiver if correct reproduction is to be obtained, i.e., the receiver pass-band must be $f_c \pm 30$ kc/s. As a general rule we may say that the receiver pass-band width is determined by the highest audio frequency modulating component, when the carrier frequency deviation is much less than the highest modulating frequency, whereas when the reverse is true the band width is determined by the frequency deviation.

There are certain advantages, notably in improved signal-to-noise ratio and reduced volume compression, to the use of frequency in place of amplitude modulation, and these are discussed more fully in the next section.

The receiver design is similar in principle to that of its amplitude modulated counterpart, except for the limiter and the converter for changing the frequency modulated carrier into an amplitude modulated carrier before detection. Some modifications may be necessary in receiving a high fidelity frequency-modulated transmission because the receiver pass-band may require to be about ten times the highest audio frequency (15 kc/s). With high fidelity A.M. transmission no increase in A.F. output is obtained by making the band-width greater than twice the highest audio frequency, and it possesses the serious disadvantage of increasing noise output.

15.2. The Advantages and Disadvantages of Frequency Modulation. Four important advantages can be gained by the use of frequency modulation instead of amplitude modulation, viz.,

(1) greater signal-to-noise ratio
(2) lower transmitter input power for a given A.F. output from the receiver
(3) less amplitude compression of the A.F. modulating signal
(4) larger service area, and smaller interference area between stations on adjacent carrier frequencies.

These advantages can only be realized under certain operating

conditions, chief of which is that reception must be confined to the direct ray [3] from the transmitter. Indirect ray communication, as in short-wave transmission over long distances, is subject to selective fading of the carrier and sidebands (see Section 3.2, Part I), and the audio frequency signal suffers severe distortion. This distortion is usually much worse with frequency than with amplitude modulation because of the large number of sidebands required to convey the correct character of the low-frequency components of the audio signal. Amplitude modulation is much less affected because there is only a pair of sidebands for each modulation frequency component. Hence this effect renders frequency modulation impracticable except on ultra-short waves. High fidelity frequency-modulated transmission with a large frequency deviation (up to ± 75 kc/s) also requires an ultra high frequency carrier.

To understand the reason for the greater signal-to-noise ratio obtained from a F.M. system it is necessary to examine the characteristics of noise, which may be caused by disturbances in, or external to, the receiver. Noise from external sources is mainly of the impulse type, and is due to atmospheric disturbances (these are not normally very serious at ultra high frequencies) or to interference from electrical machinery (the ignition system of a car, switching surges transmitted by the mains supply wiring, etc.). It often has high peak voltages and may be periodic, continuous or spasmodic. In a well-designed receiver, internal noise is due to random motion of the electrons in the conductors and the valves, the important sources being the aerial, the first tuned circuit and the first valve. Thermal (conductor) and shot (valve) noise—see Sections 4.9.2 and 4.9.3, Part I—have frequency components covering a very wide range and continually varying in amplitude. With an amplitude modulation receiver each noise voltage, in the absence of a carrier, can interact with other noise components within audible range of it to produce the characteristic A.F. hiss, and the wider the pass-band the worse is the noise. If a carrier is applied and is large enough to ensure linear detection, the noise voltages act as sidebands to the applied carrier and audible beats are now only produced between the carrier and noise, i.e., the carrier demodulates (see Section 8.10, Part I) the noise carriers and interaction between the noise components themselves is suppressed. Hence only those noise components within audio range of the carrier contribute to the noise output ; *

* It is this same principle which operates in the homodyne or reinforced carrier receiver to give increased selectivity when the amplitude of the incoming carrier is increased in the receiver.

in practice we more often find that the application of a carrier increases the noise output, and this may be due to noise on the carrier itself (from the transmitter) and to the fact that the noise voltages alone are not large enough to cause the linear detection point of the A.F. detector to be reached. However, it is still true that only those noise components within audio range of the carrier contribute to the output.

A special device, known as a limiter, is incorporated in a F.M. receiver to suppress amplitude changes of the carrier, so that noise cannot have the same effect as in an A.M. receiver. For the sake of clarity let us consider the action of a single noise frequency component, f_n kc/s, spaced an audio frequency $(f_n - f_c)$ kc/s from the carrier. By considering the carrier as a stationary vector, OA, the noise can be represented as a vector AB rotating round the carrier

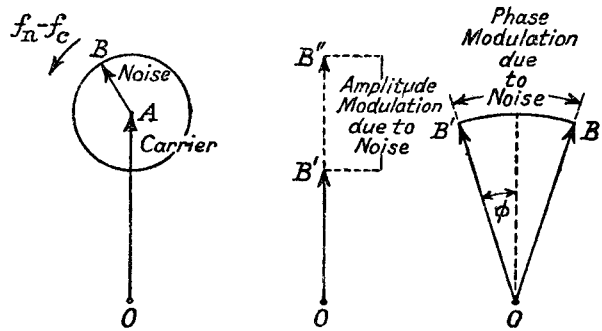

FIG. 15.2.—Amplitude and Phase Modulation of a Carrier Vector by a Single Noise Frequency.

at $(f_n - f_c)$ kc/s as illustrated in Fig. 15.2. We see that there is both amplitude and phase change of the resultant carrier vector OB; the former, which causes the noise output in the A.M. receiver, is suppressed by the limiter in the F.M. receiver, and the latter, which causes a frequency change of the carrier, produces the noise output in the F.M. receiver. A characteristic of phase modulation (see Section 1.4, Part I) is that carrier frequency deviation is directly proportional to the frequency of a constant amplitude modulating signal, so that noise sidebands near to the carrier give much less frequency deviation and consequently much less audio output from a F.M. receiver than those spaced farther from the carrier frequency. This "triangular" distribution of the effective noise sideband voltages reduces the R.M.S. noise voltage output for a maximum carrier frequency deviation of ± 15 kc/s to $\frac{1}{1{\cdot}73}$ of the noise output

from an A.M. receiver having the same maximum pass-band width of ±15 kc/s. This means a signal-to-noise power ratio three times greater than for amplitude modulation, i.e., a gain of 4·75 db. in signal-to-noise ratio. In the case of impulse noise from car ignition systems, etc., Armstrong [2] estimates an improvement of 4 to 1 (6 db.) in signal-to-noise power ratio. It is not necessary to confine the frequency deviation of the carrier to ±15 kc/s, and the signal output is proportionally increased by increasing frequency deviation in the ratio frequency deviation-to-maximum audio modulating voltage, e.g., if the carrier deviation is ±75 kc/s and the maximum audio frequency ±15 kc/s, the signal-to-noise voltage ratio is increased five times or 14 db. Taking the lower estimate for the " triangular " noise distribution, we have a total improvement in signal-to-noise power ratio of 75 to 1, or 18·75 db. The increase in receiver band width to accommodate the greater frequency deviation introduces extra noise sidebands, but if the carrier is large in comparison with the noise (at least twice the peak noise voltage) there is no increase in noise output because the phase modulation of the carrier by the additional noise sidebands is outside the audible range. When the peak carrier-to-noise ratio is less than unity, interaction occurs between the noise components, which phase modulate each other ; in this case noise is increased and signal-to-noise ratio decreased by increasing the receiver pass-band. This causes a well-defined threshold area [7] to appear round a F.M. transmitter ; outside this area better signal-to-noise ratio is obtained with reduced frequency deviation and a narrower receiver pass-band.[12] Inside this area the reverse is true.

Signal-to-noise ratio can be still further improved by the use of " pre-emphasis "—increased amplitude of the higher audio frequencies modulating the transmitter—at the transmitter followed by " de-emphasis " at the receiver. Pre-emphasis and de-emphasis can be applied to A.M. transmissions, but are less effective because all noise sideband voltages contribute equally to the noise output. An improvement in signal-to-noise power ratio of 5·4 to 1, 7·35 db.[10] is realized by pre-emphasis giving a total improvement of 405 to 1 or 26·1 db.

The second advantage of frequency modulation is that less power is required from the mains supply to the transmitter in order to produce a given audio power at the receiver output. In the power amplifier stage of an A.M. transmitter, the D.C. current must be sufficient to allow 100% modulation without serious distortion, i.e., it must be able to accommodate a carrier of twice the unmodulated

value. Since a F.M. carrier has constant amplitude it follows that, either the F.M. transmission gives twice as much effective power as the A.M. transmission for the same D.C. input power, or alternatively the same A.F. signal can be obtained at the output of the F.M. receiver by reducing the D.C. power at the transmitter by one-half. This represents a further increase in signal-to-noise power ratio of 2 to 1, giving a total improvement of 810 to 1 or 29·1 db. Successive stages of improvement are illustrated in Fig. 15.3.

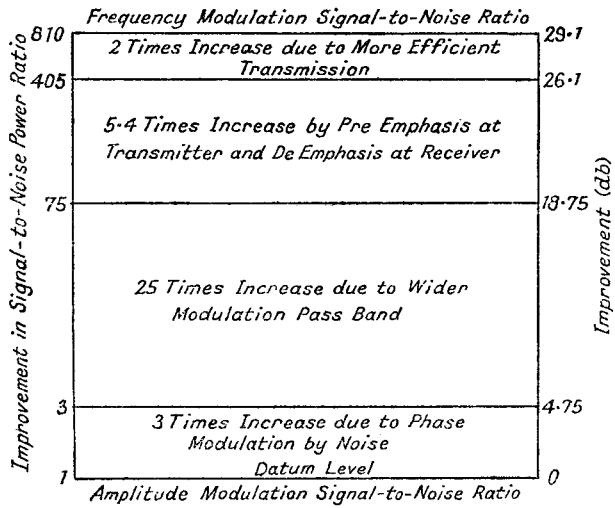

FIG. 15.3.—Successive Stages in Signal-to-Noise Ratio Improvement by the Use of Frequency Modulation.

Reduced compression of the audio signal in a F.M. transmitter really arises out of the increased signal-to-noise ratio. In an A.M. system maximum modulation percentage is limited by modulation envelope distortion to 90%, and a suitable minimum value is 5%, if low level sounds are not to be marred by noise; hence the maximum audio output voltage variation is 18 to 1, giving a power variation of 324 to 1 or 25 db. Clearly the maximum change of 70 db. between the loudest and softest orchestral passage would sound unnatural in a normal room and some compression is essential. The power ratio can, however, with advantage be raised another 20 db. to 45 db., and this is possible with F.M. because of its higher signal-to-noise ratio.

Apart from noise, a very important problem in radio communication is the separation of a desired programme from undesired programmes, and in an A.M. system this limits the closeness of

spacing between the carrier frequencies, and also the service area of a given transmitter. If the separation between the desired and an undesired carrier is equal to an audio frequency, an audible heterodyne note is produced at the receiver output, causing serious interference with the desired programme unless the desired carrier is at least ten times the undesired at the receiver aerial. This limits the service area of either transmitter, and between the two is a large area in which reception of one programme is marred by the other. Increased separation of the carrier frequencies can remove this interference outside the audio range, but the desired signal service area is still restricted by frequency inverted " monkey-chatter " due to fundamental or harmonic sideband overlap (see Section 14.5.2) from the undesired. Powerful A.M. transmitters need to be separated by at least 50 kc/s if the interference area between them is not to be large. A different state of affairs exists with two F.M. transmissions because the limiter in the receiver suppresses amplitude change. Interference, as in the case of noise, occurs due to phase modulation of the desired by the undesired carrier. This phase modulation produces an audio output of frequency equal to the carrier separation and of amplitude directly proportional to the separation frequency. Thus for small carrier separations interference is small ; it is actually most noticeable at a carrier separation of 5 kc/s,[10] for though greater separations give greater equivalent modulation the resultant output becomes less audible. We therefore find that two F.M. transmissions can be operated with small carrier spacing and yet give quite a small interference area (where the desired to undesired carrier amplitude ratio is less than 2 to 1) between them. Interference is worst when both carriers are unmodulated. Although it is possible to operate with small carrier spacing it is usually considered better to adopt a spacing slightly beyond the audio range. Even so this does not call for modification of the statement that the interference area between two F.M. transmissions is very much smaller than the area between two A.M. transmissions of comparable performance.

15.3. The Frequency Modulation Receiver. The F.M. operating frequency ranges, which must be in the ultra short-wave band for the reasons given in Section 15.2, are likely to be from 40 to 50 Mc/s and from 100 to 120 Mc/s, so that the superheterodyne method of reception is essential to achieve sufficient overall amplification. A schematic diagram of a frequency modulation receiver is shown in Fig. 15.4, and we see that it only differs from that of the amplitude modulation receiver by the inclusion of the limiter and frequency-to-amplitude modulation converter stages. The dipole

aerial is connected to a R.F. stage followed by a frequency changer with a local oscillator. After the frequency changer is a series of intermediate frequency amplifier stages, the output of which supplies the limiter. Following the limiter is a converter for changing the

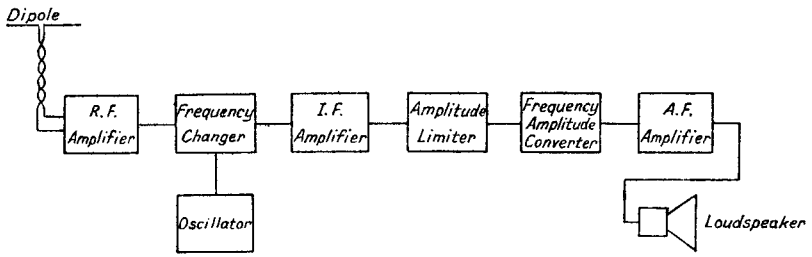

FIG. 15.4.—A Schematic Diagram of a F.M. Receiver.

frequency modulated carrier into an amplitude modulated one, which is then detected in the normal way. The detected output is amplified before it is applied to the loudspeaker.

The purpose for which the receiver is intended determines some of its design features; if it is to be used for high fidelity broadcast transmission the pass-band is wide—about ± 100 kc/s—in order to accommodate the carrier frequency deviation, whereas for communication purposes a pass-band of about ± 15 kc/s only may be necessary. The latter type of receiver has approximately the same pass-band range as a high-fidelity A.M. receiver, and there is little difference between the design of the R.F., frequency changer and I.F. stages of the two types of receiver. On the other hand, the high-fidelity F.M. system operating with large carrier frequency deviations calls for greater damping of all tuned stages, a higher intermediate frequency and, in order to obtain the same amplification, a larger number of I.F. stages. Special methods [15] may be employed to compress carrier frequency deviation after the frequency changer, so as to reduce the required number of I.F. stages. The limiter stage is an essential part of the receiver because amplitude changes of the F.M. carrier, due to noise or transmission variations, are passed on through the frequency-to-amplitude converter to the detector, which is responsive to them. The conversion of the frequency into amplitude modulation is clearly necessary to regain the original character of the audio frequency modulating voltage, which is that of amplitude variation. The A.F. stages of the receiver are identical with those of the comparable A.M. receiver.

Starting from the aerial, we shall now turn to a more detailed examination of the separate stages, illustrating the various features

with special reference to a receiver for high-fidelity transmission, having a frequency deviation of ± 75 kc/s and preset signal-tuned circuits.

15.4. The Aerial Input. This consists of a plain or V dipole aerial dimensioned so as to act as a half-wave resonant aerial approximately at the centre of the range of F.M. transmissions it is desired to accept. Its overall length is about 5% less than one-half of the wavelength of its resonant frequency because, owing to end effects, the equivalent electrical length is always greater than the physical length. Normally a dipole aerial intended to cover a range of frequencies is adjusted to resonate at the geometric mean of the extreme frequencies, but in the case of F.M. transmission covering the range 40 to 50 Mc/s, having a small ratio change of frequency, the difference between the geometric mean 44·6 Mc/s and the arithmetic mean, 45 Mc/s, is negligible. Thus the overall length of a half-wave dipole suitable for the above frequency range is given by

$$l = \frac{0{\cdot}95 \times v}{2f} \text{cms.}$$

where v = velocity of the electro-magnetic wave $\simeq 3 \times 10^{10}$ cms./sec
f = centre frequency of the range in c.p.s.

Therefore
$$l = \frac{0{\cdot}95 \times 3 \times 10^{10}}{90 \times 10^{6}} = 316 \text{ cms.}$$
$$= 10{\cdot}35 \text{ ft.}$$

If a reflector is used it is normally spaced about one-eighth to one-quarter of a wavelength away from the aerial, and it may be a half wavelength long or greater ; a length greater (by about 10%) than a half wavelength helps to give a more constant response [1.3] over the frequency range. The split centre of the dipole is taken via a low impedance ($Z_0 = 70$ to $100\ \Omega$) twin wire feeder to a centre-tapped coil coupled to the first tuned circuit of the receiver. The impedance variation of the dipole, and the transmission loss at the junction of dipole and feeder can be calculated by the methods set out in Sections 3.3.5 and 3.5.3, Part I. Motor-car ignition interference, a serious problem on ultra short waves, is mainly vertically polarized and best signal-to-noise ratio may be found with the dipole aerial horizontal.

15.5. The R.F. Amplifier Stage. The advantages of including a R.F. stage before the frequency changer are increased receiver sensitivity, signal-to-noise ratio, and selectivity against undesired I.F. responses due to interaction between undesired signals, or their

harmonics, and the oscillator, or its harmonics. The first two factors, which are interrelated, are most important. Owing to the use of a limiter stage a high degree of overall amplification (greater than for the corresponding A.M. receiver) is required, and as most of this must be obtained in the I.F. amplifier, instability is a real danger. Additional amplification at the signal frequency (it may be from 6 to 12 times with the high g_m (8 mA/volt) tetrode valve normally used for ultra-short wave amplification) is most desirable because it allows the I.F. amplification to be reduced for the same overall sensitivity. Highest sensitivity is obtained in the R.F. stage by employing optimum coupling between the feeder and first tuned circuit, a R.F. valve having a low input admittance and a high g_m, and an anode circuit having a high resonant impedance. These requirements may, however, conflict with those necessary for maximum signal-to-noise ratio and selectivity. The usual objection to optimum coupling, viz., that an appreciable reactive component is reflected into the first tuned circuit from the aerial, is much less serious at ultra high frequencies because of the feeder connection, which has a low, mainly resistive, and almost constant impedance over the tuning frequency range.

Two conflicting factors enter into the problem of obtaining greatest signal-to-noise ratio, and they arise because there are two sources of noise, the aerial-to-grid connection and the first R.F. valve itself. When valve noise predominates, greatest signal-to-noise ratio is realized by greatest possible signal voltage amplitude at the valve grid, i.e., by using optimum coupling (see Section 3.4.2, Part I) between the feeder and first tuned circuit. On the other hand, if aerial, feeder and first circuit noise is much larger than valve noise, maximum signal-to-noise ratio is realized by a coupling much greater than optimum. If it is assumed that the overall pass-band width of the receiver is independent of the selectivity of the first tuned circuit (this is certainly true of short and ultra short waves), maximum signal-to-noise ratio is obtained by dispensing with the first tuned circuit and coupling the aerial feeder direct to the grid of the first valve, at the same time neutralizing any reactive component in the aerial feeder connection by including an equal and opposite reactance. This procedure cannot, however, ordinarily be followed because of cross-modulation in the R.F. valve and the need to discriminate against signals which are not adjacent in frequency to the desired, but which might produce spurious I.F. responses in the frequency changer.

The signal-to-noise voltage ratio for optimum coupling between

aerial feeder and first tuned circuit is actually 0·707 times [16] (— 3 db.) the maximum possible signal-to-noise ratio obtained by direct coupling from aerial feeder to the grid of the first valve. This can be seen from the formula 4.50, Part I, for conductor noise, which shows that noise voltage is proportional to the square root of the effective conductor resistance. The band-width factor $(f_1 - f_2)$ in this expression is practically that of the I.F. amplifier stages and can be assumed to be unaffected by first circuit selectivity. With optimum coupling between the aerial feeder and first tuned circuit the effective resistance of the aerial feeder is doubled (see Section 3.4.2, Part I), so that the noise voltage is effectively increased by $\sqrt{2}$ or 1·414. Since greatest signal-to-valve noise ratio calls for maximum input signal, and the selectivity of the first tuned circuit is rapidly reduced when optimum coupling is exceeded (at optimum coupling it is only one-half the maximum possible), it is better from a practical point of view to use optimum coupling. It is in any case essential if it is desired to terminate the feeder correctly with its characteristic impedance.

An important feature of the R.F. valve at ultra high frequencies is its grid input admittance. This limits the transfer voltage ratio (see Section 3.4.2, Part I) from aerial feeder to the grid of the R.F. valve, and also the selectivity of the first tuned circuit. Degenerative voltage feedback from the cathode into the grid circuit through the grid-cathode interelectrode capacitance is mainly responsible for high input admittance (see Section 2.8.3, Part I). The degenerative voltage is developed in the inductance of the cathode-earth lead. Electron transit time also contributes to give a high grid input admittance. Special methods have been developed for reducing the degenerative effect of the grid-cathode capacitance by neutralizing the lead inductance. This is achieved by inserting a parallel combination of resistance and capacitance in series with the cathode earth lead and it is discussed in Sections 2.8.3 and 4.10.3, Part I. In the analysis which follows we shall assume that no special precautions are taken. In Section 2.8.3, Part I, a simplified formula for the conductance component of the input admittance is shown to be

$$G_g = g_m \omega^2 C_{gk} L_k \quad . \quad . \quad . \quad . \quad 15.1$$

where g_m = mutual conductance of the valve
C_{gk} = grid-cathode interelectrode capacitance
L_k = inductance of the cathode-earth lead.

Taking $g_m = 8$ mA/volt, $C_{gk} = 3{\cdot}5$ $\mu\mu$F, $L_k = 0{\cdot}1$ μH and

$f = 45$ Mc/s, the conductance is 224 μmhos, which is equivalent to an input parallel resistance of 4,460 Ω; an average value for this type of valve is 3,000 Ω, including electron transit time. If the valve is connected across the whole of the tuned circuit, and optimum coupling is used to the aerial feeder, the maximum possible value of resonant impedance of the tuned circuit is $\frac{3{,}000}{2}$ or 1,500 Ω. Assuming a tuning capacitance of 30 $\mu\mu$F (valve and stray wiring capacitances preclude a much lower value being used), the tuning inductance value at 45 Mc/s is 0·416 μH and the maximum effective magnification of the tuned circuit is

$$Q = \frac{R_D}{\omega L} = \frac{1{,}500}{2\pi \times 45 \times 10^6 \times 0{\cdot}416 \times 10^{-6}}$$
$$= 12{\cdot}75.$$

The pass-band width, i.e., twice the off-tune frequency at which the response of the tuned circuit falls to 0·707 of its maximum value, is given by

$$2\Delta f = \frac{f_r}{Q} = \frac{45}{12{\cdot}75} = 3{\cdot}53 \text{ Mc/s}.$$

Such a circuit could therefore be used to accept transmissions covering a range approximately from 43 to 47 Mc/s when tuned to 45 Mc/s, and it is clear that signal tuning would confer little advantage over this range, which can accommodate twenty high-fidelity F.M. transmissions having frequency deviations not exceeding ± 100 kc/s. This wide pass-band range, together with the restricted range of ultra high frequency transmission, favours preset tuning of the R.F. stage to the centre of the desired range, discrimination against adjacent transmissions being achieved in the I.F. amplifier, and variable tuning by oscillator frequency adjustment. When signal circuit tuning is employed, selectivity can be improved, at the expense usually of sensitivity and signal-to-noise ratio, by tapping the valve grid into a portion only of the tuning coil. For example, if the grid of the valve is tapped halfway down the coil the equivalent parallel damping resistance across the whole tuning coil is increased to 12,000 Ω from the valve. This is reduced to 6,000 Ω by optimum coupling to the aerial feeder so that maximum possible Q is increased to 51 and the band width reduced to 0·88 Mc/s. Reduced aerial feeder coupling could be employed to raise Q still further, and it is interesting to note that in order to produce a pass-band of 0·2 Mc/s, Q would need to be raised to $\frac{45}{0{\cdot}2} = 225$. As

a general rule an overall Q much higher than 50 would not be practicable in the first tuned circuit.

Adjustment of signal tuning may be by variation of capacitance or inductance. The disadvantage of variable capacitance tuning is that it increases the minimum tuning capacitance, reduces the already small value of tuning inductance, and also reduces the resonant impedance $\left[\frac{L}{CR}\right]$ of the tuned circuit. The latter is a more serious disadvantage in the anode circuit of the R.F. valve. Inductance tuning is usually accomplished by screwing a metal plunger in or out of the coil. The plunger, which acts as a short-circuited turn to reduce the inductance, must be of high-conductivity material (copper or brass) if it is not to reduce the Q of the coil to a very low value. This form of eddy current tuning has two disadvantages. Losses are introduced into the coil and the Q of the coil falls (rapidly at first) as the plunger or " slug " is inserted. The frequency range, which can be obtained, is limited due to the difficulty of designing a simple mechanical arrangement which will permit a high degree of coupling between coil and plunger. Stray wiring inductance, which has an effect similar to stray capacitance in the capacitively tuned circuit, also reduces the frequency range. A frequency range variation [14] of 1·5 to 1 is realizable practically, and the ratio change of Q over the same range of frequency is of the order of 0·4 to 1 for a copper plunger, and 0·3 to 1 for brass. Maximum Q is obtained at the low-frequency end of the range. The reduction in Q at the high-frequency end of the range is due to the reduction of effective inductance, the increase in the coil resistance and the resistance reflected into the coil from the plunger. Owing to this reduction in Q as tuning frequency increases, the resonant impedance is greatest at the low-frequency end of the range, and its variation over the range is generally greater than with capacitance tuning. Plotting tuning frequency against plunger position relative to the coil gives an S-shaped curve,[14] frequency change being less as the edge of the plunger is just entering the coil, being greatest when the edge is passing through the centre of the coil, and then reducing again as the edge of the plunger approaches the other end of the coil. Eccentricity of the plunger with respect to the coil appears to have very little effect on L and Q.

In the layout of the R.F. stage the usual precautions appropriate to ultra high frequency operation must be taken ; leads should be as short as possible, all earth connections taken to the same point on the chassis, and there should be adequate decoupling, by mica

capacitors, of electrodes normally carrying only D.C. or A.C. supply voltages (screens, cathodes, heaters, etc.). A typical aerial and R.F. amplifier stage with preset signal tuning is illustrated in Fig. 15.5, which is drawn to emphasize the points enumerated above. Capacitors C_3, C_4, C_6, C_7 and C_8 (mica 0·001 μF) are for by-passing radio frequencies to earth. The tuning capacitances in the grid and anode circuits are made up of the low value variable air capacitors C_2 and C_5 and the stray capacitances, consisting of the valve, wiring and coil self-capacitances, which are shown dotted as C_2' and C_5'. Alternatively the additional capacitors may be omitted and the inductance "trimmed" by using eddy current tuning with a plunger. The two capacitors C_1 are inserted in each feeder line to neutralize the inductance of L_1, which would normally

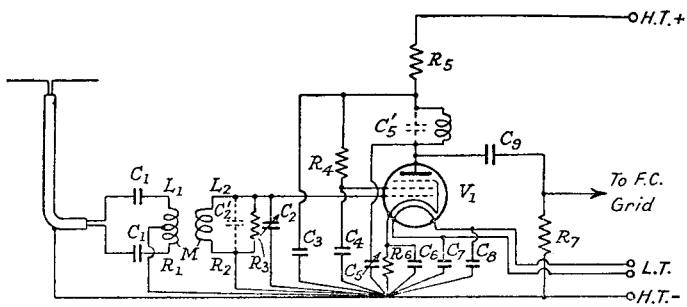

Fig. 15.5.—The Aerial and R.F. Amplifier Stage for a F.M. Receiver

[The coil in the anode of V_1 is L_3.]

mean a reactive as well as resistive termination for the feeder. They are not essential if maximum possible sensitivity and signal-to-noise ratio (with optimum coupling) are not required. The series screen resistance R_4 should be about 50,000 Ω, and if there is any tendency to parasitic oscillation a resistance of 50 Ω may be inserted between the screen pin and the junction of R_4 and C_4. The anode decoupling resistance R_5 is 1,000 Ω. A.G.C. bias can be applied to this stage, but is not desirable (and rarely necessary since the I.F. stages can provide the required control) because change of bias decreases grid input conductance and capacitance, so detuning the first tuned circuit and reducing its pass-band range. A self-bias resistance R_6 of 150 Ω is suitable.

Assuming the R.F. stage to be preset tuned to 45 Mc/s with an overall pass-band of 4 Mc/s, the details of the aerial input circuit are as follows:

Radiation resistance of dipole aerial $= 80\ \Omega$

Characteristic impedance of the aerial feeder $= 80\ \Omega$

Total inductance of the centre-tapped primary coil L_1 (any suitable value can be chosen. It should preferably be less than L_2, and, if C_1 is not used, should be as small as possible consistent with obtaining the required value of M_1 with L_2) $= 0{\cdot}28\ \mu\text{H}$

Capacitance C_1 $\left(\frac{C_1}{2}\text{ tunes } L_1 \text{ to } 45\text{ Mc/s}\right)$ $= 89\ \mu\mu\text{F}$

Two capacitors of 100 $\mu\mu$F would probably give satisfactory results.

Assumed total capacitance across secondary coil L_2, made up of 15 $\mu\mu$F from valve interelectrode and electronic capacitance and 15 $\mu\mu$F from wiring and coil self-capacitance $= 30\ \mu\mu\text{F}$

Total inductance of secondary coil L_2 $= 0{\cdot}416\ \mu\text{H}$

Assumed undamped Q of secondary circuit, Q_0 $= 150$

Resonant impedance of the undamped secondary circuit $= Q_0\omega L_2 = 17{,}630\ \Omega$

Grid input resistance, R_{g1}, of the R.F. valve at 45 Mc/s $= 3{,}000\ \Omega$

Owing to the inclusion of C_1 the aerial feeder-to-grid transformer has a tuned primary and secondary, and the Q of both these circuits influence the pass-band response. However, the Q of the primary (owing to the feeder connection) is so low that the pass-band is almost entirely determined by the Q of the secondary coil, and we need only consider the design of the grid-tuned circuit as far as pass-band characteristics are concerned. Hence, treating the aerial-grid transformer as a single tuned circuit and allowing a loss of $-1{\cdot}5$ db. at the extremes of the pass range, 43 and 47 Mc/s, we find from Fig. 4.3, Part I, that $QF = 0{\cdot}642$, or the Q of the grid-tuned circuit is required to be $Q_0'' = \dfrac{0{\cdot}642 f_m}{2\Delta f} = \dfrac{0{\cdot}642 \times 45}{4} = 7{\cdot}23$.

This includes the damping due to the aerial feeder coupling, which is optimum and therefore halves the uncoupled Q value, so that the required Q in the absence of aerial feeder coupling is

$$Q_0' = 14{\cdot}46$$

and this is equivalent to a resonant impedance of

$$R_D' = Q_0'\omega L_2 = 1{,}700\ \Omega.$$

The resonant impedance of the coil when damped by the valve is $\frac{17{,}630 \times 3{,}000}{17{,}630+3{,}000} = 2{,}560\ \Omega$, so that an additional damping resistance (R_3 in Fig. 15.5) of 5,060 Ω is needed across the tuned circuit.

The mutual inductance between L_1 and L_2 for optimum coupling (see expression on 3.21, Part I) is

$$M_1 = \frac{Z_{a1}}{\omega}\sqrt{\frac{R_2'}{R_{a1}}}$$

where Z_{a1} = total impedance of the primary circuit

$$= \sqrt{R_{a1}^2+X_{a1}^2}$$

where R_{a1} = series resistance of primary circuit and is approximately the characteristic impedance of the feeder

$$X_{a1} = \omega L_1 - \frac{2}{\omega C_1} = 0$$

R_2' = effective series resistance of the secondary circuit, including the valve and additional damping

$$= \frac{\omega L_2}{Q_0'} = 8{\cdot}12\ \Omega$$

$$\therefore\ M_1 = \frac{\sqrt{R_2'R_{a1}}}{\omega} = \frac{\sqrt{8{\cdot}12 \times 80}}{6{\cdot}28 \times 45 \times 10^6} = 0{\cdot}09\ \mu\text{H}.$$

It will be noted that the impedance reflected across the feeder terminals is resistive and equal to $\frac{\omega^2 M_1^2}{R_2'} = 80\ \Omega$.

If the coils L_1 and L_2 are wound on a $\frac{1}{2}$-in. diameter former with 16 S.W.G. copper at 10 turns per inch, the required number of turns is approximately 4 and 6 respectively.

The formula for transfer voltage ratio from the feeder to the grid of V_1 is from expression 3.20*c*, Part I.

$$T_{R\ (optimum\ coupling)} = \frac{1}{2\omega C_2\sqrt{R_{a1}R_2'}}.$$

But

$$R_2' = \frac{(\omega L_2)^2}{R_D'} = \frac{1}{(\omega C_2)^2 R_D'}.$$

$$\therefore\ T_{R\ (optimum\ coupling)} = \frac{1}{2}\sqrt{\frac{R_D'}{R_{a1}}} \quad . \quad . \quad . \quad 15.2$$

$$= \frac{1}{2}\sqrt{\frac{1{,}700}{80}}$$

$$= 2{\cdot}31.$$

We can now check the assumption made above that the double-tuned feeder-to-tuned circuit transformer has a frequency response almost the same as that for a single-tuned circuit of half the Q of the secondary tuned circuit, i.e., $\frac{1}{2}Q_0'$. From expression 7.2*b*, Part I, the modulus of the transfer impedance for two dissimilar circuits tuned to the same frequency is

$$|Z_T| = \frac{R_{D1}Q_2k\sqrt{\frac{L_2}{L_1}}}{\sqrt{[1+Q_1Q_2(k^2-F^2)]^2+(Q_1+Q_2)^2F^2}}$$

and the ratio frequency response is

$$\frac{|Z_T|_{F\neq 0}}{|Z_T|_{F=0}} = \frac{1+Q_1Q_2k^2}{\sqrt{[1+Q_1Q_2(k^2-F^2)]^2+(Q_1+Q_2)^2F^2}}$$

$$= \frac{2}{\sqrt{(2-Q_1Q_2F^2)^2+(Q_1+Q_2)^2F^2}} \quad . \quad . \quad 15.3a$$

for optimum coupling when $Q_1Q_2k^2 = 1$.
Writing the above in terms of a decibel loss

$$\text{Loss (db.)} = -20\log_{10}\frac{|Z_T|_{F=0}}{|Z_T|_{F\neq 0}}$$

$$= -10\log_{10}\frac{(2-Q_1Q_2F^2)^2+(Q_1+Q_2)^2F^2}{4} \quad . \quad . \quad 15.3b.$$

In the single tuned circuit we assumed a loss of $-1{\cdot}5$ db., which gives the expression

$$\frac{Q_0'}{2}F = 0{\cdot}642.$$

or

$$Q_0'F = Q_2F = 1{\cdot}284.$$

$$Q_1 = \frac{\omega L_1}{R_{a1}} = \frac{6{\cdot}28 \times 45 \times 0{\cdot}28}{80} = 0{\cdot}99.$$

Hence $Q_1F = 0{\cdot}088$, and $Q_1Q_2F^2 = 0{\cdot}1131$, so that

$$\text{loss (db.)} = -10\log_{10}\frac{(3{\cdot}55+1{\cdot}88)}{4} = -10\log_{10}1{\cdot}358$$

$$= -1{\cdot}32 \text{ db.}$$

The actual frequency response is therefore slightly better than that obtained on the assumption that the feeder double-tuned transformer is equivalent to a single-tuned circuit of half the secondary circuit Q value. The difference is, however, so slight as to be almost insignificant. It is interesting to note that the generalized selectivity curves of Fig. 7.7, Part I, can be applied to double-tuned

coupled circuits of dissimilar characteristics [17] but tuned to the same frequency.

The formula for thermal noise R.M.S. voltage in the first tuned circuit is (expression 4.50, Part I)

$$E_n = 1{\cdot}25 \times 10^{-10}\sqrt{R_D(f_1 - f_2)},$$

where R_D is the final resonant impedance of the secondary tuned circuit when damping from the feeder is taken into consideration, i.e., it equals $\frac{1}{2}R'_D$, and $(f_1 - f_2)$ is the overall pass-band of the receiver.

Thus
$$R_D = \frac{R_D'}{2} = 850\ \Omega,$$

and $f_1 - f_2 = 200$ kc/s for high fidelity F.M. transmission of ± 75 kc/s frequency deviation. The noise in the R.F. valve is usually expressed in the form of a resistance, and when this is known it may be added to the resonant impedance of the tuned circuit in order to calculate the total effective noise voltage at the grid of the first valve. An average value for the type of valve used is 1,500 Ω, so that the total equivalent noise resistance is 2,350 Ω and the noise voltage at the grid is

$$\begin{aligned} E_n &= 1{\cdot}25 \times 10^{-10}\sqrt{2{,}350 \times 200 \times 10^3} \\ &= 2{\cdot}71\ \mu V \\ &\equiv \frac{2{\cdot}71}{T_R} \equiv 1{\cdot}172\ \mu V \end{aligned}$$

noise output at the feeder. If it is assumed that high fidelity transmission requires a signal-to-noise ratio not less than 20 db., the receiver fulfils this requirement for all carrier voltages exceeding 11.72 μV at the feeder output. The decision not to exceed optimum coupling between feeder and first tuned circuit is seen to be justified because the valve noise resistance is greater than that of the circuit. Increased coupling reduces R_D, and hence the noise voltage at the grid of V_1, but the resulting reduction in transfer voltage ratio offsets this and increases the effective noise voltage at the output of the feeder, so reducing the overall signal-to-noise ratio. Since the reactance of L_1 is neutralized by $\frac{1}{2}C_1$, no reactance component is reflected from the feeder into the tuned circuit, and tuning of the latter is unaffected by the coupling.

Should continuous capacitance tuning be required over the range 40 to 50 Mc/s (a ratio change of 1·25), a change of capacitance of 1·563 is needed. This can be achieved by a tuning capacitor of 25 $\mu\mu$F maximum and 5 $\mu\mu$F minimum value.

Alternatively, a larger capacitor may be used with a series padding capacitor inserted to reduce its range factor. The secondary inductance L_2 must be reduced to 0·287 μH so as to resonate at 40 Mc/s with 55 $\mu\mu$F ($C_2+C_t(max.)$). To make variable tuning of value, the damping across the tuned circuit from the valve must be reduced, and we shall assume that the valve is tapped across one-third of the coil. Optimum coupling between feeder and coil must still be retained in order to terminate the feeder in 80 Ω. The capacitors C_1, neutralizing the reactance of L_1, are omitted because it is not convenient to vary them in step with C_2, and unless this is done a large reactive component is reflected into the secondary circuit as the secondary tuning frequency is changed from the resonant frequency of the primary. The unneutralized reactance of L_1 itself reflects a reactive component into the secondary, but it is shown later to be almost equivalent to a constant negative capacitance over the frequency range, and can be compensated by adding a capacitor in parallel with C_2.

For $L_2 = 0{\cdot}287$ μH, $Q_0 = 150$, $f = 45$ Mc/s, and the valve tapped across one-third of the coil, the equivalent valve damping resistance across the secondary tuned circuit ($R_{g1} = 3{,}000\ \Omega$) is 27,000 Ω

$$\therefore\ Q_0' = \frac{Q_0.27{,}000}{Q_0\omega L_2+27{,}000} = 150.\frac{27{,}000}{39{,}190} = 103{\cdot}3.$$

$$R_D' = Q_0'\omega L_2 = 103{\cdot}3 \times 81{\cdot}3 = 8{,}420\ \Omega, \text{ and } R_2' = \frac{\omega L_2}{Q_0'} = 0{\cdot}788\ \Omega.$$

Assuming $L_1 = 0{\cdot}14$ μH—it is deliberately reduced to improve feeder matching—$X_{a1} = 39{\cdot}6\ \Omega$, and

$$Z_{a1} = \sqrt{R_{a1}^2+X_{a1}^2} = \sqrt{80^2+39{\cdot}6^2} = 89{\cdot}2\ \Omega.$$

The value of M_1 for optimum coupling is

$$M_1 = \frac{Z_{a1}}{\omega}\sqrt{\frac{R_2'}{R_{a1}}} = \frac{89{\cdot}2}{6{\cdot}28 \times 45 \times 10^6}\sqrt{\frac{0{\cdot}788}{80}} = 0{\cdot}0313\ \mu\text{H}.$$

The final Q_0'' of the secondary circuit is halved by the feeder connection to 51·65 so that the pass-band width is

$$2\Delta f = \frac{45}{51{\cdot}65} = 0{\cdot}87 \text{ Mc/s}.$$

The pass-band is much larger than is required, but it must be remembered that this does not include the selectivity of the anode-tuned circuit of the R.F. amplifier, and the overall pass-band width would be about one-half this value, i.e., 0·435 Mc/s.

The overall resonant impedance of the tuned circuit is

$$R_D'' = \omega L_2 Q_0'' = 81{\cdot}3 \times 51{\cdot}65 = 4{,}200\ \Omega$$

and this is reduced to $\frac{R_D''}{9}$ across the grid of V_1. Hence the total equivalent noise resistance in the grid circuit is 1,500 (valve) +466 (circuit) = 1,966 Ω and the noise voltage is

$$E_n = 1{\cdot}25 \times 10^{-10}\sqrt{1{,}966 \times 200 \times 10^3}$$
$$= 2{\cdot}475\ \mu\text{V}.$$

The transfer voltage ratio from feeder to tuned circuit is

$$T_R = \tfrac{1}{2}\sqrt{\frac{R_D'}{R_{a1}}} = \tfrac{1}{2}\sqrt{\frac{8{,}420}{80}}.$$
$$= 5{\cdot}12.$$

The transfer voltage ratio to the grid of V_1 is one-third of this, viz., 1·706, so that the equivalent noise voltage at the output of the feeder is $\frac{2{\cdot}475}{1{\cdot}706} = 1{\cdot}45\ \mu$V; hence there is some reduction in signal-to-noise ratio and also in sensitivity due to tapping down as compared with wide-band preset tuning at 45 Mc/s.

The reactive component reflected into the secondary from the unneutralized reactance of L_1 is such as to increase the required value of tuning capacitance C_2 (see expression 3.23*b*, Part I) to

$$C_2 = \frac{C_{20}}{1 - \dfrac{\omega^2 M_1^2 X_{a1}}{\omega L_2 |Z_{a1}|^2}}$$

where C_{20} = the initial tuning capacitance with no aerial feeder coupling.

The values of C_{20}, $\frac{\omega^2 M_1^2 X_{a1}}{\omega L_2 |Z_{a1}|^2}$, C_2 and $C_2 - C_{20}$ for 40, 45 and 50 Mc/s are tabulated below:

f_r	C_{20}	$\frac{\omega^2 M_1^2 X_{a1}}{\omega L_2 \lvert Z_{a1}\rvert^2}$	C_2	$C_2 - C_{20}$
40 Mc/s	55 $\mu\mu$F	0·00397	55·22 $\mu\mu$F	0·22 $\mu\mu$F
45 ,,	43·5 ,,	0·00481	43·71 ,,	0·21 ,,
50 ,,	35·2 ,,	0·00566	35·4 ,,	0·21 ,,

The reflected reactive component is equivalent to an almost constant negative capacitance of 0·21 $\mu\mu$F over the frequency range 40 to 50 Mc/s, and can therefore be neutralized by the addition of 0·21 $\mu\mu$F across C_2.

The preset signal circuit between the R.F. and the frequency changer valves may be inserted in the anode of the former and connected by capacitance to the grid of the latter. This has the advantage of simplicity and, generally, highest stage gain from the grid of V_1 to the grid of V_2, and it is quite satisfactory when preset tuning is employed. Its disadvantage, when continuously variable tuning is used, is that of high stray capacitance ; the capacitances of both valves V_1 and V_2 are across the tuned circuit, and either transformer coupling must be used—this removes the anode-earth capacitance of V_1 from the tuned circuit—or the minimum capacitance in the aerial tuned circuit must be increased, if signal circuit ganging is to be achieved. We shall assume, therefore, that the anode tuning capacitor of Fig. 15.5 is 40 $\mu\mu$F, the extra 10 $\mu\mu$F above that of C_2 being due to the anode-earth capacitance of V_1 ; hence L_3 is 0·312 μH. The resistance R_7 is the grid leak for the frequency changer valve and also the damping resistance for widening the overall pass-band range to 4 Mc/s. The required final Q of the tuned circuit for a loss of $-$ 1·5 db. over the range 45 ± 2 Mc/s is the same as for the aerial circuit, i.e., 7·23. The coupling capacitance C_9 (500 $\mu\mu$F) is chosen to have negligible reactance in comparison with the resistance R_7, the value of which depends on the type of frequency changer used. A hexode frequency changer has a low positive grid input resistance component, R_{g2}, of the same order as that of the R.F. valve, whereas a heptode valve may present a high positive or even a negative resistance component (Section 5.8.3, Part I). For the purposes of calculation a hexode frequency changer of input resistance equal to 3,000 Ω is assumed. Taking the initial Q_0 of the tuned circuit as 150, the total damping resistance to produce a final Q_0'' of 7.23 is

$$R_T = \frac{\omega L_3 Q_0 Q_0''}{Q_0 - Q_0''} = \frac{88{\cdot}2 \times 150 \times 7{\cdot}23}{142{\cdot}77} = 670\ \Omega.$$

$$\therefore\ R_7 = \frac{R_{g2} \cdot R_T}{R_{g2} - R_T} = 862\ \Omega.$$

The overall resonant impedance of the tuned circuit is $\omega L_3 Q_0'' = 637\ \Omega$, which gives an amplification of 5·1 from the grid of V_1 to the grid of V_2 when the mutual conductance of V_1 is 8 mA/volt.

15.6. The Frequency Changer and Oscillator Stages. The frequency changer and oscillator stages are considered as one unit because they are interdependent. A hexode, heptode, pentode, or diode frequency changer may be employed, but the former is most

popular, and a typical circuit diagram of a hexode valve with a separate triode oscillator is shown in Fig. 15.6. If a pentode valve is used as a frequency changer, the oscillator voltage is usually applied to the suppressor grid. Cathode [9] application has been tried, but is normally less satisfactory because the cathode-grid inter-electrode capacitance coupling between oscillator voltage source and signal circuit causes an appreciable oscillator voltage to appear in the signal circuit and also disturbs oscillator tuning.

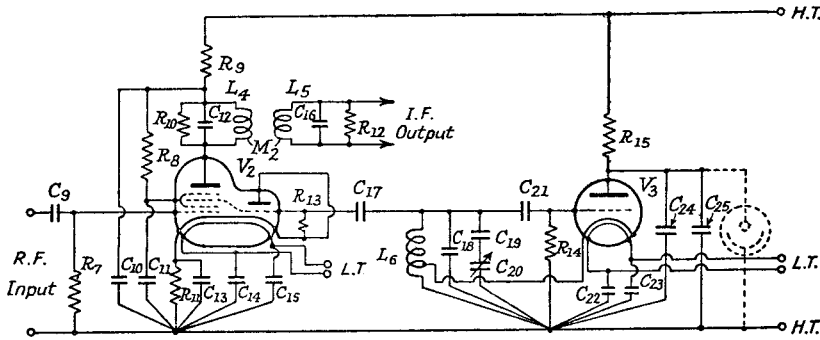

FIG. 15.6.—The Frequency Changer and Oscillator Stages of a F.M. Receiver.

The input to the frequency changer in Fig. 15.6 is the output across R_7 in Fig. 15.5, and the resistance and capacitance numbers lead on from the latter figure. Capacitors C_{10}, C_{11}, C_{13}, C_{14} and C_{15} (0·001 μF mica) by-pass radio frequencies to earth. Resistance R_8 (25,000 Ω) is the voltage-dropping resistance for the screen, R_9 (1,000 Ω) is a decoupling resistance and R_{11} (250 Ω) is the self-bias resistance. Coils L_4, L_5 and capacitors C_{12} and C_{16} are the tuning elements of the I.F. transformer, details of which are given in the next section, 15.7. The resistances R_{10} and R_{12} are damping resistances giving the required band width to the I.F. transformer.

The oscillator is a key point in the ultra high frequency superheterodyne receiver, and a high degree of frequency stability is essential for a satisfactory receiver performance. Frequency error of the oscillator has an effect on frequency modulated reception different from that on amplitude modulation. In the latter case, unless the error is large, detuning results mainly in attenuation (frequency) distortion of the A.F. output with accentuated high-frequency A.F. components producing high-pitched shrill reproduction. With frequency modulated reception, oscillator error limits the maximum permissible frequency deviation of the I.F. carrier, because it off-centres the latter with respect to the frequency-

amplitude converter. Harmonic (amplitude) distortion of the audio output—flattening of the top or bottom half of the wave shape—therefore occurs at high modulation levels (large frequency deviation). The action of the limiter removes the amplitude modulation due to off-centring, and the attentuation distortion, noted with amplitude modulation, is absent. Rapid variation of the oscillator frequency due to hum or interference voltages has no effect in an A.M. receiver because the detector is not responsive to frequency variation but only to amplitude changes. In the F.M. receiver these rapid variations are serious since the frequency-amplitude converter changes them into amplitude variation, and undesired hum or noise interference audio outputs are obtained. We see, therefore, that oscillator long- and short-period frequency stability is of much greater importance in a F.M. system.

The causes of, and remedies for, variations of oscillator frequency are considered in detail in Sections 6.6, 6.7, 6.8 and 6.9, Part I, but for the sake of completeness a brief résumé is given in this chapter. Dealing with the long-period effects, slow drift of oscillator frequency is due mainly to temperature and humidity changes. The tuning inductance and capacitance tend to increase their values with increase of temperature, and heating of the valve changes the operating conditions with consequent change of oscillator frequency. It is generally more difficult to produce a variable capacitor with a low temperature coefficient than a variable inductance, so that inductance tuning is preferable. Inductance variations with temperature result from an increase in radius and length, the first increasing and the second decreasing inductance. Reduced variation is therefore possible by suitably proportioning the coefficients of radial and axial expansion (the radial expansion coefficient should be about half that of the axial). This can be achieved by winding the coil turns loosely on the coil former and fixing the ends firmly so that radial expansion is determined by the conductor, and axial by the coil former. An alternative is to reduce both axial and radial expansion by shrinking the coil on to a former having a low coefficient of expansion, e.g., ceramic material has a coefficient of about 7×10^{-6} as compared with 17×10^{-6} per degree centigrade for copper, so that the dimensional change of such a coil construction is only about one-third of that of the coil without the coil former.

Capacitance temperature changes are due to expansion and insulation dielectric variation. Expansion effects can be reduced by accurate centring of the rotor plates of a variable capacitor or by the use of silvered mica plates in fixed capacitors. Changes of

dielectric constants are reduced by using ceramic material. Certain types of capacitors can be constructed to give a negative temperature coefficient, i.e., capacitance falls as temperature rises, and they may be used to compensate for the positive temperature coefficient of the tuning inductance or main tuning capacitance. Compensation is, however, only complete at one particular setting of the main tuning capacitance, and the temperature of the corrector capacitor together with its rate of correction must follow that of the component it is intended to compensate. Hence it is essential to aim at the highest possible stability before applying correction.

Connecting leads should be short, securely fixed and not in tension. Preliminary cyclical heating is often an aid to frequency stability. Humidity effects are rendered less serious by the use of non-hygroscopic insulation material.

Valve temperature effects are due chiefly to interelectrode dimensional changes (a capacitance variation of the order of 0·02 to 0·04 $\mu\mu$F is obtained from the initial to final operating temperature), and they can be reduced by employing loose coupling between active electrodes and the tuned circuit. In a capacitance-tuned oscillator, frequency changing with a harmonic of the oscillator reduces frequency drift from capacitance variations in inverse ratio to the harmonic employed, e.g., using the second harmonic of the oscillator as the active frequency tends to halve the capacitance-frequency drift. There are disadvantages with oscillator harmonic operation because signals separated by approximately the I.F. from the fundamental and other harmonics will produce spurious responses. Improved frequency stability may be realized by operating the oscillator at a frequency lower than the signal by an amount equal to the I.F., and this confers no disadvantages when the signal circuits have preset tuning. Supply voltage changes may cause slow or rapid changes of frequency. Heater voltage change is comparatively slow in action, affecting valve temperature, cathode emission and cathode heater resistance and capacitance. A palliative is loose coupling to the tuned circuit. Variation of H.T. supply controls frequency through its influence on the g_m and R_a of the oscillator valve, and it is largely responsible for interference frequency modulation troubles. Adequate decoupling and smoothing is an essential to stability, and feedback from the A.F. amplifier is lessened by using a push-pull output stage to the loudspeaker or even a separate H.T. supply.

The great difficulty with ultra high-frequency oscillators is to obtain sufficient amplitude of oscillation without squeggering or

dead spots in the tuning range. A separate triode-valve oscillator should be used rather than the triode section incorporated in the frequency changer, because the former generally has a higher g_m, is more stable and maintains oscillation over a frequency range more satisfactorily. The modified Colpitts circuit (see Section 6.10, Part I)—the anode-cathode and grid-cathode interelectrode capacitances act as the capacitance splitter—is often favoured as it requires no separate reaction coil. Tuned-anode or tuned-grid oscillators are not so satisfactory, because it is not easy to obtain adequate coupling between tuned and reaction coils with a reasonable size of reaction coil. An alternative circuit is the electron-coupled oscillator, and this is the type shown in Fig. 15.6. It possesses three advantages : oscillation is not difficult to maintain over a range of frequencies, negative feedback due to the impedance of that part of the tuning coil between cathode and earth, assists amplitude and frequency stability, and one side of the tuning capacitance C_{20} is earthed. The inductance of the tuning coil L_6 is 0·416 μH, and the cathode tapping on this six-turn coil ($\frac{1}{2}$-in. diam. 16 S.W.G. at 10 turns per inch) occurs at approximately two turns up from the earthed end. The tuning capacitance is made up of the grid-earth capacitance of the triode section of V_2 and V_3 (about 17 $\mu\mu$F), wiring and coil self-capacitance (about 5 $\mu\mu$F), the fixed capacitor C_{18} (7 $\mu\mu$F), and the series combination of C_{19} and C_{20}. C_{19} is a fixed capacitor of 30 $\mu\mu$F restricting the effective range factor of C_{20}, a variable air dielectric capacitor with ceramic insulating supports and minimum and maximum values of 5 and 20 $\mu\mu$F respectively. The oscillator frequency—in order to obtain greatest frequency stability —is selected to be lower than the signal frequency, and variation of C_{20} changes the oscillator frequency from 38·5 to 42·5 Mc/s (the I.F. = 4·5 Mc/s). The oscillator is coupled to the oscillation electrode of the frequency changer via the capacitance C_{17} and self-bias is provided by the resistance R_{13} (50,000 Ω). The value of C_{17} must not be made too large, otherwise the comparatively high input conductance of the oscillation grid of the frequency changer will appreciably reduce or even stop oscillation completely ; about 10 $\mu\mu$F often gives maximum voltage at the frequency changer electrode. The unused anode of the triode part of the triode hexode is returned to cathode. Constant H.T. supply to the oscillator anode is an essential requirement for frequency stability, and two decoupling capacitors are shown in Fig. 15.6 from the anode of V_3 to earth. C_{24} (0·001 μF mica) by-passes radio frequencies and C_{25} (16 μF electrolytic) any audio or hum voltages in the H.T.

supply. Better H.T. regulation and smoothing can be obtained with a gas-filled device such as a neon tube in parallel with C_{24}; C_{25} then becomes unnecessary. R_{15} must be reduced from 30,000 Ω to 10,000 Ω when the neon tube is included.

15.7. The Intermediate Frequency Amplifier. The actual value of the intermediate frequency for high fidelity F.M. transmissions (± 75 kc/s frequency deviation) must be much higher than for high fidelity A.M. transmissions. The required pass-band (200 kc/s) limits the minimum I.F. to 2 Mc/s. A low value has the advantages of greater amplification and selectivity with stability, but the possibility of spurious responses from the frequency changer is greater. These responses (see Section 5.4, Part I) are, in order of importance:

1. The image frequency on the side of the oscillator frequency opposite to the real signal and separated from the latter by twice the intermediate frequency. When image response is only likely from undesired signals in the receiver tuning range, it can be avoided by making the I.F. half this range, e.g., for a receiver covering a range 40 to 50 Mc/s, an I.F. of 5 Mc/s or greater prevents image interference from transmissions in this band.
2. Oscillator harmonic response.
3. Signal harmonic response.
4. Signal and oscillator harmonic combinations.
5. I.F. harmonic response due to the desired signal being close in frequency to an I.F. harmonic.
6. Direct I.F. response, due to an undesired signal at the fundamental or submultiple of the I.F., the latter being converted to the I.F. by the non-linear action of the frequency changer.
7. Interaction between undesired signals separated by a frequency difference equal to the I.F.
8. Cross-modulation.

A high value of I.F. assists in reducing interference from 1, 2, 3, 4 and 7 by removing the interfering signal further from the desired, and allowing R.F. selectivity to be more effective. Interference from 5 and 6 is, however, increased, though that from 5 can generally be made very small by adequate I.F. decoupling of the limiter valve, the detector-A.F. amplifier connection and the A.G.C. line. It is not likely to be serious in this instance since the maximum probable value of I.F. is about 10 Mc/s and fourth harmonic feedback is needed to cause interference in the 40 to 50 Mc/s range. Cross-modulation is rarely a serious problem and Wheeler [11] states that it is negligible in F.M. reception. There are other methods of

reducing unwanted responses ; for example, the prevention of overloading of the frequency changer by applying A.G.C. to the R.F. stage, and increased R.F. selectivity decrease effects from 3 and 4, whilst the reduction of oscillator voltage to the lowest amplitude consistent with satisfactory frequency changing decreases responses from 2 and 4.

The limiter stage requires a certain minimum input voltage (about 2 volts) in order to remove amplitude variation, and overall I.F. amplification must be such as to bring the weakest probable signal up to the limiter input minimum. The intermediate frequency must therefore be fixed at a value which will give the required overall gain without instability or mutilation of the frequency response curve. A value between 4 and 5 Mc/s is a reasonable compromise and subsequent calculations are made on the basis of an I.F. of 4·5 Mc/s.

The problem to be solved in the design of the I.F. amplifier is to obtain highest overall amplification with a frequency response having a level pass-band, little affected by bias changes on the valves, and having rapid attenuation outside the pass range. The level pass-band is a more stringent condition than freedom from instability. Sources of feedback are coupling between input and output, common I.F. impedances in valve electrode leads normally carrying only D.C. or mains A.C. currents (anode H.T. supply, screen, grid bias, cathode and heaters) and grid-anode interelectrode capacitance. The first two can be reduced to negligible proportions by suitable shielding and decoupling. Decoupling capacitors should be connected to earth by the shortest possible leads, and when used to decouple tuned circuits should be included inside the screening cans enclosing the tuning elements. Common impedance coupling can largely be eliminated by connecting decoupling capacitors for each stage to a common earth point, as was done for the R.F. and frequency changer stages. Thus we come to the basic fact that the limit to maximum overall amplification is set by feedback through the anode-grid capacitance. This effect is discussed in detail in Section 7.8, Part I, where it is shown that feedback is negative when the anode circuit is capacitive, and positive when the anode circuit is inductive. The parallel-tuned circuit has a capacitive reactance at frequencies above resonance and an inductive reactance at frequencies below resonance, so that feedback from such an anode circuit is degenerative at the higher frequencies and regenerative at the lower frequencies. Its effect on overall frequency response is to produce a lop-sided curve with greater

amplification at frequencies below resonance. The degree of degeneration or regeneration is best expressed in the form of a positive or negative input resistance (see expression 7.23*a*, Part I)

$$R_g = \frac{(G_a+G_0)^2+B_0^2}{g_m B_{ga} B_0} \quad . \quad . \quad . \quad 15.4a$$

where $G_a = \dfrac{1}{R_a}$ = anode slope conductance

G_0 = conductance of external anode circuit
B_0 = susceptance of external anode circuit
g_m = mutual conductance of valve
B_{ga} = susceptance of anode-grid capacitance
$= \omega C_{ga}$.

This resistance component has a minimum value and the condition for this is found by differentiating 15.4*a* with respect to B_0 and equating to zero. B_0 is treated as the variable because it changes rapidly in the region of resonance, from a high negative value below, through zero at resonance, to a high positive value above. G_0 over the same range is practically constant and equal to the reciprocal of the resonant impedance, i.e., $\dfrac{1}{R_D}$ or $\dfrac{1}{\omega_r LQ}$. The condition for minimum R_g is found to be

$$B_0 = \pm(G_a+G_0)$$

and

$$R_g(min.) = \frac{\pm 2(G_a+G_0)}{g_m B_{ga}} \quad . \quad . \quad . \quad . \quad 15.4b.$$

In the particular case we are considering $G_a \ll G_0$ and

$$R_g(min.) \simeq \frac{\pm 2G_0}{g_m B_{ga}} = \frac{\pm 2}{g_m B_{ga} R_D} \quad . \quad . \quad 15.4c.$$

If instead of a single-tuned circuit there is a double-tuned transformer in the anode circuit, calculation may be based on the assumption that coupling will be in the region of the critical value, and under these conditions one circuit reflects into the other a resistance equal to its initial resistance, i.e., the actual resonant impedance is half that of one tuned circuit alone and expression 15.4*c* becomes

$$R_g(min.) = \frac{\pm 4}{B_{ga} R_D g_m} \quad . \quad . \quad . \quad 15.4d.$$

If it is desired to obtain a more accurate value of $R_g(min.)$ reference should be made to Section 7.8, Part I, but expression 15.4*d* will be found to be satisfactory for all practical purposes.

In order that frequency response may be almost unaffected by

feedback, the minimum resistance component should be at least ten times the effective resonant impedance of the grid circuit, and this condition necessitates the use of a special buffer stage in the I.F. amplifier.

To obtain a flat frequency response over a given pass range it is necessary to combine single- and double-tuned overcoupled circuits, the peak of the single-tuned circuit filling in the trough of the two overcoupled circuits. Much the same effect can be obtained by the combination of a pair of overcoupled with a pair of undercoupled circuits of single-peaked response, and we shall use these principles in the design of the I.F. amplifier, the diagram of which is shown in Fig. 15.7. The frequency changer anode I.F. transformer of Fig. 15.6 is repeated in Fig. 15.7; in its anode circuit is a pair of critically coupled

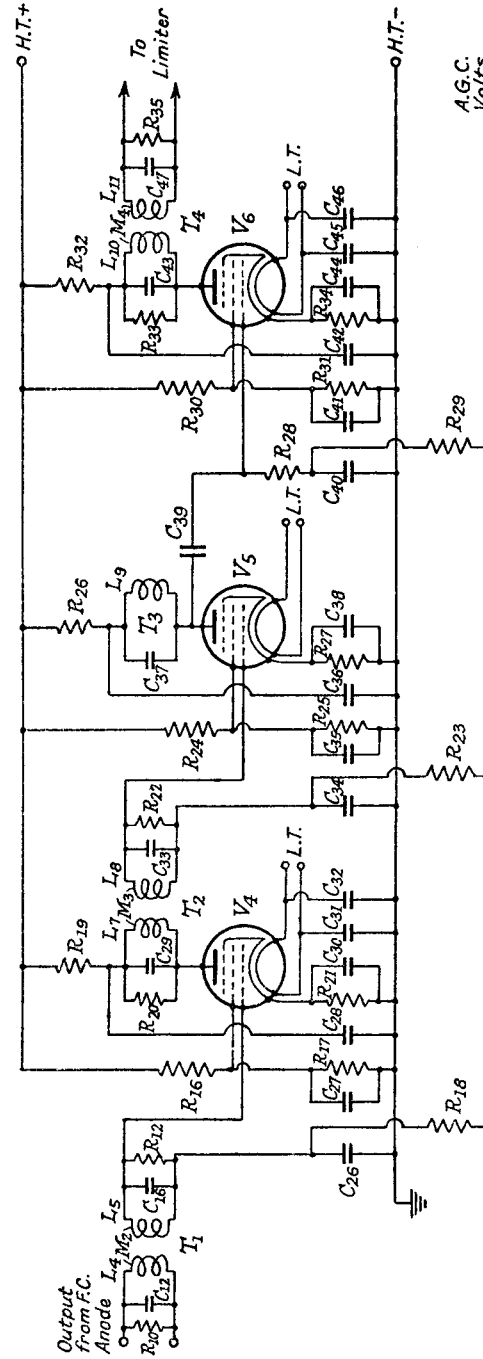

Fig. 15.7.—The I.F. Amplifier Stages of a F.M. Receiver.

supply. Better H.T. regulation and smoothing can be obtained with a gas-filled device such as a neon tube in parallel with C_{24}; C_{25} then becomes unnecessary. R_{15} must be reduced from 30,000 Ω to 10,000 Ω when the neon tube is included.

15.7. The Intermediate Frequency Amplifier. The actual value of the intermediate frequency for high fidelity F.M. transmissions ($\pm$75 kc/s frequency deviation) must be much higher than for high fidelity A.M. transmissions. The required pass-band (200 kc/s) limits the minimum I.F. to 2 Mc/s. A low value has the advantages of greater amplification and selectivity with stability, but the possibility of spurious responses from the frequency changer is greater. These responses (see Section 5.4, Part I) are, in order of importance:

1. The image frequency on the side of the oscillator frequency opposite to the real signal and separated from the latter by twice the intermediate frequency. When image response is only likely from undesired signals in the receiver tuning range, it can be avoided by making the I.F. half this range, e.g., for a receiver covering a range 40 to 50 Mc/s, an I.F. of 5 Mc/s or greater prevents image interference from transmissions in this band.
2. Oscillator harmonic response.
3. Signal harmonic response.
4. Signal and oscillator harmonic combinations.
5. I.F. harmonic response due to the desired signal being close in frequency to an I.F. harmonic.
6. Direct I.F. response, due to an undesired signal at the fundamental or submultiple of the I.F., the latter being converted to the I.F. by the non-linear action of the frequency changer.
7. Interaction between undesired signals separated by a frequency difference equal to the I.F.
8. Cross-modulation.

A high value of I.F. assists in reducing interference from 1, 2, 3, 4 and 7 by removing the interfering signal further from the desired, and allowing R.F. selectivity to be more effective. Interference from 5 and 6 is, however, increased, though that from 5 can generally be made very small by adequate I.F. decoupling of the limiter valve, the detector-A.F. amplifier connection and the A.G.C. line. It is not likely to be serious in this instance since the maximum probable value of I.F. is about 10 Mc/s and fourth harmonic feedback is needed to cause interference in the 40 to 50 Mc/s range. Cross-modulation is rarely a serious problem and Wheeler [11] states that it is negligible in F.M. reception. There are other methods of

reducing unwanted responses ; for example, the prevention of overloading of the frequency changer by applying A.G.C. to the R.F. stage, and increased R.F. selectivity decrease effects from 3 and 4, whilst the reduction of oscillator voltage to the lowest amplitude consistent with satisfactory frequency changing decreases responses from 2 and 4.

The limiter stage requires a certain minimum input voltage (about 2 volts) in order to remove amplitude variation, and overall I.F. amplification must be such as to bring the weakest probable signal up to the limiter input minimum. The intermediate frequency must therefore be fixed at a value which will give the required overall gain without instability or mutilation of the frequency response curve. A value between 4 and 5 Mc/s is a reasonable compromise and subsequent calculations are made on the basis of an I.F. of 4·5 Mc/s.

The problem to be solved in the design of the I.F. amplifier is to obtain highest overall amplification with a frequency response having a level pass-band, little affected by bias changes on the valves, and having rapid attenuation outside the pass range. The level pass-band is a more stringent condition than freedom from instability. Sources of feedback are coupling between input and output, common I.F. impedances in valve electrode leads normally carrying only D.C. or mains A.C. currents (anode H.T. supply, screen, grid bias, cathode and heaters) and grid-anode interelectrode capacitance. The first two can be reduced to negligible proportions by suitable shielding and decoupling. Decoupling capacitors should be connected to earth by the shortest possible leads, and when used to decouple tuned circuits should be included inside the screening cans enclosing the tuning elements. Common impedance coupling can largely be eliminated by connecting decoupling capacitors for each stage to a common earth point, as was done for the R.F. and frequency changer stages. Thus we come to the basic fact that the limit to maximum overall amplification is set by feedback through the anode-grid capacitance. This effect is discussed in detail in Section 7.8, Part I, where it is shown that feedback is negative when the anode circuit is capacitive, and positive when the anode circuit is inductive. The parallel-tuned circuit has a capacitive reactance at frequencies above resonance and an inductive reactance at frequencies below resonance, so that feedback from such an anode circuit is degenerative at the higher frequencies and regenerative at the lower frequencies. Its effect on overall frequency response is to produce a lop-sided curve with greater

amplification at frequencies below resonance. The degree of degeneration or regeneration is best expressed in the form of a positive or negative input resistance (see expression 7.23*a*, Part I)

$$R_g = \frac{(G_a+G_0)^2+B_0^2}{g_m B_{ga} B_0} \quad . \quad . \quad . \quad 15.4a$$

where $G_a = \dfrac{1}{R_a}$ = anode slope conductance

G_0 = conductance of external anode circuit
B_0 = susceptance of external anode circuit
g_m = mutual conductance of valve
B_{ga} = susceptance of anode-grid capacitance
$= \omega C_{ga}$.

This resistance component has a minimum value and the condition for this is found by differentiating 15.4*a* with respect to B_0 and equating to zero. B_0 is treated as the variable because it changes rapidly in the region of resonance, from a high negative value below, through zero at resonance, to a high positive value above. G_0 over the same range is practically constant and equal to the reciprocal of the resonant impedance, i.e., $\dfrac{1}{R_D}$ or $\dfrac{1}{\omega_r LQ}$. The condition for minimum R_g is found to be

$$B_0 = \pm(G_a+G_0)$$

and

$$R_g(min.) = \frac{\pm 2(G_a+G_0)}{g_m B_{ga}} \quad . \quad . \quad . \quad . \quad 15.4b.$$

In the particular case we are considering $G_a \ll G_0$ and

$$R_g(min.) \simeq \frac{\pm 2G_0}{g_m B_{ga}} = \frac{\pm 2}{g_m B_{ga} R_D} \quad . \quad . \quad 15.4c.$$

If instead of a single-tuned circuit there is a double-tuned transformer in the anode circuit, calculation may be based on the assumption that coupling will be in the region of the critical value, and under these conditions one circuit reflects into the other a resistance equal to its initial resistance, i.e., the actual resonant impedance is half that of one tuned circuit alone and expression 15.4*c* becomes

$$R_g(min.) = \frac{\pm 4}{B_{ga} R_D g_m} \quad . \quad . \quad . \quad 15.4d.$$

If it is desired to obtain a more accurate value of $R_g(min.)$ reference should be made to Section 7.8, Part I, but expression 15.4*d* will be found to be satisfactory for all practical purposes.

In order that frequency response may be almost unaffected by

feedback, the minimum resistance component should be at least ten times the effective resonant impedance of the grid circuit, and this condition necessitates the use of a special buffer stage in the I.F. amplifier.

To obtain a flat frequency response over a given pass range it is necessary to combine single- and double-tuned overcoupled circuits, the peak of the single-tuned circuit filling in the trough of the two overcoupled circuits. Much the same effect can be obtained by the combination of a pair of overcoupled with a pair of undercoupled circuits of single-peaked response, and we shall use these principles in the design of the I.F. amplifier, the diagram of which is shown in Fig. 15.7. The frequency changer anode I.F. transformer of Fig. 15.6 is repeated in Fig. 15.7; in its anode circuit is a pair of critically coupled

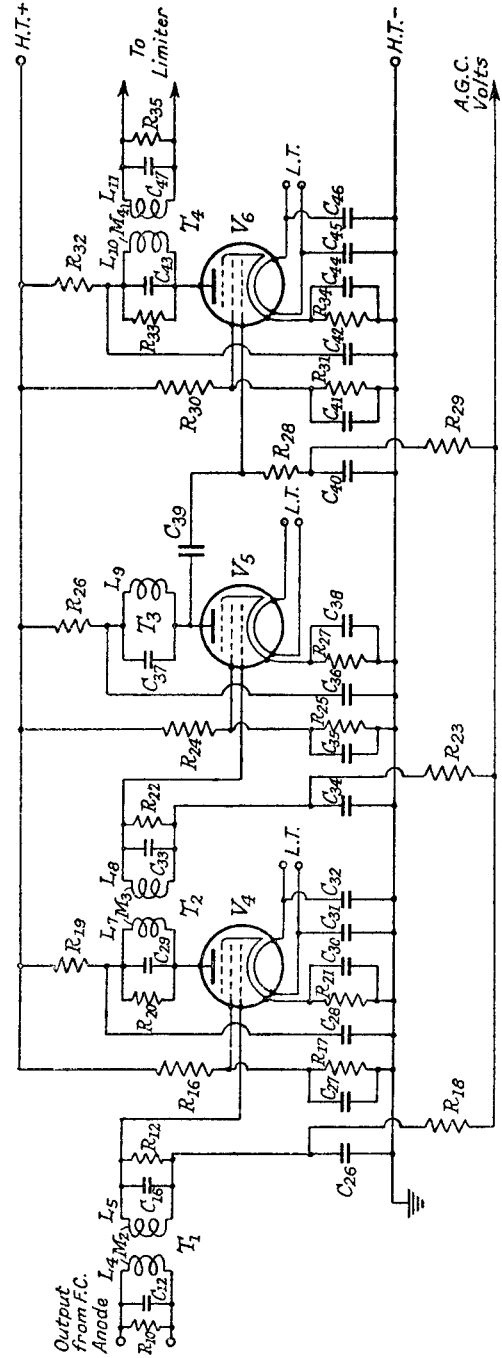

FIG. 15.7.—The I.F. Amplifier Stages of a F.M. Receiver.

tuned circuits. The first and third I.F. amplifier valves V_4 and V_6 each contain a pair of overcoupled circuits, and the second I.F. valve V_5 has a single-tuned circuit. This stage is also acting as a buffer or isolator to reduce anode-grid capacitance feedback to a negligible value. By using the generalized curves of Figs. 4.3, and 7.7, Part I, for the frequency response of single- and double-tuned circuits (the primary of each transformer has constants identical with the secondary), and assuming that transformers T_2 and T_4 are identical, we find that an almost flat pass-band response is obtained by making T_2 and T_4 overcoupled circuits of constant $Q_2k_2 = Q_4k_4 = 2$, T_1 a pair of critically coupled circuits of $Q_1k_1 = 1$, and suitably choosing Q_3 of the single-tuned circuit in the anode of V_5. k is the coupling coefficient, e.g., $\frac{M_2}{\sqrt{L_4L_5}} = \frac{M_2}{L_4}$ for T_1, and Q is the magnification of primary or secondary circuit when the other is not coupled to it. The overcoupled circuits T_2 and T_4 have maximum response at $\frac{Q_2 2\Delta f}{f_r} = \pm 1{\cdot}8$ (see the curve for $Qk = 2$, Fig. 7.7, Part I), where Δf is the frequency off-tune from f_r, the resonant or trough frequency, and the trough-to-peak ratio is -2 db. By selecting Q_2 to satisfy the above expression when $\Delta f = \pm 100$ kc/s (the maximum required semi-band width), we have

$$Q_2 = \frac{1{\cdot}8 f_r}{2\Delta f} = \frac{1{\cdot}8 \times 4{\cdot}5}{0{\cdot}2} = 40{\cdot}5.$$

This fixes the position of the frequency scale on Fig. 7.7, and the combined frequency response of the two transformers is shown as the dotted curve 1 in Fig. 15.8. The single-peaked frequency response of transformer T_1 and tuned circuit L_9C_{37} have losses of 1 and 3 db. respectively at $\frac{Q2\Delta f}{f_r}$ and if Q is selected to make this expression unity when $\Delta f = \pm 100$ kc/s, i.e.,

$$Q_1 = Q_3 = \frac{f_r}{2\Delta f} = 22{\cdot}5$$

the loss in these two circuits at 100 kc/s exactly counterbalances the gain due to T_2 and T_4. Curves 2 and 3 in Fig. 15.8 give the frequency responses for T_1 and T_3 respectively. There is not exact compensation at all frequencies in the pass-band, but the variation in the overall curve 4 does not exceed 0·7 db.

Having determined the Q values for all the circuits, we now have to select L and C values to give maximum overall amplification

and also a grid input resistance component for each valve not less than ten times the effective resonant impedance of its associated grid circuit. In designing the amplifier we shall assume that valves V_4, V_5 and V_6 are identical and have the following constants: $g_m = 2$ mA/volt, $C_{ga} = 0{\cdot}02$ $\mu\mu$F and a slope resistance R_a much

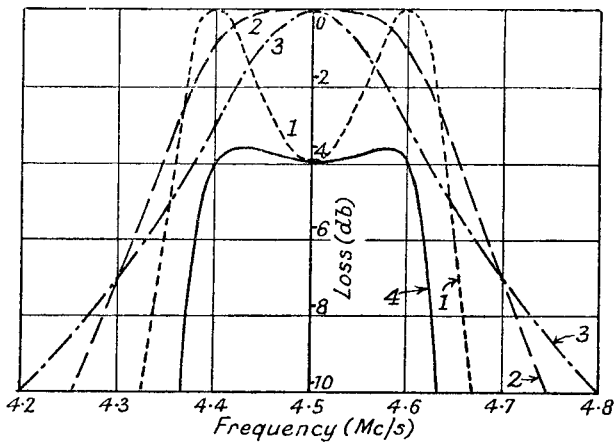

FIG. 15.8.—The Individual and Overall Frequency Responses of the I.F. Amplifier Stages of Fig. 15.7.

greater than the resonant impedance of any anode circuit. Maximum amplification in any stage is obtained by making the effective dynamic impedance $R_D = Q\omega_r L = \dfrac{Q}{\omega_r C}$ as large as possible, i.e., the tuning capacitance C should be as small as possible. A suitable minimum value is 50 $\mu\mu$F so that starting at the last I.F. amplifier with the overcoupled circuits, we have for $f_r = 4{\cdot}5$ Mc/s

$$C_{43} = C_{47} = 50\ \mu\mu\text{F}$$
$$L_{10} = L_{11} = 25\ \mu\text{H}$$
$$Q_4 = 40{\cdot}5$$
$$Q_4 k_4 = 2 \text{ or } k_4 = 0{\cdot}0494$$
$$M_4 = k_4 L_{10} = 1{\cdot}235\ \mu\text{H}.$$

The resonant impedance of either tuned circuit when not coupled to the other is

$$*R_{D4} = \frac{Q_4}{\omega_r C_{43}} = \frac{40{\cdot}5 \times 10^{12}}{6{\cdot}28 \times 4{\cdot}5 \times 10^6 \times 50} = 28{,}700\ \Omega$$

* R_{D4} is the resonant impedance of either primary or secondary alone of the transformer T_4, i.e., the numeral suffix 4 denotes the transformer number in Fig. 15.7. Similarly, R_{D3} and R_{D2} apply to transformers T_3 and T_2. The numeral suffix of Q also denotes the transformer number.

and maximum amplification at the peaks ($f_r \pm 100$ kc/s) of the frequency response of curve 1 in Fig. 15.8 is (see the expression derived from 7.3*f*, Part I)

$$*A_6 = \frac{g_m R_{D4}}{2} = 28{\cdot}7.$$

The damping resistances R_{33} and R_{35} for an initial coil Q_0 of 150 are given by

$$R_{33} = \frac{\omega L_{10} Q_0 Q_4}{Q_0 - Q_4} = \frac{706 \times 150 \times 40{\cdot}5}{150 - 40{\cdot}5} = 39{,}200\ \Omega.$$

and R_{35} has the same value if the succeeding limiter stage does not damp the circuit. In the next section a typical limiter stage is shown to have appreciable damping on the $L_{11}C_{47}$ circuit and R_{35} has to have a higher value than R_{33}.

The minimum input resistance component at the grid of V_6 is from expression 15.4*d*

$$R_{g6}(min.) = \frac{4}{g_m \omega C_{ga} R_{D4}} = \frac{4 \times 10^{12}}{2 \times 10^{-3} \times 6{\cdot}28 \times 4{\cdot}5 \times 10^6 \times 0{\cdot}02 \times 28{,}700}$$
$$= 123{,}200\ \Omega.$$

The resonant impedance of tuned circuit T_3, consisting of L_9 and C_{37}, must not therefore exceed 12,320 Ω if the overall frequency response is not to be seriously affected by feedback. But $Q_3 = 22{\cdot}5$

$$\therefore\ C_{37} = \frac{Q_3}{\omega_r R_{D3}} = \frac{22{\cdot}5 \times 10^{12}}{6{\cdot}28 \times 4{\cdot}5 \times 10^6 \times 12{,}320}\ \mu\mu\text{F}$$
$$= 64{\cdot}5\ \mu\mu\text{F}.$$
$$L_9 = 19{\cdot}4\ \mu\text{H}.$$

If $Q_0 = 150$ and C_{39} (500 $\mu\mu$F) has negligible reactance compared with R_{28}, then

$$R_{28} = \frac{\omega_r L_9 Q_0 Q_3}{Q_0 - Q_3} = \frac{549 \times 150 \times 22{\cdot}5}{127{\cdot}5}$$
$$= 14{,}550\ \Omega.$$

Maximum amplification at $f_r = 4{\cdot}5$ Mc/s is, for the single-tuned circuit,

$$A_5 = g_m R_{D3} = 24{\cdot}64.$$

* The numeral suffix to Amplification A and minimum grid input resistance $R_g(min.)$ defines the number of the valve in Fig. 15.7, with which it is associated. Thus A_6 is the amplification from the grid of V_6 to its output across the secondary of T_4, and $R_{g6}(min.)$ is the minimum grid input resistance of valve V_6.

The minimum grid input resistance

$$R_{g5}(min.) = \frac{2}{g_m \omega C_{ga} R_{D3}} = 143{,}500\ \Omega.$$

The effective resonant impedance of transformer T_2, which is identical with T_4, is $\frac{R_{D2}}{2} = \frac{R_{D4}}{2} = 14{,}350\ \Omega$, and this fulfils the condition that it should be not greater than $\frac{1}{10}R_{g5}$. All the circuit constants for T_2 are identical with those of T_4, i.e.,

$$\begin{aligned} C_{29} &= C_{33} = 50\ \mu\mu\text{F} \\ L_7 &= L_8 = 25\ \mu\text{H} \\ Q_2 &= 40{\cdot}5 \\ M_3 &= 1{\cdot}235\ \mu\text{H} \\ A_4 &= 28{\cdot}7 \text{ at the peaks } (f_r \pm 100) \text{ kc/s} \\ R_{g4}(min.) &= 123{,}200\ \Omega. \end{aligned}$$

Transformer T_1 must therefore have an effective resonant impedance not exceeding 12,320 Ω, i.e., $R_{D1} \not> 24{,}640\ \Omega$. The maximum value of R_{D1} is, however, fixed because $Q_1 = 22{\cdot}5$ $\mu\mu$F and C_{16} is not less than 50 $\mu\mu$F.

$$\therefore\ R_{D1}(max.) = \frac{Q_1}{\omega_r C_{16}} = \frac{22{\cdot}5 \times 10^{12}}{6{\cdot}28 \times 4{\cdot}5 \times 10^6 \times 50}$$
$$= 15{,}900\ \Omega.$$

This value cannot be exceeded without reducing C_{16}, but as it is less than the maximum permitted by feedback considerations it simply means that feedback has even less effect. The constants for T_1 are therefore

$$\begin{aligned} C_{12} &= C_{16} = 50\ \mu\mu\text{F} \\ L_4 &= L_5 = 25\ \mu\text{H} \\ Q_1 &= 22{\cdot}5 \\ Q_1 k_1 &= 1 \text{ or } k_1 = 0{\cdot}0445 \\ M_2 &= k_1 L_4 = 1{\cdot}11\ \mu\text{H}. \end{aligned}$$

Maximum amplification at the peak of response (f_r) for the frequency changer valve V_2 is

$$A_2 = g_c \frac{R_{D1}}{2}$$

where g_c = conversion conductance of the frequency changer valve V_2. A probable value is 0·3 mA/volt.

Hence $A_2 = 0{\cdot}3 \times \frac{15{\cdot}9}{2} = 2{\cdot}385$.

Feedback of I.F. voltage into the grid circuit of V_2 through the

anode-grid capacitance can generally be neglected because the grid circuit is tuned to a much higher frequency.

The values of R_{10} and R_{12} are

$$R_{10} = R_{12} = \frac{\omega_r L_4 Q_0 Q_1}{Q_0 - Q_1} = \frac{706 \times 150 \times 22{\cdot}5}{127{\cdot}5}$$
$$= 18{,}700\ \Omega.$$

The overall amplification from the grid of V_2 to the output of V_6, i.e., to the limiter, is

$$2{\cdot}385 \times 28{\cdot}7 \times 24{\cdot}64 \times 28{\cdot}7 \times 0{\cdot}63 = 30{,}500.$$

The factor 0·63 is included because of the 4-db. peak-to-trough loss in V_4 and V_6.

The total amplification from the grid of the R.F. valve V_1 to the output of V_6 is 30,500 × 5·1 = 155,500, and assuming a signal-to-noise ratio of 20 db., the minimum acceptable signal is 27·1 μV, which produces an output voltage from V_6 of 27·1 × 0·156 = 4·22 volts. This is adequate for operating the limiter stage, the minimum required input voltage for which is usually about 2 volts.

Suitable values for the numbered resistances and capacitances in Fig. 15.7, which have not so far been specified, are tabulated below:

Capacitances.		Resistances.	
$C_{26} = 0{\cdot}001\ \mu F$	$C_{38} = 0{\cdot}1\ \mu F$	$R_{16} = 30{,}000\ \Omega$	$R_{26} = 1{,}000\ \Omega$
$C_{27} = 0{\cdot}1\ \mu F$	$C_{39} = 0{\cdot}0005\ \mu F$	$R_{17} = 20{,}000\ \Omega$	$R_{27} = 300\ \Omega$
$C_{28} = 0{\cdot}1\ \mu F$	$C_{40} = 0{\cdot}001\ \mu F$	$R_{18} = 0{\cdot}1\ M\Omega$	$R_{29} = 0{\cdot}1\ M\Omega$
$C_{30} = 0{\cdot}1\ \mu F$	$C_{41} = 0{\cdot}1\ \mu F$	$R_{19} = 1{,}000\ \Omega$	$R_{30} = 30{,}000\ \Omega$
$C_{31} = 0{\cdot}01\ \mu F$	$C_{42} = 0{\cdot}1\ \mu F$	$R_{21} = 300\ \Omega$	$R_{31} = 20{,}000\ \Omega$
$C_{32} = 0{\cdot}01\ \mu F$	$C_{44} = 0{\cdot}1\ \mu F$	$R_{23} = 0{\cdot}1\ M\Omega$	$R_{32} = 1{,}000\ \Omega$
$C_{34} = 0{\cdot}001\ \mu F$	$C_{45} = 0{\cdot}01\ \mu F$	$R_{24} = 30{,}000\ \Omega$	$R_{34} = 300\ \Omega$
$C_{35} = 0{\cdot}1\ \mu F$	$C_{46} = 0{\cdot}01\ \mu F$	$R_{25} = 20{,}000\ \Omega$	
$C_{36} = 0{\cdot}1\ \mu F$			

The A.G.C. capacitance-resistance filters ($C_{26}R_{18}$, $C_{34}R_{23}$ and $C_{40}R_{29}$) have smaller values than their counterparts in the A.M. receiver because undesired amplitude change of the F.M. carrier, when fed back along the A.G.C. line, tends to cancel the amplitude variation of the carrier. It is a form of negative feedback. The A.G.C. voltage is often derived from the limiter stage grid circuit and the method of obtaining it is described in the next section.

15.8. The Amplitude Limiter.

15.8.1. Introduction. In order to take full advantage of F.M. transmissions, some circuit must be included in the receiver to reduce to negligible proportions any amplitude modulation of

the carrier due to noise or to variation in the overall frequency response of the pass-band. This is essential because the A.F. content of the F.M. signal is extracted by means of an amplitude detector, such as a diode, after its frequency variation has been converted to an amplitude modulation; an initial A.F. amplitude variation of the F.M. carrier is detected at the same time and produces an undesired audio output.

There are five possible types of amplitude limiter:

(1) A saturated amplifier, having an amplification factor inversely proportional to the amplitude of the input signal.

(2) A controlled local oscillator, locked by the frequency of the F.M. input but having an output voltage independent of the amplitude of the controlling signal. This type is discussed in Section 15.10.4 as it primarily acts as a frequency deviation reducer.

(3) An integrating device, having an output voltage dependent upon the frequency of the input signal but independent of its amplitude. This form of limiter is also a frequency-to-amplitude converter and is described in Sections 15.9.4 and 15.9.5.

(4) A negative feedback system which detects the amplitude modulation of the F.M. signal and uses it to supply A.G.C. bias to the I.F. valves to reduce envelope as well as carrier variations.

(5) A neutralizing device which detects the amplitude modulation and supplies it in reversed phase to the F.M. audio output so as to cancel the initial undesired amplitude variation.

15.8.2. The Saturated Amplifier Limiter. The saturated amplifier is the most common form of limiter and will be considered first. A typical circuit is shown in Fig. 15.9. The carrier input is detected by the I_gE_g characteristic of the valve and automatic bias is produced across R_{36}. A change in carrier amplitude causes a corresponding change in bias, i.e., increase of amplitude increases the negative bias across R_{36}. Provided the overall amplification to the carrier fundamental frequency is inversely proportional to the grid bias, and the bias voltage is a faithful reproduction of the amplitude modulated envelope, there is no amplitude modulation at the output. This condition can be approached by operating the valve as a Class C amplifier with an I_aE_g curve having a low bias voltage cut-off ($I_a = 0$) and a saturated characteristic for positive bias voltages. Hence the valve V_7 has low screen and anode voltages (about 40 volts). The negative (low I_a) half of the output current

wave shape is limited by the cut-off bias point, which is fixed by the screen voltage. The positive (high I_a) half is limited by anode current saturation, which is determined by the anode voltage, and, to a less extent, by damping of the input voltage peak by grid current. A low anode voltage causes the load line to operate into the " knee " of the tetrode I_aE_a characteristics and a saturated I_aE_g curve is therefore produced. The resemblance of this type of limiter to the " leaky grid " detector may be noted; it is, in fact, this form of detector, working under saturated anode current conditions, with an anode circuit tuned to the carrier fundamental instead of an aperiodic circuit accepting audio frequencies. In the " leaky grid " detector the time constant of the self-bias circuit must allow the bias change to follow exactly the modu-

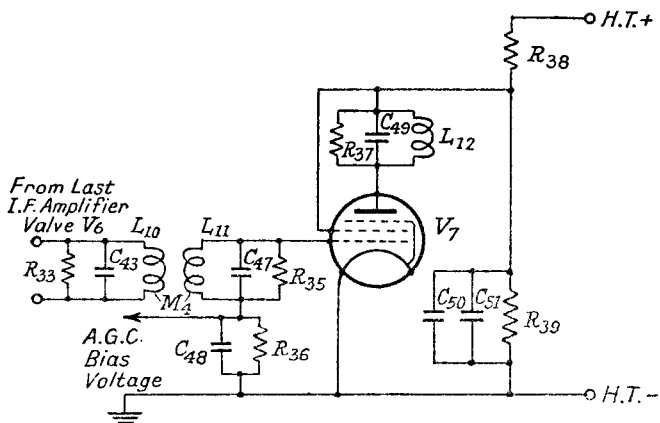

FIG. 15.9.—The Saturated Amplifier Limiter Stage.

lation envelope, and this also applies to the limiter. A suitable time constant is 10 to 20 microsecs. with $R_{36} = 0{\cdot}1$ MΩ and $C_{48} = 100$ $\mu\mu$F. If the time constant is too large, the bias is not proportional to the amplitude modulation, and if it is too small, the bias change is reduced and amplification control compensation is inadequate. Typical limiter input-output curves are shown in Fig. 15.10; curve 1 represents optimum limiting conditions with a screen and anode voltage of approximately 40 volts; output voltage falls slightly as the input voltage is increased. If anode voltage is increased, output voltage increases (curve 2), but the general shape of the curve remains unchanged unless anode voltage is considerably increased, when output voltage often falls slightly after the first maximum and then rises as the input voltage is increased.

An increase in screen voltage (curve 3) moves the limiting point to a higher input voltage, roughly in proportion to the increase in E_g, and also tends to greater variation in output voltage. R_{36} affects the rate of fall of output voltage with increase of input, a high value exaggerating the tendency to a decrease in output voltage (curve 4).

Variations in the frequency response over the pass range of tuned circuits following the limiter cause amplitude modulation of

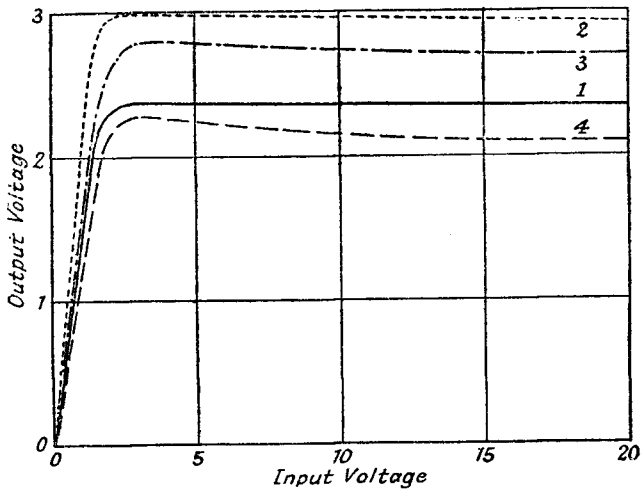

FIG. 15.10.—Input-Output Voltage Curves for the Saturated Amplifier Limiter.
Curve 1.—$E_a = E_s \simeq 40$ volts.
Curve 2.—$E_a > 40$ volts, $E_s \simeq 40$ volts.
Curve 3.—$E_a \simeq 40$ volts, $E_s > 40$ volts.
Curve 4.—$E_a = E_s \simeq 40$ volts, $R_{36} = 1\ M\Omega$.

the F.M. signal, which results in harmonic distortion of the A.F. output when the frequency deviation of the signal is large. It is essential that these circuits should have least possible variation over their pass range, whilst offering appreciable attenuation to the harmonics of the F.M. signal produced by the limiting action. If the loss of response is symmetrical on either side of the tuning points, the A.F. distortion of the output consists mainly of odd harmonics (third, fifth, etc.). Variations in the frequency response of circuits preceding the limiter are compensated by its action. A suitable value for the Q of the anode circuit of the limiter is 4·5 if it is a single-tuned circuit or 14·2 if it consists of a pair of critically coupled tuned circuits. The single circuit gives a loss of approximately — 0·15 db. (representing 1·9% change of amplitude) at

4·5 ± 0·1 Mc/s and a loss of − 16·7 db. (representing an amplitude reduction to 14·65%) at the I.F. second harmonic, 9 Mc/s. Owing to the large off-tune-to-resonant frequency ratio, the loss is calculated from expression 4.8c, Part I, using $F = \left(\frac{\omega}{\omega_r} - \frac{\omega_r}{\omega}\right)$. The corresponding values for a loss of − 0·15 db. at 4·5 ± 0·1 Mc/s with a pair of critically coupled circuits is $Q = 14{\cdot}2$ and the loss at 9 Mc/s = − 47·1 db. (an amplitude reduction to 0·44%). The coupled circuits are clearly very much better than the single circuit. The frequency-amplitude converter, which follows the limiter, can, with advantage, constitute the anode load of the latter, but it may be preceded by a separate valve amplifier. Grid current, taken by the limiter valve V_7, has a damping effect on the tuned circuit $L_{11}C_{47}$, and it is equivalent approximately to a resistance of $\frac{1}{2}R_{36}$ (see Section 8.2.5, Part I). Hence R_{35} must be such as to give a total resistance of 39,200 Ω when paralleled by 50,000 Ω, i.e.,

$$R_{35} = \frac{39{,}200 \times 50{,}000}{50{,}000 - 39{,}200} = 181{,}500\ \Omega.$$

The required low value of 40 volts for screen and anode voltage is obtained from the 250 volts H.T. supply by means of the potential divider made up of R_{38} and R_{39}, 40,000 and 10,000 Ω respectively. The decoupling capacitors C_{50} and C_{51}, 0·1 μF and 8 μF (electrolytic) respectively, by-pass R.F. and A.F., the latter being produced by the limiter action. C_{50} is required in addition to C_{51} because the latter may not be non-inductive.

Since across R_{36} in Fig. 15.9 there is a negative voltage proportional to carrier amplitude, it forms a convenient source of A.G.C. voltage for the I.F. stages of the receiver. There are disadvantages as well as advantages to controlling the R.F. valve as well. The disadvantages are that bias changes on the latter alter its input admittance and affect appreciably the damping and tuning of the aerial circuit. On the other hand, reduced output from the R.F. valve helps to prevent overloading of the frequency changer with increase of input voltage, and so reduces the possibility of spurious responses.

15.8.3. The Negative Feedback A.G.C. Limiter. The negative feedback A.G.C. limiter * principle could be applied to reinforce the action of the saturated amplifier limiter. It only involves modification of the A.G.C. filter, so as to allow the A.F. components

* Patent. R. C. A., P. F. G. Holst and L. R. Kirkwood (U.S. Application No. 441,254).

across the load resistance R_{36} in the saturated amplifier grid circuit to be passed back to the controlled valves with practically no phase shift or attenuation up to frequencies of about 5 kc/s. Decoupling capacitors C_{26}, C_{34} and C_{40} in Fig. 15.7 must be decreased to about 50 $\mu\mu$F, which means a maximum phase shift of 9° and attenuation of $-0{\cdot}1$ db. at 5 kc/s. Attentuation at 4·5 Mc/s is 43·0 db. Should any tendency to I.F. instability appear, the decoupling capacitor C_{26} should be increased first, as this has the greatest amplification after it. Any tendency to instability can often be prevented by placing C_{26} and R_{18} inside the screening can of their associated I.F. transformer. R.F. chokes may be used in place of the filter resistances to give more R.F. attenuation, but care must be exercised to see that they are properly shielded from hum, noise or R.F. pick-up. When this form of limiting is used alone, the A.G.C. voltage must be derived prior to the last I.F. stage, which is itself supplied with A.G.C. bias. If there is no controlled I.F. stage after the A.G.C. detector, amplitude limiting cannot be fully effective because the final output voltage supplies the A.G.C. bias, which must increase with increase of input voltage. Control of an I.F. amplifier following the A.G.C. detector enables a flat or falling output-input voltage characteristic to be obtained by suitably proportioning the A.G.C. bias applied to this stage.

15.8.4. The A.F. Neutralizing Limiter. The neutralizing limiter * applies the audio output from the F.M. receiver detector to the grid of a frequency changer or modulator valve such as the hexode shown in Fig. 15.11. This output consists of the desired A.F. content of the F.M. signal, amplitude modulated by noise, interference, or the selectivity characteristic of the I.F. amplifier tuned circuits. The initial undesired amplitude variation of the F.M. signal is separately detected and applied to the other grid in reverse phase to that of the undesired amplitude modulation of the desired audio output. The amplitude of the undesired audio input to the hexode grid is adjusted to neutralize or demodulate the undesired A.M. of the desired audio input. The output of the hexode valve V_1 now contains the desired audio output (free from undesired amplitude modulation) and also the undesired audio output. The latter is removed by applying the hexode output to the grid of one valve (V_2) of a pair with push-pull input and parallel output circuits. To the other valve (V_3) grid is applied a proportion of the undesired audio signal, which is just sufficient to cancel the undesired signal appearing in the parallel anode circuit from V_2.

* Patent. R. C. A. and M. G. Crosby (British Application No. 360/43).

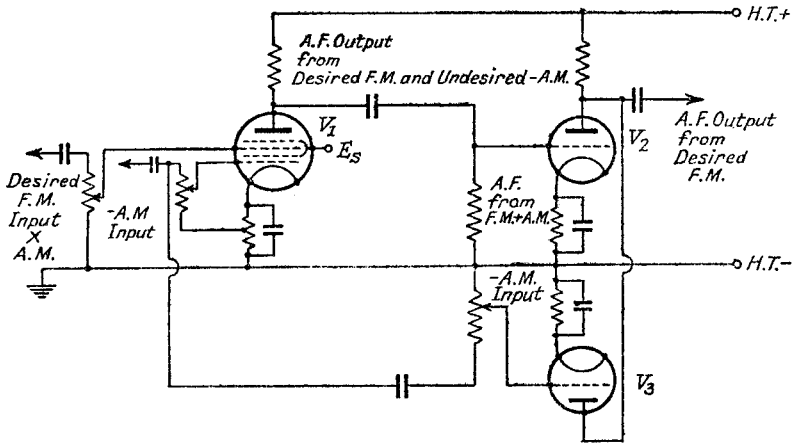

FIG. 15.11.—The A.F. Neutralizing Limiter.

15.9. The Frequency-Amplitude Converter.

15.9.1. Introduction. The chief difference between frequency and amplitude modulated reception lies in the method of making intelligible the A.F. signal conveyed in the modulation. There are two basic principles underlying methods of detecting frequency modulation, the more common system converts the frequency deviation into an amplitude change of carrier, and the resulting amplitude and frequency modulated signal is applied to an amplitude detector such as a diode. The latter is not responsive to the frequency variation and ignores it. The second method involves the use of an integrating device such as a valve charging or discharging a capacitor. The valve circuit may be of the super-regenerator, multivibrator or squegging oscillator type, and it is "triggered" by the I.F. input voltage. The duration (it must be much shorter than the period of the maximum I.F. frequency) and magnitude of the resulting pulse of current is determined solely by the valve and its associated circuit, i.e., it is practically independent of the amplitude of the "triggering" voltage. The number of pulses per second is, however, dependent on the intermediate frequency, and the mean current taken by the valve is therefore proportional to the I.F. The result at the output is an amplitude modulated signal, which is proportional to the original frequency modulation, and which can be detected by the normal methods.

We shall deal first with the frequency-amplitude converter type. The conversion must be accomplished in a linear manner, i.e., the

amplitude change is directly proportional to the frequency change, and it must be performed efficiently so that the resultant amplitude modulation is large. Many of the advantages of frequency modulation disappear if the frequency-amplitude conversion efficiency is low.

15.9.2. The Amplitude Discriminator Converter. One of the earliest methods [1] of frequency-to-amplitude conversion was to apply the F.M. signal to a circuit off-tuned from the carrier unmodulated value. For example, a parallel-tuned circuit, connected in the anode of a tetrode or pentode valve, produces an output voltage-frequency curve as shown in Fig. 15.12, when a constant-amplitude variable-frequency input voltage is applied. If this circuit is

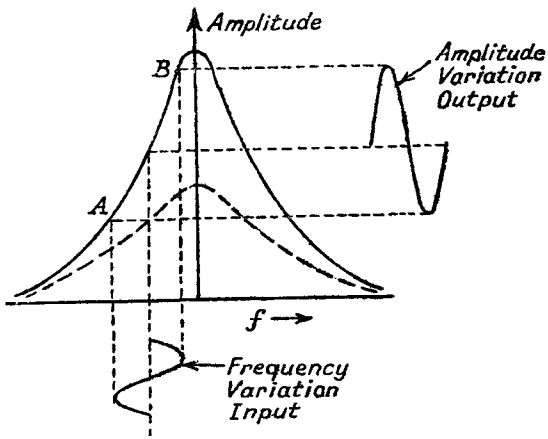

FIG. 15.12.—Frequency to Amplitude Conversion using the Selectivity Characteristics of a Parallel Tuned Circuit.

detuned (above or below) from the unmodulated carrier frequency, frequency modulation results in an output voltage of amplitude proportional to the frequency deviation of the carrier. It is, however, only linearly proportional if the carrier frequency deviation is confined to the approximately linear part AB of the curve, the centre of which occurs at a frequency, off-tune from the resonant frequency, of $\Delta f = 0{\cdot}375\frac{f_r}{Q}$. By applying the output voltage to an amplitude detector, such as a diode, an A.F. signal, corresponding to the original signal modulating the carrier, is obtained. Although variation of frequency is occurring simultaneously with change of amplitude, only the latter is detected by the diode. Hence it is possible to receive and detect a F.M. transmission on an A.M. receiver provided the latter is off-tuned from the F.M. carrier unmodulated value. This method of detection is very inefficient, partly because it is

dependent on the slope of the output voltage-frequency curve, which for practical circuits is not very high, but mainly because the tuned circuit is operated in the detuned condition with consequent reduced overall amplification. Furthermore, full advantage cannot be taken of increased frequency deviation of the carrier, for the circuit must be damped (see the dotted curve in Fig. 15.12) to increase the linear part of the curve, and conversion efficiency is reduced.

A second method of frequency-amplitude conversion suppresses one set of sidebands. In Chapter 1, Part I, a frequency modulated wave was shown to consist of a carrier vector (of frequency equal to the unmodulated value) and pairs of sidebands spaced $\pm f_{mod.}$ $\pm 2f_{mod.}$ etc., from the carrier, the odd numbered sideband pairs combining into a resultant vector at 90° to the carrier and the even pairs into

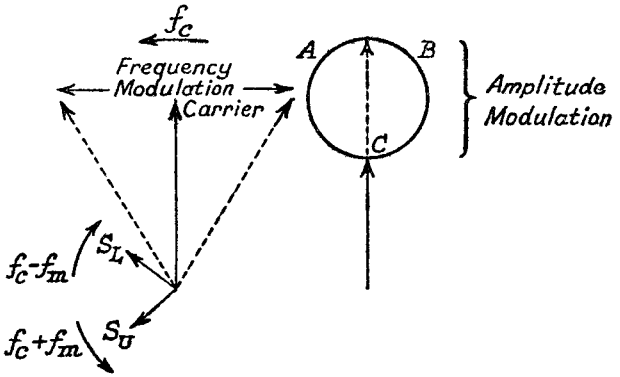

FIG. 15.13.—Frequency to Amplitude Conversion by Suppression of One of a Pair of Sidebands.

a resultant in line with the carrier. The addition of the first pair of sidebands ($f_c \pm f_{mod.}$) to the carrier gives the frequency (and amplitude) modulated carrier of Fig. 15.13, and taking this as a basis we see that suppression of one of the sidebands results in the mainly amplitude modulated carrier vector, whose locus of operation is the circle *ABC*. The amplitude modulation is not directly proportional to the original modulation even when all sideband pairs are considered, and detection of the A.M. resultant by a diode produces a distorted A.F. output containing mostly second harmonic. The suppression of one-half of the sidebands is clearly inefficient since the transmitted energy in these is not being used. Both disadvantages may be overcome by applying the F.M. wave to two channels,[4] one having a filter suppressing the upper frequency sidebands and

the other a filter suppressing the lower frequency ones. The schematic diagram is shown in Fig. 15.14. The diode detector outputs are connected in opposition so that an unmodulated carrier produces zero volts across AC. The amplitude variations of the carrier at the outputs of the two filters are in phase opposition—the upper sideband in Fig. 15.13 is subtracting from the carrier when the lower is adding—and frequency modulation causing the voltage to rise across AB reduces the voltage across BC. Thus there is a double increase in A.F. output voltage change across AC. The phase-opposing connection of the detected output also leads

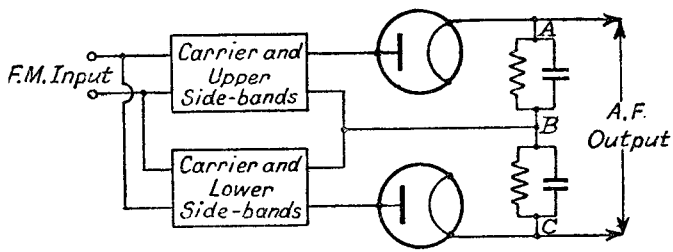

FIG. 15.14.—Frequency to Amplitude Conversion by Detection of the Carrier and Upper Sidebands, and Carrier and Lower Sidebands.

to cancellation of the second harmonic distortion in the amplitude variation, and the resultant voltage across AC is therefore a reproduction of the A.F. signal modulating the transmitter.

The third type of frequency-amplitude converter employs a frequency discriminator similar to the one used to translate frequency error into a D.C. biasing voltage for automatic frequency correction of the oscillator of a superheterodyne receiver. Either amplitude or phase discriminator (Section 13.4.2) is suitable, but the latter is almost always used in F.M. receivers because it presents fewer practical difficulties (stray capacitance coupling occurs between the two distuned circuits of the amplitude discriminator), a symmetrical characteristic can be more easily obtained, and it has a high frequency-to-amplitude conversion efficiency.

Linearity of discriminator output voltage-frequency characteristic is most important if an undistorted A.F. output is to be obtained from the F.M. signal, and this is achieved in the amplitude discriminator by satisfying the condition.

$$Q = \frac{f_1}{2\Delta f} \quad . \quad . \quad . \quad . \quad 15.5$$

where f_1 = resonant frequency of one of the off-tuned circuits

$$\Delta f = f_m - f_1 = \pm 100 \text{ kc/s}$$

and f_m = the mid frequency of the discriminator at which the D.C. output voltage is zero, i.e., it is the intermediate frequency.

Condition 15.5 is also that which gives maximum slope to the discriminator when Δf is fixed, and curve *ABODE* in Fig. 13.6*a* is therefore applicable to the frequency-amplitude converter. It is only necessary to change the frequency scale from 465 kc/s at 0 to 4·5 Mc/s, and 463 and 467 kc/s to 4·4 and 4·6 Mc/s to get the characteristic of a suitable frequency-amplitude converter for

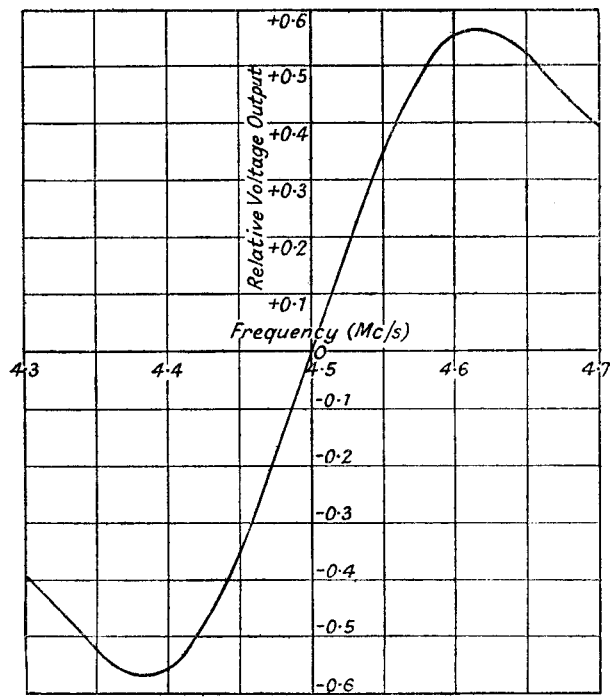

FIG. 15.15.—The Amplitude Discriminator Characteristic for Frequency-to-Amplitude Conversion.

Δf = 100 kc/s. This is done in Fig. 15.15. Calculation of the component values for the frequency-amplitude converter discriminator shown in Fig. 15.16 follows the lines set out in Section 13.4.2. The required average value of Q for the tuned circuits 1 and 2 is

$$Q = \frac{4{\cdot}5}{0{\cdot}2} = 22{\cdot}5.$$

The maximum value of the resonant impedance of either circuit is limited by the anode-to-anode capacitance, C_{a12}, of the two diodes D_1 and D_2, which forms a coupling between the two circuits.

Coupling is caused between the primaries by the anode-earth capacitance C_{aE} of the amplifier valve, and this sets a limit on the voltage transfer efficiency from primaries to secondaries. Assuming an anode-to-anode capacitance for the diodes of 1 $\mu\mu$F, we have a coupling reactance between the circuits of 35,400 Ω, so that we cannot allow the resonant impedance of either tuned circuit to exceed about 10,000 Ω. In calculating the component values for

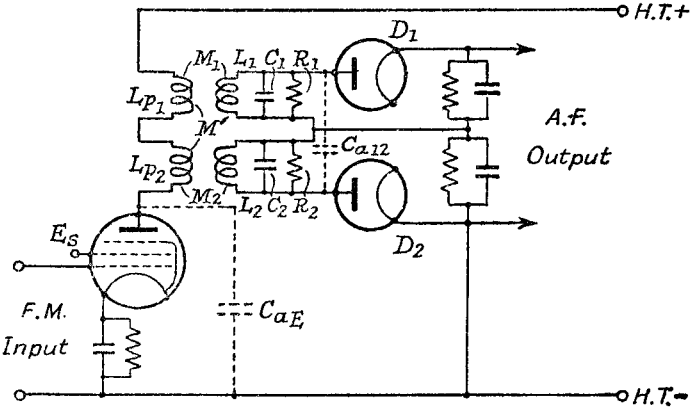

FIG. 15.16.—The Amplitude Discriminator as a Frequency-to-Amplitude Converter.

the circuits we shall take the mean frequency of 4·5 Mc/s and assume that the circuits are identical except for the values of C_1 and C_2, which are adjustable for resonance at 4·4 and 4·6 Mc/s. Calculation of the damping resistances R_1 and R_2 is made on the assumption that the frequency is f_m. The error introduced is not very large and has little practical significance. Thus

$$L = L_1 = L_2 = \frac{R_D}{\omega_m Q} = \frac{10{,}000 \times 10^6}{6{\cdot}28 \times 4{\cdot}5 \times 10^6 \times 22{\cdot}5}$$
$$= 15{\cdot}7 \ \mu\text{H}.$$
$$C_1 = 83{\cdot}2 \ \mu\mu\text{F} \ (f_1 = 4{\cdot}4 \ \text{Mc/s})$$
$$C_2 = 76{\cdot}0 \ \mu\mu\text{F} \ (f_2 = 4{\cdot}6 \ \text{Mc/s}).$$

If the anode load resistances are 0·1 MΩ, the damping due to conduction current is 50,000 Ω, so that the resonant impedance of the tuned circuit of initial $Q = 150$ and excluding R_1 is

$$R_D' = \frac{Q_0 \omega_m L . 50{,}000}{Q_0 \omega_m L + 50{,}000} = \frac{66{,}500 \times 50{,}000}{116{,}500} = 28{,}600 \ \Omega.$$

Hence $$R_1 = \frac{28{,}600 \times 10{,}000}{18{,}600} = 15{,}350 \ \Omega.$$

The reactance of an anode-earth capacitance of 15 $\mu\mu$F on the

primary side is 2,360 Ω at 4·5 Mc/s. The reflected resonant impedance across the primary is $R_D\left(\frac{M}{L}\right)^2$, and this must be much less than 2,360 Ω; let us take a value of 500 Ω. Thus

$$\frac{M}{L} = \sqrt{0{\cdot}05} = 0{\cdot}2235$$

and

$$M = 3{\cdot}51\ \mu\text{H}.$$

A possible coupling coefficient $k = \frac{M}{\sqrt{L_p L}} = 0{\cdot}35$ is attainable, so that

$$L_p = 6{\cdot}41\ \mu\text{H}.$$

The resonant frequency of C_{aE} (15 $\mu\mu$F) with the sum of the primary coil inductances, $2Lp$, is 11·48 Mc/s, which is sufficiently far away from the I.F. and the second and third harmonics of the I.F.

The slope of the frequency-amplitude conversion characteristic at the centre point O (Fig. 15.15) is given by twice expression 13.2 as

$$S(max.) = \frac{8.(22{\cdot}5)^2 100}{(4{\cdot}5 \times 10^3)^2 2^{\frac{3}{2}}} = 0{\cdot}00707.$$

The slope of the characteristic O in volts per kc/s per 1 volt peak input is for $g_m = 2$ mA/volt and $\eta_d = 0{\cdot}85$.

$$\begin{aligned} S &= 0{\cdot}00707 g_m R_D \frac{M}{L} \eta_d \\ &= 0{\cdot}00707 \times 2 \times 10^{-3} \times 10^4 \times 0{\cdot}2235 \times 0{\cdot}85 \\ &= 0{\cdot}0269 \text{ volts / kc/s off-tune / 1 volt peak input.} \end{aligned}$$

The stray capacitance coupling between the circuits can be neutralized by providing mutual inductance coupling between the coils. Cancellation is achieved by making

$$\frac{M'}{\sqrt{L_1 L_2}} = \frac{C_s}{\sqrt{C_1 C_2}}, \text{ i.e., } \frac{M'}{L} = \frac{C_s}{C_1},$$

where C_s is the total equivalent stray capacitance on the secondary side between the two tuned circuits. For cancellation M' should be in a positive direction (see Section 3.4.2, Part I); in a negative direction it adds to the coupling due to C_s.

15.9.3. The Phase Discriminator Converter.[18] Since the phase discriminator functions in a manner similar to the amplitude discriminator, converting a frequency into an amplitude change, it may be used as a frequency-to-amplitude converter in a F.M. receiver. The general behaviour of this discriminator has already been examined in Section 13.4.2, and the circuit diagram of Fig. 15.17 is very similar to that of Fig. 13.10. The valve feeding the dis-

criminator is assumed to be the limiter valve V_7. Resistances R_{37} and R_{40} are added across the primary and secondary of the phase discriminator in order to obtain the required pass-band width of ± 100 kc/s. The primary voltage is coupled to the centre-tap of the secondary through C_{52}, its voltage appearing across R_{41} and R_{42}, which are in parallel to the I.F. voltage. R.F. choke coupling (L_3 in Fig. 13.10) is not used because the extra damping due to R_{41} and R_{42} being in parallel with the primary is still insufficient to give the band width, and an additional resistance R_{37} is required.

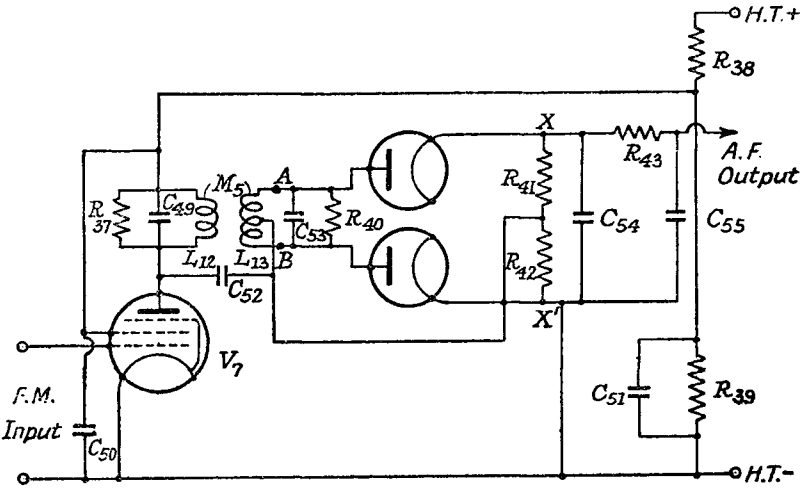

FIG. 15.17.—The Phase Discriminator as a Frequency-to-Amplitude Converter.

The characteristics required from the phase discriminator when it is to function as a converter are not exactly the same as those needed for A.F.C. purposes. Linearity of output voltage with change of frequency is all important, and maximum slope (the requirement for A.F.C.) must be sacrificed for this. To determine the shape of the characteristic and estimate the conditions for linearity of conversion over the desired pass-band range, we must turn to the fundamental equations for primary and secondary voltages set out in Section 13.4.2. These are, for the primary,

$$E_1 = g_m E_g R_{D1} \frac{1+jQ_2F}{(1+jQ_1F)(1+jQ_2F)+Q_1Q_2k^2}. \quad . \quad 15.6$$

and for the secondary

$$E_2 = g_m E_g R_{D1} \frac{-jQ_2k\sqrt{\frac{L_2}{L_1}}}{(1+jQ_1F)(1+jQ_2F)+Q_1Q_2k^2}. \quad . \quad 15.7.$$

The total voltage applied to one diode is $E_{AX} = E_1 - \frac{1}{2}E_2$ and to the other $E_{BX'} = E_1 + \frac{1}{2}E_2$, and the output voltage of the discriminator is the numerical difference between the amplitudes of E_{AX} and $E_{BX'}$ multiplied by the detection efficiency of the diodes, i.e.,

$$\begin{aligned} E_{XX'} &= \eta_d(\,|\,E_{AX}\,| - |\,E_{BX'}\,|\,) \\ &= \eta_d(\,|\,E_1 - \tfrac{1}{2}E_2\,| - |\,E_1 + \tfrac{1}{2}E_2\,|\,) \quad . \quad . \quad 15.8. \end{aligned}$$

The secondary voltage can be rewritten in terms of E_1 as

$$E_2 = E_1 \frac{-jQ_2k\sqrt{\dfrac{L_2}{L_1}}}{(1+jQ_2F)}. \quad . \quad . \quad . \quad 15.9$$

so that

$$E_{AX} = E_1\left[1+\frac{jQ_2k\sqrt{\dfrac{L_2}{L_1}}}{2(1+jQ_2F)}\right] = E_1\left[1+\frac{jQ_2k\sqrt{\dfrac{L_2}{L_1}}(1-jQ_2F)}{2[1+(Q_2F)^2]}\right]$$

or $$\frac{E_{AX}}{E_1} = 1+\frac{\alpha Q_2F}{2[1+(Q_2F)^2]} - \frac{j\alpha}{2[1+(Q_2F)^2]} \quad . \quad . \quad 15.10$$

where $\alpha = \dfrac{E_2}{E_1} = Q_2k\sqrt{\dfrac{L_2}{L_1}}$ at $F = 0$, i.e., at the mid frequency f_m.

$$\therefore \frac{|\,E_{AX}\,|}{|\,E_1\,|} = \sqrt{\left[1+\frac{\alpha Q_2F}{2[1+(Q_2F)^2]}\right]^2+\frac{\alpha^2}{4[1+(Q_2F)^2]^2}}. \quad 15.11a$$

and $$\frac{|\,E_{BX'}\,|}{|\,E_1\,|} = \sqrt{\left[1-\frac{\alpha Q_2F}{2[1+(Q_2F)^2]}\right]^2+\frac{\alpha^2}{4[1+(Q_2F)^2]^2}}. \quad 15.11b.$$

The vector relationship represented by expression 15.9 is shown in Fig. 13.11, and the variation in the length of $\dfrac{|\,E_{AX}\,|}{|\,E_1\,|}$ can be measured from this figure for different values of Q_2F and selected values of α, or alternatively it may be calculated from expression 15.11*a*. $\dfrac{|\,E_{BX'}\,|}{|\,E_1\,|}$ can be found in a similar manner, and subtracting it from $\dfrac{|\,E_{AX}\,|}{|\,E_1\,|}$ gives the relative voltage output from the discriminator if $|\,E_1\,|$ has a constant amplitude. The relative voltage output is plotted in Fig. 15.18*a* over a range of Q_2F from 0 to +2 (the other half of the curve from $Q_2F = 0$ to -2 is the same shape inverted) for $\dfrac{E_2}{E_1} = 1$, 2, 3, 4 and 6. The most noticeable

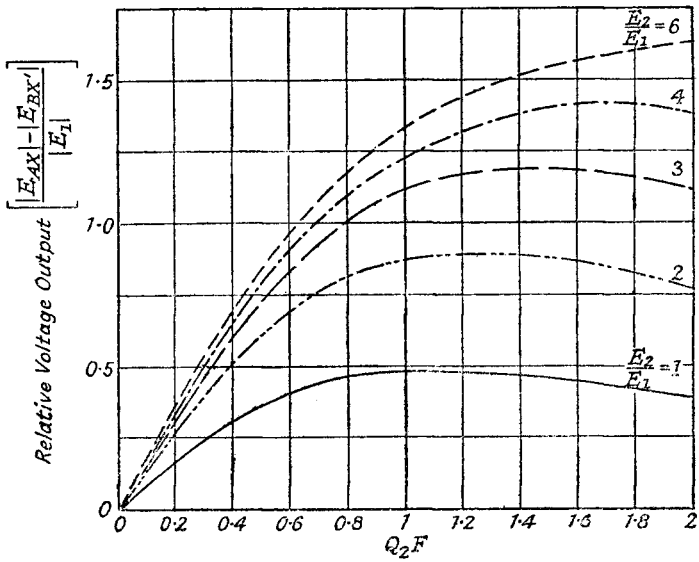

FIG. 15.18*a*.—The Variation of Phase Discriminator Output Voltage Against Frequency Off-tune from the Resonant Frequency. Primary Voltage is assumed constant.

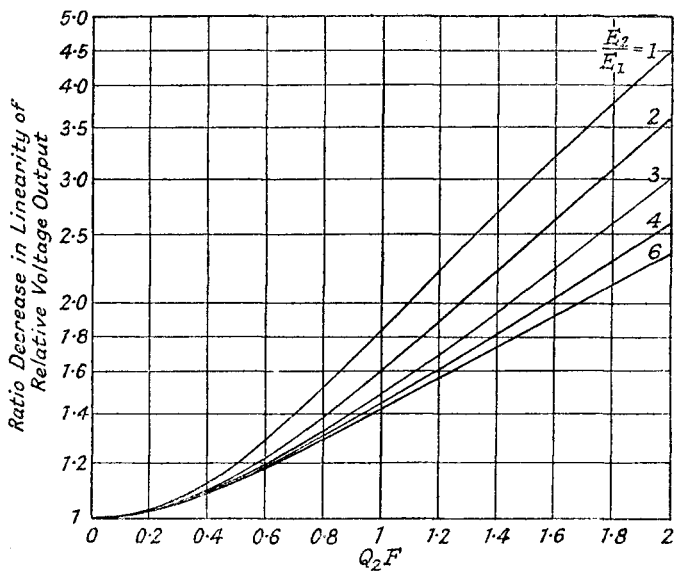

FIG. 15.18*b*.—Ratio Decrease of Linearity of Phase Discriminator Output Voltage against Off-tune Frequency. Primary Voltage assumed constant.

effect is that maximum output occurs at a large value of Q_2F as $\frac{E_2}{E_1}$ is increased, and none of the curves is truly linear. A second set of curves is drawn in Fig. 15.18*b* to show the departure from linearity, which is expressed in the form of ten times the ratio of the relative voltage output at a particular Q_2F to the voltage output at $Q_2F = 0{\cdot}1$ multiplied by the particular value of Q_2F being considered. We see from Fig. 15.18*b* that the general tendency is for the curve to become more linear as $\frac{E_2}{E_1}$ is increased, though there is not much difference between the curve for $\frac{E_2}{E_1} = 4$ and that for $\frac{E_2}{E_1} = 6$.

The divergence of these curves from the required straight line characteristic can be offset if E_1 can be made to increase with increase of Q_2F, and this is possible by a suitable choice of coupling between the secondary and primary. If we assume that $Q_1 = Q_2$ a series of curves of the ratio increase of E_1 upon its value at $f_m(F = 0)$ can be plotted against QF for different values of the coupling factor Qk. The problem is greatly complicated if Q_1 and Q_2 are not equal, because a separate set of curves must be drawn for each value of Q_1 and Q_2, and there is seldom any practical advantage to be gained by making them unequal. The ratio increase of E_1 with increase of QF is, from expression 15.6,

$$\frac{|E_1|}{|E_1|_{F=0}} = \frac{[\sqrt{1+(QF)^2}][1+Q^2k^2]}{\sqrt{[1+Q^2(k^2-F^2)]^2+4Q^2F^2}} \quad . \quad 15.12$$

and it is plotted in Fig. 15.19 as a series of curves for selected values of Qk. To find the most suitable value of Qk for compensating the ratio decrease of Fig. 15.18*b*, the curves of Fig. 15.19 should be drawn on transparent paper and placed on top of those of Fig. 15.18*b*. Any two curves which then coincide will give the conditions for a linear characteristic over the range of QF for which they are coincident. Greatest range of QF over which a linear characteristic is obtained is from 0 to 1 with $\frac{E_2}{E_1} = 2$ and $Qk = 2$. The resultant characteristic is linear up to $QF = 0{\cdot}8$ and falls away slightly at $QF = 1$ where the output is about 2% low. A slightly lower value of Qk could be chosen with some reduction of the linear range of QF, and this has the advantage of giving a higher frequency-

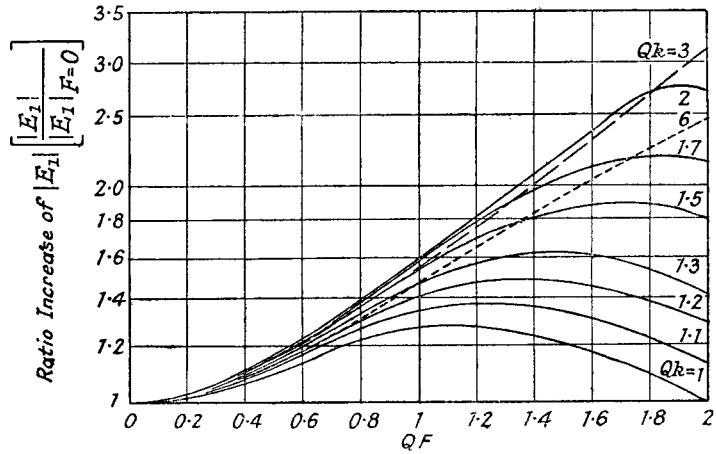

FIG. 15.19.—The Ratio Increase of Primary Voltage against Off-tune Frequency for the Phase Discriminator.

to-amplitude conversion efficiency. Thus for $Qk = 1{\cdot}5$, $\frac{E_2}{E_1} = 2$, the linear range of QF is reduced to approximately $QF = 0$ to $0{\cdot}8$, but conversion efficiency (expression 15.13) is increased in the ratio

$$\frac{1+(Qk)^2}{1+(Q_1k_1)^2} = \frac{5}{3{\cdot}25} = 1{\cdot}535,$$

provided R_{D1} is unchanged. The relative voltage output-QF characteristics for the two values of Qk, $1{\cdot}5$ and 2, are shown in Fig. 15.20. The peak of the characteristic for $Qk = 1{\cdot}5$ occurs at a much lower value of QF ($1{\cdot}5$) than that ($1{\cdot}9$) for $Qk = 2$, and this, coupled with its higher frequency-amplitude conversion efficiency, suggests the smaller value of Qk to be the better practical proposition, in spite of the reduced linear range of QF. It is interesting to note that $Qk = 2$ gives the maximum possible correction over the useful range of QF, and a linear characteristic cannot be obtained for values of $\frac{E_2}{E_1}$, which correspond to curves on Fig. 15.18*b*, having a greater reduction than the correction produced by the curve for $Qk = 2$ of Fig. 15.19. Thus a linear characteristic is unobtainable for values of $\frac{E_2}{E_1} < 2$. Correction is possible for higher values of $\frac{E_2}{E_1}$ than 2; lower values of Qk are required and the linear range of QF is reduced, e.g., $\frac{E_2}{E_1} = 3$ requires Qk to be $1{\cdot}25$ and a linear range is obtained from $QF = 0$ to $0{\cdot}85$.

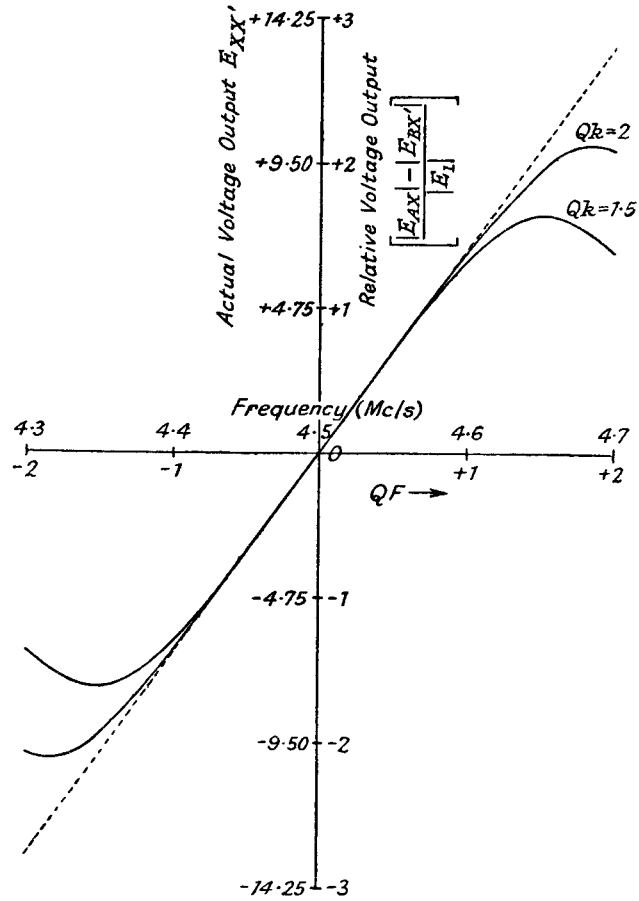

FIG. 15.20.—The Relative Voltage Output—QF Characteristic of a Phase Discriminator for $\frac{E_2}{E_1} = 2$ and $Qk = 1{\cdot}5$ and 2.

To illustrate design features the following constants are assumed :

$f_m = 4{\cdot}5$ Mc/s, carrier frequency deviation $= \pm 75$ kc/s,

$\frac{E_2}{E_1} = 2$, $Qk = 1{\cdot}5$,

hence

$$\frac{L_2}{L_1} = 1{\cdot}77.$$

Taking $QF = 1$ at $\Delta f = 100$ kc/s allows the carrier frequency deviation of ± 75 kc/s to be accommodated on the linear part of the characteristic ; and this gives

$$Q = \frac{f_m}{2\Delta f} = \frac{4{\cdot}5}{0{\cdot}2} = 22{\cdot}5$$

and

$$k = \frac{1{\cdot}5}{Q} = 0{\cdot}067.$$

In Section 13.4.2, expression 13.8 for the slope of the characteristic at O (Fig. 15.15), or the sensitivity of frequency-amplitude conversion at $f_m(F = 0)$, is

$$S_{(F=0)} = 2g_m R_{D1}\eta_d E_{g1} \frac{Q_2{}^2 k\sqrt{\frac{L_2}{L_1}}}{f_m(1+Q_1Q_2k^2)\left(1+\frac{Q_2{}^2k^2L_2}{4L_1}\right)^{\frac{1}{2}}} \quad . \quad 15.13$$

$$= g_m R_{D1}\eta_d E_{g1} \frac{2 \times 22{\cdot}5 \times 2}{4{\cdot}5 \times 10^3 \times 3{\cdot}25 \times \sqrt{2}}$$

$$= 4{\cdot}35 \times 10^{-3} g_m R_{D1}\eta_d E_{g1} \text{ volts per kc/s.}$$

Maximum sensitivity is clearly obtained when R_{D1} is as large as possible, and this means the highest possible value of L_1, which in turn is limited by the maximum practicable value of L_2. The latter is determined by the minimum permissible value of secondary tuning capacitance, which we shall assume to be 50 $\mu\mu$F. Thus referring to Fig. 15.17

$$C_{53} = 50\ \mu\mu\text{F},\ L_{13} = 25\ \mu\text{H}$$

$$L_{12} = \frac{L_{13}}{1{\cdot}77} = 14{\cdot}1\ \mu\text{H and } C_{49} = 88{\cdot}5\ \mu\mu\text{F}.$$

The higher value of primary capacitance, C_{49}, is an advantage because the stray capacitance, e.g., across R_{41} and R_{42}, is greater than across the secondary.

$$R_{D1} = \omega_m L_{12} Q = 6{\cdot}28 \times 4{\cdot}5 \times 14{\cdot}1 \times 22{\cdot}5$$
$$= 9{,}000\ \Omega.$$

If $g_m = 2$ mA/volt and $\eta_d = 0{\cdot}85$, the sensitivity of frequency-amplitude conversion is

$$S_{(F=0)} = 4{\cdot}35 \times 10^{-3} \times 2 \times 10^{-3} \times 9{,}000 \times 0{\cdot}85 \times 1$$
$$= 0{\cdot}0665 \text{ volts per kc/s per 1 volt input at the grid of } V_7.$$

The output voltage ($E_{XX'}$)-frequency characteristic of the discriminator is obtained by multiplying the vertical scale of Fig. 15.20 by 4·75, i.e., using the left-hand scale, and converting the QF scale to a frequency scale by noting that $f = 4{\cdot}5$ Mc/s at $QF = 0$ and 4·4 and 4·6 Mc/s at $QF = -1$ and $+1$ respectively.

The damping resistances R_{37} and R_{40} in Fig. 15.17 have next to

be calculated. If the diode load resistances R_{41} and R_{42} are 0·1 MΩ, the primary circuit is damped by these two in parallel (0·05 MΩ) and also by the two diode conduction currents, which are equivalent to two 0·05 MΩ in parallel, i.e., 0·025 MΩ. Hence the total damping resistance across the primary, apart from R_{37}, is equal to 0·05 MΩ in parallel with 0·025 MΩ, viz., 16,666 Ω. If the initial Q_0 of the coil is 150, the total damping resistance necessary to reduce this to 22·5 is

$$R_{tp} = \frac{\omega_m L_{12} Q_0 Q}{Q_0 - Q} = \frac{6{\cdot}28 \times 4{\cdot}5 \times 14{\cdot}1 \times 150 \times 22{\cdot}5}{127{\cdot}5}$$
$$= 10{,}600\ \Omega$$

so that $R_{37} = \dfrac{16{,}666 \times 10{,}600}{6{,}066} = 29{,}200\ \Omega.$

For the secondary side

$$R_{ts} = \frac{\omega_m L_{13} Q_0 Q}{Q_0 - Q} = 18{,}800\ \Omega$$

of which the damping resistance due to detection is that from the conduction resistances in series, i.e., 0·1 MΩ. Hence

$$R_{40} = \frac{100{,}000 \times 18{,}800}{81{,}200} = 23{,}100\ \Omega.$$

The coupling capacitor C_{52} in Fig. 15.17 is 100 μμF, the R.F. by-pass capacitor C_{54} is 50 μμF and in the R.F. filter before the A.F. amplifier $R_{43} = 0{\cdot}2$ MΩ and $C_{55} = 100$ μμF. The mutual inductance coupling M_5 between L_{12} and L_{13} is $k\sqrt{L_{12}L_{13}} = 1{\cdot}255$ μH ($k = 0{\cdot}067$).

Correct tuning and adjustment of the phase discriminator is best carried out in the manner described in Section 13.4.2. The primary and secondary, with C_{52} disconnected and coupling less than critical ($Qk < 1$), are tuned for maximum voltage across either one of the diode load resistances, R_{41} and R_{42}, when the input frequency is 4·5 Mc/s. C_{52} is now connected and the primary re-tuned for equal positive and negative D.C. voltage peaks across the two load resistances (points XX' in Fig. 15.17) at approximately equal off-tune frequencies from 4·5 Mc/s. The secondary is next tuned to produce zero D.C. voltage across XX' at 4·5 Mc/s. Finally, the mutual inductance coupling M_5 is increased until the equal positive and negative D.C. voltage peaks occur at 4·65 and 4·35 Mc/s. ($QF = 1{\cdot}5$ from Fig. 15.20.) The required linear characteristic should then be obtained.

The effect of primary and secondary mistuning on the discriminator characteristic has already been discussed in Section 13.4.2.

Variations of M_5, i.e., Qk, cause the characteristic to pass through the phases illustrated by curves 1, 2 and 3 in Fig. 15.21. Curve 1 is obtained when M_5 is too small, the linear range of QF is restricted and the peaks are close to off-tune frequencies corresponding to $QF = 1$. Curve 2 illustrates the case for the correct value of M_5, i.e., $Qk = 1{\cdot}5$, while curve 3 shows how linearity is lost by increasing M_5 beyond its optimum value, a double S-shaped characteristic

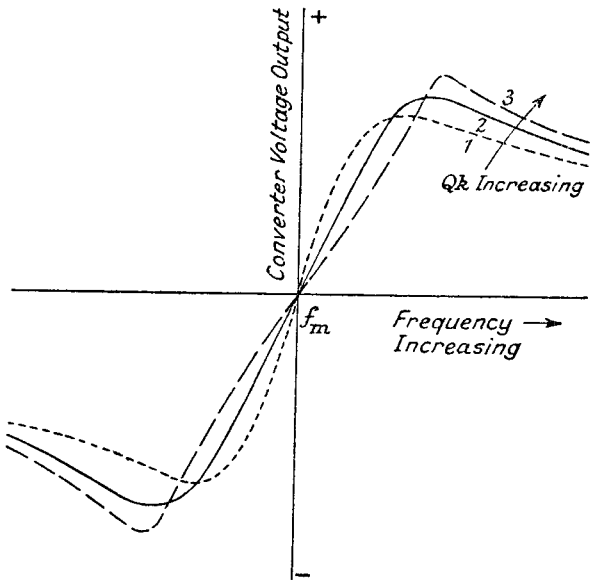

FIG. 15.21.—The Effect of increasing Mutual Inductance between Primary and Secondary of the Phase Discriminator.

Curve 1: M too small.
Curve 2: M correct for maximum linearity.
Curve 3: M too large.

being obtained. As M_5 is increased the positive and negative peaks continue to increase in amplitude.

15.9.4. The Integrating Converter. The integrating frequency-amplitude converter, which also acts as a limiter, may consist of a regenerative amplifier, a multivibrator, or a squegger oscillator, the operation of which is controlled or triggered by the intermediate frequency. All these circuits tend to produce short sharp pulses of current, the duration and amplitude of which are dependent on the circuit constants and are practically independent of the amplitude of the triggering voltage. The number of pulses produced are controlled by, and are directly proportional to, the frequency of the latter. The mean current value of these pulses is proportional

to the intermediate frequency so that the mean current amplitude varies in accordance with the frequency deviation of the I.F. carrier and reproduces the A.F. content of the latter.

An example of the regenerative* type is shown in Fig. 15.22. Two pentode valves (hexodes may equally well be employed) are used in push-pull, and regeneration is applied to one grid from the anode of the opposite valve by means of the potential divider resistances R_2 and R_3. C_1 is a coupling capacitance of fairly high value (0·001 μF) for isolating the D.C. voltage. Regeneration is critically adjusted so that the stage is very susceptible to small changes of voltage on the suppressor grids. A slight positive increase in voltage causes one valve to take a high value of anode

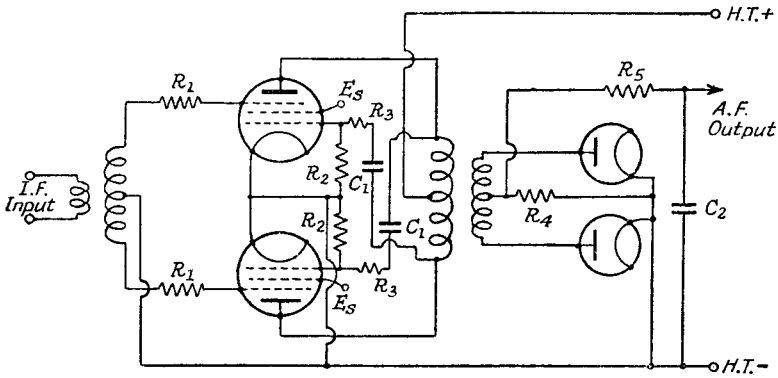

FIG. 15.22.—A Regenerator Type of Integrating Frequency-to-Amplitude Converter.

current and the other to take a small value. A large pulse of current therefore flows through the primary of the centre-tapped transformer connected to the anodes of the valves. The rate of rise and fall of anode current is very rapid and is determined solely by the regenerative circuit (the natural frequency of the primary inductance and stray capacitance is much higher than the highest intermediate frequency), so that the wave form (width and amplitude) of the current pulse is independent of the I.F. The number of pulses per second is, however, proportional to the I.F., occurring twice per cycle of the I.F. Provided the amplitude of the I.F. signal exceeds a certain minimum value, variation of amplitude has no effect, and the stage acts as an amplitude limiter. Resistances R_1 in the input grid circuit help in attaining this condition by " squaring " the tops of the I.F. signal with the aid of grid current. A double-

* Patent. R. C. A. and C. W. Hansell (British Application No. 8324/42).

diode full-wave detector is used across the secondary of the transformer in order to abstract the mean voltage variations from the A.C. voltage pulses appearing across the secondary. The mean variation of the pulse from each valve cannot be transferred through the transformer, but must be abstracted by subsequent detection. The detector must not be allowed to operate with a reservoir capacitance across its load resistance, as for an amplitude modulated signal, otherwise the capacitance fills in the gaps between the pulses (see Section 8.2.1, Part I) and there is no mean voltage variation. A resistance load is satisfactory without the reservoir capacitance as the half-wave voltage pulses appearing across it are of substantially the same shape as the section of the applied voltage wave which is producing them. Half-wave detection could be employed using the whole of the secondary as a voltage source, but it is no more efficient as regards A.F. output from a given I.F. deviation, and has the disadvantage of a large R.F. fundamental component (twice that for full-wave). This is different from the case of amplitude modulation for which half-wave detection normally gives an A.F. voltage output approximately twice that for full-wave. R_5 and C_2 form an R.F. filter between the load resistance R_4 and the first A.F. valve.

The regenerator of Fig. 15.22 may be replaced by a multivibrator, or a squegger oscillator. The squegger or blocking oscillator, shown in Fig. 15.23, has very tight coupling between its regenerator

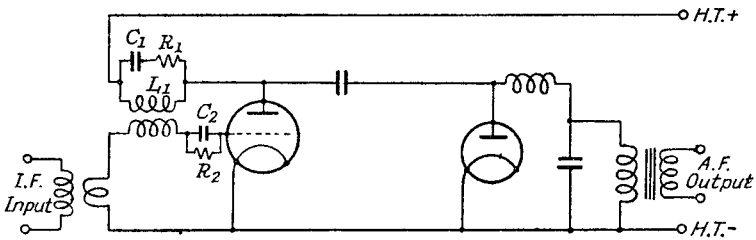

FIG. 15.23.—The Blocking Oscillator Integrator Converter.

oil and tuned circuit. Oscillation, when it occurs, is so violent that a very large pulse of grid current results and charges the capacitance C_2 to a negative voltage many times greater than the cut-off bias voltage. Oscillation ceases and only recommences after C_2 has discharged itself through R_2 to a negative voltage sufficiently small to allow oscillations to begin again. If the tuned anode is sufficiently damped—this is the function of R_1 in series with the tuning capacitance C_1—oscillations in the tuned circuit die away rapidly and there is only a single anode current pulse of short duration. The

actual period of the pulse is usually rather less than half a cycle of the normal oscillation frequency of L_1C_1, and is much less than the period of the maximum frequency of the triggering voltage. On the other hand, the time constant of the circuit R_2C_2 must be greater than the period of the minimum I.F., so that the latter can trigger the valve satisfactorily. The amplitude and duration of the anode current pulse depends on the circuit constants, and above a certain value of triggering voltage is independent of the amplitude of the latter. The mean anode current taken by the oscillator is proportional to the number of pulses, which in turn is proportional to the intermediate frequency, and the A.F. content of the I.F. signal could be obtained across a resistance placed between the tuned circuit L_1C_1 and H.T. positive. A capacitance of about 100 $\mu\mu$F would be required across the resistance to by-pass radio frequencies. Alternatively the mean value can be abstracted from the pulses by means of the diode as shown in Fig. 15.23.

Another method of producing pulses of almost constant duration and amplitude, but of number proportional to the I.F., is by means of a hexode valve, to the control and oscillator grids of which antiphase (180°) voltages are applied. The bias on the grids is adjusted so that anode current flows when there is no I.F. signal, but is quickly cut off by a differential change of voltage on the grids. Hence a short pulse of anode current occurs every half-cycle of the I.F. as the instantaneous amplitude approaches and passes through zero. There is a change in pulse width with change in I.F. amplitude and this type is less satisfactory as an amplitude limiter.

15.9.5. The Counter Type of F.M. Detector. Detection of a F.M. signal can be accomplished by using the " counter " type of detector * shown in Fig. 15.24. For the " counter " action to be satisfactory, the I.F. must have a comparatively low value, about 200 kc/s is usually chosen so that the lowest modulation frequency components (125 kc/s) are sufficiently far removed from the A.F. range of frequencies. This low I.F. necessitates double frequency changing in order to avoid image and undesired responses. The last I.F. amplifier following the limiter stage has a resistance, R_1, instead of a tuned circuit in its anode. It is biased by grid current and has low anode and screen voltages in order to " square " the top and bottom of the F.M. output signal. Capacitance C_1, initially charged by D_1 to the maximum positive square top voltage, discharges to the minimum squared voltage through R_1 and R_2, pro-

* Patent. R. C. A. and W. Van B. Roberts (British Application No. 4019/42).

ducing across the latter a negative pulse, the duration of which is adjusted to be much less than the period of the maximum F.M. signal frequency. The number of these pulses and their mean value are proportional to the F.M. signal frequency and therefore to its modulation content. Hence a mean voltage variation proportional to the frequency deviation of the I.F. appears across diode D_2 and is passed on to the A.F. amplifier. R_3 forms with diode D_2 a positive

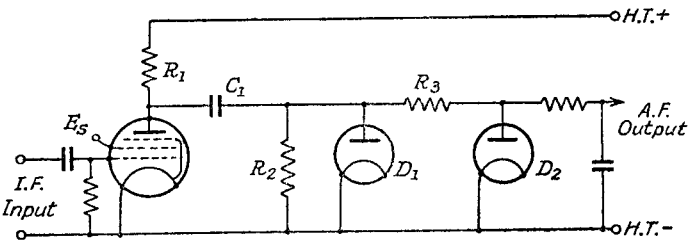

FIG. 15.24.—The Counter Type Frequency-to-Amplitude Converter.

pulse suppressor, which prevents the positive charging voltage pulse across D_1 being passed on to the A.F. amplifier.

15.9.6. The Hexode Frequency-to-Amplitude Converter. The property of electron collection possessed by the signal grid of the hexode valve (see Section 5.8.2, Part I), as the frequency of the oscillator voltage is increased, has been suggested * as a means of converting F.M. into an A.F. signal. The F.M. signal is applied to the oscillator grid, and a grid leak resistance (0·5 MΩ) and capacitance (50 $\mu\mu$F) are connected in parallel between control grid and cathode. A resistance anode load (R.F. is by-passed by a capacitance of about 50 $\mu\mu$F) is used. It is found that under suitable conditions a linear variation of grid voltage of about 0·8 volts is obtained when the signal frequency is varied from 15 to 25 Mc/s. This grid voltage variation is amplified by the valve, and the resultant A.F. appearing across the anode circuit resistance is passed on to the A.F. amplifier. The chief disadvantage of the method is the high input signal frequency required and the low conversion efficiency.

15.10. Methods of Frequency Modulation Compression in the Receiver.

15.10.1. Introduction. The use of wide-band frequency modulation has certain disadvantages from the point of view of receiver design. It is not possible to use the same I.F. transformers for high fidelity amplitude modulation—the wide pass-band admits

* Patent. R. C. A. and F. B. Stone (British Application No. 12097/42).

undesired noise components from outside the required pass range, and selectivity is inadequate—so that a receiver designed for dual operation must have two separate sets of I.F. transformer. If, however, the original frequency deviation of the F.M. signal could be compressed in the receiver from ±75 kc/s to ±15 kc/s, conversion to amplitude modulated reception would only involve a simple switching operation at the detector stage, the same transformers and I.F. amplifier circuits being used for both types of modulation. The phase discriminator stage is converted for A.M. detection by connecting the cathodes of the diodes together and taking the output for the A.F. amplifier from the centre point of the diode load resistances as shown in Fig. 15.25. The band width cannot be reduced below about ±15 kc/s, otherwise both frequency and amplitude modulation suffer from attenuation distortion of the upper audio frequencies, and high fidelity is not possible. Advantages other than that of dual operation are gained by compressing the frequency-modulated deviation ; the lower value of I.F. that is possible gives greater gain per stage and is more stable ; the method of compression generally has a limiting action on any amplitude modulation so that a separate limiter stage (with, usually, loss of amplification) is not necessary. The reduction in modulation due to compression is largely offset by the increased sensitivity of the frequency-amplitude converter discriminator made possible by the reduced band width required.

There are various methods of compressing the frequency deviation. One uses a variable reactance valve, operated from the A.F. output signal from the receiver, to frequency-modulate the local oscillator and cause its frequency to follow the frequency deviations of the input signal. For example, suppose the input carrier is frequency modulated ±75 kc/s, ranging from 45·075 to 44·925 Mc/s, the local oscillator frequency is frequency modulated to vary from 45·525 to 45·405 Mc/s (or 44·595 to 44·475) so that the resultant I.F. carrier is 465 kc/s, frequency modulated ±15 kc/s. Another method uses a frequency divider to produce the I.F. carrier and at the same time reduce the frequency deviation. A third system employs an oscillator operating at a submultiple of the input signal and locked by it. The original frequency deviation is reduced in the ratio of the submultiple to the input frequency.

15.10.2. Compression by Frequency Modulation of the Local Oscillator.[5, 6, 15] A block schematic diagram of the apparatus is shown in Fig. 15.25. The variable reactance valve may be used to correct for slow as well as rapid changes of frequency by

applying to it D.C. bias as well as A.F. voltage from the output of the discriminator; the resistance R_2 and capacitance C_2 (0·1 MΩ and 50 μμF) in the diagram form a R.F. filter. This is an important point because harmonic distortion of the A.F. output tends to occur at high output levels if the frequency deviation is not centred correctly in the frequency-amplitude converter discriminator characteristic. Amplitude limiting results because the magnitude of the reactance variation of the reactance valve is dependent on the amplitude as well as the frequency of the input signal to the discriminator. Thus an initial amplitude variation of the input signal to the latter is applied to the reactance valve to frequency-modulate the local oscillator and produce an A.F. output at the discriminator

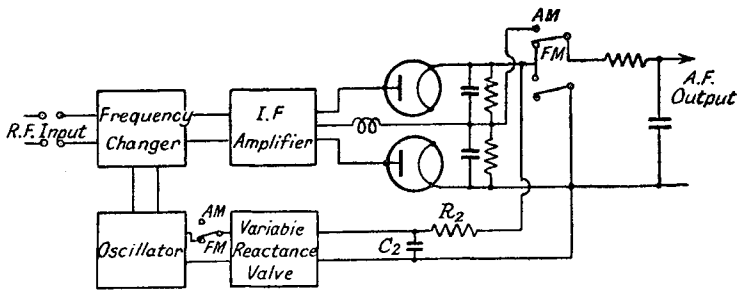

FIG. 15.25.—Frequency Deviation Compression by Frequency Modulation of the Receiver Oscillator.

180° out of phase with the A.F. output due to the initial amplitude modulation. The overall performance of the apparatus as regards signal-to-noise ratio is comparable with that of the wide-band amplifier with a saturated amplifier limiter. This type of compressor, which is an example of the negative feedback principle, possesses the advantage of reducing distortion, hum and interference produced in the I.F. amplifier.

For conversion to amplitude-modulated reception the switch is moved to position A.M. and the variable reactance valve is disconnected.

15.10.3. The Frequency Divider Compressor. The principle of frequency division* can be applied in the F.M. receiver to compress the frequency deviation, and a circuit diagram is shown in Fig. 15.26. The input frequency, 13 Mc/s, modulated ±75 kc/s, is obtained from an I.F. amplifier following the first frequency changer. This initial change of frequency is essential since a fair

* Patent. R. C. A. and M. G. Crosby (U.S. Application No. 430,348).

degree of selectivity is necessary before the frequency divider stage, which has less adjacent channel selectivity than the normal frequency changer stage. The 13 Mc/s input is applied to two frequency changer valves. The first (V_1) has an anode circuit tuned to the required I.F., e.g., 4·5 Mc/s, and its output is applied to the second I.F. amplifier and to the second frequency changer valve V_2. The anode circuit of V_2 is tuned to the sum frequency of the two intermediate frequencies, i.e., 13+4·5 = 17·5 Mc/s, and the output from this is connected to the other grid of the valve V_1, in which it reacts with the original 13 Mc/s to produce a difference frequency of

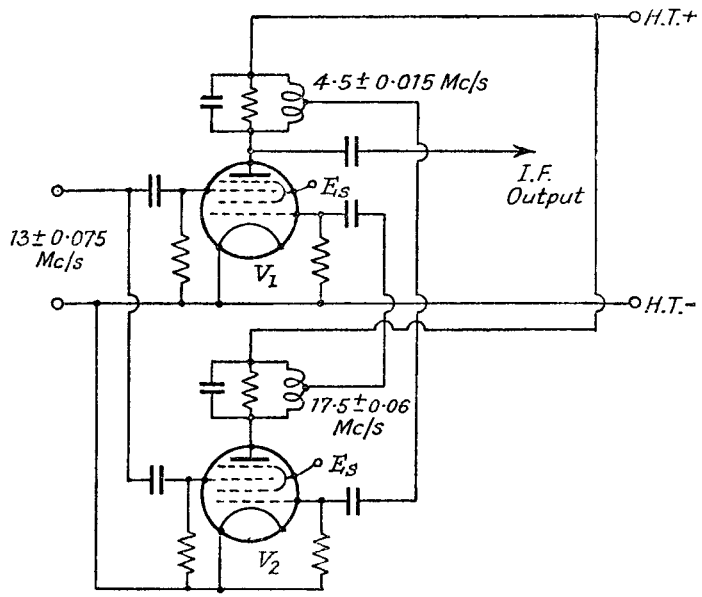

FIG. 15.26.—An Example of the Frequency Divider F.M. Compressor.

4·5 Mc/s. The extent of F.M. compression of the 4·5 Mc/s output depends on the relative selectivities of the 4·5 and 17·5 Mc/s tuned anode circuits. Equal selectivities divide the frequency deviation in equal proportions between the two frequencies, i.e., 4·5 ± 0·0375 and 17·5 ± 0·0375 Mc/s, and the degree of compression is conveniently controlled by varying the selectivity of the 17·5 Mc/s circuit. Thus, if that of the latter is reduced to one-quarter of the 4·5 Mc/s circuit, the output frequency is 4·5 Mc/s modulated ±15 kc/s. It is interesting to note that the 4·5 and 17·5 Mc/s frequencies are only generated when there is an input signal, and they disappear when it is zero. The reason for this is that the slightest shock

excitation of the 4·5 Mc/s and 17·5 Mc/s anode circuits, due to noise or switching on the 13 Mc/s signal, causes voltage components of these frequencies to appear in the circuits, and the process is self-sustaining as long as there is an input signal. The frequency divider stage has less adjacent channel selectivity than the normal frequency changer because the lower selectivity of the 17·5 Mc/s tuned circuit permits the sum frequency to be self-adjusting to a fairly wide range of input frequencies. Thus a 12 Mc/s input frequency shock-excites the 4·5 Mc/s circuit to produce a sum frequency in the anode circuit of V_2 of 16·5 Mc/s so that the second I.F. amplifier offers no selectivity against this undesired frequency. This type of compressor also acts as a limiter and is capable of smoothing out wide variations of input signal amplitude.

15.10.4. Frequency Compression by Submultiple Locked Oscillator. A method of compressing frequency modulation by means of a locked oscillator operating at a submultiple * of the I.F. has been developed, e.g., an I.F. of 4·5 Mc/s modulated ± 75 kc/s can be used to lock a submultiple oscillator of 0·9 Mc/s, the frequency modulation of which is reduced in the ratio of the fundamental frequency reduction of $\frac{1}{5}$ to ± 15 kc/s. A circuit diagram of the

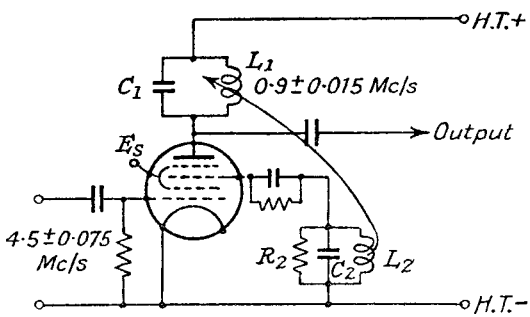

FIG. 15.27.—Compression of Frequency Deviation using a Submultiple Locked Oscillator.

apparatus is shown in Fig. 15.27. A frequency-changer type of valve is employed with the I.F. signal applied to the control grid, and the submultiple oscillation is generated by feedback from its tuned anode circuit to the oscillator grid. The regenerator circuit in the oscillator grid has a natural frequency greater than the submultiple frequency ; its inductance is $\frac{1}{5}$ or $\frac{1}{6}$ of the anode inductance L_1, and its capacitance C_2 is approximately three times that of the anode-tuning capacitance C_1.

* Patent. R. C. A. and G. L. Beers (British Application No. 2310/43).

The locking range of the submultiple oscillator is governed by the $\frac{L_1}{C_1}$ ratio and also by the damping of the anode circuits. A large $\frac{L}{C}$ ratio and heavy damping tend to increase the locking range. By a suitable choice of coupling between L_1 and L_2, and of supply voltages, the system can be made to function as a satisfactory limiter. Grid leak self-bias may be employed on the I.F. signal grid to aid limiting and provide A.G.C. voltage. The circuit is stated to possess particular advantages in reducing noise and adjacent channel interference because of its restricted locking range. Frequencies outside the selected range, which is limited to a little more than that required for the desired signal, are unable to lock and their effect is largely eliminated from the output.

BIBLIOGRAPHY

1. The Reception of Frequency Modulated Radio Signals. V. J. Andrews, *Proc. I.R.E.*, May 1932, p. 835.
2. A Method of Reducing Disturbances in Radio Signalling by a System of Frequency Modulation. E. H. Armstrong, *Proc. I.R.E.*, May 1936, p. 689.
3. Frequency Modulation Propagation Characteristics. M. G. Crosby, *Proc. I.R.E.*, June 1936, p. 898.
4. Communication by Phase Modulation. M. G. Crosby, *Proc. I.R.E.*, Feb. 1939, p. 126.
5. The Application of Negative Feedback to Frequency-Modulation Systems. J. G. Chaffee, *Proc. I.R.E.*, May 1939, p. 317.
6. Frequency Modulation. Theory of the Feedback Receiving Circuit. J. R. Carson, *Bell System Technical Journal*, July 1939, p. 395.
7. The Service Range of Frequency Modulation. M. G. Crosby, *R.C.A. Review*, Jan. 1940, p. 349.
8. A Method of Measuring Frequency Deviation. M. G. Crosby, *R.C.A. Review*, April 1940, p. 473.
9. Designing a Wide Range U.H.F. Receiver. F. W. Schor, *Q.S.T.*, Aug. 1940, p. 34.
10. N.B.C. Frequency-Modulation Field Test. R. F. Guy and R. M. Morris, *R.C.A. Review*, Oct. 1940, p. 190.
11. Two Signal Cross Modulation in a Frequency-Modulation Receiver. H. A. Wheeler, *Proc. I.R.E.*, Dec. 1940, p. 537.
12. Band Width and Readability in Frequency Modulation. M. G. Crosby, *R.C.A. Review*, Jan. 1941, p. 363.
13. The Design of Television Receiving Apparatus. B. J. Edwards, *Journal I.E.E.*, Part III, Sept. 1941, p. 191.
14. Eddy Current Tuning. C. C. Eaglesfield, *Wireless Engineer*, May 1942, p. 202.

15. Reduction of Band Width in F.M. Receivers. D. A. Bell, *Wireless Engineer*, Nov. 1942, p. 497.
16. Receiver Input Circuits. R. E. Burgess, *Wireless Engineer*, Feb. 1943, p. 66.
17. Coupled Circuit Filters. K. R. Sturley, *Wireless Engineer*, Sept. 1943, p. 426.
18. The Phase Discriminator. K. R. Sturley, *Wireless Engineer*, Feb. 1944, p. 72.
19. Frequency Modulation. K. R. Sturley, Electronic Engineering Monograph.

CHAPTER 16

TELEVISION RECEPTION

16.1. Introduction.[18, 34, 35] To obtain a clear idea of the problems involved in the reception of television signals and their conversion into an image of the original viewed object, a short description of the method of converting light, reflected from an object, into electrical impulses is necessary. Since the transmitter is, in effect, a single-channel system, it is quite incapable of conveying instantaneously the whole picture ; to do so would require a large number of links each transmitting an electrical impulse proportional to the instantaneous light intensity from a small area of the object. The actual number of transmissions would depend on the detail required from the reproduced image, fine detail necessitating the selection of light from a very small area of the object and a very large number of transmitters. Owing to its property of persistence of vision, the eye is capable of seeing a composite image even when the light components are being interrupted, provided the rate of interruption exceeds about sixteen times per second. Hence a satisfactory picture can be obtained without each transmitter being in continuous operation, as long as the electrical pulses, proportional to the light from the particular area, are transmitted at least sixteen times per second. The brightness of reproduction would be reduced in proportion to the reduced time of transmission, and flicker would be evident, but the picture would be reproduced as a whole. Since continuous transmitter operation is not essential, it is clear that the separate transmitters could be replaced by a single transmitter successively modulated by the electrical impulses derived from the light areas originally associated with individual transmitters, and this is the principle involved in television. The loss of brightness due to successive transmission can be overcome by increased efficiency of the light to electrical impulse (and vice versa) conversion at transmitter and receiver, and flicker can be removed by increasing the rate of pick-up of light from a given area.

Conversion of the light to electrical impulses and successive pick-up are normally achieved by means of a special type of cathode-ray tube, known as the iconoscope, having a mosaic screen of photo-active material, which acts like a series of minute insulated photo-electric cells. The screen consists of a thin mica plate, on one side

of which is deposited the photo-active material, and on the other a conductive coating of colloidal graphite. The image of the object to be viewed is focused on to the screen, and the coating and photo-cell elements act as a series of capacitances, which are charged to voltages proportional partly to the brightness of the light falling on the cell element and partly to the time during which the cell is activated. These minute capacitors are discharged by the action of the cathode-ray beam, which is caused to scan the sensitive side of the mica plate in a series of almost horizontal lines one below the other. The beam is eventually returned to its starting-point and the whole image is repeatedly scanned. Discharge of the photo-electric capacitance elements causes a series of voltage pulses across a resistance connected between the mica conductive coating and a similar colloidal graphite coating round the inside of the neck of the tube. These voltage pulses are actually produced by secondary electrons, released by the cathode ray beam as it passes over the photo-electric elements and collected by the tube coating, which is at the same potential as the last anode. After suitable amplification the pulses are used to modulate the transmitter.

Interlaced scanning [1] is employed because it reduces flicker and gives better definition for a given pulse-frequency spectrum. Successive line scans are spaced a line width apart, so that half the image is scanned at a time, and the gaps between the lines of one vertical scan are filled in by the lines of the next vertical scan. It is achieved automatically in the iconoscope by using an odd number of lines per complete picture, alternate vertical scans starting half a line later. The number of vertical scans, or frames, is twice the number of complete pictures and, as far as flicker is concerned, it is equivalent to doubling the number of pictures transmitted. The number of frames per second must bear an integral or fractional relationship to the mains supply frequency, otherwise flicker is produced by small A.C. voltage components from the H.T. or heater supplies, which modulate the receiver light reproducer and cause alternate bands of light and shade to wander across the picture. Hence fifty frames are transmitted per second in England and sixty in America.

To achieve a high degree of definition the number of horizontal scanning lines must be large, and to remove flicker the number of complete pictures must not be less than 25 (50 frames).[1] This entails a large number of equivalent picture elements and, for sharp contrast, a high maximum modulating frequency. The limit of the latter is half the number of picture elements scanned per

second (a sine wave has a positive and negative half), which is determined by the number of horizontal lines per complete picture and the aspect ratio (width to height) of the latter. Taking the pre-war English standard of 405 lines per picture, 25 pictures per second, and an aspect of ratio of 5 to 4, the total number of elements in a vertical side is 405 and in a horizontal $\frac{405 \times 5}{4} = 506$, so that the maximum modulating frequency is

$$\frac{405 \times 506 \times 25}{2} = 2{\cdot}56 \text{ Mc/s.}$$

An important feature of television transmission is therefore the large frequency spectrum occupied by the modulation sidebands. It is probable that development will be in the direction of even higher lines per picture, with consequent increase in sideband spectrum. In America a standard of 525 lines has already been adopted. Such a large modulation frequency spectrum can only be accommodated by using an ultra short-wave carrier frequency, such as 45 Mc/s or greater.

It is found in practice that the maximum modulating frequency, as calculated above, is actually higher [12] than is necessary because vertical resolution is less than horizontal and the number of active picture elements is less than the maximum. For example, it is possible that alternate vertical picture elements of black and white equal to one line width may be positioned such that half of each is scanned by a line. In this case the resultant pulse is equivalent to light halfway between black and white, and vertical definition is lost. It has been estimated [34] that only 65% of the total picture elements are fully effective, so that the maximum modulating frequency could be reduced from 2·56 to 1·66 Mc/s without impairing picture definition to any great extent.

In a television transmission channel, correct synthesis of the image at the receiver output is dependent on the light spot at the reproducer keeping step with the scanning spot at the transmitter, and some form of synchronizing signal must be incorporated in order to trigger the frame- and line-deflecting circuits at the correct time instants. The light signal must therefore be regularly interrupted to allow the transmission of a synchronizing signal at the end of each horizontal line and vertical frame scan. This is achieved by applying a synchronizing signal of opposite polarity to the light signal to modulate the carrier. The pre-war English [15] standard method of transmission is illustrated in Fig. 16.1. The

unmodulated carrier amplitude, corresponding to a black signal, is 30% of its maximum white amplitude, and modulation by the light signal always increases the mean carrier value. Hence average, as well as contrast brightness of picture is transmitted i.e., it contains the D.C. and A.C. components of the light signal. The synchronizing signals are transmitted by reducing carrier amplitude below its unmodulated or black value, and they have a rectangular shape. The line synchronizing pulse, which has a fundamental frequency of $405 \times 25 = 10{,}125$ c.p.s., occupies 10% of the total line period, but the carrier level is maintained at black for a further 5% to allow 15% "flyback" time for the horizontal deflecting circuits. The light signal is therefore transmitted for 85% of the total line time. At the end of a vertical (frame) scan, the vision signals are suppressed for about 10 lines, and during part of this time the frame synchronizing pulse is transmitted. It consists of a series of rectangular pulses similar to the line pulses but four times as long, i.e., two are transmitted for every line period. During the $\frac{1}{10}$th line period interval between the pulses, the carrier is restored to its unmodulated black value. The number of frame pulses are usually eight, and for the rest of the 10-line suppression period the line-synchronizing signals are continued with carrier amplitude at 30% maximum for the intervening $\frac{9}{10}$ths line periods. The synchronizing signal for odd-numbered frames occurs in the middle of a line period and for

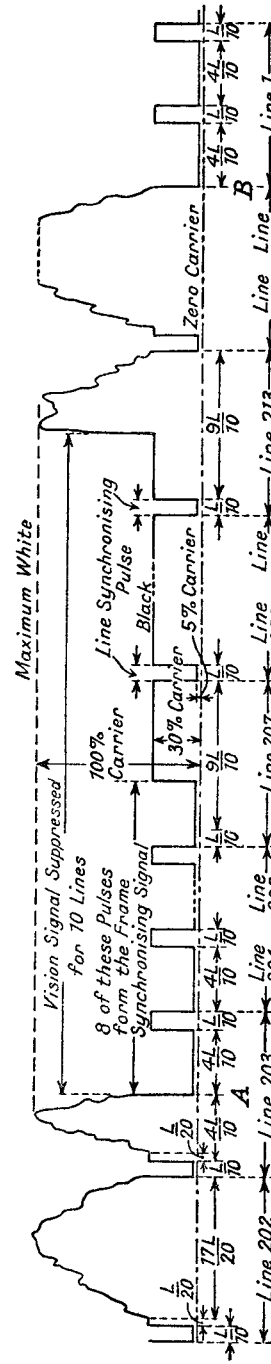

FIG. 16.1—The Waveform of the Vision Signal of the Pre-war English Transmission.

even-numbered frames at the end of a line period as shown by positions *A* and *B* in Fig. 16.1. The type of light modulation shown in this figure is known as positive modulation, and that for the synchronizing signal as negative modulation. The American system is the reverse of this, the picture modulation being negative with maximum brightness for minimum carrier, and the synchronizing modulation being positive. It is the mirror image of the English type of modulation envelope. The two systems also differ in two other respects; double sideband transmission with the associated audio* programme at a frequency 3·5 Mc/s below the television carrier, and vertical polarization of the radiated television signal are used in England, whilst vestigial sideband (the upper with 750 kc/s of the lower) transmission with the audio carrier 4·5 Mc/s above the television carrier, and horizontal polarization are standardized in America. No fundamental modifications are, however, necessary to convert the receiver from one system to the other.

Having established the form of signal broadcast by a television transmitter, we are now able to consider the essential features of a receiver for reproducing correctly an image of the object being televised.

16.2. The Essential Features of a Television Receiver. A block diagram showing the essential parts of a superheterodyne television receiver [10, 13] is given in Fig. 16.2. The dipole aerial, placed vertically if vertical polarization is used, or horizontally for horizontal polarization, has a length corresponding to half-wave resonance at approximately the centre of the frequency range covered by the vision channel. There is some attenuation of the audio signal, but little attenuation distortion because the audio sidebands cover such a small frequency range. Both signals are amplified together as far as the output of the frequency changer, the same local oscillator being used to provide the vision and audio intermediate frequencies. The anode of the frequency changer contains a special filter separating the two intermediate frequencies, but extra rejection of the audio I.F. may be required in the vision frequency I.F. amplifier in addition to the attenuation provided by the I.F. circuits. Single sideband vision reception is generally employed because a higher amplification per stage, and a more level frequency response can be obtained in the I.F. amplifier when the required band width is reduced. Proper reproduction of the

* The prefix " audio " before " programme ", " carrier " or " intermediate frequency " means the carrier or intermediate frequency which carries the audio frequency programme as sidebands.

vision signal can only be secured when the vision carrier is correctly tuned to the edge of the pass-band, and this is achieved by using the sound signal as a tuning indication. The I.F. amplifier for the audio signal usually has a pass-range about 100 kc/s wide (to allow for frequency drift of the oscillator), and correct tuning of the audio signal, within this pass-range, by variation of oscillator frequency, automatically involves correct tuning for the vision signal if the two I.F. channels are correctly aligned in the first place. The vision intermediate frequency must be carefully chosen to give an adequate pass-band without serious attenuation or phase distortion, and to avoid spurious responses, which produce chequerboard or wavy line patterns across the reproduced picture.

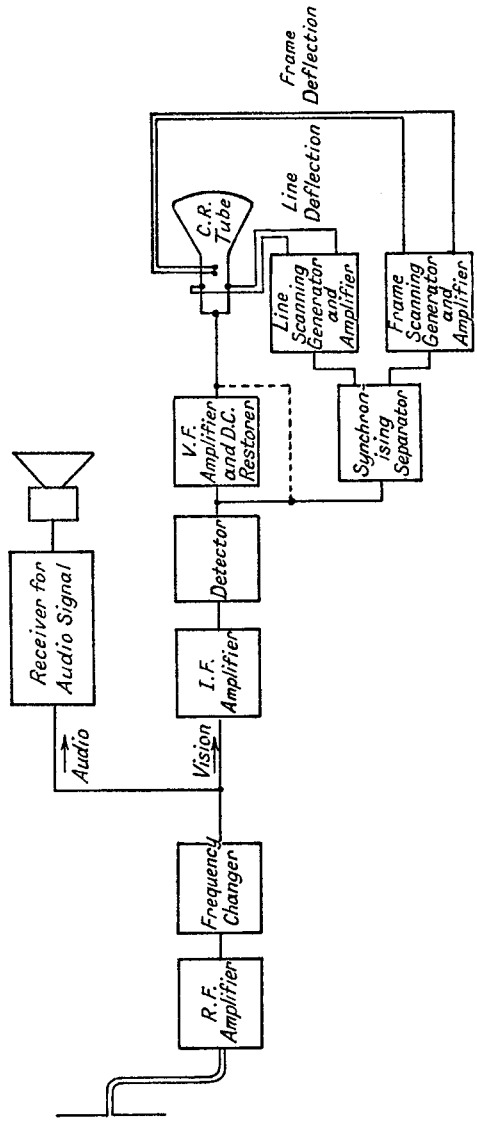

FIG. 16.2.—The Schematic Diagram of a Television Receiver.

When only a single transmission is to be received, the amplifier before the vision frequency detector may be of the fixed tuned R.F. type.[6] It has advantages over the superheterodyne that tuning is not dependent on a local oscillator, the frequency of which may drift appreciably during the first half-hour after switching on,

that a flat pass-band can be more easily obtained at the higher frequency and that it does not produce spurious interfering frequencies. Its disadvantage is that more difficulty is experienced in removing the audio signal from the vision output, because the tuned circuits in the R.F. stages cannot normally provide sufficient attenuation unless the pass-band of the vision signal is severely restricted. With this type of receiver it is usual to divide the feeder line from the aerial into two channels, and to insert a filter in the vision channel to reject the audio transmission, and a vision frequency filter in the audio channel. Additional filters may be included in the vision R.F. amplifier so as to bring about an overall attenuation of the audio signal of 40 db. It will be noticed that by this system the audio and vision signals are separated at the aerial, and common amplification of the two is not employed. Sometimes the first stage in the vision R.F. amplifier is used to amplify both audio and vision, special narrow pass-band rejection circuits being inserted to provide sufficient overall attenuation of the audio signal in the remaining stages. Another possibility with double sideband transmission is to use single sideband reception, the sideband on the opposite side of the carrier to the audio signal being accepted ; the chief difficulty with this method is that satisfactory operation depends on the R.F. circuits being, and remaining, correctly tuned.

The vision frequency detector is generally a diode, but a triode, functioning as an anode bend detector, may be used. The diode load resistance must be low, about 5,000 Ω, in order to prevent attenuation of the higher vision frequencies by the stray capacitance across it. The same is true of the anode load resistance of the vision frequency amplifier after the detector, and in this part of the apparatus special methods are adopted to neutralize the reactance of the stray capacitance. The V.F. amplifier is not usually a D.C. amplifier, and a diode or similar device is used to restore the D.C. component at the output.

The V.F. amplifier is connected to the voltage-light converter. The latter function is successfully performed by the cathode-ray tube, the beam of which is capable of intensity modulation by the application of a voltage to its grid (or gun electrode, as it is sometimes called). The grid voltage varies the density of the electrons in the beam and hence the brightness of the spot formed on the screen, a positive direction of voltage increasing brightness. The area, or focus, of the spot on the screen can be controlled by varying the D.C. current in a coil round the neck of the tube (magnetic

focusing)—a permanent magnet with a variable shunt may also be used—or by varying the voltage applied to an intermediate anode between the grid and final anode (electrostatic focusing). The diameter of the screen on which the image is formed is generally 9 or 12 inches ; the useful picture area with the 12-inch diameter cathode-ray tube is 10 inches by 8 inches. The colour of the light depends on the screen material ; the most popular colour is a bluish white obtained with a screen material of zinc sulphide or cadmium tungstate with zinc silicate.

A deflecting system is necessary to synthesize the light impulses into an intelligible picture, and arrangements must be made to deflect the beam horizontally and vertically in an identical manner to, and in step with, the scanning beam in the iconoscope. This can be achieved either by applying voltages of saw-tooth shape to deflecting plates mutually at right angles inside the C.R. tube, between the final anode and screen (electrostatic deflection), or by means of currents of saw-tooth shape in coils external to the C.R. tube (magnetic deflection). Magnetic deflection has the great advantage that it allows a much shorter tube to be used and a more compact receiver is therefore possible. The saw-tooth voltage or current generator consists usually of a resistance-capacitance charge circuit operating in conjunction with a triggering charge or discharge device, such as a blocking oscillator. The " free " frequency of the triggering action is set to a value slightly below the fundamental of the frame or line saw-tooth, and is pulled into step by means of the synchronizing pulses sent out by the transmitter. These pulses are separated from the vision signals by means of a special synchronizing separator stage, which usually incorporates a limiting action to prevent loss of synchronism due to noise or interference. A filter is employed to separate line pulses from the frame synchronizing pulse used to lock the frame-scanning generator.

The order of importance of the four types of distortion, harmonic, attenuation (frequency), phase and transient, in television reception is different from that for audio reception. Harmonic distortion has relatively little effect, but both attenuation and phase have a large influence on the picture. High-frequency cut-off attenuation distortion leads to a picture with blurred outlines giving the appearance of being out of focus, whilst high-frequency intensification in the video frequency amplifier, if carried too far (the increase should not exceed 1 db. above the average level), may result in transient distortion, i.e., damped oscillations producing a rippled effect following the trailing edge of a white or black vertical line. Low-

frequency cut-off in the V.F. amplifier causes uneven reproduction of large surfaces.

Phase distortion leads to a plastic relief type of image, a white or black vertical line being preceded by a black or white margin respectively, or, if it is excessive, multiple images may be formed. Phase distortion is zero if the time delay is constant for all the frequency components of the signal passing through the amplifier. This means that the phase angle shift between the output and input must be proportional to frequency. For example, suppose there is a constant time delay of 1 microsecond at all frequencies; this represents 1 cycle or 2π radians at 1,000 kc/s, $\frac{1}{2}$-cycle or π radians at 500 kc/s, $\frac{1}{10}$-cycle or $\frac{\pi}{5}$ radians at 100 kc/s, and so on.

Attenuation and phase distortion can occur in all stages of the receiver, but are generally greatest in the R.F. and I.F. stages, partly because there are more of them than of V.F. amplification. For a given pass-band width coupled or band-pass circuits can be designed to give less of both types of distortion than a single-tuned circuit.

We shall now examine the separate stages in the receiver, with particular reference to the English type of transmission, i.e., the vision signal is assumed to be double sideband transmission on a carrier of 45 Mc/s, with an audio programme on a carrier of 41·5 Mc/s. The required band width for adequate definition is assumed to be 78% of the maximum possible number of picture elements, i.e., $\pm 2{\cdot}56 \times 0{\cdot}78 = \pm 2$ Mc/s. Signal-to-noise ratio on full modulation (white) is to be not less than 30 db. for an input of 50 μV at the aerial. The overall amplification of the receiver is to be capable of giving 25 volts swing, peak-to-peak, at the grid of the cathode-ray tube for a fully modulated input of 50 μV at the aerial.

16.3. The Aerial Circuit.[14] Owing to the high modulation frequencies involved in television reception it is most important that reflected signals,[9] delayed in time with respect to the real signal, should be prevented from reaching the aerial input of the receiver at a strength comparable with the real signal. These delayed signals may be caused by reflections from large buildings, metal objects (aeroplane), changes in earth conductivity, or incorrectly terminated aerial feeder lines, particularly coaxial or parallel open wire lines, which have a much lower attenuation loss per unit length than twisted wire feeders. The latter have an attenuation loss of about 1 to 2 db. per wavelength as compared with 0·1 db. per wavelength for open wire lines and coaxial feeders. Particular

care must also be taken with parallel open wire lines to see that they are balanced with respect to earth for, unlike the coaxial cable with an earthed outer, they can pick up an appreciable signal voltage, which may be comparable with that picked up by the aerial itself. The signal voltages in each side of the parallel wires cancel at the receiver if the receiver input is centre-tapped to earth and the wires themselves are balanced to earth. The effect of the delayed signal depends largely on the time lag between it and the real signal; if the delay is large a " ghost " image, displaced from the real image, is produced, but, if it is small, blurring or a change in the light distribution of the image may result. For example, owing to a redistribution of the amplitude and phase of the side-bands of real and reflected signals, cancellation or intensification may change a vertical white line into black or vice versa. To gain some idea of the importance of the time delay effect, let us consider a receiver having a 12-inch diameter cathode-ray tube giving a picture area of 10 ins. by 8 ins. The speed at which the spot travels across the picture is $405 \times 25 \times 10 \times 2{\cdot}54 \div 0{\cdot}85$ (lines per picture $\times$ complete pictures per second $\times$ length of line $\div$ conversion factor allowing 15% flyback time) $= 3{\cdot}02 \times 10^5$ cms./sec. The rate of travel of the television signal in free space is 3×10^{10} cms./sec., i.e., $0{\cdot}994 \times 10^5$ times faster than the C.R. tube spot. Hence, if there are two signal paths from the transmitter to the receiver, one 276 yards (252 metres) longer than the other, the longer path signal produces a second image displaced by $\frac{1}{10}$-in. from the real image on the C.R. tube screen. Normally the best position for the aerial is vertical for vertically polarized transmission, and horizontal, one end pointing towards the transmitter, for horizontally polarized transmission, but particular site conditions—congested areas with intervening high buildings—may call for special orientation in order to reduce reflected signal interference.

The most suitable type of aerial is the dipole or V dipole. The latter has the advantage (see Sections 3.3.5 and 3.5.3, Part I) over the former of having a lower characteristic impedance and hence less variation of terminal impedance over a given frequency range. This means less transition loss at the junction of aerial and feeder. The length of the dipole is not very critical and it is usual to select a value giving resonance at the centre of the frequency range, thus the length of a dipole to resonate at 45 Mc/s is

$$\frac{\lambda}{2{\cdot}1} = \frac{3 \times 10^{10}}{45 \times 10^6 \times 2{\cdot}1} = 318 \text{ cms.} = 10 \text{ ft. } 5 \text{ ins.}$$

The factor 2·1 instead of 2 is used because, owing to end effects, the electrical length of an aerial of brass, copper or aluminium is approximately 5% greater than its physical length. For steel-rod aerials the correction factor is about 2·2. A reflector may be used behind the aerial to increase the pick-up from the transmitter and reduce interference, such as that from motor-car ignition systems, from directions on the opposite side of the aerial to the transmitter. The reflector is usually spaced from $\frac{1}{4}\lambda$ to $\frac{3}{8}\lambda$ away from the aerial, and its length may be made greater than that of the latter so as to give a broad double-humped overall frequency response. The dimensions of one such type [28] are : a main aerial 10 ft. 1 in. long with a reflector 11 ft. 1 in. long, separated by a spacing of 4 ft. 4 ins.

The aerial-to-feeder connection is generally to the centre of the dipole, though the feeder may be connected to one end of the dipole by using a special $\frac{1}{4}\lambda$ matching section,[5] made by two parallel wires $\frac{1}{4}\lambda$ long, separated by $1\frac{1}{2}$ to 2 ins. One of these wires forms an extension to the $\frac{1}{2}\lambda$ dipole and the ends of both are joined to the twin wire feeder. For twin wire shielded feeder or low impedance (80 Ω), the dipole is cut at the centre and each feeder wire goes to the end of one half-section. The distance between the two cut ends should be as small as possible compatible with satisfactory insulation; about 1 inch separation is generally adequate. Parallel wire feeders of high impedance (500 Ω) can also be connected to the centre of the aerial, but in this case the latter is not cut into two half-sections. The feeder ends are fanned out in triangular manner from their normal separation of about 2 ins. to a separation of 26 ins. in a distance of 40 ins. ($0{\cdot}15\lambda$).[30] The mouth of the isosceles triangular shape of flare is connected to be symmetrically disposed about the centre of the dipole. Coaxial feeder may also be connected to the centre of a split dipole, the outer and inner conductors being joined to the near ends of the two half-sections. This is not the most efficient method, and a standing wave is produced on the outer conductor between the points where it joins the aerial and where it is earthed. A better system is to use a transformer with a balanced primary centre-tapped to earth, and a secondary, one end of which is connected to the inner and the other to the earthed outer. An electrostatic screen is desirable to prevent capacitive coupling from the primary to the secondary, causing unbalance of the primary.

The dipole aerial should be self-supporting, or alternatively stay wires must be broken up by insulators into lengths not equal to $\frac{1}{2}\lambda$ or multiples of it. The feeder should be taken away at right

angles to a vertical dipole for a distance of about 20 ins. before turning it downwards. A shorter distance (but not less than 10 ins.[25]) may be used from aerial to the turn when necessary.

16.4. The R.F. Amplifier.[23] The design of the feeder-to-first tuned circuit connection of the receiver follows the lines set out in Section 15.5. The performance of the first R.F. valve has an influence on the design of the first tuned circuit. Maximum amplification requires the tuning capacitance of all tuned circuits to be as small as possible, so that valve grid input and anode output capacitances should be as small as possible. The input resistance of the valve at 45 Mc/s is less important than in the case of the frequency modulation receiver, because the pass-band width is very much greater and calls for heavy damping of the first tuned circuit. Mutual conductance must be as high as possible and, for minimum shot-noise resistance, total cathode current at minimum bias must be as small as possible. This means that alignment of grid and screen wires (this reduces screen current), and anode current cut-off at a comparatively low grid bias are required. The valve cannot, therefore, have a very good variable-mu characteristic and, although harmonic distortion is not so serious with a television as with an audio signal, control of amplification by grid bias variation is unlikely to be satisfactory. Another disadvantage of grid control of amplification is that it tends to vary the grid input resistance and capacitance of the valve ; this effect can be reduced by the use of an unby-passed resistance in the cathode lead as discussed in Section 4.10.3, Part I. For design purposes we shall consider the R.F. valve to have characteristics similar (except for grid input resistance which is taken as 8,000 Ω) to those of the valve in Section 15.5, viz., g_m of 8 mA/volt, input and output capacitances of approximately 10 and 8 $\mu\mu$F, and an equivalent shot-noise resistance of 1,500 Ω. Values as high as 14,000 Ω[28] for input resistance at 45 Mc/s can be obtained with special valve designs, but as long as it is greater than a certain value the chief advantage of a high resistance is that any variation from valve to valve, or due to control of amplification, has less effect when the majority of the damping is provided by a fixed resistance. A typical circuit showing the feeder to first tuned circuit coupling, and the R.F. amplifier valve is that of Fig. 16.3. The feeder is assumed to have a characteristic impedance of 80 Ω, optimum coupling is employed between the feeder coupling coil L_1 and the secondary coil L_2, the inductive reactance of L_1 is cancelled by the capacitive reactance of C_1, the tuning capacitance C_2 (consisting only of valve, wiring

and coil self-capacitances) is assumed to be 15 $\mu\mu$F. This low value of C_2 can be realized by very careful layout. We must now decide the permissible attenuation loss at the maximum off-tune frequencies of ± 2 Mc/s. For a single-tuned circuit, phase and attenuation distortion are closely related and increase of the latter increases the former. It would therefore appear that the circuit should be designed to give minimum attenuation loss; the advantages of doing this are that a lower Q value is required so that the valve grid input resistance becomes of less consequence and the noise voltage at the grid of the first R.F. valve is reduced. On the other hand, transfer voltage ratio is decreased to a greater extent than the decrease of noise voltage and a larger signal output is required from the feeder to obtain the same signal-to-noise ratio. This feature

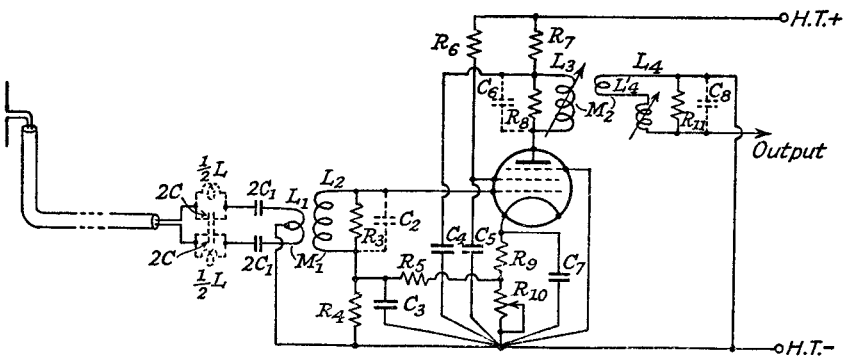

FIG. 16.3.—The Aerial and R.F. Amplifier Stage for a Television Receiver.

is illustrated later in the section. The reduction in transfer voltage ratio has practically no effect on the overall amplification of the receiver because the more constant frequency response over the pass-band range calls for less compensation in the tuned transformer stages, i.e., the coupling coefficient can be brought closer to its critical coupling value, the peak-to-trough ratio decreased and the gain of each transformer coupled stage therefore increased. The chief advantage of adopting a higher attenuation loss in the first tuned circuit (apart from greater overall sensitivity for a given signal-to-noise ratio) is that phase distortion in transformer stages giving a double-humped frequency response is in the opposite direction to that in the first tuned circuit, and it is reduced as the double-humped response is made more pronounced, i.e., coupling coefficient is increased, so that a closer approach to cancellation can be made. Usually about four transformer stages are employed and

there is therefore a tendency to obtain overcorrection of the phase distortion if the first tuned circuit has too small attenuation loss and phase distortion.

In order to estimate the effect of phase distortion, the phase angle shift and attenuation loss of a single-tuned circuit at different values of QF, i.e., different off-tune frequencies, are tabulated below. For zero phase distortion, the phase angle should be proportional to the off-tune frequency, Δf, i.e., to QF, and in the fourth row of Table 16.1, the difference between the required phase angle (proportional to Δf, and calculated by multiplying the phase angle at $QF = 0{\cdot}1$ by the ratio of the particular value of QF being considered to 0·1) and the actual phase angle is indicated.

TABLE 16.1

QF	+ 0·1	+ 0·2	+ 0·3	+ 0·4	+ 0·5
Attenuation Loss (db.)	− 0·043	− 0·17	− 0·37	− 0·64	− 0·97
Phase Angle	− 5° 43′	− 11° 19′	− 16° 42′	− 21° 48′	− 26° 34′
Phase Angle Error	0	+ 5′	+ 29′	+ 1° 7′	+ 2° 5′
QF	+ 0·6	+ 0·7	+ 0·8	+ 0·9	+ 1·0
Attenuation Loss (db.)	− 1·335	− 1·73	− 2·15	− 2·58	− 3·01
Phase Angle	− 30° 58′	− 34° 59′	− 38° 40′	− 41° 59′	− 45°
Phase Angle Error	+ 3° 25′	+ 5° 8′	+ 7° 10′	+ 9° 35′	+ 12° 18′

The time delay is greatest for the largest value of QF, and if $QF = 1$ for $\Delta f = 2$ Mc/s, the error in time delay is

$$\frac{12° \ 18'}{360} \times \frac{1}{2 \times 10^6} \text{ seconds} = 0{\cdot}0171 \ \mu \text{ secs.}$$

In Section 16.3 we showed that the spot on a typical C.R. tube for television signals travels at $3{\cdot}02 \times 10^5$ cms./sec., so that 0·0171 μ secs. corresponds to a displacement of 0·0516 mm., which will give negligible blurring of the picture. As far as the first tuned circuit is concerned we can allow an attenuation loss of − 3 db. at the maximum off-tune frequency of 2 Mc/s. A point to be watched is that compensation for this loss by doubled-humped response in subsequent stages does not introduce excessive overall phase distortion.

The final Q_2' of the secondary circuit including damping introduced by optimum coupling to the feeder of characteristic impedance 80 Ω is, for a loss of − 3 db. at $\Delta f = \pm 2$ Mc/s, given by

$$Q_2' = \frac{f_m}{2\Delta f} = \frac{45}{4} = 11{\cdot}25$$

or the Q of the secondary circuit when not coupled to L_1 is

$$Q_2 = 2Q_2' = 22{\cdot}5$$

and its resonant impedance is

$$R_{D2} = \frac{Q_2}{\omega_m C_2} = \frac{22{\cdot}5 \times 10^6}{6{\cdot}28 \times 45 \times 15} = 5{,}300\ \Omega.$$

If the initial Q_0 of the coil L_2 is 150, the total damping resistance required across L_2 is

$$R_{T2} = \frac{R_{D2}Q_0}{Q_0 - Q_2} = 6{,}240\ \Omega.$$

The input resistance of the valve provides 8,000 Ω of this so that

$$R_3 = \frac{6{,}240 \times 8{,}000}{1{,}760} = 28{,}350\ \Omega.$$

The transfer voltage ratio is (see expression 15.2)

$$T_R = \frac{1}{2}\sqrt{\frac{R_{D2}}{R_{a1}}} = \frac{1}{2}\sqrt{\frac{5{,}300}{80}} = 4{\cdot}07$$

if the feeder characteristic impedance is 80 Ω.

For optimum coupling $M_1 = \dfrac{\sqrt{R_{a1}R_2}}{\omega_m} = \dfrac{\sqrt{80 \times 10{\cdot}45}}{6{\cdot}28 \times 45} = 0{\cdot}102\ \mu\text{H}$

where $R_2 = \dfrac{\omega_m L_2}{Q_2}$ = effective series resistance of the secondary circuit.

$$C_2 = 15\mu\mu F,\ L_2 = \frac{1}{\omega^2{}_m C_2} = 0{\cdot}832\ \mu\text{H}$$

$$L_1 = 0{\cdot}416\ \mu\text{H},\ C_1 = 30\ \mu\mu\text{F}$$

$$Q_1 = \frac{\omega_m L_1}{80} = 1{\cdot}47.$$

Using expression 15.3*b* and noting that $Q_2F = 2$ and $Q_1F = 0{\cdot}1305$, we find that the actual loss at off-tune frequencies of ± 2 Mc/s is approximately $-2{\cdot}8$ db. If L_1 is made equal L_2, Q_1 is doubled and the loss at ± 2 Mc/s is reduced to $-2{\cdot}6$ db.

The equivalent total noise resistance is the sum of the overall resonant impedance of the first tuned circuit, including damping from the feeder side, and the shot-noise resistance of the valve, i.e., it equals $2{,}650 + 1{,}500 = 4{,}150\ \Omega$, so that the R.M.S. noise voltage at the grid of the first valve is

$$E_n = 1{\cdot}25 \times 10^{-10}.\ \sqrt{4{,}150 \times 4 \times 10^6}$$

$$= 16{\cdot}1\ \mu\text{V}$$

$$\equiv \frac{16{\cdot}1}{4{\cdot}07} \equiv 3{\cdot}96\ \mu\text{V on the feeder side.}$$

For satisfactory performance, signal-to-noise ratio should be of the order of 30 db., i.e., 31·6 to 1, so that the minimum acceptable signal output from the feeder is 125 μV.

If the permissible loss at 45 Mc/s is reduced to -1 db., $Q_2'F = 0{\cdot}5$, $Q_2' = 5{\cdot}62$ for $\Delta f = 2$ Mc/s, $R_{D2} = 2{,}650\ \Omega$, and

$$T_R = \frac{1}{2}\sqrt{\frac{2{,}650}{80}} = 2{\cdot}88$$

$$E_n = 1{\cdot}25 \times 10^{-10}\sqrt{(1{,}325+1{,}500) \times 4 \times 10^6}$$

$$= 13{\cdot}3\ \mu\text{V}$$

$$\equiv 4{\cdot}62\ \mu\text{V on the feeder side.}$$

Hence the minimum acceptable signal output from the feeder is 146 μV. We see, therefore, that sensitivity (for a given signal-to-noise ratio) is approximately 20% better in the case of the -3 db. attenuation loss than the -1 db. loss.

Referring to Fig. 16.3, it will be seen that control of amplification is obtained mainly by suppressor grid bias variation, the variation of control grid bias being only approximately 3% of the suppressor grid change. The reason for this dual control is that it reduces the variation of grid input resistance and capacitance with change of amplification. The same result may be realized by the use of an unby-passed resistance in the cathode circuit (see Section 4.10.3) and by variation of screen voltage[28] to obtain amplification control. When screen voltage is varied cathode self-bias is not used, but fixed bias is obtained for the controlled valves from a resistance in the main H.T. supply lead. The values of the resistances in Fig. 16.3 are

$$R_4 = 100{,}000\ \Omega, \quad R_5 = 3{,}000\ \Omega, \quad R_6 = 50{,}000\ \Omega,$$
$$R_9 = 150\ \Omega, \quad R_{10} = 20{,}000\ (max.)\ \text{variable.}$$

The decoupling capacitors, C_3, C_4, C_5, and C_7 are of mica and have values of 0·001 μF.

Before considering details of the tuned transformer in the anode circuit of the valve in Fig. 16.3, it is advantageous to obtain generalized phase-angle error curves against QF for different values of Qk in order that overall phase distortion can be estimated.

In Section 7.3, Part I, the phase angle at the output of a tuned transformer with reference to the grid input voltage for any off-tune frequency is given by rationalizing expression 7.2*a*, i.e.,

$$\phi = \tan^{-1} - \frac{(1+Q_1Q_2(k^2 - F^2))}{-(Q_1+Q_2)F} \quad . \quad . \quad 16.1$$

ϕ therefore varies from 270° to 90° as QF varies from 0 to $+\infty$ (Δf changes from 0 to $+\infty$).

As far as phase distortion is concerned, it is better to consider $QF = 0$ as the reference point, and to call the phase angle at this value 0°. To do this expression 16.1 must be inverted and given a negative sign.

$$\phi' = \tan^{-1} - \frac{(Q_1+Q_2)F}{1+Q_1Q_2(k^2 - F^2)} \quad . \quad . \quad 16.2a.$$

The negative sign is necessary because expression 16.1 shows that the phase angle is reduced as QF increases positively.

If the primary and secondary circuits are identical

$$\phi' = \tan^{-1}\frac{-2QF}{1+Q^2(k^2 - F^2)} \quad . \quad . \quad . \quad 16.2b.$$

The phase-angle error is calculated in the same way as that for the single-tuned circuit, viz., the correct phase angle is calculated by multiplying the phase angle at $QF = 0{\cdot}1$ by the ratio of the particular value of QF being considered to 0·1; the correct phase angle is subtracted from the actual phase angle to give the phase-angle error. A positive sign to the latter indicates that the required phase angle is negative and numerically less than the actual phase angle, i.e., it represents a time advance, or alternatively the time delay is less than it should be. Conversely, a negative sign means that the time delay is greater than it should be.

A series of phase-angle error curves is plotted in Fig. 16.4 against QF for different values of Qk. For reference purposes the error curve for a single-tuned circuit is also included, and is the dashed curve in the figure. An interesting point to note is that over the range from $QF = 0$ to 1 the error is positive for couplings corresponding to $Qk < 0{\cdot}7$. When $Qk = 0{\cdot}7$ the error is very small, and for $Qk > 0{\cdot}7$ the error becomes negative and reaches a maximum at about $Qk = 1$. For $Qk > 1$, the error decreases, slowly at first—there is little difference between $Qk = 1$ and 1·5.

From these curves the overall phase error for any combination of single-tuned circuits and tuned transformers can be estimated. For example, by combining a single-tuned circuit of $Q = \frac{f_m}{2\Delta f}$ with two tuned transformers of the same Q as the tuned circuit and $Qk = 1{\cdot}5$, phase distortion is almost zero over the range $QF = 0$ to 1. The maximum phase-angle error is 0° 42′ at $QF = 0{\cdot}6$. Figs. 4.3 and 7.7, Part I, show that there is some attenuation distortion with

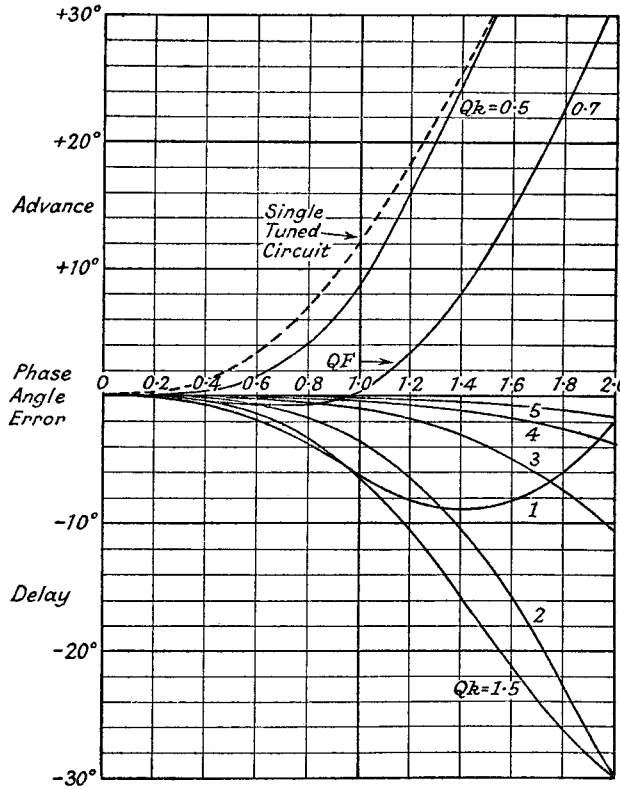

FIG. 16.4.—Phase Angle Error Curves of a Pair of Coupled Tuned Circuits for Different Values of Coupling.

this combination, the frequency response falling by 1 db. from $QF = 0$ to 1.

16.5. The Fixed Tuned R.F. Television Receiver. Let us now consider the design of the R.F. stages of a fixed tuned R.F. receiver to provide a detector input peak voltage of 5 volts. The overall amplification to produce this from a feeder output signal of 125 μV is 40,000, or 9,850 from the grid of the first valve (T_R for this feeder voltage = 4·07). A possible gain for each R.F. stage is 10, so that four stages are required. Examination of Fig. 16.4 suggests the use of four stages of coupling coefficient corresponding to $Qk = 2$ and the same Q value as the first tuned circuit, if phase distortion is to be reduced to negligible proportions. On the other hand, this combination results in a lower overall amplification and a wider pass-band than is required (less discrimination is therefore obtained against the audio signal), and a better compromise is

obtained by using four stages of coupling coefficient corresponding to $Qk = 1{\cdot}5$ and the same Q value as the first tuned circuit. Overall phase distortion is increased, but is still small enough to be negligible, and the overall frequency response variation over the frequency range corresponding to $QF = 0$ to 1 is not greater than 1 db. It actually rises from $QF = 0$ to 1 by 1 db., and at $QF = 1{\cdot}5$ and 1·75 (this corresponds to the frequency of the audio carrier), there is a loss of − 5 and − 8 db. (add to the curve in Fig. 4.3, four times the curve for $Qk = 1{\cdot}5$ in Fig. 7.7, Part I), compared to the value at $QF = 0$. The overall loss of − 8 db. at the audio carrier frequency is quite inadequate and extra filtering is necessary to increase the loss at this off-tune frequency of − 3·5 Mc/s, i.e., the audio carrier frequency of 41·5 Mc/s, to about − 40 db. Methods of achieving this are discussed at the end of the section. The rise of 1 db. in the frequency response at the edges of the pass-band is an advantage because both detector and vision frequency amplifier stages tend to have reduced amplification at the higher modulating frequencies. The overall phase-angle error is obtained by adding four times the curve for $Qk = 1{\cdot}5$ in Fig. 16.4 to the dashed curve for the single-tuned circuit, and it is tabulated below from $QF = 0$ to 1.

TABLE 16.2

QF	0	0·1	0·2	0·3	0·4	0·5
Overall Phase Angle Error	0	0	− 1′	− 9′	− 30′	− 1° 3′
QF	0·6	0·7		0·8	0·9	1·0
Overall Phase Angle Error	− 2° 4′	− 3° 38′		− 4° 56′	− 9°	− 13° 2′

Time-delay error is maximum at $QF = 1$, i.e., an off-tune frequency of 2 Mc/s, and corresponds to a displacement of 0·0546 mm. for the same speed of spot as is assumed for the single-tuned circuit calculation given earlier. Hence phase distortion is negligible.

Details of the transformer in the anode circuit of the valve in Fig. 16.3 are therefore :

$Qk = 1{\cdot}5$, $Q = \dfrac{f_m}{2\Delta f} = \dfrac{45}{4} = 11{\cdot}25$ (this is the Q of both primary and secondary circuits when not coupled together). No extra tuning capacitance is employed, it being made up of the valve, wiring and coil self-capacitances, viz., 15 $\mu\mu$F. Tuning is carried out by variation of the inductances either by means of an adjustable iron core or by eddy current (slug) tuning. L_4 is divided into two

sections, one of which is directly coupled to L_3 to provide the required coupling coefficient.

Thus
$$L_3 = L_4 = 0{\cdot}832\ \mu\text{H}$$
$$k = \frac{1{\cdot}5}{Q} = 0{\cdot}1333$$
$$M_2 = kL_3 = 0{\cdot}111\ \mu\text{H}.$$

Assuming a coupling coefficient of 0·3 between the section L_4' of the secondary and the primary L_3.

$$0{\cdot}3 = \frac{M_2}{\sqrt{L_4' \times 0{\cdot}832}} \quad \text{or} \quad L_4' = 0{\cdot}165\ \mu\text{H}.$$

The resonant impedances of primary and secondary circuits are

$$R_{D3} = R_{D4} = \frac{Q}{\omega_m C_6} = \frac{11{\cdot}25 \times 10^6}{6{\cdot}28 \times 45 \times 15} = 2{,}650\ \Omega.$$

Amplification from the grid of V_1 to the output terminals of the secondary $= g_m \frac{R_{D3}}{2} \times 0{\cdot}89 = 9{\cdot}45$ when $g_m = 8$ mA/volt. The factor 0·89 allows for the 1-db. fall from peak to trough. The required value of overall amplification is not reached in this design, and either an extra stage is needed or two of the overcoupled circuits must be replaced by two critically coupled stages.

If the initial Q_0 of L_3 and L_4 is 150, the total additional damping resistance required across the primary and secondary is

$$\frac{R_{D3}Q_0}{Q_0 - Q_1} = \frac{2{,}650 \times 150}{138{\cdot}75} = 2{,}870\ \Omega. \quad \text{Hence } R_8 = 2{,}870\ \Omega.$$

Across L_4 the second R.F. valve already provides 8,000 Ω so that

$$R_{11} = \frac{2{,}870 \times 8{,}000}{5{,}130} = 4{,}460\ \Omega.$$

Finally, we must make certain that feedback through the anode-grid interelectrode capacitance has negligible effect. From expression 15.4*d*, Section 15.7, the minimum value of grid input resistance due to anode-grid capacitance for a valve having a tuned transformer in its anode circuit is

$$R_g(min.) = \frac{\pm 4}{g_m B_{ga} R_{D3}}$$
$$= \frac{\pm 4 \times 10^6}{8{\cdot}0 \times 10^{-3} \times 6{\cdot}28 \times 45 \times 0{\cdot}02 \times 2{,}650}$$
$$= \pm 33{,}400\ \Omega$$

where $C_{ga} = 0{\cdot}02\ \mu\mu\text{F}$.

Hence feedback through the anode-grid capacitance has negligible

effect on the grid circuit, the resonant impedance of which is only 2,650 Ω.

Thus a typical fixed tuned R.F. receiver consists of four stages of amplification with overcoupled ($Qk = 1{\cdot}5$) tuned transformers in the anode circuits in association with an input tuned circuit of the same Q value. All circuits are identical except for the last secondary circuit, the damping resistance for which is adjusted to suit the detector conduction damping resistance. Estimation of this resistance is left until Section 16.7, which deals specifically with detectors for television signals.

Earlier in this section it was shown that the overall attenuation at the audio signal carrier is only -8 db., and a loss at this frequency of -40 db. is required. The most convenient way of increasing the loss at this frequency is by the insertion of a parallel circuit, tuned to the audio carrier frequency, in the feeder line from the aerial to the first tuned circuit. If a coaxial feeder is employed only one tuned circuit is needed, but if a twin wire feeder is used, balance must be maintained by using a tuned circuit, of half the resonant impedance in each line. These circuits may be inserted at some convenient point in the feeder as shown by the dotted $\frac{1}{2}L$ and $2C$ circuits in Fig. 16.3. To obtain a loss of 40 db. the sum of the resonant impedances of both tuned circuits (at 41·5 Mc/s) must be 100 times the characteristic impedance of the feeder, i.e., $\omega LQ = 8{,}000$, or if $Q = 150$ (it should be as high as possible so as to reduce the loss at the vision carrier frequency, 45 Mc/s) $L = 0{\cdot}2045$ μH and $C = 71{\cdot}8$ $\mu\mu$F. The impedance of these circuits at 45 Mc/s is from expression 4.8*b*, Part I:

$$\frac{R_D}{1+jQF} = \frac{8{,}000}{1+j150 \times \frac{7}{41{\cdot}5}} = \frac{8{,}000}{1+j25{\cdot}3} \simeq -j316.$$

Hence there is a ratio loss at 45 Mc/s due to the introduction of the filter of

$$\frac{80}{\sqrt{80^2+(316)^2}} = \frac{1}{4{\cdot}08} \equiv -12{\cdot}2 \text{ db.}$$

so that the net reduction of the audio carrier is $8 + 40 - 12{\cdot}2 = 35{\cdot}8$ db.

The impedance of the tuned circuits at the maximum negative off-tune frequency of the vision signal, viz., 43 Mc/s is

$$\frac{8{,}000}{1+j150\frac{3}{41{\cdot}5}} = \frac{8{,}000}{1+j10{\cdot}85} - j735,$$

so that there is a ratio loss of $\frac{80}{\sqrt{80^2+735^2}} \equiv -19{\cdot}32$ db.

This means that the audio signal rejector has caused attenuation and phase distortion over the pass range, the frequency response falling by — 7·12 db. from 45 to 43 Mc/s. This fall may be partially offset by the fact that the generalized selectivity curves of Fig. 7.7 ignore a frequency factor which tends to give higher amplification of the sidebands lower in frequency than the carrier, and also by the fact that the sidebands higher in frequency than the carrier are attenuated to a decreasing extent by the filter as the off-tune frequency increases. Phase distortion can be checked by finding the phase angle shift due to the filter over the range 43 to 47 Mc/s. Phase-angle error is calculated by comparing the actual phase angle against the phase angle, which should have been obtained had the change been proportional to the change from 45 to 45·1 or 44·9 to 45 Mc/s. Selected values are given in the table below.

TABLE 16.3

f (Mc/s) . . .	43	44·9	45	45·1	47
Δf, Mc/s (relative to 45 Mc/s) . . .	— 2	— 0·1	0	+ 0·1	+ 2
Phase Angle . .	— 84° 42′	— 87° 41′	— 87° 44½′	— 87° 48′	— 88° 34′
Phase Angle Shift relative to 45 Mc/s	+ 3° 2½′	+ 3½′	0	— 3½′	— 49½′
Phase Angle Error	— 1° 52½′	0	0	0	+ 20½′

It is clear from the above table that phase distortion due to the filter has negligible effect on the picture.

Another method of rejecting the audio signal, besides that of single sideband reception of the sidebands on the opposite side of the vision carrier to the audio carrier, is to use cathode feedback. A parallel circuit, tuned to the audio carrier, is included in the cathode lead of the first (or first two) R.F. valves as described in Section 7.9, Part I.

16.6. The Superheterodyne Television Receiver.

16.6.1. Introduction. The chief advantage of the superheterodyne over the tuned R.F. receiver is that it can more conveniently select any one of a number of different carrier frequency transmissions. This is more important in America where there are five television bands covering a range from 44 to 90 Mc/s. The disadvantages of the superheterodyne are poor signal-to-noise [27] ratio (particularly when no R.F. stage precedes the frequency changer), a tuning stability dependent on the frequency stability of a local oscillator, and the production of spurious frequencies,

which may be fed back to the input of the receiver to cause interference with the picture.

Signal-to-noise ratio in a superheterodyne having no R.F. amplifying stages is low because the frequency changer generally produces more noise and gives less amplification to the signal than a R.F. amplifier. The local oscillator, too, adds its own quota to the total noise. The special types of frequency changer, such as the hexode or heptode, take a much larger cathode current than a R.F. amplifier valve and their equivalent shot-noise resistance is consequently very high (of the order of 0·25 MΩ). Hence they are not very suitable for use in receivers employing no R.F. stage. American practice, which often omits the R.F. stages, uses a pentode frequency changer with the local oscillator voltage applied to the grid-cathode circuit. This is the most efficient method of frequency changing for a given total cathode current, and the equivalent noise resistance can be reduced to quite a low value (about 10,000 Ω) when a high g_m pentode is used. A still lower equivalent noise resistance (about 7,000 Ω) can be obtained by using a triode valve as a frequency changer, but its conversion gain is low—it may be less than unity—so that higher amplification is needed from the I.F. stages to achieve a given sensitivity.

In the superheterodyne receiver it is normal to accept audio and vision signals up to the frequency changer output and to provide two separate I.F. channels. Frequency stability of the local oscillator is therefore more important from the point of view of the audio than of the vision signal, because the tuned circuits in the audio I.F. amplifier have much sharper selectivity. They may, however, be given a wider pass-band (±50 to ±100 kc/s) than that (±20 kc/s) normally required for high fidelity amplitude modulated reception. There is usually a slight reduction in signal-to-noise ratio with the wider pass-band. Discrimination against the audio signal is carried out in the vision I.F. amplifier by means of special rejection circuits.

Full discussion of the types of interference frequencies produced by the frequency changer is found in Section 5.4, Part I, and Section 15.7. The chief cause of interference with the television signal is I.F. harmonic feedback into the signal circuits. These I.F. harmonics can be produced in the I.F. amplifier and are normally present across the detector load resistance in the form of a R.F. ripple. If these fall within the television signal pass-band and are fed back into the signal circuits, they may cause chequerboard patterns or alternate streaks of light and shade to appear across

the picture. The effect can be reduced to negligible proportions by careful shielding of components likely to produce I.F. harmonics, decoupling of all circuits (frequency changer, I.F. amplifier, detector to V.F. amplifier connection, and the V.F. amplifier) so as to prevent I.F. harmonics from entering the H.T. supply. Careful selection of the intermediate frequency and reduction of the I.F. amplifier pass-band by employing single sideband reception are also important.

Single sideband I.F. reception is almost a necessity in the superheterodyne, if adequate amplification and selectivity are to be obtained with a level frequency response over the pass-band range. This calls for careful tuning, otherwise there may be serious phase distortion producing a picture in relief, or attenuation distortion with loss of definition. Generally the best tuning position is with the carrier tuned outside the pass range to a point where amplification is one-half maximum. There can never be an abrupt cut-off outside the pass range, and double sideband reception of the lower modulation frequencies nearest the carrier occurs. Unless the carrier is detuned to about one-half amplitude, this double sideband reception results at the detector output in an accentuated low-frequency response with an apparent lack of definition. The English system of double sideband transmission allows selection of either sideband to be made; since the sound signal is lower in frequency than the vision, better discrimination against it can be realized in the vision I.F. amplifier by using the upper vision sideband. Vestigial sideband transmission (the upper vision sideband with 750 kc/s of the lower sideband) has been adopted in America and the vision I.F. carrier is tuned outside the level part of the I.F. pass range to one-half amplitude. The vision and audio I.F. amplifiers are lined up together so that when the audio signal is correctly tuned, the vision carrier is correctly located on the side of the I.F. response curve, i.e., the output from the audio receiver acts as a tuning indication. Vestigial sideband transmission is used in preference to single sideband because it is difficult to achieve a sharp cut-off of all sidebands below the carrier frequency without appreciable phase distortion of those above the carrier.

To demonstrate the design features of a superheterodyne receiver, we shall consider the American system of television transmissions, each in different, sometimes adjacent, frequency bands, because it leads to a more complex receiver than does the single English transmission. Each frequency band is 6 Mc/s wide, the vision carrier is 1·25 Mc/s from the lowest frequency of the 6 Mc/s pass-band, e.g., the carrier frequency for the band 44 to 50 Mc/s, is

45·25 Mc/s. Vestigial sideband transmission provides for 750 kc/s of the lower vision sideband and 4 Mc/s of the upper. The associated audio carrier is 4·5 Mc/s above the vision carrier, viz., 49·75 Mc/s for the band specified, and 0·25 Mc/s from the upper edge of the 6 Mc/s band. There are four other television bands, 50 to 56, 66 to 72, 78 to 84, and 84 to 90 Mc/s, and it will be seen that first and last pairs are adjacent. This means that filters must be included in the vision I.F. amplifier to discriminate not only against the associated audio carrier but also against the audio carrier of the adjacent lower frequency band, for this carrier is only 1·5 Mc/s below the vision carrier.

16.6.2. The Frequency Changer Stage. The design of a R.F. stage preceding the frequency changer of a superheterodyne receiver is identical with that of a R.F. stage in a tuned R.F. receiver, and no further discussion is needed. Whether or not the frequency changer is preceded by a R.F. stage (or stages) depends on the type of frequency changer. If it is a heptode or hexode, a R.F. stage is essential. On the other hand, if a pentode of high g_m is used with oscillator application to the grid-cathode circuit, the equivalent noise voltage is not so much greater than that of the tuned R.F. receiver in Section 16.4. In order to make comparison between the relative noise voltages at the grid of the first valve in the two types of receiver, we shall consider the same total pass-band width as in Section 16.4, viz., 4 Mc/s. If the R.F. valve cited in that section is used as a frequency changer, it will have a conversion conductance approximately equal to $\frac{1}{4}g_m$, i.e., 2 mA per volt; its shot-noise resistance as a frequency changer is therefore four times its resistance as an amplifier, i.e., 6,000 Ω. Allowing for an equivalent shot-noise resistance of 2,000 Ω for the oscillator valve, we have a total shot-noise resistance of 8,000 Ω for the valve as a frequency changer. If the feeder-first tuned circuit coupling is the same as that in Section 16.4 having a loss of 3 db., the noise voltage at the grid of the frequency changer is

$$\begin{aligned} E_n &= 1{\cdot}25 \times 10^{-10}\sqrt{(8{,}000+2{,}650) \times 4 \times 10^6} \\ &= 25{\cdot}8\ \mu\text{V}, \end{aligned}$$

which is 1·6 times greater than that of the valve as a R.F. amplifier. This is not a large increase and it could be tolerated except for receivers operating at the edge of the service area of a transmitter. It should, however, be noted that as g_c is only $\frac{1}{4}g_m$, greater I.F. amplification is needed for the same overall gain as the tuned R.F. receiver. Since the pass-band width and minimum tuning

capacitance are the same for both types of receiver, the amplification of each I.F. stage cannot exceed that of a R.F. stage, so that an extra stage is needed in the superheterodyne receiver.

A heptode or hexode frequency changer has an equivalent shot-noise resistance of about 0·25 MΩ, hence the noise voltage at the grid of this type of valve is

$$E_n = 1{\cdot}25 \times 10^{-10} \times \sqrt{(250{,}000+2{,}650) \times 4 \times 10^6}$$
$$= 125{\cdot}6\ \mu\text{V},$$

which is 7·8 times greater than for the R.F. amplifier. The need for a R.F. amplifier in this case is obvious. Suppose we include the first R.F. stage of Section 16.5 before the frequency changer. The equivalent noise resistance in the frequency changer grid is 251,325 Ω (note that the resonant impedance of the secondary of the tuned transformer of Fig. 16.3 is $\frac{R_{D^4}}{2} = 1{,}325\ \Omega$), and

$$E_n = 1{\cdot}25 \times 10^{-10}\sqrt{251{,}325 \times 4 \times 10^6} = 125{\cdot}3\ \mu\text{V}.$$

The additional equivalent noise voltage at the grid of the R.F. valve is this voltage divided by the gain (9·45) of the R.F. stage, i.e., 13·28 μV. The total equivalent noise voltage at the grid of the R.F. valve, including that due to R.F. valve and first tuned circuit, is

$$E_n = \sqrt{(16{\cdot}1)^2+(13{\cdot}28)^2} = 20{\cdot}85\ \mu\text{V},$$

which is half-way between that of the R.F. valve used as an amplifier and that of the same valve used as a frequency changer. The use of two R.F. stages before the frequency changer reduces the equivalent frequency changer noise voltage at the grid of the first R.F. valve to 1·405, which makes practically no difference to the total noise voltage.

Another method of calculating the overall effect of noise in the frequency changer valve is to refer the total equivalent noise resistance in its grid circuit to the grid circuit of the R.F. valve by dividing the resistance by the square of the gain of the R.F. stage. The gain must be squared because noise resistance is proportional to the square of the noise voltage. Thus the equivalent frequency changer noise resistance at the grid of the R.F. valve is 2,810, giving a total resistance of 4,150+2,810 = 6,960 or

$$E_n = 1{\cdot}25 \times 10^{-10}\sqrt{6{,}960 \times 4 \times 10^6} = 20{\cdot}85\ \mu\text{V}.$$

For two R.F. stages the frequency changer equivalent shot-noise resistance falls to 31·6 Ω.

Turning now to the design of the frequency changer stage,

a circuit typical of American practice is shown in Fig. 16.5, for two of the five television bands. The dipole aerial is coupled through a transformer with a centre-tapped primary to a coaxial feeder; an electrostatic screen is included between primary and secondary. The coaxial feeder has the advantage of simplifying the push-button switching because one side is earthed. The receiver end of the feeder is connected through push-button switches (PB1 for band 1 and PB2 for band 2, etc.) to a primary coil L_1 coupled to two tuned circuits L_2C_2 and L_3C_3. The first tuned circuit increases selectivity against the image and other undesired signal frequencies, and also acts as an isolator to reduce the possibility of re-radiation of the local oscillator. Compared with the single coupling between feeder and grid-tuned circuit of Section 16.4, this double-tuned circuit coupling gives much sharper selectivity outside the pass-band for the same fall in response at the edges of the band; transfer voltage ratio is, however, usually reduced by inserting the circuit L_2C_2. Optimum coupling is employed between L_1 and L_2 and often between L_2 and L_3, and for a given pass-band response the value of L_2 can be varied without affecting the overall transfer voltage ratio of the filter. This may be proved as follows:

The transfer voltage ratio from feeder to C_2 is

$$\frac{E_2}{E_1} = \frac{1}{2}\sqrt{\frac{R_{D2}}{R_{a1}}} \quad . \quad . \quad . \quad . \quad 16.3$$

where R_{D2} = resonant impedance of L_2C_2 when coupled to, and including the damping from L_3C_3.

and R_{a1} = characteristic impedance of the feeder.

In order to make use of tuned transformer theory as developed in Chapter 7, Part I, we must imagine that the voltage E_2 is being produced by a constant current generator supplying the parallel circuit formed by L_2C_2. Assuming that optimum coupling is employed between L_1 and L_2, the resonant impedance of L_2C_2 (including the damping effects from L_1 and L_3C_3) is $\frac{1}{2}R_{D2}$. Hence the current from the fictitious constant current generator is

$$I = \frac{E_2}{\frac{1}{2}R_{D2}} \quad . \quad . \quad . \quad . \quad 16.4.$$

The transfer impedance from L_2C_2 to L_3C_3 from the current generator is (expression 7.3*a*, Part I) at f_m

$$Z_T = \frac{R_{D2}Q_3k\sqrt{\frac{L_3}{L_2}}}{2} = \frac{\sqrt{R_{D2}R_{D3}}}{2} \quad . \quad . \quad 16.5.$$

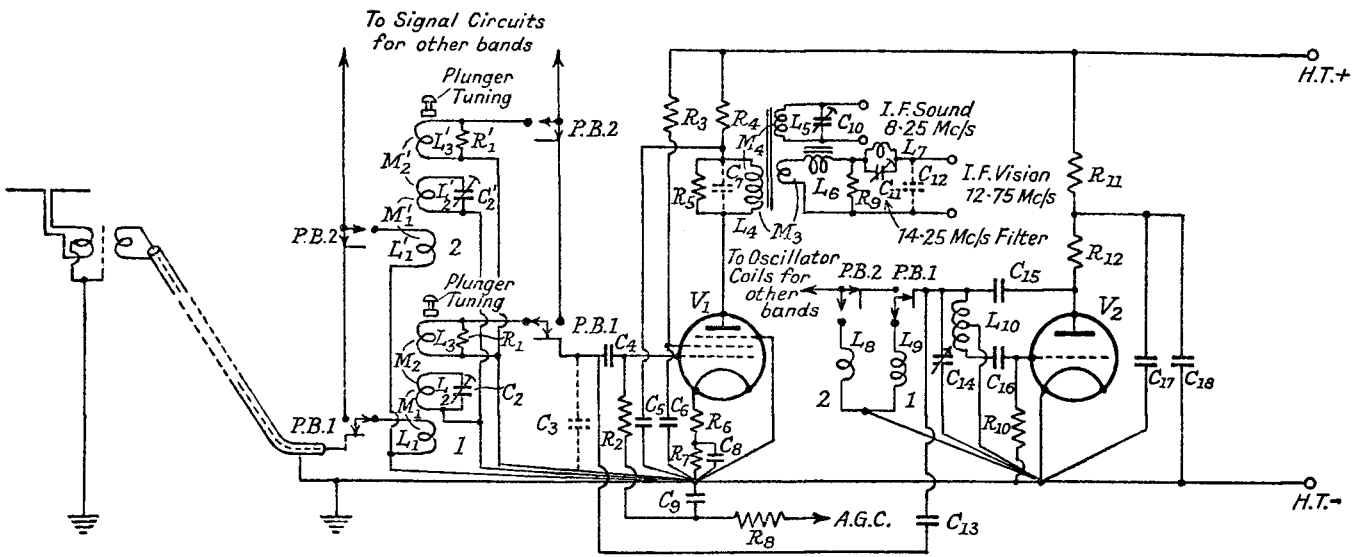

Fig. 16.5.—The Aerial and Frequency Changer Stages of a Superheterodyne Television Receiver.

The voltage across C_3 is

$$E_3 = IZ_T = I\frac{\sqrt{R_{D2}R_{D3}}}{2}$$

Replacing I by 16.4

$$E_3 = E_2\sqrt{\frac{R_{D3}}{R_{D2}}}$$

and E_2 from 16.3

$$\frac{E_3}{E_1} = \frac{1}{2}\sqrt{\frac{R_{D3}}{R_{a1}}} \quad . \quad . \quad . \quad . \quad 16.6$$

which is independent of R_{D2}. Now Q_2 and Q_3 determine the overall selectivity, and for constant selectivity (constant pass-band range) the product Q_2Q_3 must be constant, which means that Q_2 must be constant when L_2 only is varied. But

$$L_2 = \frac{R_{D2}}{\omega Q_2} \propto R_{D2} \text{ when } Q_2 \text{ is constant,}$$

so that variation of L_2 has no effect on transfer voltage when pass-band response is fixed.

Let us now compare a double coupling filter having a loss of — 3 db. at the edge of the pass-band with the single coupling of Section 16.4. Taking $Q_2 = Q_3$ (this is generally the most economical condition) and referring to Fig. 7.7, Part I, we see that for — 3 db. loss at optimum coupling ($Qk = 1$ curve), $QF \simeq 1{\cdot}4$, so that for $\Delta f = 2$ Mc/s

$$Q = \frac{1{\cdot}4 \times 45}{4} = 15{\cdot}75.$$

If $C_3 = 15\ \mu\mu$F, $R_{D3} = 3{,}700\ \Omega$, $L_3 = 0{\cdot}832\ \mu$H, and overall transfer voltage ratio is $\frac{1}{2}\sqrt{\frac{3{,}700}{80}} = 3{\cdot}4$, which is less than that (4·07) for the single coupling of Section 16.4. On the other hand, the loss at (for example) 11·3 Mc/s off-tune ($QF = 7{\cdot}9$) is — 30 db. as compared with — 18 db. (Fig. 4.3, Part I) for the single circuit.

If $L_2 = \frac{1}{2}.L_3 = 0{\cdot}416\ \mu$H, and $Q_2 = Q_3 = 15{\cdot}75$, the mutual inductance coupling between L_2 and L_3 is determined from $k = \frac{1}{Q} = \frac{1}{15{\cdot}75} = 0{\cdot}0635$, i.e., $M_2 = k\sqrt{L_2L_3} = 0{\cdot}0374\ \mu$H. The value of M_1 is obtained from the resistance $\frac{\omega^2 M_1^2}{R_{a1}}$ (see expression 3.18, Part I, when $R_{a1} \gg X_{a1}$), which, in association with

ωL_2, must give a Q of 15·75 (neglecting losses in L_2). Thus, when $\omega L_1 \ll R_{a1}$, $\omega L_2/\omega^2 M_1^2/R_{a1} = 15{\cdot}75$ gives $M_1 = 0{\cdot}063$ μH. In order to satisfy the condition that $\omega L_1 \ll R_{a1}$, L_1 should be as small as possible ; it is fixed by the maximum possible coupling coefficient, which may be taken as 0·4. Thus

$$k = 0{\cdot}4 = \frac{M_1}{\sqrt{L_1 L_2}}$$

or $$L_1 = 0{\cdot}1085\ \mu\text{H}$$

and $$\omega L_1 = 30{\cdot}7\ \Omega.$$

The chief effect of L_1 is to introduce a reactive as well as resistive component into the L_2C_2 circuit, but this may be compensated by retuning L_2C_2. In the above example the circuit L_2C_2 is assumed to be tuned to 45 Mc/s in order to facilitate comparison with previous calculations based on the English transmission. For the American system the circuit is capacitance-tuned to the centre of each band, e.g., 47 Mc/s for the 44 to 50 Mc/s band. The grid coil L_3 must be made as large as possible in order to obtain maximum transfer voltage ratio, and no tuning capacitance other than the wiring and valve capacitance, shown dotted as C_3, is used. Tuning of this circuit is accomplished by eddy current tuning of L_3. The plunger is inserted at the end of L_3 opposite to L_2, so that variation of L_3 has practically no effect on L_2 or the mutual inductance coupling M_2 between L_3 and L_2. The coils L_1, L_2 and L_3 are usually all wound on the same former, M_1 being adjusted for optimum coupling between L_1 and L_2, and M_2 for the correct pass-band width of 4·5 Mc/s, which covers both vision and audio sidebands. The push-button switching is arranged so that all but the coils associated with the particular band are disconnected.

The grid input resistance of the frequency changer will be comparable with its resistance as an amplifier, and its value will determine the value of resistance R_1 in parallel with L_3. It is quite common American practice to apply A.G.C. to the television receiver, and when the frequency-changer valve is controlled it is important that its input resistance and capacitance should not vary appreciably with change of bias, otherwise the grid circuit is off-tuned and its pass-band reduced as bias is increased. Accordingly an unby-passed resistance R_6 (about 50 Ω) is included in the cathode lead as described in Section 4.10.3. This resistance introduces negative feedback, and reduces the conversion gain of the frequency changer to about 65% of its value without the resistor. It increases input resistance, which means that R_1 must be decreased, and changes

of input resistance therefore have less effect. Mutual inductance or capacitance coupling is employed between the oscillator and grid-tuned circuit to produce an oscillator peak voltage of 3 volts between grid and cathode of the frequency changer. The latter may have cathode self-bias as in Fig. 16.5, or when A.G.C. is not applied it may be biased by grid current. The extra damping due to grid conduction current is negligible compared with the input resistance of the valve if a comparatively high grid leak, R_2 (0·5 MΩ) is employed.

The values of the other components in the frequency changer section of Fig. 16.5 are

$$R_3 = 50{,}000\ \Omega, \quad R_4 = 1{,}000\ \Omega, \quad R_6 = 50\ \Omega,$$
$$R_7 = 300\ \Omega, \quad R_8 = 0{\cdot}5\ \text{M}\Omega.$$
$$C_2 = 30\ \mu\mu\text{F}\ (max.), \quad C_4 = 50\ \mu\mu\text{F}, \quad C_5 = 0{\cdot}001\ \mu\text{F},$$
$$C_6 = 0{\cdot}001\ \mu\text{F}, \quad C_8 = 0{\cdot}001\ \mu\text{F}, \quad C_9 = 0{\cdot}01\ \mu\text{F}.$$

The heater leads are not shown in the diagram, but they are decoupled to earth by 0·001 μF mica capacitors.

16.6.3. The Oscillator. A separator oscillator valve is almost an essential requirement for the high frequencies involved in television reception, because it is not possible to obtain a high enough g_m and low enough R_a for satisfactory operation from a triode and frequency changer combined in the same bulb. The types of oscillator circuit most often used are the Hartley or Colpitts, or modified forms of these. In most cases fine tuning is carried out by means of a small trimmer capacitance, $C_{14}(2 - 5\ \mu\mu\text{F})$ in Fig. 16.5, across a part of the coil from anode or grid to earth. With the modified Hartley circuit of Fig. 15.6, the trimmer is placed across the whole coil.

Frequency stability is all important and care should be taken to carry out the principles laid down in Section 6.9, Part I, and Section 15.6. A negative temperature coefficient capacitor may finally be connected across a whole or part of the coil to compensate for the fall in frequency, which is associated with the normal increase in inductance and capacitance as the temperature rises. From the point of view of stability, oscillator frequency should be less than the signal frequency, but in American receivers it is generally greater than the signal frequency because this gives a lower I.F. for the sound signal. The disadvantage of the lower oscillator frequency is that the image frequency falls in a short wave range normally occupied by a large number of transmissions.

Change of range of oscillator frequency is usually accomplished

by switching coils in parallel with a part of the main tuning coil by push-button switches as shown in Fig. 16.5. Coupling to the frequency changer is by capacitance C_{13} (about 2 to 5 $\mu\mu$F) or by mutual inductance from the oscillator to signal circuit. This is possible because correct adjustment of oscillator amplitude can be made for each television band since the signal circuits are preset tuned. Typical values for the remaining components of the oscillator circuit are

$$R_{10} = 50{,}000\ \Omega, \quad R_{11} = 5{,}000\ \Omega, \quad R_{12} = 15{,}000\ \Omega.$$
$$C_{15} = C_{16} = 20\ \mu\mu\text{F}, \ C_{17} = 0{\cdot}001\ \mu\text{F (mica)}, \ C_{18} = 2\ \mu\text{F (paper)}.$$

The capacitance C_{18} is intended to decouple the oscillator from any low-frequency components present in the H.T. source.

16.6.4. The I.F. Amplifier. The most serious form of interference in television superheterodyne reception is that from intermediate frequency harmonics, and not, as in sound broadcast reception on medium and short waves, that from oscillator harmonic and image signal responses. Provided the oscillator frequency is greater than the signal frequency, image signal response presents hardly any problem, though it may become more important as more use is made of the ultra high-frequency band. With the English system of audio signal lower than the vision, the lower oscillator frequency has the advantage of giving an audio I.F. lower than the vision I.F.

Referring to the English system of audio and vision carriers at 41·5 and 45 Mc/s, it is clear that an I.F. equal to the difference (or a multiple of this) between the two carriers, viz., 3·5, 7, 10·5, 14 Mc/s, etc., should be avoided. Since feedback of I.F. harmonics is the greatest source of interference, a submultiple frequency of the vision carrier, 22·5, 15, 11·25, 9 and 7·5 Mc/s, must not be employed for the vision I.F. carrier. The width of the vision sidebands, 2 Mc/s, precludes the use of a low I.F., and too high a value is unsatisfactory because it is then more difficult to discriminate against the associated audio signal, and also to I.F. harmonics, which happen to fall in the I.F. range. On the other hand, image signal response is reduced by a high I.F. From the point of view of overall amplification it does not matter what value of I.F. is chosen when the pass-band width and minimum tuning capacitance are fixed, because the resonant impedances of any tuned circuits are then independent of f_m, e.g.,

$$R_D = \frac{Q}{\omega C}$$

and for a fixed pass-band width QF = constant, A,

hence $$Q = \frac{Af_m}{2\Delta f}.$$

Therefore $$R_D = \frac{Af_m}{2\pi f_m 2\Delta f C} = \frac{B}{\Delta f C} \propto \frac{1}{\Delta f C} = \text{constant}$$

when Δf and C are constant.

For a vision frequency band from 43 to 47 Mc/s, we find I.F. harmonic interference is possible over the following frequency ranges, 8·6 to 9·4, 10·75 to 11·75, 14·33 to 15·66, 21·5 to 23·5 Mc/s—we need not consider lower than the 5th submultiple—with clear reception from 9·4 to 10·75 (1·35), 11·75 to 14·33 (2·58), and 15·66 to 21·5 (4·83) Mc/s. Assuming single sideband I.F. reception (2 Mc/s total pass-band) with the upper sideband, a vision I.F. carrier of about 12 Mc/s is the lowest possible value; the I.F. audio carrier would be 8·5 Mc/s. Actually a lower I.F. (4·25 Mc/s with audio at 750 kc/s) has been successfully employed with narrowed sideband response. However, the general trend of television development is towards greater picture detail so that an I.F. of the order of 12 Mc/s is a better proposition. In America the vision I.F. carrier has been standardized at 12·75 Mc/s with 8·25 Mc/s for its associated audio carrier.

The circuits employed in the I.F. amplifier may consist of single-tuned circuits, having staggered resonant frequencies to cover the wide pass-band, coupled tuned circuits, or band-pass filters of the derived type with rejection frequencies for the associated audio programme and any other transmission likely to cause interference. The objection to single-tuned circuits with staggered resonant frequencies is that overall amplification is lower than for coupled circuits of the same pass-band width, and there is a danger of overloading the last stage in the amplifier unless the last tuned circuit has a flat frequency response over the pass range. Band-pass filters [10] generally require a low terminating impedance to give a practical value of capacitance element, and therefore stage gain tends to be low. Coupled tuned circuits [29] are the most popular type.

Coupled tuned circuits provide two possible methods of obtaining a flat overall frequency response; either each pair can be designed for a substantially flat response, or a combination of single- and double-peaked responses may be used. The former involves heavy damping and low Q values with consequent low amplification per stage; a combination of single- and double-peak responses is

therefore preferable because greater amplification can be realized. Overall phase distortion can also be reduced by suitably combining single- and double-peaked circuits, the distortion in single-peaked circuits often being in the opposite direction to that in double-peaked circuits. Excessive double-peaked response must be avoided, otherwise phase distortion (see Table 16.4) may become excessive ; for best compensation of attenuation distortion the value of QF at which the peak occurs should correspond to the edge of the pass-band, i.e., Δf remains the same as the peak moves farther from the mid-frequency, and Q must be increased to satisfy the higher value of QF. Mutual inductance or capacitance coupling may be provided between the tuned circuits ; the advantages of capacitance coupling are that inductance tuning can be carried out without affecting the coupling, and adjustment of one side only of the response curve with respect to the mid-frequency is possible. However, mutual inductance coupling can be made almost independent of inductance tuning if the mutual inductance is obtained by coupling a part only of one coil to the other, and adjustment of one side only of the response curve is possible by variation of the resonant frequency of either circuit, i.e., by varying coil inductance. If the stray capacitances across primary and secondary coils can be controlled within as good a limit as the inductances, tuning may be dispensed with ; alternatively one circuit only may have variable tuning and be made to compensate for variations in the other one. If capacitance tuning is used in the latter case, it is better included on the secondary side because the input capacitance of a valve is generally higher than its output capacitance. The trimmer capacitance has a certain minimum value and the ratio increase in tuning capacitance is less, and therefore the ratio decrease in amplification less, by adding the trimmer to the higher initial capacitance circuit. Lower stage gain is, of course, inevitable with capacitance tuning.

To estimate the overall amplification required of the I.F. stages, let us imagine that the aerial circuit and frequency changer valve are as in Section 16.6.2, and that an output of 5 volts peak is required at the detector. The equivalent noise voltage at the grid of the frequency changer is 25·8 μV, so that a signal-to-noise ratio of 30 db. fixes the minimum input signal at 817 μV, and the total amplification required from the grid of the frequency changer to the detector is $\frac{5 \times 10^6}{817} = 6{,}130$. Allowing a frequency changer conversion gain $\frac{1}{4}$ that of an I.F. stage and an I.F. stage gain of 13, we need three stages of I.F. amplification after the frequency changer,

and four pairs of I.F. coupled circuits. The pass-band of the R.F. tuned circuit before the frequency changer is wider than the I.F. pass-band (it has to include the audio signal as well), and we shall therefore neglect its effect on the overall frequency response in and around the I.F. pass range.

The design of the I.F. amplifier, which is detailed below, is considered with respect to the American form of multichannel vestigial sideband transmission, so that the vision I.F. carrier has to be tuned to a point on the side of the overall selectivity curve where the frequency response is one-half that of the average response over the pass-band. As 750 kc/s of the lower sideband is transmitted, it means that the flat pass-band response should begin about 500 kc/s above the vision I.F. carrier, the upper limit of the sidebands is 4 Mc/s, giving an effective overall pass-band of 3·5 Mc/s. Taking the band 50 to 56 Mc/s, for which the vision carrier is 51·25 Mc/s, the maximum upper sideband frequency, 55·25 Mc/s, and the associated audio carrier frequency, 55·75 Mc/s, an oscillator frequency of 64 Mc/s gives an I.F. vision carrier of 12·75 Mc/s, and a vision pass range from 12·25 to 8·75 Mc/s with a mid-frequency of 10·5 Mc/s. The associated audio carrier is 8·25 Mc/s and there is also the audio carrier (49·75 Mc/s) of the adjacent transmission producing an I.F. of 14·25 Mc/s. Special discrimination is needed against both these frequencies, and the filter circuits needed to suppress them may have considerable influence on the frequency response of the vision pass-band, particularly at the edges; the I.F. coupled circuits should therefore be designed in association with the filters. This, however, tends to mask some of the properties of the coupled circuits, and in this section we shall consider the performance of the latter only, leaving to the next section an examination of the I.F. amplifier with special filters, but noting that an overall response peaked at the edges of the pass-band will be an advantage in compensating for the attenuation caused by the filters.

When selecting the desired response of each pair of coupled circuits, we cannot afford to have single-peaked couplings less than critical because this entails loss of stage gain (maximum transfer impedance for couplings less than critical equals $\frac{R_{D1}Q_2k\sqrt{\frac{L_2}{L_1}}}{1+Q_1Q_2k^2}$). However, the overall reduction of amplification is usually less than the stage gain reduction due to using under-coupled circuits, since

a level pass-band response calls for increased coupling in the double-peaked circuits and also a higher Q value, which therefore tends to give a higher trough stage gain at the mid-frequency, f_m. For the four pairs of coupled circuits, let us select three of $Qk = 1{\cdot}5$, each having a peak-to-trough ratio of 0·7 db. with the peaks at $QF = \pm 1{\cdot}12$ (see Section 7.3, Part I), and one of $Qk = 1$ with a fall of − 1·8 db. at $QF = \pm 1{\cdot}2$. If Q is chosen to satisfy the values of QF quoted above at $\Delta f = \pm 1{\cdot}75$ (the total required pass-band is 3·5 Mc/s), there is a rise in the frequency response curve from the mid-frequency (10·5 Mc/s) to the edges of the pass-band. Maximum response of +0·9 db. occurs at $\Delta f = \pm 1{\cdot}45$ Mc/s and at $\Delta f = \pm 1{\cdot}75$ Mc/s the response is +0·3 db. with respect to that at the mid-frequency. As stated above, this increase is an aid when the sound signal filters are incorporated. Component values for the coupled circuits are as follows: taking first the overcoupled circuits ($Qk = 1{\cdot}5$), $QF = 1{\cdot}12$ at $\Delta f = 1{\cdot}75$ Mc/s gives

$$Q = \frac{1{\cdot}12 f_m}{2\Delta f} = \frac{1{\cdot}12 \times 10{\cdot}5}{3{\cdot}5} = 3{\cdot}36.$$

For maximum stage gain the tuning capacitance must be a minimum and this may be taken as 15 $\mu\mu$F. Referring to the typical I.F. amplifier circuit of Fig. 16.6 (valve V_4 stage), $C_{34} = C_{35} = 15$ $\mu\mu$F, $L_{17} = L_{18} = 15{\cdot}3$ μH, $k = \frac{1{\cdot}5}{Q} = 0{\cdot}446$, $M_6 = 0{\cdot}446 \times 15{\cdot}3 = 6{\cdot}82$ μH and

$$R_D = \frac{Q}{\omega C_{34}} = \frac{3{\cdot}36 \times 10^6}{6{\cdot}28 \times 10{\cdot}5 \times 15} = 3{,}400\ \Omega.$$

If the g_m of the I.F. valve is 8 mA/volt, the stage gain at the peaks of the frequency response is $\frac{1}{2} g_m R_D = \frac{8 \times 3{,}400}{2 \times 10^3} = 13{\cdot}6$, or at 10·5 Mc/s is $13{\cdot}6 \times 0{\cdot}923 = 12{\cdot}55$ (the factor 0·923 takes into account the trough to peak ratio of − 0·7 db.). The damping resistances R_{25} and R_{28} are calculated, using the method applied for the R.F. amplifier in Section 16.5; the valve input resistances are much higher, approximately in proportion to the reciprocal of the square of the frequency ratio, i.e., about 100,000 Ω. If grid-bias control of the I.F. valve is employed some method of stabilizing grid input capacitance is necessary, and in Fig. 16.6 negative feedback stabilization with the unby-passed resistances R_{17} and R_{26} (about 50 Ω) is shown. The values of the anode decoupling resistances (R_{16} and R_{24}) are 1,000 Ω, the screen potential dividers, $R_{14}R_{15}$ and $R_{22}R_{23}$, consist of 30,000 and 20,000 Ω resistances, the

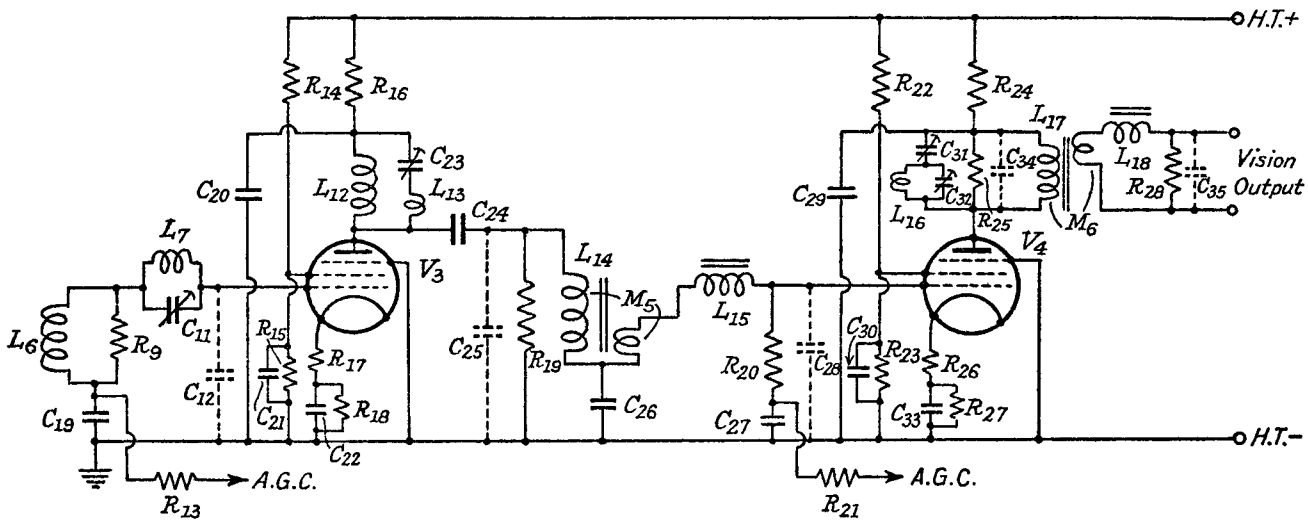

FIG. 16.6.—I.F. Amplifier Circuits of a Television Receiver with Audio Signal Rejector Circuits.

bias resistances R_{18} and R_{27} are 150 Ω, and decoupling capacitances C_{20}, C_{21}, C_{22}, etc., are 0·01 μF (mica). The A.G.C. filter for the valve V_3 stage is made up of C_{19} (0·1 to 0·5 μF) and R_{13} (0·5 MΩ).

For the critically coupled stage $QF = 1{\cdot}2$, $Q = 3{\cdot}6$, and $R_D = 3{,}640\ \Omega$ (C_7 and C_{12} in Fig. 16.5 are 15 $\mu\mu$F), which gives a stage gain for the frequency changer of 3·64 if $g_c = 2$ mA/volt. The total overall amplification is therefore 7,200 times, which more than satisfies the requirement originally postulated. This calculated gain ignores the reduction in amplification due to the negative feedback caused by resistances R_{17} and R_{26} in Fig. 16.6. Stage gain may be reduced to 75% of its normal value by the inclusion of these resistances, and when they are used an extra I.F. stage will be needed to reach the desired overall amplification of 6,130 times.

Since the gains of the I.F. amplifier stages are comparable with those of the tuned R.F. amplifier, and the mid-frequency is only one-quarter of the signal frequency, it follows that anode-grid interelectrode capacitance feedback, which was very small in the case of the R.F. amplifier, will be negligible in the I.F. amplifier.

Phase distortion can be checked in the manner described in Section 16.4. Since single sideband reception is being used the reference point is no longer the mid-frequency 10·5 Mc/s, but the vision carrier frequency 12·75 Mc/s and the curves in Fig. 16.4 are not applicable. The phase angles, derived from expression 16.2*b*, are tabulated on page 398 against QF for the two values of coupling $Qk = 1$ and 1·5. The modulation frequency corresponding to each QF value, and the phase angle error are also listed. The correct angle for zero distortion is calculated for the circuits of $Qk = 1{\cdot}5$ by subtracting from 68° 24′ the phase angle difference between $QF = +1{\cdot}45$ and $+1{\cdot}4$ multiplied by 20 times the difference between the particular value of QF being considered and $QF = 1{\cdot}45$. The latter value does not quite correspond to the vision I.F. carrier frequency (12·75 Mc/s), which gives $QF = 1{\cdot}44$, but is sufficiently close for all practical purposes. Similarly, for the critically coupled circuit of $Qk = 1$, $QF = 1{\cdot}55$ is taken as the reference point though $QF = 1{\cdot}545$ actually gives the vision carrier frequency.

The overall phase angle error is obtained by multiplying the error for $Qk = 1{\cdot}5$ by 3, and adding to it the error for $Qk = 1$. Thus at modulation frequencies of 3 and 4 Mc/s the overall errors are $-87°$ ($-106°+19°$) and $-104°$ ($-133°+29°$), and these correspond to time delays of 0·0805 and 0·0723 μ secs. respectively, which are satisfactory. Maximum time delay occurs at a modulation frequency at 3 Mc/s.

TABLE 16.4

QF.	$f_{mod.}$ (Mc/s).	Φ (actual).	Phase Angle Error.	$f_{mod.}$ (Mc/s).	Φ (actual).	Phase Angle Error.
+ 1·55	0	− 97° 24′	—	—	—	—
+ 1·5	0·07	− 94° 46′	0	—	—	—
+ 1·45	—	—	—	0	− 68° 24′	—
+ 1·4	0·21	− 89° 11′	+ 0° 19′	0·06	− 65° 16′	0
+ 1·3	0·35	− 83° 12′	+ 1° 2′	0·22	− 59° 2′	− 0° 2′
+ 1·2	0·5	− 76° 52′	+ 2° 6′	0·375	− 52′ 59′	− 0° 15′
+ 1·1	0·65	− 70° 15′	+ 3° 27′	0·53	− 47° 10′	− 0° 42′
+ 1·0	0·8	− 63° 26′	+ 5°	0·70	− 41° 38′	− 1° 26′
+ 0·8	1·1	− 49° 38′	+ 8° 16′	1·0	− 31° 29′	− 3° 49′
+ 0·6	1·375	− 36° 12′	+ 11° 10′	1·31	− 22° 33′	− 7° 25′
+ 0·4	1·73	− 23° 30′	+ 13° 20′	1·625	− 14° 31′	− 11° 55′
+ 0·2	1·96	− 11° 32′	+ 14° 46′	1·94	− 7° 6′	− 17° 2′
0	2·25	0	+ 15° 46′	2·25	0	− 22° 28′
− 0·2	2·54	+ 11° 32′	+ 16° 46′	2·56	+ 7° 6′	− 27° 54′
− 0·4	2·83	+ 23° 30′	+ 18° 12′	2·875	+ 14° 31′	− 33° 1′
− 0·6	3·125	+ 36° 12′	+ 20° 22′	3·19	+ 22° 33′	− 37° 31′
− 0·8	3·365	+ 49° 38′	+ 23° 16′	3·5	+ 31° 29′	− 41° 7′
− 1·0	3·71	+ 63° 26′	+ 26° 32′	3·81	+ 41° 38′	− 43° 30′
− 1·1	3·85	+ 70° 15′	+ 28° 5′	3·98	+ 47° 10′	− 44° 14′
− 1·2	4·0	+ 76° 52′	+ 29° 26′	4·125	+ 52° 59′	− 44° 41′
Qk	1	1	1	1·5	1·5	1·5

Expression 7.2*c*, Part I, enables the attenuation at the two audio carrier frequencies of 8·25 and 14·25 Mc/s to be calculated, and they are tabulated below. The reference point for 0 db. is taken as the value of $| Z_T |$ at f_m and not the maximum value as is done in Section 7.4, Part I. Thus for three circuits of $Qk = 1{\cdot}5$ and one of $Qk = 1$, the following results are obtained.

TABLE 16.5

Audio Carrier Frequency (Mc/s).	Δf (Mc/s).	QF	Qk	Attenuation per stage (db.).	Total Attenuation (db.).
8·25	− 2·25	− 1·44	1·5	+ 0·4	− 2·66
		− 1·545	1·0	− 3·86	
14·25	+ 3·75	+ 2·4	1·5	− 4·44	− 24·12
		+ 2·58	1·0	− 10·8	− 24·12

A positive sign in the above represents a gain and a negative sign a loss. A point to be noted is that the vision carrier frequency loss

is the same as that at the lower audio carrier, viz., — 2·66 db., and it is not sufficient to reduce the carrier to half amplitude (— 6 db.); however, the trap circuits for 14·25 Mc/s will introduce a loss at this frequency and the total loss at 12·75 Mc/s will be greater than that shown for 8·75 Mc/s in the table.

It is clear from the above that the attenuation at 8·25 and 14·25 Mc/s is insufficient, and we shall now consider the types of filter for rejecting these frequencies.

16.6.5. Audio Signal I.F. Filter Circuits.[24] Special care has to be exercised in the design of filter circuits required for suppressing undesired audio transmissions, otherwise the vision signal pass-band response may be seriously affected by the addition of the filter or trap circuit. It is better to employ a number of filters, each having equal attenuation at the rejection frequency rather than a single filter of the same total attenuation, because a series of filters produces a much sharper attenuation characteristic with less attenuation and phase distortion at the edges of the vision pass-band. To avoid cross-modulation the filters should be incorporated in the early stages of the I.F. amplifier.

The filter generally consists of a series or parallel circuit, tuned to the frequency it is desired to reject, and examples of some of the methods employed are shown in Figs. 16.5 and 16.6. In Fig. 16.5, L_5C_{10} is a resonant circuit coupled to the primary of the first pair of coupled circuits and acting as an absorber and also pick-up circuit for the associated audio signal. L_7C_{11} is a parallel resonant circuit which forms with the secondary tuning capacitance, C_{12}, a potential divider. A series resonant circuit, $L_{13}C_{23}$ in Fig. 16.6 may be included in parallel with the primary or secondary to act as a shunt to the rejection frequency, and yet another type is the series parallel circuit, C_{31} and $L_{16}C_{32}$, of Fig. 16.6. The parallel section $L_{16}C_{32}$ is tuned to the mid-frequency of the vision pass-band, and C_{31} is adjusted for resonance with the inductive reactance of $L_{16}C_{32}$ at the lower audio carrier; it can only be used to reject frequencies lower than the vision frequencies, and if it is desired to reject higher frequencies C_{31} must be replaced by an inductance. Combined inductance and capacitance coupling may also be used to provide a rejection frequency; in Fig. 16.6 M_5 and C_{26} form a series resonant circuit, which reduces the coupling to zero at the resonant frequency. The sign of M must be positive (see Section 3.4.2, Part I).

Let us now examine in detail the absorber type of filter, L_5C_{10} in Fig. 16.5, assuming that it is coupled only to L_4, and therefore

has negligible effect on the L_6C_{12} circuit. This is not difficult to achieve in practice, particularly when L_6 is split into a coupling and main section, with the latter separate from the former as shown in Fig. 16.5. The filtering action of the L_5C_{10} circuit is accomplished by virtue of the impedance it reflects into the L_4C_7 circuit; this impedance has resistive and reactive components (see Section 7.6, Part I) of $\frac{\omega^2 M_4{}^2}{R'_5{}^2+X_5{}^2}R'_5$ and $-\frac{\omega^2 M_4{}^2 X_5}{R'_5{}^2+X_5{}^2}$ respectively, where R'_5 is the series resistance component of L_5 and C_{10}, and X_5 is the series reactance component, i.e., $\omega L_5 - \frac{1}{\omega C_{10}}$. It will be seen that the reflected reactive component is negative (capacitive) when X_5 is inductive, a condition occurring when the applied frequency is greater than the resonant frequency of L_5C_{10}. The reverse is true when the frequency is less than the resonant frequency of L_5C_{10}.

This reflected impedance from L_5C_{10} modifies the transfer impedance formula of expression 7.2*a*, Part I, to

$$Z_T = \frac{-jR_{D1}Q_2k\sqrt{\frac{L_2}{L_1}}}{[1+A+j(Q_1F+B)][1+jQ_2F]+Q_1Q_2k^2} \quad . \quad 16.7a$$

where $$A = \frac{\omega^2 M_4{}^2 R'_5}{(R'_5{}^2+X_5{}^2)R_1'}$$

and $$B = -\frac{\omega^2 M_4{}^2 X_5}{(R'_5{}^2+X_5{}^2)R_1'}$$

where R_1' is the equivalent series resistance of the primary of the transformer and is associated with Q_1.

Section 7.6, Part I, shows that the reflected impedance from L_5C_{10} effectively is in series with L_4, and the sign given to B in expression 16.7*a* is positive if the resonant frequency of L_5C_{10} is above the mid-frequency of the coupled circuits and negative if it is below. Assuming identical coupled circuits as for Section 16.6.4, expression 16.7*a* reduces to

$$Z_T = \frac{-jR_DQk}{[1+A+j(QF+B)][1+jQF]+Q^2k^2}$$

$$|Z_T| = \frac{R_DQk}{\sqrt{[1+Q^2(k^2-F^2)+A-BQF]^2+[2QF+AQF+B]^2}} \quad . \quad 16.7b.$$

It should be noted that L_5C_{10} has the same effect whether it is coupled to L_4 or L_6, when these two circuits are identical.

The ratio loss introduced by filter at any frequency is therefore

$$\frac{|Z_T|_{+filter}}{|Z_T|} = \sqrt{\frac{[1+Q^2(k^2-F^2)]^2+[2QF]^2}{[1+Q^2(k^2-F^2)+A-BQF]^2+[2QF+AQF+B]^2}}$$

or
$$\text{loss} = -20\log_{10}\frac{|Z_T|}{|Z_T|_{+filter}} \text{ db.}$$

$$= -10\log_{10}\frac{[1+Q^2(k^2-F^2)+A-BQF]^2+[2QF+AQF+B]^2}{[1+Q^2(k^2-F^2)]^2+[2QF]^2} \quad 16.8.$$

If the coupled circuits L_4C_7 and L_6C_{12} are the critically coupled pair of the previous section, $Qk = 1$, the value of QF corresponding to the frequency, 8·25 Mc/s, to which L_5C_{10} is tuned, is $-1{\cdot}545$. Replacing Qk and QF in expression 16.8 by these numerical values and noting that $B = 0$, for X_5 is zero when L_5C_{10} is resonant,

$$\text{Loss} = -10\log_{10}\frac{[-0{\cdot}390+A_0]^2+[-(2+A_0)1{\cdot}545]^2}{[-0{\cdot}390]^2+[3{\cdot}09]^2}$$

$$= -10\log_{10}\frac{9{\cdot}712+8{\cdot}78A_0+3{\cdot}39A_0^2}{9{\cdot}712}$$

$$= -10\log_{10}\frac{1{,}541{\cdot}3}{9{\cdot}712} \equiv -22 \text{ db.}$$

if
$$A_0 = 20 = \frac{\omega^2 M_4^2}{R_5' R_1'}.$$

This is a satisfactory value for the attenuation of a single filter circuit provided the effect on the vision pass-band is small. This can be checked as follows: at a frequency above the resonant frequency of L_5C_{10}, the series impedance of this circuit can be written $Z_5 = R_5(1+jQ_5F')$, where $F' = \frac{2\Delta f'}{f_5}$, $\Delta f'$ is the frequency off-tune from the resonant frequency f_5 of L_5C_{10} and $Q_5 = \frac{\omega_5 L_5}{R_5'}$; it is convenient to neglect the variation of ωM_4 over the frequency range considered—the error is not large and in any case the principle is applied in calculating Z_T and Z_5. Hence the value of A in expression 16.8 at frequencies above f_5 is

$$A = \frac{A_0}{1+(Q_5F')^2}$$

and
$$B = -\frac{A_0Q_5F'}{1+(Q_5F')^2} = -AQ_5F'.$$

As an example, let us calculate the additional filter loss at the edge

of the vision pass-band, 8·75 Mc/s, for $Q_5 = 120$, $f_5 = 8{\cdot}25$ Mc/s,

$$F' = \frac{+2 \times 0{\cdot}5}{8{\cdot}25} = +0{\cdot}1212, \quad Q_5F' = +14{\cdot}58, \quad A = \frac{20}{213} = 0{\cdot}094,$$

$$B = AQ_5F' = -1{\cdot}37, \quad QF = \frac{-1{\cdot}545 \times 1{\cdot}75}{2{\cdot}25} = -1{\cdot}2.$$

Loss

$$= -10 \log_{10} \frac{[0{\cdot}56 + 0{\cdot}094 - 1{\cdot}37 \times 1{\cdot}2]^2 + [-2{\cdot}4 - 0{\cdot}094 \times 1{\cdot}2 - 1{\cdot}37]^2}{6{\cdot}064}$$

$$= -10 \log_{10} \frac{16}{6{\cdot}064} \equiv -4{\cdot}2 \text{ db.}$$

This procedure can be repeated for other frequencies and other values of Q_5. The additional attenuation at selected frequencies for two values of Q_5, 120 and 200 is tabulated below for the pair of overcoupled circuits ($Qk = 1{\cdot}5$) as well as the critically coupled circuits. A_0 is constant at 20, so that the additional attenuation at the rejection frequency 8·25 Mc/s is practically constant at − 22 db. A positive sign before the attenuation value indicates a gain and a negative a loss.

TABLE 16.6

f (Mc/s).	Additional Attenuation (db.) due to Filter.				Coupled Circuits only.	Overall Response Coupled Circuits plus Filter.	
10·5	− 0·08	− 0·06	− 0·02	negligible	0	− 0·06	0
9·25	− 1·46	− 0·12	− 0·74	− 0·4	+ 0·52	+ 0·40	+ 0·48
8·75	− 4·2	− 1·93	− 2·52	− 0·8	+ 0·7	− 1·23	− 0·1
8·25	− 22	− 21·76	− 22	− 21·76	+ 0·4	− 21·36	− 21·36
Qk	1	1·5	1	1·5	1·5	1·5	1·5
Q_5	120	120	200	200		120	200

The need for the highest possible value for Q_5 is plainly shown by the table, but an almost more important feature is the reduced attenuation at the edge of the vision pass-band brought about by using overcoupled circuits. The response of the overcoupled circuits of $Qk = 1{\cdot}5$ is set out in the sixth column, and in the seventh and eighth the overall frequency response of overcoupled circuits and filter is shown. An almost flat response is obtained for $Q_5 = 200$, but the more likely practical value of Q_5 is 120, and this produces a maximum variation of 1·63 db. over the range from 10·5 to 8·75 Mc/s. A slight reduction and better distribution of the

frequency response variation can be obtained by combining the frequency response of the absorber and coupled circuits with that of another pair of coupled circuits of $Qk = 1{\cdot}5$; the combined response ($Q_5 = 120$) then varies from $+0{\cdot}92$ db. at 9·25 to $-0{\cdot}53$ db. at 8·75 Mc/s. If a more level frequency response is desired over the pass-band the attenuation at the rejection frequency must be reduced; for example, if A_0 is reduced to 10, the following results are obtained with the overcoupled circuits:

TABLE 16.7

$Qk = 1{\cdot}5$, $QF = -1{\cdot}12$ at $\Delta f = -1{\cdot}75$ Mc/s, $f_m = 10{\cdot}5$ Mc/s, $A_0 = 10$, $Q_5 = 120$

f (Mc/s).	Attenuation (db.).	Coupled Circuits plus Filter.
10·5	0	0
9·25	− 0·15	+ 0·37
8·75	− 0·68	+ 0·02
8·25	− 16·3	− 15·9

The advantage of using more filters (three would be required instead of two for an overall attenuation of not less than − 40 db.), to obtain a given attenuation is clearly shown.

Since the overcoupled circuits of $Qk = 1{\cdot}5$ produce a better pass-band frequency response than the critically coupled circuits, it is necessary to see if greater couplings might with advantage be employed. Thus the frequency response for a coupling of $Qk = 2$ has a peak of $+1{\cdot}95$ db. at $QF = \pm 1{\cdot}732$ compared with the trough value at $QF = 0$, and letting this value of QF correspond to $\Delta f = -1{\cdot}75$ ($f = 8{\cdot}75$ Mc/s), the following results are obtained for $A_0 = 20$.

TABLE 16.8

$Qk = 2$, $QF = -1{\cdot}732$ at $\Delta f = -1{\cdot}75$ Mc/s, $f_m = 10{\cdot}5$ Mc/s, $A_0 = 20$

f (Mc/s).	Attenuation (db.).		Coupled Circuits only.	Overall Response Coupled Circuits plus Filter.	
10·5	Very small	Very small	0	0	0
9·25	+ 0·24	+ 0·25	+ 1·4	+ 1·64	+ 1·65
8·75	− 1·9	− 0·75	+ 1·95	− 0·05	+ 1·20
8·25	− 21·5	− 21·5	+ 1	− 20·5	− 20·5
Q_5	120	200		120	200

Comparing the above with Table 16.6, when $Q_5 = 120$, there is little to choose between the two values of coupling as far as overall frequency response variation is concerned, but the smaller value ($Qk = 1{\cdot}5$) is preferable because it is possible in combination with another pair of coupled circuits to achieve a better frequency response distribution relative to 10·5 Mc/s. Overall frequency response for $Q_5 = 200$ is less satisfactory when $Qk = 2$.

A point which has to be considered is the frequency response variation for the half pass-band above 10·5 Mc/s. If filters are included to suppress the adjacent audio signal of 14·25 Mc/s, they can be made to correct the effect of the 8·25 Mc/s filter on the frequency response of the upper half pass-band. Alternatively, if no upper frequency filters are required, the mid-frequency of the pairs of coupled circuits not associated with the 8·25 Mc/s filters can be reduced in order to correct for the rise in response from the overcoupled circuits to which the filters are connected. If a 14·25 Mc/s absorber filter is required, expression 16.8 can be used for calculating its attenuation, because B and QF have the same sign—it is positive instead of negative—over the range 14·25 to 10·5 Mc/s, and the numerator is unaffected when the signs of both are changed. The attenuation at selected frequencies for $Qk = 1{\cdot}5$, $Q_5 = 120$ and 200, $A_0 = 70$ is tabulated below :

TABLE 16.9

$Qk = 1{\cdot}5$, $QF = +\ 1{\cdot}12$ at $\Delta f = +\ 1{\cdot}75$ Mc/s, $f_m = 10{\cdot}5$ Mc/s, $A_0 = 70$

f (Mc/s).	Attenuation (db.).		Coupled Circuits only.	Coupled Circuits plus Filter.	
10·5	− 0·51	− 0·2	0	− 0·51	− 0·2
11·75	− 1·25	− 0·34	+ 0·52	− 0·73	+ 0·18
12·25	− 3·3	− 1·5	+ 0·7	− 2·6	− 0·8
12·75	− 6·25	− 3·7	+ 0·4	− 5·85	− 3·3
14·25	− 30·7	− 30·7	− 4·4	− 35·1	− 35·1
Q_5	120	200		120	200

The combined frequency response of coupled circuit and filter causes a too rapid fall in frequency response when $Q_5 = 120$—the overall response at the vision carrier frequency, 12·75 Mc/s, must not be more than 6 db. below the average response—and satisfactory performance could only be obtained at $Q_5 = 200$ if two filters are used. If more filters are possible, e.g., three, the value of A_0 can be reduced to 30, which gives a maximum attenuation of − 18·0 db.

and a satisfactory frequency response for $Q_s = 120$, as shown in Table 16.10.

TABLE 16.10

$Qk = 1{\cdot}5$, $QF = +\ 1{\cdot}12$ at $\Delta f = +\ 1{\cdot}75$ Mc/s, $f_m = 10{\cdot}5$ Mc/s, $A_0 = 30$, $Q_s = 120$

f (Mc/s).	Attenuation (db.).	Coupled Circuits plus Filter.
10·5	− 0·1	− 0·1
11·75	− 0·18	+ 0·34
12·25	− 0·88	− 0·18
12·75	− 2·52	− 2·12
14·25	− 23·56	− 27·96

If we assume that three of the four pairs of coupled circuits in the I.F. amplifier have absorber filters with attenuation characteristics as set out in Tables 16.7 and 16.10, the overall frequency response of the three circuits is that given in the second column of Table 16.11. If the fourth pair of coupled circuits has a coupling corresponding to $Qk = 1{\cdot}355$, $f_m = 10{\cdot}75$ Mc/s, $QF = 0{\cdot}91$ at $\Delta f = 2$ Mc/s, it has the attenuation characteristic shown in the third column. Overall I.F. frequency response of the four pairs is shown in the fourth column.

TABLE 16.11

f (Mc/s).	Attenuation (db.).	Attenuation of Special Circuit.	Overall Attenuation.
8·25	− 47·7	+ 0·26	− 47·44
8·75	+ 0·06	+ 0·4	+ 0·46
9·25	+ 1·11	+ 0·3	+ 1·41
10·5	− 0·3	+ 0·05	+ 0·25
11·75	+ 1·02	+ 0·14	+ 1·16
12·25	− 0·54	+ 0·3	− 0·24
12·75	− 6·36	+ 0·4	− 5·96
14·25	− 83·88	− 1·05	− 84·93

The overall I.F. amplifier frequency response has a variation of about ± 1 db. over the pass range, with a response at the vision carrier frequency of almost exactly that required, viz., − 6 db. Attenuation is more than that specified at 8·25 Mc/s, and at 14·25 Mc/s.

To show the method of calculating the component values for

the absorber filters we shall assume that the primaries and secondaries of the three pairs of coupled circuits are identical, i.e., in Figs. 16.5 and 16.6, $C_7 = C_{12} = C_{25} = C_{28} = C_{34} = C_{35} = 15\ \mu\mu F$, the inductances L_4, L_6, etc., are equal to 15·3 μH, $Qk = 1{\cdot}5$, $QF = \pm 1{\cdot}12$ at $\Delta f = \pm 1{\cdot}75$ Mc/s, $f_m = 10{\cdot}5$ Mc/s, $Q = 3{\cdot}36$.

(*a*) 8·25 *Mc/s Filter.*

Let $C_{10} = 15\ \mu\mu F$, $Q_5 = 120$.

$$L_5 = \frac{10^{-6}}{(6{\cdot}28 \times 8{\cdot}25)^2 \times 15} = 24{\cdot}8\ \mu H.$$

$$R_5' = \frac{1}{Q_5 \omega_5 C_{10}} = \frac{10^6}{120 \times 6{\cdot}28 \times 8{\cdot}25 \times 15} = 10{\cdot}7\ \Omega.$$

$$* R_1' = \frac{1}{Q \omega_m C_7} = \frac{10^6}{3{\cdot}36 \times 6{\cdot}28 \times 10{\cdot}5 \times 15} = 300\ \Omega.$$

$$A_0 = 10 = \frac{\omega_5^2 M_4^2}{R_1' R_5'}.$$

$$M_4 = \frac{10^{-6}\sqrt{10 \times 10{\cdot}7 \times 300}}{6{\cdot}28 \times 8{\cdot}25} = 3{\cdot}46\ \mu H.$$

$$k_4 = \frac{M_4}{\sqrt{L_4 L_5}} = \frac{3{\cdot}46}{\sqrt{15{\cdot}3 \times 24{\cdot}8}} = 0{\cdot}177.$$

(*b*) 14·25 *Mc/s.*

If $C_{10} = 15\ \mu\mu F$, $L_5 = 8{\cdot}35\ \mu H$, $Q_5 = 120$, $R_5' = 6{\cdot}2\ \Omega$

$$A_0 = 30$$

$$M_4 = \frac{10^{-6}\sqrt{30 \times 6{\cdot}2 \times 300}}{6{\cdot}28 \times 14{\cdot}25} = 2{\cdot}63\ \mu H.$$

$$k_4 = \frac{2{\cdot}63}{\sqrt{15{\cdot}3 \times 8{\cdot}35}} = 0{\cdot}233.$$

As described in Section 16.6.4, phase distortion can be derived from the phase angle,

$$\phi = \tan^{-1}\left[-\frac{2QF + AQF + B}{1 + Q^2(k^2 - F^2) + A - BQF}\right].$$

The second type of filter is the parallel resonant circuit-capacitance potential divider formed by $L_7 C_{11}$ and C_{12} in Fig. 16.6. Actually C_{12} is not the total tuning capacitance of the $L_6 C_{12}$ circuit,

* Note that R_1' is the equivalent series resistance of the $L_4 C_7 R_5$ circuit in Fig. 16.5, and the value of Q used is that calculated in Section 16.6.4 for the overcoupled circuits of $Qk = 1{\cdot}5$.

but is the wiring and valve input capacitance and so will have a value of about 10 $\mu\mu$F. For rejection at 14·25 Mc/s, the resonant impedance R_{D7} of L_7C_{11} at this frequency must be approximately 10 times the reactance C_{12}, or

$$R_{D7} = 10\,\frac{1}{\omega_7 C_{12}} = 10\frac{10^6}{6{\cdot}28 \times 14{\cdot}25 \times 10} = 11{,}150\ \Omega.$$

The impedance of the L_7C_{11} circuit at any frequency is $\dfrac{R_{D7}}{1+jQ_7F}$ and it can be resolved into a resistance and reactive component of $R_S = \dfrac{R_{D7}}{1+(Q_7F)^2}$ and $X_S = \dfrac{-R_{D7}Q_7F}{1+(Q_7F)^2}$, where Q_7 is the Q of the circuit, $F = \dfrac{\Delta f}{f_7}$ and Δf = frequency off-tune from the resonant frequency, f_7 (in this case 14·25 Mc/s). The attenuation due to this type of filter is $20\log_{10}\dfrac{\dfrac{1}{\omega C_{12}}}{\sqrt{R_S{}^2+\left(X_S-\dfrac{1}{\omega C_{12}}\right)^2}}$, and when Q_7 is large it reduces to $20\log_{10}\dfrac{1}{X_S\omega C_{12}-1}$ for all frequencies except those close to series resonance of L_7C_{11} with C_{12}. Table 16.12 gives the attenuation at the selected frequencies for $Q_7 = 120$ and 200.

TABLE 16.12

$R_{D7} = 11{,}150\ \Omega$. $f_7 = 14{\cdot}25$ Mc/s.

f (Mc/s).	$\frac{1}{\omega C_{12}}$	X_S	db.	X_S.	db.
10·5	1,512	+ 176·5	+ 1·08	+ 106	+ 0·64
11·75	1,352	+ 265	+ 1·9	+ 159	+ 1·08
12·25	1,298	+ 331	+ 2·54	+ 199	+ 1·44
12·75	1,245	+ 442	+ 3·8	+ 265	+ 2·1
14·25	1,115	0	− 20·04	0	− 20·04
Q_7		120	120	200	200

The chief point of interest is that over the pass range there is a gain instead of loss ; this is due to the fact that the L_7C_{11} circuit appears as an inductive reactance at frequencies below resonance, and eventually it forms with C_{12} a series resonant circuit. This series resonance occurs at about $Q_7F = -9{\cdot}5$, and there is a peak in the

filter response at this frequency, 13·68 Mc/s for $Q_7 = 120$. Between 13·7 and 14·25 Mc/s the response falls away sharply to a maximum loss of — 20·04 db. The rise in response over the pass-band can be used to compensate for any fall in response due to the coupled circuits. The filter circuit is a part of the tuning of the secondary and it reduces the capacitive reactance of C_{12} over the pass-band range. This means that the factor $(1+jQ_2F)$ in the denominator of the transfer impedance expression is increased to $(1+j(Q_2F+x))$ and Z_T is therefore reduced, an effect which tends to offset the increase in frequency response due to the filter itself. Again, it can be observed that the filter has least influence on the pass range when Q_7 is large. If this type of filter is used for rejecting 8·25 Mc/s, X_S is negative, the range 10·5 to 8·75 shows a fall in response, and there is no series resonance peak. The results for $R_{D7} = 19{,}250\ \Omega$, $f_r = 8{\cdot}25$ Mc/s, $Q_7 = 120$ are :

TABLE 16.13

f (Mc/s).	$\frac{1}{\omega C_{11}}$	X_S	db.
10·5	1,512	— 295	— 1·54
9·25	1,715	— 663	— 2·84
8·75	1,815	— 1,325	— 4·56
8·25	1,925	0	— 20·04

In this case the filter reduces the factor $(1+jQ_2F)$ in the denominator of Z_T to $(1+j(Q_2F - x))$ and thus tends to offset the fall in response due to the filter.

The values of L_7 and C_{11} are calculated from R_{D7} and Q_7; thus for 14·25 Mc/s

$$L_7 = \frac{R_{D7}}{\omega_7 Q_7} = \frac{11{,}150 \times 10^{-6}}{6{\cdot}28 \times 14{\cdot}25 \times 120} = 1{\cdot}035\ \mu\text{H}$$

$$C_{11} = 120\ \mu\mu\text{F}$$

and for 8·25 Mc/s

$$L_7 = \frac{19{,}250 \times 10^{-6}}{6{\cdot}28 \times 8{\cdot}25 \times 120} = 3{\cdot}09\ \mu\text{H}$$

$$C_{11} = 120\ \mu\mu\text{F}.$$

The series resonant circuit filter, exemplified by $L_{13}C_{23}$ in Fig. 16.6, acts as a shunt in parallel with the primary impedance, and the attenuation it produces may be calculated from the ratio

of its impedance to the sum of its impedance and the primary impedance. The latter, from expression 7.7*d*, Part I, is

$$Z_p = \frac{R_{D1}(1+jQF)}{1+Q^2(k^2-F^2)+2jQF}$$

and taking the previous component values for the $Qk = 1{\cdot}5$ coupled circuits, the primary impedance at 8·25 Mc/s is

$$\begin{aligned} Z_p &= \frac{3{,}400(1-1{\cdot}44j)(1{\cdot}17+2{\cdot}88j)}{(1{\cdot}17)^2+(2{\cdot}88)^2} \\ &= \frac{3{,}400}{9{\cdot}67}(5{\cdot}32+1{\cdot}193j) \\ &= 1{,}870+420j. \end{aligned}$$

For $Q_{13}=120$, $C_{23} = 7{\cdot}5\ \mu\mu$F, $L_{13} = 49{\cdot}5\ \mu$H, the additional attenuation at 8·25 Mc/s is $20\log_{10}\dfrac{21{\cdot}4}{\sqrt{(1{,}891{\cdot}4)^2+(420)^2}} = -39{\cdot}12$ db. for $R'_{13} = \dfrac{\omega_{13}L_{13}}{Q_{13}} = 21{\cdot}4\ \Omega$. At other frequencies the impedance of the series circuit is $R'_{13}(1+jQ_{13}F')$ where $F' = \dfrac{2\Delta f}{f_{13}}$, so that at 10·5 Mc/s it is $21{\cdot}4(1+65{\cdot}5j) \simeq 1{,}400j$. Hence there is a loss of $20\log_{10}\dfrac{1{,}400}{\sqrt{(3{,}400)^2+(1{,}400)^2}} = -8{\cdot}4$ db. at the centre of the pass range. It is only possible to reduce this loss by increasing L_{13} because the impedance at 10·5 Mc/s is approximately equal to $jR'_{13}Q_{13}F' = j\omega_{13}L_{13}F'$. Such a large value of loss could hardly be tolerated and the series parallel filter $L_{16}C_{32}$ and C_{31} in Fig. 16.6 is preferable. The parallel section is resonant at 10·5 Mc/s and has therefore an inductive reactance at 8·25 Mc/s. Series resonance is obtained by this inductive reactance in combination with C_{31}. Let us assume that the resonant impedance R_{D16} of $L_{16}C_{32}$ at 10·5 Mc/s is 170,000 Ω—this involves a loss of − 0·16 db.—and that Q_{16} is 120; we therefore find that

$$L_{16} = \frac{170{,}000\times10^{-6}}{120\times6{\cdot}28\times10{\cdot}5} = 21{\cdot}5\ \mu\text{H}$$

and

$$C_{32} = 10{\cdot}7\ \mu\mu\text{F}.$$

The reactance of this circuit at 8·25 Mc/s ($Q_{16}F' = -51{\cdot}4$) is

$$-j\frac{R_{D16}Q_{16}F'}{1+(Q_{16}F')^2} = +j3{,}310\ \Omega.$$

and the capacitance value for C_{31} is

$$C_{31} = \frac{10^6}{6{\cdot}28\times8{\cdot}25\times3{,}310} = 5{\cdot}84\ \mu\mu\text{F}.$$

The series impedance of the filter at 8·25 Mc/s is the resistance component of the impedance of $L_{16}C_{32}$, i.e.,

$$\frac{R_{D16}}{1+(Q_{16}F')^2} = \frac{170{,}000}{2{,}640} = 64{\cdot}5\ \Omega$$

which causes an attenuation of

$$20\log_{10}\frac{64{\cdot}5}{|Z_p + 64{\cdot}5|} = 20\log_{10}\frac{64{\cdot}5}{\sqrt{(1{,}934{\cdot}5)^2+(420)^2}} = -29{\cdot}72\ \text{db.}$$

This type of filter is less satisfactory for suppressing frequencies above the vision pass-band because the reactance of $L_{16}C_{32}$ is capacitive and series resonance can only be obtained at a higher frequency by replacing C_{31} by an inductance, the performance of which is considerably modified by its inherent self capacitance.

It is worth noting that the effect of the series or series-parallel filter circuit is the same whether it is connected across primary or secondary provided the latter are identical.

The rejection circuit formed by a resonant coupling between the primary and secondary is illustrated by M_5 in combination with C_{26} in Fig. 16.6. The performance of the resonant coupling can be calculated by replacing k in Z_T by $\frac{\left(M_5 - \frac{1}{\omega^2 C_{26}}\right)}{\sqrt{L_{14}.L_{15}}}$ and C_{26} is chosen to satisfy the expression

$$f = 14{\cdot}25 \text{ or } 8{\cdot}25 = \frac{1}{2\pi\sqrt{M_5 C_{26}}}.$$

Appreciable values of attenuation can be obtained by this method because M_5 has no resistance component and the resistance of the resonant coupling is determined only by the losses in C_{26}. On the other hand, the frequency response at the edges of the pass-band may be considerably affected.

Cathode feedback (Section 7.9, Part I) may also be used for suppression purposes, but to be fully effective the valve to which it is applied must not have grid-bias control.

16.7. The Detector Stage. The vision frequency detector stage is a modified form of the audio frequency detector, the modifications being rendered necessary by the much larger range of modulation frequencies (2 to 4 Mc/s as compared with 18 kc/s for audio signals). Both reservoir capacitance and load resistance must be small, otherwise the higher modulation frequencies are severely attenuated. Consequently detection efficiency is low; it is of the order of 50% for a single diode half-wave detector, provided that

the diode is designed to have a low anode-cathode capacitance and a low conduction resistance. The anode-cathode capacitance in conjunction with the low value of reservoir capacitance acts as a potential divider to reduce the effective R.F. voltage applied to the diode. A small value of anode-cathode capacitance calls for a large anode-cathode spacing, but this increases the diode conduction resistance, so that a compromise is necessary. Typical values for the anode-cathode capacitance and conduction resistance of a television diode detector are 1·5 to 2 $\mu\mu$F and 1,000 Ω respectively. Both R.F. and superheterodyne receivers need special filters between the diode output and the vision frequency amplifier, though the need for filtering is less urgent in the R.F. than in the superheterodyne receiver, because feedback of I.F. harmonics into the signal circuits, which leads to serious interference with the picture, does not arise. Feedback of R.F. carrier is undesirable, but can only cause regeneration or degeneration, apart from harmonic distortion when large peak signals are applied to the V.F. amplifier. Regeneration can, of course, become serious if the receiver is brought near the point of oscillation (it may cause appreciable attenuation distortion), but such a situation rarely arises if normal precautions are taken.

Of the three types of diode detector circuit, the half-wave, the full-wave and voltage doubler, the former is the most popular on account of simplicity and, compared with the full-wave detector, less loss of amplification from input to output. The chief merit of the full-wave detector is that the vision carrier fundamental is cancelled, and only its harmonics have to be filtered from the output of the V.F. amplifier. The input voltage applied to each diode of the full-wave detector is halved by the centre tap, but detection efficiency (η_d) is higher at about 70%. Thus the overall output-to-input voltage ratio is about 0·35 compared with 0·5 for the half-wave detector. Another disadvantage of the full-wave detector is that the centre-tapped output coil must be electrically balanced to earth, otherwise cancellation of the carrier fundamental is not realized. The voltage doubling type of detector is more useful when it is desired to operate the C.R. tube direct from the detector. For examples of this see Fig. 11.4*c*, and the alternative form provided by V_1 and V_2 in Fig. 11.12; the latter type is better than the former because there is less R.F. ripple across the reservoir capacitance C_1. Conduction current damping is twice that of the half-wave detector so that the equivalent damping resistance is approximately one-half the load resistance (see below).

An example of the half-wave detector is shown in Fig. 16.7. Damping of the tuned circuit feeding the detector is very much greater than in the case of the A.F. detector because of the low load resistance, 5,000 Ω, but this is not a serious disadvantage as the tuned circuit must be heavily damped to secure the wide pass-band. Since the detection efficiency is 50%, the conduction current damping resistance may be taken as equal to the load resistance (Section 8.2.5, Part I), and any additional damping resistance must be calculated with this in mind. The direction of the diode connections depends on the type of modulation and the number of V.F. amplifier stages. The circuit of Fig. 16.7 is suitable for detecting the English system of positive modulation with direct connection from detector to C.R. tube, or with an even number of V.F. stages between detector and C.R. tube. The same circuit can be used for the American system of negative modulation if an odd number of V.F. stages is employed ;

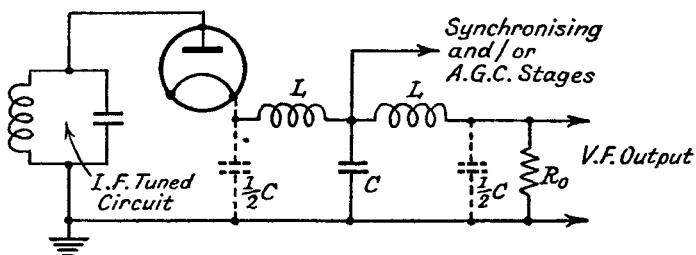

FIG. 16.7.—The Vision Signal Detector of a Television Receiver.

the anode-cathode connections of the diode must be reversed if direct connection or an even number of V.F. stages is desired between detector and C.R. tube. A two-stage low-pass filter is shown between the detector and its V.F. output, and the values of L and C may be calculated from the normal filter formulæ for constant k structures. Thus

$$L = \frac{R_0}{\pi f_c} \text{ and } C = \frac{1}{\pi f_c R_0}$$

where f_c = the cut-off frequency
and R_0 = the characteristic and terminating resistance of the filter. Generally the value of the reservoir capacitance, which is the capacitance $\frac{1}{2}C$ of the shunt arm of the π section filter, shown in Fig. 16.7, is fixed by stray capacitance at not less than 10 $\mu\mu$F, and this in turn limits the maximum value of R_0 and f_c. From the point of view of detection efficiency R_0 should be as large as possible ; small attenuation distortion over the pass-range calls for a high

value of f_c, though it must not be so high as to cause insufficient filtering of the I.F. A suitable compromise for 2 Mc/s pass-band is $R_0 = 5{,}000\ \Omega$ and $f_c = 3{\cdot}18$ Mc/s, i.e., approximately one and a half times the maximum vision frequency of 2 Mc/s, with $C = 20\ \mu\mu$F and $L = 500\ \mu$H. For the higher definition 4 Mc/s pass-band, R_0 must be reduced to 3,000 Ω, thereby increasing f_c to 5·3 Mc/s with $C = 20\ \mu\mu$F and $L = 180\ \mu$H.

Attenuation and phase distortion for a low-pass filter have been examined in considerable detail elsewhere,[31, 32] and it is not proposed to do more than state the formulae involved and the probable performance of a suitable filter. The attenuation in decibels of a correctly terminated single section constant k low-pass filter $\left(R_0 = \sqrt{\frac{L}{C}}\right)$ is

$$\left.\begin{aligned}\alpha &= -20\log_{10}\left|\frac{\sqrt{1+\frac{Z_1}{4Z_2}}+\sqrt{\frac{Z_1}{4Z_2}}}{\sqrt{1+\frac{Z_1}{4Z_2}}-\sqrt{\frac{Z_1}{4Z_2}}}\right| \\ &= -20\log_{10}\left|\left(\sqrt{1+\frac{Z_1}{4Z_2}}+\sqrt{\frac{Z_1}{4Z_2}}\right)^2\right|\end{aligned}\right\} \quad . \quad . \quad 16.9$$

and the phase angle

$$\beta = \tan^{-1}\frac{j\text{ part of }\left(\sqrt{1+\frac{Z_1}{4Z_2}}+\sqrt{\frac{Z_1}{4Z_2}}\right)^2}{\text{real part of above}} \quad . \quad . \quad 16.10$$

where Z_1 = impedance of a full series arm $= \omega L$

and Z_2 = impedance of a full shunt arm $= \dfrac{1}{\omega C}$.

Thus if L contains no resistive component

$$\frac{Z_1}{4Z_2} = \frac{j\omega L}{4\frac{1}{j\omega C}} = -\frac{\omega^2 LC}{4} = -\left(\frac{f}{f_c}\right)^2$$

for $f_c = \dfrac{1}{\pi\sqrt{LC}}$. On the other hand, if L has a resistive component R,

$$\frac{Z_1}{4Z_2} = \frac{(R+j\omega L)j\omega C}{4} = -\frac{\omega^2 LC}{4}\left(\frac{R}{j\omega L}+1\right) = \left(\frac{f}{f_c}\right)^2\left[\frac{j}{Q}-1\right]$$

$$= \left(\frac{f}{f_c}\right)^2\sqrt{\frac{1}{Q^2}+1}\,.\,\underline{/\tan^{-1}\left(-\frac{1}{Q}\right)} \quad . \quad . \quad . \quad . \quad 16.11.$$

To illustrate the use of the formulae 16.9 and 16.10, we shall take two cases :

(1) $\frac{Z_1}{4Z_2}=1\underline{/180°}=-1$, and (2) $\frac{Z_1}{4Z_2}=1{\cdot}2\underline{/150°}=-1{\cdot}04+0{\cdot}6j$.

(1) $\frac{Z_1}{4Z_2}=1\underline{/180°}$. This corresponds to cut-off frequency and zero resistance in the L and C arms.

$$\left(\sqrt{1+\frac{Z_1}{4Z_2}}+\sqrt{\frac{Z_1}{4Z_2}}\right)^2=(\sqrt{-1})^2=-1=1\underline{/\tan^{-1}(-1)}=1\underline{/180°}.$$

Therefore $\alpha = 20 \log_{10} 1 = 0$ db.
$\beta = \tan^{-1}(-1) = 180°$.

(2) $\frac{Z_1}{4Z_2} = 1{\cdot}2\underline{/150°} = -1{\cdot}04+0{\cdot}6j$. This corresponds to a frequency greater than cut-off with $Q = \frac{\omega L}{R} = -\cot\phi = 1{\cdot}732$

$$\left(\sqrt{1+\frac{Z_1}{4Z_2}}+\sqrt{\frac{Z_1}{4Z_2}}\right)^2 = (\sqrt{-0{\cdot}04+0{\cdot}6j}+\sqrt{-1{\cdot}04+0{\cdot}6j})^2$$
$$= -1{\cdot}08+1{\cdot}2j+2\sqrt{-0{\cdot}3184-0{\cdot}648j}\ *$$
$$= -1{\cdot}08+1{\cdot}2j-0{\cdot}898+1{\cdot}444j$$
$$= 3{\cdot}31\underline{/125°\ 48'}$$

i.e., $\alpha = -10{\cdot}4$ db., $\beta = 125°\ 48'$.

Phase and attenuation distortion is affected by the Q of the coil L of the series arm, and Q is not easy to assess because it varies from a low value at the low-frequency end of the pass-band to a comparatively high value at the high-frequency end, e.g., 2 to 3 at 1 kc/s to 100 at 4 Mc/s. However, provided the maximum vision frequency does not exceed about $0{\cdot}75f_c$, attenuation distortion is usually negligible for normal Q values. Suppose Q at 4 Mc/s = 100, and $f_c = 5{\cdot}3$ Mc/s, then

$$\frac{Z_1}{4Z_2} = \left(\frac{f}{f_c}\right)^2\sqrt{\frac{1}{Q^2}+1}\Big/\underline{\tan^{-1}-\frac{1}{Q}}$$
$$= \left(\frac{4}{5{\cdot}3}\right)^2\sqrt{1+(0{\cdot}01)^2}\,\underline{/\tan^{-1}-0{\cdot}01}$$
$$= 0{\cdot}57\underline{/179°\ 25'}.$$

---

* Note $\sqrt{-0{\cdot}3184-0{\cdot}648j} = \sqrt{\sqrt{(0{\cdot}3184)^2+(0{\cdot}648)^2}}\Big/\underline{\tfrac{1}{2}\tan^{-1}\frac{-0{\cdot}648}{-0{\cdot}3184}}$
$= 0{\cdot}85\underline{/121°\ 56'}$
$= -0{\cdot}449+0{\cdot}722j$

The above value of $\frac{Z_1}{4Z_2}$, when replaced in expression 16.9, gives a loss of $-0{\cdot}2$ db. at 4 Mc/s, which is negligible.

At the vision I.F. carrier 12·75 Mc/s if Q is unchanged,

$$\frac{Z_1}{4Z_2} = \left(\frac{f}{f_c}\right)^2 \underline{/179^\circ\ 25'} = 5{\cdot}8\ \underline{/179^\circ\ 25'}$$

and the loss for this value of $\frac{Z_1}{4Z_2}$ is found to be $-26{\cdot}6$ db.

For the two-section filter of Fig. 16.7, the loss at the vision I.F. carrier is twice this. There can be large variations in phase angle of $\frac{Z_1}{4Z_2}$ with practically no effect on the attenuation in the cut-off region.

Greatest variation of frequency response over the pass-band is caused by reflection losses due to the mismatch between the filter input image impedance and the equivalent A.C. impedance of the diode, consisting of its slope resistance and anode-cathode inter-electrode capacitance in parallel. The diode slope resistance R_d' is generally about 1,500 Ω, and the anode-cathode capacitance of 2 $\mu\mu$F has only a very small effect because its reactance (19,950 Ω at 4 Mc/s) is very small compared with 1,500 Ω. The input image impedance Z' of the π section filter varies over the pass-band in accordance with the formula

$$Z' = \frac{R_0}{\sqrt{1 - \left(\frac{f}{f_c}\right)^2}} \quad . \quad . \quad . \quad 16.12$$

and the reflection loss due to mismatch is

$$\text{loss} = -20 \log_{10} \frac{1 + \frac{Z'}{R_d'}}{2\sqrt{\frac{Z'}{R_d'}}} \text{db.} \quad . \quad . \quad 16.13$$

and it is tabulated on page 416 for $R_d' = 1{,}500\ \Omega$, $R_0 = 3{,}000\ \Omega$, and $f_c = 5{\cdot}3$ Mc/s.

Reflection mismatch loss increases as the V.F. frequency increases because the input impedance of the π section increases. A T-section filter would have advantages in this respect because its input impedance falls over the pass-band from 3,000 Ω to zero at $f = f_c$. This will cause the loss to decrease with increase of frequency until Z' falls below R_d', and the V.F. response will thus tend to increase. The T-section filter cannot, however, be used because

TABLE 16.14

$\frac{f}{f_c}$	0	0·1	0·2	0·3	0·4	0·5	0·6	0·7	0·8	0·9
f(Mc/s) .	0	0·53	1·06	1·59	2·12	2·65	3·18	3·71	4·24	4·77
Z' (ohms) .	3,000	3,020	3,060	3,145	3,275	3,465	3,750	4,200	5,000	6,880
Loss (db.) .	−0·5	−0·51	−0·52	−0·58	−0·64	−0·74	−0·86	−1·08	−1·48	−2·32
Loss (db.) referred to $f = 0$	0	−0·01	−0·02	−0·08	−0·14	−0·24	−0·36	−0·58	−0·98	−1·82

the stray capacitance $\frac{1}{2}C$ across the output of the diode and input of the filter cannot be eliminated. There is no phase shift due to the mismatch if the reactive component of the diode A.C. impedance is negligible, i.e., if the diode anode-cathode capacitive reactance is large compared with R_d'.

Phase distortion in the filter itself can be estimated by noting the departure of the phase angle (expression 16.10) from a linear relationship to frequency. It will be found to be greatest when there is no resistive component in the shunt and series arms of the filter, so that we shall gain an idea of the likely phase distortion by studying this condition, for which $\frac{Z_1}{4Z_2} = \left(\frac{f}{f_c}\right)^2 \underline{/180°} = -\left(\frac{f}{f_c}\right)^2$, where $\frac{f}{f_c} < 1$. Hence

$$\left(\sqrt{1+\frac{Z_1}{4Z_2}}+\sqrt{\frac{Z_1}{4Z_2}}\right)^2 = \left(\sqrt{1-\left(\frac{f}{f_c}\right)^2}+\sqrt{-\left(\frac{f}{f_c}\right)^2}\right)^2$$

$$= \left(\sqrt{1-\left(\frac{f}{f_c}\right)^2}+j\frac{f}{f_c}\right)^2$$

$$= 1-2\left(\frac{f}{f_c}\right)^2+j\frac{2f}{f_c}\sqrt{1-\left(\frac{f}{f_c}\right)^2} \quad . \quad 16.14.$$

From which the phase angle

$$\beta = \tan^{-1}\frac{\frac{2f}{f_c}\sqrt{1-\left(\frac{f}{f_c}\right)^2}}{1-2\left(\frac{f}{f_c}\right)^2} \quad . \quad . \quad . \quad 16.15.$$

The phase angle and phase-angle error are given in Table 16.15 over the pass range of the filter for $f_c = 5{\cdot}3$ Mc/s. The correct phase angle is given by $\beta = \tan^{-1}\frac{2f}{f_c}$ radians $= 57°\ 18'\ \tan^{-1}\frac{f}{f_c}$ degrees.

TABLE 16.15

$\frac{f}{f_c}$	0·1	0·2	0·3	0·4	0·5
f (Mc/s). . .	0·53	1·06	1·59	2·12	2·65
Phase Angle .	11° 26′	23° 2′	34° 53′	47° 9′	60°
Error . . .	1′	+ 0° 8′	+ 0° 34′	+ 1° 19′	+ 2° 42′

$\frac{f}{f_c}$	0·6	0·7	0·8	0·9	1·0
f (Mc/s). . .	3·18	3·71	4·24	4·77	5·3
Phase Angle .	73° 46′	88° 51′	106° 14′	128° 19′	180°
Error . . .	+ 5° 11′	+ 8° 38′	+ 14° 39′	+ 25° 17′	+ 65° 24′

The phase angle and phase-angle error is positive, so that there is a time delay amounting to approximately

$$\frac{12}{360 \times 4} = 0{\cdot}00833\ \mu \text{ secs. at } 4 \text{ Mc/s.}$$

This is very small compared with that caused by the I.F. amplifier.

In the example taken for high definition transmission, viz., maximum vision frequency 4 Mc/s, $R_0 = 3{,}000\ \Omega$, $f_c = 5{\cdot}3$ Mc/s, and a two-section filter, frequency response shows a loss of about $2 \times (-0{\cdot}8$ (mismatch) $- 0{\cdot}2$ (filter, loss due to Q of coil)), i.e., $-2{\cdot}0$ db. from low to high frequencies and time delay amounts to 0·01666 μ secs. at the highest vision frequency.

The double value of shunt capacitance (20 $\mu\mu$F) required at the junction of the two sections of the filter makes this a suitable point for connecting other circuits, such as the synchronizing and A.G.C. stage, which use the detector output as their source of voltage. Care must be exercised to keep the stray and self-capacitances of the filter inductances L to a minimum, because the parallel resonant circuit so formed, though increasing discrimination against a narrow band of frequencies, offers less attenuation to frequencies higher than this band. Alternatively the resonant frequency may be controlled and used to increase the effectiveness of the filter at the vision I.F. carrier fundamental (or second harmonic in the case of full-wave detection).

A.G.C. bias control, which may be derived from the detector output, is quite often employed in American receivers, but has not proved necessary with the single English transmission. The chief advantage of automatic gain control in television reception is for smoothing out variations in signal strength due to a swinging aerial

or lead-in (this is prevented by firm fixing), or to reflections from nearby moving objects, e.g., aeroplane flutter effect. It is also useful for stabilizing output when tuning from one transmission to another. The source of A.G.C. voltage must be the synchronizing pulse section of the carrier and not the vision signal section because the vision voltage varies between wide limits and depends on the average black or white content of the image. For the American system of negative modulation with synchronizing pulses applied at maximum carrier amplitude, A.G.C. voltage may be obtained by connecting a diode and its load resistance across the central capacitance C of the filter as shown in Fig. 16.8. The time constant of the load resistance R_1 and reservoir capacitance C_1 is sufficiently large to ensure that the A.G.C. diode acts as a peak voltage detector of the positive synchronizing pulses. The D.C. output voltage is positive

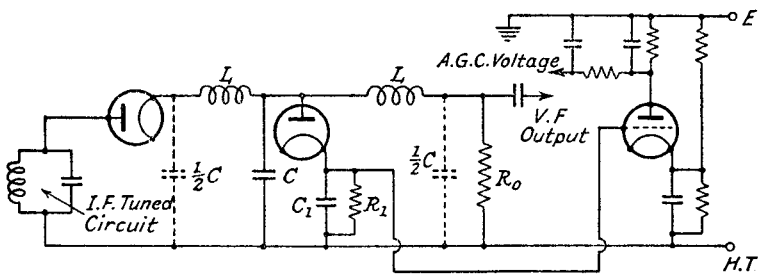

FIG. 16.8.—A Method of obtaining A.G.C. for the American Negative Modulation Transmission System.
[For H.T. read H.T. −]

and a phase-reversing valve must be used to change it to a negative voltage. The phase-reversing valve, which also acts as an amplifier, is connected between the earth line of the R.F. receiver and a source of negative voltage as shown in Fig. 16.8. If two stages of V.F. amplification are used the vision detector connections must be reversed for the American negative modulation, i.e., the cathode is connected to the R.F. voltage source and the anode to the vision detector filter. The synchronizing pulses are now negative and the A.G.C. diode connections must also be reversed. The D.C. voltage appearing across R_1 has the correct polarity for applying direct to the R.F. valves. Much the same principle may be applied to obtain A.G.C. from the English positive modulation system.

It should be noted that the initial curvature of the vision detector characteristic reduces the synchronizing pulse of the English transmission and the white signal of the American. Vestigial and single sideband reception inevitably produce some harmonic distortion of

the vision frequency signal, but as explained previously, this type of distortion is much less important in television than in audio frequency reception.

Anode bend detection may be used in order to gain some amplification of the detected output voltage. Its chief disadvantage is its non-linear detection characteristic and restricted input signal handling capacity, though both effects can be mitigated by the use of negative feedback. Cathode self-bias cannot be employed because the average carrier level varies with the image brightness. A special compensating anode circuit is included to provide the required vision frequency response, and it is similar to those described in the next section.

16.8. Vision Frequency Amplification.[2, 16]

16.8.1. Introduction. Cathode ray tubes reproducing television images require a peak-to-peak signal voltage of about 25 volts for reproducing the full range of brightness from black to white. It is not normally possible to obtain this voltage direct from a detector stage without overloading the last R.F. or I.F. stage of the receiver, since the synchronizing pulses increase the required detected output voltage amplitude by another 43% (30% carrier represents black) to 35·75 volts peak-to-peak. Hence, allowing for a detection efficiency of 50%, the R.F. or I.F. voltage needs to be 71·5 volts. At least one stage of vision frequency amplification is needed between the detector and C.R. tube. The wide range of frequencies, from D.C. to 4 Mc/s, which are present in the vision frequency output from the detector, creates difficulties in the design of the V.F. amplifier. The D.C. component is essential for correct reproduction of the image as it provides the datum of average brightness, e.g., the average light content of the picture is reduced in passing from an outdoor to indoor scene, and this change can only be appreciated if the D.C. component is present at the grid of the C.R. tube reproducer. It would be possible to use a D.C. amplifier V.F. stage, but this generally leads to a more complicated power supply system, particularly if more than one stage of V.F. amplification is employed. Fortunately D.C. amplification is not essential because a diode connected across the output of the V.F. stage can be used to restore the D.C. component lost in the amplifier. Failure to restore this component also tends to make the flyback trace of the frame deflection visible across the image.

Increase of the reactances of the coupling and self-bias capacitances in the V.F. amplifier cause loss of low-frequency response and

phase distortion, which results in a brightness variation in a vertical direction when a white or black square is being transmitted. High-frequency attenuation due to stray and valve capacitances leads to a loss of horizontal detail. Phase distortion is not often a serious problem at the high-frequency end of the range and is usually negligible in comparison with that introduced in the R.F. and I.F. stages, because the number of reactances and therefore the total phase shift is small. Although minimum attenuation and phase distortion are not necessarily achieved at the same time, a flat high-frequency response generally results in small-phase distortion. At low frequencies phase distortion is more serious because a phase-angle error of 1° represents a time error of 55·5 μ secs. (16·78 cms. error on the C.R. tube screen) at 50 c.p.s., and it is preferable to aim at minimum phase rather than minimum attenuation distortion. A point always to be remembered when more than one V.F. stage is involved is that each stage should be compensated to give satisfactory phase and attenuation distortion independently of any other. It is most unwise to try and correct in one stage the deficiencies of several others.

There is another form of distortion to which V.F. amplifiers are susceptible, and that is transient distortion. It is caused by a transient pulse setting up damped oscillations in the LC circuit formed by the inductance used for compensating high-frequency loss, and the stray capacitance with which it is associated. It is a function of high-frequency response, and is liable to be produced when there is a peak exceeding 1 db. in the response curve. It causes a rippled effect on the picture immediately following a sharp transition from black to white, or vice versa. For this reason the ratio $\frac{L}{CR^2}$ of the components used in a single stage V.F. amplifier should not exceed about 0·5. Since frequency response variations are additive it may be necessary to reduce the value of $\frac{L}{CR^2}$ if more stages than one are used.

Tetrode or pentode valves (often of the power output type with normal operating anode current of 30 mA) are universally employed in the V.F. stages of a television receiver, partly because they give much greater amplification than triodes, but also because they have a low anode-grid interelectrode capacitance and therefore reflect a much smaller value of capacitance into their grid circuits. Harmonic distortion is relatively unimportant so that there is no advantage in using triodes.

We shall now consider the V.F. amplifier under three headings, viz., its performance at high frequencies, its performance at low frequencies, and the method of restoring the D.C. component to its output. It is convenient to start at the high-frequency end of the V.F. range because this determines overall performance by limiting the maximum value of resistance in the anode circuit, which in turn fixes maximum amplification.

16.8.2. High-Frequency Performance. Loss of high-frequency response in a V.F. amplifier is caused by wiring, valve input and output, and C.R. tube input capacitances, the values of which

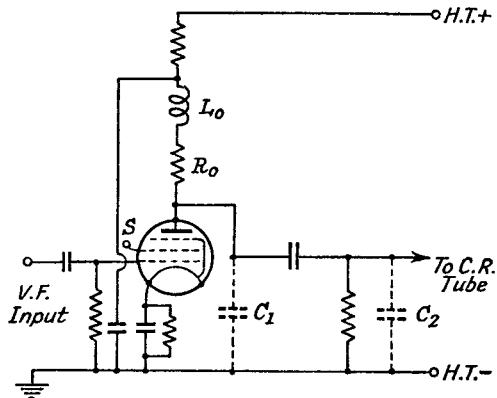

FIG. 16.9*a*.—A Typical V.F. Amplifier Circuit.

are about 5, 10, 10, and 15 $\mu\mu$F respectively, making a total stray capacitance of 30 $\mu\mu$F across the anode circuit of the last V.F. amplifier valve. At high frequencies the reactance of this capacitance falls to a low value, e.g., at 3·5 Mc/s it is 1,515 Ω, and this

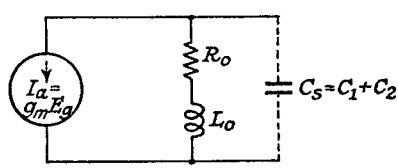

FIG. 16.9*b*.—The Equivalent Circuit for Fig. 16.9*a*.

limits the maximum value of the anode load resistance R_0 to not more than 1,500 Ω if — 3 db. loss is tolerable at this frequency. The circuit for this condition is that of Fig. 16.9*a* with $L_0 = 0$; its equivalent, assuming $L_0 = 0$ and R_a to be much greater than

R_0, is that of Fig. 16.9*b*. The amplification of the stage at any frequency, f, is therefore

$$A = \frac{g_m R_0}{1+j\omega C_s R_0} \quad . \quad . \quad . \quad . \quad 16.16a$$

where C_s = total stray capacitance of the anode circuit.

$$= C_1 \quad C_2.$$

Let $$f_0 = \frac{1}{2\pi R_0 C_s}, \text{ then}$$

$$A = \frac{g_m R_0}{1+j\frac{f}{f_0}} \quad . \quad . \quad . \quad . \quad 16.16b.$$

The amplification at any frequency compared with the maximum amplification $A_{max.}$ at the lower middle frequencies is

$$\frac{A}{A_{max.}} = \frac{1}{1+j\frac{f}{f_0}}$$

and the attenuation at any frequency is

$$20 \log_{10} \frac{|A|}{A_{max.}} = -10 \log_{10} \left(1+\left(\frac{f}{f_0}\right)^2\right).$$

It is plotted in Fig. 16.10*a* as the curve marked $\frac{L_0}{C_s R_0^2} = 0$.

The phase shift at any frequency is

$$\phi = -\tan^{-1} \omega C_s R_0 = -\tan^{-1} \frac{f}{f_0} \quad . \quad . \quad 16.17$$

and the departure from the linear phase relationship is given by

$$\Delta\phi = -\tan^{-1} \frac{f}{f_0} - \left(-57° 18' \frac{f}{f_0}\right) \quad . \quad . \quad 16.18$$

and it is plotted in Fig. 16.10*b* as the curve for $\frac{L_0}{C_s R_0^2} = 0$. This curve is actually identical with the dashed curve for the single-tuned circuit shown in Fig. 16.4. The attenuation curve is also the same. It may be noted that when f is small, $\phi = -\tan^{-1} \frac{f}{f_0} \simeq \frac{f}{f_0} \propto f$, so that if this relationship were continued for all frequencies ϕ would equal $\frac{-f}{f_0}$ radians or $-57° 18' \frac{f}{f_0}$. The required phase angle is greater than the actual phase angle for all frequencies, so that $\Delta\phi$ is positive, i.e., there is insufficient time delay of each frequency vector to maintain the linear relationship. If we take the highest vision

frequency as 3·5 Mc/s, and permit a loss of − 1 db. at this frequency, we have $f_0 = 7{\cdot}0$ Mc/s $\left(\text{see Fig. 16.10}a,\ \frac{f}{f_0} \simeq 0{\cdot}5 \text{ for } -1 \text{ db. loss}\right)$, so that R cannot exceed 757 Ω. If the g_m of the valve is 10 mA/volt, overall gain is 7·57, which is low. Phase-angle error at $f = \frac{1}{2}f_0$ is from Fig. 16.10b $\left(\frac{L_0}{C_s R_0^2} = 0\right) + 2° 5'$, corresponding to a time advance of 0·00166 μ secs., which is negligible. The most serious disadvantage of the uncompensated circuit is therefore its low maximum amplification. It is possible to increase maximum amplification, without increasing attenuation or phase distortion, by neutralizing the stray capacitive reactance with an inductance L_0 in series with R_0 as shown in Fig. 16.9a. From expression 4.4, Part I, the load impedance is

$$Z_0 = \frac{R_0 + j\omega[L_0(1 - \omega^2 L_0 C_s) - C_s R_0^2]}{[1 - \omega^2 L_0 C_s]^2 + [\omega C_s R_0]^2} \quad . \quad . \quad 16.19a$$

$$= R_0 \left[\frac{1 + \frac{j\omega L_0}{R_0}\left[1 - \omega^2 L_0 C_s - \frac{C_s R_0^2}{L_0}\right]}{[1 - \omega^2 L_0 C_s]^2 + [\omega C_s R_0]^2}\right].$$

If $\omega_r = \frac{1}{\sqrt{L_0 C_s}}$, $\frac{\omega L_0}{R_0} = \frac{f}{f_r}\frac{1}{R_0}\sqrt{\frac{L_0}{C_s}}$, and $\omega C_s R_0 = \frac{f}{f_r} R_0 \sqrt{\frac{C_s}{L_0}}$

$$\therefore\ Z_0 = R_0 \frac{1 + j\frac{f}{f_r}\alpha\left[1 - \left(\frac{f}{f_r}\right)^2 - \frac{1}{\alpha^2}\right]}{\left[1 - \left(\frac{f}{f_r}\right)^2\right]^2 + \left[\frac{f}{f_r}\cdot\frac{1}{\alpha}\right]^2} \quad . \quad 16.19b$$

where $\alpha = \frac{1}{R_0}\sqrt{\frac{L_0}{C_s}} = \frac{f_0}{f_r}$, for $f_0 = \frac{1}{2\pi R_0 C_s}$.

From the above, the attenuation at any frequency compared with the value at the lower middle frequencies is

$$20 \log_{10} \frac{|Z_0|}{R_0} = +10 \log_{10} \frac{1 + \left[\frac{f}{f_r}\alpha\right]^2\left[1 - \left(\frac{f}{f_r}\right)^2 - \frac{1}{\alpha^2}\right]^2}{\left[\left[1 - \left(\frac{f}{f_r}\right)^2\right]^2 + \left(\frac{f}{f_r}\frac{1}{\alpha}\right)^2\right]^2}$$

$$= +10 \log_{10} \frac{1 + \left[\frac{f}{f_0}\alpha^2\right]^2\left[1 - \left(\frac{f}{f_0}\alpha\right)^2 - \frac{1}{\alpha^2}\right]^2}{\left[\left[1 - \left(\frac{f}{f_0}\alpha\right)^2\right]^2 + \left[\frac{f}{f_0}\right]^2\right]^2} \quad . \quad 16.20a$$

$$\phi = +\tan^{-1}\frac{f}{f_r}\alpha\left[1-\left(\frac{f}{f_r}\right)^2-\frac{1}{\alpha^2}\right]$$

$$= +\tan^{-1}\frac{f}{f_0}\alpha^2\left[1-\left(\frac{f}{f_0}\alpha\right)^2-\frac{1}{\alpha^2}\right] \quad . \quad . \quad . \quad 16.20b$$

and $$\Delta\phi = \tan^{-1}\frac{f}{f_r}\alpha\left[1-\left(\frac{f}{f_r}\right)^2-\frac{1}{\alpha^2}\right]-57^\circ\ 18'\frac{f}{f_r}\alpha\left(1-\frac{1}{\alpha^2}\right)$$

$$= \tan^{-1}\frac{f}{f_0}\alpha^2\left[1-\left(\frac{f}{f_0}\alpha\right)^2-\frac{1}{\alpha^2}\right]-57^\circ\ 18'\frac{f}{f_0}\alpha^2\left(1-\frac{1}{\alpha^2}\right). \quad 16.20c.$$

Attenuation and phase-angle error, $\Delta\phi$, are plotted in Figs. 16.10*a* and 16.10*b* against the ratio of actual frequency to f_0, for various values of $\alpha^2\left[\frac{L_0}{C_sR_0^2}\right]$, where $f_0 = \frac{1}{2\pi R_0 C_s}$. The frequency f_0 is used

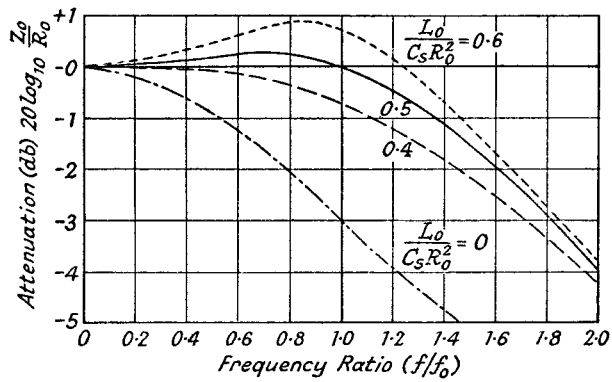

FIG. 16.10*a*.—The Attenuation Characteristics of an Inductance Compensated V.F. Amplifier.

as a parameter, rather than f_r, because it allows direct comparison with the uncompensated case, and also L_0 is the essential variable. It will be noted that for the values of α chosen and $\frac{f}{f_0} < 1{\cdot}8$, the actual phase angle is negative and greater than the required, hence phase-angle error is negative, indicating too much delay on each frequency vector. The most suitable value of $\frac{L_0}{C_sR_0^2}$ as regards frequency response is 0·5, but phase distortion is less for $\frac{L_0}{C_sR_0^2} = 0{\cdot}4$. Frequency response for $\frac{L_0}{C_sR_0^2} = 0{\cdot}5$ is almost level to $\frac{f}{f_0} = 1$, so

that 3·5 Mc/s may be considered as corresponding to $\frac{f}{f_0} = 1$. Hence

$$R_0 = \frac{1}{2\pi f_0 C_s} = \frac{10^{12}}{6{\cdot}28 \times 3{\cdot}5 \times 10^6 \times 30} = 1{,}515\ \Omega$$

$$L_0 = 0{\cdot}5 C_s R_0^2 = \frac{0{\cdot}5 \times 30 \times (1{,}515)^2}{10^6 \times 10^6} = 34{\cdot}5\ \mu\text{H},$$

and the amplification of the compensated stage is double that of the uncompensated. Phase-angle error is $-\ 8°\ 12'$, and corresponds to a time delay of 0·0065 μ secs.; it is greater than that for the uncompensated circuit, but is still negligibly small. If a large

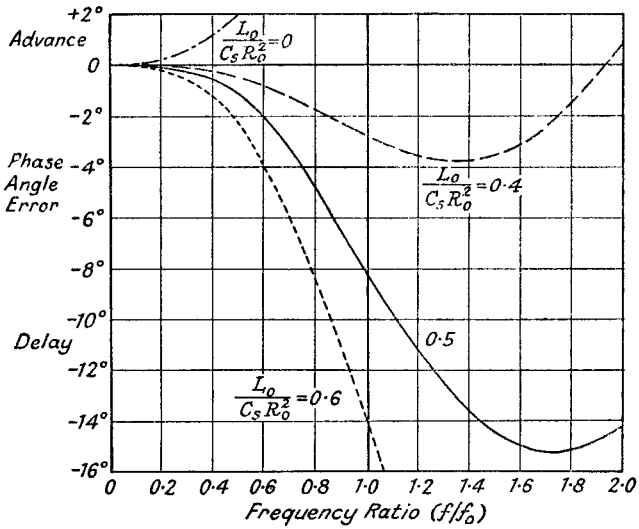

FIG. 16.10*b*.—Phase Angle Error Curves for the Inductance Compensated V.F. Amplifier.

number of V.F. stages is required and phase-angle error, which is additive from stage to stage, must be reduced, $\frac{L_0}{C_s R_0^2} = 0{\cdot}4$ is more suitable. For satisfactory frequency response, $\frac{f}{f_0} = 0{\cdot}6$ should correspond to the highest vision frequency, and this reduces the maximum permissible value of R_0 to 910 Ω; overall amplification is reduced to 60% of the value at $\frac{L_0}{C_s R_0^2} = 0{\cdot}5$. Values of $\frac{L_0}{C_s R_0^2}$ greater than 0·5 are unlikely to be satisfactory as attenuation and phase distortion are increased. The rising frequency response characteristic tends also to introduce transient distortion.

Another type of compensated circuit is shown in Fig. 16.11 ; it is sometimes known as the series peaking circuit, the circuit of

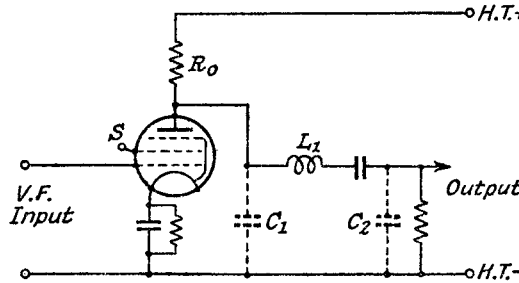

FIG. 16.11.—The Series Peaking Compensated v.f. Amplifier.

Fig. 16.9*a* being called the shunt peaking circuit. The circuit functions as a low-pass filter and the ratio of output-to-input voltage is

$$\frac{E_0}{E_g} = g_m \frac{R_0 \dfrac{\dfrac{1}{j\omega C_1}\left(j\omega L_1 + \dfrac{1}{j\omega C_2}\right)}{j\omega L_1 + \dfrac{1}{j\omega C_1} + \dfrac{1}{j\omega C_2}}}{R_0 + \dfrac{\dfrac{1}{j\omega C_1}\left(j\omega L_1 + \dfrac{1}{j\omega C_2}\right)}{j\omega L_1 + \dfrac{1}{j\omega C_1} + \dfrac{1}{j\omega C_2}}} \cdot \frac{\dfrac{1}{j\omega C_2}}{j\omega L_1 + \dfrac{1}{j\omega C_2}} \quad . \quad . \quad 16.21a.$$

$$= g_m \frac{\dfrac{-R_0}{\omega^2 C_1 C_2}}{R_0\left(j\omega L_1 + \dfrac{1}{j\omega C_1} + \dfrac{1}{j\omega C_2}\right) + \dfrac{1}{j\omega C_1}\left(j\omega L_1 + \dfrac{1}{j\omega C_2}\right)} \quad . \quad 16.21b.$$

Let $R_0 = \dfrac{1}{\omega_0 C_1 \sqrt{2m}}$ and $L_1 = \dfrac{1}{2\omega_0{}^2 C_1}$, where $\dfrac{C_2}{C_1} = m$ and $C_2 + C_1 = C_s$.

Hence $\dfrac{1}{C_1} = \omega_0 R_0 \sqrt{2m}$, $\dfrac{1}{C_2} = \omega_0 R_0 \sqrt{\dfrac{2}{m}}$ and $L_1 = \dfrac{R_0}{\omega_0}\sqrt{\dfrac{m}{2}}$. Replacing L_1, C_1 and C_2 in 16.21*b* by these expressions

$$\frac{E_0}{E_g} = g_m R_0 \frac{\left(-2\dfrac{\omega_0{}^2}{\omega^2}\right)}{\left[m - \dfrac{2\omega_0{}^2}{\omega^2}\right] + j\left[\dfrac{\omega}{\omega_0}\sqrt{\dfrac{m}{2}} - \dfrac{\omega_0}{\omega}\left(\sqrt{2m} + \sqrt{\dfrac{2}{m}}\right)\right]} \quad . \quad 16.21c.$$

The most satisfactory overall performance is obtained for $m = 2$, when

$$\frac{E_0}{E_g} = g_m R_0 \frac{\left[-2\frac{f_0^2}{f^2}\right]\left[2\left(1-\frac{f_0^2}{f^2}\right) - j\left(\frac{f}{f_0} - 3\frac{f_0}{f}\right)\right]}{\left[2\left(1-\frac{f_0^2}{f^2}\right)\right]^2 + \left[\frac{f}{f_0} - 3\frac{f_0}{f}\right]^2} \quad . \quad 16.21d.$$

The attenuation characteristic is obtained by plotting

$$10 \log_{10} \frac{4\frac{f_0^4}{f^4}}{\left[2\left(1-\frac{f_0^2}{f^2}\right)\right]^2 + \left[\frac{f}{f_0} - 3\frac{f_0}{f}\right]^2} \quad . \quad . \quad 16.22$$

against $\frac{f}{f_0}$ as in Fig. 16.12*a* (curve 1). Over the pass range up to $f = f_0$ it is similar to the "shunt peaking" circuit for $\frac{L_0}{C_s R_0^2} = 0{\cdot}5$,

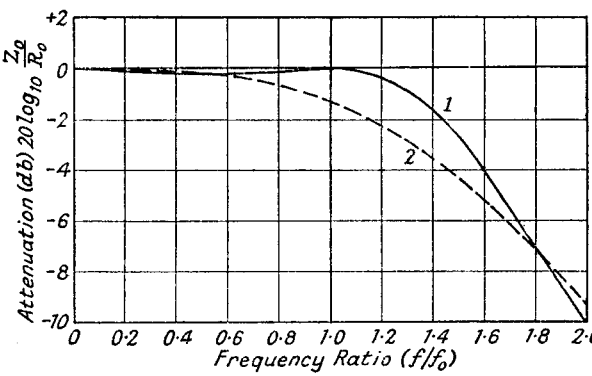

FIG. 16.12*a*.—Attenuation Characteristics of Compensated V.F. Amplifiers.
1. Series Peaking Circuit.
2. Combined Shunt and Series Peaking Circuit.

but at frequencies above f_0 it has the advantage of more rapid attenuation. The phase angle

$$\phi = \tan^{-1} \frac{-\left(\frac{f}{f_0} - 3\frac{f_0}{f}\right)}{2\left(1-\frac{f_0^2}{f^2}\right)} \simeq -57° 18' \frac{3}{2}\frac{f}{f_0} \text{ when } f \ll f_0$$

and phase-angle error is

$$\Delta\phi = \tan^{-1} \frac{-\left(\frac{f}{f_0} - 3\frac{f_0}{f}\right)}{2\left(1-\frac{f_0^2}{f^2}\right)} + 57° 18' \frac{3}{2}\frac{f}{f_0} \quad . \quad . \quad 16.23$$

which is plotted against $\frac{f}{f_0}$ in Fig. 16.12*b* (curve 1). Phase-angle error is very small over the pass range up to $f = f_0$ and is much less

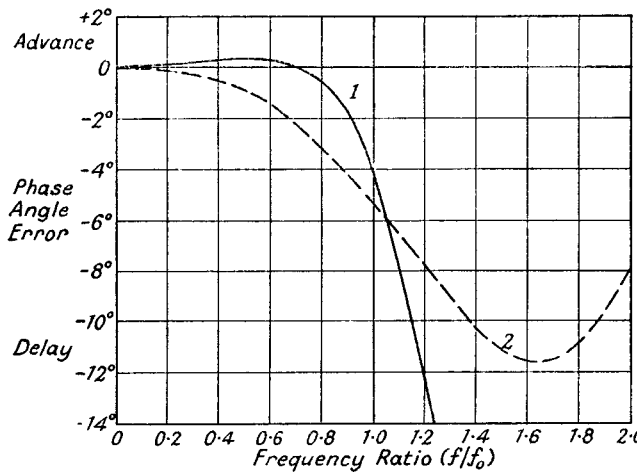

FIG. 16.12*b*.—Phase Angle Error Curves of Compensated V.F. Amplifiers.
1. Series Peaking Circuit.
2. Combined Shunt and Series Peaking Circuit.

than that of the previous case. If C_s and f_0 have the same values as those for the shunt peaking circuit, $R_0 = \frac{1}{2\omega_0 C_1} = \frac{3}{2\omega_0 C_s} = 2{,}270\ \Omega$; hence amplification is 1·5 times as great as for the previous case.

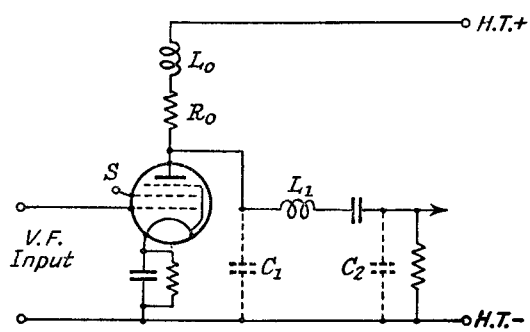

FIG. 16.13.—The Combined Shunt and Series Peaking Compensated V.F. Amplifier.

The net increase in amplification may not be as large as 1·5 because it may be necessary to add a trimmer capacitance to either C_1 or

C_2 to obtain the required ratio of $\frac{C_2}{C_1} = 2$, and this increases C_s and so reduces amplification. Values of $m < 2$ tend to give a more peaked frequency response, whilst values greater than 2 tend to cause a more rapid fall at high frequencies. The resistance component of L_1 has little effect on performance provided it is not more than $\frac{1}{20}\omega L_1$.

Still greater amplification can be obtained by combining the shunt and series peaking circuits as in Fig. 16.13. The expression for the ratio of output-to-input voltage is found by replacing R_0 by $R_0+j\omega L_0$ in 16.21*b*, thus

$$\frac{E_0}{E_g}=g_m\frac{-\dfrac{(R_0+j\omega L_0)}{\omega^2 C_1 C_2}}{(R_0+j\omega L_0)\left(j\omega L_1+\dfrac{1}{j\omega C_1}+\dfrac{1}{j\omega C_2}\right)+\dfrac{1}{j\omega C_1}\left(j\omega L_1+\dfrac{1}{j\omega C_2}\right)} \quad . 16.24a.$$

The following relationships between R_0, L_0, L_1, C_1 and C_2 are suggested as providing a satisfactory frequency and phase characteristic.

$$R_0 = \frac{1{\cdot}8}{\omega_0 C_s}, \quad C_s = C_1+C_2, \quad C_1 = \frac{C_2}{m}, \quad m = 2,$$

i.e.,
$$C_1 = \frac{1}{1{\cdot}66\omega_0 R_0}; \quad C_2 = \frac{1}{0{\cdot}833\omega_0 R_0}.$$

$$L_0 = 0{\cdot}12 C_s R_0^2 = \frac{0{\cdot}216 R_0}{\omega_0}$$

$$L_1 = 0{\cdot}52 C_s R_0^2 = \frac{0{\cdot}937 R_0}{\omega_0}.$$

Inserting these values in 16.24*a*, we get

$$\frac{E_0}{E_g} = \frac{g_m R_0 1{\cdot}387\dfrac{f_0^2}{f^2}\left(1+j0{\cdot}216\dfrac{f}{f_0}\right)}{1{\cdot}387\dfrac{f_0^2}{f^2}+0{\cdot}202\dfrac{f^2}{f_0^2}-2{\cdot}099+j\left(2{\cdot}5\dfrac{f_0}{f}-0{\cdot}937\dfrac{f}{f_0}\right)} \quad . 16.24b.$$

The attenuation characteristic, curve 2 in Fig. 16.12*a*, is obtained by plotting

$$10\log_{10}\frac{1{\cdot}92\dfrac{f_0^4}{f^4}\left(1+0{\cdot}0467\dfrac{f^2}{f_0^2}\right)}{\left[1{\cdot}387\dfrac{f_0^2}{f^2}+0{\cdot}202\dfrac{f^2}{f_0^2}-2{\cdot}099\right]^2+\left[2{\cdot}5\dfrac{f_0}{f}-0{\cdot}937\dfrac{f}{f_0}\right]^2} \quad . 16.25$$

against $\frac{f}{f_0}$; the phase angle is

$$\phi = \tan^{-1}\frac{-2{\cdot}2\frac{f_0}{f}+0{\cdot}484\frac{f}{f_0}+0{\cdot}0437\frac{f^3}{{f_0}^3}}{1{\cdot}387\frac{{f_0}^2}{f^2}-1{\cdot}559}$$

$$= 57^\circ\ 18' \times -1{\cdot}589\frac{f}{f_0} \text{ when } f \ll f_0.$$

Phase-angle error is

$$\Delta\phi = \tan^{-1}\frac{-2{\cdot}2\frac{f_0}{f}+0{\cdot}484\frac{f}{f_0}+0{\cdot}0437\frac{f^3}{{f_0}^3}}{1{\cdot}387\frac{{f_0}^2}{f^2}-1{\cdot}559}+57^\circ\ 18' \times 1{\cdot}589\frac{f}{f_0} \quad . \quad 16.26$$

and it is plotted in Fig. 16.12*b* as curve 2. For the particular component relationships chosen, neither attenuation nor phase characteristics are as good as those for the previous circuit. Allowing a loss of -1 db., $\frac{f}{f_0} = 0{\cdot}9$ for $f = 3{\cdot}5$ Mc/s gives

$$R_0 = \frac{1{\cdot}8 \times 0{\cdot}9 \times 10^6}{6{\cdot}28 \times 3{\cdot}5 \times 30} = 2{,}455\ \Omega.$$

Hence amplification is slightly higher for this combination of shunt and series peaking circuits.

There are many other possible forms of compensated circuit, including varieties of the constant k low-pass filter prototype and m-derived structures, and reference should be made to Bibliography 26.

The values of C_1 and C_2 can be measured by means of a circuit magnification or Q meter, or may be calculated by noting the frequency at which the amplification of the uncompensated amplifier falls to 0·707 of its maximum value, and by using the fact that $R_0 = \frac{1}{\omega C}$ at this frequency.

Measurement of the amplification characteristic of a V.F. amplifier can be made, using the C.R. tube grid as a diode detector and noting the variation in amplifier input voltage necessary to preserve constant C.R. tube grid current. The phase shift characteristic can be noted by applying the input and output voltages of the amplifier to a horizontal and a vertical deflector plate of a C.R. tube. If the input and output voltages are adjusted to give equal amplitudes of deflection, 0°, 180°, 360°, etc., phase angles are denoted by a

straight line at 45° and 135°, and phase angles of 90°, 270°, etc., by a circle. Alternatively, a calibrated phase-shifting network consisting of a resistance and capacitance can be included in the input or output lines so as to recover the 0° straight line condition.

16.8.3. Low Frequency Performance. Frequencies below 10 kc/s contribute very little to the horizontal detail of the picture but do affect vertical detail. Poor low-frequency performance affects background intensity causing it to vary from top to bottom of the picture, e.g., a transmitted all-white screen is reproduced as a screen gradually shading from white to grey from top to bottom, or vice versa. Phase distortion, which is caused by the increasing reactance of coupling and self-bias capacitors as the frequency is

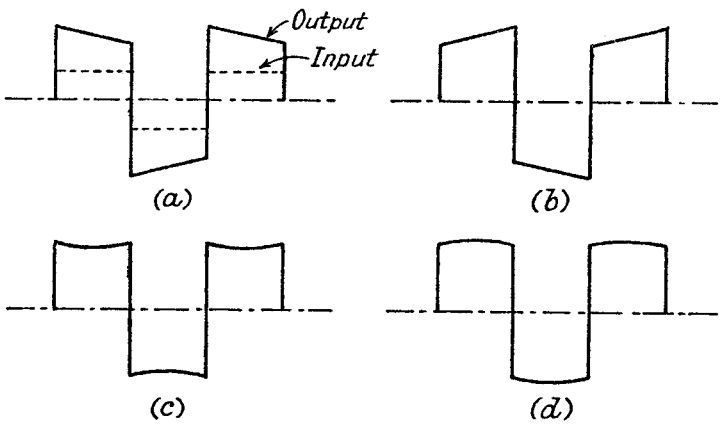

FIG. 16.14.—Examples of Phase and Attenuation Distortion of a Square Wave Input Signal.

decreased, is much more serious than attenuation distortion. A coupling capacitance of 0·1 μF and resistance of 0·5 MΩ in the grid circuit of a V.F. amplifier produce a frequency response at 50 c.p.s. of 99·82% of the maximum, but the phase shift is $\tan^{-1}\frac{3{\cdot}18}{50} = 3°\ 38'$, which is equivalent to a time advance of $\frac{3°\ 38' \times 10^6}{360 \times 50} = 201{\cdot}5\ \mu$ secs. The effect of phase distortion is more conveniently examined by applying an input voltage of square wave shape rather than a single-frequency voltage, and examples of types of distorted output wave shapes which may be obtained are shown in Figs. 16.14*a*, 16.14*b*, 16.14*c* and 16.14*d*. A square-shaped voltage wave applied to the coupling capacitance and resist-

ance in the grid circuit of a V.F. amplifier produces across the resistance the wave shape shown in Fig. 16.14*a*, the trailing ends of the upper and lower parts of the original square wave being tilted towards the centre line. The distorted section is part of an exponential curve $E\varepsilon^{\frac{-t}{R_g C_c}}$. If the wave has a fundamental frequency of 50 c.p.s. and C_c and R_g are 0·1 μF and 0·5 MΩ, the percentage fall in voltage from leading to trailing edge is $\left(1 - \varepsilon^{\frac{-20}{100}}\right) 100\% = 18{\cdot}2\%$ $\left(\text{note that } t = \frac{1}{2 \times 50} \text{ secs.}\right)$; for a fundamental frequency of 25 c.p.s., the percentage fall is 33%. This voltage fall can be reduced either by increasing C_c or R_g, or by including a compensating circuit in the anode of the V.F. amplifier. The maximum value of R_g is limited to about 0·5 MΩ by considerations of valve life, so that only C_c can be increased. Making $C_c = 0{\cdot}5\,\mu$F reduces the fall to 3·92% at 50 c.p.s. and 7·69% at 25 c.p.s., which would generally be regarded as satisfactory. The increased bulk of C_c would tend to increase the input earth capacitance of the V.F. amplifier and so affect high-frequency response.

It is possible to produce a compensating tilt in the opposite direction by means of a decoupling capacitance (C_s in Fig. 16.15)

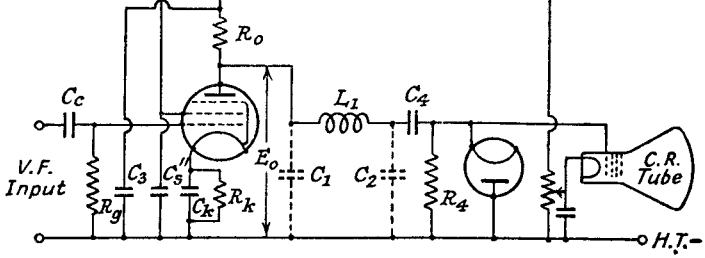

FIG. 16.15.—A Circuit for Improving the V.F. Amplifier Response to a Square Wave and for Restoring the D.C. Component of the Vision Signal.

in the anode circuit of the V.F. amplifier. A square wave of input voltage at the grid is caused by C_s in association with R_0 to have the output voltage wave shape of Fig. 16.14*b*, and exact compensation of grid circuit distortion can be achieved by a suitable choice of C_s provided R_s is much larger (about 10 times) than the reactance of C_s at the square wave fundamental frequency. Analysis of the circuit of Fig. 16.15 shows that amplification is

$$\frac{E_0}{E_g} = g_m\left(R_0+\frac{1}{jpC_3}\right)\left(\frac{R_g}{R_g+\frac{1}{jpC_c}}\right) \quad . \quad . \quad 16.27a$$

when $R_3 \gg \frac{1}{pC_3}$, and $R_4 \gg R_0$

$$\frac{E_0}{E_g} = g_m R_g\left(R_0+\frac{1}{jpC_3}\right)\frac{R_g-\frac{1}{jpC_c}}{R_g{}^2+\left(\frac{1}{pC_c}\right)^2}$$

$$= \frac{g_m R_g}{R_g{}^2+\left(\frac{1}{pC_c}\right)^2}\left[R_0R_g+\frac{1}{p^2C_3C_c}-\frac{j}{p}\left(\frac{R_g}{C_3}-\frac{R_0}{C_c}\right)\right] \quad . \quad 16.27b.$$

Phase distortion is, therefore, completely cancelled by making the time constant of the grid circuit equal to that of the anode circuit, i.e., $R_gC_c = R_0C_3$, provided R_3 can be neglected. The anode decoupling circuit is primarily a phase distortion compensator, and though it does tend to cancel attenuation distortion—it has a rising low-frequency response as frequency is decreased—it may not be sufficient to produce zero overall attenuation distortion. An example of the wave shape to be expected from a phase-corrected stage having a decreasing low-frequency response [8] is illustrated in Fig. 16.14*c*, and in Fig. 16.14*d* is shown the waveform resulting from a rising low-frequency response.

When R_3 is comparable with the reactance of C_3—this occurs as the frequency approaches a very low value such as 5 c.p.s.—expression 16.27*a* is modified to

$$\frac{E_0}{E_g} = g_m\left(R_0+\frac{R_3}{1+jpC_3R_3}\right)\left(\frac{R_g}{R_g+\frac{1}{jpC_c}}\right)$$

$$= g_m\left(\frac{R_0+R_3+jpC_3R_3R_0}{1+jpC_3R_3}\right)\left(\frac{R_g}{R_g+\frac{1}{jpC_c}}\right)$$

$$= g_m(R_0+R_3)\left(\frac{1+\frac{jpC_3R_3R_0}{R_0+R_3}}{1+jpC_3R_3}\right)\frac{R_gjpC_c}{(1+jpC_cR_g)} \quad . \quad 16.27c.$$

Exact phase compensation is no longer possible because rationalization of 16.27*c* produces a j term in the numerator of

$$j\left[1+\frac{p^2C_3R_3{}^2}{R_0+R_3}(C_3R_0-C_cR_g)\right]$$

and a real term of

$$p\left[C_cR_g\left(1+\frac{p^2C_3{}^2R_3{}^2R_0}{R_0+R_3}\right)+C_3R_3\frac{R_3}{R_0+R_3}\right].$$

Hence the phase angle can neither be made constant nor proportional to p, i.e., to frequency.

If $\dfrac{C_3R_3R_0}{R_3+R_0}=C_cR_g$, expression 16.27c becomes

$$\frac{E_0}{E_g}=\frac{g_mR_0}{1+\dfrac{1}{jpC_3R_3}},$$

i.e., phase and attenuation distortion is a function of C_3 and R_3 and is independent of the grid circuit. There is, therefore, little advantage in using C_3 and R_3 for correcting grid circuit distortion unless the time constant of the decoupling capacitance and resistance can be made much greater than that of the grid circuit. Hence R_3 should be given its highest possible value, and this is generally 5,000 Ω (a very high value cannot be considered because it reduces the D.C. anode voltage of the V.F. amplifier). If $R_g=0{\cdot}5$ MΩ, $C_c=0{\cdot}1$ μF, $R_0=2{,}500$ Ω and $R_3=5{,}000$ Ω

$$C_3=\frac{R_gC_c(R_0+R_3)}{R_0R_3}=30\ \mu\text{F}$$

$$C_3R_3=0{\cdot}15\text{ secs.}=3C_cR_g.$$

Thus the use of the compensating decoupling circuit has reduced the frequency for a given loss and the phase shift to a third of its value for the uncompensated stage, i.e., a frequency of $\frac{50}{3}$ or 16·66 c.p.s. now suffers a phase shift of 3° 38′ and amplifier response at this same frequency is 99·82% of its maximum value.

The bias voltage for the V.F. amplifier may be derived from a fixed voltage source; it may be provided by the anode current passing through a cathode resistance, or by grid current produced by the input signal. Fixed bias voltage has the advantage that a simple filter circuit (for hum voltages) can be designed to produce very small phase and attenuation distortion of the signal, but it does not compensate for H.T. supply voltage changes; the grid resistance R_g must therefore be limited to a lower value than with cathode self-bias. Cathode self-bias causes phase and attenuation distortion at low frequencies unless the shunt capacitor C_k in Fig. 16.15 is made very large, e.g., 200 to 1,000 μF. Low-frequency performance is improved by omitting C_k, but there is a large reduction in amplification, and high-frequency performance is affected

because stray capacitance across R_k tends to reduce the degeneration at high frequencies. Grid current biasing from the signal voltage has the advantage of retaining the D.C. component of the signal in the V.F. anode current, but there is a danger of taking too large an anode current when the signal ceases.

Phase and attenuation distortion from the cathode self-bias circuit can be compensated by a suitable choice of decoupling capacitance and resistance in the anode circuit. Since $R_a \gg Z_0$

$$\frac{E_0}{E_g} = \frac{g_m Z_0}{1+g_m Z_k}$$

where $$Z_0 = R_0 + \frac{R_3}{1+jpC_3R_3}$$

and $$Z_k = \frac{R_k}{1+jpC_kR_k}.$$

In order that the decoupling circuit may exactly compensate for the self-bias circuit

$$\frac{E_0}{E_g} = g_m R_0 = \frac{g_m Z_0}{1+g_m Z_k}$$

i.e., $$(1+g_m Z_k) = \frac{Z_0}{R_0}$$

or $$1+\frac{g_m R_k}{1+jpC_kR_k} = 1+\frac{R_3}{R_0(1+jpC_3R_3)}.$$

Hence equating imaginary and real terms

$$C_kR_k = C_3R_3$$

$$g_m R_k = \frac{R_3}{R_0}$$

or $$g_m R_0 = \frac{R_3}{R_k} = \frac{C_k}{C_3} \quad . \quad . \quad . \quad 16.28.$$

Typical values for C_k and R_k are 25 μF and 150 Ω, so that for $g_m = 10$ mA/volt and $R_0 = 2{,}500\ \Omega$, $C_3 = 1\ \mu$F and $R_3 = 3{,}750\ \Omega$.

The following is the normal procedure for cathode circuit correction. C_kR_k and R_0 are given their specified values, C_3 is made about 1 μF and R_3 about 5,000 Ω. A 10 kc/s input voltage is applied and the amplification noted—at this frequency the reactances of C_k and C_3 are negligibly small. C_k and C_3 are next removed and R_3 adjusted to give the same overall amplification as previously. R_3 is then measured and C_3 calculated from $C_3 = \frac{C_kR_k}{R_3}$.

The screen circuit, like the cathode circuit, can also produce

attenuation and phase distortion and it may be compensated by the anode decoupling circuit. Exact compensation is obtained by equating expressions for B and for x in Sections 9.3.5 and 6, thus

$$\frac{R_3}{R_s'} = \frac{C_s''}{C_3} = \frac{R_0}{R_{SG}}$$

where R_s' = external resistance in the screen H.T. path

C_s'' = screen decoupling capacitance

R_{SG} = slope resistance of the screen electrode $= \dfrac{\Delta E_s}{\Delta I_s}$.

It is clearly not possible to compensate for the grid, cathode and screen circuits in one stage, and it is usual when more than one stage is employed to use the decoupling circuit of one stage for grid circuit correction, one for cathode self-bias and one for screen circuit correction. Screen circuit components generally have less effect on attenuation and phase distortion than cathode self-bias components. When only one stage of V.F. amplification is employed, grid circuit correction may be used and the bias derived from a fixed voltage source, or the time constant of the grid circuit (R_gC_c) may be made as large as possible and cathode self-bias distortion corrected in the anode circuit. Low-frequency performance will generally be found satisfactory if phase and attenuation is small down to a frequency of 25 c.p.s.

Motor boating is sometimes a problem, more particularly with a large number of V.F. stages, and great care must be taken to ensure that the power supply has a low impedance, i.e., large smoothing capacitors are needed. In extreme cases it may be necessary to reduce the grid coupling capacitors so as to attenuate very low frequencies.

16.8.4. Restoration of the D.C. Component. The need for restoring the D.C. component of the vision signal has been stressed in Section 16.8.1. If this component is absent, the vision output wave automatically centres itself so that " positive " and " negative " areas are equal, as shown beneath the beam current-grid voltage curve of the C.R. tube in Fig. 16.16. The bias position is A and the combined V.F. and synchronizing input signal automatically centres itself on the line AB. Thus position 1 corresponds to a maximum white line and position 2 to a black line. This means that the correct black position (line DF, the start of the synchronizing pulses) is variable in relation to the bias line AB and contrast is lost. The D.C. component can be restored if a variable positive bias just cancelling the difference in voltage, E_d, between

the correct black line HG and the vision signal black line DF is included in the grid circuit of the cathode ray tube. This can be accomplished by using a diode connected as shown in Fig. 16.15, to act as a peak voltage detector of the " negative " half of the vision A.C. wave, i.e., on the synchronizing pulse side. If the time constant of the coupling capacitance C_4 and diode load resistance, R_4, which is also the coupling resistance to the C.R. tube, is made sufficiently large, the bias produced across R_4 is nearly equal to the negative peak voltage, E_1, of the input wave. By suitable location of the bias point A, DF can be made to coincide with GH as shown in position 3. The time constant must not, however, be so large that it makes the bias change sluggish to changes of picture background brightness. A time constant of 0·1 second is suitable; too low a value causes noticeable lack of contrast.

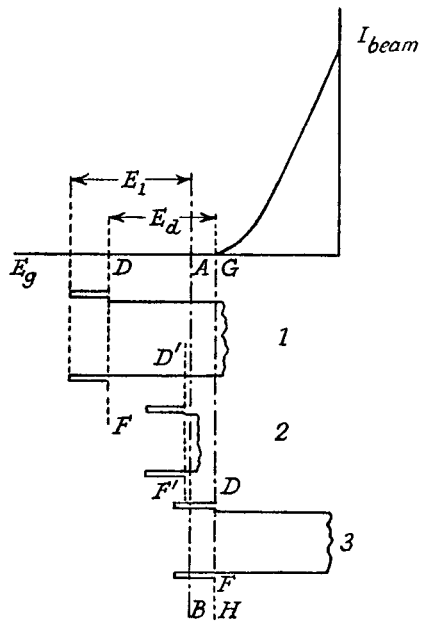

FIG. 16.16.—A Diagram Illustrating the Need for Restoring the D.C. Component of the Vision Signal.

The action of the diode bias also tends to restore the downward tilt of a square wave input (Fig. 16.14a) due to phase and attenuation distortion in the V.F. amplifier, the direction of the variable diode bias being opposite to the wave tilt. In order to obtain this correction, the time constant C_4R_4 must be not greater than that of circuit being corrected but must be much greater than the period of the line frequency.

It is possible to use the last V.F. amplifier as a D.C. restorer if the cathode ray tube grid can be directly connected to the amplifier anode, i.e., the cathode of the C.R. tube cannot be at vision receiver earth potential but must be connected to a potential divider across the receiver H.T. supply. The amplifier valve is operated as a cumulative-grid detector with zero standing bias, and D.C. restoration occurs by grid current detection. There are three serious objections to the method: if the receiver rectifier heats up more quickly than the V.F. amplifier, positive bias is applied to the C.R.

tube grid, screen voltage tends to vary with changes of grid bias, and screen voltage must be reduced to prevent excessive anode dissipation in the absence of a signal, and this leads to a reduction in amplification.

With positive modulation transmission a biased diode limiter (see Section 12.9) may be incorporated to suppress " snowflake " interference on the picture. The diode is non-conductive for normal signals but peaked interference voltages cause it to conduct and apply a negative pulse to the C.R. tube grid, thus blacking out on interference. With negative modulation, peaks of interference automatically black-out the picture at the spot where they occur.

16.9. Synchronizing Pulse Separation.

16.9.1. Introduction. Two actions are involved in synchronizing pulse separation : the first, known as amplitude separation, divides the I.F. or V.F. signal into vision and pulse components and rejects the former ; the second, known as frequency separation, divides the synchronizing voltage into frame and line pulses, which are then used to lock the frame and line scanning generators employed for deflecting the C.R. tube spot across the screen. Synchronism can be established with the scanning generator " free " frequency fast or slow, but slow running is preferable because stable locking is possible over a wider range of frequencies than if the generator frequency is fast. Correct polarity of synchronizing pulse is essential, and this depends on the type of scanning generator and the point at which the pulse is applied. If it is injected into the grid circuit of a slow-running generator, it must usually be in a positive direction, the start of the pulse, where it joins the vision component, being negative. With the American system of negative modulation and the V.F. detector connected as in Fig. 16.7, an even number of phase reversals must be included between the detector output and the scanning generator. The English system of positive modulation calls for an odd number of phase reversals between the detector output (Fig. 16.7) and the scanning generators, because the initial synchronizing pulse is in a negative direction.

For most satisfactory synchronization the free frequency of the scanning generator is set about half-way between the correct and " fall-out " frequency, so that the generator is held in synchronism when its free frequency varies in either direction. Variations of frequency are caused by supply voltage fluctuations, and hum or noise voltages injected into the scanning generator circuits. An adequately smoothed H.T. supply is most necessary, and if iron-cored

coils are used in the generator circuit they must be carefully screened from sources of A.C. mains magnetic field. Hum and noise voltages tend to affect interlacing, causing unequal spacing or weaving of interlacing lines. Limitation of pulse amplitude in a positive direction is advisable in order to reduce the effect of peaked noise pulses of large amplitude and short duration. The advantage of this limiting is particularly marked at the edge of the service area of a television transmission, and a steady picture can often be obtained from a signal one-fifth to one-tenth of that which is required to provide a steady picture when no limiter is employed. The voltages required for synchronizing depend on the type of scanning generator employed. The blocking or squegger oscillator requires from 5 to 15 volts, the multivibrator 0·5 to 2 volts, and about the same is needed for the gas-filled relay.

The line and frame pulses must be filtered from each other, and feedback between the two scanning generators must be prevented, otherwise the frame is liable to be triggered by the line, and interlacing is erratic.

16.9.2. Amplitude Separation of the Vision and Synchronizing Components.[4, 7] Separation of the synchronizing pulses from the vision component of the television signal can be accomplished by using a detector type of valve, such as a diode, leaky grid or anode bend, and the principles involved are very similar to those of the amplitude limiter of the F.M. receiver. The input to the

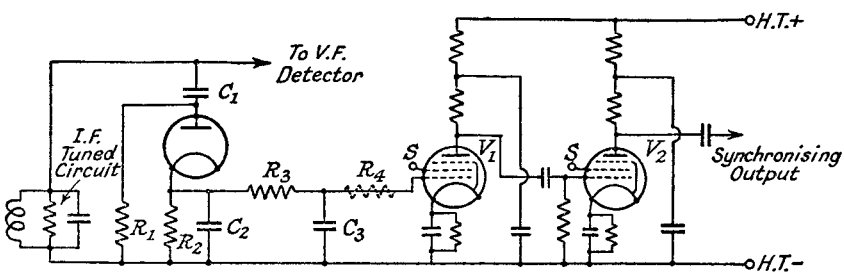

FIG. 16.17*a*.—Separation of the Synchronizing Signals from the Vision Signal for the American Type of Negative Modulation Transmission.

amplitude separator may be taken from the output of the last I.F. valve, the V.F. detector or a V.F. amplifier stage. An example of the diode separator operating from the I.F. output is shown in Fig. 16.17*a*, the circuit is only suitable for the American system in which the synchronizing pulses occur at maximum carrier. The time constant of the coupling capacitance C_1 (0·05 to 0·1 μF) and

resistance R_1 (0·5 to 1 MΩ) is large in order that the D.C. bias voltage across R_1 shall remain almost constant at a value slightly higher than the start of the synchronizing pulse. The latter causes the diode to conduct and produce across R_2 (3,000 Ω to 5,000 Ω) a voltage wave similar in shape to the synchronizing pulse. The by-pass capacitance C_2 (100 $\mu\mu$F) is to assist in removing I.F. ripple and V.F. voltages from the output, and additional filtering is provided by R_3 (2,000 Ω) and C_3 (100 $\mu\mu$F). The output voltage across C_3 is directly connected to an amplifier valve biased almost to the anode current cut-off point, which is given a low negative value by using a low anode voltage [3] if the valve is a triode, or low screen voltage if a tetrode. A resistance R_4 (0·1 MΩ) can be included in series with the grid of the amplifier valve to limit the pulse amplitude in a positive direction. The amplitude of the pulse and any interference, which is superimposed on it or breaks through the vision

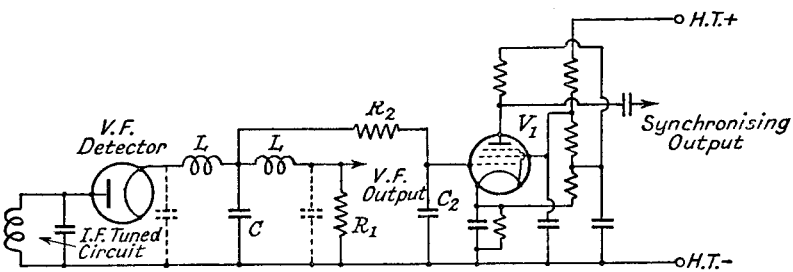

FIG. 16.17*b*.—An Anode Bend Type of Synchronizing Signal Separator for the English System of Positive Modulation

signal, cannot greatly exceed the cut-off bias voltage because grid current in association with R_4 prevents the grid of the amplifier becoming appreciably positive. The synchronizing pulse is in a positive direction across R_2 and an additional phase reversal is necessary after V_1 to regain the positive direction. This is provided by including a second valve V_2. The latter can be omitted if the diode connections are reversed and the bias on V_1 adjusted to a value sufficient to prevent grid current flowing. Pulse amplitude limitation is then brought about by anode current cut-off. Fig. 16.17*b* shows the anode bend type of separator. It may be supplied from the V.F. detector output if the English system of positive transmission is being received and the detector is connected to give a positive vision signal. The valve is biased into cut-off and the vision component is cut off by the action of the grid series resistance R_2 (0·1 MΩ) and grid current. Screen voltage, which controls the

cut-off bias voltage, has a comparatively low value (30 to 40 volts), so that the pulse amplitude is limited, with consequent reduction in interference from noise. Not only is the vision component cut-off by the action of the grid circuit, but it may also be cut off by using a low anode voltage to produce a flat-topped $I_a E_g$ characteristic at grid voltages near zero and in the positive bias region. A triode valve is not likely to be satisfactory in this type of separator because the vision component may be transferred from the grid to the anode circuit through the anode-grid capacitance. Phase reversal of the pulse direction occurs in valve V_1, which therefore gives a positive pulse output. The leaky grid amplitude separator, shown in Fig. 16.17*c*, will function with a V.F. input voltage provided the synchronizing pulses are positive. Low anode and screen

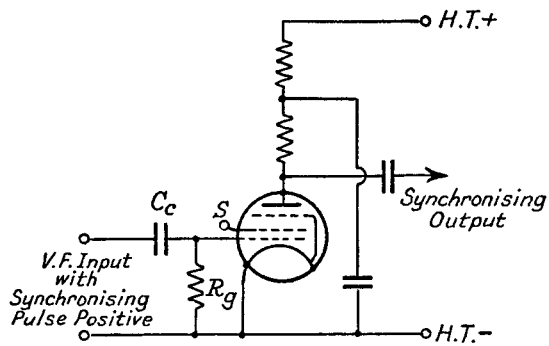

FIG. 16.17*c*.—The Leaky Grid Synchronizing Signal Separator.

voltages are employed to limit pulse amplitude and noise interference. The time constant of the grid circuit is sufficiently high (about 0·05 seconds) to prevent rapid changes of bias voltage due to the vision components. In order to obtain at the separator output a satisfactory synchronizing pulse shape independent of the vision signal, the input synchronizing amplitude should exceed a voltage equal to the cut-off bias of the valve. The latter may be operated from the I.F. output when the television signal has negative modulation. An additional phase reversing stage is necessary to convert the pulse output to a positive direction.

16.9.3. Frequency Separation of the Frame and Line Pulses. The frame and line synchronizing pulses must be separated from each other, and interaction between the scanning generators (particularly from line to frame) must be prevented, otherwise erratic interlacing occurs. Normal filter circuits do not provide

sufficient discrimination without severe mutilation of the pulse wave shape. Attenuation and phase distortion adversely affect the higher harmonic pulse components which control the slope of its leading edge. The latter should be as sharp as possible or synchronism becomes dependent on pulse amplitude and is liable to be affected by interference superimposed on the leading edge. The most satisfactory form of filter for selecting the line pulse has proved to be the differentiator type. This may consist either of a high resistance and an inductance, or a capacitance and a low resistance to which is applied a voltage of synchronizing pulse shape, the output voltage in the first case being that across the reactance and in the second that across the low resistance. The first is provided by a tetrode valve, which has an inductance in its anode circuit, and to the input of which is applied the rectangular synchronizing pulses. The tetrode, owing to its high slope resistance, produces an anode current wave identical in shape to the input voltage wave, and there appears across the inductance a voltage, the shape of which is a differential of the current wave $\left(E_L = L\frac{dI_a}{dt}\right)$. The actual voltage wave shape depends on the resistance component of the inductance, and if this is small it is a sharp pulse of much shorter duration than the rectangular synchronizing pulse, as shown in Fig. 16.18*a*. Increased resistance in the inductance causes a pulse of longer duration, slower rate of rise and smaller amplitude. There is a similar pulse in the opposite direction on the downstroke of the synchronizing pulse, but this has no effect on the scanning generator, being in the wrong direction for triggering it. For the second differentiator circuit the reactance of the capacitance at the fundamental frequency of the synchronizing pulse must be large compared with the output and generator resistance. Hence the valve supplying the voltage of synchronizing pulse shape must be a triode. The voltage appearing across the output resistance is a function of circulating current, which, if the total resistance is low, is a function of the differential of the applied voltage. These differentiator filters may also be considered from the angle of circuits having a frequency response proportional to frequency; the fundamental and lower harmonic components of the pulse have reduced amplification compared with the higher harmonics, thus tending to sharpen the leading edge of the pulse and reduce its duration. The inductance differentiator is more commonly used, and the line synchronizing output pulse may be obtained from a secondary coil connected to it. Phase reversal is then possible without an extra

valve stage. Line synchronizing is carried on during the frame synchronizing pulse in order that the first few visible lines at the beginning of a new frame may not be jumbled while the line scanning generator is being pulled into synchronism.

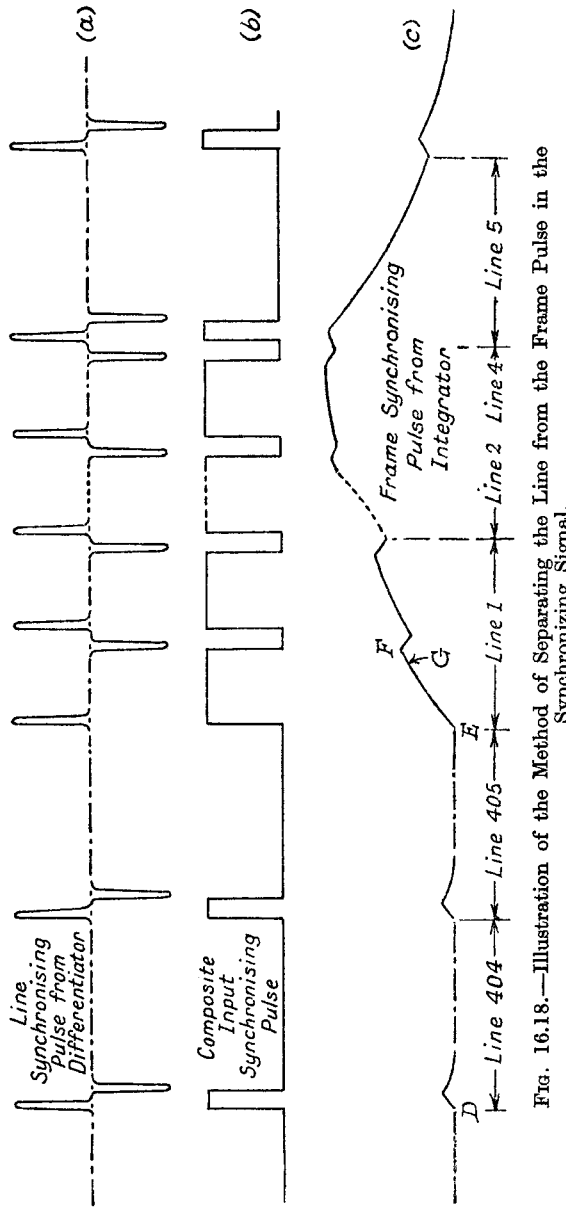

FIG. 16.18.—Illustration of the Method of Separating the Line from the Frame Pulse in the Synchronizing Signal.

The frame synchronizing pulse is separated from the line by using an integrator circuit, consisting of a parallel combination of resistance and capacitance, to which is applied through a high resistance a voltage of synchronizing pulse shape. The frame output voltage is taken across the RC combination, and is an integral function $\left(E_c = \int \frac{Idt}{C}\right)$ of the current through the capacitance. The frequency response of this circuit is the opposite of the differentiator, attenuation of the higher harmonic components of the pulse occurring. The voltage wave shape across the integrator circuit is shown beneath the synchronizing input wave shape in Fig. 16.18c. The line pulses produce a voltage across the integrator, but it is small because the line pulse duration is only 10% of the total line time and is insufficient to synchronize the frame scanning generator. The frame pulse of much longer duration (40% of the line time) produces a large voltage component as shown by the section EF in Fig. 16.18c. Synchronism should take place on the first up-stroke at about the point G.

A circuit diagram of a typical frequency separator is shown in Fig. 16.19. The inductance L_1 forms the differentiator for the line

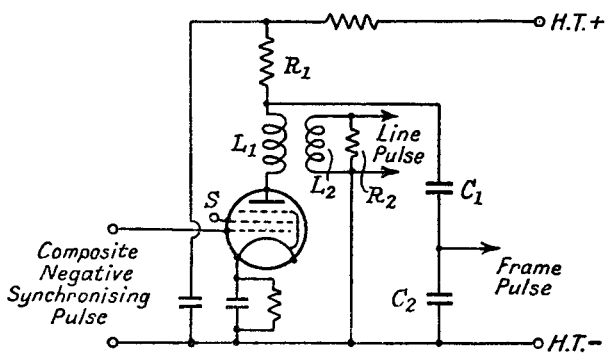

FIG. 16.19.—A Circuit for Separating the Line from the Frame Pulse in the Synchronizing Signal.

synchronizing pulses, which are taken from the secondary coil L_2 to the line scanning generator. A comparatively low resistance R_2 (3,000 to 5,000 Ω) is connected across L_2 to prevent damped oscillations occurring due to resonance of L_1 or L_2 with the stray capacitance. The frame integrator circuit is provided by R_1 (10,000 Ω) in parallel with C_1 and C_2 in series. C_1 is about one-tenth of C_2 (0·025 μF) and there is therefore a reduction in pulse amplitude. The chief advantage of this capacitance divider is that

C_2 can also be the grid blocking capacitor of a blocking oscillator acting as the frame scanning generator : a negative direction of synchronizing pulse is required at the input to the valve in order to give the required positive direction to the frame output pulse. The transformer connection between L_1 and L_2 allows phase reversal of the line synchronizing pulse, so that either a positive or negative input pulse could be used if only line synchronizing has to be considered.

Another form [28] of frequency separator is illustrated in Fig. 16.20. The valve, a pentode, is supplied from the output of a V.F. amplifier giving a negative vision signal and positive synchronizing pulse, and it operates as a leaky-grid detector to separate vision from synchronizing signals in the same manner as the circuit of Fig. 16.17c. The

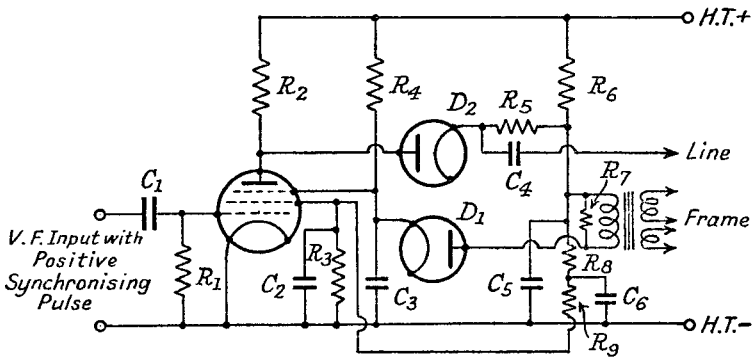

FIG. 16.20.—A Circuit for Separating the Line from the Frame Pulse in the Synchronizing Signal.

line and frame pulses at the output of the valve are therefore in a negative direction and they are taken from two separate electrodes, the anode and suppressor grid respectively ; hence the possibility of interaction between line and frame scanning generators is almost negligible.

The suppressor grid external resistance R_4 (0·25 MΩ) is high, and this produces a saturated suppressor grid current-input grid voltage characteristic with a change from cut-off to the saturated current condition for 0·75 to 1 volts change of grid bias. Frame pulse amplitude is therefore limited in a positive as well as negative current direction. The resistance R_4 and capacitance C_3 (0·0003 μF) form the integrator circuit, and the voltage pulses due to the line synchronizing (see section *DE* of the frame voltage integrated wave in Fig. 16.18c) are removed from the frame pulse by the biased diode

separator D_1, the anode of which is slightly negative with respect to the cathode in the intervals between frame synchronizing pulses. Phase reversal of the frame output signal is obtained by the transformer connection to the scanning generator coils. The line output pulse is not differentiated but appears in almost the original rectangular form across the anode load resistance R_3, which has a much lower value (5,000 Ω) than the suppressor grid resistance R_4, in order to prevent attenuation of the higher harmonic components. A diode D_2, connected in the opposite way to D_1, acts as an amplitude limiter. As the line pulse amplitude is increasing, the anode voltage is decreasing and the voltage on the anode of diode D_2 eventually falls below that of the cathode, causing the diode current in the output resistance R_5 (5,000 Ω) to become zero. Any increase in line amplitude produces no further change of voltage across R_5. The line synchronizing pulse is in a negative direction and the equivalent of a phase reversal is achieved by injecting it into the cathode instead of the grid circuit of the scanning generator. Component values for this type of amplitude separator are as follows :

Component	C_1	C_2	C_3	C_4	C_5	C_6
Value .	0·001 μF	2 μF(elec.)	0·0003 μF	0·1 μF	0·1 μF	2 μF(elec.)
Component	R_1	R_2	R_3	R_4		R_5
Value .	5MΩ	5,000 Ω	15,000 Ω	0·25 MΩ		5,000Ω
Component	R_6	R_7	R_8	R_9		
Value .	5,000 Ω	10,000 Ω	5,000 Ω	70,000 Ω		

The H.T. voltage is between 300 and 350 volts.

16.10. The Scanning Generator.

16.10.1. Introduction. The voltage or current needed to produce the electric or magnetic field for deflecting the C.R. tube beam is usually obtained from an amplifier to which is applied a voltage from a scanning generator. The shape of the output voltage required from the latter depends on the method of deflection employed ; if it is electrostatic, by voltages of saw-tooth shape applied to deflector plates mutually perpendicular inside the C.R. tube, a voltage of saw-tooth shape is required from the scanning generator. On the other hand, electromagnetic deflection, by a current of saw-tooth shape in coils mutually perpendicular outside the C.R. tube, requires from the scanning generator an output voltage of pulse form or a combination of pulse and saw-tooth shape (see Section 16.11.1). The most important features required of the scanning generator are : (1) the frequency and amplitude of its

output voltage should be stable (little affected by supply voltage and temperature changes) and yet susceptible to manual control, (2) synchronism should be easy to establish and (3) the output wave shape should conform to that required by the deflection amplifier (in the case of electro-static deflection the saw-tooth output voltage should be linear, i.e., its instantaneous amplitude should be proportional to time). The scanning generator normally consists of a resistance-capacitance charge circuit, across which the saw-tooth voltage is developed, and a device for periodically discharging or charging the capacitance. The pulse-shaped voltage may be obtained from the discharge current of the capacitance or from some part of the discharge oscillator circuit. The discharge device may be a gas-filled relay valve, a multivibrator (relaxation oscillator), or a blocking oscillator.

16.10.2. The Gas-Filled Relay Valve Scanning Generator. The gas-filled relay valve is not now used to any great extent in television scanning generators because it is more erratic in performance—free running frequency and amplitude are affected by gas pressure, which is a function of temperature—has a shorter life and is more costly than the high vacuum valve multivibrator or blocking

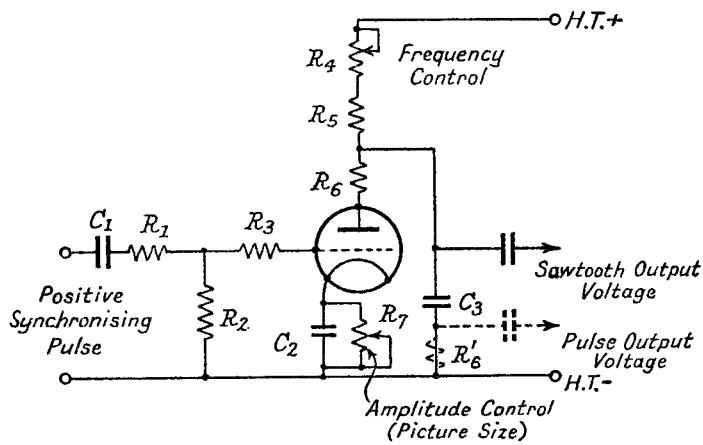

FIG. 16.21.—The Circuit for a Gas-Filled Valve Scanning Generator.

oscillator. Fig. 16.21 shows a circuit suitable for the gas-filled valve. The charge circuit consists of two resistances, R_4 and R_5, 2 MΩ and 0·5 MΩ respectively, and the capacitance C_3. R_4 is variable, providing means of controlling the rate of charge of C_3, and hence the frequency of the output voltage. The value of C_3 is about 0·25 μF and 0·0005 μF respectively for the frame and line frequencies. The

voltage-time curve is exponential, but an almost linear saw-tooth shape can be obtained by having a discharge voltage of 10% or less of the H.T. voltage applied to the charge circuit. A characteristic of the gas-filled valve is that as soon as the gas is ionized it becomes practically a short circuit across C_3, and to prevent destruction of the cathode the maximum discharge current must be limited by including R_6 in the discharge circuit. The anode voltage at which the gas ionizes—it is known as the striking voltage—depends on the grid bias voltage, and it is increased by increasing the negative bias. Once ionization has taken place the grid is surrounded by a sheath of positive ions (gas atoms with a deficiency of electrons), and it has no further control. The positive ions cause grid current to flow, and to prevent overheating of the grid R_3 (20,000 Ω) is inserted as a grid current limiter. The valve continues to take anode current until the anode voltage falls below the ionizing potential of the gas (approximately 15 volts for mercury vapour and argon), when current ceases. This voltage, known as the extinction voltage, should be as low as possible because it subtracts from the " linear " part of the exponential curve and reduces the maximum permissible saw-tooth amplitude. When conduction ceases, the grid loses its positive ion sheath and takes full control, preventing anode current until the striking voltage is once again reached. The ratio of the change in striking voltage to change of grid voltage producing it is known as the control ratio and is generally about 20. The anode current limiting resistance R_6 has a value from 100 to 500 Ω; it must not be increased unduly, otherwise the time of discharge (the flyback time) is prolonged and the output amplitude reduced by the voltage drop across R_6. R_6 may be included between C_3 and earth as shown dotted in Fig. 16.21, when a pulse voltage (developed across R_6') or a combination of pulse and saw-tooth voltage (developed across C_3 and R_6') is required for the input to the deflection amplifier. Control of output voltage amplitude is achieved by variation of the cathode bias provided by R_7 (5,000 Ω variable), which is paralleled by C_2 (25 μF). Frequency is also varied, but R_7 is primarily an amplitude control, increase of R_7 increasing amplitude. The D.C. current component of the deflection amplifier can with advantage be diverted through R_7 so as to give a more constant biasing action. R_1 and R_2 are adjusted to suit synchronizing input requirements. The larger R_1 is made the less likelihood is there of feedback from one scanning generator to the other through the synchronizing separator stage.

16.10.3. The Multivibrator Scanning Generator. More stable operation is obtained from a high vacuum discharge device, and television scanning generators are almost entirely confined to the multivibrator or the blocking oscillator type of discharge unit. The chief advantage of the multivibrator is that, besides the valves, only resistance and capacitance elements are involved in the circuit. On the other hand, the output voltage wave shape is more easily controlled in the blocking oscillator, which does, however, require a more complicated and costly circuit because of the transformer oscillatory circuit. The absence of inductance (apart from that of the leads) gives the multivibrator low inertia and makes it susceptible to quite small synchronizing voltages (of the order of 0·1 volts). This confers disadvantages as well as advantages, and special care is needed in layout in order to prevent electrostatic pick-up of

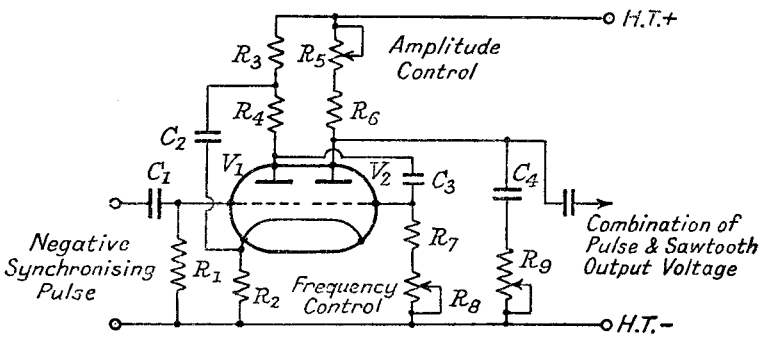

FIG. 16.22.—A Multivibrator Scanning Generator.

unwanted impulses and interaction between line and frame generators, both of which tend to cause loss of synchronism. The blocking oscillator requires about 5 volts for synchronizing and is less affected by undesired impulses. An example of the multivibrator scanning generator is given in Fig. 16.22. Two triode valves (V_1 and V_2) are used with a resistance in the common cathode circuit as the coupling unit. The second valve V_2 acts as the discharge device across the capacitance C_4 of the (R_5 and R_6) C_4 charge circuit. The action of the multivibrator is as follows: when the H.T. is initially applied to the circuit the anode voltage of V_1 rises more rapidly than that of V_2 because the time constant of the decoupling circuit R_3C_2 is smaller than the time constant of the anode circuit of V_2. A bias voltage is established across R_2, and

this prevents the flow of anode current in V_2 until the anode voltage reaches a certain value. As soon as V_2 starts to take current, the bias voltage across R_2 is increased and the anode current of V_1 falls, thus causing its anode voltage to rise. A positive voltage pulse is therefore transmitted through C_3 to the grid of V_2, and this further increases the current taken by V_2. The action is cumulative and leads to a rapid discharge of C_4. The valves return to the condition obtaining initially because the falling anode voltage on V_2 reduces the rate of rise of anode current and eventually reverses it, causing the bias voltage across R_2 to be reduced, the anode current of V_1 to be increased, its anode voltage to be reduced and a negative voltage pulse to be applied to V_2. The action is again cumulative and V_2 rapidly becomes non-conductive. Control of the multivibrator frequency within the limits required of a television scanning generator is achieved by varying the time constant of the grid circuit of V_2 (resistance R_8). Amplitude control is provided by varying the H.T. voltage applied to V_2, or the charging resistance R_5; since discharge results from a decrease in the anode current of V_1, a negative synchronizing pulse is required at the grid of this valve. Typical values for the circuit constants of a multivibrator scanning generator for frame and line are:

Component . .	R_2	R_3	R_4	R_5
Frame . . .	500 Ω	50,000 Ω	100,000 Ω	2 MΩ
Line . . .	500 Ω	50,000 Ω	50,000 Ω	2 MΩ

Component . .	R_6	R_7	R_8	R_9
Frame . . .	0·5 MΩ	0·5 MΩ	1 MΩ	5,000 Ω
Line . . .	0·5 MΩ	25,000 Ω	50,000 Ω	10,000 Ω

Component . .	C_1	C_2	C_3	C_4
Frame . . .	1 μF	2 μF	0·01 μF	0·1 μF
Line . . .	0·1 μF	0·1 μF	0·001 μF	0·0005 μF

A saw-tooth, pulse or combination of these voltages can be obtained at the output. When magnetic deflection is employed, R_9 is generally made variable in order to allow adjustment of the deflecting current for the nearest approach to linearity of deflection. The decoupling capacitance C_2 for the anode circuit of the first valve can be taken to H.T. negative, but the cathode connection [11] shown in Fig. 16.22 gives a more satisfactory performance because it prevents the anode current degenerative feedback caused when the A.C. component of the anode current of V_1 is allowed to flow through R_2.

16.10.4. The Blocking Oscillator Scanning Generator. Any oscillator which derives its bias by grid current flowing in a resistance-capacitance combination, the time constant of which is much greater than the period of the normal oscillation, can be made to function as a blocking or squegger oscillator if very tight coupling is employed between the oscillator coils. The very large grid current pulse, caused by overcoupling, charges the grid bias capacitance to a negative voltage (with reference to the grid electrode) considerably greater than that required to cut off the anode current of the oscillator. Oscillation, therefore, ceases and cannot begin again until the capacitance has discharged through the grid leak resistance to a voltage low enough to permit anode current to flow. The cycle of operations, consisting of oscillation followed by a quiescent period, is then repeated. The length of time during which the valve anode current is cut off depends on the time constant of the grid self-biasing circuit and the degree of coupling, the greater either of these the longer is the quiescent period. When oscillation commences there may be one or a number of oscillation cycles, the actual number depending on the damping of the tuned circuit and its L/C ratio, a large L/C ratio and heavy damping tending to a single cycle of oscillation ; damping must not be made too large, otherwise it may prevent the blocked condition being realized. Single pulse oscillation is desired in the blocking oscillator scanning generator and the highest possible L/C ratio is therefore required. Generally no tuning capacitance is employed other than that due to stray capacitance. The important advantages of this type of oscillator are that (1) the blocking frequency is relatively stable and only slightly affected by supply and temperature variations, (2) synchronism is easily maintained by a positive synchronizing voltage applied to the grid circuit, (3) pulse and saw-tooth voltages are generated and (4) the discharge or flyback time can be controlled by variation of the normal oscillation frequency of the tuned circuit.

An example of the blocking oscillator is shown in Fig. 16.23*a*, and the shapes of the voltage waves occurring across the different parts of the circuit are shown in Fig. 16.23*b*. The pentode valve in Fig. 16.23*a* performs two rôles : the control and screen grids act as the grid and anode of a blocking oscillator, and the anode-cathode circuit as the discharge device for the capacitance C_3, which is charged from the H.T. supply through the resistances R_3 and R_4. The anode current is zero during the quiescent period of the oscillator and only flows when the positive oscillation pulse of the blocking

oscillator part renders the whole valve conductive. A saw-tooth voltage is developed across C_3 or a combination of pulse and saw-tooth if R_5 is included. The synchronizing input voltage is applied through a coupling coil L_3 connected to the oscillator coils. Fig. 16.23*b* shows the impulse nature of the voltages E_{L_1} and E_{L_2} across the grid and screen coils respectively—these voltages are, of course, 180° out-of-phase with each other. A large value of tuning capacitance produces the lightly damped train of oscillations shown by the dotted E_{L_1} curve and may result in a second current pulse in the anode circuit, causing a second saw-tooth voltage as shown by dotted E_{C_2} curve in the figure. Linearity of saw-tooth voltage across C_3 requires the H.T. voltage to be at least ten times the amplitude (peak-to-peak) of the saw-tooth output voltage. Changing the rate of charge of C_3 by varying R_3 controls the amplitude of the saw-tooth, frequency being governed entirely by the control

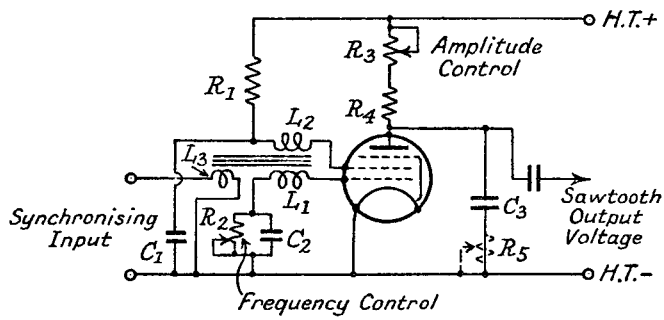

FIG. 16.23*a*.—A Blocking Oscillator Scanning Generator.

grid circuit time constant, i.e., by variation of R_2. It is seen from Fig. 16.23*b* that the exponential discharge curve of capacitance C_2 approximates to the saw-tooth voltage shape, and if this shape of output voltage is required the pentode discharge section and the charge circuit can be omitted, the output voltage being taken across C_2. The voltage wave shape will not be linear as long as the discharge voltage for C_2 is zero, but the resistance R_2 can be returned to H.T. positive instead of to zero with consequent improvement in linearity. The effect of connecting R_2 to a positive voltage E is illustrated by the dashed curve on Fig. 16.23*b*, it is equivalent to increasing the H.T. voltage on the anode charge circuit of a gas-filled valve generator.

Suitable component values for the circuit of Fig. 16.23*a* are :

Component	R_1	R_2	R_3	R_4
Frame . . .	20,000 Ω	0·25 MΩ (var.)	2 MΩ (var.)	0·5 MΩ
Line . . .	20,000 Ω	0·25 MΩ (var.)	2 MΩ (var.)	0·5 MΩ

Component	R_5	C_1	C_2	C_3
Frame . . .	5,000 Ω	2 μF	0·1 μF	0·1 μF
Line . . .	10,000 Ω	0·1 μF	0·0005 μF	0·0005 μF

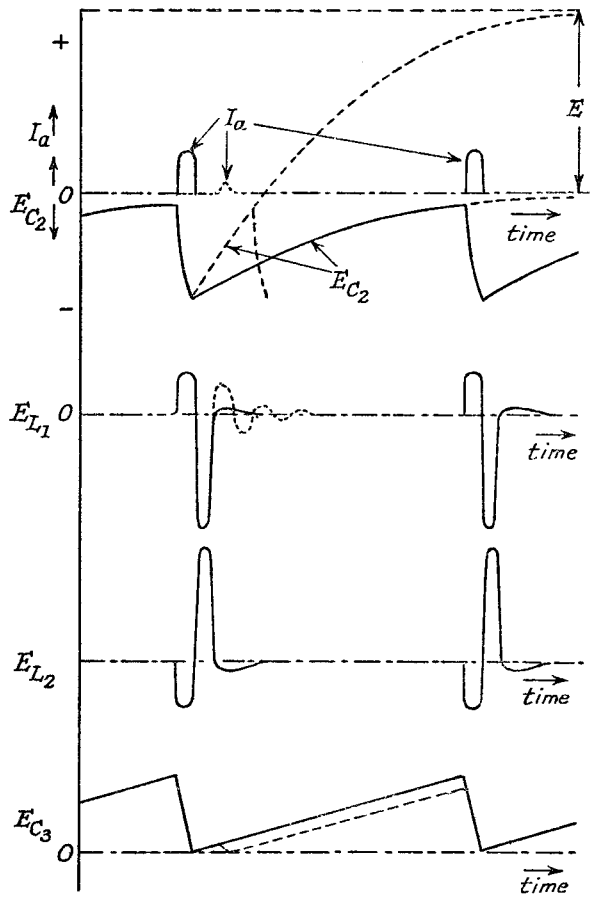

FIG. 16.23*b*.—Voltage and Current Waveforms in a Blocking Oscillator.

An alternative form [28] of blocking oscillator suitable as a line scanning generator producing a pulse output voltage is illustrated in Fig. 16.24. Synchronizing is effected by a negative pulse applied to the cathode circuit. The free frequency is controlled by variation

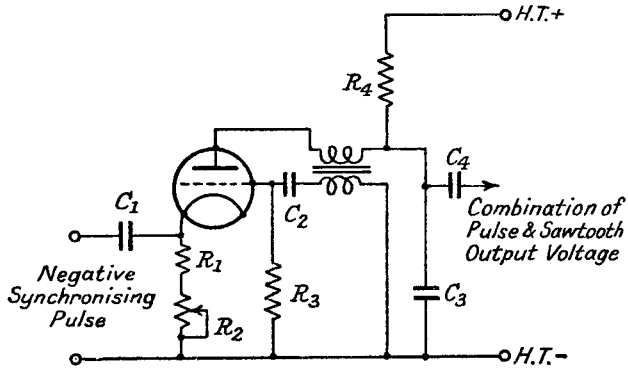

FIG. 16.24.—An Alternative Form of Blocking Oscillator Scanning Generator suitable for the Frame Scan.

of the resistance R_2 in the cathode circuit. Component values are as follows :

$R_1 = 1{,}000\ \Omega$, $R_2 = 3{,}000\ \Omega$, $R_3 = 0{\cdot}15\ \text{M}\Omega$, $R_4 = 0{\cdot}25\ \text{M}\Omega$, $C_1 = 0{\cdot}1\ \mu\text{F}$, $C_2 = 0{\cdot}0005\ \mu\text{F}$, $C_3 = 0{\cdot}002\ \mu\text{F}$, $C_4 = 0{\cdot}01\ \mu\text{F}$.

The resonant frequency of the inductance of the anode or grid coil, whichever is the larger, of the coupling transformer, and the stray capacitance determines the flyback time of the output voltage wave shape, and it should be not less than ten times the fundamental saw-tooth frequency. The frequency must not be made too high otherwise the discharging capability of the generator is reduced, because the maximum current taken by a high vacuum valve is very much less than that of a gas-filled valve. A resonant frequency of about 1,000 c.p.s. is suitable for the frame scanning generator, and an intervalve or output transformer of 1 to 2 turns ratio will usually fulfil this rôle satisfactorily. The line scanning generator requires a resonant frequency of 150 to 200 kc/s.

16.11. The Deflecting Circuits and Amplifiers.

16.11.1. Introduction. Deflection of the C.R. tube beam may be accomplished electrostatically or electromagnetically. Whilst both methods have their advantages and disadvantages, magnetic deflection is generally to be preferred. The chief point in favour of electrostatic deflection is that it deflects not only the electrons, but also the negative ions (atoms of residual gas to which electrons have attached themselves) contained in the C.R. tube beam. The negative ions have much greater mass than the electrons, and if they are allowed continuously to bombard a small area of the screen they destroy its luminosity. A magnetic deflecting field has much less influence on the ions than on the electrons, so that the ionic beam

tends to remain at the centre of the screen and cause an " ionic burn " or dark spot. The disadvantages of electrostatic deflection are that a long C.R. tube is required, comparatively high deflecting voltages (about 850 volts peak-to-peak on each plate) are needed, and there is distortion of the spot at the edges of the picture due to the non-uniform electric lens action between the deflector plates. A long C.R. tube means a more bulky cabinet and increased tube and cabinet cost. High deflecting voltages call for a high voltage H.T. supply with valves and capacitance components suitable for high voltage operation. Push-pull deflection is essential to prevent trapezium distortion. A further disadvantage of electrostatic deflection is that the coupling capacitances from the deflection amplifier to the plates must be capable of withstanding about 7,000 volts because the voltage between plates and earth is the same as from the C.R. tube anode to earth.

The advantages of magnetic deflection are reduced size of C.R. tube, beam distortion or defocusing during deflection is small, and the deflection amplifier can be operated from a low voltage supply (300 volts). The disadvantages of magnetic deflection are the negative ion burn, the higher deflecting power required, and the high induced voltage caused by the flyback of the line deflection current.

For electrostatic deflection a saw-tooth voltage must be applied to the deflector plates of the C.R. tube; electromagnetic deflection requires a saw-tooth current through the deflector coils. The actual shape of the input voltage to the magnetic deflection amplifier depends on the slope resistance of the amplifier valve. If it is a tetrode or pentode of high R_a, the input voltage shape should be saw-tooth because the current wave shape is independent of the external load. On the other hand, the input voltage shape to

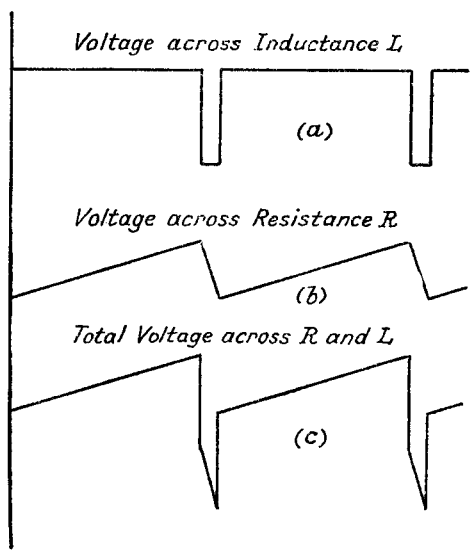

FIG. 16.25.—The Voltage Waveform required across a Coil to give a Saw-tooth Current Waveform through the Coil.

a triode of low R_a needs to be a combination of pulse and saw-tooth shape. The actual voltage required across the inductive part, as distinct from the whole coil, including the resistive component, is of rectangular pulse shape as shown in Fig. 16.25*a*. Integration of this shape $\left(I = \frac{\int E}{L} dt\right)$ gives a saw-tooth current shape through the coil, and this saw-tooth current produces a saw-tooth voltage across the resistance component of the coil and the valve slope resistance (Figs. 16.25*b*). The input voltage shape must be equivalent to the sum of these two as shown by Fig. 16.25*c*, and it is obtained by adjusting a resistance in series with the charge capacitance as described in Section 16.10.

16.11.2. Electrostatic Deflection. The distance through which the beam of a C.R. tube is deflected by a voltage applied to a flat plate parallel to the beam is directly proportional to the length of the plate, its distance from the screen and the deflecting voltage ; it is inversely proportional to the distance from the plate to the beam axis and to the voltage between the cathode and last anode of the C.R. tube.

Deflection of the C.R. tube beam by a saw-tooth voltage applied to one deflecting plate results in a variation of the mean potential difference between the last anode and the deflecting plate. This varies the speed of the electrons in the beam, causing them to travel faster when the deflecting voltage is increasing positively and to travel slower when the latter is decreasing negatively. When the electrons are travelling faster, they are under the influence of a deflecting field from a plate at right angles to the first plate for a shorter time, and the beam deflection due to the second plate voltage is therefore becoming less when the first plate voltage is rising positively. This results in trapezium distortion of the picture. It can be overcome by using push-pull deflection to both pairs of plates ; the mean voltage between the plates and last anode is zero because a positive voltage on one is counterbalanced by a negative on the other.

An example of a push-pull deflection amplifier is shown in Fig. 16.26. For a satisfactory linear saw-tooth with rapid flyback, the amplifiers should have small attenuation and phase distortion up to at least the 10th harmonic of the saw-tooth fundamental frequency ; this is adequate for a 10% flyback time, but there is slight distortion of the last 10% of the forward stroke. If the frequency range is extended to the 15th harmonic, the saw-tooth voltage is practically linear. Reversal of phase of the

input voltage for the second valve V_2 is obtained from the output voltage of V_1, stepped down in the frame amplifier by the potential divider action of R_6 and R_7. The ratio $\frac{R_7}{R_6+R_7}$ is approximately equal to the stage gain of V_1. A resistance potential divider is not satisfactory for the line deflection amplifier because the input capacitance of V_2 (including the Miller effect of anode-grid capacitance) has a comparatively low reactance. R_6 is therefore replaced by a variable capacitance, which forms a potential divider with the input capacitance of V_2. R_7 is fixed and has a value much greater than the grid input reactance of V_2. Other possible methods of achieving phase reversal are discussed in Section 10.8.2.

In the frame deflecting amplifier C_3 and C_5 are often omitted, because unless they are made very large they cause attenuation

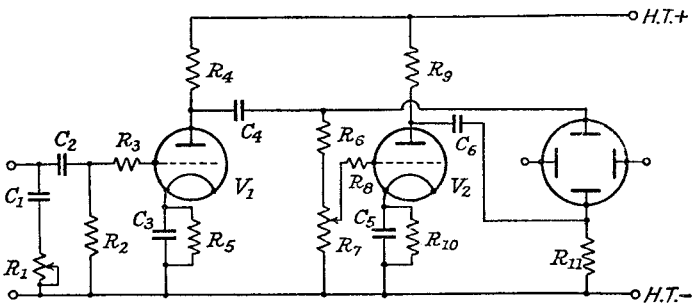

FIG. 16.26.—A Push-Pull Amplifier for Electrostatic Deflection of the Cathode Ray Beam.

and phase distortion of the lower frequency components of the saw-tooth. A larger anode load resistance is permissible in the frame than in the line amplifier since the reactance of stray capacitance is much greater at the frame frequencies, and this helps to reduce the loss of amplification due to the unby-passed cathode bias resistances R_5 and R_{10}. If the valves V_1 and V_2 are accurately matched a common bias resistance can be employed and the degenerative cathode voltages then cancel each other. Some improvement in the wave shape (distorted by attenuation and phase shift of the higher frequency components due to stray capacitance) of the line deflecting voltage can be secured by applying a combination of saw-tooth and pulse input voltage. This is achieved by inserting the resistance R_1 in series with the charge capacitance C_1. Typical component values for the frame and line amplifier are listed on page 458.

Component	C_1	C_2	C_3	C_4	C_5	C_6
Frame .	0·5 μF	0·25 μF	0	0·1 μF	0	0·1 μF
Line .	0·003 μF	0·01 μF	0·1 μF	0·002 μF	0·1 μF	0·002 μF

All capacitances except C_3 and C_5 should be 1,000-volt working.

Component	R_1	R_2	R_3	R_4	R_5	R_6
Frame .	0	2 MΩ	500 Ω	0·2 MΩ	10,000 Ω	4 MΩ
Line . .	400 Ω	1 MΩ	500 Ω	0·1 MΩ	5,000 Ω	—

Component	R_7	R_8	R_9	R_{10}	R_{11}
Frame .	1 MΩ (var.)	500 Ω	0·2 MΩ	10,000	5 MΩ
Line . .	1 MΩ (fixed)	500 Ω	0·1 MΩ	5,000Ω	5 MΩ

In the line deflecting amplifier R_6 is replaced by a variable capacitance of 10 $\mu\mu$F, and a resistance of 5 MΩ is included from the top deflecting plate to earth. The H.T. voltage required is 1,200 to 1,500 volts.

Step-up transformer coupling with a centre-tapped secondary may be used instead of push-pull R.C. coupling. The important point to observe is that the primary reactance of the frame transformer must be large compared with the valve slope resistance, in order that reactance variation with frequency shall have little effect. Leakage inductance and stray capacitance are the chief factors in the line deflection transformer, and primary to secondary coupling must be high and stray capacitance low.

16.11.3. Electromagnetic Deflection. Magnetic deflection of the C.R. tube beam is directly proportional to the length (in the beam axis direction) of the magnetic field, the distance from the coil to the screen and the flux density of the field; it is inversely proportional to the square root of the voltage between the cathode and last anode of the C.R. tube. Two pairs of coils are used at right angles to each other on the neck of the tube. The coils, of saddle shape, are surrounded by a magnetic yoke of C type laminations as shown in Fig. 16.27. The saddle shape of coil gives a field of maximum intensity with uniform distribution at right angles to the coil. A non-uniform field leads to "barrel" or "pincushion" distortion [20] of the picture with convex or concave edges. The electron travels in a direction perpendicular to the magnetic field, and either convex or concave field shape is obtained according to the way in which the magnetic lines of force are bent: step-down transformer coupling is employed from the valve to the coils as this prevents permanent deflection of the beam by the valve anode current, and also allows the inductance of the line deflecting coil to be smaller, with consequent reduction of the induced voltage on the flyback. It is easier to insulate the primary of a transformer

against high voltages than a deflecting coil. A low inductance deflecting coil of larger gauge wire is also stronger mechanically than a coil of many turns of fine wire. For maximum deflection the coil should be as long as possible, but it must not be made so long that the beam strikes the neck of the C.R. tube before reaching the full extent of its travel on the screen. Beam cut-off is overcome by reducing the coil length from the cathode end of the tube, if the other end of the coil is touching the flare. An average value for coil length is $1\frac{3}{4}$ ins. The line and frame coils, mounted one above the other, are surrounded by a yoke of magnetic material which concentrates and makes the field more uniform. The yoke, which may be circular [17] or square in section, consists of laminations held in a frame (this is omitted in Fig. 16.27). An air gap of $\frac{1}{8}$ in. to $\frac{1}{4}$ in. is often included between the two halves of a C-type core.

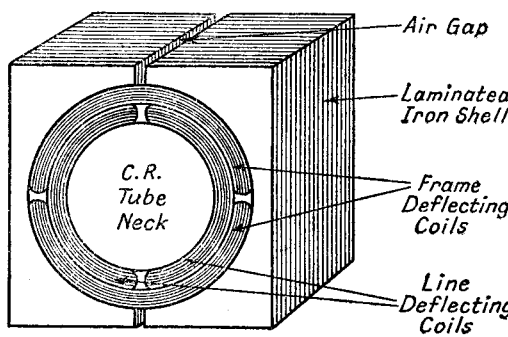

FIG. 16.27.—Coil Shape for Electromagnetic Deflection of the Cathode Ray Beam.

Each coil is wound on a special former [22] to give the saddle shape. Generally the separate layers are rectangular in shape and the turns decrease in size from the outside to the inside of the layer. The number of turns in each of the two line deflecting coils is of the order of 100 to 150 and in each of the frame coils 500 to 800. Adjacent ends of the line and frame deflecting coils are separated by about $\frac{1}{4}$ in.

The deflection amplifier may have either a tetrode or a triode valve. The tetrode has the advantage of requiring a much smaller input voltage for a given output current change, but the triode gives less distortion; however, distortion from the tetrode can be reduced by applying negative feedback. A triode valve (or tetrode with screen and anode joined) is often used in the frame amplifier, and a tetrode in the line amplifier. A typical line deflection amplifier is shown in Fig. 16.28. A combination of saw-tooth and pulse input

voltage is required to produce a saw-tooth current through the deflecting coils. The valve is a high g_m tetrode having a normal D.C. dissipative power at the anode of 15 to 20 watts. A resistance R_2 (1,000 Ω) is included close to the grid pin of the valve to act as a suppressor of parasitic oscillations, to which high g_m valves are liable. The total H.T. voltage is about 320 volts, but the screen voltage is limited to a maximum of 250 volts by the resistance R_3 (5,000 Ω); the decoupling capacitance C_3 is 0·1 μF. Decoupling of the amplifier from the H.T. supply is provided by R_4 (250 Ω variable) and R_5 (500 Ω) in series together with the capacitance C_2 (16 μF). The variable resistance R_4 varies the screen and anode voltage of the tetrode, and so controls the amplitude of the line deflecting current, i.e., it varies the width of the picture. The self-bias circuit consists of R_6 (about 150 Ω) and C_4 (25 μF). The

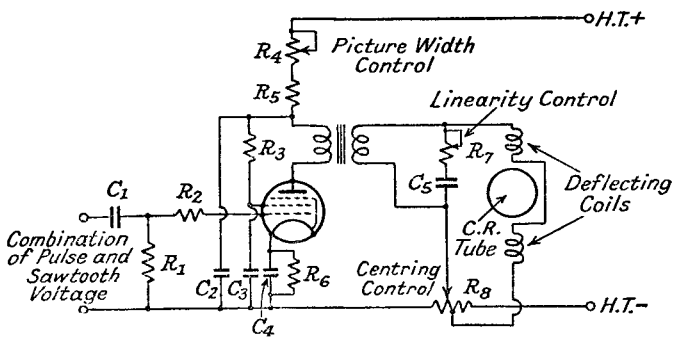

FIG. 16.28.—A Typical Line Deflection Amplifier for Electromagnetic Deflection of the Cathode Ray Beam.

output transformer has a step-down ratio of about 8 to 1, the primary inductance should be about ten times the reflected inductance due to the deflecting coils, in order that transformer volt-ampere efficiency may be high. Referred to the secondary side, this means that the ratio of secondary to deflecting coil inductance should be 10 to 1. Considerations of leakage inductance and winding capacitance (both are increased by using a large primary inductance, and cause loss of efficiency as well as distortion of the saw-tooth current) generally dictate a lower ratio, of the order of 5 to 1. Across the secondary is included a special circuit to limit the inverse voltage induced by the rapid change of current during the flyback period. The component values of this absorber circuit are $R_7 = 5{,}000\ \Omega$, $C_5 = 0{\cdot}005\ \mu$F. Part of R_7 may be variable in order to assist linearization of the saw-tooth current as it approaches

the flyback point. Centring of the picture can be achieved by means of the centre-tapped potential divider R_8 (20 Ω) in the main H.T. supply to the deflecting amplifier. It is not absolutely essential with magnetic focusing because the picture can be centred by movement of the focus coil.

The frame amplifier circuit may be similar to that shown in Fig. 16.28. Decoupling capacitances need to be much greater than those for the line amplifier, for example, C_2 should be about 32 μF, C_3 16 μF and C_4 100 μF. The C_5R_7 absorber circuit is no longer required since the rate of change of current on the flyback is much slower than for the line, and the inverse induced voltage is therefore very much less. To prevent excessive peak currents in the valve due to the reduced load reactance at the frame frequency, the frame deflecting coils have a higher inductance than the line (about fifty times as large) and a higher step-down ratio (12 to 1) is employed. A valve having a higher anode D.C. dissipative power is generally necessary to accommodate the higher peak currents due to the lower load reactance. A triode or tetrode with screen and anode joined together may be used, but this introduces only minor changes in circuit detail, e.g., R_3 and C_3 are no longer required.

16.12. Power Supplies and Focusing of the C.R. Tube.[33]

16.12.1. Introduction.[19] The H.T. supply to the vision receiver, scanning generators and deflection amplifier can be obtained from the same power unit. The latter needs no special comment since it has a comparatively low output voltage (about 400 volts across the reservoir capacitance), and its design follows the lines set out in Chapter 11. The rectifier and smoothing choke must be capable of handling a current of 150 to 200 mA, and great care must be exercised to ensure adequate smoothing and decoupling, because scanning generator and deflection amplifier current changes are large. These are liable to interact upon each other and the vision amplifier if decoupling is insufficient; furthermore, hum voltages in the H.T. supply tend to cause erratic interlacing.

The C.R. tube requires a high-voltage H.T. supply (5,000 volts), but the load current is small, being little more than that taken by the potential divider providing the various auxiliary anode voltages. Consequently a resistance-capacitance filter can be employed for smoothing purposes. The number of auxiliary anodes (other than the last) is governed by the type of focusing; electrostatic focusing generally needs two, whilst none is required with magnetic focusing.

Electrostatic focusing has the advantage that temperature

changes have negligible effect and hardly any adjustment is entailed after the initial setting. On the other hand, it concentrates negative ions as well as electrons, causing ion burn unless electrostatic deflection is used. Extra decoupling capacitances and resistances are needed in the potential divider supplying the auxiliary anodes. Centring is only possible by means of a shift potential on the deflecting plates or a shift current through the deflecting coils.

Magnetic focusing has the advantage of giving a much higher beam current with less negative ion concentration than electrostatic focusing, and a much brighter picture results. Another advantage is that movement of the focus coil controls the centring of the picture and obviates the necessity for shift voltages or currents. Its chief disadvantages are that the focus coil takes power and that focus tends to drift from the cold to normal running condition due to a change in coil resistance.

16.12.2. Electrostatic Focusing and the C.R. Tube Power Supply. An example of the C.R. tube power supply for an electrostatically focused tube is shown in Fig. 16.29. The A.C. supply voltage is obtained from a 4,000-volt (R.M.S.) secondary winding, and half-wave rectification is used because it is very suitable for

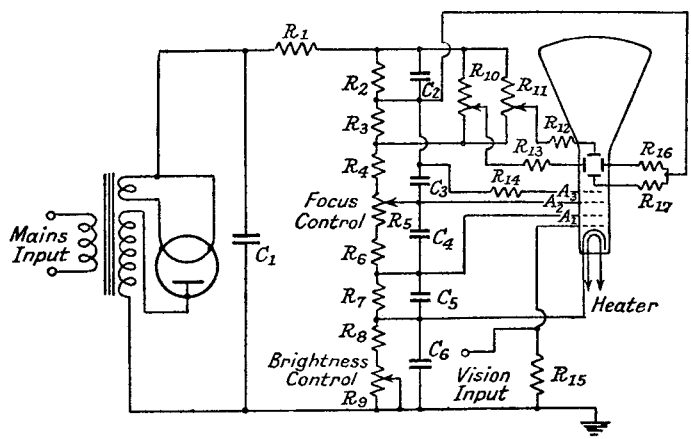

FIG. 16.29.—A Power Supply Circuit for a Cathode Ray Tube having Electrostatic Focusing and Deflection.

high voltage low current D.C. outputs. The anode of the rectifier is connected to one side of the secondary winding, and the cathode to the H.T. positive lead of the D.C. supply; hence the maximum voltage between the heater winding to earth is the peak A.C. voltage output of the high voltage secondary winding. If the cathode of

the rectifier is connected to the high-voltage winding, both heater winding and heater end of the high-voltage winding must be capable of withstanding nearly twice the peak A.C. voltage to earth, viz., 11,000 volts, because on the negative half-cycle the maximum voltage from heater winding to earth is the sum of the peak A.C. voltage across the high-voltage secondary and the D.C. voltage across the reservoir capacitance C_1. The C.R. tube has three anodes, A_1, A_2 and A_3, requiring approximately 400, 1,500 and 5,000 volts respectively to cathode. A_3 is connected to the junction of R_2 and R_3, across which are connected the shift potential dividers, R_{10} and R_{11}, for one of each pair of deflecting plates. The latter are connected to the push-pull deflection amplifier by capacitances, which must be capable of withstanding 7,000 volts. A resistance, R_{14} (0·1 MΩ), is inserted between A_3 and the supply to limit current in the event of a short circuit of A_3 to earth. R_5 controls the voltage applied to A_2 and provides focus adjustment. R_9 varies the cathode bias and so controls the average brightness of the picture. The vision input is applied between the C.R. tube grid and earth.

The values of the resistances and capacitances (the voltages in brackets indicate the required working values for the capacitances) in the potential divider for the anode voltages are listed below ; the former are calculated on the assumption that the C.R. tube electrode currents are negligible.

Component	R_1	R_2	R_3	R_4	R_5	R_6	R_7	R_8
Value (MΩ)	0·5	0·5	0·5	2	0·5 (var.)	0·25	0·25	0·01

Component	R_9	R_{10}	R_{11}	R_{12}	R_{13}	R_{14}	R_{16}	R_{17}
Value (MΩ)	0·1 (var.)	0·5 (var.)	0·5 (var.)	5	5	0·1	5	5

Component	C_1	C_2	C_3	C_4	C_5	C_6
Value (μF)	0·1 (7,000)	1 (500)	1 (2,500)	1 (1,500)	1 (500)	4 (250)

When wiring the high voltage power supply, leads should be well spaced from each other and earth, and high voltage cable should be used for the output leads to A_2, A_3 and the deflector plates. It is advisable to include a safety switch attached to the back of the receiver so that C_1 is automatically short-circuited when the back is removed for inspection purposes.

16.12.3. Magnetic Focusing and the C.R. Tube Power Supply.[21] The H.T. supply to the C.R. tube is greatly simplified by employing magnetic focusing. Only one anode (this may be provided by a graphite coating on the inside of the bulb) is required, or if two are used the first is at a low voltage (300 to 400 volts),

which can be obtained from the low voltage H.T. supply. A resistance shunt R_1 is shown across the reservoir capacitance C_1 in Fig. 16.30, as it provides cathode bias through R_2 and R_3 for the tube, and also discharges C_1 after the receiver has been switched off. R_1 has a value of about 10 MΩ, R_2 20,000 Ω and R_3 0·25 MΩ, C_1 is 0·1 μF (7,000-volt) and C_2 is 4 μF (250-volt). A safety resistance R_4 (0·1 MΩ) is inserted in series with the lead to the anode, which is formed by a conducting graphite coating inside the C.R. tube. Additional resistance-capacitance smoothing is not required, partly because the load current and the ripple voltage across C_1 are so small, and partly because hum voltages on the last anode have much less effect than on intermediate anodes. If the shunt resistance R_1 is not included, cathode bias can be derived from the low voltage H.T. supply. The vision input is applied across R_5.

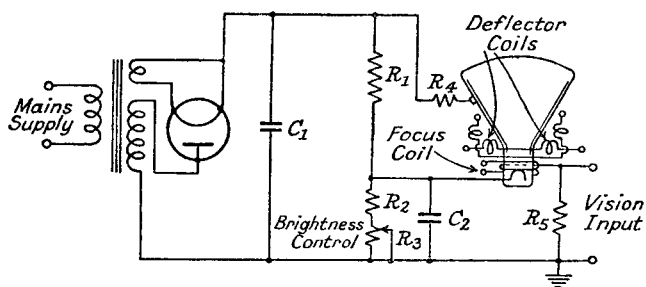

FIG. 16.30.—A Power Supply Circuit for a Cathode Ray Tube having Electromagnetic Focusing and Deflection.

Magnetic focusing may be provided by a permanent magnet with a variable shunt or by a coil wrapped round the tube so that its axis coincides with that of the beam. The former is seldom used because it is more costly and less easy to adjust. The focus coil may have a low resistance and be placed in series with the low voltage supply, or it may have a high resistance and be placed across it. The former is preferable because it is easier to construct, is more robust, and is less liable to current change from the cold to normal operating condition. The coil is connected in series with the H.T. supply to the scanning generators and deflection amplifiers; the current from the vision receiver should not be included because it varies when gain adjustments are made. It is shunted by a fixed and variable resistance in series, the latter providing focus control. A soft iron shell with an air gap normally encloses the coil so as to produce a uniform concentrated magnetic field; Fig. 16.31 is an example of the type of construction. The soft-iron shell, made in

two halves which slide over the coil as shown, has an external diameter of about 4 ins. and is about $1\frac{1}{2}$ ins. deep. The air-gap is 1 cm. (approximately 0·4 in.) long and about 600 ampere-turns are required for focusing. Centring of the picture can be achieved by

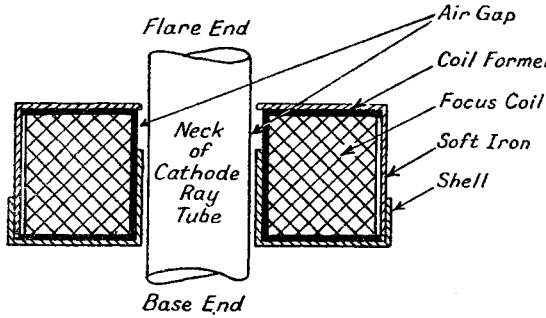

FIG. 16.31.—An Example of a Magnetic Focusing Coil.

altering the position of the coil, which may be mounted on gimbals and provided with adjusting and locking screws.

Magnetic fields from the mains transformer can affect C.R. tube and scanning generators, and the transformer must be located as far as possible from this part of the equipment, if necessary, being orientated so as to produce minimum field interference. For the same reason the flux density of the transformer core should not be allowed to exceed 50,000 lines per sq. in. Owing to the power supplied by the transformer and the rectifier units adequate ventilation is absolutely necessary. The actual voltage required of the high voltage secondary can be reduced by connecting its negative lead to the positive of the low voltage supply, cathode bias for the C.R. tube being obtained from the low voltage supply.

BIBLIOGRAPHY

1. A Study of Television Image Characteristics, Part II. E. W. Engstrom, *Proc. I.R.E.*, April 1935, p. 295.
2. Correction Circuits for Amplifiers. O. E. Keall, *Marconi Review*, May–June 1935, p. 15, Sept.–Oct. 1935, p. 9.
3. Synchronizing in Television. W. T. Cocking, *Wireless World*, Jan. 22nd, 1937, p. 74.
4. The Television Receiver. W. T. Cocking, *Wireless World*, May 14th, 1937, p. 475.
5. Television Aerials. H. B. Dent, *Wireless World*, May 28th, 1937, p. 506.
6. The Wireless World Television Receiver. W. T. Cocking, *Wireless World*, July 2nd, 1937, p. 2, to July 30th, 1937, p. 98.
7. Television Scanning and Synchronizing. P. D. Tyers, *Wireless World*, Aug. 6th, 1937, p. 115.

8. Some Notes on Video Amplifier Design. A. Preisman, *R.C.A. Review*, April 1938, p. 421.
9. Effect of the Receiving Antenna on Television Reception Fidelity. S. W. Seeley, *R.C.A. Review*, April 1938, p. 433.
10. Television Receivers. E. W. Engstrom and R. S. Holmes, *Electronics*, April 1938, p. 28, to Aug. 1938, p. 18.
11. Television Topics, *Wireless World*, April 21st, 1938, p. 354.
12. The Line Structure of Television Images. H. A. Wheeler and A. V. Loughren, *Proc. I.R.E.*, May 1938, p. 540.
13. Laboratory Television Receiver. D. Fink, *Electronics*, July 1938, p. 16, to Dec. 1938, p. 16.
14. Aerial Coupling Systems for Television. W. E. Benham, *Wireless Engineer*, Oct. 1938, p. 555.
15. The Marconi-E.M.I. Television System. Part I: The Transmitted Wave Form. A. D. Blumlein, *Journal I.E.E.*, Dec. 1938, p. 758.
16. Analysis and Design of Video Amplifiers. S. W. Seeley and C. N. Kimball, *R.C.A. Review*, Jan. 1939, p. 290.
17. Television Deflection Circuits. E. W. Engstrom and R. S. Holmes, *Electronics*, Jan. 1939, p. 19.
18. A Television Bibliography. *Electronics*, March 1939, p. 47.
19. Power for Television Receivers. E. W. Engstrom and R. S. Holmes, *Electronics*, April 1939, p. 22.
20. Line Deflectors. D. V. Ridgeway, *Wireless World*, June 15th, 1939, p. 550.
21. Magnetic Television Receiver. W. T. Cocking, *Wireless World*, June 29th, 1939, p. 602, to July 20th, 1939, p. 57.
22. Scanning Coil Construction. P. D. Tyres, *Wireless World*, Sept. 14th, p. 248, and Sept. 21st, 1939, p. 279.
23. Television Signal Frequency Circuit Considerations. G. Mountjoy, *R.C.A. Review*, Oct. 1939, p. 204.
24. Simplified Television I.F. Systems. G. Mountjoy, *R.C.A. Review*, Jan. 1940, p. 299.
25. Ultra-Short-Wave Aerial Systems. F. R. W. Strafford, *Wireless World*, April 1940, p. 224.
26. Video Output Systems. D. E. Foster and J. A. Rankin, *R.C.A. Review*, April 1941, p. 409.
27. Fluctuations in Space Charge Limited Currents at Moderately High Frequencies, Part V. W. A. Harris, *R.C.A. Review*, April 1941, p. 505.
28. The Design of Television Receiving Apparatus. B. J. Edwards, *Journal I.E.E.*, Part III, Sept. 1941, p. 191.
29. Coupling Circuits as Band-Pass Filters. E. K. Sandeman, *Wireless Engineer*, Sept., p. 361, Oct., p. 406, Nov., p. 450, Dec., p. 492, 1941.
30. Short Wave Dipole Aerials. N. Wells, *Wireless Engineer*, May 1943, p. 219.
31. *Transmission Circuits for Telephonic Communication*. K. S. Johnson. D. Van Nostrand. Text-book.
32. *Transmission Networks and Wave Filters*. T. E. Shea. D. Van Nostrand. Text-book.
33. *The Cathode Ray Tube*. G. Parr. Chapman & Hall. Text-book.
34. *Electron Optics in Television*. I. G. Maloff and D. W. Epstein. McGraw Hill. Text-book.
35. *Principles of Television Engineering*. D. Fink. McGraw Hill. Text-book.

APPENDIX 3A*

THÉVENIN'S THEOREM

A MOST important and useful theorem in the analysis of circuits is that enunciated by Thévenin. It states that if an impedance is connected between any two points in a network consisting of linear impedances, the resulting (steady state) current through the impedance is the ratio of the open circuit voltage across the two points (before the impedance is connected) to the sum of the connecting impedance and the impedance of the network looking in from the two points. Taking the valve equivalent circuit of

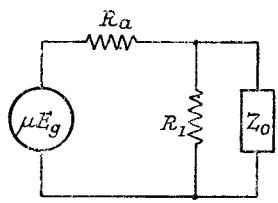

FIG. 3A.1.—A Valve Generator Circuit supplying a Resistance and Impedance in Parallel.

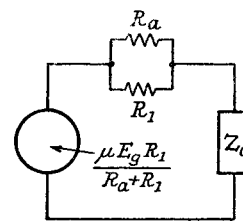

FIG. 3A.2.—The Thévenin Equivalent of Fig. 3A.1.

Fig. 3A.1, it means that the equivalent generator has a generated voltage of $\frac{\mu E_g R_1}{R_a+R_1}$ and an internal impedance of R_a and R_1 in parallel as shown in Fig. 3A.2.

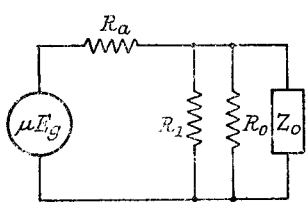

FIG. 3A.3.—A more Complicated Valve Generator Circuit.

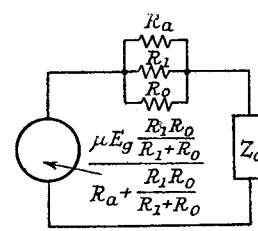

FIG. 3A.4.—The Thévenin Equivalent of FIG. 3A.3.

* Appendix 1A and 2A appear in Part I.

The proof is as follows:

For Fig. 3A.1

$$E_0 = \frac{\mu E_g \dfrac{R_1 Z_0}{R_1 + Z_0}}{R_a + \dfrac{R_1 Z_0}{R_1 + Z_0}} = \frac{\mu E_g R_1 Z_0}{R_a(R_1 + Z_0) + R_1 Z_0}$$

and for Fig. 3A.2

$$E_0 = \frac{\dfrac{\mu E_g R_1}{R_a + R_1} Z_0}{\dfrac{R_a R_1}{R_a + R_1} + Z_0} = \frac{\mu E_g R_1 Z_0}{R_a R_1 + Z_0(R_a + R_1)}$$

which is identical with the result obtained from direct analysis.

The same method may be used to show that the two circuits given in Figs. 3A.3 and 3A.4 produce the same result as far as the output voltage across, and current in, Z_0 are concerned.

INDEX

THE END